



Sustainable Stabilisation of Expansive Road Pavement Foundations, Pavement thickness Optimisation and Defects Analysis



Submitted by
Samuel Yaw Owusu Amakye (GMICE)
Student No: 19042147

A thesis submitted in partial fulfilment of the requirements of the
University of the West of England, Bristol for the degree of Doctor of
Philosophy (PhD) In Civil Engineering



Department of Engineering, Design and Mathematics, Faculty of Environment and Technology,
University of the West of England, United Kingdom
April 2023

Supervisors

Dr Samuel Jonah Abbey (DoS) and Dr Colin Anthony Booth (Supervisor)

Funding

This Research Did Not Receive Any Specific Grant From Funding Agencies In The Public,
Commercial or Not-For-Profit Sector

This submission is in compliance with requirements for the completion of a PhD research program at the University of the West of England (UWE), Bristol, as specified in the academic regulations and procedures 2018/2019. This report is sectioned into nine main chapters

CERTIFICATE OF RESEARCH

This is to certify that, except where specific references are made, the work described in this thesis is the result of work carried out by the candidate. Neither this thesis nor any part of it has been presented or is currently submitted in candidature for any other degree at any other university

Samuel Yaw Owusu Amakye
(Candidate Signature)

Date

Dr Samuel Jonah Abbey
(Director of Studies Signature)

Date

Dr Colin Anthony Booth
(Supervisor Signature)

Date

ACKNOWLEDGEMENTS

The author would like to thank the leadership of Jacobs Engineering Inc. for their support during this research. The author would like to specifically express his heartfelt gratitude and appreciation to Dr Samuel Jonah Abbey and Dr Colin Booth who has been of great support from the start to the finish of this research. Their good counsel, advice and guidance based on their in-depth knowledge of the subject area of this study kept me on track during the time of this research and I would like to say I'm grateful. I also say thank you to Prof. Jonathan Oti for the massive support given to me during the publication of my work I say God richly bless him.

The author also says thank you to Andrew Geary, the team leader of Geosciences, Emma Brown and Adrian Rose who are the Earth Sciences Laboratory technicians and Atul Vadgama who is a senior technician at the concrete laboratory for the support given me during my laboratory experiments. And last but not least, I would like to say thank you to my family especially my wife Adwoa Amakye and my sister Deborah Amakye for the words of encouragement and support through this journey, I'm very grateful.

LIST OF PUBLICATIONS

S/N	Publication Title	Links
1	Road Pavement Defect Investigation Using Treated and Untreated Expansive Road Subgrade Materials with Varying Plasticity Index	https://doi.org/10.1016/j.treng.2022.100123
2	DMRB Flexible Road Pavement Design Using Re-Engineered Expansive Road Subgrade Materials with Varying Plasticity Index	https://doi.org/10.3390/geotechnics2020018
3	Road Pavement Thickness and Construction Depth Optimization Using Treated and Untreated Artificially-Synthesized Expansive Road Subgrade Materials with Varying Plasticity Index	https://doi.org/10.3390/ma15082773
4	Enhancing the Engineering Properties of Subgrade Materials Using Processed Waste: A Review	https://doi.org/10.3390/geotechnics1020015
5	Understanding the Performance of Expansive Subgrade Materials Treated With Non-traditional Stabilisers: A Review	https://doi.org/10.1016/j.clet.2021.100159
6	Consistency and Mechanical Properties of Sustainable Concrete Blended with Brick Dust Waste Cementitious Materials	https://doi.org/10.1007/s42452-021-04430-w
7	Mechanical Properties and Microstructure of Fibre-Reinforced Clay Blended with By-Product Cementitious Materials	https://doi.org/10.3390/geosciences10060241
8	Performance of Sustainable Road Pavements Founded on Clay Subgrades Treated with Eco-Friendly Cementitious Materials	https://doi.org/10.3390/su141912588

ABSTRACT

Expansive road subgrade has been in existence for decades resulting in major road pavement defects, high maintenance/construction costs and detrimental environmental effects associated with using traditional cement and lime in subgrade stabilisation. Taking a sustainable approach, this research aims to address these issues using waste and industrial by-products (i.e. brick dust waste (BDW), ground granulated blast-furnace slag (GGBS), recycled plastic (RP) and recycled glass (RG) as partial replacements for cement and lime in subgrade stabilisation. The study investigates the sample characteristics, mineral structure, Atterberg limit, compaction, California Bearing Ratio (CBR), swell and microstructural properties of treated and untreated expansive subgrade materials.

Sustainable waste materials and industrial by-products at proportions of 23.5%GGBS, 23.5%RP, 23.5%RG, 23.5%BDW and 11.75%GGBS, 11.75%RP, 11.75%RG, 11.75%BDW were used to achieve the optimum results. This reduced 20%Cement and 8%Lime (control mix design) to 2.5%Cement and 2%Lime. The 2.5%Cement was later eliminated and GGBS increased to 26% to see the effect on subgrade. Untreated high plasticity index (PI) (103) subgrade recorded Optimum Moisture Content (OMC) of 34.46% with a standard deviation (SD) of 23.41% and Maximum Dry Density (MDD) of 1.25Mg/m³ (SD=0.31%). A Liquid Limit (LL) of 131.26% (SD=18.18%) and Plastic Limit (PL) of 28.74% (SD=1.85%) were also recorded for untreated high PI subgrade. Untreated extremely high PI subgrade (249) recorded higher OMC of 40.97% (SD=9.42%) and MDD of 1.17 Mg/m³ (SD=0.28%) with much higher LL of 294.07% (SD=48.48%) and PL of 45.38% (SD=1.13%). CBR values for untreated subgrade increased from 0.6% (SD=4.38%) to 109% (SD=34.10%) and 200% (SD=53%) and up to 220% (SD=54%) after 28 and 90 days of curing when 20%Cement+8% Lime were partially replaced with 23.5%GGBS, 11.75%GGBS+11.75%BDW and 26%GGBS. Swell values reduced from 56.76% (SD=7.72%) to 0.04% (SD=0.01%) after 20%Cement+8%Lime were partially replaced with 23.5%GGBS and 11.75%GGBS+11.75%BDW translating into reduced pavement thickness and depth of construction when pavement design was conducted in the study.

Road pavement thickness of 700mm and depth of construction of 800mm recorded for untreated subgrade with CBR values less than 2% reduced to 40mm and 50mm with CBR values between 80-100% when 20%Cement+8%Lime were partially replaced with 23.5%GGBS and 11.75%GGBS +11.75%BDW. Pavement design conducted using CBR values between 80-100% achieved for waste-treated subgrade in accordance with Design Manual for Roads and Bridges (DMRB) recorded a slight reduction in pavement thickness with reduced stresses responsible for pavement defects. A gradual reduction in CBR values from 230% (SD=54.61%) to 16% (SD=29.81%) for high PI subgrade and from 200% (SD=47.79%) to 15% (SD=20.44%) for extremely high PI subgrade was observed after ten (10) wetting-drying cycles when 20%Cement+8%Lime was partially replaced with 23.5%GGBS and 11.75%GGBS+11.75%BDW. These acceptable CBR values achieved for wetting-drying cycle were due to the formation of high Calcium Silicate Hydrate (CSH) gel in the mix where up to 44.87% (SD=11.98%) of calcium (Ca) was recorded after 28 days of curing. Mix design 2%Lime+2.5%Cement+23.5%GGBS was selected as the optimised and most viable mix design in this study followed by mix design 2%Lime+2.5%Cement+11.75%GGBS+11.75%BDW due to their ability to achieve acceptable results for the set objectives including reduced Life Cycle Cost (LCC).

Furthermore, a 55% reduction in LCC (£268,433,336) was observed for a kilometre (km) of road subgrade treated using 23.5%GGBS; whilst a high LCC of £488,754,774 was recorded for a km of road subgrade removed and replaced with foreign materials. Sustainably treated subgrade using 23.5%GGBS recorded 21% lower embodied carbon (0.0018 Co₂e/kg); whilst subgrade treated using 20%Cement+8%Lime recorded high embodied carbon of 0.0084 Co₂e/kg. Based on these findings, the study concluded that the engineering properties of expansive subgrade can be enhanced with reduced pavement thickness/construction depth, defects, carbon emission and overall LCC using sustainable waste as additives in subgrade stabilisation. However, the findings are based entirely on laboratory generated data and not field data. Therefore, as a next step, and before widespread uptake is considered, it is important that the findings are tested and verified in real-life field settings.

SYMBOLS AND ABBREVIATIONS

ASS	Artificially Synthesised Subgrade
BCS	Black Cotton Soil
BDW	Brick Dust Waste
C-A-H	Calcium-Aluminate-Hydrate
CBR	California Bearing Ratio
CCP	Coal Combustion Products
CCP	Coal Combustion Products
CDA	Cow Dung Ash
CDW	Construction and Demolition Waste
CMA	Cold Mix Asphalt
Co₂	Carbon Dioxide
C-S-H	Calcium Silicate Hydrate
DEHA	Diethylhydroxylamine
DMRB	Design Manual for Roads and Bridges
DSC	Differential Scanning Calorimetry
EDX	Energy Dispersion X-Ray
EPMA	Electron Probe Micro-Analyser
EU	European Union
EUAC	Uniform Annual Costs
GGBS	Ground Granulated Blast-Furnace Slag
HBM	Hydraulic Bound Material
HBM	Hydraulic Bound Mixture
HDPE	High-Density Polyethylene
HMA	Hot Mix Asphalt
KM	Kilometre
LCCA	Life Cycle Cost Analysis
LDPE	Low-Density Polyethylene
LL	Liquid Limit
MDD	Maximum Dry Density
Mt	Metric Tonne
NPV	Net Present Value
OMC	Optimum Moisture Content

Symbols and Abbreviations

OPC	Ordinary Portland Cement
PC	Portland Cement
PETE	Polyethene Terephthalate
PL	Plastic Limit
RG	Recycled Glass
RHA	Rice Husk Ash
RP	Recycled Plastic
SBD	Solid-State Backscattered Detector
SCBA	Sugarcane Bagasse Ash
SD	Standard Deviation
SEM	Scanning Electron Microscopy
SL	Shrinkage Limit
TGA	Thermo Gravimetric Analysis
ToT	Tetrahedral Octohedral Tetrahedral
TSCS	Thin Surface Course System
UCS	Unconfined Compressive Strength
UN	United Nations
UNSDG	United Nations Sustainable Development Goals
VA	Volcanic Ash
VDOT	Virginia Department of Transport
WHO	World Health Organisation
WMA	Warm Mix Asphalt
XRD	X-Ray Diffraction

Table of Content

Table of Content

CERTIFICATE OF RESEARCH.....	i
ACKNOWLEDGEMENTS	ii
LIST OF PUBLICATIONS	iii
ABSTRACT	iv
SYMBOLS AND ABBREVIATIONS	v
1. CHAPTER 1 – INTRODUCTION	1
1.1 BACKGROUND OF THE RESEARCH	1
1.2 PROBLEM STATEMENT.....	4
1.3 RESEARCH AIM AND OBJECTIVES	5
1.3.1 Aim	5
1.3.2 Objectives	5
1.4 ANTICIPATED IMPACT OF THE RESEARCH.....	6
1.4.1 Climate change.....	6
1.4.2 The United Nations Sustainable Development Goals (UNSDGs).	7
1.5 STRUCTURE OF THESIS	9
1.6 CHAPTER SUMMARY.....	10
2. CHAPTER 2 – LITERATURE REVIEW	11
2.1 SOIL.....	11
2.2 EXPANSIVE SOIL	14
2.3 CHARACTERISTICS AND MINERALS OF CLAY SOIL.....	17
2.3.1 Structure of Clay Minerals.....	19
2.3.2 Kaolinite and Attapulgite Group	22
2.3.3 Chlorite and Mica Group.....	23
2.3.4 Smectite, Illite and Vermiculite Group.....	24
2.4. IDENTIFICATION OF CLAY MINERALS.....	25
2.4.1 Scanning Electron Microscopy (SEM):	26
2.4.2 Energy Dispersion X-ray (EDX):	27
2.5 EXPANSIVE SUBGRADE STABILISATION	28
2.6 PROCESSED WASTE MATERIALS	35
2.6.1 Sustainability of Using Processed Waste in Subgrade Stabilisation.....	40
2.6.2 Effect of Process Waste on The Engineering Properties of Road Subgrade	41

Table of Content

2.7 BRICK DUST WASTE (BDW).....	44
2.8 GROUND GRANULATED BLAST-FURNACE SLAG (GGBS).....	47
2.9 PLASTICS.....	49
2.10 RECYCLED GLASS.....	51
2.11 PORTLAND CEMENT	53
2.12 HYDRAULIC LIME	57
2.13 CATION EXCHANGE AND FLOCCULATION-AGGLOMERATION	60
2.14 POZZOLANIC AND CARBONATION REACTIONS	60
2.15 ROAD PAVEMENT THICKNESS AND CONSTRUCTION DEPTH OPTIMISATION	61
2.15.1 Flexible, Flexible Composite and Rigid Pavements	62
2.16 ECONOMIC APPRAISAL	64
2.17 CHAPTER SUMMARY.....	65
3. CHAPTER 3 – MATERIALS	66
3.1 BENTONITE CLAY	66
3.2 KAOLINITE (CHINA CLAY)	67
3.3 PORTLAND CEMENT	67
3.4 QUICK LIME	68
3.5 BRICK DUST WASTE.....	69
3.6 GROUND GRANULATED BLAST-FURNACE SLAG (GGBS).....	70
3.7 RECYCLED PLASTIC.....	71
3.8 RECYCLED GLASS	72
3.9 CHAPTER SUMMARY.....	76
4. CHAPTER 4 – METHODOLOGY AND RESEARCH DESIGN	77
4.1 SOIL SAMPLING AND MATERIAL CHARACTERISATION	78
4.2 PRELIMINARY TESTS	78
4.2.1 - Moisture content	78
4.2.2 - Atterberg limits.....	79
4.3 PROCTOR COMPACTION TEST.....	86
4.4 MIX DESIGN.....	89
4.4.1 Preliminary Mix design and Mix Optimisation	89
4.5 CBR TEST SPECIMEN PREPARATION.....	92
4.6 LABORATORY TESTING	99
4.6.1 California Bearing Ratio (CBR)	99

Table of Content

4.6.2 CBR Test for Untreated Artificially Synthesised Subgrade (ASS).....	102
4.6.3 CBR Test for Treated Artificially Synthesised Subgrade (ASS)	102
4.6.4 Swell Test	103
4.6.5 Durability Test – Wetting-drying Cycle	110
4.6.6 Microstructural Properties of Treated Subgrade Materials.....	111
4.7 ROAD PAVEMENT ANALYSIS AND ECONOMIC APPRAISAL	113
4.7.1 DMRB Road Pavement Design	113
4.7.2 Road Pavement Thickness and Construction Depth Optimisation.....	114
4.7.3 Road Pavement Defect Analysis	117
4.8 ECONOMIC APPRAISAL	122
4.8.1 Life Cycle Cost (LCC) Estimate	122
4.9 LIMITATIONS	126
4.10 CHAPTER SUMMARY.....	127
5. CHAPTER 5 – RESULTS AND DISCUSSION	128
5.1 COMPACTION AND ATTERBERG LIMITS FOR UNTREATED ASS MATERIALS.....	128
5.2 CALIFORNIA BEARING RATIO (CBR).....	130
5.2.1 Untreated Artificially Synthesised Subgrade Materials	130
5.2.2 CBR for Artificially Synthesised Subgrade Treated with Cement and Lime	132
5.2.3 CBR for ASS materials treated with sustainable materials	135
5.3 SWELL FOR ASS MATERIALS.....	156
5.3.1 Treated and Untreated Artificially Synthesised Subgrade Materials	156
5.3.2 Swell Test in Accordance with BS EN 13286-47:2021	159
5.3.3 Variation in Swell Using BDW In Accordance with BS EN 13286-47:2021	163
5.3.4 Variation in Swell Using GGBS In Accordance with BS EN 13286-47:2021	167
5.3.5 Variation in Swell Using Recycled Plastic in Accordance with BS EN 13286-47:2021.....	171
5.3.6 Variation in Swell Using Recycled Glass In Accordance with BS EN 13286- 47:2021.....	175
5.3.7 Variation in Swell Using GGBS and Recycled Plastic In Accordance with BS EN 13286-47:2021	179

Table of Content

5.3.8 Variation in Swell Using GGBS and Recycled Glass In Accordance with BS EN 13286-47:2021.....	183
5.3.9 Variation in Swell Using GGBS and Brick Dust Waste (BDW) In Accordance with BS EN 13286-47:2021.....	188
5.4 Swell test in accordance with BS EN 13286-49:2004	193
5.5 DURABILITY TEST - WETTING-DRYING CYCLE	195
5.6 MICROSTRUCTURAL PROPERTIES.....	204
5.7 ROAD PAVEMENT THICKNESS AND CONSTRUCTION DEPTH OPTIMISATION	211
5.7.1 Variation in Pavement Thickness and Construction Depth	211
5.7.2 Sustainable Treated – Soaked and Un-soaked CBR.....	212
5.8 ROAD CONSTRUCTION DEPTH OPTIMISATION	229
5.8.1 Treated and Untreated ASS Materials	229
5.9 DMRB PAVEMENT DESIGN	240
5.10 ROAD PAVEMENT DEFECT ANALYSIS	248
5.10.1 Stress Effect on Treated and Untreated ASS Materials.....	248
5.10.2 Permanent Deformation, Fatigue and Rutting Failure for Treated and Untreated ASS Materials	277
5.11 ECONOMIC APPRAISAL	285
5.11.1 Variation in Cost of Using Sustainable Waste or Cement and Lime	285
5.12 CLASSIFICATION OF PARAMETERS AND EMBODIED CARBON	297
5.13 UNITED NATIONS SUSTAINABLE DEVELOPMENT GOALS (UNSDGs) .	298
5.14 CHAPTER SUMMARY.....	302
6. CHAPTER 6 – CONCLUSIONS AND RECOMMENDATIONS.....	303
6.1 INTRODUCTION	303
6.2 REVIEW OF RESEARCH OBJECTIVES.....	303
6.2.1 Objective One	303
6.2.2 Objective Two	303
6.2.3 Objective Three	303
6.2.4 Objective Four	304
6.2.5 Objective Five	304
6.2.6 Objective Six.....	304
6.2.7 Objective Seven.....	304
6.3 RESEARCH LIMITATIONS.....	304

Table of Content

6.3.1 Research Results and Conclusions	304
6.3.2 Limited Literature in the Research Area	304
6.3.3 Sample Size.....	305
6.3.4 Data Analysis.....	305
6.3.5 Limited CBR Moulds	305
6.3.6 Limited Swell Apparatus	306
6.3.7 Delays in Delivery of Materials.....	306
6.3.8 Financial Constraints	307
6.4 REVIEW OF RESEARCH FINDINGS	307
6.4.1 Preliminary Findings	307
6.4.2 California Bearing Ratio (CBR)	307
6.4.3 Swell	307
6.4.4 Durability.....	307
6.4.5 Microstructural Properties.....	308
6.4.6 Road pavement Analysis	308
6.4.7 Economic Appraisal	308
6.4.8 Environmental Effects.....	308
6.5 IMPLICATIONS OF THE RESEARCH FINDINGS.....	309
6.6 CONTRIBUTION TO THE BODY OF KNOWLEDGE	309
6.7 CONCLUSIONS.....	310
6.7.1 Ranking of Treatments	310
6.7.2 Enhancement of Engineering Properties	311
6.7.3 Effect on Road Pavement.....	313
6.7.4 Microstructural Analysis	314
6.7.5 Cost Effects	315
6.7.6 Environmental and Sustainability.....	316
6.8 RECOMMENDATIONS.....	317
6.8.1 Recommendations for Clients and Decision-makers	317
6.8.2 Recommendations for Designers.....	317
6.8.3 Recommendations for Road Contractors.....	317
6.8.4 Recommendations for Policy-makers	317
6.8.5 Recommendation for Future Research.....	318
6.9 CHAPTER SUMMARY.....	318

Table of Content

REFERENCES.....	320
APPENDIXES	358
Appendix 1: Preliminary test	358
Appendix 1.1 Data table for Figure 82	358
Appendix 1.2 Data table for Figure 83	358
Appendix 2: California Bearing Ratio (CBR)	358
Appendix 2.1 Data table for Figures 85 – 94.....	358
Appendix 3: Swell	360
Appendix 3.1 Data tables for Figures 95 - 111	360
Appendix 3.2 Data table for Figures 112 - 114.....	361
Appendix 4: Durability test - wetting-drying cycle.....	362
Appendix 4.1 Data table for Figures 115 – 122.....	362
Appendix 5 : Calculation	364
Appendix 5.1 Defect calculations procedure for Figures 186 – 197	364
Appendix 6 Economic appraisal.....	365
Appendix 6.1 Cost calculations procedure used for Figures 239 – 247	365
Appendix 6.2 Agency and user cost data.....	368
Appendix 6.3 Estimated maintenance, rehabilitation cost and discount rate	368
Appendix 6.4 Life cycle cost analysis calculations procedure	368
Appendix 6.4.1 LCCA treated subgrade	368
Appendix 6.4.2 LCCA calculation subgrade removal and replacement	369
Appendix 7 Laboratory photos	370
Appendix 7.1 Research limitations.....	370
Appendix 7.2 Preliminary test process.....	376
Appendix 7.3 California Bearing Ratio sample preparation and testing	378
Appendix 7.4 Wetting-drying sample preparation and testing process	380
Appendix 7.5 SEM and EDX.....	381
Appendix 8 Publications.....	391
Appendix 8.1 Publications (Journal).....	391

List of Figures

List of Figures

Figure 1.1: Shrink-Swell potential areas in the UK and areas in the US where soils are susceptibility soils to swelling	1
Figure 1.2: Distribution of expansive clay in South Africa.....	2
Figure 1.3: Typical wet expansive soil.....	1
Figure 1.4: Typical dry expansive soil typical dry expansive soil.....	1
Figure 1.5: Uplifting of flexible pavement	2
Figure 1.6: Typical longitudinal crack on road pavement	2
Figure 1.7: Differential settlement due to expansive	3
Figure 1.8: Slope failure of embankment caused by expansive soil.....	3
Figure 1.9: Objective and chapter correlation.....	6
Figure 1.10: Sustainable Development Venn diagram	9
Figure 2.1: Production of kaolinite from Devon and Cornwall from 1748 to 2001.....	13
Figure 2.2: Wyoming bentonite production from 1921 to 2012.....	14
Figure 2.3: Mechanism of expansive soils showing expansion of expansive soil due to water adsorption in (B) and shrinkage expansive soil due to dryness	16
Figure 2.4: Bentonite clay structure.....	20
Figure 2.5; Kaolinite clay structure	21
Figure 2.6; Clay mineral structure	21
Figure 2.7: The testing process of SEM analysis	27
Figure 2.8: The testing process of Energy Dispersion X-ray	28
Figure 2.9: Cement stabilisation process in road construction	30
Figure 2.10: Fly ash stabilisation process in road construction	30
Figure 2.11: Lime stabilisation process in road construction.....	31
Figure 2.12: Construction and demolition waste, geogrid and textile used in road construction	31
Figure 2.13: Application process of binder agent in real-life road construction	32
Figure 2.14: Projected waste generation, by region Mt per year	37
Figure 2.15: Modes of the utilisation of fly ash in the year 2014-15	38
Figure 2.16: Utilisation of fly ash in areas of engineering.....	39
Figure 2.17: Modes of fly ash utilisation in 2012-13.	40
Figure 2.18: Contribution of the top 10 countries in global CO ₂ emission in 2008....	41
Figure 2.19: Stockpile of brick waste.....	46
Figure 2.20: Recycling of brick waste to produce brick dust waste	46
Figure 2.21: Ground Granulated Blast-furnace Slag (GGBS) stockpile.....	48
Figure 2.22: Schematic diagram of the manufacturing process of GGBS	48
Figure 2.23: Waste plastics bottles and other types of plastic waste	50
Figure 2.24: Plastic recycling process	51
Figure 2.25: Difference between flexible and rigid pavement.....	63
Figure 3.1: Package of the bentonite clay used in this study.....	66
Figure 3.2: Bentonite clay used in this study	66
Figure 3.3: Package of the kaolinite clay used in this study	67

List of Figures

Figure 3.4: Kaolinite clay used in this study	67
Figure 3.5: Package of the cement used in this study	68
Figure 3.6: Cement used in this study	68
Figure 3.7: Package of the Lime used in this study	69
Figure 3.8: Lime used in this study	69
Figure 3.9: The package of the brick dust waste used in this study	70
Figure 3.10: Brick dust waste used in this study	70
Figure 3.11: The package of the GGBS used in this study.....	71
Figure 3.12: GGBS used in this study	71
Figure 3.13: Package of the recycled plastic used in this study	72
Figure 3.14: Recycled plastic used in this study.....	72
Figure 3.15: The package of the glass grits used in this study.....	73
Figure 3.16: The recycled glass grits used in this study	73
Figure 3.17: Particle size distribution of materials used in this study	74
Figure 4.1: Research methodological process	77
Figure 4.2: Laboratory test process and how plastic limit samples were prepared ..	83
Figure 4.3: Laboratory test process and how liquid limit samples were prepared	86
Figure 4.4: Laboratory testing process and how proctor compaction samples were prepared	88
Figure 4.5: Moisture content control chart (VDOT).....	94
Figure 4.6: Untreated un-soaked ASS CBR sample preparation process	95
Figure 4.7: Untreated soaked ASS CBR sample preparation process	96
Figure 4.8: Treated un-soaked ASS CBR sample preparation process	97
Figure 4.9: Treated soaked ASS CBR sample preparation process	98
Figure 4.10: CBR testing process (a) CBR apparatus used in this study (b) CBR Mould with surcharge weight and transducer during testing (C) Extruding CBR sample using hydraulic jack after testing is complete.	101
Figure 4.11: Untreated swell testing process in accordance with BS EN 13286-47:2021.....	105
Figure 4.12: Treated swell testing process in accordance with BS EN 13286-47:2021	106
Figure 4.13: Consolidometer apparatus used in this research	108
Figure 4.14: Swell set-up for treated and untreated ASS materials.....	109
Figure 4.15: Treated and untreated ASS1 (High plasticity subgrade) and ASS2 (Extremely high plasticity subgrade) samples after swell test.	109
Figure 4.16: Describes how samples are mounted.	112
Figure 4.17: Stub holder for the SEM chamber.	112
Figure 4.18: Gold Sputter Coating Unit.	112
Figure 4.19: Treated Artificially Synthesised Subgrade (ASS) material mounted and ready for SEM and EDX analysis.....	112
Figure 4.20: Three-layer flexible composite pavement structure	114
Figure 4.21: Class 3 design – single foundation layer	115
Figure 4.22: Nomograph for determining the design thickness for flexible pavement	116

List of Figures

Figure 4.23: Pavement deflection in tensile and compressive stress in the pavement structure.....	120
Figure 4.24: Types of stresses within a road pavement structure	120
Figure 4.25: Types of road pavement failures.	121
Figure 4.26: The five sections of the RealCost Switchboard	125
Figure 4.27: Example of expenditure stream.....	125
Figure 5.1: Proctor compaction test results	129
Figure 5.2: Atterberg limit test results against plasticity index	130
Figure 5.3: Plasticity index chart	130
Figure 5.4: Results for untreated ASS materials where B is Bentonite and K is Kaolinite.....	132
Figure 5.5: Control mix for treated Artificially Synthesised Subgrade.....	135
Figure 5.6: CBR results for the various treated, soaked and un-soaked ASS materials at varying curing ages	138
Figure 5.7: CBR results for the various treated, soaked and un-soaked ASS materials at varying curing ages	142
Figure 5.8: CBR results for the various treated, soaked and un-soaked ASS materials at varying curing ages	145
Figure 5.9: CBR results for the various treated, soaked and un-soaked ASS materials at varying curing ages	147
Figure 5.10: CBR results for the various treated, soaked and un-soaked ASS materials at varying curing ages	150
Figure 5.11: CBR results for the various treated, soaked and un-soaked ASS materials at varying curing ages	152
Figure 5.12: CBR results for the various treated, soaked and un-soaked ASS materials at varying curing ages	155
Figure 5.13: CBR results for best performing mixes and mix without cement cured and tested after 90 days	156
Figure 5.14: Swell results for untreated ASS materials only.....	160
Figure 5.15: Treated ASS materials using cement and lime as binders	161
Figure 5.16: Combined results of treated and untreated ASS materials for comparison purposes	161
Figure 5.17: 4 days cement and lime treated swell values and soaked CBR	162
Figure 5.18: Swell results for ASS samples treated using 23.5% BDW	165
Figure 5.19: Combined results of treated and untreated ASS materials.....	165
Figure 5.20: 4 days swell values for sustainable treated ASS and soaked CBR	166
Figure 5.21: swell results for ASS samples treated using 23.5% GGBS.....	169
Figure 5.22: Combined results of treated and untreated ASS materials.....	169
Figure 5.23: 4 days swell values for sustainable treated ASS and soaked CBR	170
Figure 5.24: Swell results for ASS samples treated using 23.5% recycled plastic .	173
Figure 5.25: Combined results of treated and untreated ASS materials.....	173
Figure 5.26: 4 days swell values for sustainable treated ASS and soaked CBR	174
Figure 5.27: Swell results for ASS samples treated using 23.5% recycled glass ...	177
Figure 5.28: Combined results of treated and untreated ASS materials.....	177

List of Figures

Figure 5.29: 4 days swell values for sustainable treated ASS and soaked CBR	178
Figure 5.30: swell results for ASS samples treated using 11.75% GGBS and 11.75% recycled plastic	181
Figure 5.31: combined results of treated and untreated ASS materials	181
Figure 5.32: 4 days swell values for sustainable treated ASS and soaked CBR	182
Figure 5.33: swell results for ASS samples treated using 11.75% GGBS and 11.75% recycled glass	185
Figure 5.34: combined results of treated and untreated ASS materials	186
Figure 5.35: 4 days swell values for sustainable treated ASS and soaked CBR	187
Figure 5.36: Swell results for ASS samples treated using 11.75% GGBS and 11.75% BDW	190
Figure 5.37: Combined results of treated and untreated ASS materials for comparison purposes	191
Figure 5.38: 4 days swell values for sustainable treated ASS and soaked CBR	192
Figure 5.39: Swell results for untreated ASS materials after 28 days	194
Figure 5.40: Swell results for treated ASS materials after 28 days	195
Figure 5.41: Combined swell results for untreated and treated ASS materials after 28 days	195
Figure 5.42: Wetting-drying cycle results for subgrade 1 composed of GGBS after 28 days of curing	199
Figure 5.43: Wetting-drying cycle results for subgrade 2 composed of GGBS after 28 days of curing	200
Figure 5.44: Wetting-drying cycle results for subgrade 1 composed of GGBS and BDW after 28 days of curing	200
Figure 5.45: Wetting-drying cycle results for subgrade 2 composed of GGBS and BDW after 28 days of curing	200
Figure 5.46: Sample mass for subgrade 1 composed of GGBS after 28 days of curing	201
Figure 5.47: Sample mass for subgrade 2 composed of GGBS after 28 days of curing	201
Figure 5.48: Sample mass for subgrade 1 composed of GGBS and BDW after 28 days of curing	202
Figure 5.49: Sample mass for subgrade 2 composed of GGBS and BDW after 28 days of curing	202
Figure 5.50: Oven dry sample exhibiting cracks similar to a typical existing naturally dry expansive	203
Figure 5.51: Loose subgrade particles as a result of the disintegration of binders due to high temperature	203
Figure 5.52: Eroded subgrade sample due to cyclic wetting	203
Figure 5.53: Ca, Si, Al responsible for strength gain	208
Figure 5.54: ASS samples with dark green colour formed during the hydration process to produce C-S-H gel responsible for strength gain	209
Figure 5.55: SEM image and EDX results for ASS1 + 8% lime + 20% cement after 7 days of curing	210

List of Figures

Figure 5.56: SEM image and EDX results for ASS1+ 8% lime + 20% cement after 28 days of curing	210
Figure 5.57: SEM image and EDX results for ASS2 + 8% lime + 20% cement after 7 days of curing	210
Figure 5.58: SEM image and EDX results for ASS2+ 8% lime + 20% cement after 28 days of curing	210
Figure 5.59: Untreated ASS Swell values against pavement thickness	214
Figure 5.60: Treated swell values against pavement thickness	215
Figure 5.61: Untreated ASS Swell values against the depth of construction	215
Figure 5.62: Treated swell values against the depth of construction	216
Figure 5.63: Road pavement thickness optimisation for un-soaked treated and untreated subgrade materials	218
Figure 5.64: Road pavement thickness optimisation for un-soaked treated and untreated subgrade materials	220
Figure 5.65: Road pavement thickness optimisation for un-soaked treated and untreated subgrade materials	222
Figure 5.66: Road pavement thickness optimisation for soaked treated and untreated ASS materials	224
Figure 5.67: Road pavement thickness optimisation for soaked treated and untreated ASS materials	226
Figure 5.68: Road pavement thickness optimisation for soaked treated and untreated ASS materials	228
Figure 5.69: Road pavement construction depth optimisation for un-soaked treated and untreated ASS materials	230
Figure 5.70: Road pavement construction depth optimisation for un-soaked treated and untreated ASS materials	232
Figure 5.71: Road pavement construction depth optimisation for un-soaked treated and untreated ASS materials	234
Figure 5.72: Road pavement construction depth optimisation soaked treated and untreated ASS materials	236
Figure 5.73: Road pavement construction depth optimisation soaked treated and untreated ASS materials	238
Figure 5.74: Road pavement construction depth optimisation soaked treated and untreated ASS materials	240
Figure 5.75: Results of road pavement designed using DMRB for traffic 3msa and 8msa	243
Figure 5.76: Results of road pavement designed using DMRB for traffic 60msa and 100msa	245
Figure 5.77: Summary of DMRB road pavement design using various design traffic and CBR values	247
Figure 5.78: Stresses and Kenpave results for untreated soaked ASS materials ..	252
Figure 5.79: Stresses and Kenpave results for treated ASS materials using cement and lime	255

List of Figures

Figure 5.80: Stresses and Kenpave results for treated ASS materials using sustainable waste materials.....	258
Figure 5.81: Stresses and Kenpave results for treated ASS materials using sustainable waste materials.....	261
Figure 5.82: Stresses and Kenpave results for treated ASS materials using sustainable waste materials.....	264
Figure 5.83: Stresses and Kenpave results for treated ASS materials using sustainable waste materials.....	267
Figure 5.84: Stresses and Kenpave results for treated ASS materials using sustainable waste materials.....	270
Figure 5.85: Stresses and Kenpave results for treated ASS materials using sustainable waste materials.....	273
Figure 5.86: Stresses and Kenpave results for treated ASS materials using sustainable waste materials.....	276
Figure 5.87: Permanent deformation results for treated and untreated ASS materials	278
Figure 5.88: Permanent deformation results for treated ASS materials	279
Figure 5.89: Permanent deformation results for ASS materials	279
Figure 5.90: Permanent deformation results for ASS materials	280
Figure 5.91: Permanent deformation results for ASS materials	280
Figure 5.92: Permanent deformation results for treated and untreated ASS materials	281
Figure 5.93: Fatigue and rutting failure for treated and untreated ASS materials...	282
Figure 5.94: Fatigue and rutting failure for treated ASS materials.....	282
Figure 5.95: Fatigue and rutting failure for treated ASS materials.....	283
Figure 5.96: Fatigue and rutting failure for treated ASS materials.....	283
Figure 5.97: Fatigue and rutting failure for treated ASS materials.....	284
Figure 5.98: Fatigue and rutting failure for treated ASS materials.....	284
Figure 5.99: Discount rate, estimated maintenance and rehabilitation cost	287
Figure 5.100: LCCA for lime and cement treated ASS against subgrade removal and replacement.....	288
Figure 5.101: LCCA for sustainable treated ASS against subgrade removal and replacement.....	289
Figure 5.102: LCCA for sustainable treated ASS against subgrade removal and replacement.....	290
Figure 5.103: LCCA for sustainable treated ASS against subgrade removal and replacement.....	291
Figure 5.104: LCCA for sustainable treated ASS against subgrade removal and replacement.....	292
Figure 5.105: LCCA for sustainable treated ASS against subgrade removal and replacement.....	293
Figure 5.106: LCCA for sustainable treated ASS against subgrade removal and replacement.....	294

List of Figures

Figure 5.107: LCCA for sustainable treated ASS against subgrade removal and replacement..... 295

Figure 5.108: LCCA for sustainable treated ASS against subgrade removal and replacement..... 296

List of Tables

List of Tables

Table 2.1: Swelling potential of soils based on liquid limit	16
Table 2.2: Classification of shrink potentials based on plasticity index	16
Table 2.3: Relation of soil index properties and probably volume change for highly plastic soils	17
Table 2.4: Values of thickness, planar diameter, specific surface area and cation exchange capacity of clay minerals	17
Table 2.5: Typical values for cation exchange capacities.....	22
Table 2.6: Advantages of insitu treated subgrade and disadvantages of removal and replacement of subgrade	33
Table 2.7: Fly ash production and use in the year 2001	37
Table 2.8: Major industrial solid wastes generated in India	38
Table 2.9: CCP production around the world (Heidrich et al., 2013).	39
Table 2.10: Summary of findings of improved engineering properties of expansive subgrade stabilised using various types of processed waste.	43
Table 2.11: Summary of findings of improved engineering properties of subgrade using cement	56
Table 2.12: Summary of findings of improved engineering properties of subgrade using lime	59
Table 3.1: Oxide and some chemical composition of Bentonite, Kaolinite clay and the binders used in this study	73
Table 3.2: Consistency limits, chemical and physical properties of kaolinite, Bentonite, Portland cement, lime, brick waste plastic and glass.....	75
Table 4.1: Atterberg limit results for untreated subgrade materials	80
Table 4.2: Apparatus needed for Atterberg Limit Test.....	80
Table 4.3: Plastic limit results for untreated subgrade materials	81
Table 4.4: Liquid limit results for untreated subgrade materials	84
Table 4.5: Proctor compaction data for untreated subgrade materials	87
Table 4.6: Preliminary Mix design and Mix Optimisation used in this study	91
Table 4.7: Hydraulic Bound Base Materials (HBM).	117
Table 4.8: Description of parameters used in LCCA	124
Table 5.1: United Nations Sustainable Development Goals.....	298
Table 5.2: Summary results of all parameters described in this research	300

List of Equations

List of Equations

Equation 1 Moisture content.....	79
Equation 2 Plasticity index	80
Equation 3 Plastic Limit	81
Equation 4 Liquid Limit	84
Equation 5 Linear expansion.....	108
Equation 6 Surface Resilient Modulus.....	119
Equation 7 Subbase Resilient Modulus.....	119
Equation 8 Subgrade Resilient Modulus	119
Equation 9 Fatigue	119
Equation 10 Permanent deformation.....	119
Equation 11 Rutting Life Prediction	119
Equation 12 Initial Cons.Cost	124
Equation 13 Discount Rate.....	124

CHAPTER 1 – INTRODUCTION

Chapter 1 explains the background of the research, its aim and objectives, and the methodologies used. It also describes the impact and contribution to knowledge and a brief description of the structure of the thesis.

1.1 BACKGROUND OF THE RESEARCH

Expansive soils have the potential to swell when wet and shrink when dry (Abbey *et al.*, 2019). The clay mineral smectite found in expansive soils usually exhibits evident volume change with changes in moisture content, causing major structural and geotechnical challenges worldwide (Wu *et al.*, 2019). Structures built on expansive clay soils develop defects due to swell-shrink activities causing fissures in the structure (Pritchard *et al.*, 2013; Khademi *et al.*, 2016 and Abbey *et al.*, 2019). Each year, damage caused by expansive soils in buildings and infrastructural systems are more than the damage caused by floods, hurricanes, tornadoes, and earthquakes combined (Wu *et al.*, 2019; López-Lara *et al.*, 2017). Over the past 10 years, the negative impacts of expansive soils have cost the UK economy an estimated amount of £3 billion making it the most damaging geohazard (Jones *et al.*, 2019).

Subgrade materials refer to the ground or soil underneath a road or pavement and oftentimes, these materials do not have sufficient capacity to support the weight of the road pavement and the traffic load and will require some modification and re-engineering to enhance their capacity to support traffic loads. So, when the subgrade materials are made up of expansive soil they are termed Expansive subgrades, which leads to early distress within the pavement causing the premature failures of the road pavement structure. The common method of treating expansive subgrades involves the use of chemical stabilisation techniques, these techniques have reportedly been used to address the problems associated with expansive subgrades for many years (Jalal *et al.*, 2020). Chemical stabilisation involves adding different types of admixtures, such as lime and Ordinary Portland cement (OPC) among others, as binders to stabilise soil (Rivera *et al.*, 2020). CEM I cement type is popularly used to improve the engineering properties of expansive subgrade materials (Abbey *et al.*, 2017; Abbey *et al.*, 2018).

Chapter 1 – Introduction

Before the introduction of cement, lime was mostly used in subgrade stabilization, and it has proven to be an effective modification agent for the stabilization of highway and airport pavement subgrade. However, apart from cement and lime, other materials including fly ash, bituminous, rice husk ash, lime, construction and demolition waste, electrical and thermal waste, geotextile fabrics and recycled waste can be used as admixtures in this process (Rivera *et al.*, 2020). The addition of these materials as admixtures can alter the geotechnical properties of expansive soil, such as the strength, bearing capacity, hydraulic conductivity, compressibility, workability, durability and swelling potentials (Cabezas *et al.*, 2019). The use of waste in soil stabilisation provides environmental and economic advantages (Zorluer *et al.*, 2020). In civil engineering applications, knowing the California Bearing Ratio (CBR) of road subgrade is very important in determining the thickness and materials to be used during construction. Good California Bearing Ratio (CBR) and swelling results were achieved when 80% lime was used in the expansive subgrade stabilization for flexible pavement, and 3–8% of lime was used to improve high plasticity clays (Ingles *et al.*, 1972). Figure 1.1 shows areas in the UK and the US that are susceptible to swell-shrink effects and Figure 1.2 shows the distribution of expansive clay in South Africa. Figure 1.3 and Figure 1.4 show a typical low-strength expansive soil with high potential for swelling and shrinkage and road pavement defects caused by expansive subgrade. Figure 1.5 - Figure 1.8 shows road pavement defects caused by expansive subgrade materials.

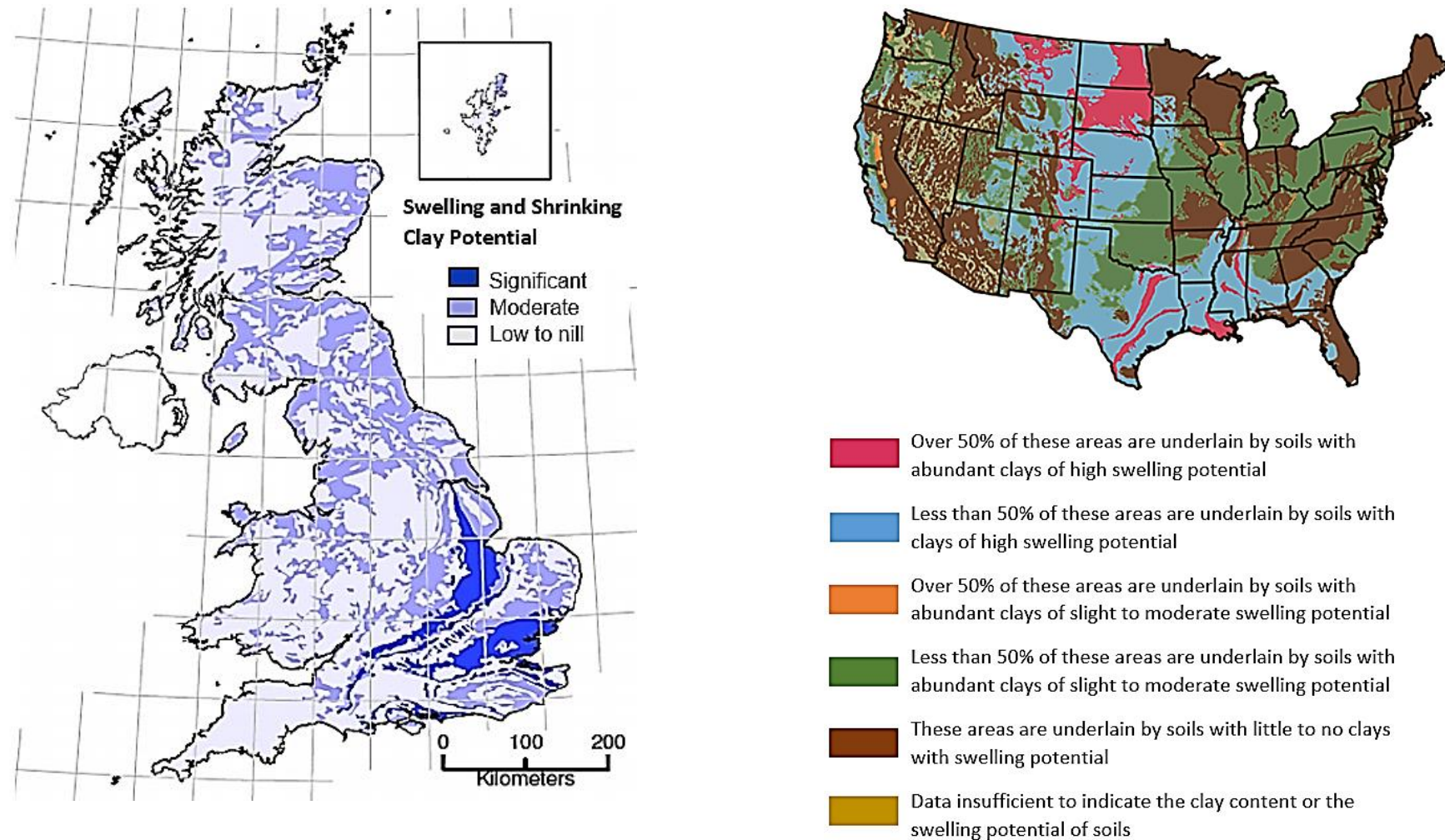


Figure 1.1: Shrink-Swell potential areas in the UK (Jones and Jefferson, 2012) and areas in the US where soils are susceptibility soils to swelling (Wang et al., 2016)

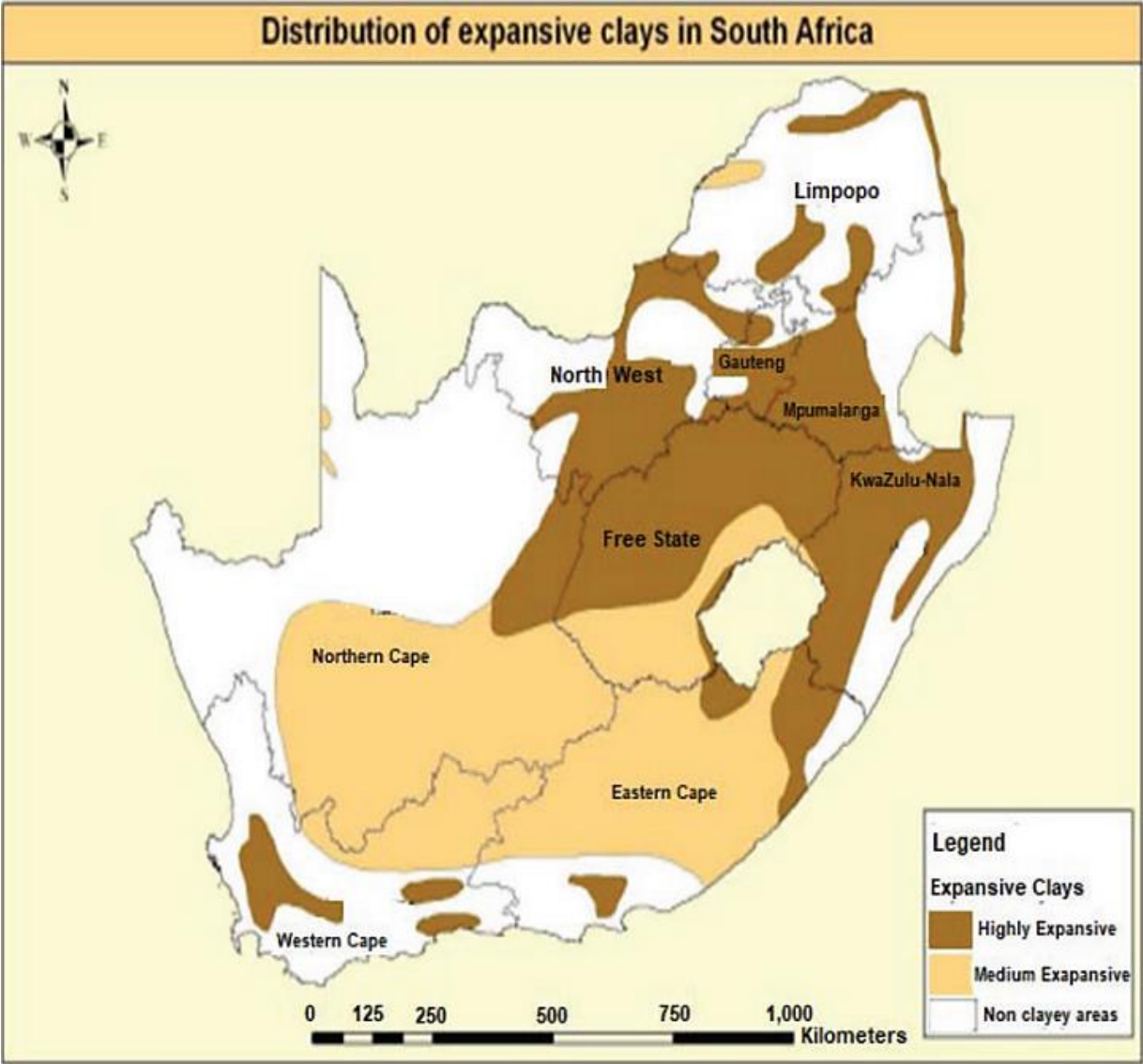


Figure 1.2: Distribution of expansive clay in South Africa (Aneke *et al.*, 2019)



Figure 1.3: Typical wet expansive soil
(Hossain *et al.*, 2019)



Figure 1.4: Typical dry expansive soil typical dry expansive soil
(British Geological Survey, 2021)



Figure 1.5:Uplifting of flexible pavement
(White *et al.*, 2021)



Figure 1.6:Typical longitudinal crack on road pavement
(The geological society, 2012)



Figure 1.7: Differential settlement due to expansive subgrade (U.S. Department of Transport, 2020)



Figure 1.8: Slope failure of embankment caused by expansive soil (Jalal *et al.*, 2020)

1.2 PROBLEM STATEMENT

Expansive soils expand and shrink with changes in moisture content within the soil causing defects in roads pavements, houses, embankments and structures to the tune of billions of pounds worldwide (Pritchard *et al.*, 2013; Khademi *et al.*, 2016; López-Lara *et al.*, 2017; Wu *et al.*, 2019; Jones, 2019 and Abbey *et al.*, 2019;) (Figure 1.5 – Figure 1.8). The process of modifying and re-engineering the subgrade materials or road pavement to make them suitable for use in construction is referred to as subgrade stabilisation. cement and lime have been successfully used for decades to stabilise road subgrade materials because of their higher binding and particle binding properties compared to other materials. After water, concrete is the most widely used material on the planet and is considered the most destructive material on Earth (López-Lara *et al.*, 2017). During cement production, a large amount (4-8%) of the world's CO₂ destroys natural resources such as limestone and vegetation, discharging waste sludge and wastewater from concrete batch plants which have harmful effects on the water ecosystem (Federica *et al.*, 2014).

It is clear that the production and use of cement and lime in subgrade stabilisation are associated with a high carbon footprint and are not environmentally friendly. Due to these global challenges, this research seeks to develop a more sustainable approach to stabilise expansive road subgrade materials for use in road construction. Therefore, the study will explore the use of sustainable waste materials and industrial by-products. An economic appraisal will conduct to investigate the cost of stabilising expansive road subgrade using waste materials in comparison with the cost of using cement and lime. Furthermore, the study will carry out road pavement thickness and construction depth optimisation to determine the effect of treating subgrade using waste materials in road construction. Lastly, a durability test will be conducted on stabilised subgrade materials. Stabilising expansive subgrade materials using waste to improve the engineering properties of road subgrade would create a robust understanding of the use of sustainable waste materials in road subgrade stabilisation. This would increase the prospects of introducing possible changes to the current road subgrade stabilisation practices based on the findings, decisions, and recommendations of this research.

1.3 RESEARCH AIM AND OBJECTIVES

1.3.1 Aim

This research aims to stabilise expansive road subgrade materials using sustainable waste and industrial by-products to obtain a desirable and acceptable subgrade strength (CBR), reduced pavement thickness and construction depth similar to cement and or lime stabilised road subgrade. The study aims to carry out durability and defects analysis to determine the effect of wetting-drying cycles and repeated traffic loadings on road subgrade stabilised using sustainable waste materials. Furthermore, the research aims to conduct road pavement design using CBR values achieved for waste-stabilised road subgrade and economic appraisal using the LCCA approach and compare the cost effects and benefits of using sustainable waste materials to the cost of using unsustainable materials (cement and lime), against the environmental effect (carbon emission) associated with cement and lime production.

1.3.2 Objectives

The objectives of the research are as follows:

1. Carry out detailed laboratory testing on stabilised and unstabilised expansive road subgrade materials with varying plasticity index used for the engineering of sustainably stabilise expansive road subgrade materials. Investigate the key engineering properties of stabilised expansive road subgrade materials including California Bearing Ratio (CBR) test and swell test.
2. Conduct microstructural analysis on treated expansive road subgrade using Scanning Electron Microscopy (SEM) and Energy Dispersion X-ray (EDX) to determine the elemental composition of treated expansive road subgrade materials.
3. Carry out road pavement thickness and construction depth optimisation. Conduct road pavement design using DMRB to determine the effect of sustainably stabilised expansive road subgrade on the thickness and construction depth of road pavement. Carry out road pavement defect analysis

Chapter 1 – Introduction

to determine how sustainably stabilised expansive road subgrades are affected or can withstand/prevent defects within the pavement structure.

4. Establish the durability of sustainably stabilised expansive road subgrade materials by carryout a wetting-drying cycle test to determine the ability of treated subgrade to withstand harsh weather conditions.
5. Conduct economic appraisal using the Life Cycle Cost Analysis (LCCA) approach to determine the cost-effects and cost-benefits of using sustainable waste materials in expansive road subgrade stabilisation.
6. Establish the environmental effects of using sustainable waste materials in road subgrade stabilisation compared with using unsustainable materials by determining the embodied carbon of each binder used in this study. Figure 1.9 shows the correlation between the objectives and chapters of this study.

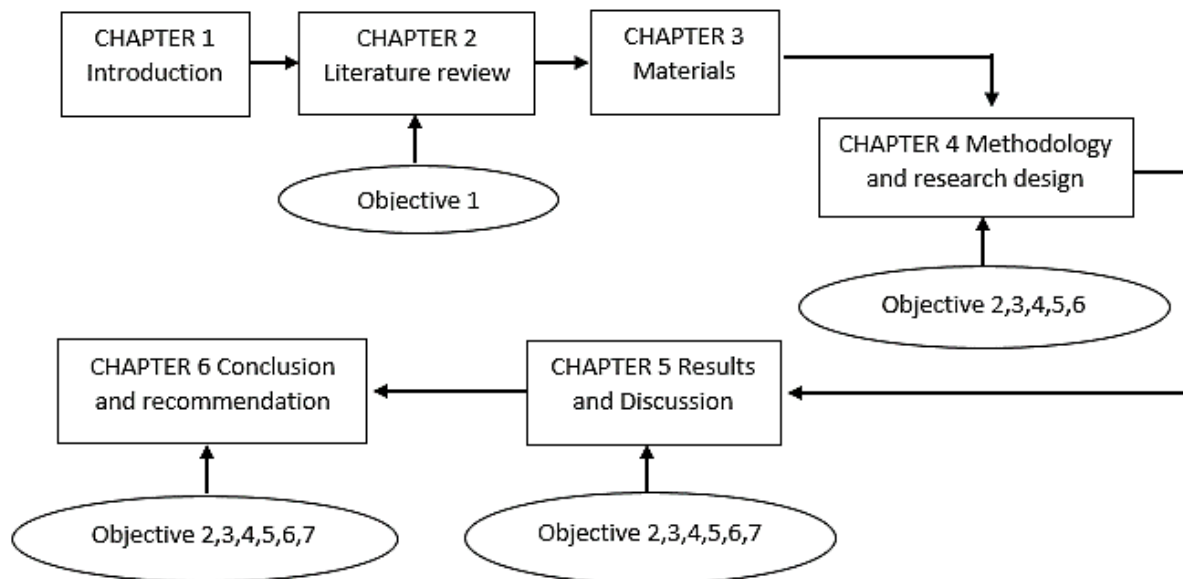


Figure 1.9: Objective and chapter correlation

1.4 ANTICIPATED IMPACT OF THE RESEARCH

1.4.1 Climate change

The entire globe is battling climate change and the findings of this research will help speed up the efforts by many countries and organisations including the United Nations (UN) and the World Health Organisation (WHO) in the fight against climate change (The World Health Organisation, 2021; United Nations (UN), 2021). The challenges

Chapter 1 – Introduction

the world is facing today with climate change are a result of the high greenhouse gases emitted into the atmosphere due to human activities, especially in the civil engineering and construction sector. Some of the causes of global warming include the production and use of unsustainable construction materials such as cement and lime which have a high demand for energy and natural resources like clinker, however, they are associated with very high carbon dioxide (CO₂) emission. The dumping of waste materials in landfills by humans also has a great impact on the environment leading to the current climate change we experience.

According to the World Health Organisation (WHO) (2021) report on climate change in the Western Pacific, it is estimated that climate change will cause an additional 250,000 deaths annually between 2030 to 2050 (The World Health Organisation, 2021 and United Nations (UN) 2021). The United Nations (UN) 2021 report on climate change states that countries are committing to net-zero emission by 2050, and about half of the emission cuts must be in place by 2030 to keep global warming below 1.5°C (The World Health Organisation (WHO), 2021; United Nations (UN), 2021). This research provides solutions to how waste materials dumped at landfills can be used in road construction to reduce the overreliance on traditional binders such as cement and lime which has contributed greatly to the recent climate change we experience.

1.4.2 The United Nations Sustainable Development Goals (UNSDGs).

Findings from this research are the way forward to the future of sustainable engineering and industrial revolution which forms part of the United Nations Sustainable Development Goals (UNSDG) (UNSDG, 2022). The finding from this research will help the drive towards achieving the sustainable development paradigm of the United Nations (UN) which focuses on the four intertwined dimensions of sustainable development– society, environment, culture and economy. The concept of sustainable development was described by the 1987 Brundtland Commission Report as “*development that meets the needs of the present without compromising the ability of future generations to meet their own needs.*” Sustainable development has been intergraded into many global frameworks and conventions related to the key areas of sustainable development such as Climate change – Article 6 of the United Nations Framework Convention on Climate Change, Biodiversity – Article 13 of

Chapter 1 – Introduction

Convention on Biological Diversity and Disaster Risk Reduction – Sendai Framework for Disaster Risk Reduction 2015-2030 (Convention on Biological Diversity, 2021 and Disaster Risk Reduction, 2015).

1.4.3.1 Society (Social Sustainability): the ability of a society or any social system to achieve good social well-being. This research provides a solution to a sustainable and cost-effective way of road subgrade stabilisation using waste materials dumped in landfills instead of using traditional cement and lime in subgrade stabilisation. This will benefit society through the reduction of greenhouse gas emissions into the atmosphere during cement production (responsible for climate change) and reducing the amount of waste dumped in landfills. Through the utilisation of waste materials in road construction, as prescribed in this study, governments will save money on the purchase of disinfectants to fumigate landfills, whilst eradicating the outbreak of diseases in society, which can be caused by the contaminated landfills.

1.4.3.2 Economy (Economic Sustainability): the ability of a county to use its resources efficiently and responsibly so that it can operate in a sustainable manner to consistently produce an operational profit. Findings from this research will help countries to save money and make a profit for use in other ventures to improve the economy through the utilisation of waste materials dumped in landfills in road stabilisation. Instead of using cement and lime which are expensive and associated with negative environmental effects.

1.4.3.3 Environment (Environmental Sustainability): this means living within the means of our natural resources and consuming these natural resources at a sustainable rate. Findings from this research will help reduce our over-reliance on scarce natural resources such as clinker used in cement production, to the use of waste materials in road construction. This will as save the environment from further human destruction due to the high demand for cement. Figure 1.10 shows a Venn diagram of how the four dimensions of sustainable development intertwine.

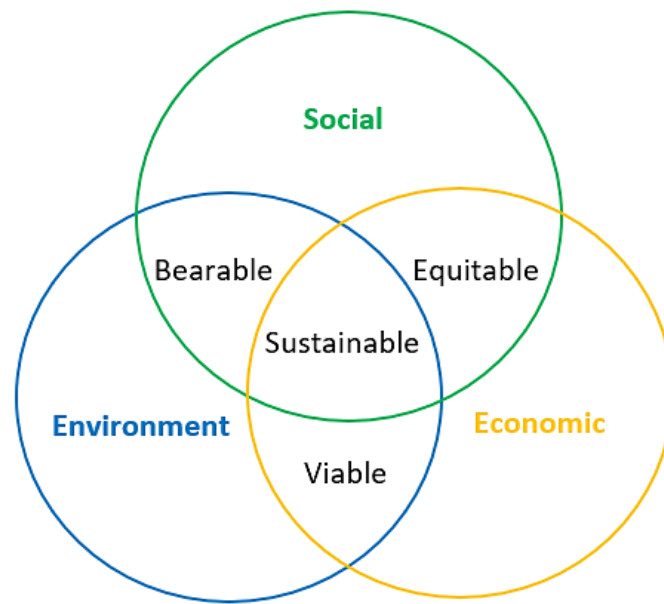


Figure 1.10: Sustainable Development Venn diagram
(ConceptDraw, 2022)

1.5 STRUCTURE OF THESIS

The body of the thesis consists of nine chapters and their arrangements are as follows;

Chapter 1 introduces the research and the report. It discusses the background of the research and the basis in a contextualised manner. The chapter expands on the nature of the problem of road pavement defects due to expansive subgrade material. The chapter summarises the main aims and objectives of the research methodology used to address the problem. This chapter further captures the researcher's view of the impact of the research work in the UK and its contribution to global knowledge.

Chapter 2 reviews existing literature on road subgrade stabilisation to establish the level of current knowledge and thinking to provide an intellectual contest of the research. A critical review of the current techniques used in subgrade stabilisation are outlined in this chapter.

Chapter 3 describes the materials used and their characterisation, including details regarding their current usage in road subgrade stabilisation, their sources, chemical and oxide compositions, some physical properties, and particle size distribution.

Chapter 4 outlines the method and research design used in this research and the analytical techniques for the formulation of mix designs. In addition, the sample

Chapter 1 – Introduction

preparation process, the test for engineering properties, such as CBR, Swell, microstructural analysis, durability tests such as wetting-drying cycles, road pavement defect analysis, optimisation of road pavement and road construction depth, cost analysis using the LCCA approach are presented in this chapter. Chapter 4 describes the process and the types of road pavement analysis, and the guidance used such as DMRB road pavement design, road pavement thickness and construction depth optimisation and road pavement defect analysis. The chapter also describes the process and how the various materials and software applications used in this research were adopted. The chapter also outlines the process of economic appraisal and the approach techniques used in the research such as the Life Cycle Cost Analysis (LCCA) approach. The chapter compared the cost effects and benefits of using sustainable waste materials in road subgrade stabilisation against unsustainable materials such as cement and lime.

Chapter 5 describes the detailed results obtained from the research work for the various test including the pavement and cost analysis conducted in this study. In this chapter, the analytical results are discussed, based on the physical observations and the correlation derived from this research. Next, the chapter shows the engineering performance of the laboratory tests and discusses the pavement and cost analysis conducted using various parameters based on this research.

Chapter 6 is the final chapter of the thesis, and it summarises the main conclusions and recommendations of the research work suggesting new areas for further research.

1.6 CHAPTER SUMMARY

Chapter 1 gives an in-depth background of the research, its impacts on the environment and climate change and how the research helps to achieve the United Nations Sustainable Development Goals (UNSDGs). The aim, objectives, methodology used, and structure of the thesis are fully described in this chapter.

Chapter 2 presents some literature on the theories and techniques in subgrade stabilisation to establish the status of current knowledge to provide an intellectual context for the research. The review aims to provide knowledge and information surrounding soil and expansive subgrade stabilisation, which influence the development of this research.

CHAPTER 2 – LITERATURE REVIEW

2.1 SOIL

Soils are the extreme outer part of the Earth's crust. They are regarded as the 'skin of the earth'. Soils are formed over time under chemical, physical and biological processes where rocks and sediments are influenced by five factors: parent materials, biota, relief, climate and time (Dokuchaev, 1883). According to Garrison *et al.* (2021), soil can be defined as the biologically active, porous medium that has developed in the uppermost layer of the earth's crust. Civil engineers define soil as a natural aggregate material or grain that can be separated by such gentle mechanical means as agitation in water (Terzaghi *et al.*, 1996). Soils are classified and categorised based on their grain shape, size and aggregate properties. The most significant aggregate properties of soil are its density (non-cohesive soil) and consistency (cohesive soil). Cohesive soils such as (clay soils) <0.002mm are sticky silt and their strength depends on the surface tension of capillary water. Non-cohesive soils such as gravel 4.75-75mm or sand 0.42mm have a particle size that does not bond together. In addition, soils serve as a natural medium to support plants' growth because they serve as a natural reservoir of water and nutrients for plants and facilitate the cycling of carbon and other elements through the global ecosystem.

Kaolinite is a white or grey mineral which is the main constituent in the manufacturing of China clay (Bristow, 1994 and 1993). China clay production in Devon and Cornwall, South-west England was 2.5 Mt per year representing approximately 10% of the world's output. Companies producing kaolinite clay include IMERYS, Goonvean and WBB Minerals. IMERYS account for 25% of the world's total China clay production of 24.4 Mt both in Devon and Cornwall and in the USA, Brazil and New Zealand (Bristow, 1994 and 1993). There are approximately 9 tonnes of waste rock and debris production for 1 tonne of China clay product and the clay-bearing ground in Cornwall covers approximately 40km² (Geography, 2010). According to Wilson. (2003), 87% and 30% of the over 60 grades of China clay produced in Cornwall are exported through the port of Par and Fowey respectively. The paper, ceramic and performance mineral market dominated the sales of kaolinite from Devon and Cornwall with 75% paper, 13% ceramics, and 12% performance mineral (mainly for paint, rubber and plastics) (Thurlow, 2001). There has been uninterrupted mining and processing of

Chapter 2 – Literature Review

China clay for a wide range of markets since the discovery in 1746 at Tregonning Hill near Helston, Cornwall by William Cookworthy. In the early 1900s, China clay was utilised in porcelain and tableware mainly in paper production as a filler and coating pigment (Wilson, 2003). The production of China clay exceeded 0.5 Mt for the first time and by 1900, 60% of the sales were for the paper industry. Kaolinite are soft clays which cannot be used on their own in construction and would require treatment to make them suitable for use. Alrubaye *et al.* (2016) used various percentages of lime (3%, 5%, 7% and 9%) and 4% silica fume to stabilise soft kaolinite to improve its engineering properties. Figure 2.1 shows China's clay production from 1748 to 2001.

The original name for Bentonite was 'mineral soap' or 'soap clay'. A pioneering geologist known as Wilbur C. Knight came to Wyoming in 1897 and served as state geologist, first used the name taylorite for bentonite in an article "the engineering and mineral journal (1897)" who made the first shipment of bentonite in 1888 (Sutherland, 2014). The highest quality bentonite was found in the upper Cretaceous Mowry Shale. Bentonite that swells contains a high concentration of sodium ions and will substantially increase in volume when it comes into contact with water. The bentonite in Wyoming originated from intense, explosive volcanism associated with the emplacement of the Idaho batholith in what is known as Idaho (Sutherland, 2014). Bentonite was first produced at \$25 per ton in 1888 by William Taylor from a property near Rock Creek. Taylor shipped 5,400 tonnes of bentonite from the quarry to buyers across the country. Bentonite pit was opened near Newcastle and Wyoming in 1897 and the total output for the year amounted to 150 tonnes. Bentonite production from 1921 to 1937 showed a substantial overall increase in both volume and total value (Sutherland, 2014).

Bentonite Clays are an absorbent swelling clay formed from the weathering of volcanic ash in seawater (Sutherland, 2014). As a swelling clay, bentonite possesses the ability to absorb large amounts of water leading to an increase in volume making bentonite beds unstable grounds for road construction and buildings (Sutherland, 2014). In fresh exposures, bentonite is pale or white-blue or green, they can turn to cream and yellow colour, brown or red by further wreathing of the exposure (Sutherland, 2014). There are three types of bentonites namely sodium bentonite, calcium bentonite and potassium bentonite. Sodium bentonite expands when wet and can absorb moisture

Chapter 2 – Literature Review

several times as its dry mass in water (Odom, 1984). Sodium bentonites are often used in drilling mud for boreholes, lining the base of landfills gas and oil wells for geotechnical and environmental investigations due to their excellent colloidal properties (Hosterman *et al.*, 1992). Bentonites are used as sealants due to their swelling property, providing a self-sealing and low permeability barrier (Hosterman *et al.*, 1992).

Calcium bentonites are a useful adsorbent of ions fats and oils in solution. It is classified as one of the earliest cleaning agents and the main active ingredient of Fuller's Earth (Lagaly, 1995). Calcium bentonite can be converted to sodium bentonite by a process called ion exchange (Lagaly, 1995). This process involves the addition of 5-10% of a soluble sodium salt such as sodium carbonate to wet bentonite, mixing well and allowing time for the ion exchange to take place and water to remove the exchanged calcium (Christidis *et al.*, 2006; Eisenhour *et al.*, 2009). Some properties may not be fully equivalent to those of natural bentonite due to viscosity and fluid loss of suspensions of sodium-beneficiated calcium bentonite (Odom, 1984). Potassium bentonite also known as k-bentonite or potash bentonite are illite clay rich in potassium formed from the alteration of smectic clay (McCarty *et al.*, 2009). Illite is a high-charge ToT clay mineral with sheets bounding relatively strongly by more numerous potassium ions, so it is not a swelling clay and has few industrial uses (Nesse, 2000). Figure 2.2 shows Wyoming bentonite production from 1921 to 2012.

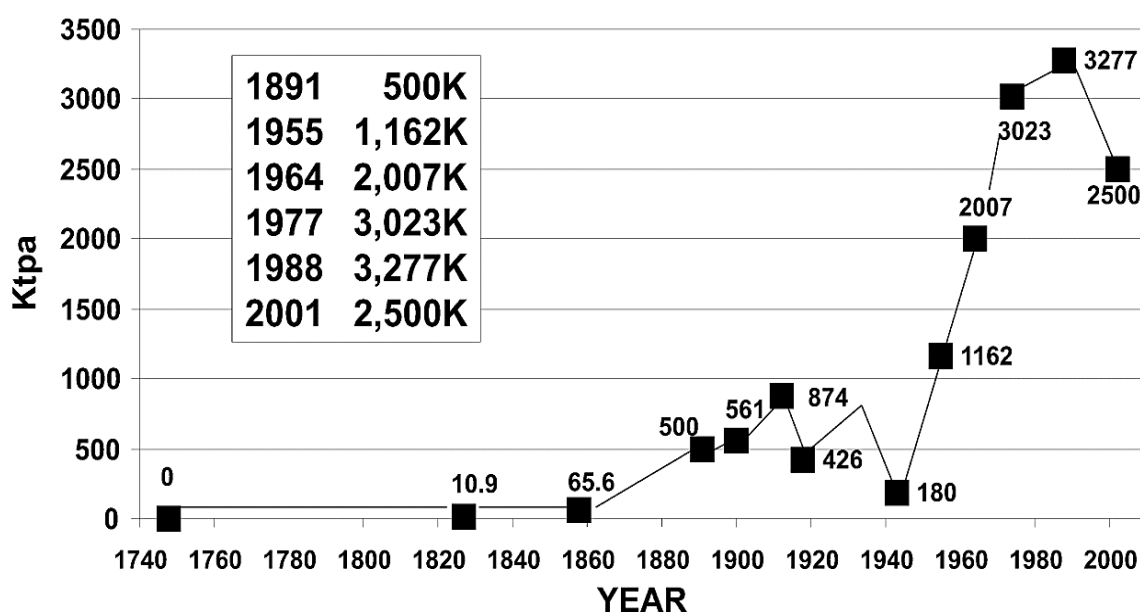


Figure 2.1: Production of kaolinite from Devon and Cornwall from 1748 to 2001 (Wilson *et al.*, 2003)

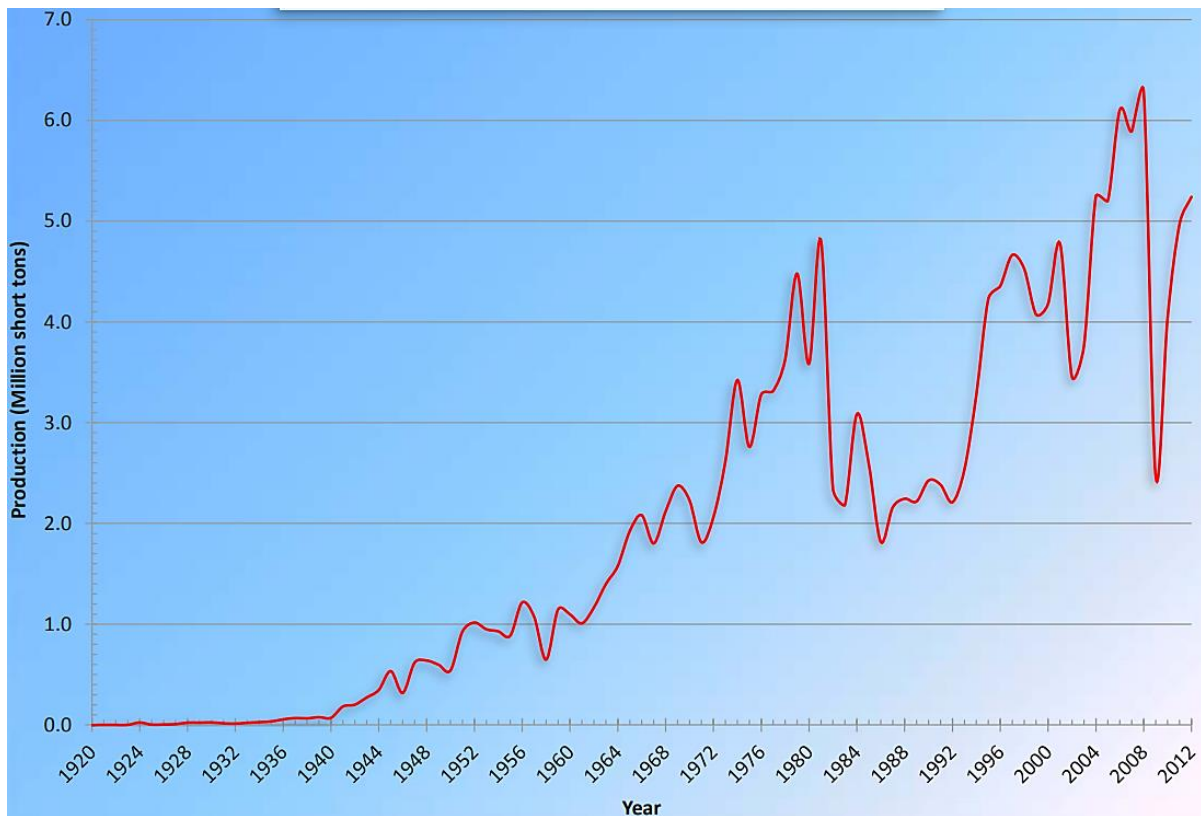


Figure 2.2: Wyoming bentonite production from 1921 to 2012 (Sutherland, 2014)

2.2 EXPANSIVE SOIL

Expansive soils are composed of high percentage of clay minerals such as montmorillonite expandable illite and vermiculite, with their liquid limit exceeding 50% and the plasticity index exceeding 30% (Elarabi, 2010). The swelling ability of expansive soils are dependent on the total internal and external areas of their mineral particles. A small amount of swell can occur as a result of the enlargement of the capillary films in clay minerals when water absorbs through their outer surface (Al-Rawas *et al.*, 2006). Expansive soils are highly plastic soils that typically contain clay minerals such as montmorillonite that attract and absorb water (Mitchell *et al.*, 2005). Water molecules in expansive soils absorb into the gaps between the clay plates when the soil is introduced to water, causing the soil to absorb more water as the moisture content increase, forcing the plates further apart (Zaid, 2017). A study conducted by Reda *et al.* (2016) reveals that, expansive soils contain smectite clay materials which at the microscopic level look like layered sheets due to their moisture-retaining abilities (See Figure 2.3) (Reda *et al.*, 2016). The diffused double layer influences the engineering properties of clayey soil, especially the hydraulic conductivity (Besq *et al.*,

Chapter 2 – Literature Review

2003). The swelling potential of expansive clay soils are due to the adsorption of water into the interlayer region due to surface forces that can cause clay minerals to swell (Mitchell *et al.*, 2005). Osmosis is the known process through which clay minerals can swell as a result of the movement of solvents through a semi-permeable membrane from a region of higher concentration to a region of lower concentration (Mokni *et al.*, 2009).

A net expansion is produced in the crystal structure of montmorillonite when water moves into the interlayer regions in response to the interlayer cations (Mitchell *et al.*, 2005). It is common for sodium montmorillonite to adsorb water into the interlayer region, they usually exhibit greater swelling compared to calcium montmorillonite. Sodium ions in the interlayer region cause greater osmotic pressure than calcium (Janovák *et al.*, 2009). Unlike kaolinite, illite and calcium montmorillonite, the crystal of sodium montmorillonite expands which can be observed by x-ray diffraction (Janovák *et al.*, 2009; Mitchell *et al.*, 2005). Expansive soil although exerts large pressure against non-yielding structures; can also exhibit high shrink-swell with changes in moisture content which can cause damage and deformation to road pavement structures (Mitchell *et al.*, 2005). Figure 2.3 illustrates the mechanism of expansive soils. Expansive soils are classified using their properties such as plastic index and liquid limit. Table 2.1 Swelling potential of soils based on the liquid limit, Table 2.2 shows the classification of shrink potentials of expansive soil based on their plasticity index and Table 2.3 shows the relation of soil index properties and probably volume change for highly plastic soil and Table 2.4 shows the values of thickness, planar diameter, specific surface area and cation exchange capacity of clay minerals.

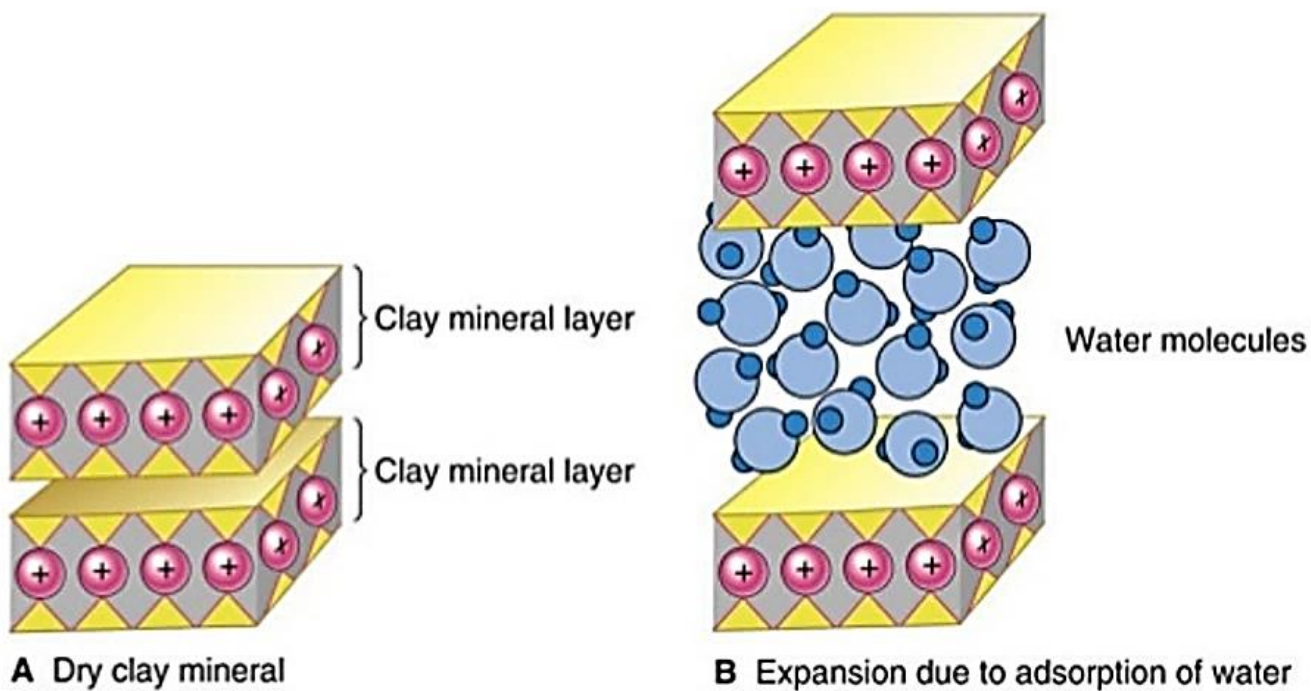


Figure 2.3: Mechanism of expansive soils showing expansion of expansive soil due to water adsorption in (B) and shrinkage expansive soil due to dryness (Harraz *et al.*, 2016)

Table 2.1: Swelling potential of soils based on liquid limit (Dakshanamurthy *et al.*, 1973)

Liquid limit	Classification
0-20	Non-Swelling
20-35	Low-Swelling
35-50	Medium-Swelling
50-70	High-Swelling
70-90	Very High-Swelling
>90	Extra High-Swelling

Table 2.2: Classification of shrink potentials based on plasticity index (Jones and Jefferson, 2012)

I_p (%)	Clay Fraction (<0.002mm)	Shrinkage potential
>35	>95	Very High
22-48	60-95	High
12-32	30-60	Medium
<18	<30	Low

Where I_p = Plasticity Index

Chapter 2 – Literature Review

Table 2.3: Relation of soil index properties and probably volume change for highly plastic soils (ACPA Concrete Pavement Technology Series) (2021)

Data from Index Tests ¹			Estimation of probable expansion ² , percent total volume change (dry to saturated condition)	Degree of expansion
Colloid Content (percent minus 0.00004 in. (0.001mm) (ASTM D422))	Plasticity Index (ASTMD4318)	Shrinkage Limit Percent (ASTM D427)		
> 28	> 35	> 11	> 30	Very High
20 - 31	24 - 41	7 - 12	20 - 30	High
13 - 23	15 - 28	10 - 16	10 - 20	Medium
< 15	< 8	< 15	< 10	Low

¹. All three index tests should be considered in estimating expansive properties. ². Based on a vertical loading of 1.0 psi (0.007 MPa). For higher loadings, the amount of expansion is reduced, depending on the load and the clay characteristics.

Table 2.4: Values of thickness, planar diameter, specific surface area and cation exchange capacity of clay minerals (Baker *et al.*, 2017; Uddin *et al.*, 2017)

Edge View	Typical Thickness (nm)	Planar Diameter (nm)	Specific Surface Area (SSA) (m ² /kg)	Cation Exchange Capacity (CEC) (meq/100g)
Kaolinite	100	10-1,000	10-15	3-18
Halloysite	-	-	-	5-40
Chlorite	30	100-2,000	70-90	10-40
Illite	20	100-2,000	80-120	10-40
Montmorillonite (Bentonite)	2	10-1,000	700-800	60-150
Vermiculite	-	-	-	100-215

2.3 CHARACTERISTICS AND MINERALS OF CLAY SOIL

It is important in this research to understand the characteristics and behaviour of clay minerals and how they impact road pavement as subgrade materials. This section looks at how clay minerals influence the formation of carbonates, hydroxides and oxides, sulphates, swelling and double-layer formation. Clay minerals are a diverse group of hydrous layer aluminosilicates that constitutes the greater part of the phyllosilicate family of minerals. They are fine-grained sediments and rocks (mudrocks, shales, claystone, clayey siltstones, clayey oozes and argillites) (Huggett, 2015) Geologist commonly defines clay soils as hydrous layer aluminosilicates with particle size < 2µm, while engineering and soil scientists define clay as any mineral particle < 4µm (Huggett, 2015). Clays are normally classified according to their layer type and because of their particle size, clay minerals are not easily identified by optical

Chapter 2 – Literature Review

methods (Huggett, 2015). The mineral structures of clay go through a geometric arrangement of atoms and ions with time and these transformations as a result of weathering (Huggett, 2015).

Clay minerals act as ‘chemical sponges’ which hold water and dissolved plant nutrients weathered from other minerals (Mitchell *et al.*, 2005; Sposito, 2008). This results in the presence of an unbalanced electrical positively charged surface of clay grains with other surfaces acting as negatively charged (Sposito, 2008; Waltham, 2009; Mitchell *et al.*, 2005). Clay minerals attract water molecules by way of surface adsorption which is the process where ions and water are not attracted deep inside the clay grains (Mitchell *et al.*, 2005; Sposito, 2008). The presence of clay minerals (typical clay) are important in engineering because they dominate the soil’s behaviour and clays sometimes contain organic minerals like dolomite, feldspar, calcite, mica, gibbsite and pyrite (Lekha *et al.*, 1998; Venugopal, 1992; Mitchell *et al.*, 2005; Sposito, 2008). These non-clay materials such as pyrite can be problematic during engineering applications because of the high amount of pyrite oxidises to form gypsum (Mitchell *et al.*, 2005; Sposito, 2008). The adsorption properties of clay minerals are replicated when the decay of dead plants and animals in the soil are promoted by organic matter from soil microbes (Yang *et al.*, 2009; Czerewko *et al.*, 2003).

Some chemical compositions of organic materials can influence the sorption properties of soil (Wang *et al.*, 2007). Extra admixtures were used with cement by Chen *et al.* (2006) to stabilise soft soil with high organic content which can control soil-borne pathogens through several mechanisms such as the release of fungi-toxic compounds, and the generation of fungistatic (Lockwood, 1977). Research has found aliphatic carbon to be a dominant sorbing phase of clay soils with organic matter composition (Liang *et al.*, 2006; Wang *et al.*, 2007). The chemical foundation, geometric arrangements of the atoms, ions and the electrical forces of clay minerals that bind them together are responsible for the determination of the properties and composition of the mineral (Klein *et al.*, 1985; Mitchell *et al.*, 2005). Clay minerals belong to the larger class of sheet silicates known as phyllosilicates, and their sheet arrangement within the alumina-silicate layers varies resulting in variable physical and chemical properties that differentiate the clay mineral classes (See Figure 2.6) (Wang *et al.*, 2007).

2.3.1 Structure of Clay Minerals

Clay structures are composed of two units (octahedral sheet and tetrahedra sheet) (Gopal *et al.*, 2000). The tetrahedral sheets are composed of silicon-oxygen tetrahedral linked to neighbouring tetrahedra by sharing three corners resulting in a hexagonal network (Uddin *et al.*, 2017). The remaining fourth corner of each tetrahedron forms a part of the adjacent octahedral sheet (Uddin *et al.*, 2017). The octahedral sheets are usually composed of aluminium or magnesium in six-fold coordination with oxygen from the tetrahedral sheet and with hydroxyl (Chen *et al.*, 2009). The two sheets together form layers and individual octahedra are linked laterally by sharing edges (Ke *et al.*, 2005). Vander Waals and electrostatic forces or hydrogen bonding may join individual layers each other in a clay crystallite interlayer cation (Gopal *et al.*, 2000; Mitchell *et al.*, 2005; Ke *et al.*, 2005; Chen *et al.*, 2009; Uddin *et al.*, 2017). Complex chemistry can arise from ionic substitution in any of these sheets due to replacing the primary source of both negative and positive charges in clay minerals (Gopal *et al.*, 2000). When cations are small enough to enter into tetrahedral coordination with oxygen cations like Fe^{3+} and Al^{3+} , they can substitute for Si^{4+} in the tetrahedral sheet (Bentabol *et al.*, 2009).

A gain of only one negative charge is achieved with the substitution of one Al^{3+} for a Si^{4+} in the tetrahedron and a cation such as Mg^{2+} , Fe^{2+} , Fe^{3+} , Li^+ , Ni^{2+} , Cu^{2+} and other medium-sized cations can substitute for Al^{3+} in the octahedral sheet (Varma, 2002). Negatively charged layers are produced from such substitution and a replacement of a lower valence cation by one with a higher valence (Fe^{2+} by Fe^{3+}) resulting in a gain of one positive charge (Bentabol *et al.*, 2009). Chemical bonding between layers is achieved by balancing cations between the layers exhibiting substitution that results in both positive and negative charges (Janovák *et al.*, 2009). Clay minerals structures have double layers on their surface due to swelling and comprise electrically charged colloidal particles. Clay minerals surfaces are negatively charged and cations adsorb into this surface (Janovák *et al.*, 2009). The importance of the double layer of the clays are dependent on the particle size in the clay mineral (Mitchell *et al.*, 2005). The double layer of clay minerals are about 30nm (Mitchell *et al.*, 2005; Janovák *et al.*, 2009; Mokni *et al.*, 2009). The double layer in clay minerals causes two clay mineral particles to repel against each other on approach. Hence the double layers of different particles may overlap each other and control flocculation and dispersion (Mitchell *et al.*, 2005).

Chapter 2 – Literature Review

In simple terms, calcium ions in the interlayer region compress the double layer (divalency Ca^{2+}) bringing the sheets closer together to prevent water absorption to reduce swelling. However, sodium ions (monovalency Na^+) swell more easily (Mitchell *et al.*, 2005; Janovák *et al.*, 2009; Mokni *et al.*, 2009). The increasing negative charges observed in the soil system due to cation exchange is result from unbalanced ionic substitution and broken bonds of soil particle edges within the clay mineral lattice (Bailey, 1998). The net charge of the mineral is determined by a balance in the electron loss and gain within the structure (Sposito, 2008). Clay minerals are divided into groups which include the Kaolinite, the Mica, the Illite, the Chlorite, the Smectite, the Vermiculite and the Attapulgite groups (Mokni *et al.*, 2009). These groups help in the understanding of how the structural sheet of clay minerals forms the clay structure (Bailey, 1998; Mitchell *et al.*, 2005; Sposito, 2008). Figure 2.4 shows the bentonite clay structure, Figure 2.5 shows the kaolinite clay structure, Figure 2.6 shows the Clay mineral structure and Table 2.5 shows typical values for cation exchange capacities

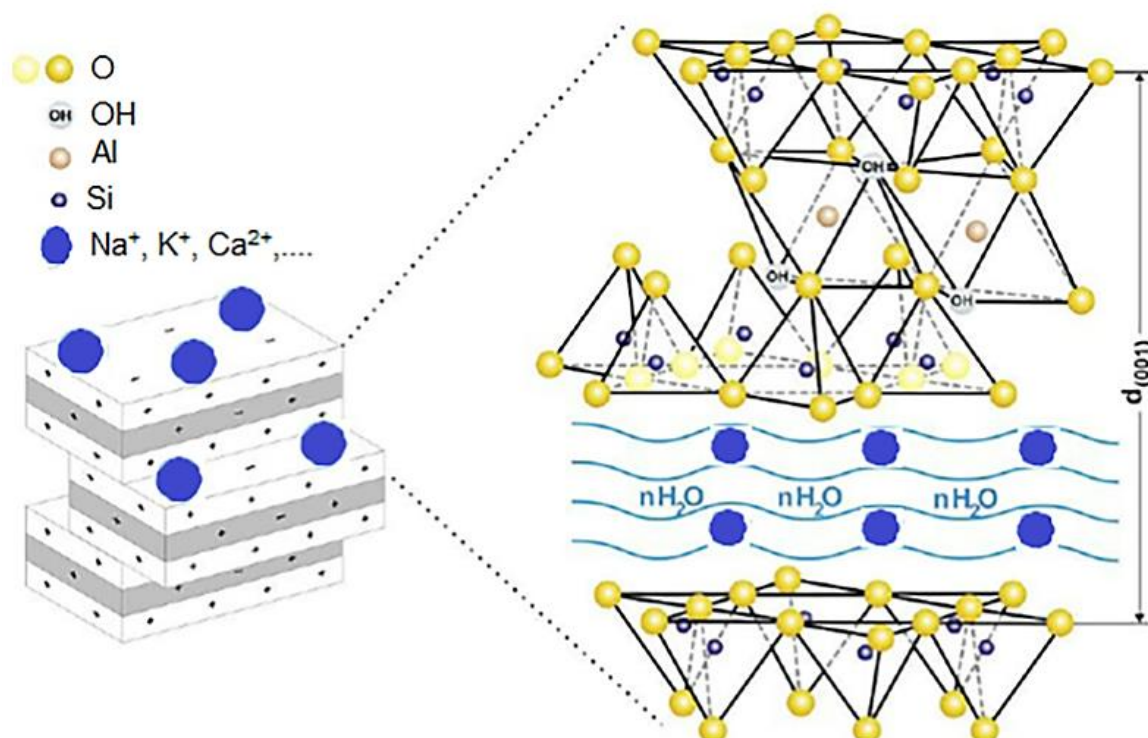


Figure 2.4: Bentonite clay structure (Bananezhad *et al.*, 2019)

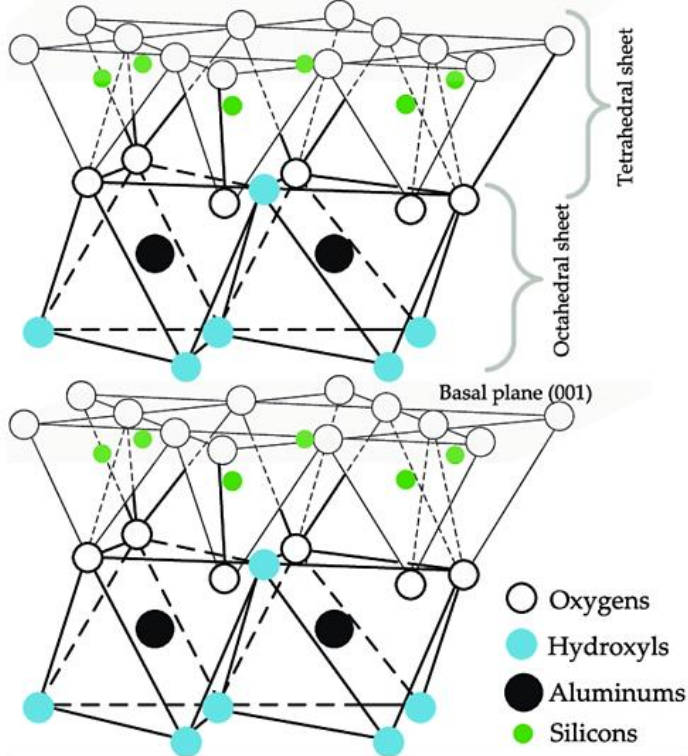


Figure 2.5; Kaolinite clay structure (Jaradat et al., 2017)

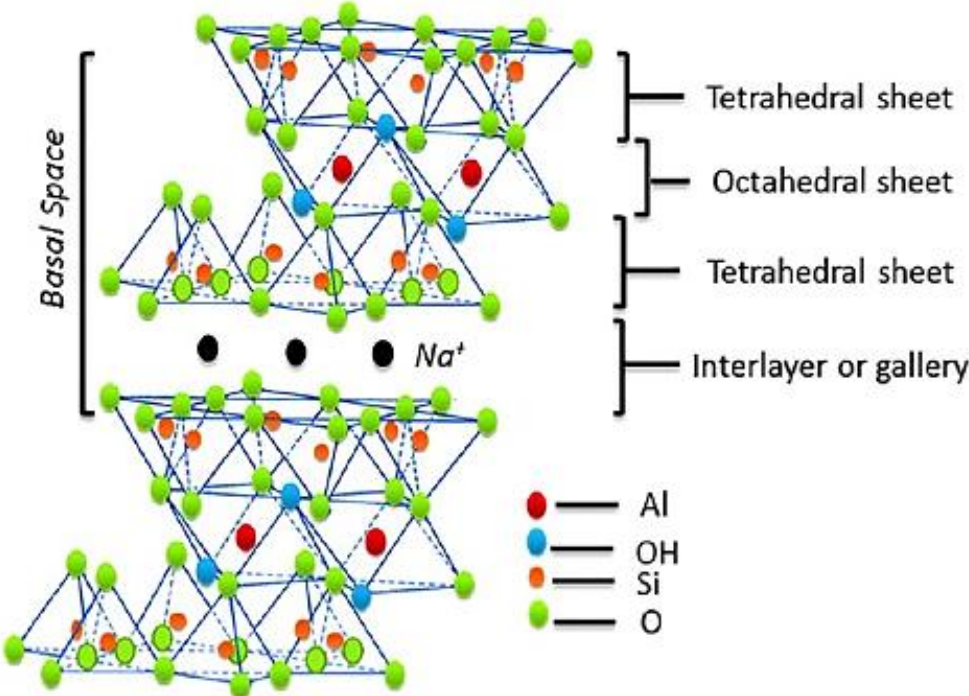


Figure 2.6; Clay mineral structure (Nuruzzaman et al., 2016)

Chapter 2 – Literature Review

Table 2.5: Typical values for cation exchange capacities (Uddin *et al.*, 2017)

Liquid limit	meq/100g
Kaolinite	3-18
Halloysite	5-40
Chlorite	10-40
Illite	10-40
Montmorillonite	60-150
Vermiculite	100-215

2.3.2 Kaolinite and Attapulgite Group

In this group, the tetrahedral sheets are occupied by silicon and the octahedral sheets by aluminium. In kaolinite, the tetrahedral sheet carries a small permanent negative charge due to the isomorphous substitution of Si^{4+} by Al^{3+} leaving a single negative charge for each substitution (Giese *et al.*, 1986; Costanzo *et al.*, 1990). The formula $\text{Al}_2\text{Si}_2\text{O}_5(\text{OH})_4$ is used to express the chemical composition of kaolinite and the octahedral sheet and crystal edges of kaolinite have a pH-dependent variable charge (Lackovic *et al.*, 2003; Srivastava *et al.*, 2005). This allows electrostatic interaction with positively charged ions because the tetrahedral sheets of clay are permanently negatively charged (Lackovic *et al.*, 2003; Srivastava *et al.*, 2005). However, this permanent charge is a minor component in kaolinite-type of clays because the layers exposed OH groups and may exhibit acid-based behaviour (Papini *et al.*, 2002; Hizal, 2006). Kaolinites are natural soil with a higher density of hydroxyl groups than clay minerals of the smectite group and its interlayer chemistry is much less developed in comparison with smectites.

The structure of kaolinite is a 1:1 dioctahedral layered mineral whose layers are formed of silicon tetrahedral sheets linked to aluminium octahedral sheets. The stacked layers are linked by Van der Waals and hydrogen bonds making it difficult to access the alumino group (Al-OH) of the interlayer spaces (Letaief, 2005; Letaief *et al.*, 2008). Kaolinite clay is named after a locality in China called Kaolin, which invented porcelain (known as China clay) using the local clay mineral. Attapulgites are crystalline hydrated magnesium aluminium silicate with a unique three-dimensional structure and have a fibrous morphology (Yang *et al.*, 2009; Sun *et al.*, 2009). Attapulgite mineral has a special property that smectite lack as it is stable in a saltwater environment and as a drilling fluid. Attapulgite resembles clay minerals more than amphiboles. Attapulgite clays are composed of a finer-like morphology with an ideal

Chapter 2 – Literature Review

structural formula $\text{Si}_8\text{O}_{20}\text{Mg}_5(\text{Al})(\text{OH})_2(\text{H}_2\text{O})_4 \cdot 4\text{H}_2\text{O}$ (Yang *et al.*, 2009; Sun *et al.*, 2009). The mica group (Figure 2.6) is a representation of the joining of two tetrahedral sheets with one from each side and one octahedral sheet which produces a three-sheet mineral type called 2:1. The mica group typically represent an electrically neutral 2:1 type mineral in which adjacent layers are joined to each other by Van der Waals bonds.

2.3.3 Chlorite and Mica Group

The structure of micas is similar to that of talc and pyrophyllite, the only difference is the substitution of Al^{3+} for Si^{4+} in every fourth tetrahedral site results in an excess of one negative charge per formula unit. Monovalent cations satisfy the negative charge, primarily K^+ , that resides on interlayer sites between the 2:1 layer (Waltham, 2009). A strong bond is formed between adjoining tetrahedral sheets by the interlayer cation which limits the expansion of the mineral. The mica group is subdivided into tri- and dioctahedral minerals according to cation substitutions in the octahedral sheet and within the interlayer (Sposito, 2008; Waltham, 2009). The trioctahedral group of micas contains interlayer K^+ cations and is represented by phlogopite $[\text{KMg}_3(\text{AlSi}_3\text{O}_{10})(\text{OH})_2]$ with Mg^{2+} occupying the octahedral sites and biotite, which contains both Fe^{2+} and Mg^{2+} in the octahedron. Muscovite $[\text{KAl}_2(\text{AlSi}_3\text{O}_{10})(\text{F},\text{OH})_2]$, or $(\text{KF})_2(\text{Al}_2\text{O}_3)_3(\text{SiO}_2)_6(\text{H}_2\text{O})$ is a dioctahedral mica (Sposito, 2008) containing Al^{3+} in the octahedral sheet and K^+ in the interlayer, while paragonite exhibits similar dioctahedral coordination with interlayer K^+ and Na^+ cations (Sposito, 2008 and Waltham, 2009). Mica in the clay fraction exhibits poorer crystallinity higher water content, lower K^+ and possible substitutions of Fe^{2+} and Fe^{3+} in the octahedral sheets and Ca^{2+} in the interlayer.

Micas occur in an unweathered state in the sand and silt fractions which is inherited from the parent material. Other cations (such as Vanadium, lithium, titanium, chromium, and manganese) occur in varying amounts in these fine-grained micas (Sposito, 2008; Waltham, 2009). Chlorites are mineral groups that exhibit a basic 2:1 layer structure which is similar to that of pyrophyllite, but with an interlayer brucite or gibbsite-like sheet which forms a 2:1:1 structural arrangement. This clay mineral is the weathering product of mafic silicates (such as Olivine, Labradorite and Biotite) and is

Chapter 2 – Literature Review

stable in cool, dry or temperate climates and occurs along with illite (Sposito, 2008; Zanazzi *et al.*, 2009; Lázár *et al.*, 2009; Waltham, 2009). A variety of cation species may exhibit in these brucites or gibbsite-like islands that contribute to a large number of mineral species within the chlorite group (Sposito, 2008; Zanazzi *et al.*, 2009; Lázár *et al.*, 2009; Waltham, 2009). Chlorites are generally non-expansive minerals because there is adsorption within the interlayer space and their cation exchange capacity and surface charge densities are low (Sposito, 2008; Zanazzi *et al.*, 2009; Lázár *et al.*, 2009; Waltham, 2009). The cation exchange capacity and surface charge densities of chlorite are low and the negative charge generated by isomorphous substitution is compensated by brucite (Mg Hydroxide) of ten positive charges due to isomorphous exchange of Mg^{2+} by Al^{3+} (Sposito, 2008; Zanazzi *et al.*, 2009; Lázár *et al.*, 2009; Waltham, 2009).

2.3.4 Smectite, Illite and Vermiculite Group

The occurrence of weathering products of mafic silicates are termed smectite clay and are stable in a temperate climate. Smectite clay belongs to the family of dioctahedral layers, lattice silicate with a 2:1 structure and montmorillonite is a common member of this group. A Vander Waals holds together the 2:1 layers in the smectites with weak cation-to-oxygen linkages (Gates *et al.*, 2009; Wolters *et al.*, 2009; Benhammou *et al.*, 2009). Expansion of the crystal lattice is allowed as the mineral hydrates due to the presence of exchangeable cations located between water molecules in the interlayer. Basal spacing between layers can approach 2nm under dry conditions when the mineral is saturated with water (Gates *et al.*, 2009; Wolters *et al.*, 2009; Benhammou *et al.*, 2009). Smectites such as bentonite are used in civil and environmental engineering, and in the oil drilling and chemistry industry. Engineers find smectite clays problematic due to their propensity for cracks to form and the general instability of the soil surface. The expansion and contraction behaviour of smectites is known as shrink-swell potential.

Smectite has a very high negative surface charge which is partially compensated by hydrated cations positioned in the interlayer spacing of the solid. In most cases, smectite has a large cation exchange capacity and high specific area and swells in the presence of water or polar organic molecules (Klopprogge *et al.*, 1999; Guimarães *et*

Chapter 2 – Literature Review

al., 2009). The physical properties of the smectite may change due to the fifth inorganic cation of smectites being replaced by large alkylammonium ions. The swelling ability, high surface area and high cation exchange capacity of the smectite family have made it the subject of many investigations. Sodium smectite and calcium smectite are the two main varieties of the smectite family and can absorb up to 18 layers of water molecules between layers of clay (Tonle *et al.*, 2003). Although Calcium smectite are commonly used as drilling mud, the most preferred clay mineral for drilling mud is sodium smectite (Gates *et al.*, 2009; Wolters *et al.*, 2009; Benhammou *et al.*, 2009). When sodium smectite is used in drilling, it creates a protective clay liner for the prevention of seepage of groundwater into residential basements. Sodium smectite is also used in for hazardous waste landfills to guard against future groundwater contamination or as a commercial clay absorbent to soak up liquid spills (Gates *et al.*, 2009; Wolters *et al.*, 2009; Benhammou *et al.*, 2009).

Vermiculites are formed as a result of weathered mica replacing interlayer K^+ with hydrated exchangeable cations. The clay group is mostly used as an additive for the retention of water in potted plants and sometimes as protective materials for shipping packages (Marwa *et al.*, 2009; Chmielarz *et al.*, 2009). Vermiculite exists as an Al^{3+} dominated dioctahedral and to a lesser extent, Mg^{2+} dominated trioctahedral mineral. Vermiculite can be present in mixed-layer clays (chlorite and mica). The 2:1 layers in vermiculite are held together by the strong bonding of the interlayer cations which reduces expansion (Marwa *et al.*, 2009; Chmielarz *et al.*, 2009). Vermiculites have a high cation exchange capacity which are weak (K^+ and NH_4^+). Exchangeable cations, water molecules, tetrahedral charge, preliminary Mg^{2+} and Ca^{2+} are firmly absorbed within the interlayer space of vermiculites. Each formula unit of vermiculite is derived from a charge of 0.6 – 0.9 per formula unit in the minerals by tetrahedral substitution of Al^{3+} for Si^{4+} (Marwa *et al.*, 2009; Chmielarz *et al.*, 2009).

2.4. IDENTIFICATION OF CLAY MINERALS

Microstructural properties of clay are the properties influencing the physical properties such as hardness, strength, high/low-temperature behaviour, toughness wear resistance etc (Benhammou *et al.*, 2009). Microstructural properties can be determined by conducting Scanning Electron Microscopy (SEM). However, the

Chapter 2 – Literature Review

identification and quantification of clay minerals are carried out using Energy Dispersion X-ray (EDX), X-Ray Diffraction (XRD), Solid-state Backscattered Detector (SBD) and Thermo Gravimetric Analysis (TGA).

2.4.1 Scanning Electron Microscopy (SEM): this is the primary tool for resolving 2D-3D image processing and analysis and has various magnification and resolution ranges depending on the equipment type. SEM analysis is used to access the morphology, chemical composition, crystalline structure and orientation of materials making up the sample (Goldstein *et al.*, 2003; Covelli *et al.*, 2009; Migliavacca *et al.*, 2009). Sample preparation for SEM is easy because SEM only required samples to be conductive. The electrons are made up of a focused beam of high-energy electrons to generate a variety of signals at the surface of solid specimens. (Goldstein *et al.*, 2003; Covelli *et al.*, 2009; Migliavacca *et al.*, 2009). The capability of SEM to perform analysis of selected point locations on samples is useful in quantitatively or semi-quantitatively determination of chemical compositions (EDX).

SEM is one of the most used instruments in research due to the combination of high magnification, larger depth of focus, greater resolution and easy observation of samples (Goldstein *et al.*, 2003; Covelli *et al.*, 2009; Migliavacca *et al.*, 2009). During thermal methods, specific clay minerals lose their structural OH water known as thermogravimetric analysis (TGA) based on the characteristic temperature regions. The enthalpy are associated with the dihydroxylation reaction also known as the differential scanning calorimetry (DSC) and the mineral quantities are estimated from comparisons of the OH- or enthalpy fractions measured and the standard quantities of representative pure minerals (Serapiglia *et al.*, 2009; Rauma, 2009).

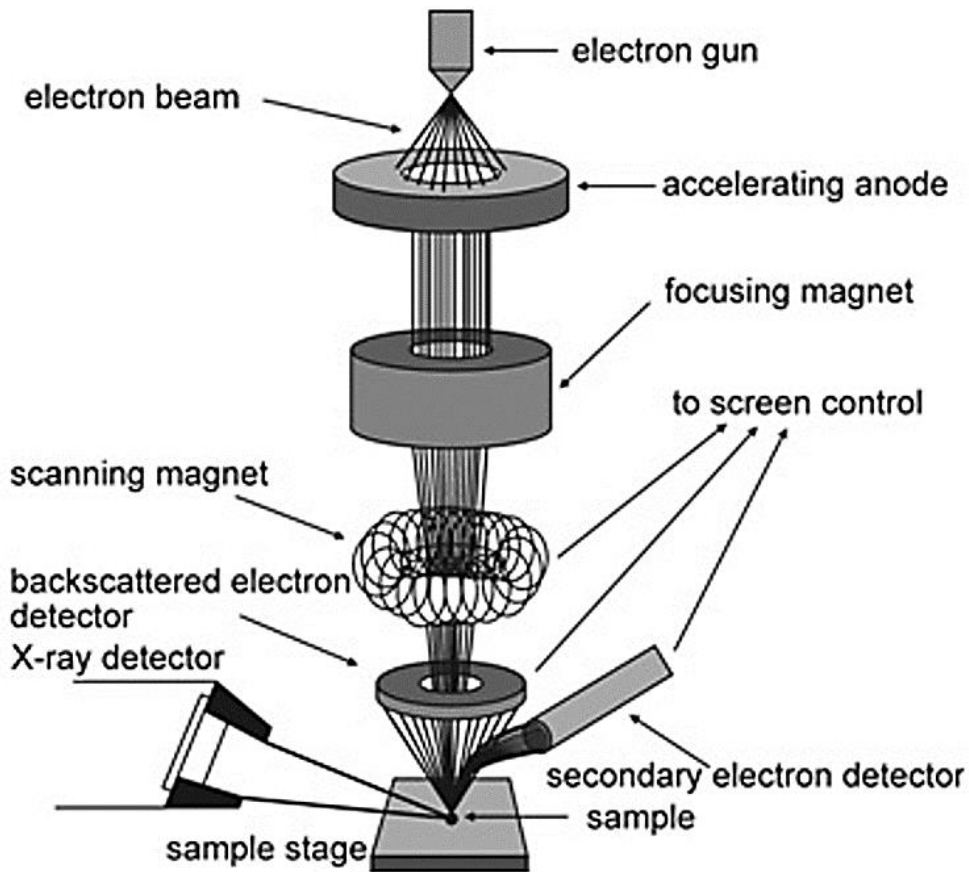


Figure 2.7: The testing process of SEM analysis (Havancsák, 2021)

2.4.2 Energy Dispersion X-ray (EDX): this analysis uses a beam inside a scanning electron microscope to displace electrons from their energy levels (Osman *et al.*, 2003; Lal, 2006; Bhaskaran *et al.*, 2009). EDX techniques are successfully used alongside SEM in the application as an analytical detection technique. A high-energy electron from an outer shell occupies a position vacated by an ejected inner shell electron, accompanied by X-ray emission. X-rays with unique amounts of energy are released by atoms of each element during the electron transfer process. The energies of the X-rays emitted can be used to identify the elements (Osman *et al.*, 2003; Lal, 2006; Bhaskaran *et al.*, 2009;). Unlike SEM, Energy Dispersion X-ray (EDX) analysis gives concrete evidence of particle identification. The identification of minerals with overlapping d-spacing regions is based on specific diffraction peak shifts and the energy of the beam is typically in the range of 10-20keV (Osman *et al.*, 2003; Lal, 2006; He, 2009).

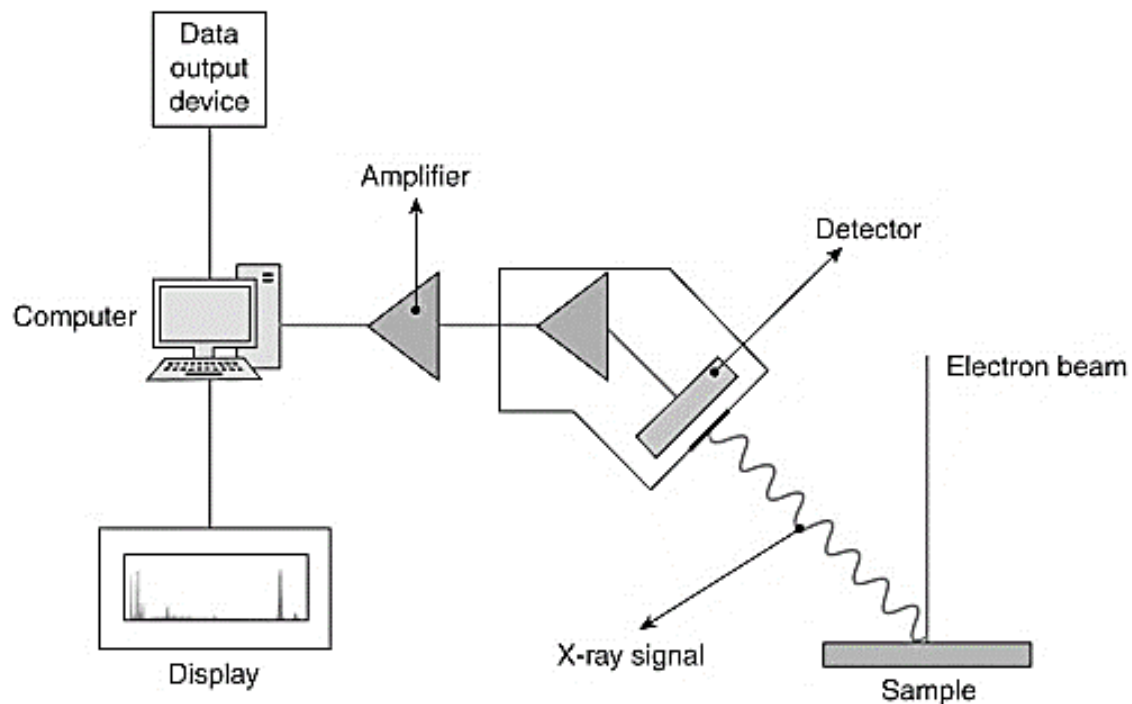


Figure 2.8: The testing process of Energy Dispersion X-ray (Colpan *et al.*, 2018)

2.5 EXPANSIVE SUBGRADE STABILISATION

Subgrade materials refer to the original ground or soil underneath a road pavement (Reddi *et al.*, 2000). Many times, these materials do not have sufficient capacity to support the weight of the road pavements and the traffic loads and will require some sort of modification and re-engineering to enhance their capacity to support load (Ikeagwuani *et al.*, 2019). Expansive subgrade means when road subgrade materials are made up of expansive clay soil (Afrin *et al.*, 2017). In civil engineering practice, expansive soils are stabilised using chemical stabilisation techniques. Chemical stabilisation is the process of adding binder/additives materials to soil (expansive soils) as a way of treatment to make them usable for use in civil engineering and construction (Afrin *et al.*, 2017). Many geotechnical solutions such as soil treatment and modification have been adopted to overcome the problems of expansive subgrade materials (Jawad *et al.*, 2014). Soil stabilisation techniques via chemical stabilisation have been used in addressing the problems associated with expansive subgrade materials (Ikeagwuani *et al.*, 2019). In this study, chemical subgrade stabilisation techniques were used to stabilise expansive road subgrade materials. Chemical subgrade stabilisation is the process of adding chemicals to improve the engineering

Chapter 2 – Literature Review

properties of expansive subgrade material (Afrin *et al.*, 2017). The treatment of expansive subgrade using lime and other additives to improve its engineering properties has been effective for road pavement construction (Reddi *et al.*, 2000).

The addition of these chemicals changes the gradation and physico-synthetics within and around the soil particles promoting cation exchange which leads to flocculation and agglomeration of the expansive soil particles (Jawad *et al.*, 2014). Cement, fly ash, bituminous, rice husk ash, lime, construction and demolition waste, electrical and thermal waste, geotextile fabrics and recycled waste can be used as admixtures (Lucena *et al.*, 2014). The addition of these materials as admixtures can alter the geotechnical properties of expansive soil such as strength, bearing capacity, hydraulic conductivity, compressibility, workability, durability and swelling potential (Cabezas *et al.*, 2019). Chemical subgrade stabilisation is an effective technique to improve expansive subgrade (Phanikumar *et al.*, 2020). An investigation into the application of stabilisation of wastewater sludge proves that cement, lime and bitumen can be used as subgrade materials (Lucena *et al.*, 2014). During chemical road subgrade stabilisation, the shear strength of the expansive subgrade improves when stabilisers react with water within the soil leading to an increase in the stiffness of the soil (Phanikumar *et al.*, 2020). Expansive subgrade can be removed and replaced with higher-quality fill. However, this simple concept can be very expensive and unsustainable compared to chemical stabilisation techniques. Figure 2.9 – Figure 2.12 show different road subgrade stabilisation processes. Figure 2.13 and Table 2.6 show real-life insitu subgrade stabilisation processes.



Figure 2.9: Cement stabilisation process in road construction (Pleasants Construction, Inc, 2020)



Figure 2.10: Fly ash stabilisation process in road construction (Beeghly *et al.*, 2003)



Figure 2.11: Lime stabilisation process in road construction (Saranya *et al.*, 2017)



Figure 2.12: Construction and demolition waste, geogrid and textile used in road construction (ABG Geosynthetics, 2020)

Chapter 2 – Literature Review

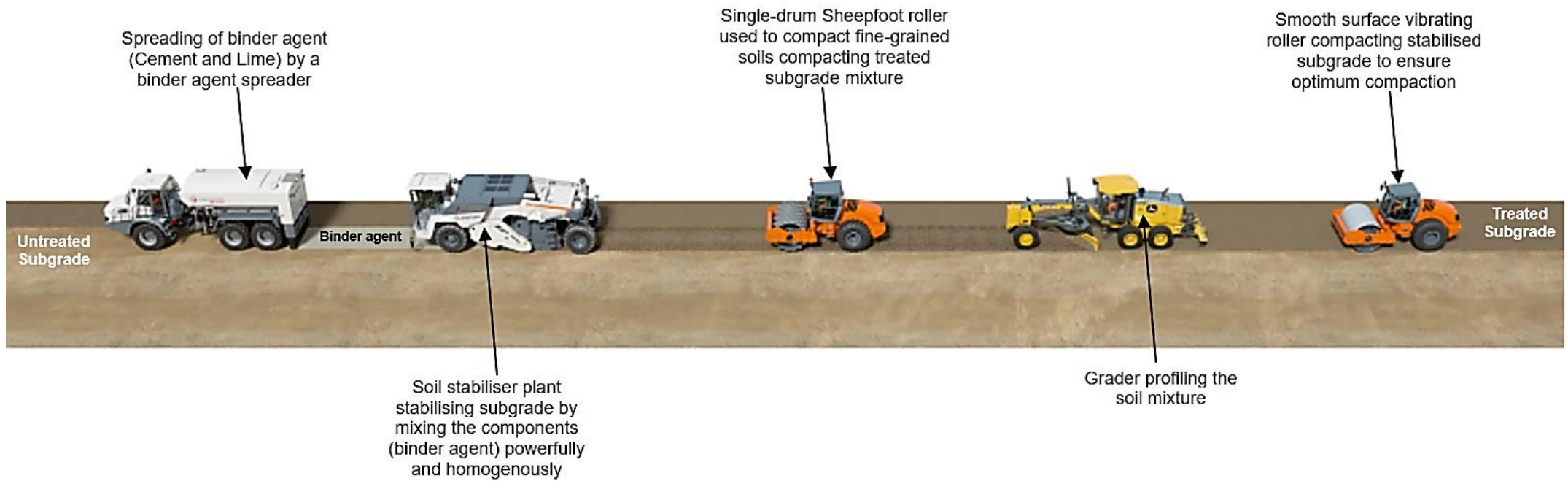


Figure 2.13: Application process of binder agent in real-life road construction (Wirtgen-group.com, 2021)

Chapter 2 – Literature Review

Table 2.6: Advantages of insitu treated subgrade and disadvantages of removal and replacement of subgrade

Cement/lime treated subgrade

- Less time, less cost Reduce environmental impact
- Improves the workability of subgrade of soil.
- Reduces plasticity and shrink/swell potential
- Reduce moisture susceptibility and migration
- Increase speed of construction
- Increase bearing capacity compared to untreated subgrade
- Promotes soil drying
- Provides significant improvement to the working platform
- Uses onsite soil rather than removal and replacement
- Provides permanent soil modification (no leaching)
- Does not require mellowing period



Insitu soil stabilisation process (Wirtgen-group.com, 2021)



Insitu soil treatment process in mixing chamber (Wirtgen-group.com, 2021)

Removal and Replacement



- Time-consuming
- Very costly
- Greater environmental impact

Removal and replacement of expansive subgrade with imported materials (Valley Trading and Roadpacker, 2021)

Chapter 2 – Literature Review

2.6 PROCESSED WASTE MATERIALS

Various kinds of waste materials are generated worldwide as a result of human activities. Due to our inability to recycle all the waste society produces, a large section of these waste materials are dumped in landfills and others are dumped in water bodies contributing to some of the environmental problems society faces today. Over the past decades, more than 80 billion tonnes of waste have been produced worldwide and it is still growing (Laura, 2018). Countries such as China Malaysia and Cambodia have been buying recyclable trash from the first world's Western nations. However, in 2018, Malaysia and China sent back about 4900 tonnes of plastic and paper waste to the USA, UK, Australia and Canada because China could not recycle all the waste and they end up in landfills (Laura, 2018). According to The World Bank, (2021), the world generates 2.01 billion tonnes of municipal solid waste annually and it is expected to grow to 3.40 billion tonnes by 2050. To mitigate the problem, many strategies have been implemented, including recycling incineration. However, these strategies are not enough to deal effectively with all the waste we produce. This has encouraged the use of processed waste in the engineering and construction sector to construct roads, pavements, and buildings. However, the availability of processed waste in high quantities for use in subgrade stabilisation and their associated environmental effects have been questioned (Chakraborty *et al.*, 2014). Before waste materials can be used in subgrade stabilisation, the waste must, first of all, be processed to remove toxic chemicals and contamination to make them suitable for use as an additive in road construction (Hoornweg *et al.*, 2012).

Using processed waste in subgrade stabilisation is arguably the new trend in chemical stabilisation to reduce the amount of greenhouse gas emissions and the environmental effects associated with cement production (Chakraborty *et al.*, 2014). The United States Department of Transportation, in 2021, stated that a considerable amount of processed waste is produced around the world for use in various engineering activities. Other studies have also shown that there are enough processed industrial by-products and waste materials available to meet the current demands for subgrade stabilisation and the processing of these waste materials are cheaper and more sustainable compared to the cost of cement, Lime and its production (Chakraborty *et al.*, 2014). Over 20 million metric tonnes (22 million tonnes) of fly ash

Chapter 2 – Literature Review

are used annually in a variety of engineering applications typically highway engineering (United States Department of Transportation, 2017). The use of GGBS at high volumes as supplementary cementitious materials is good from an environmental point of view. The higher the amount of GGBS used to replace cement in soil stabilisation, the lesser the carbon footprint is expected due to the lower cement content used (Onn *et al.*, 2019). The use of processed waste (such as fly ash) has significant environmental benefits including a net reduction in energy use and greenhouse gas emission. Sixty-two million metric tonnes (68 million tonnes) of fly ash were produced in 2001 and only 20 million metric tonnes (22 million tonnes) or 32% of the total production was used (United States Department of Transportation, 2017). The total production of hypo-sludge in Bangladesh which is capable of replacing cement is equivalent to $550,000 \times 6 = 3,300,000\text{kg}$ per year.

A reduction in the amount of coal combustion products that must be disposed of in landfills has been observed due to their use in subgrade stabilisation (United States Department of Transportation, 2017). The use of waste in soil stabilisation provides environmental and economic advantages (Zorluer *et al.*, 2020). According to the World Bank (2012) report, about 1.3 billion tonnes of solid waste are generated by cities globally each year and the volume is expected to increase to about 2.2 billion tonnes by 2025 (Hoornweg *et al.*, 2012). Statistics have shown approximately 780 million tonnes of waste are generated worldwide this includes coal combustion products (CCP), such as fly ash, bottom ash, cenospheres, conditioned ash and flue gas desulphurization gypsum (Kumal *et al.*, 2014). Out of these, the largest CCP of 395 million tonnes were produced by China, 118 million tonnes by North America, 105 million tonnes by India, 52.6 million tonnes by Europe, 31.1 million tonnes by Africa and a minor contribution from the Middle East (Heidrich *et al.*, 2013). Motz *et al.* (2015) state approximately 400 million tonnes of GGBS are produced annually worldwide while the production of steel slag is around 350 million tonnes. Studies have shown that an estimated 70 -120 million tonnes per year of red mud are produced worldwide (Motz *et al.*, 2015). While an estimated 100 – 280 million tonnes of phosphogypsum are produced every year (Tayibi *et al.*, 2009).

Chapter 2 – Literature Review

Cement kiln dust of approximately 510 – 680 million tonnes are produced yearly (Kumal *et al.*, 2014). India had a fly ash production of about 163.56 million tonnes per year in 2014, which increased to 184.14 million tonnes in 2014 (Central Electricity Authority, 2014, 2015). Figure 2.14 shows the projected waste generation, by region Mt per year showing a gradual increase in waste generation year by year Table 2.7 shows the 2001 fly ash production and use showing the underutilisation of fly ash. Table 2.8 shows the major industrial solid wastes generated in India. Figure 2.15 shows the modes of the utilisation of fly ash in the year 2014-15. Figure 2.16 shows the utilisation of fly ash in areas of engineering. Table 2.9 shows the coal combustion products (CCP) production around the world, and Figure 2.17 shows the modes of fly ash utilisation in 2012-13.

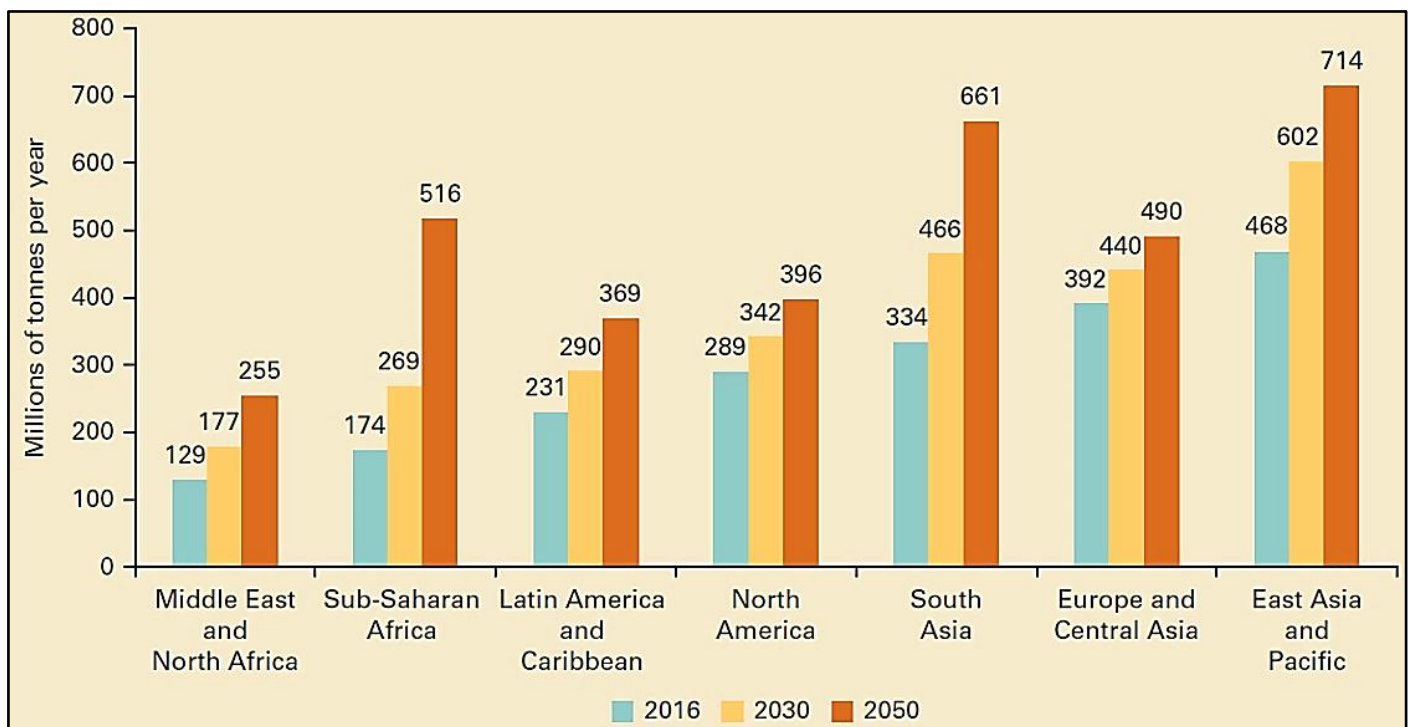


Figure 2.14: Projected waste generation, by region Mt per year (The World Bank, 2021)

Table 2.7: Fly ash production and use in the year 2001
(United States Department of Transportation, 2001)

	Million metric tonnes	Million short tonnes	Percent
Produced	61.84	68.12	100
Used	19.98	22.00	32.3

Chapter 2 – Literature Review

Table 2.8: Major industrial solid wastes generated in India (James *et al.*, 2016)

Solid waste	Fly Ash	GGBS	Steel slag	Red mud	Lime sludge	Lead-zinc slag	Phosphorus furnace slag	PG	Jarosite	Kimberlite	Mine rejects
Annual production (million tonnes)	184.14	10	12	4.71	4.5	0.5	0.5	11	0.6	0.6	750

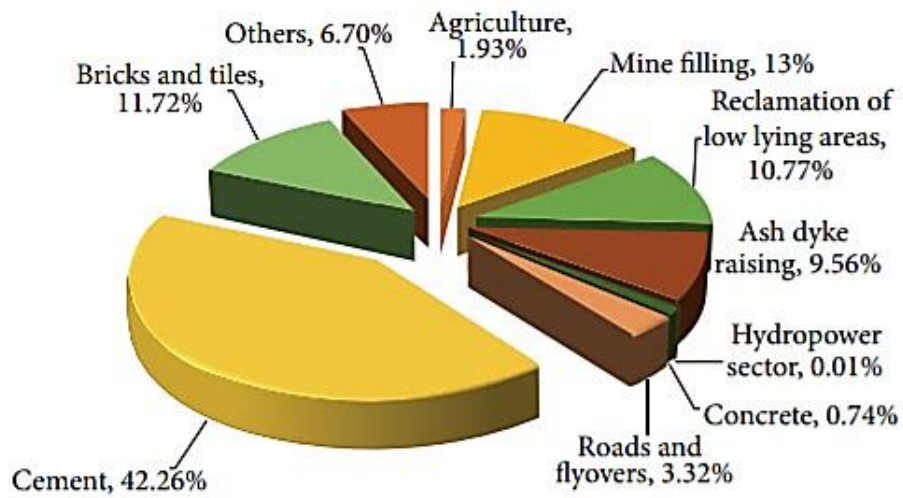


Figure 2.15: Modes of the utilisation of fly ash in the year 2014-15 (Central Electricity Authority, 2014)

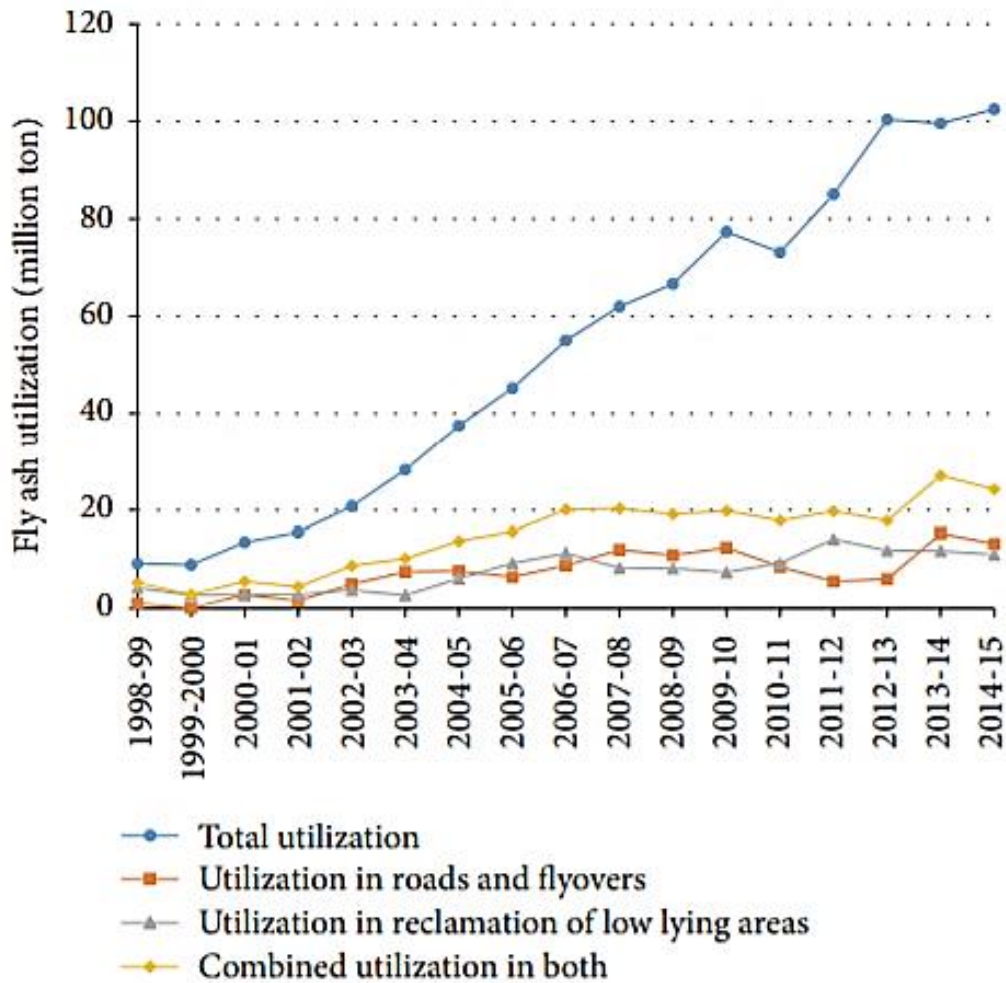


Figure 2.16: Utilisation of fly ash in areas of engineering (James et al., 2016)

Table 2.9: CCP production around the world (Heidrich et al., 2013).

Country/Region	CCP Production (Mt)	CCP Utilisation (Mt)	Utilisation rate (%)	CCP Production /Person (Mt)	CCP Utilisation/Person (Mt)
Australia	13.1	6.0	45.8	0.60	0.27
Canada	6.8	2.3	33.8	0.20	0.07
China	395	265	67.1	0.20	0.20
Europe	52.6	47.8	90.9	0.11	0.10
India	105	14.5	13.8	0.09	0.01
Japan	11.1	10.7	96.4	0.09	0.08
The Middle East and Africa	32.2	3.4	10.6	0.02	0.01
United States	118	49.7	42.1	0.37	0.16
Other Asia	16.7	11.1	66.5	0.05	0.03
Russian Federation	26.6	5.0	18.8	0.19	0.04

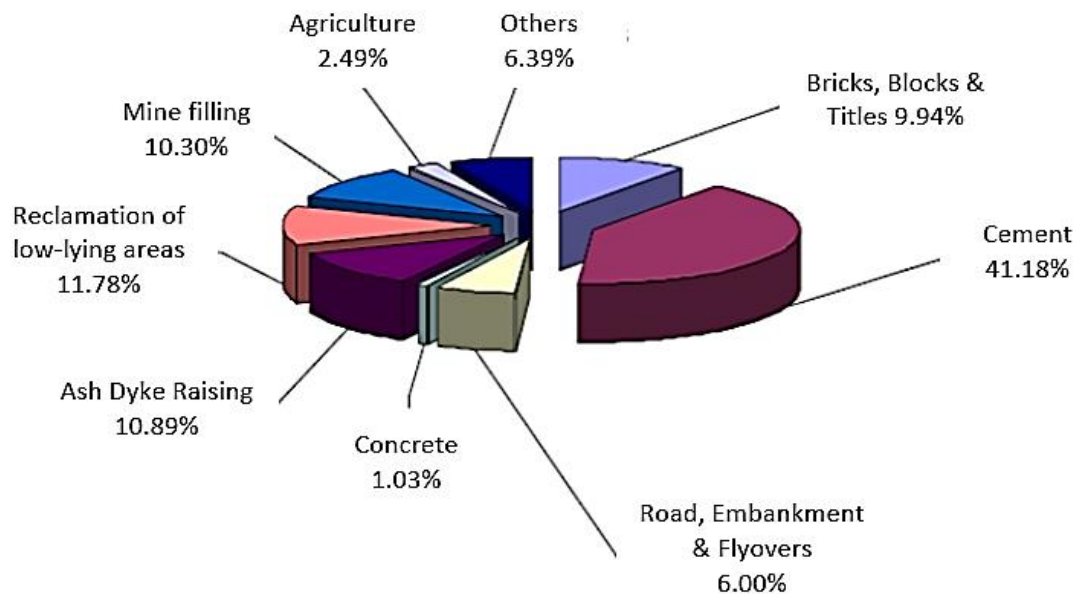


Figure 2.17: Modes of fly ash utilisation in 2012-13 (Central Electricity Authority, 2014).

2.6.1 Sustainability of Using Processed Waste in Subgrade Stabilisation

Climate change has been a huge challenge to the world and many efforts have been made to remedy the situation by ensuring a more sustainable way of production, especially in the construction sector to reduce greenhouse gas emissions (Booth *et al.*, 2012). According to Benhelal *et al.* (2013), 7% of the world's CO₂ emission comes from cement and lime production due to the high demand for cement and lime. One tonne of CO₂ is emitted for every tonne of cement produced (Onn *et al.*, 2019). During cement production, 50% of the carbon is emitted as a result of the calcination of the raw materials and 50% of the energy used (Geng *et al.*, 2019). Recent studies have shown the efforts made by many countries to mitigate carbon emissions in cement plants. However, the problem of greenhouse gas emissions persists and the total replacement of cement and lime with sustainable waste materials can help mitigate the problem and reduce the associated environmental problems (Onn *et al.*, 2019). Some concerns have been raised about the availability and the production of processed wastes including their associated environmental effects, such as CO₂ emission and high energy consumption.

However, the environmental impact associated with the production of processed waste is far less compared to the problems associated with the use of cement and its

production. Using GGBS in high volumes as supplementary cementitious materials is good from an environmental point of view (Onn *et al.*, 2019). The higher the amount of GGBS used in replacing cement in soil stabilisation the less carbon footprint is expected due to the reduction in the use of cement (Onn *et al.*, 2019). Furthermore, the use of processed waste such as fly ash has significant environmental benefits including a net reduction in energy use and greenhouse gas emission. Figure 2.18 shows the contribution of the top ten countries to global CO₂ emissions in 2008.

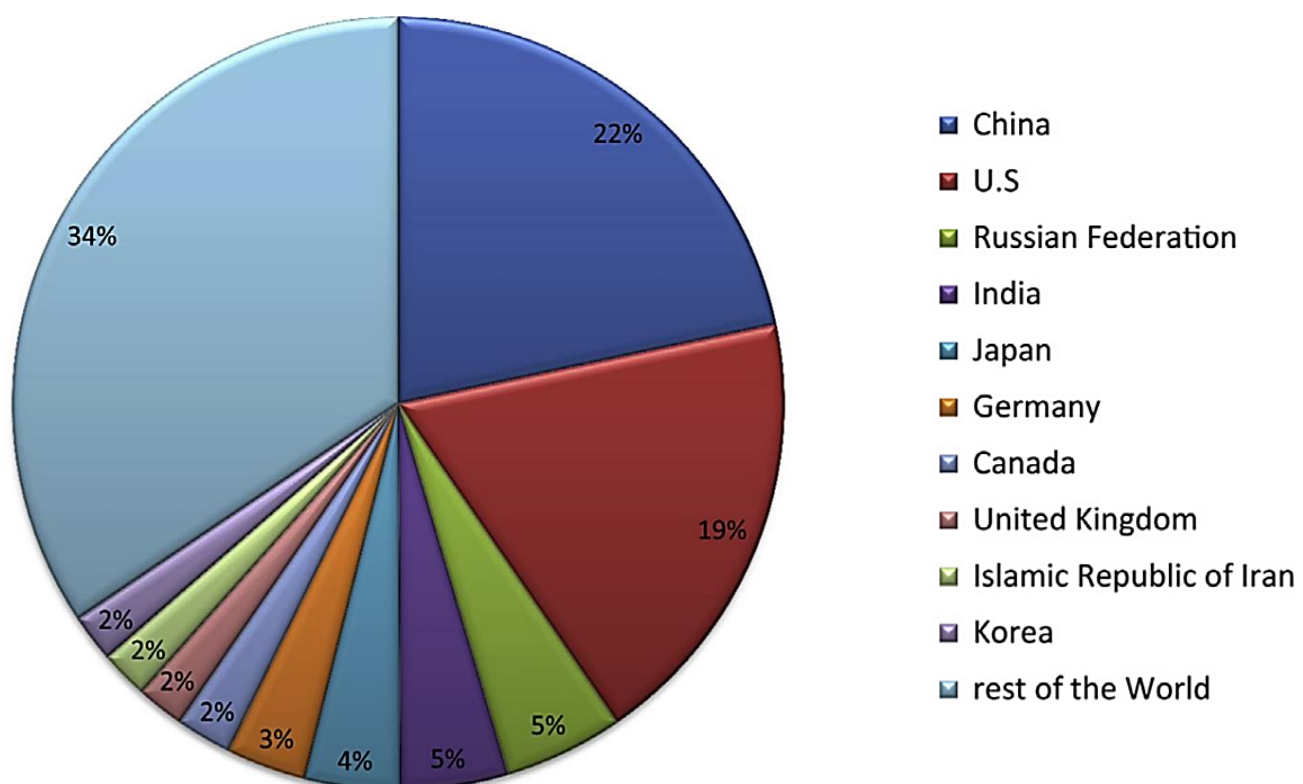


Figure 2.18: Contribution of the top 10 countries in global CO₂ emission in 2008 (International Energy Agency 2010)

2.6.2 Effect of Process Waste on The Engineering Properties of Road

Subgrade

Processed waste, such as brick dust waste (BDW), among others, can improve the engineering properties of road subgrade materials. BDW is mainly sourced from the cutting and demolition of brick and brick structures. Brick dust waste has been reportedly used in various studies to stabilise expansive road subgrade material. According to Anand *et al.* (2014), the California Bearing Ratio (CBR) value increased to over 400% and a high Unconfined Compressive Strength (UCS) was achieved when an optimum brick dust waste (BDW) content of 40% was used during expansive subgrade stabilisation. Compressive strength and CBR of soil reached their maximum

Chapter 2 – Literature Review

values based on the standard compaction test when an optimum content of 40% BDW was used in subgrade stabilisation in accordance with ASTM D2166/D2166M-13 and ASTM D1883-14. Other studies have shown an increase in CBR values at optimum BDW content from 5% to 20% (Al-Baidhani *et al.*, 2019). Best stabilisation effects were obtained with brick dust waste at an optimum content of 50% (Sachin *et al.*, 2014).

A reduction in swell linear shrinkage and compaction water content was recorded when an optimum content of 50% brick dust waste was used in subgrade stabilisation (Teja *et al.*, 2018). Good CBR and swelling results were achieved when 20% of brick dust waste proportions were used in expansive subgrade stabilisation for flexible pavement (Reddy *et al.*, 2018). Unconfined compressive strength increased with the addition of 30% brick dust waste and began to decrease at 40% brick waste in accordance with ASTM D2166/D2166M-13 (Hairulla *et al.*, 2016). Studies on the use of brick waste as a partial replacement for cement in expansive subgrade stabilisation have shown that the optimum or the highest proportion of brick waste used in subgrade stabilisation to achieve good engineering properties of soil is up to 50%. Brick dust waste proportion from 5%, 10%, 15%, 20% and 25% was used in subgrade stabilisation and the results obtained are as follows CBR 7.36, 8.54, 13.70, 19.13 and 7.36. UCS 0.60 kg/cm², 2.60 kg/cm², 4.31 kg/cm² and 2.84 kg/cm², respectively. Unconfined compressive strength increased with the addition of 30% brick dust waste and began to decrease at 40% brick waste (Hairulla *et al.*, 2016). Table 2.10 shows a summary of findings of improved engineering properties of expansive subgrade stabilised using various types of processed waste.

Chapter 2 – Literature Review

Table 2.10: Summary of findings of improved engineering properties of expansive subgrade stabilised using various types of processed waste.

Waste Type	Content (%) /Ratio	Information Source	Test Type	Results: UCS (kN/m ²), CBR (%), Swell (mm), Shrinkage (%)	Standards
Brick dust	30-50	Teja <i>et al.</i> , 2018	CBR and UCS increased	CBR = 19 & UCS = 20	ASTM D1883-16
Brick dust	30-50	Bhavsar <i>et al.</i> , 2014	Shrinkage reduced	Shrinkage = 23.7 to 7.3	IS 2720
Brick dust	0-16	Kumar <i>et al.</i> , 2018	CBR increased	CBR = 7.9	ASTM D1883-16
Brick dust	10-30	Khan <i>et al.</i> , 2020	CBR increased	CBR = 4.6	BS1377
Brick dust	5-25	Kumar <i>et al.</i> , 2016	UCS and CBR increased	UCS = 3544 & CBR = 21.90	IS:2720 part 16
Brick dust	0-30	Pokale <i>et al.</i> , 2015	UCS increased & swell decreased	UCS = 297.76 & Swell = 23.98	IS:2720 Part X1991
Brick dust	10-50	Pundir <i>et al.</i> , 2017	Swell reduced & CBR increased	Swell = 0 & CBR = 12.54	IS 2720
Brick dust	10-30	Rizwan <i>et al.</i> , 2019	CBR increased	CBR = 7.4	IS:2720 part 16
Brick dust	30-50	Kinjal <i>et al.</i> , 2018	CBR improved from	CBR = 1.6 to 6.8	IS:2720 Part 16
Brick dust	10-40	Hairulla <i>et al.</i> , 2016	UCS improved	UCS = 197	IS:2720 Part 16
Brick dust	10-20	Rank <i>et al.</i> , 2020	UCS improved	UCS = 142.2	IS:2720 Part 16
Brick dust	10-20	Rank <i>et al.</i> , 2020	CBR improved	CBR = 2.86	ASTM D1883-16
Brick dust	10-20	Rank <i>et al.</i> , 2020	Swell decreased	Swell = 0.83	1977STM D1883-16
Brick dust	10-20	Rank <i>et al.</i> , 2020	Shear strength improved	UCS = 67.15	BS 1377-1:2016
GGBS	5-10	Estabragh <i>et al.</i> , 2020	UCS increased with	5% and 10% GGBS	IS:4332 Part 5 (1970)
GGBS	70 ratio	Sharma <i>et al.</i> , 2016	UCS increased	UCS = 450	IS:2720 Part 16
GGBS	0-30	Prasad <i>et al.</i> , 2019	CBR increased	CBR = 2.69	IS:2720 Part 10-1991
GGBS	0-30	Duyu <i>et al.</i> , 2015	UCS increased	UCS = 263.5	IS:2720 Part 16
GGBS	3-9	Yadu <i>et al.</i> , 2013	CBR increased	CBR = 2.05 to 8.29	IS:2720 Part 40-
GGBS	3-12	Yadu <i>et al.</i> , 2013	Swell reduced	Swell = 67 and 21	1977STM D1883-16
Plastic waste	0.0-1.0	Ashraf <i>et al.</i> , 2011	CBR values increased	CBR = 1.967 to 2.479	IS:2720 Part 16
Plastic waste	0-1.5	Wani <i>et al.</i> , 2021	UCS and CBR increased	UCS = 40 and CBR = 2.35	IS-2720: Part 7
Polypropylene	0.5-2	Prasad <i>et al.</i> , 2019	CBR increased	CBR = 8.51	IS:2720 Part 16
Polypropylene	0.05-0.25	Tang <i>et al.</i> , 2007	UCS increased	UCS = 1280	IS 2720 part 10
Polypropylene	0.2-0.5	Tharini <i>et al.</i> , 2020	Swell reduced considerably	Swell = 21.73	IS:2720 Part 40-1977
Polypropylene	0.5-2	Murthi <i>et al.</i> , 2021	Swell pressure reduced	Swell = 110 to 59	IS:2720 Part 40-1977
Polypropylene	0.1-1.3	Tomar <i>et al.</i> , 2020	UCS increased	UCS = 338.7	IS 2720 part 10
Polypropylene	0-1.4	Vakili <i>et al.</i> , 2018	UCS increased by	UCS = 29.87	IS:4332 Part 5 (1970)
Polypropylene	0.05-0.30	Ding <i>et al.</i> , 2018	UCS decreased	UCS = 600 to 330	IS:4332 Part 5 (1970)

Chapter 2 – Literature Review

2.7 BRICK DUST WASTE (BDW)

Brick dust waste is recycled waste materials mostly sourced from demolishing of buildings made with clay bricks or as a by-product after the manufacturing, cutting, and fabrication process of fired clay bricks. Brick dust waste contains crystalline silica which is a deadly substance. Wet brick dust after wet cutting is collected in hessian bags to allow the water to drain out and later be transported and dumped in a landfill (Kinuthia *et al.*, 2011). Brick dust waste is classified as part of construction and demolition waste which makes up about 14% of the volume of waste generated during construction (Malek *et al.*, 2007). Construction and Demolition Waste (CDW) are unwanted materials from construction activities such as new construction, renovation and demolition (Bektas, 2007). One of the voluminous and heaviest waste streams generated in the EU is Construction and Demolition Waste (CDW), this accounts for approximately 25% - 30% of the total waste stream generated in the EU and an annual CDW generation of 200 million tonnes generated each year in Europe (Müller, 2004; European Commission, 2016). European Commission reported CDW as the largest waste stream in the European Union (EU) in 2017 and accounts for more than 350 million tonnes/year excluding excavated soil and dredging spoil (European Commission, 2017).

According to Mülller (2006), CDW is made up of 42-92% of typical CDW mass and 30-80% of brick and tiles materials. CDW consist of materials such as bricks, wood, gypsum, glass concrete, plastic, metals, asbestos, solvents and excavated soil (European Commission, 2016). Brick was first used in Mesopotamia (now Iraq) as a sun-dried brick in 4500 BC and is still being used in the 21st century (Campbell, 2003). Recently, efficient ways of brick making are being adopted with the aim of reducing waste thanks to technology and research. However, there are still millions of tonnes of brick waste around the world. According to Mazumder *et al.* (2006), developing countries discard 13% of the world's total brick waste normally stockpiled or dumped in landfills Figure 2.19. These wastes can be used as raw materials in sustainable production. Brick Dust Waste (BDW) is manufactured by the calcination of alumina-silicate clay which is ground into fine powder giving it pozzolanic properties and can be used as cement replacement in road subgrade stabilisation (Kartini *et al.*, 2012). A reduction in effective grinding time and specific weight of a blend can occur while

Chapter 2 – Literature Review

setting time increases when brick waste is blended with cement in a mix (Naceri, 2009).

During production, a liquid phase is formed when clay bricks are highly fired at a temperature of about 1000°C to 1100°C, which solidifies to an amorphous glass phase when it cools. This gives it high pozzolanic properties such as pulverised fuel ash (O'Farrel *et al.*, 2001). This glassy phase cements the crystalline and other phases that make up the brick and enhances the resistance to chemical attack in cementitious mixtures (Wild *et al.*, 1996). Pozzolans are materials that contain alumina/silica, which react to form new compounds (Calcium silicate hydrate (C-S-H) and Calcium aluminium Hydrates (C-A-H) when lime is added and have the ability to modify the properties of a lime mixture (Rogers, 2011). Pozzolans of siliceous and aluminous materials (possess little or no cementitious value) in a finely divided form react chemically with the right amount of water with calcium hydrate at ordinary temperature to form compounds that possess the properties of cement (O'Farrell *et al.*, 2001). The addition of pozzolanic materials (e.g. brick waste) to a soil mix will enhance the properties; hence, speeding up setting time and increasing the strength and durability of soil (Rogers, 2011). Pozzolanic reaction enables the formation of a secondary C-S-H gel, which fills up voids and improves the internal structure and increases durability and strength. According to Rogers (2011), Greeks in ancient days constructed durable structures using volcanic ash from Santorini Island in the Aegean Sea.

There are two characteristics of pozzolans (the ability to form insoluble products with binding properties and the ability to react with lime) (Rogers, 2011). Some pozzolanic features are exhibited in clay materials especially when they are burnt between the temperature of 600°C and 900°C, and are grounded to form a powder (Figure 2.20). During the process of making a material pozzolanic, its crystal structures are destroyed and water content in their interlayers is removed. Studies have shown that high pozzolanic activities are observed when kaolinite clay is heated around a temperature of 600°C to form metakaolin (a dehydrated clay mineral) (Bektas *et al.*, 2008). According to Naceri (2009), an increase in strength was observed for blends composed of up to 10% by-weight brick waste after 90 days of curing.



Figure 2.19: Stockpile of brick waste (Crisands.com, 2022)



Figure 2.20: Recycling of brick waste to produce brick dust waste (YiFan concrete crusher, 2012)

2.8 GROUND GRANULATED BLAST-FURNACE SLAG (GGBS)

GGBS is a by-product of the iron manufacturing process. GGBS is collected from a blast furnace as a molten liquid. These by-products are mostly dumped in landfills which can lead to environmental effects (Higgins *et al.*, 1998). GGBS can be processed and used in subgrade stabilisation for road construction to solve the problem of landfills and reduce construction costs (Hewlett, 2003). During the processing of GGBS, GGBS molten liquid solidifies to form a crystalline material with virtually no cementitious properties when allowed to cool slowly. However, when it is rapidly quenched in water (granulated) it remains in a glassy, non-crystalline and is a latent hydraulic binder (Taylor, 1997). GGBS is sometimes grounded into powder form for use as a supplementary binder in many cement applications to enhance durability (Escalante-Garcia and Sharp, 2004). The alkaline properties of Portland cement, lime and other activators such as sulphates, chlorides and alkali silicates are sufficient to activate the cementitious properties of GGBS. According to Telling *et al.*, (1989, 1993), additional alumina, calcium, silica and magnesia are introduced to the system with the addition of GGBS (Oner and Akyuz, 2007). Lime and GGBS used in soil stabilisation have proven to be effective in the stabilisation of kaolinite clay with strength improvement at 7 days and 28 days (Wild *et al.*, 1998; Higgins *et al.*, 1998).

In various engineering applications, GGBS is mostly used in addition to lime to improve durability, workability, and economic benefits (Hewlett, 2003). Lime is used with GGBS because the strength development of GGBS alone is very slow under standard 20°C curing conditions compared to other conventional stabilisers (Escalante-Garcia and Sharp, 2004). The factor that affects the strength of GGBS when used as a binder is the rate of quenching which influences the glass content. Studies have shown that the higher the amount of GGBS blend, the greater the hydraulic activity (Hewlett, 2003). Strength increases with alumina (Al_2O_3) content and calcium oxide (CaO) compensated by a large amount of magnesia (MgO) when a constant amount of GGBS is added to a mix. However, a decrease in silica (SiO_2) can be recorded with the addition of less GGBS content (Frearson and Higgins, 1992). Figure 2.21 shows Ground Granulated Blast-furnace Slag (GGBS) stockpile and Figure 2.22 shows a schematic diagram of the manufacturing process of GGBS.



Figure 2.21: Ground Granulated Blast-furnace Slag (GGBS) stockpile (Steel360, 2019)

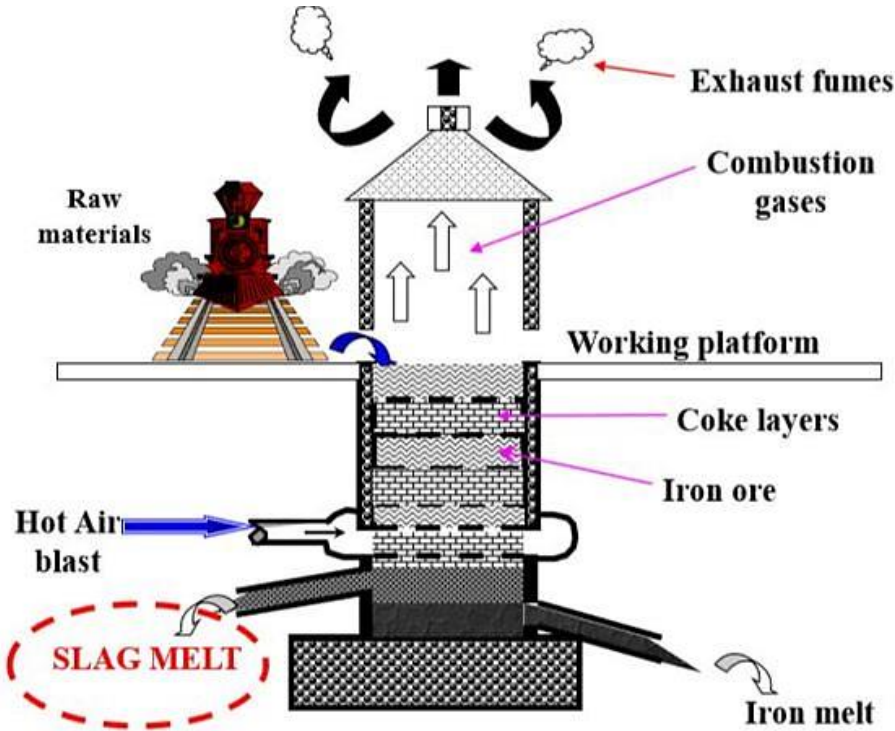


Figure 2.22: Schematic diagram of the manufacturing process of GGBS (Oti, 2010)

2.9 PLASTICS

Plastic is any synthetic or semisynthetic organic polymer sometimes of high molecular weight and is usually derived from petrochemicals. Thermoplastics and thermosetting are types of polymers and the name “plastic” refers to the plasticity and ability to deform without breaking. Thermosetting polymers solidify into a permanent shape. They are amorphous and considered to have infinite molecular weight while thermoplastics can be heated and remoulded repeatedly (Kassa *et al.*, 2020). Plastic always includes carbon and hydrogen which improve performance, polymer may contain other additives like plasticizers, stabilisers, ultraviolet (UV) absorbing material, lubricants, and flame retardants. The chemical composition, properties and mechanical properties of plastic can be altered during production with the addition of colourants, plasticisers, stabilisers, fillers, and reinforcements (Kassa *et al.*, 2020). Plastics are composed of a network of molecular monomers that bond together to form macromolecules and are usually referred to by acronyms for their chemical formulas (Kassa *et al.*, 2020). Polyethylene terephthalate (PETE) is mostly used for soft plastic drinks and ridged containers. High-density polyethylene (HDPE) is used to make milk and water jugs and soda bottles. Low-density polyethylene (LDPE) is used in cellophane wrap, diaper liners and squeeze bottles (Kassa *et al.*, 2020). Light thermoplastic resin (PP) is used in packaging, pipes, tubes and coating.

The properties of plastics and the ease of plastic production have made the use of plastic popular and have become part of our everyday lives. Plastics are used for various purposes such as packaging, building construction water transportation, packaging, telecommunication, medicine, education, agriculture etc. This has increased the demand for plastics to meet our modern-day lifestyle which has increased plastic waste. The world produces 381 million tonnes of plastic waste each year and is set to double by 2034 (Plastic in the Ocean, 2021). According to “Plastic in the Ocean” statistics for 2020-2021, about 8 million pieces of plastic make their way into our oceans and there are 5.25 trillion macro and micro pieces of plastic in our ocean and 46,000 pieces in every square mile of ocean, weighing up to 269,000 tonnes. Plastics such as polythene used in shopping are non-degradable, which means it does not break naturally in landfills and can stay in the ground for years hence contaminating the ground and leading to environmental problems. Statistics have

Chapter 2 – Literature Review

shown that the US alone produces over 230 million tonnes of plastic each year and less than 25% of that waste is recycled (Plastic in the Ocean, 2021).

The breakdown of plastic bottles can release DEHA, a type of carcinogen that can cause reproductive problems, liver issues and weight loss. Using plastic waste and recycled plastic in road construction will reduce the challenges the world is facing when it comes to the use of plastics and their disposal. Plastic wastes are used in various studies as an additive to stabilise expansive road subgrade material. CBR value of 3.04% was achieved for soil stabilised with up to 2% plastic strip and UCS values of up to 316.4kN were achieved (Kassa *et al.*, 2020). Figure 2.23 shows waste plastic bottles and other types of plastic waste at the waste disposal site in Thilafushi, part of the Maldives and Figure 2.24 shows plastic recycling process.



Figure 2.23: Waste plastics bottles and other types of plastic waste (Theguardian.com)



Figure 2.24: Plastic recycling process (Bezner, 2013)

2.10 RECYCLED GLASS

Glass is a state of matter and soil produced by cooling molten material so that the internal arrangement of atoms or molecules remains in a random or disordered state, similar to the arrangement in a liquid (Bezner, 2013). Other studies also defined glass as a silica-based product of inorganic, non-crystalline amorphous solid material fusion obtained by cooling down molten inorganic materials to a rigid condition (Brooks *et al.*, 1973). Glass has broad practical and technological properties which include longstanding function in decorative applications such as windows, tableware and household appliances. Glass grits transmits, reflects and refract light, all qualities that can be enhanced through cutting and polishing for use in optical lenses, prisms, fine glassware and optical fibres for high-speed data transmission that uses light. Natural glass has been in existence as early as 75,000 BC long before human beings learnt how to make glass, they used natural glass to fashion knives, arrowheads and other useful articles (Douglas *et al.*, 1972). The most common natural glass is obsidian which is formed when the heat of volcanos melts rocks, such as granite, which then becomes glassy upon cooling.

Chapter 2 – Literature Review

Other natural glasses are pumice, a glassy foam produced from lava, fulgurites, glass tubes formed by lightning striking sand or sandy soil and tektites, lumps or beads of glass probably formed during meteoric impacts (Kampfer *et al.*, 1966). Manmade or synthetic glass has existed as far back as 4000 B.C.E and may have been a by-product of copper smelting or pottery glazing (Kampfer *et al.*, 1966). Ancient glasses were based on silica (sand), modified with considerable amounts of various metal oxides, mainly soda (Na_2O) and lime (CaO). However ancient glass was usually coloured and opaque due to the presence of various impurities, in contrast, most modern glass has the useful property of transparency (Kolb *et al.*, 1988). Glass is composed of three basic types of ingredients namely formers, fluxes and stabilizers. Glass former is the key component in the structure of a glassy material (Kampfer *et al.*, 1966). The former used in most glasses is silica (SiO_2). It is difficult to melt pure silica due to its extremely high melting point (1,723°C) fluxes are sometimes added to reduce the melting temperature (Kampfer *et al.*, 1966). Other glass formers with much lower melting points (400°C - 600°C) are boric oxide (B_2O_3) and phosphorus pentoxide (P_2O_5) but they dissolve in water and have limited usefulness (Rogers *et al.*, 1948). Stabilisers are added to make glass stronger and more durable (Philips, 1981). The most common stabiliser is lime (CaO), but others are magnesia (MgO), baria (BaO) and litharge (PbO).

Glass grits used in this research are high-quality glass grains resulting from the specialised processing of selected glass cullet. The angular profile of crushed glass grit allows for aggressive surface profiling. Glass grits deliver very low grit embedment and are therefore regularly specified as a secondary process to remove embedment caused by other friable abrasives is suitable for blasting of all non-ferrous metals, weld seams prior to inspection. The special effect of the angular particles in crushed glass grit allows for aggressive surface profiling and removal of coatings such as epoxy, paint, alkyds, vinyl, polyurea, coal tar and elastomers. Glass grit is normally used as abrasive blasting. There are different arrays of silica-based glass but the most ordinary glazing and container glass is referred to as soda-lime glass or soda-lime-silica glass. The type of glass accounts for approximately 90% of all manufactured glass and is most commonly used in windowpanes, glass containers for beverages and food and various other goods.

2.11 PORTLAND CEMENT

Cement is popularly used to improve the engineering properties of subgrade materials (Lucena *et al.*, 2014; Abbey *et al.*, 2017; Saha *et al.*, 2017; Abbey *et al.*, 2018; Morales *et al.*, 2019). Portland cement is a common subgrade stabilisation material popularly used to improve the engineering properties of subgrade materials. It is a finely ground powder (hydraulic binder) that becomes solid when mixed with water through a process known as hydration (Neville, 2011). This hydraulic binder is derived through the crushing, milling and proportioning of raw materials such as calcareous/limestones/chalk rock and clay/shale. Hydration is the chemical combination of Portland cement compounds and water to form sub-microscopic crystals. In other words, hydration in cement is the process of solidification and strengthening of cement when it comes in contact with water. This results in a combination of Portland cement compounds and water to form sub-microscopic crystals (Dadsetan, 2015). During the manufacturing process, the raw materials are mixed intermittently in appropriate proportions to form powder through a dry process or slurry (wet process) (Neville, 2011).

The materials are burnt in a large rotary kiln at a temperature of up to 1450°C or 2600°F. After heating, the slurry undergoes some chemical and physical changes to produce greyish-black pellets which fuse partially into balls called cement clinker (Neville, 2011). The cement clinker is cooled, pulverized and gypsum is added to regulate setting time or prevent flash setting (rapid stiffening of the cement paste). The alumina and iron present in the mix act as a fluxing agent which lowers the melting point of silica from 3000°F to 2600°F (c). The mixture is then ground into extremely fine powder to produce Portland cement. Cement clinker is an intermediary product of cement production and a multiconstituent substance composed of four main clinker phases, known as tri- and dicalcium-silicates ($3\text{CaO}\cdot\text{SiO}_2$ and $2\text{CaO}\cdot\text{SiO}_2$), tricalcium-aluminate ($3\text{CaO}\cdot\text{Al}_2\text{O}_3$) and tetracalcium aluminoferrite ($4\text{CaO}\cdot\text{Al}_2\text{O}_3\cdot\text{Fe}_2\text{O}_3$), usually together with some unreacted CaO (free lime). Cement clinker is made by mineralogical transformation of a precisely specified mixture of raw materials based on oxides of calcium, silicon, aluminium and iron and small quantities of other elements (Kassa *et al.*, 2020). The basic constituents of cement are lime (CaO), silica (SiO_2) and alumina (Al_2O_3) and the hydration rate of Portland cement follows the sequence;

Chapter 2 – Literature Review

Tricalcium aluminate (C₃A) → Tricalcium silicate (C₃S) → Tetrecalcium alumino-ferrite (C₄AF) → Dicalcium silicate (C₂S) (Kassa *et al.*, 2020).

Tricalcium aluminate (C₃A): is a minor component and the most basic about 5-15% in volume and releases high amount of heat in the first few days. It has a significant contribution to early and rapid hydration products such as ettringite.

Tricalcium aluminate (C₃A) contributes slightly to the early strength development without calcium hydroxide (Ca(OH)₂) and is resistant to sulphates (Kassa *et al.*, 2020). The most reactive of the four phases is the strongly exothermic reaction from the C₃A hydration. However, it does not last long. Tricalcium aluminate (C₃A) occurs in Portland cement clinker as an 'interstitial phase' crystalizing the melt to obtain liquid at the peak kiln processing temperature (1400°C-1450°C) to facilitate the formation of the desired silicate phases (Kassa *et al.*, 2020).

Tricalcium silicate (C₃S): hydrates and hardens rapidly, it is a major component of PC which constitutes the silicate phase, and the bulk of the hydration products (calcium silicate hydrate gel (C-S-H gel) and calcium hydroxide (Ca(OH)₂) during the hydration of PC (Kassa *et al.*, 2020). The primary responsibility of C₃S is to develop strength at an early age (1 – 28 days)

Tetrecalcium alumino-ferrite (C₄AF): is a minor component of about 5% which contributes to little hydration. It hydrates quickly with the addition of water and slows down when a layer of iron hydroxide gel is formed (Kassa *et al.*, 2020). This becomes a coat on the ferrite and acts as a barrier that prevents further reaction and reduces clinkering temperature (Kassa *et al.*, 2020).

Hydrates and hardens slowly, it is the second component of PC (20-30%) and constitutes the silicate phase. It provides a significant contribution to hydration products (C-S-H gel) and Ca(OH)₂ (Kassa *et al.*, 2020). The dicalcium silicate phase is responsible for strength development at later ages (28 days on) and hydrates at a slower rate compared to (C₃S) (Kassa *et al.*, 2020). In road construction, using cement as a stabilisation agent is accepted and, in some situations, the use of cement and other conventional stabilisers can be avoided based on the design. High strength again is observed in subgrade specimens in the formation of a Portland cement gel matrix that binds together the soil particles and the bonding of the surface-active

Chapter 2 – Literature Review

particles within the soil (Prusinski and Bhattacharja, 1999). Studies have shown that Portland cement at high levels in soil stabilisation improves the surface coating and reduces erosion with a considerable influence on improving the resistance of soil vulnerability to frost attack (Bekhiti *et al.*, 2019). However, the permeability of the soil to allow the natural passage of moisture is reduced significantly (Bhattacharja, 1999; Walker, 2000; Lyons, 2010 and Prusinski).

In subgrade stabilisation, the amount of Portland cement used is in the range of 4% and 15% to increase strength and resist erosion depending on the grading and characteristics of the subgrade material (Walker, 2000). Generally, cement is suitable for the stabilisation of the subgrade with a low plasticity index ranging between 2% and 30%, this is because clay presence in the subgrade limits the effectiveness of cement during stabilisation (Gooding *et al.*, 1995). According to Nasir and Fall, (2009), a high pH of 12-13 can occur during cement hydration and C-S-H production as alkalis become solubilised due to pozzolanic reactions (Lea, 1980; Lin *et al.*, 2004). The high pH can lead to a reaction between hydroxides and silica derived from clayey soils which results in the development of a gel phase. The gel-phase act as a cementing agent similar to the reaction between lime and soil. Swell potential was reduced to 15.5% with the addition of cement proportions of 5, 7.5 and 10% (Bekhiti *et al.*, 2019).

Chemical stabilisation was investigated by adding 0%, 4%, 6%, 8%, 10%, 12%, 15% or 20% cement by weight of soil achieving a UCS value of 6MPa (Bahar *et al.*, 2004). UCS increased when ordinary Portland cement was used in subgrade stabilisation at proportions of 10%, 15% and 20% (Liang *et al.*, 2020). Subgrade material strength was improved from 564.87KPa to 636.19 KPa, 649.26 KPa, 673.34 KPa and 707.37 KPa respectively when Portland cement proportion 1,5, 3, 6 and 9% was added during the stabilisation process (Nazari *et al.*, 2021). CBR values of subgrade materials increased to upto 60% with an increase in cement content when cement proportions of 3%, 5%, 7%, 9% and 11% were used during road subgrade stabilisation in accordance with ASTM D 1883-67 (Pongsivasathit *et al.*, 2019). The compressive strength of specimens with 15% and 22% cement increased by 14.2%, and 7.8%, for 30, days respectively in accordance with ASTM D2166 (Meng *et al.*, 2017). Table 2.11 shows a summary of findings of improved engineering properties of subgrade using cement.

Chapter 2 – Literature Review

Table 2.11: Summary of findings of improved engineering properties of subgrade using cement

Waste Type	Content (%) /Ratio	Information Source	Test Type	Results: UCS (kPa)	Standards
Cement	8-33	Miura <i>et al.</i> , 2001	UCS increased	165	IS:2720 part 16
Cement	0-16	Al-Tabbaa <i>et al.</i> , 2003	UCS increased	1400-7550	IS:2720 part 16
Cement	1.5-7	Jauberthie <i>et al.</i> , 2010	UCS increased	1700 to 2300	IS:2720 part 16
Cement	0-10	Consoli <i>et al.</i> , 2009	UCS increased	400 and 1020	IS:2720 Part-16
Cement	5-8	Tang <i>et al.</i> , 2007	UCS increased	630 and 1280	IS:2720 part 16
Cement	3-12	Ding <i>et al.</i> , 2018	UCS decreased	480 to 150	IS:2720 part 16
Cement	0-10	Balkis <i>et al.</i> , 2019	CBR increased	22% – 69%	ASTM-D1883-07
Cement	0-5	Cabalar <i>et al.</i> , 2014	CBR increased	1.50% – 136.89%	ASTM-D1883-07
Cement	2-12	Edi <i>et al.</i> , 2018	CBR increased	2.54% - 59%	ASTM-D1883-07

Chapter 2 – Literature Review

2.12 HYDRAULIC LIME

Natural hydraulic lime is produced by burning a form of low-grade limestone containing silica and alumina which, above certain temperatures, are combined with calcium oxide (Venkatarama, 1998). The resulting silicates and aluminates impart hydraulic properties to the product. Lime was widely used in road subgrade stabilisation and applications before Portland cement was manufactured. Quicklime and hydraulic lime are the most common lime used in subgrade stabilisation. Lime has over the years been tested and proven to be a good agent for the modification and stabilisation of highway and airport pavement subgrade (Venkatarama, 1998). The addition of lime in subgrade stabilisation improves strength, workability, stiffness, and enhances durability. Unlike cement, lime works well with clay minerals in soils and the least amount of lime treatment in dry and temporarily modified soils produces a working platform for the construction of temporary roads (Lepore *et al.*, 2009). A plasticity index greater than 10% and minimum clay content of 10% are desirable. According to studies conducted by Boardman *et al.* (2001), Sakr *et al.* (2009), and Bell (1996), soil with a plasticity index between 20% and 30% with a liquid limit from 25% to 50% is recommended for lime stabilisation in most civil engineering applications. An optimum lime dosage of between 6-12% by dry weight is suitable and will increase the compressive strength of expansive soil (Houben, 1994; Norton, 1997; Venkatarama, 1998; Lepore *et al.*, 2009). Unlike cement, lime is slow in achieving its strength hence curing period of lime stabilised subgrade should be at least three times more than cement stabilised subgrade.

The liquid limit of soil may decrease and the plastic limit may increase when lime is added to the soil (Lepore *et al.*, 2009). This will lead to a reduction in the plasticity index of the soil hence increasing workability. When soil is stabilised with lime, a lime-soil reaction takes place which may change the moisture to density relationship of the soil due to the addition of more lime (Lepore *et al.*, 2009). The reaction may lead to a decrease in maximum dry density and an increase in optimum moisture content of the soil. certain clay with a highly negative-charge surface such as plastic clays reacts with lime to attract free cations (positively charged ions) and water dipoles (Lepore *et al.*, 2009). This lime-soil reaction forms a highly diffused water layer around the plastic clay particles. This separates the particles causing instability and weakness in plastic clay. The morphology and mineralogy of clay influence the extent of separation

Chapter 2 – Literature Review

depending on the amount of water present in the clay soil. (Little, 1987; Lime-Treated Soil Construction Manual, 2004). Cation exchange and flocculation-agglomeration reactions take place when lime is added to natural fine-grain soil. This reaction produces an immediate improvement in the soil plasticity, workability, uncured strength and load-deformation properties (Osula, 1996; Prusinski and Bhattacharja, 1999; Sakr *et al.*, 2009).

Lime stabilisation can be classified as immediate and long-term. However, immediate modification effects are achieved without curing due to the cation exchange and flocculation-agglomeration reactions that occur when lime is mixed with soil (Bell, 1996). Long-term stabilisation effects occur during and after curing for improvement in strength and durability (Ingles *et al.*, 1972). These effects are generated as a result of pozzolanic reactions which occur depending on the characteristics of the soil being treated, forming various cementing agents that further increase mixture strength and durability depending on curing time and temperature (Bell, 1996; Consoli *et al.*, 2009). A gradual increase in strength is observed and continuous for a long period of time. Temperatures of 16°C and below reduce the reaction while higher temperatures accelerate the reaction (Ingles *et al.*, 1972). Lime can also react with atmospheric carbon dioxide to form a relatively insoluble carbonate which negatively affects the stabilisation process. Ingles *et al.* (1987) used 1% of lime for every 10% of clay content in the soil. Jha *et al.* (2019) used 6% of lime to stabilise expansive subgrade. 4 to 6% lime proportion was adopted to achieve the best performance of expansive subgrade material (Wang *et al.*, 2019).

Swell potentials of lime-stabilised soil decreased from 90.1% to 0.2% with the addition of 5% lime (Hozatlioglu *et al.*, 2021). The Swell percentage of soil was reduced to zero with the addition of 6% lime (Al-Rawas *et al.*, 2005). Swell percentage was reduced significantly when 4% lime content was added to expansive soil (Phanikumar *et al.*, 2020). UCS values increased between 400-1503 KPa at 56 days of curing for 6% and 9% lime proportions when 4%, 6%, and 9% hydrated lime were used to stabilise expansive subgrade material in accordance with ASTM D2166/D2166M-13. Table 2.12 shows a summary of some findings of improved engineering properties of subgrade using lime.

Chapter 2 – Literature Review

Table 2.12: Summary of findings of improved engineering properties of subgrade using lime

Waste Type	Content (%) /Ratio	Information Source	Test Type	Results: UCS	Standards
Lime	3-9	Kumar <i>et al.</i> , 2016	UCS and CBR increased	3544 N/mm ² & 21.90	IS:2720 part 16
Lime	2	Oviya <i>et al.</i> , 2016	CBR and UCS	6.1 & 350kN/m ²	ASTM D 1883-67
Lime	1-4	Kulkarni <i>et al.</i> , 2016	Swell reduced & CBR increased	16 and 2.26	IS:2720 Part 40
Lime	1-4	Al-Tabbaa <i>et al.</i> , 2003	UCS increased	1400-7550kPa	IS:2720 part 16
Lime	1.5-7	Jauberthie <i>et al.</i> , 2010	UCS ranged from	0.8Mpa to 1.0MPa	IS:2720 part 16

Chapter 2 – Literature Review

2.13 CATION EXCHANGE AND FLOCCULATION-AGGLOMERATION

Cation exchange and flocculation-agglomeration reactions occur rapidly when lime is mixed with soil. The general order of replaceability of the cations is given by the Lyotropic series, $\text{Na}^+ < \text{K}^+ \ll \text{Mg}^{++} < \text{Ca}^{++}$ (Bell, 1990, Osula, 1996, Bell 1996, Prusinski and Bhattacharja, 1999; Consoli *et al.*, 2009). In cation exchange, higher valence cations replace those of lower valency and larger cations replace smaller cations of the same valency. The addition of lime to the soil in sufficient quantities supplies excess Ca^{++} which replaces the weaker metallic cations from the exchange complex of the soil (Consoli *et al.*, 2009). A reduction in the size of diffused water layer may occur during cation exchange. This allows clay particles to flocculate i.e come more closely to each other (Little, 1987). An apparent change in texture occurs as a result of flocculation and agglomeration. During this reaction, clay particles agglomerate or clump together into large-sized particles (Terrel *et al.*, 1979). Flocculation and agglomeration occur as a result of an increased electrolyte content of the pore water and as a result of ion exchange and are responsible for soil modification (Little, 1987). The reaction gives rise to a significant reduction and stabilisation of the adsorbed water layer causing an increase in the internal friction among the agglomerates (Terrel *et al.*, 1979). This gives greater shear strength and workability due to the change in texture from plastic clay to a friable, sand-like material.

2.14 POZZOLANIC AND CARBONATION REACTIONS

Pozzolanic reaction takes place between lime, water, soil silica and alumina that forms various cementing-type materials such as calcium-silicate-hydrate (C-S-H) and calcium-aluminate-hydrate (C-A-H). A variety of cement-like compounds are formed between lime and certain clay minerals during pozzolanic reaction to bind soil particles together and reduce water absorption by clay particles (Bell, 1996; Consoli *et al.*, 2009). The stabilisation behaviour of a soil lime mixture is caused by the flocculation of the clay particles that aggregate together to form larger-size particles that create new cementing materials due to the pozzolanic reaction of lime with the clay minerals. A significant increase in pH is observed during lime-soil reactions which increase the solubilities of silica and alumina (Little, 1987). Pozzolanic reaction continuous as long as enough residual calcium from lime remains in the system and the pH remains high enough to maintain solubility (Bell, 1996; Consoli *et al.*, 2009). Lime carbonation is an

unpleasant reaction that may occur during lime-clay mixtures. During this reaction, lime reacts with carbon dioxide from the atmosphere to form calcium carbonate instead of cementitious C-A-H and C-S-H.

The strength of some soil-lime stabilised systems may increase for the modification of their porous system as a result of the hardening of lime (Taylor, 1997; Shih *et al.*, 1999). Free water and calcium carbonate are the main products of the carbonation reaction. The carbonation process is controlled by two mechanisms: carbon dioxide from the air through the porous system up to the reaction front and the reaction of the diffused carbon dioxide with Ca(OH)_2 (Taylor, 1997 and Van Balen, 2005). The behaviours of conventional and unconventional materials are unpredictable because the extent to which they react in stabilised soil is influenced by the natural soil properties and the stabilising agent (Consoli *et al.*, 2009). Therefore, it is imperative to understand the reaction mechanism in stabilised soil and the stabilising agent.

2.15 ROAD PAVEMENT THICKNESS AND CONSTRUCTION DEPTH OPTIMISATION

Road pavement design is the major component in road construction and forms nearly one-third or half of the total cost of construction which includes the surface course and any underlying base or subbase layers (Paul *et al.*, 2014). Road pavement design process was used to determine the material composition and thickness of the different layers within a pavement structure required to accommodate a given loading regime (Paul *et al.*, 2014). Road pavement thickness optimisation is the process of delivering the most economical and sustainable road design while striking a balance between reducing pavement thickness with increased trafficking performance (Dhir OBE *et al.*, 2019). Pavement thickness includes the total thickness of asphalt including the various layer compositions on the subgrade (Dhir OBE *et al.*, 2019). There are three types of pavement and including fully flexible, flexible composite and rigid pavements (Dhir OBE *et al.*, 2019). During pavement design, many factors affect the selection of pavement types for construction these include initial cost, availability of good materials, cost of maintenance, environmental conditions and traffic intensity (Paul *et al.*, 2014). Pavement designs are focused on the structural design of new pavement based on the CBR value of the subgrade. Road pavement structures are made up of

multiple layers of proposed and compacted materials, in different thicknesses and in both unbound and bound forms, which together form a structure that primarily supports vehicle loads as well as provides a smooth riding quality (Dhir OBE *et al.*, 2019).

2.15.1 Flexible, Flexible Composite and Rigid Pavements

Pavement structures made up of a combination of aggregate and bitumen are termed flexible pavement, it is heated and blended precisely and then put and compacted on a bed of granular layer (Parry *et al.*, 1999). Flexible-composite pavements are pavement structures where asphalt is laid on a hydraulic-bound material (HBM). These pavements transfer the load to the subgrade through the combination of layers (Parry *et al.*, 1999). Flexible pavements require proper maintenance to avoid crumbling due to heavy traffic load because it is made up of asphalt whose viscous nature permits plastic distortion. Although almost all asphalt pavements are constructed on a gravel base, some ‘full; depth’ asphalt surfaces are constructed directly on the subgrade. There are three different classifications of asphalt depending on temperature: (i) Hot mix asphalt (HMA); (ii) Warm mix asphalt (WMA) and (iii) Cold mix asphalt (CMA) (Parry *et al.*, 1999). Rigid pavements comprise a combination of aggregates and cement, it is blended precisely and then put and compacted on a bed of granular layer (Parry *et al.*, 1999). Rigid road pavement has no subbase and is non-flexible, they are constructed from reinforced concrete rigid road consisting of three layers. Rigid pavements are mostly used to build airport runways and highways and typically provide heavy-duty industrial floor slabs, ports and dock plant pavements and heavy high-traffic park or concluding pavements (Parry *et al.*, 1999).

Rigid pavements are designed as long-lasting structures with high-quality surfaces for a ride for the purpose of safe driving (Parry *et al.*, 1999). The structural layers of rigid pavement transmit traffic load to the subgrade. A description of the various layers of road pavements are outlined as follows; Surface course: is a carefully proportioned mixture of bitumen-bound minerals mixed to the required specification. It provides skid resistance, weather resistance and low traffic noise. It can withstand traffic load and transfer the load to lower layers (Parry *et al.*, 1999). The base course is the area immediately under the surface course. The materials used in a base course are extremely high quality as the base course lies close underneath the pavement surface

Chapter 2 – Literature Review

and is subjected to severe loading (Parry *et al.*, 1999). The Subbase course is the lower layer of the road pavement and is made up of cement-bound granular materials containing crushed rock or gravel. It is the foundation of the road, and it transfers the load from above to lower layers (Parry *et al.*, 1999). The subgrade is the existing ground whether improved by stabilisation or compacted to the appropriate level of strength required to carry traffic load (Parry *et al.*, 1999).

In situations where subgrade materials are not strong enough on their own, a capping course can be provided as a construction platform to work on. Capping courses are generally a layer of granular product from crushed rock quarry and recycled materials. In some circumstances depending on the particular need of the road being built, a pavement structure may require a Binder course at the lower part of the surfacing (Parry *et al.*, 1999). Binder Course carries part of the load the surface course carries and helps to waterproof lower layers. Binder courses are made up of a type of asphalt concrete with different gradings of aggregate types and quantities (Parry *et al.*, 1999). The results achieved in this study are applicable to flexible pavements, flexible composite and rigid Pavements. Figure 2.25 shows the difference between flexible and rigid pavement.

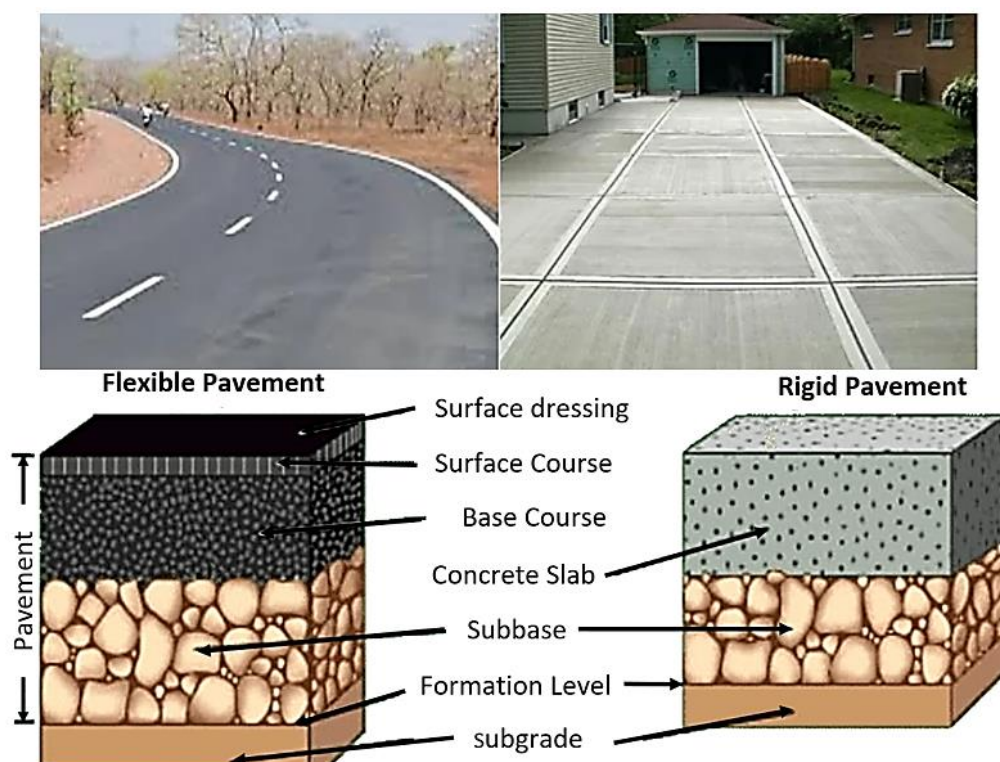


Figure 2.25: Difference between flexible and rigid pavement (Allaboutengineering, 2022)

2.16 ECONOMIC APPRAISAL

Economic appraisal is the process of investigating the cost-benefit and effects of an assertion by conducting LCC on the asset. LCCA serves as a tool for operators and service owners to enable them to determine the most appropriate solution for their requirements (White *et al.*, 2013). It uses economic principles to compare the cost or value of competing options based on the long-term, net benefit to a society or asset owner (Walls *et al.*, 1998). In estimating the life cost of an asset, LCCA takes into account initial agency cost, discounted future costs and other relevant costs where they are known (Rangaraju *et al.*, 2008). The concept of LCCA was first introduced in the 1930s as part of federal legislation regarding flood control and later into highway construction projects (Wild *et al.*, 2001). LCCA has been used in the comparison of many different road pavement structure designs and municipal infrastructure such as roads and bridges (Val *et al.*, 2003; Zakeri *et al.*, 2015). The approach has also been used to analyse the life cycle cost of Portland cement concrete pavement (Wild *et al.*, 2001). The approach has been used to compare rigid and flexible pavement design (Rangaraju *et al.*, 2008) and used in road and airport pavement maintenance interventions (Gendreau *et al.*, 1998; Giustozzi *et al.*, 2012).

LCCA allow objective comparison of solutions with high construction cost, long life and low maintenance requirements against other structurally equivalent and visible options that are less expensive to initially construct but have higher maintenance requirements for flexible pavement (White *et al.*, 2013). With help of technology, many life cycle cost analysis software programs have been developed to make LCCA easy and simple, while minimising human errors. For four decades, many life cycle cost methods have been developed by various agencies, industries and universities. However, the most noticeable pavement life cycle cost analyst program and methods have been developed and are being used by Pennsylvania, Maryland, Alabama, and Ohio (Wild *et al.*, 2001). In the general theory of LCCA, several studies (Gendreau *et al.*, 1998; Giustozzi *et al.*, 2012) have been undertaken to detail the appropriate junctures to maintain the structural integrity of the pavement at a minimum financial cost to the asset owner. Expansive road subgrade can influence the life cycle cost of road pavement in many ways. This is because expansive road subgrades are weak and require modification. These modifications can sometimes affect the life cycle cost of the road pavement.

2.17 CHAPTER SUMMARY

Chapter 2 outlined a detailed literature review in the subject area of this research giving theories and techniques used in road subgrade and soil stabilisation. The chapter also presented the characteristics and mineralogy of expansive subgrade materials, the use of processed waste and its availability for use in road subgrade stabilisation, and the environmental effect associated with using cement and lime compared with using waste materials. The chapter presented current knowledge and techniques used in road subgrade stabilisation to provide an intellectual context for the research.

Chapter 3 gives detailed information on the materials used, this includes their particle size distribution, materials source, physical properties, and oxide/chemical compositions. The basic characterisation of these materials was carried out in accordance with the British standard and other internationally accepted engineering standards in line with the UK road construction regulations.

CHAPTER 3 – MATERIALS

3.1 BENTONITE CLAY

The term bentonite is used to describe a rock with high plastic swelling clay belonging to the smectite mineral group. Bentonite is generated from the alteration of volcanic ash, predominantly made up of smectite minerals usually montmorillonite (Barbieri *et al.*, 2022). Road subgrade made up of bentonite has the lowest CBR and MDD values and a high plasticity index (PI) (Rahman *et al.*, 2021). Bentonite exhibited high water holding capacity with an increase in OMC, and MDD up to 15% as bentonite content increased (Thakur *et al.*, 2018). CBR value reduces drastically with the addition of bentonite in a mix, an increase in cohesion and a reduction in the angle of internal friction was observed with an increase in bentonite content in a mix (Thakur *et al.*, 2018). The Bentonite clay used in this research was high-quality sodium bentonite selectively mined and processed in Wyoming. The clay was a multi-purpose suspending, emulsifying, and binding agent used in industrial products with a minimum dry particle size of 65% passing 200 mesh (74 microns), a viscosity of 8-30cps and a pH of 8.5 to 10.5. The clay was a Hydrous aluminium silicate made up of clay mineral montmorillonite which contains small portions of feldspar, calcite and quartz. The clay was supplied by Potclays Ltd, Brickkiln Lane, Etruria, Stoke-on-Trent England. The oxide, chemical composition, consistency limits and other properties of bentonite used in this research are shown in Table 3.1 and Table 3.2. Figure 3.2 shows bentonite clay used in this study research.



Figure 3.1: Package of the bentonite clay used in this study



Figure 3.2: Bentonite clay used in this study

3.2 KAOLINITE (CHINA CLAY)

Kaolinite soil is formed by the weathering or hydrothermal alteration of aluminosilicate minerals. These are rocks rich in feldspar and are a common source of kaolinite. In order to form ions such as Na, K, Ca, Mg and Fe kaolinite must first be leached away by the weathering process, favoured by acidic conditions (low pH). The plasticity of kaolinite is very poor and is often used in conjunction with additives, and shrinkage (Abbey *et al.*, 2020). The Kaolinite used in this research is a hydrated aluminium silicate crystal mineral formed over many million years by the hydrothermal decomposition of granite rocks with the chemical formula $Al_2Si_2O_5(OH)_4$. It was manufactured by IMERYS and supplied by Potclays Ltd, Brickkiln Lane, Etruria, Stoke-on-Trent England. The oxide, chemical composition, consistency limits and other properties of kaolinite used in this research are shown in Table 3.1 and Table 3.2. Figure 3.4 show the kaolinite clay used in this study.



Figure 3.3: Package of the kaolinite clay used in this study

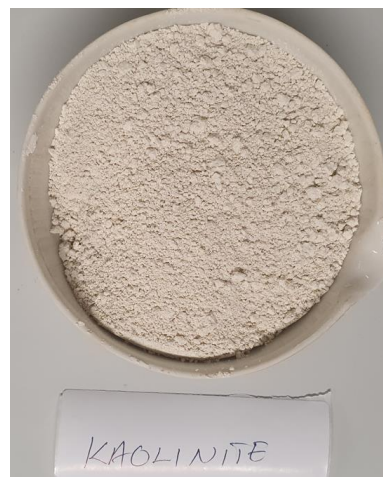


Figure 3.4: Kaolinite clay used in this study

3.3 PORTLAND CEMENT

Portland cement is a common road subgrade stabilisation material used to improve the engineering properties of subgrade materials. It is a finely ground powder (hydraulic binder) that becomes solid when mixed with water through a process called hydration (Neville *et al.*, 2011). During the hydration process, a cement gel called calcium silicate hydrate gel (C-S-H) is produced. This gel binds soil particles together and is responsible for strength gain (Prusinski *et al.*, 1999). The Portland cement used in this research was a Dragon Alfa Portland cement in compliance with BS EN 197-1:2019 CEM I 42.5R with high strength at early stages and was supplied by Decking delivery Morton farm, Old Gloucester Road, Thornbury, BS35 3UF, UK. CEM I

Chapter 3 – Materials

Portland cement are the most widely specified in the UK and is used in various applications from mortar, concrete, and render soil stabilisation to the manufacture of pre-cast units such as blocks, bricks, pipes and tiles. The oxide, chemical composition, consistency limits and other properties of Portland cement used in this research are shown in Table 3.1 and Table 3.2. Figure 3.6 shows the cement used in this study.



Figure 3.5: Package of the cement used in this study

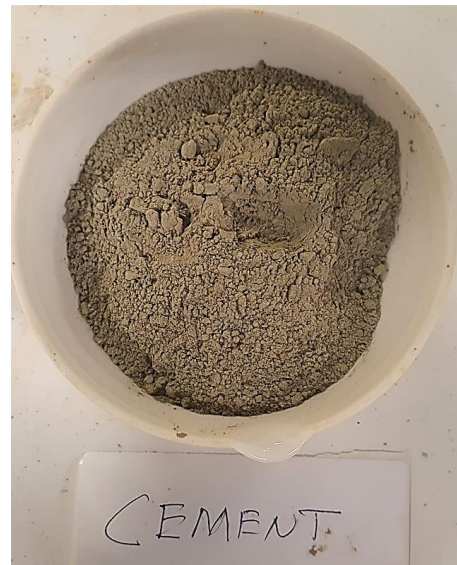


Figure 3.6: Cement used in this study

3.4 QUICK LIME

Lime is a calcium-containing inorganic mineral composed primarily of oxides and hydroxides usually calcium oxide and calcium hydroxide. Lime can be sourced from other calcareous materials such as aragonite, chalk, coral, marble and shall. The Lime used in this research was calcium oxide (CaO) commonly known as quicklime manufactured by Saint-Astier and in compliance with BS EN 459-1-2015. The lime was supplied by Womersley's Ltd, Ravensthorpe Industrial Estate, Low Mill Lane, Ravensthorpe, West Yorkshire, WF13 3LN UK. The oxide, chemical composition, consistency limits and other properties of hydraulic lime used in this research are shown in Table 3.1 and Table 3.2. Figure 3.8 shows the Lime used in this study.

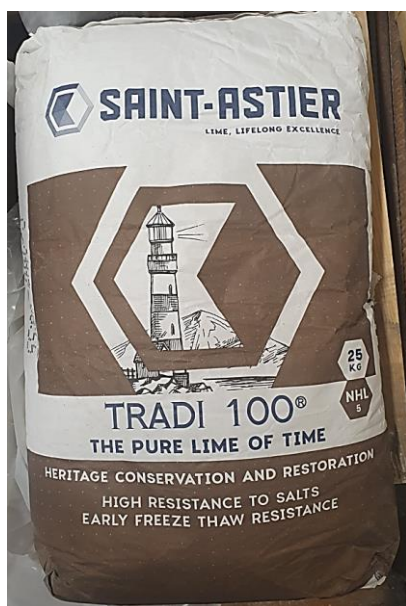


Figure 3.7: Package of the Lime used in this study



Figure 3.8: Lime used in this study

3.5 BRICK DUST WASTE

Brick dust waste is brick waste from demolition waste grounded in powdered form. Brick dust waste possesses pozzolans which can enhance the engineering properties of subgrade materials (Lihua *et al.*, 2020). Pozzolans are materials that contain high silica and/or alumina content that reacts chemically when mixed with lime to form a compound with cementitious properties (Walker *et al.*, 2011). Adding pozzolanic brick dust waste to lime will create an initial set in the soil giving it the early stage strength and overall strength when soil samples are cured (Spence *et al.*, 1983). According to Anand *et al.*, (2014), CBR value increased to over 400% and a high UCS was achieved when an optimum brick dust waste content of 40% was used during expansive subgrade stabilisation. Compressive strength and CBR of soil reached their maximum values based on the standard compaction test when an optimum content of 40% BDW was used in subgrade stabilisation in accordance with ASTM D2166/D2166M-13 and ASTM D1883-14 (Walker *et al.*, 2011). Other studies have shown an increase in CBR values at optimum BDW content from 5% to 20% (Al-Baidhani *et al.*, 2019).

The BDW used in this research was a red coloured pozzolan manufactured by Cornish Lime Company in accordance with BS EN 771-1:2011 + A1:2015 and supplied by Celtic Sustainable Ltd, Unit 9 Parc Teifi Business Park Cardigan UK. The oxide, chemical composition, consistency limits and other properties of BDW used in this

research are shown in Table 3.1 and Table 3.2. Figure 3.10 shows the brick dust waste used in this study.

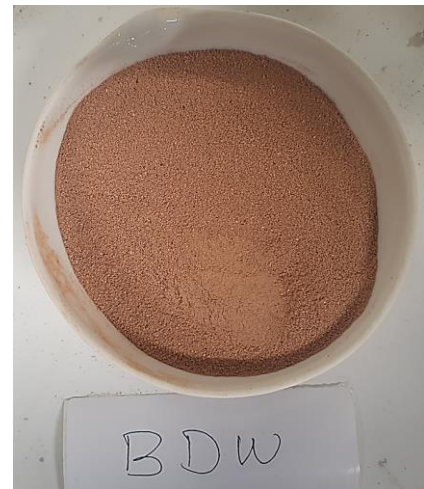


Figure 3.9: The package of the brick dust waste used in this study Figure 3.10: Brick dust waste used in this study

3.6 GROUND GRANULATED BLAST-FURNACE SLAG (GGBS)

The GGBS is a latent hydraulic binder normally mixed with cement and water for construction purposes. The GGBS consist of non-crystalline oxides of aluminium, calcium, silicon and magnesium together with sulfur compounds and small quantities of alkalis (Wild *et al.*, 1998). GGBS is a by-product of steel manufacturing process and has been successfully used in various studies as cement replacement to stabilise expansive road subgrade material (Obuzor *et al.*, 2012). The first application of GGBS-based stabiliser combination in road pavement construction in the UK was on the A421 Tingwick bypass in Buckinghamshire, and on the A130 road near London (Wild *et al.*, 1998). The engineering properties of expansive soil were improved with the addition of up to 7.5% GGBS (Corrêa-Silva *et al.*, 2020).

Subgrade materials were stabilised with 16% GGBS and the results obtained show an increase in UCS value over time to 1500kN/m² in accordance with ASTM 1633 (Obuzor *et al.*, 2012). The addition of 6% GGBS to a lime-treated soil reduced swell from 8% to 0% (Celik *et al.*, 2013). High compressive strength of 14.2kPa, 89kPa, 211.9kPa and 656 kPa was achieved when GGBS proportions of 6%, 12%, 18% and 24% were used in subgrade stabilisation after 28 days of curing (Gokul *et al.*, 2020). The GGBS used in this research was a Francis Flower finely ground white powder insoluble in water in accordance with BS EN 15167-1:2006. It was supplied by Francis Flower, Gurney Slade, Radstock, Somerset BA3 4UU. The oxide, chemical

composition, consistency limits and other properties of GGBS used in this research are shown in Table 3.1 and Table 3.2. Figure 3.12 shows the GGBS used in this study.



Figure 3.11: The package of the GGBS used in this study



Figure 3.12: GGBS used in this study

3.7 RECYCLED PLASTIC

Plastic waste has been successfully used in various studies as an additive to stabilise expansive road subgrade material. CBR value of 3.04% was achieved for soil stabilised with up to 2% plastic strip and UCS values of up to 316.4kN were achieved (Kassa *et al.*, 2020). Synthetic fibres such as polypropylene have been reportedly used in various studies as an additive to stabilise expansive road subgrade material. The recycled plastic used in this research was high-definition super-strong lightweight plastic pellets with a melting temperature of over 100°C. They are long-lasting and mold/mildew resistant. The pellets are safe to use and are slightly more irregular in shape than virgin material. The plastic pellets are manufactured and supplied by Poli Plastics Pellets Ltd, Monor farmhouse, Hawarden, Flintshire, CH5 3PL, UK. The oxide, chemical composition, consistency limits and other properties of the plastic used in this research are shown in Table 3.1 and Table 3.2. Figure 3.14 shows the Recycled plastic used in this study.



Figure 3.13: Package of the recycled plastic used in this study

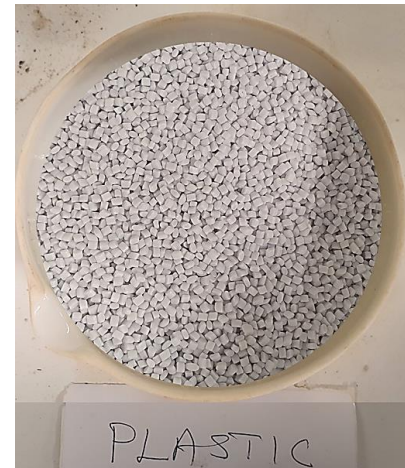


Figure 3.14: Recycled plastic used in this study

3.8 RECYCLED GLASS

Glass grits used in this research are angular and subangular abrasive glass particles with the ability to cut coatings exceptionally well when used in abrasive blasting. The glass does not contain significant chlorides and has a much lower dust generation with many health and safety benefits (Syed *et al.*, 2020). Glass grits are free from silicates and heavy metals meaning it is a safe product for use. Glass grits used in this research are non-toxic and inert, unlike copper and other metal. Glass grits can be used when working in and around environmentally sensitive areas (such as watercourses, marina's, etc.) because the media is completely inert and will pose no environmental risks should spillage occur (Ateş *et al.*, 2016). Ground waste recycled glass was used as a partial replacement for clay used in fired brick manufacturing, the glass acted as a flux in the mix reducing firing temperature (Abbey *et al.*, 2020).

The health and safety of the glass grits used in this research are guaranteed unlike other minerals-based abrasives, glass has no detectable “free” or “crystalline” silica, greatly reducing the potential health hazards for the user and eliminates users from silicosis, a lung-damaging disease which can be fatal. The glass grits are completely non-sharp and can be handled without the risk of cutting. The glass grits used in this research were a course grade with a particle size of 1.0mm – 3.0mm (1000 to 3000µm). It was manufactured by Centurywise Ltd in accordance with BSI PAS102 and under ISO 9001 quality control systems and supplied by Centurywise Ltd, Unit 2 Bridge House, Stuart road Bredbury, Stockport, Greater Manchester, SK6 2SR. The oxide, chemical composition, consistency limits and other properties of glass grit used

in this research are shown in Table 3.1 and Table 3.2. Figure 3.16 shows the recycled glass grits used in this study.



Figure 3.15: The package of the glass grits used in this study Figure 3.16: Recycled glass grits used in this study

Table 3.1: Oxide and some chemical composition of Bentonite, Kaolinite clay and the binders used in this study (Datasheet from suppliers)

Oxide	SiO ₂	Al ₂ O ₃	Fe ₂ O ₃	FeO	MgO	CaO	K ₂ O	SO ₃	TiO ₂	Na ₂ O	BaO	Cr ₂ O ₃	Trace	L.O.I
Bentonite Clay(%)	63.02	21.08	3.25	0.35	2.67	0.65	-	-	-	2.57	-	-	0.72	5.64
Kaolinite Clay (%)	48.5	36.0	1.00	-	0.30	0.05	2.15	-	0.06	0.15	-	-	-	11.7
Cement (%)	20	6.0	3.0	-	4.21	63	-	2.30	-	-	-	-	-	0.80
GGBS (%)	35.35	11.59	0.35	-	8.04	41.99	-	0.23	-	-	-	-	-	-
Lime (%)	3.25	0.19	0.16	-	0.45	89.2	0.01	2.05	-	-	-	-	-	-
BDW (%)	52	41	0.7	-	0.12	4.32	0.53	0.33	0.65	0.05	-	-	-	2.01
Plastic (%)	45.47	12.11	1.04	-	-	38.49	0.94	0.43	-	-	-	-	-	-
Glass (%)	72.20	1.50	0.07	-	1.30	10.90	0.45	0.16	0.06	13.30	0.04	0.02	-	-

These components are important in ensuring high strength gain through pozzolanic reaction and the production of calcium silicate hydrate (C-S-H) and calcium aluminate hydrate (C-A-H) gel. The SiO₂, Al₂O₃ elements are the basic constituents of cement and lime and when added to clay particles produce hydrated gels of C-S-H and C-A-H responsible for strength gain. The reasonably high Magnesium Oxide (MgO) content in GGBS also contributes to high strength in the mix with an increase in curing age. GGBS-MgO stabilised soil could gain higher unconfined compressive strength relative to the Portland cement stabilised soils (Yi et al., 2012). MgO acts as an effective alkali activator of GGBS, achieving higher 28 day compressive strength (Yi et al., 2014). Figure 3.17 shows the particle size distribution of materials used in this study.

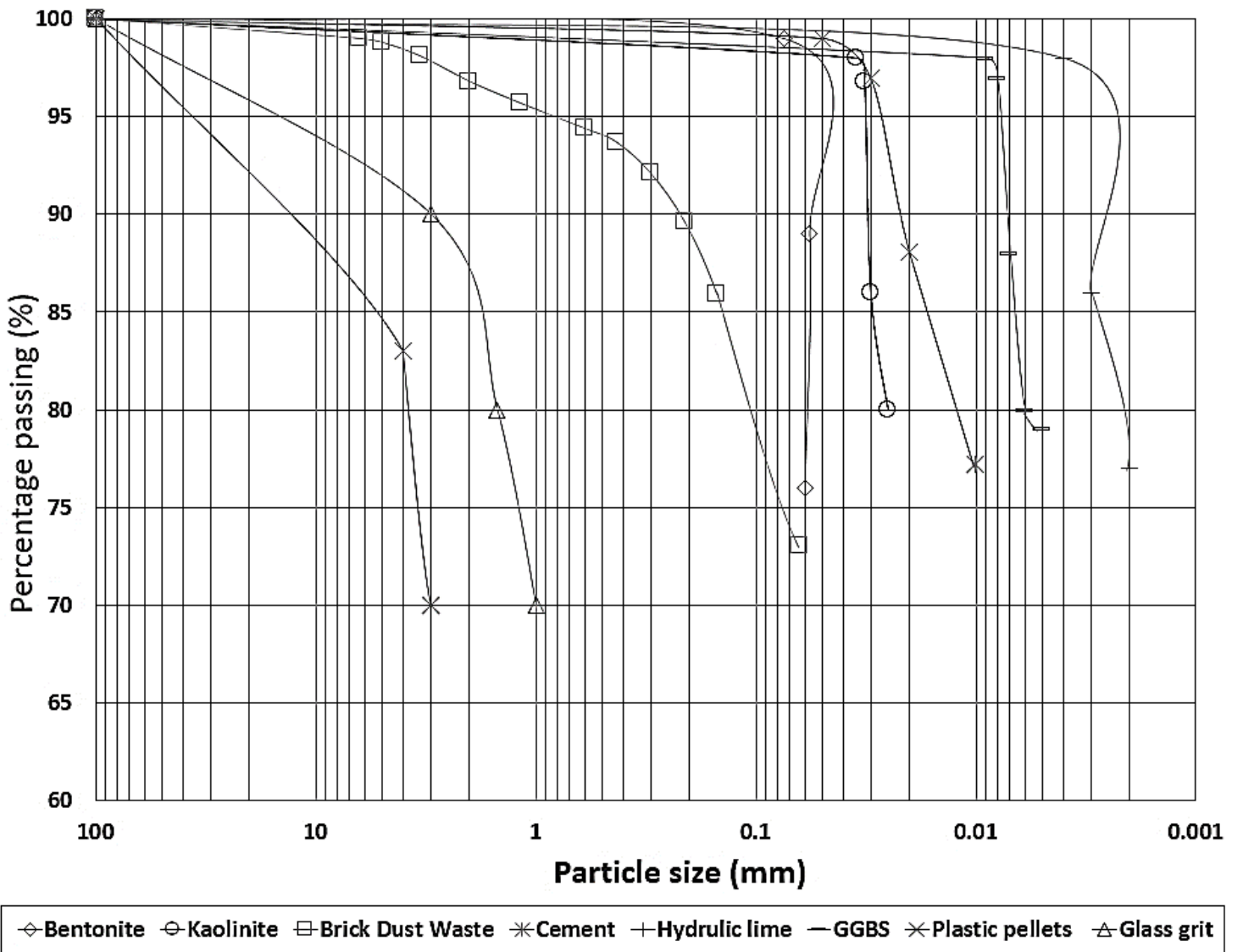


Figure 3.17: Particle size distribution of materials used in this study

Chapter 3 – Materials

Table 3.2: Consistency limits, chemical and physical properties of kaolinite, Bentonite, Portland cement, lime, brick waste plastic and glass

Properties	Description							
	KC	BC	PC	LIME	BDW	GGBS	PLASTIC	GLASS
Consistency limits								
Liquid limit w_L (%)	59	310	-	-	-	-	-	-
Plastic limit w_P (%)	28	49	-	-	-	-	-	-
Plasticity index I_P (%)	31	261	-	-	Non-plastic	-	-	-
Others								
Appearance	Fine powder	Fine powder	Fine powder	Fine powder	Fine powder	Fine powder	Solid	Solid
Colour	Greyish-white	Beige	Grey	White	Brick red	Off white	Light grey	Multi-coloured
Trade name	China clay	Bentonite	CEMEX Cement	Hydraulic Lincolnshire Lime	Brick dust	GGBS	Plastic pellets	Glass grit
Mean particle size (micron)	25-35	60-74	1 – 50	2-4	-	5-92	3000-4000	1000-3000
Odour	Earthy odour	Odourless	Odourless	slight earthy odour	Odourless	Odourless	Odourless	Odourless
Boiling point (°C)	-	-	>1000	580	-	>1700	-	-
Melting point (°C)	1750	1550	>1250	580	<850°	>1200	165	1300C
Flashpoint (°C)	-	-21	Not flammable	-	>450	-	275	-
Vapour pressure (°C)	-	-	>1250	>450	>450	-	-	<700
Viscosity	-	8-30 cps	1450 mPas @ 20°C	>450°C	-	110cPs	-	-
P84 demand (mass %)	-	0.44	-	-	-	-	-	-
Casting concentration (mass% solids)	0.4	-	-	-	-	-	-	-
Concentration	-	7.0	-	-	-	-	-	-
Casting Rate (mm ² min ⁻¹)	3.0	-	-	-	-	-	-	-
Brightness (%)	81.0	81.0	-	-	-	-	-	-
Water absorption	-	16.0	-	-	-	-	-	-
Density	2.4	2.5 at 20°C	2800 – 3200kg/m ³	-	-	2.4-2.8 g/cm ³	1.1 g/cm ³	2.53
Bulk density	-	1.18glcc	1100 – 1600kg/ m ³	0.43 – 0.48 g/cm ³	-	-	-	1.5 kgs/dm ³
Maximum dry density (kN/m ³)	1430	11.8	-	-	1.5	-	-	-
Optimum moisture content (OMC) (%)	-	-	-	-	17	-	-	-
Relative density	1.8 g/cm ³	2.7 g/cm ³	2.75g/cm ³	2.24	0.9-1.6	10	>1.0	2.45kgs/dm ³
Specific gravity	2.7	2.20	-	2.3	-	-	-	2500
Specific surface	-	-	-	300-1500 m ² /kg	-	-	-	-
Particle size distribution	-	-	-	99% <90 μ	-	-	-	-
pH	6 at 25°C	8.5	pH of wet cement 12 - 14	12.4, approx. 2g/l	-	When wet, up to 12	6-8	7.2
Solubility in water (g/l)	Insoluble	Insoluble	0.1	1844.9 mg/L	Negligible	<1	Insoluble	Insoluble
Natural moisture content (%)	28	14	-	-	-	-	-	-
Autoignition temperature °C	-	-	-	No relative self-ignition temperature below 400°C	-	-	>340	-
Notation								
BC – Bentonite clay KC – Kaolinite clay PC - Portland cement BDW - Brick dust waste GGBS - Ground Granulated Blast-furnace Slag								

3.9 CHAPTER SUMMARY

Chapter 3 introduced the type of materials used in this research, their sources, particle size distribution, physical properties, and oxide/chemical compositions. The chapter also mentioned the constituents present in the sustainable waste materials used such as pozzolans in brick dust waste (BDW) and the presence of calcium, silicon and magnesium in GGBS that are responsible for improving road subgrade. Furthermore, the chapter mentioned how CBR values of weak subgrade were enhanced in other studies using waste materials.

Chapter 4 outlines the research methodological process and analytical techniques used to achieve the set aim of this study. The chapter includes details of preliminary tests, mix design, and test sample preparation. The chapter also describes laboratory tests for the engineering properties such as moisture content and Atterberg limit test, swell test, California Bearing Ratio (CBR) test and microstructural analysis. The research methodological process is shown in Figure 4.1.

CHAPTER 4 – METHODOLOGY AND RESEARCH DESIGN

The research methodological process and analytical techniques below were used to achieve the set aim of this research. The method includes conducting preliminary tests, mix design, and test sample preparation, moisture content, Atterberg limit test, swell test, California Bearing Ratio (CBR) test and microstructural analysis. The methodology shows the various processes of conducting road pavement and life cycle cost analysis in this research. Figure 4.1 shows the research methodological process.

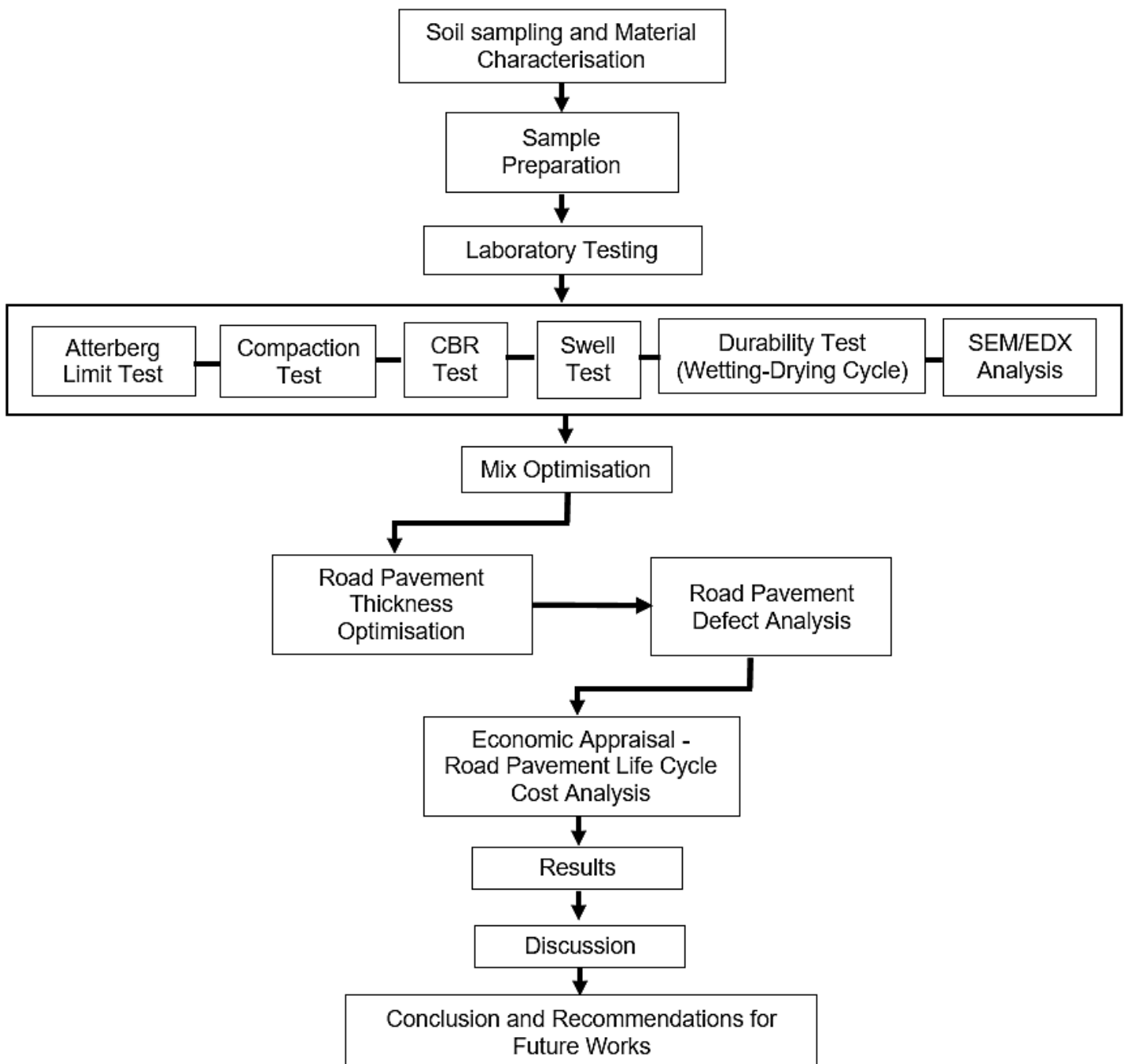


Figure 4.1: Research methodological process

4.1 SOIL SAMPLING AND MATERIAL CHARACTERISATION

In this section, the process of soil sample preparation and the characterisation of the materials used in this research are outlined. The target materials are bentonite and kaolinite clay and the binders used include BDW, GGBS, Recycled Plastic and Recycled Glass. These waste materials were locally sourced from suppliers after detoxification and decontamination in accordance with relevant standards. Materials characterisation to determine the physical properties, particle size distribution, chemical compositions, mineralogy composition, oxide composition and others in accordance with the relevant standards were provided by the supplier in the form of datasheets. This information was used to describe the characteristics of each material and assisted in the completion of a comprehensive health and safety risk assessment for this study. Two ASS materials were formulated for use in this study. These subgrade materials consist of a mixture of untreated bentonite and kaolinite at various percentages by weight of the total sample to form subgrade materials with varying plasticity index and with properties similar to that of a naturally existing expansive clay subgrade material. The two Artificially Synthesised Subgrade (ASS) materials were formed in proportions of ASS1 (25% Bentonite, 75% Kaolinite) and ASS2 (75% Bentonite, 25% kaolinite) respectively.

4.2 PRELIMINARY TESTS

4.2.1 - Moisture content

Moisture content tests of the various types of ASS materials was conducted and used as a guide and a control standard for the classification of specimen used for the laboratory test. Moisture content for ASS materials composed of various proportions of bentonite and kaolinite was determined using the oven-drying method in accordance with BS EN ISO 17892-1-2014. Each of the two types of ASS material was placed separately in an empty container after the weight of the empty container was weighed and recorded. ASS specimen was placed in the container and the weight of the container and soil were recorded. The container and the soil were put in the oven to dry for 24 hours at a temperature of 105⁰C to 110⁰C. The oven-dry method was adopted because according to BS 1924-1:2018, it is the most convenient and the materials used are unlikely to be affected by heating at 105⁰C. The specimen was removed after drying and allowed to cool and the weight was recorded. The moisture

content for the various ASS materials was determined and plotted against the Maximum Dry Density (MDD) to determine the Optimum Moisture Content (OMC) of the various ASS materials. The moisture content of the subgrade materials was calculated as a percentage of the dry weight of the soil using Equation 1

$$\text{Equation 1..... Moisture content (MC)} = \frac{M_m}{M_D} \times 100$$

Where:

M_m = Mass of moisture M_D = Mass of the oven-dried specimen

4.2.2 - Atterberg limits

Atterberg limits are also known as consistency limits, this classification method was developed by a Swedish soil physicist called Albert Mauritz Atterberg in 1911 (Lal, 2006). The method defines the boundaries of four states of soil in terms of 'limits' to measure the plasticity range of soil specimens in numerical terms and to determine the states of consistency of the soil. In clay soils, there is a range of moisture contents within which clay becomes plastic. Knowing the Atterberg limits of soil helps to understand the nature of fine-grained soil, to distinguish between silt and clay and the different types of silt and clay. Depending on the water content of the soil, four states of consistencies may occur: solid, Semi-solid, plastic and liquid. Each state of consistency and behaviour presents different engineering properties. A gradual increase in water content in the soil would result in changes in the consistency of the clay soil from semi-solid to a plastic state and lastly to a liquid state. Hence, the change in soil behaviour can be determined based on the boundaries between each state. The plastic limit (PL), liquid limit (LL) and shrinkage limit (SL) of soil are collectively referred to as Atterberg or consistency limit of the soil specimen. The consistency values of a soil specimen can be influenced by the various parameters of soil such as particle size distribution and specific surface area due to the differences in their water absorption potentials. Table 4.1 shows Atterberg limit results for untreated subgrade materials, Equation 2 shows the formula for calculating plasticity index and Table 4.2 shows the apparatus used in the Atterberg limit in this study.

Table 4.1: Atterberg limit results for untreated subgrade materials

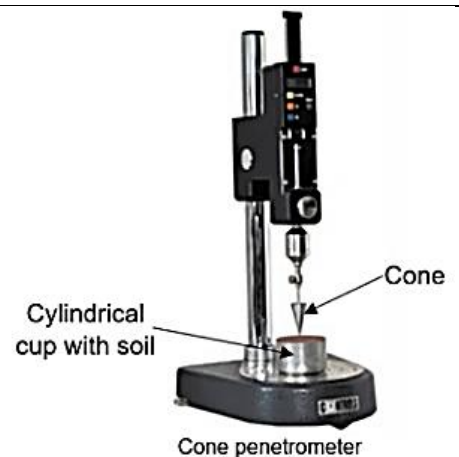
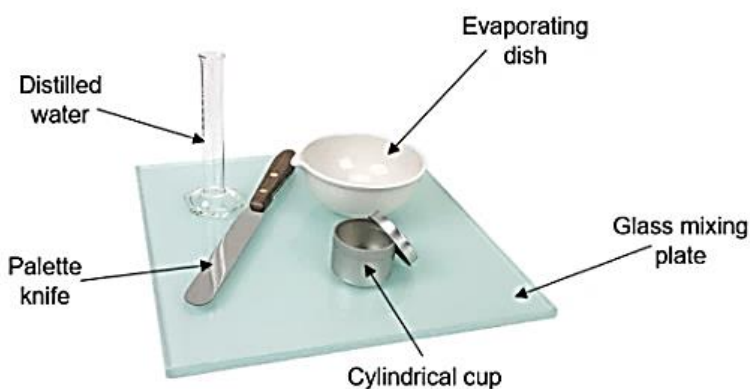
Parameters	ASS1 (25%Bentonite + 75% Kaolinite)	ASS2 (75%Bentonite + 25% Kaolinite)
Liquid Limit (LL)	131.26	294.07
Plastic Limit (PL)	28.74	45.38
Plasticity Index	102.52	248.69

$$\text{Equation 2} \dots \dots \dots \text{Plasticity index (PI) = Liquid Limit (LL) - Plastic Limit (PL)}$$

Table 4.2: Apparatus needed for Atterberg Limit Test

Equipment	
<ul style="list-style-type: none"> Penetrometer apparatus and flat glass plate Metal cup, 55mm diameter and 40mm deep Wash bottle containing distilled water 	<ul style="list-style-type: none"> Palette knives or spatulas Moisture content apparatus

Description



4.2.2.1 - Plastic limit (PL)

The PL state of soil is classified as the minimum moisture content at which the soil can be deformed plastically or the condition at which the soil can be remoulded to any shape without any development or cracks. A PL test was conducted on ASS materials in accordance with BS EN ISO 17892-12:2018+A1:2021. Plastic limit results in this research were used as part of the calculations to determine the plasticity index of the various ASS materials. Air-dried ASS material of about 20g was weighed and a measured amount of water was added and mixed in an evaporation dish and then transferred onto a glass plate. The pH level of the water used was measured as 6.64

which falls within the range required for sample preparation as specified in BS 1924-1:2018. The soils were allowed to partially dry on the plate, so they become plastic enough to be shaped into a ball (Abbey *et al.*, 2020). The ball was moulded and rolled between the palms of the hand until the heat of the palm dried the soil for significant slight cracks to appear on the surface of the soil.

The moulded rolled soil specimen was then divided into two equal halves of about 10g each. Each half of the rolled soil was further divided into four equal parts to be treated separately. By applying uniform and continuous rolling pressure, each part of the four-soil specimen was rolled in between the palms into rods or thinner threads. With a diameter of about 3mm with strikes of about 80 to 90 per minute, where the soil specimen starts to crumble due to lack of plasticity. The crumbled soil was transferred into suitable numbered containers that meet the requirements in BS 1924-1:2018 for moisture content determination after the weight of the container was recorded. The specimen was placed in the container and the weight of the container and specimen were also recorded. The container with the specimen was placed in the oven for 24 hours at a temperature of 105⁰C. The specimen and container were allowed to cool for 20 hours after drying in the oven and their weights were recorded for plastic limit determination. Equation 3 Shows the formula for calculating plastic Limit, Table 4.3 shows Plastic limit results for untreated subgrade materials and Figure 4.2 (a) – (h) shows the laboratory test process and how plastic limit samples were prepared.

Equation 3.....Plastic Limit (PL) = $\left(\frac{m_2-m_3}{m_3-m_1}\right) \times 100$

Where:
 m2 = Mass of wet soil + container, m3 = Mass of dry soil + container
 and m1 = Mass of container

Table 4.3: Plastic limit results for untreated subgrade materials

Parameters	ASS1 (25%Bentonite + 75% Kaolinite)	ASS2 (75%Bentonite + 25% Kaolinite)
Plastic Limit (PL)	28.74	45.38



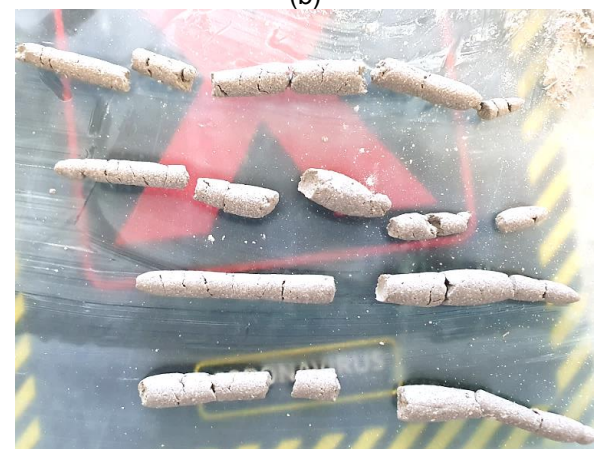
(a)



(b)



(c)



(d)



(e)



(f)



(g)



(h)

Figure 4.2: Laboratory test process and how plastic limit samples were prepared

(a) ASS in plastic limit state **(b)** Dividing rolled plastic limit state ASS ball into two for rolling between the palms **(c)** Rolling specimen into rods between the palms until specimen cracks/breaks **(d)** Rolled specimen rods **(e)** Rolled specimen rods in a container ready for oven-drying **(f)** Specimen and container on scale **(g)** Specimen in the oven **(h)** Oven-dried specimen in a container

4.2.2.2 - Liquid limit (LL)

Liquid limit is the state at which a fine-grained soil (ASS material) flows on its own weight. Liquid limit (w_L or LL) is expressed as the water content at which the soil stops acting as a plastic solid and starts acting like a liquid. In this study, the cone penetration method was used to determine the liquid limit of all types of ASS in accordance with BS EN ISO 17892-12:2018+A1:2021. The test was based on the measurement of penetration of a specific cone standard mass and dimensions into the soil sample. The liquid limit was expressed as the water content which corresponds to a cone penetration of 20mm. Liquid limit was plotted against plasticity index to determine the level of plasticity of the various ASS Materials (Abbey *et al.*, 2020). The cone penetration method was used in this research to determine the liquid limit of all types of ASS materials. The test was based on the measurement of penetration of a specific cone standard mass and dimensions into the soil sample. The liquid limit was expressed as the water content which corresponds to a cone penetration of 20mm. Air-dried artificially synthesised Subgrade (ASS) material composed of various proportions of kaolinite and Bentonite of about 300g was weighed and placed on a glass plate.

Dried ASS was mixed thoroughly by hand until homogeneity was achieved after which a measured amount of water was added and mixed using palette knives to form a paste. The pH level of the water used was measured as 6.64 which falls within the range required for sample preparation as specified in BS 1924-1:2018. ASS paste was transferred to a brass cylindrical cup carefully to ensure no voids are allowed. The surface of the brass cup filled with the ASS paste was flattened to the brim of the cup ready for the fall cone penetration test. The ASS sample and the brass cup were placed centrally under the cone penetration apparatus and making sure the pointed part of the cone penetrator was hung directly at the centre with the tip just in contact with the surface of the sample. The dial gauge on the cone penetrometer apparatus was adjusted to zero and an automatic timer was set for five seconds. The cone was released to penetrate the soil sample paste and the reading on the dial gauge was recorded. The process was repeated for all three types of ASS, and moisture content was measured by taking about 10g of the ASS sample in the brass cup from the area penetrated by the cone, using the tip of a small spatula. The collected sample was placed in numbered containers that meet the requirements in BS 1924-1:2018. The container plus wet samples were weighed, recorded and oven-dried for 24 hours. The container plus dry samples were weighed, and the values were recorded. Table 4.4 shows Liquid limit results for untreated subgrade materials, and Figure 4.3 (a) – (h) shows the laboratory test process and how liquid limit samples were prepared. Equation 4 Shows the formula for calculating Liquid Limit and Table 4.4 shows the Liquid limit for untreated subgrade materials.

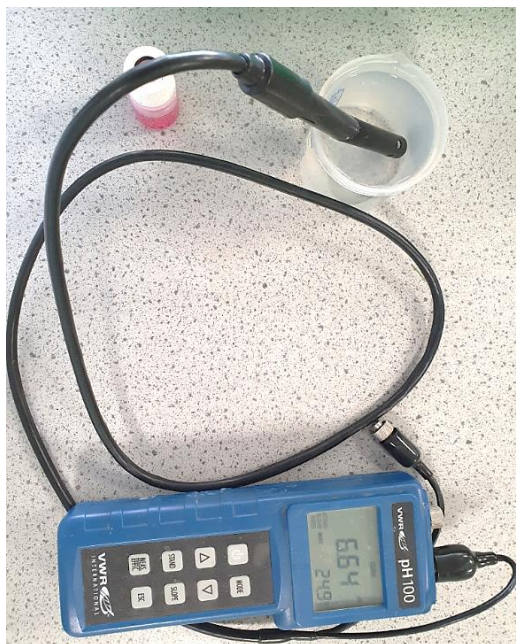
$$\text{Equation 4..... Liquid Limit (LL)} = \left(\frac{m_2 - m_3}{m_3 - m_1} \right) \times 100$$

Where:

m_2 = Mass of wet soil + container, m_3 = Mass of dry soil + container
and m_1 = Mass of container

Table 4.4: Liquid limit results for untreated subgrade materials

Parameters	ASS1 (25%Bentonite + 75% Kaolinite)	ASS2 (75%Bentonite + 25% Kaolinite)
Liquid Limit (LL)	131.26	294.07



(a)



(b)



(c)



(d)





Figure 4.3: Laboratory test process and how liquid limit samples were prepared
(a) Testing pH level of water used (b) Soil at liquid limit state (c) Cone penetration process during liquid limit test (d) Taking specimen after cone penetration for liquid limit test (e) Specimen and container on a scale (f) Wet specimen in containers ready for oven-drying (g) Specimen in the oven (h) Oven-dried specimen in containers

4.3 PROCTOR COMPACTION TEST

Proctor compaction test was conducted in this research to determine the moisture content and target dry density values of the various types of subgrade materials used in accordance with BS 1377- 4:1990 and BS EN ISO 17892-1-2014. The test was conducted to establish the compaction characteristics (optimum moisture content (OMC) and maximum dry density (MDD)) of untreated ASS materials. The compaction mould plus base without the collar was weighed and the value was recorded. A measured amount of ASS material was mixed with different percentages of water and mixed at different moisture content levels. The ASS subgrade material was placed in a proctor test mould with a collar in three different layers and with the help of a 2.5kg hammer, twenty-seven blows were applied at different areas of the surface of each layer to ensure even distribution of force. After the last layer was compacted, the collar was carefully removed, and the compacted ASS subgrade material was trimmed off using a pallet knife so that it was completely even with the top of the mould.

The compacted ASS subgrade material with the mould and the base was weighed and the value was recorded. The base of the mould was detached, and the compacted ASS material was extruded from the mould using a mechanical extruder. A sample was collected from the centre of the compacted ASS subgrade material and placed in

Chapter 4 – Methodology and Research Design

a numbered container after the weight of the empty container was recorded. The weight of the container with the compacted ASS subgrade material was recorded, and the process was repeated for all types of ASS subgrade materials. Figure 4.4 (a) – (h) shows the laboratory testing process and how proctor compaction samples were prepared. Table 4.5 Proctor compaction data for untreated subgrade materials.

Table 4.5: Proctor compaction data for untreated subgrade materials

Subgrade Type	Moisture Content	Dry density
ASS1 (25%Bentonite + 75% Kaolinite)	65.37	0.519
	34.46	1.254
	17.96	0.760
	13.81	0.735
ASS2 (75%Bentonite + 25% Kaolinite)	59.84	0.525
	49.80	1.033
	40.97	1.174
	39.39	0.826



(a)



(b)



(c)



(d)



(e)



(f)



(g)



(h)

Figure 4.4: Laboratory testing process and how proctor compaction samples were prepared

- (a) Empty mould used for the test (b) Weighed ASS ready for mixing with water (c) Process of compacting soil in layers (d) Trimming off the sample to make even with the top of the mould (e) Weighing compacted soil in mould plus base (f) Extruding compacted soil using hydraulic jack (g) Splitting compacted soil sample (h) Taking specimen from the middle of sample for oven-drying.

4.4 MIX DESIGN

This section describes the process of selecting and identifying suitable ingredients to determine the mix proportion of additives and binders for use in expansive subgrade stabilisation to obtain high strength and maximise the performance of subgrade materials used in road construction.

4.4.1 Preliminary Mix Design and Mix Optimisation

To establish mix designs for use in this research, the engineering properties of ASS materials were first of all investigated. California Bearing Ratio (CBR) test was conducted for untreated ASS materials to establish their bearing capacity and shrink-swell potentials on their own without any treatment. The results achieved showed a very low CBR and high swell potentials which are not suitable for use as subgrade materials in road pavement construction (IAN73/06). After establishing the swell and bearing capacity of untreated ASS materials, it was necessary to improve their engineering properties by adding traditional binders (cement and lime) at varying proportions to establish a control mix. To achieve the control mix, a benchmark subgrade CBR value of 80% capable of carrying heavy traffic load of 5443kg was adopted as the worst-case scenario which complies with the CBR method recommended by the California State of Highways (The Constructor Building Ideas (TCBI), 2021).

According to Southern Testing, (2021), a high-quality subgrade normally has a CBR value between 80-100% maximum. The range of cement and lime proportions used to formulate the control mix was recommended by Design Manual for Roads and Bridges (DMRB) HA 74/07. This range of cement and lime proportions was increased gradually until a CBR value of 80% was achieved. After a series of preliminary investigations using varying additive proportions to achieve a CBR value of 80%, a binder proportion of 8% lime + 20% cement achieved a CBR of 80% after 7 days of curing at normal room temperature of $20 \pm 2^{\circ}\text{C}$. Using such a high stabiliser dosage of cement and lime in subgrade stabilisation is unsustainable and expensive due to the cost of cement and lime and their associated environmental effects during production. This called for the reengineering of more sustainable and cost-effective subgrade materials by partially replacing cement and lime using sustainable waste materials.

After establishing the control mix, waste materials and industrial by-products (GGBS, BDW, Recycled Plastic and Recycled Glass) were investigated to establish their potential for use as a partial replacement for cement and lime. The aim was to achieve high CBR value and low swell potential by partially replacing cement and lime with waste materials normally dump in landfills. After trying several proportions of each waste material on their own in the mix, it was observed that the mix design composed of a high amount of 23.5% GGBS achieved a very high bearing capacity (CBR) and low swell compared with the other sustainable binders. Due to this observation, another laboratory-engineered mix design was formulated by adding 11.75%GGBS which is half of the 23.5%GGBS to the other sustainable mix design which was without GGBS content to enhance and improve the engineering properties of ASS materials.

Through this discovery, an optimised mix design was achieved with a reduction in cement and lime proportions from 8%lime + 20%cement (control mix) to 2%lime + 2.5%cement, while achieving a CBR value of 80% and a drastic reduction in swell (0.01%). To ensure the results achieved in this research are correct, accurate and reliable for use in road construction, two or three samples were made for each mix design per test and their average CBR value was recorded and used in the analysis. Samples were prepared for the best-performing mix to conduct wetting-drying test to determine the durability of the subgrade after 28 days of curing. The best-performing mix samples were further cured for 90 days to see the impact of long-term curing on sustainably treated subgrade materials using waste. Furthermore, cement was eliminated in the best-performing mix and GGBS increased to 26% and cured for 90 days to see the effect of the absence of cement and long and long-term curing on sustainably treated subgrade materials. A total of 318 samples were prepared and tested in this study. Table 4.6 shows the optimisation process from the control mix formulation until the optimised mix design was achieved.

Chapter 4 – Methodology and Research Design

Table 4.6: Preliminary Mix design and Mix Optimisation used in this study

ASS Subgrade types	Sustainable mix design						Curing days	CBR (%)	Soaked CBR (%)
	Mix proportion in (%) by weight								
	Lime	Cement	GGBS	Plastic	Glass	BDW			
ASS1	x	x	x	x	x	x	x	8	x
ASS2	x	x	x	x	x	x	x	9	x
ASS1	2	5	x	x	x	x	7	22	x
ASS2	2	5	x	x	x	x	7	14	x
ASS1	4	10	x	x	x	x	7	28	x
ASS2	4	10	x	x	x	x	7	20	x
ASS1	6	15	x	x	x	x	7	19	x
ASS2	6	15	x	x	x	x	7	21	x
ASS1	8	20	x	x	x	x	7	80	x
ASS2	8	20	x	x	x	x	28	80	x
ASS1	2	2.5	23.5	x	x	x	7	70	79
ASS2	2	2.5	23.5	x	x	x	7	73	46
ASS1	2	2.5	23.5	x	x	x	28	92	97
ASS2	2	2.5	23.5	x	x	x	28	68	65
ASS1	2	2.5	x	23.5	x	x	7	13	12
ASS2	2	2.5	x	23.5	x	x	7	12	6
ASS1	2	2.5	x	23.5	x	x	28	13	8
ASS2	2	2.5	x	23.5	x	x	28	8	3
ASS1	2	2.5	x	x	23.5	x	7	14	17
ASS2	2	2.5	x	x	23.5	x	7	11	3
ASS1	2	2.5	x	x	23.5	x	28	16	11
ASS2	2	2.5	x	x	23.5	x	28	8	4
ASS1	2	2.5	x	x	x	23.5	7	23	17
ASS2	2	2.5	x	x	x	23.5	7	14	18
ASS1	2	2.5	x	x	x	23.5	28	26	28
ASS2	2	2.5	x	x	x	23.5	28	18	17
ASS1	2	2.5	11.75	11.75	x	x	7	44	59
ASS2	2	2.5	11.75	11.75	x	x	7	21	47
ASS1	2	2.5	11.75	11.75	x	x	28	82	93
ASS2	2	2.5	11.75	11.75	x	x	28	51	50
ASS1	2	2.5	11.75	x	11.75	x	7	51	59

ASS Subgrade types	Sustainable mix design						Curing days	CBR (%)	Soaked CBR (%)
	Mix proportion in (%) by weight								
	Lime	Cement	GGBS	Plastic	Glass	BDW			
ASS2	2	2.5	11.75	x	11.75	x	7	21	31
ASS1	2	2.5	11.75	x	11.75	x	28	80	72
ASS2	2	2.5	11.75	x	11.75	x	28	46	46
ASS1	2	2.5	11.75	x	x	11.75	7	61	61
ASS2	2	2.5	11.75	x	x	11.75	7	27	16
ASS1	2	2.5	11.75	x	x	11.75	28	109	67
ASS2	2	2.5	11.75	x	x	11.75	28	44	24
ASS1	2	2.5	11.75	x	x	11.75	90	180	x
ASS2	2	2.5	11.75	x	x	11.75	90	120	x
ASS1	2	2.5	23.5	x	x	x	90	200	x
ASS2	2	2.5	23.5	x	x	x	90	96	x
ASS1	2	x	26	x	x	x	90	220	x
ASS2	2	x	26	x	x	x	90	98	x

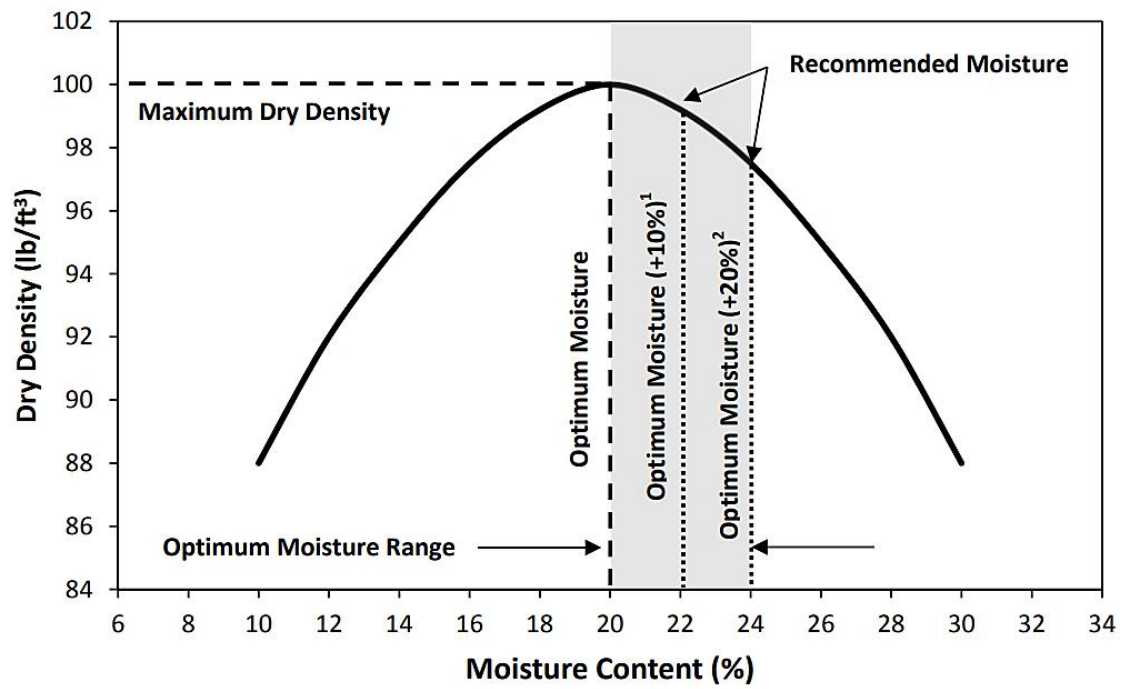
Where: ASS = Artificially Synthesised Subgrade, GGBS = Ground Granulated Blast-furnace Slag, BDW = Brick Dust Waste, ASS1 (25%Bentonite + 75% Kaolinite), ASS2 (75%Bentonite + 25% Kaolinite)

4.5 CBR TEST SPECIMEN PREPARATION

CBR test samples were prepared for all two types of ASS materials (treated and untreated), after determining the total sample mass of (4kg) required to achieve a fully compacted CBR mould using trial mixes. The binder percentages were calculated based on the total sample mass and dry mixed by hand until homogeneity was achieved. A measured amount of water was gradually added based on the OMC achieved during the proctor compaction test. Continuous hand mixing was carried out until a uniform mixture was formed and the mixture looks and feels dry at OMC during the preparation of treated ASS materials due to the addition of binders (cement, lime, BDW, GGBS, plastic, glass) which can sometimes imbibe a lot of water. A recommended amount of water within the range of 10-20% above the OMC of untreated ASS materials was added to the original moisture content (OMC) achieved during the proctor compaction test in accordance with BS EN ISO 17892-1-2014, BS

EN 13286-47:2012 and section 3/9 of Virginia Department of Transport (VDOT) document.

A CBR mould (152mm diameter X 178mm high) with a collar was weighed on a scale without the collar and the weight was recorded. The collar was later attached to the mould and the uniformly mixed ASS material (4kg) was divided into three equal parts and placed in layers in the mould during compaction. Each part was placed in the CBR mould and with the help of a mechanical compactor fitted with a 2.5kg rammer, 62 blows were applied at different areas of the surface of each layer to ensure even distribution of force. After the last layer was compacted, the mould containing the compacted sample was detached from the mechanical compactor. The collar was carefully removed, and the compacted ASS material was trimmed off using a pallet knife so that it was completely even with the top of the mould. The compacted ASS material with the mould and the base was weighed and the value was recorded. At this stage, untreated ASS materials were tested for soaked and un-soaked CBR without curing. Also, treated ASS samples were wrapped in an airtight plastic bag while in the CBR mould ready for curing at room temperature of $20\pm 2^{\circ}\text{C}$ for 7 and 28 days respectively. Figure 4.5 shows the recommended OMC range in the Virginia Department of Transport (VDOT) document. Figure 4.6 and Figure 4.7 shows the test sample preparation process for untreated soaked and un-soaked ASS materials and Figure 4.8 and Figure 4.9 shows the test sample preparation process for treated soaked and un-soaked ASS materials.



¹Acceptable Range = Up to 20% above Optimum Moisture
²Recommended Range = 10% to 20% above Optimum Moisture

Figure 4.5: Moisture content control chart (VDOT) (2016)

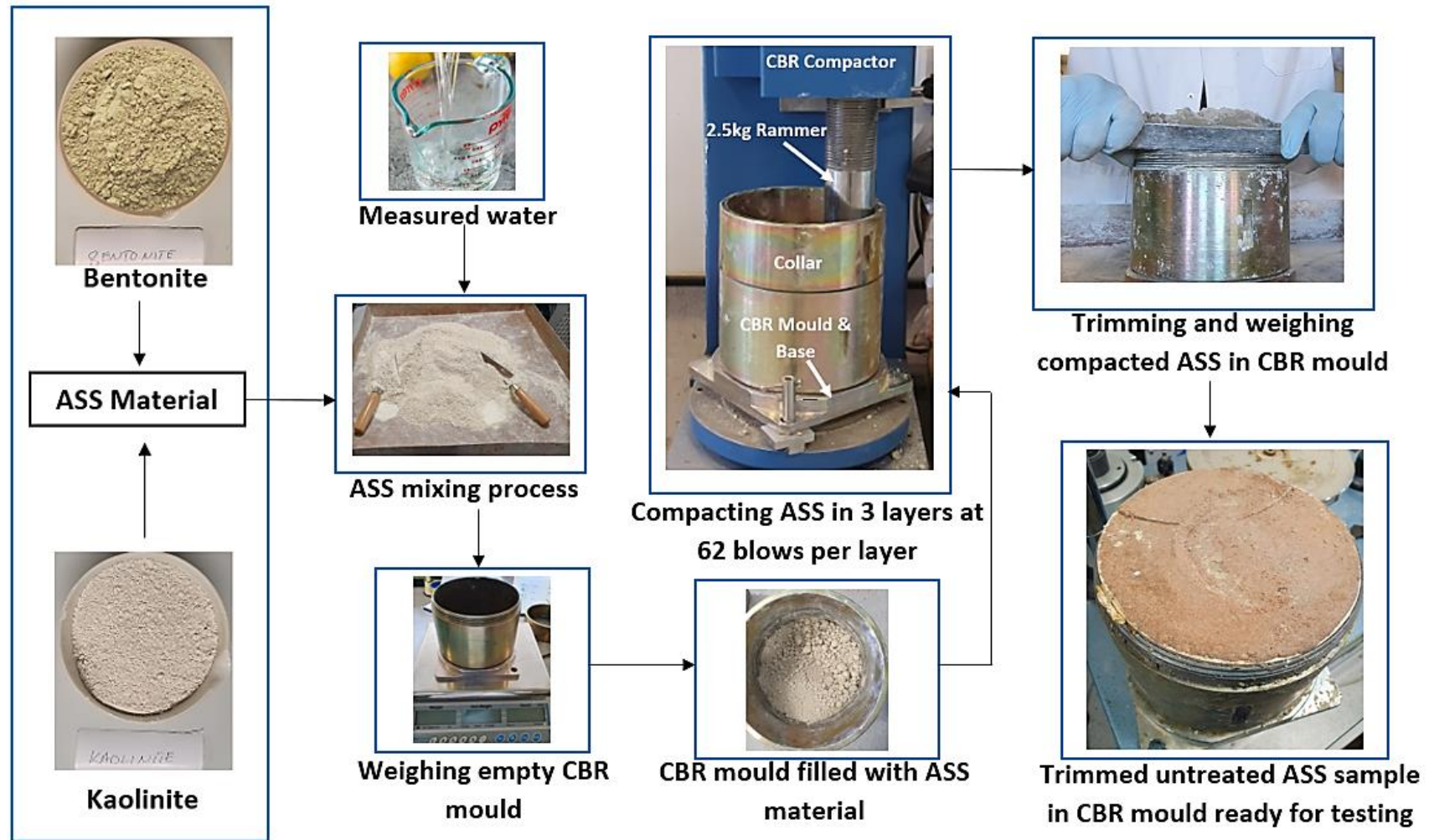


Figure 4.6: Untreated un-soaked ASS CBR sample preparation process

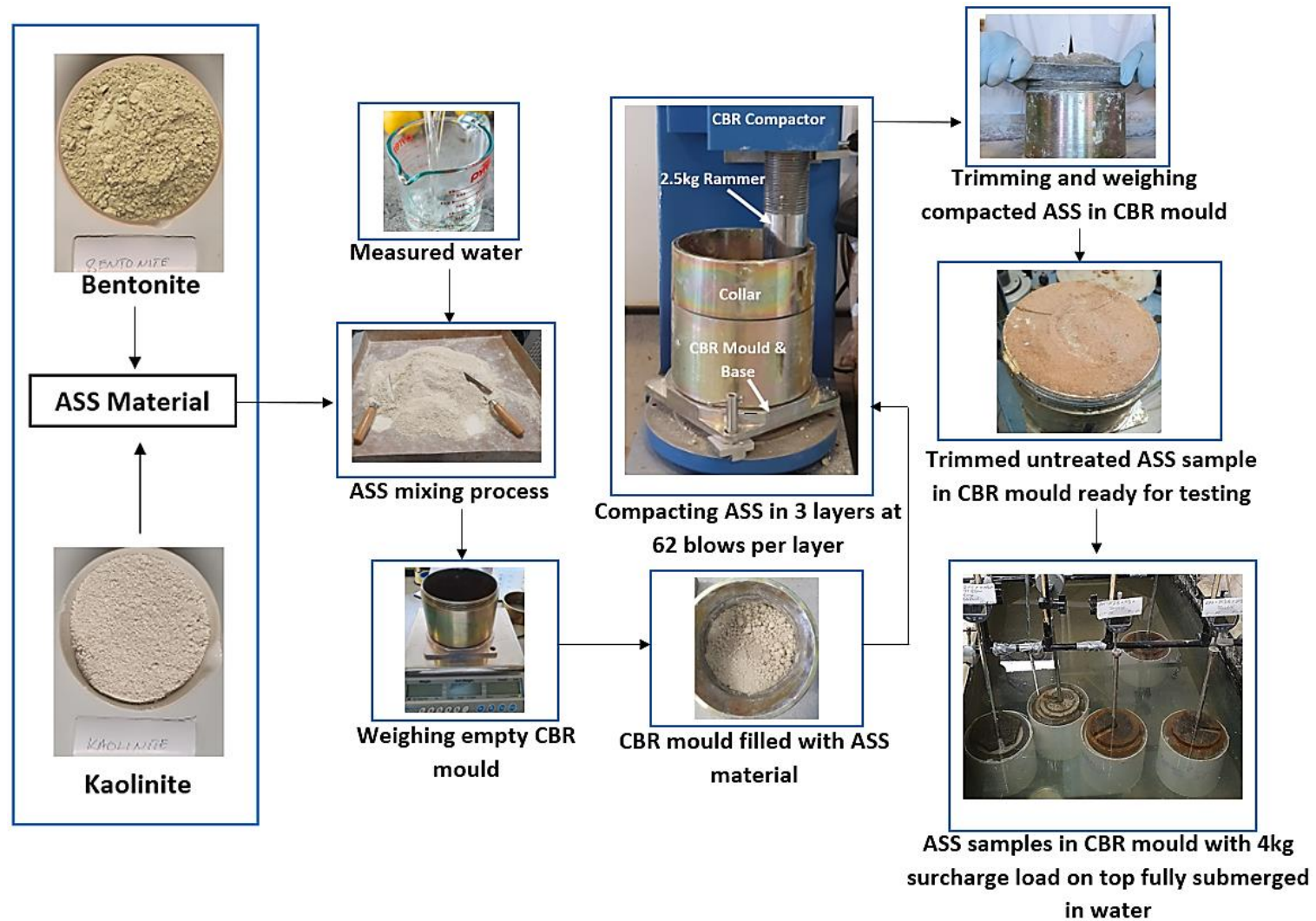


Figure 4.7: Untreated soaked ASS CBR sample preparation process

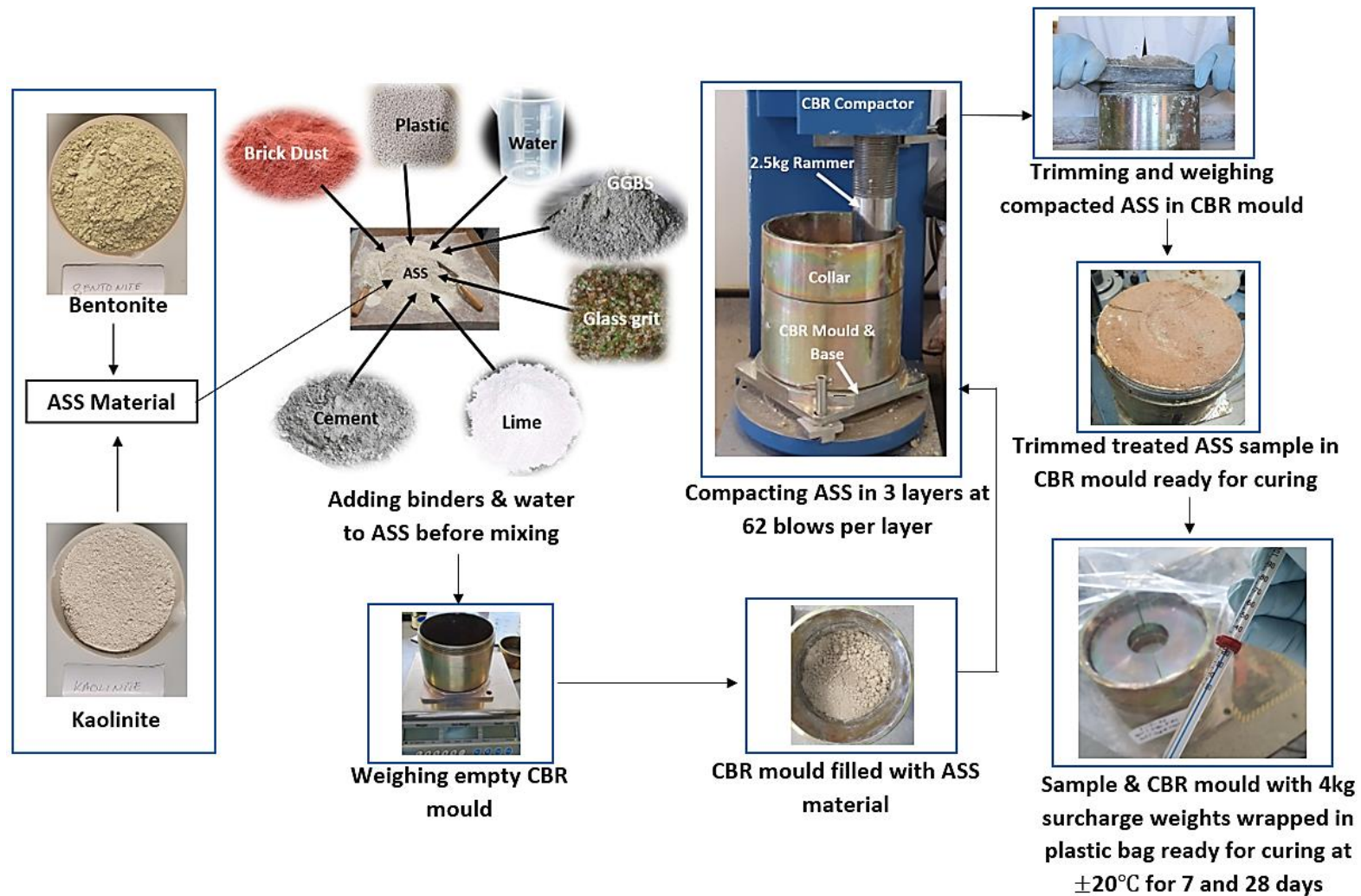


Figure 4.8: Treated un-soaked ASS CBR sample preparation process

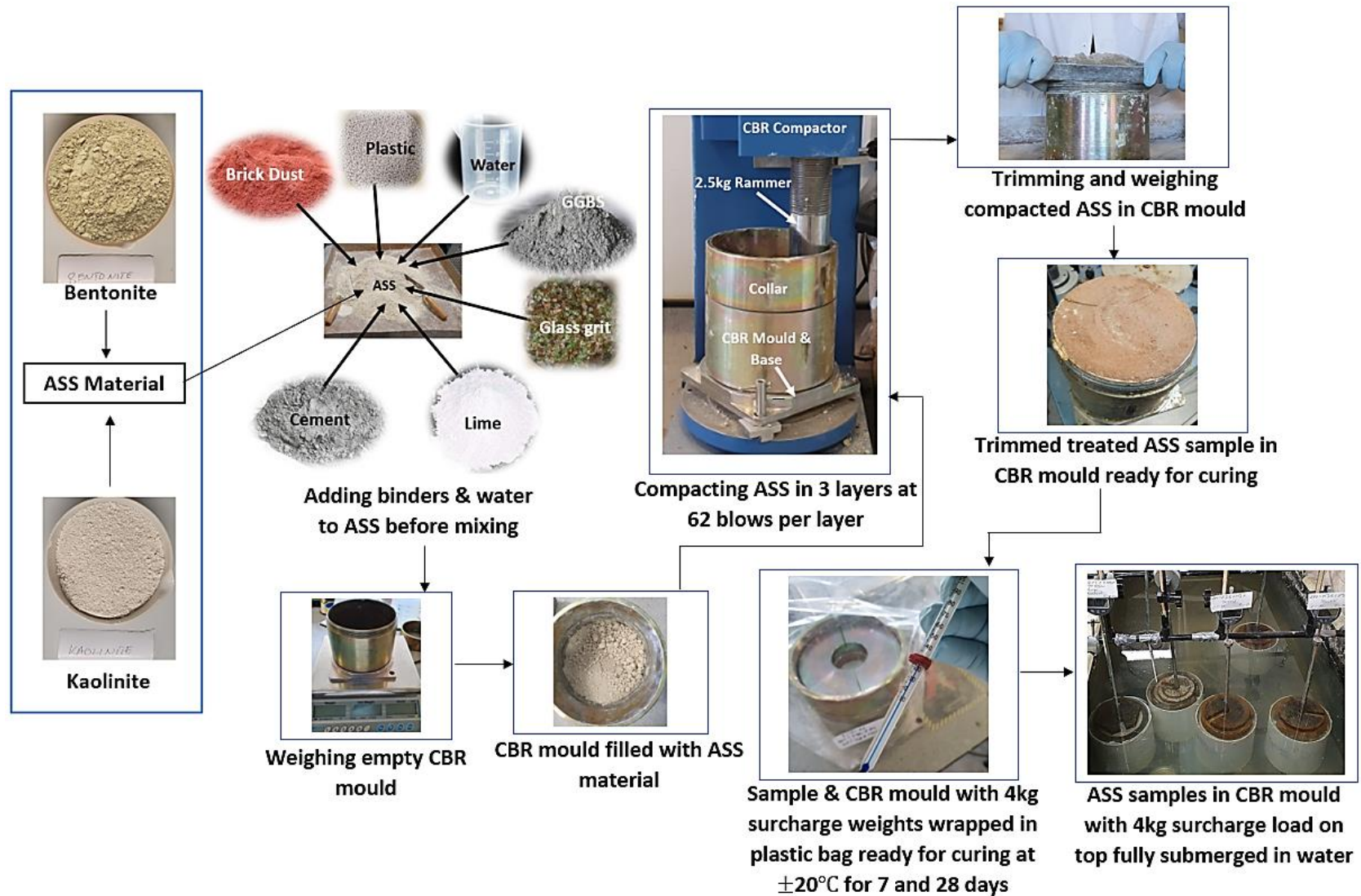


Figure 4.9: Treated soaked ASS CBR sample preparation process

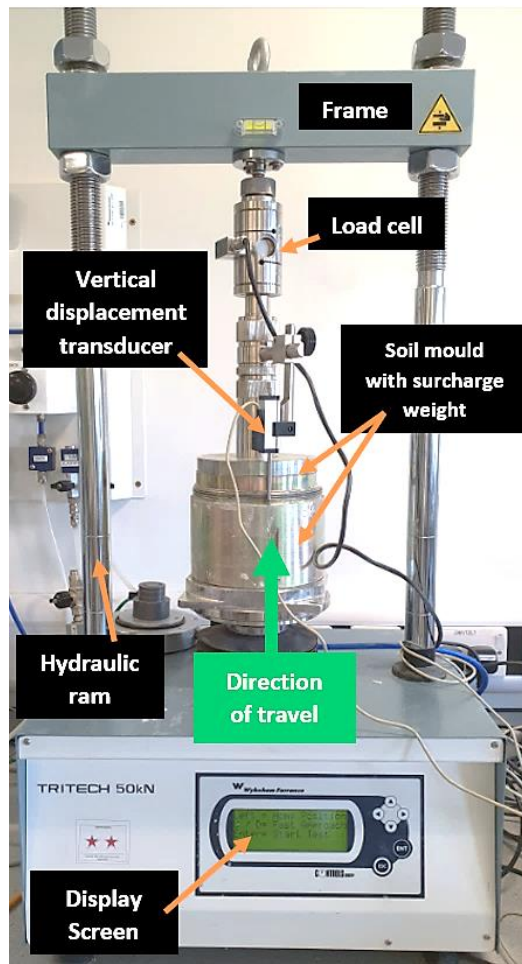
4.6 LABORATORY TESTING

4.6.1 California Bearing Ratio (CBR)

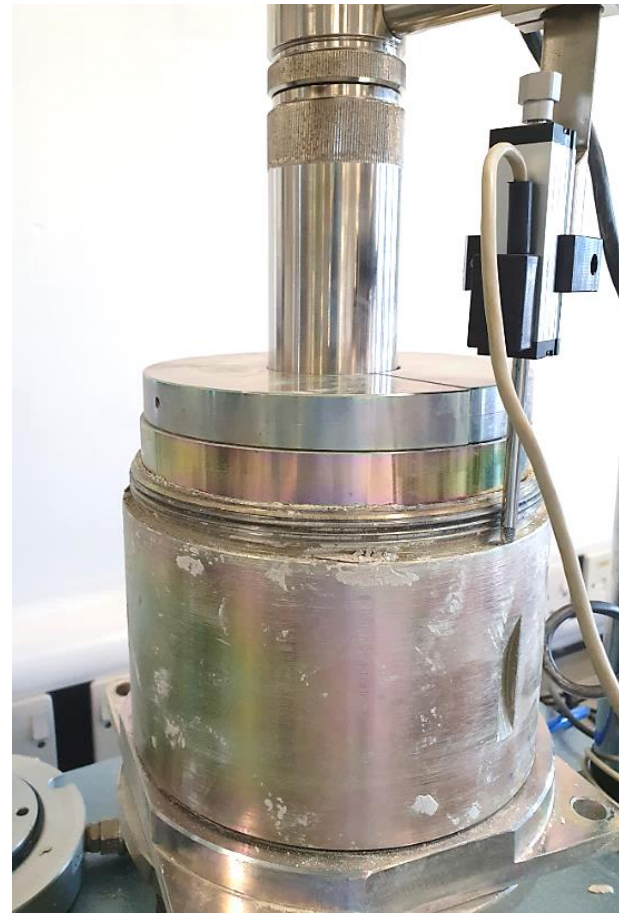
California Bearing Ratio is a penetration test conducted to evaluate the strength and bearing capacity of road subgrade material. Knowing the CBR value of subgrade material prior to any road construction influences the design and construction of road pavement. According to BS EN 13286-47:2012, ASTM D1883-16 and AASHTO T193, the classification of a road in terms of pavement thickness and how much traffic a road can carry are dependent on the CBR value of the subgrade material. A typical CBR value of 2% equates to clay, while some sands may have a CBR value of 10%. A high-quality subgrade normally has a CBR value between 80-100% maximum (Southern Testing, 2021). According to relevant road pavement design guides such as Design Manual for Roads and Bridges (DMRB) and Indian Roads Congress - IRC-37-2001, the higher the CBR value the thinner the road pavement and the lower the CBR value the thicker the road pavement. During road pavement design thicker pavements are mostly recommended to compensate for the low CBR value of weak road subgrade material to enable it to carry traffic load. According to the constructor building ideas (TCBI), 2021 document on flexible pavement design by the CBR method shows that CBR of 2% would require a road pavement thickness of 700mm to carry heavy traffic (5443kg) while of CBR of 80% would require pavement thickness of 70mm to withstand heavy traffic load (5443kg). Subgrade CBR values <2% are unacceptable for use in road construction and required engineering or modification to make them suitable for road construction (DMRB, 2021 and The Constructor Building Ideas (TCBI), 2021). This means that CBR values affect the design, overall thickness and eventually the cost of road construction and must be taken seriously during a road project.

CBR test in this research was carried out for ASS1 and ASS2 types (treated and untreated) to determine their bearing capacity in accordance with BS 13377-4:1990 and BS EN 13286-47:2021 using the DMRB CD 226 and DMRB HA 74/07 as a guide. The process used also satisfies AASHTO T193-13-2021 and ASTM D 1883-16. The test was conducted to evaluate the subgrade strength of road and pavement by determining the ratio of force per unit area required to penetrate a soil mass with a standard circular plunger. Before testing for CBR, two surcharge weights of 2.5kg each

were placed on top of the sample. The surcharge weights are equivalent to the weight of the road pavement expected above the subgrade in the final design. ASS material in the mould with surcharge weights on top was placed in the CBR test apparatus. The CBR test apparatus is made up of a plunger (50mm diameter and fits through an annulus) attached to a frame, and an electric motor drives a ram which pushes the sample in the mould upwards onto the plunger. The penetration force is measured by a load cell mounted above the plunger. The load cell is a transducer used to create an electric signal whose magnitude is directly proportional to the force being measured. A vertical displacement transducer provides a reading of the penetration. The plunger provides a surcharge weight equivalent to the weight of road pavement expected above the soil in the final design. The CBR test apparatus is connected to a computer that records the CBR data. The test was conducted for treated and untreated Artificially Synthesised Subgrade (ASS) samples. The samples were later extruded from the mould using a mechanical extruder and discarded. Figure 4.10 (a) – (c) shows CBR sample preparation and testing process used in this study.



(a)



(b)



(c)

Figure 4.10: CBR testing process (a) CBR apparatus used in this study (b) CBR Mould with surcharge weight and transducer during testing (c) Extruding CBR sample using hydraulic jack after testing is complete.

4.6.2 CBR Test for Untreated Artificially Synthesised Subgrade (ASS)

CBR test samples were prepared and tested for all types of untreated expansive ASS subgrade material in accordance with the relevant standards following the step-by-step procedure outlined elsewhere (sections 4.5 and 4.6.1) of this study. The aim of conducting CBR test on untreated expansive Artificially Synthesised Subgrade (ASS) materials was to determine their bearing capacity for use as subgrade materials without any modification, re-engineering or treatment. Untreated-un-soaked ASS Samples were tested for CBR immediately after compaction without soaking. The same samples were prepared and soaked immediately after compaction for 96 hours (4 days) at a temperature of $20\pm 2^{\circ}\text{C}$ at a level that the sample was fully immersed in water in accordance with BS EN 13286-47:2021 and their CBR values were determined. The idea of conducting soaked CBR in this research was to simulate the effect and behaviour of untreated expansive subgrade in the event of a flood and how the subgrade material would behave when the air voids are filled with water.

4.6.3 CBR Test for Treated Artificially Synthesised Subgrade (ASS)

Expansive subgrade materials are mostly treated because they do not have the capacity to support the weight of the road pavement and traffic load and would normally require some form of modification or re-engineering to enhance their capacity to carry and support the load. In this study, all ASS materials were re-engineered and modified using chemical stabilisation techniques to increase their bearing capacity and reduce swell. Cement and lime were used as additives in a controlled mix to improve the engineering properties of ASS materials whiles reducing their swelling potential. The cement and lime used were later replaced with sustainable waste materials with the aim of reducing the environmental effect associated with the use of cement and lime. Portland cement and lime have been used to improve the engineering properties of subgrade materials. During the hydration process, a cement gel matrix is produced called calcium silicate hydrate (C-S-H) and calcium-aluminate-hydrate (C-A-H)), which binds subgrade particles together and is responsible for strength gain (Neville *et al.*, 2011). According to Walker *et al.* (2000) and Gooding *et al.* 2021, a cement range of 4 and 15% was used to enhance the engineering properties of subgrade materials.

A lime soil reaction takes place when soil mixed with lime changes the moisture and density relationship of the soil. This reaction triggers a lime hydration process and with

the help of calcium, releases cementitious products (calcium-silicate-hydrate (C-S-H) and calcium-aluminate-hydrate (C-A-H)) responsible for strength increase in the subgrade (Abbey *et al.*, 2021). In this study, a measured amount of cement, lime and water were added to the ASS materials and mixed until homogeneity was formed. CBR test samples were prepared from the mix in accordance with the relevant standards following the step-by-step procedure outlined in Sections 4.5 and 4.6.1 of this report. Samples were made for all types of ASS material and tested for un-soaked CBR after 7 and 28 days of curing at room temperature of $20 \pm 2^\circ\text{C}$ and soaked CBR tests were conducted on samples soaked in water for 96 hours (4 days) after 7 and 28 days curing at room temperature of $20 \pm 2^\circ\text{C}$ in accordance with BS EN 13286-47:2021.

4.6.4 Swell Test

In this research, swell tests were conducted for all treated and untreated ASS materials in accordance with BS EN 13286-47:2021 and BS EN 13286-49:2004, respectively. The aim of conducting two swell tests was to compare the swell potentials of ASS materials after a long and short period of soaking in water (28 days swell BS EN 13286-49:2004 and 4 days swell BS EN 13286-47:2021).

4.6.4.1 Swell Test in Accordance with BS EN 13286-47:2021

During swell testing, in accordance with BS EN 13286-47:2021, CBR samples were prepared as described in section 4.5. The joints of the base and collar of the mould were sealed with silicon to avoid penetration of water through the side of the mould during soaking (immersion). For untreated CBR samples, the swell test was conducted immediately after the samples were prepared. However, treated CBR samples were cured at room temperature of $20 \pm 2^\circ\text{C}$ for 7 and 28 days, respectively, for the binders to react before conducting the swell test on them. A CBR swell filter paper was put on the top of the sample followed by a perforated swell plate and surcharge weights (4kg). The CBR swell assembly were placed inside an empty tank. A dial gauge (measuring vertical expansion) was attached to a metal bar fitted to the tank with the plunger adjusted to come in contact with the swell plate. The empty tank with the CBR swell assembly was then filled with water until the CBR assembly was completely submerged in water. The dial gauge was then zeroed to begin measuring vertical

expansion, with the help of a regulated heater inside the tank, the temperature of the water was set to a constant $20\pm 2^{\circ}\text{C}$. Dial gauge readings were recorded daily for a soaking period of 4 days and at the end of the soaking period, the recorded results were used to calculate the final swell as a percentage of the initial height of the specimen. Figure 4.11 and Figure 4.12 shows untreated and treated swell testing process.

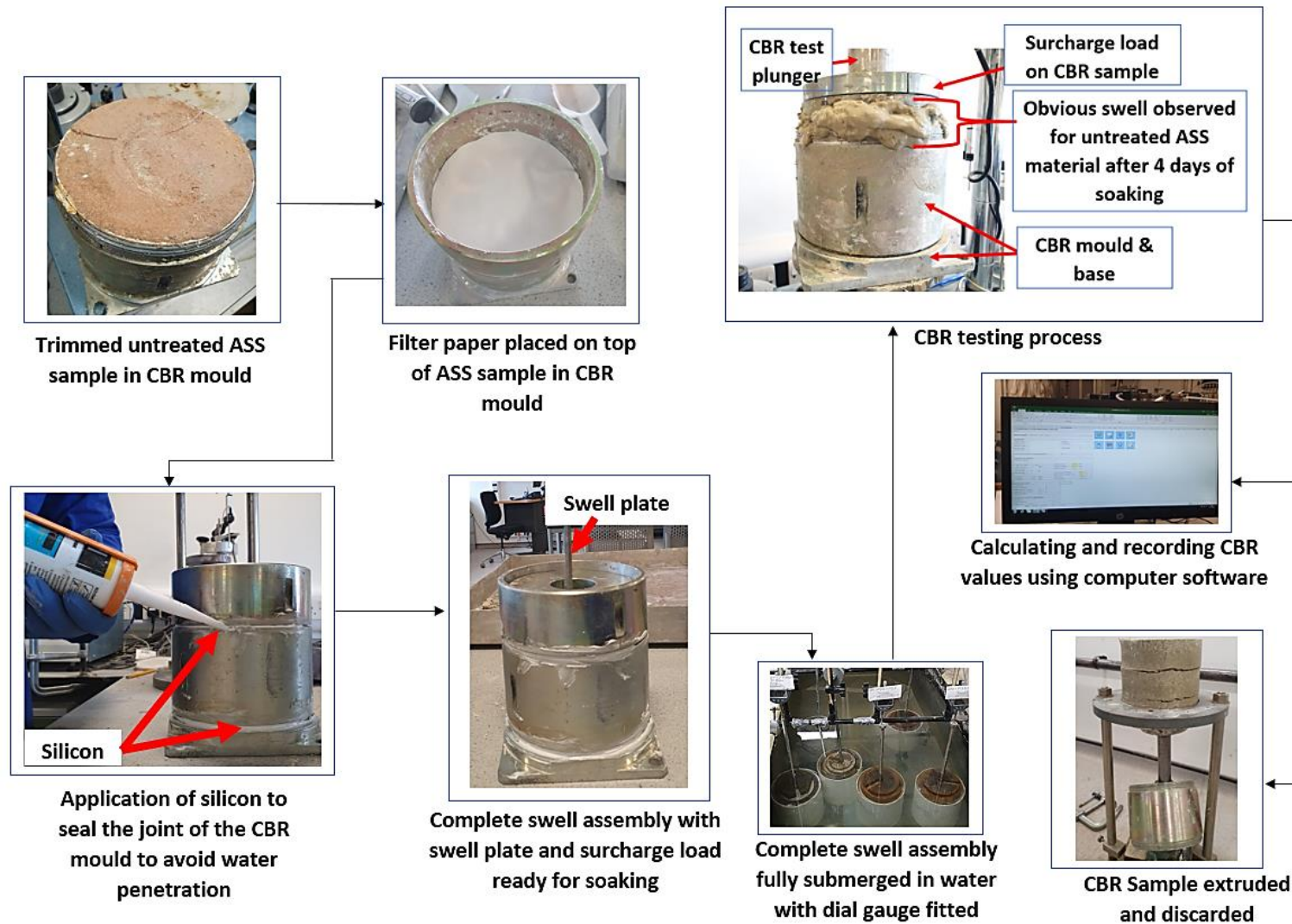


Figure 4.11: Untreated swell testing process in accordance with BS EN 13286-47:2021

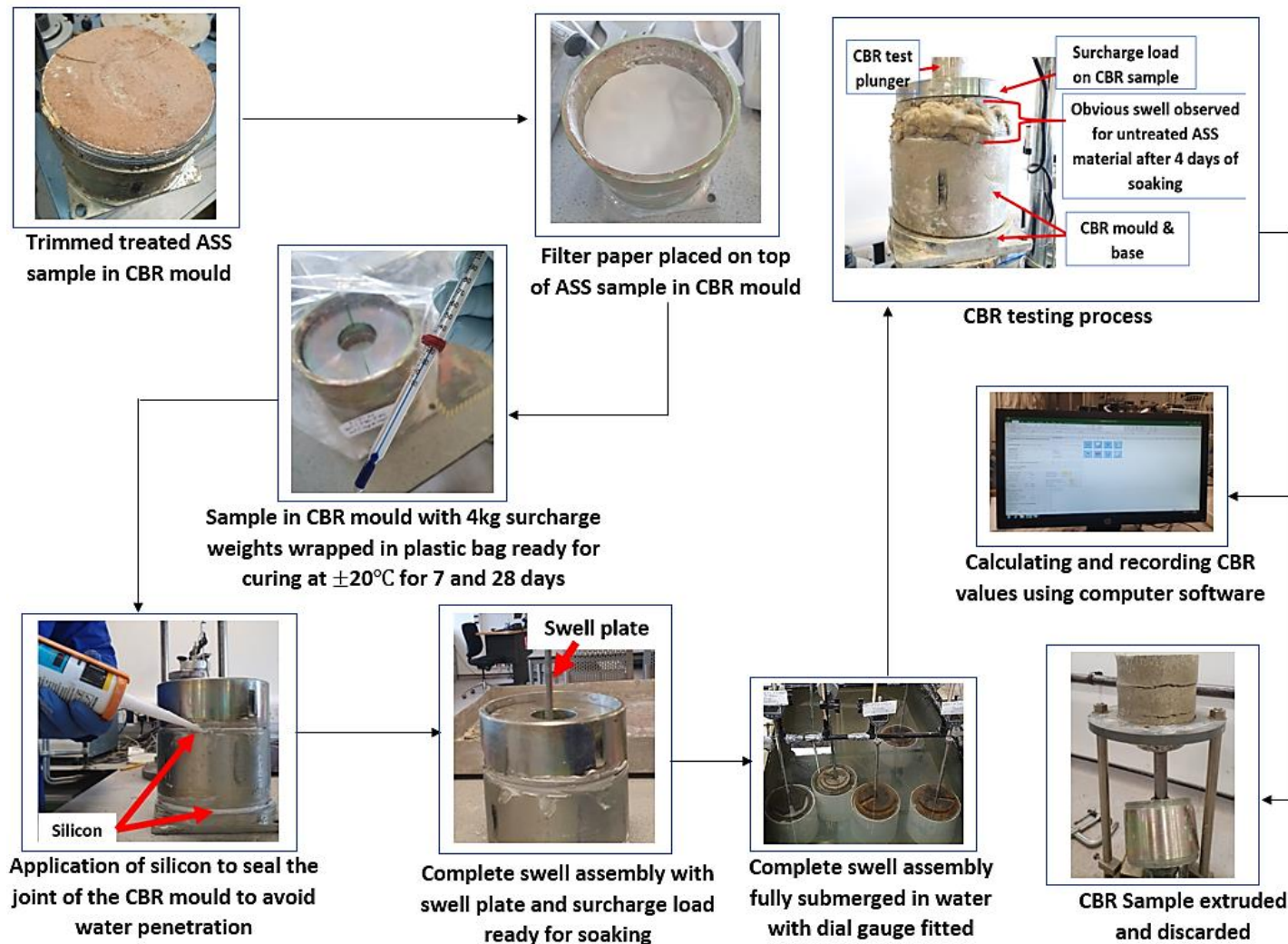


Figure 4.12: Treated swell testing process in accordance with BS EN 13286-47:2021

4.8.10.2 Swell Test in Accordance with BS EN 13286-49:2004

At this stage, swell tests were conducted on both untreated and treated ASS materials only using the control mix for comparison purposes to investigate the longer swell limit (28 days soaking) of treated and untreated ASS materials. The swell behaviour for untreated and treated expansive ASS materials was tested using the linear expansion measurement method in accordance with BS EN 13286-49:2004. At this stage, the amount of swell or expansion observed in the various ASS materials was measured using a self-contained basic swell consolidometer apparatus. The apparatus includes a stainless-steel compaction ring with a diameter of 2.42, two porous stones (top porous stone diameter 61.5mm, 6.35mm thick and bottom porous stone diameter 84mm, 6.35mm thick), a loading weight of 2.87 kPa and a dial gauge. Treated and untreated ASS materials were weighed with a total mass of 100g with or without binder inclusive and compacted into a stainless-steel compaction ring. The compacted samples are placed in the consolidometer between the two porous stones which allows water to seep through and come in contact with the soil specimen in the stainless-steel ring.

A loading weight to produce 2.87kPa was placed on top of the porous stone on the sample and a dial gauge indicator was set to the initial sample height with the tip of the plunger touching the top of the loading weight. The dial gauge reading was set to zero and the consolidometer was filled with water to begin the test. Untreated ASS subgrade materials were tested for swell immediately after compaction without curing. Treated ASS subgrade materials were wrapped in cling film and cured at room temperature of $20 \pm 2^\circ\text{C}$ for 7 and 28 days before testing for swell. The aim of wrapping treated samples in cling film was to slow the rate of water evaporation from the sample and allow the binders to chemically react in anticipation of reducing the swelling potential of the subgrade materials. Dial gauge readings of the amount of swell were recorded daily for 28 days and the data was analysed to establish the swelling potentials of both treated and untreated ASS materials using Equation 5. Figure 4.13 and Figure 4.14 show obvious swell after soaked CBR test, consolidometer apparatus, compacted swell samples in stainless-steel compaction ring, Swell set-up for treated and untreated ASS materials and samples after the swell test. Figure 4.15 shows

Chapter 4 – Methodology and Research Design

treated and untreated ASS1 (High plasticity subgrade) and ASS2 (Extremely high plasticity subgrade) samples after swell test.

Equation 5..... Linear expansion (%) = $\frac{\Delta L}{L} \times 100$

Where

L = Length of specimen (mm)

ΔL = change in length (mm)

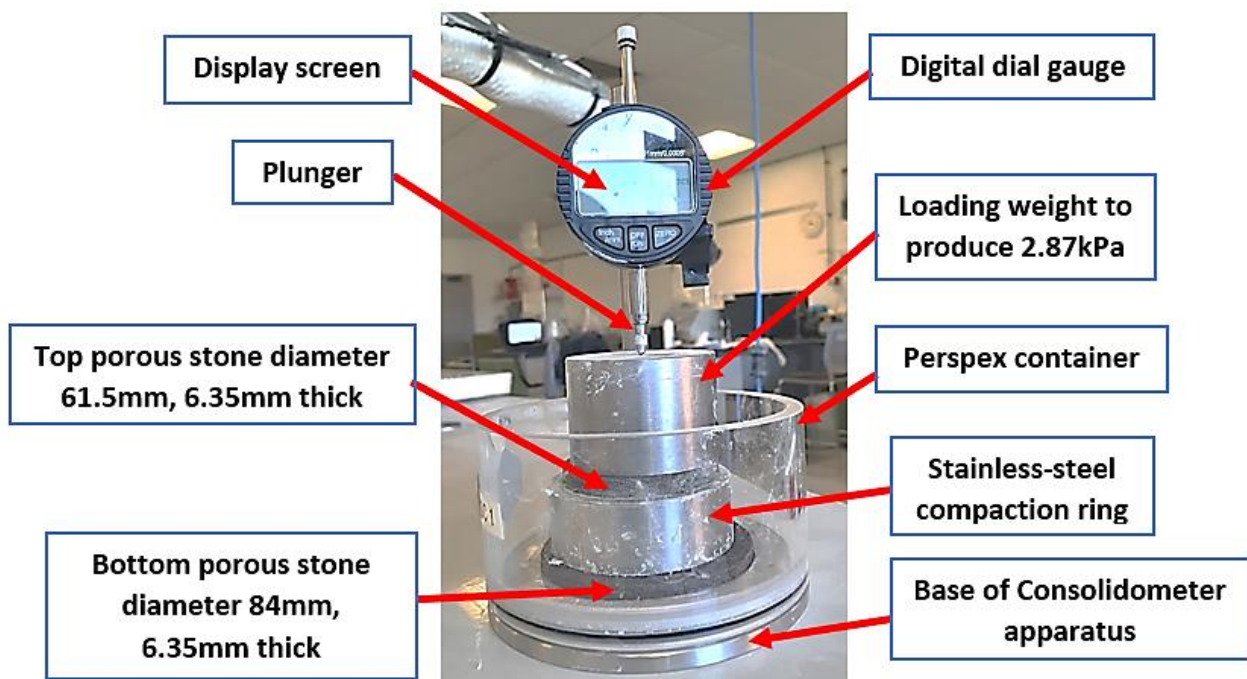


Figure 4.13: Consolidometer apparatus used in this research



Figure 4.14: Swell set-up for treated and untreated ASS materials

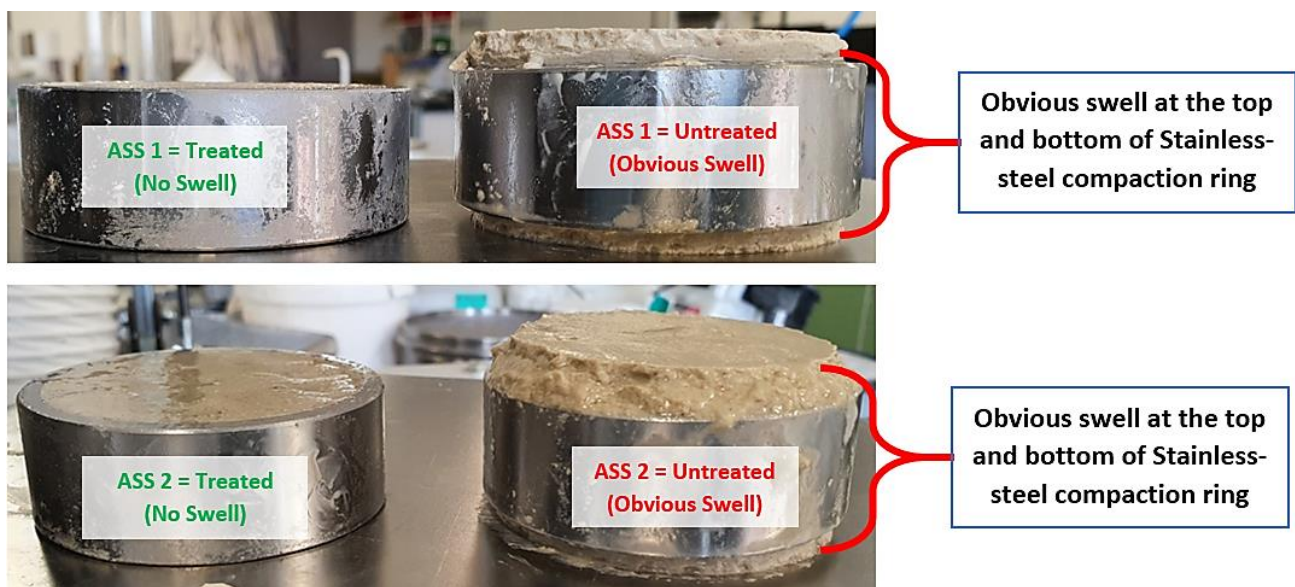


Figure 4.15: Treated and untreated ASS1 (High plasticity subgrade) and ASS2 (Extremely high plasticity subgrade) samples after swell test.

4.6.5 Durability Test – Wetting-drying Cycle

Wetting-drying cycle test was conducted in this research for the best performing mix design following the wetting and drying procedure outlined in ASTM D559/D559M – 15. Wetting-drying cycles were conducted in this research to simulate the effect of repeated wetting and drying cycles on treated road subgrade materials during the wet (flood) and dry (drought) seasons. CBR samples were prepared in compliance with BS EN 13286-47-2021, wrapped in clingfilm and cured for 28 days ready for wetting-drying cycle test. After curing the samples, the clingfilm was removed and the samples were wrapped using duct tape leaving the top and bottom of the sample. This was done to hold the sample together in one piece during the wetting-drying cycles test. All CBR samples were submerged in water for 5 hours at a room temperature of $20 \pm 2^\circ\text{C}$ to simulate flood during heavy rainfall. After 5 hours of soaking, the samples were removed and weighed, and their mass was recorded per the procedure outlined in ASTM D559/D559M – 15. After the soaking, one sample was set aside for CBR test (wetting-cycle No 1) and the CBR value was recorded.

The remaining soaked samples were then placed in an oven at a temperature of $71 \pm 3^\circ\text{C}$ for a period of 42 hours to simulate extreme dryness (drought) or high temperature in accordance with the procedure outlined in ASTM D559/D559M – 15. After 42 hours the dry samples were removed, and their mass was recorded. After drying in the oven, one sample was set aside for CBR test (drying-cycle No 1) and the CBR value was recorded. This procedure constitutes one cycle (48 hours) of wetting and drying per ASTM D559/D559M – 15. The process was repeated until all 10 cycles were achieved. The purpose of conducting wetting-drying test in this research was to ascertain the durability of expansive subgrade materials treated using sustainable waste. And to establish at which cycle of wetting or drying the CBR value of the subgrade materials becomes unsuitable for use in road construction. A normal subgrade has a CBR value between 80-100% (Southern Testing Environmental and Geotechnical, 2020). According to The Constructor Building Ideas (TCBI), (2021), subgrade with CBR value $< 2\%$ is unacceptable for use in road construction and would require modification or treatment.

4.6.6 Microstructural Properties of Treated Subgrade Materials

Microstructural investigations were conducted to understand the morphology of the cementitious materials and homogeneity and compactness of the stabilised subgrade. These properties are determined by conducting SEM analysis, EDX analysis, Radar detection, and Mises strain test among others. SEM analysis results in a study conducted by Parihar *et al.* (2020) show a high C-S-H gel development resulting in high strength after adding 6% of limited leather waste ash (LLWA) in a mix. EDX patterns show high formation of calcium silicate hydrate (C-S-H) gel after 28 days when expansive soil was stabilised with 20% GGBS (Sharma *et al.*, 2016). In this study, analyses were conducted to determine the elemental composition of stabilised ASS materials providing high-resolution imaging for identifying and evaluating the materials' surface structure, contaminants, flaws or corrosion, unknown particles, the cause of failure and interaction between materials.

After testing the CBR samples, a piece of the sample was taken and attached to tabs using glue and sputter gold coated for convenient viewing and rendering. A combination of SEM and EDX analysis provides a better understanding of the surface material and the elemental composition of a sample allowing for a more quantitative result offering chemical composition and elemental investigation to provide a comprehensive evaluation of the results. The SEM and EDX equipment used in this research are FEI Quanta 650 field emission scanning electron microscope and Oxford Instruments Aztec Energy EDX system using an X-Max 50 detector with a coverage area of 50mm² and a sputter Coater Emscope SC500 gold sputter coating unit. Figure 4.16 (a) – (c) describes how samples are mounted, Figure 4.17 shows the stub holder for the SEM chamber, Figure 4.18 shows Gold Sputter Coating Unit and Figure 4.19 shows treated ASS samples ready for SEM and EDX tests. Figure 4.1 shows the research methodological process.

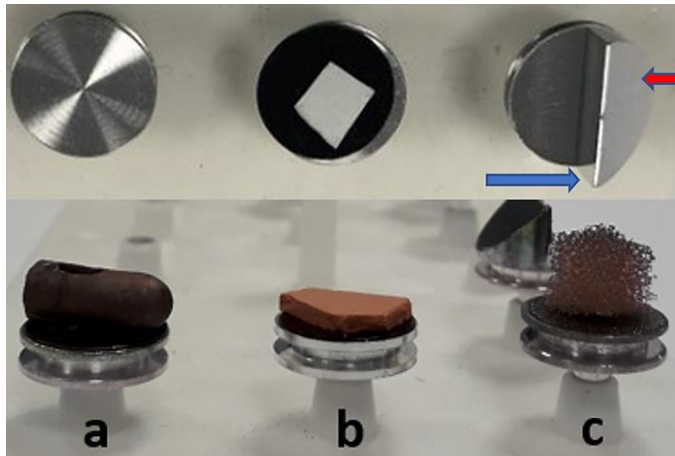


Figure 4.16: Describes how samples are mounted.

(a) Samples are mounted on standard aluminium stubs 13mm in diameter. The stub has a groove at the side to facilitate handling using forceps. **(b)** Aluminium stub with a double-sided adhesive black conductive carbon tab. A piece of filter paper has been cut to size and pressed down at the corners using forceps onto the tab. **(c)** This stub allows one to see a transverse view. The sample is mounted against the vertical face (blue arrow). The red arrow indicates a 45° angle face.

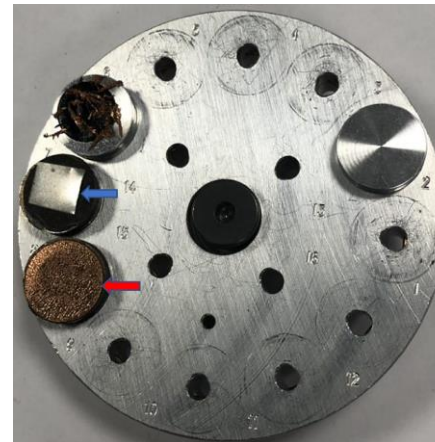


Figure 4.17: Stub holder for the SEM chamber.

Stub holder for the SEM chamber. The blue arrow indicates a piece of metal which requires no further preparation. The red arrow shows a non-conductive sample which has been sputter coated with gold to make it conductive.



Figure 4.18: Gold Sputter Coating Unit.



Figure 4.19: Treated Artificially Synthesised Subgrade (ASS) material mounted and ready for SEM and EDX analysis.

4.7 ROAD PAVEMENT ANALYSIS

4.7 ROAD PAVEMENT ANALYSIS AND ECONOMIC APPRAISAL

4.7.1 DMRB Road Pavement Design

Road pavement thickness optimisation was carried out in this research using various pavement design approaches for varying CBR values and traffic loads to establish the best-performing mix design in terms of CBR values and pavement thickness. A selected range of CBR values (low, medium and high) obtained from this study was used in the pavement thickness optimisation process. Design traffic 3msa, 8msa, 60msa, 100msa and CBR value of 3% for mix-design ASS2 +2% lime +2.5% cement + 23.5% glass, soaked after 7 days of curing, CBR value of 8% for ASS1 +2% lime + 2.5% cement + 23.5% plastic soaked after 28 days of curing and CBR value of 109% for ASS1 + 2% lime + 2.5% cement + 11.75% GGBS + 11.75% BDW after 28 days of curing were used in the optimisation process. The Design Manual for Roads and Bridges (DMRB) CD 226, HD 26/06, IAN 73/06 and the CBR method recommended by the California State of Highways (The Constructor Building Ideas (TCBI), 2021) were used as a guide in this study. Using different pavement design approaches, these guidelines were used to establish the effects of varying CBR values on road pavement thickness. During the process, the most viable mix design was established based on the best performing pavement in terms of strength, durability and performance of the road pavement structure without compromising relevant standards. CBR values and the mix design used include stiffness modulus above 30MPa in accordance with IAN73/06.

A flexible composite pavement construction with performance design Class 3 was adopted due to its durability and cost-effectiveness compared to a fully flexible pavement. Heavy-duty road pavements are usually built using flexible composite pavement options because it provides the same quality as fully flexible pavement. Composite pavement structures have a Cement Bound Granular Materials (CBGM) base with an asphalt overlay. This research used a three-layer flexible composite pavement structure (Figure 4.20) to determine the thickness and stiffness modulus for the various pavement layers. Based on the design, a hydraulic bound class (B) CBGM B – C8/10 (or T3) was adopted as subbase materials (See Table 4.7). A Hydraulic Bound Mixture (HBM) was adopted as base material and a Hot Rolled Asphalt (HRA) was adopted as surface material for the various layers of the road pavement in

4.7 ROAD PAVEMENT ANALYSIS

accordance with DMRB CD 226. Figure 4.21 shows Class 3 design – single foundation layer (IAN 73/06) and Figure 4.22 shows the nomograph for determining the design thickness for flexible pavement (DMRB CD 226).

4.7.2 Road Pavement Thickness and Construction Depth Optimisation

Pavement thickness optimisation was conducted according to the CBR method recommended by the California State of Highways (The Constructor Building Ideas) using CBR values achieved in this study. Road pavement thickness optimisation was carried out to cater for light traffic (3175kg), medium traffic (4082kg) and heavy traffic (5443kg) using the pavement thickness determination chart in compliance with the CBR method recommended by the California State of Highways. Road pavement construction depths and their corresponding CBR values for various traffic classifications were also investigated. The aim was to see the effect of varying CBR values and traffic loads on pavement thickness and construction depth. The pavement thickness determination chart recommended by the California State of Highways was used as a guide to determine light, medium, and heavy traffic classification for the construction depth determination (The Constructor Building Ideas (TCBI)).

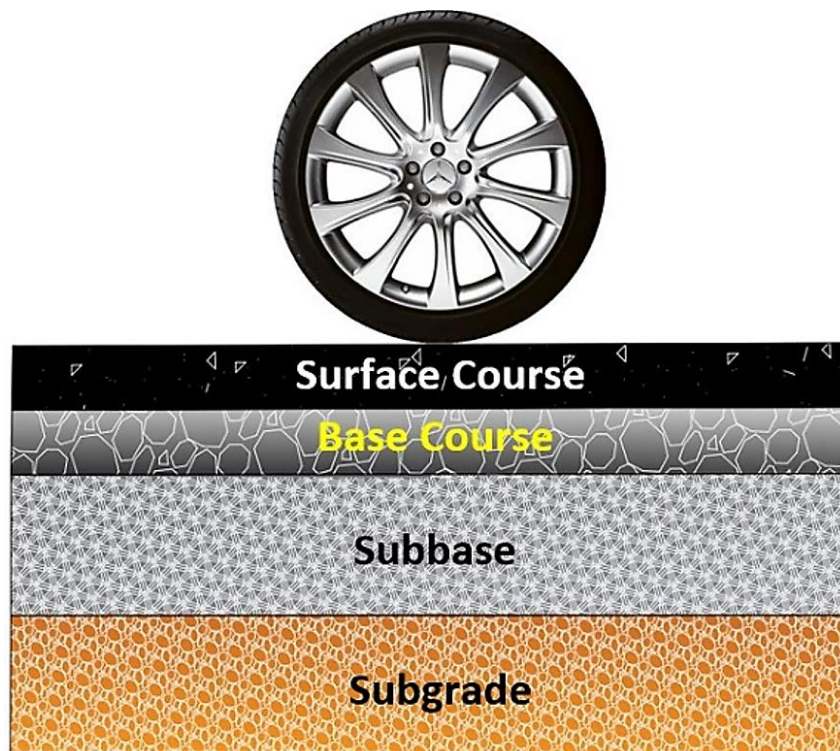


Figure 4.20: Three-layer flexible composite pavement structure

4.7 ROAD PAVEMENT ANALYSIS

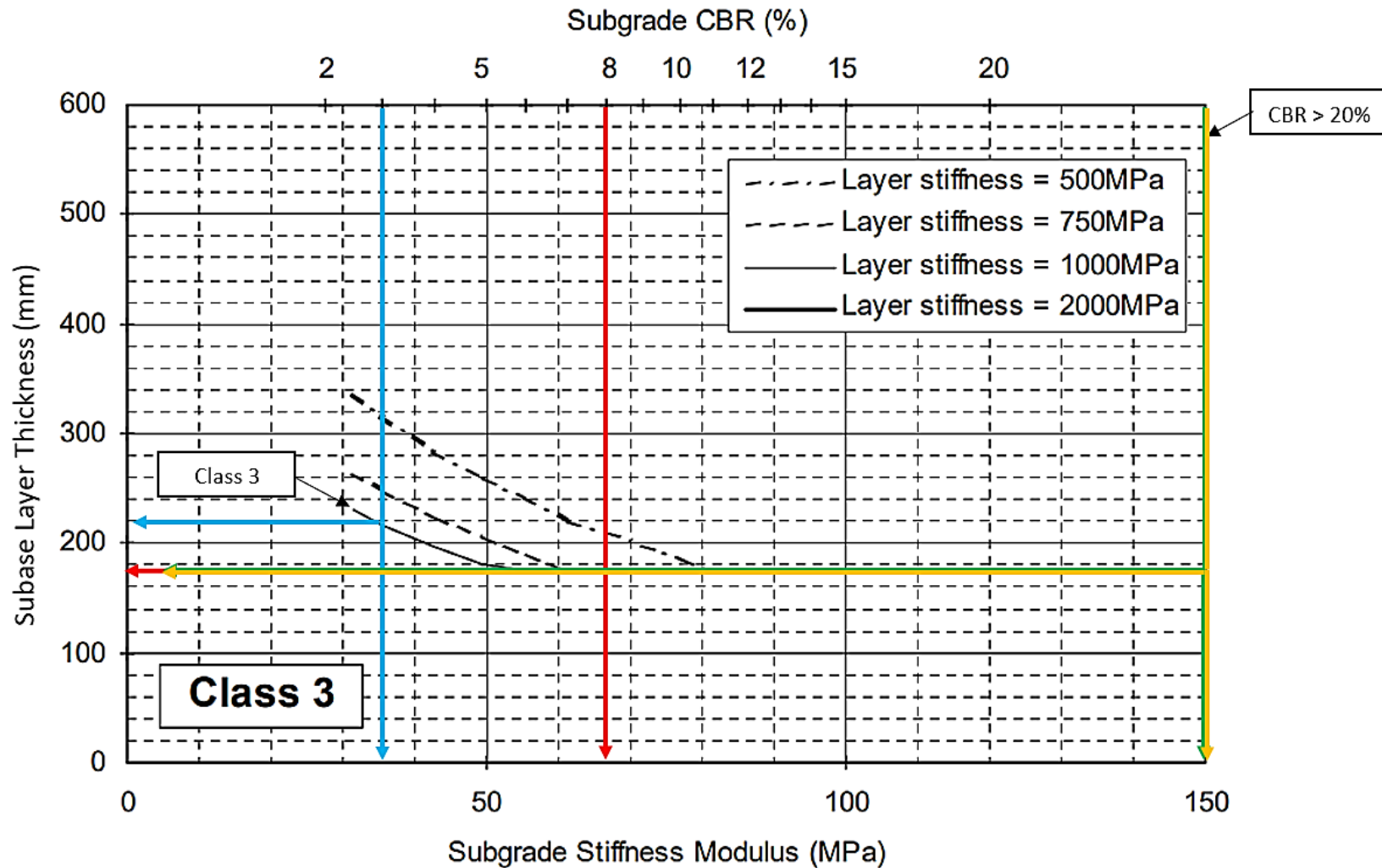


Figure 4.21: Class 3 design – single foundation layer (IAN 73/06)

4.7 ROAD PAVEMENT ANALYSIS

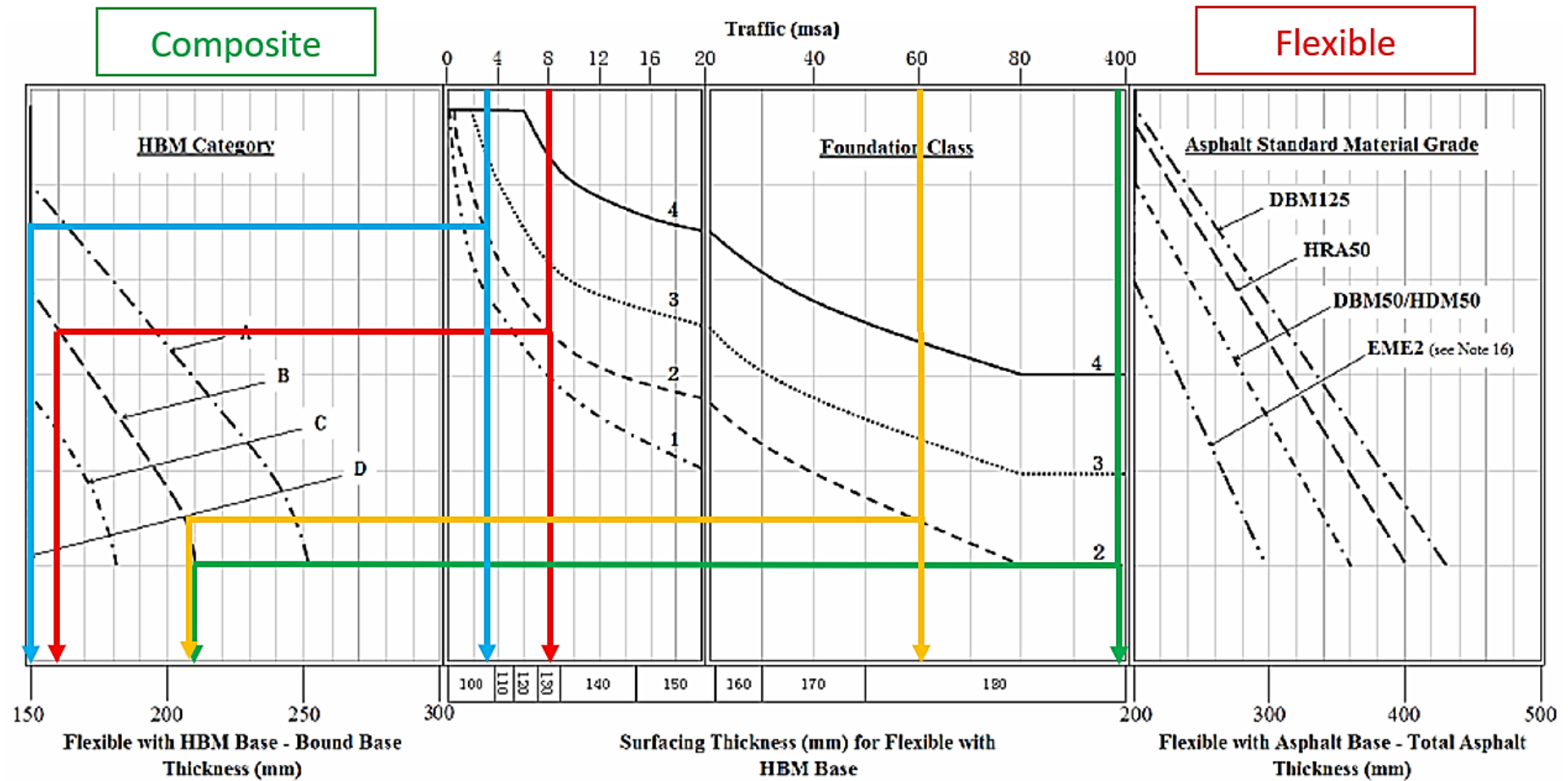


Figure 4.22: Nomograph for determining the design thickness for flexible pavement (DMRB CD 226)

4.7 ROAD PAVEMENT ANALYSIS

Table 4.7: Hydraulic Bound Base Materials (HBM) (DMRB CD 226).

HBM Category	A	B	C	D
Crushed rock coarse aggregate: (using aggregate with a coefficient of thermal expansion $<10 \times 10^{-6}$ per $^{\circ}\text{C}$)	-	CBGM B – C8/10 (or T3) SBM B1 – C9/12 (or T3) FABM1 – C9/12 (or T3)	CBGM B – C12/15 (or T4) SBM B1 – C12/16 (or T4) FABM1 – C12/16 (or T4)	CBGM B – C16/20 (or T5) SBM B1 – C15/20 (or T5) FABM1 – C15/20 (or T5)
Gravel coarse aggregate: (using aggregate with a coefficient of thermal expansion $\geq 10 \times 10^{-6}$ per $^{\circ}\text{C}$)	CBGM B – C8/10 (or T3) SBM B1 – C9/12 (or T3) FABM1 – C9/12 (or T3)	CBGM B – C12/15 (or T4) SBM B1 – C12/16 (or T4) FABM1 – C12/16 (or T4)	CBGM B – C16/20 (or T5) SBM B1 – C15/20 (or T5) FABM1 – C15/120 (or T5)	-
Pavement layers		Materials Description		
Surface course		Hot Rolled Asphalt (HRA)		
Base course		Hydraulic Bound Mixture (HBM)		
Subbase		Cement Bound Granular Mixture (CBGM)		

4.7.3 Road Pavement Defect Analysis

Road pavement defect analysis in this research was conducted using a selected mix design and CBR values achieved in this current research to evaluate their durability when used as road pavement subgrade materials. The CBR values used would determine the level of stresses and their behaviours within the pavement structure. The intensity of these stress and stains determines the type of defect and how long it would take for the defect to occur within the pavement structure. Some of these damages include fatigue, rutting and deformation in the pavement. Fatigue is the ability of an object or material to withstand concentrated stresses before it fails completely (Lowa State University, 2021). Rutting is the surface or longitudinal depression that occurs in the wheel paths of flexible pavement and deformation is the change in a road surface from the originally intended profile (Lowa State University, 2021).

In this research fatigue, rutting and deformation analyses were conducted to determine the effect of varying CBR values and how they affect the pavement structure using KENPAVE software. KENPAVE provides a solution for elastic multilayer pavement systems under a circular loaded area. The software is designed to analyse different wheel configurations under linear elastic, nonlinear elastic, and visco-elastic layer behaviours. KENPAVE software was used to analyse a three-layer pavement system at the bottom of the asphalt layer and the vertical compressive strain on the top of the subgrade at four points. The loaded areas were determined using the same radius

4.7 ROAD PAVEMENT ANALYSIS

and contact pressure (tyre inflation pressure). Materials adopted for the various layers include a bituminous surfacing material - Thin Surface Course System (TSCS), granular base and subbase material - Dense Macadam Binder and subbase Course (DBM50) respectively. The subgrade CBR values achieved for high plasticity Artificially Synthesised expansive subgrade stabilised using cement and lime were used in the analyses to see the effect of stabilised high plasticity subgrade on pavement fatigue, rutting and deformation.

A traffic design of 30msa (Light traffic) and 80msa (Heavy traffic) was adopted with a single axle dual wheel load configuration. A contact radius of 10.4cm and contact pressure of 586KPa on a circular loaded area was adopted. The pavement was assumed to behave as a linear elastic structure with Poisson's ratio of 0.35 for all the layers and 0.4 for the subgrade. The critical stress and strain are estimated in the pavement layers at radial distances of 13cm away from the centre of the wheel load. Vertical compression strain above the subgrade and tensile strain at the bottom of the bituminous layer were considered critical conditions for the pavement system. Resilient modulus M_{R1} , of the bituminous layer, was considered to be 1350MPa for a standard UK asphalt material at temperatures 20°C and 5Hz in accordance with DMRB CD226. Resilient modulus of the subgrade, subbase and base were estimated using CBR values of Artificially Synthesised Subgrade (ASS) materials achieved in this research and calculated using Equation 6, Equation 7 and Equation 8 in Box 4. 1 (IRC, 2001). Resilient modulus is a measure of the elastic behaviour of pavement under repeated loadings and helps characterise different materials used in the construction of pavement under simulated field conditions. Values for long-term elastic stiffness modulus 4700MPa of standard UK asphalt material (DBM50) used in the analytical design were adopted in accordance with DMRB HD 26/06. Equation 9, Equation 10 and Equation 11 (Box 4. 1) used by Asphalt Institute and IRC were adopted to calculate the allowable load repetition for fatigue, permanent deformation, and rutting life of the road pavement. Repeated loading is the number of loadings required to initial fatigue crack, before fatigue crack can be initiated, three basic factors are required. (i) The loading pattern must contain minimum and maximum peak values with large enough variation or fluctuation.

4.7 ROAD PAVEMENT ANALYSIS

The peak values may be in tension or compression which may change over time, but the reverse loading cycle must be sufficient to initiate a crack. (ii) peak stress must be very high, if peak stresses are low, they may not initiate crack (iii) the materials must experience a sufficiently large number of cycles of the applied stress. The higher the stress concentration the more likely a crack may initiate (Lowa State University, 2021). Fatigues are usually associated with tensile stresses, but fatigue cracks have been reported due to compressive loads, hence the greater the applied stress range, the shorter the life (Fleck *et al.*, 1985). Tensile and compressive stress values used in this research were derived from KENPAVE after the analysis. Figure 4.23 shows Pavement deflection in tensile and compressive stress in the pavement structure. Figure 4.24 shows the types of stresses within a road pavement structure. Figure 4.25 shows the types of road pavement failures and shows pavement details and responses for the actual tyre contact area for selected ASS materials.

Box 4. 1: Detailed description of equations

Equation 6 Surface Resilient Modulus ----- $M_{R1} = 17.6 \times CBR^{0.64}$

Equation 7: Subbase Resilient Modulus ----- $M_{R2} = E3 \times 0.2 \times h^{0.45}$

Equation 8: Subgrade Resilient Modulus ----- $M_{R3} = 17.6 \times CBR^{0.64}$

Where M_{R1} is the resilient modulus of base course, M_{R2} resilient modulus of subbase course, M_{R3} resilient modulus of subgrade

Damage Analysis

Equation 9: Fatigue ----- $N_{fatigue} = f_1(\epsilon_t)^{-f_2} (E_1)^{-f_3}$

Equation 10: Permanent deformation----- $N_{permanent\ deformation} = f_4 E^{-9} (\epsilon_c)^{-f_5}$

Where ϵ_t is the tensile strain at the bottom of the asphalt layer, and E_1 is the modulus of the asphalt layer, and ϵ_c is compressive strain at the top of the subgrade layer, and f_{1-5} are empirical values used by Asphalt Institute for these calculations.

Rutting Life Prediction

Equation 11: Rutting Life Prediction----- $N = 4.1656 \times 10^{-08} \times \left(\frac{1}{\epsilon_c}\right)^{4.5337}$

Where N = Number of cumulative standard axles
 ϵ_c = Compressive strain in the subgrade

4.7 ROAD PAVEMENT ANALYSIS

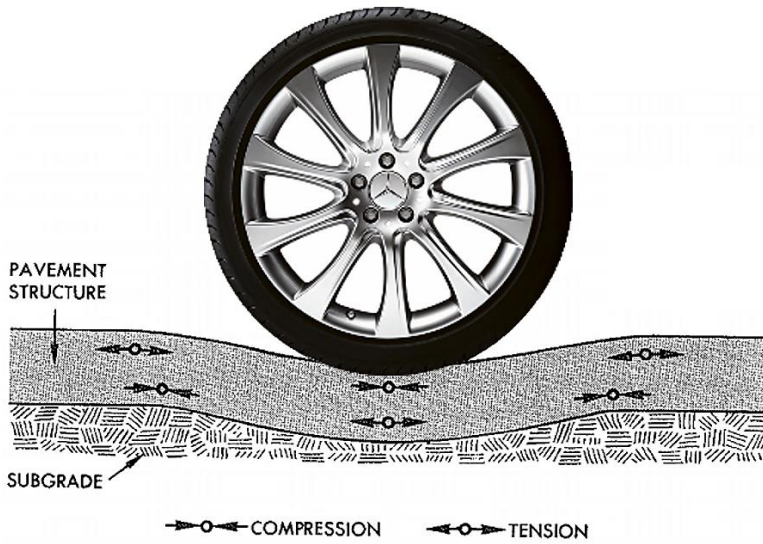


Figure 4.23: Pavement deflection in tensile and compressive stress in the pavement structure (IRC-37, 2021).

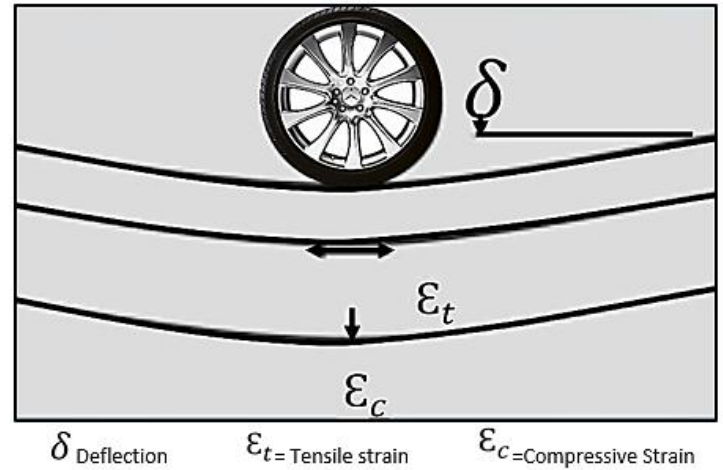


Figure 4.24: Types of stresses within a road pavement structure (IRC-37, 2021).

4.7 ROAD PAVEMENT ANALYSIS

Longitudinal Cracking



Transverse Cracking



Alligator Cracking



Potholes



Raveling



Block Cracking



Edge Cracking



Joint Reflection Cracking



Slippage Cracking



Figure 4.25: Types of road pavement failures (Ahmad *et al.*, 2018).

4.8 ECONOMIC APPRAISAL

4.8.1 Life Cycle Cost (LCC) Estimate

Economic appraisal in this research was conducted using the Life Cycle Cost Analysis (LCCA) approach to determine the cost effects and benefits of using waste materials in road pavement subgrade stabilisation in accordance with BS ISO 15686-5:2017. Comparing the cost of stabilising road subgrade materials to the removal and replacement of expansive or weak subgrade materials during road construction. LCCA involves the calculations of the true cost of an asset over its useful or design life. Life Cycle Cost Analysis serves as a tool for operators and service owners to enable them to determine the most appropriate solution for their requirements. The components of LCCA comprises initial construction costs, user cost and maintenance costs. The concept of LCCA was first introduced in the 1930s as part of federal legislation regarding flood control and later into highway construction projects (Wild *et al.*, 2001). Prices of the binders used in this research were investigated and cost analysis was carried out to determine the cost of each mix design to establish the best performing mix design for a typical design period of 35 years to compare the LCC per kilometre of road with treated (sustainable waste materials) subgrade material with a kilometre of road with subgrade removed and replaced with imported materials. Economic appraisal for optimised road pavement structure in this research can inform road contractors on the choice of binder proportions and pavement structure to adopt when they encounter expansive subgrade with similar characteristics to that used in this study.

The cost of materials was investigated using current market prices (2022) for the number of materials used to stabilise expansive subgrade material for each mix design. The cost of the binders used to stabilise a square meter area of road subgrade was calculated based on the binder percentages used in the mix design. To arrive at the total cost of stabilising a kilometre of road subgrade, plant cost was considered and estimated using (Newmarket Plant Hire (NPH)) Group document andecoinvent, 2022 to get product and materials data for the analysis. LCC analysis was based on economic principles to compare the cost of constructing road pavement using the approach of stabilising or removal and replacement of expansive road subgrade materials. LCC comparison for these road construction approaches was conducted

using a range of design traffic to determine the long-term cost and economic viability of road pavement structures designed based on the CBR values achieved for ASS materials using RealCost 2.5 software. The software was created to provide an instructional tool for pavement design decision-makers to investigate the effects of cost, service life and economic inputs on life cycle cost. According to Babashamsi *et al.* (2016), the LCCA method is utilised by several agencies due to its realistic analysis of pavement economics. The software allows pavement designers to incorporate life-cycle costs into their pavement investment decisions. The software was used to calculate the life cycle values for agency and user costs associated with construction and rehabilitation. Furthermore, according to Babashamsi *et al.* (2016), the LCCA method has been utilised by several agencies due to its realistic analysis of pavement economics.

Conducting LCCA for road pavement can help the designer put in place measures to reduce pavement life cycle costs and impact on users and identify opportunities to reduce agency and user costs throughout the pavement life cycle. This would help inform and guide decision-making for policy planning or design. In this research, the Net Present Value (NPV) indices shown in Equation 12 in Box 4. 2 were used to project the initial costs, maintenance cost rehabilitation cost and salvage value of the road. A discount rate factor was applied to calculate the time value of money. Net Present Value (NPV) is the discounted monetary value of expected net benefits that is, assigned to benefits and costs, discounting future benefits and costs. This is done using an appropriate discount rate and subtracting the sum of discount costs from the sum of discounted benefits. The discount rate was calculated using Equation 13 in Box 4. 2. The RealCost software was used to calculate all the parameters used in the Life Cycle Cost analysis. Table 4.8 shows the description of the parameters used in LCCA. Figure 4.26 shows the five sections of the RealCost Switchboard used for data input and results. Figure 4.27 shows an example of an expenditure stream diagram for a 35-year life road pavement.

Table 4.8: Description of parameters used in LCCA

Parameters	Description
Initial construction cost (ICC)	Initial construction costs are derived from bid records of projects constructed in the past and are presented in unit prices.
Maintenance and Rehabilitation cost (M&R)	Cost to keep pavement in use through service life derived from historical records of actual pavement M&R costs and activities of previously constructed projects
Salvage Value (SV)	Evaluation of the pavement structure beyond the analysis period and determine if the road pavement has a useful life at the end of the life analysis period.
Discount Rate (DR)	The rough difference between interest and inflation rates is used to indicate the real value of money over time.
Life Cycle Cost (LCC)	ICC + (M&R x DR)

Box 4. 2: Detail description of equations

Equation 12 : Initial Cons.Cost ---NPV = Initial Cons.Cost + $\sum_{k=1}^N \text{Future Cost}_K$
 $\left[\frac{1}{(1+i)^{n_k}} \right] - \text{Salvage Value} \left[\frac{1}{(1+i)^{n_e}} \right]$

Where:

N = number of future costs incurred over the analysis period

i = discount rate in the present

n_k = number of years from the initial construction to the K^{th} expenditure

n_e = analysis period in years.

Equation 13: Discount Rate -----Discount Rate = $\left[\frac{\text{interest} - \text{inflation}}{1 + \text{inflation}} \right]$

Where:

interest = Expected interest rate

inflation = Expected inflation rate.

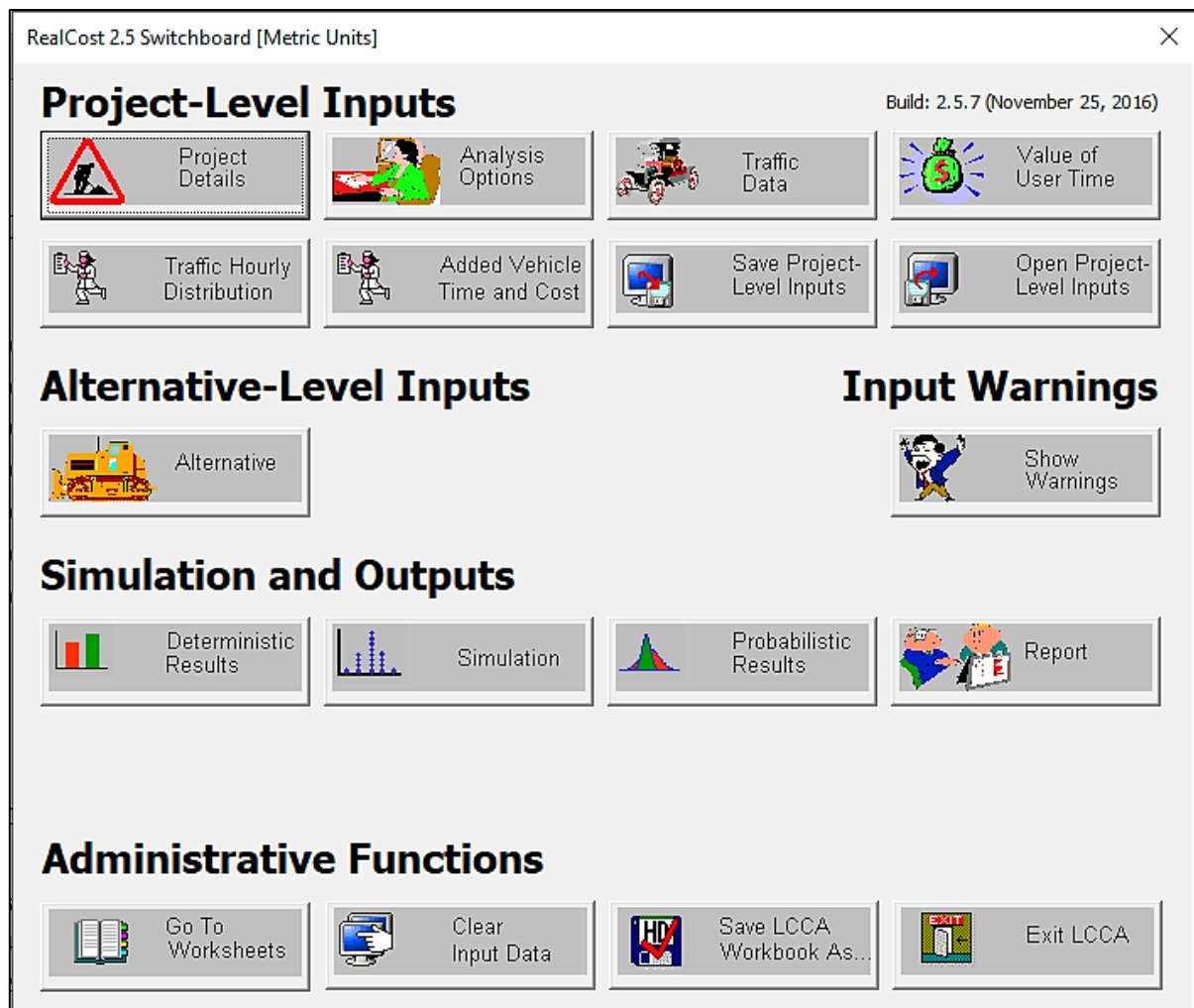


Figure 4.26: The five sections of the RealCost Switchboard

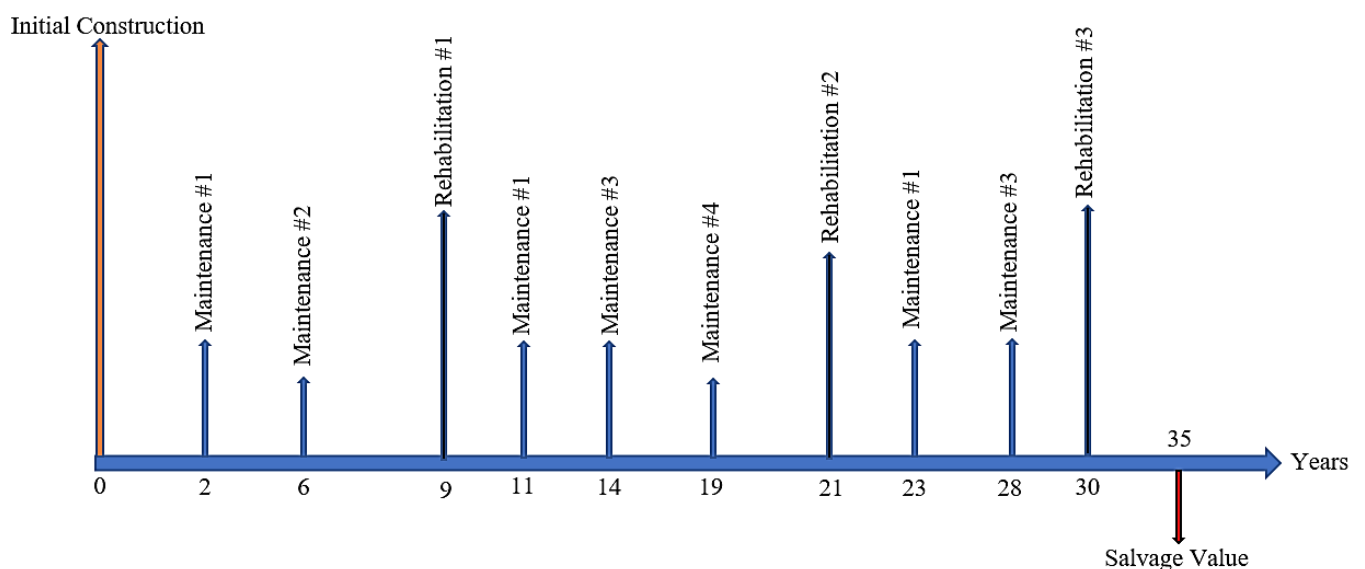


Figure 4.27: Example of expenditure stream

4.9 LIMITATIONS

The research method used in this study has lots of advantages and gives the researcher control over the experiment. However, there are some limitations to the experimental method used in the current research and these are as follows;

1. **Human and machine error:** the methodology used in this research are subject to possible human errors due to the levels of variable control. Human errors could reveal information about other variables hence invalidating the results of the research. Also, machine errors due to incorrect calibration, faulty equipment and power fluctuation could affect experimental results.
2. **Unrealistic data:** because the research method used in this study gives the researcher total control over the data, there could be a possibility of corrupted data. Data can still seem authentic even though they are corrupted or inaccurate and the experimental results of the research cannot be achieved in a real-life environment.
3. **Consume a lot of time and money:** the method used in the research is time-consuming due to the many tests that need to be carried out to ensure all areas are investigated. Also, during these tests, each variable must be isolated and investigated hence more materials would be required leading to the consumption of large financial resources.
4. **Other constraints:** apart from human errors, there could be other environmental constraints such as allergy, inability to withstand loud noise from machines, extractors and high heat from ovens. Also, the experimental method requires lots of manual handling and the researcher needs to be physically fit to carry out these tasks. These situations could create a distraction to the researcher that could eventually influence the results.
5. **Data manipulation:** the research method used in this current study gives room to the researcher to manipulate results. This is because the researcher has too much control over the process and even though manipulated results could give sensible and reasonable observations, they may not provide realistic results for future use.

4.10 CHAPTER SUMMARY

Chapter 4 presented an in-depth step-by-step methodological process used to achieve the set aim of this research. The chapter showed how the soils were sampled, the process of preliminary testing (moisture content and Atterberg limit test) of subgrade materials, how the various mix design was formulated from preliminary to optimised mix, and the process of California Bearing Ratio (CBR) test sample preparation. The chapter also describes the process of swell test, durability test (wetting-drying cycles) and microstructural analysis process. The standards used to conduct these tests and analyses were described and adhered to in this chapter to ensure the results obtained are valid and widely accepted. The Chapter also introduced and described the process of conducting road pavement thickness and construction depth optimisation and road pavement defect analysis. The chapter gives details of the selected mix design, the design traffic load adopted and the various road pavement design standards used in this research and the parameters adopted for the DMRB road pavement design and the pavement defect analysis. Furthermore, the chapter describes the software application used in this research.

Chapter 4 introduced the process and techniques of conducting economic appraisal in the research were described in this chapter 6. The chapter throws more light on the cost analysis approach used (Life Cycle Cost Analysis (LCCA) and how this approach has benefited the industry. The chapter referred to how the LCCA process has been used in other projects and the benefits it brings to a project. Furthermore, the chapter described the parameters and formulas used in the various stages of calculating the LCC. Finally, the chapter describes the cost analysis software used in this research to calculate all the parameters needed to complete a whole Life Cycle Cost Analysis (LCCA).Chapter 4 describes the process and the types of road pavement analysis, and the guidance used such as DMRB road pavement design, road pavement thickness and construction depth optimisation and road pavement defect analysis. The chapter also describes the process and how the various materials and software applications used in this research were adopted.

Chapter 5 gives a detailed description of the results obtained in this research are shown in this chapter. This includes details of the various laboratory test results for all Artificially Synthesised Subgrade (ASS) materials outlined in this chapter.

CHAPTER 5 – RESULTS AND DISCUSSION

5.1 COMPACTION AND ATTERBERG LIMITS FOR UNTREATED ASS

MATERIALS

The results obtained show a high Optimum Moisture Content (OMC) and Maximum Dry Density (MDD) for ASS1 (25% Bentonite and 75% Kaolinite) and ASS2 (75% Bentonite and 25% Kaolinite). An OMC of 34.46% was achieved for ASS1 and an OMC of 40.97 was achieved for ASS2. The maximum dry density (MDD) recorded for ASS1 was 1.25 Mg/m³ followed by 1.17 Mg/m³ for ASS2, respectively. A liquid limit (LL) of 131.26% was recorded for ASS1 followed by a Liquid limit of 294.07% for ASS2. The plastic limit of 28.74% achieved for ASS1 increased to 45.38% for ASS2. These results influenced the plasticity index of ASS materials to increase from 102.52% for ASS1 to 248.69% for ASS2. The plasticity index chart shows that ASS1 (25% Bentonite and 75% Kaolinite) falls under soils with a high plasticity index within category 'C' above the A-line making ASS1 a soil with high clay content. The plasticity index chart also shows that ASS2 (75% Bentonite and 25% Kaolinite) falls under soils with extremely high plasticity index within category 'C' above the A-line making ASS2 a soil with extremely high clay content.

The increase and decrease in proctor compaction and Atterberg limit test results observed in the various ASS materials are a result of high/low bentonite content in the mixture. Bentonite clays are very expansive with high plasticity and imbibe a lot of water which can result in high OMC and very low MDD. After the preliminary test, the results show high plasticity for ASS1 (25% Bentonite and 75% Kaolinite) and extremely high plasticity for ASS 3 (75% Bentonite and 25% Kaolinite) respectively. the highest MDD was recorded for ASS1 with high kaolinite content. This increase in dry density could be a result of high kaolinite in the mixture. Accorded to Arefnia et al. (2014), pure kaolinite observed the highest dry density due to the specific gravity of kaolinite clay. The gradual increase in plasticity index as bentonite proportion increases can be attributed to the high clay content or the high plasticity nature of bentonite. According to Abbey et al. (2020), the gradual increase in the percentage of bentonite clay in a mixture increases the plasticity index of the soil mix. Bentonites, however, are highly water absorbent and have high shrinkage and swell characteristics (Asad et al., 2013). The results obtained by Srikanth et al. (2016) in a

Chapter 5 – Results and Discussion

study conducted on the characteristics of sand-bentonite mixtures state that the plasticity characteristics of sand-bentonite mixture depend upon the clay content and the type of clay mineral present in the bentonite. Figure 5.1 shows proctor compaction results, Figure 5.2 shows Atterberg limit test results against plasticity index and Figure 5.3 shows plasticity index chart.

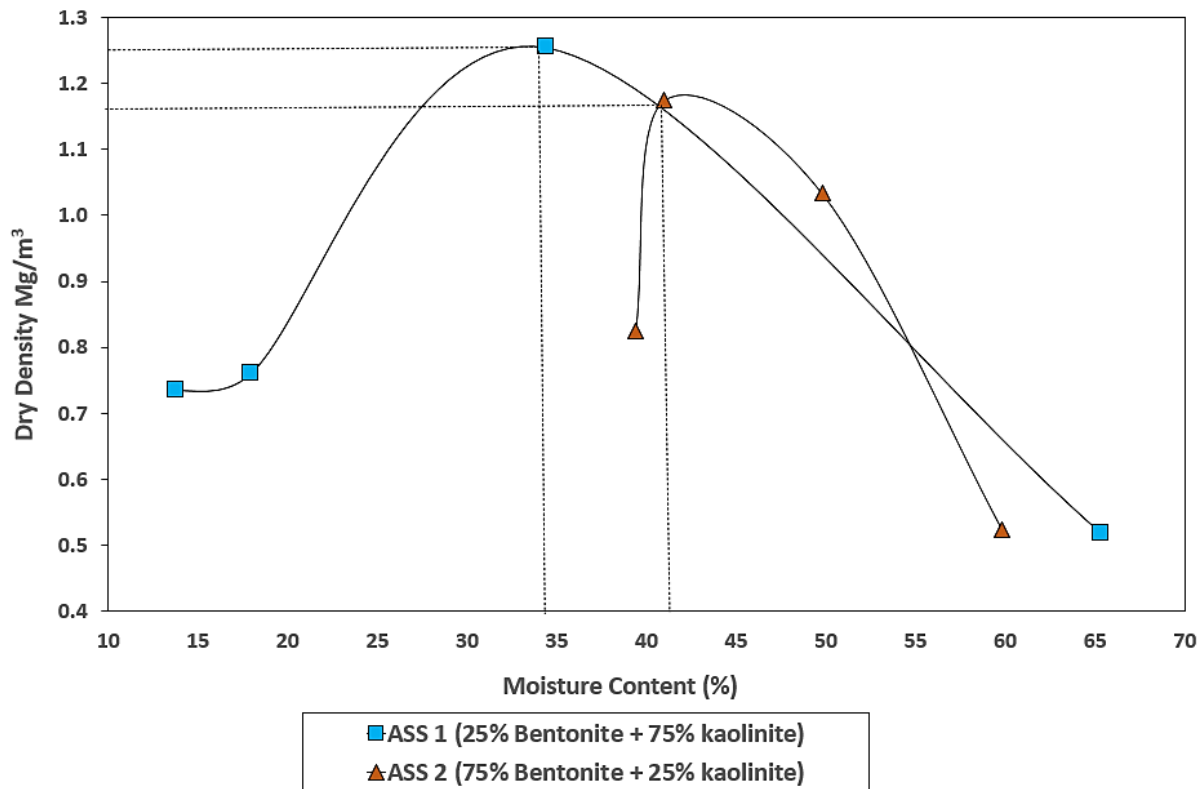


Figure 5.1: Proctor compaction test results

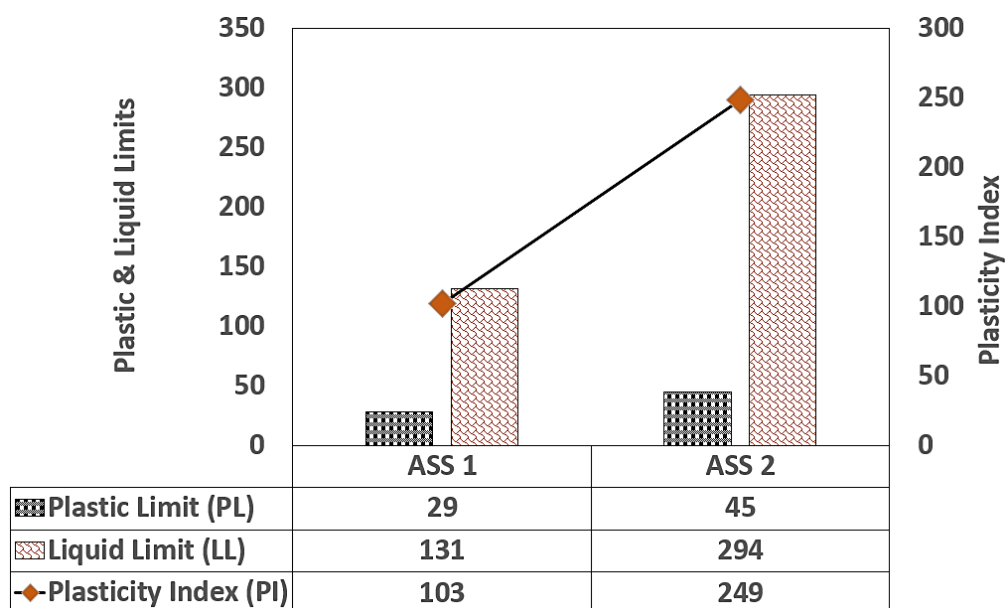


Figure 5.2: Atterberg limit test results against plasticity index

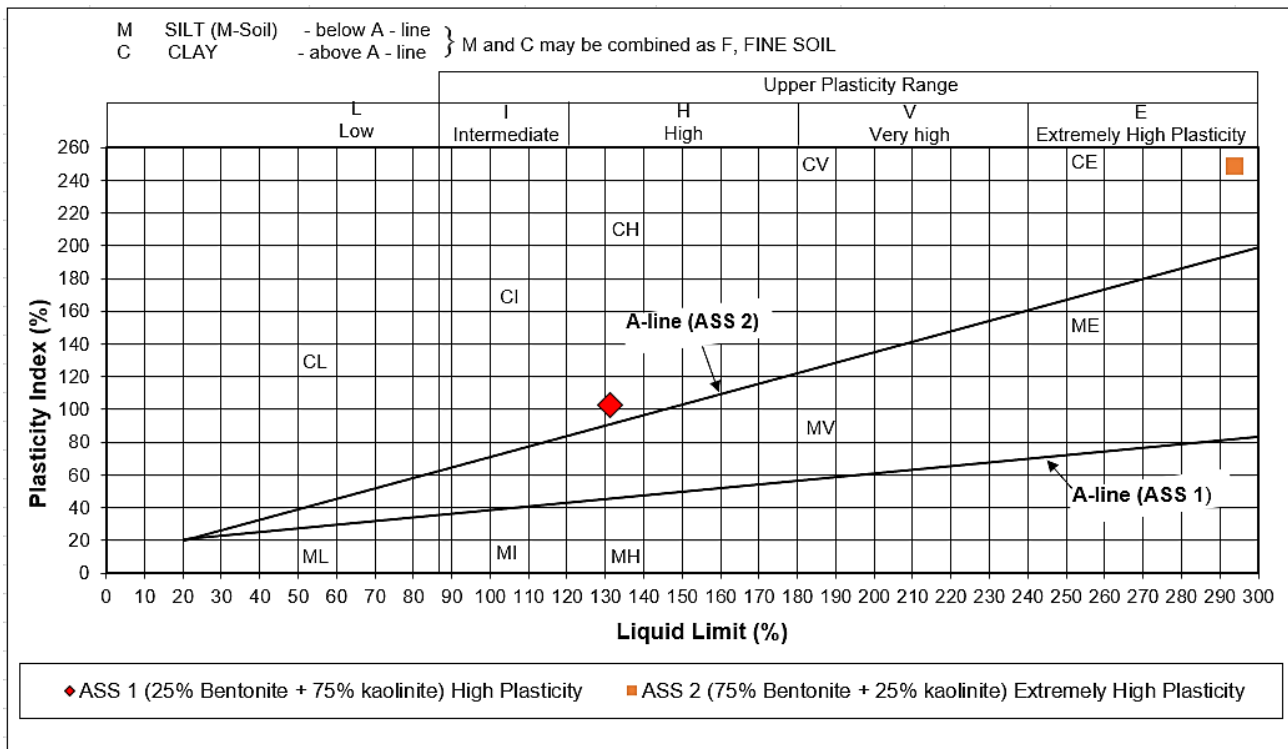


Figure 5.3: Plasticity index chart

5.2 CALIFORNIA BEARING RATIO (CBR)

5.2.1 Untreated Artificially Synthesised Subgrade Materials

A CBR value of 9% was recorded for untreated ASS2 (75%Bentonite + 25%Kaolinite) and a reduction in CBR values to 1.3% was recorded after untreated ASS2 was soaked in water for 4 days. These samples represent the highest CBR values recorded for untreated and untreated-soaked ASS materials in this study. ASS1 (25% Bentonite and 75% Kaolinite) also achieved a CBR value of 8% for untreated-un-soaked samples followed by CBR values of 0.6% recorded for untreated soaked ASS materials respectively. It was observed that only CBR values for un-soaked samples crossed the 2% limit line making them suitable for use in road construction. Soaked ASS samples could not meet the criteria for use in road construction. Figure 5.4 shows the CBR results for ASS materials used in this study.

5.2.1.1 Variation in CBR values

Several studies have reported that expansive subgrade materials exhibit evident volume changes with the potential to swell and shrink with changes in moisture content due to the presence of clay minerals (Reda et al., 2016). This highly expansive subgrade material does not have the capacity to support the weight of the road pavement and traffic load and will normally require some form of modification or re-engineering to enhance its capacity to support load. High and extremely high plasticity subgrade materials ASS1 and ASS after testing for soaked and un-soaked CBR indicated the highest CBR value recorded for ASS2 soaked and un-soaked CBR followed by ASS1. The highest CBR values of 9% and 1.3% (soaked) recorded for ASS2 were due to the high bentonite content in the mixture. A reasonably high CBR value of 8% for un-soaked and 0.6% (soaked) was achieved by ASS1 (25% Bentonite and 75% Kaolinite). The low CBR values observed for soaked ASS1 of 0.6% followed by soaked ASS2 with a CBR value of 1.3% indicated that high and extremely high plasticity subgrade materials have low bearing capacity when they come in contact with water. However, ASS2 composed of high bentonite content recorded the highest soaked CBR value of 1.3% compared with ASS1 with a CBR value of 0.6%. According to Rabab'ah et al., (2021), CBR value for expansive non-stabilised soils was as low as 1.8%, indicating that the expansive soil had very low strength and stabilisation is needed before use in pavement construction.

CBR values achieved expansive soil was 6.29% (Hastuty et al., 2020). This shows that ASS samples with high bentonite content recorded high soaked CBR values even though they are very expansive when they come in contact with water. Bentonites are expansive soils that have high plasticity, low permeability and high swelling potential (Estabragh et al., 2016). During the laboratory experiment, a naturally high bearing capacity (CBR) was observed for untreated bentonite even though they exhibit very high shrink-swell potentials. However, this naturally high bearing capacity of bentonite was affected by the addition of binders to reduce its swelling potentials in a mixture resulting in a reduction in CBR value with an increase in bentonite content in treated ASS samples. According to Schanz et al., (2015), pure bentonite has a high CBR value, which equates to 35.8%. Gratchev et al., (2018) confirmed that soils with high plasticity index exhibit reasonable CBR values. This confirms the findings in this research that, bentonite subgrade materials exhibit naturally high CBR values. Even

though some value of CBR was recorded for soaked and un-soaked ASS samples, these values are unacceptable for use in road construction because they fall below the 2% CBR mark. According to IAN73/06, CBR values below 2% are not acceptable for use as subgrade materials in road construction and will require some modification or re-engineering to make them suitable for use. This confirms that expansive subgrade materials with high and extremely high plasticity index do not have the capacity to support the weight of the road pavement and traffic load and will normally require some form of modification or re-engineering to enhance their capacity to support load.

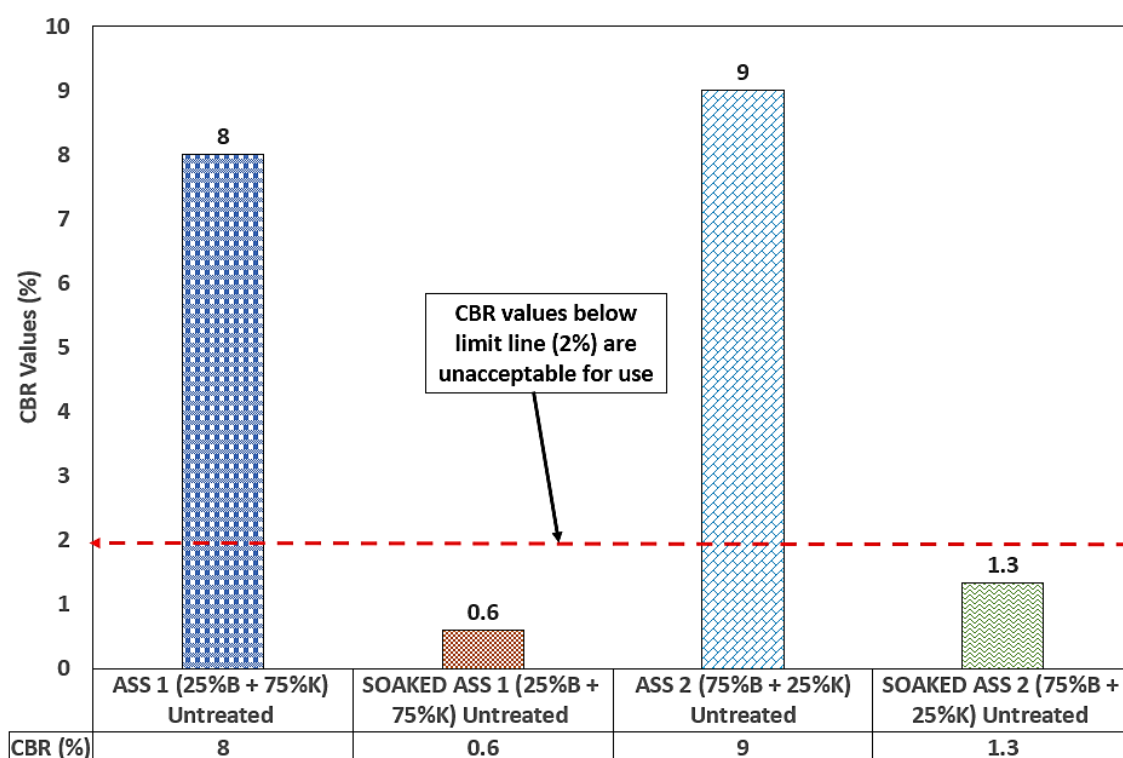


Figure 5.4: Results for untreated ASS materials where B is Bentonite and K is Kaolinite

5.2.2 CBR for Artificially Synthesised Subgrade Treated with Cement and Lime

5.2.2.1 Control Mix

The highest CBR value of 96% was recorded for ASS1 (25% Bentonite and 75% Kaolinite) treated with cement and lime after 28 days of curing, followed by a CBR value of 80% for ASS1(25% Bentonite and 75% Kaolinite) after 7 days of curing at room temperature of $20 \pm 2^\circ\text{C}$. Treated ASS2 (75% Bentonite and 25% Kaolinite) with cement and lime recorded a CBR value of 38% after 7 days of curing followed by a later increase in CBR value of 80% after 28 days of curing. Soaked ASS samples

treated with cement and lime recorded relatively low CBR values compared with treated un-soaked ASS samples. The highest CBR value recorded for soaked ASS samples was 61% recorded for ASS2, which was soaked after 28 days of curing, followed by ASS1 at 50% after 28 days of curing. ASS1 treated and soaked after 7 days of curing achieved a CBR value of 45% followed by ASS2 of 34% after 7 days of curing at room temperature of $20 \pm 2^\circ\text{C}$. It was observed that CBR values for all samples crossed the 2% limit line making them suitable for use in road construction. Figure 5.5 shows CBR results for the various treated, soaked and un-soaked ASS materials at varying curing ages.

The CBR values of expansive road subgrade materials in this research were increased using cement and lime as binders during the stabilisation process. ASS1 treated using 8% lime and 20% cement recorded the highest CBR value for soaked (50%) and un-soaked (96%) after 28 days of curing while ASS2 with high bentonite content treated with 8% lime and 20% cement recording a CBR value of 80% after 28 days of curing. This confirms that the naturally high bearing capacity of bentonite can be affected by the addition of binder in a mixture leading to a reduction in CBR value. This reduction in CBR for a treated sample as bentonite content increased was observed in a study conducted by Thakur et al. (2018) on treated subgrade materials which saw a reduction in CBR values from 15.41% to 3.56% as bentonite content in a mix increase from 5%, 10%, 15%, 20% and 25%, respectively. According to Abbey et al., (2020), traditional cement and lime are popularly used to enhance the engineering properties of subgrade materials and other soil stabilisation purposes. The addition of 3% cement with 1% nano-silica and nano-alumina resulted in a 196% and 164% increase in the soaked CBR of the nontreated clay (Karimiazar et al., 2022). Unconfined compressive strength (UCS) was increased when cement was used in subgrade stabilisation at proportions of 10% 15% and 20% (Liang et al., 2020) subgrade materials were improved from 564.78 kPa to 636.19kPa (Nazari et al., 2021). Lepore et al. (2009) also recorded that an optimum lime dosage between 6-12% by dry weight is suitable to enhance the engineering properties of subgrade materials.

A gradual increase in CBR value with an increase in curing age was observed for all ASS samples both soaked and un-soaked at a temperature of $20 \pm 2^\circ\text{C}$. This shows that CBR values increase with respect to curing age when subgrade materials are

stabilised using cement and lime as binders. Hence, the longer the curing time the higher the CBR value. Cement and lime have been reportedly used in the stabilisation of expansive subgrade materials in many instances which have yielded very good CBR results. Highly effective clay stabilisation is also provided by Portland cement, generally with the advantage of high strength gain (Athanasopoulouet, 2016). The high CBR value observed with an increase in curing age can be attributed to the formation of calcium silicate hydrate (C-S-H) gel and calcium aluminate hydrate (C-A-H) gel also referred to as Tobermorite in the mixture.

Tobermorite are chemicals composed of calcium silicate hydrate minerals and are responsible for detoxification and strength gain in a mix. During the hydration process in a cement/lime mix under normal room temperature, cementitious products are released (C-S-H and C-A-H gel) which are responsible for strength gain in the mixture (Faith et al., 2007). According to Zhang et al. (2014), High long-term temperatures can affect the strength behaviour of cement-stabilised clays. The continuous formation of C-S-H gel with an increase in curing age within a pore structure can contribute to strength development in a mix, the higher the C-S-H gel the high the strength in the samples (Abbey et al., 2020). The formation of C-S-H and C-A-H gel in this research acted as a binding agent responsible for strength gain and high CBR value of the subgrade materials. According to Ingles et al. (1987), Portland cement with lime in the presence of water forms hydraulic compounds. Unlike untreated ASS samples, CBR values for soaked-treated samples decreased with an increase in bentonite (highly plastic clay) content can be linked to the effect of the addition of binders and the weak compression nature of clay when they come in contact with water. Treated ASS samples both soaked and un-soaked crossed the 2% CBR line making them good enough for use in road construction in accordance with IAN73/06. Cement and lime stabilisation are traditional means of improving the engineering properties of soil for use as both base and subbase materials (Olutoge et al., 2018). This confirms that using cement and lime as binders in road subgrade stabilisation can good CBR yield results that can be used in road construction.

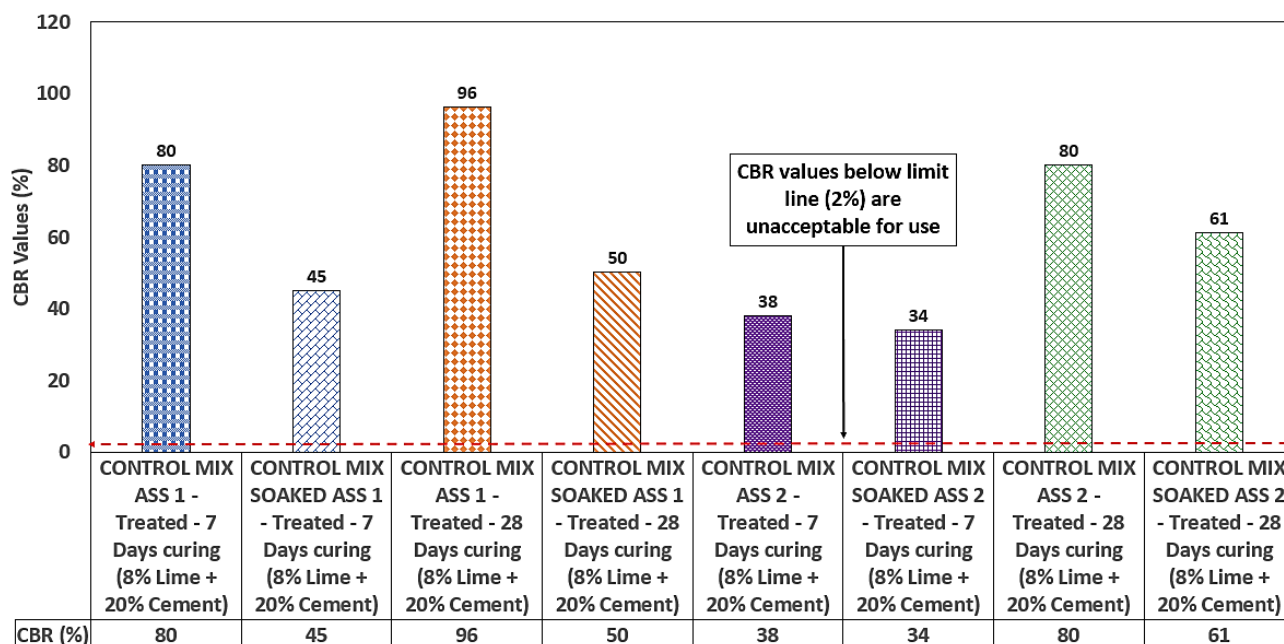


Figure 5.5: Control mix for treated Artificially Synthesised Subgrade

5.2.3 CBR for ASS materials treated with sustainable materials

5.2.3.1 Brick Dust Waste

A reasonably high CBR value was recorded for ASS materials treated using 23.5% Brick Dust Waste (BDW) as partial replacement for cement and lime in the mix. It was observed that soaked samples exhibited high CBR values compared with un-soaked samples. The highest CBR value of 28% was recorded for soaked treated samples after 28 days of curing followed by ASS1 with CBR values of 26% after 28 days of curing. ASS1 also recorded a CBR value of 23% after 7 days of curing and later recorded a reduction in CBR values of 17% after the sample was soaked in water at room temperature of $20 \pm 2^\circ\text{C}$ for 4 days. ASS2 was cured for 7 days and recorded CBR values of 14%. However, ASS2 soaked after 7 days of curing and ASS2 cured for 28 days both recorded CBR values of 18%. This was followed by a 1% reduction in CBR value for ASS2 soaked after 28 days of curing which recorded a CBR value of 17%. It was observed that CBR values for all samples crossed the 2% limit line making them suitable for use in road construction. Figure 5.6 shows CBR results for the various treated, soaked and un-soaked ASS materials at varying curing ages.

The use of sustainable waste materials in road subgrade stabilisation was considered in this research due to the cost, and environmental effects associated with cement and

lime production. Fly ash, bituminous, rice husk ash, lime, construction and demolition waste, electrical and thermal waste, geotextile fabrics and recycled waste can be used as admixtures in this process (Rivera et al., 2020). Very high CBR values were recorded for all ASS materials soaked and un-soaked with an increase in curing age for un-soaked ASS when 23.5% BDW was used as a partial replacement for cement and lime in a mixture. Zhu et al. (2020) stated that clay brick wastes are a potential partial cement replacement. It was found that the addition of brick dust resulted in an increase in the soil strength between 1.7 and 2.3 times with respect to the non-stabilised materials (Hidalgo et al., 2019). The high CBR values observed for ASS materials can be attributed to the pozzolanic reaction responsible for the formation of C-S-H and C-A-H gel due to the presence of BDW in the mixture which acted as a binding agent responsible for strength gain and the high CBR value of the subgrade materials (Rogers et al., 2011).

Pozzolans are materials such as BDW that contain alumina/silica which reacts to form new compounds (Calcium silicate hydrate (C-S-H) and Calcium aluminium Hydrates (C-A-H) when lime is added and have the ability to modify the properties of a lime mixture (Rogers, 2011). BDW exhibits pozzolanic properties, which can be used as cement replacement in road subgrade stabilisation (Kartini et al., 2012). According to O'Farrel et al. (2001), the liquid phase is formed during the production of BDW when clay bricks are highly fired at a temperature of about 1000°C to 1100°C, which solidifies to an amorphous glass phase when it cools and gives it high pozzolanic properties. Pozzolans of siliceous and aluminous materials (possess little or no cementitious value) in a finely divided form reacts chemically with the right amount of water with calcium hydrate at ordinary temperature to form compounds that possess the properties of cement (O'Farrell et al., 2001). The addition of pozzolanic materials (Brick waste) to a soil mix will enhance the properties hence speeding upsetting time and increasing the strength and durability of soil (Rogers, 2011). Pozzolanic reaction enables the formation of a secondary C-S-H gel, which fills up voids and improves the internal structure and increases durability and strength.

The highest CBR value 26% for un-soaked ASS samples was recorded for ASS1 after 28 days of the curing temperature of 20±2°C. Followed by ASS1 of 23% after 7 days

of curing under normal room temperature of $20\pm 2^{\circ}\text{C}$. This shows an increase in CBR values as curing age increases. This same trend was observed for ASS2 with a CBR value of 14% after 7 days of curing and 18% after 28 days of curing under normal room temperature of $20\pm 2^{\circ}\text{C}$. This shows that the addition of BDW in the mix does not affect strength development with respect to curing age. Soaked ASS samples recorded high CBR values of 17% after 7 days of curing followed by an overall highest CBR for both soaked and un-soaked ASS of 28% after 28 days of curing. This shows that very high CBR values can be obtained when high plasticity subgrade materials composed of high BDW content are subjected to a long period of soaking at normal room temperature of $20\pm 2^{\circ}\text{C}$. Soaked CBR samples composed red-brick powder recorded high CBR value of 15% (Salimah et al., 2021). According to a study conducted by Blayi et al. (2020), the maximum soaked CBR value was achieved by a mixture composed of the highest brick powder (BP) of 20%. Soaked CBR values increase from 4% to 8% only with the addition of brick dust (Mir et al., 2019).

The Soaked CBR value of 21.17% achieved using brick dust was higher than that of black cotton soil at 2.4% (Tiwari et al., 2018). Un-soaked ASS2 composed of high bentonite content after 7 days of curing recorded the lowest CBR value of 14% even though there was an increase in CBR value of 18% after 28 curing these CBR values are nowhere close to what was achieved for ASS1 after 7 and 28 days curing. Also, ASS2 un-soaked achieved low CBR compared to ASS1 un-soaked. this could be attributed to the high presence of bentonite in the mix which exhibits low bearing capacity when in contact with binders. This reduction in CBR for treated samples as bentonite content increased was observed in a study conducted by Thakur et al. (2018) on treated subgrade materials which saw a reduction in CBR values from 15.41% to 3.56% as bentonite content in a mix increase from 5%, 10%, 15%, 20% and 25%. After the analysis, it was observed that the highest CBR values of 28% achieved for soaked ASS1 after 28 days of curing with 23.5% BDW used as partial replacement for cement and lime did not even match up to the lowest CBR values of 34% obtained for soaked ASS2 sample after 7 days using traditional lime and cement only as binders. However, the results achieved are greater than 2% making them usable in road construction as subgrade materials according to IAN73/06.

The addition of brick dust increased the soil strength and its suitable materials for use in practical applications in construction (Hidalgo et al., 2019). As part of the commitment of many countries to reduce greenhouse gas emissions, using brick waste as binders in place of cement and lime in subgrade stabilisation will help reduce the greenhouse gas emitted to the atmosphere due to cement and lime production as well as reduce the environmental effect associated with a brick stockpile and landfill. According to the World Health Organisation (WHO) (2021) report on climate change in the Western Pacific, it is estimated that climate change will cause an additional 250,000 deaths annually between 2030 to 2050. However, countries are committing to net-zero emissions by 2050, and about half of the emission cuts must be in place by 2030 to keep global warming below 1.5°C (The United Nations, 2021).

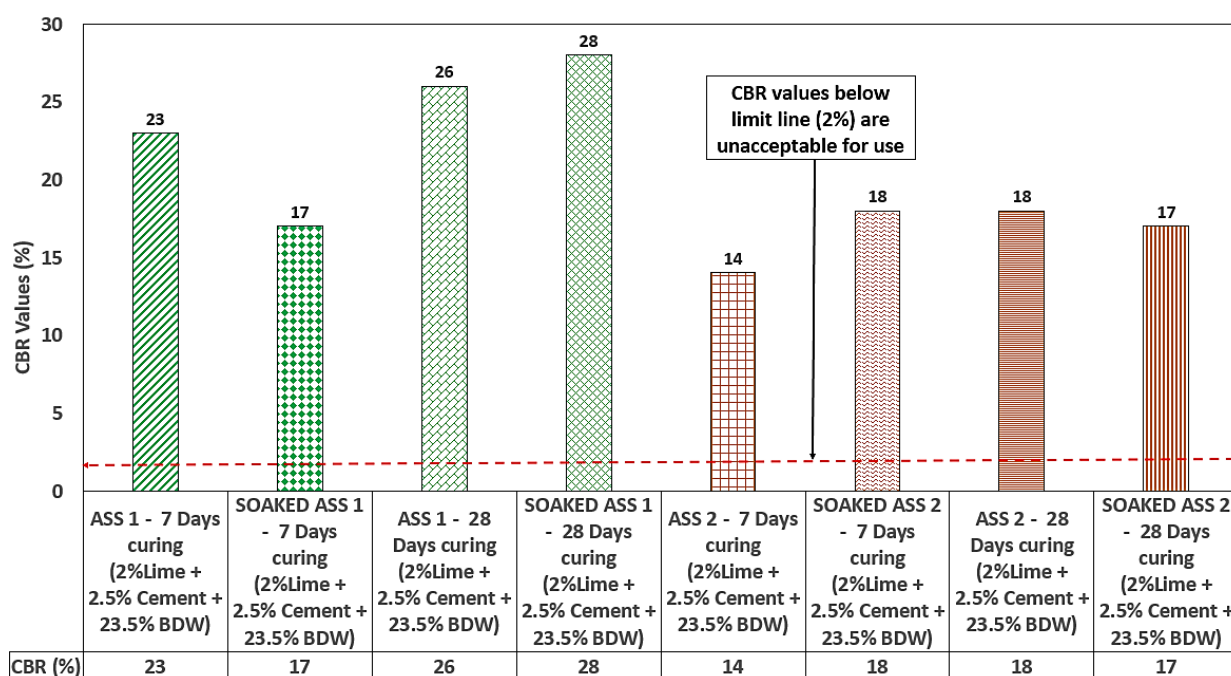


Figure 5.6: CBR results for the various treated, soaked and un-soaked ASS materials at varying curing ages

5.2.3.2 Ground Granulated Blast-furnace Slag (GGBS)

A high CBR value was recorded for ASS materials treated using 23.5% GGBS as partial replacement for cement and lime in the mix. Very high CBR values of 97% were recorded for soaked ASS1 sample after 28 days of curing when 23.5% GGBS was used to partially replace cement and lime in the mix. This high CBR value was also observed for ASS1, which recorded CBR values of 92% after 28 days of curing at room temperature of $20 \pm 2^\circ\text{C}$. A CBR value of 79% was recorded for soaked ASS

samples soaked after 7 days of curing and a CBR of 70% was recorded for ASS1 sample after 7 days of curing. A reduction in CBR values of 46% was observed for ASS2 soaked after 7 days of curing compared CBR value of 73% recorded for ASS2 after 7 days of curing. ASS2 cured for 28 days recorded a CBR value of 68% followed by a slight reduction in CBR value of 65% for ASS2 soaked after 28 days of curing at room temperature of $20\pm 2^{\circ}\text{C}$. It observed that CBR values for all samples crossed the 2% limit line making them suitable for use in road construction. Figure 5.7 shows CBR results for the various treated, soaked and un-soaked ASS materials at varying curing ages.

GGBS has been reportedly used as binders in road subgrade stabilisation to improve the engineering properties of road subgrade materials. The application of GGBS is a useful material for soil stabilisation (Saravanan et al., 2017). Extremely high CBR values were recorded for ASS materials due to the high GGBS content of 23.5%GGBS used as partial replacement for cement and lime in the mix. These extremely high CBR values achieved could be attributed to the high amount of GGBS present in the mix. Strength in expansive soil stabilisation increased with the addition of 20% GGBS for the curing periods of 7 and 14 days and up to 40% for the curing period of 28 days (Sharma et al., 2012). High compressive strength up to 100Mpa was observed after 7, 14 and 28 days of curing when high GGBS content of 60% was added to the mix (Saludung et al., 2018). Soaked and un-soaked CBR of soil-lime and GGBS samples increased by 9.02% and 8%, respectively, with an increase in lime and GGBS content and found maximum UCS value at proportions of 6% lime and 10% GGBS (Darsi et al., 2021). GGBS are highly cementations and high in strength-enhancing compounds calcium silicate hydrate (C-S-H) which improves strength and durability in a mix. Studies have shown that the higher the amount of GGBS blend, the greater the hydraulic activity (Hewlett, 2003).

The addition of a minimal amount of 2% lime and 2.5% cement to the mix in this research also contributed to the high strength gain of ASS materials because GGBS works well with the addition of lime. The alkaline properties of Portland cement, lime and other activators, such as sulphates, chlorides and alkali silicates, are sufficient to activate the cementitious properties of GGBS (Oner and Akyuz, 2007). The process of adding GGBS and lime induces the calcium silicate hydrate bond in the soil to

accelerate the formation of cementitious substances in the soil during curing under standard room temperature of $20\pm 2^{\circ}\text{C}$. (Saravanan et al., 2017). Adding lime to GGBS helps in strength development because GGBS alone in a mix exhibits very slow strength development under standard 20°C curing conditions compared to other conventional stabilisers (Escalante-Garcia and Sharp, 2004). GGBS and lime react chemically with the right amount of water at ordinary temperature to form compounds that possess the properties of cement (O'Farrell et al., 2001). CBR values for un-soaked ASS1 (high plasticity subgrade) material in this research increased with an increase in curing age. Un-soaked CBR values were found to be higher than soaked CBR values with the addition of GGBS in a mixture (Rabbani et al., 2012). 25% GGBS achieved higher CBR values of 35% compared to other percentages and at 28 days it had shown maximum values than other curing periods (Rao et al., 2012).

The engineering properties of expansive soil were improved with the addition of up to 7.5% GGBS (Corrêa-Silva et al., 2020). Subgrade materials were stabilised with 16% GGBS and the results obtained show an increase in UCS value over time to 1500kN/m^2 in accordance with ASTM 1633 (Obuzor et al., 2012). The addition of 6% GGBS to a lime-treated soil reduced swell from 8% to 0% (Celik et al., 2013). High compressive strength of 14.2kPa, 89kPa, 211.9kPa and 656 kPa was achieved when GGBS proportions of 6%, 12%, 18% and 24% were used in subgrade stabilisation after 28 days of curing (Gokul et al., 2020). Unlike ASS1, ASS2 (extremely high plasticity subgrade) with high bentonite of 75% saw a reduction in CBR values with an increase in curing age for un-soaked ASS sample. However, an increase in CBR value was observed for soaked ASS2 samples with an increase in curing age. This observation shows that CBR values for extremely high ASS materials (ASS2) with high GGBS content reduce with an increase in curing age and increase with an increase in curing age when soaked. Soaked CBR values increased by about 400% and 28% with the addition of an optimum amount of GGBS (Yadu et al., 2013).

The decrease in CBR value with an increase in curing age for ASS2 (extremely high plasticity subgrade) with respect to an increase in curing age could be a result of high GGBS content in the mix. CBR value of Black Cotton soil (very high plasticity) further decreased from 5.16% to 4.93% with an increase in GGBS from 16% to 20% in the mixture (Patel et al., 2019). Soaked ASS1 recorded the highest CBR value of 97%

after 28 days of curing. This confirms the study conducted by Gali et al. (2018), where the CBR value of soil-GGBS mix was higher in soaked conditions compared to unsoaked conditions. The CBR values achieved for using GGBS are extremely high and in the same range as using cement and lime only (Control mix) in a mixture. This means GGBS can be used in place of cement and lime. Overall CBR values achieved for ASS2 both soaked and un-soaked are on-the-low due to the high bentonite content and extremely high plasticity nature of ASS2. During the laboratory experiment, a naturally high bearing capacity (CBR) was observed for untreated bentonite even though they exhibit very high shrink-swell potentials. According to Schanz et al. (2015), pure bentonite has a high CBR value and soils with high plasticity index exhibit reasonable CBR values (Gratchev et al., 2018).

CBR values achieved for adding 2.35%GGBS are higher than that of 23.5% BDW even though they are all acceptable for use in road construction. CBR values for the addition of 23.5% GGBS in a mixture are greater than 2% making them usable in road construction as subgrade materials according to IAN73/06. As part of the commitment of many countries to reduce greenhouse gas emissions, using GGBS as binders in place of cement and lime in subgrade stabilisation will help reduce the greenhouse gas emitted to the atmosphere due to cement and lime production as well as reduce the environmental effect associated with brick stockpile and landfill. The use of GGBS binders at high volumes as supplementary cementitious materials are good from an environmental point of view; hence, the higher the amount of GGBS used in replacing cement in soil stabilisation the lesser the carbon footprint (Onn et al., 2019).

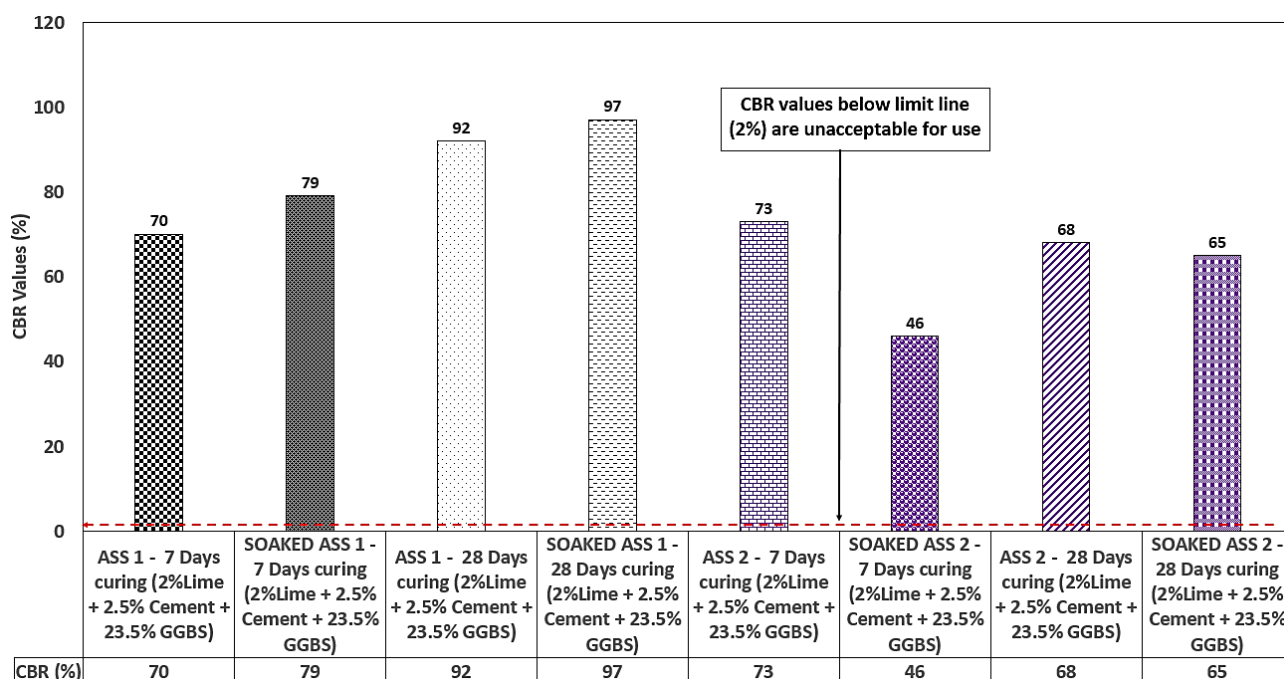


Figure 5.7: CBR results for the various treated, soaked and un-soaked ASS materials at varying curing ages

5.2.3.3 Recycled Plastic

High CBR value was recorded for ASS materials treated using 23.5% recycled plastic as partial replacement for cement and lime in the mix. CBR value of 13% was recorded for ASS1 after 7 and 28 days of curing. This was followed by a 1% reduction in CBR value to 12% for ASS1 sample soaked after 7 days of curing. ASS2 also recorded a CBR value of 12% after 7 days of curing and later observed a drastic reduction in CBR values to 6% after the ASS2 sample was soaked after 7 days of curing. ASS1 recorded CBR values of 8% after the sample was soaked in water after 285 days of curing. ASS2 also recorded 8% CBR value after the sample was cured for 28 days at room temperature of $20 \pm 2^\circ\text{C}$. A very low CBR value of 3% slightly above the limit line was observed for ASS2 sample after 28 days of curing. It was observed that CBR values for all samples crossed the 2% limit line making them suitable for use in road construction. Figure 5.8 shows CBR results for the various treated, soaked and un-soaked ASS materials at varying curing ages.

Plastic waste produced due to human activities has become a major problem to deal with using plastic in road subgrade stabilisation will help reduce the environmental effect associated with plastic waste. The world produces 381 million tonnes of plastic waste each year and is set to double by 2034 (Plastic in the Ocean, 2021). After stabilising expansive road subgrade materials using high recycled plastic waste

content as a partial replacement for cement and lime shows a high CBR value usable in road construction. Soil stabilisation using plastic waste can be used in embankment and road pavement layers to improve the soil strength value (Gardete et al., 2020). Waste plastics were used by Ashraf et al. (2011), to stabilise soil and the results show a reasonably high CBR value Un-soaked. ASS1 samples (high plasticity subgrade) composed of 23.5% plastic waste recorded the highest CBR value of 13% after 7 and 28 days. Apart from the small amount of C-S-H gel formed due to the 2% lime and 2.5% cement addition in the mix, the plastic granules/pellets, interlocking during sample compaction (mechanical stabilisation) are also responsible for strength gain. Mechanical stabilisation can be possible by interlocking granular binders with soil-aggregate particles during the compaction process (Mishra et al., 2017).

However, un-soaked ASS2 with high bentonite content recorded a reduction in CBR value from 12% at 7 days to 8% after 28 days of curing. A decline in soaked CBR values with an increase in curing age with observed. This shows no indication of CBR increase with respect to curing age because plastic does not react with cement and lime to form C-S-H gel to increase CBR in a mixture. However, the minimal amount of cement (2.5%) and lime (2%) was responsible for the generally low CBR values achieved because no C-H-S gel was formed to increase the strength. The reduction in soaked CBR could be a result of the granular nature of recycled plastic used in this study, granular materials are weak in compression when soaked because they have open structures that allow water and air to penetrate through during soaking. Granular soils are basically crumbed structures with open structures that allow water and air to penetrate through the soil (Bo et al., 2015). Stabilising expansive soil using plastic waste strips and lime has a greater influence on the plasticity and strength parameters of the soil (Amena et al., 2022). Plastic polypropylene fibre mixed with lime can be used to stabilise clay soil (Amena et al., 2021). A combination of cement and lime resulted in a significant increase in UCS (Hassan et al., 2021). Even though the plastic used in this research is granular, the generally low CBR values of 13%, 12%, 8%, 6% and 3% achieved for ASS samples with high plastic content compared with GGBS are lower than the range of CBR range for sand and gravel.

According to section 3/9 of the Virginia Department of Transport (VDOT) (2016), sands are more granular and grain better and will generally have a CBR value between 15% and 35%. Soaked ASS2 samples after 28 days recorded the lowest CBR or 3% only 1% beyond the 2% mark for acceptable CBR value. This shows that high plasticity subgrade materials stabilised with a high amount of plastic are very weak when soaked in water. CBR values for all ASS samples with the addition of 23.5% recycled plastic waste in a mixture are greater than 2% making them usable in road construction as subgrade materials according to IAN73/06. However, the CBR values recorded are very low compared with CBR values achieved for using a high amount of GGBS and BDW. As part of the commitment of many countries to reduce greenhouse gas emissions, using recycled plastic waste as binders to partially replace cement and lime in subgrade stabilisation will help reduce the greenhouse gas emitted to the atmosphere due to cement and lime production as well as reduce the environmental effect associated with landfill.

According to “Plastic in the Ocean” statistics for 2020-2021, about 8 million pieces of plastic make their way into our oceans and there are 5.25 trillion macro and micro pieces of plastic in our ocean and 46,000 places in every square mile of ocean, weighing up to 269,000 tonnes. By partially replacing Portland cement with recycled waste plastic, this design may have the potential to contribute to reduced carbon emissions (Schaefer et al., 2017). Plastics are one of the leading waste materials found suitable for the purpose of subgrade stabilisation. They reduce the cost of stabilisation at a large rate and using plastic for this purpose simultaneously solves the challenge of improper plastic recycling (Kassa et al., 2020). Sustainability and environmental benefits can be achieved when recycled materials/by-products are used efficiently in road construction (El-Badawy et al., 2019).

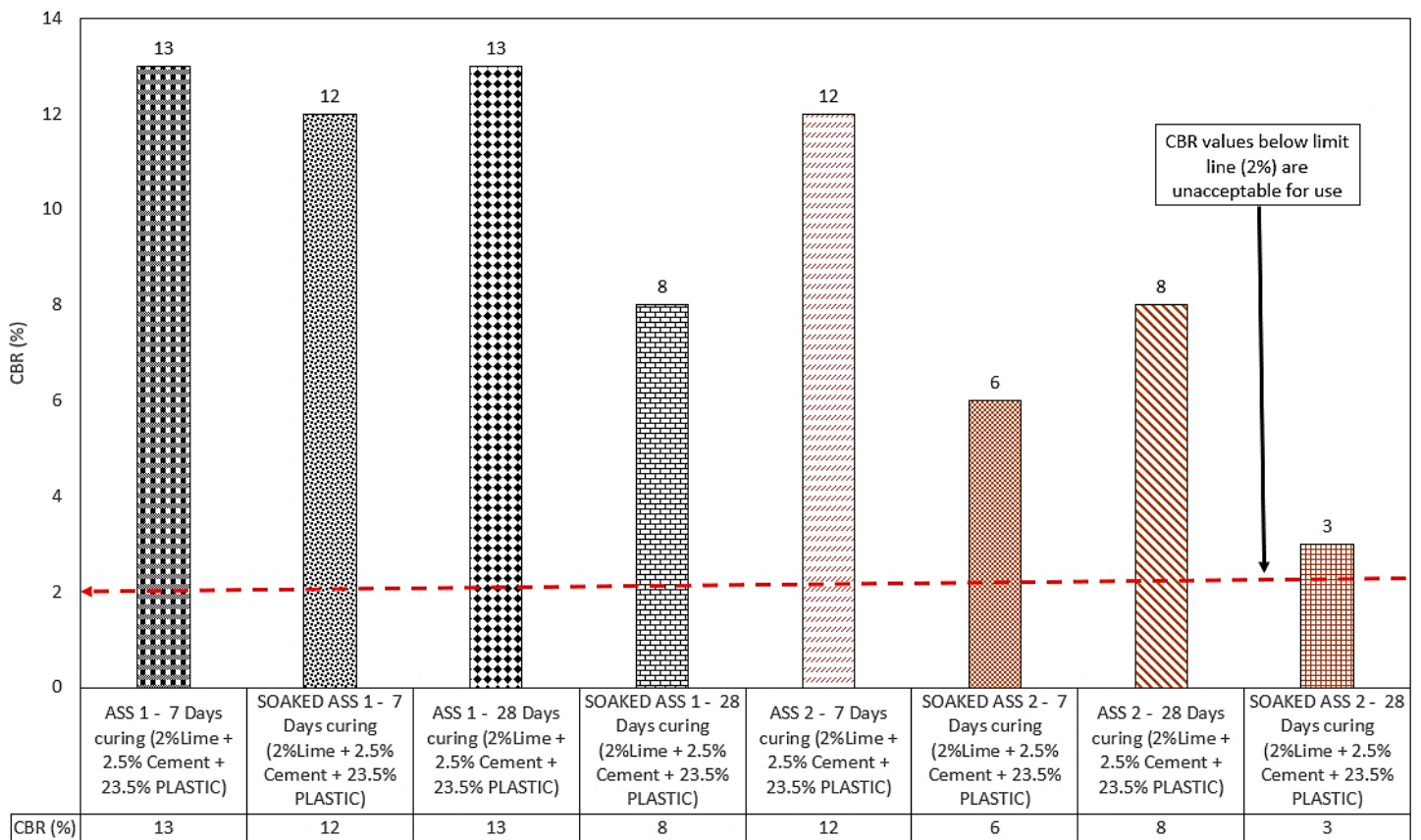


Figure 5.8: CBR results for the various treated, soaked and un-soaked ASS materials at varying curing ages

5.2.3.4 Recycled Glass

A reasonably high CBR value was recorded for ASS materials treated using 23.5% recycled glass as partial replacement for cement and lime in the mix. The highest CBR of 17% was recorded for ASS1 soaked after 7 days of curing followed by a CBR value of 16 for ASS1 cured for 28 days. ASS1 sample recorded a CBR value of 14% after 7 days of curing, meanwhile ASS1 soaked after 28 days of curing and ASS2 cured for 7 days recorded a CBR value of 11%. ASS2 cured for 28 days recorded a CBR value of 8% and ASS2 soaked after 7 and 28 days of curing recorded a CBR value of 3% and 4% slightly above the limit line. It was observed that CBR values for all samples crossed the 2% limit line making them suitable for use in road construction. Figure 5.9 shows CBR results for the various treated, soaked and un-soaked ASS materials at varying curing ages.

Glass waste dumped in landfills has been a major challenge facing today. Recycling glass and using them in road construction and other construction activities would reduce the environmental issues associated with glass landfills. In this study, 23.5%

of recycled glass used in a mixture recorded CBR values usable in road construction. A generally low CBR value in the range between 17% and 3% was recorded for all ASS samples soaked and un-soaked with a reduction in CBR up to 3% with the addition of recycled glass. According to Hastuty et al. (2020), CBR values at a mixture of 2% limestone and 10% slag was 8.86% and the variation of a mixture of 4% limestone and 10% glass recorded a CBR of 10.5%. This confirms that CBR values do not increase significantly with the addition of a glass of any sort in subgrade stabilisation. The highest CBR value of 17% was recorded for soaked ASS1 sample after 7 days of curing and a gradual increase in CBR value with an increase in curing age was observed for un-soaked ASS1 samples. However, a reduction in CBR values with an increase in curing age was observed for ASS2 with high bentonite content. This could be due to the effect of binders on high bentonite content and observed in other mixtures as mentioned and confirmed in the study earlier.

This highest soaked CBR value of 17% for ASS1 after 7 days of curing was reduced to 11% after 28 days of curing. soaked ASS2 recorded a CBR value of 3% after 7 days of curing with a little increase in CBR value of 4% after 28 days. This shows that CBR does not increase with respect to curing age because glass does not react with cement and lime to form C-S-H gel to increase CBR value in a mixture. However, the little amount of cement (2.5%) and lime (2%) was responsible for the generally low CBR values achieved for ASS samples. Overall, the CBR values achieved for 23.5% recycled glass were in the same range as CBR values for recycled plastic waste but were very low compared with the CBR values achieved for 23.5% BDW and 23.5% GGBS used in the mixture. Soaked ASS2 recorded very low CBR of 3% at 7 days and 4% after 28 days making them weak for use as a subgrade material even though they could be used. Recycled glass can be used in subgrade stabilisation to achieve some level of CBR, however higher levels of CBR can be achieved using GGBS and BDW. CBR values achieved for all ASS samples with the addition of 23.5% recycled glass waste in a mixture are greater than 2% making them usable in road construction as subgrade materials according to IAN73/06 (2020).

As part of the commitment of many countries to reduce greenhouse gas emissions, using recycled glass waste in subgrade stabilisation would reduce the greenhouse gas emitted to the atmosphere. And reduce the environmental effect associated with

landfill and cement and lime production. Using glass waste normally dumped in landfills would reduce greenhouse gas emissions and the environmental effect that emanates from glass landfills. Using glass produced from recycled glass reduced related air pollution by 20% and related water pollution by 50% and reduced the space in landfills (World Wide Fund for Nature, 2021).

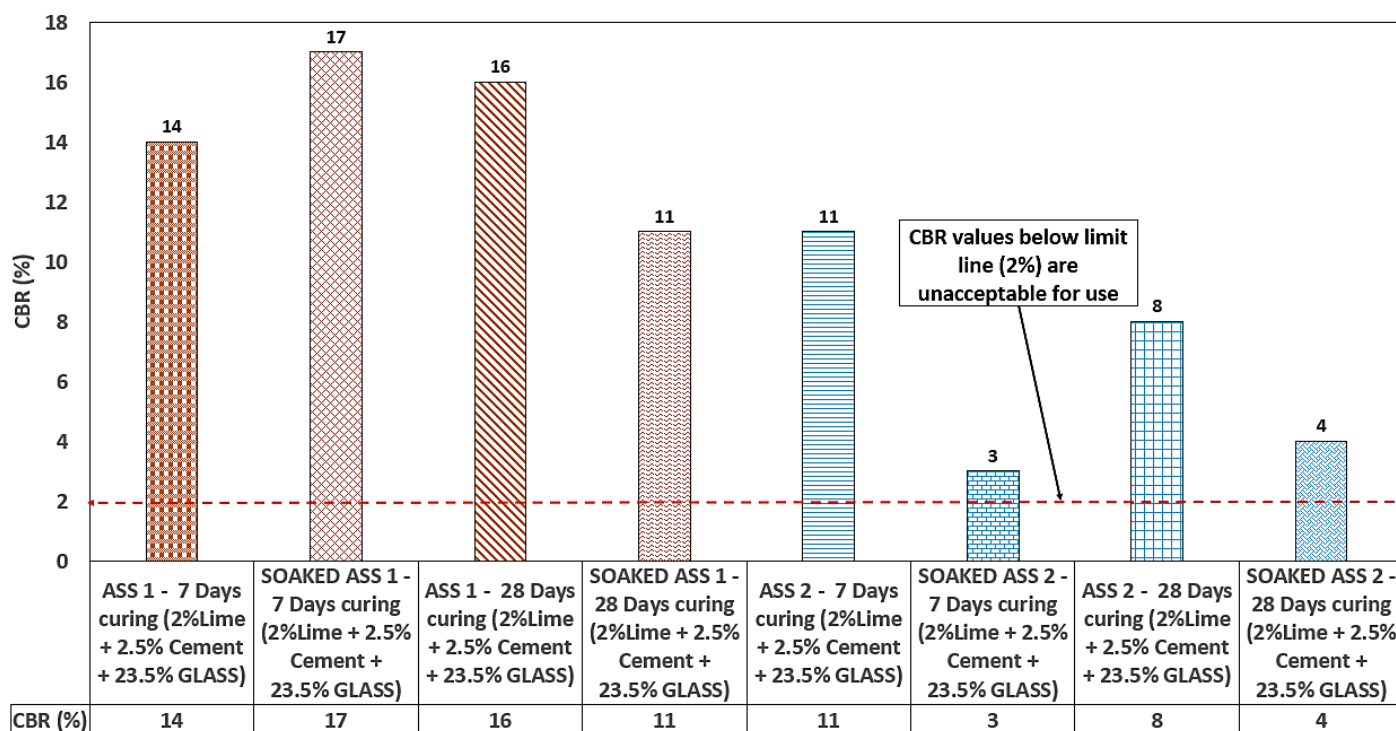


Figure 5.9: CBR results for the various treated, soaked and un-soaked ASS materials at varying curing ages

5.2.3.5 GGBS and Recycled Plastic

High CBR value was recorded for ASS materials treated using 11.75% GGBS and 11.75% recycled plastic as partial replacement for cement and lime in the mix. A very high CBR value of 93% was recorded for ASS1 samples soaked after 28 days of curing followed by a CBR value of 82% for ASS1 cured for 28 days. ASS1 sample soaked after 7 days of curing recorded a CBR value of 59% and ASS1 cured for 7 days recorded a CBR value of 44%. A CBR value of 51% was recorded for ASS2 after 28 days and ASS2 soaked after 28 days of curing recorded a CBR of 50% respectively. ASS2 soaked after 7 days of curing recorded a CBR value of 47% and a reduction in CBR value of 21% was observed for ASS2 after 7 days of curing at room temperature of $20 \pm 2^\circ\text{C}$. It was observed that CBR values for all samples crossed the 2% limit line making them suitable for use in road construction. Figure 5.10 shows CBR results for the various treated, soaked and un-soaked ASS materials at varying curing ages.

After conducting CBR test for ASS materials using individual sustainable binders at very high percentages, it was observed that GGBS achieved extremely high CBR values making GGBS the best performing binder in this study. Due to this reason, GGBS was added to each mix design by half the weight of the individual sustainable binders with the aim of achieving higher CBR values for ASS mix designs. 11.75% GGBS was added to 11.75% recycled plastic in a mixture and the results show very high CBR values with the highest CBR value of 93% and the lowest CBR value of 21% compared with the previous addition of 23.5% recycled plastic only which achieved a highest CBR value of 13% and a lowest CBR value of 3% the mix. It was found that the presence of GGBS in the mixes significantly increased the compressive strength of geopolymer (Saludung et al., 2018). GGBS are rich in calcium, the main reaction product of C-S-H gel responsible for strength development (Sasui et al., 2019).

The highest CBR value of 13% was recorded for ASS1 after 7 and 28 days with the addition of a higher proportion of 23.5% recycled plastic increased drastically to 44% after 7 days and 82% after 28 days of curing with the addition of GGBS. The lowest CBR values of 6% after 7 days and 3% after 28 days were recorded for soaked ASS2 samples with the addition of a higher proportion of 23.5% recycled plastic shot up to CBR values of 47% after 7 days and 50% after 28 days of curing. This shows that CBR values have significantly improved with the addition of GGBS which contains high amounts of C-S-H gel responsible for strength increase. GGBS contains a high amount of calcium forming C-S-H gel which contributed to strength development (Saludung et al., 2018). It was found that with the increase in GGBS content, the CBR also increased up to the immediate formation of cemented products by hydration which increases the density of soil (Narendra et al., 2017). CBR values increase significantly with the addition of 10% GGBS in black cotton soil stabilisation (Darsi et al., 2021). Adding 15% GGBS to 1% polypropylene plastic fibre to expansive soil increased CBR values (Prasad, et al., 2019). Expansive soil subgrade flexible pavement was improved by 90.48% with the addition of GGBS as a binder when compared with untreated expansive soil subgrade flexible pavement (Prasad, et al., 2019). It was observed that the strength improvement of sodium bentonite, black cotton clay and organic clay depends on the amount of GGBS in the mix (Narendra et al., 2017).

An increase in CBR values with an increase in curing age was observed for both soaked and un-soaked ASS samples. However, the CBR values recorded for un-soaked ASS samples are higher compared with CBR values for soaked ASS samples. The lowest CBR value of 21% was recorded for ASS2 with high bentonite content after 7 days of curing which later increased to 51% after 28 days and can be increased further by increasing the GGBS content in the mix. An increase in CBR values was observed with an increase in GGBS (Kumar et al., 2020), and studies have revealed that using GGBS waste materials has the potential to modify the properties of clays (Narendra et al., 2017). It could be observed that CBR values for both soaked and un-soaked ASS2 composed of high bentonite content are on the low, due to the high amount of bentonite in the mix. According to Schanz et al., (2015), pure bentonite has a high CBR value, which equates to 35.8%. Gratchev et al., (2018) confirmed that soils with high plasticity index exhibit reasonable CBR values. CBR values achieved for all ASS samples with the addition of 11.75%GGBS and 11.75% recycled plastic waste in a mixture are greater than 2% making them usable in road construction as subgrade materials according to IAN73/06. As part of the commitment of many countries to reduce greenhouse gas emissions. Using GGBS and recycled plastic waste as binders to partially replace cement and lime in subgrade stabilisation would reduce construction costs, greenhouse gas emissions and the environmental effect associated with landfills. GGBS can be utilised as an alternative to reduce the construction cost of the road, particularly in the rural areas of developing countries (Prasad, et al., 2019).

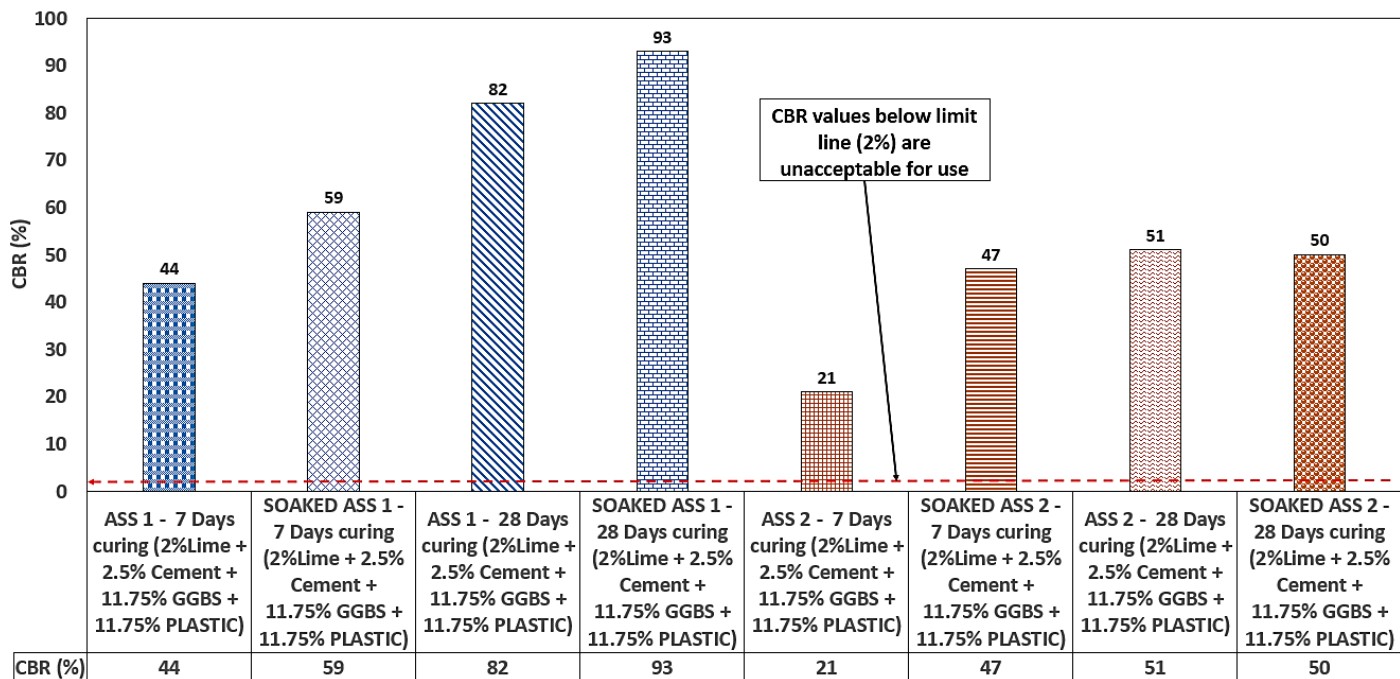


Figure 5.10: CBR results for the various treated, soaked and un-soaked ASS materials at varying curing ages

5.2.3.6 GGBS and Recycled Glass

Acceptable CBR value was recorded for ASS materials treated using 11.75% GGBS and 11.75% recycled glass as partial replacement for cement and lime in the mix. A very high CBR value of 80% was recorded for ASS1 after 28 days of curing followed by a slight reduction in CBR values of 72% for ASS1 soaked after 28 days of curing. ASS1 sample cured for 7 days recorded a CBR value of 51% and later recorded a higher CBR value of 59% after soaking for 7 days at room temperature of $20 \pm 2^\circ\text{C}$. ASS2 soaked and un-soaked after 28 days of curing recorded a CBR value of 46%. However, ASS2 recorded a CBR value of 21% after 7 days of curing and later recorded a higher CBR value of 31% when soaked in water after 7 days of curing at room temperature of $20 \pm 2^\circ\text{C}$. It was observed that CBR values for all samples crossed the 2% limit line making them suitable for use in road construction. Figure 5.11 shows CBR results for the various treated, soaked and un-soaked ASS materials at varying curing ages.

After 11.75% GGBS was added to 11.75% recycled glass in a mixture, the results show very high CBR values with the highest CBR value of 80% and the lowest CBR value of 21%. Compared with the previous addition of 23.5% recycled glass only which achieved the highest CBR value of 17% and a lowest CBR value of 3% of the mix.

This indicated that the addition of GGBS to the mixture has significantly improved the CBR value of the subgrade material. It was found that the presence of GGBS in the mixes significantly increased the compressive strength of geopolymer (Saludung et al., 2018). GGBS are rich in calcium, the main reaction product of C-S-H gel responsible for strength development (Sasui et al., 2019). GGBS contains a high amount of silica that upon activation with excess calcium form C-S-H gel which contributed to strength development (Saludung et al., 2018). It was found that with the increase in GGBS content, the CBR also increased up to the immediate formation of cemented products by hydration which increases the density of soil (Narendra et al., 2017). CBR values increase significantly with the addition of 10% GGBS in black cotton soil stabilisation (Darsi et al., 2021). Adding 15% GGBS to 1% polypropylene plastic fibre to expansive soil increased CBR values (Prasad, et al., 2019).

Expansive soil subgrade flexible pavement was improved by 90.48% with the addition of GGBS as a binder when compared with untreated expansive soil subgrade flexible pavement (Prasad, et al., 2019). An increase in CBR values with an increase in curing age was observed for both soaked and un-soaked ASS samples. However, the CBR values recorded for un-soaked ASS samples are higher compared with CBR values for soaked ASS samples. The lowest CBR value of 21% recorded for un-soaked ASS2 with high bentonite content after 7 days of curing later increased to 46% after 28 days can be increased further by increasing the GGBS content in the mix. An increase in CBR values was observed with an increase in GGBS (Kumar et al., 2020) and studies have revealed that using GGBS waste materials has the potential to modify the properties of clays (Narendra et al., 2017). It could be observed that CBR values for both soaked and un-soaked ASS2 composed of high bentonite content are on the low, due to the high amount of bentonite in the mix. It could be observed that CBR values achieved for 11.75% GGBS and 11.75% recycled glass are in the same range compared with CBR values achieved for 11.75% GGBS and 11.75% recycled plastic waste. This confirms that plastic pellets and glass grits used in this research behave in a similar manner due to their granular nature when used as binders in subgrade stabilisation. Mixing of randomly oriented glass and plastic granules to soil samples may be considered the same in soil stabilisation (Subash et al., 2016).

Even though the glass grits used in this research are randomly oriented and do not react chemically with other binders to form cementitious materials (C-S-H gel), their interlocking (mechanical stabilisation) within the mixture was not enough to increase the CBR value of subgrade materials. CBR values achieved for all ASS samples with the addition of 11.75% GGBS and 11.75% recycled glass waste in a mixture are greater than 2% making them usable in road construction as subgrade materials according to IAN73/06. As part of the commitment of many countries to reduce greenhouse gas emissions, and the environmental effect associated with landfills and overall road construction costs, GGBS and recycled glass waste can be used as binders to partially replace cement and lime in subgrade stabilisation. and the. GGBS can be utilised as an alternative to reduce the construction cost of the road, particularly in the rural areas of developing countries (Prasad, et al., 2019).

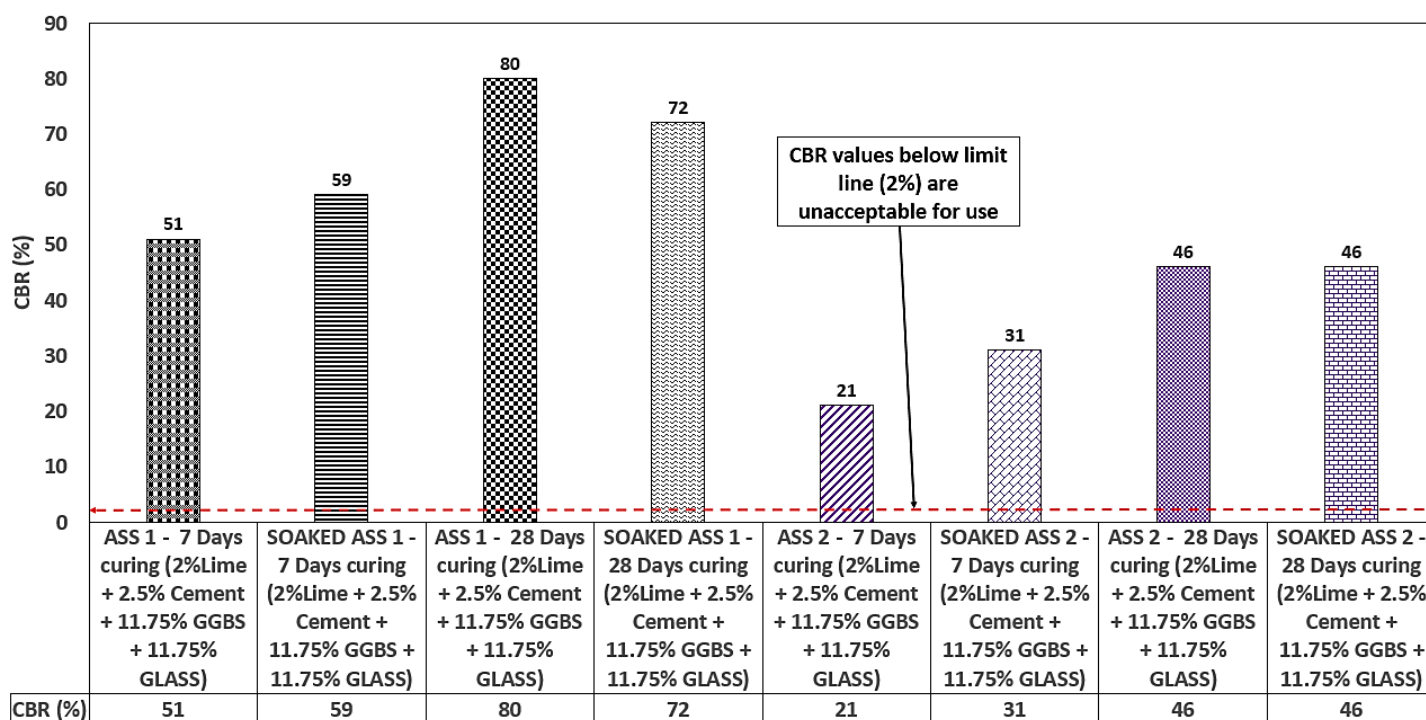


Figure 5.11: CBR results for the various treated, soaked and un-soaked ASS materials at varying curing ages

5.2.3.7 GGBS and Brick Dust Waste (BDW)

CBR value was recorded for ASS materials treated using 11.75% GGBS and 11.75% BDW as partial replacement for cement and lime in the mix. An extremely high CBR value of 109% was recorded for ASS1 after 28 days of curing with a slight reduction in CBR value of 97% for ASS1 sample when soaked after 28 days of curing at room temperature of $20 \pm 2^\circ\text{C}$. A CBR value of 61% was recorded for both ASS1 soaked

and un-soaked after 7 days of curing. ASS2 sample after 28 days of curing recorded a CBR value of 44% and later recorded a reduction in CBR value of 24% after it was soaked in water after 28 days of curing. ASS2 recorded a CBR value of 27% after 7 days of curing and when later soaked in water after 7 days of curing at room temperature of $20 \pm 2^\circ\text{C}$ recorded a CBR value of 16%. It was observed that CBR values for all samples crossed the 2% limit line making them suitable for use in road construction. Figure 5.12 shows CBR results for the various treated, soaked and un-soaked ASS materials at varying curing ages.

Adding GGB and BDW as partial replacements for cement and lime in stabilising ASS materials observed extremely high CBR values for soaked and un-soaked ASS1 after 28 days of curing. An increase in CBR value with an increase in curing age was observed for both soaked and un-soaked ASS materials and the highest CBR value of 109% in this research was recorded for un-soaked ASS1 after 28 days of curing. Soaked ASS1 after 28 days also recorded a very high CBR value of 97% after 28 days. This shows that C-S-H gel formation increases with an increase in curing age when GGBS and BDW are used as binders in a mix. The highest CBR value of lime and red brick powder was found in the 15% mixture, while the CBR-un-soaked result of red brick powder has the highest CBR value of 19.2% (Salimah et al., 2021). BDW are pozzolanic materials that form C-S-H gel responsible for strength gain in a mixture. GGBS is high in calcium and forms C-S-H gel during the hydration process for strength gain in a mixture. It was found that the addition of brick dust increased the soil strength between 1.7 and 2.3 times with respect to the non-stabilised materials (Hidalgo et al., 2019). The high CBR values observed for ASS materials can be attributed to the pozzolanic reaction responsible for the formation of C-S-H and C-A-H gel due to the presence of BDW in the mixture which acted as a binding agent responsible for strength gain and the high CBR value of the subgrade materials (Hewlett, 2003).

Pozzolans are materials such as BDW that contain alumina/silica which reacts to form new compounds (Calcium silicate hydrate (C-S-H) and Calcium aluminium Hydrates (C-A-H) when lime is added and have the ability to modify the properties of a lime mixture (Rogers, 2011). BDW exhibits pozzolanic properties which can be used as cement replacement in road subgrade stabilisation (Kartini et al., 2012). GGBS are

highly cementations and high in strength-enhancing compounds calcium silicate hydrate (C-S-H) which improves strength and durability in a mix. Studies have shown that the higher the amount of GGBS blend, the greater the hydraulic activity (Hewlett, 2003). The addition of a little amount of 2% lime and 2.5% cement to the mix in this research also contributed to the high strength gain of ASS materials because GGBS works well with the addition of lime. The alkaline properties of Portland cement, lime and other activators such as sulphates, chlorides and alkali silicates are sufficient to activate the cementitious properties of GGBS (One et al., 2007). Adding GGBS and lime induces the calcium silicate hydrate bond in the soil to accelerate the formation of cementitious substances in the soil during curing under standard room temperature of $20\pm 2^{\circ}\text{C}$. (Saravanan et al., 2017).

Adding lime to GGBS helps in strength development because GGBS alone in a mix exhibits very slow strength development under standard 20°C curing conditions compared to other conventional stabilisers (Escalante-Garcia and Sharp, 2004). GGBS and lime react chemically with the right amount of water at ordinary temperature to form compounds that possess the properties of cement (O'Farrell et al., 2001). Soaked and un-soaked ASS1 recorded a CBR value of 61% after 7 days of curing. This shows that CBR values for high plasticity subgrades ASS1 do not increase by soaking in water after 7 days of curing. However, a later increase in CBR values was observed after 28 days of curing. When compared with un-soaked ASS1, ASS2 soaked and un-soaked recorded low CBR values. This could be a result of high bentonite content in ASS2 (extremely high plasticity index). The lowest CBR value was recorded for soaked ASS2 after 7 days of curing. However, all CBR values achieved for all ASS samples with the addition of 11.75%GGBS and 11.75% BDW in a mixture are greater than 2% making them usable in road construction as subgrade materials according to IAN73/06. As part of the commitment of many countries to reduce greenhouse gas emissions, and the environmental effect associated with landfills and overall road construction costs, GGBS and BDW can be used as binders to partially replace cement and lime in subgrade stabilisation.

GGBS can be utilised as an alternative to reduce the construction cost of the road, particularly in the rural areas of developing countries (Prasad, et al., 2019). The use of GGBS binders at high volumes as supplementary cementitious materials are good

from the environmental point of view, hence the higher the amount of GGBS used in replacing cement in soil stabilisation the lesser the carbon footprint (Onn et al., 2019). The addition of brick dust resulted in an increase in the soil strength and its suitable materials for use in practical applications in construction (Hidalgo et al., 2019). Using brick waste as binders in place of cement and lime in subgrade stabilisation will help reduce the greenhouse gas emitted to the atmosphere due to cement and lime production as well as reduce the environmental effect associated with brick stockpiles and landfills.

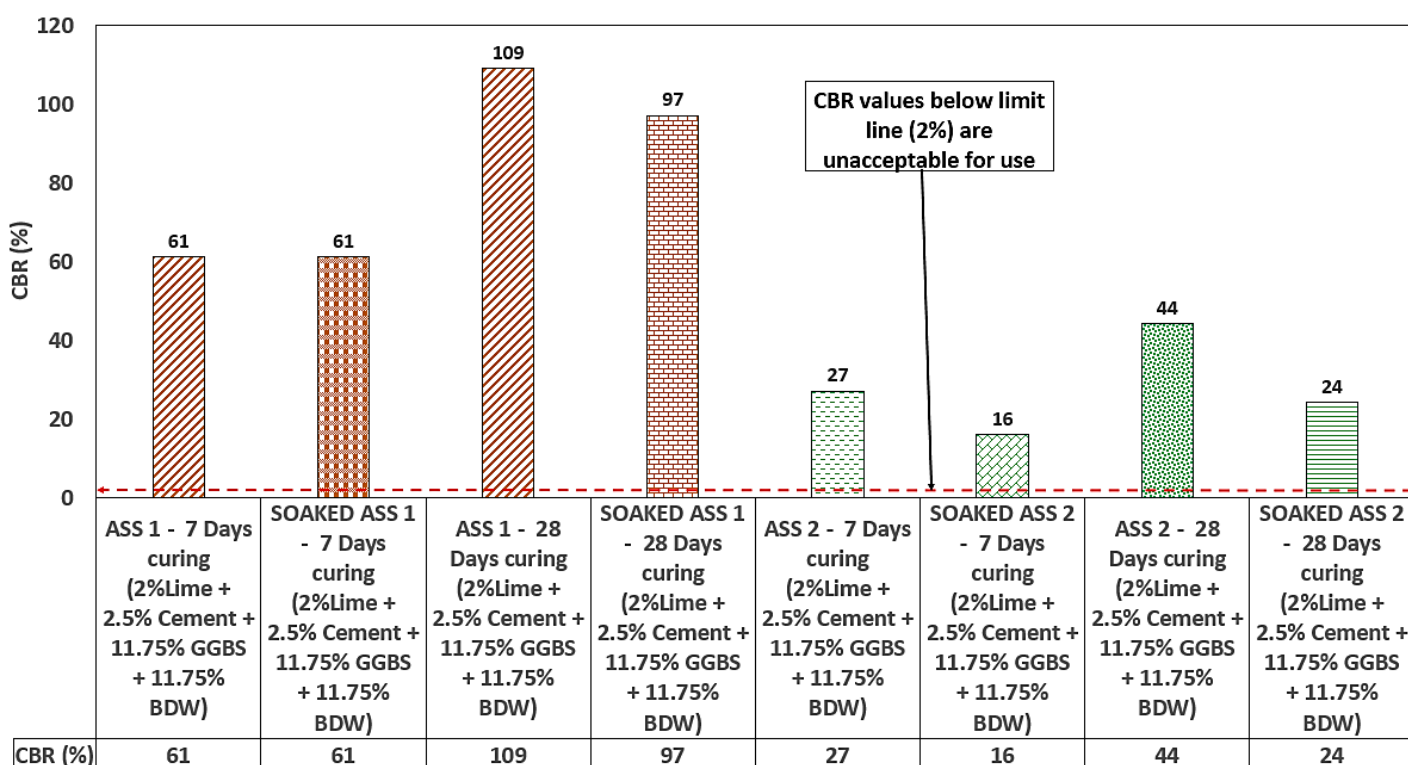


Figure 5.12: CBR results for the various treated, soaked and un-soaked ASS materials at varying curing ages

5.2.3.8 CBR for Best-performing Mixes After 90 Days of Curing

Best performing mixes recorded extremely high CBR values of 180% and 120% for ASS1 and 2 + 2%Lime +2.5% cement +11.75%GGBS+11.75%BDW, 200% and 96% for ASS1 and 2 + 2%Lime +2.5% cement +23.5%GGBS after 90 days of curing. The highest CBR value of 220% was observed for ASS1+ 2%Lime + 26%GGBS with total elimination of cement in the mix. A CBR value of 98% was recorded for ASS2+ 2%Lime + 26%GGBS, respectively. Figure 5.13 shows CBR results for best-performing mixes and mixes without cement cured and tested after 90 days. The very

high CBR values recorded for the best performing mixes after 90 days of curing could be attributed to the long curing period. This proves that subgrade materials treated using GGBS and BDW accumulate strength with increased curing age. The highest CBR value of 220% recorded for mix design without cement but high GGBS content and a little lime shows that GGBS is capable of improving the engineering properties of subgrade materials after a longer period of curing (Escalante-Garcia and Sharp, 2004).

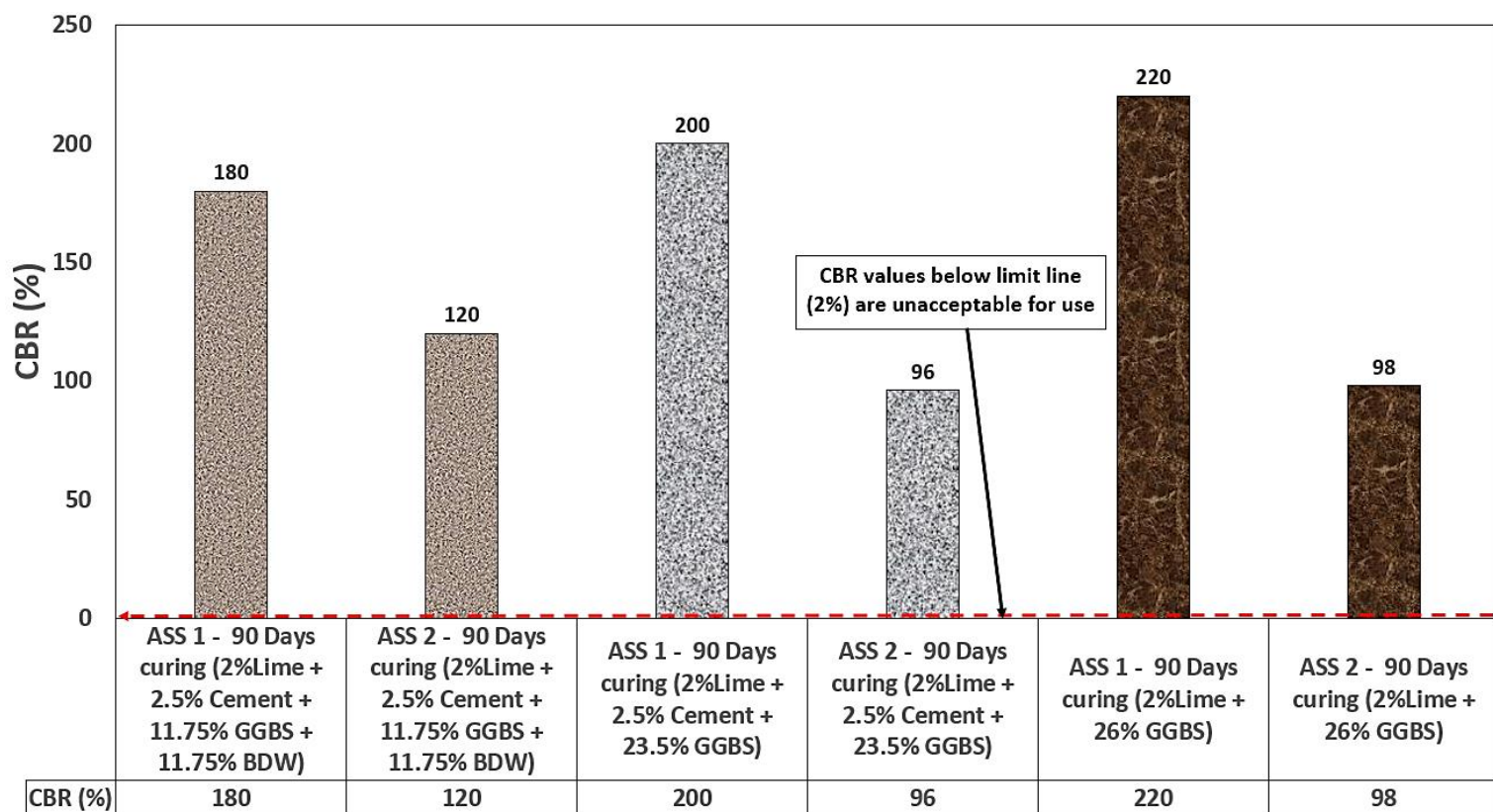


Figure 5.13: CBR results for best performing mixes and mix without cement cured and tested after 90 days

5.3 SWELL FOR ASS MATERIALS

5.3.1 Treated and Untreated Artificially Synthesised Subgrade Materials

Swell test in this research was conducted in accordance with two different standards BS EN 13286-47:2021 and BS EN 13286-49:2004 with the aim of comparing short-term swelling and long-term swelling pressure of untreated ASS materials. BS EN 13286-47:2021 recommend soaking CBR samples and measuring swell for a period of 4 days (96 hours). So, in order to investigate the extent of swell for ASS materials beyond 4 days, BS EN 13286-49:2004 standard for testing was used to measure the swell of ASS samples after 28 days. After the treatment, it was observed that swell

potentials reduced drastically with the addition of 8% lime and 20% cement as binders in the mixture. The swelling potential of ASS samples using BS EN 13286-49:2004 reduced drastically after 28 days of soaking. Untreated ASS2 (75% Bentonite and 25% Kaolinite) with the highest swell percentage of 56.76% reduced to 0.2% after treating ASS materials using cement and lime.

Untreated ASS1 (25% Bentonite and 75% Kaolinite) with an unacceptable swell value of 35.92% reduced to 0.04% after curing using cement and lime as binders. The lowest swell value of 0.04% was recorded for ASS1. However, a swell value of 0.2% (even though acceptable) was recorded for ASS2 with the highest amount of bentonite (extremely high plasticity index) content. This indicates very high swell potentials for subgrade materials with high plasticity index. Swell values for treated ASS materials using BS EN 13286-47:2021 recorded acceptable swell values of 0.06% for ASS2 and 0.04 % for ASS1 after 7 and 28 days of curing. ASS1 of 4.11% was reduced to 0.03% after 7 and to 0.02% after 28 days of curing. This shows that adding high cement and lime content to a mix can reduce the swell potentials of expansive subgrade making them usable as subgrade materials. Swell potentials were reduced by 42.5% at 4% lime and by 46.4% at 20% cement (Phanikumar et al., 2015). Using cement and lime reduces the plasticity index of ASS materials leading to swell potential reduction. This was responsible for the low swell values recorded for ASS1 and 2 after 7 and 28 days of curing. According to Abbey et al. (2020), the addition of 5% and 8% cement after 28 days of curing saw a reduction in plasticity index resulting in decreased swell pressure of the bentonite-kaolinite mixed clays.

A dosage of 6% lime reduced swelling pressure by 27% with a later reduction of 96% in swell pressure (Kechouane et al., 2015). The reduction in swell value observed with an increase in curing age can be attributed to the formation of calcium silicate hydrate (C-S-H) gel and calcium aluminate hydrate (C-A-H) gel also referred to as Tobermorite in the mixture. During the hydration process in a cement/lime mix under normal room temperature, cementitious products are released (C-S-H and C-A-H gel) which are responsible for strength gain and reduced swell pressure in the mixture. According to Zhang et al (2014), the continuous formation of C-S-H gel with an increase in curing age within a pore structure contributes to reduced swell pressure hence the higher the C-S-H gel the lower the swell pressure in the samples (Abbey et al., 2020). After

comparing untreated ASS with treated ASS materials swell pressure for ASS materials was reduced drastically using cement and lime. the mixing of cement in the soil improved swell potential by 70% (Hindu et al., 2015). Comparing soaked CBR with swell values shows the highest swell value of 0.06% for treated ASS2 after 7 days of curing recorded the lowest CBR value of 34% and later recorded the highest CBR value of 61% with further reduction in swell values of 0.04% after 28 days of curing.

A similar trend was observed for ASS1 swell value of 0.03% recorded the second-lowest CBR value of 45% after 7 days of curing and later recorded the second-highest CBR value of 50% with further reduction in swell values of 0.02% after 28 days of curing. This trend shows that a reduction in swell pressure results in an increase in CBR value for ASS materials and vice versa. Mixing cement in the soil improved the CBR values and decreased the swelling potential of the soil (Hindu et al., 2015). The addition of lime reduced free swelling from 80.00% to 6.70% and increased CBR value from 1.20% to 86.70% (Ismail et al., 2013). The addition of 10% lime makes black cotton soil non-plastic, non-swelling and attains increased CBR values (Rao et al., 2021). Comparing treated ASS materials with treated CBR values it was observed that all treated swell values are $< 2.5\%$ and CBR values are $> 2\%$ making all ASS samples suitable for use in road construction. According to standard practice, subgrade swell $> 2.5\%$ are unacceptable and would require treatment or removal and replacement (Troy, 2016). IAN73/06 states that CBR values $> 2\%$ are accepted for use in road construction as subgrade materials.

Even though cement and lime can be used in subgrades stabilisation, they are associated with high costs and high CO₂ emissions. Due to this, they are not sustainable, and their use must be discouraged by finding novel binders as a replacement. Cement and lime production consume very high energy and heavily pollute the environment through CO₂ emission. A large number of CO₂ emissions were produced by the decomposition of calcium carbonate in the lime production process (Zhang et al., 2019). Climate change and carbon emissions are the main environmental issue for the cement and lime industry (Environmental Agency, 2020). Using non-traditional stabilisers in subgrade stabilisation has proven to be more environmentally friendly, cheaper and effective in improving the engineering properties of expansive subgrade materials (Kassa et al., 2020). Using waste materials in

subgrade stabilisation will reduce overall project costs and greenhouse gas emissions while saving landfill space.

5.3.2 Swell Test in Accordance with BS EN 13286-47:2021

After conducting swell test using BS EN 13286-47:2021, high swell potentials were recorded for untreated ASS1 and 2. However, ASS2 composed of high bentonite content recorded the highest swell with a swell value of 5.03% followed by untreated ASS2 of 4.11%, respectively. This shows that high and extremely high plasticity subgrade materials (ASS1 and 2) have very high swell potentials and swell potentials increase with an increase in bentonite content in a mix. A maximum swell value of 5.03% was recorded for ASS2 (75% Bentonite + 25% kaolinite) without treatment, followed by ASS1 (25% Bentonite + 75% kaolinite) which recorded a swell value of 4.11%. A gradual increase in swell was observed for ASS1 and 2 on day 1 of 1.83% and 1.29% and later increased to 4.06% and 3.36% on day 2, the sample later increased in swell on day 3 of 4.64% and 3.87% and finally increased to 5.03% and 4.11% at day 4, respectively. It was observed that ASS1 and 2 crossed the limit line making them unsuitable for use as subgrade materials in road construction. After cement and lime were used as binders to treat ASS materials, swell at the end of day 4 reduced from 5.03% to 0.06% and 0.04% for ASS2 after 7 and 28 days of curing. Swell value for ASS1 was reduced from 4.11% to 0.02% after treating ASS1 using lime and cement as binders.

A gradual reduction of ASS samples was observed on day 1 with a 0.01% and 0.02% increase and later with a 0.01%, 0.02%, 0.03 and 0.04% on day 2, this trend continued until day 4 with a maximum swell value of 0.06% for ASS2, 0.04% for ASS1 after 28 days curing followed by a swell of 0.02% for ASS1 after 7 and 28 days curing at room temperature of $20 \pm 2^\circ\text{C}$. A drastic reduction in swell potential was observed with treated ASS materials way below the limit line with the highest swell value of 0.06% after comparing treated and untreated ASS samples after 7 and 28 days of curing. From the comparison, it can be seen that treated ASS materials using cement and lime are below the limit line and are suitable for use as subgrade materials in road construction while untreated ASS materials above the limit line are not suitable for use as subgrade materials in road construction. Figure 5.14 shows swell results for

untreated ASS materials only, Figure 5.15 shows treated ASS materials using cement and lime as binders and Figure 5.16 shows combined results of treated and untreated ASS materials for comparison purposes. Figure 5.17 shows 4 days of cement and lime treated swell values and soaked CBR values.

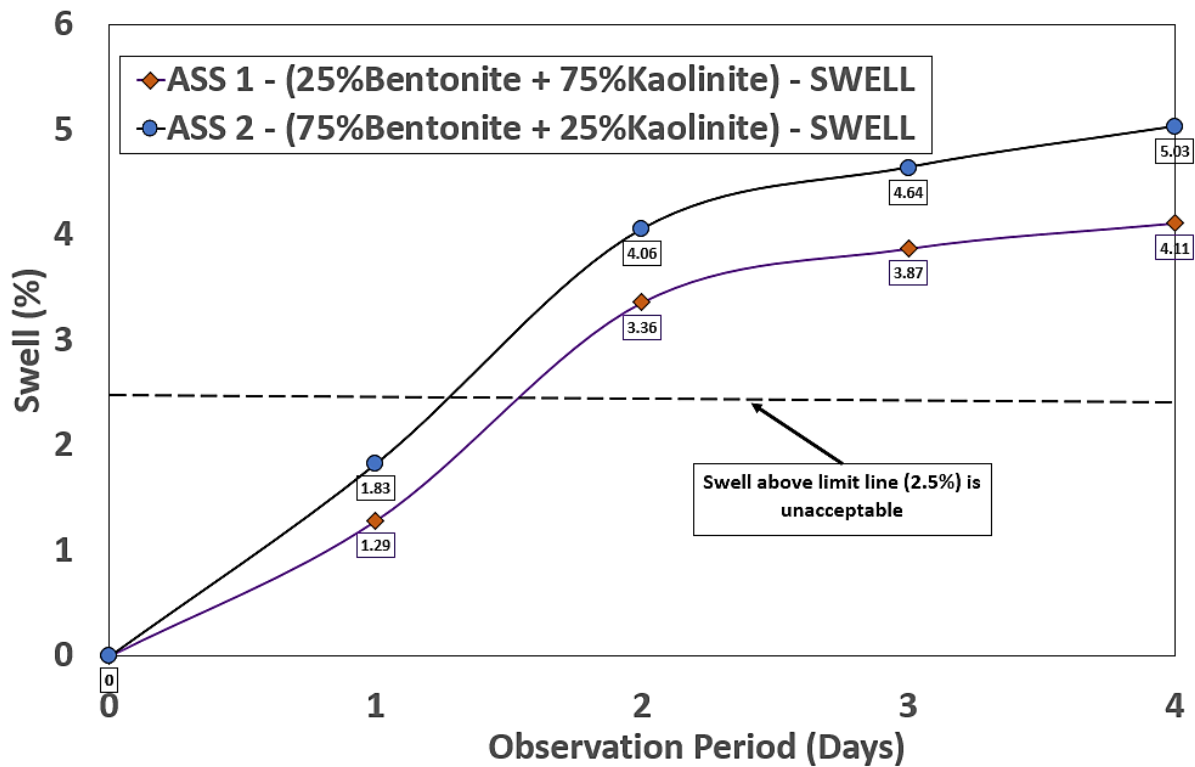


Figure 5.14: Swell results for untreated ASS materials only

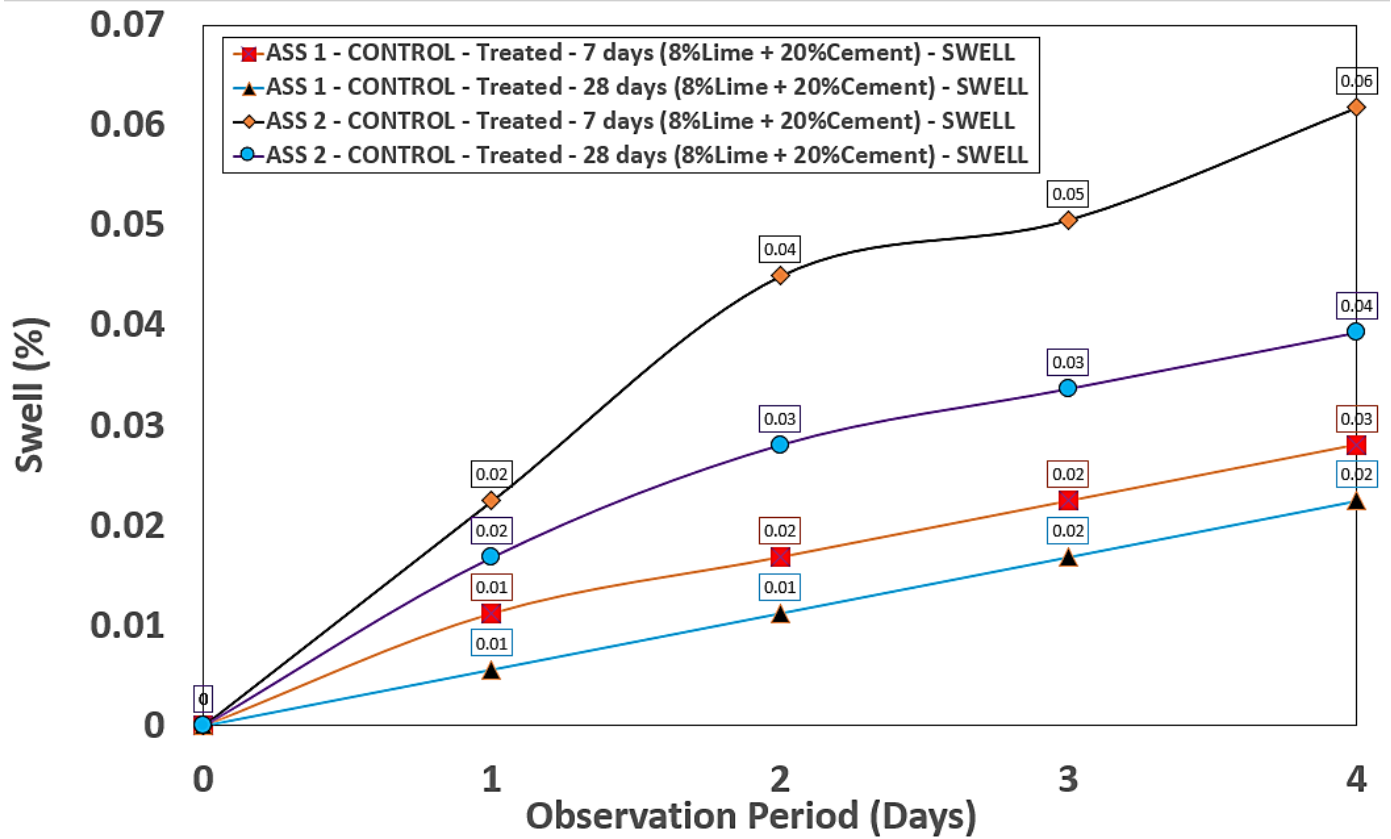


Figure 5.15: Treated ASS materials using cement and lime as binders

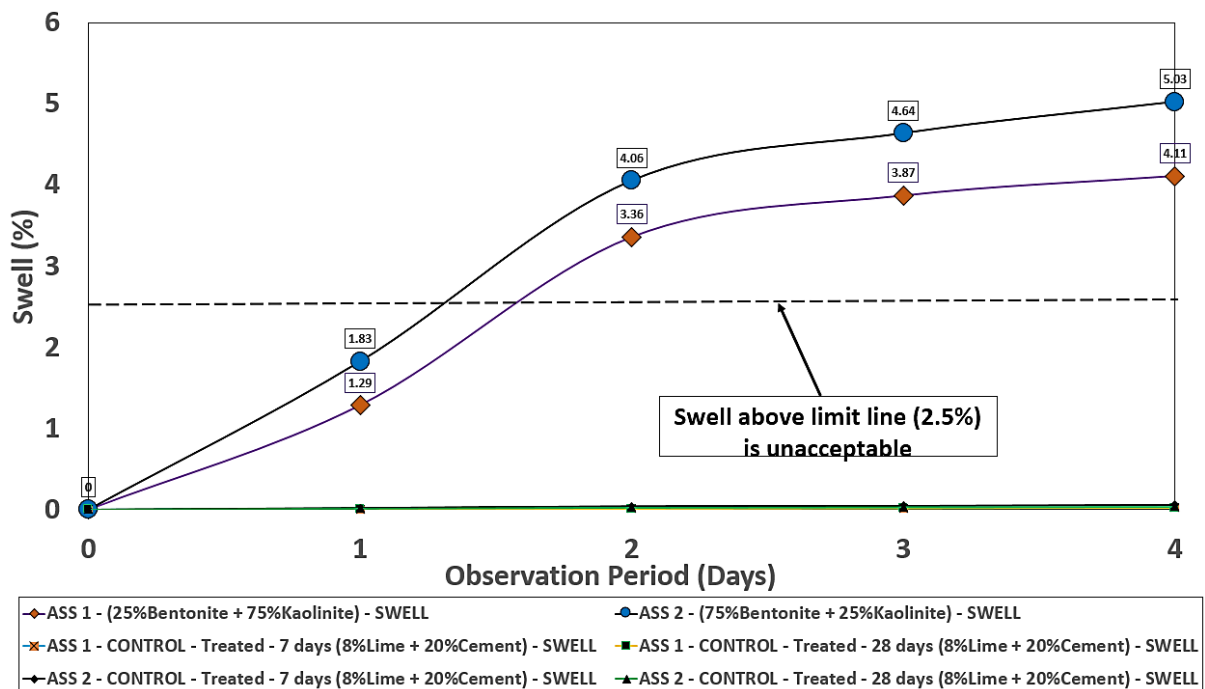


Figure 5.16: Combined results of treated and untreated ASS materials for comparison purposes

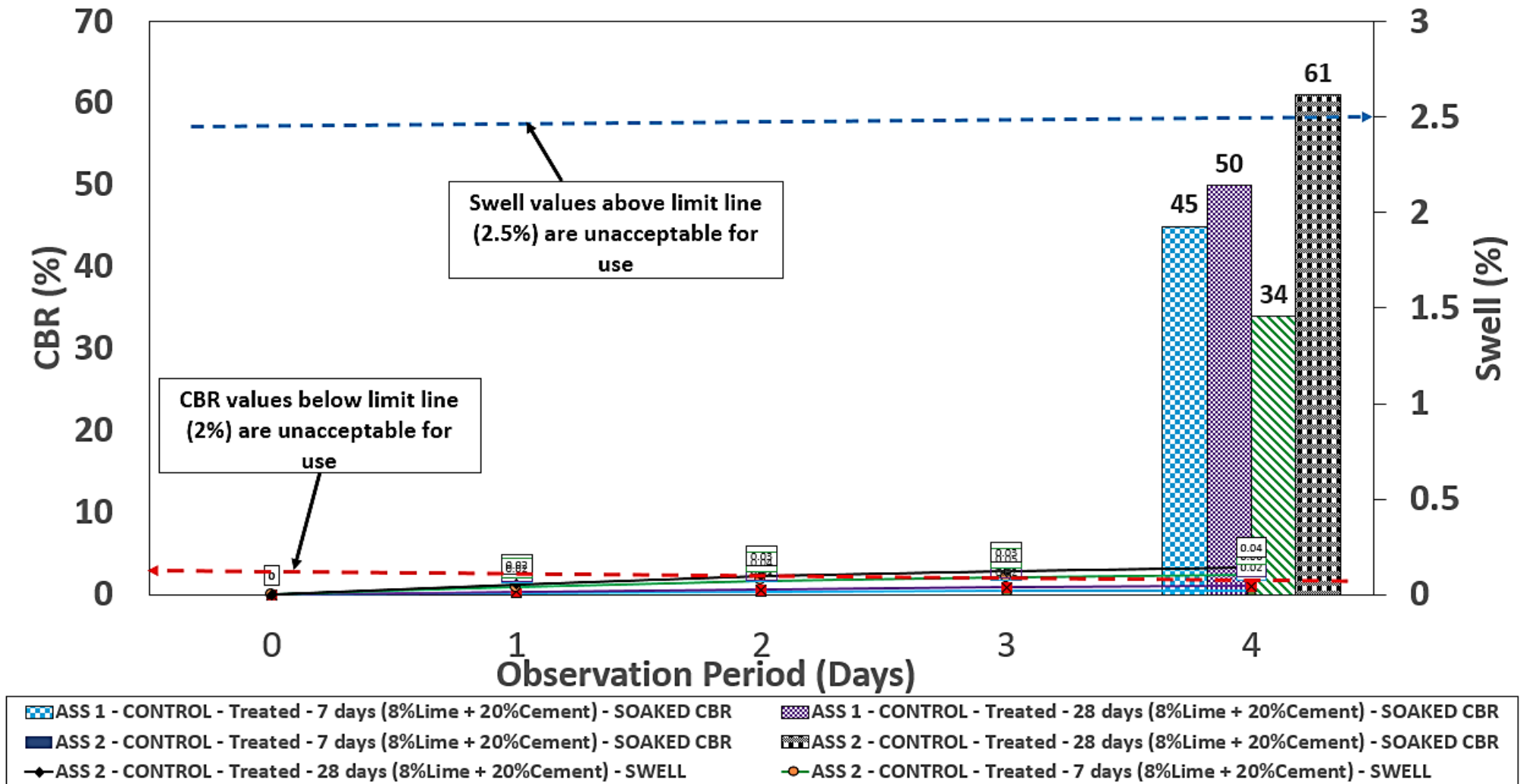


Figure 5.17: 4 days cement and lime treated swell values and soaked CBR

5.3.3 Variation in Swell Using BDW In Accordance with BS EN 13286-47:2021

A reduction in swell was recorded for all ASS samples after 7 and 28 days of curing. The highest ASS value was recorded for ASS2 with a swell value of 0.63% at the end of day 4 followed by ASS1 of 0.58% at day 4. A sharp increase in swell value was recorded on day 1 for all ASS samples with swell values of 0.59%, 0.51%, 0.45% and 0.31%, respectively, after 7 and 28 days of curing at room temperature of $20 \pm 2^\circ\text{C}$. Swell values began to stabilise on day 2 through till day 4 with the maximum swell values of 0.63 for ASS2 and 0.58 for ASS1. After comparing untreated ASS samples with samples treated using BDW, it was observed that ASS values recorded for treated ASS materials are below the limit line making them suitable for use as subgrade materials in road construction.

A reduction in swell values was achieved after stabilising expansive ASS materials using BDW. ASS2 (extremely plastic) with an unacceptable swell value of 5.03% was reduced to 0.53% and 0.51% after 7 and 28 days of curing. It was observed that ASS2 after 7 days recorded the highest swell of 0.63% followed by ASS2 with a swell of 0.61% after 28 days. ASS1 recorded a swell value of 0.58% after 7 days of curing and later swell was reduced to 0.56% after 28 days of curing. This shows a decrease in swell pressure with an increase in curing age for ASS1 and 2. Brick dust significantly decreased the swell potential of soil with an increase in curing age (Michael et al., 2016). This shows that BDW has the potential to reduce swell in expansive subgrade materials and improve its engineering properties. Studies have shown that partial replacement for cement in expansive subgrade stabilisation with BDW achieved good engineering properties (Lihua et al., 2020). The addition of 50% BDW reduced swell liner shrinkage in subgrade stabilisation (Ali et al., 2014). After comparing swell values for treated ASS using BDW to untreated ASS it was observed that ASS treated using BDW are $< 2.5\%$ making them acceptable for use as subgrade material according to Troy, (2022).

It was observed that ASS1 recorded the lowest swell value of 0.56% after 28 days of curing with the highest soaked CBR value of 28%. The highest swell value of 0.63% recorded for ASS2 with high bentonite content after 7 days of curing recorded the lowest soaked CBR value of 18%. This shows an increase in CBR value with a decrease in swell potentials for ASS samples. Comparing the swell values for BDW

treated ASS samples with cement and lime (control) treated ASS samples, observation showed that swell values for cement and lime treated ASS samples were very low. The lowest swell for cement treated sample was 0.02% and the highest was 0.06% while the lowest swell for BDW treated sample was 0.56% and the highest was 0.63%. However, swell values achieved for BDW-treated ASS samples are acceptable for use in road construction. CBR increased to over 400% when an optimum brick dust waste (BDW) of 40% was used during expansive subgrade stabilisation (Anand et al., 2014). CBR increased with BDW content from 5% to 20% (Al-Baidhani et al., 2019). Good CBR and swell results were achieved when 20% of brick dust waste was used in expansive subgrade stabilisation for flexible pavement (Reddy et al., 2018).

The low swell and high CBR values observed for ASS materials can be attributed to the pozzolanic reaction responsible for the formation of C-S-H and C-A-H gel due to the presence of BDW in the mixture which acted as a binding agent responsible for strength gain and high CBR value of the subgrade materials (Consoli et al., 2009). Pozzolans are materials such as BDW that contain alumina/silica which reacts to form new compounds (Calcium silicate hydrate (C-S-H) and Calcium aluminium Hydrates (C-A-H) when lime is added and have the ability to modify the properties of a lime mixture (Rogers, 2011). Brick Dust Waste (BDW) exhibits pozzolanic properties which can be used as cement replacement in road subgrade stabilisation (Kartini et al., 2012). Using BDW as cement and lime replacement in subgrade stabilisation would reduce overall construction costs, reduce CO₂ emission due to cement and lime production and ease the pressure on scarce raw materials such as clinker used in cement production. Blended stabilisers achieved better performance and results suggest the technological, economic and environmental advantages of using brick dust to achieve sustainable infrastructure development (Kinuthia et al., 2011). Figure 5.18 shows swell results for ASS samples treated using 23.5% BDW as partial replacement for cement and lime in the mix Figure 5.19 shows combined results of treated and untreated ASS materials for comparison purposes. Figure 5.20 shows 4 days swell values at the various points of the curve for sustainable treated ASS and soaked CBR values.

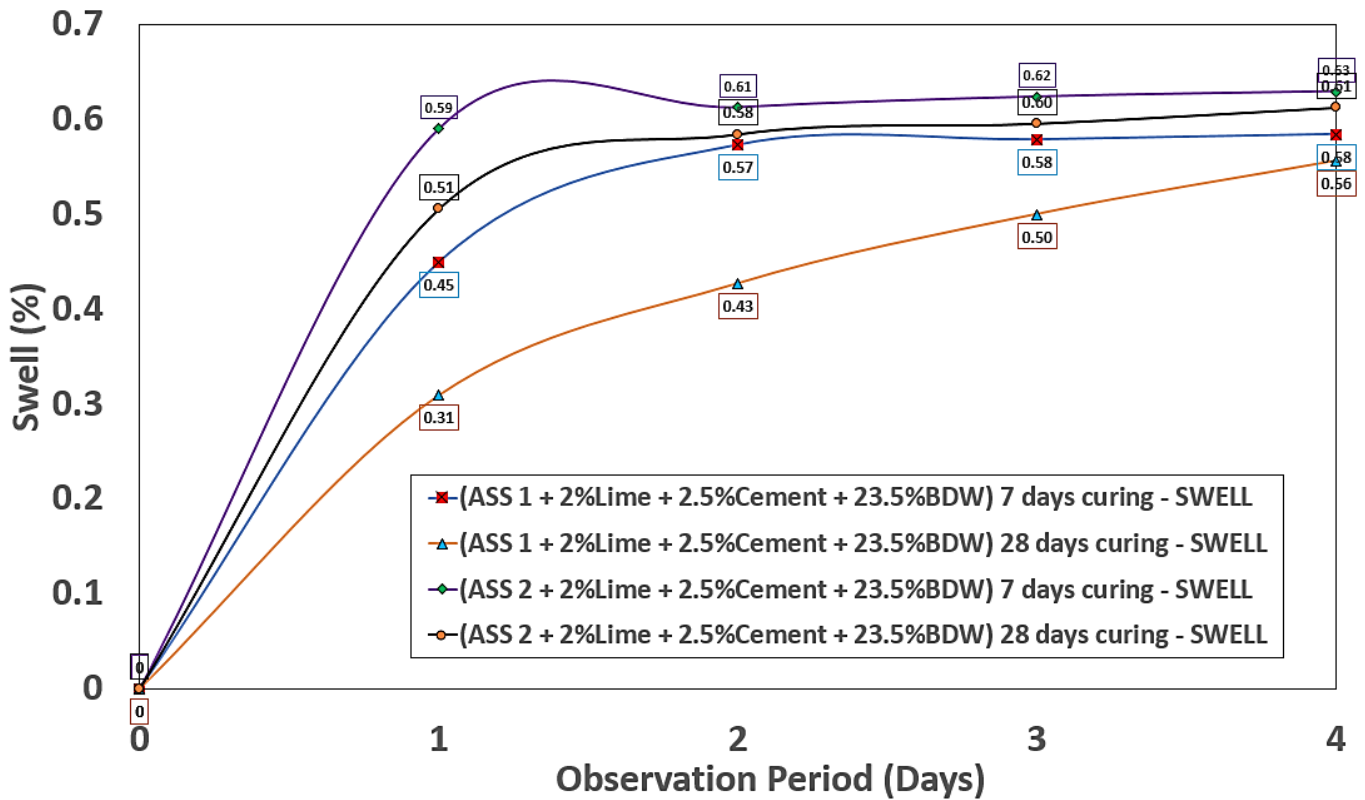


Figure 5.18: Swell results for ASS samples treated using 23.5% BDW

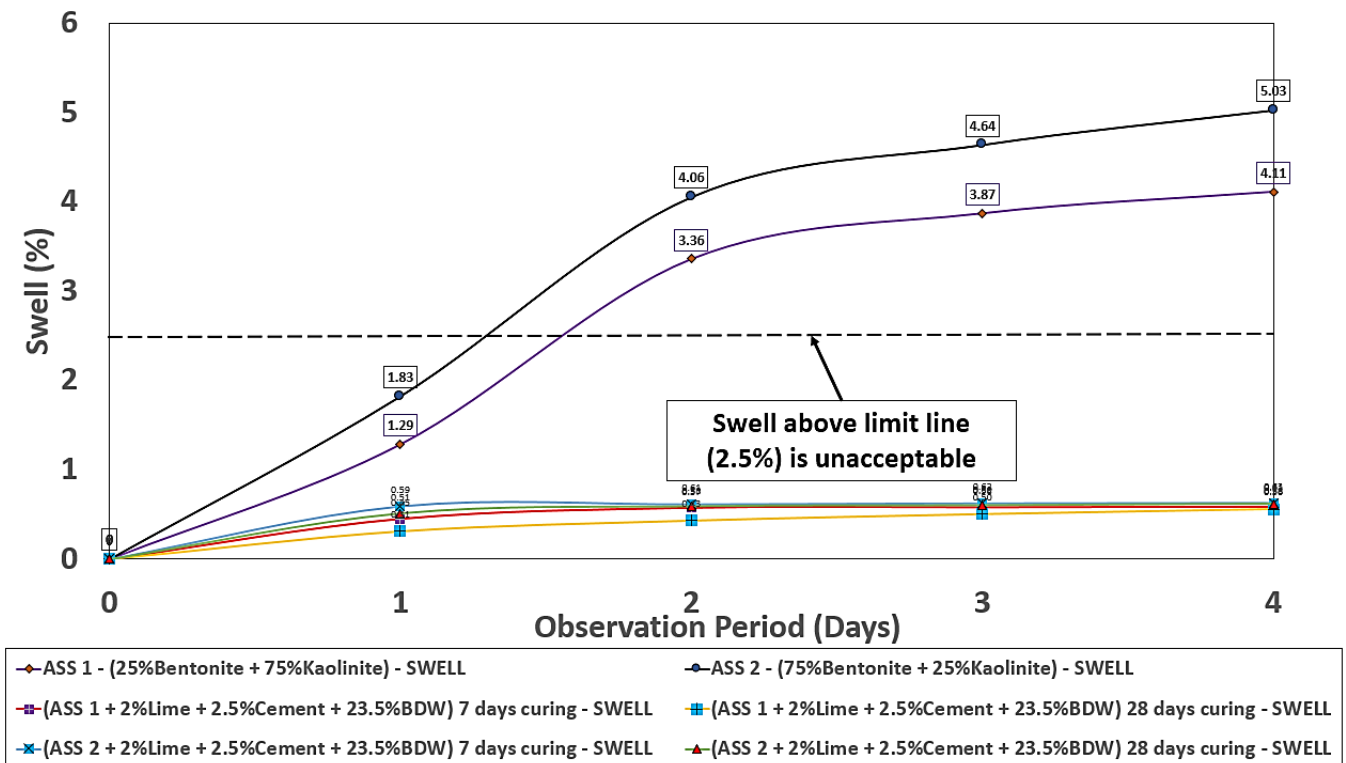


Figure 5.19: Combined results of treated and untreated ASS materials

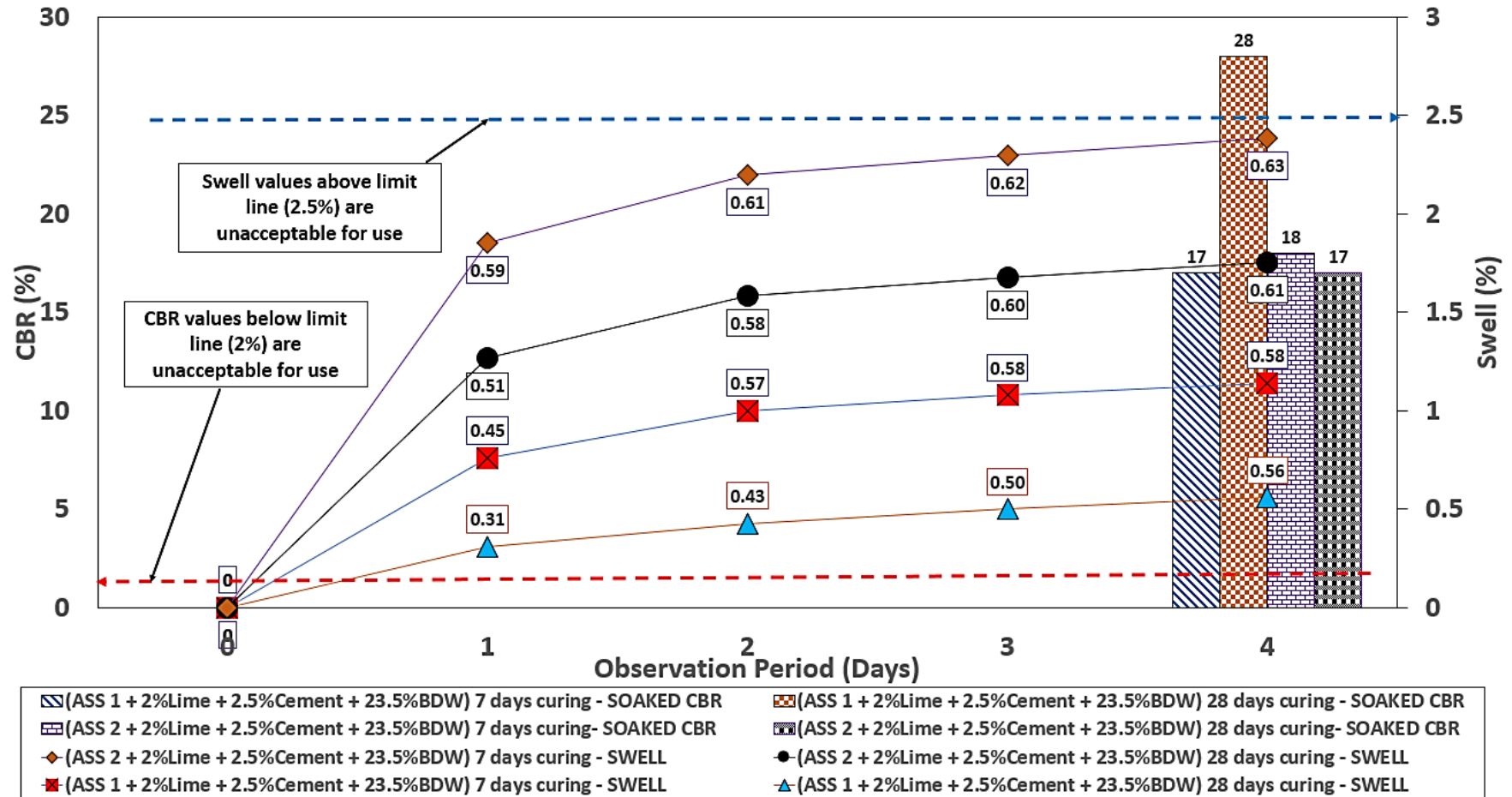


Figure 5.20: 4 days swell values for sustainable treated ASS and soaked CBR

5.3.4 Variation in Swell Using GGBS In Accordance with BS EN 13286-47:2021

A reduction in swell potential was observed for ASS materials treated using 23.5% GGBS as partial replacement for cement and lime in the mix. The highest swell value of 0.50% for ASS2 on day 4 and the lowest swell value was recorded for ASS1 at 0.32% at the end of day 4. A gradual increase in swell values was observed from day 1 to day 4 with small values of 0.46% for ASS1 after 7 days of curing, and 0.32% for ASS1 after 28 days of curing all on day 4. ASS2 recorded swell values of 0.50% and 0.43% after day 7 and 28 days of curing at room temperature of $20 \pm 2^\circ\text{C}$. After comparing untreated ASS samples with samples treated with GGBS, it was observed that ASS values recorded for treated ASS materials are below the limit line making them suitable for use as subgrade materials in road construction. Figure 5.21 shows swell results for ASS samples treated using 23.5% GGBS as partial replacement for cement and lime in the mix. Figure 5.22 shows the combined results of treated and untreated ASS materials for comparison purposes.

GGBS has been reported to be a binder with high calcium content with the ability to reduce swell potentials and increase strength in expansive subgrade. GGBS are rich in calcium, the main reaction product of C-S-H gel responsible for strength development (Sasui et al., 2019). ASS materials were stabilised using a high amount of 23.5% GGBS as partial replacement for cement and lime and the reductions saw an improvement in the engineering properties of expansive subgrade. A reduction in swell value with an increase in curing age was observed for ASS samples. ASS2 after 7 days of curing recorded the highest swell of 0.50% followed by ASS2 with a swell value of 0.47% after 28 days of curing. ASS1 recorded a swell value of 0.46% after 7 days of curing and later swell was reduced to 0.32% after 28 days of curing. This shows a decrease in swell pressure with an increase in curing age for ASS1 and 2. The decrease in swell for ASS samples are as a result of high calcium content in GGBS. Calcium is the main ingredient for the formation of C-S-H gel responsible for the swell reduction and strength gain in a mix. GGBS contains a high amount of calcium forming C-S-H gel which contributed to strength development (Saludung et al., 2018). It was found that with the increase in GGBS content, the CBR also increased up to the immediate formation of cemented products by hydration which increases the density of soil (Narendra et al., 2017). CBR values increase significantly with the addition of 10% GGBS in black cotton soil stabilisation (Darsi et al., 2021).

Adding 15% GGBS to expansive soil increased CBR values (Prasad et al., 2019). Expansive soil subgrade flexible pavement was improved by 90.48% with the addition of GGBS as a binder when compared with untreated expansive soil subgrade flexible pavement (Prasad et al., 2019).

Comparing the swell values for GGBS treated ASS samples with cement and lime (control) and BDW treated ASS samples, It was observed that swell values for cement and lime treated ASS samples were very low. The lowest swell for cement-treated sample was 0.02% and the highest was 0.06% while the lowest swell for BDW treated sample was 0.56% and the highest was 0.63%. However, the lowest swell for GGBS treated sample was 0.32% and the highest was 0.50%. even though cement and lime recorded very low swell values, GGBS samples had the lowest swell compared with BDW samples. The swell values achieved for GGBS-treated ASS samples are acceptable for use in road construction. ASS2 after 7 days of curing recorded the highest swell value of 0.50% and the lowest soaked CBR value of 46% and ASS1 with the lowest swell value of 0.32% recorded the highest soaked CBR value of 97%. Hence, a reduction in swell pressure using GGBS as a binder in a mix translates to very high soaked CBR values usable in road construction. According to standard practice, subgrade swell >2.5% are unacceptable and would require treatment or removal and replacement (Troy, 2016). IAN73/06 states that CBR values >2% are accepted for use in road construction as subgrade materials. Even though cement and lime can be used in subgrade stabilisation, they are associated with high costs and high CO₂ emissions. Figure 5.23 shows 4 days swell values at the various points of the curve for sustainable treated ASS and soaked CBR for comparison.

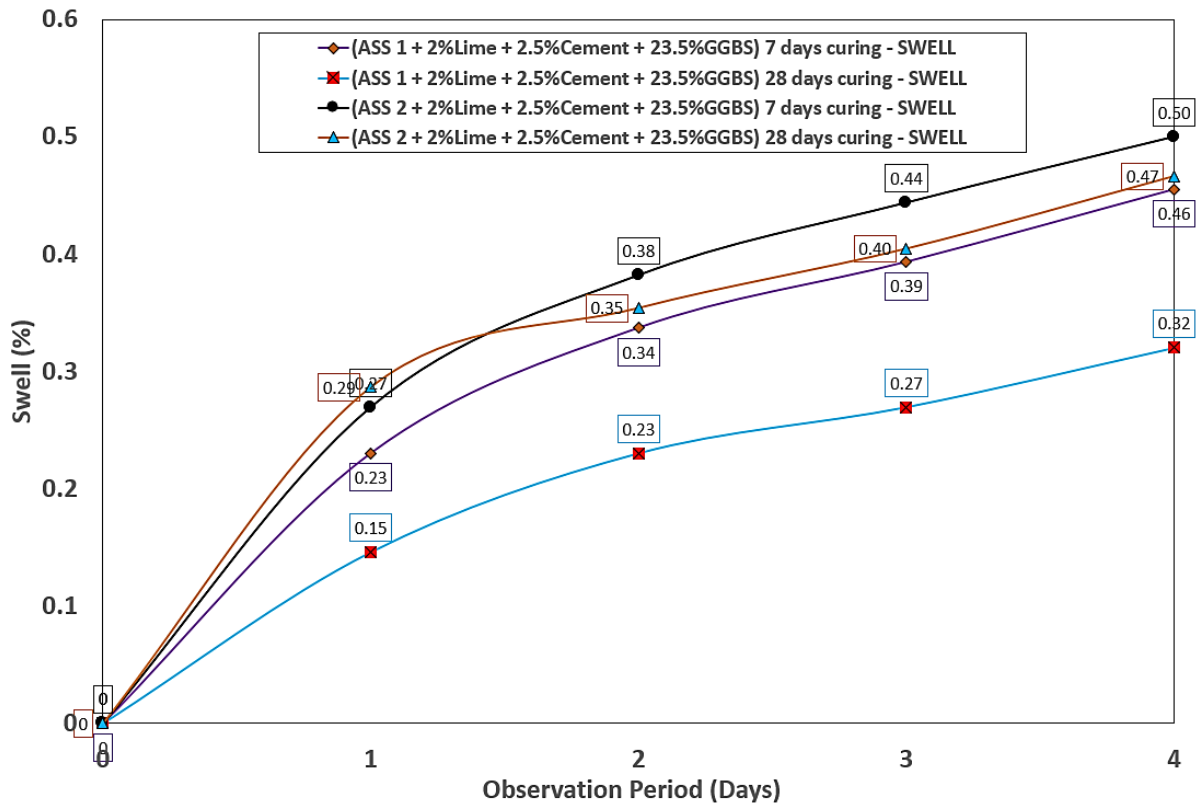


Figure 5.21: swell results for ASS samples treated using 23.5% GGBS

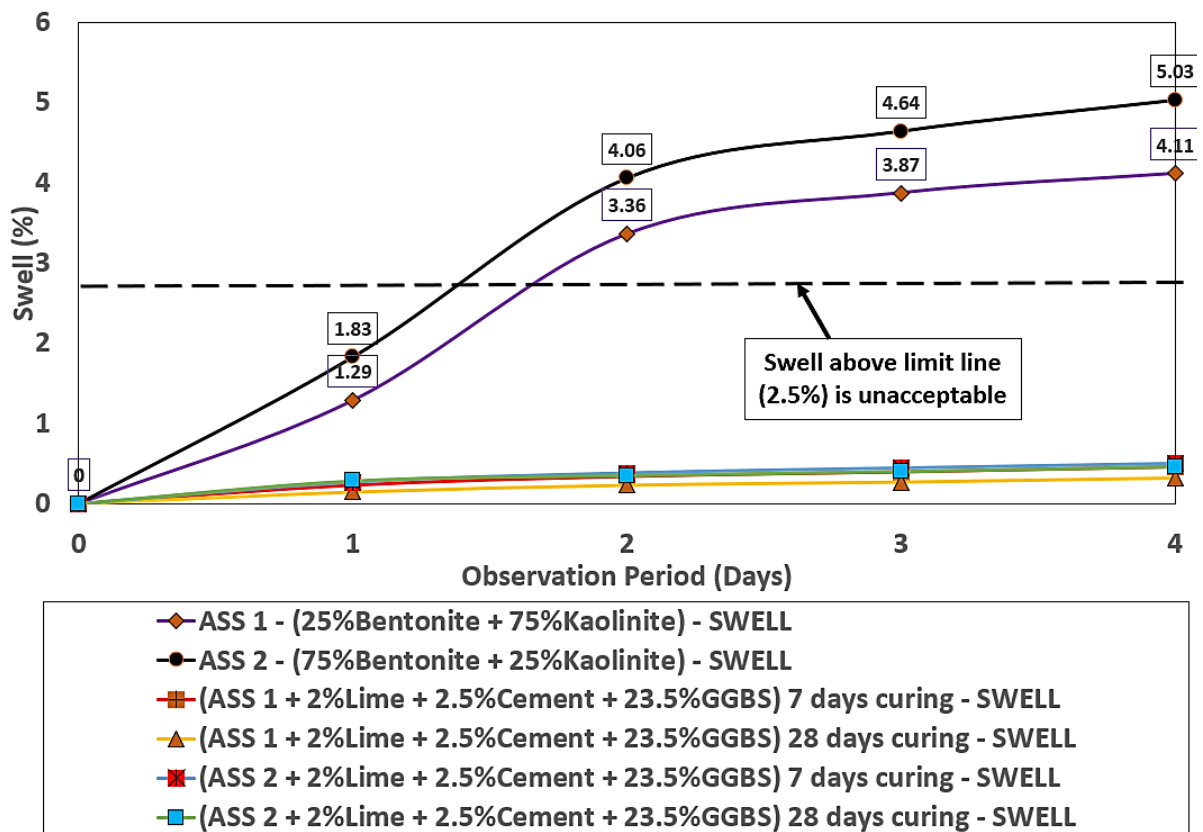


Figure 5.22: Combined results of treated and untreated ASS materials

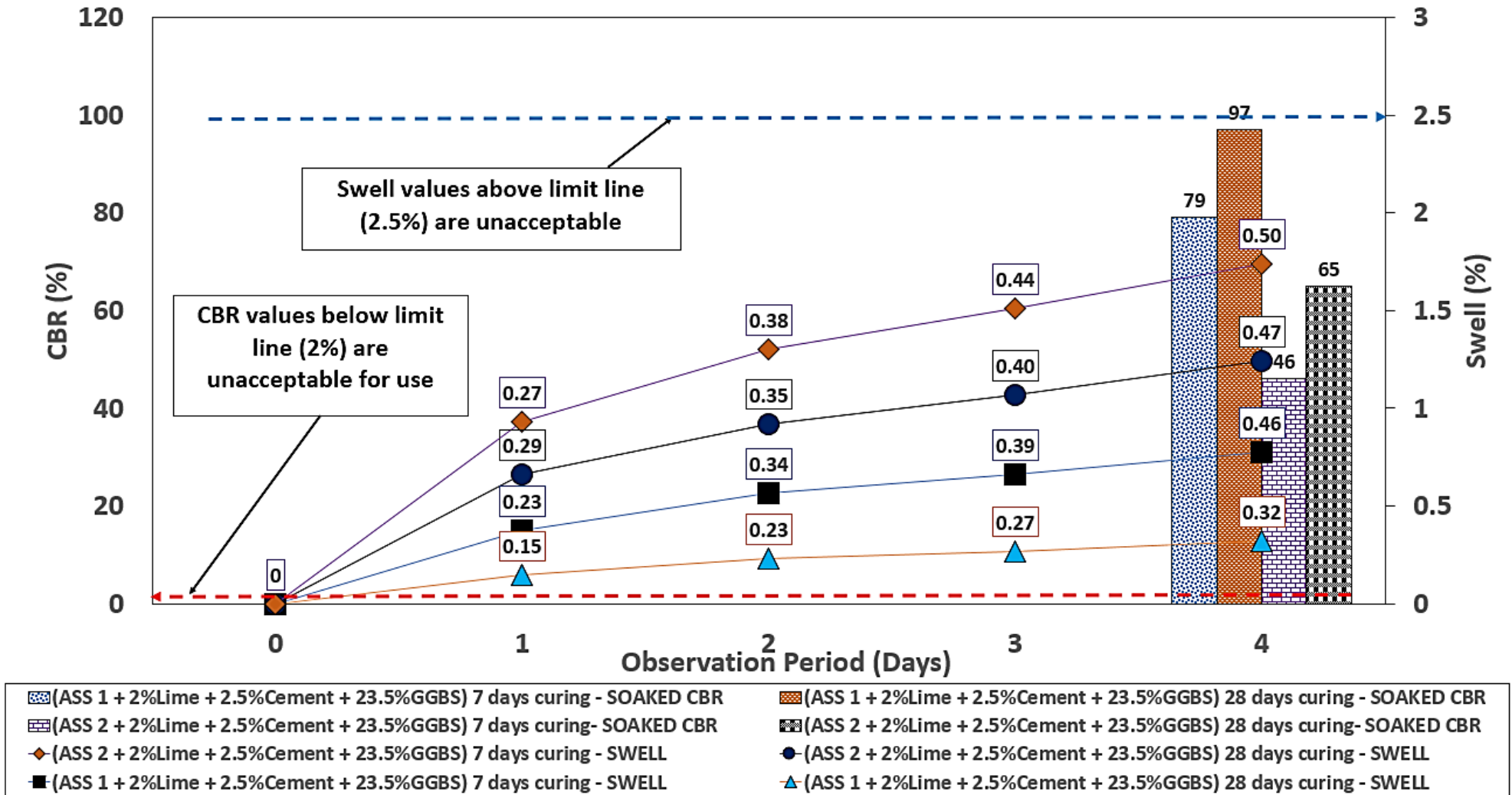


Figure 5.23: 4 days swell values for sustainable treated ASS and soaked CBR

5.3.5 Variation in Swell Using Recycled Plastic in Accordance with BS EN 13286-47:2021

A reduction in swell potential was observed for ASS materials treated using 23.5% recycled plastic as partial replacement for cement and lime in the mix. The highest swell value of 0.61% for ASS2 at end of day 4 and the lowest swell value was recorded for ASS1 at 0.51% at the end of day 4. A gradual increase in swell values was observed from day 1 to day 4 with swell values of 0.56% for ASS1 after 7 days of curing, and 0.51% for ASS1 after 28 days of curing all on day 4. ASS2 recorded swell values of 0.59% and 0.61% after day 7 and 28 days of curing at room temperature of $20 \pm 2^\circ\text{C}$. After comparing untreated ASS samples with samples treated with recycled plastic, it was observed that ASS values recorded for treated ASS materials are below the limit line making them suitable for use as subgrade materials in road construction. Figure 5.24 shows swell results for ASS samples treated using 23.5% recycled plastic as partial replacement for cement and lime in the mix. Figure 5.25 shows the combined results of treated and untreated ASS materials for comparison purposes.

Recycled plastic waste has been used in subgrade stabilisation and has proven to be successful. Soil stabilisation using plastic waste can be used in embankment and road pavement layers to improve the soil strength value (Gardete et al., 2020). Waste plastics were used by Ashraf et al. (2011), to stabilise soil and the results show a reasonably high CBR value Un-soaked. ASS materials were stabilised using a high amount of 23.5% recycled plastic waste as partial replacement for cement and lime. The reductions improved the engineering properties of expansive subgrade. A reduction in swell value with an increase in curing age was observed for ASS samples. ASS2 after 7 days of curing recorded the highest swell of 0.61% followed by ASS2 with a swell value of 0.59% after 28 days of curing. ASS1 recorded a swell value of 0.56% after 7 days of curing and later swell was reduced to 0.51% after 28 days of curing. This shows a decrease in swell pressure with an increase in curing age for ASS1 and 2. ASS1 sample with low bentonite content recorded the lowest swell. Plastic does not react with cement and lime to form C-S-H gel responsible for the swell reduction. However, the minimal amount of cement (2.5%) and lime (2%) was responsible for the low swell values achieved.

It was observed that the swell values obtained for ASS samples are lower than those of untreated ASS samples and are acceptable for use in road construction. Comparing the swell values for recycled plastic waste treated ASS samples with cement and lime (control), BDW and GGBS treated ASS samples, It was observed that swell values for ASS samples treated with plastic are within the range of BDW. It was observed that the swell values achieved do not correspond with CBR values with respect to curing ages. The highest swell value of 0.61 for ASS2 after 7 days recorded a soaked CBR value of 6% and ASS2 after 28 days with a swell value of 0.59% recorded the lowest CBR value of 3%. This shows that recycled plastic-treated ASS samples exhibit low swell values but are weak in compression. Hence, the samples exhibit low bearing capacity with low swell values due to the granular nature of the plastic used in the study. A substantial reduction in free swell of soil was observed due to the addition of plastic strips (Kassa et al., 2020). Granular soils are basically crumbed structures with open structures that allow water and air to penetrate through the soil (Bo et al., 2015). Comparing treated ASS materials with treated CBR values it was observed that swell values are $< 2.5\%$ and CBR values are $>2\%$ making all ASS samples suitable for use in road construction.

According to standard practice, subgrade swell $>2.5\%$ are unacceptable and would require treatment or removal and replacement (Troy, 2016). IAN73/06 states that CBR values $>2\%$ are accepted for use in road construction as subgrade materials. Stabilising expansive soil using plastic waste will simultaneously solve improper recycling (Kassa et al., 2020). As part of the commitment of many countries to reduce greenhouse gas emissions, using recycled plastic waste as binders to partially replace cement and lime in subgrade stabilisation will help reduce the greenhouse gas emitted to the atmosphere due to cement and lime production as well as reduce the environmental effect associated with landfill. According to “Plastic in the Ocean” statistics for 2020-2021, about 8 million pieces of plastic make their way into our oceans and there are 5.25 trillion macro and micro pieces of plastic in our ocean and 46,000 pieces in every square mile of ocean, weighing up to 269,000 tonnes. By partially replacing Portland cement with recycled waste plastic, this design may have the potential to contribute to reduced carbon emissions (Schaefer et al., 2017). Plastics are one of the leading waste materials found suitable for subgrade stabilisation. They reduce the cost of stabilisation at a large rate and using plastic for

Chapter 5 – Results and Discussion

this purpose simultaneously solves the challenge of improper plastic recycling (Kassa et al., 2020). Figure 5.26 shows 4 days swell values at the various points of the curve for sustainable treated ASS and soaked CBR for comparison.

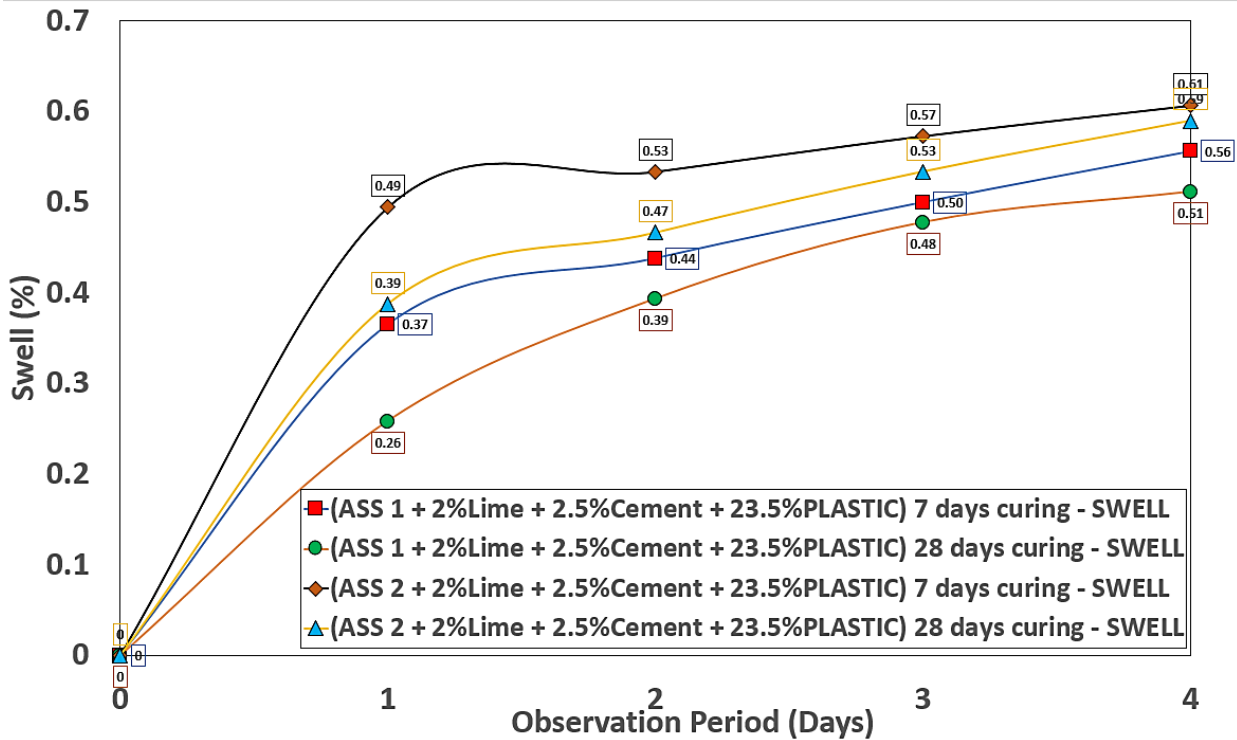


Figure 5.24: Swell results for ASS samples treated using 23.5% recycled plastic

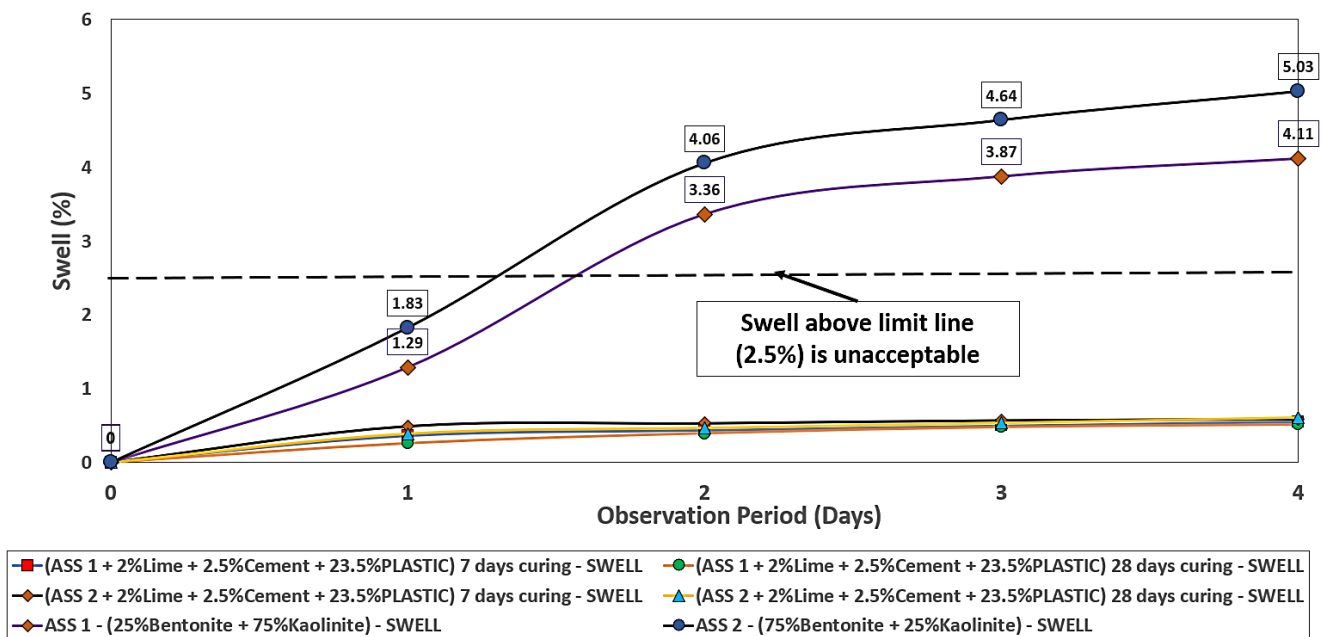


Figure 5.25: Combined results of treated and untreated ASS materials

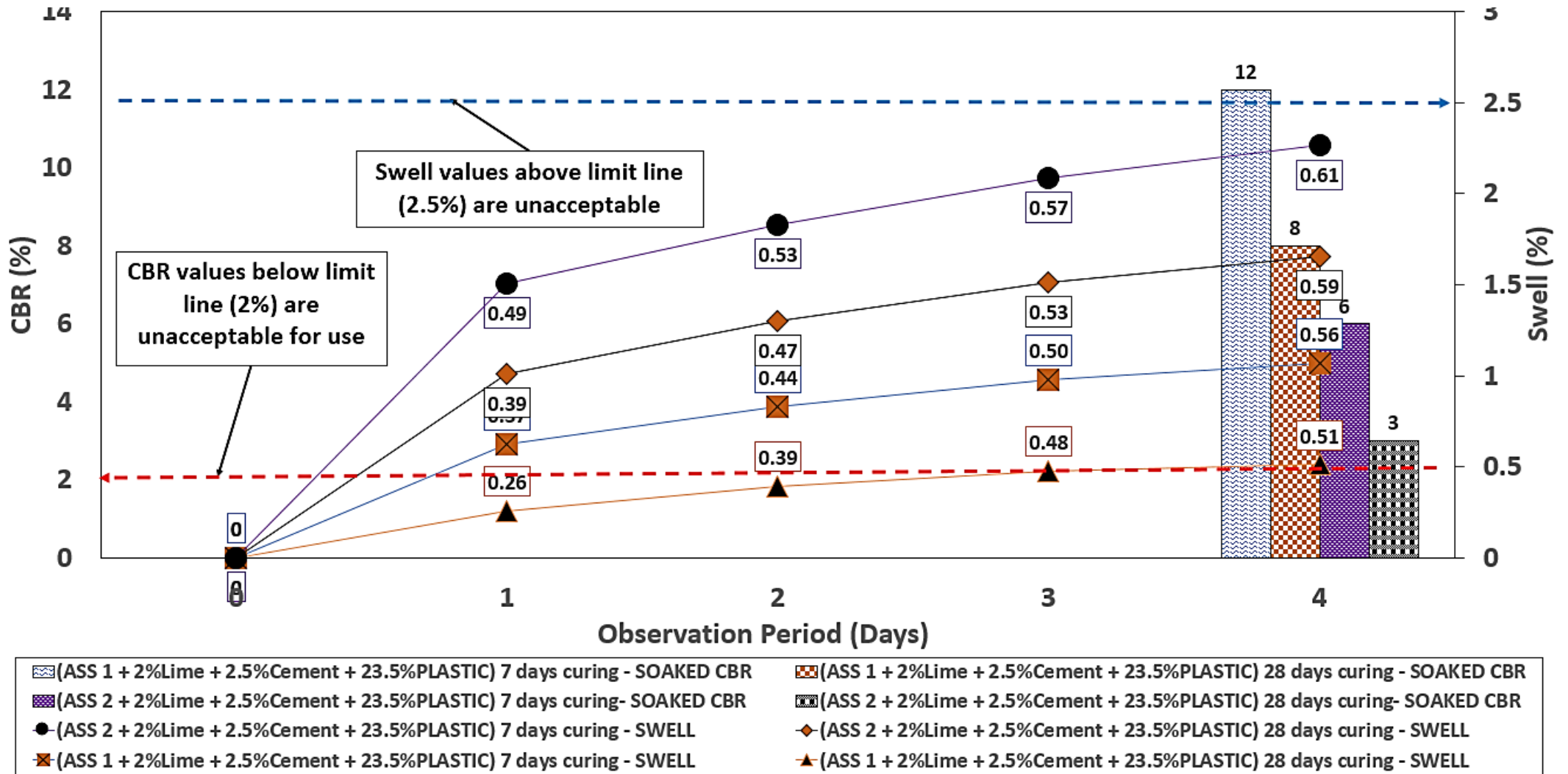


Figure 5.26: 4 days swell values for sustainable treated ASS and soaked CBR

5.3.6 Variation in Swell Using Recycled Glass In Accordance with BS EN 13286-47:2021

A reduction in swell potential was observed for ASS materials treated using 23.5% recycled glass as partial replacement for cement and lime in the mix. The highest swell value of 0.64% for ASS2 at end of day 4 and the lowest swell value was recorded for ASS1 at 0.46% at the end of day 4. A gradual increase in swell values was observed from day 1 to day 4 with swell values of 0.52% for ASS1 after 7 days of curing, and 0.46% for ASS1 after 28 days of curing all on day 4. ASS2 recorded swell values of 0.64% and 0.57% after day 7 and 28 days of curing at room temperature of $20 \pm 2^\circ\text{C}$. After comparing untreated ASS samples with samples treated with recycled glass, it was observed that ASS values recorded for treated ASS materials are below the limit line making them suitable for use as subgrade materials in road construction. Figure 5.27 shows swell results for ASS samples treated using 23.5% recycled glass as partial replacement for cement and lime in the mix. Figure 5.28 shows combined results of treated and untreated ASS materials for comparison purposes.

Swell reduction with an increase in curing age was observed for ASS samples. ASS2 after 7 days of curing recorded the highest swell of 0.64% followed by ASS2 with a swell value of 0.57% after 28 days of curing. ASS1 recorded a swell value of 0.52% after 7 days of curing and later swell reduced to 0.46% after 28 days of curing. This shows a decrease in swell pressure with an increase in curing age for ASS1 and 2. ASS1 sample with low bentonite content recorded the lowest swell after 28 days. The reduction in swell values observed could be attributed to the formation of some small amount of C-S-H gel with the addition of 2%lime and 2.5% cement in the mix because plastics do not react with cement and lime to form C-S-H gel responsible for the swell reduction. it was observed that the swell values achieved do not correspond with CBR values with respect to curing ages. The highest swell value of 0.64% for ASS2 after 7 days of curing recorded a soaked CBR value of 3% and ASS2 after 28 days with a swell value of 0.57% recorded the lowest CBR value of 4%. This shows that recycled glass-treated ASS samples exhibit low swell vales but are weak in compression. Hence, the samples exhibit low bearing capacity with low swell values due to the granular nature of the glass used in this study.

According to Hastuty et al. (2020), CBR values at a mixture of 2% limestone and 10% slag was 8.86% and the variation of a mixture of 4% limestone and 10% glass was recorded as a CBR of 10.5%. This confirms that CBR values do not increase significantly with the addition of a glass of any sort in subgrade stabilisation. Granular soils are basically crumbed structures with open structures that allow water and air to penetrate through the soil (Bo et al., 2015). Comparing treated ASS materials with treated CBR values, swell values are $< 2.5\%$ and CBR values are $>2\%$, making all ASS samples suitable for road construction. According to standard practice, subgrade swell $>2.5\%$ are unacceptable and would require treatment or removal and replacement (Troy, 2016). IAN73/06 states that CBR values $>2\%$ are accepted for use in road construction as subgrade materials. As part of the commitment of many countries to reduce greenhouse gas emissions, using recycled glass waste as binders to partially replace cement and lime in subgrade stabilisation would reduce the greenhouse gas emitted to the atmosphere due to cement and lime production as well as reduce the environmental effect associated with landfill. Using glass waste normally dumped at a landfill would reduce greenhouse gas emissions and the environmental effect emanating from glass landfills. Using glass produced from recycled glass reduced related air pollution by 20% and related water pollution by 50% and reduced the space in landfills (World wide Fund for Nature, 2021). The use of recycled materials is a key element in generating sustainable pavement designs to save natural resources, and reduce energy, greenhouse gas emission and costs (Zhao et al., 2021). Figure 5.29 shows 4 days swell values at the various points of the curve for sustainable treated ASS and soaked CBR for comparison.

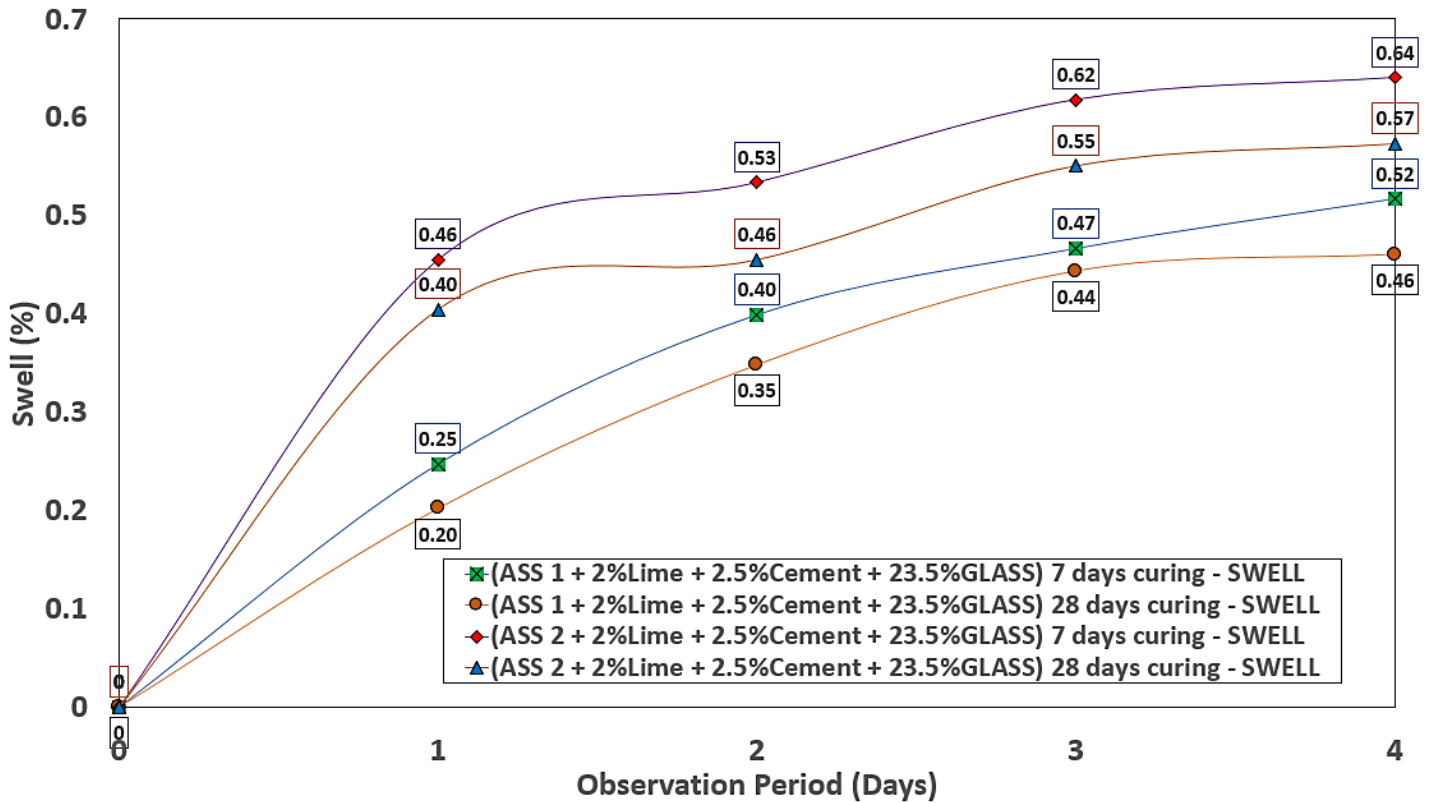


Figure 5.27: Swell results for ASS samples treated using 23.5% recycled glass

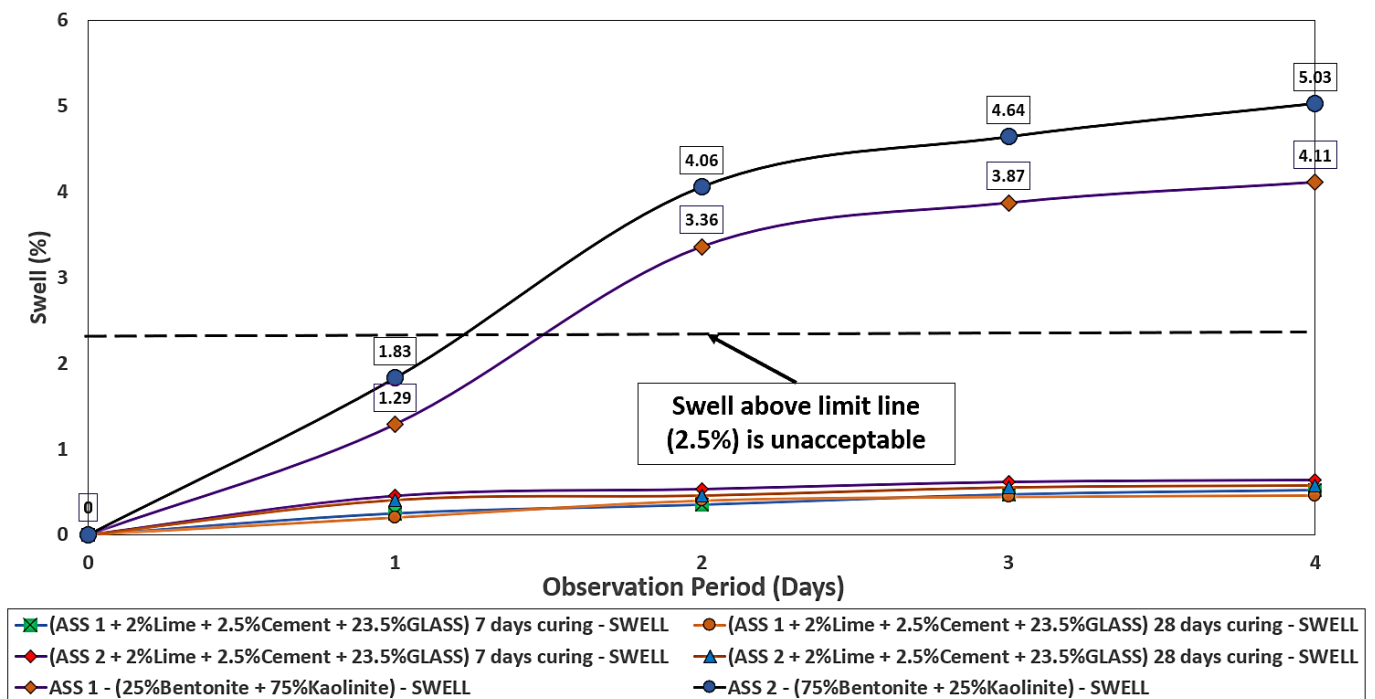


Figure 5.28: Combined results of treated and untreated ASS materials

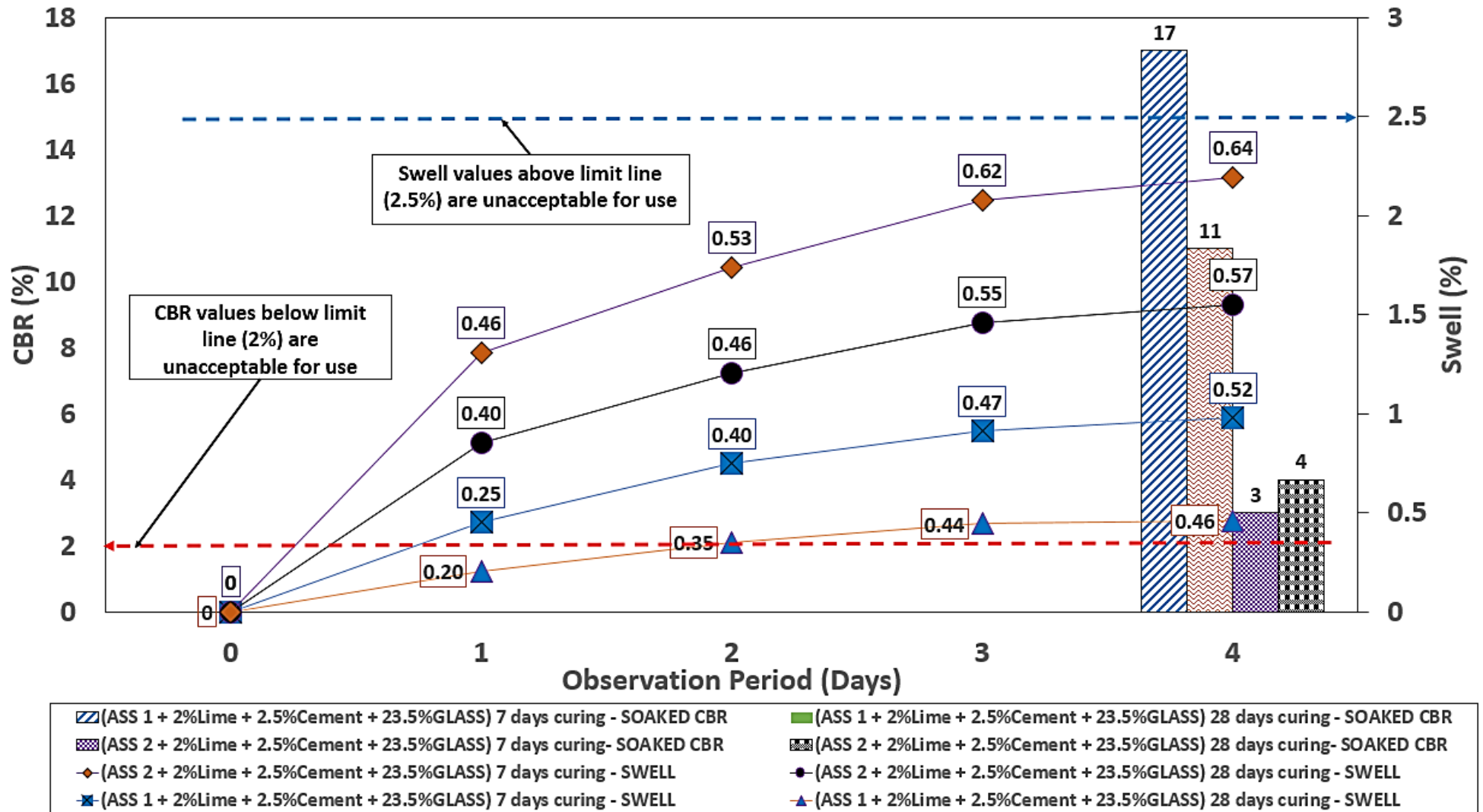


Figure 5.29: 4 days swell values for sustainable treated ASS and soaked CBR

5.3.7 Variation in Swell Using GGBS and Recycled Plastic In Accordance with BS EN 13286-47:2021

A reduction in swell potential was observed for ASS materials treated using 11.75% GGBS and 11.75% recycled plastic as partial replacements for cement and lime in the mix. The highest swell value of 0.94% was achieved for ASS2 at end of day 4 and the lowest swell value was recorded for ASS 0.37 at the end of day 4. A gradual increase in swell values was observed from day 1 to day 4 with swell values of 0.47% for ASS1 after 7 days of curing, and 0.38% for ASS1 after 28 days of curing all on day 4. ASS2 recorded swell values of 0.94% and 0.37% after day 7 and 28 days of curing at room temperature of $20 \pm 2^\circ\text{C}$. After comparing untreated ASS samples with those treated with GGBS and recycled plastic, it was observed that ASS values recorded for treated ASS materials are below the limit line making them suitable for use as subgrade materials in road construction. Figure 5.30 shows swell results for ASS samples treated using 11.75% GGBS and 11.75% recycled plastic as partial replacement for cement and lime in the mix. Figure 5.31 shows combined results of treated and untreated ASS materials for comparison purposes.

It was observed during a swell test conducted for ASS materials using individual sustainable binders at very high percentages of GGBS and plastic in the mix achieved low swell values. Due to this reason, GGBS and plastic were added to the ASS sample at percentages of 11.75% GGBS and 11.75% recycled plastic respectively. After the swell test, ASS samples recorded low swell values which are acceptable for use in road construction. ASS2 (high bentonite content after 7 days of curing recorded the highest swell value of 0.94% and ASS2 after 28 days recorded a swell value of 0.47%. ASS1 with less bentonite content observed the lowest swell value of 0.36% after 28 days of curing. this shows a reduction in swell value with an increase in curing age observed for ASS samples. Comparing the swell values with untreated ASS samples shows that, ASS samples treated using GGBS and Recycled Plastic Waste recorded low swell. The reduction in swell values observed could be attributed to the formation of some small amount of C-S-H gel with the addition of GGBS in the mix because plastics do not chemically react with other binders to form C-S-H gel responsible for strength gain and swell reduction (Sasui et al., 2019).

GGBS contains a high amount of calcium forming C-S-H gel which contributed to strength development (Saludung et al., 2018). It was found that the presence of GGBS in the mixes significantly increased the compressive strength of geopolymer (Saludung et al., 2018). It was observed that the swell values achieved correspond with CBR values with respect to curing ages. The highest swell value of 0.94% for ASS2 after 7 days of curing recorded a soaked CBR value of 47% and ASS2 after 28 days with a swell value of 0.47% recorded the lowest CBR value of 50%. ASS1 with the lowest swell value of 0.36% recorded the highest soaked CBR value of 93%. This shows that CBR values have significantly improved with the addition of GGBS which contains high amounts of C-S-H gel responsible for the swell reduction in the expansive subgrade. The increase in GGBS content increased CBR values in a mix (Narendra et al., 2017). The addition of GGBS in a mix reduced the free swell index and swelling pressure by about 67% and 21% from its un-stabilised counterparts (Yadu et al., 2013). The Swell values achieved for all ASS samples with the addition of 11.75%GGBS and 11.75% recycled plastic waste in a mixture are acceptable and usable in road construction as subgrade materials. According to standard practice, subgrade swell $>2.5\%$ are unacceptable and would require treatment or removal and replacement (Troy, 2016).

As part of the commitment of many countries to reduce greenhouse gas emissions. Using GGBS and recycled plastic waste as binders to partially replace cement and lime in subgrade stabilisation would reduce construction costs, greenhouse gas emissions and the environmental effect associated with landfills. GGBS can be utilised as an alternative to reduce the construction cost of the road, particularly in the rural areas of developing countries (Prasad et al., 2019). Partially replacing Portland cement with recycled waste plastic, this design may have the potential to contribute to reduced carbon emissions (Schaefer et al., 2017). Plastics are one of the leading waste materials found suitable for the purpose of subgrade stabilisation. They reduce the cost of stabilisation at a large rate and using plastic for this purpose simultaneously solves the challenge of improper plastic recycling (Kassa et al., 2020). Using recycled materials is a key element in generating sustainable pavement designs to save natural resources, and reduce energy, greenhouse gas emission and costs (Zhao et al., 2021). Figure 5.32 shows 4 days swell values at the various points of the curve for sustainable treated ASS and soaked CBR for comparison.

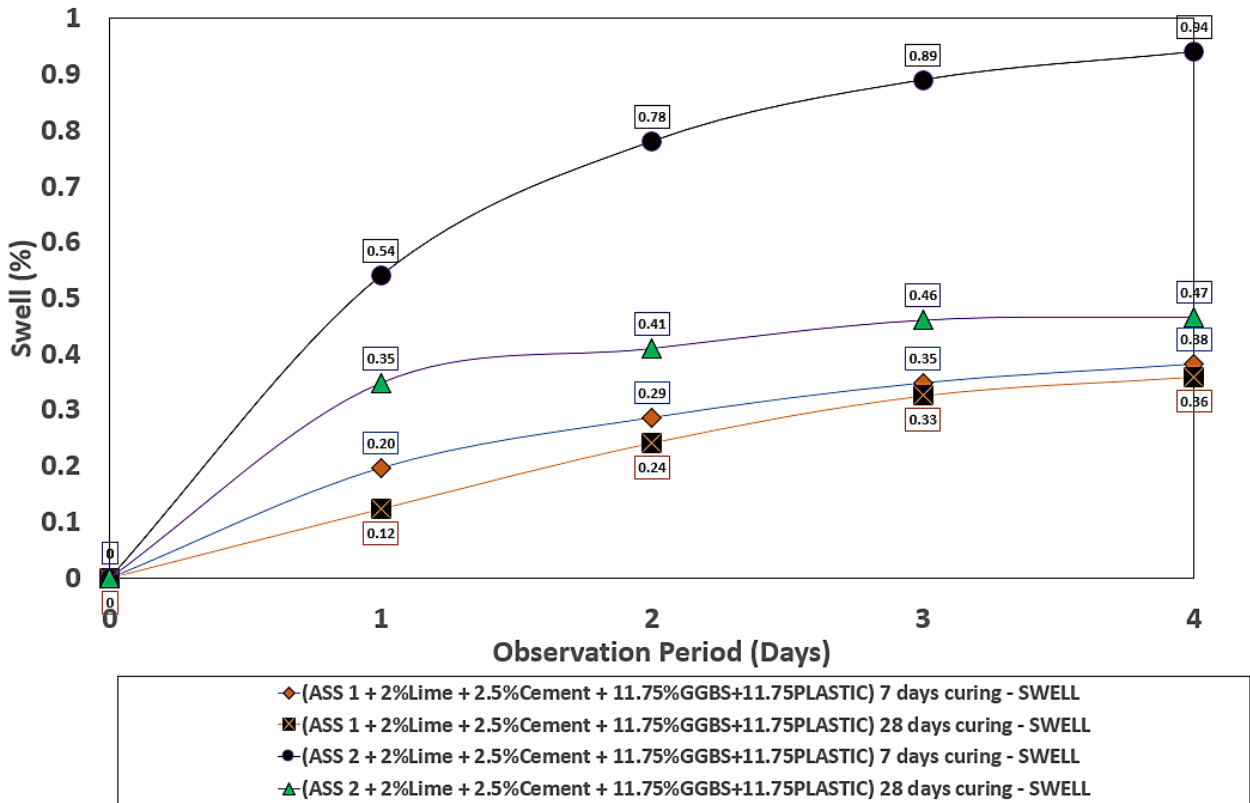


Figure 5.30: swell results for ASS samples treated using 11.75% GGBS and 11.75% recycled plastic

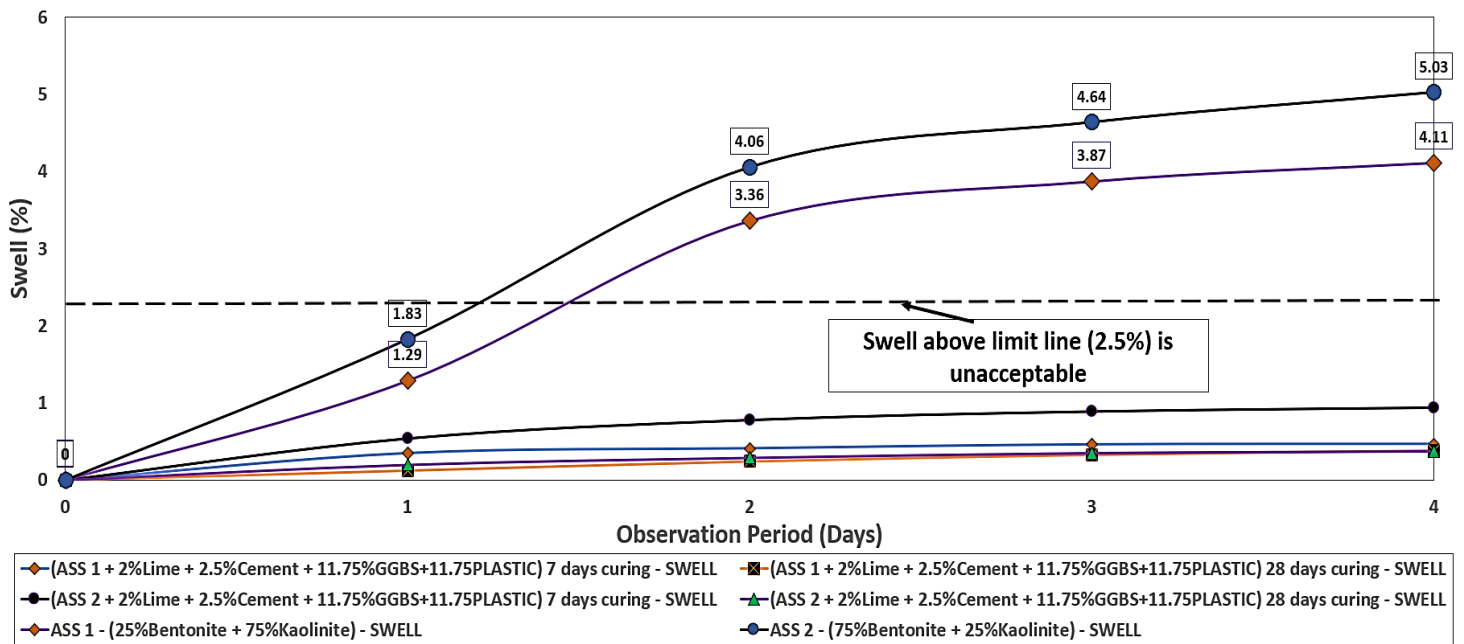


Figure 5.31: combined results of treated and untreated ASS materials

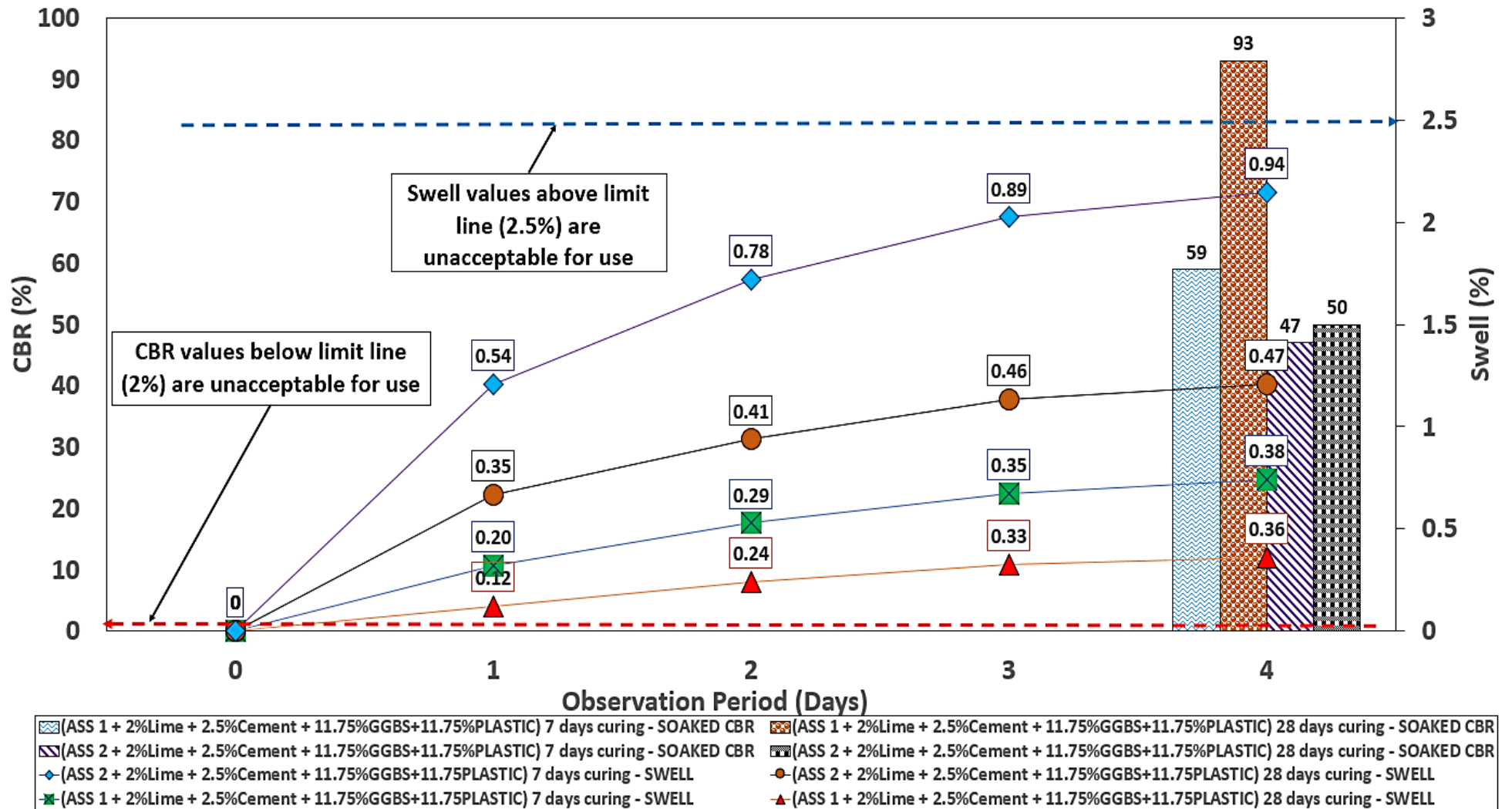


Figure 5.32: 4 days swell values for sustainable treated ASS and soaked CBR

5.3.8 Variation in Swell Using GGBS and Recycled Glass In Accordance with BS EN 13286-47:2021

A reduction in swell potential was observed for ASS materials treated using 11.75% GGBS and 11.75% recycled glass as partial replacements for cement and lime in the mix. The highest swell value of 0.56% for ASS2 at end of day 4 and the lowest swell value was recorded for ASS1 at 0.40% at the end of day 4. A gradual increase in swell values was observed from day 1 to day 4 with small values of 0.50% for ASS1 after 7 days of curing, and 0.40% for ASS1 after 28 days of curing all on day 4. ASS2 recorded swell values of 0.56% and 0.40% after day 7 and 28 days of curing at room temperature of $20 \pm 2^\circ\text{C}$. After comparing untreated ASS samples with samples treated with GGBS and recycled glass, it was observed that ASS values recorded for treated ASS materials are below the limit line making them suitable for use as subgrade materials in road construction. Figure 5.33 shows swell results for ASS samples treated using 11.75% GGBS and 11.75% recycled glass as partial replacement for cement and lime in the mix. Figure 5.34 shows combined results of treated and untreated ASS materials for comparison purposes.

Stabilising ASS materials using 11.75% GGBS and 11.75% recycled glass yielded improved swell results usable in road construction. After the swell test, ASS2 (high bentonite content after 7 days of curing recorded the highest swell value of 0.56% and ASS2 after 28 days recorded a swell value of 0.50%. ASS1 with less bentonite content observed the lowest swell value of 0.41% after 28 days of curing. This shows a reduction in swell value with an increase in curing age observed for ASS samples. Comparing the swell values with untreated ASS samples shows that, ASS samples treated using GGBS and recycled glass waste recorded low swell. The reduction in swell values observed could be attributed to the formation of some small amount of C-S-H gel with the addition of GGBS in the mix because glass does not chemically react with other binders to form C-S-H gel responsible for strength gain and swell reduction. GGBS are rich in calcium, the main reaction product of C-S-H gel responsible for strength development and a reduction in swell (Sasui et al., 2019). It was found that the presence of GGBS in the mixes significantly increased the compressive strength of geopolymer (Saludung et al., 2018).

Swell values for ASS materials stabilised using GGBS and Recycled Glass Waste were compared with untreated ASS materials and the results of low swell values for treated ASS samples were acceptable for use in road construction. It was observed that the swell values achieved corresponded with CBR values with respect to curing ages. The highest swell value of 0.56% for ASS2 after 7 days of curing recorded a soaked CBR value of 31% and ASS2 after 28 days with a swell value of 0.50% recorded the lowest CBR value of 46%. ASS1 with the lowest swell value of 0.39% recorded the highest soaked CBR value of 72%. This shows that the highest swell values recorded the lowest CBR values and the lowest swell recorded the highest CBR value, respectively. Adding GGBS to glass significantly improved the engineering properties of ASS materials. GGBS contain high amounts of C-S-H gel responsible for the swell reduction in the expansive subgrade. The Swell values achieved for all ASS samples with the addition of 11.75%GGBS and 11.75% recycled glass waste in a mixture are acceptable for use in road construction as subgrade materials. According to standard practice (Troy, 2016), subgrade swell >2.5% are unacceptable and would require treatment or removal and replacement (Troy, 2016).

As part of the commitment of many countries to reduce greenhouse gas emissions. Using GGBS and recycled glass waste as binders to partially replace cement and lime in subgrade stabilisation would reduce construction costs, greenhouse gas emissions and the environmental effect associated with landfills. GGBS was used as an alternative to reduce road construction costs (Prasad, et al., 2019). Using glass waste normally dumped in landfills would reduce greenhouse gas emissions and the environmental effect emanating from glass landfills. Using glass produced from recycled glass reduced related air pollution by 20% and related water pollution by 50% and reduced the space in landfills (Worldwide Fund for Nature, 2021). The use of recycled materials is a key element in generating sustainable pavement designs to save natural resources, and reduce energy, greenhouse gas emission and costs (Zhao et al., 2021). Figure 5.35 shows 4 days swell values at the various points of the curve for sustainable treated ASS and soaked CBR for comparison.

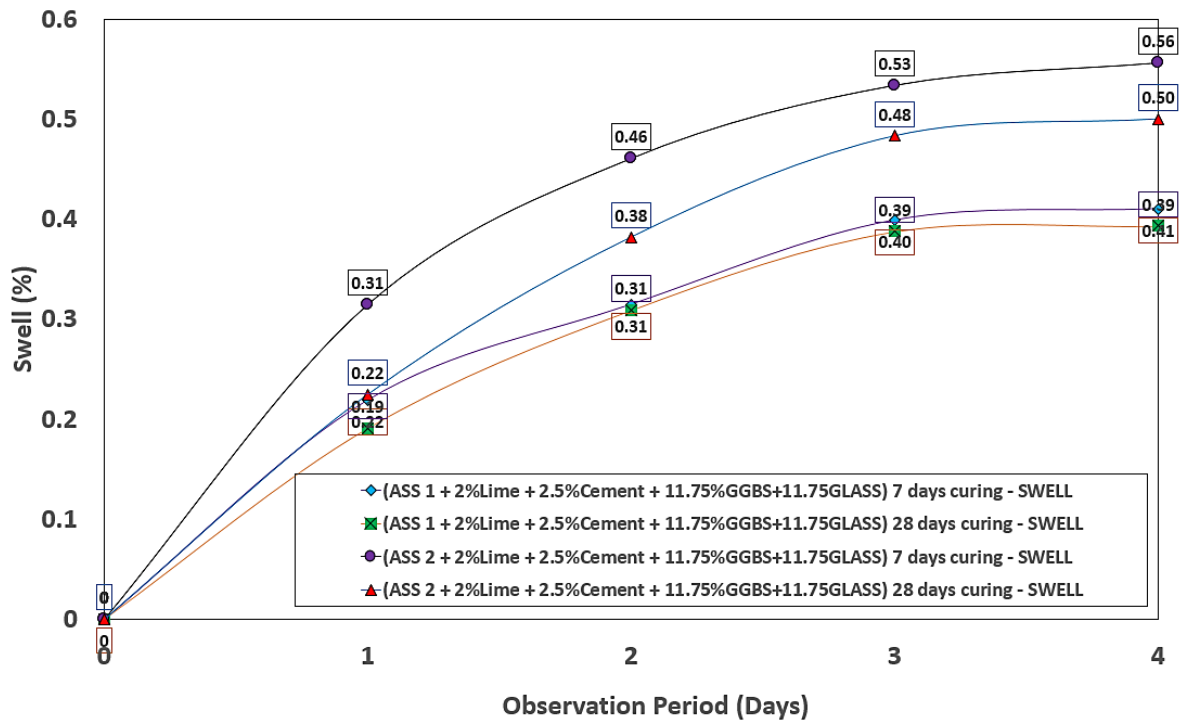


Figure 5.33: swell results for ASS samples treated using 11.75% GGBS and 11.75% recycled glass

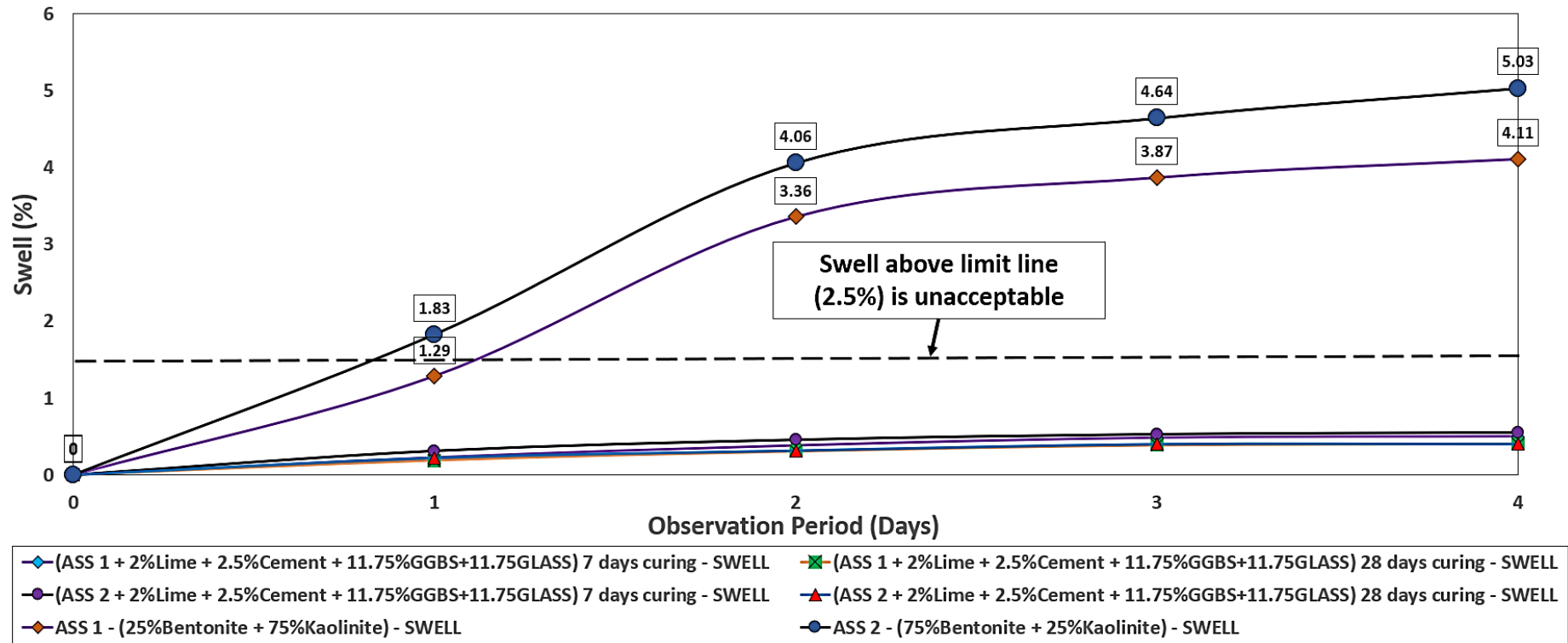


Figure 5.34: combined results of treated and untreated ASS materials

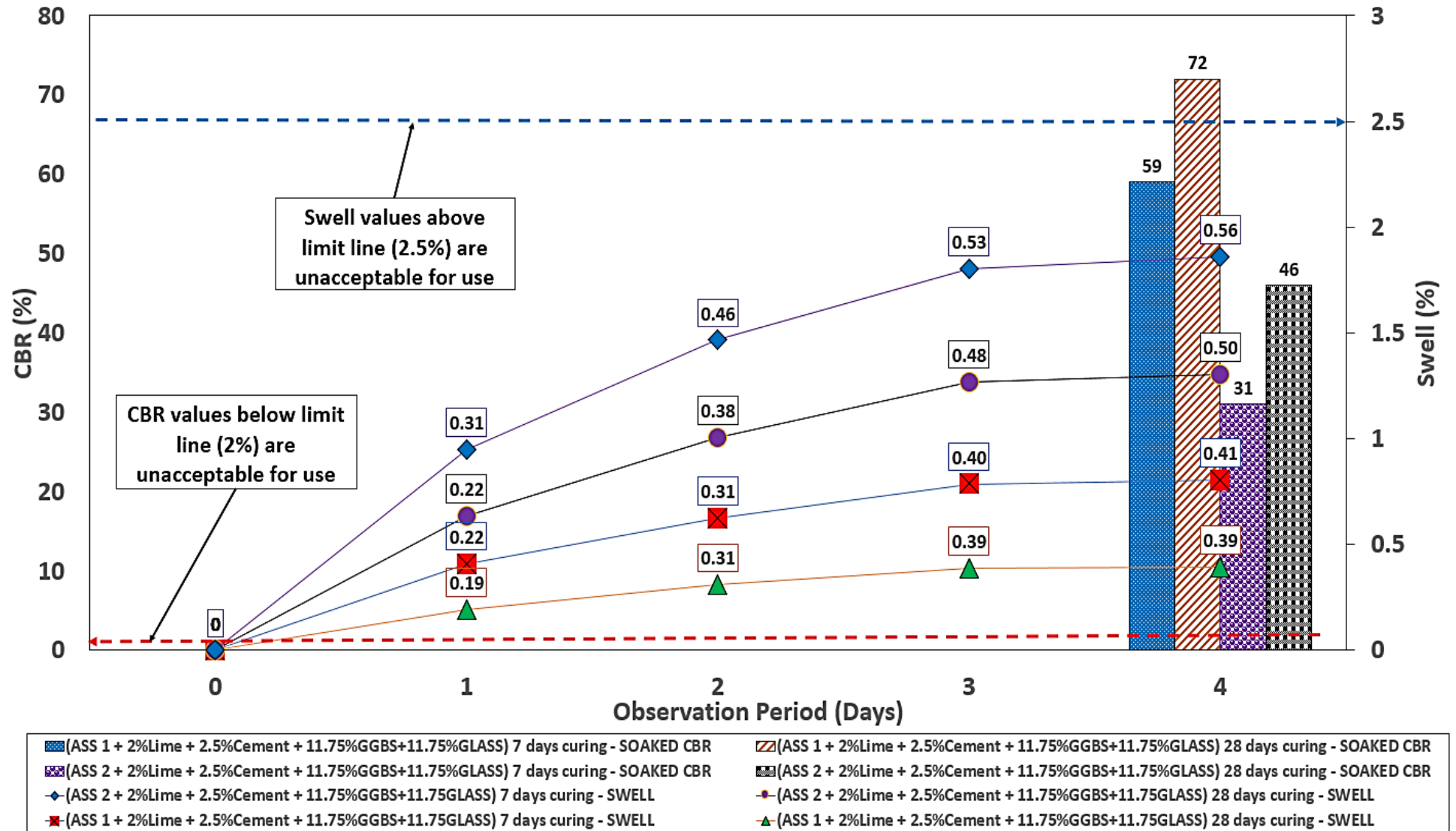


Figure 5.35: 4 days swell values for sustainable treated ASS and soaked CBR

5.3.9 Variation in Swell Using GGBS and Brick Dust Waste (BDW) In Accordance with BS EN 13286-47:2021

A reduction in swell potential was observed for ASS materials treated using 11.75% GGBS and 11.75 BDW as partial replacement for cement and lime in the mix. The highest swell value of 0.54% for ASS2 at the end of day 4 and the lowest swell value was recorded for ASS1 at 0.49 at the end of day 4. A gradual increase in swell values was observed from day 1 to day 4 with swell values of 0.51% for ASS1 after 7 days of curing, and 0.52% for ASS1 after 28 days of curing all on day 4. ASS2 recorded swell values of 0.54% and 0.49% after day 7 and 28 days of curing at room temperature of $20 \pm 2^\circ\text{C}$. After comparing untreated ASS samples with samples treated with GGBS and recycled BDW, it was observed that ASS values recorded for treated ASS materials are below the limit line making them suitable for use as subgrade materials in road construction. Figure 5.36 shows swell results for ASS samples treated using 11.75% GGBS and 11.75% recycled BDW as partial replacement for cement and lime in the mix. Figure 5.37 Shows combined results of treated and untreated ASS materials for comparison purposes.

GGBS and BDW proportions of 11.75% GGBS and 11.75% BDW were used as binders in ASS materials and the swell results obtained were good for use in road construction. ASS2 (high bentonite content after 7 days of curing recorded the highest swell value of 0.54% and ASS2 after 28 days recorded a swell value of 0.49%. ASS1 with less bentonite content observed the lowest swell value of 0.42% after 28 days of curing. This shows a reduction in swell value with an increase in curing age observed for ASS samples. Comparing the swell values with untreated ASS samples shows that, ASS samples treated using GGBS and BDW recorded low swell. The reduction in swell values observed could be attributed to the formation of some small amount of C-S-H gel with the addition of GGBS and BDW in the mix GGBS are highly cementations and high in strength enhancing compounds calcium silicate hydrate (C-S-H) which improves strength and durability in a mix. BDW are pozzolanic materials that form C-S-H gel responsible for strength gain in a mixture. GGBS is high in calcium and forms C-S-H gel during the hydration process for strength gain in a mixture. It was found that the addition of brick dust increased the soil strength between 1.7-2.3 times with respect to the non-stabilised materials (Hidalgo et al., 2019). Pozzolanic reaction is responsible for the formation of C-S-H and C-A-H gel due to the presence of BDW

in the mixture, which acted as a binding agent responsible for strength gain and high CBR value of the subgrade materials.

Pozzolans are materials (such as BDW) that contain alumina/silica which reacts to form new compounds (Calcium silicate hydrate (C-S-H) and Calcium aluminium hydrates (C-A-H) when lime is added and have the ability to modify the properties of a lime mixture (Rogers, 2011). BDW exhibits pozzolanic properties which can be used as cement replacement in road subgrade stabilisation (Kartini et al., 2012). GGBS are highly cementations and high in strength-enhancing compounds calcium silicate hydrate (C-S-H) which improves strength and durability in a mix. Studies have shown that the higher the amount of GGBS blend, the greater the hydraulic activity (Hewlett, 2003). GGBS are highly cementations and high in strength-enhancing compounds calcium silicate hydrate (C-S-H), which improves strength and durability in a mix. Studies have shown that the higher the amount of GGBS blend, the greater the hydraulic activity (Hewlett, 2003). After comparing treated ASS swell values using GGBS and BDW as binders with untreated ASS swell, it was observed that treated ASS using GGBS and BDW recorded very low swell values usable in road construction. It was observed that the swell values achieved corresponded with CBR values with respect to curing ages. The highest swell value of 0.54% for ASS2 after 7 days of curing recorded the lowest soaked CBR value of 16% and ASS2 after 28 days with a swell value of 0.49% recorded the lowest CBR value of 24%. ASS1 with the lowest swell value of 0.42% recorded the highest soaked CBR value of 97%.

This shows that the highest swell values recorded the lowest CBR values and the lowest swell recorded the highest CBR value respectively. All swell values achieved for ASS samples with the addition of 11.75%GGBS and 11.75% BDW in a mixture are < 2.5% and acceptable for use as subgrade materials in road construction. Any swell >2.5% is unacceptable and would require treatment or removal and replacement (Troy, 2016). As part of the commitment of many countries to reduce greenhouse gas emissions, the environmental effect associated with landfills and overall road construction costs, GGBS and BDW can be used as binders to partially replace cement and lime in subgrade stabilisation (Prasad et al., 2019). The use of GGBS binders at high volumes as supplementary cementitious materials are good from the environmental point of view; hence, the higher the amount of GGBS used in replacing

cement in soil stabilisation the lesser the carbon footprint (Onn et al., 2019). The addition of brick dust resulted in an increase in the soil strength and its suitable materials for use in practical applications in construction (Hidalgo et al., 2019). Using brick waste as binders in place of cement and lime in subgrade stabilisation will help reduce the greenhouse gas emitted to the atmosphere due to cement and lime production as well as reduce the environmental effect associated with a brick stockpile and landfill. According to the World Health Organisation (WHO) 2021 report on climate change in the Western Pacific, it is estimated that climate change will cause an additional 250,000 deaths annually between 2030 to 2050. However, countries are committing to net-zero emissions by 2050, and about half of emission cuts must be in place by 2030 to keep global warming below 1.5°C (The United Nations, 2021). Figure 5.38 4 days swell values for sustainable treated ASS and soaked CBR.

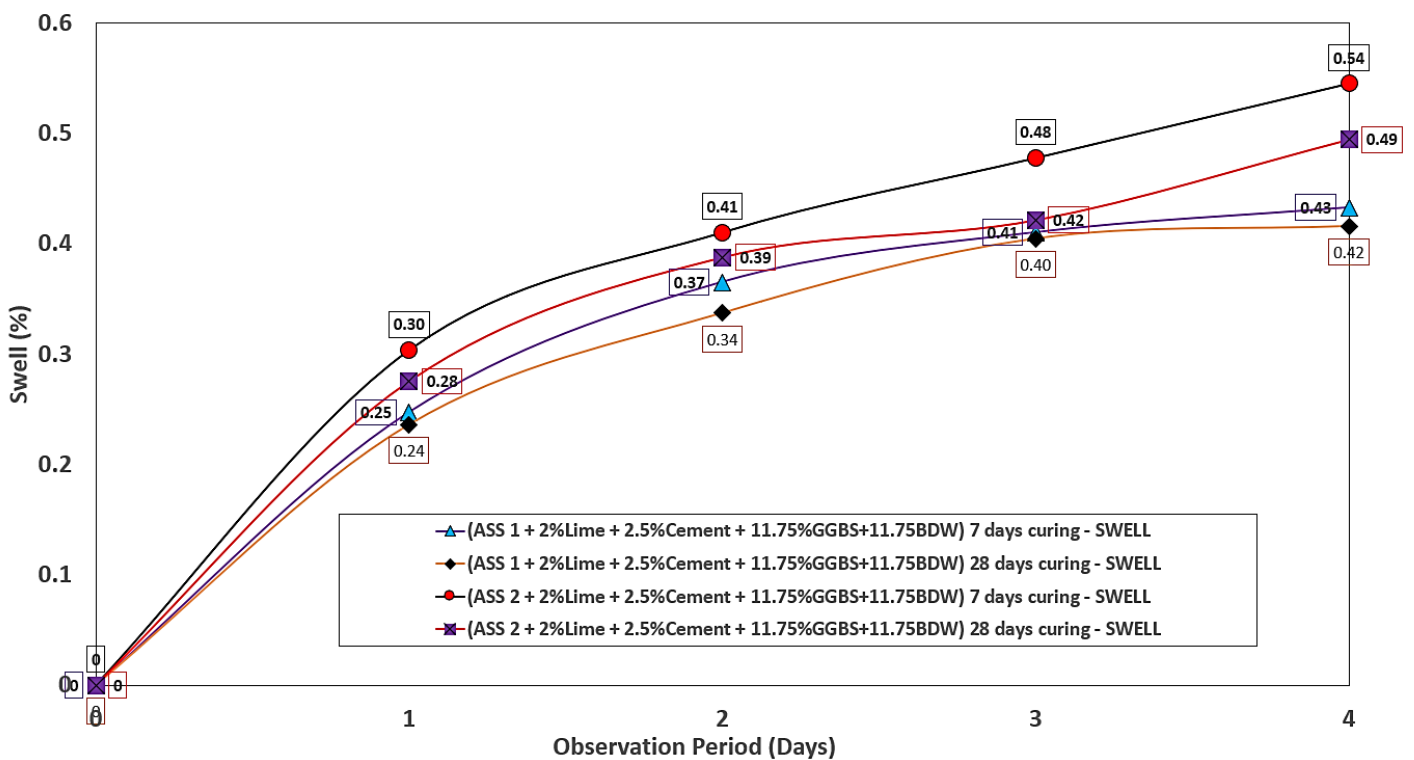


Figure 5.36: Swell results for ASS samples treated using 11.75% GGBS and 11.75% BDW

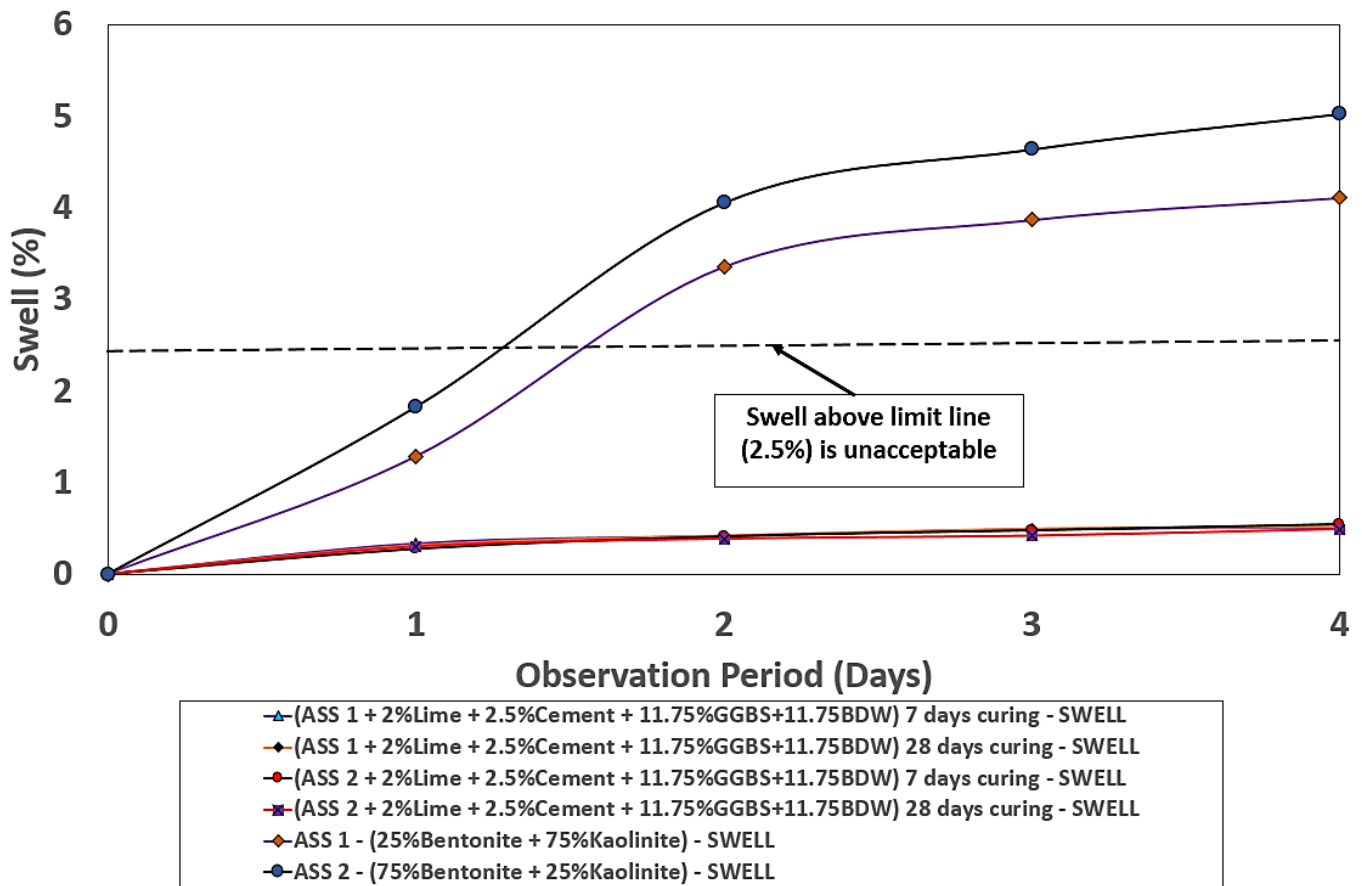


Figure 5.37: Combined results of treated and untreated ASS materials for comparison purposes

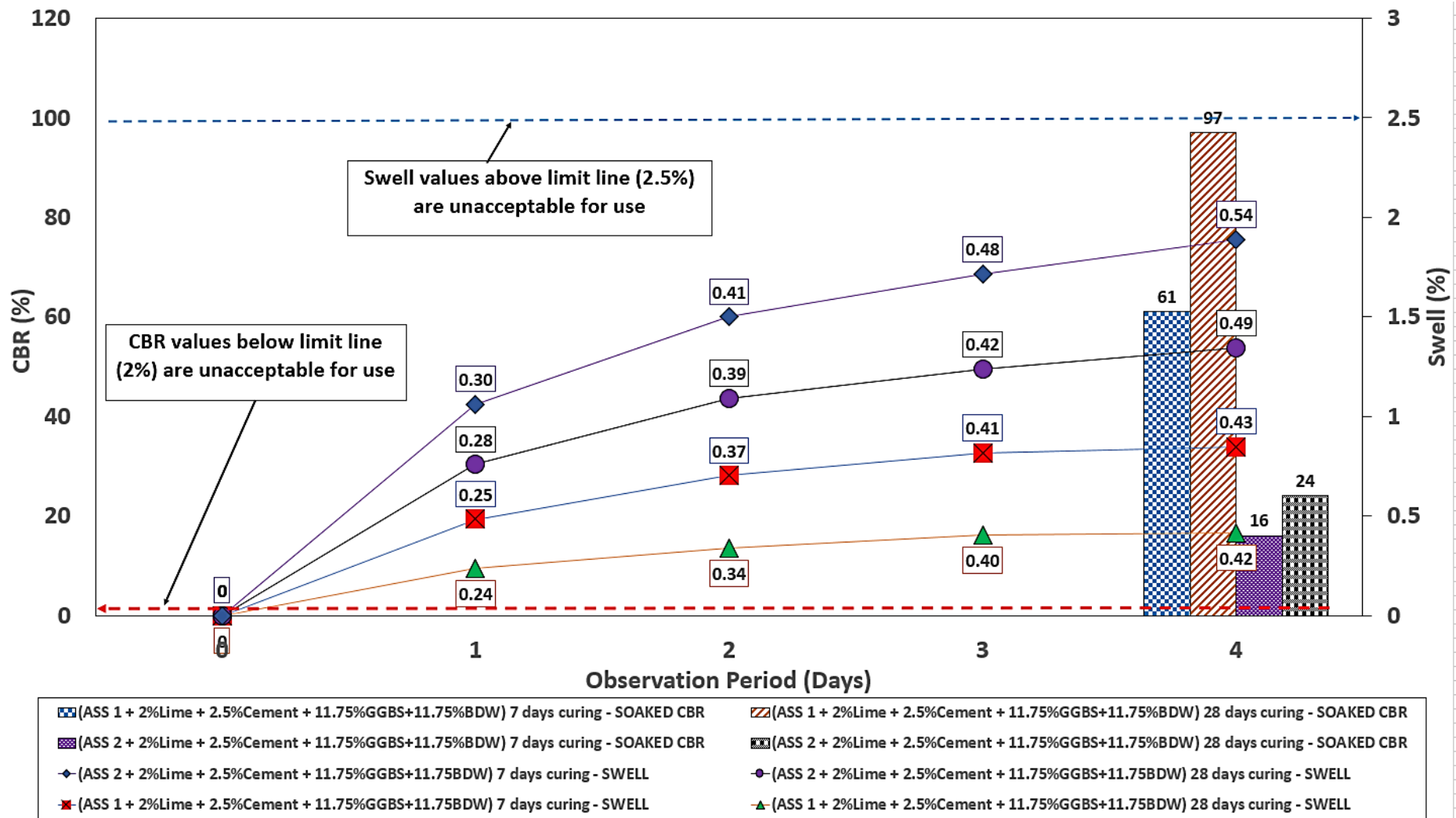


Figure 5.38: 4 days swell values for sustainable treated ASS and soaked CBR

5.4 Swell test in accordance with BS EN 13286-49:2004

Swell conducted using BS EN 13286-49:2004 shows that ASS materials began to swell after day 1 and ASS1 continue to swell until day 14 where no further swell was observed till the end of 28 days. ASS2 continues to swell until day 3 with a slight reduction in swell on day 4 and a rise in swell on day 5 until no further swell was recorded till the end of 28 days. The highest swell percentage of 56.76% was recorded for ASS2 (75% Bentonite and 25% Kaolinite) and the lowest swell percentage of 35.92% for ASS1 (25% Bentonite and 75% Kaolinite) all after 28 days of curing.

ASS materials began to swell after day 1 and ASS1 continue to swell until day 14 when no further swell was observed until day 28. ASS2 continues to swell until day 3 with a slight reduction in swell on day 4 and a rise in swell on day 5 until no further swell was recorded until day 28. The highest swell percentage of 56.76% was recorded for ASS2 (75% Bentonite and 25% Kaolinite) and the lowest swell percentage of 35.92% for ASS1 (25% Bentonite and 75% Kaolinite) whiles ASS2. The swelling potential of ASS reduced drastically from 56.76% for untreated ASS2 (75% Bentonite and 25% Kaolinite) to 0.2% after treating ASS materials using cement and lime. The lowest swell value of 0.04% was recorded for ASS1 compared with ASS2. However, a swell value of 0.2% recorded for ASS2 was the highest recorded for treated ASS samples. Swell values recorded for treated ASS materials in this research fall below the unacceptable 2.5% swell limit. Hence, all treated ASS materials in the study meet the standard for use as subgrade materials in road construction.

This indicates a high swell with an increase in bentonite content and proves that extremely high and high plasticity subgrade materials exhibit very high swell potentials. Swell results achieved for BS EN 13286-47:2021 and BS EN 13286-49:2004 do not meet the standard for use as subgrade material. According to standard practice, subgrade swell >2.5% are unacceptable and would require treatment or removal and replacement (Troy, 2016). Diman et al. (2008) state that bentonites are known to have very high swelling pressures. Sodium bentonite clays are widely known for their high swelling characteristics. A typical sodium bentonite clay has the ability to absorb 4-5 times its own weight in water and can swell 5-15 times its dry volume at full-unconfined saturation (ASTM D5890).

Bentonite clays have high swelling capacity in low electrolyte water solutions i.e the bentonite swell in water to a volume several times the original dry clay volume (Oy et al., 1998). Bentonite absorbs water to a greater extent than any other ordinary plastic clay consequently, it swells depending on the change in its moisture content (Diman et al., 2008). Bentonite has low hydraulic conductivity and high swelling capacity (Wan et al., 2020). A high CBR value was observed for ASS2 (extremely high plasticity) composed of high bentonite content even though it recorded the shiest swell potential. However, the swell and CBR values obtained for ASS1 and 2 are unsuitable for road construction. Swell values for all ASS materials after 4 and 28 days of soaking were greater than 2.5% making them unacceptable for use as road subgrade in road construction and will require modification or re-engineering. Figure 5.39 shows swell results for untreated ASS materials after 28 days. Figure 5.40 shows swell results for treated ASS materials after 28 days and Figure 5.41 shows the combined swell results for untreated and treated ASS materials after 28 days for easy comparison.

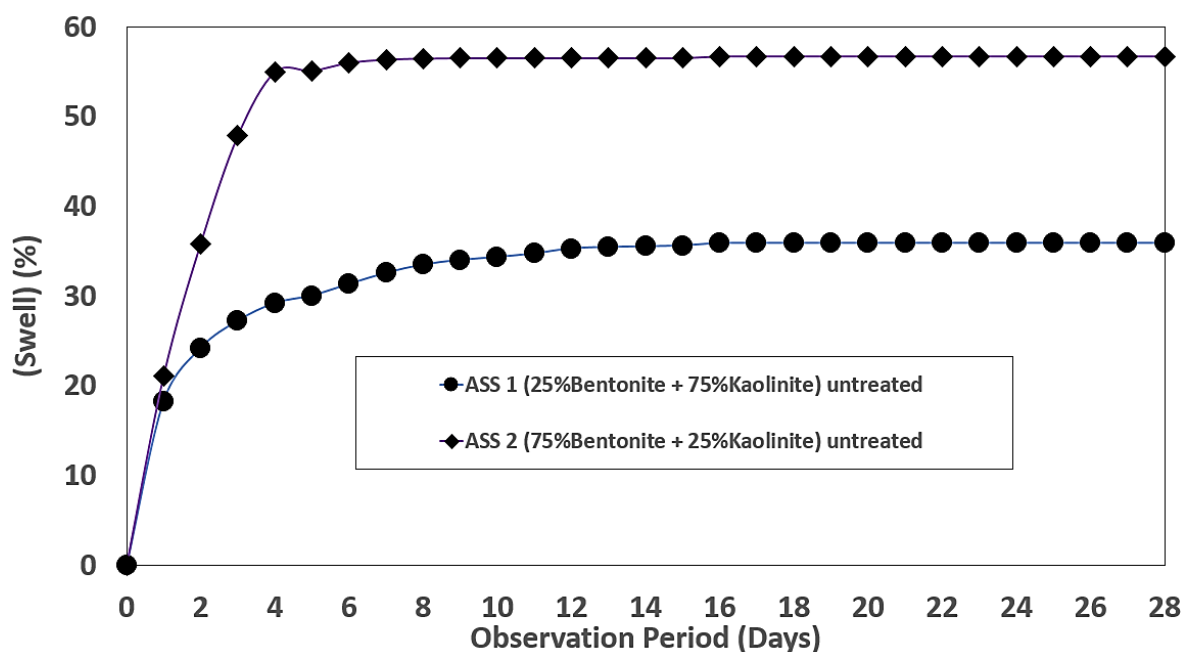


Figure 5.39: Swell results for untreated ASS materials after 28 days

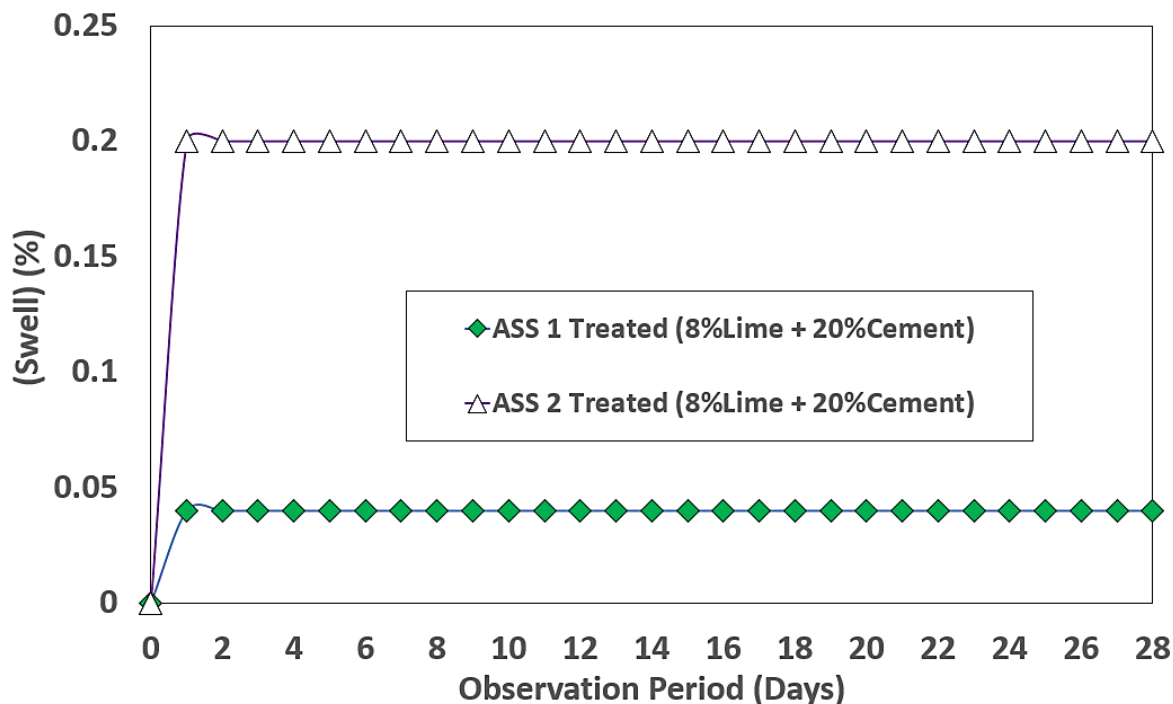


Figure 5.40: Swell results for treated ASS materials after 28 days

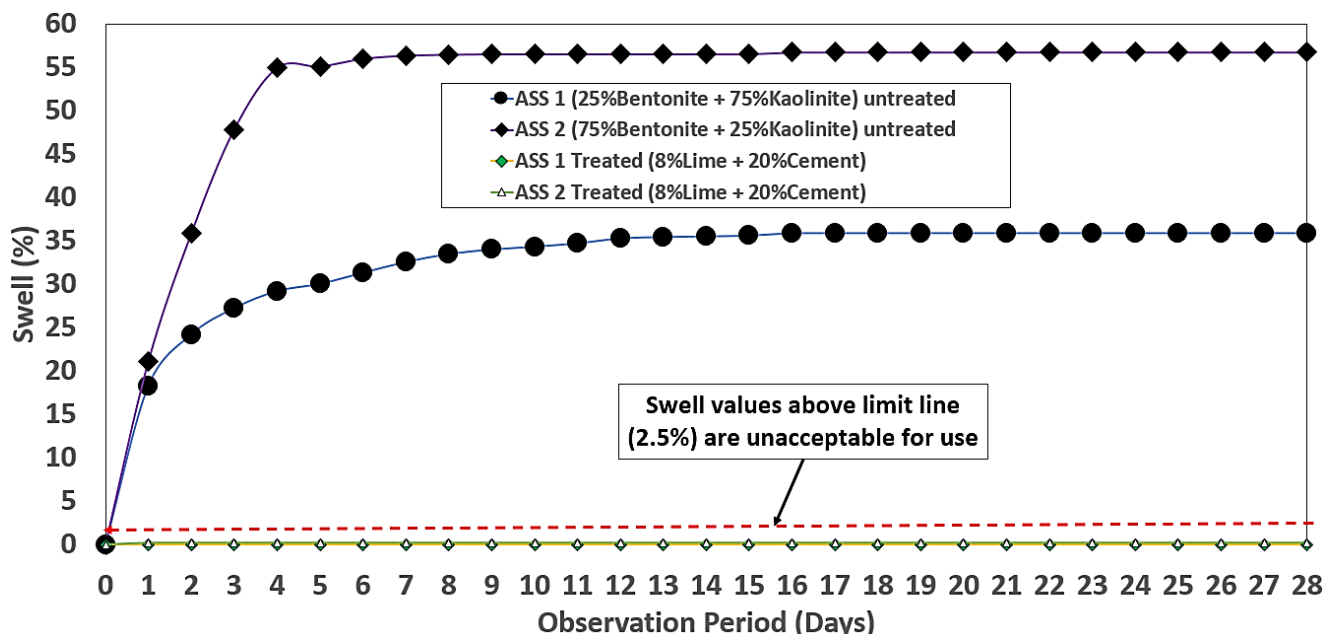


Figure 5.41: Combined swell results for untreated and treated ASS materials after 28 days

5.5 DURABILITY TEST - WETTING-DRYING CYCLE

A reduction in CBR values was observed for all subgrade samples both wet and dry with extremely high CBR values recorded for dry samples. ASS1 + 2%Lime + 2.5% Cement + 23.5%GGBS after 28 days recorded the highest dry CBR values of 230% and a lowest CBR value of 70%. Wet samples recorded the highest CBR value of

180% and a lowest CBR value of 52%. ASS2 + 2%Lime + 2.5% Cement + 23.5%GGBS after 28 days recorded the highest dry CBR values of 200%, and a lowest CBR value of 43%. Wet CBR values recorded include 100%, 83%, 70%, 56%, 43%, 42%, 33%, 29%, 27% and 23%. ASS1 + 2%Lime + 2.5% Cement + 11.75%GGBS + 11.75%BDW after 28 days recorded dry CBR values of 190%, 180%, 110%, 98%, 93%, 88%, 79%, 70%, 69% and 58%. Wet CBR recorded 120%, 89%, 88%, 83%, 78%, 69%, 58%, 46%, 39% and 16%. ASS2 + 2%Lime + 2.5% Cement + 11.75%GGBS + 11.75%BDW) after 28 days recorded dry CBR values of 84%, 79%, 70%, 66%, 58%, 45%, 38%, 33%, 23% and 19%. Wetting sample recorded CBR values of 79%, 67%, 52%, 51%, 45%, 38%, 33%, 27%, 19% and 15%. The mass of wet samples was greater compared to the mass of dry samples. However, a gradual reduction in mass was observed for both wetting and drying samples as cycle number increased. Figure 5.42 - Figure 5.45 shows CBR results for subgrade materials after the wetting-drying cycle test. Figure 5.46 - Figure 5.49 shows the results of mass for wetting-drying samples.

After the conducting wetting-drying cycle on subgrade samples, deeper cracks were observed for ASS2 (extremely high plasticity index) composed of a high percentage (75%) of bentonite compared to ASS1 (25% bentonite). This was due to the high shrinkage potential because of the high amount of bentonite content in the mix. Weight loss in the samples was observed for all mix designs as the number of cycles increased (Harichane et al., 2010). The significant loss in mass of the samples was observed from cycles 3 through to cycle 10 for both wet and dry samples. This weight loss was a result of the sample eroding and falling off due to repeated wetting and drying causing the binders to weaken leading to the disintegration of the subgrade particles. Binders used in subgrade stabilisation disintegrate and losses their binding ability to hold soil particles together when exposed to extreme heat. According to Zihms et al. (2013), high temperature affects mass loss of soil leading to a decrease in particle size with increasing heat. A drastic drop in sample mass after oven drying was observed. However, during the wetting process (soaking) the samples regained some weight due to water filling the air voids in the samples and water is denser than air. The occurrence of mass loss was due to the evaporation of moisture out of the sample during oven drying at $71 \pm 3^\circ\text{C}$ creating cracks and air voids within the sample hence reducing the mass of the sample (Tu et al., 2022).

Cracking after different numbers of wetting-drying cycles was obtained in the subgrade (Tu et al., 2022). According to the British Lime Association, (2015), more moisture loss was observed through evaporation due to heat in soil stabilisation using cement, lime and GGBS. There are two stages of cracks at the end of the drying process of high plasticity index subgrade: The stage of rapid growth and the stage of steady state, these stages affect the strength of the soil and reduced soil mass (Tu et al., 2022). This is what happens to naturally existing high plasticity index subgrade materials when they come under extremely high temperatures, especially in tropical areas. When oven-dry samples were submerged in water during the wetting cycle process, water quickly occupied the air voids expelling the air from within the sample hence increasing the mass of the sample because water is denser than air. The bearing capacity (CBR) of the subgrade samples began to decrease with an increase in the number of cycles. This observation confirms the findings by Hu et al. (2019), which state that subjecting soil to wetting-drying cycles caused the decrease in soil strength. The CBR value of ASS2 (extremely high plasticity index) composed of a high percentage (75%) of bentonite was less compared to ASS1 (25% bentonite).

The reduction in CBR values was observed for all subgrade samples with an increase in wetting-drying cycles. The reduction in CBR value as wetting-drying increases could be attributed to the repeated swelling and shrinkage due to the wetting-drying cycle process resulting in weakness within the core of the samples (Hu et al., 2019). Very high CBR values more than twice as high compared with wet samples were recorded for dry cycle samples. The extremely high CBR observed in dry cycles was due to the ability of highly plasticity index soil (clay) to harden when they come in contact with elevated temperatures. This occurrence could be observed during the process of pot making. The early people discovered in the 29,000 – 25,000BC that clay becomes hard and maintains its shape when mixed with water and cooked in fire (Lesley, 2022). When clay comes in contact with high heat, it undergoes major physical and chemical changes where the clay change from soluble clay to hard insoluble ceramic (Lesley, 2022). The hardening of the clay (high plasticity index soil) increased the bearing capacity (CBR) of the soil, hence, the high CBR values were recorded for drying-cycle samples. The low CBR values recorded for wet-cycle samples compared with dry-cycle samples could be due to the fact that high plasticity index (clay) is weak when

they come in contact with water. Overall, the CBR values recorded for ASS2 (extremely high plasticity index) were lower compared with ASS1.

This was due to the high amount of bentonite content in the mix making it expansive and weak in compression. Subgrade materials with high bentonite content have low CBR values and subgrade mix design composed of high GGBS content (23.5%) recorded the highest CBR values for the wetting-drying cycle test making it the best performing mix for the wetting-drying test. The high CBR values achieved with the addition of high amounts of GGBS in the mix. GGBS are rich in calcium, the main reaction product of Calcium Silicate Hydrate (CSH) gel responsible for strength gain in a mix. GGBS are highly cementitious and high in strength-enhancing compounds (Roger, 2011). Studies have shown that the higher the amount of GGBS blend the greater the strength and durability of the mix (Hewlett, 2003). This shows that subgrade material treated using a high amount of GGBS (23.5%) as binder can withstand a large number of wetting-drying cycles and still maintain very high CBR values required for use in road construction. The addition of an equal proportion of GGBS and BDW exhibited good CBR values usable in road construction at the end of the wetting-drying cycle testing process. Brick Dust Waste (BDW) are pozzolanic materials that can form CSH gel to increase strength in a mix.

It was found that the addition of brick dust increased soil strength between 1.7 - 2.3 times (Hidalgo et al., 2019). Pozzolanic materials like BDW contain alumina/silica which reacts to form new compounds (calcium silicate hydrate (CSH) and calcium aluminium hydrate (CAH) gel when lime is added (Roger, 2011). According to According to The Constructor Building Ideas (TCBI), (2021), subgrades with CBR value < 2% are unsuitable for use in road construction and would require modification or re-engineering. The results show that CBR values achieved for all subgrade samples after the wetting-drying cycles test are very good and greater than 2% making them suitable for use in road construction. Hence, expansive subgrade materials treated with GGBS and BDW are highly durable and can withstand harsh weather conduction without losing their strength. Figure 5.42 - Figure 5.45 Wetting-drying cycle results for ASS1 and 2. Figure 5.46 - Figure 5.49 shows sample mass for ASS1 and 2. Figure 5.50 - Figure 5.52 shows oven dry sample exhibiting cracks similar to a typical existing naturally dry expansive. Loose subgrade particles as a result of the

Chapter 5 – Results and Discussion

disintegration of binders due to high temperature. Air bubbles coming from cracks due to water filling the air voids during the wetting process immediately after oven drying and eroded subgrade sample due to cyclic wetting.

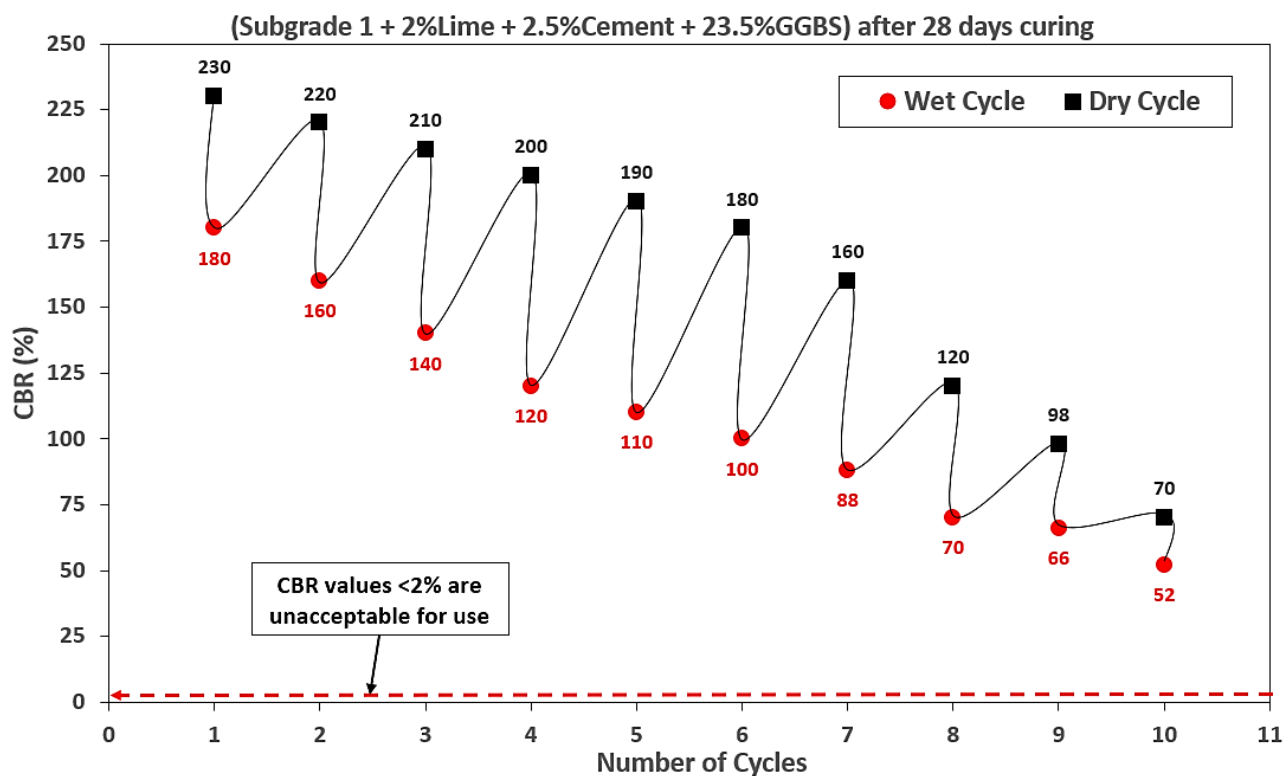
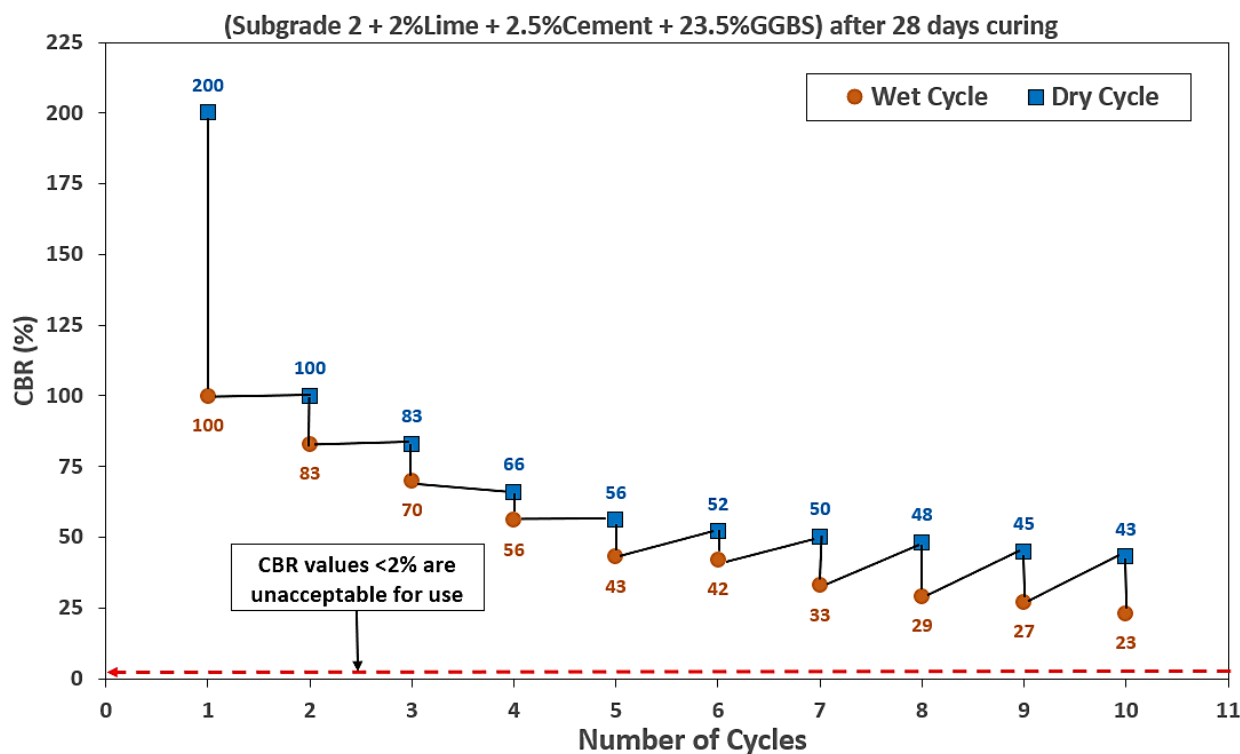


Figure 5.42: Wetting-drying cycle results for subgrade 1 composed of GGBS after 28 days of curing



Chapter 5 – Results and Discussion

Figure 5.43: Wetting-drying cycle results for subgrade 2 composed of GGBS after 28 days of curing

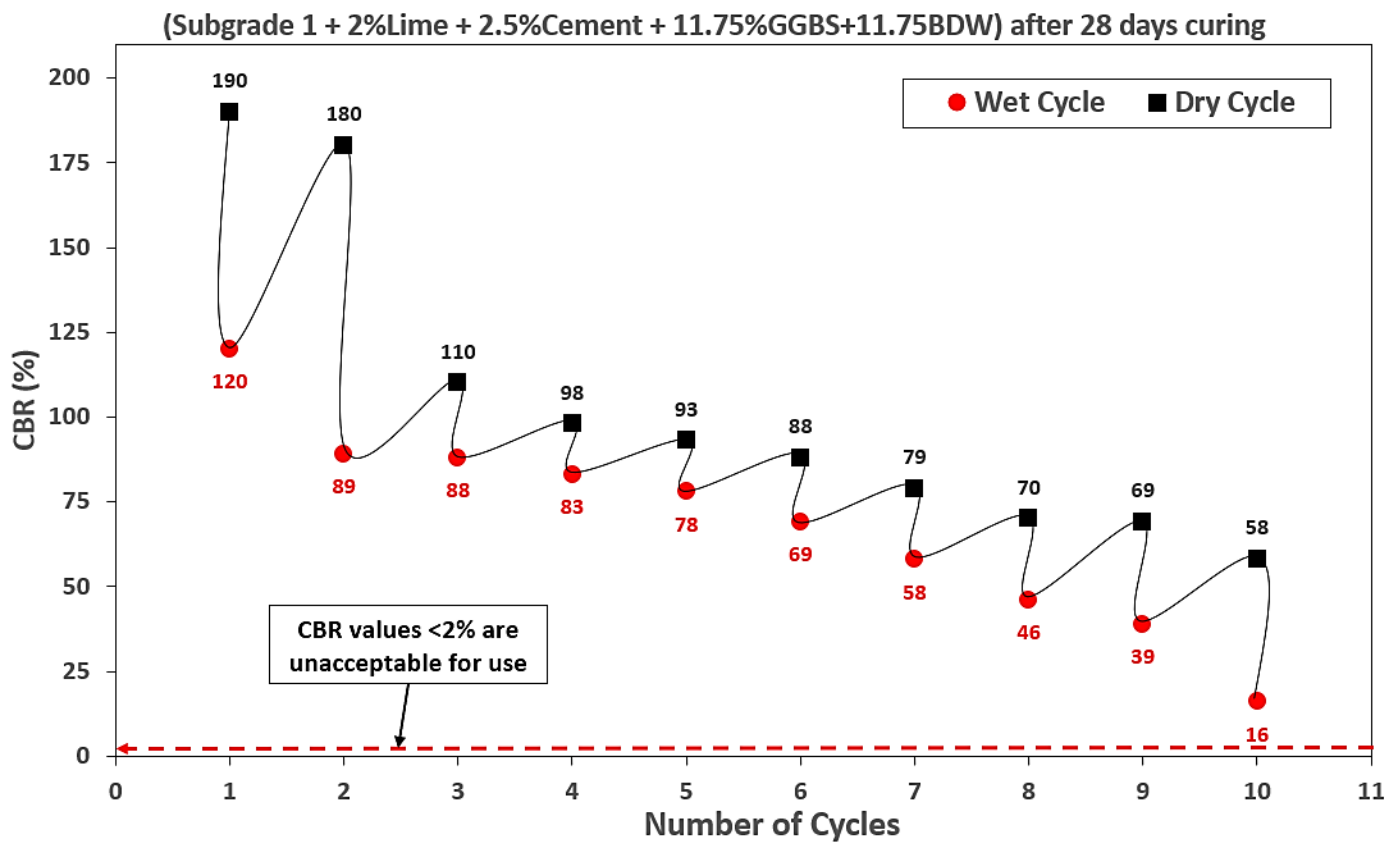


Figure 5.44: Wetting-drying cycle results for subgrade 1 composed of GGBS and BDW after 28 days of curing

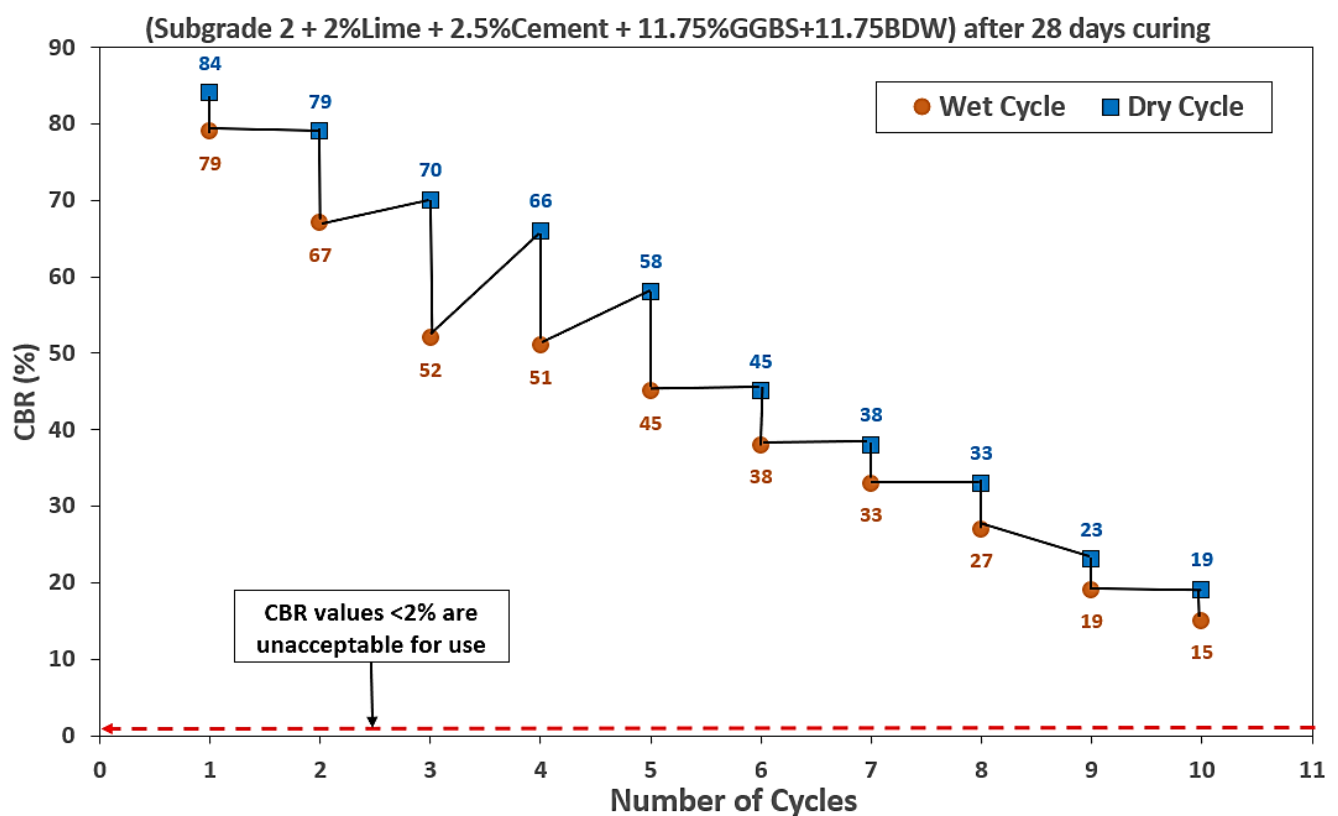


Figure 5.45: Wetting-drying cycle results for subgrade 2 composed of GGBS and BDW after 28 days of curing

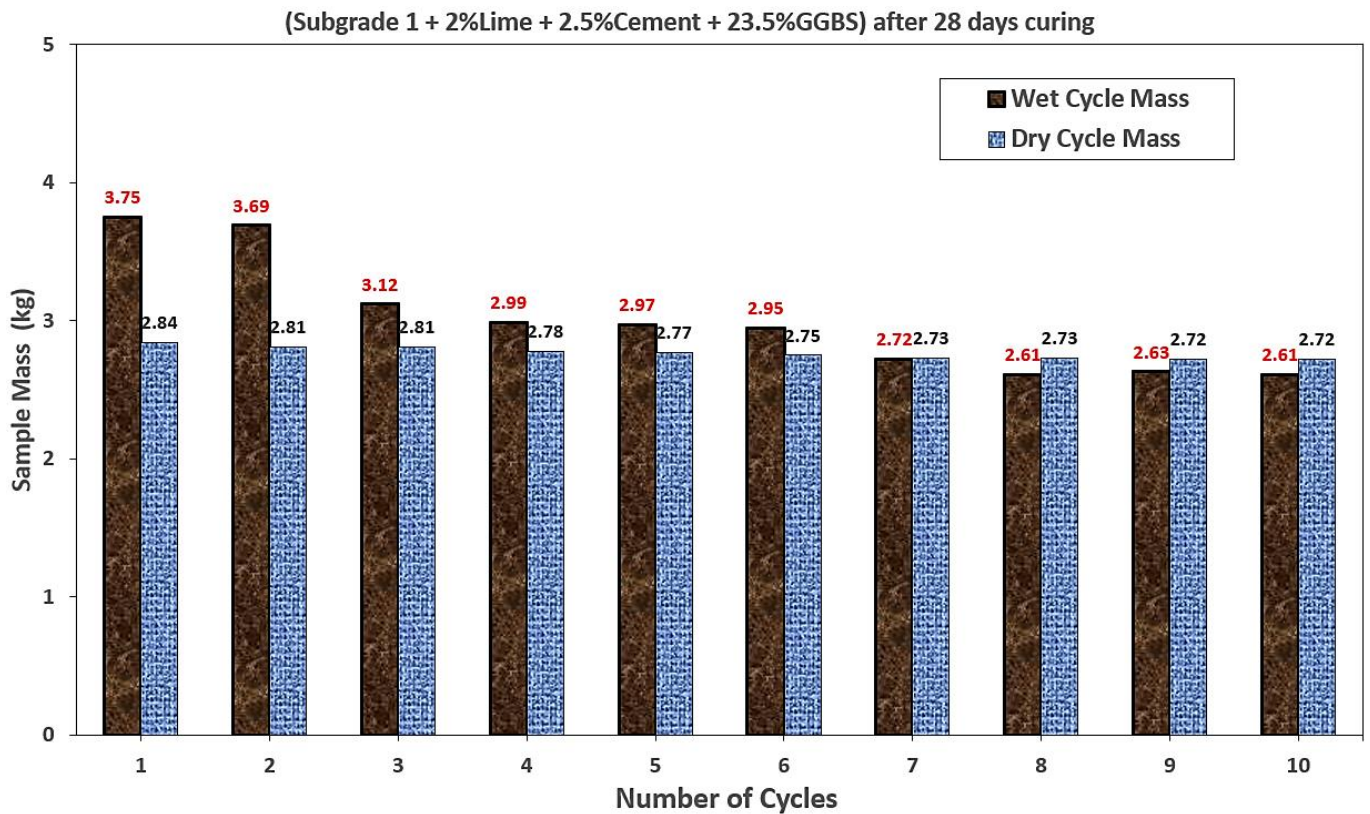


Figure 5.46: Sample mass for subgrade 1 composed of GGBS after 28 days of curing

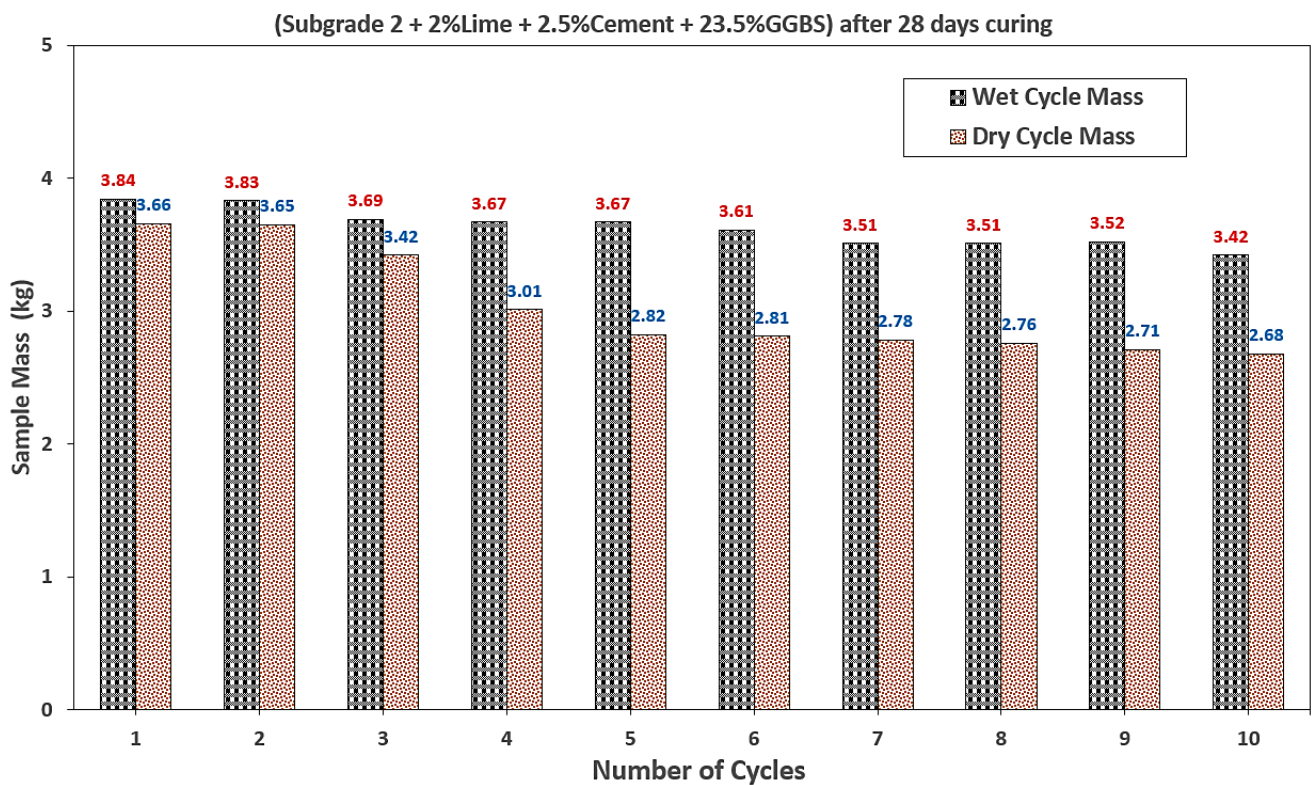


Figure 5.47: Sample mass for subgrade 2 composed of GGBS after 28 days of curing

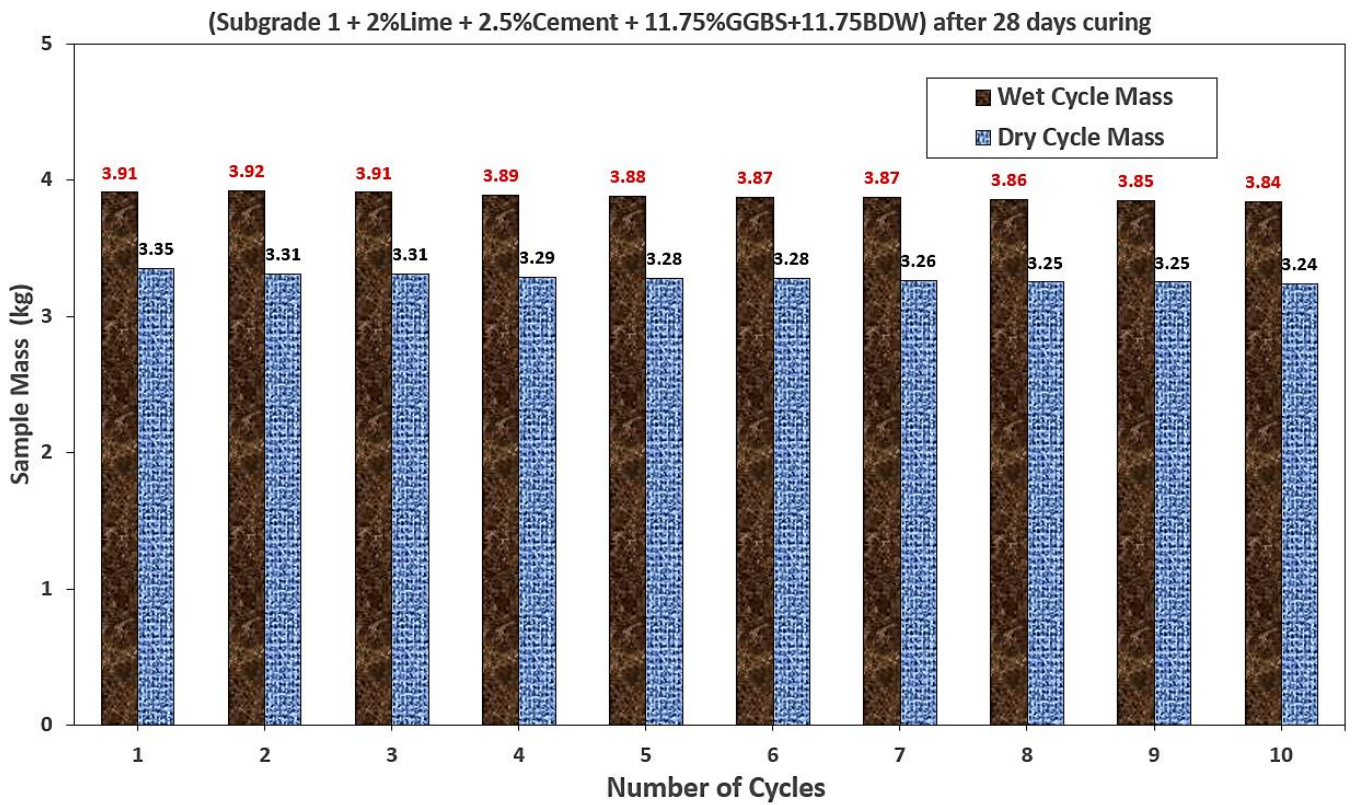


Figure 5.48: Sample mass for subgrade 1 composed of GGBS and BDW after 28 days of curing

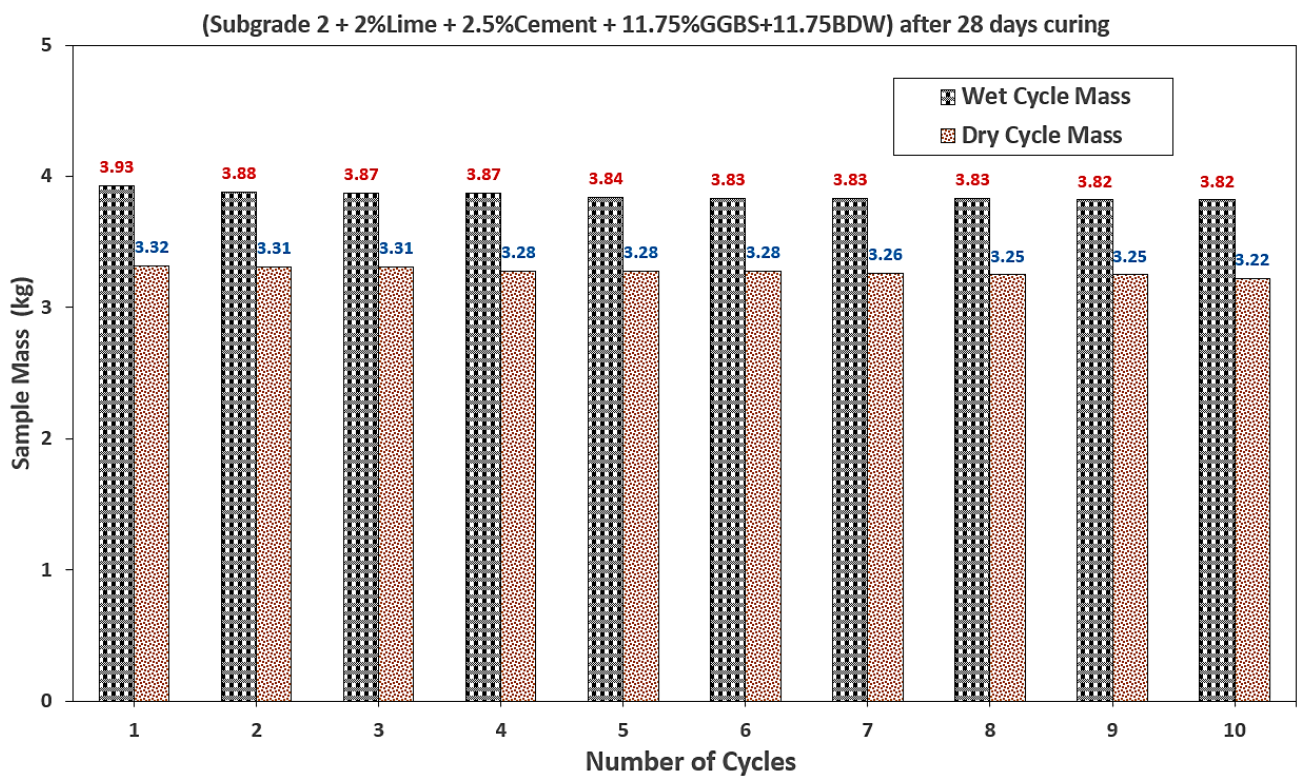


Figure 5.49: Sample mass for subgrade 2 composed of GGBS and BDW after 28 days of curing



Figure 5.50: Oven dry sample exhibiting cracks similar to a typical existing naturally dry expansive

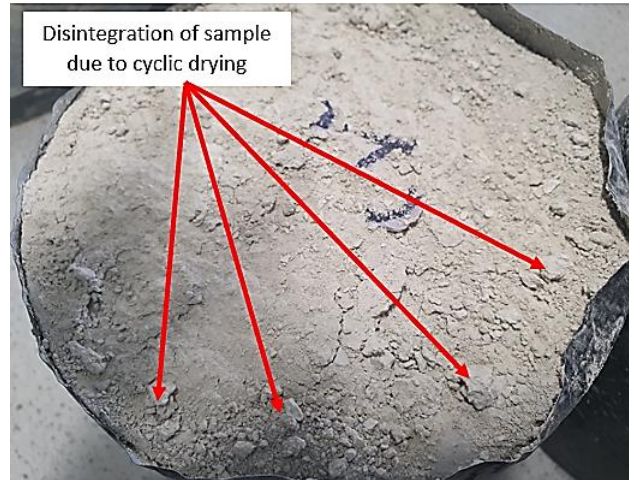


Figure 5.51: Disintegration of sample due to cyclic drying
Loose subgrade particles as a result of the disintegration of binders due to high temperature



Figure 5.52: Eroding of sample due to cyclic wetting

5.6 MICROSTRUCTURAL PROPERTIES

In this study, the SEM images and EDX results (Figure 5.55 - Figure 5.58 and Appendix 7.5 SEM and EDX) for treated ASS samples show the formation of calcium silicate hydrate (C-S-H) gel and calcium aluminate hydrate (C-A-H) gel with an increase in curing age. A clear presence of high Ca-Si-Al elements responsible for the formation of tobermorite gel was observed from the SEM Map for the various chemical compositions in different areas of the ASS materials. At the end of 7 days of curing, ASS1 and ASS2 were treated using 8% lime + 20% cement recorded with the formation of 16.21% Calcium and 21.96% Calcium respectively. All ASS Samples cured for 28 days exhibited a very high presence of C-S-H and C-A-H gel. At the end of 28 days of curing ASS1 and ASS2 treated using 8% lime + 20% cement, the formation of 16.21% Calcium observed after 7 days for ASS1 increased to 24.75%, and 21.96% Calcium formed in 7 days for ASS2 increased to 33.08% respectively. The highest Calcium of 44.87% was recorded for ASS1 + 2%Lime + 2.5%cement + 11.75%GGBS +11.75%BDW after 28 days of curing and the lowest Calcium of 2.77% was observed for ASS1 + 2%Lime + 2.5%cement + 11.75%GGBS +11.75%Plastic after 7 days of curing.

ASS1 + 2%Lime + 2.5%cement + 23.5% Glass after 7 days of curing recorded the highest Silicon of 50.28%. the lowest Silicon of 4.54% was observed for ASS1 + 2%Lime + 2.5%cement + 11.75%GGBS + 11.75%BDW after 7 days curing. ASS1 + 2%Lime + 2.5%cement + 23.5%Plastic after 28 days of curing also recorded the highest Aluminium of 26.76%. ASS1 + 2%Lime + 2.5%cement + 11.75%GGBS +11.75%Glass and ASS2 + 2%Lime + 2.5%cement + 23.5% BDW after 28 days of curing recorded the lowest Aluminium of 2.34%. Figure 5.53 shows detailed results of calcium silicon and aluminium oxides for treated ASS materials. Figure 5.54 shows ASS samples with dark green colour formed during the hydration process to produce C-S-H gel responsible for strength gain. Figure 5.55 – Figure 5.58 and Appendix 7.5 SEM and EDX shows detailed results of SEM images and EDX results for treated ASS samples at various points of the sample after 7 and 28 days of curing ages. The best performing mixes after 90 days curing ASS1 + 2%Lime + 2.5%cement + 11.75%GGBS + 11.75% BDW and ASS + 2%Lime + 2.5%cement + 23.5%GGBS recorded 26.09% Calcium, 22.13% Silicon and 12.57% Aluminium. ASS2 + 2%Lime + 2.5%cement + 11.75%GGBS + 11.75%BDW and ASS + 2%Lime + 2.5%cement + 23.5% GGBS

recorded 12.28% Calcium, 40.06% Silicon and 20.52%. Samples without cement (ASS1 + 2%Lime + 26%GGBS recorded Calcium 11.16% Silicon 34.12% and Aluminium 29.41%. Further details for ASS+2%Lime+2.5%Cement+23.5%GGBS and more can be found in Figure 5.55 – Figure 5.58 and Appendix 7.5 SEM and EDX.

High Ca-Si-Al, which is the main ingredient for the formation of C-S-H gel responsible for strength development, was observed in all ASS materials with an increase in curing age. The continuous formation of C-S-H gel with an increase in curing age within a pore structure can contribute to strength development in a mix, the higher the C-S-H gel the high the strength in the samples (Abbey et al., 2020). The highest calcium (Ca) oxide was found in mix design with high GGBS and BDW content (2% lime + 2.5% cement + 11.75% GGBS + 11.75% BDW) after 28 days of curing. The high formation of Ca in this mix was due to the presence of GGBS rich in Calcium and BDW pozzolanic materials. These two binders with a high ability to form C-S-H gel coming together in a mixture after a long curing period recorded the highest CBR value of 109% and very low swell values in this research due to the high C-S-H gel found in the mix. The SEM micrograph and XRD results show that the formation of C-S-H gel became prominent as GGBS increased (Saludung et al., 2018). BDW are pozzolanic materials that form C-S-H gel responsible for strength gain in a mixture. GGBS is high in calcium and forms C-S-H gel during the hydration process for strength gain in a mixture (Hidalgo et al., 2019). GGBS are rich in calcium, the main reaction product of C-S-H gel responsible for strength development (Sasui et al., 2019).

Soaked CBR values increased by about 400% and 28% with the addition of an optimum amount of GGBS (Yadu et al., 2013). Pozzolans are materials such as BDW that contain alumina/silica which reacts to form new compounds (Calcium Silicate Hydrate and Calcium Aluminium Hydrates when lime is added and have the ability to modify the properties of a lime mixture (Rogers, 2011). Brick Dust Waste (BDW) exhibits pozzolanic properties, which can be used as cement replacement in road subgrade stabilisation (Kartini et al., 2012). GGBS are highly cementations and high in strength-enhancing compounds which improve strength and durability in a mix. Studies have shown that the higher the amount of GGBS blend, the greater the hydraulic activity (Hewlett, 2003). Although the formation of high C-S-H gel although good can harm the sample under high temperature. Therefore, too much formation of

C-S-H may harm the structure of the specimen at high temperatures due to decomposition (Saludung et al., 2018).

The highest Silicon (Si) was recorded for mix design with very high glass content (2% lime + 2.5% cement + 23.5% Glass) after 7 days of curing. This observation of high silicon in mixtures with high glass content can be attributed to the high silicon content in glass. Silicon dioxides (SiO₂) are a common fundamental constituent of glass because glass is made from chemically-pure silica (Chawla et al., 1993). High silicon oxide often refers to high purity silica glass (Wang et al., 2011). High Aluminum (Al) oxide was recorded for mix design with very high glass content (2% lime + 2.5% cement + 23.5% Plastic) after 28 days of curing. The formation of aluminium in the mix could be due to the hydration process of cement and lime. Furthermore, aluminium oxides are formed during cement and lime hydration to generate calcium carbonate hydrate (Zhang et al., 2011). The reasonably high Magnesium Oxide (MgO) content in GGBS also contributed to high strength in the mix with an increase in curing age. It was observed that ASS1 2% Lime + 2.5% Cement + 23.5% GGBS after 7 days of curing recorded Mg of 1.49%. Mg increased up to 4.74% at a later curing age of 28 days.

Extremely high plasticity subgrade ASS2 2% Lime + 2.5% Cement + 23.5% GGBS after 7 days of curing recorded Mg of 0.66% which later increased to 3.69%. This shows that ASS2 (extremely high plasticity) recorded lower Mg at 7 and 28 days compared with ASS1 (high plasticity). This shows that Mg decreases with an increase in plasticity index. GGBS-MgO stabilised soil could gain higher unconfined compressive strength relative to the Portland cement stabilised soils (Yi et al., 2012). MgO acts as an effective alkali activator of GGBS, achieving higher 28-day compressive strength (Yi et al., 2014). Although higher carbon was recorded for other mixtures, the high carbon oxide (C) found in mixtures containing recycled plastic could be due to the plastic content in the mix because plastics are basically full of carbon. High carbon oxides (C) were found in the mixtures containing high plastic content and the carbon oxide increased with an increase in curing age. ASS1 2% Lime + 2.5% Cement + 23.5% Plastic after 7 days of curing recorded C of 19.82% and later increased to 21.71% after 28 days of curing. Low carbon content was observed for ASS2 (extremely high plasticity) with a slight increase with increase in curing age. ASS2 2% Lime + 2.5%

Cement + 23.5% Plastic after 7 days recorded carbon of 5.06% and later increased to 18.1% after 28 days of curing. Plastics are carbon more specifically because almost all plastics are fossil carbon locked up in polymer form (Zhu et al., 2021).

The high CSH gel formation observed for the best performing mixes composed of GGBS and BDW was due to the formation of high calcium, Silica and Aluminium found in the mix. The high strength of samples without cement composed of high GGBS content and a small amount of lime shows that GGBS and lime only can be used in subgrade stabilisation to improve their engineering properties. During the laboratory test, an obvious dark green colour change was observed in ASS samples containing GGBS with very high CBR and low swell values. About 90% of the sample changed to dark green with increased GGBS content and curing age. After investigating this colour reaction (SEM and EDX analysis) it was confirmed that the dark green emanates from carbonation due to the formation of carbon minerals or C-S-H gel during the hydration process. It was observed that the more the dark green colour the higher the CBR value.

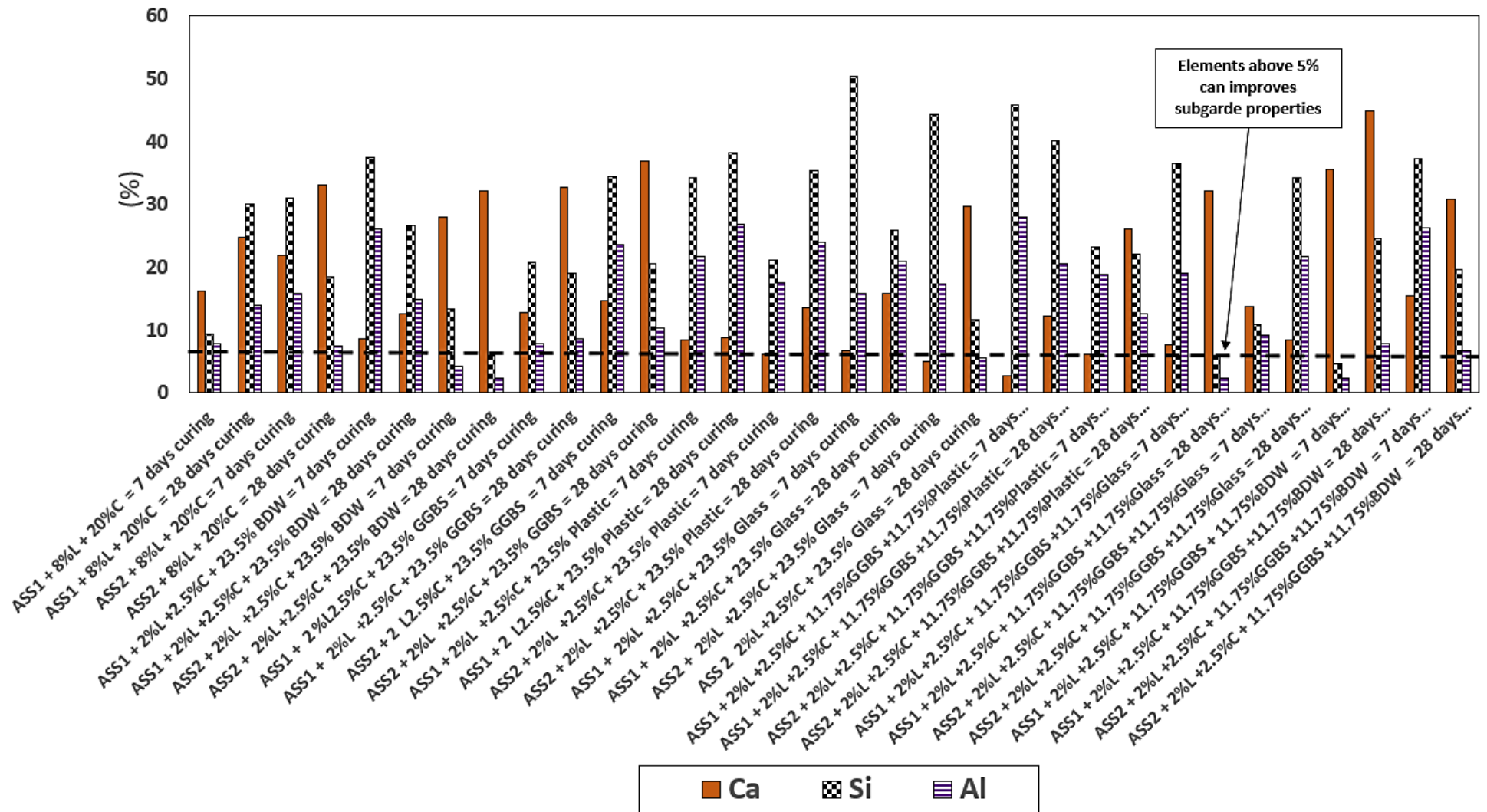


Figure 5.53: Ca, Si, Al responsible for strength gain

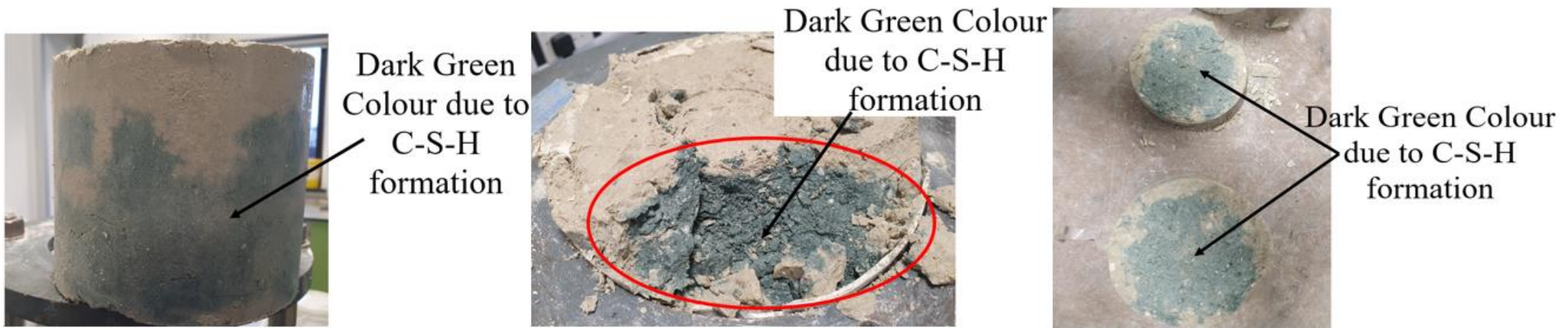


Figure 5.54: ASS samples with dark green colour formed during the hydration process to produce C-S-H gel responsible for strength gain

Chapter 5 – Results and Discussion

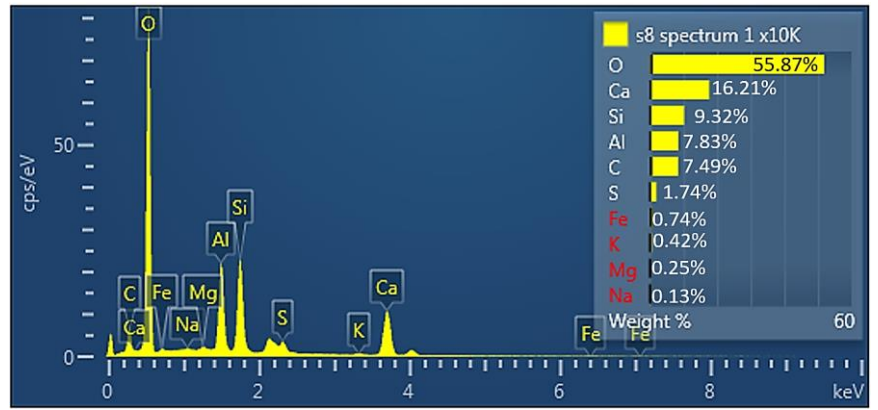
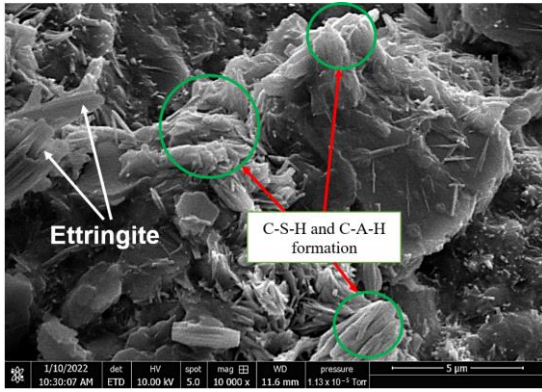


Figure 5.55: SEM image and EDX results for ASS1 + 8% lime + 20% cement after 7 days of curing

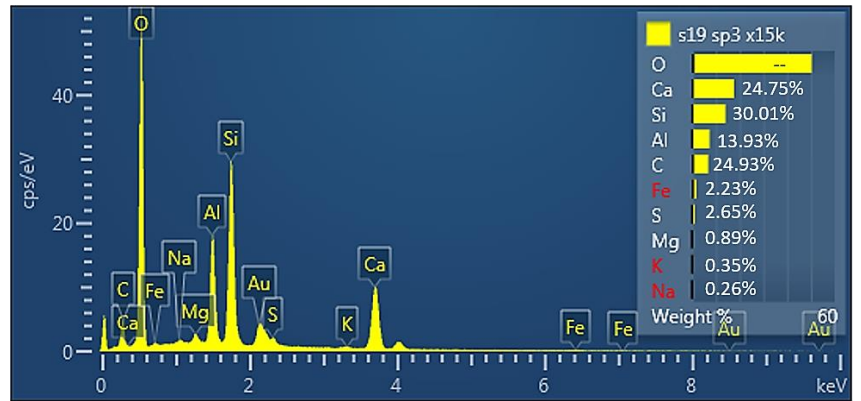
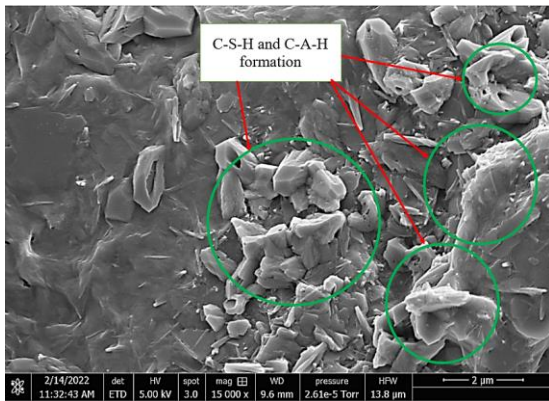


Figure 5.56: SEM image and EDX results for ASS1+ 8% lime + 20% cement after 28 days of curing

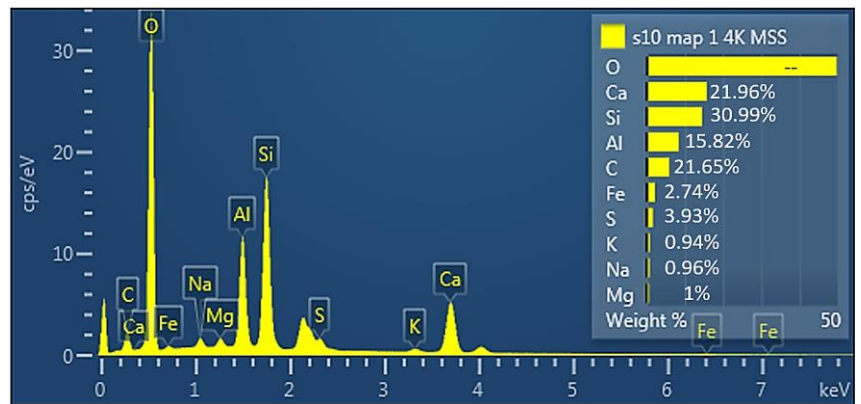
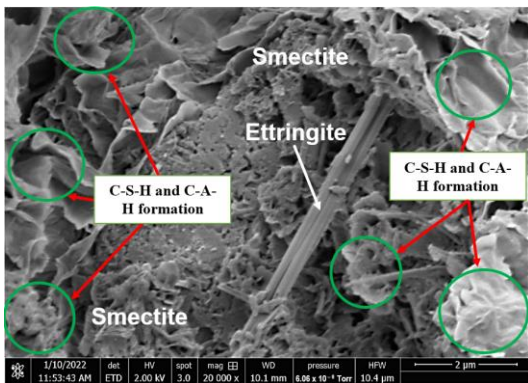


Figure 5.57: SEM image and EDX results for ASS2 + 8% lime + 20% cement after 7 days of curing

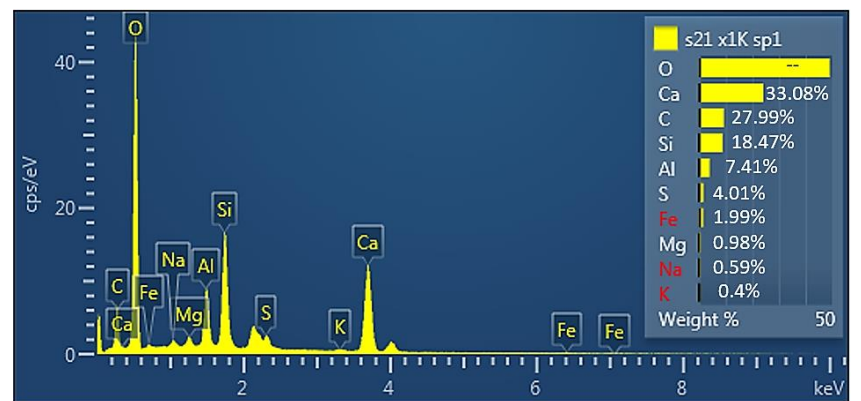
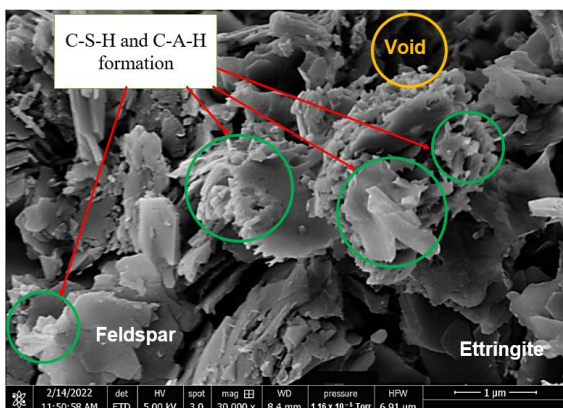


Figure 5.58: SEM image and EDX results for ASS2+ 8% lime + 20% cement after 28 days of curing

5.7 ROAD PAVEMENT THICKNESS AND CONSTRUCTION DEPTH OPTIMISATION

5.7.1 Variation in Pavement Thickness and Construction Depth

5.7.1.1 Un-soaked Treated and Untreated ASS Materials

Pavement thickness optimisation was conducted for treated and un-soaked ASS materials after 7 and 28 days of curing and untreated ASS materials shows a reduction in road pavement thickness with an increase in CBR value for all ASS samples. An increase in pavement thickness was observed when traffic loads increased from light, medium to heavy traffic for all ASS materials. It was observed that CBR values for all ASS samples are greater than 2% making them suitable for use as subgrade materials in road construction. Road construction depth optimisation conducted for treated-unsoaked ASS materials after 7 and 28 days of curing and untreated ASS materials shows a reduction in road construction depth with an increase in CBR value for all ASS samples. An increase in construction depth was observed when traffic load increased for light, medium to heavy traffic for all ASS materials. It was observed that CBR values for all un-soaked ASS samples are greater than 2% making their depth of construction accepted for use in road construction. ASS samples with a CBR value of 8% recorded the deepest depth of construction of 205mm, 240mm and 400mm for light, medium and heavy traffic loads.

After conducting road pavement thickness and construction depth optimisation using CBR values achieved in this study, a reduction in road pavement thickness and depth of construction with an increase in CBR value was observed. Hence the higher the CBR value the thinner the pavement thickness and the shallower the depth of construction. A significant difference in pavement thickness and depth of construction was observed between using the lowest and the highest CBR value and between light and heavy traffic types. 19% increase in CBR value reflected in a reduction in the overall thickness and life cycle cost of a road in Uganda (Melling et al., 2017). According to the Constructor Building Ideas, (2021), pavement thickness is determined by the subgrade strength and it's good to make the subgrade as strong as possible. Pavements are built to a set thickness dependent only on the subgrade quality, being independent of anticipated traffic (Dawson et al., 2008). It was more economical to design road pavement for the existing subgrade capacity than to import

or raise the subgrade support by using an extra-thicker subbase (Li et al., 1964). It was observed that heavy traffic load requires thicker pavement to be able to carry traffic load and light traffic load requires thinner pavement.

This is to ensure the road pavement withstands deformation and can sustain the weight of heavy traffic during its design life. Pavement design involves determining a pavement thickness that can sustain the heaviest traffic load over an extended design life without additional structure (National Asphalt Pavement Association, 2019). Nunn et al. (1997), road pavements are designed for predicted levels of traffic to control deterioration due to the accumulation of small amounts of damage caused by the passage of each vehicle. Pavement with less than about 180mm of asphalt deforms at a high rate but thicker pavement deforms at a lesser rate (Nunn et al., 1997). Untreated un-soaked ASS samples with a CBR of 8% for ASA 1 and 9% for ASS2 recorded thicker pavement and construction depth. After treating ASS materials using cement and lime (Control), CBR value shot up to 80% and 96% for ASS1 after 7 and 28 days of curing due to the formation of C-S-H gel responsible for strength gain. This translated to a drastic reduction in road pavement and construction depth.

5.7.2 Sustainable Treated – Soaked and Un-soaked CBR

ASS materials treated using sustainable waste materials also recorded thinner pavement thickness with an increase in CBR values at various binder proportions and curing ages. ASS1 was treated using 23.5% Brick Dust Waste as a partial replacement for cement and lime with a CBR value of 23% after 7 days of curing at room temperature of $20 \pm 2^\circ\text{C}$ recorded pavement thickness of 150mm, 170mm and 190mm for light, medium and heavy traffic load. Untreated ASS, glass and plastic on their own with little cement and lime used as binders to stabilise ASS materials recorded thickest pavement of 260mm, 280mm and 320mm for light, medium and heavy traffic. They also recorded the deepest construction depth of 205mm, 240mm and 400mm due to their low CBR values at the end of 7 and 28 days of curing. Glass and plastic do not react with cement and lime to form C-S-H gel to increase CBR in a mixture. However, the minimal amount of cement (2.5%) and lime (2%) was responsible for the generally low CBR values achieved because no C-H-S gel was formed to increase the strength. The acceptable CBR and their resultant pavement thickness for glass and plastic could

have been obtained due to the interlocking of the granular (plastic and glass) materials.

The very high CBR values achieved for using a high amount of 23.5% GGBS only and the addition of 11.75% GGBS to BDW in a mixture record the thinnest pavement thickness of 40mm for light, medium and heavy traffic loads and construction depth of 50mm, 55mm and 80mm for light, medium and heavy traffic. The CBR values are expected to increase with the inclusion of brick kiln dust in stabilised soil, helping to decrease the design thickness of subgrade and hence decreasing the overall construction cost (Mehta et al., 2019). Pavement thickness and construction depth began to reduce with the addition of 11.75% GGBS to each mix due to their high calcium responsible for the formation of C-S-H gel. GGBS are rich in calcium, the main reaction product of C-S-H gel responsible for strength development (Sasui et al., 2019). Stabilising subgrade using waste materials such as GGBS will increase the load-bearing capacity of the subgrade for heavy-wheeled vehicle traffic and reduce the cost of pavement (Joshi et al., 2021). All pavement thickness and construction depths achieved for un-soaked ASS samples are good and acceptable for use in road construction because their CBR values are $>2\%$. According to relevant guidance, such as the IAN73/06, CBR values less than 2% are unacceptable for use in road construction and would require modification or treatment to improve their engineering properties. Soaked ASS samples recorded very low CBR for untreated samples $<2\%$ making them unacceptable for use in road construction. treated soaked ASS samples recorded low CBR even though acceptable which translates to thicker pavements and deeper construction depth.

Soaked ASS samples treated using 23.5% glass with CBR 3% recorded thicker pavement of 450mm, 490, and 540mm for light, medium and heavy traffic loads. It also recorded a corresponding construction depth of 350mm, 400mm and 610mm for light, medium and heavy traffic loads, respectively. A reduction in the swell was observed with a reduction in pavement thickness after comparing pavement thickness for soaked ASS samples with their swell values. A similar observation was found for depth of construction with deduced corresponding to reduced swell for soaked ASS samples. Hence, the higher the swell potentials of subgrade materials the thicker and deeper the pavement and vice versa. Lower CBR and swell values are allowed at

Chapter 5 – Results and Discussion

greater depth as the wheel-load stresses are more widely distributed (O'Flaherty et al., 1961). Figure 5.59 shows untreated ASS Swell values against pavement thickness. Figure 5.60 shows treated swell values against pavement thickness. Figure 5.61 shows untreated ASS Swell values against the depth of construction. Figure 5.62 shows treated swell values against the depth of construction. Further details on ASS1 treated using 11.75% and 23.5% GGBS, recycled plastic, glass and BDW including road pavement thickness optimisation for un-soaked treated and untreated subgrade materials in accordance with California state of highways guidance are shown in Figure 5.63 - Figure 5.65.

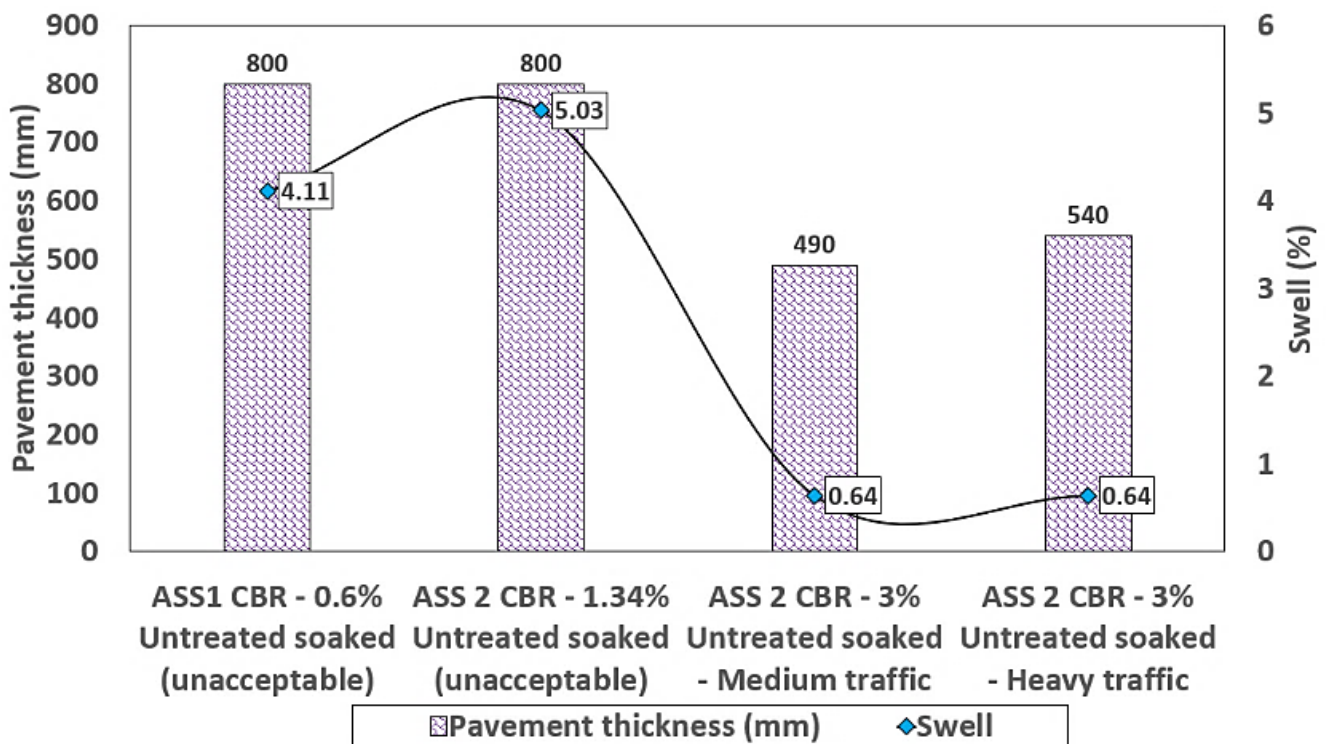


Figure 5.59: Untreated ASS Swell values against pavement thickness

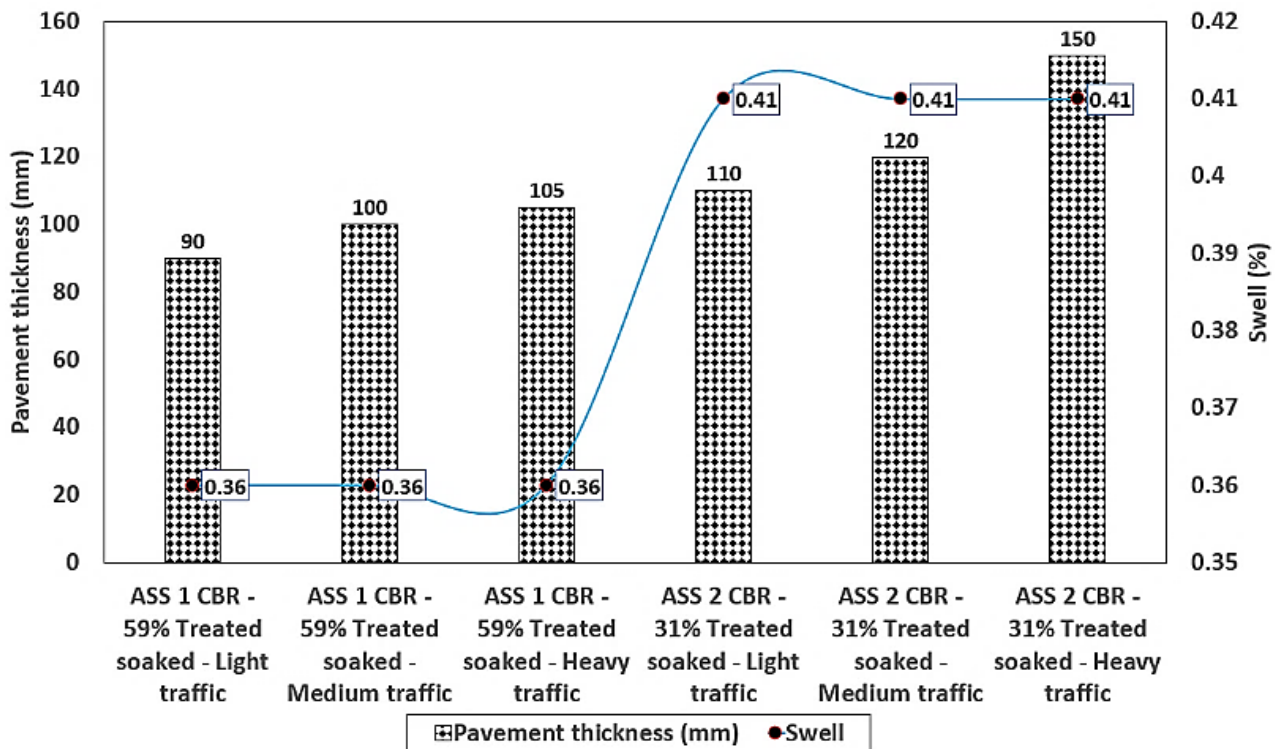


Figure 5.60: Treated swell values against pavement thickness

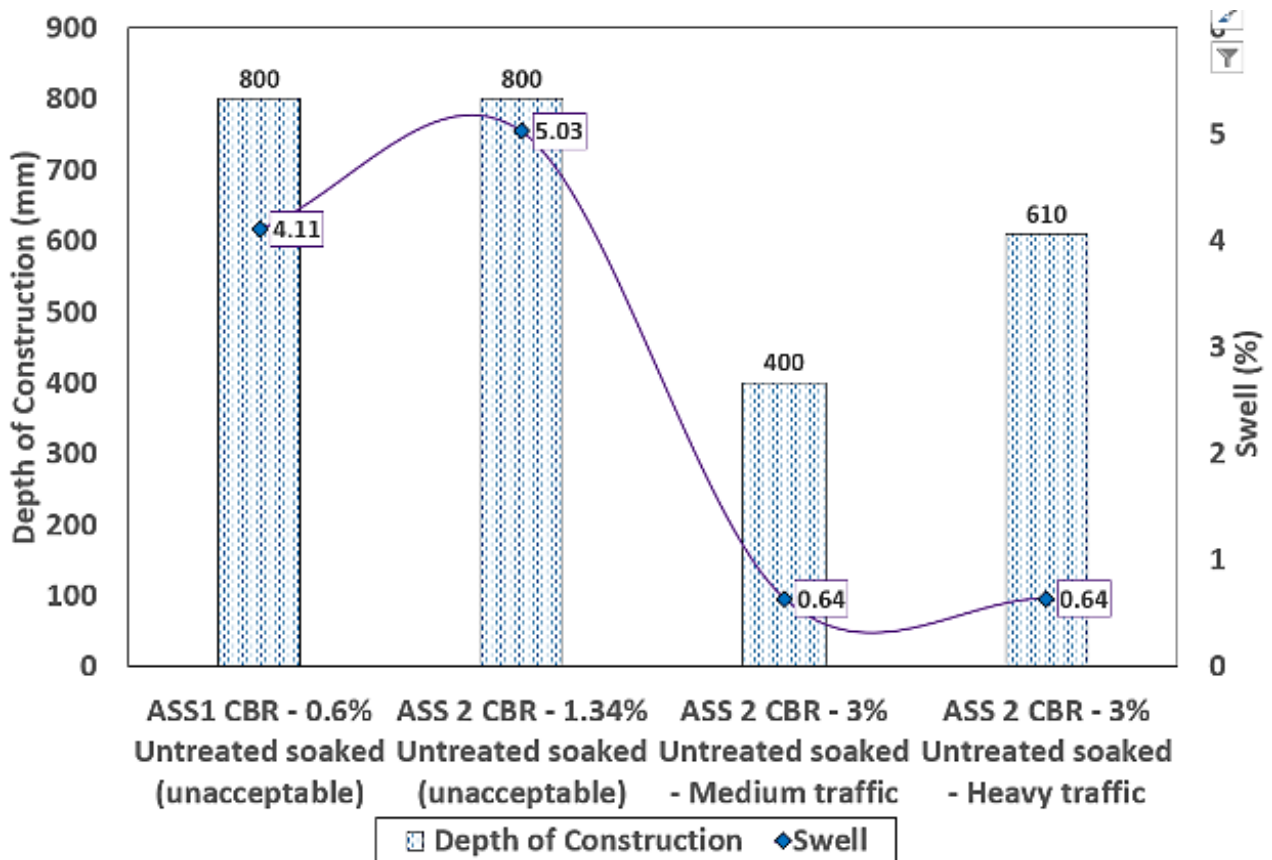


Figure 5.61: Untreated ASS Swell values against the depth of construction

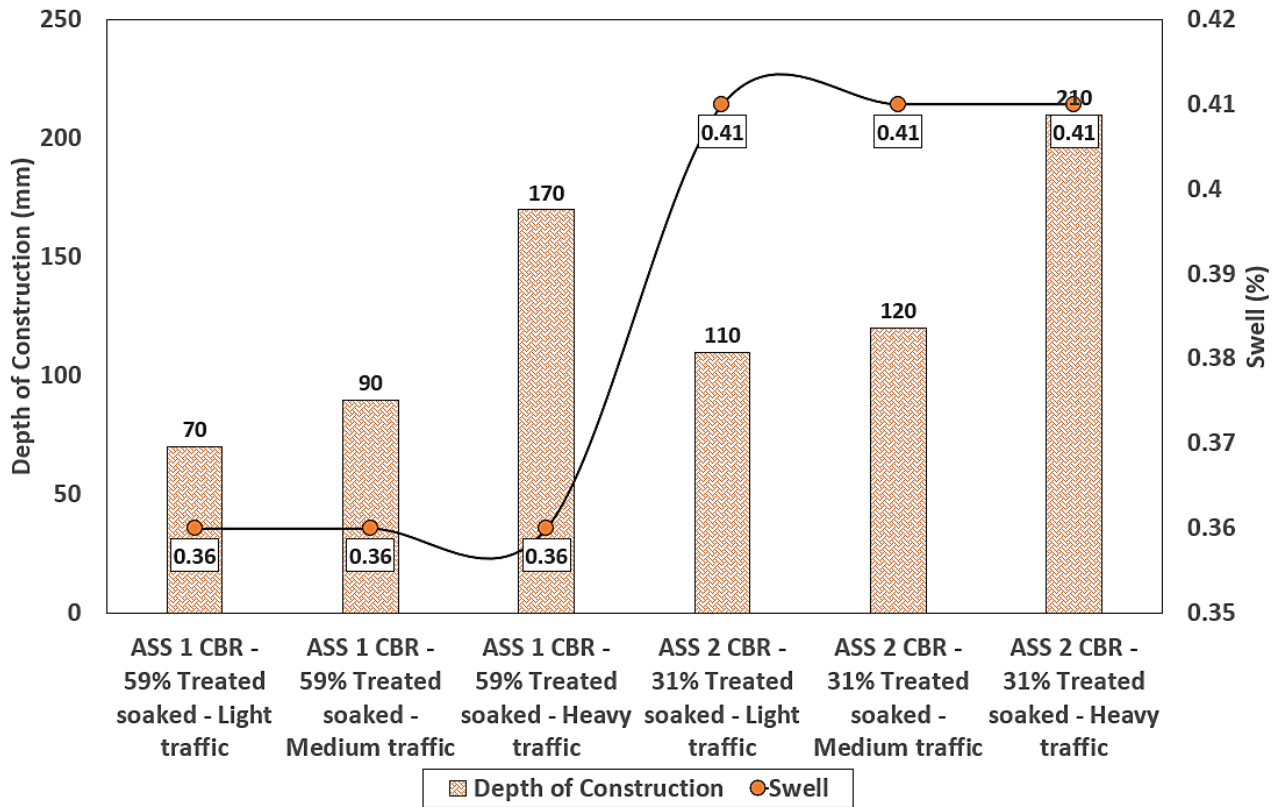
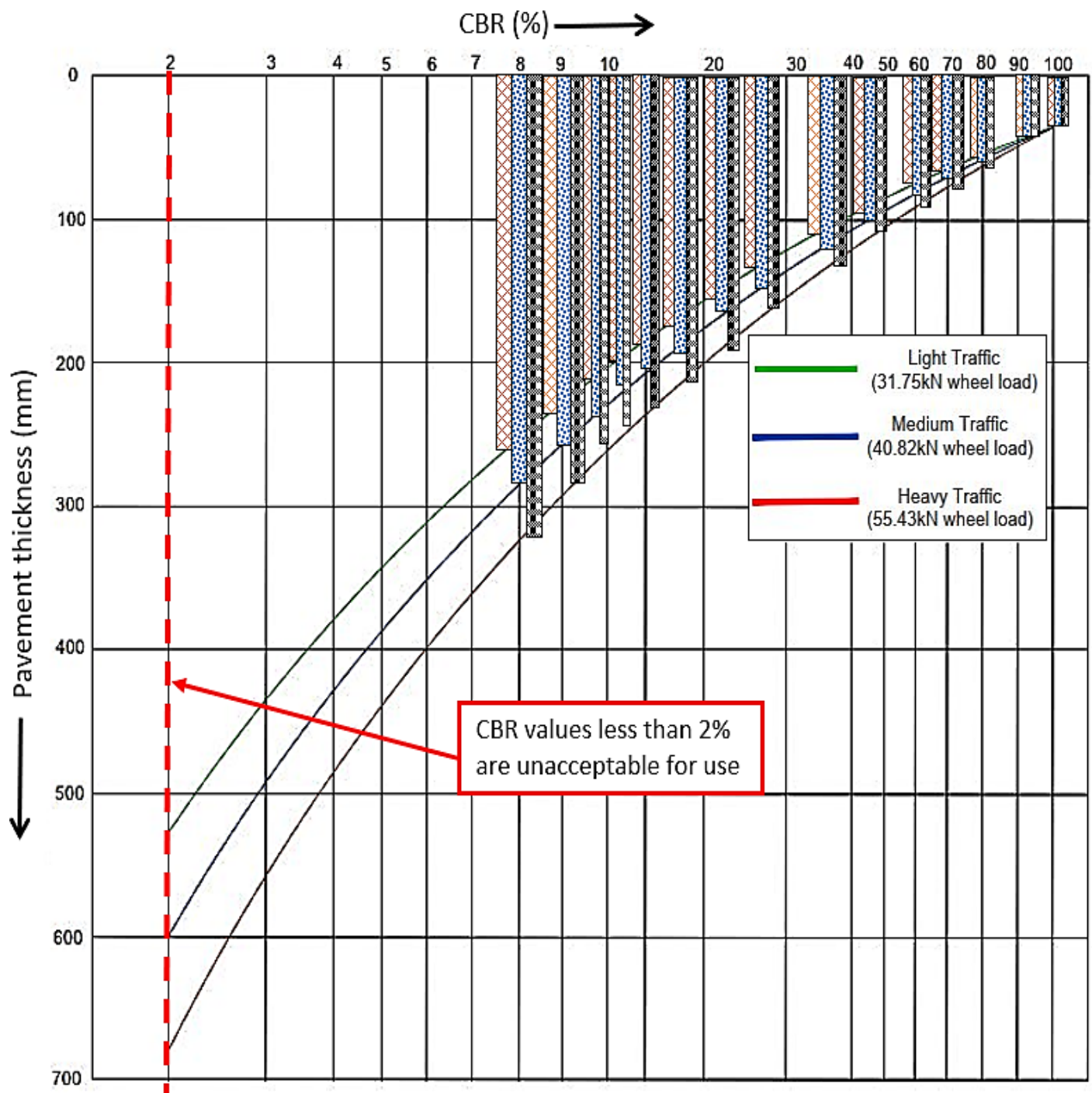


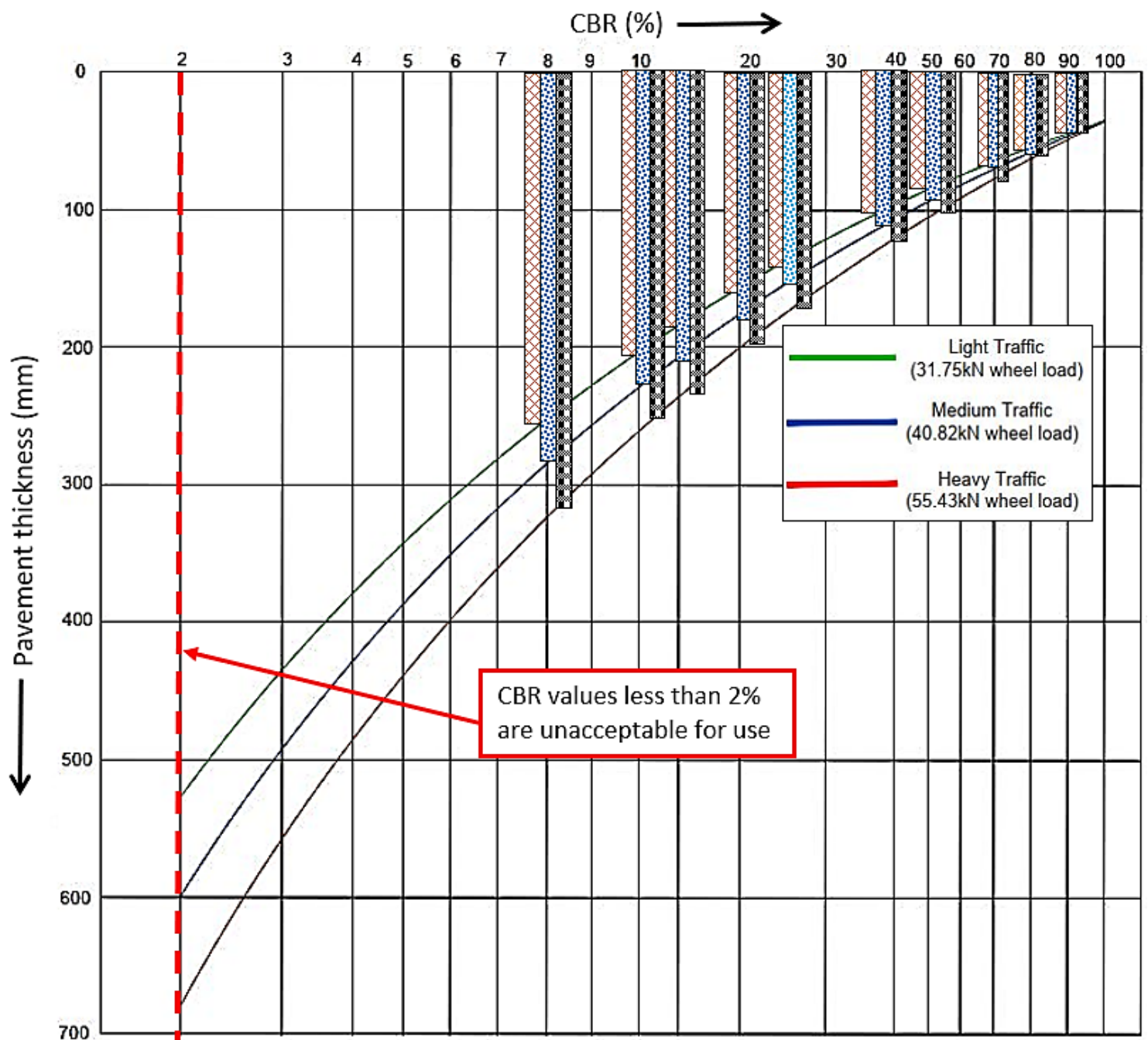
Figure 5.62: Treated swell values against the depth of construction



Chapter 5 – Results and Discussion

<ul style="list-style-type: none"> ☒ ASS 1 (25%B+75%K) CBR - 8% - Light traffic - Pavement Thickness = 260mm ☒ ASS 1 (25%B+75%K) CBR - 8% - Medium traffic - Pavement Thickness = 280mm ☒ ASS 1 (25%B+75%K) CBR - 8% - Heavy traffic - Pavement Thickness = 320mm
<ul style="list-style-type: none"> ☒ ASS 2 (75%B+25%K) CBR 9% - Light traffic - Pavement Thickness = 230mm ☒ ASS 2 (75%B+25%K) CBR 9% - Medium traffic - Pavement Thickness = 260mm ☒ ASS 2 (75%B+25%K) CBR -9% - Heavy traffic - Pavement Thickness = 280mm
<ul style="list-style-type: none"> ☒ CONTROL (ASS 1 + 8%L+20%C) = CBR 80% 7 days curing - Light traffic - Pavement Thickness = 50mm ☒ CONTROL (ASS 1 + 8%L+20%C) = CBR 80% 7 days curing- Medium traffic - Pavement Thickness = 55mm ☒ CONTROL (ASS 1 + 8%L+20%C) = CBR 80% 7 days curing - Heavy traffic - Pavement Thickness = 60mm
<ul style="list-style-type: none"> ☒ CONTROL (ASS 1 + 8%L+20%C) = CBR 96% 28 days curing - Light traffic - Pavement Thickness = 40mm ☒ CONTROL (ASS 1 + 8%L+20%C) = CBR 96% 28 days curing - Medium traffic - Pavement Thickness = 42mm ☒ CONTROL (ASS 1 + 8%L+20%C) = CBR 96% 28 days curing - Heavy traffic - Pavement Thickness = 44mm
<ul style="list-style-type: none"> ☒ CONTROL (ASS 2 + 8%L+20%C) = CBR 38% 7 days curing - Light traffic - Pavement Thickness = 110mm ☒ CONTROL (ASS 2 + 8%L+20%C) = CBR 38% 7 days curing - Medium traffic - Pavement Thickness = 120mm ☒ CONTROL (ASS 2 + 8%L+20%C) = CBR 38% 7 days curing - Heavy traffic - Pavement Thickness = 130mm
<ul style="list-style-type: none"> ☒ (ASS 1 +2%L+2.5%C+23.5%PLASTIC) = CBR 13% 28 days curing - Light traffic - Pavement Thickness = 200mm ☒ (ASS 1 +2%L+2.5%C+23.5%PLASTIC) = CBR 13% 28 days curing - Medium traffic - Pavement Thickness = 215mm ☒ (ASS 1 +2%L+2.5%C+23.5%PLASTIC) = CBR 13% 28 days curing - Heavy traffic - Pavement Thickness = 240mm
<ul style="list-style-type: none"> ☒ (ASS 2 +2%L+2.5%C+23.5%PLASTIC) = CBR 12% 7 days curing - Light traffic - Pavement Thickness = 215mm ☒ (ASS 2 +2%L+2.5%C+23.5%PLASTIC) = CBR 12% 7 days curing - Medium traffic - Pavement Thickness = 250mm ☒ (ASS 2 +2%L+2.5%C+23.5%PLASTIC) = CBR 12% 7 days curing - Heavy traffic - Pavement Thickness = 260mm
<ul style="list-style-type: none"> ☒ (ASS 1 +2%L+2.5%C+11.75%GGBS+11.75%PLASTIC) = CBR 44% 7 days curing - Light traffic - Pavement Thickness = 100mm ☒ (ASS 1 +2%L+2.5%C+11.75%GGBS+11.75%PLASTIC) = CBR 44% 7 days curing - Medium traffic - Pavement Thickness = 110mm ☒ (ASS 1 +2%L+2.5%C+11.75%GGBS+11.75%PLASTIC) = CBR 44% 7 days curing - Heavy traffic - Pavement Thickness = 120mm
<ul style="list-style-type: none"> ☒ (ASS 1 +2%L+2.5%C+23.5%BDW) = CBR 23% 7 days curing - Light traffic - Light traffic - Pavement Thickness = 150mm ☒ (ASS 1 +2%L+2.5%C+23.5%BDW) = CBR 23% 7 days curing - Medium traffic - Medium traffic - Pavement Thickness = 170mm ☒ (ASS 1 +2%L+2.5%C+23.5%BDW) = CBR 23% 7 days curing - Heavy traffic - Heavy traffic - Pavement Thickness = 190mm
<ul style="list-style-type: none"> ☒ (ASS 2 +2%L+2.5%C+23.5%BDW) = CBR 14% 7 days curing - Light traffic - Light traffic - Pavement Thickness = 185mm ☒ (ASS 2 +2%L+2.5%C+23.5%BDW) = CBR 14% 7 days curing - Medium traffic - Medium traffic - Pavement Thickness = 205mm ☒ (ASS 2 +2%L+2.5%C+23.5%BDW) = CBR 14% 7 days curing - Heavy traffic - Heavy traffic - Pavement Thickness = 240mm
<ul style="list-style-type: none"> ☒ (ASS 1 +2%L+2.5%C+11.75%GGBS+11.75%BDW) = CBR 61% 7 days curing - Light traffic - Pavement Thickness = 70mm ☒ (ASS 1 +2%L+2.5%C+11.75%GGBS+11.75%BDW) = CBR 61% 7 days curing - Medium traffic - Pavement Thickness = 75mm ☒ (ASS 1 +2%L+2.5%C+11.75%GGBS+11.75%BDW) = CBR 61% 7 days curing - Heavy traffic - Pavement Thickness = 80mm
<ul style="list-style-type: none"> ☒ (ASS 1 +2%L+2.5%C+11.75%GGBS+11.75%BDW) = CBR 109% 28 days curing - Light traffic - Pavement Thickness = 40mm ☒ (ASS 1 +2%L+2.5%C+11.75%GGBS+11.75%BDW) = CBR 109% 28 days curing - Medium traffic - Pavement Thickness = 40mm ☒ (ASS 1 +2%L+2.5%C+11.75%GGBS+11.75%BDW) = CBR 109% 28 days curing - Heavy traffic - Pavement Thickness = 40mm
<ul style="list-style-type: none"> ☒ (ASS 2 +2%L+2.5%C+11.75%GGBS+11.75%BDW) = CBR 27% 7 days curing - Light traffic - Pavement Thickness = 145mm ☒ (ASS 2 +2%L+2.5%C+11.75%GGBS+11.75%BDW) = CBR 27% 7 days curing - Medium traffic - Pavement Thickness = 150mm ☒ (ASS 2 +2%L+2.5%C+11.75%GGBS+11.75%BDW) = CBR 27% 7 days curing - Heavy traffic - Pavement Thickness = 160mm
<ul style="list-style-type: none"> ☒ (ASS 1 +2%L+2.5%C+23.5%GGBS) = CBR 70% 7 days curing - Light traffic - Pavement Thickness = 60mm ☒ (ASS 1 +2%L+2.5%C+23.5%GGBS) = CBR 70% 7 days curing - Medium traffic - Pavement Thickness = 70mm ☒ (ASS 1 +2%L+2.5%C+23.5%GGBS) = CBR 70% 7 days curing - Heavy traffic - Pavement Thickness = 80mm
<ul style="list-style-type: none"> ☒ (ASS 1 +2%L+2.5%C+23.5%GLASS) = CBR 16% 28 days curing - Light traffic - Pavement Thickness = 185mm ☒ (ASS 1 +2%L+2.5%C+23.5%GLASS) = CBR 16% 28 days curing - Medium traffic - Pavement Thickness = 190mm ☒ (ASS 1 +2%L+2.5%C+23.5%GLASS) = CBR 16 % 28 days curing - Heavy traffic - Pavement Thickness = 210mm

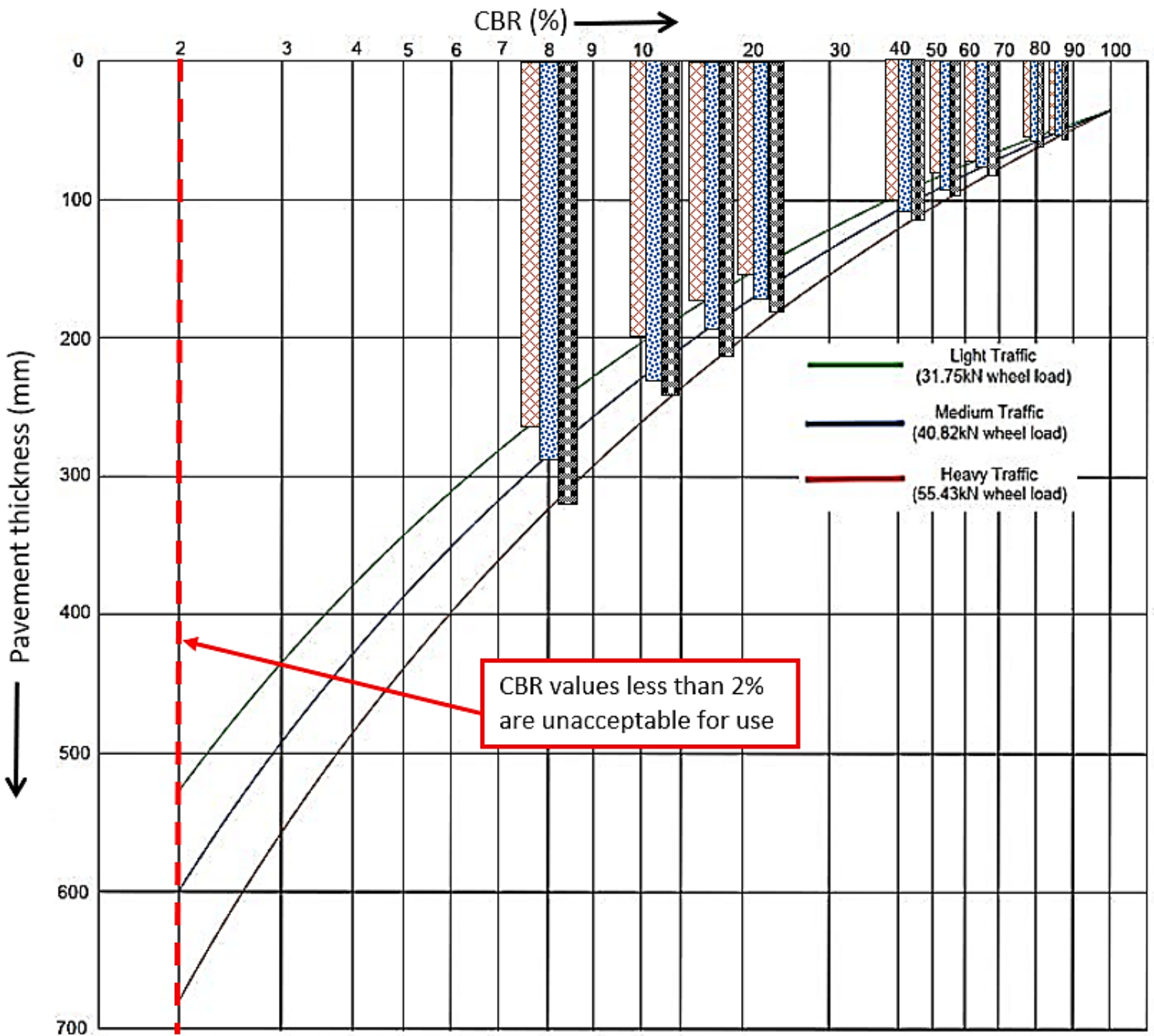
Figure 5.63: Road pavement thickness optimisation for un-soaked treated and untreated subgrade materials



Chapter 5 – Results and Discussion

<p>☒ CONTROL (ASS 2 + 8%L+20%C) = CBR 80% 28 days curing - Light traffic - Pavement Thickness = 50mm</p> <p>☒ CONTROL (ASS 2 + 8%L+20%C) = CBR 80% 28 days curing - Medium traffic - Pavement Thickness = 55mm</p> <p>☒ CONTROL (ASS 2 + 8%L+20%C) = CBR 80% 28 days curing - Heavy traffic - Pavement Thickness = 60mm</p>
<p>☒ (ASS 1 +2%L+2.5%C+23.5%PLASTIC) = CBR 13% 7 days curing - Light traffic - Pavement Thickness = 190mm</p> <p>☒ (ASS 1 +2%L+2.5%C+23.5%PLASTIC) = CBR 13% 7 days curing - Medium traffic - Pavement Thickness = 210mm</p> <p>☒ (ASS 1 +2%L+2.5%C+23.5%PLASTIC) = CBR 13% 7 days curing - Heavy traffic - Pavement Thickness = 220mm</p>
<p>☒ (ASS 2 +2%L+2.5%C+23.5%PLASTIC) = CBR 8 % 28 days curing - Light traffic - Pavement Thickness = 260mm</p> <p>☒ (ASS 2 +2%L+2.5%C+23.5%PLASTIC) = CBR 8 % 28 days curing - Medium traffic - Pavement Thickness = 280mm</p> <p>☒ (ASS 2 +2%L+2.5%C+23.5%PLASTIC) = CBR 8 % 28 days curing - Heavy traffic - Pavement Thickness = 320mm</p>
<p>☒ (ASS 2 +2%L+2.5%C+11.75%GGBS+11.75%PLASTIC) = CBR 21% 7 days curing - Light traffic - Pavement Thickness = 170mm</p> <p>☒ (ASS 2 +2%L+2.5%C+11.75%GGBS+11.75%PLASTIC) = CBR 21% 7 days curing - Medium traffic - Pavement Thickness = 180mm</p> <p>☒ (ASS 2 +2%L+2.5%C+11.75%GGBS+11.75%PLASTIC) = CBR 21% 7 days curing - Heavy traffic - Pavement Thickness = 200mm</p>
<p>☒ (ASS 2 +2%L+2.5%C+11.75%GGBS+11.75%PLASTIC) = CBR 51% 28 days curing - Light traffic - Pavement Thickness = 80mm</p> <p>☒ (ASS 2 +2%L+2.5%C+11.75%GGBS+11.75%PLASTIC) = CBR 51 % 28 days curing - Medium traffic - Pavement Thickness = 90mm</p> <p>☒ (ASS 2 +2%L+2.5%C+11.75%GGBS+11.75%PLASTIC) = CBR 51 % 28 days curing - Heavy traffic - Pavement Thickness = 100mm</p>
<p>☒ (ASS 1 +2%L+2.5%C+23.5%BDW) = CBR 26% 28 days curing - Light traffic - Light traffic - Pavement Thickness = 140mm</p> <p>☒ (ASS 1 +2%L+2.5%C+23.5%BDW) = CBR 26% 28 days curing - Medium traffic - Medium traffic - Pavement Thickness = 160mm</p> <p>☒ (ASS 1 +2%L+2.5%C+23.5%BDW) = CBR 26% 28 days curing - Heavy traffic - Heavy traffic - Pavement Thickness = 170mm</p>
<p>☒ (ASS 2 +2%L+2.5%C+11.75%GGBS+11.75%BDW) = CBR 44% 28 days curing - Light traffic - Pavement Thickness = 100mm</p> <p>☒ (ASS 2 +2%L+2.5%C+11.75%GGBS+11.75%BDW) = CBR 44% 28 days curing - Medium traffic - Pavement Thickness = 110mm</p> <p>☒ (ASS 2 +2%L+2.5%C+11.75%GGBS+11.75%BDW) = CBR 44 % 28 days curing - Heavy traffic - Pavement Thickness = 120mm</p>
<p>☒ (ASS 1 +2%L+2.5%C+23.5%GGBS) = CBR 92% 28 days curing - Light traffic - Pavement Thickness = 40mm</p> <p>☒ (ASS 1 +2%L+2.5%C+23.5%GGBS) = CBR 92% 28 days curing - Medium traffic - Pavement Thickness = 40mm</p> <p>☒ (ASS 1 +2%L+2.5%C+23.5%GGBS) = CBR 92% 28 days curing - Heavy traffic - Pavement Thickness = 40mm</p>
<p>☒ (ASS 2 +2%L+2.5%C+23.5%GGBS) = CBR 73% 7 days curing - Light traffic - Pavement Thickness = 60mm</p> <p>☒ (ASS 2 +2%L+2.5%C+23.5%GGBS) = CBR 73% 7 days curing - Medium traffic - Pavement Thickness = 70mm</p> <p>☒ (ASS 2 +2%L+2.5%C+23.5%GGBS) = CBR 73% 7 days curing - Heavy traffic - Pavement Thickness = 80mm</p>
<p>☒ (ASS 2 +2%L+2.5%C+23.5%GLASS) = CBR 11% 7 days curing - Light traffic - Pavement Thickness = 205mm</p> <p>☒ (ASS 2 +2%L+2.5%C+23.5%GLASS) = CBR 11% 7 days curing - Medium traffic - Pavement Thickness = 210mm</p> <p>☒ (ASS 2 +2%L+2.5%C+23.5%GLASS) = CBR 11% 7 days curing - Heavy traffic - Pavement Thickness = 250mm</p>

Figure 5.64: Road pavement thickness optimisation for un-soaked treated and untreated subgrade materials

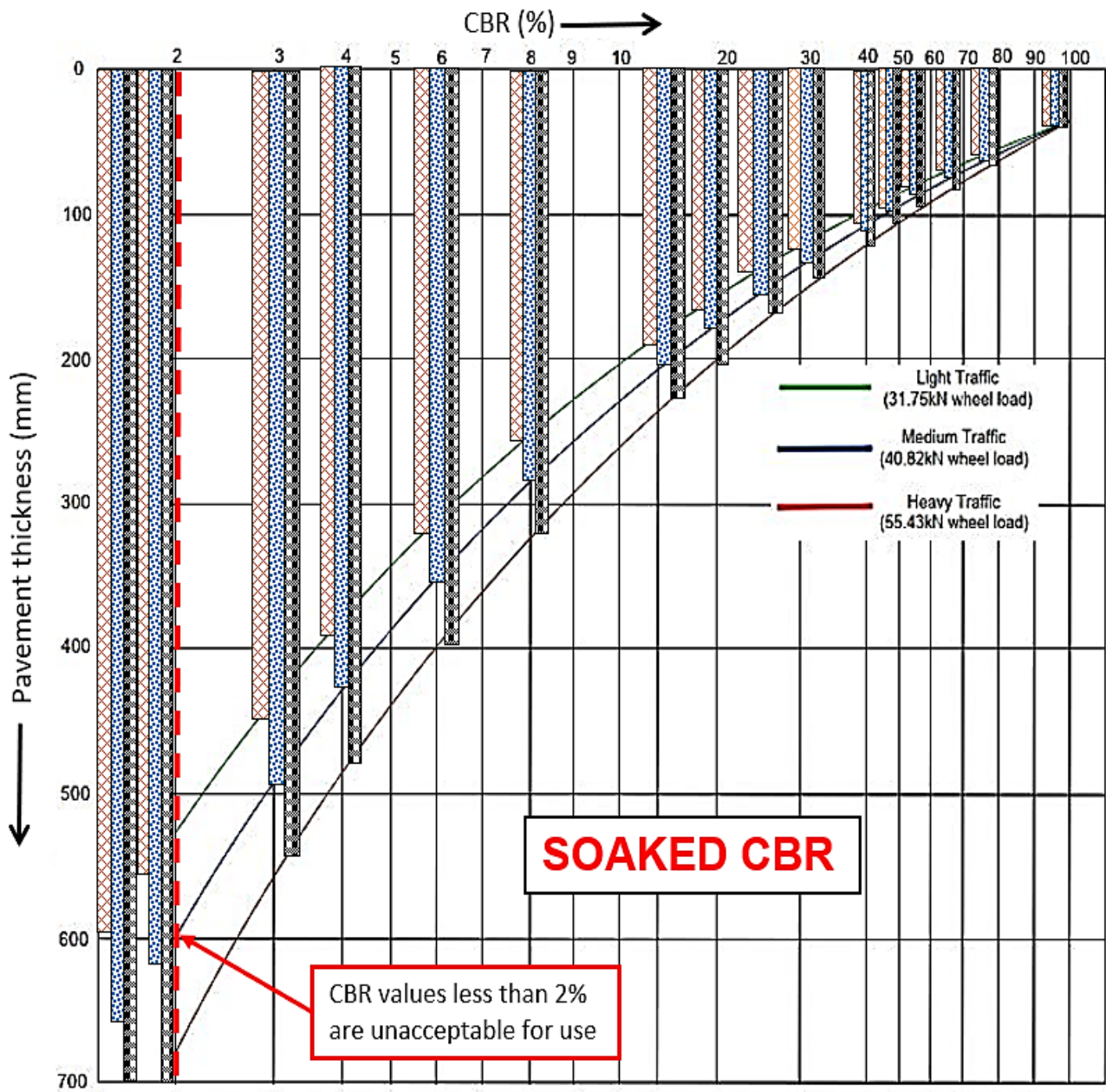


Chapter 5 – Results and Discussion

<ul style="list-style-type: none"> ☒ (ASS 2 +2%L+2.5%C+23.5%GLASS) = CBR 8% 28 days curing - Light traffic - Pavement Thickness = 260mm ☒ (ASS 2 +2%L+2.5%C+23.5%GLASS) = CBR 8% 28 days curing - Medium traffic - Pavement Thickness = 280mm ■ (ASS 2 +2%L+2.5%C+23.5%GLASS) = CBR 8% 28 days curing - Heavy traffic - Pavement Thickness = 320mm
<ul style="list-style-type: none"> ☒ (ASS 1 +2%L+2.5%C+23.5%GLASS) = CBR 14% 7 days curing - Light traffic - Pavement Thickness = 185mm ☒ (ASS 1 +2%L+2.5%C+23.5%GLASS) = CBR 14% 7 days curing - Medium traffic - Pavement Thickness = 205mm ■ (ASS 1 +2%L+2.5%C+23.5%GLASS) = CBR 14% 7 days curing - Heavy traffic - Pavement Thickness = 240mm
<ul style="list-style-type: none"> ☒ (ASS 1 +2%L+2.5%C+11.75%GGBS+11.75%GLASS) = CBR 51% 7 days curing - Light traffic - Pavement Thickness = 80mm ☒ (ASS 1 +2%L+2.5%C+11.75%GGBS+11.75%GLASS) = CBR 51% 7 days curing - Medium traffic - Pavement Thickness = 90mm ☒ (ASS 1 +2%L+2.5%C+11.75%GGBS+11.75%GLASS) = CBR 51% 7 days curing - Heavy traffic - Pavement Thickness = 100mm
<ul style="list-style-type: none"> ☒ (ASS 2 +2%L+2.5%C+11.75%GGBS+11.75%GLASS) = CBR 21% 7 days curing - Light traffic - Pavement Thickness = 170mm ☒ (ASS 2 +2%L+2.5%C+11.75%GGBS+11.75%GLASS) = CBR 21% 7 days curing - Medium traffic - Pavement Thickness = 180mm ■ (ASS 2 +2%L+2.5%C+11.75%GGBS+11.75%GLASS) = CBR 21% 7 days curing - Heavy traffic - Pavement Thickness = 200mm
<ul style="list-style-type: none"> ☒ (ASS 1 +2%L+2.5%C+11.75%GGBS+11.75%GLASS) = CBR 80% 28 days curing - Light traffic - Pavement Thickness = 50mm ☒ (ASS 1 +2%L+2.5%C+11.75%GGBS+11.75%GLASS) = CBR 80% 28 days curing - Medium traffic - Pavement Thickness = 55mm ■ (ASS 1 +2%L+2.5%C+11.75%GGBS+11.75%GLASS) = CBR 80% 28 days curing - Heavy traffic - Pavement Thickness = 60mm
<ul style="list-style-type: none"> ☒ (ASS 2 +2%L+2.5%C+11.75%GGBS+11.75%GLASS) = CBR 46% 28 days curing - Light traffic - Pavement Thickness = 100mm ☒ (ASS 2 +2%L+2.5%C+11.75%GGBS+11.75%GLASS) = CBR 46% 28 days curing - Medium traffic - Pavement Thickness = 110mm ☒ (ASS 2 +2%L+2.5%C+11.75%GGBS+11.75%GLASS) = CBR 46% 28 days curing - Heavy traffic - Pavement Thickness = 120mm
<ul style="list-style-type: none"> ☒ (ASS 2 +2%L+2.5%C+23.5%GGBS) = CBR 68% 28 days curing - Light traffic - Pavement Thickness = 70mm ☒ (ASS 2 +2%L+2.5%C+23.5%GGBS) = CBR 68% 28 days curing - Medium traffic - Pavement Thickness = 80mm ☒ (ASS 2 +2%L+2.5%C+23.5%GGBS) = CBR 68% 28 days curing - Heavy traffic - Pavement Thickness = 90mm
<ul style="list-style-type: none"> ☒ (ASS 2 +2%L+2.5%C+23.5%BDW) = CBR 18% 28 days curing - Light traffic - Light traffic - Pavement Thickness = 170mm ☒ (ASS 2 +2%L+2.5%C+23.5%BDW) = CBR 18% 28 days curing - Medium traffic - Medium traffic - Pavement Thickness = 180mm ☒ (ASS 2 +2%L+2.5%C+23.5%BDW) = CBR 18% 28 days curing - Heavy traffic - Heavy traffic - Pavement Thickness = 200mm
<ul style="list-style-type: none"> ☒ (ASS 1 +2%L+2.5%C+11.75%GGBS+11.75%PLASTIC) = CBR 82% 28 days curing - Light traffic - Pavement Thickness = 30mm ☒ (ASS 1 +2%L+2.5%C+11.75%GGBS+11.75%PLASTIC) = CBR 82% 28 days curing - Medium traffic - Pavement Thickness = 40mm ☒ (ASS 1 +2%L+2.5%C+11.75%GGBS+11.75%PLASTIC) = CBR 82% 28 days curing - Heavy traffic - Pavement Thickness = 45mm

Figure 5.65: Road pavement thickness optimisation for un-soaked treated and untreated subgrade materials

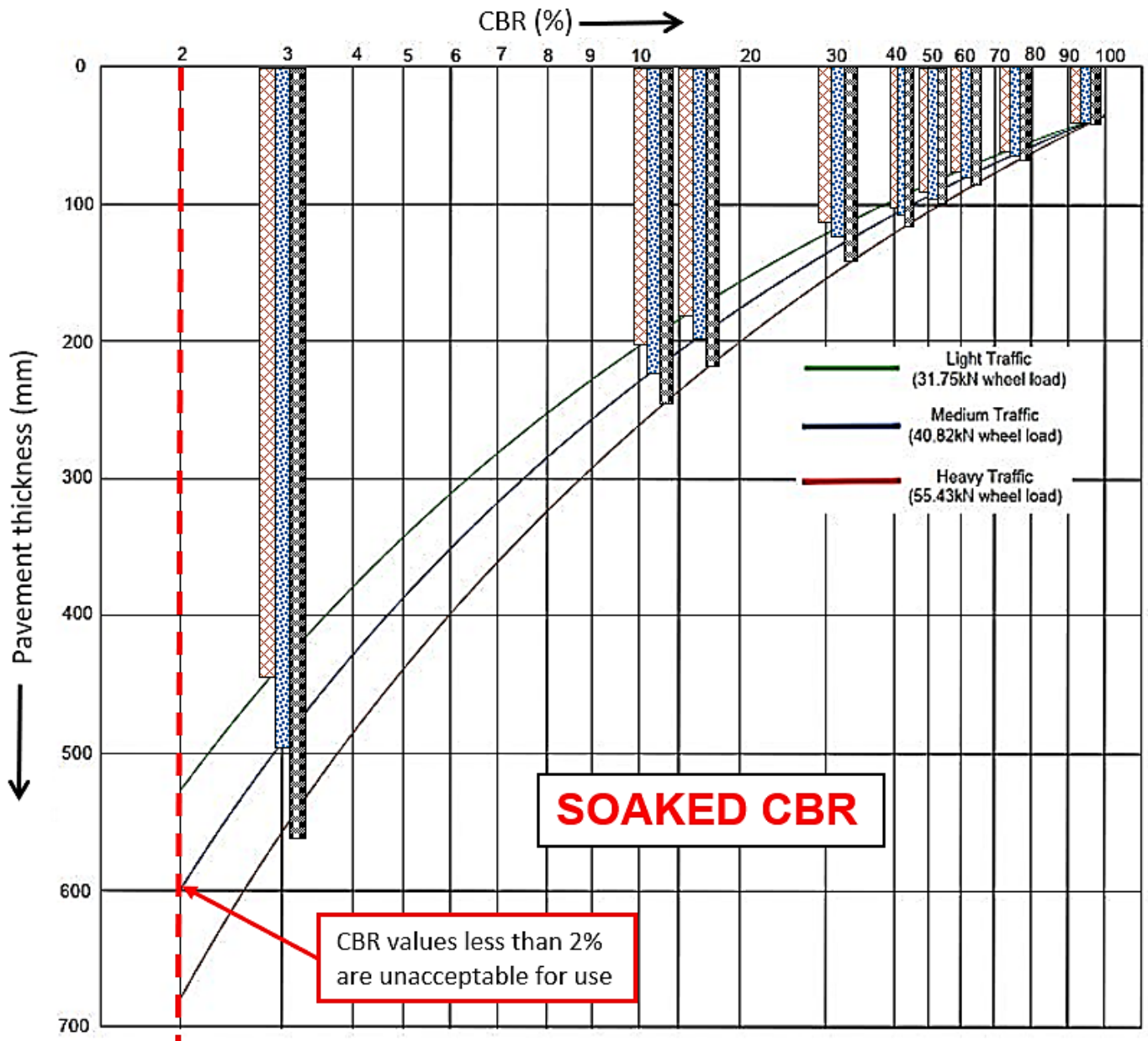
. More details on subgrade treated using 11.75% and 23.5% GGBS, recycled plastic, glass waste and Brick Dust Waste are shown in Figure 5.66 – Figure 5.68.



Chapter 5 – Results and Discussion

☑ CONTROL (ASS 1 + 8%L+20%C) = CBR 45% SOAKED after 7 days curing- Light traffic - Pavement Thickness = 90mm
☑ CONTROL (ASS 1 + 8%L+20%C) = CBR 45% SOAKED after 7 days curing - Medium traffic - Pavement Thickness = 100mm
☑ CONTROL (ASS 1 + 8%L+20%C) = CBR 45% SOAKED after 7 days curing - Heavy traffic - Pavement Thickness = 110mm
☑ CONTROL (ASS 1 + 8%L+20%C) = CBR 50% SOAKED after 28 days curing- Light traffic - Pavement Thickness = 80mm
☑ CONTROL (ASS 1 + 8%L+20%C) = CBR 50% SOAKED after 28 days curing - Medium traffic - Pavement Thickness = 90mm
☑ CONTROL (ASS 1 + 8%L+20%C) = CBR 50% SOAKED after 28 days curing - Heavy traffic - Pavement Thickness = 100mm
☑ CONTROL (ASS 2 + 8%L+20%C) = CBR 34% SOAKED after 7 days curing- Light traffic - Pavement Thickness = 130mm
☑ CONTROL (ASS 2 + 8%L+20%C) = CBR 34% SOAKED after 7 days curing - Medium traffic - Pavement Thickness = 140mm
☑ CONTROL (ASS 2 + 8%L+20%C) = CBR 34% SOAKED after 7 days curing - Heavy traffic - Pavement Thickness = 150mm
☑ ASS1 (25%B+75%K) CBR - 0.6%SOAKED - Light traffic - Pavement Thickness = 600mm (UNACCEPTABLE FOR USE)
☑ ASS1 (25%B+75%K) CBR - 0.6%SOAKED - Medium traffic - Pavement Thickness = 650mm (UNACCEPTABLE FOR USE)
☑ ASS1 (25%B+75%K) CBR - 0.6%SOAKED - Heavy traffic - Pavement Thickness = 700mm (UNACCEPTABLE FOR USE)
☑ ASS 2 (75%B+25%K) CBR 1.34% SOAKED - Light traffic - Pavement Thickness = 550mm (UNACCEPTABLE FOR USE)
☑ ASS 2 (75%B+25%K) CBR 1.34% SOAKED - Medium traffic - Pavement Thickness = 610mm (UNACCEPTABLE FOR USE)
☑ ASS 2 (75%B+25%K) CBR 1.34% SOAKED - Heavy traffic - Pavement Thickness = 700mm (UNACCEPTABLE FOR USE)
☑ (ASS 2 +2%L+2.5%C+23.5%GLASS)= CBR 3% SOAKED after 7 days curing - Light traffic - Pavement Thickness = 450mm
☑ (ASS 2 +2%L+2.5%C+23.5%GLASS) = CBR 3% SOAKED after 7 days curing - Medium traffic - Pavement Thickness = 490mm
☑ (ASS 2 +2%L+2.5%C+23.5%GLASS) = CBR 3% SOAKED after 7 days curing - Heavy traffic - Pavement Thickness = 540mm
☑ (ASS 2 +2%L+2.5%C+23.5%GLASS) = CBR 4% SOAKED after 28 days curing - Light traffic - Pavement Thickness = 390mm
☑ (ASS 2 +2%L+2.5%C+23.5%GLASS) = CBR 4% SOAKED after 28 days curing - Medium traffic - Pavement Thickness = 430mm
☑ (ASS 2 +2%L+2.5%C+23.5%GLASS) = CBR 4% SOAKED after 28 days curing - Heavy traffic - Pavement Thickness = 490mm
☑ (ASS 2 +2%L+2.5%C+11.75%GGBS+11.75%GLASS) = CBR 46% SOAKED after 28 days curing - Light traffic - Pavement Thickness = 100mm
☑ (ASS 2 +2%L+2.5%C+11.75%GGBS+11.75%GLASS) = CBR 46% SOAKED after 28 days curing - Medium traffic - Pavement Thickness = 110mm
☑ (ASS 2 +2%L+2.5%C+11.75%GGBS+11.75%GLASS) = CBR 46% SOAKED after 28 days curing - Heavy traffic - Pavement Thickness = 120mm
☑ (ASS 2 +2%L+2.5%C+23.5%PLASTIC) = CBR 6% SOAKED after 7 days curing - Light traffic - Pavement Thickness = 320mm
☑ (ASS 2 +2%L+2.5%C+23.5%PLASTIC) = CBR 6% SOAKED after 7 days curing - Medium traffic - Pavement Thickness = 350mm
☑ (ASS 2 +2%L+2.5%C+23.5%PLASTIC) = CBR 6% SOAKED after 7 days curing - Heavy traffic - Pavement Thickness = 400mm
☑ (ASS 1 +2%L+2.5%C+23.5%PLASTIC) = CBR 8% SOAKED after 28 days curing - Light traffic - Pavement Thickness = 260mm
☑ (ASS 1 +2%L+2.5%C+23.5%PLASTIC) = CBR 8% SOAKED after 28 days curing - Medium traffic - Pavement Thickness = 280mm
☑ (ASS 1 +2%L+2.5%C+23.5%PLASTIC) = CBR 8% SOAKED after 28 days curing - Heavy traffic - Pavement Thickness = 320mm
☑ (ASS 1 +2%L+2.5%C+23.5%BDW) = CBR 17% SOAKED after 7 days curing- Light traffic - Pavement Thickness = 190mm
☑ (ASS 1 +2%L+2.5%C+23.5%BDW) = CBR 17% SOAKED after 7 days curing - Medium traffic - Pavement Thickness = 200mm
☑ (ASS 1 +2%L+2.5%C+23.5%BDW) = CBR 17% SOAKED after 7 days curing - Heavy traffic - Pavement Thickness = 230mm
☑ (ASS 2 +2%L+2.5%C+23.5%BDW) = CBR 18% SOAKED after 7 days curing- Light traffic - Pavement Thickness = 170mm
☑ (ASS 2 +2%L+2.5%C+23.5%BDW) = CBR 18% SOAKED after 7 days curing - Medium traffic - Pavement Thickness = 180mm
☑ (ASS 2 +2%L+2.5%C+23.5%BDW) = CBR 18% SOAKED after 7 days curing - Heavy traffic - Pavement Thickness = 200mm
☑ (ASS 2 +2%L+2.5%C+11.75%GGBS+11.75%BDW) = CBR 24% SOAKED after 28 days curing - Light traffic - Pavement Thickness = 140mm
☑ (ASS 2 +2%L+2.5%C+11.75%GGBS+11.75%BDW) = CBR 24% SOAKED after 28 days curing - Medium traffic - Pavement Thickness = 160mm
☑ (ASS 2 +2%L+2.5%C+11.75%GGBS+11.75%BDW) = CBR 24% SOAKED after 28 days curing - Heavy traffic - Pavement Thickness = 180mm
☑ (ASS 1 +2%L+2.5%C+23.5%GGBS) = CBR 79% SOAKED after 7 days curing - Light traffic - Pavement Thickness = 50mm
☑ (ASS 1 +2%L+2.5%C+23.5%GGBS) = CBR 79% SOAKED after 7 days curing - Medium traffic - Pavement Thickness = 55mm
☑ (ASS 1 +2%L+2.5%C+23.5%GGBS) = CBR 79% SOAKED after 7 days curing - Heavy traffic - Pavement Thickness = 60mm
☑ (ASS 1 +2%L+2.5%C+23.5%GGBS) = CBR 97% SOAKED after 28 days curing - Light traffic - Pavement Thickness = 40mm
☑ (ASS 1 +2%L+2.5%C+23.5%GGBS) = CBR 97% SOAKED after 28 days curing - Medium traffic - Pavement Thickness = 40mm
☑ (ASS 1 +2%L+2.5%C+23.5%GGBS) = CBR 97% SOAKED after 28 days curing - Heavy traffic - Pavement Thickness = 40mm
☑ (ASS 2 +2%L+2.5%C+23.5%GGBS) = CBR 65% SOAKED after 28 days curing - Light traffic - Pavement Thickness = 70mm
☑ (ASS 2 +2%L+2.5%C+23.5%GGBS) = CBR 65% SOAKED after 28 days curing - Medium traffic - Pavement Thickness = 80mm
☑ (ASS 2 +2%L+2.5%C+23.5%GGBS) = CBR 65% SOAKED after 28 days curing - Heavy traffic - Pavement Thickness = 90mm

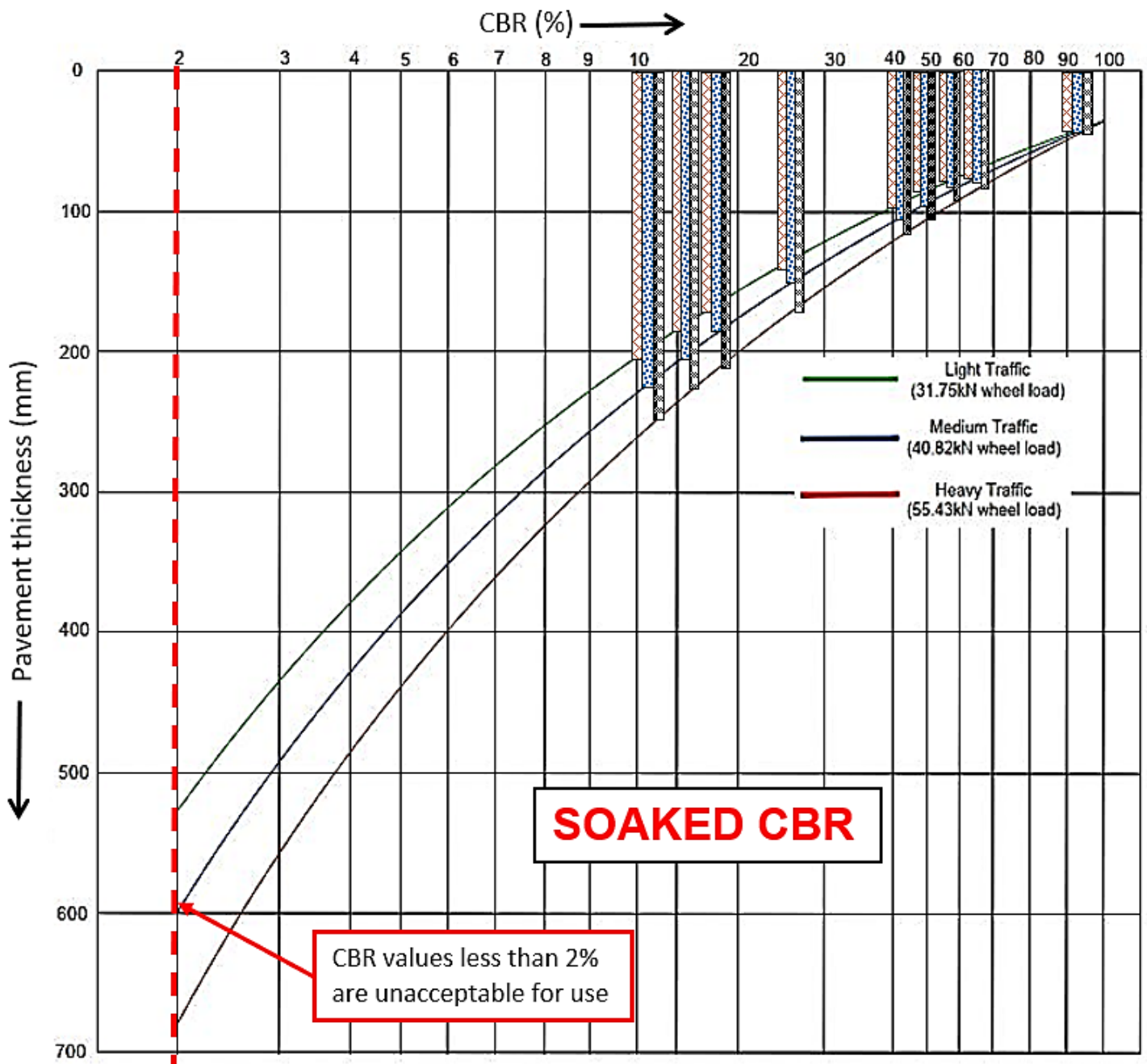
Figure 5.66: Road pavement thickness optimisation for soaked treated and untreated ASS materials



Chapter 5 – Results and Discussion

☒ CONTROL (ASS 2 + 8%L+20%C) = CBR 61% SOAKED after 28 days curing- Light traffic - Pavement Thickness = 70mm
☒ CONTROL (ASS 2 + 8%L+20%C) = CBR 61% SOAKED after 28 days curing - Medium traffic - Pavement Thickness = 75mm
■ CONTROL (ASS 2 + 8%L+20%C) = CBR 61% SOAKED after 28 days curing - Heavy traffic - Pavement Thickness = 80mm
☒ (ASS 1 +2%L+2.5%C+23.5%PLASTIC) = CBR 12% SOAKED after 7 days curing - Light traffic - Pavement Thickness = 200mm
☒ (ASS 1 +2%L+2.5%C+23.5%PLASTIC) = CBR 12% SOAKED after 7 days curing - Medium traffic - Pavement Thickness = 220mm
☒ (ASS 1 +2%L+2.5%C+23.5%PLASTIC) = CBR 12% SOAKED after 7 days curing - Heavy traffic - Pavement Thickness = 250mm
☒ (ASS 2 +2%L+2.5%C+23.5%PLASTIC) = CBR 3 % SOAKED after 28 days curing - Light traffic - Pavement Thickness = 450mm
☒ (ASS 2 +2%L+2.5%C+23.5%PLASTIC) = CBR 3 % SOAKED after 28 days curing - Medium traffic - Pavement Thickness = 490mm
■ (ASS 2 +2%L+2.5%C+23.5%PLASTIC) = CBR 3% SOAKED after 28 days curing - Heavy traffic - Pavement Thickness = 540mm
☒ (ASS 2 +2%L+2.5%C+11.75%GGBS+11.75%PLASTIC) = CBR 50% SOAKED after 28 days curing - Light traffic - Pavement Thickness = 80mm
☒ (ASS 2 +2%L+2.5%C+11.75%GGBS+11.75%PLASTIC) = CBR 50 % SOAKED after 28 days curing - Medium traffic - Pavement Thickness = 90mm
■ (ASS 2 +2%L+2.5%C+11.75%GGBS+11.75%PLASTIC) = CBR 50 % SOAKED after 28 days curing - Heavy traffic - Pavement Thickness = 100mm
☒ (ASS 1 +2%L+2.5%C+23.5%GLASS) = CBR 17% SOAKED after 7 days curing - Light traffic - Pavement Thickness = 190mm
☒ (ASS 1 +2%L+2.5%C+23.5%GLASS) = CBR 17% SOAKED after 7 days curing - Medium traffic - Pavement Thickness = 200mm
■ (ASS 1 +2%L+2.5%C+23.5%GLASS) = CBR 17% SOAKED after 7 days curing - Heavy traffic - Pavement Thickness = 230mm
☒ (ASS 2 +2%L+2.5%C+11.75%GGBS+11.75%GLASS) = CBR 31% SOAKED after 7 days curing - Light traffic - Pavement Thickness = 110mm
☒ (ASS 2 +2%L+2.5%C+11.75%GGBS+11.75%GLASS) = CBR 31% SOAKED after 7 days curing - Medium traffic - Pavement Thickness = 120mm
☒ (ASS 2 +2%L+2.5%C+11.75%GGBS+11.75%GLASS) = CBR 31% SOAKED after 7 days curing - Heavy traffic - Pavement Thickness = 150mm
☒ (ASS 1 +2%L+2.5%C+11.75%GGBS+11.75%GLASS)= CBR 72% SOAKED after 28 days curing - Light traffic - Pavement Thickness = 50mm
☒ (ASS 1 +2%L+2.5%C+11.75%GGBS+11.75%GLASS) = CBR 72% SOAKED after 28 days curing - Medium traffic - Pavement Thickness = 55mm
■ (ASS 1 +2%L+2.5%C+11.75%GGBS+11.75%GLASS) = CBR 72% SOAKED after 28 days curing - Heavy traffic - Pavement Thickness = 60mm
☒ (ASS 2 +2%L+2.5%C+23.5%GGBS) = CBR 46% SOAKED after 7 days curing - Light traffic - Pavement Thickness = 100mm
☒ (ASS 2 +2%L+2.5%C+23.5%GGBS) = CBR 46% SOAKED after 7 days curing - Medium traffic - Pavement Thickness = 105mm
■ (ASS 2 +2%L+2.5%C+23.5%GGBS) = CBR 46% SOAKED after 7 days curing - Heavy traffic - Pavement Thickness = 110mm
☒ (ASS 1 +2%L+2.5%C+11.75%GGBS+11.75%BDW) = CBR 97% SOAKED after 28 days curing - Light traffic - Pavement Thickness = 40mm
☒ (ASS 1 +2%L+2.5%C+11.75%GGBS+11.75%BDW) = CBR 97% SOAKED after 28 days curing - Medium traffic - Pavement Thickness = 40mm
■ (ASS 1 +2%L+2.5%C+11.75%GGBS+11.75%BDW) = CBR 97% SOAKED after 28 days curing - Heavy traffic - Pavement Thickness = 40mm

Figure 5.67: Road pavement thickness optimisation for soaked treated and untreated ASS materials



Chapter 5 – Results and Discussion

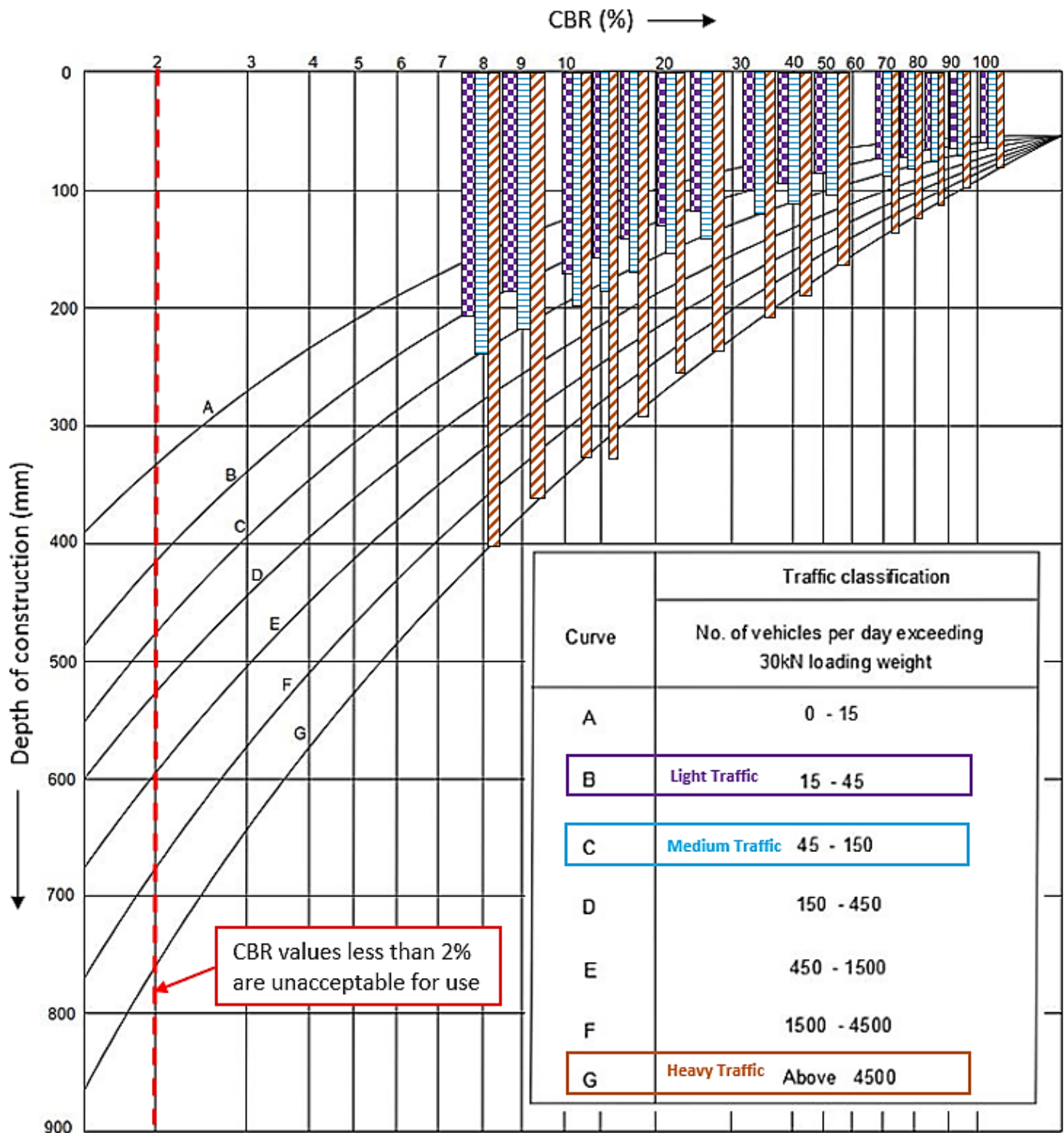
☒ (ASS 1 +2%L+2.5%C+11.75%GGBS+11.75%GLASS) = CBR 59% SOAKED after 7 days curing - Light traffic - Pavement Thickness = 90mm
☒ (ASS 1 +2%L+2.5%C+11.75%GGBS+11.75%GLASS) = CBR 59% SOAKED after 7 days curing - Medium traffic - Pavement Thickness = 100mm
☒ (ASS 1 +2%L+2.5%C+11.75%GGBS+11.75%GLASS) = CBR 59% SOAKED after 7 days curing - Heavy traffic - Pavement Thickness = 105mm
☒ (ASS 1 +2%L+2.5%C+23.5%GLASS) = CBR 11 % SOAKED after 28 days curing - Light traffic - Pavement Thickness = 205mm
☒ (ASS 1 +2%L+2.5%C+23.5%GLASS)= CBR 11 % SOAKED after 28 days curing - Medium traffic - Pavement Thickness = 220mm
☒ (ASS 1 +2%L+2.5%C+23.5%GLASS) = CBR 11% SOAKED after 28 days curing - Heavy traffic - Pavement Thickness = 250mm
☒ (ASS 1 +2%L+2.5%C+23.5%BDW) = CBR 28% SOAKED after 28 days curing- Light traffic - Pavement Thickness = 140mm
☒ (ASS 1 +2%L+2.5%C+23.5%BDW) = CBR 28% SOAKED after 28 days curing - Medium traffic - Pavement Thickness = 150mm
☒ (ASS 1 +2%L+2.5%C+23.5%BDW) = CBR 28% SOAKED after 28 days curing - Heavy traffic - Pavement Thickness = 180mm
☒ (ASS 2 +2%L+2.5%C+23.5%BDW) = CBR 17% SOAKED after 28 days curing- Light traffic - Pavement Thickness = 190mm
☒ (ASS 2 +2%L+2.5%C+23.5%BDW) = CBR 17 % SOAKED after 28 days curing - Medium traffic - Pavement Thickness = 200mm
■ (ASS 2 +2%L+2.5%C+23.5%BDW) = CBR 17 % SOAKED after 28 days curing - Heavy traffic - Pavement Thickness = 230mm
☒ (ASS 1 +2%L+2.5%C+11.75%GGBS+11.75%BDW) = CBR 61% SOAKED after 7 days curing - Light traffic - Pavement Thickness = 70mm
☒ (ASS 1 +2%L+2.5%C+11.75%GGBS+11.75%BDW) = CBR 61% SOAKED after 7 days curing - Medium traffic - Pavement Thickness = 75mm
☒ (ASS 1 +2%L+2.5%C+11.75%GGBS+11.75%BDW) = CBR 61% SOAKED after 7 days curing - Heavy traffic - Pavement Thickness = 80mm
☒ (ASS 2 +2%L+2.5%C+11.75%GGBS+11.75%BDW) = CBR 16% SOAKED after 7 days curing - Light traffic - Pavement Thickness = 190mm
☒ (ASS 2 +2%L+2.5%C+11.75%GGBS+11.75%BDW) = CBR 16% SOAKED after 7 days curing - Medium traffic - Pavement Thickness = 200mm
☒ (ASS 2 +2%L+2.5%C+11.75%GGBS+11.75%BDW) = CBR 16% SOAKED after 7 days curing - Heavy traffic - Pavement Thickness = 230mm
☒ (ASS 2 +2%L+2.5%C+11.75%GGBS+11.75%PLASTIC) = CBR 47% SOAKED after 7 days curing - Light traffic - Pavement Thickness = 100mm
☒ (ASS 2 +2%L+2.5%C+11.75%GGBS+11.75%PLASTIC) = CBR 47% SOAKED after 7 days curing - Medium traffic - Pavement Thickness = 105mm
☒ (ASS 2 +2%L+2.5%C+11.75%GGBS+11.75%PLASTIC) = CBR 47% SOAKED after 7 days curing - Heavy traffic - Pavement Thickness = 110mm
☒ (ASS 1 +2%L+2.5%C+11.75%GGBS+11.75%PLASTIC) = CBR 59% SOAKED after 7 days curing - Light traffic - Pavement Thickness = 90mm
☒ (ASS 1 +2%L+2.5%C+11.75%GGBS+11.75%PLASTIC) = CBR 59% SOAKED after 7 days curing - Medium traffic - Pavement Thickness = 100mm
■ (ASS 1 +2%L+2.5%C+11.75%GGBS+11.75%PLASTIC) = CBR 59% SOAKED after 7 days curing - Heavy traffic - Pavement Thickness = 105mm
☒ (ASS 1 +2%L+2.5%C+11.75%GGBS+11.75%PLASTIC) = CBR 93% SOAKED after 28 days curing - Light traffic - Pavement Thickness = 40mm
☒ (ASS 1 +2%L+2.5%C+11.75%GGBS+11.75%PLASTIC) = CBR 93% SOAKED after 28 days curing - Medium traffic - Pavement Thickness = 40mm
■ (ASS 1 +2%L+2.5%C+11.75%GGBS+11.75%PLASTIC) = CBR 93% SOAKED after 28 days curing - Heavy traffic - Pavement Thickness = 40mm

Figure 5.68: Road pavement thickness optimisation for soaked treated and untreated ASS materials

5.8 ROAD CONSTRUCTION DEPTH OPTIMISATION

5.8.1 Treated and Untreated ASS Materials

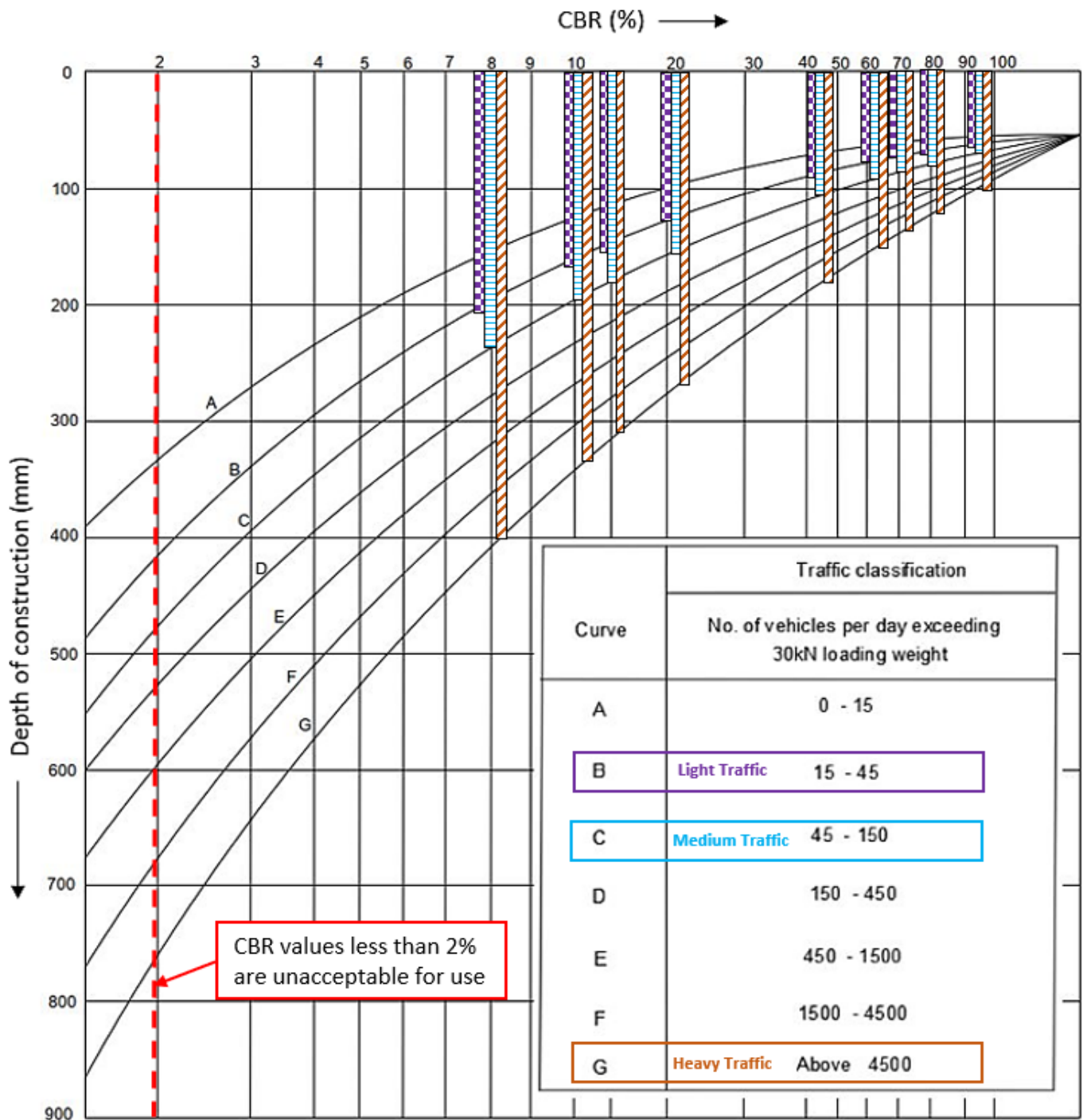
Results for subgrade treated using 11.75% and 23.5% GGBS, recycled glass, plastic and BDW are shown in Figure 5.69 - Figure 5.71.



Chapter 5 – Results and Discussion

<ul style="list-style-type: none"> ☒ ASS 1 (25%B + 75%K) CBR 8% - Light traffic - Depth of Construction = 205mm ☐ ASS 1 (25%B + 75%K) CBR 8% - Medium traffic - Depth of Construction = 240mm ■ ASS 1 (25%B + 75%K) CBR 8% - Heavy traffic - Depth of Construction = 400mm
<ul style="list-style-type: none"> ☒ ASS 2 (75%B+25%K) CBR 9% - Light traffic - Depth of Construction = 190mm ☐ ASS 2 (75%B+25%K) CBR 9% - Medium traffic - Depth of Construction = 210mm ☒ ASS 2 (75%B+25%K) CBR 9% - Heavy traffic - Depth of Construction = 380mm
<ul style="list-style-type: none"> ☒ CONTROL (ASS 2 + 8%L+20%C) = CBR 38% 7 days curing - Light traffic - Depth of Construction = 100mm ☐ CONTROL (ASS 2 + 8%L+20%C) = CBR 38% 7 days curing - Medium traffic - Depth of Construction = 110mm ☒ CONTROL (ASS 2 + 8%L+20%C) = CBR 38% 7 days curing - Heavy traffic - Depth of Construction = 200mm
<ul style="list-style-type: none"> ☒ CONTROL (ASS 2 + 8%L+20%C) = CBR 80% 28 days curing - Light traffic - Depth of Construction = 60mm ☐ CONTROL (ASS 2 + 8%L+20%C) = CBR 80% 28 days curing - Medium traffic - Depth of Construction = 70mm ■ CONTROL (ASS 2 + 8%L+20%C) = CBR 80% 28 days curing - Heavy traffic - Depth of Construction = 120mm
<ul style="list-style-type: none"> ☒ (ASS 1 +2%L+2.5%C+23.5%PLASTIC) = CBR 13% 7 days curing - Light traffic - Depth of Construction = 150mm ☐ (ASS 1 +2%L+2.5%C+23.5%PLASTIC) = CBR 13% 7 days curing - Medium traffic - Depth of Construction = 190mm ☒ (ASS 1 +2%L+2.5%C+23.5%PLASTIC) = CBR 13% 7 days curing - Heavy traffic - Depth of Construction = 340mm
<ul style="list-style-type: none"> ☒ (ASS 2 +2%L+2.5%C+23.5%PLASTIC) = CBR 12% 7 days curing - Light traffic - Depth of Construction = 180mm ☐ (ASS 2 +2%L+2.5%C+23.5%PLASTIC) = CBR 12% 7 days curing - Medium traffic - Depth of Construction = 190mm ☒ (ASS 2 +2%L+2.5%C+23.5%PLASTIC) = CBR 12% 7 days curing - Heavy traffic - Depth of Construction = 310mm
<ul style="list-style-type: none"> ☒ (ASS 1 +2%L+2.5%C+11.75%GGBS+11.75%PLASTIC) = CBR 82% 28 days curing - Light traffic - Depth of Construction = 50mm ☐ (ASS 1 +2%L+2.5%C+11.75%GGBS+11.75%PLASTIC) = CBR 82% 28 days curing - Medium traffic - Depth of Construction = 60mm ☒ (ASS 1 +2%L+2.5%C+11.75%GGBS+11.75%PLASTIC) = CBR 82% 28 days curing - Heavy traffic - Depth of Construction = 110mm
<ul style="list-style-type: none"> ☒ (ASS 1 +2%L+2.5%C+23.5%BDW) = CBR 26% 28 days curing - Light traffic - Depth of Construction = 120mm ☐ (ASS 1 +2%L+2.5%C+23.5%BDW) = CBR 26% 28 days curing - Medium traffic - Depth of Construction = 140mm ■ (ASS 1 +2%L+2.5%C+23.5%BDW) = CBR 26% 28 days curing - Heavy traffic - Depth of Construction = 230mm
<ul style="list-style-type: none"> ☒ (ASS 2 +2%L+2.5%C+23.5%BDW) = CBR 18% 28 days curing - Light traffic - Depth of Construction = 150mm ☐ (ASS 2 +2%L+2.5%C+23.5%BDW) = CBR 18% 28 days curing - Medium traffic - Depth of Construction = 170mm ☒ (ASS 2 +2%L+2.5%C+23.5%BDW) = CBR 18% 28 days curing - Heavy traffic - Depth of Construction = 290mm
<ul style="list-style-type: none"> ☒ (ASS 2 +2%L+2.5%C+11.75%GGBS+11.75%BDW) = CBR 44% 28 days curing - Light traffic - Depth of Construction = 90mm ☐ (ASS 2 +2%L+2.5%C+11.75%GGBS+11.75%BDW) = CBR 44% 28 days curing - Medium traffic - Depth of Construction = 110mm ■ (ASS 2 +2%L+2.5%C+11.75%GGBS+11.75%BDW) = CBR 44% 28 days curing - Heavy traffic - Depth of Construction = 190mm
<ul style="list-style-type: none"> ☒ (ASS 1 +2%L+2.5%C+11.75%GGBS+11.75%BDW) = CBR 109% 28 days curing - Light traffic - Depth of Construction = 50mm ☐ (ASS 1 +2%L+2.5%C+11.75%GGBS+11.75%BDW) = CBR 109% 28 days curing - Medium traffic - Depth of Construction = 55mm ■ (ASS 1 +2%L+2.5%C+11.75%GGBS+11.75%BDW) = CBR 109% 28 days curing - Heavy traffic - Depth of Construction = 80mm
<ul style="list-style-type: none"> ☒ (ASS 1 +2%L+2.5%C+11.75%GGBS+11.75%GLASS) = CBR 51% 7 days curing - Light traffic - Depth of Construction = 90mm ☐ (ASS 1 +2%L+2.5%C+11.75%GGBS+11.75%GLASS) = CBR 51% 7 days curing - Medium traffic - Depth of Construction = 100mm ■ (ASS 1 +2%L+2.5%C+11.75%GGBS+11.75%GLASS) = CBR 51% 7 days curing - Heavy traffic - Depth of Construction = 180mm
<ul style="list-style-type: none"> ☒ (ASS 2 +2%L+2.5%C+11.75%GGBS+11.75%GLASS) = CBR 21% 7 days curing - Light traffic - Depth of Construction = 120mm ☐ (ASS 2 +2%L+2.5%C+11.75%GGBS+11.75%GLASS) = CBR 21% 7 days curing - Medium traffic - Depth of Construction = 150mm ■ (ASS 2 +2%L+2.5%C+11.75%GGBS+11.75%GLASS) = CBR 21% 7 days curing - Heavy traffic - Depth of Construction = 280mm
<ul style="list-style-type: none"> ☒ (ASS 1 +2%L+2.5%C+23.5%GGBS) = CBR 92% 28 days curing - Light traffic - Depth of Construction = 50mm ☐ (ASS 1 +2%L+2.5%C+23.5%GGBS) = CBR 92% 28 days curing - Medium traffic - Depth of Construction = 60mm ☒ (ASS 1 +2%L+2.5%C+23.5%GGBS) = CBR 92% 28 days curing - Heavy traffic - Depth of Construction = 90mm
<ul style="list-style-type: none"> ■ (ASS 2 +2%L+2.5%C+23.5%GGBS) = CBR 73% 7 days curing - Light traffic - Depth of Construction = 70mm ☐ (ASS 2 +2%L+2.5%C+23.5%GGBS) = CBR 73% 7 days curing - Medium traffic - Depth of Construction = 90mm ☒ (ASS 2 +2%L+2.5%C+23.5%GGBS) = CBR 73% 7 days curing - Heavy traffic - Depth of Construction = 150mm

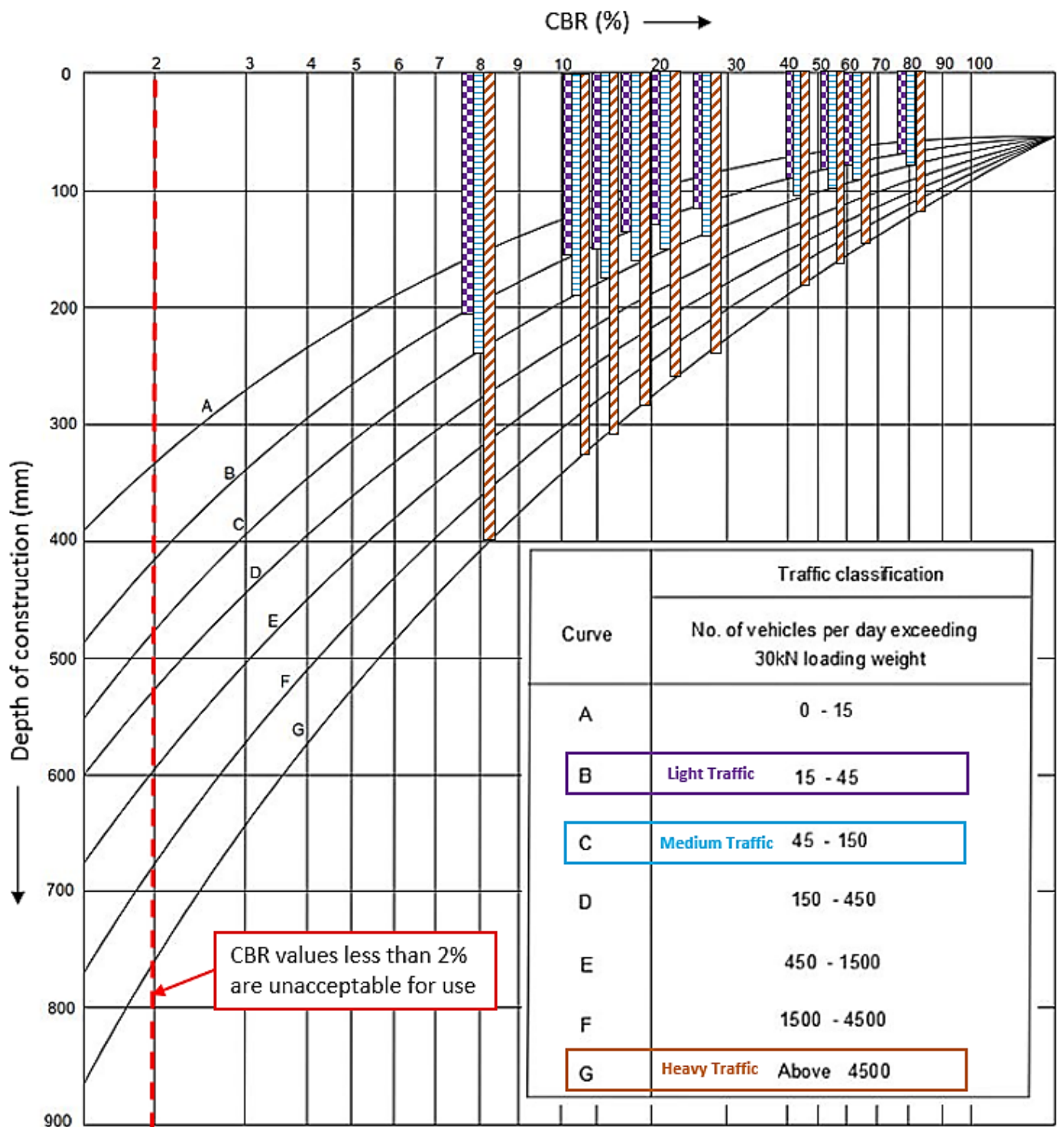
Figure 5.69: Road pavement construction depth optimisation for un-soaked treated and untreated ASS materials



Chapter 5 – Results and Discussion

☒ CONTROL (ASS 1 + 8%L+20%C) = CBR 80% 7 days curing - Light traffic - Depth of Construction = 60mm
☒ CONTROL (ASS 1 + 8%L+20%C) = CBR 80% 7 days curing - Medium traffic - Depth of Construction = 70mm
☒ CONTROL (ASS 1 + 8%L+20%C) = CBR 80% 7 days curing - Heavy traffic - Depth of Construction = 120mm
☒ CONTROL (ASS 1 + 8%L+20%C) = CBR 96% 28 days curing - Light traffic - Depth of Construction = 50mm
☒ CONTROL (ASS 1 + 8%L+20%C) = CBR 96% 28 days curing - Medium traffic - Depth of Construction = 60mm
☒ CONTROL (ASS 1 + 8%L+20%C) = CBR 96% 28 days curing - Heavy traffic - Depth of Construction = 100mm
☒ (ASS 2 +2%L+2.5%C+23.5%PLASTIC) = CBR 8% 28 days curing - Light traffic - Depth of Construction = 205mm
☒ (ASS 2 +2%L+2.5%C+23.5%PLASTIC) = CBR 8% 28 days curing - Medium traffic - Depth of Construction = 240mm
☒ (ASS 2 +2%L+2.5%C+23.5%PLASTIC) = CBR 8% 28 days curing - Heavy traffic - Depth of Construction = 400mm
☒ (ASS 1 +2%L+2.5%C+11.75%GGBS+11.75%PLASTIC) = CBR 44% 7 days curing - Light traffic - Depth of Construction = 90mm
☒ (ASS 1 +2%L+2.5%C+11.75%GGBS+11.75%PLASTIC) = CBR 44% 7 days curing - Medium traffic - Depth of Construction = 110mm
☒ (ASS 1 +2%L+2.5%C+11.75%GGBS+11.75%PLASTIC) = CBR 44% 7 days curing - Heavy traffic - Depth of Construction = 190mm
☒ (ASS 2 +2%L+2.5%C+23.5%GLASS) = CBR 11% 7 days curing - Light traffic - Depth of Construction = 170mm
☒ (ASS 2 +2%L+2.5%C+23.5%GLASS) = CBR 11% 7 days curing - Medium traffic - Depth of Construction = 190mm
☒ (ASS 2 +2%L+2.5%C+23.5%GLASS) = CBR 11% 7 days curing - Heavy traffic - Depth of Construction = 320mm
☒ (ASS 1 +2%L+2.5%C+23.5%GLASS) = CBR 14% 7 days curing - Light traffic - Depth of Construction = 150mm
☒ (ASS 1 +2%L+2.5%C+23.5%GLASS) = CBR 14% 7 days curing - Medium traffic - Depth of Construction = 180mm
☒ (ASS 1 +2%L+2.5%C+23.5%GLASS) = CBR 14% 7 days curing - Heavy traffic - Depth of Construction = 310mm
☒ (ASS 2 +2%L+2.5%C+23.5%GGBS) = CBR 68% 28 days curing - Light traffic - Depth of Construction = 80mm
☒ (ASS 2 +2%L+2.5%C+23.5%GGBS) = CBR 68% 28 days curing - Medium traffic - Depth of Construction = 90mm
☒ (ASS 2 +2%L+2.5%C+23.5%GGBS) = CBR 68% 28 days curing - Heavy traffic - Depth of Construction = 170mm
☒ (ASS 1 +2%L+2.5%C+23.5%GGBS) = CBR 70% 7 days curing - Light traffic - Depth of Construction = 70mm
☒ (ASS 1 +2%L+2.5%C+23.5%GGBS) = CBR 70% 7 days curing - Medium traffic - Depth of Construction = 80mm
☒ (ASS 1 +2%L+2.5%C+23.5%GGBS) = CBR 70% 7 days curing - Heavy traffic - Depth of Construction = 150mm
☒ (ASS 1 +2%L+2.5%C+23.5%BDW) = CBR 23% 7 days curing - Light traffic - Depth of Construction = 130mm
☒ (ASS 1 +2%L+2.5%C+23.5%BDW) = CBR 23% 7 days curing - Medium traffic - Depth of Construction = 150mm
☒ (ASS 1 +2%L+2.5%C+23.5%BDW) = CBR 23% 7 days curing - Heavy traffic - Depth of Construction = 280mm

Figure 5.70: Road pavement construction depth optimisation for un-soaked treated and untreated ASS materials



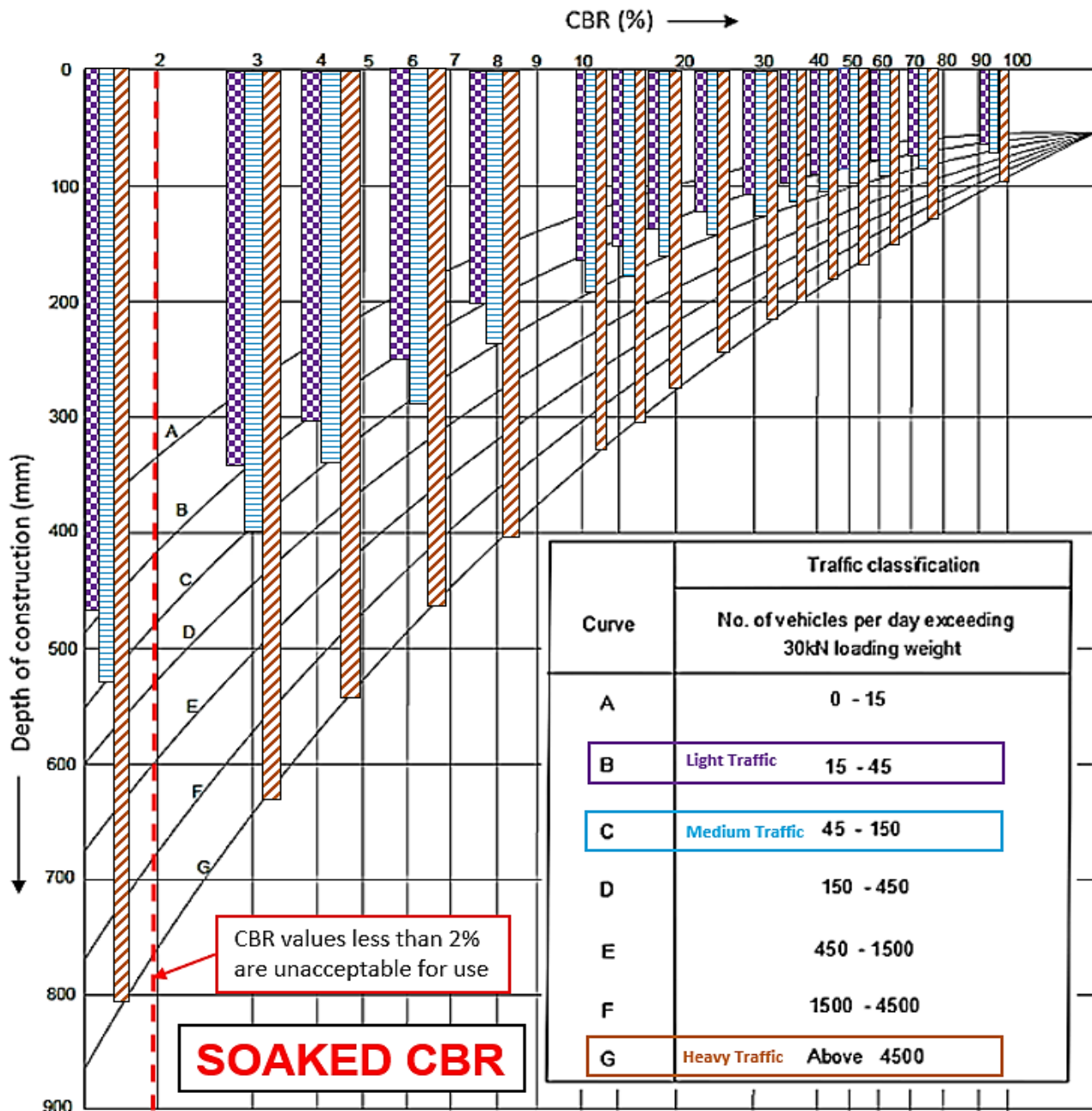
Chapter 5 – Results and Discussion

☒ (ASS 2 +2%L+2.5%C+23.5%GLASS) = CBR 8% 28 days curing - Light traffic - Depth of Construction = 205mm
☒ (ASS 2 +2%L+2.5%C+23.5%GLASS) = CBR 8% 28 days curing - Medium traffic - Depth of Construction = 240mm
■ (ASS 2 +2%L+2.5%C+23.5%GLASS) = CBR 8% 28 days curing - Heavy traffic - Depth of Construction = 400mm
☒ (ASS 1 +2%L+2.5%C+23.5%PLASTIC) = CBR 13% 28 days curing - Light traffic - Depth of Construction = 160mm
☒ (ASS 1 +2%L+2.5%C+23.5%PLASTIC) = CBR 13% 28 days curing - Medium traffic - Depth of Construction = 190mm
■ (ASS 1 +2%L+2.5%C+23.5%PLASTIC) = CBR 13% 28 days curing - Heavy traffic - Depth of Construction = 310mm
☒ (ASS 2 +2%L+2.5%C+11.75%GGBS+11.75%PLASTIC) = CBR 21% 7 days curing - Light traffic - Depth of Construction = 120mm
☒ (ASS 2 +2%L+2.5%C+11.75%GGBS+11.75%PLASTIC) = CBR 21% 7 days curing - Medium traffic - Depth of Construction = 150mm
☒ (ASS 2 +2%L+2.5%C+11.75%GGBS+11.75%PLASTIC) = CBR 21% 7 days curing - Heavy traffic - Depth of Construction = 280mm
⊗ (ASS 2 +2%L+2.5%C+11.75%GGBS+11.75%PLASTIC) = CBR 51% 28 days curing - Light traffic - Depth of Construction = 90mm
☒ (ASS 2 +2%L+2.5%C+11.75%GGBS+11.75%PLASTIC) = CBR 51% 28 days curing - Medium traffic - Depth of Construction = 100mm
■ (ASS 2 +2%L+2.5%C+11.75%GGBS+11.75%PLASTIC) = CBR 51% 28 days curing - Heavy traffic - Depth of Construction = 180mm
☒ (ASS 2 +2%L+2.5%C+23.5%BDW) = CBR 14% 7 days curing - Light traffic - Depth of Construction = 150mm
☒ (ASS 2 +2%L+2.5%C+23.5%BDW) = CBR 14% 7 days curing - Medium traffic - Depth of Construction = 180mm
☒ (ASS 2 +2%L+2.5%C+23.5%BDW) = CBR 14% 7 days curing - Heavy traffic - Depth of Construction = 310mm
☒ (ASS 2 +2%L+2.5%C+11.75%GGBS+11.75%BDW) = CBR 27% 7 days curing - Light traffic - Depth of Construction = 110mm
☒ (ASS 2 +2%L+2.5%C+11.75%GGBS+11.75%BDW) = CBR 27% 7 days curing - Medium traffic - Depth of Construction = 130mm
■ (ASS 2 +2%L+2.5%C+11.75%GGBS+11.75%BDW) = CBR 27% 7 days curing - Heavy traffic - Depth of Construction = 240mm
☒ (ASS 1 +2%L+2.5%C+11.75%GGBS+11.75%BDW) = CBR 61% 7 days curing - Light traffic - Depth of Construction = 70mm
☒ (ASS 1 +2%L+2.5%C+11.75%GGBS+11.75%BDW) = CBR 61% 7 days curing - Medium traffic - Depth of Construction = 80mm
■ (ASS 1 +2%L+2.5%C+11.75%GGBS+11.75%BDW) = CBR 61% 7 days curing - Heavy traffic - Depth of Construction = 140mm
☒ (ASS 1 +2%L+2.5%C+23.5%GLASS) = CBR 16% 28 days curing - Light traffic - Depth of Construction = 130mm
☒ (ASS 1 +2%L+2.5%C+23.5%GLASS) = CBR 16% 28 days curing - Medium traffic - Depth of Construction = 170mm
■ (ASS 1 +2%L+2.5%C+23.5%GLASS) = CBR 16% 28 days curing - Heavy traffic - Depth of Construction = 290mm
☒ (ASS 2 +2%L+2.5%C+11.75%GGBS+11.75%GLASS) = CBR 46% 28 days curing - Light traffic - Depth of Construction = 90mm
☒ (ASS 2 +2%L+2.5%C+11.75%GGBS+11.75%GLASS) = CBR 46% 28 days curing - Medium traffic - Depth of Construction = 100mm
☒ (ASS 2 +2%L+2.5%C+11.75%GGBS+11.75%GLASS) = CBR 46% 28 days curing - Heavy traffic - Depth of Construction = 190mm
☒ (ASS 1 +2%L+2.5%C+11.75%GGBS+11.75%GLASS) = CBR 80% 28 days curing - Light traffic - Depth of Construction = 60mm
☒ (ASS 1 +2%L+2.5%C+11.75%GGBS+11.75%GLASS) = CBR 80% 28 days curing - Medium traffic - Depth of Construction = 70mm
■ (ASS 1 +2%L+2.5%C+11.75%GGBS+11.75%GLASS) = CBR 80% 28 days curing - Heavy traffic - Depth of Construction = 120mm

Figure 5.71: Road pavement construction depth optimisation for un-soaked treated and untreated ASS materials

Chapter 5 – Results and Discussion

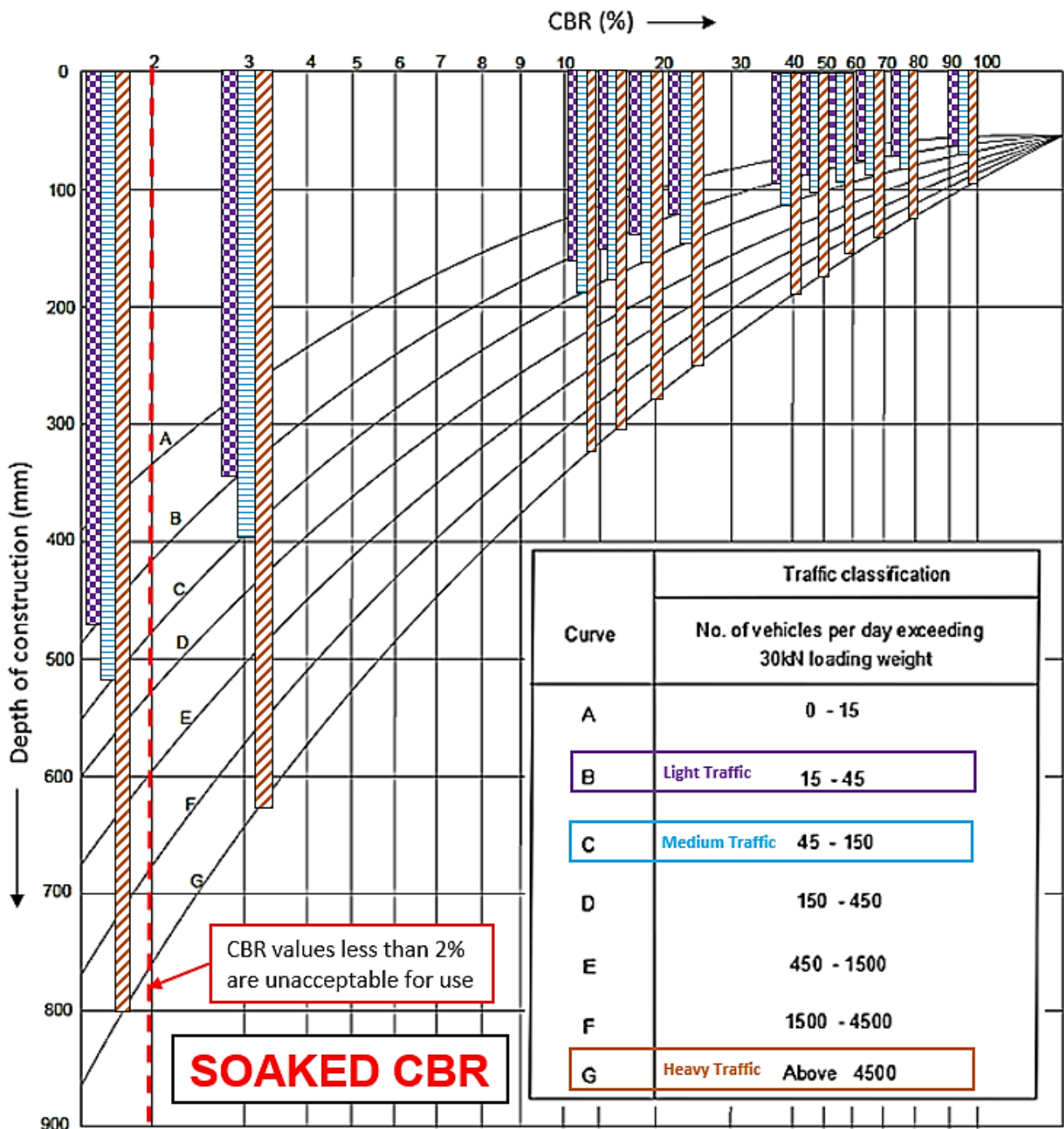
Figure 5.72 - Figure 5.74 shows road pavement construction depth optimisation soaked treated and untreated ASS materials using 11.75% and 23.5% recycled plastic and glass, GGBS and BDW in accordance with California State of Highways guidance 2021.



Chapter 5 – Results and Discussion

☒ ASS 1 (25%B + 75%K) CBR 0.6% SOAKED - Light traffic - Depth of Construction = 480mm (UNACCEPTABLE)
☐ ASS 1 (25%B + 75%K) CBR 0.6% SOAKED- Medium traffic - Depth of Construction = 510mm (UNACCEPTABLE)
☑ ASS 1 (25%B + 75%K) CBR 0.6% SOAKED- Heavy traffic - Depth of Construction = 800mm (UNACCEPTABLE)
☒ CONTROL (ASS 1 + 8%L+20%C) = CBR 50% SOAKED 28 days curing - Light traffic - Depth of Construction = 80mm
☐ CONTROL (ASS 1 + 8%L+20%C) = CBR 50% SOAKED 28 days curing - Medium traffic - Depth of Construction = 90mm
☑ CONTROL (ASS 1 + 8%L+20%C) = CBR 50% SOAKED 28 days curing - Heavy traffic - Depth of Construction = 180mm
☒ CONTROL (ASS 2 + 8%L+20%C) = CBR 34% SOAKED after 7 days curing - Light traffic - Depth of Construction = 100mm
☐ CONTROL (ASS 2 + 8%L+20%C) = CBR 34% SOAKED after 7 days curing - Medium traffic - Depth of Construction = 110mm
☑ CONTROL (ASS 2 + 8%L+20%C) = CBR 34% SOAKED after 7 days curing - Heavy traffic - Depth of Construction = 200mm
☒ CONTROL (ASS 2 + 8%L+20%C) = CBR 61% SOAKED after 28 days curing - Light traffic - Depth of Construction = 70mm
☐ CONTROL (ASS 2 + 8%L+20%C) = CBR 61% SOAKED after 28 days curing - Medium traffic - Depth of Construction = 80mm
☑ CONTROL (ASS 2 + 8%L+20%C) = CBR 61% SOAKED after 28 days curing - Heavy traffic - Depth of Construction = 140mm
☒ (ASS 1 +2%L+2.5%C+23.5%GLASS) = CBR 17% SOAKED after 7 days curing - Light traffic - Depth of Construction = 140mm
☐ (ASS 1 +2%L+2.5%C+23.5%GLASS) = CBR 17% SOAKED after 7 days curing - Medium traffic - Depth of Construction = 150mm
☑ (ASS 1 +2%L+2.5%C+23.5%GLASS) = CBR 17% SOAKED after 7 days curing - Heavy traffic - Depth of Construction = 290mm
☒ (ASS 1 +2%L+2.5%C+23.5%GLASS) = CBR 11% SOAKED after 28 days curing - Light traffic - Depth of Construction = 170mm
☐ (ASS 1 +2%L+2.5%C+23.5%GLASS)= CBR 11% SOAKED after 28 days curing - Medium traffic - Depth of Construction = 190mm
☑ (ASS 1 +2%L+2.5%C+23.5%GLASS) = CBR 11% SOAKED after 28 days curing - Heavy traffic - Depth of Construction = 320mm
☒ (ASS 1 +2%L+2.5%C+11.75%GGBS+11.75%GLASS)= CBR 72% SOAKED after 28 days curing - Light traffic - Depth of Construction = 60mm
☐ (ASS 1 +2%L+2.5%C+11.75%GGBS+11.75%GLASS) = CBR 72% SOAKED after 28 days curing - Medium traffic - Depth of Construction = 70mm
☑ (ASS 1 +2%L+2.5%C+11.75%GGBS+11.75%GLASS) = CBR 72% SOAKED after 28 days curing - Heavy traffic - Depth of Construction = 130mm
☒ (ASS 2 +2%L+2.5%C+23.5%GLASS)= CBR 3% SOAKED after 7 days curing - Light traffic - Depth of Construction = 350mm
☐ (ASS 2 +2%L+2.5%C+23.5%GLASS) = CBR 3% SOAKED after 7 days curing - Medium traffic - Depth of Construction = 400mm
☑ (ASS 2 +2%L+2.5%C+23.5%GLASS) = CBR 3% SOAKED after 7 days curing - Heavy traffic - Depth of Construction = 610mm
☒ (ASS 2 +2%L+2.5%C+23.5%GLASS) = CBR 4% SOAKED after 28 days curing - Light traffic - Depth of Construction = 300mm
☐ (ASS 2 +2%L+2.5%C+23.5%GLASS) = CBR 4% SOAKED after 28 days curing - Medium traffic - Depth of Construction = 320mm
☑ (ASS 2 +2%L+2.5%C+23.5%GLASS) = CBR 4% SOAKED after 28 days curing - Heavy traffic - Depth of Construction = 520mm
☒ (ASS 2 +2%L+2.5%C+11.75%GGBS+11.75%GLASS) = CBR 31% SOAKED after 7 days curing - Light traffic - Depth of Construction = 110mm
☐ (ASS 2 +2%L+2.5%C+11.75%GGBS+11.75%GLASS) = CBR 31% SOAKED after 7 days curing - Medium traffic - Depth of Construction = 120mm
☑ (ASS 2 +2%L+2.5%C+11.75%GGBS+11.75%GLASS) = CBR 31% SOAKED after 7 days curing - Heavy traffic - Depth of Construction = 210mm
☒ (ASS 2 +2%L+2.5%C+23.5%PLASTIC) = CBR 6% SOAKED after 7 days curing - Light traffic - Depth of Construction = 250mm
☐ (ASS 2 +2%L+2.5%C+23.5%PLASTIC) = CBR 6% SOAKED after 7 days curing - Medium traffic - Depth of Construction = 280mm
☑ (ASS 2 +2%L+2.5%C+23.5%PLASTIC) = CBR 6% SOAKED after 7 days curing - Heavy traffic - Depth of Construction = 480mm
☒ (ASS 1 +2%L+2.5%C+23.5%PLASTIC) = CBR 8% SOAKED after 28 days curing - Light traffic - Depth of Construction = 205mm
☐ (ASS 1 +2%L+2.5%C+23.5%PLASTIC) = CBR 8% SOAKED after 28 days curing - Medium traffic - Depth of Construction = 240mm
☑ (ASS 1 +2%L+2.5%C+23.5%PLASTIC) = CBR 8% SOAKED after 28 days curing - Heavy traffic - Depth of Construction = 400mm
☒ (ASS 1 +2%L+2.5%C+23.5%BDW) = CBR 17% SOAKED after 7 days curing - Light traffic - Depth of Construction = 150mm
☐ (ASS 1 +2%L+2.5%C+23.5%BDW) = CBR 17% SOAKED after 7 days curing - Medium traffic - Depth of Construction = 190mm
☑ (ASS 1 +2%L+2.5%C+23.5%BDW) = CBR 17% SOAKED after 7 days curing - Heavy traffic - Depth of Construction = 300mm
☒ (ASS 1 +2%L+2.5%C+23.5%BDW) = CBR 28% SOAKED after 28 days curing - Light traffic - Depth of Construction = 120mm
☐ (ASS 1 +2%L+2.5%C+23.5%BDW) = CBR 28% SOAKED after 28 days curing - Medium traffic - Depth of Construction = 130mm
☑ (ASS 1 +2%L+2.5%C+23.5%BDW) = CBR 28% SOAKED after 28 days curing - Heavy traffic - Depth of Construction = 250mm
☒ (ASS 2 +2%L+2.5%C+23.5%GGBS) = CBR 46% SOAKED after 7 days curing - Light traffic - Depth of Construction = 90mm
☐ (ASS 2 +2%L+2.5%C+23.5%GGBS) = CBR 46% SOAKED after 7 days curing - Medium traffic - Depth of Construction = 100mm
☑ (ASS 2 +2%L+2.5%C+23.5%GGBS) = CBR 46% SOAKED after 7 days curing - Heavy traffic - Depth of Construction = 190mm
☒ (ASS 1 +2%L+2.5%C+23.5%GGBS) = CBR 97 % SOAKED after 28 days curing - Light traffic - Depth of Construction = 50mm
☐ (ASS 1 +2%L+2.5%C+23.5%GGBS) = CBR 97 % SOAKED after 28 days curing - Medium traffic - Depth of Construction = 60mm
☑ (ASS 1 +2%L+2.5%C+23.5%GGBS) = CBR 97 % SOAKED after 28 days curing - Heavy traffic - Depth of Construction = 100mm

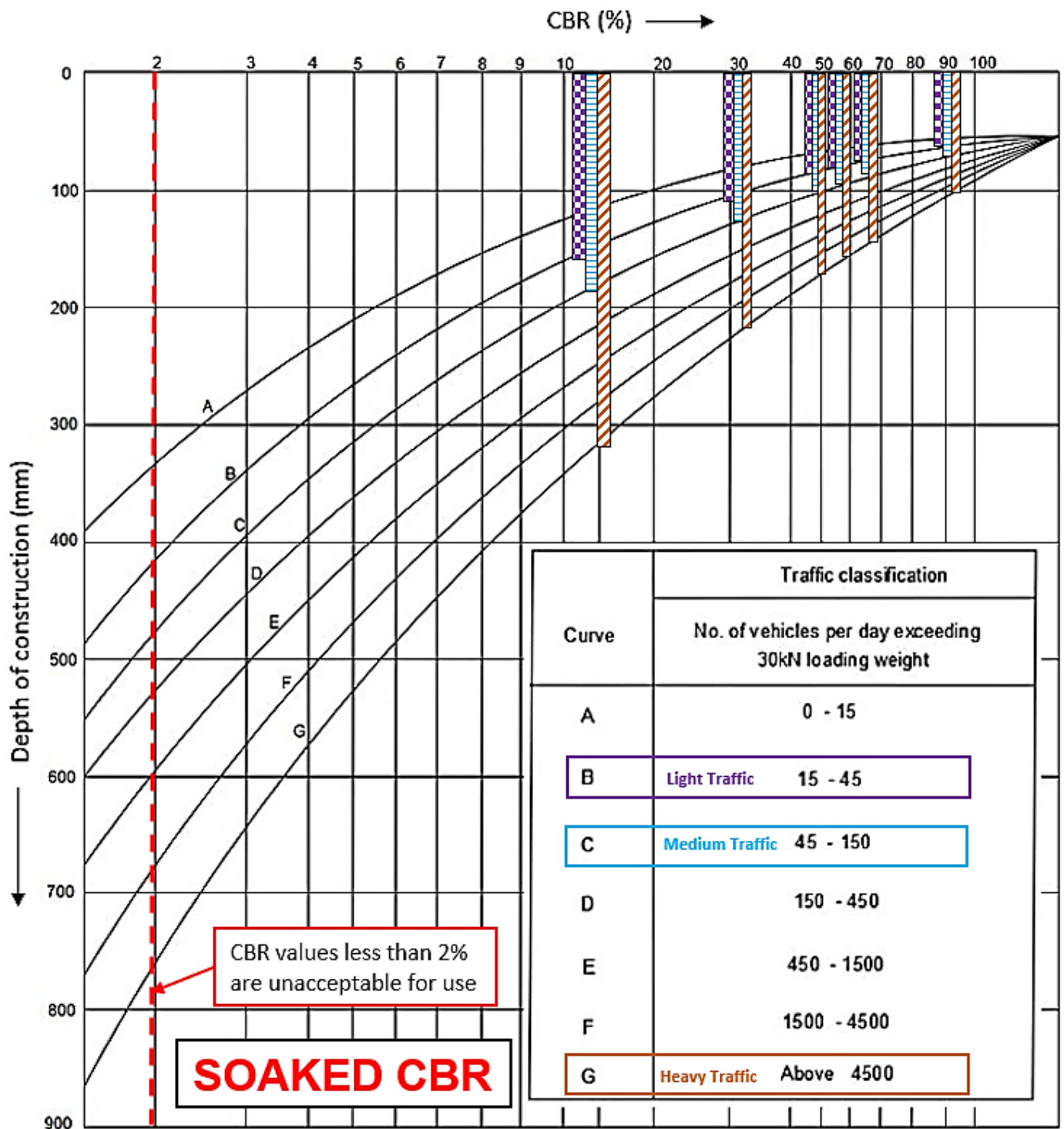
Figure 5.72: Road pavement construction depth optimisation soaked treated and untreated ASS materials



Chapter 5 – Results and Discussion

<ul style="list-style-type: none"> ☒ CONTROL (ASS 1 + 8%L+20%C) = CBR 45% SOAKED after 7 days curing - Light traffic - Depth of Construction = 90mm ☐ CONTROL (ASS 1 + 8%L+20%C) = CBR 45% SOAKED after 7 days curing - Medium traffic - Depth of Construction = 110mm ☑ CONTROL (ASS 1 + 8%L+20%C) = CBR 45% SOAKED after 7 days curing - Heavy traffic - Depth of Construction = 190mm
<ul style="list-style-type: none"> ☒ ASS 2 (75%B+25%K) CBR 1.34% SOAKED - Light traffic - Depth of Construction = 490mm (UNACCEPTABLE) ☐ ASS 2 (75%B+25%K) CBR 1.34% SOAKED - Medium traffic - Depth of Construction = 510mm (UNACCEPTABLE) ☑ ASS 2 (75%B+25%K) CBR 1.34% SOAKED - Heavy traffic - Depth of Construction = 800mm (UNACCEPTABLE)
<ul style="list-style-type: none"> ☒ (ASS 2 +2%L+2.5%C+23.5%PLASTIC) = CBR 3% SOAKED after 28 days curing - Light traffic - Depth of Construction = 350mm ☐ (ASS 2 +2%L+2.5%C+23.5%PLASTIC) = CBR 3% SOAKED after 28 days curing - Medium traffic - Depth of Construction = 400mm ☑ (ASS 2 +2%L+2.5%C+23.5%PLASTIC) = CBR 3% SOAKED after 28 days curing - Heavy traffic - Depth of Construction = 610mm
<ul style="list-style-type: none"> ☒ (ASS 1 +2%L+2.5%C+11.75%GGBS+11.75%PLASTIC) = CBR 59% SOAKED after 7 days curing - Light traffic - Depth of Construction = 70mm ☐ (ASS 1 +2%L+2.5%C+11.75%GGBS+11.75%PLASTIC) = CBR 59% SOAKED after 7 days curing - Medium traffic - Depth of Construction = 90mm ☑ (ASS 1 +2%L+2.5%C+11.75%GGBS+11.75%PLASTIC) = CBR 59% SOAKED after 7 days curing - Heavy traffic - Depth of Construction = 170mm
<ul style="list-style-type: none"> ☒ (ASS 2 +2%L+2.5%C+11.75%GGBS+11.75%PLASTIC) = CBR 47% SOAKED after 7 days curing - Light traffic - Depth of Construction = 80mm ☐ (ASS 2 +2%L+2.5%C+11.75%GGBS+11.75%PLASTIC) = CBR 47% SOAKED after 7 days curing - Medium traffic - Depth of Construction = 100mm ☑ (ASS 2 +2%L+2.5%C+11.75%GGBS+11.75%PLASTIC) = CBR 47% SOAKED after 7 days curing - Heavy traffic - Depth of Construction = 180mm
<ul style="list-style-type: none"> ☒ (ASS 2 +2%L+2.5%C+11.75%GGBS+11.75%PLASTIC) = CBR 50% SOAKED after 28 days curing - Light traffic - Depth of Construction = 80mm ☐ (ASS 2 +2%L+2.5%C+11.75%GGBS+11.75%PLASTIC) = CBR 50% SOAKED after 28 days curing - Medium traffic - Depth of Construction = 90mm ☑ (ASS 2 +2%L+2.5%C+11.75%GGBS+11.75%PLASTIC) = CBR 50% SOAKED after 28 days curing - Heavy traffic - Depth of Construction = 180mm
<ul style="list-style-type: none"> ☒ (ASS 2 +2%L+2.5%C+23.5%BDW) = CBR 17% SOAKED after 28 days curing - Light traffic - Depth of Construction = 150mm ☐ (ASS 2 +2%L+2.5%C+23.5%BDW) = CBR 17% SOAKED after 28 days curing - Medium traffic - Depth of Construction = 190mm ☑ (ASS 2 +2%L+2.5%C+23.5%BDW) = CBR 17% SOAKED after 28 days curing - Heavy traffic - Depth of Construction = 300mm
<ul style="list-style-type: none"> ☒ (ASS 2 +2%L+2.5%C+23.5%BDW) = CBR 18% SOAKED after 7 days curing - Light traffic - Depth of Construction = 140mm ☐ (ASS 2 +2%L+2.5%C+23.5%BDW) = CBR 18% SOAKED after 7 days curing - Medium traffic - Depth of Construction = 180mm ☑ (ASS 2 +2%L+2.5%C+23.5%BDW) = CBR 18% SOAKED after 7 days curing - Heavy traffic - Depth of Construction = 290mm
<ul style="list-style-type: none"> ☒ (ASS 1 +2%L+2.5%C+11.75%GGBS+11.75%BDW) = CBR 97% SOAKED after 28 days curing - Light traffic - Depth of Construction = 50mm ☐ (ASS 1 +2%L+2.5%C+11.75%GGBS+11.75%BDW) = CBR 97% SOAKED after 28 days curing - Medium traffic - Depth of Construction = 60mm ☑ (ASS 1 +2%L+2.5%C+11.75%GGBS+11.75%BDW) = CBR 97% SOAKED after 28 days curing - Heavy traffic - Depth of Construction = 90mm
<ul style="list-style-type: none"> ☒ (ASS 2 +2%L+2.5%C+11.75%GGBS+11.75%BDW) = CBR 16% SOAKED after 7 days curing - Light traffic - Depth of Construction = 130mm ☐ (ASS 2 +2%L+2.5%C+11.75%GGBS+11.75%BDW) = CBR 16% SOAKED after 7 days curing - Medium traffic - Depth of Construction = 170mm ☑ (ASS 2 +2%L+2.5%C+11.75%GGBS+11.75%BDW) = CBR 16% SOAKED after 7 days curing - Heavy traffic - Depth of Construction = 290mm
<ul style="list-style-type: none"> ☒ (ASS 2 +2%L+2.5%C+11.75%GGBS+11.75%BDW) = CBR 24% SOAKED after 28 days curing - Light traffic - Depth of Construction = 110mm ☐ (ASS 2 +2%L+2.5%C+11.75%GGBS+11.75%BDW) = CBR 24% SOAKED after 28 days curing - Medium traffic - Depth of Construction = 150mm ☑ (ASS 2 +2%L+2.5%C+11.75%GGBS+11.75%BDW) = CBR 24% SOAKED after 28 days curing - Heavy traffic - Depth of Construction = 250mm
<ul style="list-style-type: none"> ☒ (ASS 2 +2%L+2.5%C+23.5%GGBS) = CBR 65% SOAKED after 28 days curing - Light traffic - Depth of Construction = 80mm ☐ (ASS 2 +2%L+2.5%C+23.5%GGBS) = CBR 65% SOAKED after 28 days curing - Medium traffic - Depth of Construction = 90mm ☑ (ASS 2 +2%L+2.5%C+23.5%GGBS) = CBR 65% SOAKED after 28 days curing - Heavy traffic - Depth of Construction = 150mm
<ul style="list-style-type: none"> ☒ (ASS 1 +2%L+2.5%C+23.5%GGBS) = CBR 79% SOAKED after 7 days curing - Light traffic - Depth of Construction = 70mm ☐ (ASS 1 +2%L+2.5%C+23.5%GGBS) = CBR 79% SOAKED after 7 days curing - Medium traffic - Depth of Construction = 80mm ☑ (ASS 1 +2%L+2.5%C+23.5%GGBS) = CBR 79% SOAKED after 7 days curing - Heavy traffic - Depth of Construction = 120mm

Figure 5.73: Road pavement construction depth optimisation soaked treated and untreated ASS materials



☒ (ASS 1 +2%L+2.5%C+23.5%PLASTIC) = CBR 12% SOAKED after 7 days curing - Light traffic - Depth of Construction = 160mm
☐ (ASS 1 +2%L+2.5%C+23.5%PLASTIC) = CBR 12% SOAKED after 7 days curing - Medium traffic - Depth of Construction = 190mm
☑ (ASS 1 +2%L+2.5%C+23.5%PLASTIC) = CBR 12% SOAKED after 7 days curing - Heavy traffic - Depth of Construction = 310mm
☒ (ASS 1 +2%L+2.5%C+11.75%GGBS+11.75%PLASTIC) = CBR 93% SOAKED after 28 days curing - Light traffic - Depth of Construction = 50mm
☐ (ASS 1 +2%L+2.5%C+11.75%GGBS+11.75%PLASTIC) = CBR 93% SOAKED after 28 days curing - Medium traffic - Depth of Construction = 60mm
☑ (ASS 1 +2%L+2.5%C+11.75%GGBS+11.75%PLASTIC) = CBR 93% SOAKED after 28 days curing - Heavy traffic - Depth of Construction = 100mm
☒ (ASS 2 +2%L+2.5%C+11.75%GGBS+11.75%PLASTIC) = CBR 50% SOAKED after 28 days curing - Light traffic - Depth of Construction = 80mm
☐ (ASS 2 +2%L+2.5%C+11.75%GGBS+11.75%PLASTIC) = CBR 50% SOAKED after 28 days curing - Medium traffic - Depth of Construction = 90mm
☑ (ASS 2 +2%L+2.5%C+11.75%GGBS+11.75%PLASTIC) = CBR 50% SOAKED after 28 days curing - Heavy traffic - Depth of Construction = 180mm
☒ (ASS 1 +2%L+2.5%C+11.75%GGBS+11.75%GLASS) = CBR 59% SOAKED after 7 days curing - Light traffic - Depth of Construction = 70mm
☐ (ASS 1 +2%L+2.5%C+11.75%GGBS+11.75%GLASS) = CBR 59% SOAKED after 7 days curing - Medium traffic - Depth of Construction = 90mm
☑ (ASS 1 +2%L+2.5%C+11.75%GGBS+11.75%GLASS) = CBR 59% SOAKED after 7 days curing - Heavy traffic - Depth of Construction = 170mm
☒ (ASS 2 +2%L+2.5%C+11.75%GGBS+11.75%GLASS) = CBR 46% SOAKED after 28 days curing - Light traffic - Depth of Construction = 90mm
☐ (ASS 2 +2%L+2.5%C+11.75%GGBS+11.75%GLASS) = CBR 46% SOAKED after 28 days curing - Medium traffic - Depth of Construction = 100mm
☑ (ASS 2 +2%L+2.5%C+11.75%GGBS+11.75%GLASS) = CBR 46% SOAKED after 28 days curing - Heavy traffic - Depth of Construction = 190mm
☒ (ASS 1 +2%L+2.5%C+11.75%GGBS+11.75%BDW) = CBR 61% SOAKED after 7 days curing - Light traffic - Depth of Construction = 70mm
☐ (ASS 1 +2%L+2.5%C+11.75%GGBS+11.75%BDW) = CBR 61% SOAKED after 7 days curing - Medium traffic - Depth of Construction = 80mm
☑ (ASS 1 +2%L+2.5%C+11.75%GGBS+11.75%BDW) = CBR 61% SOAKED after 7 days curing - Heavy traffic - Depth of Construction = 140mm

Figure 5.74: Road pavement construction depth optimisation soaked treated and untreated ASS materials

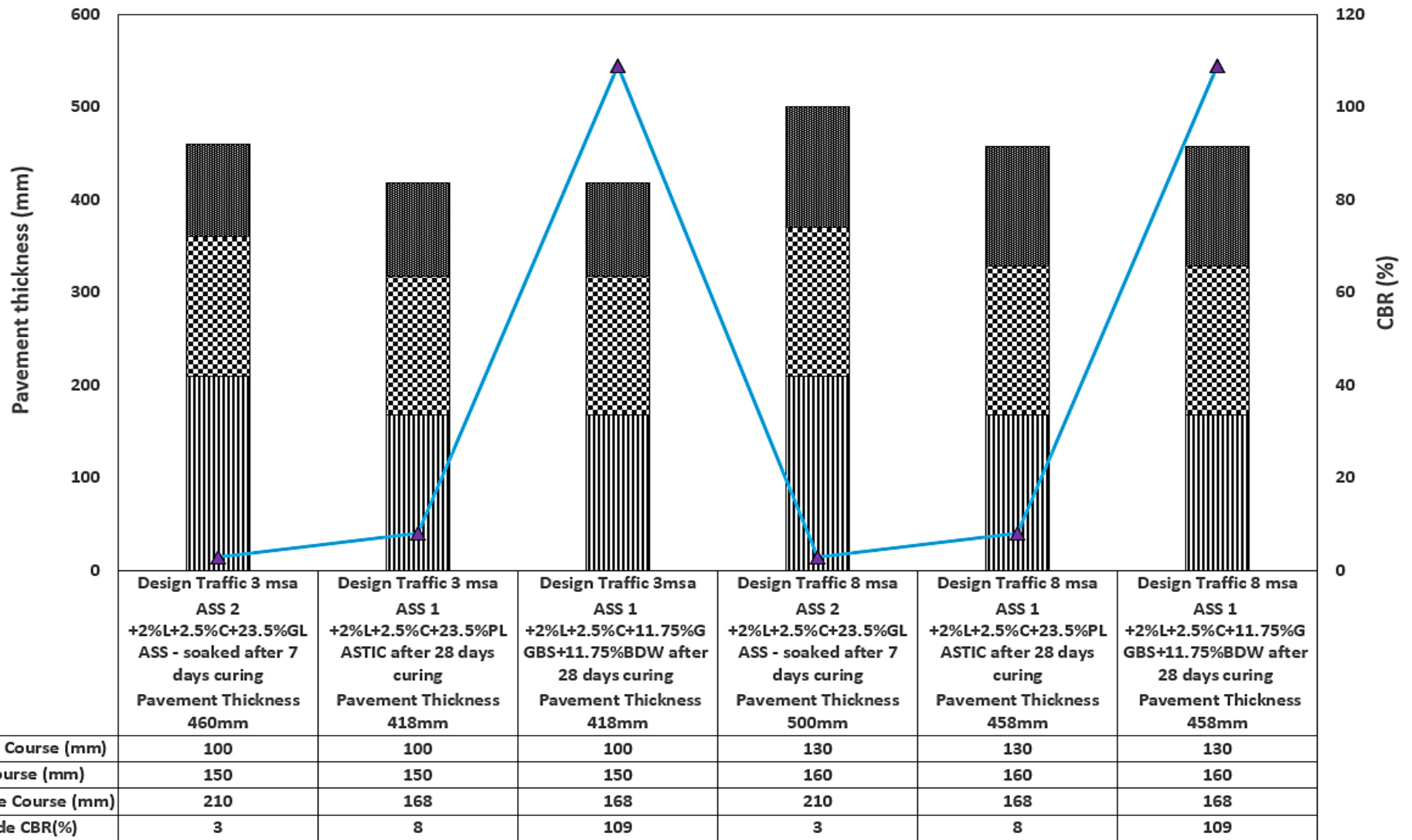
5.9 DMRB PAVEMENT DESIGN

An increase in road pavement thickness was observed with an increase in CBR values and design traffic. It was observed that the subbase course of the road pavement influences the increase and or reduction of pavement thickness. A slight reduction in subbase course thickness was observed as the CBR value increased from 3% to 8% however, subbase course thickness remained the same even with a CBR value as high as 109%. The thickness of the base and surface course remains the same as specified by DMRB standards for the various traffic loads.

Design Manual for Roads and Bridges (DMRB) (2021) road pavement design guidance used in this research was to validate the findings in this research that, higher CBR translate to thinner pavement. After carrying out DMRB pavement design, a reduction in pavement thickness and an increase in CBR values were observed for ASS1 and with design traffic 3msa, 8msa, 60msa and 100msa, respectively. increase CBR value which will considerably reduce total pavement thickness and hence the

total cost of the project (Otoko et al., 2014). 19% increase in CBR value reflected in a reduction in the overall thickness and life cycle cost of a road in Uganda (Melling et al., 2017). According to the Constructor Building Ideas, (2021), pavement thickness is determined by the subgrade strength and it's good to make the subgrade as strong as possible. Pavements are built to a set thickness dependent only on the subgrade quality, being independent of anticipated traffic (Dawson et al., 2008). only a little change in pavement thickness was observed using DMRB in road design compared to using other pavement design guidance. This change in pavement thickness was mostly due to the change in thickness in the subbase layer.

A significant change in pavement thickness can only be observed for subgrade CBR values from 2 - 5% when using DMRB in road pavement design guidance. This is because the subbase layer forms a major of the road pavement structure and the class 3 subbase chart offers the thicker subbase layer only for subgrade CBR values between 2 - 10.5% after which subbase thickness remains the same (180mm). Hence, no significant change in pavement thickness was observed even with a CBR value of 100%. The reduction in pavement thickness with an increase in CBR value observed using DMRB guidance validates the earlier statement that, high CBR translate to thinner pavement. High CBR values were achieved using sustainable waste materials in this research recorded thinner pavement thickness. The thickest pavement recorded using selected CBR values was 600mm (100msa) with a CBR value of 3% and the thinnest was 418mm (3msa) with a CBR value of 109%. Due to the low CBR values (5%) a thicker pavement was required to limit the pavement deterioration rate due to stresses (Parry et al., 1999). The thickness of asphalt layers is necessary to limit stresses and reduce the severity of reflective cracking. Figure 5.75 - Figure 5.76 shows detailed results of road pavement designed using DMRB and Figure 5.77 shows a summary of DMRB road pavement design using various design traffic and CBR values achieved in this study.



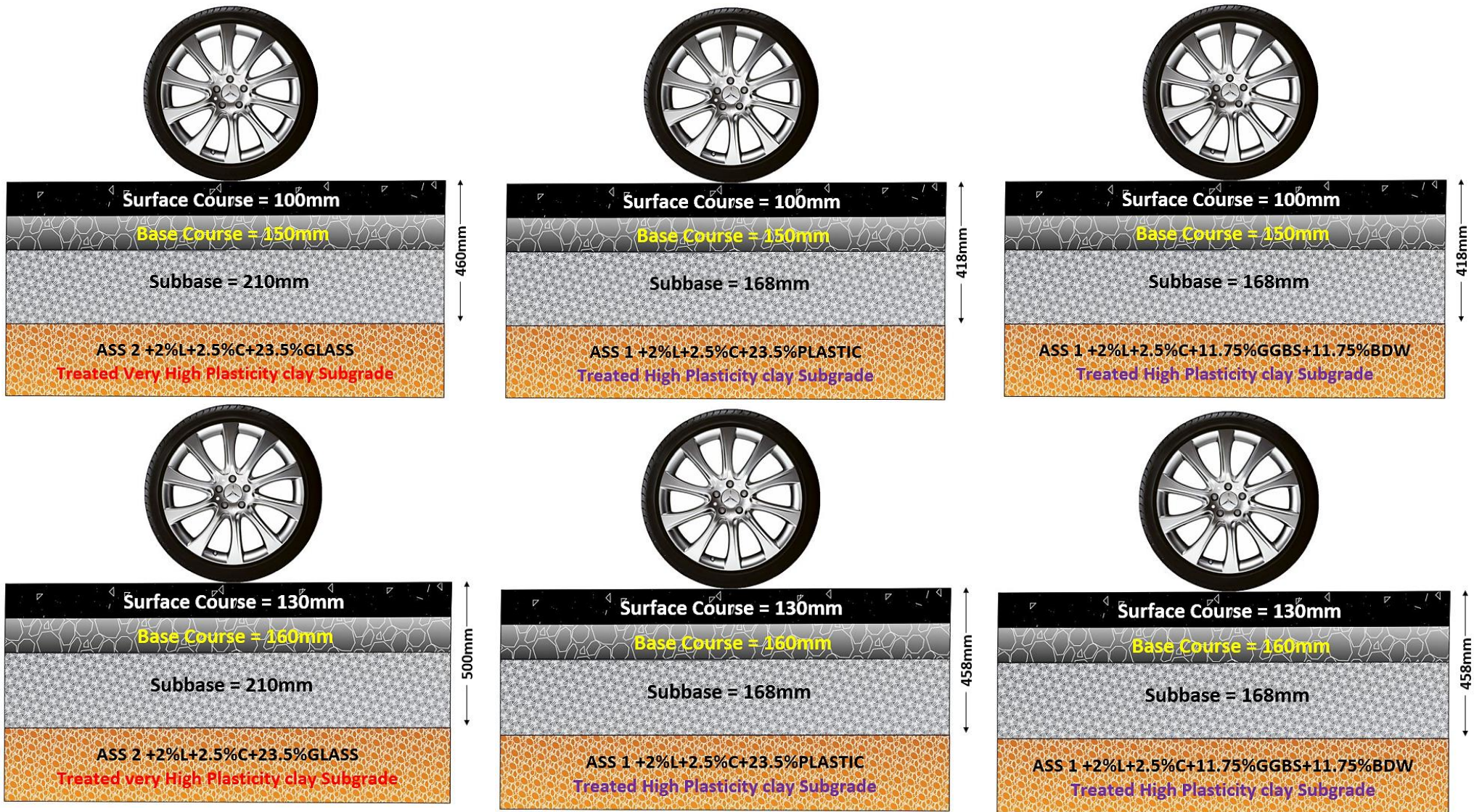
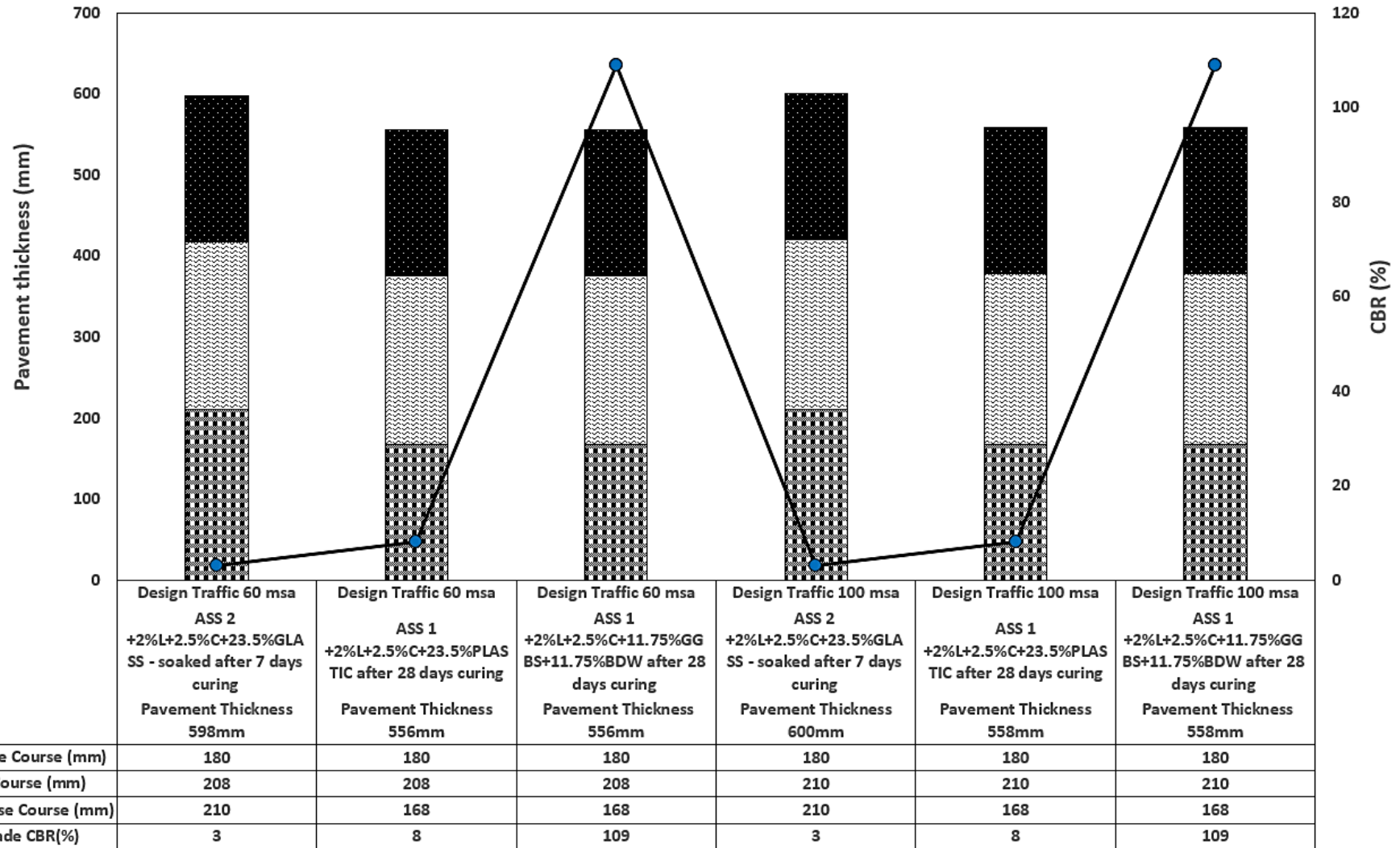


Figure 5.75: Results of road pavement designed using DMRB for traffic 3msa and 8msa



Chapter 5 – Results and Discussion

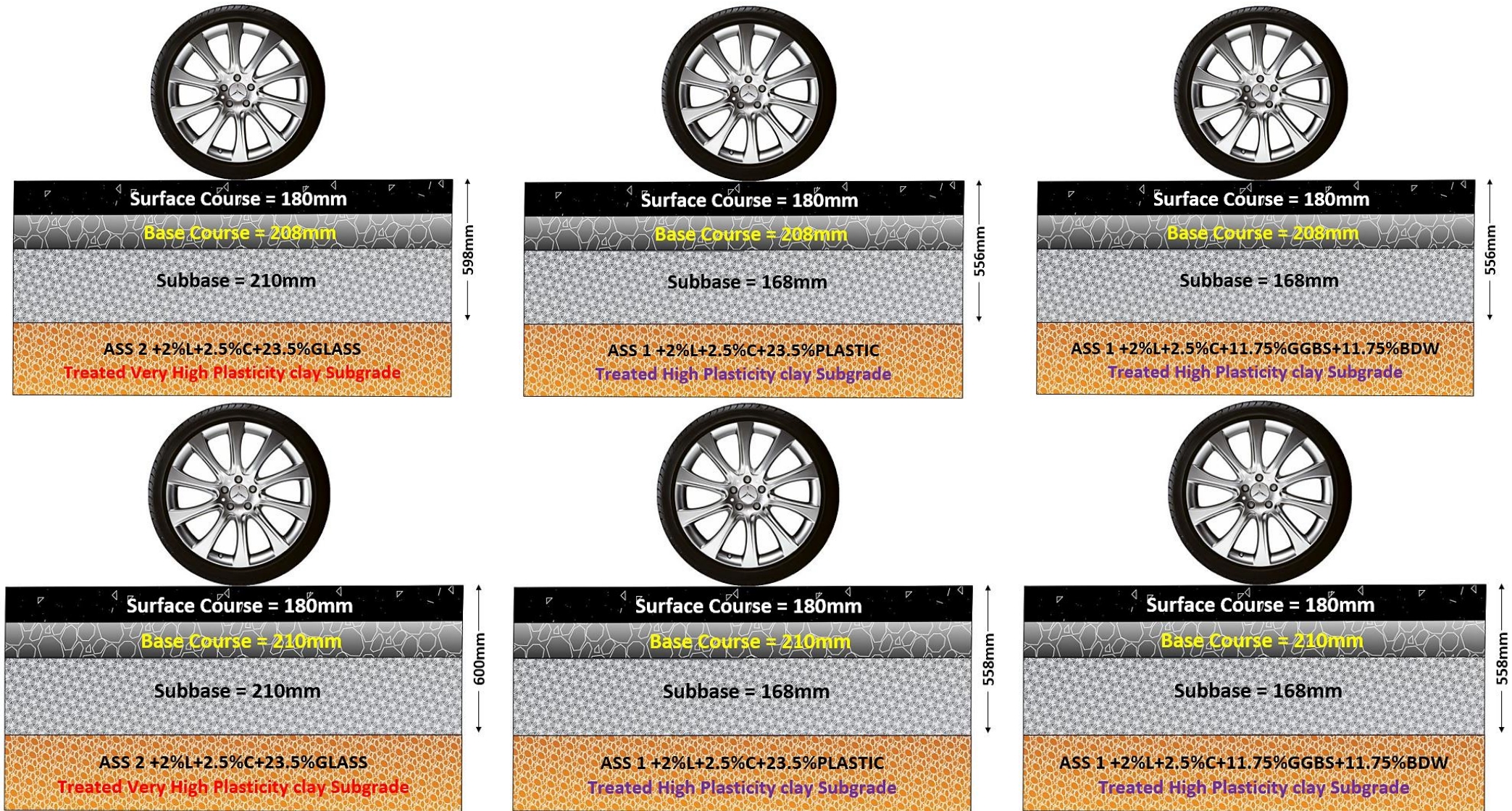


Figure 5.76: Results of road pavement designed using DMRB for traffic 60msa and 100msa

Chapter 5 – Results and Discussion

ASS1 (25% Bentonite + 75% Kaolinite) High Plasticity							
Flexible Pavement Layers	Material	Thickness (mm)	Treated	Curing (Days)	Soaked	CBR (%)	Design Traffic (msa)
Surface Course	HRA	130					
Base Course	HBM	160					
Subbase	CBGM	180					
Subgrade	ASS	∞					
Total pavement thickness		470					
(ASS1+ 2L+2.5C+23.5BDW) High Plasticity							
Flexible Pavement Layers	Material	Thickness (mm)	Treated	Curing (Days)	Soaked	CBR (%)	Design Traffic (msa)
Surface Course	HRA	180					
Base Course	HBM	210					
Subbase	CBGM	180					
Subgrade	ASS	∞					
Total pavement thickness		570					

ASS2 (75% Bentonite + 25% Kaolinite) Extremely High Plasticity							
Flexible Pavement Layers	Material	Thickness (mm)	Treated	Curing (Days)	Soaked	CBR (%)	Design Traffic (msa)
Surface Course	HRA	130					
Base Course	HBM	160					
Subbase	CBGM	180					
Subgrade	ASS	∞	×	×	×	9	8
Total pavement thickness		470					
(ASS2+ 2L+2.5C+23.5BDW) Extremely High Plasticity							
Flexible Pavement Layers	Material	Thickness (mm)	Treated	Curing (Days)	Soaked	CBR (%)	Design Traffic (msa)
Surface Course	HRA	180					
Base Course	HBM	210					
Subbase	CBGM	180					
Subgrade	ASS	∞					
Total pavement thickness		570	√	7	×	14	100

Chapter 5 – Results and Discussion

(ASS1+ 2L+2.5C+23.5GGBS) High Plasticity							
Flexible Pavement Layers	Material	Thickness (mm)	Treated	Curing (Days)	Soaked	CBR (%)	Design Traffic (msa)
Surface Course	HRA	100					
Base Course	HBM	150					
Subbase	CBGM	180					
Subgrade	ASS	∞					
Total pavement thickness		430	√	7	×	70	3

(ASS2+ 2L+2.5C+23.5GGBS) Extremely High Plasticity							
Flexible Pavement Layers	Material	Thickness (mm)	Treated	Curing (Days)	Soaked	CBR (%)	Design Traffic (msa)
Surface Course	HRA	130					
Base Course	HBM	150					
Subbase	CBGM	180					
Subgrade	ASS	∞					
Total pavement thickness		460	√	7	×	73	8

(ASS1+ 2L+2.5C+23.5PLASTIC) High Plasticity							
Flexible Pavement Layers	Material	Thickness (mm)	Treated	Curing (Days)	Soaked	CBR (%)	Design Traffic (msa)
Surface Course	HRA	180					
Base Course	HBM	210					
Subbase	CBGM	180					
Subgrade	ASS	∞					
Total pavement thickness		570	√	28	×	13	60

(ASS2+ 2L+2.5C+23.5PLASTIC) Extremely High Plasticity							
Flexible Pavement Layers	Material	Thickness (mm)	Treated	Curing (Days)	Soaked	CBR (%)	Design Traffic (msa)
Surface Course	HRA	180					
Base Course	HBM	210					
Subbase	CBGM	180					
Subgrade	ASS	∞					
Total pavement thickness		470	√	28	×	6	100

NOTE: **HRA** = Hot Rolled Asphalt **ASS** = Artificially Synthesised Subgrade **HBM** = Hydraulic Bound mixture **CBGM** = Cement Bound Granular Mixture

Figure 5.77: Summary of DMRB road pavement design using various design traffic and CBR values

5.10 ROAD PAVEMENT DEFECT ANALYSIS

5.10.1 Stress Effect on Treated and Untreated ASS Materials

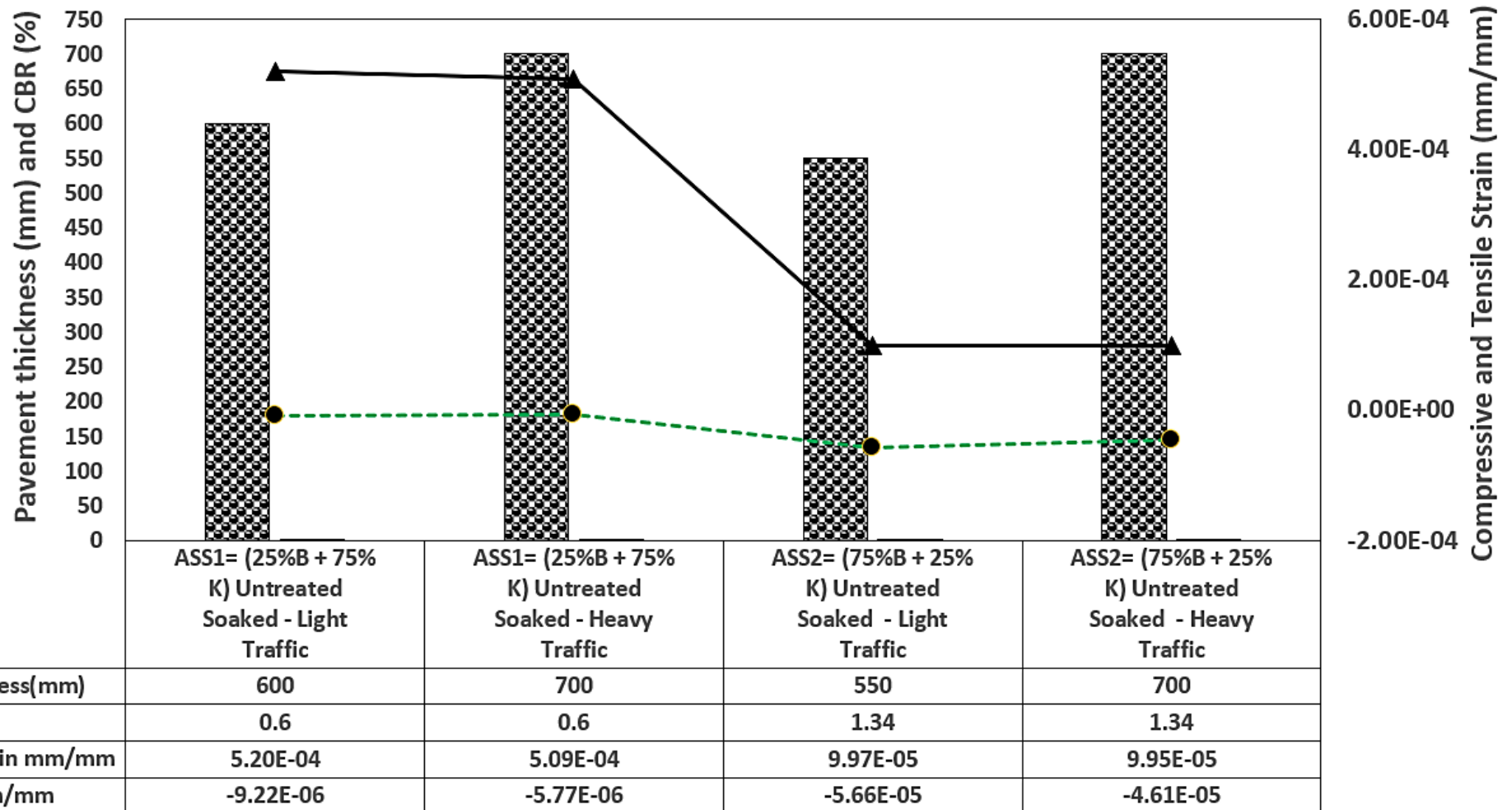
After conducting KENPAVE analysis on subgrade materials, the results showed that stresses within road pavement subgrade increase with an increase in pavement thickness and a reduction in CBR value. Untreated ASS1 soaked without curing with a CBR value of 0.6% for light and heavy traffic recorded a very high compressive strain of $5.20\text{E}-04$ for light traffic, $5.09\text{E}-04$ for heavy traffic, a tensile strain of $-9.22\text{E}-06$ for light traffic, $-5.77\text{E}-06$ for heavy traffic load. A high potential for pavement damage was observed with an increase in compressive and tensile strain for light traffic in untreated ASS material as CBR values of 0.6% for ASS1. These stresses began to decrease when CBR values for untreated ASS1 increased to 1.34%. CBR values recorded for untreated ASS1 and 2 for heavy traffic exhibited high compressive and tensile strains responsible for pavement damage. However, these stresses reduce as CBR values increase. Overall, very high CBR values with low compressive and tensile strain responsible for pavement damage were recorded for treated ASS materials for light and heavy traffic loads compared with untreated ASS materials. This means that treated ASS materials with very high CBR values can withstand pavement defects for longer compared with untreated ASS with low CBR values.

An increase in compressive and tensile strain was observed with an increase in pavement thickness due to low CBR values for light and heavy traffic load 7 and 28 days treated ASS materials. The reduction in stresses with an increase in CBR values proves that stabilising ASS materials using sustainable waste can reduce pavement defects. Waste plastic is the type of material to use for improving the performance of flexible pavements against rutting (Dhiman et al., 2021). For fatigue crack to initiate in road pavement structure peak stress (compressive and tensile) must be very high, if peak stresses are low they may not initiate a crack. The higher the stress concentration the more likely a crack may initiate and the greater the applied stress range, the shorter the pavement life (Fleck et al., 1985; Iowa State University, 2021). This means the higher the CBR value the least likely a defect may occur in the road pavement structure. These are the reasons why pavement thickness increases with low CBR values to cater for reduced stresses in the pavement structure to prolong the life of

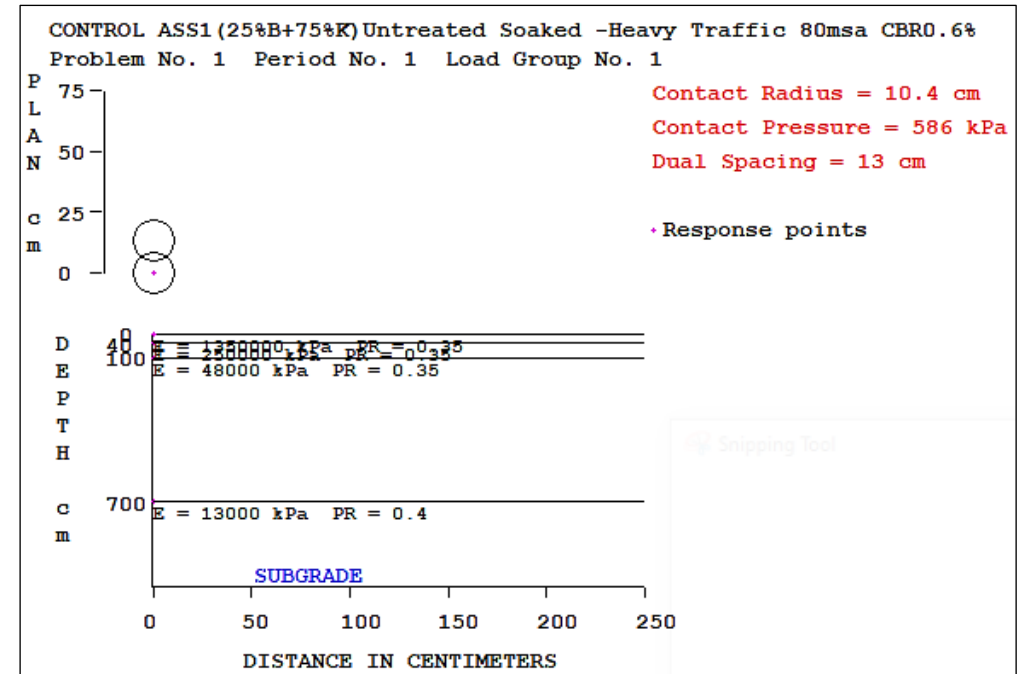
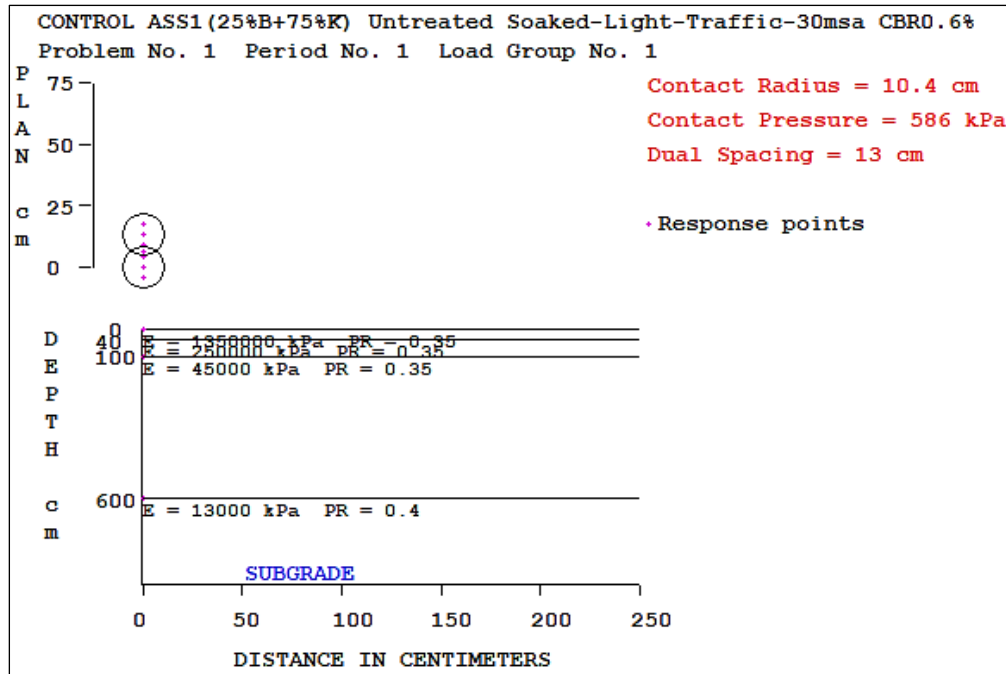
the road pavement. Pavement with less than about 180mm of asphalt deforms at a high rate but thicker pavement deforms at a lesser rate (Nunn et al., 1997).

A reduction in elastic modulus within subgrade materials with increased stresses was observed for ASS materials. Untreated ASS1 (high plasticity) with a CBR value of 0.6 recorded an elastic modulus of 13000kPa and ASS2 (extremely high plasticity) with a CBR value of 1.34% recorded an elastic modulus of 21000kPa. This shows that the higher the CBR value the higher the elastic modulus and vice versa. Elastic modulus is the ratio of the force exerted upon a substance or body to the resultant deformation (Lowa State University, 2021). This means the higher the elastic modulus the lesser deformation can occur within the pavement structure. Furthermore, observation indicated that ASS2 (extremely high plasticity) exhibited high elastic modulus even though they have high swelling potential. This confirms the findings in this research that high plasticity subgrade with high bentonite content exhibits high bearing capacity. However, due to their high swell potentials, they are prone to deformation when used as subgrade materials.

High plasticity clays involve the formation of surface cracks (Aubeny et al., 2002). According to Putri et al., (2012), high plasticity clay exhibit, high modulus since clay shrinks and becomes very stiff when dry. ASS1 with low plasticity compared with ASS2 recorded very high CBR values and elastic modulus resulting in less stress within the subgrade that can cause deformation. Very high elastic modulus was recorded when untreated ASS materials were treated using sustainable waste materials which resulted in low stresses within the subgrade. However, a reduction in elastic modulus for treated ASS materials with observed with a reduction in CBR values. Detailed results for compressive and tensile strain results for treated and untreated ASS materials at various curing ages using 11.75% GGBS, recycled plastic, glass and BDW are Figure 5.78 - Figure 5.86. A high elastic modulus was recorded for treated ASS samples with high CBR values for light and heavy traffic loads, respectively, and higher elastic modulus was observed for low CBR subgrade with thicker pavement.



Chapter 5 – Results and Discussion



Chapter 5 – Results and Discussion

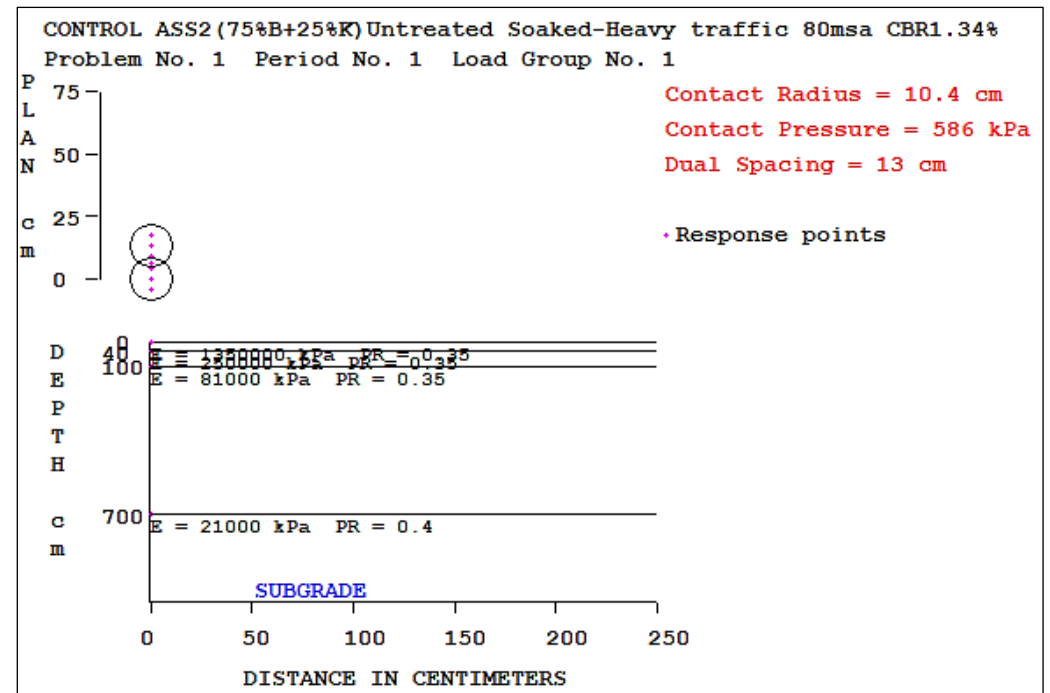
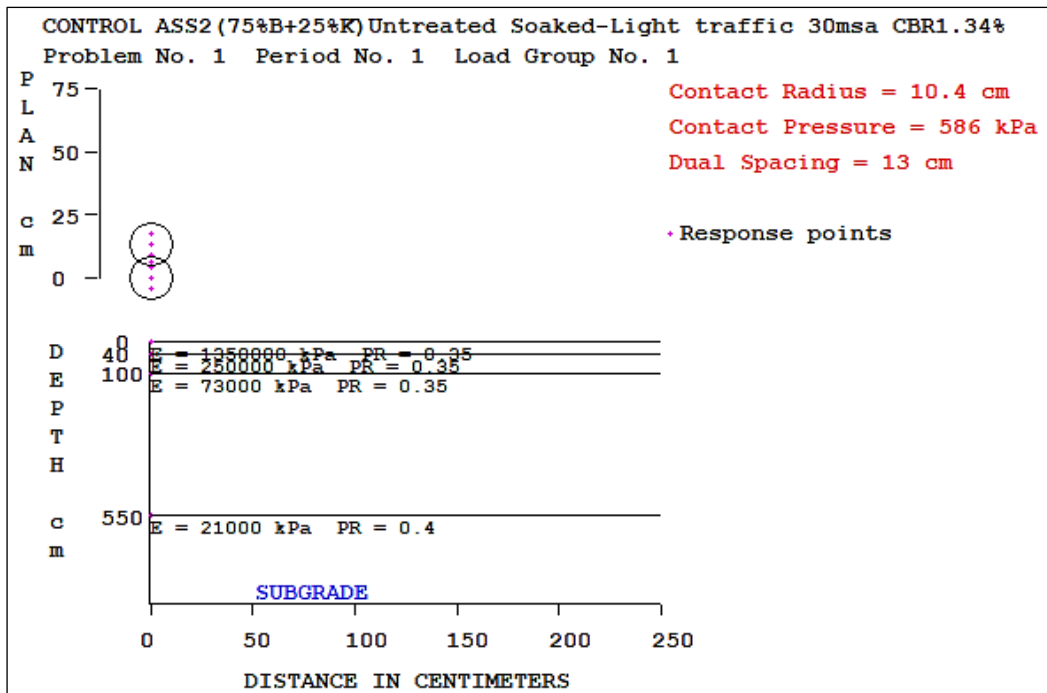
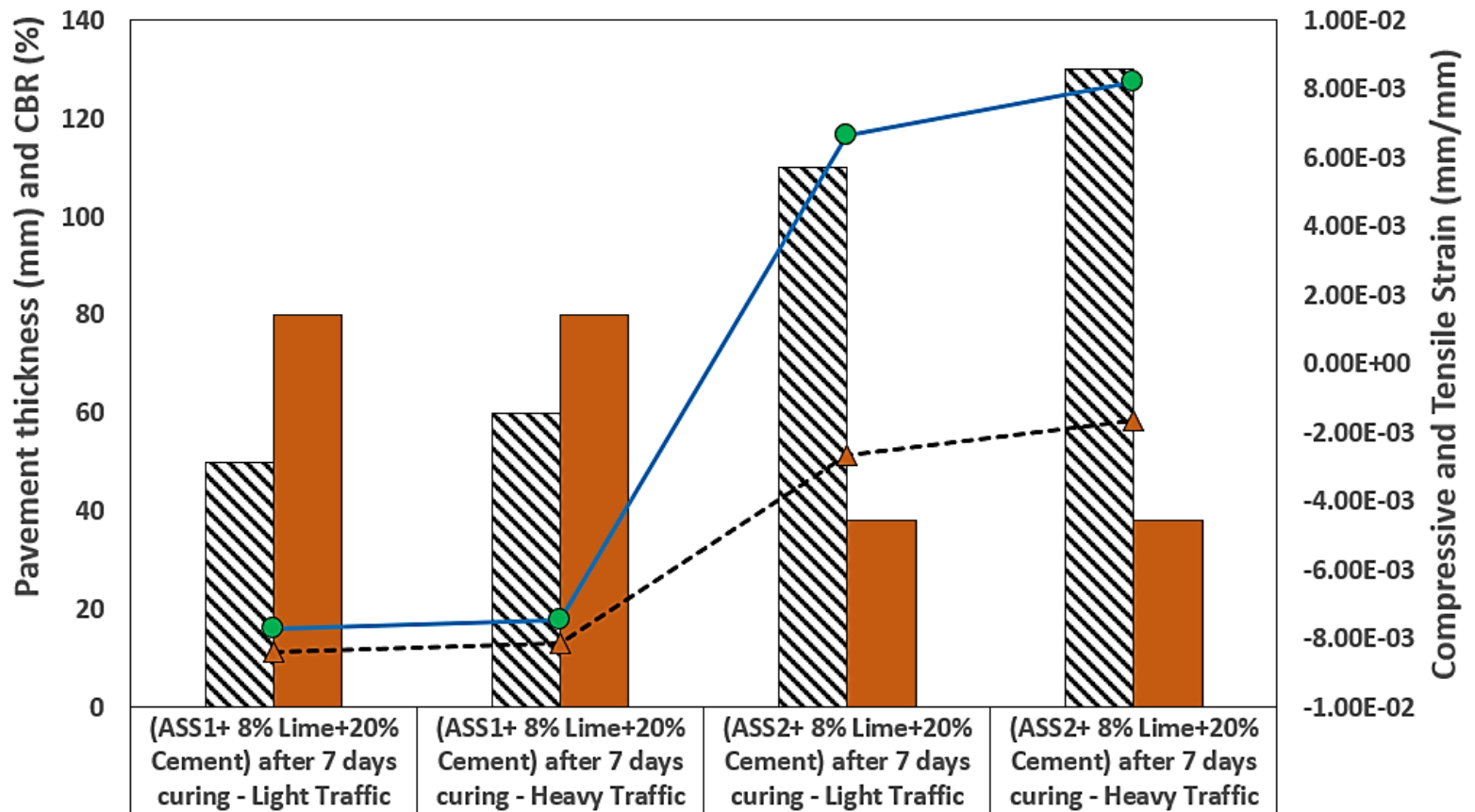
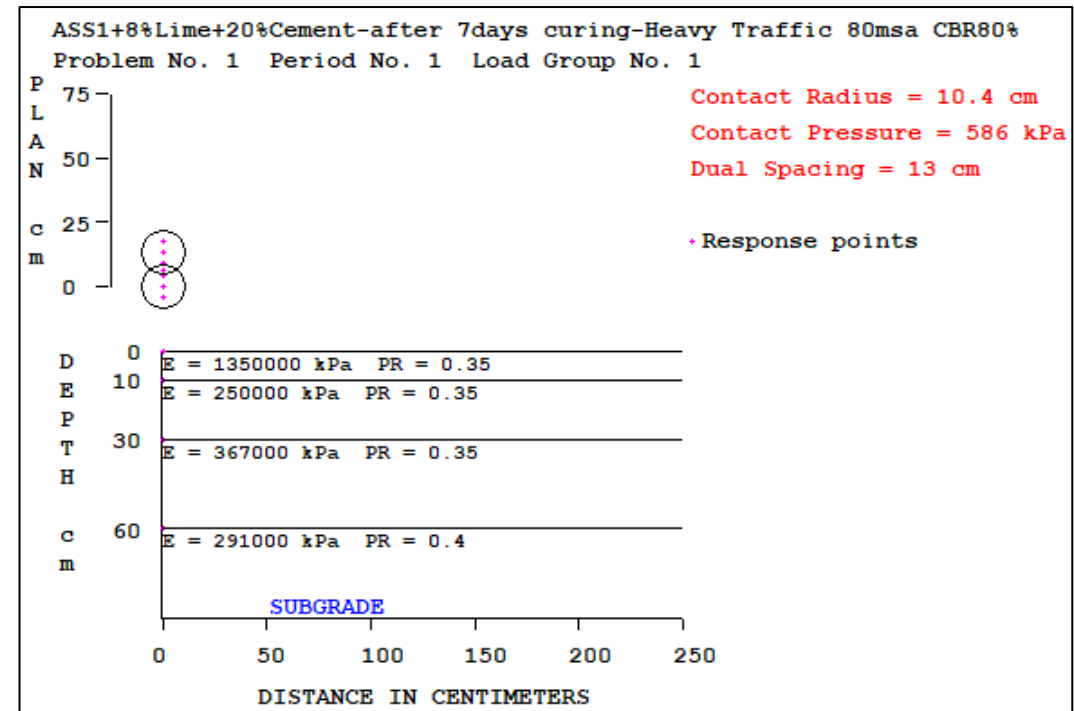
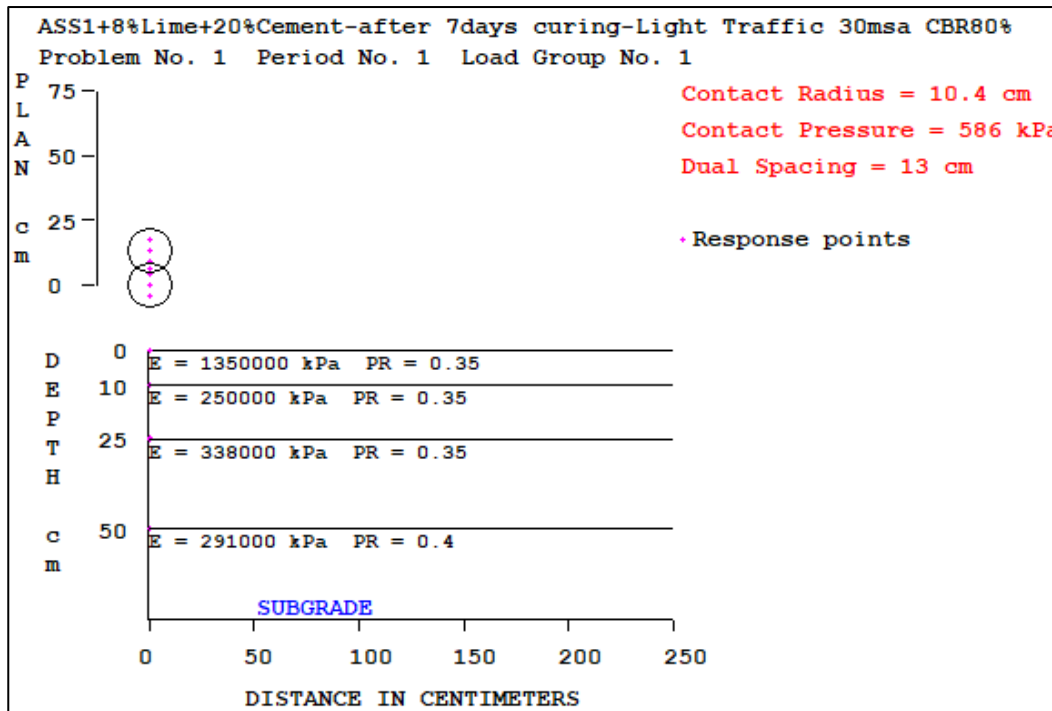


Figure 5.78: Stresses and Kenpave results for untreated soaked ASS materials



▨ Pavement Thickness(mm)	50	60	110	130
■ CBR(%)	80	80	38	38
● Compressive Strain mm/mm	6.86E-04	6.87E-04	9.29E-03	9.83E-03
▲ Tensile strain mm/mm	-8.41E-03	-8.15E-03	-2.65E-03	-1.64E-03

Chapter 5 – Results and Discussion



Chapter 5 – Results and Discussion

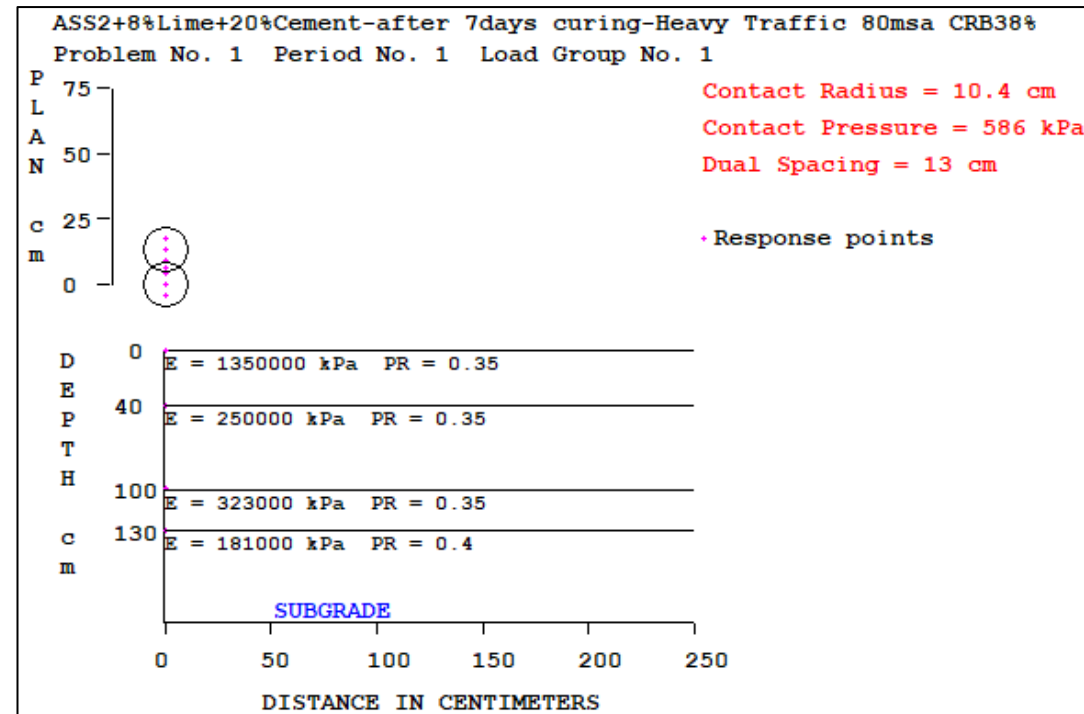
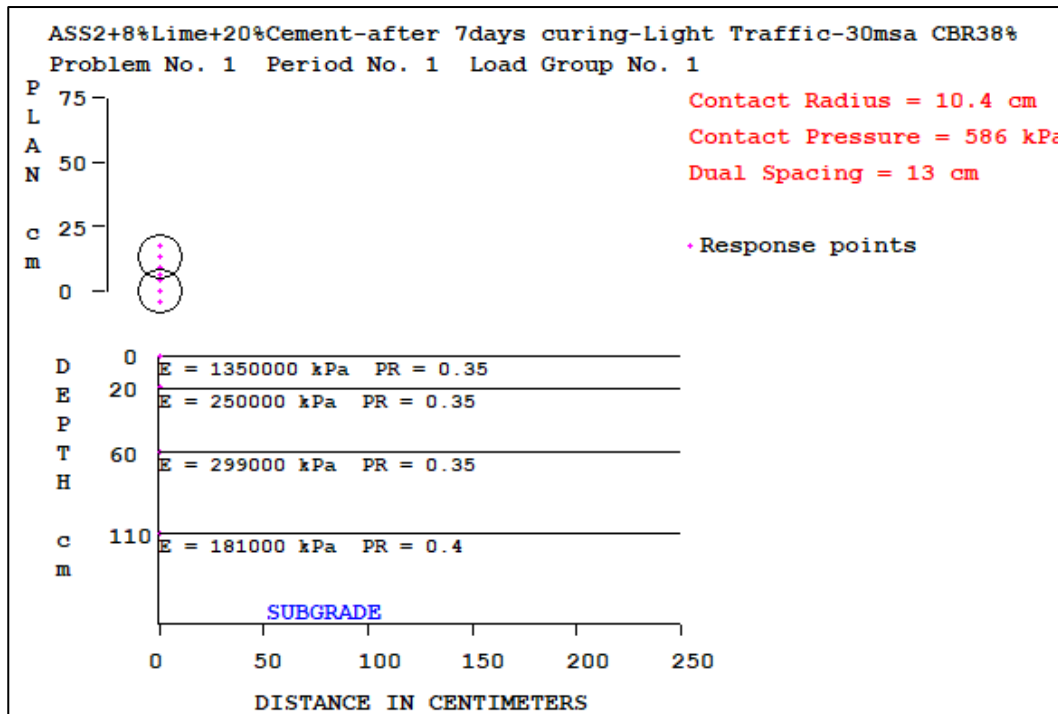
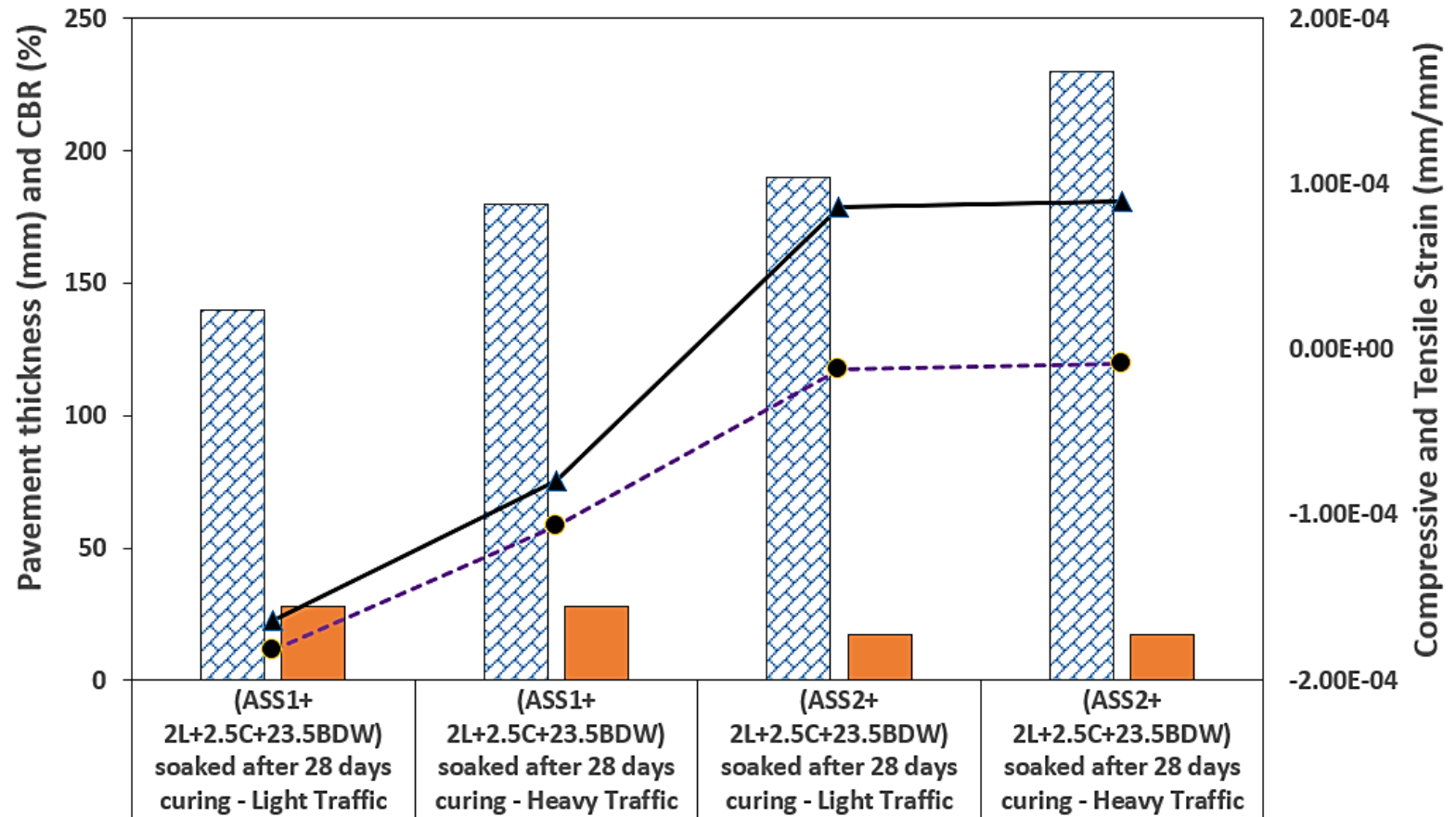
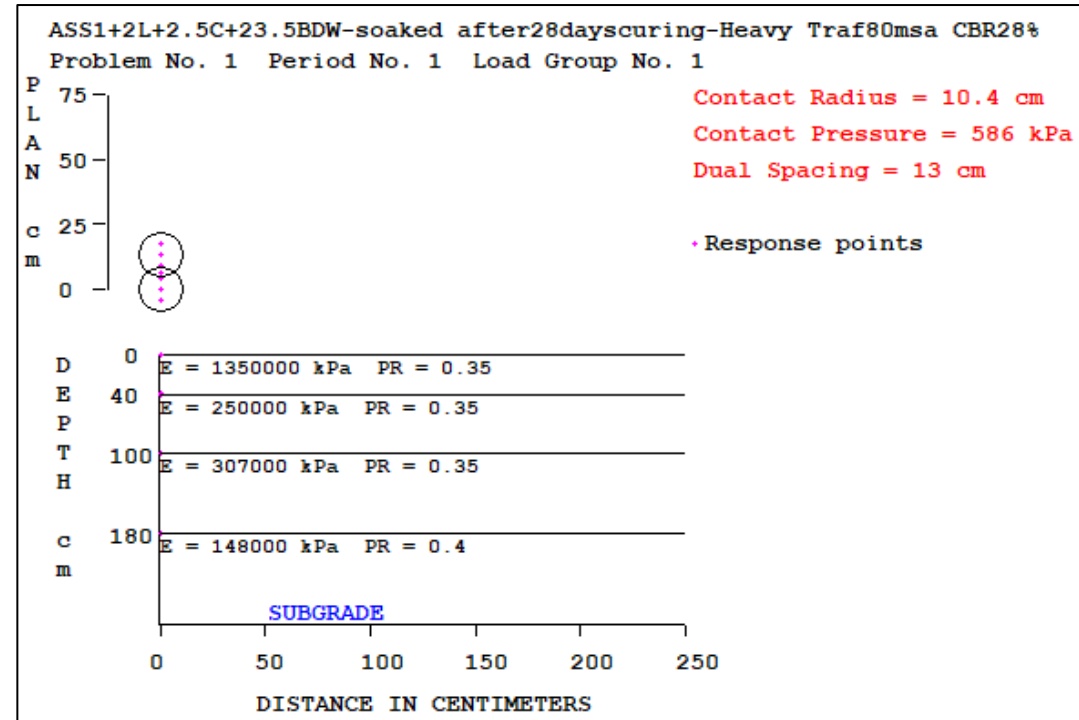
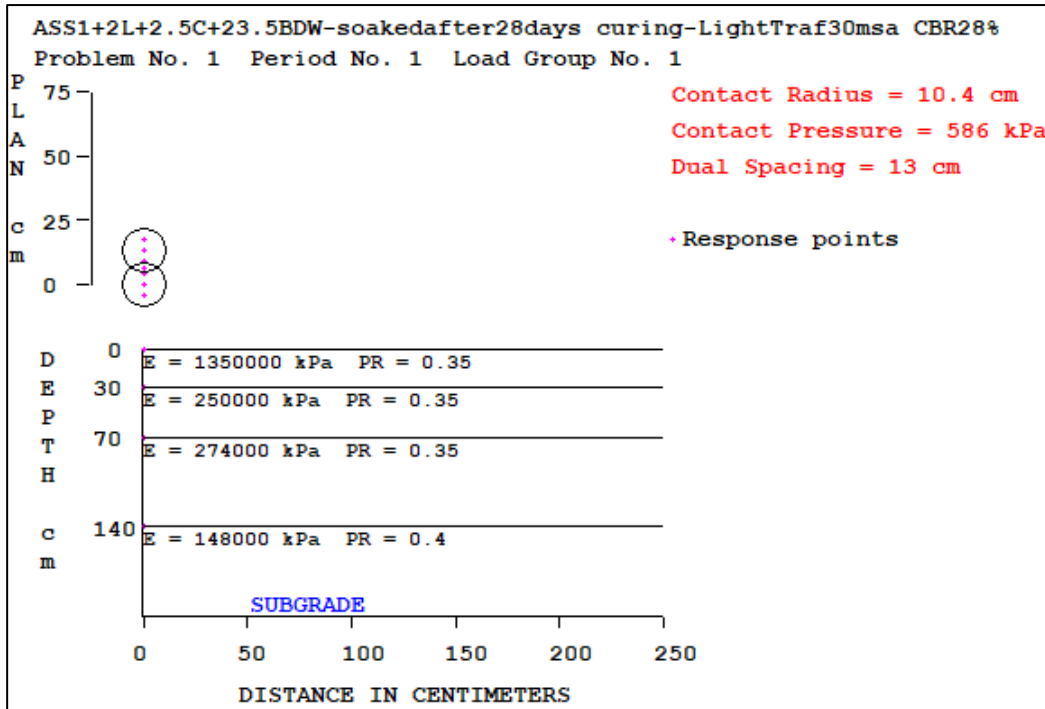


Figure 5.79: Stresses and Kenpave results for treated ASS materials using cement and lime



Pavement Thickness(mm)	140	180	190	230
CBR(%)	28	28	17	17
Compressive Strain mm/mm	1.81E-05	2.80E-05	9.83E-05	9.81E-05
Tensile strain mm/mm	-1.82E-04	-1.07E-04	-1.22E-05	-8.52E-06

Chapter 5 – Results and Discussion



Chapter 5 – Results and Discussion

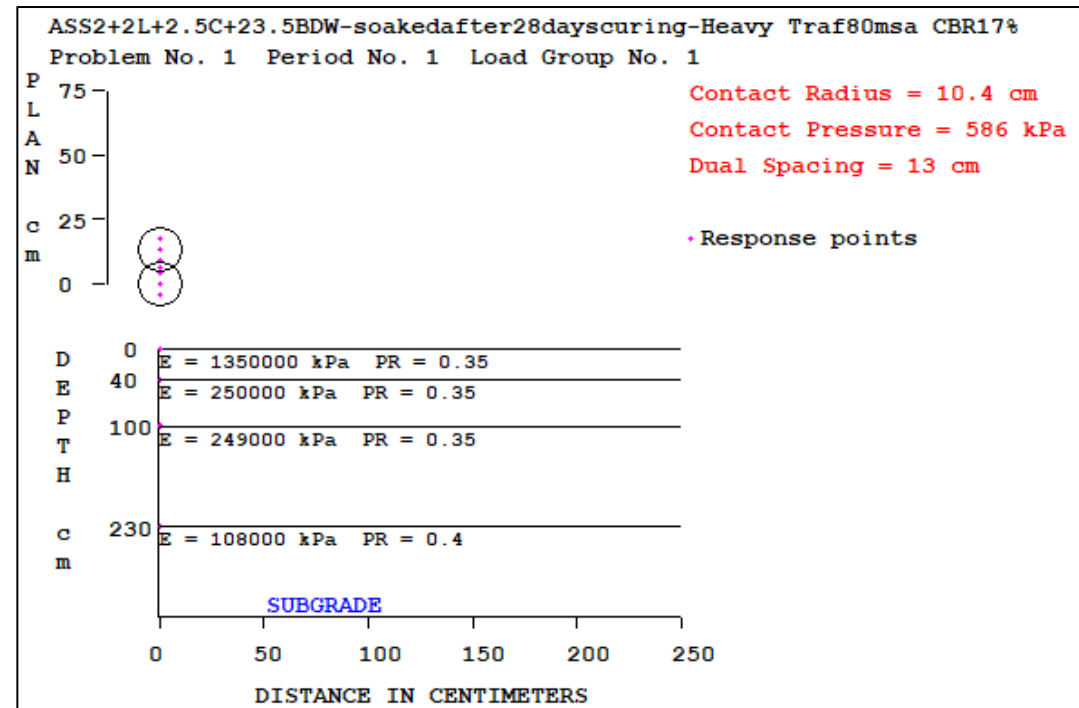
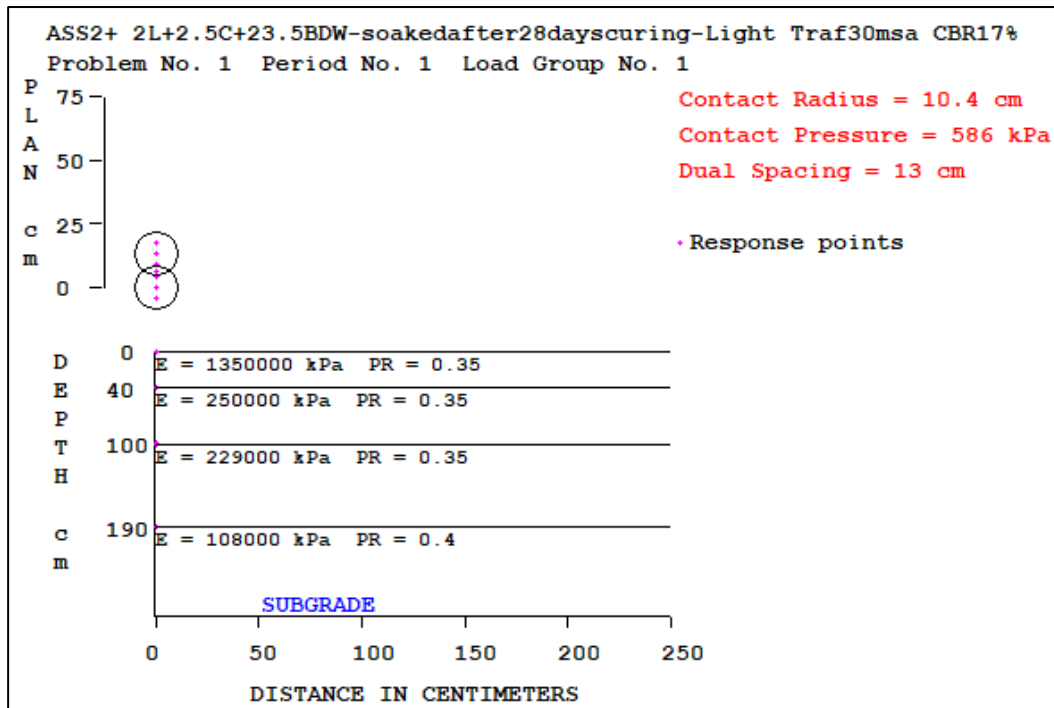
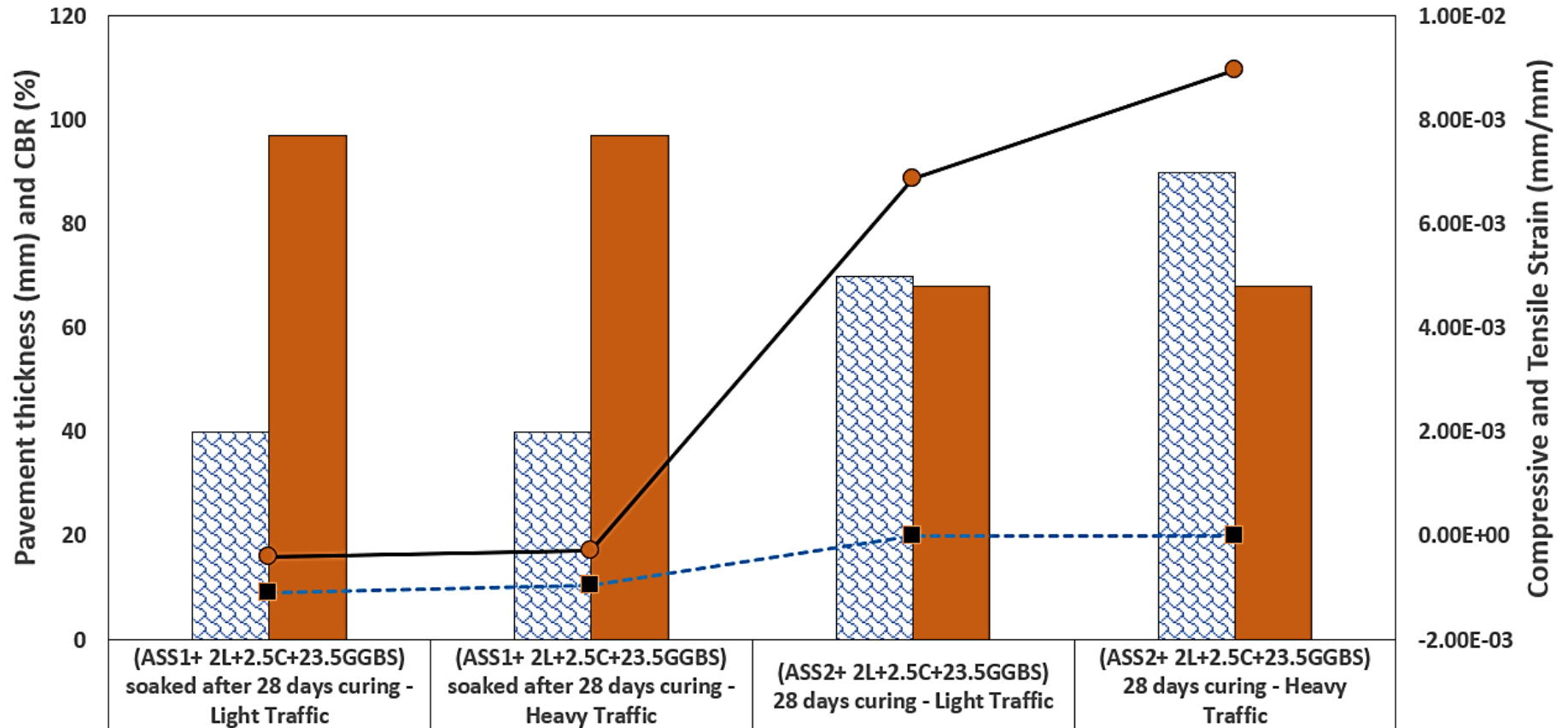
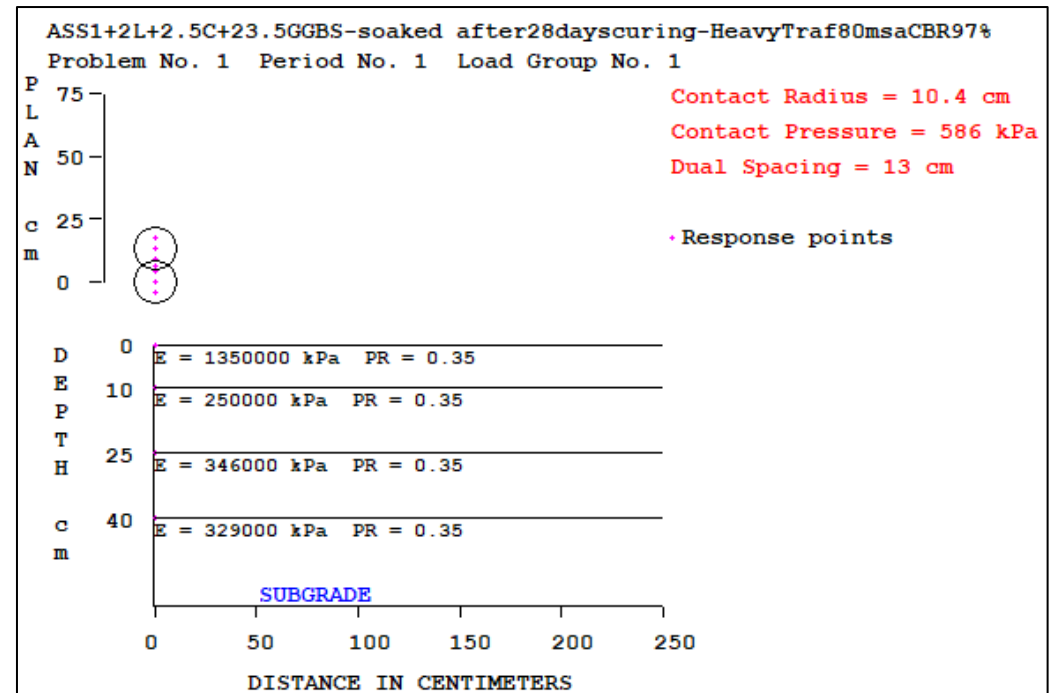
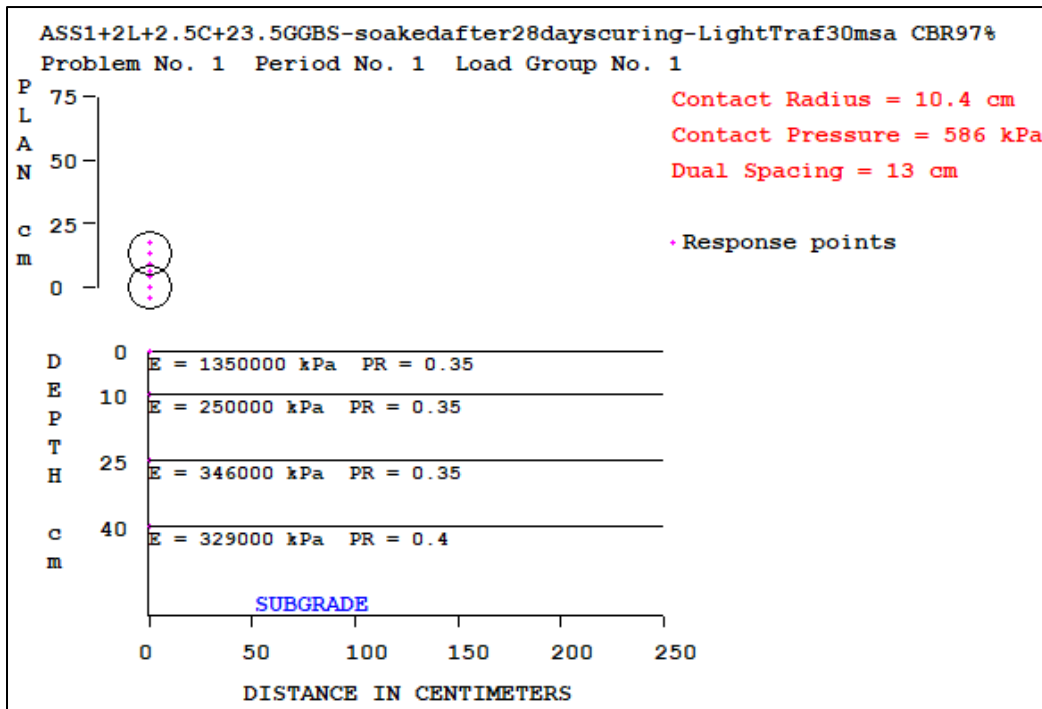


Figure 5.80: Stresses and Kenpave results for treated ASS materials using sustainable waste materials



Pavement Thickness(mm)	40	40	70	90
CBR(%)	97	97	68	68
Compressive Strain mm/mm	6.86E-04	6.86E-04	6.87E-03	8.97E-03
Tensile strain mm/mm	-1.09E-03	-9.59E-04	-5.05E-06	-2.85E-06

Chapter 5 – Results and Discussion



Chapter 5 – Results and Discussion

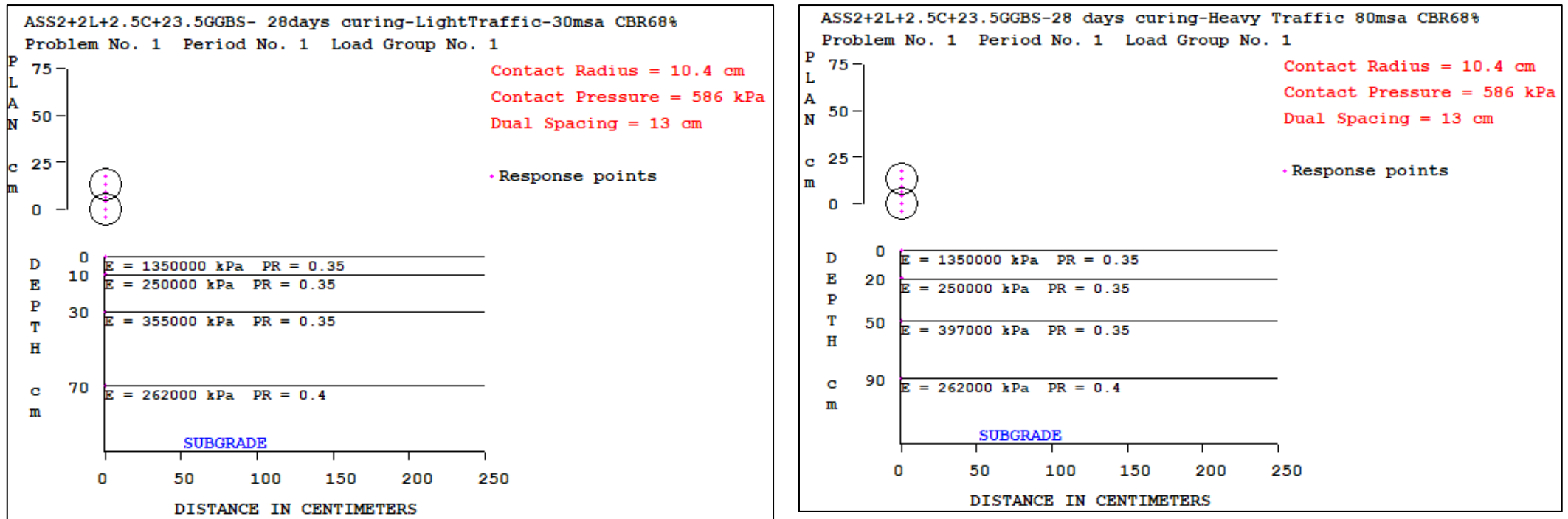
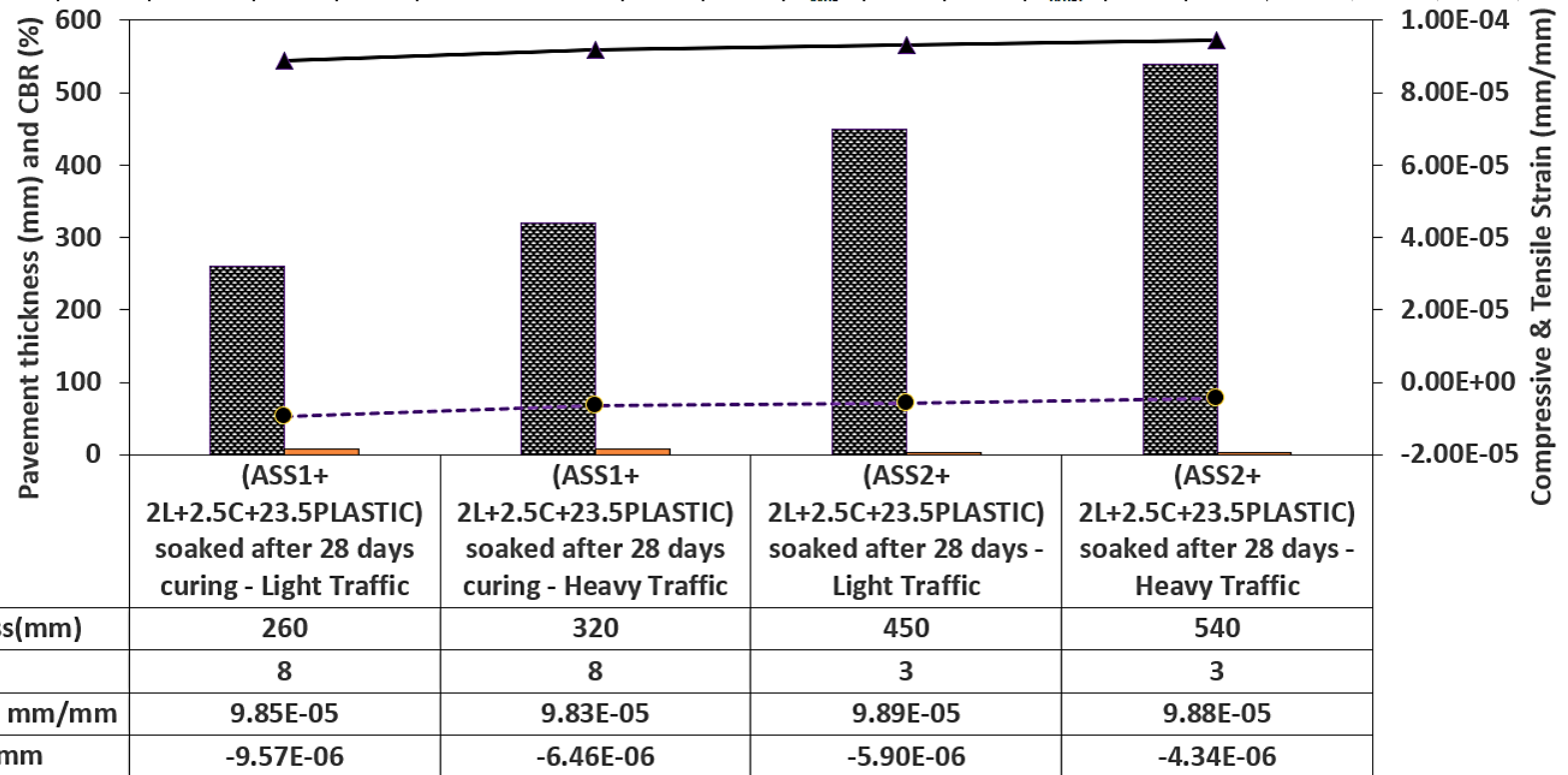
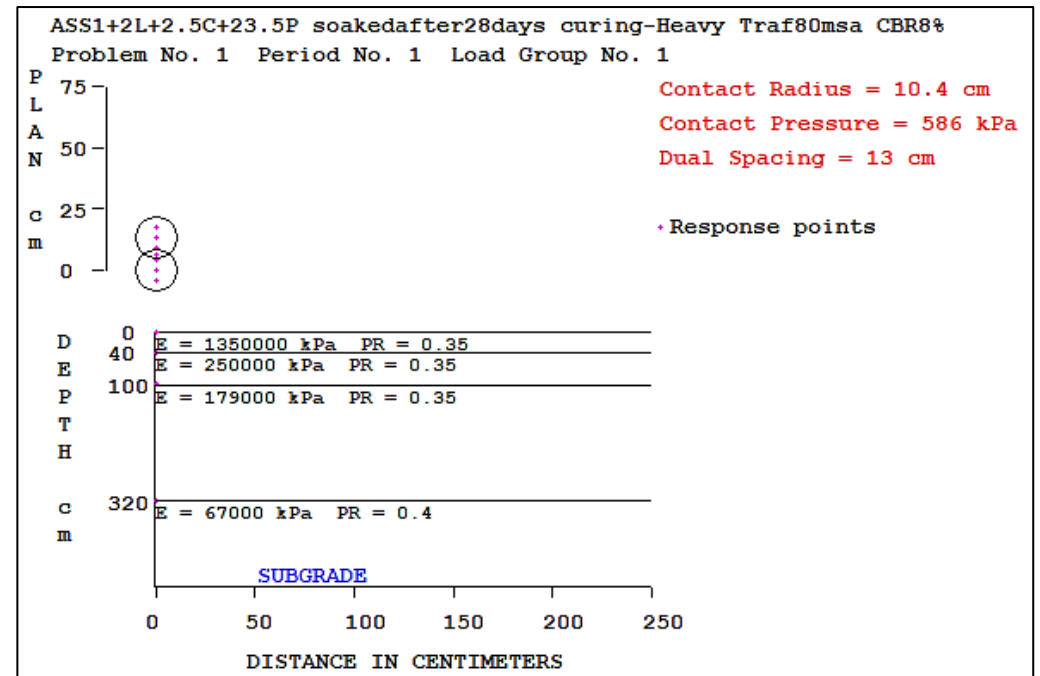
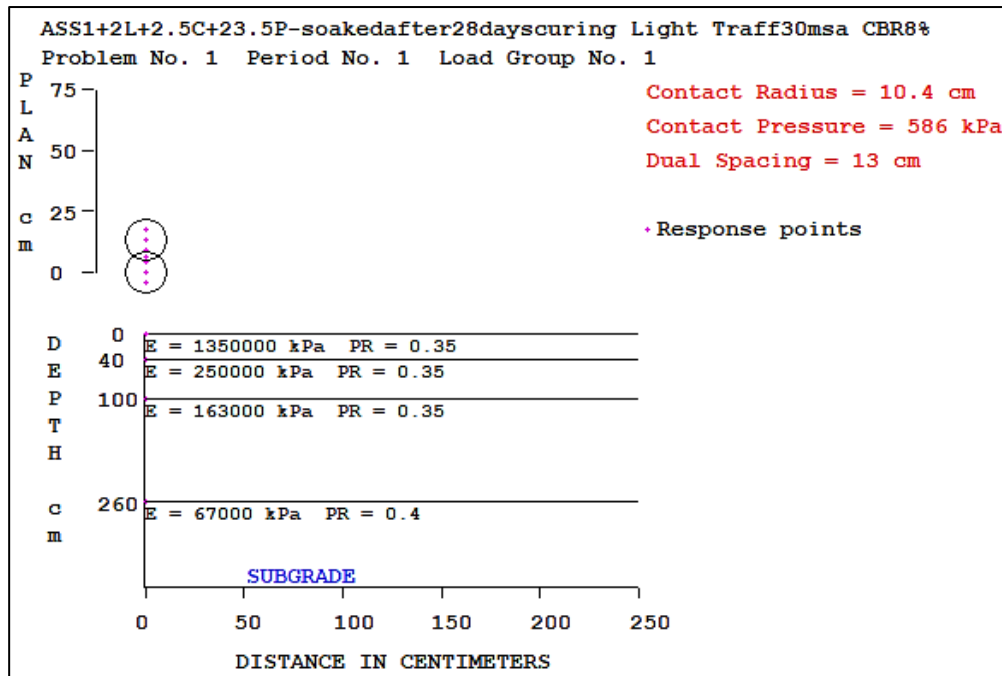


Figure 5.81: Stresses and Kenpave results for treated ASS materials using sustainable waste materials

Chapter 5 – Results and Discussion



Chapter 5 – Results and Discussion



Chapter 5 – Results and Discussion

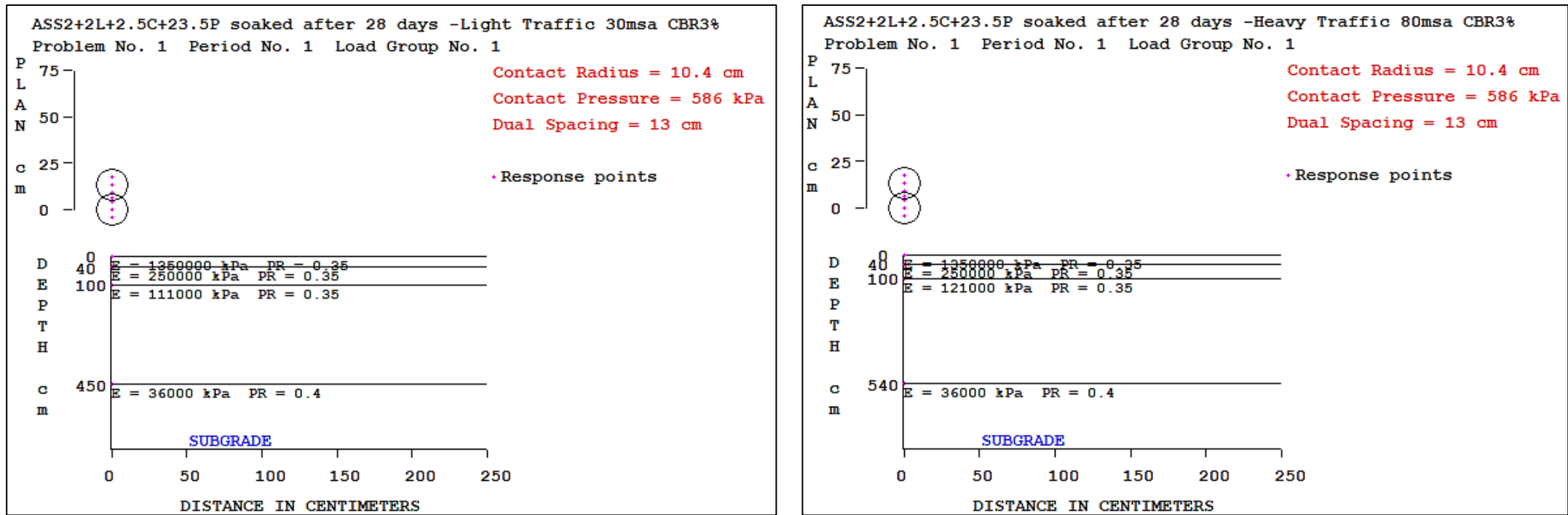
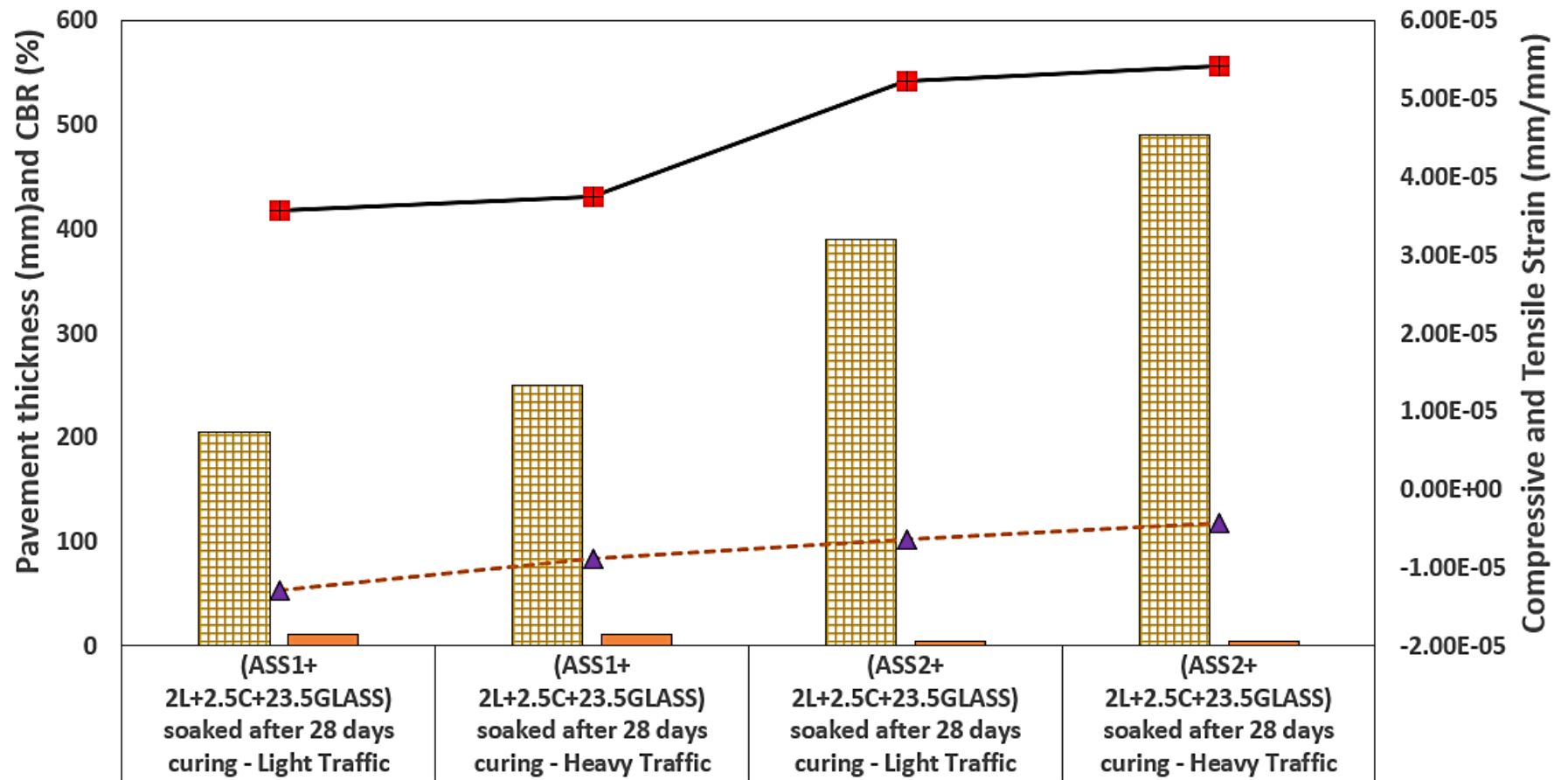
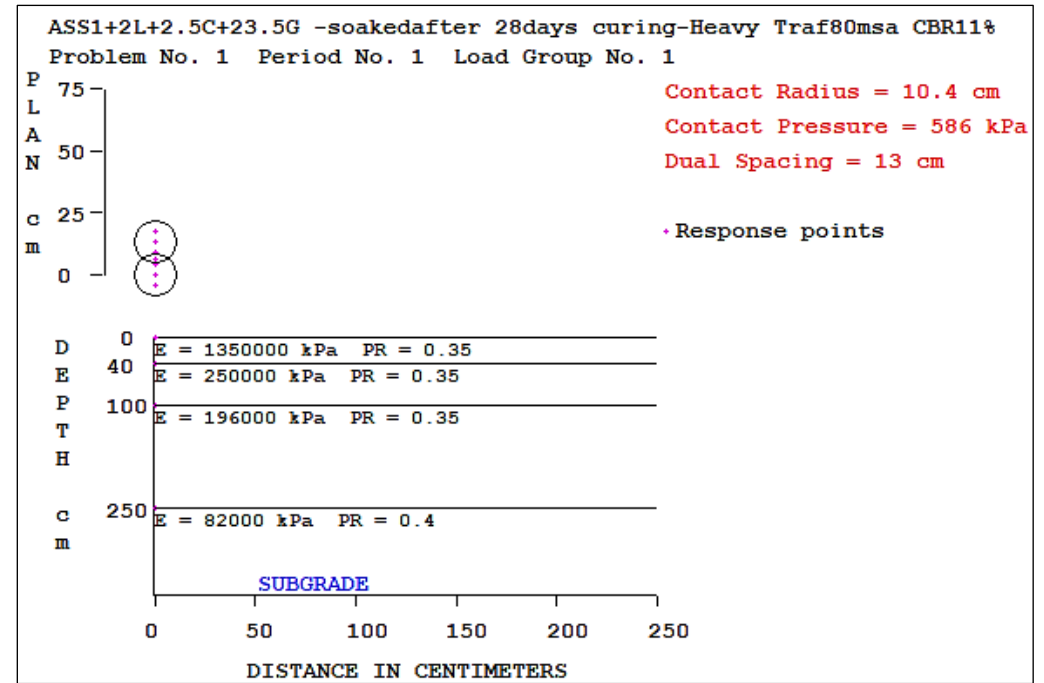
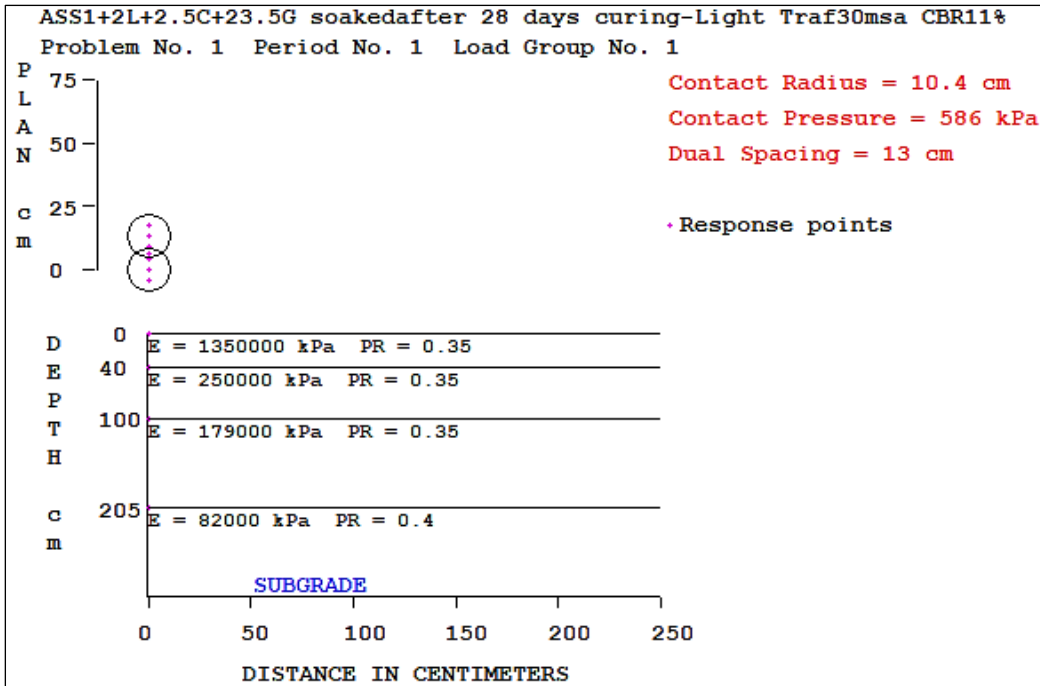


Figure 5.82: Stresses and Kenpave results for treated ASS materials using sustainable waste materials



Pavement Thickness(mm)	205	250	390	490
CBR(%)	11	11	4	4
Compressive Strain mm/mm	4.85E-05	4.63E-05	5.88E-05	5.86E-05
Tensile strain mm/mm	-1.29E-05	-8.90E-06	-6.48E-06	-4.36E-06

Chapter 5 – Results and Discussion



Chapter 5 – Results and Discussion

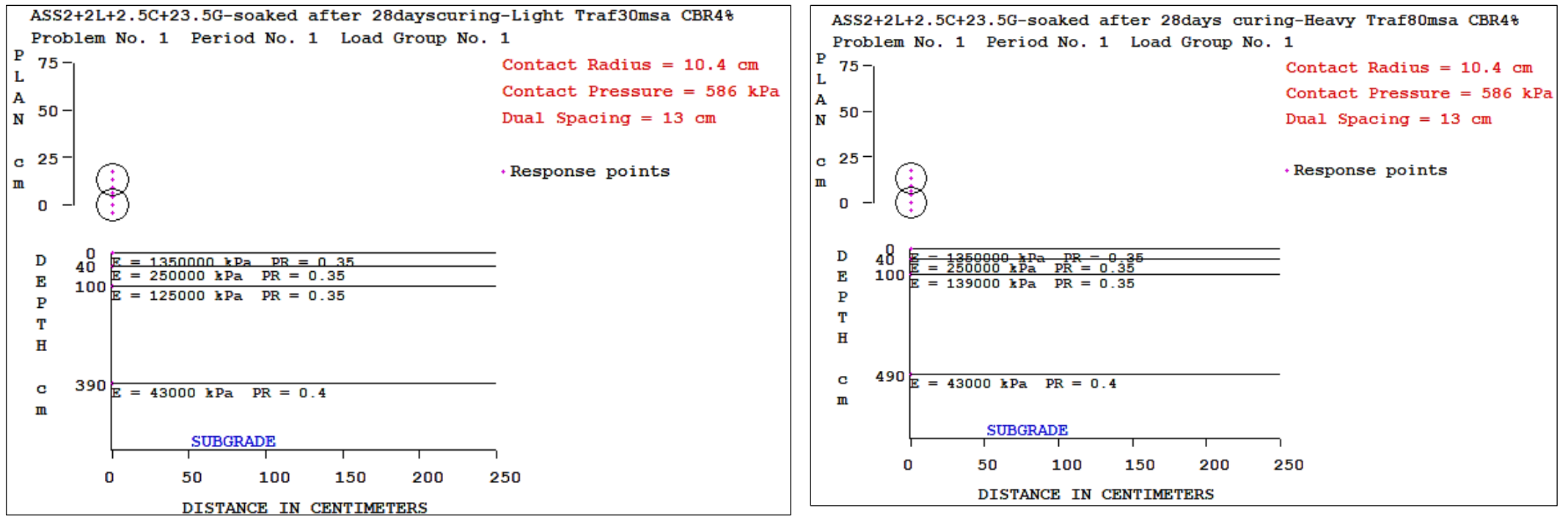
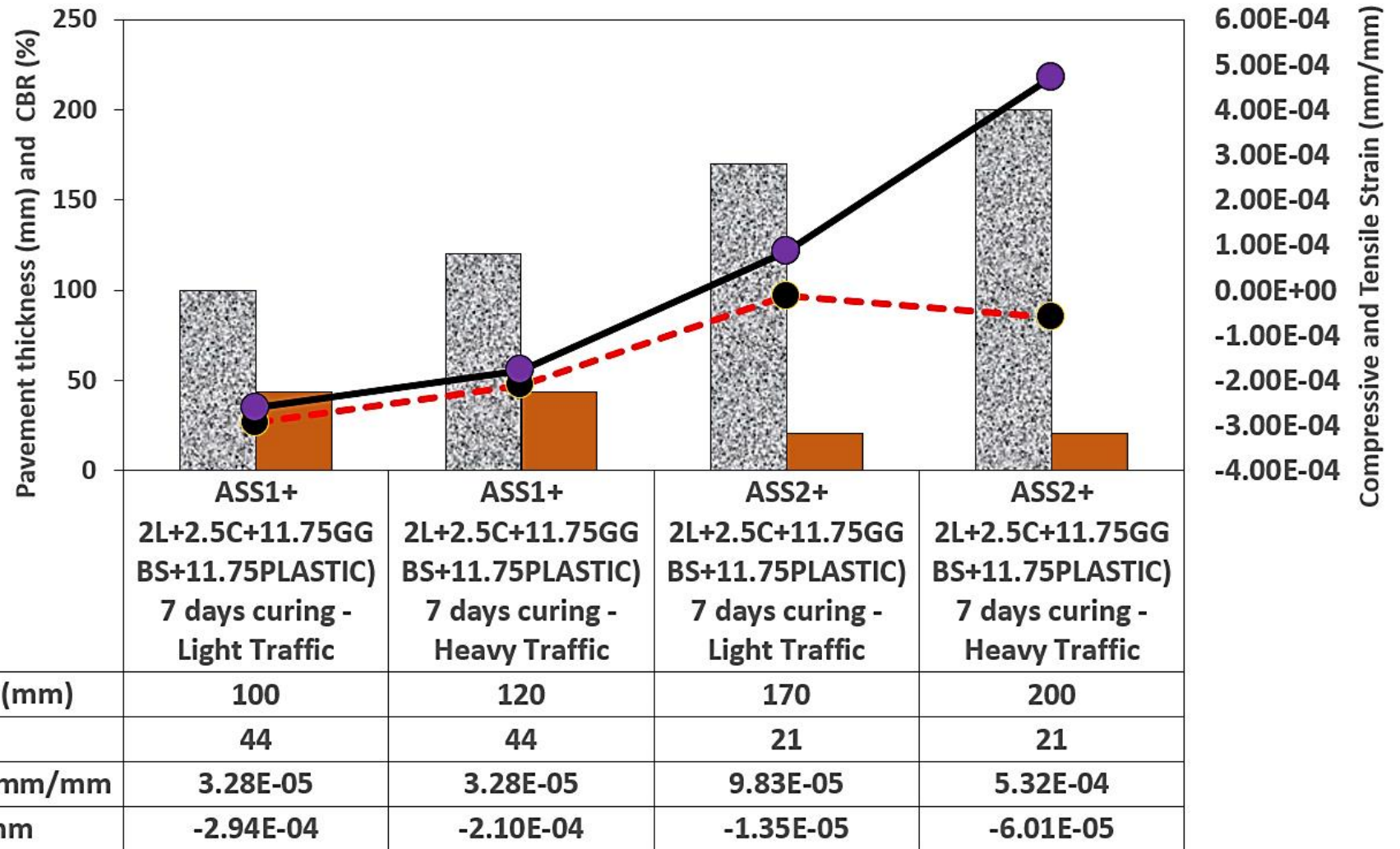
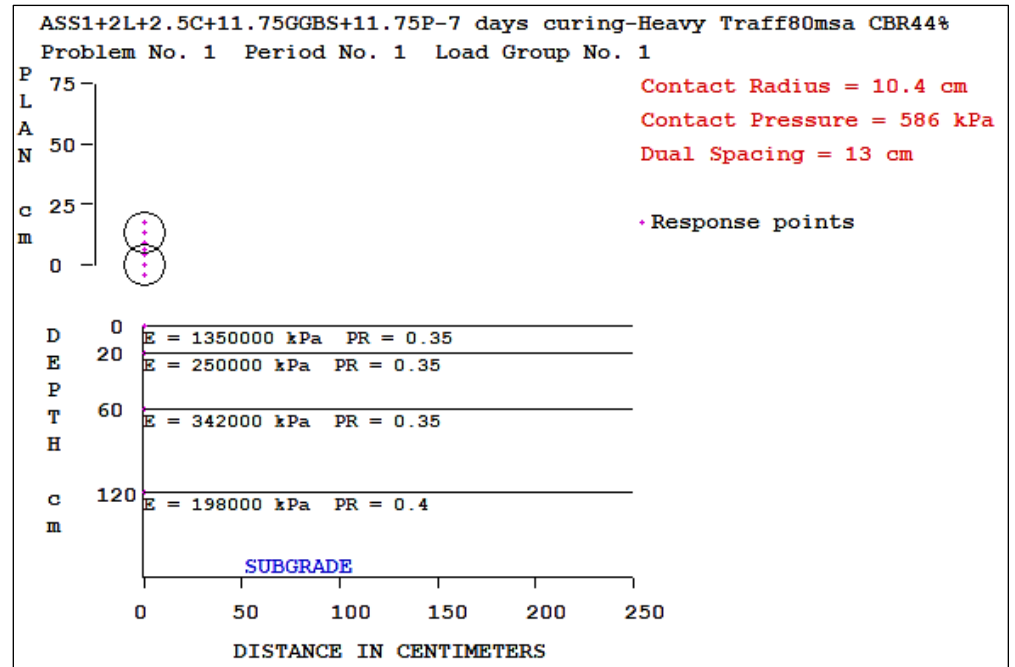
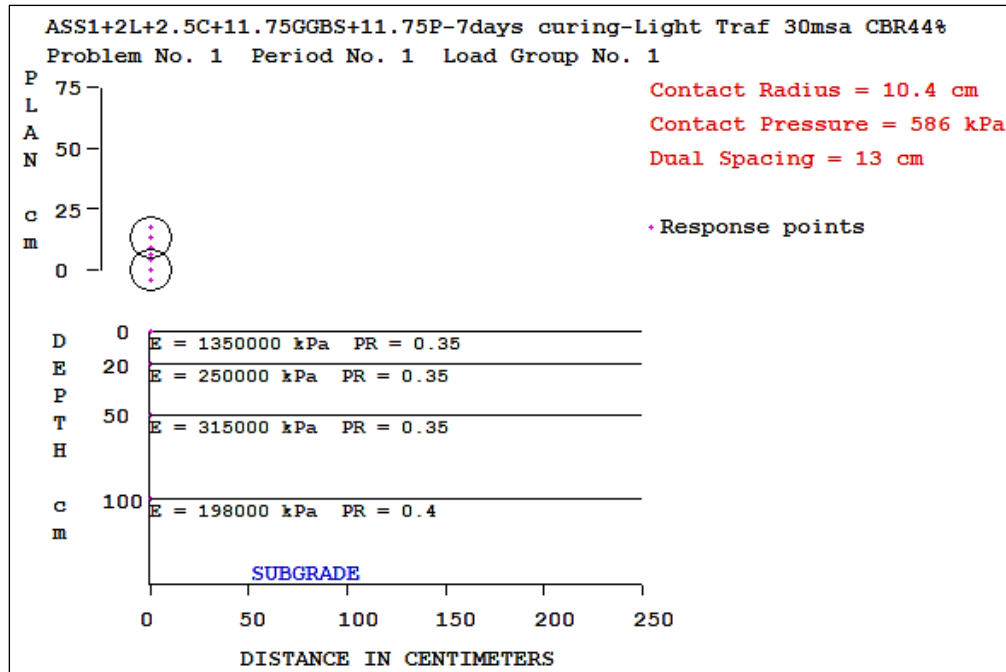


Figure 5.83: Stresses and Kenpave results for treated ASS materials using sustainable waste materials



Chapter 5 – Results and Discussion



Chapter 5 – Results and Discussion

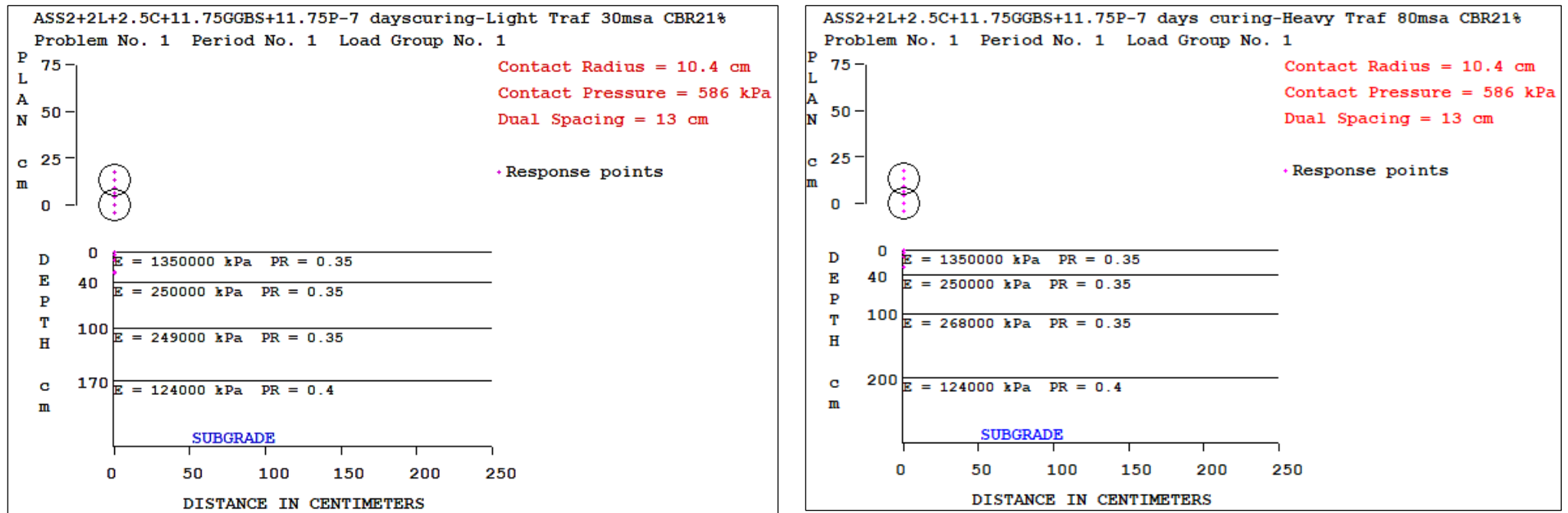
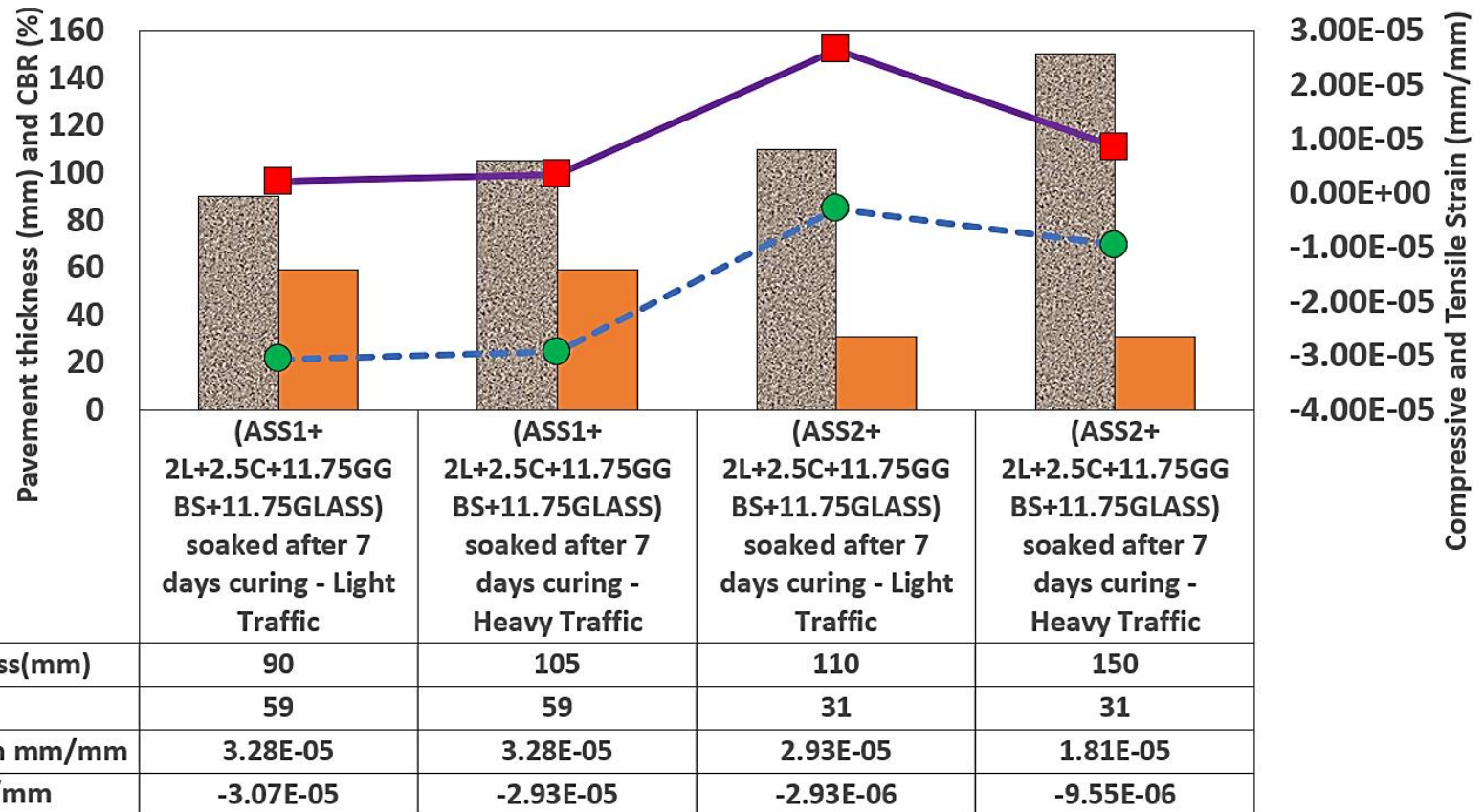
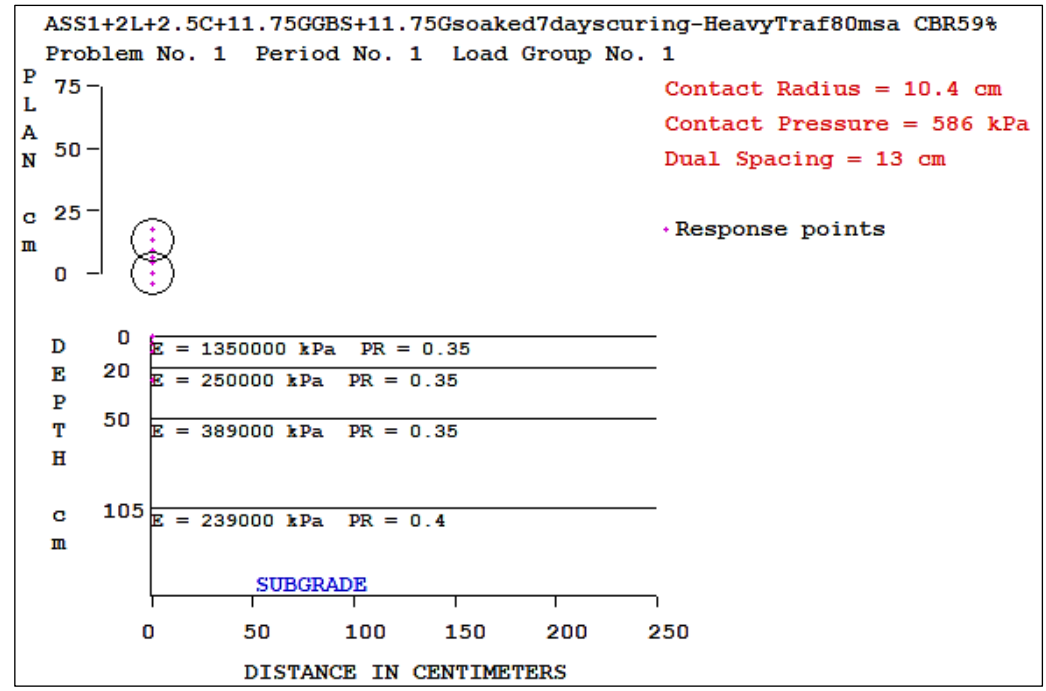
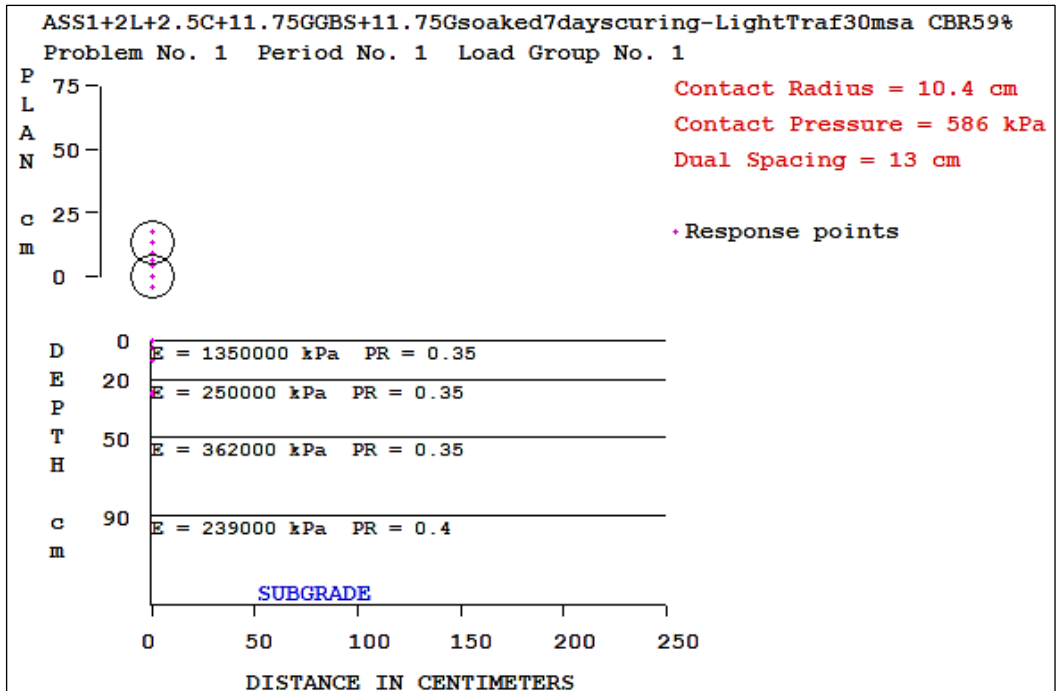


Figure 5.84: Stresses and Kenpave results for treated ASS materials using sustainable waste materials



Chapter 5 – Results and Discussion



Chapter 5 – Results and Discussion

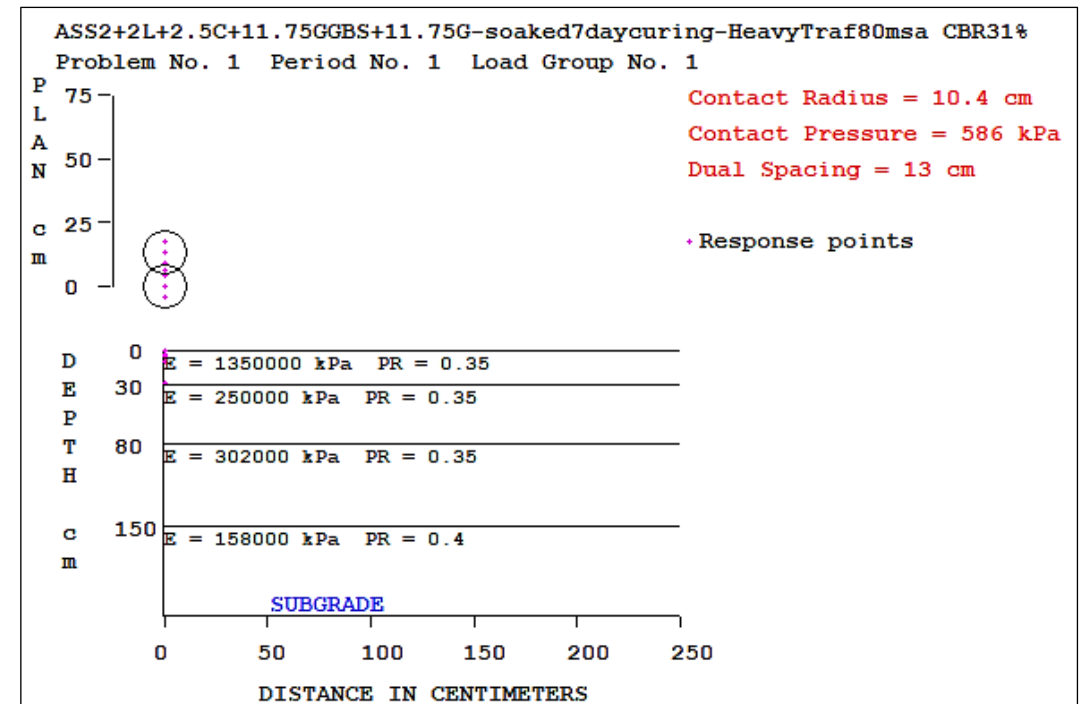
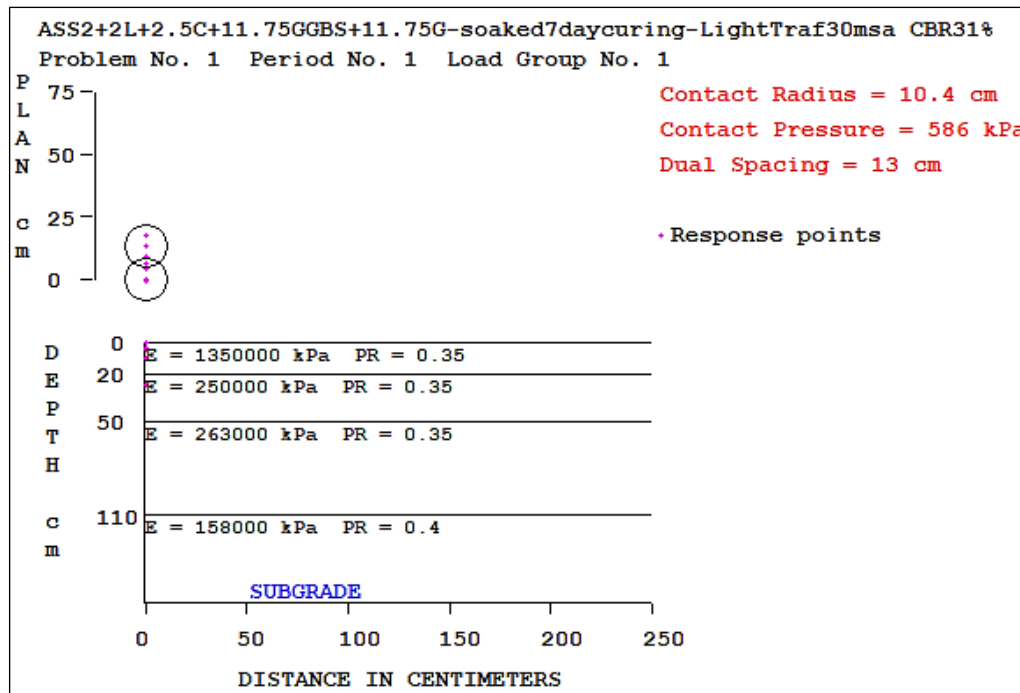
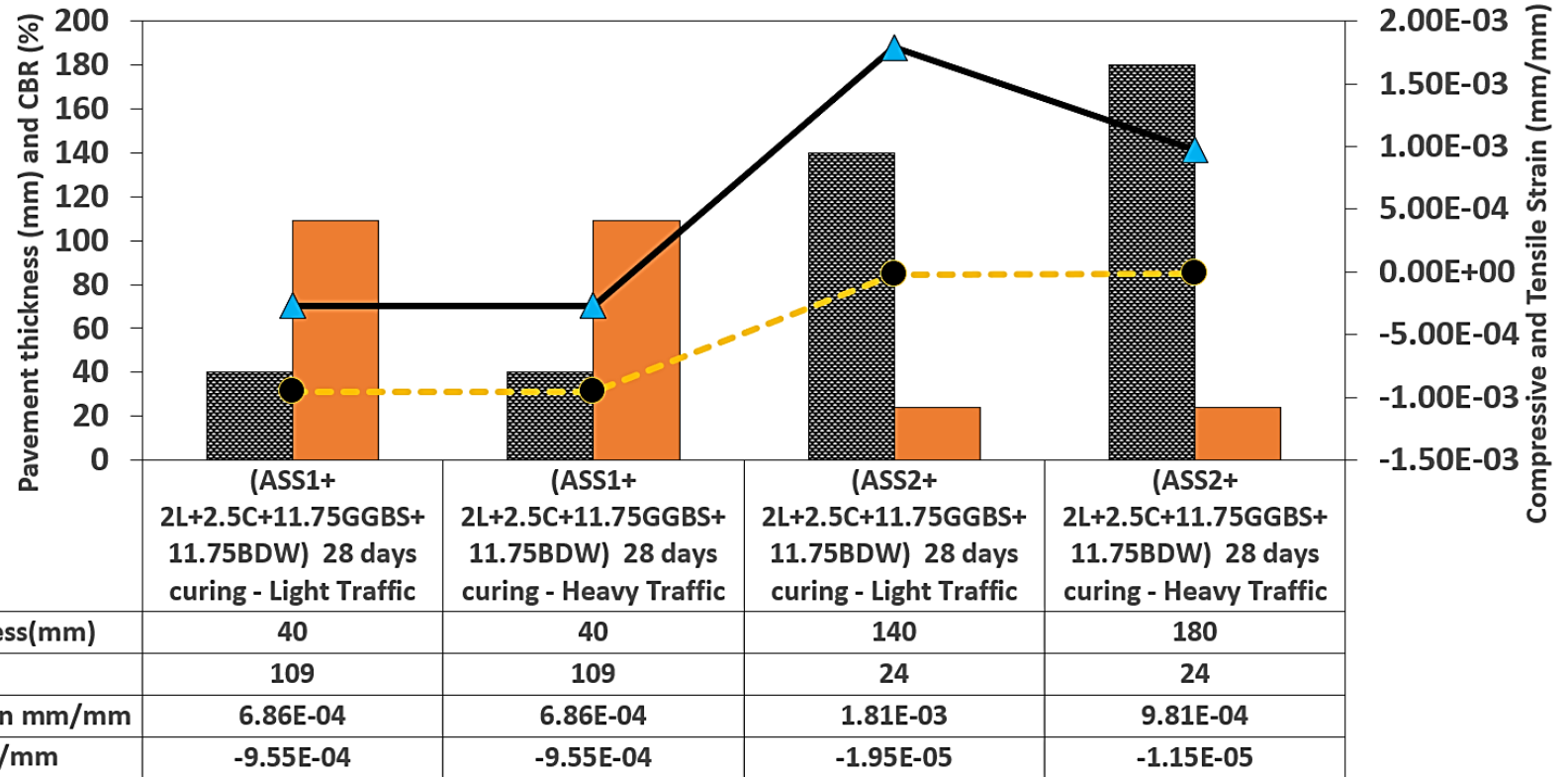
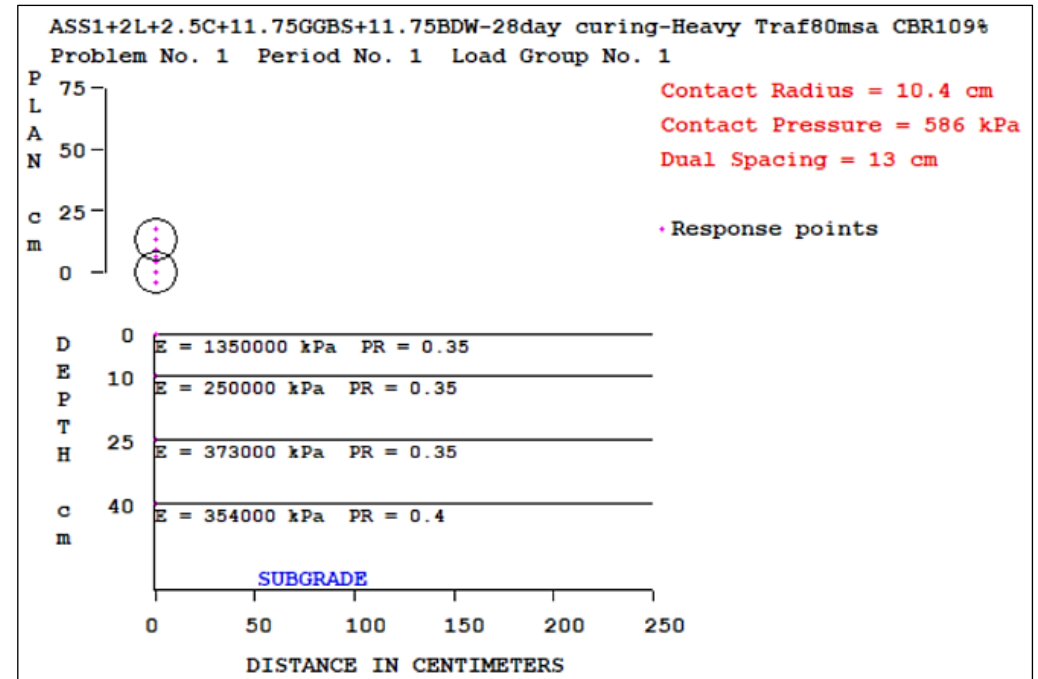
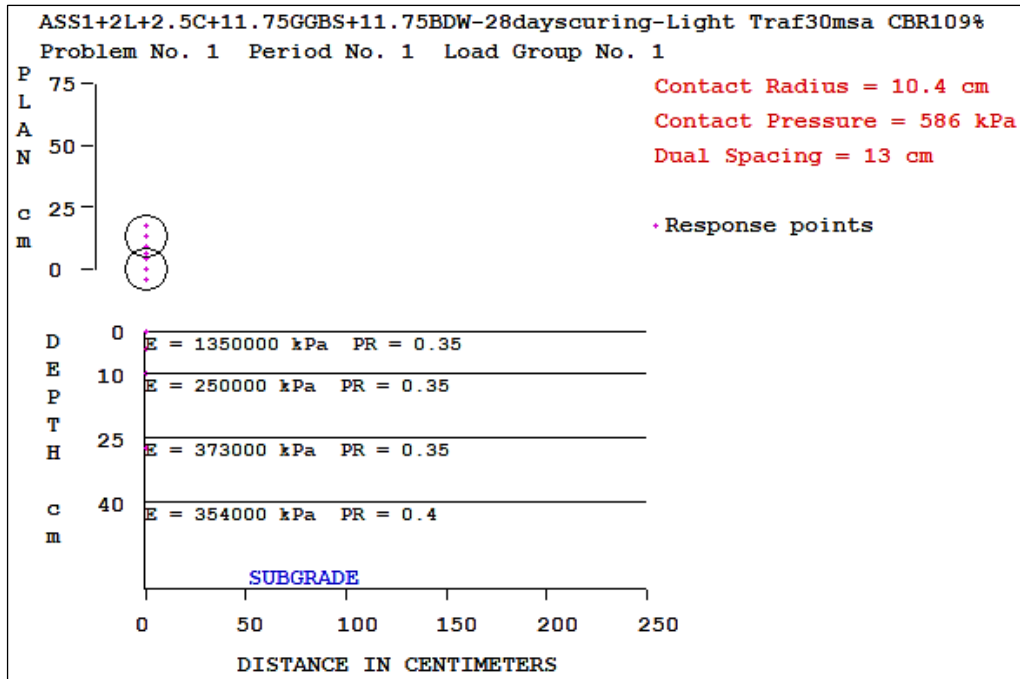


Figure 5.85: Stresses and Kenpave results for treated ASS materials using sustainable waste materials



Chapter 5 – Results and Discussion



Chapter 5 – Results and Discussion

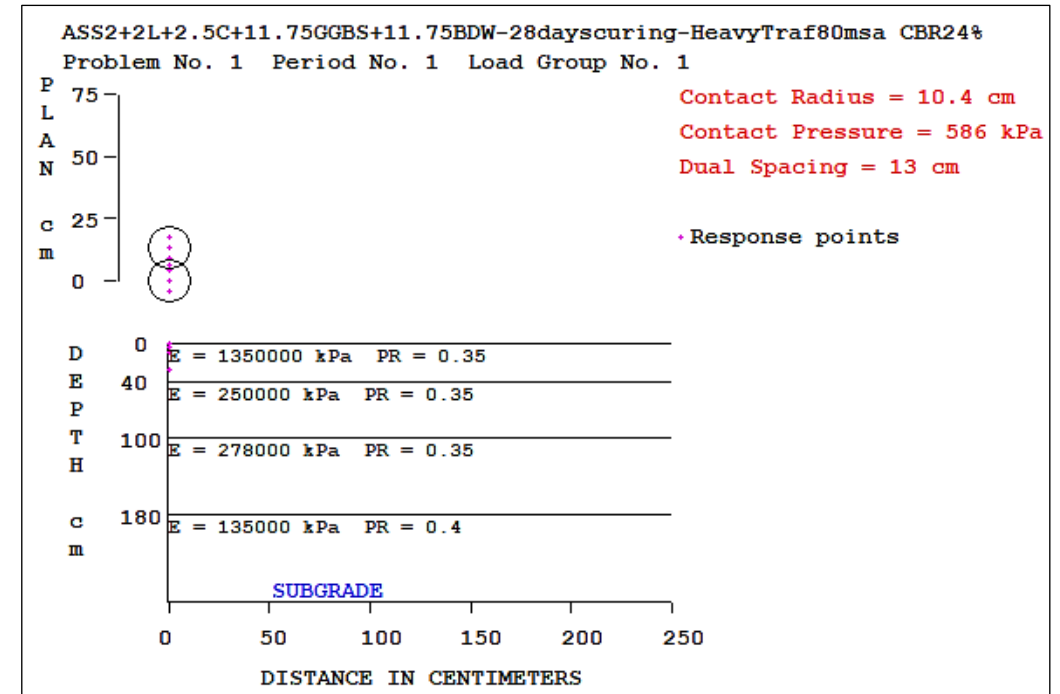
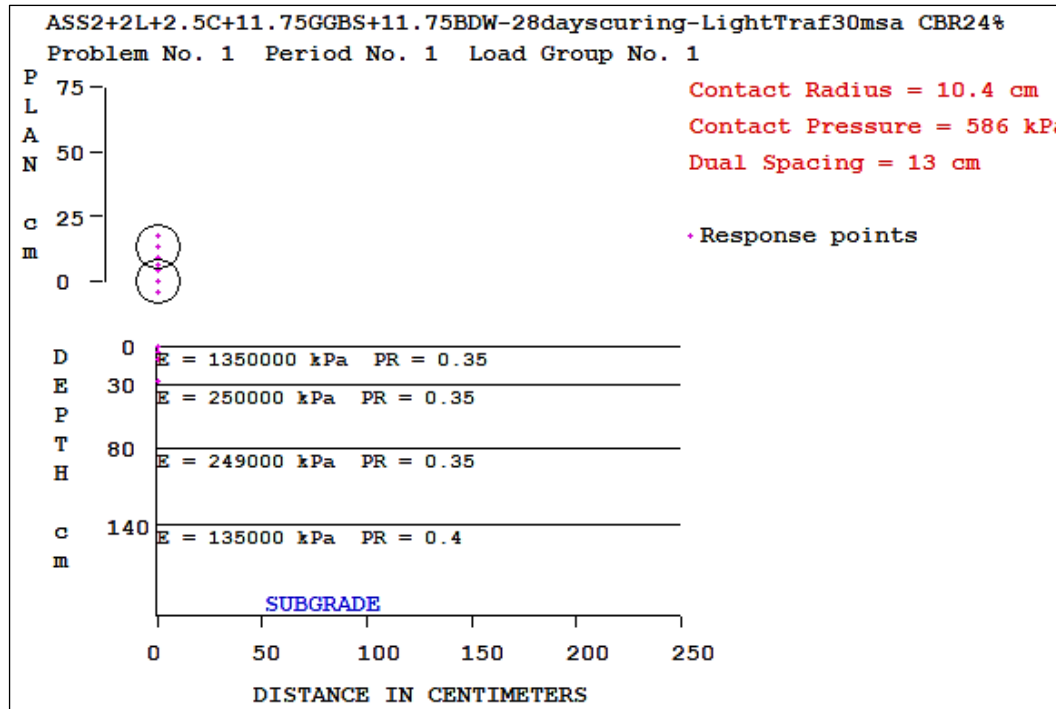


Figure 5.86: Stresses and Kenpave results for treated ASS materials using sustainable waste materials

5.10.2 Permanent Deformation, Fatigue and Rutting Failure for Treated and Untreated ASS Materials

A high allowable number of load repetitions to reach permanent deformation was observed in subgrade materials with high CBR values. While a lower allowable number of load repetitions to reach permanent deformation was recorded for subgrade materials with lower CBR values. An increase in load repetition was observed as traffic load increased. An increase in load repetition to reach fatigue and rutting failure with an increase in CBR value was observed for all ASS materials. Untreated soaked ASS1 with a CBR value of 0.6% recorded failure load repetition of $3.22E+09$ for light traffic fatigue, $1.51E+10$ for heavy traffic fatigue, $5.91E+43$ for light traffic rutting life and $5.67E+34$ for heavy traffic rutting life.

An allowable number of load repetitions to reach fatigue, rutting and permanent deformation for light and heavy traffic load recorded for untreated ASS1 CBR 8% reduced for untreated ASS2 CBR 5% and later increased when CBR for untreated ASS 3 increase to 9%. An allowable number of load repetitions to reach fatigue for light and heavy traffic load was recorded for 7 days treated ASS1 CBR 80% and ASS2 60% decreased when CBR value decreased to 30% for 7 days treated ASS 3. An allowable number of load repetitions to reach rutting failure for light and heavy traffic load recorded for 7 days treated ASS1 CBR 80% and ASS2 60% also decreased when CBR value decreased to 30% for 7 days treated ASS 3. An allowable number of load repetitions to reach permanent deformation for light and heavy traffic load recorded for 7 days treated ASS1 CBR 80% and ASS2 60% decreased with a decrease in CBR value to 30% for 7 days treated ASS 3. This was the case for treated 7 and 28 days CBR values, the allowable number of load repetitions reduces with a reduction in CBR value and increases with an increase in CBR value.

This means subgrade materials with high CBR can withstand fatigue, rutting and permanent deformation for a long time before failure occurs compared with subgrade materials with low CBR values. High cycle load repetition means the applied cyclical stresses are low and failure occurs after many cycles, typically more than 10,000 cycles (Lowa State University, 2021). Low cycle load repetition involves higher applied cyclical stresses. Failure occurs after fewer cycles because the stresses involved are

Chapter 5 – Results and Discussion

above the materials yield stress both elastic and plastic deformation (Lowa State University, 2021). Figure 5.87 - Figure 5.92 shows permanent deformation results for treated and untreated ASS materials for 11.75% GGBS, recycled plastic, glass and BDW. Figure 5.93 – Figure 5.98 show more details for fatigue and rutting failure for treated ASS materials using 11.75% GGBS, recycled plastic, BDW.

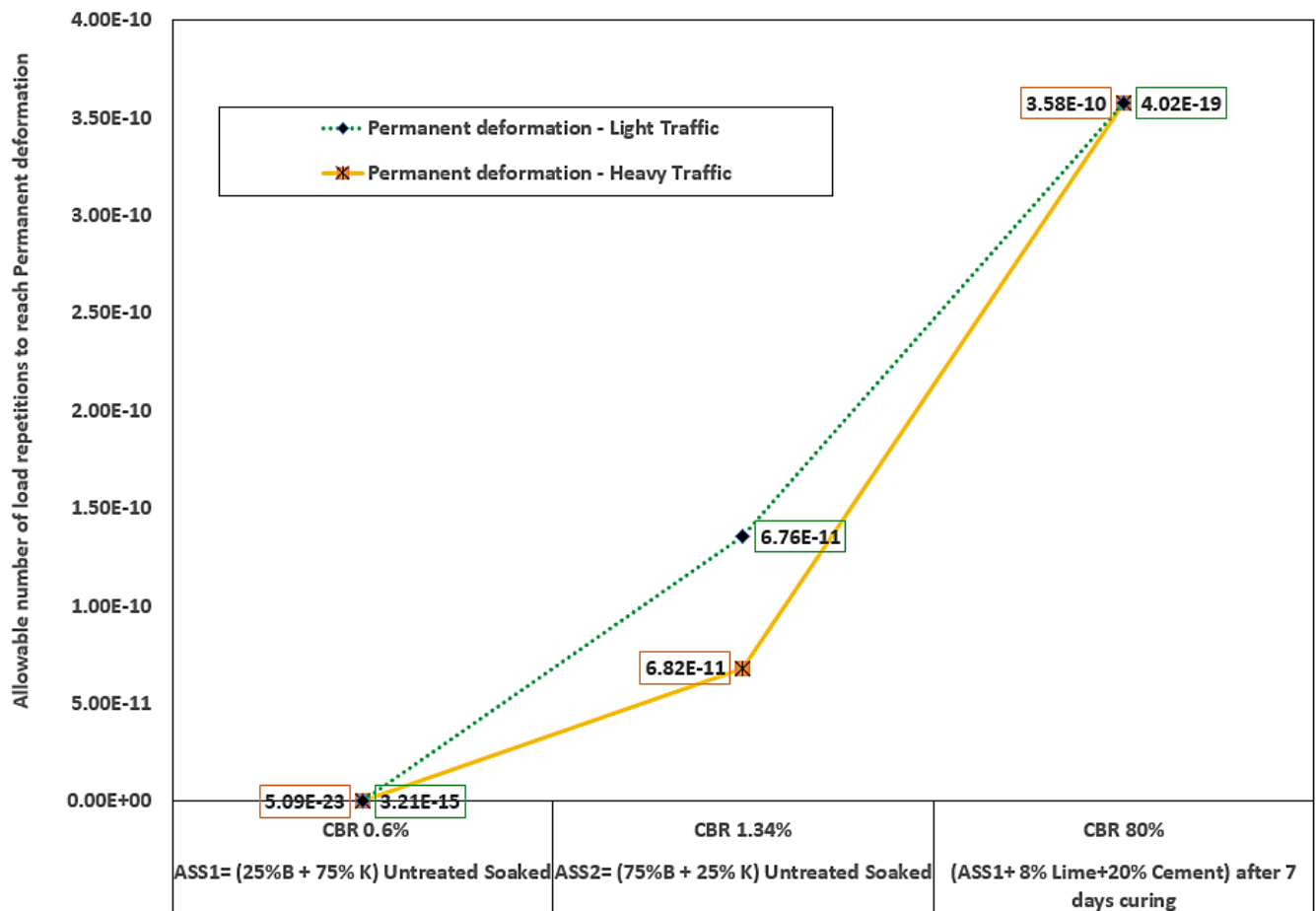


Figure 5.87: Permanent deformation results for treated and untreated ASS materials

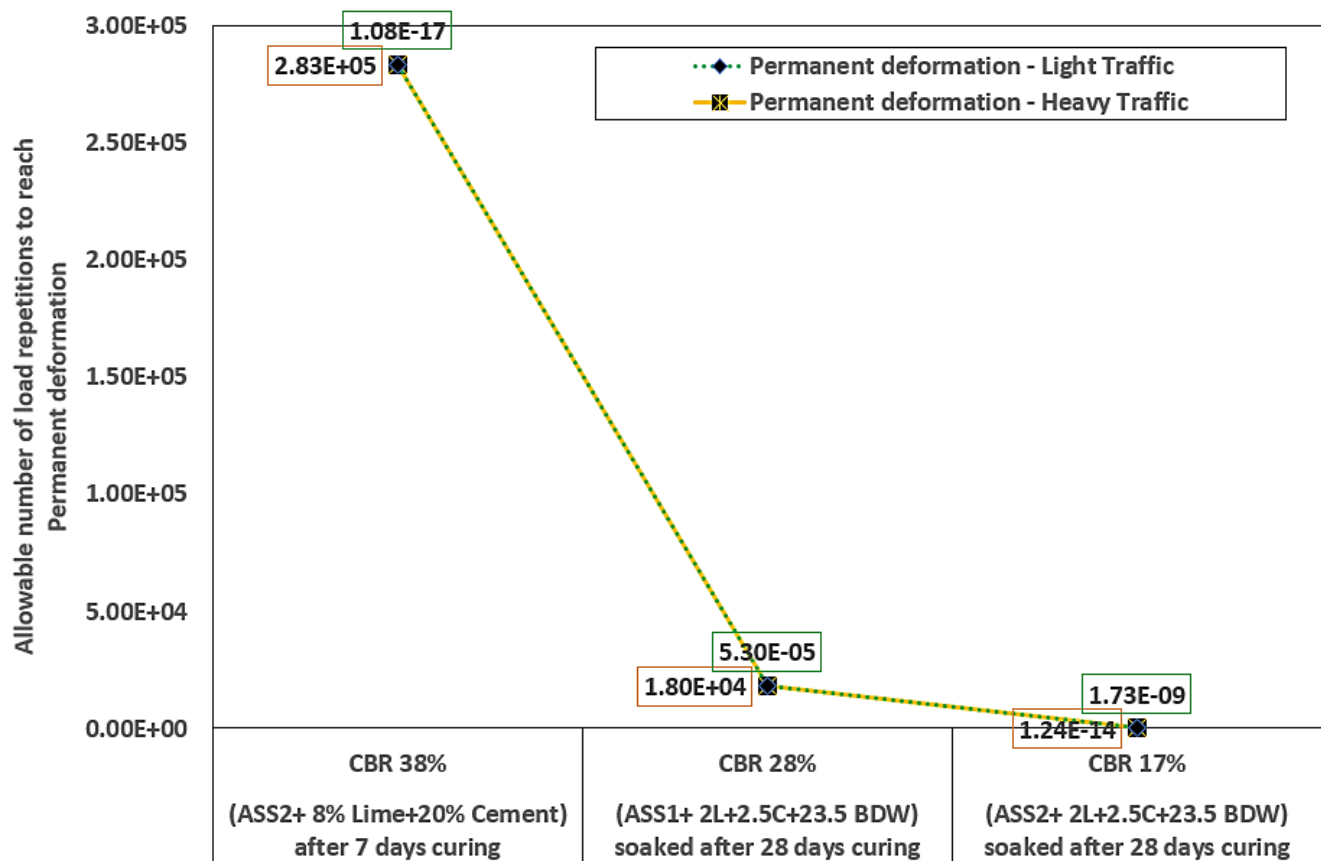


Figure 5.88: Permanent deformation results for treated ASS materials

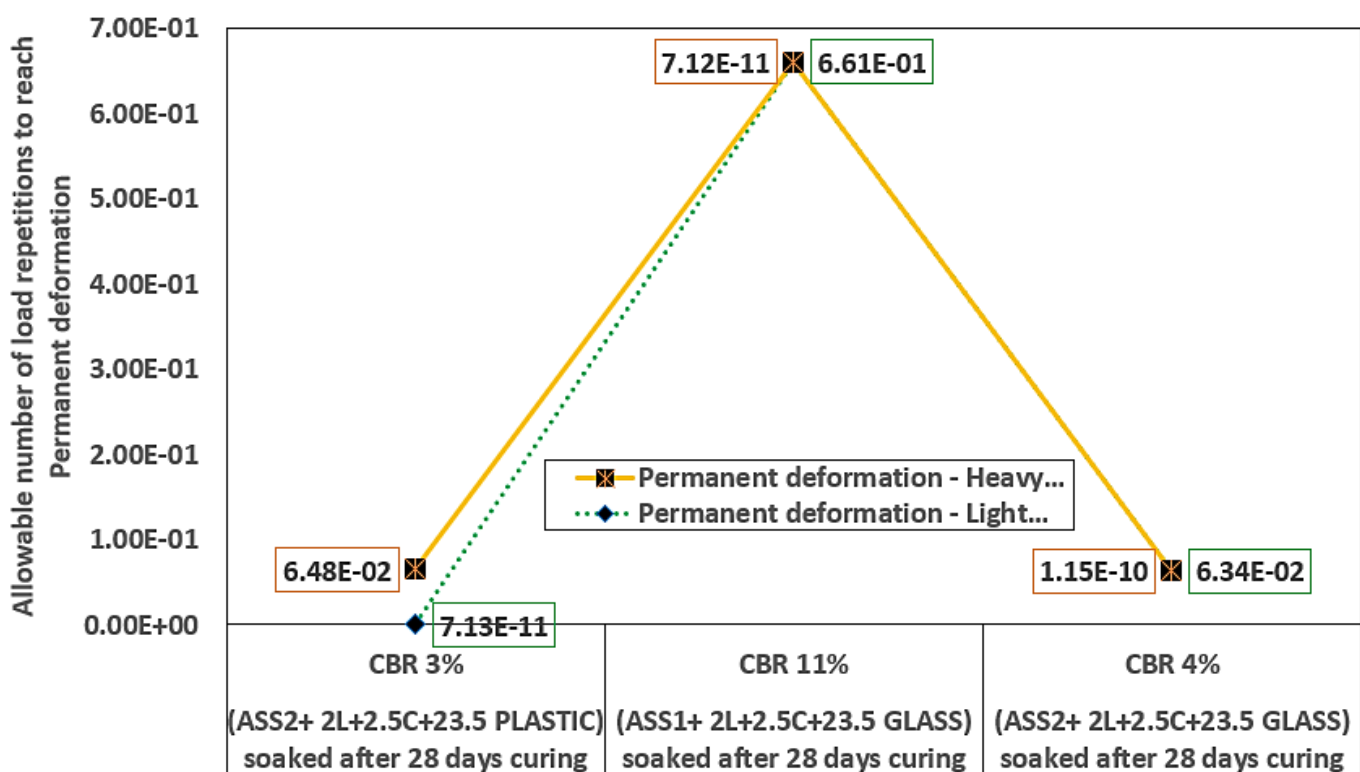


Figure 5.89: Permanent deformation results for ASS materials

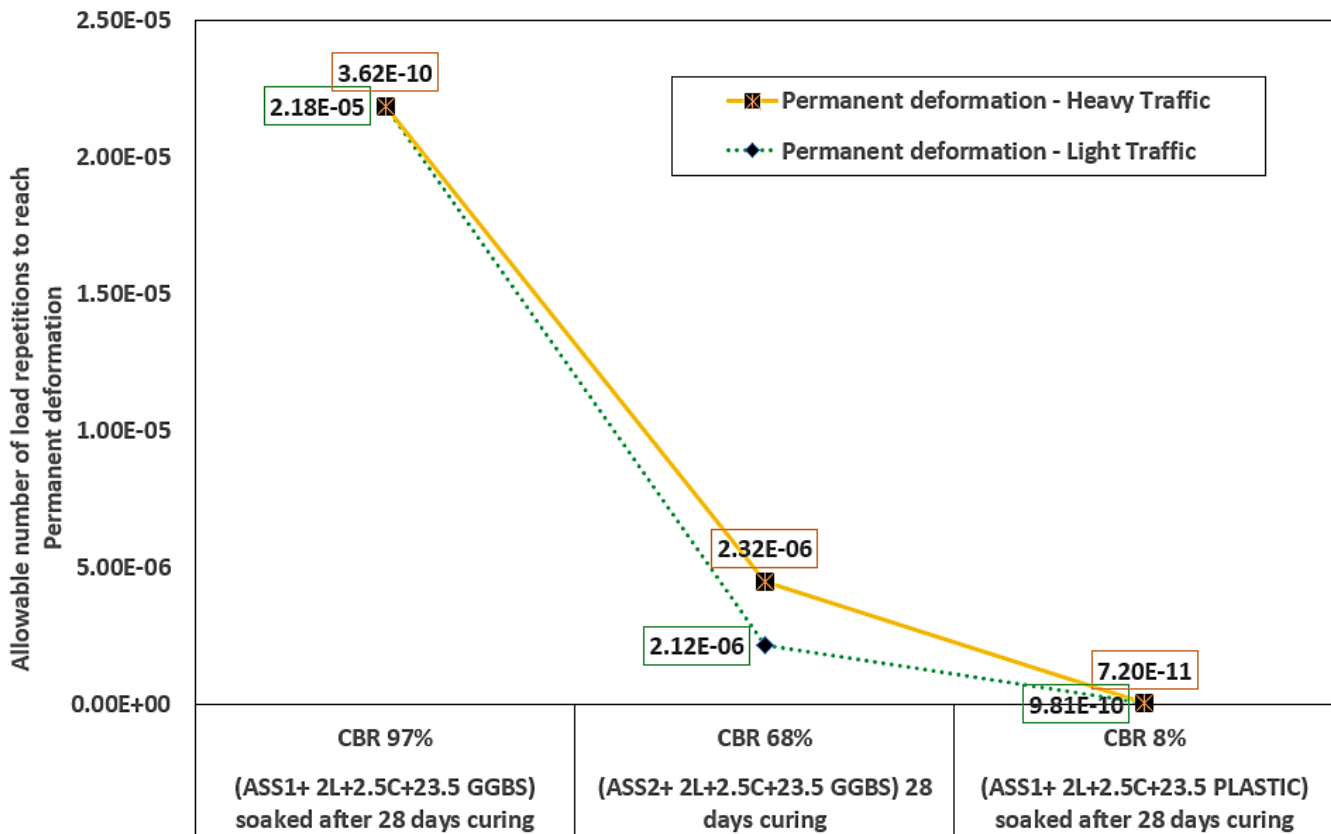


Figure 5.90: Permanent deformation results for ASS materials

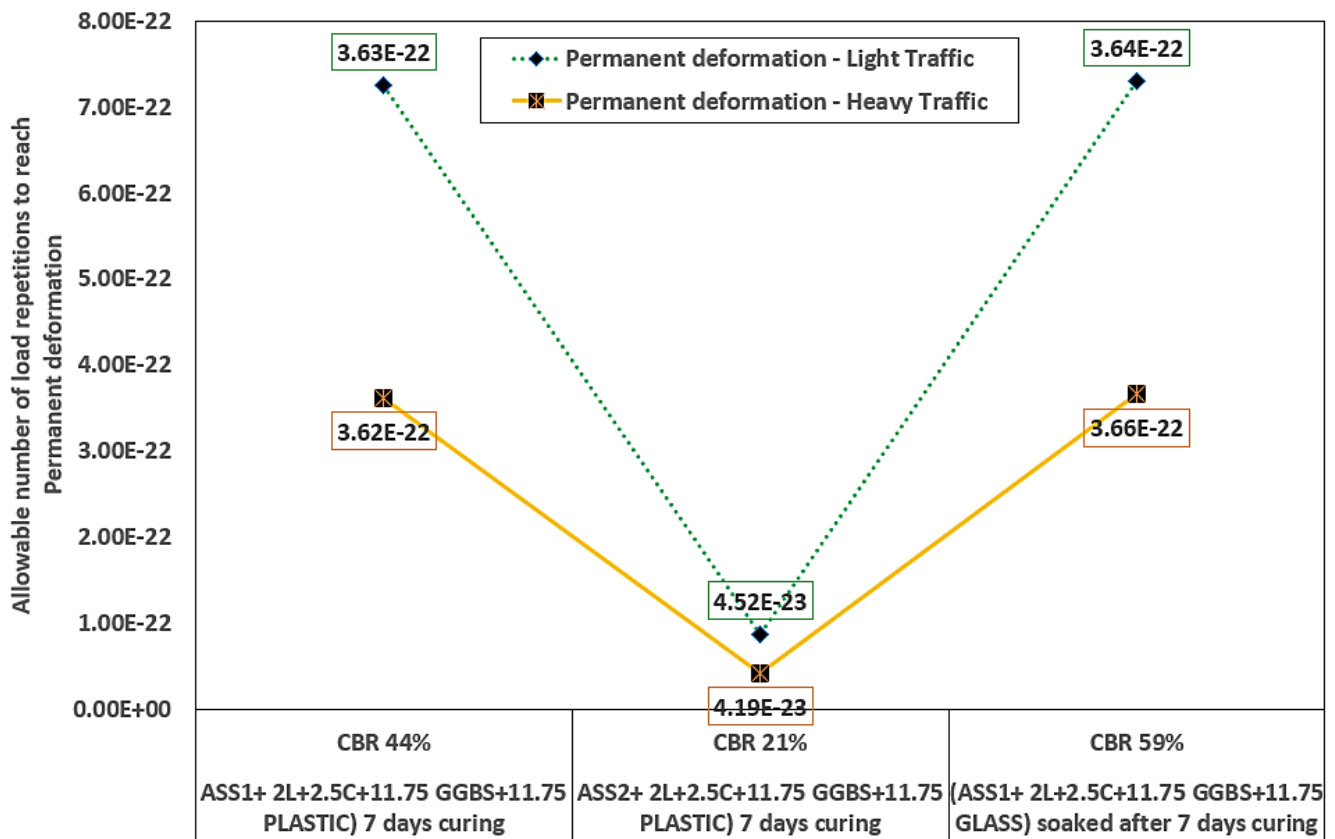


Figure 5.91: Permanent deformation results for ASS materials

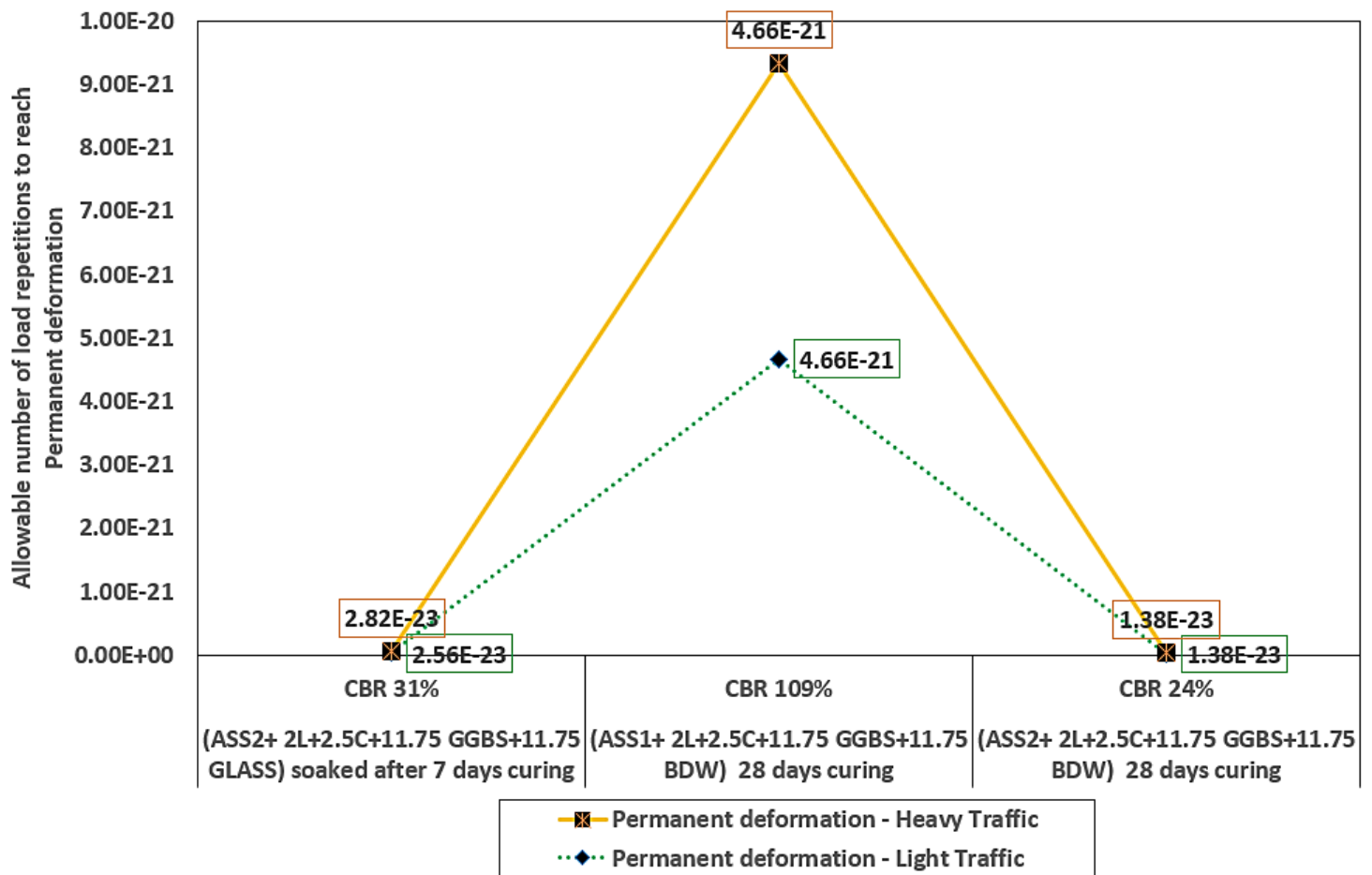


Figure 5.92: Permanent deformation results for treated and untreated ASS materials

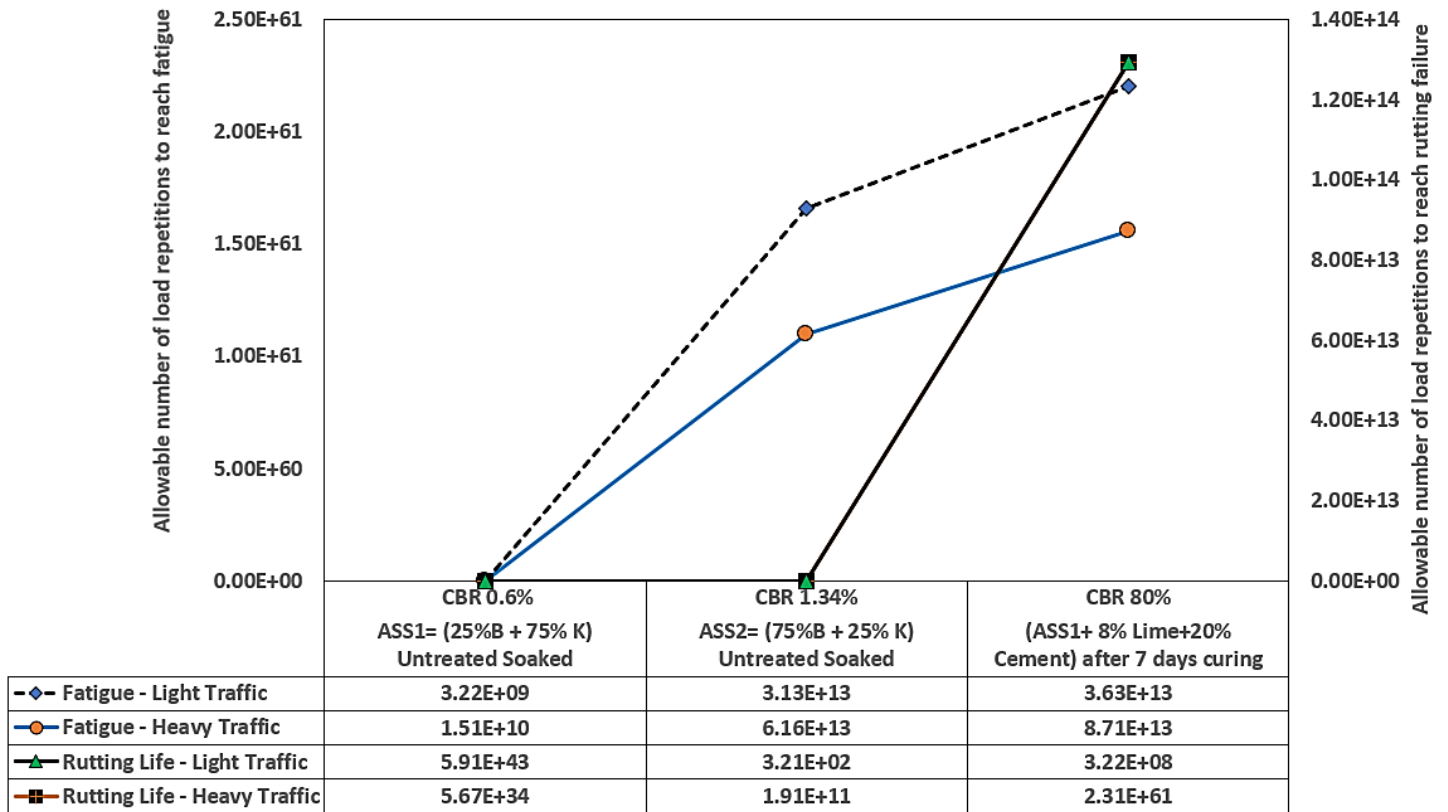


Figure 5.93: Fatigue and rutting failure for treated and untreated ASS materials

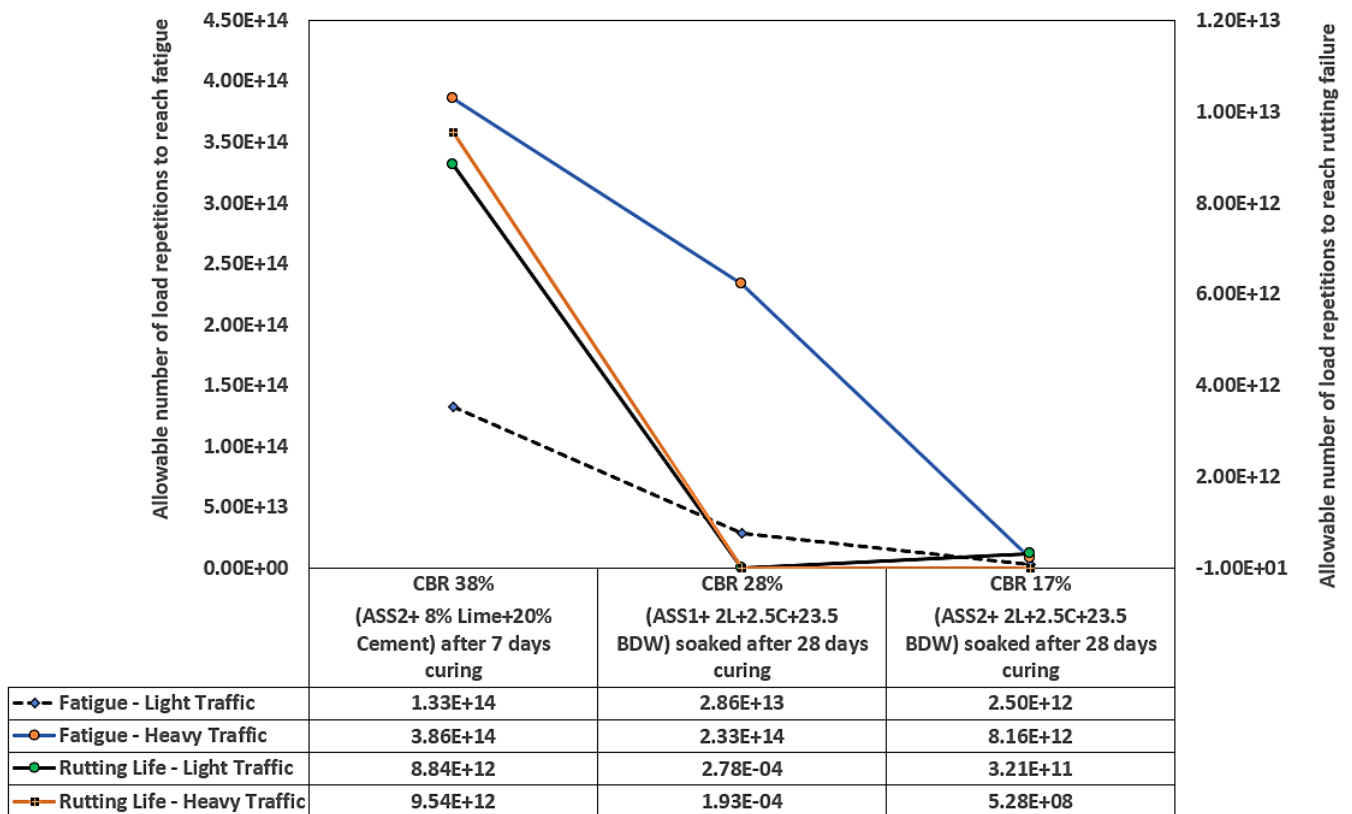


Figure 5.94: Fatigue and rutting failure for treated ASS materials

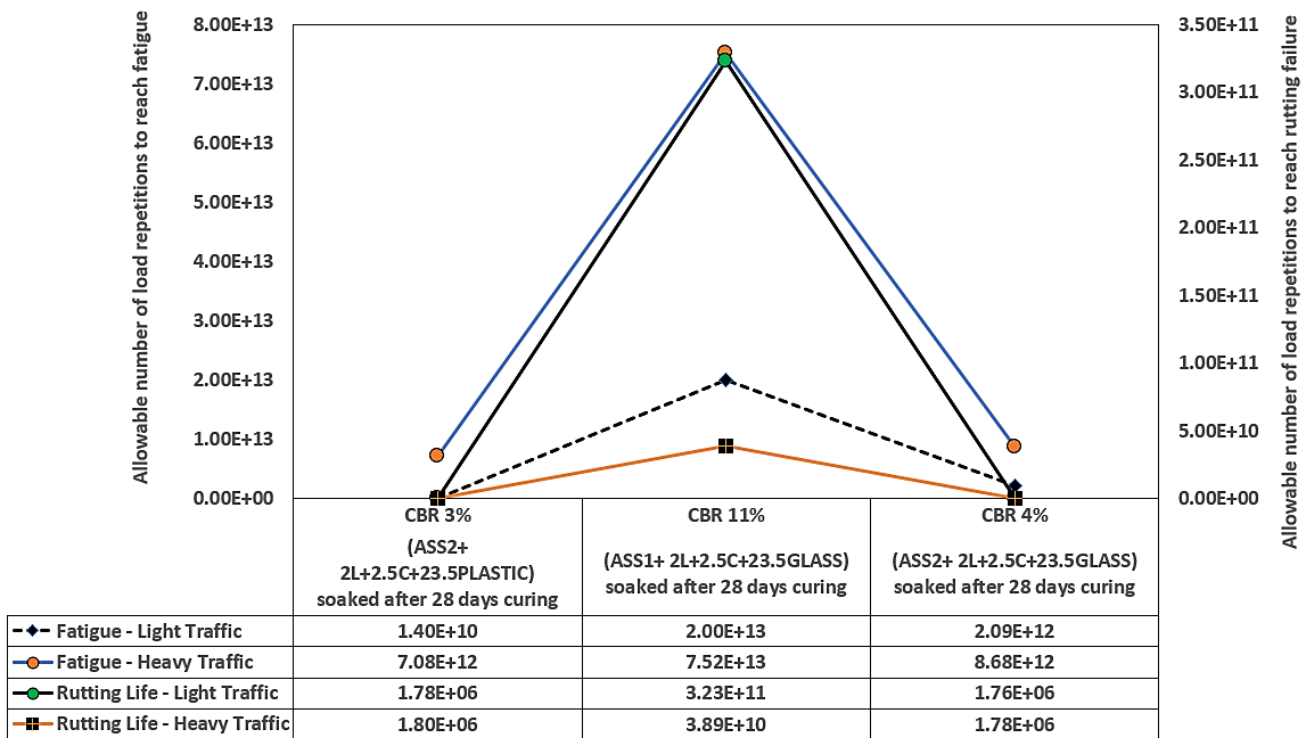


Figure 5.95: Fatigue and rutting failure for treated ASS materials

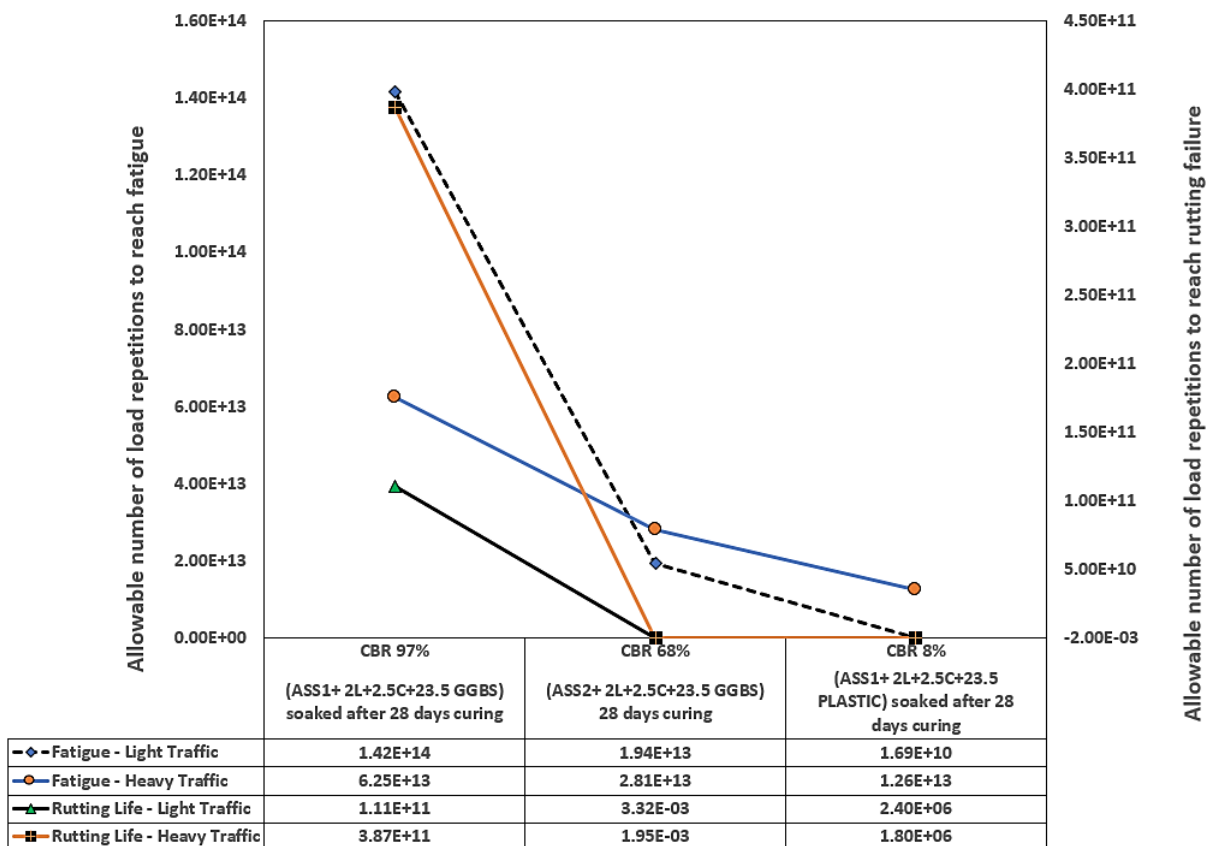


Figure 5.96: Fatigue and rutting failure for treated ASS materials

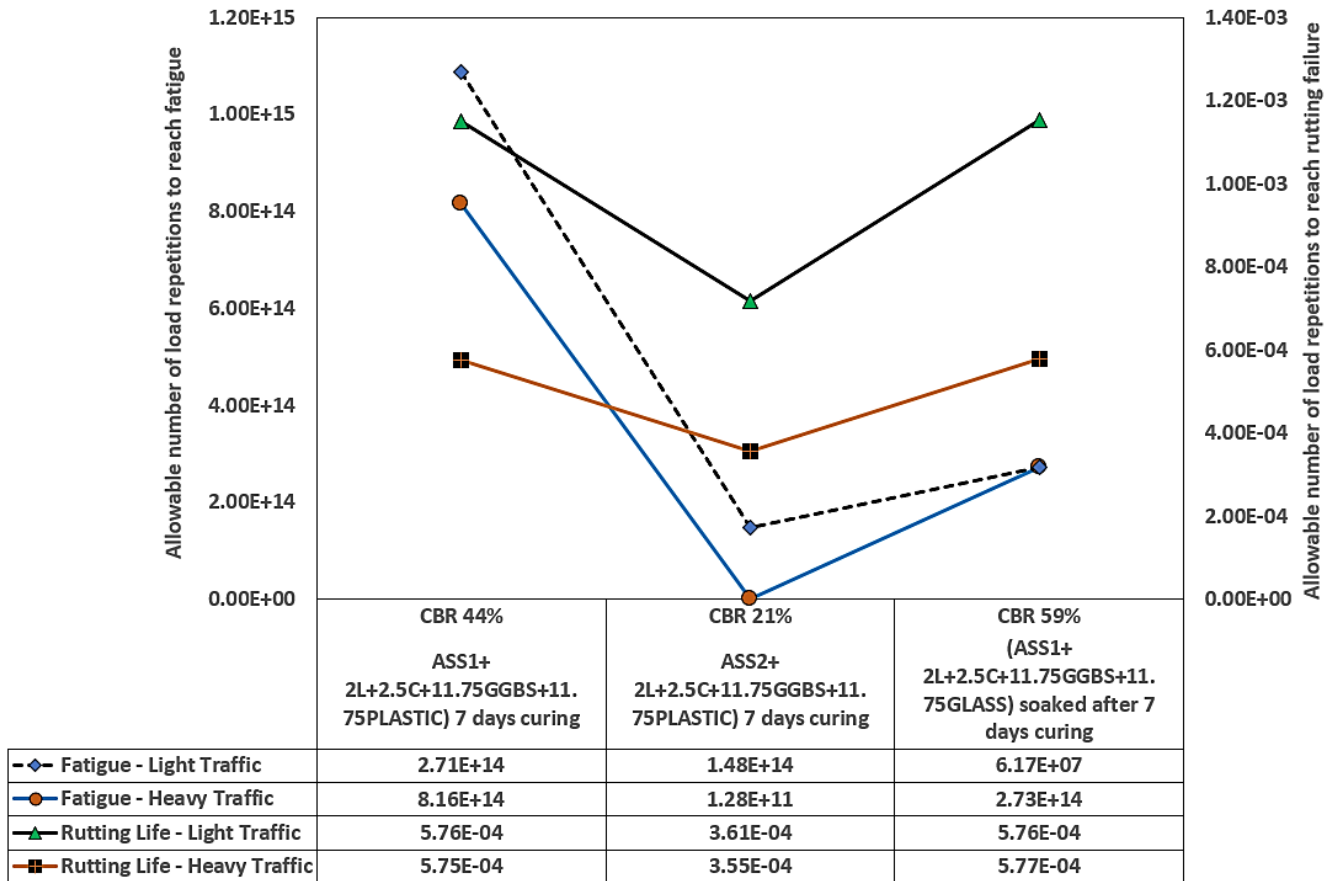


Figure 5.97: Fatigue and rutting failure for treated ASS materials

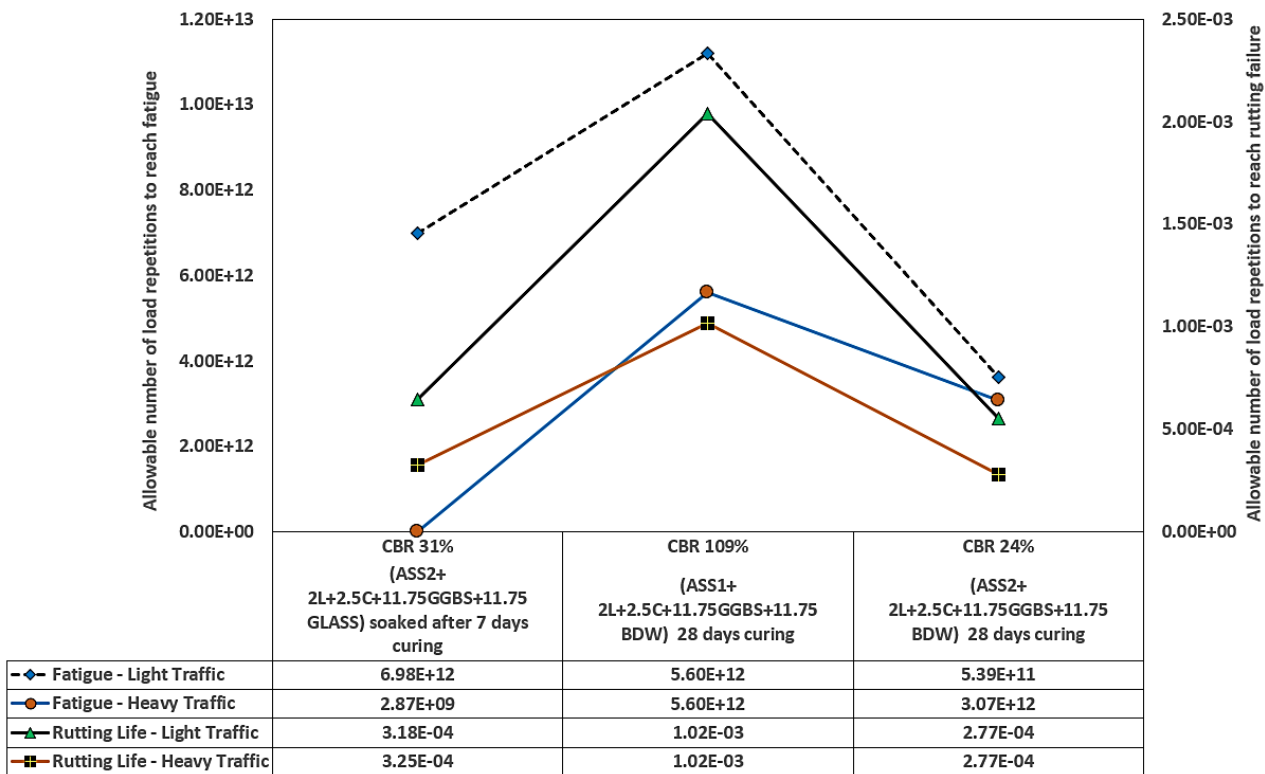


Figure 5.98: Fatigue and rutting failure for treated ASS materials

5.11 ECONOMIC APPRAISAL

5.11.1 Variation in Cost of Using Sustainable Waste or Cement and Lime

A rise in maintenance and rehabilitation costs with a rise in the discount rate was observed with an increase in the road age. A huge rehabilitation and maintenance cost was observed at a later age (Years 28 and 30). After the LCCA, a huge difference in cost was observed between subgrade materials stabilised using cement and lime and subgrade materials removed and replaced with foreign material, the most expensive approach. The cost of using sustainable waste materials exceeded the cost of using cement and lime in subgrade stabilisation however they are economical. Stabilisation exhibited a high unit cost but was moderately economical (Cote et al., 2012). The environmental benefits (such as low carbon emissions and environmental pollution) are far greater compared to using cement and lime which are associated with high carbon emissions and environmental pollution.

Stabilising pavement subgrades using cement has proved to be very costly and unsustainable due to the amount of carbon dioxide (CO₂) emitted during cement production (Abbey et al., 2017). However, using waste materials in road subgrade stabilisation will enhance the engineering properties of expansive soils while reducing environmental effects and overall construction costs (Kassa et al., 2020). Using GGBS in high volumes as supplementary cementitious materials is good from an environmental point of view (Onn et al., 2019). The higher the amount of GGBS used in replacing cement in soil stabilisation the less carbon footprint is expected due to the reduction in the use of cement (Onn et al., 2019). The use of processed waste (such as fly ash) has significant environmental benefits including a net reduction in energy use and greenhouse gas emission. The use of recycled materials may not only provide less costly alternatives for subgrade stabilisation, but their use may also alleviate landfill disposal challenges (Bandara et al., 2013). The LCC for subgrade stabilisation and subgrade removal and preplacement was greatly influenced by the initial cost at year zero.

According to Fuller et al., (2016), land acquisition, renovation, modification, construction and equipment can increase the initial cost during LCCA. It is more economical to design road pavement for the existing subgrade capacity than to import

or raise the subgrade support by using an extra-thicker subbase (Li et al., 1964). This shows that the initial cost incurred during the construction of road pavement can influence the life cycle cost of the road. Even though maintenance and rehabilitation costs began to increase gradually for road pavement with stabilised subgrade for all binder types after year zero, a high maintenance cost compared to rehabilitation cost was observed followed by a drop in the cost of salvage value at year 35 was observed. A very high initial cost at year zero was recorded for road subgrade removal and replacement followed by a gradual increase in maintenance and rehabilitation cost and a drop in salvage value. This high initial cost was responsible for the overall high cost of removing and replacing subgrade materials. the cost of removing and replacing rod subgrade materials was almost three times the cost of stabilising subgrade materials.

According to Cole et al. (2013), the high cost of removing and replacing subgrade is influenced by the disposal options, availability and cost of replacement materials, cost of equipment and operations. Compared to cut-and-fill, lime treatments are less than 1/3 of the cost of remove-and-replace subgrade (Cole et al., 2013).

The subgrade treatment technique works better for construction loads and is less costly (Cole et al., 2013).

The highest cost of £269,087,587 for stabilising a square meter of road subgrade using sustainable waste materials was recorded for a design mix of 2% lime + 2.5% cement + 11.75% GGBS + 11.75% Plastic due to the high cost of plastic pellets used in this study. The lowest cost of £268,344,106 for stabilising a square meter of road subgrade was recorded for the control mix (8% Lime + 20% Cement) due to the low cost of cement used in this research even though they are associated with high greenhouse gas emissions. Portland cement and lime are low-cost and effective for soil stabilisation (Ramaji et al., 2012). Using cement and lime in subgrade stabilisation is far cheaper (Chandola et al., 2001). Using waste materials in subgrade stabilisation is economical and less harmful to the environment. Figure 5.99 shows the assumed discount rate, and estimated maintenance and rehabilitation cost which is applicable to all types of roads with good subgrade. The changes in the total LCC emanates from whether the subgrade was removed and replaced or stabilised using cement, lime or waste materials. Figure 5.100 shows LCCA for lime and cement-treated ASS against

Chapter 5 – Results and Discussion

subgrade removal and replacement. Figure 5.101 - Figure 5.108 shows the LCC comparison between sustainable subgrade stabilisation and subgrade removal and replacement cost.

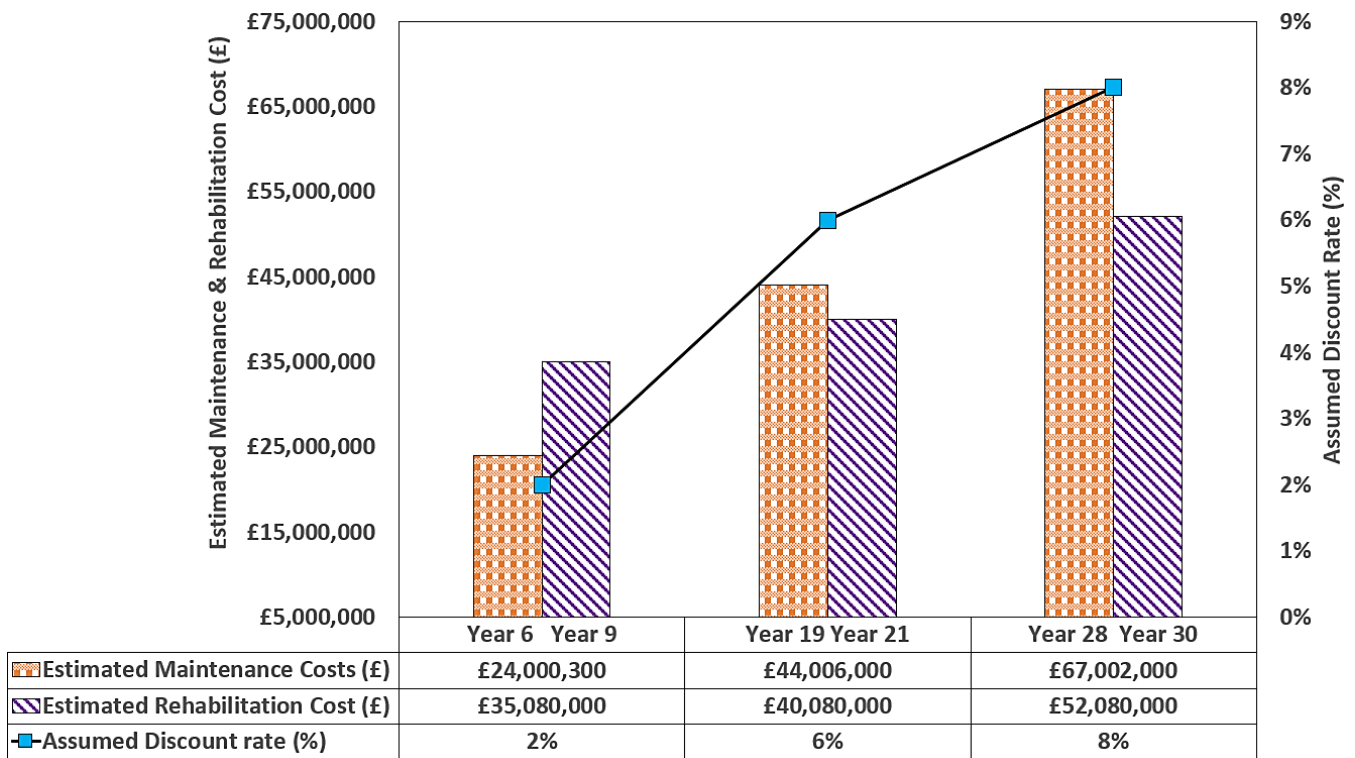
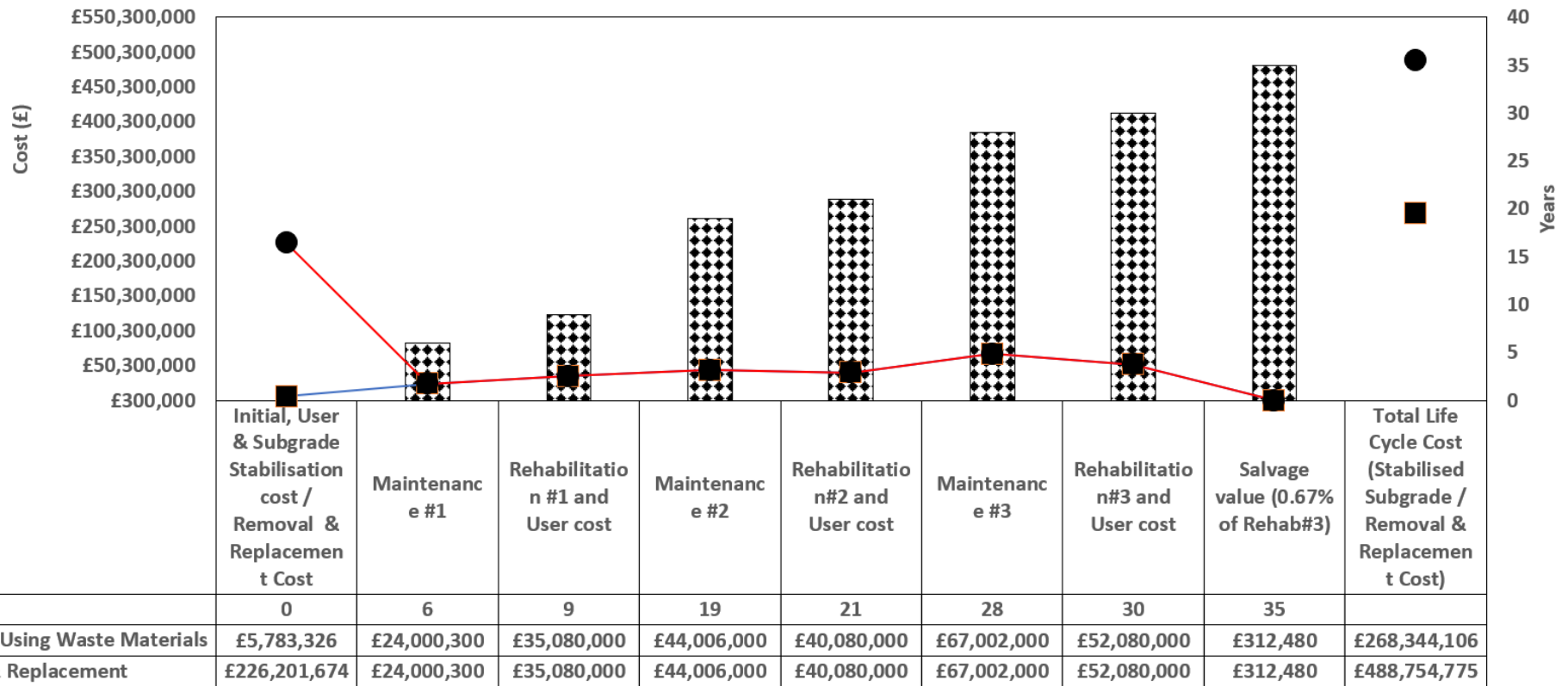


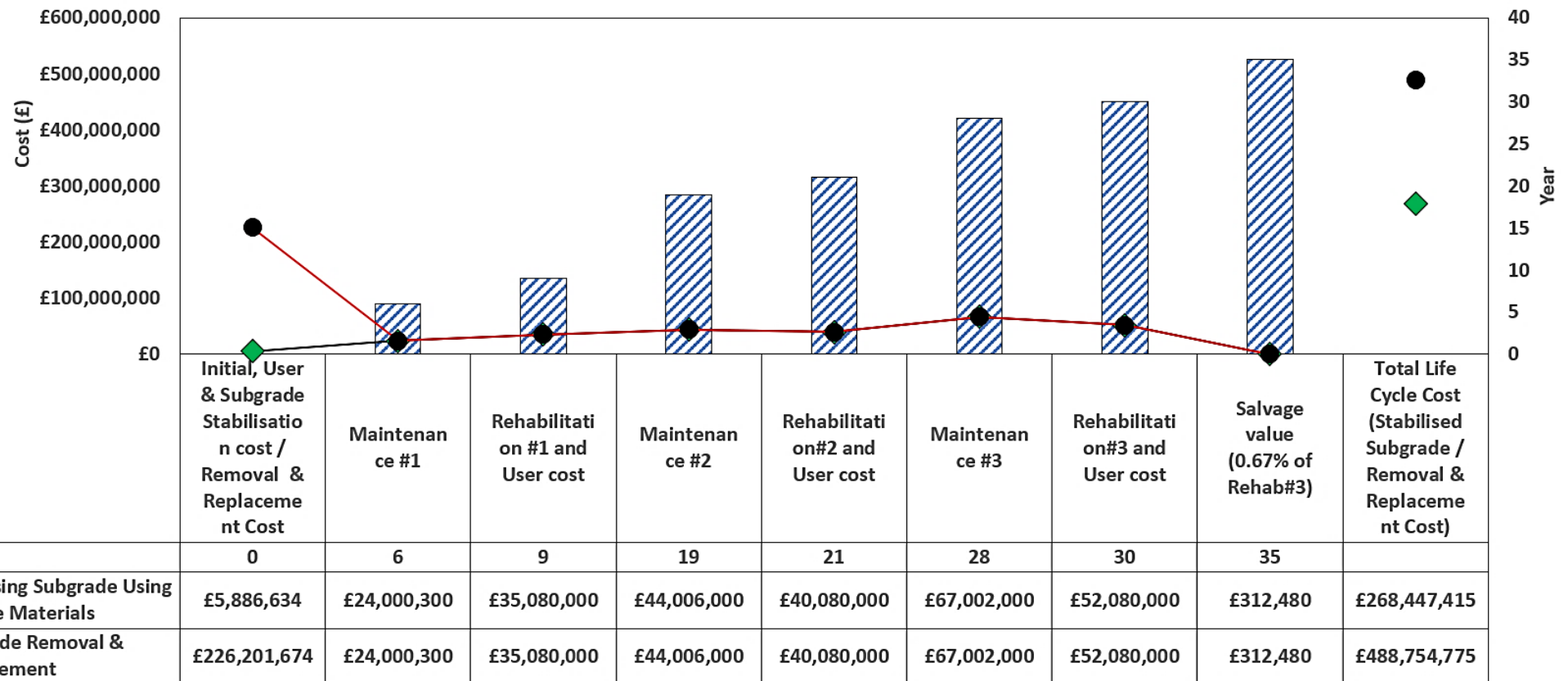
Figure 5.99: Discount rate, estimated maintenance and rehabilitation cost



**Stabilisation Subgrade Using 8%Lime + 20%Cement (CONTROL MIX)
Against Subgrade Removal and Replacement**

Figure 5.100: LCCA for lime and cement treated ASS against subgrade removal and replacement

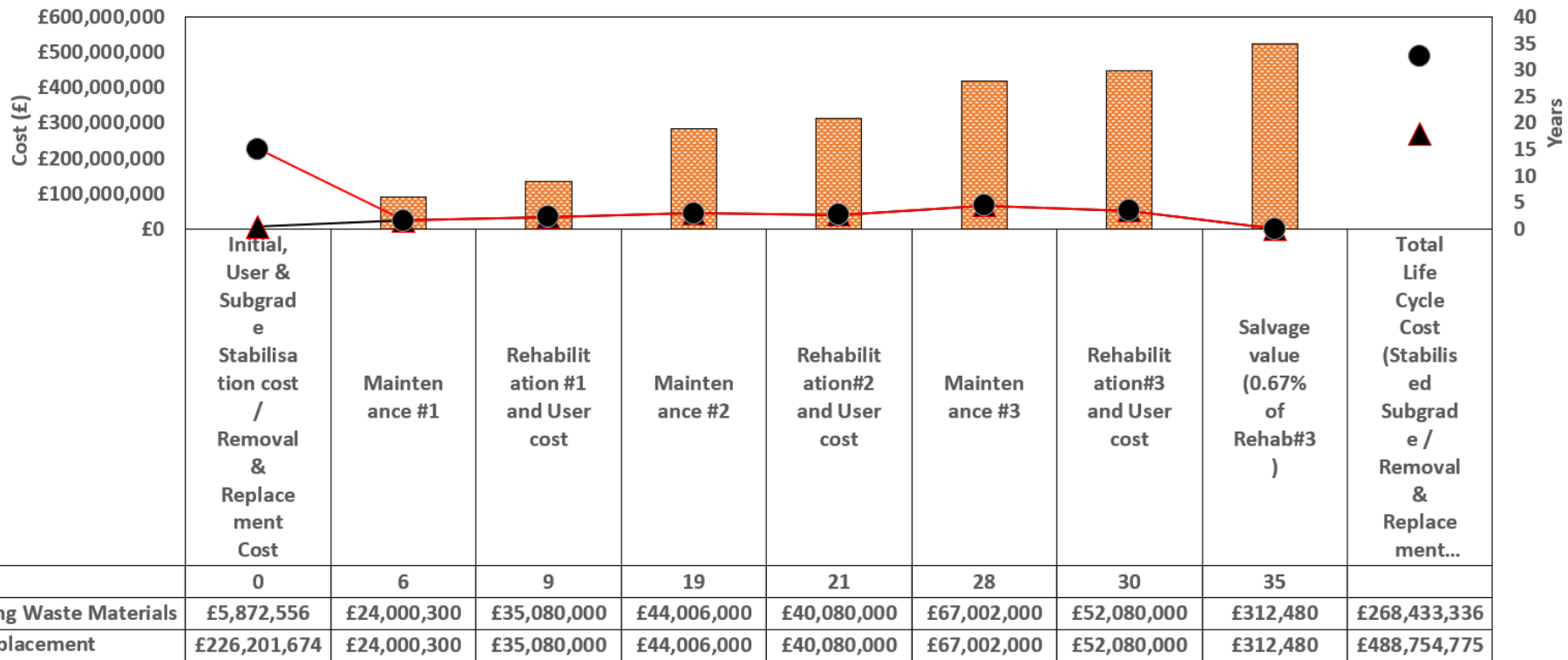
Chapter 5 – Results and Discussion



Stabilising Road Subgrade Using 2%Lime + 2.5%Cement + 23.5%BDW Against Subgrade Removal and Replacement

Figure 5.101: LCCA for sustainable treated ASS against subgrade removal and replacement

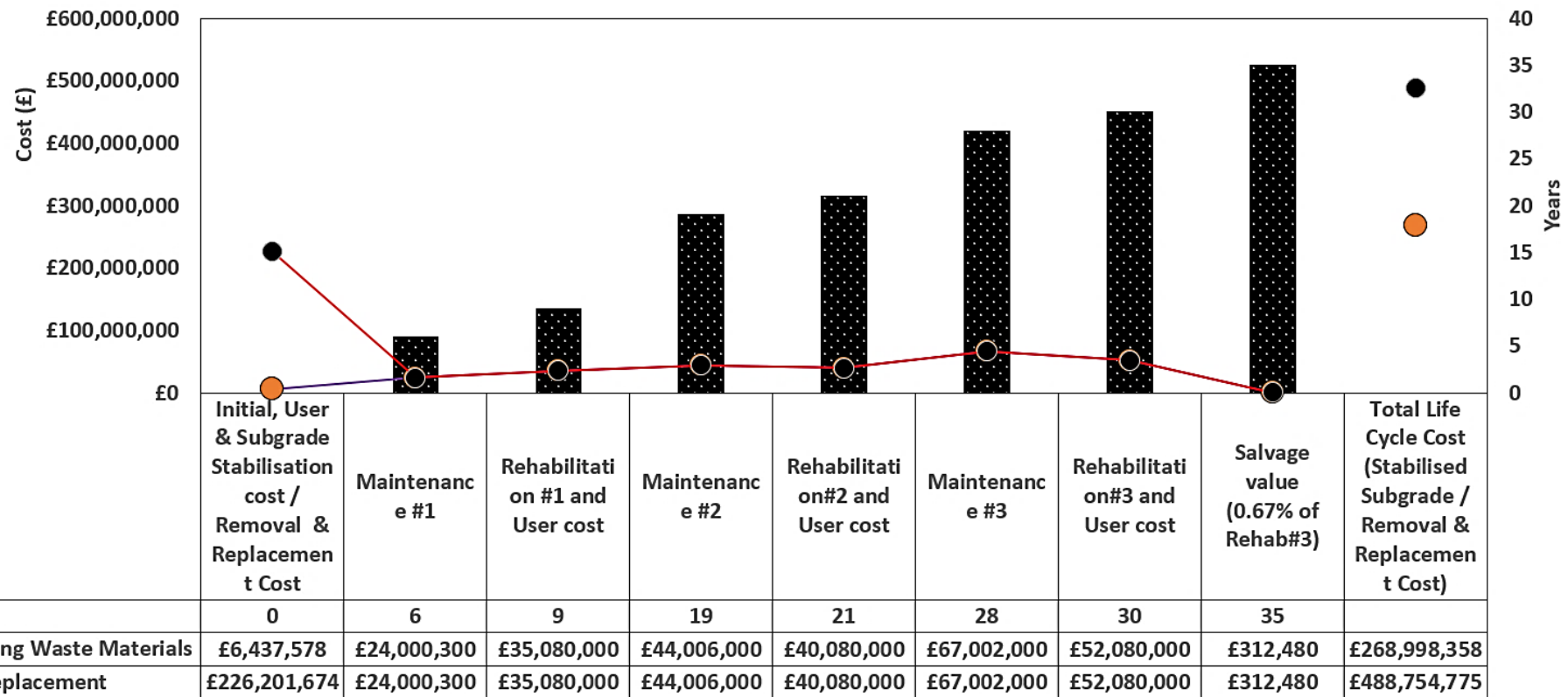
Chapter 5 – Results and Discussion



Stabilising Road Subgrade Using 2%Lime + 2.5%Cement + 23.5%GGBS Against Subgrade Removal and Replacement

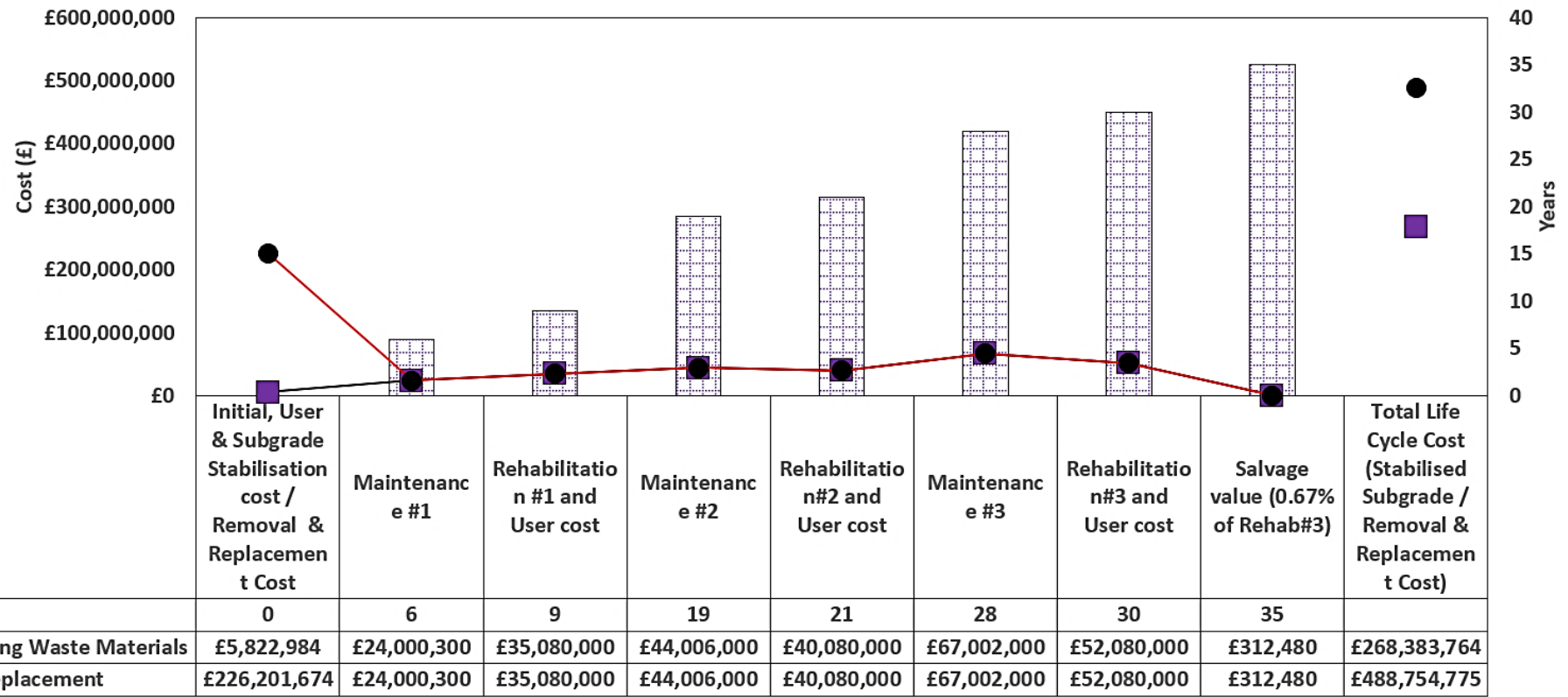
Figure 5.102: LCCA for sustainable treated ASS against subgrade removal and replacement

Chapter 5 – Results and Discussion



Stabilising Road Subgrade Using 2%Lime + 2.5%Cement + 23.5%PLASTIC Against Subgrade Removal and Replacement

Figure 5.103: LCCA for sustainable treated ASS against subgrade removal and replacement



Stabilising Road Subgrade Using 2%Lime + 2.5%Cement + 23.5%GLASS Against Subgrade Removal and Replacement

Figure 5.104: LCCA for sustainable treated ASS against subgrade removal and replacement

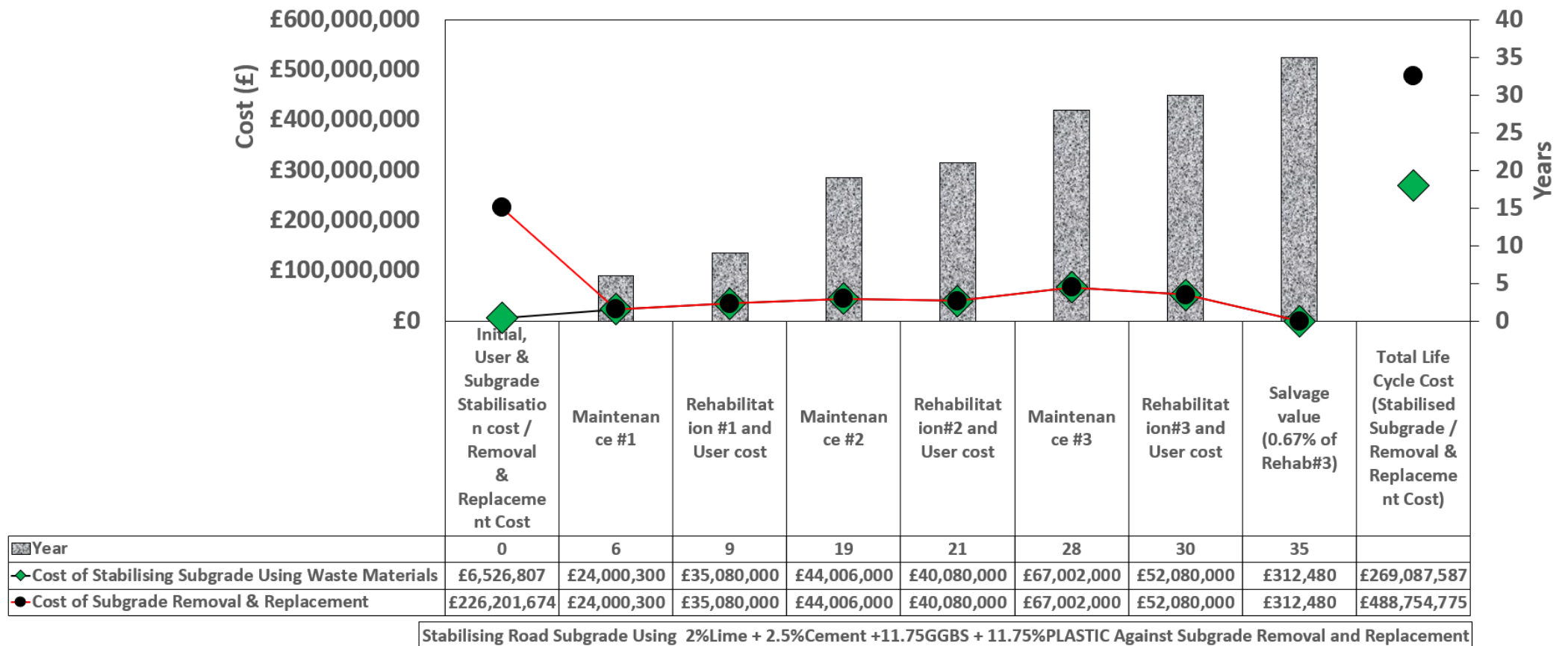


Figure 5.105: LCCA for sustainable treated ASS against subgrade removal and replacement

Chapter 5 – Results and Discussion

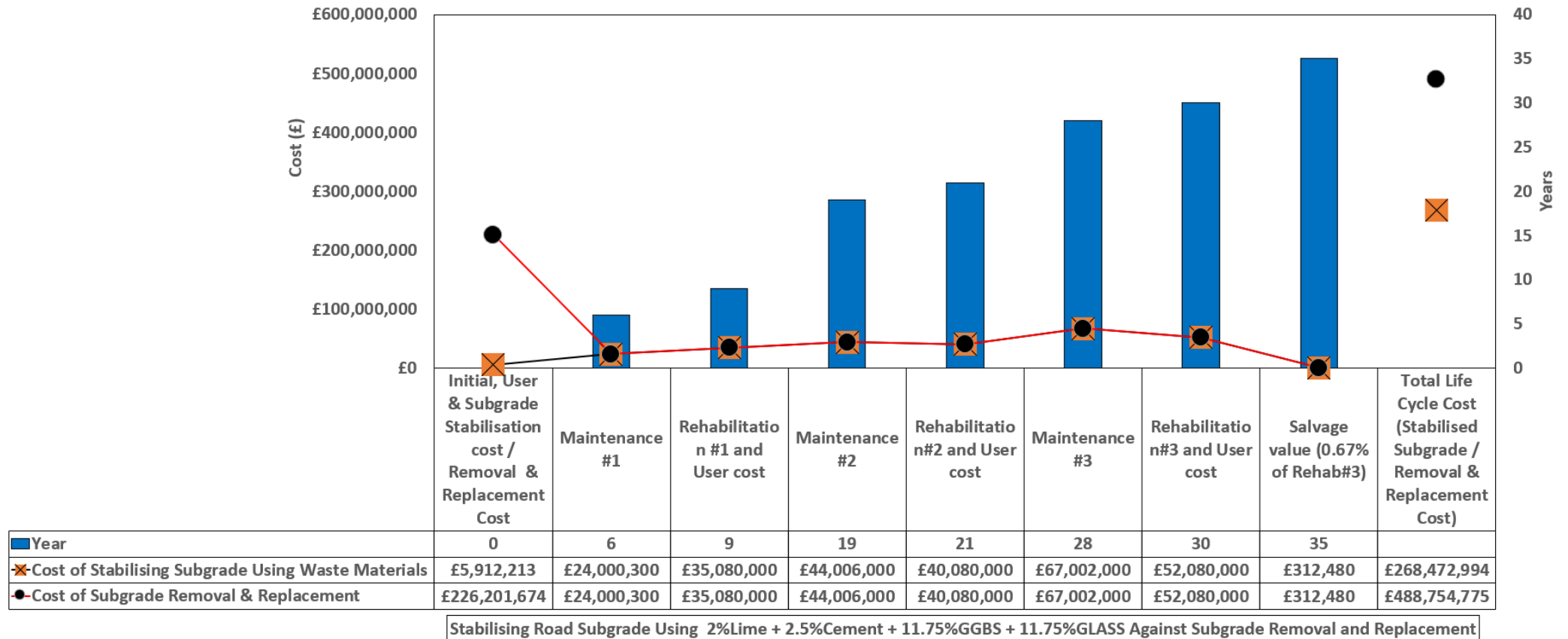
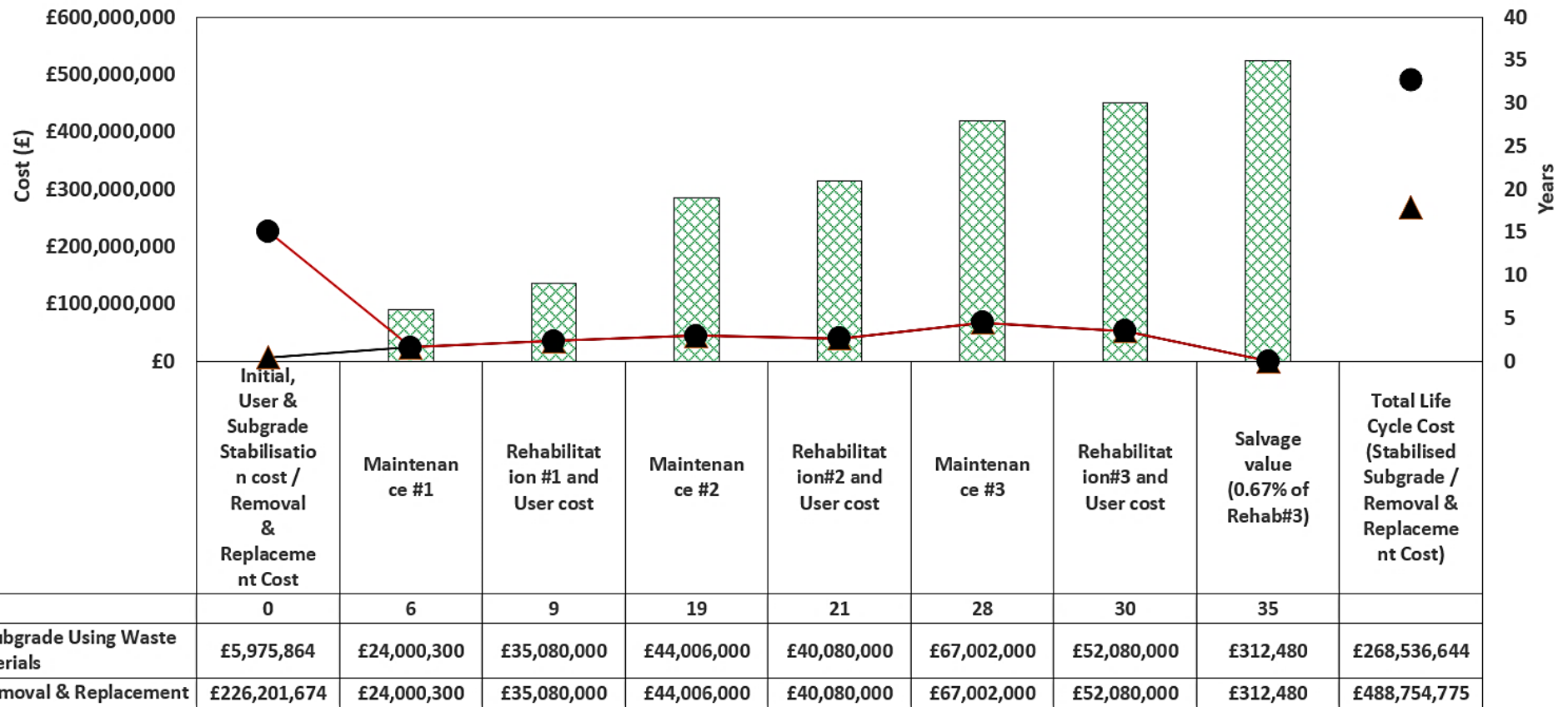


Figure 5.106: LCCA for sustainable treated ASS against subgrade removal and replacement

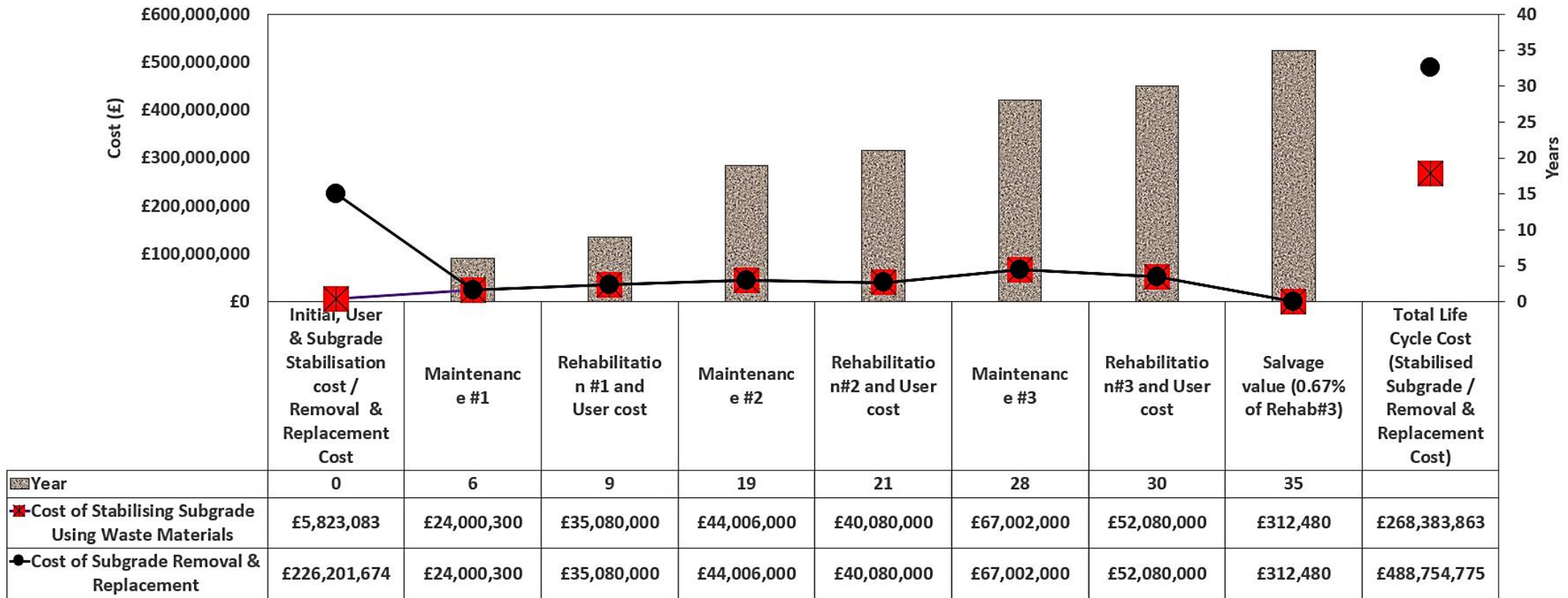
Chapter 5 – Results and Discussion



Stabilising Road Subgrade Using 2%Lime + 2.5%Cement + 11.75%GGBS + 11.75%BDW Against Subgrade Removal and Replacement

Figure 5.107: LCCA for sustainable treated ASS against subgrade removal and replacement

Chapter 5 – Results and Discussion



Stabilising Road Subgrade Using 2%Lime + 26%GGBS Against Subgrade Removal and Replacement

Figure 5.108: LCCA for sustainable treated ASS against subgrade removal and replacement

5.12 CLASSIFICATION OF PARAMETERS AND EMBODIED CARBON

The lowest embodied carbon was recorded for mix design 2%Lime+26%GGBS (0.0011 Co₂e/kg) compared with the control mix 8%Lime+20%Cement of 0.0084 Co₂e/kg. However, sustainably stabilised mix recorded low embodied carbon except for mix designs containing plastic. The highest embodied carbon of 0.0107 Co₂e/kg was recorded for 2%Lime +2.5%Cement +11.75%GGBS +11.75%Plastic as a result of the plastic. Plastic has very high embodied carbon. This confirms EDX findings in this research which shows that high carbon was recorded for other mixtures, the high carbon (C) found in mixtures containing recycled plastic could be due to the plastic content in the mix because plastics are full of carbon. Zhu *et al.*, (2021) stated that plastics are carbon more specifically because almost all plastics are fossil carbon locked up in polymer form. Mix design 2%Lime +2.5%Cement +11.75%GGBS +11.75%BDW recorded a LCC of £268,536,644.10. However, the Control mix of 8% Lime + 20% Cement recorded the lowest Life Cycle Cost (£268,344,106.46) for treated subgrade followed by mix design without cement (2%Lime+26%GGBS) of £268,383,863.20. There is no significant difference in their LCC which means using waste materials in subgrade stabilisation is the best option to achieve more sustainable construction. Even though traditional cement and lime are cheaper compared to sustainable waste-treated subgrade, they are none-environmentally friendly and unsustainable due to their high embodied carbon and greenhouse gas emissions.

5.13 UNITED NATIONS SUSTAINABLE DEVELOPMENT GOALS (UNSDGs)

Reaching the goal set by the United Nations as part of the UNSD agender is very crucial and steps have been taken by many countries to achieve these goals. Findings of this research would help achieve the following United Nation Sustainable Development Goals:

Table 5.1: United Nations Sustainable Development Goals achieved by this research

UNSDG Goal/target	Focus	Findings from research
Goal 9	Industry, Innovation, and infrastructure: inclusive and sustainable industrialisation together with innovation and infrastructure to accelerate the 2030 target to scale up investment in scientific research and innovation.	This research provides solutions for sustainable and innovative ways of road construction using waste materials. The quality of the sustainable and innovative ways of road construction used in this research meets the required standards so quality is not compromised. Findings in this research would lead to more economical infrastructure (cheaper/affordable) due to the use of waste materials in the research.
Target 9.1	Develop of quality, reliable, sustainable and resilient infrastructure.	This research encourages the development of quality, reliable, sustainable and resilient infrastructure to support economic development and well-being with a focus on affordable and equitable access for all.
Target 9.4	Upgrading infrastructure to make them sustainable.	The research looks at upgrading infrastructure to make them sustainable, with increased resource-use efficiency and greater adoption of clean and environmentally sound technologies by the end of 2030.
Goal 12	Responsible Consumption and Production: Ensure sustainable consumption and production patterns. This means doing more and better with less and decoupling economic growth from environmental	This research provide solutions for sustainable consumption and environmental degradation (this study uses waste inserted of raw materials) and low-carbon for green economies (this study uses less or no cement to reduce carbon emission)

UNSDG Goal/target	Focus	Findings from research
	degradation, increasing resource efficiency, promoting sustainable lifestyles and transitioning towards a low-carbon and green economy	
Target 12.2	encourage the drive towards achieving sustainable management and efficient use of natural resources	Encourage the drive towards achieving sustainable management and efficient use of natural resources (this study uses waste inserted cement which is produced using natural resources (clinker)).
Target 12.4	Achieve the environmentally sound management of waste	This study uses waste in road construction, and significantly reduce the release CO ₂ into the air, and toxic into water bodies and the ground (solutions from this study will reduce carbon emission, the release of wastewater (chemical) from cement plants into soil and water bodies by using waste materials in road construction inserted of cement).
Target 12.5	Sustainably reduce waste generation through prevention, reduction, recycling and reuse	finding from this study would reduce waste generation by using recycled waste materials in road construction.
Goal 13	Climate Action taking urgent actions to combat climate change and its impacts	Findings from this research will reduce the impact of climate change by using less cement and lime in road construction to reduce global warming from the heat generated by cement plants during cement production.

Chapter 5 – Results

Table 5.2: Summary results of all parameters described in this research

Subgrade Type		Binder composition	Curing age range (days)	CBR Range (%)	Traffic Load (kN)	Traffic Class	Road Pavement Thickness (mm)	Road Pavement Cons. Depth (mm)	Embodied Carbon for binders (Co ₂ e/kg) (BSRIA Guide 2022)	Life Cycle Cost (LCC) 35 years	
High	Extremely high									Treated subgrade	Subgrade Removal & Replacement
ASS1	ASS2	8%L+20%C (control)	7 – 28	38 – 96	31.75	Light	40 – 110	50 – 100	0.0084	£268,344,106	£488,754,774
					40.82	Medium	42 – 120	60 – 110			
					55.43	Heavy	44 - 130	100 – 200			
ASS1	ASS2	2%L+2.5%C+23.5%BDW	7 – 28	17 – 23	31.75	Light	150 – 180	110 – 120	0.0036	£268,447,414	£488,754,774
					40.82	Medium	160 – 210	150 – 160			
					55.43	Heavy	190 – 240	220 – 310			
ASS1	ASS2	2%L+2.5%C+23.5%GGBS	7 – 28	46 – 97	31.75	Light	50 – 90	50 – 90	0.0018	£268,433,336	£488,754,774
					40.82	Medium	51 – 100	60 – 110			
					55.43	Heavy	52 – 110	100 – 190			
ASS1	ASS2	2%L+2.5%C+23.5%PL	7 – 28	3 – 13	31.75	Light	190 – 440	170 – 350	0.0195	£268,998,357	£488,754,774
					40.82	Medium	210 – 490	200 – 400			
					55.43	Heavy	240 – 550	320 – 650			
ASS1	ASS2	2%L+2.5%C+23.5%GL	7 – 28	3 – 17	31.75	Light	180 – 440	150 – 350	0.0069	£268,383,764	£488,754,774
					40.82	Medium	200 – 490	160 – 400			
					55.43	Heavy	220 - 550	290 – 650			
ASS1	ASS2	2%L+2.5%C+11.75%GGBS+11.75%BDW	7 – 28	16 - 109	31.75	Light	40 – 180	50 – 150	0.0028	£268,536,644	£488,754,774
					40.82	Medium	40 – 220	52 – 190			
					55.43	Heavy	40 – 240	70 – 290			
ASS1	ASS2	2%L+2.5%C+11.75%GGBS+11.75%PL	7 – 28	44 - 93	31.75	Light	50 – 100	50 – 90	0.0107	£269,087,587	£488,754,774
					40.82	Medium	51 – 110	60 – 110			
					55.43	Heavy	52 – 120	100 – 190			
ASS1	ASS2	2%L+2.5%C+11.75%GGBS+11.75%GLASS	7 – 28	21 – 80	31.75	Light	50 – 160	60 – 120	0.0072	£268,472,993	£488,754,774
					40.82	Medium	51 – 180	70 – 150			
					55.43	Heavy	52 – 190	130 – 250			
ASS1	ASS2	2%L+2.5%C+23.5%BDW	90	120 – 180	31.75	Light	40	50	0.0036	£268,447,414	£488,754,774
					40.82	Medium	40	50			
					55.43	Heavy	40	50			
ASS1	ASS2	2%L+2.5%C+23.5%GGBS	90	96 – 200	31.75	Light	40	50	0.0018	£268,433,336	£488,754,774
					40.82	Medium	40	50			

Chapter 5 – Results

Subgrade Type		Binder composition	Curing age range (days)	CBR Range (%)	Traffic Load (kN)	Traffic Class	Road Pavement Thickness (mm)	Road Pavement Cons. Depth (mm)	Embodied Carbon for binders (Co ₂ e/kg) (BSRIA Guide 2022)	Life Cycle Cost (LCC) 35 years	
High	Extremely high									Treated subgrade	Subgrade Removal & Replacement
					55.43	Heavy	40	50			
					31.75	Light	40	50			
ASS1	ASS2	2%Lime+26%GGBS	90	98 – 220	40.82	Medium	40	50	0.0011	£268,383,863	£488,754,774
					55.43	Heavy	40	50			

Where: L = Lime, GGBS = Ground Granulated Blast-furnace Slag, C = Cement, PL = Plastic, GL = Glass and BDW = Brick Dust Waste

Chapter 7 – Conclusion and Recommendation

5.14 CHAPTER SUMMARY

Chapter 5 presented detailed results and discussion of all the tests and analyses conducted to achieve the aim of this research. The dynamics of the results for Atterberg limits Compaction, California Bearing Ratio (CBR), Swell, Durability (Wetting-drying cycles), Microstructural analysis (SEM and EDX), Road pavement thickness and construction depth optimisation, Road pavement defect analysis, DMRB road pavement design, Economic appraisal and embodied carbon were presented in this chapter. The chapter presented a critical analysis and investigations of the dynamics of results achieved in this research and what influenced these results. Furthermore, the chapter referenced similar studies by comparing their results to the research results to buttress, support or disagree with the results of the research. It was observed during the discussion that, all results obtained are within the range of other studies conducted in the subject area in accordance with the standards used in this study. Finally, the chapter concluded that waste materials used as binder/additive agents in this research can improve the engineering properties of road subgrade materials making them useable in road construction. the chapter also emphasised how the results could help achieve some of the UNSDGs by reducing carbon emissions, and overall construction costs using waste materials in road subgrade stabilisation.

Chapter 6 summarises the main conclusions and recommendations of the research work suggesting new areas for further research. The chapter also describes the limitations of this research.

CHAPTER 6 – CONCLUSIONS AND RECOMMENDATIONS

6.1 INTRODUCTION

Chapter 6 presents conclusions of the findings in this research to address the problem of road defects due to expansive road subgrade. The benefits and effects of using sustainable waste materials to reduce the environmental effects of using traditional cement and lime in subgrade stabilisation were summarised in this chapter. Furthermore, the chapter presented conclusions on the analysis carried out on road pavement thickness and construction depth optimisation, Road pavement design using DMRB, economic appraisal and embodied carbon using sustainably treated subgrade materials. Thus, this research has great benefits in terms of technology, economy and environment. Finally, the chapter presented research recommendations for future works.

6.2 REVIEW OF RESEARCH OBJECTIVES

6.2.1 Objective One

Objective one was successfully carried out in this research by providing an intellectual context to achieve the set aim of the research. Even though an in-depth literature review to establish the level of current knowledge on expansive road subgrade stabilisation was addressed in the current study, there were limited or no studies conducted in the area of road pavement design using DMRB and road pavement thickness and construction depth optimisation. This research gap identified has been addressed in this research.

6.2.2 Objective Two

Laboratory tests were conducted in this research in accordance with relevant standards to Investigate the key engineering properties of treated and untreated expansive road subgrade materials. Atterberg limit test, compaction test, California Bearing Ratio (CBR) test and swell test were successfully conducted.

6.2.3 Objective Three

Investigating the microstructural properties of treated subgrade was well carried out achieving good results in this research. The Scanning Electron Microscopy (SEM) and Energy Dispersion X-ray (EDX) method were used to determine the elemental composition of treated expansive road subgrade materials.

Chapter 7 – Conclusion and Recommendation

6.2.4 Objective Four

Road pavement thickness and construction depth optimisation, and road pavement design using DMRB were successfully conducted in compliance with relevant standards and guidelines. The effect of sustainably stabilised expansive road subgrade on the thickness and construction depth of road pavement and road pavement defect using waste materials in subgrade treated was well established.

6.2.5 Objective Five

The durability of sustainably stabilised expansive road subgrade materials was established in this study. The study investigated the durability of treated subgrade using waste materials by carryout a wetting-drying cycle test. Good results were achieved with a decline in CBR values as the cycle number increased.

6.2.6 Objective Six

Life Cycle Cost Analysis (LCCA) was successfully carried out to determine the cost-effects and cost-benefits of using sustainable waste materials in expansive road subgrade stabilisation. The cost dynamics of using waste-treated subgrade compared with subgrade removal and replacement were discussed in the current research.

6.2.7 Objective Seven

The environmental effects and benefits of using sustainable waste materials in road subgrade stabilisation were addressed. The embodied carbon of each binder used in this study was investigated and the UNSDGs achieved in this current research were presented.

6.3 RESEARCH LIMITATIONS

6.3.1 Research Results and Conclusions

The results achieved in this study are experimental results based on laboratory testing and numerical analysis and not real-life field test results. Therefore, the results achieved in this research could defer in a real-life field test. Hence the researcher acknowledges that the findings of this current research could be tested in the field in future studies.

6.3.2 Limited Literature in the Research Area

There was limited literature or previous studies in the area of road pavement thickness, construction depth optimisation and DMRB road pavement design. This made it

Chapter 7 – Conclusion and Recommendation

difficult for the researcher to cite other studies. However, this limitation exposed the research gap that needs filling, hence the novelty of the current research.

6.3.3 Sample Size

The sample size set for this research was very high and was not easy for the researcher to make all these samples. However, for the research results to be considered a true representation, a large sample size was necessary. At a point during the stage of wetting-drying cycles sample preparation, the mechanical compactor broke down and the researcher had to compact CBR samples manually. This could affect the wetting-drying CBR results due to human error and uniform compaction pressure due to fatigue. However, the results achieved in this study are within the range when compared with results achieved in other wetting-dry studies using similar parameters used in this research. Hence this limitation did not significantly impact the conclusions of this research.

6.3.4 Data Analysis

The software applications used in this research were sourced by the researcher as the university could not provide software applications need for use by the researcher. The researcher aimed to conduct finite element analysis on treated subgrade materials using the Abaqus software application, to investigate the stress distributions within the treated subgrade when traffic load is applied. However, this was not possible because the specification of the researcher's laptop computer provided by the university was too low to run the number of nodes. Also, the Abaqus licence installed on the campus computers are student licences and limited to a small number of nodes and loan laptops do not have Abaqus installed on them. So the researcher could not carry out this analysis. However, this limitation did not stop the researcher or affect the conclusions of the research as KENPAV software was sourced by the researcher and used in place of Abaqus to carry out these analyses.

6.3.5 Limited CBR Moulds

During California Bearing Ratio (CBR) sample preparation, there was limited number of CBR mould available to share with other students. The researcher could only make one sample a day and be cured in the mould for up to 28 days. Meaning other students who need to use the CBR mould would have to wait for 28 days for the researcher's sample to cure. This was a huge setback and the researcher could not have made

Chapter 7 – Conclusion and Recommendation

and cured a total of 318 samples within the time frame of the PhD research. Due to this challenge, the researcher found an innovative way to line the inside of the CBR mould using PVC pipes so that freshly compacted CBR samples can be extruded from the mould and cured separately. So, the mould can be used multiple times a day. This limitation did not significantly impact the conclusions of this study because the researcher validated the results for CBR samples cured in PVC pipes by making a total of 8 samples where four samples were cured in CBR mould and the remaining 4 samples cured in PVC pipes. After testing the samples in the CBR mould and PVC pipes, similar results were achieved with a difference of about $\pm 3\%$. The average of these results was used as the true representation of the findings in this study. This confirms that CBR results achieved in this research using PVC pipes are suitable for use. See Appendix 7.1 Research limitations.

6.3.6 Limited Swell Apparatus

They were not enough swell setup apparatus such as dial gauge holders and cross bars for mounting dial gauge on the swell tank. Also due to the limited CBR mould, swell samples were tested in the confines of a PVC pipe. The researcher fabricated cross bars and swell plates using scrap metals and plastics to ensure the research can be completed within the stipulated time of the PhD programme. There was no significant impact of this limitation on the conclusions drawn in this research. The researcher validated the results by conducting swell test using a CBR mould and compared the results to swell test carried out using PVC plastic and the results were similar ($\pm 2\%$). See Appendix 7.1 Research limitations.

6.3.7 Delays in Delivery of Materials

At the start of this research, the university supplied the researcher with materials until a certain point in the research when the researcher was asked to provide their own materials for the research. During this time, materials ordered by the university could sometimes delay for months causing a lot of inconvenience for the researcher in meeting the research limestones. Regardless of these delays, the conclusions drawn in this research were not affected as the researcher worked hard despite the delays to meet the milestones set for the PhD programme.

6.3.8 Financial Constraints

Due to the high cost of some materials used in this study, the researcher was financially drained due to the large sample size and the increase in the price of goods and services in recent times. However high cost of some materials used in this study did not affect the conclusions of the study because quality materials were purchased and the right quantity was used throughout the laboratory stage of this research to ensure good and valid results are achieved.

6.4 REVIEW OF RESEARCH FINDINGS

6.4.1 Preliminary Findings

High liquid limit, plastic limit and plasticity index were recorded for subgrade materials (ASS2) composed of high bentonite content. this shows that the amount of bentonite present in the mix can influence the moisture content of the subgrade materials. this means bentonite imbibes water and has high swell potential.

6.4.2 California Bearing Ratio (CBR)

Untreated subgrade materials unsoaked recorded very low CBR values with their soaked CBR values below 2% making them unacceptable for use. Despite the low CBR values achieved for untreated subgrade materials, using waste materials in treating the subgrade improved their CBR significantly making them usable in road construction.

6.4.3 Swell

Swell test results achieved for untreated subgrade materials were high and above the unacceptable limit of 2.5%, hence cannot be used and requires treatment. However, a drastic reduction in swell was observed after treating subgrade using sustainable waste materials. These swell values were below the unacceptable limit and are suitable for use.

6.4.4 Durability

Durability tests carried out using the wetting-drying cycle approach saw a gradual reduction in CBR values after each cycle. however, at the end of the ten cycles, the CBR values recorded for both wet cycle and dry cycles were above the unacceptable limit of 2%. This shows that subgrade treated using waste materials are durable and can withstand repeated wet and dry weather conditions for many years.

Chapter 7 – Conclusion and Recommendation

6.4.5 Microstructural Properties

The microstructural properties of the treated subgrade exhibited high formation of CSH gel responsible for strength gain. This confirms that waste materials have the ability to enhance the engineering properties of subgrade materials and can be used as partial replacements for cement and lime.

6.4.6 Road pavement Analysis

Road pavement thickness and depth of construction were reduced when waste materials were used in subgrade treatment. This shows that using waste materials to improve the strength and bearing capacity of road subgrade could result in a reduction of road pavement thickness and depth of construction, hence reducing overall road construction cost. Good CBR values were achieved for use in the design of road pavement using the DMRB guide when waste materials were used in road subgrade treatment. The result showed a slight reduction in pavement thickness for varying traffic designs. In determining the ability of waste-treated subgrade to withstand defects, a road pavement defect analysis was conducted. The results showed a reduction in stresses, permanent deformation, Fatigue and rutting failure after treating subgrade using waste materials.

6.4.7 Economic Appraisal

The long-term cost of road projects are very important and must be considered during the design stage. This research conducted a Life cycle Cost analysis (LCCA) for treated and untreated road subgrade. At the end of the analysis, it was observed that waste-treated subgrade recorded the lowest Life cycle Cost. This means long-term cost reduction of road projects could be achieved using waste materials in subgrade stabilisation.

6.4.8 Environmental Effects

The environmental benefits of using waste materials in subgrade stabilisation were investigated by calculating the embodied carbon for all waste materials used in this research. The lowest embodied carbon was recorded for subgrade treated using sustainable waste materials. Furthermore, findings in the current research achieved some of the United Nations Sustainable Development Goals (UNSDGs) and when implemented would lead to a greener and cleaner way of construction.

6.5 IMPLICATIONS OF THE RESEARCH FINDINGS

Findings from this research provide sustainable and environmentally friendly solutions to solving the problems of road pavement defects caused by expansive subgrade and the high cost of road construction. The research findings show the feasibility of using waste materials in road subgrade stabilisation to reduce road pavement thickness and construction depth and road pavement defects. The research findings also sustainable solutions to the environmental and climate change problems associated with stabilising expansive road subgrade using traditional cement and lime. The findings provide sustainable and eco-friendly alternatives to cement and lime to reduce the over-reliance on natural resources such as clinker. The findings of this study also address the problem of landfill by providing ways to use waste materials normally dumped in landfill during road construction. Findings from this research provide sustainable solutions to deal with the problem of carbon dioxide emission. Very high amounts of carbon dioxide are emitted into the atmosphere each year due to cement and lime production leading to the current climate change challenges. Using waste materials as partial replacement for cement and lime in road subgrade treatment would reduce the use of cement and lime hence reducing carbon dioxide emission. The findings of this research achieved some of the United Nations Sustainable Development Goals (UNSDGs) focused on reducing greenhouse gas emissions, winning the fight against climate change, and protecting the planet.

6.6 CONTRIBUTION TO THE BODY OF KNOWLEDGE

- Little or no attention has been devoted to the use of waste and industrial by-products as cement and lime replacement in the engineering of road pavement design to withstand the deteriorating effect due to traffic load and investigate pavement thickness and construction depth. This research has contributed to filling this gap by investigating and finding possible use of waste and industrial by-products in subgrade stabilisation to reduce road pavement thickness, construction depth and the deteriorating effect of road pavement due to traffic load.
- There are several pavement design techniques available to determine the thickness of road pavement for specific designs, but no method specifically established the exact mix design of waste materials required in road subgrade

Chapter 7 – Conclusion and Recommendation

stabilisation to achieve reduced pavement and construction depths for expansive subgrades with varying plasticity index. And this is one of the key findings and contributions of the research to the body of knowledge.

- The area of elimination or reduction of defects in road pavement structure for high plasticity index subgrade stabilised using waste materials has not been explored. This research has contributed to fill this gap by reducing road pavement defects for high plasticity index subgrade stabilised using waste materials.
- Little or no attention has been devoted to reducing the Life Cycle Cost Analysis (LCCA) of road pavement by using sustainable waste materials as partial replacements for cement and lime in expansive road subgrade stabilisation. This research has contributed to filling this gap by conducting a Life Cycle Cost Analysis (LCCA) of road pavement by using sustainable waste materials as partial replacement for cement and lime in expansive road subgrade stabilisation.

6.7 CONCLUSIONS

The findings of this research show the possibility of improving the engineering properties of expansive road subgrade materials using waste materials normally dumped in landfills while saving the environment and reducing defects, pavement thickness and Life Cycle Cost (LCC) of roads. The conclusions of this research are as follows:

6.7.1 Ranking of Treatments

After treating expansive road subgrade using waste materials, mix proportion 2%Lime + 2.5% Cement + 23.5% GGBS with unsoaked CBR value of 92%, soaked CBR value of 97% after 28 days of curing and swell value of 0.32% after 4 days of soaking and CBR value of 200% was recorded after 90 days of curing makes mix design composed of 23.5%GGBS the best performing mix in this study. The second-best performing mix was recorded for mix proportion 2%Lime + 2.5% Cement + 11.75% BDW + 11.75%GGBS which achieved unsoaked CBR value of 109%, soaked CBR value of 67% after 28 days of curing and swell value of 0.42% after 4 days of soaking. The mix further recorded a CBR value of 180% after 90 days of curing respectively. Mix proportion 2%Lime + 2.5% Cement + 23.5%Plastic recorded unsoaked CBR values

Chapter 7 – Conclusion and Recommendation

of 13%, soaked CBR value of 12% after 28 days of curing and swell value of 0.59% after 4 days of soaking. Followed by mix proportion 2%Lime + 2.5% Cement + 23.5% Glass with unsoaked CBR value of 16%, soaked CBR value of 11% after 28 days of curing and swell value of 0.46% making mix design composed of recycled plastic and glass the worst performing mix in this study.

The treatment ranking proves that GGBS is the best-performing additive/binder in this research due to its ability to improve the engineering properties of subgrade materials resulting in very high CBR and low swell values when added to a mix design. The high CBR values recorded for mix designs composed of GGBS resulted in the reduction in pavement thickness, depth of construction and LCC of road pavement. Furthermore, stresses within the subgrade responsible for pavement defects such as fatigue, rutting and permanent deformation were reduced for mix designs composed of GGBS due to its ability to increase CBR values and reduce swell of expansive road subgrade.

6.7.2 Enhancement of Engineering Properties

The engineering properties of expansive subgrade materials were enhanced with the addition of sustainable waste materials. Further details of how the engineering properties of expansive subgrade were improved are as follows:

1. The engineering properties of expansive road subgrade were improved as CBR values for ASS materials increased with an increase in curing age after using sustainable waste materials as binders in subgrade stabilisation. Very high CBR values were recorded for all ASS materials soaked and un-soaked with an increase in curing age with the addition of waste materials proving that sustainable waste materials can be used as partial replacement for cement and lime in a mixture.
2. Cement and lime can partially be replaced with sustainable waste materials such as GGBS can be used due to their ability to exhibit extremely high CBR values for ASS materials due to the high amount of calcium present in GGBS responsible for the formation of C-S-H and C-A-H gel. Adding BDW to GGBS in a mix would escalate the engineering performance of stabilised road subgrade because BDW are pozzolans that activate pozzolanic reaction

Chapter 7 – Conclusion and Recommendation

responsible for the formation of C-S-H and C-A-H gel, which acted as a binding agent responsible for strength gain in subgrade materials.

3. Untreated bentonite exhibited a naturally high bearing capacity even though they are highly susceptible to swelling. However, their naturally high CBR was affected by the addition of binders leading to a reduction in the bearing capacity of expansive subgrade materials composed of high bentonite content.
4. A reduction in CBR value with an increase in swell was observed for extremely high bentonite subgrade material (ASS2). There was no indication of CBR values increase with respect to curing age for mixtures composed of recycled glass or plastic because glass or plastic do not react with cement and lime to form C-S-H gel to increase CBR in a mixture. However, their interlock ability during the mechanical stabilisation (compaction) process helped with strength increase in subgrade materials.
5. Soaked CBR samples generally observed a reduction in CBR value with high swell values compared with un-soaked CBR samples. CBR values for soaked samples composed of high recycled plastic or glass content were generally low with a high swell value due to their granular nature allowing air and water to pass through.
6. Extremely high plasticity and high plasticity subgrade materials exhibit very high swell potentials and the addition of sustainable binders reduced swell and improved other engineering properties of expansive subgrade. Subgrade stabilised using sustainable waste materials and industrial by-products are durable and can withstand wetting-drying conditions for several cycles without losing their strength. CBR values obtained for sustainably treated subgrade of wetting-drying cycles were very high and suitable for use in subgrade stabilisation.

Chapter 7 – Conclusion and Recommendation

6.7.3 Effect on Road Pavement

The used of sustainable waste materials improved the engineering properties of expansive subgrade and the resulting effects are as follows:

1. Besides improving the engineering properties of expansive subgrade using sustainable waste materials, the improvement resulted in a reduction in pavement thickness and depth of construction with an increase in CBR values using various pavement design guidance.
2. A significant difference in pavement thickness and depth of construction was observed between using the lowest and the highest CBR value and between light and heavy traffic types. Hence, the higher the CBR value the thinner the pavement thickness and the shallower the depth of construction.
3. The thinnest pavement and shallowest construction depth was recorded for the best performing mix ASS1+ 2% lime + 2.5% Cement + 11.75% GGBS + 11.75% BDW after 28 days of curing with a CBR of 109%. Similar to this observation was found for depth of construction, which saw a reduction corresponding to reduced swell for soaked ASS samples. Hence, the higher the swell potential of subgrade materials the thicker and deeper the pavement and vice versa.
4. A reduction in swell value was observed with a reduction in pavement thickness and construction depth after comparing pavement thickness for soaked ASS samples with their swell values it was observed. A reduction in pavement thickness and construction depth achieved in this research proves that sustainable waste materials can be used to achieve thinner pavement through subgrade stabilisation.
5. A high potential for pavement damage was observed with an increase in stresses within the road subgrade due to weak subgrade. A decrease in these stresses within the subgrade was observed with an increase in the CBR value of the subgrade using sustainable waste materials. This means that sustainably treated expansive with very high CBR values can withstand pavement defects for longer compared with untreated ASS with low CBR values.

Chapter 7 – Conclusion and Recommendation

6. Increased stresses were observed with an increase in pavement thickness due to low CBR values. Therefore, subgrades with low CBR values have thicker pavement to help reduce the stresses within the subgrade emanating from traffic load.
7. This study established that the higher the stress concentration the more likely a crack may initiate and the greater the applied stress range, the shorter the pavement life. This means subgrade materials with high CBR can withstand fatigue, rutting and permanent deformation for a long time before failure occurs compared with subgrade materials with low CBR values. In addition, load repetition achieved for various pavements shows the number of times cyclical stresses can be applied before the pavement finally fail under repeated load.

6.7.4 Microstructural Analysis

Expansive subgrade materials treated using waste materials as binders developed strength and high bearing capacity. Details of the strength improvement observed after conducting microstructural analysis are as follows:

1. SEM and EDX analysis shows high formation of C-S-H gel with the addition of sustainable waste materials as binders. The formation of additional C-S-H gel through the pozzolanic process was due to the addition of BDW which is a pozzolanic material.
2. High amounts of C-S-H gels were formed for samples composed of high GGBS due to the high Calcium and silica content in GGBS responsible for strength gain.
3. Higher C-S-H gels are formed with an increase in curing age for subgrade materials treated using sustainable waste. The presence of other elements apart from Calcium (Ca) are of low contribution to the hydraulic activity of the system.
4. Ettringites responsible for expansion in road subgrade were found in all samples but predominantly in a sample composed of high bentonite content.

6.7.5 Cost Effects

The Life Cycle Cost (LCC) of road pavement was affected after stabilising expansive subgrade using sustainable waste materials as detailed as follows:

1. The Life Cycle Cost (LCC) of road pavement with subgrade stabilised using sustainable waste materials show a rise in maintenance and rehabilitation costs with a rise in the discount rate as the age of the road increase. A huge rehabilitation and maintenance cost was observed at the later age in years 28 and 30 years of the road.
2. The LCC for subgrade stabilisation using sustainable waste and subgrade removal and replacement was greatly influenced by the initial cost at year 0. This shows that the initial cost incurred during the construction of road pavement can influence the LCC of the road.
3. The high cost of subgrade removal and replacement was influenced by the disposal options, availability and cost of replacement materials, and cost of equipment and operations.
4. The highest LCC cost for stabilising a square meter of road subgrade using sustainable waste materials was recorded for a mix design of 2% lime + 2.5% cement + 11.75% GGBS + 11.75% Plastic due to the high cost of plastic used in this study. After the LCCA, a huge difference in cost was observed between subgrade materials stabilised using sustainable waste materials and subgrade materials removed and replaced with foreign material. The cost of using sustainable waste materials exceeded the cost of using cement and lime in subgrade stabilisation however they are economical and environmentally friendly.
5. The lowest LCC was recorded for traditional cement and lime (control mix) treated subgrade. However, there was no significant difference between the LCC of the cheapest sustainably treated subgrade and the LCC of the control mix. This makes using waste materials an option in road construction due to their environmental benefits.

Chapter 7 – Conclusion and Recommendation

6.7.6 Environmental and Sustainability

The effect of these research findings on the environment and sustainability of the process are outlined as follows:

1. This study has shown that using cement and lime as binders in subgrade stabilisation are associated with high emissions from cement and lime production and the energy used in this process. Using sustainable waste materials in road subgrade stabilisation would help reduce cost and the environmental damage (carbon emission) due to cement and lime production. This would also help curtail the climate change problem society faces today.
2. This research achieved some of the UNSDGs including Goal 9 - Industry, Innovation, and Infrastructure, Goal 12 - Responsible Consumption and Production and Goal 13 - Climate Action. Achieving these goals would help in the fight against climate change to achieve a more sustainable and carbon-free environment.
3. Waste materials used as binders in place of cement and lime in subgrade stabilisation will help reduce the greenhouse gas emitted to the atmosphere due to cement and lime production as well as reduce the environmental effect associated with brick stockpiles and landfills.
4. The sustainable material combinations used as binders through this research for road subgrade stabilisation would reduce the demand for cement and lime leading to more sustainable and greener road construction.
5. The sustainable waste materials used in this research provided an alternative to traditional cement and lime. The addition of GGBS provided more effective and sustainable ways to achieve even higher engineering properties than cement and lime provide. Hence, using waste materials like GGBS would reduce the demand for cement and lime which would translate to a reduction in cement and lime production and its associated emission.
6. Sustainable stabilised subgrade recorded the lowest embodied carbon compared with traditional cement and lime which are associated with high

Chapter 7 – Conclusion and Recommendation

greenhouse gas emissions and are non-environmentally friendly. These findings prove that using sustainable waste materials in subgrade stabilisation would help reduce the effect of climate change due to carbon emissions during road construction.

6.8 RECOMMENDATIONS

6.8.1 Recommendations for Clients and Decision-makers

Clients and decision-makers must investigate the Life Cycle Cost (LCC) of road projects before making any investment decisions. Clients can save money and make informed decisions by achieving cheaper Life Cycle Costs (LCC) of road using waste materials in subgrade treatment.

6.8.2 Recommendations for Designers

When expansive subgrade materials are encountered on site, road designers recommend the use of waste materials in subgrade stabilisation to the client to push the drive towards sustainable road construction. Designers can give discounts on road projects using waste materials as stabilisation agents. Institutionalising a significant percentage discount for such projects across all consultancy firms would encourage clients to invest in sustainable projects to reduce carbon emissions due to the use of cement and lime.

6.8.3 Recommendations for Road Contractors

Expansive soil encounters on-site during road construction should be stabilised or treated using sustainable waste materials. Road constructors who propose to use waste materials in road construction should be given special consideration during the bidding process. This would encourage construction companies to move towards a more sustainable and eco-friendly way of construction.

6.8.4 Recommendations for Policy-makers

Policy-makers can review the current road construction regulation to identify the hindrance and bottlenecks that resist the use of waste materials in road construction. Removing these hindrances would encourage clients, contractors and designers to consider an eco-friendly way for wider application in construction.

Chapter 7 – Conclusion and Recommendation

6.8.5 Recommendation for Future Research

Even though this research investigated a wide range of parameters related to expansive road subgrade stabilisation and their cost effects, there are still areas and scopes that can further be investigated based on the finding of this current research.

The following recommendation is outlined for further work:

1. The mix composition of the best performing mixes and the worst performing mixes can be changed to determine their effect on the engineering properties of subgrade materials.
2. Further investigation into the use of cheaper sustainable waste materials can be done to further reduce the cost of road subgrade stabilisation
3. Durability tests like freezing and thawing, sulphate attack, water adsorption and water permeability can be conducted on the various mix design to ascertain the durability of the various mixtures.
4. Samples with low CBR values can be cured for longer periods (such as 56 and 90 days) to see their true strength.
5. Other sustainable waste materials like road cam, fly ash, rice husk etc can be used in subgrade stabilisation to see their effect in improving their engineering properties.

6.9 CHAPTER SUMMARY

The conclusions drawn in the current study were presented in Chapter 9. The chapter presents a summarised conclusion on the ability of waste materials to enhance of engineering properties of subgrade, the effect of using waste materials as stabilisation agents on road pavement, and how the microstructural properties of subgrade improved with the addition of waste materials as binders. Chapter 9 also concluded the cost effect and benefit (Life Cycle Cost Analysis (LCCA)) of stabilising subgrade materials using waste which are normally dumped in landfill. Furthermore, the environmental benefits and sustainability of using waste materials in road subgrade treatment were mentioned in this chapter. Finally, the chapter concluded that using waste materials in road subgrade stabilisation can improve subgrade strength, reduce road pavement thickness and construction depth, reduce road pavement defects, reduce negative environmental effects due to carbon emission, reduce the Life Cycle

Chapter 7 – Conclusion and Recommendation

Cost of road and provide a sustainable and eco-friendly way of road subgrade stabilisation. The chapter presented recommendations for clients, decision-makers, designers, contractors, and policy-makers. Areas for further research based on the finding of this current study were also recommended in this chapter.

REFERENCES

1. A Chart to Estimate CBR of Plastic Soils: A Case-Study from Queensland, *Australia*,
2. Abbey, S. J., Eyo, E. U. and Ng'ambi, S. (2019). Swell and Microstructural Characteristics of High-Plasticity Clay Blended with Cement. *Bulletin of Engineering Geology and the Environment*, 79(4), 2119–2130.
<https://doi.org/10.1007/s10064-019-01621-z>
3. Abbey, S. J., Ngambi, S. and Ganjian, E. (2017). Development of Strength Models for Prediction of Unconfined Compressive Strength of Cement/By-product Material Improved Soils. *Geotechnical Testing Journal*, 40(6), 20160138. <https://doi.org/10.1520/GTJ20160138>
4. Abbey, S., Olubanwo, A., Ngambi, S. and Tetteh, F. K. (2018). Strength and Hydraulic Conductivity of Cement and By-Product Cementitious Materials Improved Soil. *International Journal of Applied Engineering Research*, 13(0973–4562), 8684–8694.
5. Abbey, S.J., Eyo, E.U. and Jeremiah, J.J. (2021). Experimental Study On Early Age Characteristics of Lime-GGBS-Treated Gypseous Clays Under Wet-dry Cycles. *Geotechnics*, 1, 0019.
6. ABG Geosynthetics, 2020. Creative Geosynthetic Engineering.
<http://www.abg-geosynthetics.com/products/abgrid.html>. (Accessed 15 June 2020).
7. ACPA Concrete Pavement Technology Series. (2021) Expansive Soil.
<http://1204075.sites.myregisteredsite.com/downloads/TS/EB204P/TS204.2P.pdf>
8. Afrin, H. (2017). A Review on Different Types Soil Stabilization Techniques. *International Journal of Transportation Engineering and Technology*, 3(2), 19.
<https://doi.org/10.11648/j.ijtet.20170302.12>
9. Ahmad, T. and Khawaja, H. (2018). Review of Low-temperature Crack (LTC) Developments in Asphalt Pavements, *The International Journal of Multiphysics* 12 (2) (2018). 169–188, <https://doi.org/10.21152/1750-9548.12.2.169>.
10. Al-Baidhani, A. A. and Al-Taie, A. (2019). Review of Brick Waste in Expansive Soil Stabilization and Other Civil Engineering Applications. *Journal of*

References

- Geotechnical Studies*, 4(3), 14–23.
<http://matjournals.in/index.php/JoGS/article/view/4305>
11. Ali, A.A., Abde, M. and Esraa, M.A. (2014). Re-use of Waste Marble Dust In The Production of Cement and Concrete, *Construction and Building Materials*.
<https://doi.org/10.1016/j.conbuildmat.2013.09.005>.
 12. Allaboutengineering, 2022. <https://allabouteng.com/difference-between-flexible-pavement-and-rigid-pavement/> (accessed on 22 January 2022).
 13. Al-Rawas, A. A. and Goosen, M. F. A. (2006). *Expansive Soils*. CRC Press.
<https://doi.org/10.1201/9780203968079>
 14. Al-Rawas, A. A., Hago, A. W. and Al-Sarmi, H. (2005). Effect of Lime, Cement And Sarooj (Artificial Pozzolan) On The Swelling Potential of An Expansive Soil From Oman. *Building and Environment*, 40(5), 681–687.
<https://doi.org/10.1016/j.buildenv.2004.08.028>
 15. Alrubaye, A. J., Hasan, M. and Fattah, M. Y. (2016). Improving Geotechnical Characteristics of Kaolin Soil Using Silica Fume and Lime. *Special Topics & Reviews in Porous Media: An International Journal*, 7(1), 77–85.
<https://doi.org/10.1615/SpecialTopicsRevPorousMedia.v7.i1.70>
 16. Al-Tabbaa, A. and Evans, C. (2003). Deep Soil Mixing In The UK: Geoenvironmental Research And Recent Applications. *Land Contamination and Reclamation*, 11(1), 1–14. <https://doi.org/10.2462/09670513.620>
 17. Amena, S. (2021). Experimental Study on the Effect of Plastic Waste Strips and Waste Brick Powder on Strength Parameters of Expansive Soils. *Heliyon*, 7(11), e08278. <https://doi.org/10.1016/j.heliyon.2021.e08278>
 18. Amena, S. and Chakeri, D. (2022). A Study on The Effects of Plastic Waste Strips and Lime on Strength Characteristics of Expansive Soil. *Advances in Civil Engineering*, 2022, 1–6. <https://doi.org/10.1155/2022/6952525>
 19. American Association of State Highway and Transportation Officials. (2022). *AASHTO T265 – Standard Method of test for laboratory determination of moisture content of soil* (pp. 1–5).
 20. American Association of State Highway and Transportation Officials. (2022). *AASHTO T90 – standard method of test for determining the plastic limit and plasticity index of soils*.1–6)

References

21. American Association of State Highway and Transportation Officials. (2021). *AASHTO T193-13 – Standard method of test for the California bearing ratio*. 1–12.
22. Anand, G., Agrawal, S. and Dobriyal, A. (2014). Stabilisation of Cohesive Soil Using Demolished Brick Waste. *Innovations and Advances in Civil Engineering towards Green and Sustainable Systems*.
23. Aneke, F., Hassan, M. and Moubarak, A. (2019). Shear strength behaviour of stabilised unsaturated expansive subgrade soil for highway backfill. *Bituminous Mixture and Pavements VII. Nikolaidis & Manthos (Eds) Conference: Bituminous Mixture and Pavement*.
24. Arefnia, A., Momeni, E., Jahed Armaghni, D., Anuar Kassim, K. and Ahmad, K. (2014). Effect of Tire Derived Aggregate on Maximum Dry Density of Kaolin. *Jurnal Teknologi*, 66(1). <https://doi.org/10.11113/jt.v66.1704>
25. Asad, Md. A., Kar, S., Ahmeduzzaman, M. and Hassan, Md. R. (2013). Suitability of Bentonite Clay: An Analytical Approach. *Earth Sciences*, 2(3), 88. <https://doi.org/10.11648/j.earth.20130203.13>
26. Ashraf, A., Sunil, S., Dhanya, J., Joseph, M., Varghese, M. and Veena, M. (2011). Soil Stabilisation Using Raw Plastic Bottles. *Proceedings of Indian Geotechnical Conference*.
27. ASTM International. (2017). *ASTM D4318-17e1 Standard Test Methods for Liquid Limit, Plastic Limit, and Plasticity Index of Soils*. 1–20.
28. ASTM International. (2019). ASTM D2216-19 Standard Test Methods for Laboratory Determination of Water (Moisture) Content of Soil and Rock by Mass. In *ASTM International* (pp. 1–7).
29. ASTM International. (2019). ASTM-D5890 › Standard Test Method for Swell Index of Clay Mineral Component of Geosynthetic Clay Liners. In *ASTM International* (pp. 1–7).
30. Ateş, A. (2016). Mechanical properties of sandy soils reinforced with cement and randomly distributed glass fibres (GRC). *Compos. Part B Eng.* 96, 295–304.
31. Athanasopoulou, A. (2016). The Role of Curing Period on the Engineering Characteristics of A Cement-Stabilized Soil. *Romanian Journal of Transport Infrastructure*, 5(1), 38–52. <https://doi.org/10.1515/rjti-2016-0041>

References

32. Aubeny, C. and Lytton, R. (2002). Properties of High-Plasticity Clays. <https://static.tti.tamu.edu/tti.tamu.edu/documents/2100-2.pdf>
33. Babashamsi, P., Md Yusoff, N. I., Ceylan, H., Md Nor, N. G. and Salarzadeh Jenatabadi, H. (2016). Evaluation of Pavement Life Cycle Cost Analysis: Review and Analysis. *International Journal of Pavement Research and Technology*, 9(4), 241–254. <https://doi.org/10.1016/j.ijprt.2016.08.004>
34. Bahar, R., Benazzoug, M. and Kenai, S. (2004). Performance of Compacted Cement-Stabilised Soil. *Cement and Concrete Composites*, 26(7), 811–820. <https://doi.org/10.1016/j.cemconcomp.2004.01.003>
35. Balkıs, A. and Macid, S. (2019). Effect of Cement Amount on CBR Values of Different Soil . *Avrupa Bilim ve Teknoloji Dergisi* , (16) , 809-815 . DOI: 10.31590/ejosat.588990
36. Bailey, S. W. (1988). Hydrous Phyllosilicates. *American Mineralogical Society*, Washington DC. <https://doi.org/10.1180/claymin.1989.024.4.11>
37. Baker, M. L., Baas, J. H., Malarkey, J., Jacinto, R. S., Craig, M. J., Kane, I. A. and Barker, S. (2017). The Effect of Clay Type on The Properties of Cohesive Sediment Gravity Flows and Their Deposits. *Journal of Sedimentary Research*, 87(11), 1176–1195. <https://doi.org/10.2110/jsr.2017.63>
38. Bananezhad, B., Islami, M. R., Ghonchepour, E., Mostafavi, H., Tikdari, A. M. and Rafiei, H. R. (2019). Bentonite Clay As An Efficient Substrate for The Synthesis of The Super Stable and Recoverable Magnetic Nanocomposite of Palladium (Fe₃O₄/Bentonite-Pd). *Polyhedron*, 162, 192–200. <https://doi.org/10.1016/j.poly.2019.01.054>
39. Bandara, N., Elin, J., Binoy, T. H. (216 C.E.). Performance Evaluation of Subgrade Stabilization with Recycled Materials. *National Concrete Pavement Technology Center*. <https://cptechcenter.org/ncc-projects/performance-evaluation-of-subgrade-stabilization-with-recycled-materials/>
40. Barbieri, D. M., Lou, B., Dyke, R. J., Chen, H., Zhao, P., Memon, S. A. and Hoff, I. (2022). Calcium Bentonite and Sodium Bentonite As Stabilizers for Roads Unbound. *Cleaner Engineering and Technology*, 6, 100372. <https://doi.org/10.1016/j.clet.2021.100372>
41. Beeghly, J.H., 2003. Recent Experiences With Lime-Fly Ash Stabilisation of Pavement Subgrade Soils Base, and Recycled Asphalt. In: *International Ash Utilisation Symposium*, p. 8.

References

42. Bekhiti, M., Trouzine, H. and Rabehi, M. (2019). Influence of Waste Tire Rubber Fibers on Swelling Behavior, Unconfined Compressive Strength and Ductility of Cement Stabilized Bentonite Clay Soil. *Construction and Building Materials*, 208, 304–313. <https://doi.org/10.1016/j.conbuildmat.2019.03.011>
43. Bektas, F. (2007). Use of Ground Clay Brick as A Supplementary Cementitious Material In Concrete Hydration Characteristics, Mechanical Properties, And ASR Durability. PhD thesis. 1 – 149. <https://doi.org/10.31274/rtd-180813-6631>
44. Bell, F. G. (1996). Lime Stabilization of Clay Minerals And Soils. *Engineering Geology*, 42(4), 223–237. [https://doi.org/10.1016/0013-7952\(96\)00028-2](https://doi.org/10.1016/0013-7952(96)00028-2)
45. Bell, F. G. and Coulthard, J M. (1990). Stabilization of Clay Soils with Lime. *National Academies, Science Engineering and Medicine*, 7(3), 125–140. <https://trid.trb.org/view/353305>
46. Benhammou, A., Tanouti, B., Nibou, L., Yaacoubi, A. and Bonnet, J.-P. (2009). Mineralogical and Physicochemical Investigation of Mg-Smectite from Jbel Ghassoul, Morocco. *Clays and Clay Minerals*, 57(2), 264–270. <https://doi.org/10.1346/CCMN.2009.0570212>
47. Benhelal, E., Zahedi, G., Shamsaei, E. and Bahadori, A. (2013). Global Strategies and Potentials To Curb CO₂ Emissions In Cement Industry. *Journal of Cleaner Production*, 51, 142–161. <https://doi.org/10.1016/j.jclepro.2012.10.049>
48. Bentabol, M., Ruiz Cruz, M. D. and Huertas, F. J. (2009). Isomorphous Substitution vs. Defect Density In Hydrothermally Synthesized (200 °C) Fe³⁺, Ga³⁺ and Cr³⁺-Substituted Kaolinites. *Applied Clay Science*, 45(1–2), 36–43. <https://doi.org/10.1016/j.clay.2009.04.004>
49. Besq, A., Malfoy, C., Pantet, A., Monnet, P. and Righi, D. (2003). Physicochemical Characterisation and Flow Properties of Some Bentonite Muds. *Applied Clay Science*, 23(5–6), 275–286. [https://doi.org/10.1016/S0169-1317\(03\)00127-3](https://doi.org/10.1016/S0169-1317(03)00127-3)
50. Bezner. (2022). Waste Management Solutions. *Bezner.Com*. <https://www.bezner.com/>
51. Bhaskaran, M., Sriram, S., Holland, A. S. and Evans, P. J. (2009). Characterisation of Nickel Silicide Thin Films By Spectroscopy And

References

- Microscopy Techniques. *Micron*, 40(1), 99–103.
<https://doi.org/10.1016/j.micron.2007.12.008>
52. Blayi, R. A., Sherwani, A. F. H., Ibrahim, H. H. and Abdullah, S. J. (2020). Stabilization of High-Plasticity Silt Using Waste Brick Powder. *SN Applied Sciences*, 2(12), 1989. <https://doi.org/10.1007/s42452-020-03814-8>
53. Bo, M. W., Arulrajah, A., Choa, V., Horpibulsuk, S. and Disfani, M. M. (2015). Deep Compaction of Granular Fills in a Land Reclamation Project by Dynamic and Vibratory Compaction Techniques. In *Ground Improvement Case Histories*. 263–274. <https://doi.org/10.1016/B978-0-08-100698-6.00008-8>
54. Boardman, D. I, Glendinning, S., and Rogers, C. D. F. (2001). Development of Stabilisation and Solidification In Lime–Clay Mixes. *Géotechnique*, 51(6), 533–543. <https://doi.org/10.1680/geot.2001.51.6.533>
55. Booth, C., Hammond, F., Lamond, J. and Proverbs, D. (2012). Solutions For Climate Change Challenges For The Built Environment. *Innovation in the Built Environment*.
56. Bristow, C. M. (1993). The Genesis of the China Clays of South-West England - A Multistage Story. In *Kaolin Genesis and Utilization*. Clay Minerals Society. <https://doi.org/10.1346/CMS-SP-1.8>
57. Bristow, C. M. (1994). Historical and Geological Aspects of The China Clay Industry of Southeast England. *Transactions of the Royal Geological Society of Cornwall*, 247–314.
58. British Geological Survey, (2021) <https://www.bgs.ac.uk/geology-projects/shallow-geohazards/clay-shrink-swell/> (accessed 17th August 2021).
59. British Lime Association. (2015). *Soil stabilisation with lime, cement and other binders*.
60. British Standard. (2004). BS EN 13286-49:2004 - Unbound and Hydraulically Bound Mixtures - Accelerated Swelling Test for Soil Treated By Lime and/or Hydraulic Binder. In *British Standard*.
61. British Standard. (2021). BS EN ISO 17892-12:2018+A1:2021 - Geotechnical Investigation and Testing. Laboratory Testing of Soil Determination of Liquid and Plastic Limits. In *British Standard*.
62. British Standards. (1990). BS 1377-4:1990 Methods of Test for Soils for Civil Engineering Purposes - Compaction-Related Tests. In *British Standards*. British Standards.

References

63. British Standards. (2010). Unbound and Hydraulically Bound Mixtures - Test Methods for Laboratory Reference Density and Water Content. Proctor Compaction. In *British Standards*. British Standards.
64. British Standards. (2014). BS EN ISO 17892-1:2014 Geotechnical Investigation and Testing - Laboratory Testing of Soil. Determination of Water Content. *British Standards*.
65. British Standards. (2018). BS 1924-1:2018 - Hydraulically Bound and Stabilized Materials for Civil Engineering Purposes - Sampling, Sample Preparation and Testing of Materials Before Treatment. In *British Standards*.
66. Brooks, J., A. (1973). Glass. *Journal of Glass Studies*, 17, 176–213.
67. Cabalar, A. and Karabash, Z. (2015). California Bearing Ratio of a sub-base materials modified with tire buffings and cement addition. *Journal of Testing and Evaluation*, 43(6). DOI: 10.1520/JTE20130070.
68. Cabezas, R. and Cataldo, C. (2019). Influence of Chemical Stabilization Method and Its Effective Additive Concentration (EAC) In Non-Pavement Roads. A Study In Andesite-Based Soils. *Cogent Engineering*, 6(1). <https://doi.org/10.1080/23311916.2019.1592658>
69. Campbell W. P. and William. P. (2003). Brick - A World History (1st ed.). *Thames and Hudson*, London.
70. Celik, E. and Nalbantoglu, Z. (2013). Effects of Ground Granulated Blastfurnace Slag (GGBS) On The Swelling Properties of Lime-Stabilized Sulfate-Bearing Soils. *Engineering Geology*, 163, 20–25. <https://doi.org/10.1016/j.enggeo.2013.05.016>
71. Central Electricity Authority. (1987). Report of The World Commission On Environment And Development. In *United Nations*. United Nations.
72. Central Electricity Authority. (2015). Central Electricity Authority, Report on Fly Ash Generation at Coal/Lignite Based Thermal Power Station and Its Utilization in the Country for the Year 2014-15.
73. Chakraborty, S., Mahmud, T., Islam, M.M. and Islam, M.S. (2014). Use of Paper Industry Waste In Making Low Cost Concrete. *2nd International Conference on Advances in Civil Engineering*, 1–6. https://www.researchgate.net/publication/293810073_Use_of_Paper_Industry_Waste_in_Making_Low_Cost_Concrete

References

74. Chandola, S. P. (2001). A Textbook of Transportation Engineering - For civil Engineering Students of All Indian Universities and Practicing Engineers (1st ed.). *Schand*.
75. Chawla, L. S. and Gupta R. K. (1993). Materials Selection for Corrosion Control. *ASM International*, 327–328.
76. Chen, H. and Wang, Q. (2006). The Behaviour of Organic Matter In The Process of Soft Soil Stabilization Using Cement. *Bulletin of Engineering Geology and the Environment*, 65(4), 445–448.
<https://doi.org/10.1007/s10064-005-0030-1>
77. Chen, K., and Kurgan, L. (2009). Investigation of Atomic Level Patterns in Protein—Small Ligand Interactions. *PLoS ONE*, 4(2), e4473.
<https://doi.org/10.1371/journal.pone.0004473>
78. Cheng, Y. and Huang, X. (2019). Effect of Mineral Additives on the Behavior of an Expansive Soil for Use in Highway Subgrade Soils. *Applied Sciences*, 9(1), 30. <https://doi.org/10.3390/app9010030>
79. Chmielarz, L., Kuśtrowski, P., Piwowarska, Z., Dudek, B., Gil, B. and Michalik, M. (2009). Montmorillonite, Vermiculite and Saponite Based Porous Clay Heterostructures Modified With Transition Metals As Catalysts for the DeNOx Process. *Applied Catalysis B: Environmental*, 88(3–4), 331–340.
<https://doi.org/10.1016/j.apcatb.2008.11.001>
80. Christidis, G. E., Blum, A. E., and Eberl, D. D. (2006). Influence of Layer Charge and Charge Distribution of Smectites On The Flow Behaviour and Swelling of Bentonites. *Applied Clay Science*, 34(1–4), 125–138.
<https://doi.org/10.1016/j.clay.2006.05.008>
81. Cole, L. (2013). Subgrade Improvement Options - Performance Study and Cost Comparison. *Carmeuse natural chemicals*. 1 – 35.
82. Colpan, C. O., Nalbant, Y. and Ercelik, M. (2018). Fundamentals of Fuel Cell Technologies. In *Comprehensive Energy Systems* (pp. 1107–1130). Elsevier.
<https://doi.org/10.1016/B978-0-12-809597-3.00446-6>
83. ConceptDraw. (2022). Sustainable Development Venn Diagram. In *Sustainable Development Venn diagram*. Conceptdraw.
<https://www.conceptdraw.com/examples/venn-diagram-for-sustainable-development>

References

84. Consoli, N. C., da Silva Lopes, L., Foppa, D. and Heineck, K. S. (2009). Key Parameters Dictating Strength of Lime/Cement-Treated Soils. *Proceedings of the Institution of Civil Engineers - Geotechnical Engineering*, 162(2), 111–118. <https://doi.org/10.1680/geng.2009.162.2.111>
85. Convention on Biological Diversity. (2021). Article 13. Public Education and Awareness. In *Convention on Biological Diversity*.
86. Corrêa-Silva, M., Miranda, T., Rouainia, M., Araújo, N., Glendinning, S. and Cristelo, N. (2020). Geomechanical Behaviour of a Soft Soil Stabilised with Alkali-Activated Blast-Furnace Slags. *Journal of Cleaner Production*, 267, 122017. <https://doi.org/10.1016/j.jclepro.2020.122017>.
87. Costanzo P. M. and Giese R.F. (1990). Ordered and Disordered Organic Intercalates of 8.4-Å, Synthetically Hydrated Kaolinite. *Clays and Clay Minerals*, 38(2), 160–170.
88. Cote, B., Robinson, B., Gabr, M. A. and Borden, R. H. (2013). Performance-Cost Analysis of Stabilized Undercut Subgrades. *Journal of Construction Engineering and Management*, 139(2), 121–127. [https://doi.org/10.1061/\(ASCE\)CO.1943-7862.0000572](https://doi.org/10.1061/(ASCE)CO.1943-7862.0000572)
89. Covelli, D., Hernández-Cruz, D., Haines, B. M., Munoz, V., Omotoso, O., Mikula, R. and Urquhart, S. (2009). NEXAFS Microscopy Studies of The Association of Hydrocarbon Thin Films With Fine Clay Particles. *Journal of Electron Spectroscopy and Related Phenomena*, 173(1), 1–6. <https://doi.org/10.1016/j.elspec.2009.02.012>
90. Crisands. (2022). Recycled Bricks. *Crisands.Com*.
91. Czerewko, M. A., Cripps, J. C., Reid, J. M. and Duffell, C. G. (2003). Sulfur Species In Geological Materials—Sources And Quantification. *Cement and Concrete Composites*, 25(7), 657–671. [https://doi.org/10.1016/S0958-9465\(02\)00066-5](https://doi.org/10.1016/S0958-9465(02)00066-5)
92. Dadsetan, S. (2015). Utilisation of Supplementary Cementitious Materials in High Performance Self-Compacting Concrete. *Google Scholar*.
93. Dakshanamurthy, V., and Raman, V. (1973). A Simple Method of Identifying an Expansive Soil. *Soils and Foundations*, 13(1), 97–104. <https://doi.org/10.3208/sandf1972.13.97>
94. Darsi, B. P., Molugaram, K. and Madiraju, S. V. H. (2021). Subgrade Black Cotton Soil Stabilization Using Ground Granulated Blast-Furnace Slag

References

- (GGBS) and Lime, an Inorganic Mineral. *The 2nd International Electronic Conference on Mineral Science*, 15. <https://doi.org/10.3390/iecms2021-09390>
95. Dawson, A., Kolisoja, P. and Vuorimies, N. (2008). Understanding Low-volume Pavement Response to Heavy Traffic Loading. *Institute of Earth and Foundation Structure*, 1–47.
96. Design Manual for Roads and Bridges (DMRB). (2021). CD 226 - Design for New Pavement Construction. In *Standards For Highways*.
97. Dhiman, A. and Arora, N. (2021). Improving Rutting Resistance of Flexible Pavement Structure By Using Waste Plastic. *IOP Conference Series: Earth and Environmental Science*, 889(1), 012030. <https://doi.org/10.1088/1755-1315/889/1/012030>
98. Dhir OBE, R., K., Brito, J., Silva, R., V. and Lye, C., Q. (2019). Use of Recycled Aggregates in Road Pavement Applications. In *Sustainable Construction Materials* 451–494 <https://doi.org/10.1016/B978-0-08-100985-7.00012-1>
99. Diman, S. F. and Wijeyesekera, D.C. (2008). Swelling Characteristics of Bentonite Clay Mats. *Proceedings of the AC&T*, 179 – 185
100. Dokuchaev, V. (1883). Russian Chernozem, *Saint Petersburg*
101. Douglas, R. W. and Frank, S. (1972). A History of Glass Making. *G. T. Foulis and Co.Ltd.*
102. Ecoinvent. (2021). For The Availability of Environmental Data Worldwide. In *Ecoinvent*.
103. Eisenhour, D. D. and Brown, R. K. (2009). Bentonite and Its Impact On Modern Life. *Elements*, 5(2), 83–88. <https://doi.org/10.2113/gselements.5.2.83>
104. Elarabi, H. (2010). Damage Mechanism of Expansive Soils Damage Mechanism of Expansive Soils. *Conference: 2nd International Conference on Geotechnical Engineering*.
105. El-Badawy, S. M., Gabr, A. R. and Abd El-Hakim, R. T. (2019). Recycled Materials and By-Products for Pavement Construction. In *Handbook of Ecomaterials* 2177–2198. https://doi.org/10.1007/978-3-319-68255-6_168
106. Environmental Agency. (2020). Business and Environment Report: Environmental Outlook for The Cement, Lime And Minerals Sector. In *Environmental Agency*.

References

107. Escalante-Garcia, J. I. and Sharp, J. H. (2004). The Chemical Composition and Microstructure of Hydration Products In Blended Cements. *Cement and Concrete Composites*, 26(8), 967–976.
<https://doi.org/10.1016/j.cemconcomp.2004.02.036>
108. Estabragh, A. R., Jahani, A., Javadi, A. A. and Babalar, M. (2022). Assessment of Different Agents for Stabilisation of A Clay Soil. *International Journal of Pavement Engineering*, 23(2), 160–170.
<https://doi.org/10.1080/10298436.2020.1736293>
109. Estabragh, A. R., Khosravi, F. and Javadi, A. A. (2016). Effect of Thermal History on The Properties of Bentonite. *Environmental Earth Sciences*, 75(8), 657. <https://doi.org/10.1007/s12665-016-5416-9>
110. Etim, R. K., Ekpo, D. U., Attah, I. C. and Onyelowe, K. C. E. (2021). Effect of Micro Sized Quarry Dust Particle on The Compaction and Strength Properties of Cement Stabilized Lateritic Soil. *Cleaner Materials*, 2, 100023.
<https://doi.org/10.1016/j.clema.2021.100023>
111. Edi, H., Wardani, P. and Muntohar, A. (2018). The effect of cement stabilisation on the strength of the Bawen’s siltstone. MATEC Web of Conference. ICRMCE. 195, 03012.
<https://doi.org/10.1051/matecconf/201819503012>
112. European Commission. (2016). EU Construction and Demolition Waste Management Protocol. In *European Commission*.1–52).
113. European Commission. (2017). Efficient Use of Mixed Waste-Improving Management of Construction and Demolition Waste – Final Report. In *European Commission*. EU publications.
114. Faith. (2007). Use Of Ground Clay Brick As A Supplementary Cementitious Material In Concrete Hydration Characteristics, Mechanical Properties, and ASR Durability. *PhD thesis*. Iowa state University.
<https://lib.dr.iastate.edu/cgi/viewcontent.cgi?referer=&httpsredir=1&article=1091&context=rtd>. (accessed: 20 July 2020).
115. Federica, C., Idiano, D. and Massimo, G. (2014). Sustainable Management of Waste-to-Energy Facilities. *Renewable and Sustainable Energy Reviews*, 33, 719–728. <https://doi.org/10.1016/j.rser.2014.02.015>

References

116. Fleck, N. A., Shin, C. S. and Smith, R. A. (1985). Fatigue Crack Growth Under Compressive Loading. *Engineering Fracture Mechanics*, 21(1), 173–185. [https://doi.org/10.1016/0013-7944\(85\)90063-3](https://doi.org/10.1016/0013-7944(85)90063-3)
117. Fleck, N. A., Shin, C. S. and Smith, R. A. (1985). Fatigue Crack Growth Under Compressive Loading. *Engineering Fracture Mechanics*, 21(1), 173–185. [https://doi.org/10.1016/0013-7944\(85\)90063-3](https://doi.org/10.1016/0013-7944(85)90063-3)
118. Frearson, J. P. H. and Higgins, D. D. (1992). Sulfate Resistance of Mortars Containing Ground Granulated Blast-Furnace Slag with Variable Alumina Content. “*SP-132: Fly Ash, Silica Fume, Slag, and Natural Pozzolans and Natural Pozzolans in Concrete - Proceedings Fourth Interna.*” <https://doi.org/10.14359/1237>
119. Fuller, S. (2016). Life-Cycle Cost Analysis (LCCA). *National Institute of Standards and Technology (NIST)*. <https://www.wbdg.org/resources/life-cycle-cost-analysis-lcca>
120. Gali, M. L. and Rao, R. (2018). Problematic Soils and Geoenvironmental Concerns. *Problematic Soils and Geoenvironmental Concerns*.
121. Gardete, D. and Luzia, R. (2020). Experimental Study on Soils Stabilized with Two Types of Plastic Waste. *KnE Engineering*. <https://doi.org/10.18502/keg.v5i6.7020>.
122. Garrison, S. (2021). Encyclopedia Britannica. *Encyclopedia*
123. Gates, W. P., Bouazza, A. and Churchman, G. J. (2009). Bentonite Clay Keeps Pollutants at Bay. *Elements*, 5(2), 105–110. <https://doi.org/10.2113/gselements.5.2.105>.
124. Gendreau, M. and Soriano, P. (1998). Airport Pavement Management Systems: An Appraisal of Existing Methodologies. *Transportation Research Part A: Policy and Practice*, 32(3), 197–214. [https://doi.org/10.1016/S0965-8564\(97\)00008-6](https://doi.org/10.1016/S0965-8564(97)00008-6).
125. Geng, Y., Wang, Z., Shen, L., and Zhao, J. (2019). Calculating of CO₂ Emission Factors For Chinese Cement Production Based on Inorganic Carbon and Organic Carbon. *Journal of Cleaner Production*, 217, 503–509. <https://doi.org/10.1016/j.jclepro.2019.01.224>.
126. Geography, 2010. Photograph every grid square. [https://www.geography.org.uk/photo/1836872#:~:text=Nine%20tonnes%20of%](https://www.geography.org.uk/photo/1836872#:~:text=Nine%20tonnes%20of%20)

References

- 20waste%20rock,some%2060%20grades%20are%20produced. (accessed 31th March 2023).
127. Giese, R.F. and Costanzo, P.M. (1986). Behaviour of Water on The Surface of Kaolin Minerals: In Geochemical Processes At Mineral Surfaces. *American Chemical Society Symposium Series 323*, 37–53.
128. Giustozzi, F., Crispino, M. and Flintsch, G. (2012). Multi-Attribute Life Cycle Assessment of Preventive Maintenance Treatments on Road Pavements For Achieving Environmental Sustainability. *The International Journal of Life Cycle Assessment*, 17(4), 409–419.
<https://doi.org/10.1007/s11367-011-0375-6>
129. Gokul, V., Steffi, D. A., Kaviya, R., Harni, C. V. and Dharani, S. M. A. (2021). Alkali Activation of Clayey Soil Using GGBS and NaOH. *Materials Today: Proceedings*, 43, 1707–1713.
<https://doi.org/10.1016/j.matpr.2020.10.044>
130. Goldstein, J. I., Newbury, D. E., Michael, J. R., Ritchie, N. W. M., Scott, J. H. J. and Joy, D. C. (2003). Scanning Electron Microscopy and X-Ray Microanalysis (3rd ed.). *Springer New York*. <https://doi.org/10.1007/978-1-4939-6676-9>
131. Gooding, D.E. and Thomas, T (1995). The Potential of Cement-Stabilised Building Blocks as an Urban Building Material in Developing Countries. In *Economics*.
132. Gopal R. and Rao, A.S.R. (2006). Basic and Applied Soil Mechanics. *New Age International*.
133. Gratchev, I., Pitawala, S., Gurung., and Monteiro, E. (2018).
134. Guimarães, A. M. F., Ciminelli, V. S. T., and Vasconcelos, W. L. (2009). Smectite Organofunctionlised With Thiol Group For Adsorption of Heavy Metal Ions. *Applied Clay Science* 42(3-4). P.410-414.
doi.org/10.1016/j.clay.2008.04.006
135. Hairulla, and Betaubun, P. (2016). The Effect of Using Brick Waste to the Stabilization of Soft Soil Due to the Unconfined Compression. *Journal of Basic and Applied Scientific Research*, 6(2), 1–8.
136. Harichane, K., Ghrici, M., Wiam, K. and Missoum, H. (2010). Effect of the Combination of Lime and Natural Pozzolana on the Durability of Clayey Soils. *Electronic Journal of Geotechnical Engineering* 15, 15, 1194–1209.

References

137. Harraz, H. (2016). Beneficiation and Mineral Processing of Clay Minerals.
138. Hassan, H. J. A., Rasul, J. and Samin, M. (2021). Effects of Plastic Waste Materials on Geotechnical Properties of Clayey Soil. *Transportation Infrastructure Geotechnology*, 8(3), 390–413. <https://doi.org/10.1007/s40515-020-00145-4>
139. Hastuty, I. P., Roesyanto., Anas, M. R. and Nasution, A. (2020). Soil Improvement For Clay With Limestone and Glass Slag Based on CBR Value. *IOP Conference Series: Materials Science and Engineering*, 801(1), 012007. <https://doi.org/10.1088/1757-899X/801/1/012007>
140. Havancsák, K. (2021). High-resolution Scanning Electron Microscopy. <https://www.technoorg.hu/news-and-events/articles/high-resolution-scanning-electron-microscopy-1/>.
141. He, B. B. (2009). Two-Dimensional X-Ray Diffraction. *John Wiley and Sons, Inc.* <https://doi.org/10.1002/9780470502648>
142. Heidrich, C., Feuerborn, H. and Weir, A. (2013). Coal Combustion Production: A Global Perspective. *In Proceedings of the World of Coal Ash Conference*, Lexington, KY, USA, 22–25.
143. Hewlett, P. (1998). *Lea's Chemistry of Cement and Concrete*. Elsevier. <https://doi.org/10.1016/B978-0-7506-6256-7.X5007-3>
144. Hidalgo, C., Carvajal, G. and Muñoz, F. (2019). Laboratory Evaluation of Finely Milled Brick Debris as a Soil Stabilizer. *Sustainability*, 11(4), 967. <https://doi.org/10.3390/su11040967>
145. Higgins, D.D., Kinuthia, J. M. and Wild, S. (1998). Soil Stabilization using Lime-Activated Ground Granulated Blast Furnace Slag. “*SP-178: Sixth CANMET/ACI/JCI Conference: Fly Ash, Silica Fume, Slag and Natural Pozzolans in Concrete.*” <https://doi.org/10.14359/6023>
146. Highways Agency. (2020). Interim Advice Note (IAN) 73/06 – Design Guidance for road pavement Foundations. *Highways Agency*.
147. Hindu, A. K., Khaskheli, G. B. and Korejo, R (2015). Improving CBR Value and Swelling Potentials of Jamshoro Soil By Cement. *Conference: 7th Reginal Symposium on Infrastructure Development At: Department of Civil Engineering, Kasetsart University.*

References

148. Hizal, J. and Apak, R. (2006). Modelling of Cadmium(II) Adsorption on Kaolinite-Based Clays In The Absence And Presence of Humic Acid. *Applied Clay Science*, 32(3–4), 232–244. <https://doi.org/10.1016/j.clay.2006.02.002>
149. Hoornweg, D. and Bhada-Tata, P. (2012). What a Waste: A Global Review of Solid Waste Management Urban development series; *knowledge papers no. 15*. World Bank Group.
150. Hossain, A., Sultana, N., Bhowmic, S., Hoque, M.S. and Shantana, F.A. (2019) Modification of Expansive Soil Using Recycled Plastic Bottle Chips. *Journal of Geotechnical Studies*, 7 – 13 (3) <https://doi.org/10.5281/zenodo.336695>
151. Hosterman, J. W. and Patterson, S. H, (1992). Bentonite and Fuller's Earth Resources of The United States.
152. Houben, H. and Guillard, H. (1989). Earth Construction. *Practical Action Publishing*. <https://doi.org/10.3362/9781780444826>
153. Hozatlıoğlu D. T., Yilmaz, I. (2021). Shallow Mixing and Column Performances of Lime, Fly Ash and Gypsum On The Stabilization of Swelling Soils. *Engineering Geology*, 280, 105931. <https://doi.org/10.1016/j.enggeo.2020.105931>
154. Hu, Z., Peng, K., Li, L., Ma, Q., Xiao, H., Li, Z. and Ai, P. (2019). Effect of Wetting-Drying Cycles on Mechanical Behaviour and Electrical Resistivity of Unsaturated Subgrade Soil. *Advances in Civil Engineering*, 2019, 1–10. <https://doi.org/10.1155/2019/3465327>
155. Huggett, J. M. (2015). Clay Minerals. In *Reference Module in Earth Systems and Environmental Sciences*. <https://doi.org/10.1016/B978-0-12-409548-9.09519-1>
156. Ikeagwuani, C. C. and Nwonu, D. C. (2019). Emerging Trends In Expansive Soil Stabilisation: A Review. *Journal of Rock Mechanics and Geotechnical Engineering*, 11(2), 423–440. <https://doi.org/10.1016/j.jrmge.2018.08.013>
157. Indian Roads Congress. (2001). Indian Roads Congress - IRC-37-2001: *Guidelines for the design of flexible pavements*.
158. Ingles, O. G. and M. J. B. (1972). Soil stabilization. *Principles and Practice*.

References

159. Ingles, O. H. (1987). Soil stabilisation Chapter 38. In: Bell, F. G (Ed.). *Ground Engineer's Reference Book*, 381–3826.
160. International Energy Agency (IEA). (2010). CO₂ Emission for Combustion Highlights. *International Energy Agency (IEA)*.
161. Ismaiel, H. A. H. and Badry, M. M. (2013). Lime Chemical Stabilisation of Expansive Deposits Exposed at El-Kawther Quarter, Sohag Region, Egypt. *Geosciences*, 89–98.
162. ISO. (2017). ISO 15686-5:2017 Buildings and Constructed Assets — Service Life Planning — Part 5: Life-Cycle Costing. In *ISO*.
163. Jalal, F. E., Xu, Y., Jamhiri, B. and Memon, S. A. (2020). On The Recent Trends in Expansive Soil Stabilization Using Calcium-Based Stabilizer Materials (CSMs): A Comprehensive Review. *Advances in Materials Science and Engineering*, 2020, 1–23. <https://doi.org/10.1155/2020/1510969>
164. James, J. and Pandian, P. K. (2016). Industrial Wastes as Auxiliary Additives to Cement/Lime Stabilization of Soils. *Advances in Civil Engineering*, 2016, 1–17. <https://doi.org/10.1155/2016/1267391>
165. James, K. and Mitchell, K. S. (2005). *Fundamentals of Soil Behavior* (3rd ed.) John Wiley and Sons, New Jersey, USA.
166. Janovák, L., Varga, J., Kemény, L. and Dékány, I. (2009). Swelling Properties of Copolymer Hydrogels In The Presence of Montmorillonite And Alkylammonium Montmorillonite. *Applied Clay Science*, 43(2), 260–270. <https://doi.org/10.1016/j.clay.2008.08.002>
167. Jaradat, K. A., Darbari, Z., Elbakhshwan, M., Abdelaziz, S. L., Gill, S. K., Dooryhee, E. and Ecker, L. E. (2017). Heating-Freezing Effects on The Orientation of Kaolin Clay Particles. *Applied Clay Science*, 150, 163–174. <https://doi.org/10.1016/j.clay.2017.09.028>
168. Jauberthie, R., Rendell, F., Rangeard, D. and Molez, L. (2010). Stabilisation of Estuarine Silt with Lime and/or Cement. *Applied Clay Science*, 50(3), 395–400. <https://doi.org/10.1016/j.clay.2010.09.004>
169. Jawad, T. I., Taha, R. M., Majeed, H., Zaid, A. and Tanveer, K. (2014). Soil Stabilization Using Lime: Advantages, Disadvantages and Proposing a Potential Alternative. *Research Journal of Applied Sciences, Engineering and Technology*, 8(4), 510–520. <https://doi.org/10.19026/rjaset.8.1000>

References

170. Jha, A. K. and Sivapullaiah, P. v. (2020). Lime Stabilization of Soil: A Physico-Chemical and Micro-Mechanistic Perspective. *Indian Geotechnical Journal*, 50(3), 339–347. <https://doi.org/10.1007/s40098-019-00371-9>
171. Jones, L. D. and Jefferson, I. (2012). Chapter 33 Expansive Soils. *Institution of Civil Engineers' Manuals Series*. ICE Publishing, pp. 413-441
172. Jones, L. D. and Jefferson, I. (2019). *Chapter C5 - Expansive Soils*. *Institution of Civil Engineers' Manuals Series*. ICE Manuals, 1 – 46
173. Joshi, H. N. (2021). Improvement of Subgrade Using GGBS and Cement For Pavement. *International Journal of Engineering Development and Research*, 9(3), 1–11.
174. Kampfer, F. and Beyer, K., G. (1966). Glass: A World History, The Story of 4000 Years of Fine Glass-Making. *Studio Vista*, 1–315.
175. Karimiazar, J., Sharifi Teshnizi, E., Mirzababaei, M., Mahdad, M. and Arjmandzadeh, R. (2022). California Bearing Ratio of A Reactive Clay Treated with Nano-Additives and Cement. *Journal of Materials in Civil Engineering*, 34(2). [https://doi.org/10.1061/\(ASCE\)MT.1943-5533.0004028](https://doi.org/10.1061/(ASCE)MT.1943-5533.0004028)
176. Kartini; K., Rohaidah; M. N. and Zuraini; Z. A. (2012). Performance of Ground Clay Bricks as Partial Cement Replacement in Grade 30 Concrete. *Zenodo*, 1–4.
177. Kassa, R. B., Workie, T., Abdela, A., Fekade, M., Saleh, M. and Dejene, Y. (2020). Soil Stabilization Using Waste Plastic Materials. *Open Journal of Civil Engineering*, 10(01), 55–68. <https://doi.org/10.4236/ojce.2020.101006>
178. Ke, Y. C. and Stroeve, P. (2005). Polymer-Layered Silicate and Silica Nanocomposites. *Elsevier*. <https://doi.org/10.1016/B978-0-444-51570-4.X5000-9>
179. Kechouane, Z. and Nechnech, A. (2015). Characterization of An Expansive Clay Treated with Lime: Effect of Compaction On The Swelling Pressure. *AIP Conference Proceedings 1653, 020057*. <https://doi.org/10.1063/1.4914248>
180. Khademi, F. and Budiman, J., (2016). Expansive Soil: Causes and Treatments. *I-Manager's Journal on Civil Engineering*, 6(3), 1. <https://doi.org/10.26634/jce.6.3.8083>

References

181. Khan, R. and Sonthwal, V. K. (2020). Soil Stabilization using Brick Kiln Dust and waste Coir Fibre. *International Journal of Recent Technology and Engineering (IJRTE)*, 8(2), 2574–2578.
<https://doi.org/10.35940/ijrte.B1834.078219>
182. Khan, T. A., Taha, M. R., Khan, M. M., Shah, S. A. R., Aslam, M. A., Waqar, A., Khan, A. R. and Waseem, M. (2020). Strength and Volume Change Characteristics of Clayey Soils: Performance Evaluation of Enzymes. *Minerals*, 10(1), 52. <https://doi.org/10.3390/min10010052>
183. Kinjal, C.C., Padvī, H.S., Patel, H. V., Patel, J. A. and Tandel, J. (2018). Literature Review of Soil Stabilisation Using Different Materials. *Int. J. Tech. Innov. Mod. Eng. Sci.*
184. Kinuthia, J. M. and Nidzam, R. M. (2011). Towards Zero Industrial Waste: Utilisation of Brick Dust Waste In Sustainable Construction. *Waste Management*, 31(8), 1867–1878.
<https://doi.org/10.1016/j.wasman.2011.03.020>
185. Klein, C. and Hurlbut, C. S. (1985). Manual of Mineralogy (20th ed.). *Manual of Mineralogy*.
186. Klopogge, J. T. (1999). Synthesis of Smectite Clay Minerals: A Critical Review. *Clays and Clay Minerals*, 47(5), 529–554.
<https://doi.org/10.1346/CCMN.1999.0470501>
187. Knight, W. C. (1897). Mineral soap. *Engineering and Mining Journal*, 600.
188. Kolb, K., E. and Kolb, D., K (1988). *Glass: its many facets*.
189. Kulkarni, A. P., Sawant, M. K., Battul, V. V. and Shindepatil, M. S (2016). Black Cotton Soil Stabilization Using Bagasse Ash and Lime. *International Journal of Civil Engineering and Technology*, 7(6), 460–471.
190. Kumal, P., Rajour, A. and Siddiqui, R. (2014). Biological Remediation of Alkaline Cement Kiln Dust for Sustainable Development. *Industrial, Medical and Environmental Application of Microorganisms*, 52–58.
191. Kumar, A. B. G., Agrawal, S. and Dobriyal, A. (2018). Stabilization of Cohesive Soil Using Demolished Brick Waste. *Innovations and Advances in Civil Engineering Towards Green and Sustainable Systems*.
192. Kumar, A., Kumar, A. and Ved, P. (2016). Stabilization of Expansive Soil with Lime and Brick Dust. *Int. J. All Res. Educ. Sci*, 4(9).

References

193. Kumar, J. K. and Kumar, V. P. (2020). Experimental analysis of soil stabilization using e-waste. *Materials Today: Proceedings*, 22, 456–459. <https://doi.org/10.1016/j.matpr.2019.07.716>
194. Lackovic, K., Angove, M. J., Wells, J. D. and Johnson, B. B. (2003). Modeling the Adsorption of Cd(II) onto Muloorina illite and Related Clay Minerals. *Journal of Colloid and Interface Science*, 257(1), 31–40. [https://doi.org/10.1016/S0021-9797\(02\)00031-0](https://doi.org/10.1016/S0021-9797(02)00031-0)
195. Lagaly, G. (1995). Surface and Interlayer Reactions: Bentonites As Adsorbents In Churchman. *Proceedings of the 10th International Clay Conference*, 137–144.
196. Lal, R. (2006). Encyclopaedia of Soil Science Vol. 1, Second Edition. *CRC Press*, 276–290.
197. Laura, P. (2018). China's Ban on Trash Imports Shifts Waste Crisis to Southeast Asia. In *National Geographic*. <https://www.nationalgeographic.com/environment/article/china-ban-plastic-trash-imports-shifts-waste-crisis-southeast-asia-malaysia>
198. Lázár, K., Máthé, Z., Földvári, M., Németh, T. and Mell, P. (2009). Various Stages of Oxidation of Chlorite As Reflected in the Fe²⁺ and Fe³⁺ Proportions In The Mössbauer Spectra of Minerals In Boda Claystone. *Hyperfine Interactions*, 190(1–3), 129–133. <https://doi.org/10.1007/s10751-009-9974-z>
199. Lea, F. M. (1980). The chemistry of cement and concrete (3rd ed.).
200. Lekha, V. S., Rajan, P., Sehgal, J. L and Gajbhiye, K. S. (1998). Sand Mineralogical Investigation and Mineral Weathering Index (MWI) of Selected Soils of Kerala. *Indian Soc. Sci*, 46, 675–682.
201. Lepore, B. J., Thompson, A. M. and Petersen, A. (2009). Impact of Polyacrylamide Delivery Method With Lime or Gypsum for Soil And Nutrient Stabilization. *Journal of Soil and Water Conservation*, 64(3), 223–231. <https://doi.org/10.2489/jswc.64.3.223>
202. Lesley, 2022 The pottery wheel. <https://thepotterywheel.com/what-happens-to-clay-when-it-is-fired/> (accessed 16th July 2022).
203. Letaief, S. and Detellier, C. (2005). Reactivity of Kaolinite In Ionic Liquids: Preparation and Characterization of a 1-ethyl Pyridinium Chloride–

References

- kaolinite Intercalate. *Journal of Materials Chemistry*, 15(44), 4734.
<https://doi.org/10.1039/b511282f>
204. Letaief, S., Tonle I. K., Diaco, T. and Detellier, C. (2008). Nanohybrid Materials From Interlayer Functionalization of Kaolinite. Application To The Electrochemical Per Concentration of Cyanide. *Applied Clay Science*. 42(1-2), 95-101.
205. Li, S. (1964). Heavy Duty Pavements. *South Dakota School of Mines and Technology*.
206. Liang, C., Dang, Z., Xiao, B., Huang, W. and Liu, C. (2006). Equilibrium Sorption of Phenanthrene By Soil Humic Acids. *Chemosphere*, 63(11), 1961–1968. <https://doi.org/10.1016/j.chemosphere.2005.09.065>
207. Liang, S., Chen, J., Guo, M., Feng, D., Liu, L. and Qi, T. (2020). Utilization of Pretreated Municipal Solid Waste Incineration Fly Ash For Cement-Stabilized Soil. *Waste Management*, 105, 425–432.
<https://doi.org/10.1016/j.wasman.2020.02.017>
208. Lihua Z, and Zengmie, Z. (2020) Reuse of clay brick waste in mortar and concrete. Hindawi. *Adv Mater Sci Eng*. pp 7, 5.
<https://doi.org/https://doi.org/10.1155/2020/6326178>
209. Lime-Treated Soil Construction Manual. (2004). Lime stabilisation and Lime Modification. 247. *National Lime Association*, 1–41.
https://www.graymont.com/sites/default/files/pdf/tech_paper/lime_treated_soil_construction_manual.pdf
210. Lin, K. L., Wang, K. S., Tzeng, B. Y. and Lin, C. Y. (2004). The Hydration Characteristics and Utilization of Slag Obtained By The Vitrification of MSWI Fly Ash. *Waste Management*, 24(2), 199–205.
[https://doi.org/10.1016/S0956-053X\(03\)00131-4](https://doi.org/10.1016/S0956-053X(03)00131-4)
211. Little, D. L. (1987). Fundamentals of the stabilisation of soil with lime. *International Lime Association*.
212. Lockwood, J. L. (1977). Fungistasis In Soils. *Biological Reviews*, 52(1), 1–43. <https://doi.org/10.1111/j.1469-185X.1977.tb01344.x>
213. López-Lara, T., Hernández-Zaragoza, J. B., Horta-Rangel, J., Rojas-González, E., López-Ayala, S. and Castaño, V. M. (2017). Expansion Reduction of Clayey Soils Through Surcharge Application and Lime

References

- Treatment. *Case Studies in Construction Materials*, 7, 102–109.
<https://doi.org/10.1016/j.cscm.2017.06.003>
214. Iowa State University. (2022). Fatigue Properties. <https://www.nde-ed.org/Physics/Materials/Mechanical/FractureToughness.xhtml>
215. Lucena, L. C. de F. L., Juca, J. F. T., Soares, J. B. and Tavares Marinho Filho, P. G. (2014). Use of Wastewater Sludge For Base And Subbase of Road Pavements. *Transportation Research Part D: Transport and Environment*, 33, 210–219. <https://doi.org/10.1016/j.trd.2014.06.007>
216. Lyons, A. (2010). *Materials for Architects and Builders* (4th ed.). Butterworth-Heinemann - Elsevier.
https://kashanu.ac.ir/Files/Content/9781856175197_Materials_for_Architects_and_Builders.pdf
217. Malek, B., Igbal, M. and Ibrahim, A. (2007). Use of Selected Waste Materials In Concrete Mixes. *Waste Management*, 27(12), 1870–1876.
<https://doi.org/10.1016/j.wasman.2006.07.026>
218. Marwa, E. M. M., Hillier, S., Rice, C. M. and Meharg, A. A. (2009). Mineralogical and Chemical Characterization of Some Vermiculites From The Mozambique Belt of Tanzania for Agricultural Use. *Clay Minerals*, 44(1), 1–17.
<https://doi.org/10.1180/claymin.2009.044.1.1>
219. Mazumder, A. R., Kabir, A. and Yazdani, N. (2006). Performance of Overburnt Distorted Bricks as Aggregates in Pavement Works. *Journal of Materials in Civil Engineering*, 18(6), 777–785.
[https://doi.org/10.1061/\(ASCE\)0899-1561\(2006\)18:6\(777\)](https://doi.org/10.1061/(ASCE)0899-1561(2006)18:6(777))
220. McCarty, D. K., Sakharov, B. A. and Drits, V. A. (2009). New Insights Into Smectite Illitization: A Zoned K-Bentonite Revisited. *American Mineralogist*, 94. 11–12, 1653–1671. <https://doi.org/10.2138/am.2009.3260>
221. Mehta, K., Akshit, M. and Kumar, A. (2019). Performance Evaluation of Cement Stabilized and Fiber Reinforced Surkhi/Brick Kiln Dust-Clay Mixes as A Highway Sub-Grade Material. *International Journal of Modern Trends in Engineering and Research*, 1–19.
222. Melling, H., Tusabe, K., Jjuuko, S. and Kalumba, D. (2017). Designing a paved road using geogrids to reduce the thickness of the pavement layers. <https://www.researchgate.net/publication/320774837>.

References

223. Meng, T., Qiang, Y., Hu, A., Xu, C. and Lin, L. (2017). Effect Of Compound Nano-CaCO₃ Addition On Strength Development And Microstructure of Cement-Stabilized Soil In The Marine Environment. *Construction and Building Materials*, 151, 775–781. <https://doi.org/10.1016/j.conbuildmat.2017.06.016>
224. Michael, T. S. S. and K. A. (2016). Expansive Soil Stabilisation Using Industrial Solid Waste A Review. *International Conference on Recent Trends in Engineering and Science*, 508–516.
225. Migliavacca, D. M., Teixeira, E. C., Gervasoni, F., Conceição, R. V. and Rodriguez, M. T. R. (2009). Characterization of Wet Precipitation by X-ray Diffraction (XRD) and Scanning Electron Microscopy (SEM) in the Metropolitan Area of Porto Alegre, Brazil. *Journal of Hazardous Materials*, 171(1–3), 230–240. <https://doi.org/10.1016/j.jhazmat.2009.05.135>
226. Mir, S. M. and Sharma, N (2019). Effect of Brick Kiln Dust and Alccofine 1101 on UCS and CBR Values of Clayey Soil. *International Journal of Innovation Research in Science, Engineering and Technology*, 8(12), 1–9.
227. Mishra, U. (2017). Enhancement in Subgrade Soil Strength Using Glass Powder as Discrete Fiber: A review. *International Research Journal of Engineering and Technology (IRJET)*, 4(4), 1–10.
228. Miura, M., Horpibulsuk, S. and Nagaraj, T. S. (2001). Soils and Foundations. *Japanese Geotechnical Society*, 41(5), 1–33.
229. Mokni, N., Olivella, S. and Alonso, E. E. (2010). Swelling In Clayey Soils Induced By The Presence of Salt Crystals. *Applied Clay Science*, 47(1–2), 105–112. <https://doi.org/10.1016/j.clay.2009.01.005>
230. Morales, D., Romero-Esquinas, A., Fernández-Ledesma, E., Fernández, J. and Jiménez, J. (2019). Feasible Use of Colliery Spoils As Subbase Layer For Low-Traffic Roads. *Construction and Building Materials*, 229, 116910. <https://doi.org/10.1016/j.conbuildmat.2019.116910>
231. Motz, H., Ehrenberg, A. and Mudersbach, D. (2015). Dry Solidification With Heat Recovery of Ferrous Slag. *Mineral Processing and Extractive Metallurgy*, 124(2), 67–75. <https://doi.org/10.1179/1743285514Y.0000000082>
232. Müller A, H. (2006). Recycling of Construction and Demolition Waste- Status and new utilisation methods. *Chair of Mineral Processing of Building Materials and Reuse*.

References

233. Müller, A. H. (2004). Lightweight Aggregates from Masonry Rubble. *239. Müller A. H.*, 97–106.
234. Murthi, P., Saravanan, R. and Poongodi, K. (2021). Studies On The Impact of Polypropylene And Silica Fume Blended Combination On The Material Behaviour of Black Cotton Soil. *Materials Today: Proceedings*, 39, 621–626. <https://doi.org/10.1016/j.matpr.2020.09.004>
235. Naceri, A. and Hamina, M. C. (2009). Use of Waste Brick As A Partial Replacement of Cement In Mortar. *Waste Management*, 29(8), 2378–2384. <https://doi.org/10.1016/j.wasman.2009.03.026>
236. Narendra, K. and Prasad A. D. (2017). Effect of Ground Granulated Blast Furnace Slag on Expansive Soils Under Static Loading. *Engineering Science Technology*, 3(1), 2455–2062.
237. Nasir, O. and Fall, M. (2010). Coupling Binder Hydration, Temperature and Compressive Strength Development of Underground Cemented Paste Backfill At Early Ages. *Tunnelling and Underground Space Technology*, 25(1), 9–20. <https://doi.org/10.1016/j.tust.2009.07.008>
238. National Asphalt Pavement Association. (2019). Quality Improvement Series 123. In *National Asphalt Pavement Association*.
239. National Highways. (2021). DMRB Volume 4 Section 1 Part 6 (HA 74/07) Geotechnics and drainage. In *Earthworks*.
240. Nazari, Z., Tabarsa, A. and Latifi, N. (2021). Effect of Compaction Delay on The Strength and Consolidation Properties of Cement-Stabilized Subgrade Soil. *Transportation Geotechnics*, 27, 100495. <https://doi.org/10.1016/j.trgeo.2020.100495>
241. Nesse, W. D. 2000. Introduction to Mineralogy. xiii + 442 pp. New York, Oxford: Oxford University Press. *Geological Magazine*, 139(4), 489–492. <https://doi.org/10.1017/S0016756802246798>
242. Neville, A. M. (2011). Properties of Concrete (5th ed.). *The Royal Academy of Engineering*.
243. Newmarket Plant Hire (NPH) Group. (2018). Plant and Tool Hire Rates. In 253. *Newmarket Plant Hire (NPH) Group*.
244. Norton, J. (1997). Building with Earth: A handbook (2nd ed.). *Intermediate Technology Publications*.

References

245. Nunn, M. E. Brown. A., Weston, D. and Nicholls, J. C. (1997). Design of Long-Life Flexible Pavements for Heavy Traffic. *British Aggregate Construction Materials, Industry, and the Refined Bitumen Association*.
246. Nuruzzaman, Md., Rahman, M. M., Liu, Y. and Naidu, R. (2016). Nanoencapsulation, Nano-guard for Pesticides: A New Window for Safe Application. *Journal of Agricultural and Food Chemistry*, 64(7), 1447–1483. <https://doi.org/10.1021/acs.jafc.5b05214>
247. Nyuk, H. W., Su, Fi. and Raymond, W. (2003). Life Cycle Cost Analysis of Rooftop Gardens In Singapore. *Building and Environment*, 38(3), 499–509. [https://doi.org/10.1016/S0360-1323\(02\)00131-2](https://doi.org/10.1016/S0360-1323(02)00131-2)
248. O'Farrell, M., Wild, S. and Sabir, B. B. (2001). Pore Size Distribution And Compressive Strength of Waste Clay Brick Mortar. *Cement and Concrete Composites*, 23(1), 81–91. [https://doi.org/10.1016/S0958-9465\(00\)00070-6](https://doi.org/10.1016/S0958-9465(00)00070-6)
249. Obuzor, G. N., Kinuthia, J. M. and Robinson, R. B. (2012). Soil Stabilisation with Lime-Activated-GGBS—A Mitigation To Flooding Effects On Road Structural Layers/Embankments Constructed On Floodplains. *Engineering Geology*, 151, 112–119. <https://doi.org/10.1016/j.enggeo.2012.09.010>
250. Odom, I. R. (1984). Smectite Clay Minerals: Properties and Uses. *Philosophical Transactions of the Royal Society of London. Series A, Mathematical and Physical Sciences*, 311(1517), 391–409. <https://doi.org/10.1098/rsta.1984.0036>
251. O'Flaherty, C. A., David, H. T. and Davidson, D. T. (1961). Relationship Between the California Bearing Ratio and The Unconfined Compressive Strength of Sand-Cement Mixtures. *Proceedings of the Iowa Academy of Science*, 68(1), 341–356. <https://scholarworks.uni.edu/pias/vol68/iss1/52>
252. Oner, A. and Akyuz, S. (2007). An Experimental Study on Optimum Usage of GGBS for the Compressive Strength of Concrete. *Cement and Concrete Composites*, 29(6), 505–514. <https://doi.org/10.1016/j.cemconcomp.2007.01.001>
253. Onn, C. C., Mo, K. H., Radwan, M. K. H., Liew, W. H., Ng, C. G. and Yusoff, S. (2019). Strength, Carbon Footprint and Cost Considerations of Mortar Blends with High Volume Ground Granulated Blast Furnace Slag. *Sustainability*, 11(24), 7194. <https://doi.org/10.3390/su11247194>

References

254. Oreto, C., Veropalumbo, R., Viscione, N., Biacardo, A. and Russo, F. (2001). Investigating the environmental impacts and engineering performance of road asphalt pavement mixtures made up of jet grouting waste and reclaimed asphalt pavement. *Environ. Res.*198-111277.
255. Osman, M. A., Ploetze, M. and Suter, U. W. (2003). Surface Treatment of Clay Minerals ? Thermal Stability, Basal-Plane Spacing and Surface Coverage. *Journal of Materials Chemistry*, 13(9), 2359.
<https://doi.org/10.1039/b302331a>
256. Osula, D. O. A. (1996). A Comparative Evaluation of Cement and Lime Modification of Laterite. *Engineering Geology*, 42(1), 71–81.
[https://doi.org/10.1016/0013-7952\(95\)00067-4](https://doi.org/10.1016/0013-7952(95)00067-4)
257. Oti, J.E. (2010). The Development of Unfired Clay Building Materials for Sustainable Building Construction.
https://unilearn.southwales.ac.uk/webapps/blackboard/content/listContent.jsp?course_id=_141532_1&content_id=_2997727_1&mode=reset (accessed on 15 February 2021).
258. Otoko, G. R. and Pedro, P. P (2014). Cement Stabilisation of Laterite and Chikoko Soils Using Waste Rubber Fiber. *International Journal of Engineering Science and Research Technology*.
259. Oviya, R. and Manikandan, R (2016). An Experimental Investigation on Stabilising The Soil Using Rice Husk Ash With Lime As An Admixture. *International Journal of Informative and Futuristic Research*.
260. Oy, P. (1998). Bentonite Swelling Pressure In Strong NaCl Solutions. *Ola Karnland Clay Technology*, 1–34.
<https://www.osti.gov/etdweb/servlets/purl/605607>
261. Papini, M. P. and Majone, M. (2002). Modelling of Heavy Metal Adsorption at Clay Surfaces. *Encyclopaedia of Surface and Colloid Science*, 3483–3498.
262. Parihar, N. S. and Gupta, A. K. (2020). Strength and Microstructural Behavior of Expansive Soil Treated with Limed Leather Waste Ash. *International Journal of Innovative Technology and Exploring Engineering*, 4(9), 604–609. <https://doi.org/10.35940/ijitee.D9072.029420>
263. Parry, A. R., Phillips, S. J., Potter, J. F. and Nunn, M. E. (1999). Design and Performance of Flexible Composite Road Pavements. *Proceedings of the*

References

- Institution of Civil Engineers - Transport*, 135(1), 9–16.
<https://doi.org/10.1680/itrans.1999.31282>
264. Parry, A.R., Phillips, S.J., Potter, J.F., Nunn, M.E. Design and Performance of Flexible Composite Road Pavements. *Proc. Inst. Civ.Eng.—Transp.* 1999, 135, 9–16
265. Patel, S., Solanki, C. H. and Reddy, K. R. (2021). Proceedings of the Indian Geotechnical Conference 2019. *Springer Singapore*.
<https://doi.org/10.1007/978-981-33-6370-0>
266. Paul, A. (2014). Pavement Design In Road Construction – Design Parameters. *Pavement Design in Road Construction*.
<https://civildigital.com/pavement-design-road-construction-design-parameters/>
267. Peltonen, C., Marcussen, Ø., Bjørlykke, K. and Jahren, J. (2009). Clay Mineral Diagenesis and Quartz Cementation In Mudstones: The Effects of Smectite To Illite Reaction On Rock Properties. *Marine and Petroleum Geology*, 26(6), 887–898. <https://doi.org/10.1016/j.marpetgeo.2008.01.021>
268. Phanikumar, B. R. and Ramanjaneya Raju, E. (2020). Compaction and Strength Characteristics of An Expansive Clay Stabilised With Lime Sludge And Cement. *Soils and Foundations*, 60(1), 129–138.
<https://doi.org/10.1016/j.sandf.2020.01.007>
269. Phanikumar, B. R., Sreedharan, R. and Aniruddh, C. (2015). Swell-Compressibility Characteristics of Lime-Blended And Cement-Blended Expansive Clays – A Comparative Study. *Geomechanics and Geoengineering*, 10(2), 153–162.
<https://doi.org/10.1080/17486025.2014.902120>
270. Philips, P. (1981). The Encyclopaedia of glass. *Glass Encyclopedia*.
271. Plastic in the Ocean. (2021). Plastic in the Ocean Statistics 2020-2021. In *condor*. condor.
272. Pleasants Construction, Inc. Soil stabilisation and soil modification. <https://pleasantsconstruction.com/services/soil-cement-soil-stabilization/>. (Accessed 15 June 2020).
273. Pokale, K. R., Borkar, Y. R. and Jichkar, R. R. (2015). Experimental Investigation for Stabilization of Black Cotton Soil By using waste material Dust. *Int. Res. J. Eng. Technol*, 2.

References

274. Pongsivasathit, S., Horpibulsuk, S. and Piyaphipat, S. (2019). Assessment of Mechanical Properties of Cement Stabilized Soils. *Case Studies in Construction Materials*, 11, e00301. <https://doi.org/10.1016/j.cscm.2019.e00301>
275. Prasad, S. D., Prasad, V. and Raju, P. (2019). Stabilisation of Black Cotton Soil Using Ground Granulated Blast Furnace Slag And Plastic Fibers. *International Journal of Recent Technology and Engineering (IJRTE)*, 7(6C2). <https://www.ijrte.org/wp-content/uploads/papers/v7i6c2/F11150476C219.pdf>
276. Pritchard., O. G., Hallett, S. H. and Farewell, T S (2013). Soil Movement In The UK – Impacts On Critical Infrastructure. *Infrastructure Transitions Research Consortium Working Paper Series*, 1–74.
277. Prusinski, J. R. and Bhattacharja, S. (1999). Effectiveness of Portland Cement and Lime in Stabilizing Clay Soils. *Transportation Research Record: Journal of the Transportation Research Board*, 1652(1), 215–227. <https://doi.org/10.3141/1652-28>
278. Pundir, N. and Trivedi, M. K. (2017). Improvement of Pavement Soil Subgrade by Using Burnt Brick Dust. *International Journal for Research in Applied Science and Engineering Technology*, 5(5), 218–221.
279. Putri, E. E., Kameswara, N. S. V. and Mannan, M. A. (2012). Evaluation of Modulus of Elasticity and Modulus of Subgrade Reaction of Soils Using CBR Test. *Journal of Civil Engineering Research*, 2(1), 34–40. <https://doi.org/10.5923/j.jce.20120201.05>
280. Rabab'ah, S., al Hattamleh, O., Aldeeky, H. and Abu Alfoul, B. (2021). Effect of Glass Fiber On the Properties of Expansive Soil And Its Utilization As Subgrade Reinforcement In Pavement Applications. *Case Studies in Construction Materials*, 14, e00485. <https://doi.org/10.1016/j.cscm.2020.e00485>
281. Rabbani, P., Daghigh, Y., Reza Atrechian, M., Karimi, M. and Tolooyan, A. (2012). The Potential of Lime and Grand Granulated Blast Furnace Slag (GGBFS) Mixture for Stabilisation of Desert Silty Sands. *Journal of Civil Engineering Research*, 2(6), 108–119. <https://doi.org/10.5923/j.jce.20120206.07>

References

282. Rahman, I. U., Raheel, M., Wajahat Ali Khawaja, M., Khan, R., Li, J., Khan, A. and Khan, M. T. (2021). Characterization of Engineering Properties of Weak Subgrade Soils with Different Pozzolanic and Cementitious Additives. *Case Studies in Construction Materials*, 15, e00676. <https://doi.org/10.1016/j.cscm.2021.e00676>
283. Ramaji, A. E. (2012). A Review on Soil Stabilisation Using Low-Cost Methods. *Journal of Applied Science Research*, 8(4), 2193–2196.
284. Rangaraju, P. R., Amirkhanian, S. and GÜven, Z. (2008). Life Cycle Cost Analysis for Pavement Type Selection; Report Number FHWA-SC-08-01; Clemson University: Clemson, SC, USA, 2008.
285. Rank, K., Bhandari, J. and Mehta, J. V. (2020). Using Brick Dust Manufacturing Waste and Cement Dust Manufacturing Waste as Stabilizing Material for Expansive Soil. *International Journal of Emerging Technologies and Innovative Research*, 7(2), 525–531. <https://www.jetir.org/view?paper=JETIR2002078>
286. Rao, C. H., Naidu, G. P. and Satyanayana, P. V. (2012). Application of GGBS Stabilized Redmud in Road Construction. *IOSR Journal of Engineering*, 02(08), 14–20. <https://doi.org/10.9790/3021-02841420>
287. Rauma, M. and Johanson, G. (2009). Comparison of the Thermogravimetric Analysis (TGA) and Franz Cell Methods to Assess Dermal Diffusion of Volatile Chemicals. *Toxicology in Vitro*, 23(5), 919–926. <https://doi.org/10.1016/j.tiv.2009.04.003>
288. Reda, A., Ibrahim, E. and Houssami, L. (2016). A Cure for Swelling. *Dar Al-Handasah*. <https://dar.com/news/details/a-cure-for-swelling>
289. Reddi, L. and Inyang, H. I. (2000). *Geoenvironmental Engineering: Principles and Applications*. CRC Press, Taylor and Francis Group, USA. <https://ostad.nit.ac.ir/payaidea/ospic/file8601.pdf>
290. Reddy, S. S., Prasad, N. and Krishna, N. (2018). Lime-Stabilized Black Cotton Soil and Brick Powder Mixture as Subbase Material. *Advances in Civil Engineering*, 2018, 1–5. <https://doi.org/10.1155/2018/5834685>
291. Rivera, J. F., Orobio, A., Mejía de Gutiérrez, R. and Cristelo, N. (2020). Clayey Soil Stabilization Using Alkali-Activated Cementitious Materials. *Materiales de Construcción*, 70(337), 211. <https://doi.org/10.3989/mc.2020.07519>

References

292. Roadpacker solutions. (2021). Soil Stabilisation. *Roadpacker Solutions Ltd.* <https://roadpackersolutions.com/>
293. Rogers, F. (1948). *5000 Years of Glass, etc.*
294. Rogers, S. B. (2011). Evaluation and Testing of Brick Dust as a Pozzolanic Additive to Lime Mortars for Architectural Conservation. *Penn Libraries University of Pennsylvania*. 1 – 203
https://repository.upenn.edu/cgi/viewcontent.cgi?article=1178&context=hp_theses
295. Sachin, N. and Bhavsar, A. J. P. (2014). Analysis of Swelling and Shrinkage Properties of Expansive Soil using Brick Dust as a Stabilizer. *International Journal of Emerging Technology and Advanced Engineering*, 4(12), 1.
296. Saha, D. C. and Mandal, J. N. (2017). Laboratory Investigations on Reclaimed Asphalt Pavement (RAP) for Using It As Base Course of Flexible Pavement. *Procedia Engineering*, 189, 434–439.
<https://doi.org/10.1016/j.proeng.2017.05.069>.
297. Sakr, M. A., Shahin, M. A. and Metwally, Y. M. (2009). Utilization of Lime for Stabilizing Soft Clay Soil of High Organic Content. *Geotechnical and Geological Engineering*, 27(1), 105–113. <https://doi.org/10.1007/s10706-008-9215-2>
298. Salimah, A., Hazmi, M., Fathur Rouf Hasan, M., Agung, P. A. M. and Yelvi, . (2021). A Comparative Study Of Red Brick Powder And Lime As Soft Soil Stabilizer. *F1000Research*, 10, 777.
<https://doi.org/10.12688/f1000research.27835.1>
299. Saludung, A., Ogawa, Y., and Kawai, K. (2018). Microstructure And Mechanical Properties of FA/GGBS-Based Geopolymer. *MATEC Web of Conferences*, 195, 01013. <https://doi.org/10.1051/matecconf/201819501013>
300. Saranya, K., Jeevitha, J. and Varshini, T. (2017). A Review on Application of Chemical Additives In Soil Stabilisation. *International Research Journal of Engineering and Technology (IRJET)* 4 (3). pp 2395-0072.
301. Saravanan, R., Udhayakumar, T., Dinesh, S., Venkatasubramanian, C. and Muthu, D. (2017). Effect of Addition of GGBS and Lime in Soil Stabilisation for Stabilising Local Village Roads in Thanjavur Region. *IOP*

References

- Conference Series: Earth and Environmental Science*, 80, 012060.
<https://doi.org/10.1088/1755-1315/80/1/012060>
302. Sasui, S., Kim, G., Nam, J., Koyama, T. and Chansomsak, S. (2019). Strength and Microstructure of Class-C Fly Ash and GGBS Blend Geopolymer Activated in NaOH andamp; NaOH + Na₂SiO₃. *Materials*, 13(1), 59.
<https://doi.org/10.3390/ma13010059>
303. Schaefer, C. E., Kupwade-Patil, K., Ortega, M., Soriano, C., Büyüköztürk, O., White, A. E., and Short, M. P. (2017). Irradiated Recycled Plastic as A Concrete Additive For Improved Chemo-Mechanical Properties And Lower Carbon Footprint. *Waste Management*, 71, 426–439.
<https://doi.org/10.1016/j.wasman.2017.09.033>
304. Schanz, T. and Elsayw, M. D. (2015). Swelling Characteristics and Shear Strength of Highly Expansive Clay–Lime Mixtures: A Comparative Study. *Arabian Journal of Geosciences*, 8(10), 7919–7927.
<https://doi.org/10.1007/s12517-014-1703-5>
305. Serapiglia, M. J., Cameron, K. D., Stipanovic, A. J. and Smart, L. B. (2009). Analysis of Biomass Composition Using High-Resolution Thermogravimetric Analysis and Percent Bark Content for the Selection of Shrub Willow Bioenergy Crop Varieties. *BioEnergy Research*, 2(1–2), 1–9.
<https://doi.org/10.1007/s12155-008-9028-4>
306. Sharma, A. K. and Sivapullaiah, P. V. (2016). Ground Granulated Blast Furnace Slag Amended Fly Ash as An Expansive Soil Stabilizer. *Soils and Foundations*, 56(2), 205–212. <https://doi.org/10.1016/j.sandf.2016.02.004>
307. Sharma, A. and Puvvadi, S. (2012). Improvement of Strength of Expansive Soil with Waste Granulated Blast Furnace Slag. *GeoCongress 2012*, 3920–3928. <https://doi.org/10.1061/9780784412121.402>
308. Shih, S. M., Ho, C. S., Song, Y. S. and Lin, J. P. (1999). Kinetics of the Reaction of Ca(OH)₂ with CO₂ at Low Temperature. *Industrial and Engineering Chemistry Research*, 38(4), 1316–1322.
<https://doi.org/10.1021/ie980508z>
309. Southern Testing Environmental and Geotechnical. (2020). CBR Test. *ST Consult*. <https://www.southerntesting.co.uk/services/ground-site-investigation-consultants/cbr-test/>

References

310. Spence, R.J.S. and Cook, D.J. (1983). Building materials in developing countries. *Wiley*, London.
311. Sposito, G. (2008). The Chemistry of Soils (2nd ed.). *Oxford University Press*.
312. Srikanth, V. and Mishra, A. K. (2016). A Laboratory Study on the Geotechnical Characteristics of Sand–Bentonite Mixtures and the Role of Particle Size of Sand. *International Journal of Geosynthetics and Ground Engineering*, 2(1), 3. <https://doi.org/10.1007/s40891-015-0043-1>
313. Srivastava, P., Singh, B. and Angove, M. (2005). Competitive Adsorption Behavior of Heavy Metals on Kaolinite. *Journal of Colloid and Interface Science*, 290(1), 28–38. <https://doi.org/10.1016/j.jcis.2005.04.036>
314. Steel360, (2019), Granulation of blast Furnace Slag. *360 Editor*. <https://www.steel-360.com/technology-next/dry-granulation-of-blast-furnace-slag>.
315. Subash, K., Sukesh, S., Sreerag, R., Jino, J., Dilna, S. V. and Deeraj, A. D, (2016), Stabilization of Black Cotton Soil using Glass and Plastic Granules, *International Journal Of Engineering Research & Technology (IJERT)* 5(4) <http://dx.doi.org/10.17577/IJERTV5IS040842>
316. Sun, L.-H., Yang, Z.-G., and Li, X.-H. (2009). Effects of The Treatment of Attapulgite and Filler Contents on Tensile Properties of PTFE and Attapulgite Reinforced Fabric Composites. *Composites Part A: Applied Science and Manufacturing*, 40(11), 1785–1791. <https://doi.org/10.1016/j.compositesa.2009.08.014>
317. Sutherland, W. M. (2014). Wyoming Bentonite. *Wyoming State Geological Survey*, Summary Report. 1- 4. <https://www.wsgs.wyo.gov/products/wsgs-2014-bentonite-summary.pdf>
318. Syed, M. and Guharay, A. (2020). Stabilization of Expansive Soil Reinforced with Polypropylene and Glass Fiber In Cement And Alkali Activated Binder. In *Advancements in Unsaturated Soil Mechanics*; Hoyos, L., Shehata, H., Eds.; Springer International Publishing: Cham, Switzerland, pp. 41–55.
319. Tang, C., Shi, B., Gao, W., Chen, F. and Cai, Y. (2007). Strength and Mechanical Behavior of Short Polypropylene Fiber Reinforced and Cement

References

- Stabilized Clayey Soil. *Geotextiles and Geomembranes*, 25(3), 194–202.
<https://doi.org/10.1016/j.geotexmem.2006.11.002>
320. Tayibi, H., Choura, M., López, F. A., Alguacil, F. J. and López-Delgado, A. (2009). Environmental Impact and Management of Phosphogypsum. *Journal of Environmental Management*, 90(8), 2377–2386.
<https://doi.org/10.1016/j.jenvman.2009.03.007>
321. Taylor, H. F. W. (1997). Cement Chemistry 2nd Edition. *ICE Virtual Library*. Thomas Telford Publishing. <https://doi.org/10.1680/cc.25929>
322. Teja, S. L., Kumar, S. S. and Needhidasan, S. (2018). Stabilization of Expansive Soil Using Brick Dust. *International Journal of Pure and Applied Mathematics*, 119(17), 1–8. <https://acadpubl.eu/hub/2018-119-17/4/375.pdf>
323. Telling, B. and Brandstetr, J. (1989). Present State and Future of Alkali-Activated Slag Concretes. *American Concrete Institute*, 114 - 1519.
324. Telling, B. and Brandstetter, J. (1993). Clinker Free Concrete Based on Alkali Activated Slag. *Mineral Admixtures in Cement and Concrete*, 7, 296–341.
325. Terrel, R. L., Epps, J. A., Barenberg, E. J., Mitchell, J. K. and Thompson, M. R. (1979). Soil Stabilization in Pavement Structures. *A User's Manual*.
326. Terzaghi, K. and Peck R, B., Gholamreza, M (1996). Soil Mechanics in Engineering Practice 3rd Edition. *Wiley-Interscience Publication*. 1 – 533.
327. Thakur, Y. and Yadav, R. K. (2018). Effect of Bentonite Clay On Compaction, CBR and Shear Behaviour of Narmada Sand. *International Research Journal of Engineering and Technology (IRJET)*, 5(3), 1–5.
<https://www.irjet.net/archives/V5/i3/IRJET-V5I3484.pdf>
328. Tharini, Ali, N., Raj, V. S., Anto. and Srinivasan. (2020). Effect of Polypropylene Fibre on Swelling Behaviour of Black Cotton Soil. *Materials Today: Proceedings*. <https://doi.org/10.1016/j.matpr.2020.09.356>
329. The British Standards Institution. (2012). BS EN 13286-47:2012 - Unbound and Hydraulically Bound Mixtures. Test Method for The Determination of California Bearing Ratio, Immediate Bearing Index and Linear Swelling. In *The British Standards Institution*. The British Standards Institution.

References

330. The Constructor Building Ideas (TCBI). (2021). Flexible Pavement Design by California Bearing Ratio (CBR) Method. *The Constructor Building Ideas (TCBI)*. <https://theconstructor.org/transportation/flexible-pavement-design-cbr-method/11442/>
331. The geological society, 2012. <https://www.geolsoc.org.uk/Geoscientist/Archive/March-2014/Cracking-up-in-Lincolnshire> (accessed on 16 March 2021).
332. The United Nations. (2021). United Nation Sustainable Development Goals. <https://sdgs.un.org/goals>
333. The World Bank. (2021). What A Waste 2.0 A Global Snapshot of Solid Waste Management to 2050. https://datatopics.worldbank.org/what-a-waste/trends_in_solid_waste_management.html
334. The World Health Organisation. (2021). Climate Change. <https://www.who.int/westernpacific/health-topics/climate-change>
335. Theguardian.com. (2021). Waste Plastics Bottles And Other Types of Plastic Waste. *Pinterest*. <https://www.pinterest.co.uk/pin/maldives-rubbish-island-turns-paradise-into-dump--136585801174778480/>
336. Thoft-Christensen, P. (2012). Infrastructures and Life-Cycle Cost-Benefit Analysis. *Structure and Infrastructure Engineering*, 8(5), 507–516. <https://doi.org/10.1080/15732479.2010.539070>
337. Thurlow, C. (2001). China Clay From Cornwall And Devon-The Modern China Clay Industry (3rd ed.). *Cornish Hillside publications*. 1 – 48.
338. Tiwari, N. and Prasad, C. D. (2018). Effect of Lime and Brick Dust on Compaction and Swelling Property of Black Cotton Soil. *International Journal of Engineering Development And Research*, 6(2), 1–5.
339. Tomar, A., Sharma, T. and Singh, S. (2020). Strength Properties And Durability of Clay Soil Treated With Mixture of Nano Silica And Polypropylene Fiber. *Materials Today: Proceedings*, 26, 3449–3457. <https://doi.org/10.1016/j.matpr.2019.12.239>
340. Tonle, I. K., Ngameni, E., Njopwouo, D., Carteret, C. and Walcarius, A. (2003). Functionalization of Natural Smectite-Type Clays by Grafting With Organosilanes: Physico-Chemical Characterization And Application To Mercury (Ii) Uptake. *Physical Chemistry Chemical Physics*, 5(21), 4951. <https://doi.org/10.1039/b308787e>

References

341. Troy, A. (2016). Subgrade Reactivity Considerations In Pavement Design. In *Industry Articles*. In Industry Articles.
342. Tu, Y., Zhang, R., Zhong, Z. and Chai, H. (2022). The Strength Behavior and Desiccation Crack Development of Silty Clay Subjected to Wetting–Drying Cycles. *Frontiers in Earth Science*, 10. <https://doi.org/10.3389/feart.2022.852820>
343. U.S. Department of Transport, 2020. Federal Highway Administration: chapter 3.0. Geotechnical aspects of pavements reference manual. <https://www.fhwa.dot.gov/engineering/geotech/pubs/05037/03a.cfm>. (Accessed 13 April 2020).
344. Uddin, F. (2017). Montmorillonite: An Introduction to Properties and Utilization. In *Current Topics in the Utilization of Clay in Industrial and Medical Applications*. <https://doi.org/10.5772/intechopen.77987>
345. United Nations (2015). Sendai Framework for Disaster Risk Reduction 2015-2030. <https://www.undrr.org/>
346. United Nations. (1992). United Nations Framework Convention on Climate Change. https://unfccc.int/files/essential_background/background_publications_htmlpdf/application/pdf/conveng.pdf
347. United States Department of Transportation. (2017). Pavements. *Federal Highway Administration*. <https://www.fhwa.dot.gov/pavement/recycling/fach01.cfm>
348. Vakili, A. H., Ghasemi, J., bin Selamat, M. R., Salimi, M. and Farhadi, M. S. (2018). Internal Erosional Behaviour of Dispersive Clay Stabilized with Lignosulfonate And Reinforced With Polypropylene Fiber. *Construction and Building Materials*, 193, 405–415. <https://doi.org/10.1016/j.conbuildmat.2018.10.213>
349. Val, D. V. and Stewart, M. G. (2003). Life-Cycle Cost Analysis of Reinforced Concrete Structures In Marine Environments. *Structural Safety*, 25(4), 343–362. [https://doi.org/10.1016/S0167-4730\(03\)00014-6](https://doi.org/10.1016/S0167-4730(03)00014-6)
350. Valley Trading. (2021). Professional Site Clearance. *Valley Trading*. <https://www.valleytrading.co.uk/the-importance-of-a-professional-site-clearance/>.

References

351. Van Balen, K., (2005). Carbonation Reaction of Lime, Kinetics at Ambient Temperature. *Cement and Concrete Research*. 35 (4), 647-657.
352. Varma, R. S. (2002). Clay and Clay-Supported Reagents In Organic Synthesis. *Tetrahedron*, 58(7), 1235–1255. [https://doi.org/10.1016/S0040-4020\(01\)01216-9](https://doi.org/10.1016/S0040-4020(01)01216-9)
353. Venkatarama, R. B. V. and Lokras, S. S. (1998). Steam-Cured Stabilised Soil Blocks for Masonry Construction. *Energy and Buildings*, 29(1), 29–33. [https://doi.org/10.1016/S0378-7788\(98\)00033-4](https://doi.org/10.1016/S0378-7788(98)00033-4)
354. Venugopal, K. R. (1992). Study of Coarse Fraction In The Groundmass of Ferruginous Soil and Assessing The Parent Material and The Nature of Soil Formation. 40(4), 885–887.
355. Virginia Department of Transport (VDOT). (2016). Construction and Acceptance Testing of Subgrade Material. <https://pdf4pro.com/amp/view/construction-and-acceptance-testing-of-1fa6ed.html>
356. Walker, P. (2000). Review and Experimental Comparison of Erosion Tests for Earth Blocks. *8th International Conference on the Study and Conservation of Earth Architecture*.
357. Walker, R., Pavia, S. (2011). Physical Properties of Pozzolans and Their Influence on The Properties of Lime-Pozzolan Paste, *Materials and Structural*, <http://hdl.handle.net/2262/58454>. (accessed on 16 July 2020)
358. Walls, J., Smith, M. R. (1998). Life-Cycle Cost Analysis in Pavement Design; Interim Technical Bulletin. *Sciences Engineering medicine*. Federal Highway Administration. 1 - 121
359. Waltham, T. (2009). *Fundamentals of Engineering Geology* (3rd ed.). CRC Press. 1 – 104
360. Wan, Y., Guo, D., Hui, X., Liu, L., and Yao, Y. (2020). Studies on Hydration Swelling and Bound Water Type of Sodium and Polymer-Modified Calcium Bentonite. *Advances in Polymer Technology*, 2020, 1–11. <https://doi.org/10.1155/2020/9361795>
361. Wang, J. X. (2016). Expansive Soil and Practice in Foundation Engineering. *PhD Thesis*, P.E. Programs of Civil Engineering Programs Louisiana Tech University, USA

References

362. Wang, R., Zheng, S. and Ping, Y. (2011). Polymer Matrix composition and technology. *A volume in Woodhead Publishing Series in Composite Science and Engineering*. Woodhead Publishing Ltd.
363. Wang, X., Cook, R., Tao, S. and Xing, B. (2007). Sorption of Organic Contaminants By Biopolymers: Role of Polarity, Structure and Domain Spatial Arrangement. *Chemosphere*, 66(8), 1476–1484.
<https://doi.org/10.1016/j.chemosphere.2006.09.004>
364. Wang, Y., Guo, P., Li, X., Lin, H., Liu, Y. and Yuan, H. (2019). Behavior of Fiber-Reinforced and Lime-Stabilized Clayey Soil in Triaxial Tests. *Applied Sciences*, 9(5), 900. <https://doi.org/10.3390/app9050900>
365. Wani, I. A., Sheikh, I. M., Maqbool, T. and Kumar, V. (2021). Experimental Investigation on Using Plastic Wastes To Enhance Several Engineering Properties of Soil Through Stabilization. *Materials Today: Proceedings*, 45, 4571–4574. <https://doi.org/10.1016/j.matpr.2021.01.006>
366. White, J. D. and Vennapusa, P. (2013). Low-cost Rural Surface Alternatives: Literature Review and Recommendations. *InTrans Project Reports*. 28.
367. Wild, S., Khatib, J. M. and Jones, A. (1996). Relative Strength, Pozzolanic Activity and Cement Hydration In Superplasticised Metakaolin Concrete. *Cement and Concrete Research*, 26(10), 1537–1544.
[https://doi.org/10.1016/0008-8846\(96\)00148-2](https://doi.org/10.1016/0008-8846(96)00148-2)
368. Wild, S., Kinuthia, J. M., Jones, G. I. and Higgins, D. D. (1998). Effects of Partial Substitution of Lime with Ground Granulated Blast Furnace Slag (GGBS) on The Strength Properties of Lime-Stabilised Sulphate-Bearing Clay Soils. *Engineering Geology*, 51(1), 37–53. [https://doi.org/10.1016/S0013-7952\(98\)00039-8](https://doi.org/10.1016/S0013-7952(98)00039-8)
369. Wild, W. J., Waalkes, S. and Harrison, R. (2001). Life Cycle Cost Analysis of Portland Cement Concrete Pavements. *Technical Report Documentation Report No. FHWA/TX-00/0-1739-1*
370. Wilson, I. R. (2003). Current World Status of Kaolin from South-West England. *Geoscience in South-West England*, 10, 417–423.
http://ussher.org.uk/wp-content/uploads/journal/2003/06-Wilson_2003.pdf
371. Wirtgen.com. (2021). Soil Stabilization. <https://www.wirtgen-group.com/en-gb/applications/earthworks/soil-stabilisation/>

References

372. Wolters, F., Lagaly, G., Kahr, G., Nueeshch, R. and Emmerich, K. (2009). A Comprehensive Characterization of Dioctahedral Smectites. *Clays and Clay Minerals*, 57(1), 115–133.
<https://doi.org/10.1346/CCMN.2009.0570111>
373. World Wide Fund for Nature. (2021). *World Wide Fund for Nature*.
374. Wu, J., Liu, Q., Deng, Y., Yu, X., Feng, Q. and Yan, C. (2019). Expansive Soil Modified By Waste Steel Slag and Its Application In Subbase Layer of Highways. *Soils and Foundations*, 59(4), 955–965.
<https://doi.org/10.1016/j.sandf.2019.03.009>
375. Yadu, L. and Tripathi, R. K. (2013). Effects of Granulated Blast Furnace Slag in the Engineering Behaviour of Stabilized Soft Soil. *Procedia Engineering*, 51, 125–131. <https://doi.org/10.1016/j.proeng.2013.01.019>
376. Yang, C., Chen, Y., Peng, P., Li, C., Chang, X. and Wu, Y. (2009). Trace Element Transformations and Partitioning During The Roasting of Pyrite Ores In The Sulfuric Acid Industry. *Journal of Hazardous Materials*, 167(1–3), 835–845. <https://doi.org/10.1016/j.jhazmat.2009.01.067>
377. Yi, Y., Liska, M. and Al-Tabbaa, A. (2012). Initial Investigation Into The Use of GGBS-MgO in Soil Stabilisation. *Grouting and Deep Mixing 2012*, 444–453. <https://doi.org/10.1061/9780784412350.0030>
378. Yi, Y., Liska, M. and Al-Tabbaa, A. (2014). Properties and Microstructure of GGBS–Magnesia Pastes. *Advances in Cement Research*, 26(2), 114–122. <https://doi.org/10.1680/adcr.13.00005>
379. YiFan concrete crusher. (2012). Mobile Construction Waste Recycling Equipment. <http://www.recycling-concrete.com/news/133.html>
380. Zaid, A. (2017). Swelling Expansion and Dilation of Soil. LinkedIn <https://www.slideshare.net/AhmedZaid11/swelling-expansion-and-dilation-of-soil>
381. Zakeri, B. and Syri, S. (2015). Electrical Energy Storage Systems: A Comparative Life Cycle Cost Analysis. *Renewable and Sustainable Energy Reviews*, 42, 569–596. <https://doi.org/10.1016/j.rser.2014.10.011>
382. Zanazzi, P., Francesco Comodi, P., Nazzareni, S., Andreozzi, G. and Battista. (2009). Thermal Behaviour of Chlorite: An In Situ Single-Crystal and Powder Diffraction Study. *European Journal of Mineralogy*, 21(3), 581–589. <https://doi.org/10.1127/0935-1221/2009/0021-1928>

References

383. Zhang, H. (2011). Building Materials In Civil Engineering. *A volume in Woodhead Publishing Series in Composite Science and Engineering*.
384. Zhang, R. J., Lu, Y. T., Tan, T. S., Phoon, K. K. and Santoso, A. M. (2014). Long-Term Effect of Curing Temperature on the Strength Behavior of Cement-Stabilized Clay. *Journal of Geotechnical and Geoenvironmental Engineering*, 140(8). [https://doi.org/10.1061/\(ASCE\)GT.1943-5606.0001144](https://doi.org/10.1061/(ASCE)GT.1943-5606.0001144)
385. Zhang, R., Long, M. and Zheng, J. (2019). Comparison of Environmental Impacts of Two Alternative Stabilization Techniques on Expansive Soil Slopes. *Advances in Civil Engineering*, 2019, 1–13. <https://doi.org/10.1155/2019/9454929>
386. Zhao, Y., Goulias, D. and Peterson, D. (2021). Recycled Asphalt Pavement Materials in Transport Pavement Infrastructure: Sustainability Analysis and Metrics. *Sustainability*, 13(14), 8071. <https://doi.org/10.3390/su13148071>
387. Zhu, L. and Zhu, Z. (2020). Reuse of Clay Brick Waste in Mortar and Concrete. *Advances in Materials Science and Engineering*, 2020, 1–11. <https://doi.org/10.1155/2020/6326178>
388. Zhu, X. (2021). The Plastic Cycle – An Unknown Branch of the Carbon Cycle. *Frontiers in Marine Science*, 7. <https://doi.org/10.3389/fmars.2020.609243>
389. Zihms, S. G., Switzer, C., Karstunen, M. and Tarantino, A. (2013). Understanding The Effect of High Temperature Processes on The Engineering Properties of Soils. *Proceedings of the 18th International Conference on Soil Mechanics and Geotechnical Engineering*, 1–1.
390. Zorluer, I. and Gucek, S. (2020). The Usability of Industrial Wastes On Soil Stabilization. *Revista de La Construcción*, 80–89. <https://doi.org/10.7764/rdlc.19.1.80-89>.

APPENDIXES

Appendix 1: Preliminary test

Appendix 1.1 Data table for Figure 82

Data for Proctor compaction data for untreated subgrade materials

Subgrade Type	Moisture Content	Dry density
ASS1 (25%Bentonite + 75% Kaolinite)	65.37	0.519
	34.46	1.254
	17.96	0.760
	13.81	0.735
ASS2 (75%Bentonite + 25% Kaolinite)	59.84	0.525
	49.80	1.033
	40.97	1.174
	39.39	0.826

Appendix 1.2 Data table for Figure 83

Data Table for Atterberg limit data for untreated subgrade materials

Parameters	ASS1 (25%Bentonite + 75% Kaolinite)	ASS2 (75%Bentonite + 25% Kaolinite)
Liquid Limit (LL)	131.26	294.07
Plastic Limit (PL)	28.74	45.38
Plasticity Index	102.52	248.69

Appendix 2: California Bearing Ratio (CBR)

Appendix 2.1 Data table for Figures 85 – 94

Data Table for California Bearing Ratio (CBR) for all samples tested in this research

ASS Subgrade types	Sustainable mix design						Curing days	CBR (%)	Soaked CBR (%)
	Mix proportion in (%) by weight								
	Lime	Cement	GGBS	Plastic	Glass	BDW			
ASS1 untreated	x	x	x	x	x	x	x	8	x
ASS2 untreated	x	x	x	x	x	x	x	9	x
ASS1	8	20	x	x	x	x	7	80	x

Appendixes

ASS Subgrade types	Sustainable mix design						Curing days	CBR (%)	Soaked CBR (%)
	Mix proportion in (%) by weight								
	Lime	Cement	GGBS	Plastic	Glass	BDW			
Control									
ASS2 Control	8	20	x	x	x	x	7	80	x
ASS1	2	2.5	23.5	x	x	x	7	70	79
ASS2	2	2.5	23.5	x	x	x	7	73	46
ASS1	2	2.5	23.5	x	x	x	28	92	97
ASS2	2	2.5	23.5	x	x	x	28	68	65
ASS1	2	2.5	x	23.5	x	x	7	13	12
ASS2	2	2.5	x	23.5	x	x	7	12	6
ASS1	2	2.5	x	23.5	x	x	28	13	8
ASS2	2	2.5	x	23.5	x	x	28	8	3
ASS1	2	2.5	x	x	23.5	x	7	14	17
ASS2	2	2.5	x	x	23.5	x	7	11	3
ASS1	2	2.5	x	x	23.5	x	28	16	11
ASS2	2	2.5	x	x	23.5	x	28	8	4
ASS1	2	2.5	x	x	x	23.5	7	23	17
ASS2	2	2.5	x	x	x	23.5	7	14	18
ASS1	2	2.5	x	x	x	23.5	28	26	28
ASS2	2	2.5	x	x	x	23.5	28	18	17
ASS1	2	2.5	11.75	11.75	x	x	7	44	59
ASS2	2	2.5	11.75	11.75	x	x	7	21	47
ASS1	2	2.5	11.75	11.75	x	x	28	82	93
ASS2	2	2.5	11.75	11.75	x	x	28	51	50
ASS1	2	2.5	11.75	x	11.75	x	7	51	59
ASS2	2	2.5	11.75	x	11.75	x	7	21	31
ASS1	2	2.5	11.75	x	11.75	x	28	80	72
ASS2	2	2.5	11.75	x	11.75	x	28	46	46
ASS1	2	2.5	11.75	x	x	11.75	7	61	61
ASS2	2	2.5	11.75	x	x	11.75	7	27	16
ASS1	2	2.5	11.75	x	x	11.75	28	109	67
ASS2	2	2.5	11.75	x	x	11.75	28	44	24
ASS1	2	2.5	11.75	x	x	11.75	90	180	x

Appendixes

ASS Subgrade types	Sustainable mix design						Curing days	CBR (%)	Soaked CBR (%)
	Mix proportion in (%) by weight								
	Lime	Cement	GGBS	Plastic	Glass	BDW			
ASS2	2	2.5	11.75	x	x	11.75	90	120	x
ASS1	2	2.5	23.5	x	x	x	90	200	x
ASS2	2	2.5	23.5	x	x	x	90	96	x
ASS1	2	x	26	x	x	x	90	220	x
ASS2	2	x	26	x	x	x	90	98	x

Where: ASS = Artificially Synthesised Subgrade material, GGBS = Ground Granulated Blast-furnace Slag, BDW = Brick Dust Waste, ASS1 (25%Bentonite + 75% Kaolinite), ASS2 (75%Bentonite + 25% Kaolinite)

Appendix 3: Swell

Appendix 3.1 Data tables for Figures 95 - 111

Data Table Swell test data in accordance with BS EN 13286-47:2021

Mix design	Curing days	Observation Period (Days)			
		1	2	3	4
		Swell (%)			
ASS1 untreated	x	1.29	3.36	3.87	4.11
ASS2 untreated	x	1.83	4.06	4.64	5.03
ASS1 + 8%Lime + 20% Cement - CONTROL	7	0.01	0.02	0.02	0.03
	28	0.01	0.01	0.02	0.02
ASS2 + 8%Lime + 20%Cement - CONTROL	7	0.02	0.04	0.05	0.06
	28	0.02	0.03	0.03	0.04
ASS1 + 2%Lime + 2.5% Cement + 23.5%BDW	7	0.45	0.57	0.58	0.58
	28	0.31	0.43	0.50	0.56
ASS2 + 2%Lime + 2.5% Cement + 23.5%BDW	7	0.59	0.61	0.62	0.63
	28	0.51	0.58	0.60	0.61
ASS1 + 2%Lime + 2.5%Cement + 23.5%GGBS	7	0.23	0.34	0.39	0.46
	28	0.15	0.23	0.27	0.32
ASS2 + 2%Lime + 2.5%Cement + 23.5%GGBS	7	0.27	0.38	0.44	0.50
	28	0.29	0.35	0.40	0.47
ASS1 + 2%Lime + 2.5% Cement + 23.5% PLASTIC	7	0.37	0.44	0.50	0.56
	28	0.26	0.39	0.48	0.51
ASS2 + 2%Lime + 2.5% Cement + 23.5% PLASTIC	7	0.49	0.53	0.57	0.61
	28	0.39	0.47	0.53	0.59
ASS1 + 2%Lime + 2.5%Cement + 23.5%GLASS	7	0.25	0.40	0.47	0.52
	28	0.20	0.35	0.44	0.46

Appendixes

ASS2 + 2%Lime + 2.5%Cement + 23.5%GLASS	7	0.46	0.53	0.62	0.64
	28	0.40	0.46	0.55	0.57
ASS1 + 2%Lime + 2.5% Cement + 11.75% GGBS +11.75 PLASTIC	7	0.20	0.29	0.35	0.38
	28	0.12	0.24	0.33	0.36
ASS2 + 2%Lime + 2.5% Cement + 11.75% GGBS +11.75 PLASTIC	7	0.54	0.78	0.89	0.94
	28	0.35	0.41	0.46	0.47
ASS1 + 2%Lime + 2.5% Cement + 11.75% GGBS +11.75% GLASS	7	0.22	0.31	0.40	0.41
	28	0.19	0.31	0.39	0.39
ASS2 + 2%Lime + 2.5% Cement + 11.75% GGBS +11.75% GLASS	7	0.31	0.46	0.53	0.56
	28	0.22	0.38	0.48	0.50
ASS1 + 2%Lime + 2.5%Cement + 11.75%GGBS+11.75BDW	7	0.25	0.37	0.41	0.43
	28	0.24	0.34	0.40	0.42
ASS2 + 2%Lime + 2.5%Cement + 11.75%GGBS+11.75BDW	7	0.30	0.41	0.48	0.54
	28	0.28	0.39	0.42	0.49

Where: ASS = Artificially Synthesised Subgrade material, GGBS = Ground Granulated Blast-furnace Slag, BDW = Brick Dust Waste, ASS1 (25%Bentonite + 75% Kaolinite), ASS2 (75%Bentonite + 25% Kaolinite)

Appendix 3.2 Data table for Figures 112 - 114

Data Table for Swell test in accordance with BS EN 13286-49:2004

Untreated				Treated			
Mix design	Observation Period (Days)	Curing days	Swell (%)	Mix design	Observation Period (Days)	Curing days	Swell (%)
ASS1	1	x	18.32	ASS1 + 8% Lime + 20% Cement	1	7	0.04
ASS2			21.12	ASS2 + 8% Lime + 20% Cement			0.2
ASS1	2	x	24.24	ASS1 + 8% Lime + 20% Cement	2	7	0.04
ASS2			35.88	ASS2 + 8% Lime + 20% Cement			0.2
ASS1	3	x	27.28	ASS1 + 8% Lime + 20% Cement	3	7	0.04
ASS2			47.88	ASS2 + 8% Lime + 20% Cement			0.2
ASS1	4	x	29.24	ASS1 + 8% Lime + 20% Cement	4	7	0.04
ASS2			55.00	ASS2 + 8% Lime + 20% Cement			0.2
ASS1	5	x	30.08	ASS1 + 8% Lime + 20% Cement	5	7	0.04
ASS2			55.16	ASS2 + 8% Lime + 20% Cement			0.2
ASS1	6	x	31.36	ASS1 + 8% Lime + 20% Cement	6	7	0.04
ASS2			56.04	ASS2 + 8% Lime + 20% Cement			0.2
ASS1	7	x	32.60	ASS1 + 8% Lime + 20% Cement	7	7	0.04
ASS2			56.04	ASS2 + 8% Lime + 20% Cement			0.2
ASS1	8	x	33.52	ASS1 + 8% Lime + 20% Cement	8	7	0.04
ASS2			56.40	ASS2 + 8% Lime + 20% Cement			0.2
ASS1	9	x	33.52	ASS1 + 8% Lime + 20% Cement	9	7	0.04
ASS2			56.52	ASS2 + 8% Lime + 20% Cement			0.2
ASS1	10	x	34.04	ASS1 + 8% Lime + 20% Cement	10	7	0.04
ASS2			56.56	ASS2 + 8% Lime + 20% Cement			0.2
ASS1	11	x	34.36	ASS1 + 8% Lime + 20% Cement	11	7	0.04
ASS2			56.56	ASS2 + 8% Lime + 20% Cement			0.2

Appendixes

ASS1	12	x	34.76	ASS1 + 8% Lime + 20% Cement	12	7	0.04
ASS2			56.56	ASS2 + 8% Lime + 20% Cement			0.2
ASS1	13	x	35.32	ASS1 + 8% Lime + 20% Cement	13	7	0.04
ASS2			56.56	ASS2 + 8% Lime + 20% Cement			0.2
ASS1	14	x	35.48	ASS1 + 8% Lime + 20% Cement	14	7	0.04
ASS2			56.56	ASS2 + 8% Lime + 20% Cement			0.2
ASS1	15	x	35.56	ASS1 + 8% Lime + 20% Cement	15	7	0.04
ASS2			56.56	ASS2 + 8% Lime + 20% Cement			0.2
ASS1	16	x	35.64	ASS1 + 8% Lime + 20% Cement	16	7	0.04
ASS2			56.56	ASS2 + 8% Lime + 20% Cement			0.2
ASS1	17	x	35.92	ASS1 + 8% Lime + 20% Cement	17	7	0.04
ASS2			56.56	ASS2 + 8% Lime + 20% Cement			0.2
ASS1	18	x	35.92	ASS1 + 8% Lime + 20% Cement	18	7	0.04
ASS2			56.56	ASS2 + 8% Lime + 20% Cement			0.2
ASS1	19	x	35.92	ASS1 + 8% Lime + 20% Cement	19	7	0.04
ASS2			56.56	ASS2 + 8% Lime + 20% Cement			0.2
ASS1	20	x	35.92	ASS1 + 8% Lime + 20% Cement	20	7	0.04
ASS2			56.56	ASS2 + 8% Lime + 20% Cement			0.2
ASS1	21	x	35.92	ASS1 + 8% Lime + 20% Cement	21	7	0.04
ASS2			56.56	ASS2 + 8% Lime + 20% Cement			0.2
ASS1	22	x	35.92	ASS1 + 8% Lime + 20% Cement	22	7	0.04
ASS2			56.56	ASS2 + 8% Lime + 20% Cement			0.2
ASS1	23	x	35.92	ASS1 + 8% Lime + 20% Cement	23	7	0.04
ASS2			56.56	ASS2 + 8% Lime + 20% Cement			0.2
ASS1	24	x	35.92	ASS1 + 8% Lime + 20% Cement	24	7	0.04
ASS2			56.56	ASS2 + 8% Lime + 20% Cement			0.2
ASS1	25	x	35.92	ASS1 + 8% Lime + 20% Cement	25	7	0.04
ASS2			56.56	ASS2 + 8% Lime + 20% Cement			0.2
ASS1	26	x	35.92	ASS1 + 8% Lime + 20% Cement	26	7	0.04
ASS2			56.56	ASS2 + 8% Lime + 20% Cement			0.2
ASS1	27	x	35.92	ASS1 + 8% Lime + 20% Cement	27	7	0.04
ASS2			56.56	ASS2 + 8% Lime + 20% Cement			0.2
ASS1	28	x	35.92	ASS1 + 8% Lime + 20% Cement	28	7	0.04
ASS2			56.56	ASS2 + 8% Lime + 20% Cement			0.2

Where, ASS1 (25%Bentonite + 75% Kaolinite), ASS2 (75%Bentonite + 25% Kaolinite)

Appendix 4: Durability test - wetting-drying cycle

Appendix 4.1 Data table for Figures 115 – 122

Data Table for Durability Test - Wetting-drying Cycle

Cycle No	Mix design	Curing days	Wet Cycle	Dry Cycle	Wet Cycle Mass	Dry Cycle Mass
2% Lime + 2.5% Cement + 23.5% GGBS						
1	ASS1	28	180	230	3.75	2.84
2	ASS1	28	160	220	3.69	2.81
3	ASS1	28	140	210	3.12	2.81

Appendixes

4	ASS1	28	120	200	2.99	2.78
5	ASS1	28	110	190	2.97	2.77
6	ASS1	28	100	180	2.95	2.75
7	ASS1	28	88	160	2.72	2.73
8	ASS1	28	70	120	2.61	2.73
9	ASS1	28	66	98	2.63	2.72
10	ASS1	28	52	70	2.61	2.72
1	ASS2	28	100	200	3.84	3.66
2	ASS2	28	83	100	3.83	3.65
3	ASS2	28	70	83	3.69	3.42
4	ASS2	28	56	66	3.67	3.01
5	ASS2	28	43	56	3.67	2.82
6	ASS2	28	42	52	3.61	2.81
7	ASS2	28	33	50	3.51	2.78
8	ASS2	28	29	48	3.51	2.76
9	ASS2	28	27	45	3.52	2.71
10	ASS2	28	23	43	3.42	2.68
2%Lime + 2.5%Cement + 11.75%GGBS+11.75BDW						
1	ASS1	28	120	190	3.91	3.35
2	ASS1	28	89	180	3.92	3.31
3	ASS1	28	88	110	3.91	3.31
4	ASS1	28	83	98	3.89	3.29
5	ASS1	28	78	93	3.88	3.28
6	ASS1	28	69	88	3.87	3.28
7	ASS1	28	58	79	3.87	3.26
8	ASS1	28	46	70	3.86	3.25
9	ASS1	28	39	69	3.85	3.25
10	ASS1	28	16	58	3.84	3.24
1	ASS2	28	79	84	3.93	3.32
2	ASS2	28	67	79	3.88	3.31
3	ASS2	28	52	70	3.87	3.31
4	ASS2	28	51	66	3.87	3.28
5	ASS2	28	45	58	3.84	3.28
6	ASS2	28	38	45	3.83	3.28
7	ASS2	28	33	38	3.83	3.26
8	ASS2	28	27	33	3.83	3.25
9	ASS2	28	19	23	3.82	3.25
10	ASS2	28	15	19	3.82	3.22
Where, ASS1 (25%Bentonite + 75% Kaolinite), ASS2 (75%Bentonite + 25% Kaolinite)						

Appendix 5 : Calculation

Appendix 5.1 Defect calculations procedure for Figures 186 – 197

Fatigue

$$N_{fatigue} = f_1(\epsilon_t)^{-f_2} (E_1)^{-f_3}$$

ASS1 (25% Bentonite + 75% Kaolinite) untreated soaked CBR = 0.6% Light Traffic

$$0.0796(9.2E - 05)^{-3.291}(1350)^{-0.854} = 3.22E+09$$

ASS1 + 2%Lime + 2.5% Cement + 23.5 GGBS Soaked 28days curing CBR = 97% Light Traffic

$$0.0796(3.58E - 06)^{-3.291}(1350)^{-0.854} = 3.58E-06$$

Permanent deformation

$$N_{permanent\ deformation} = f_4 E^{-9} (\epsilon_c)^{-f_5}$$

ASS1 + 2%Lime + 2.5% Cement + 23.5%BDW Soaked 28 days curing CBR 17% Heavy Traffic

$$1.37E-09 \times 1350^{-9} (6.81E - 06)^{-4.477} = 1.24E-14$$

ASS2 + 2%Lime + 2.5% Cement + 11.75%GGBS + 11.75%Plastic 7 days curing CBR 21% Heavy Traffic

$$1.37E-09 \times 1350^{-9} (5.32E - 04)^{-4.477} = 4.19E-23$$

Rutting Life Prediction

$$N = 4.1656 \times 10^{-08} \times \left[\frac{1}{\epsilon_c}\right]^{4.5337}$$

ASS1 + 2%Lime + 2.5% Cement + 23.5%Plastic Soaked after 28 days of curing CBR 8% Light Traffic

$$4.1656 \times 10^{-08} \times \left[\frac{1}{5.57E-06}\right]^{4.5337} = 2.40E+06$$

ASS2 + 2%Lime + 2.5% Cement + 23.5%Glass Soaked after 28 days of curing CBR 4% Light Traffic

$$4.1656 \times 10^{-08} \times \left[\frac{1}{9.88E-04}\right]^{4.5337} = 1.76E+06$$

Appendixes

Appendix 6 Economic appraisal

Appendix 6.1 Cost calculations procedure used for Figures 239 – 247

Data Table for Cost calculations for binder per mix design

Mix design	Binder	Mass of binder (kg)/mix design	Mass of binder/ cubic meter (kg)	Mass of binder/ km (kg)	Unit price (£) 25kg	20% VAT of 25kg	Price (£) per 25kg + (20%) VAT	Price (£) per kg + VAT	Estimated delivery charge (£) (2%)	Cost (£) per kg	Cost of Binder (£)/mix design	Cost of binder (£)/square meter	Cost (£) of binder per km of road	Overall cost (£) of binder per km of road
ASS+ 8%Lime + 20%Cement (CONTROL)	Lime	0.32	0.065	64800	£13.40	£2.68	£16.08	£0.64	£0.013	£0.656	£2.050	£0.13	£132,852.96	£182,325.82
	Cement	0.8	0.162	162000	£4.99	£1.00	£5.99	£0.24	£0.005	£0.24	£0.305	£0.05	£49,472.86	
ASS+ 2L+2.5C+23.5BDW	Lime	0.08	0.016	16200	£13.40	£2.68	£16.08	£0.64	£0.01	£0.66	£8.201	£0.13	£132,852.96	£285,633.86
	Cement	0.1	0.020	20250	£4.99	£1.00	£5.99	£0.24	£0.00	£0.24	£2.443	£0.05	£49,472.86	
	BDW	0.94	0.190	190350	£10.42	£2.08	£12.50	£0.50	£0.010	£0.51	£0.543	£0.10	£103,308.05	
ASS+ 2L+2.5C+23.5GGBS	Lime	0.08	0.0162	16200	£13.40	£2.68	£16.08	£0.64	£0.01	£0.66	£8.201	£0.13	£132,852.96	£271,555.42
	Cement	0.1	0.02025	20250	£4.99	£1.00	£5.99	£0.24	£0.00	£0.24	£2.443	£0.05	£49,472.86	
	GGBS	0.94	0.19035	190350	£9.00	£1.80	£10.80	£0.43	£0.01	£0.44	£0.469	£0.09	£89,229.60	
ASS+ 2L+2.5C+23.5PLASTIC	Lime	0.08	0.0162	16200	£13.40	£2.68	£16.08	£0.64	£0.01	£0.66	£8.201	£0.13	£132,852.96	£836,577.07
	Cement	0.1	0.02025	20250	£4.99	£1.00	£5.99	£0.24	£0.00	£0.24	£2.443	£0.05	£49,472.86	
	PLASTIC	0.94	0.19035	190350	£65.99	£13.20	£79.19	£3.17	£0.06	£3.23	£3.437	£0.65	£654,251.26	
ASS+ 2L+2.5C+23.5GLASS	Lime	0.08	0.0162	16200	£13.40	£2.68	£16.08	£0.64	£0.01	£0.66	£8.201	£0.13	£132,852.96	£221,983.42
	Cement	0.1	0.02025	20250	£4.99	£1.00	£5.99	£0.24	£0.00	£0.24	£2.443	£0.05	£49,472.86	
	GLASS	0.94	0.19035	190350	£4	£0.80	£4.80	£0.19	£0.00	£0.20	£0.208	£0.04	£39,657.60	
ASS+ 2L+2.5C+11.75GGBS+11.75PLASTIC	Lime	0.08	0.0162	16200	£13.40	£2.68	£16.08	£0.64	£0.01	£0.66	£8.201	£0.13	£132,852.96	£925,806.67
	Cement	0.1	0.02025	20250	£4.99	£1.00	£5.99	£0.24	£0.00	£0.24	£2.443	£0.05	£49,472.86	
	GGBS	0.47	0.095175	95175	£9.00	£1.80	£10.80	£0.43	£0.01	£0.44	£0.938	£0.09	£89,229.60	
	PLASTIC	0.47	0.095175	95175	£65.99	£13.198	£79.19	£3.17	£0.06	£3.23	£6.874	£0.65	£654,251.26	
	Lime	0.08	0.0162	16200	£13.40	£2.68	£16.08	£0.64	£0.01	£0.66	£8.201	£0.13	£132,852.96	£311,213.02

Appendixes

Mix design	Binder	Mass of binder (kg)/mix design	Mass of binder/ cubic meter (kg)	Mass of binder/ km (kg)	Unit price (£) 25kg	20% VAT of 25kg	Price (£) per 25kg + (20%) VAT	Price (£) per kg + VAT	Estimated delivery charge (£) (2%)	Cost (£) per kg	Cost of Binder (£)/mix design	Cost of binder (£)/square meter	Cost (£) of binder per km of road	Overall cost (£) of binder per km of road
ASS+ 2L+2.5C+11.75GGBS+11.75GLASS	Cement	0.1	0.02025	20250	£4.99	£1.00	£5.99	£0.24	£0.00	£0.24	£2.443	£0.05	£49,472.86	
	GGBS	0.47	0.095175	95175	£9.00	£1.80	£10.80	£0.43	£0.01	£0.44	£0.938	£0.09	£89,229.60	
	GLASS	0.47	0.095175	95175	£4	£0.80	£4.80	£0.19	£0.00	£0.20	£0.417	£0.04	£39,657.60	
ASS+ 2L+2.5C+11.75GGBS+11.75BDW	Lime	0.08	0.0162	16200	£13.40	£2.68	£16.08	£0.64	£0.01	£0.66	£8.201	£0.13	£132,852.96	£374,863.46
	Cement	0.1	0.02025	20250	£4.99	£1.00	£5.99	£0.24	£0.00	£0.24	£2.443	£0.05	£49,472.86	
	GGBS	0.47	0.095175	95175	£9.00	£1.80	£10.80	£0.43	£0.01	£0.44	£0.938	£0.09	£89,229.60	
	BDW	0.47	0.095175	95175	£10.42	£2.08	£12.50	£0.50	£0.01	£0.51	£1.085	£0.10	£103,308.05	
ASS+ 2L+26GGBS	Lime	0.08	0.0162	16200	£13.40	£2.68	£16.08	£0.64	£0.01	£0.66	£8.201	£0.13	£132,852.96	£222,082.56
	GGBS	0.94	0.19035	190350	£9.00	£1.80	£10.80	£0.43	£0.01	£0.44	£0.469	£0.09	£89,229.60	

Appendixes

Appendix 6.2 Agency and user cost data.

Data Table from RealCost Software

Total Cost	Alternative 1		Alternative 2	
	Agency Cost	User Cost	Agency Cost	User Cost
Undiscounted	£6,000,000.00	£80,000.06	£7,200,000.0	£133,000.
Sum			0	43
Net Present Value	£5,521,000.40	£80,000.06	£6,632,000.9	£133,000.
			1	43
EUAC	£295,000.82	£4,000.29	£355,000.37	£7,000.15
Lowest Net Present Value User Cost		Alternative 1		

Appendix 6.3 Estimated maintenance, rehabilitation cost and discount rate

Data Table from RealCost Software

Year	Estimated Maintenance Costs (£)	Estimated Rehabilitation Cost (£)	Assumed Discount Rate (%)
Year 6 Year 9	24,000,300	35,080,000.06	2%
Year 19 Year 21	44,006,000	40,080,000.06	6%
Year 28 Year 30	67,002,000	52,080,000.06	8%

Appendix 6.4 Life cycle cost analysis calculations procedure

Appendix 6.4.1 LCCA treated subgrade

LCCA calculation using treated subgrade - 8%Lime + 20%Cement (CONTROL MIX) as an example

1. Initial Cost Year 0 = Alternative 1 (Net Present Value Agency Cost) + Alternative 1 (User Cost) + Overall cost of binder per square km of road = £5,783,326.28
2. Maintenance #1 Cost Year 6 = £24,000,300
3. Rehabilitation #1 Cost Year 9 = £35,080,000.06
4. Maintenance #2 Cost Year 19 = £44,006,000
5. Rehabilitation #2 Cost Year 21 = £40,080,000.06
6. Maintenance #3 Cost Year 30 = £67,002,000

Appendixes

7. Rehabilitation #3 Cost Year 35 = 52,080,000.06
8. Salvage value (0.67% of Rehab#3) Year 35 = £312,480
9. Total Life Cycle Cost (Stabilised Subgrade) = £268,344,106.46

Appendix 6.4.2 LCCA calculation subgrade removal and replacement

Data Table for removal and replacement of square km subgrade

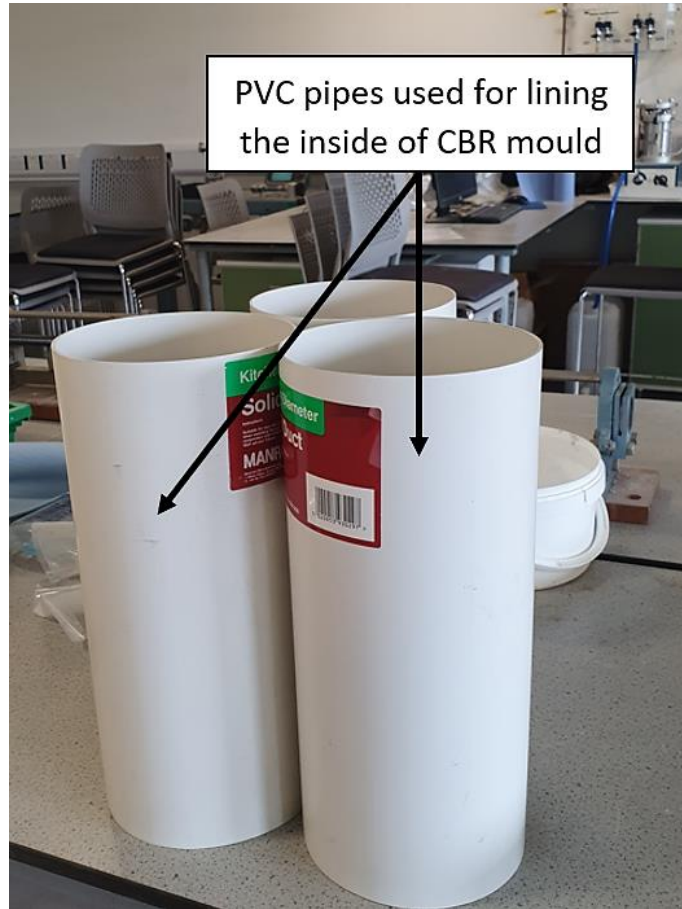
Item	Cost (Estimate)
Cost of plant hire and operation	£20,600,450.00
Cost of transporting excavated materials & dumping site fees	£60,000,235.00
Cost of buying and transporting granular materials to the site	£200,000,224.00
The total cost of removing and replacing a square km of subgrade	£220,600,674.00

Initial Cost Year 0 = Alternative 1 - Net Present Value + Alternative 1 - User Cost +
Overall cost of binder per square km of road

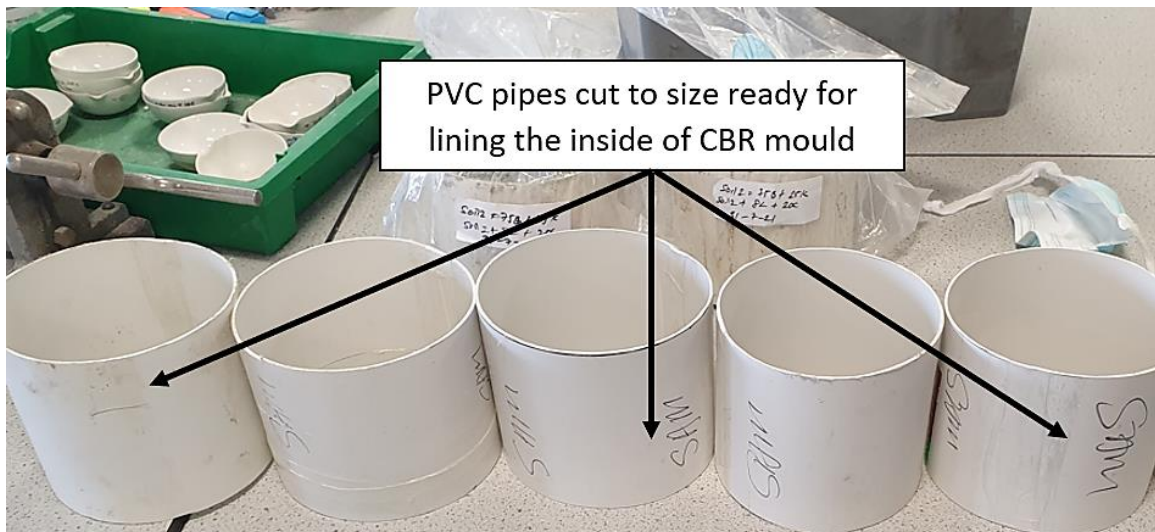
1. Initial Cost Year 0 = Alternative 1 (Net Present Value Agency Cost) +
Alternative 1 (User Cost) + Total cost removing and replacing a square km of
road subgrade = 226,201,674.46
2. Maintenance #1 Cost Year 6 = £24,000,300
3. Rehabilitation #1 Cost Year 9 = £35,080,000.06
4. Maintenance #2 Cost Year 19 = £44,006,000
5. Rehabilitation #2 Cost Year 21 = £40,080,000.06
6. Maintenance #3 Cost Year 30 = £67,002,000
7. Rehabilitation #3 Cost Year 35 = 52,080,000.06
8. Salvage value (0.67% of Rehab#3) Year 35 = £312,480
9. Total Life cycle cost (Subgrade Removed & replaced) = £488,754,774.64

Appendix 7 Laboratory photos

Appendix 7.1 Research limitations



PVC pipes were used for lining the inside of CBR mould

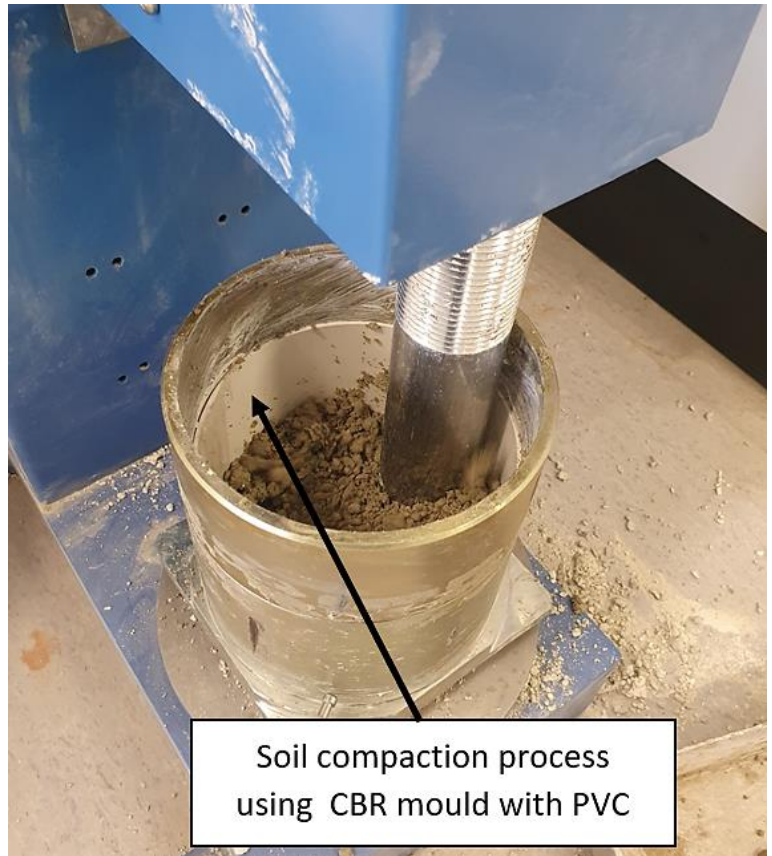


PVC pipes cut to size ready for lining the inside of the CBR mould

Appendixes



CBR mould with PVC lining ready for soil compaction



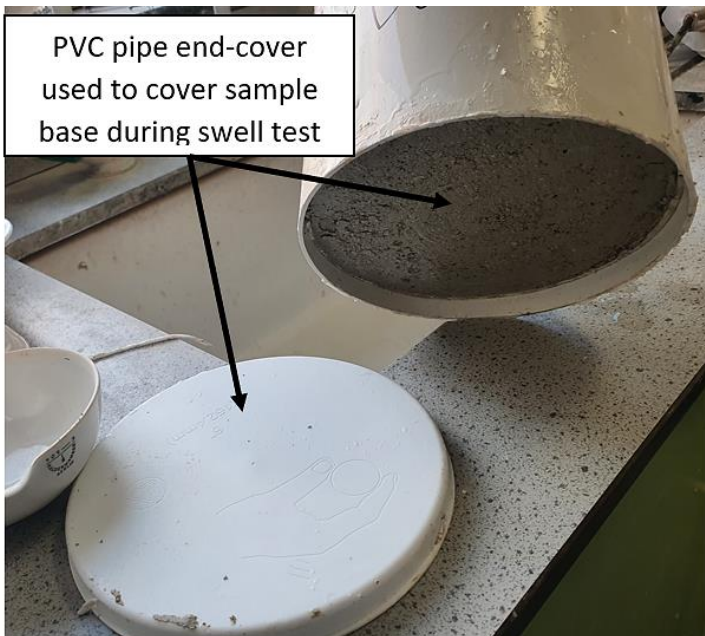
Soil compaction process using CBR mould with PVC



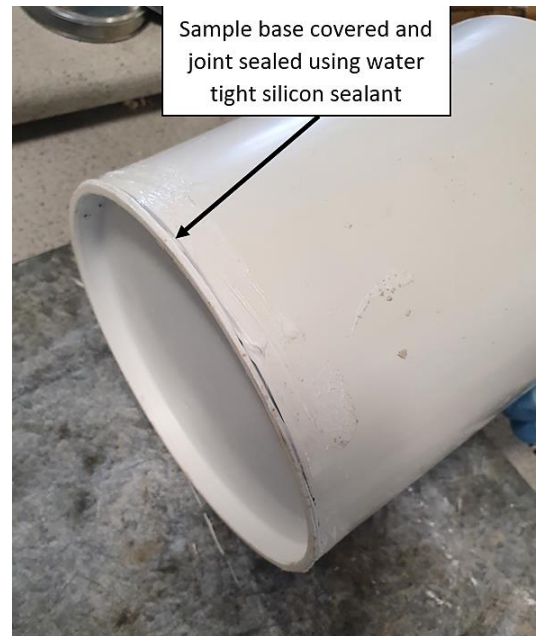
Extruding compacted soil inside PVC pipe ready for curing



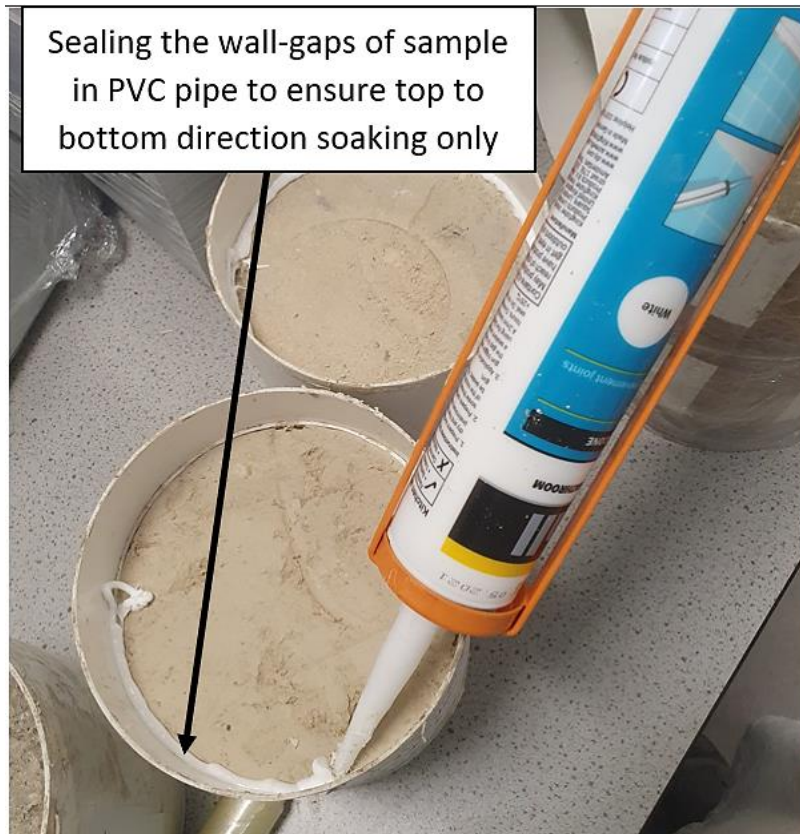
Curing process of extruded compacted soil in PVC pipe wrapped in cling film



PVC pipe end-cover used to cover sample base during swell test



Sample base covered and joint sealed using water-tight silicon sealant



Sealing the wall gaps of sample in PVC pipe to ensure top to bottom direction soaking only



Researcher fabricating swell plates for swell test



Researcher fabricating swell plates for swell test

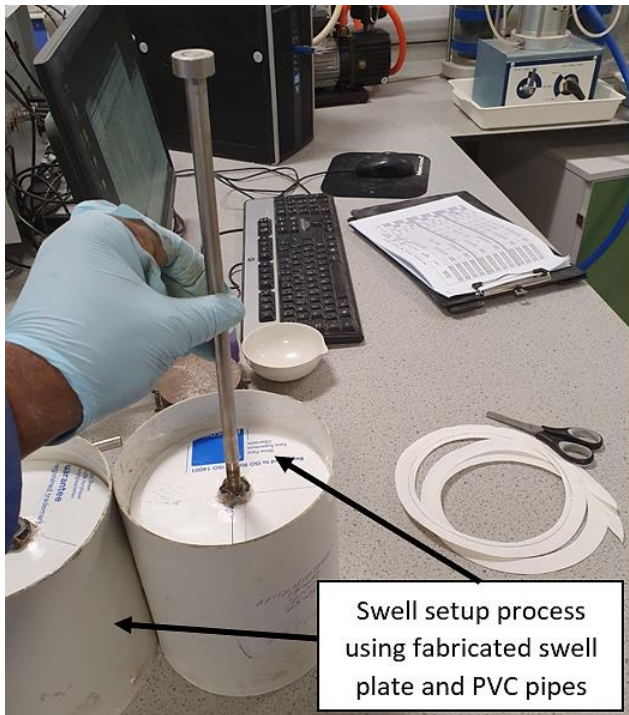
Appendixes



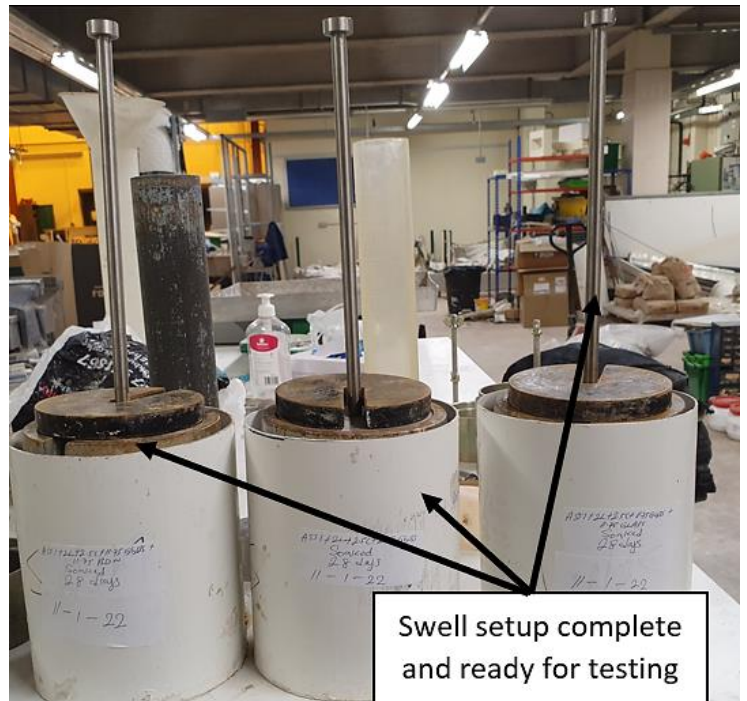
Researcher fabricating swell plates for swell test



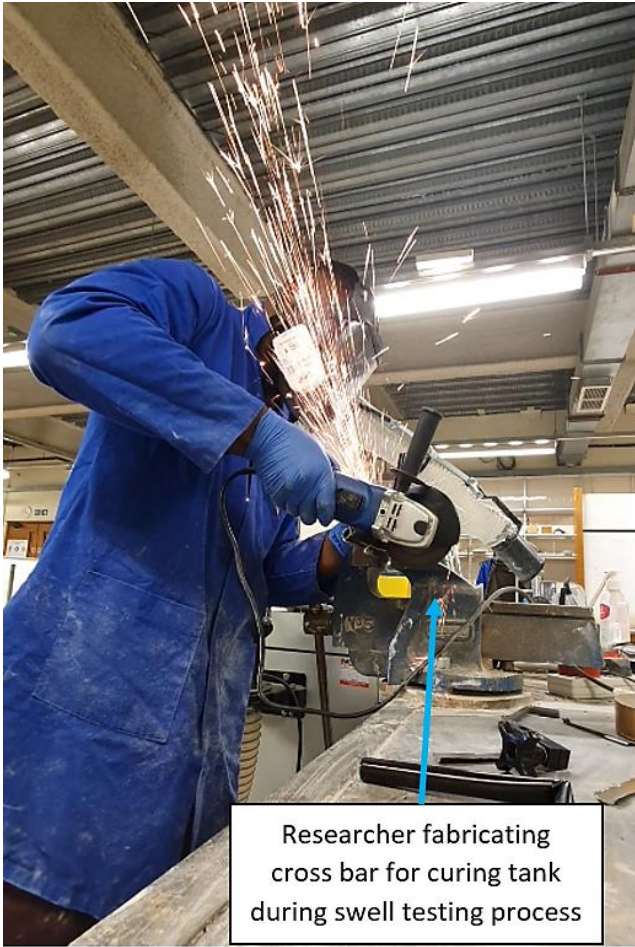
Researcher fabricating swell plates for swell test



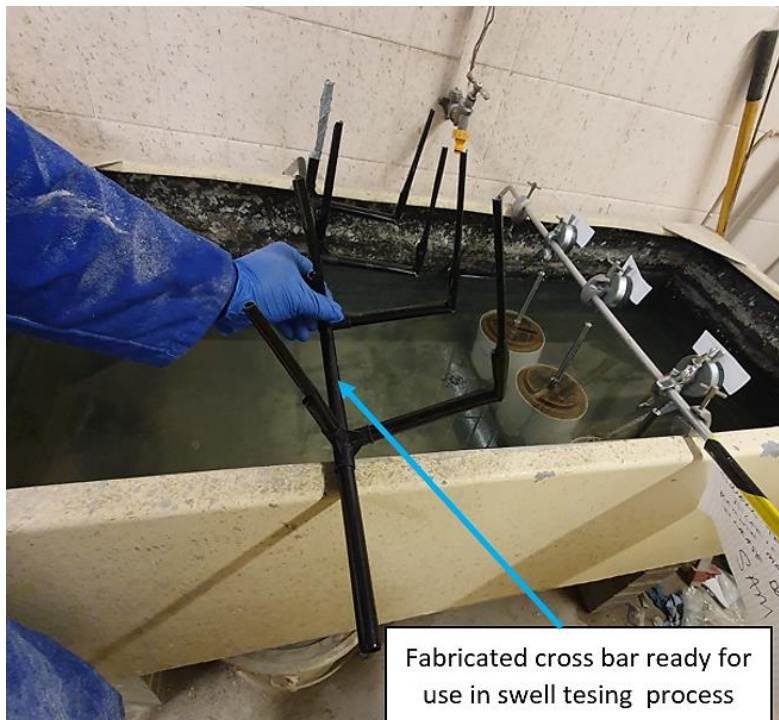
Swell setup process using the fabricated swell plate and PVC pipes



Swell setup complete and ready for testing



Researcher fabricating crossbar for curing tank during the swell testing process



Fabricated cross bar ready for use in swell testing process



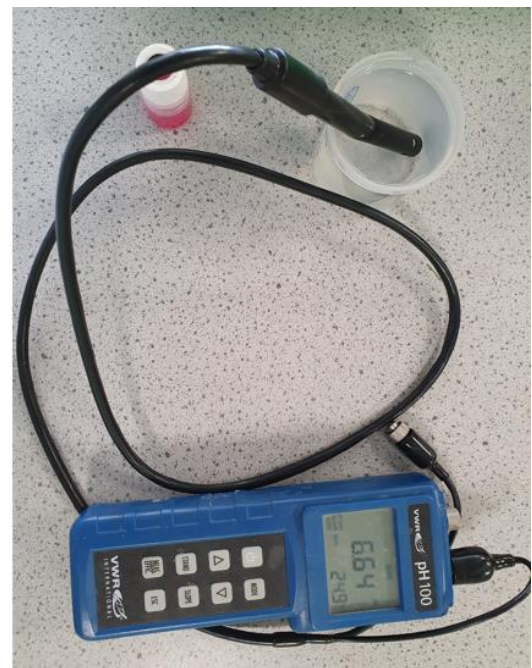
Swell setup using fabricated cross bar, PVC pipes and swell plates

Swell setup using the fabricated crossbar, PVC pipes and swell plates

Appendix 7.2 Preliminary test process



Testing the pH of water used in the mixture



pH value of water used in the mixture

Appendixes



Plastic Limit testing process



Liquid Limit testing process



Proctor compaction test sample preparation



Proctor compaction test sample preparation

Appendix 7.3 California Bearing Ratio sample preparation and testing



Brick dust waste and other binders added to subgrade material during the mixing process



Recycled glass grits and other binders added to subgrade material during the mixing process



Recycled plastic pellets and other binders added to subgrade material during the mixing process



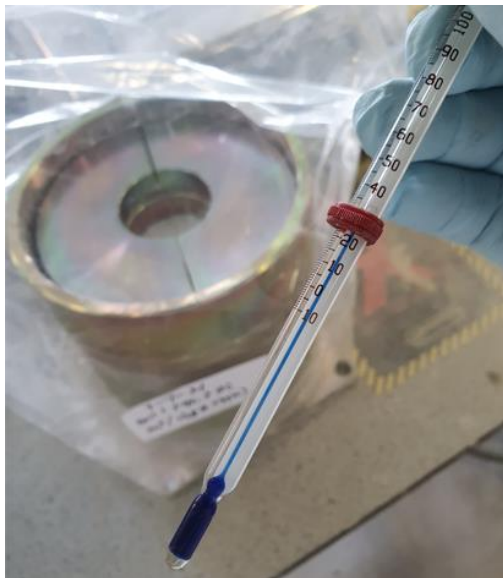
The mixing process of treated subgrade materials



Manual CBR test sample compaction Process



Trimming CBR test sample



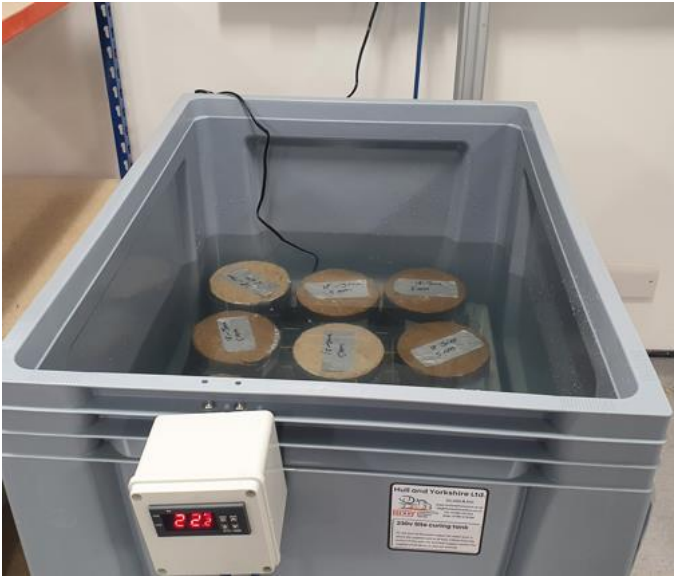
Curing CBR test sample



Sealing joints of CBR mould with sample using silicon gel ready for swell test



Appendix 7.4 Wetting-drying sample preparation and testing process



Soaking CBR samples for wetting cycle test



CBR sample eroded after due to cyclic wetting



Oven-drying samples for drying cycle test



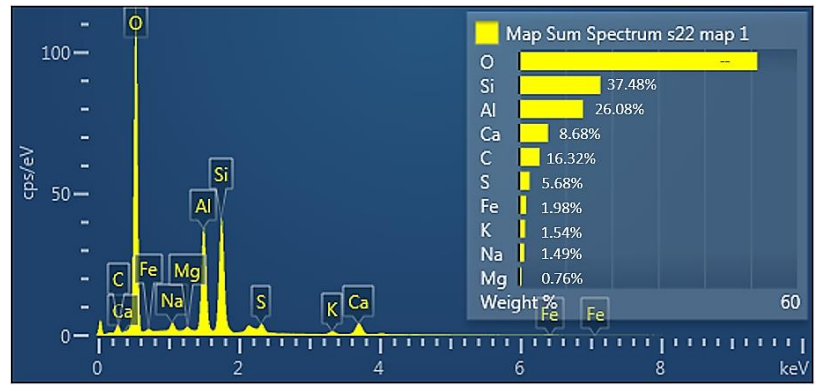
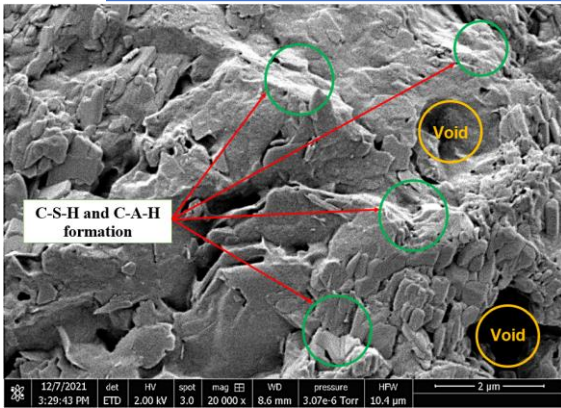
CBR sample cracking due to cyclic drying

Appendix 7.5 SEM and EDX

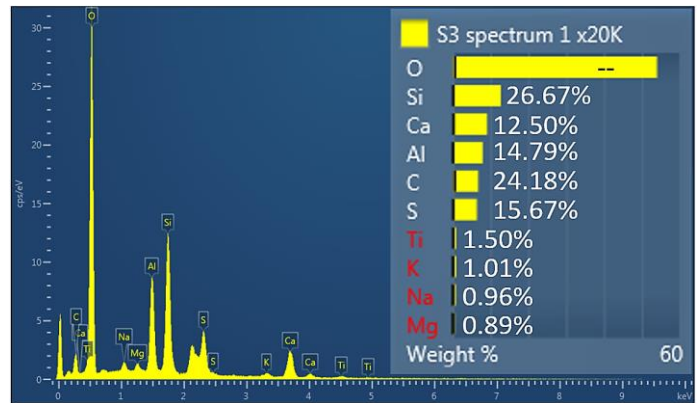
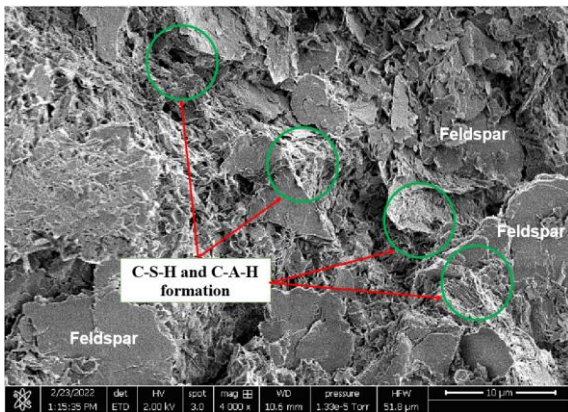


SEM and EDX samples prepared and ready for testing

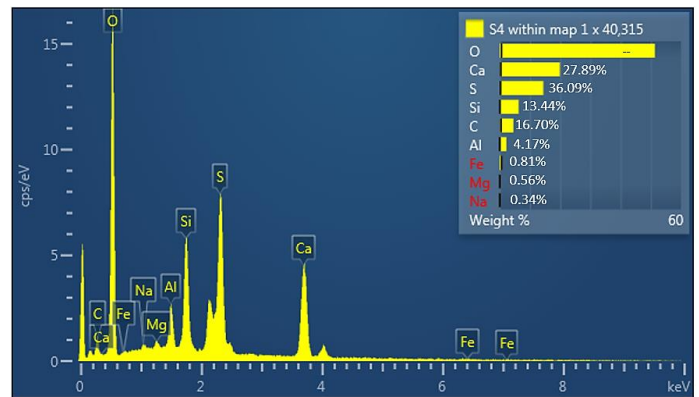
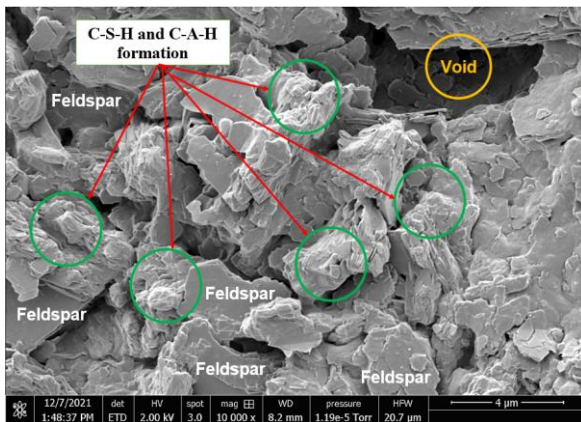
Appendixes



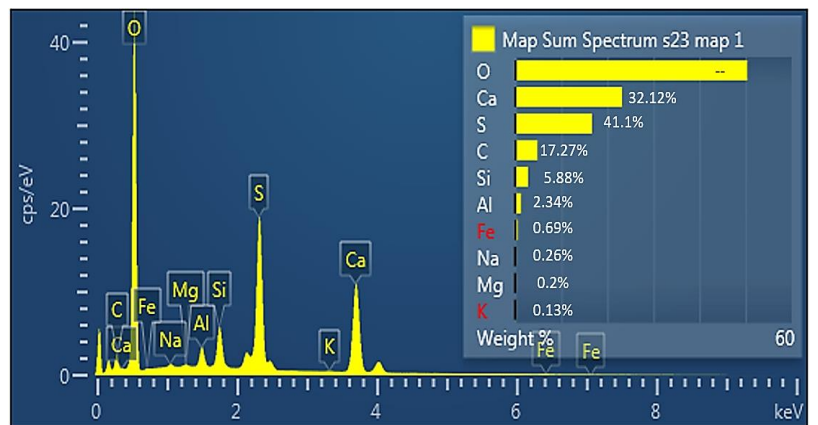
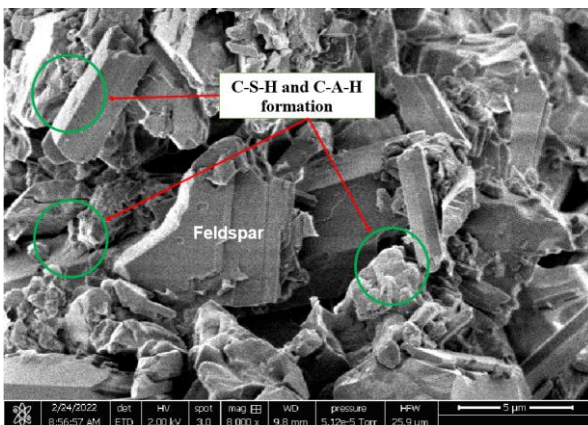
SEM image and EDX results for ASS1+2% Lime 2.5% Cement + 23.5%BDW after 7 days of curing



SEM image and EDX results for ASS1+2% Lime 2.5% Cement + 23.5%BDW after 28 days of curing

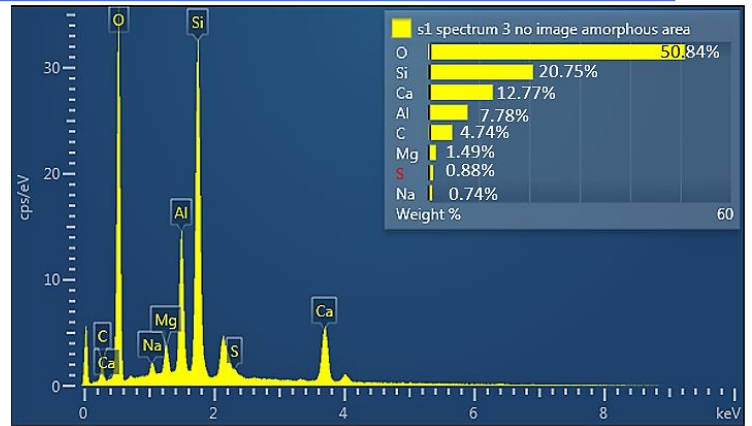
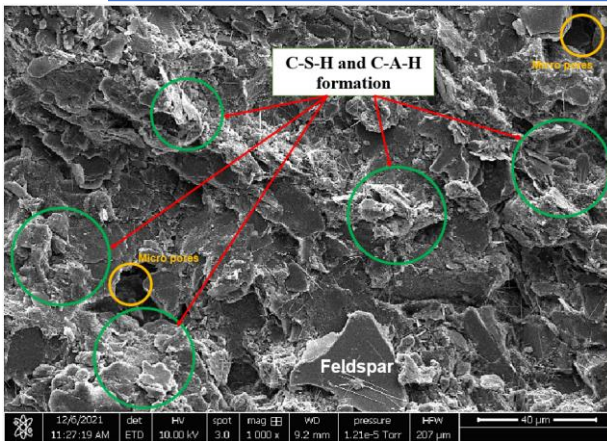


SEM image and EDX results for ASS2+2% Lime 2.5% Cement + 23.5%BDW after 7 days of curing

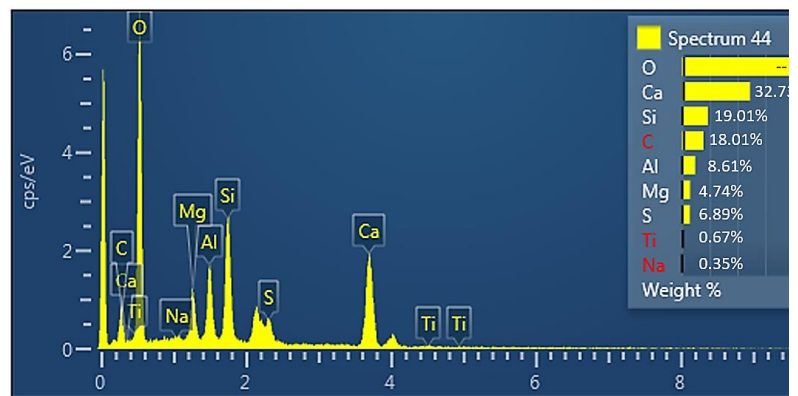
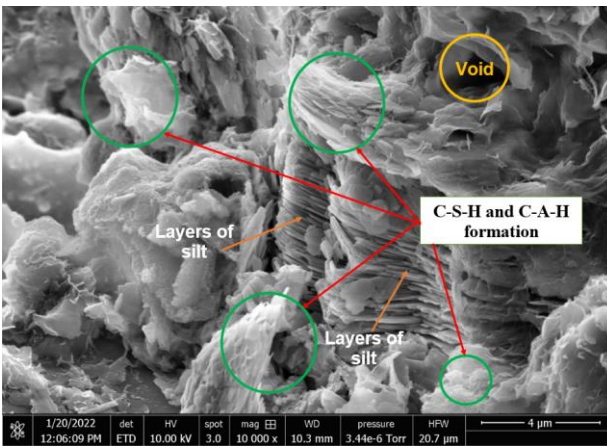


SEM image and EDX results for ASS2+2% Lime + 2.5% Cement + 23.5%BDW after 28 Days curing

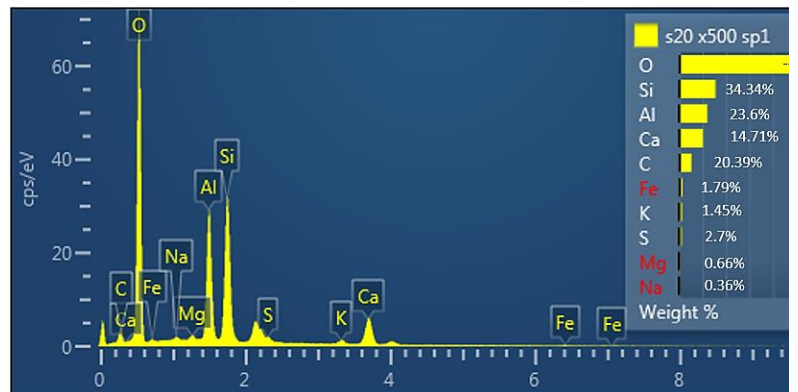
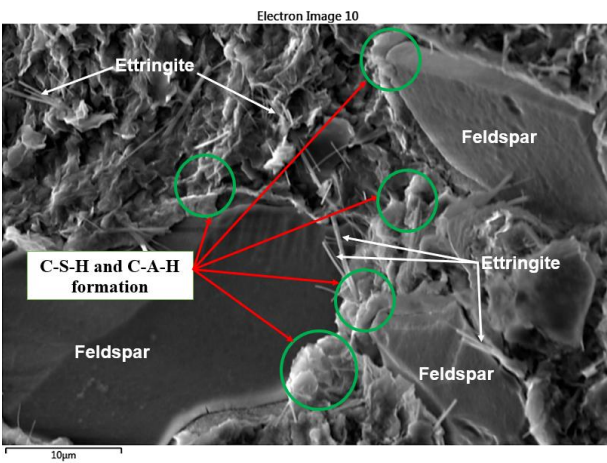
Appendixes



SEM image and EDX results for ASS1+2%Lime+2.5%Cement+23.5%GGBS after 7 days of curing

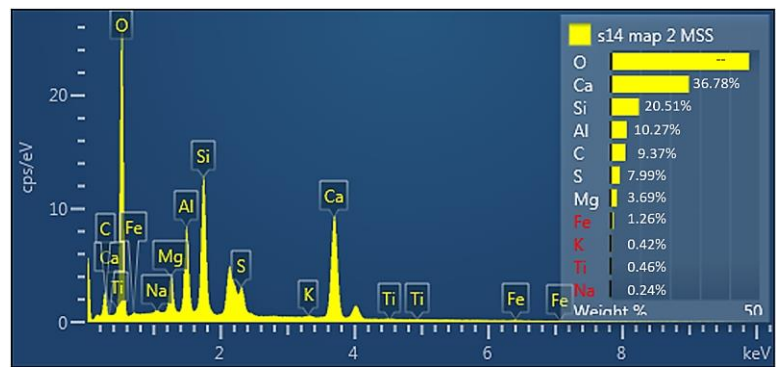
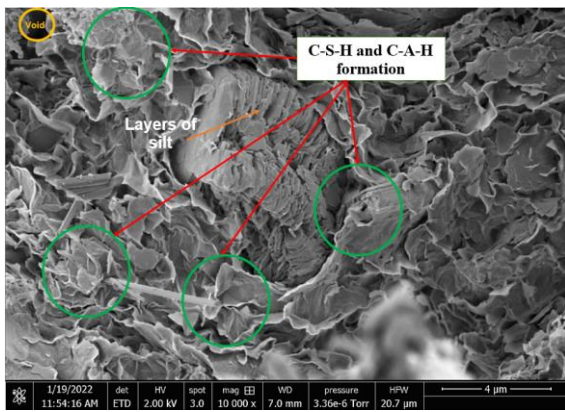


SEM image and EDX results for ASS1+2%Lime+2.5%Cement+23.5%GGBS after 28 days of curing

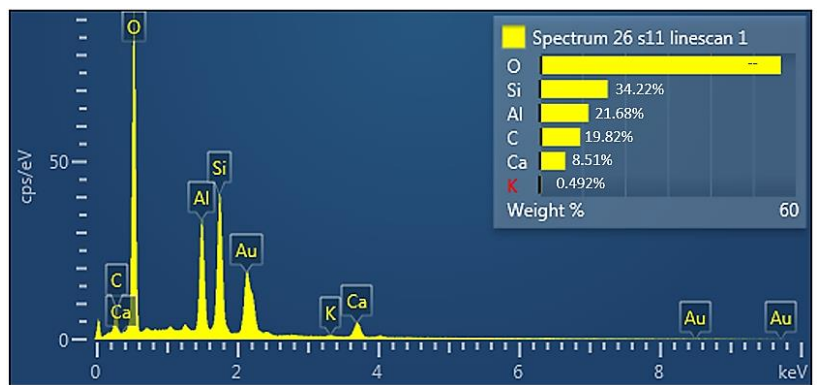
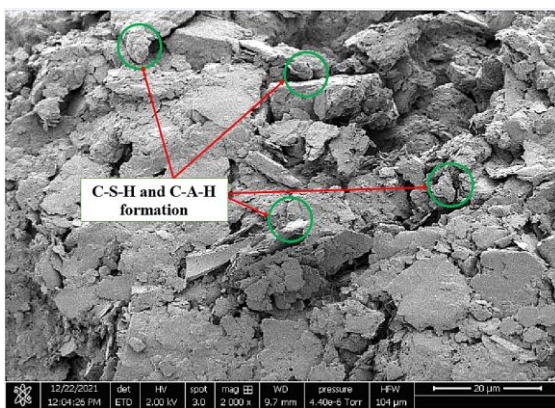


SEM image and EDX results for ASS2+2%Lime+2.5%Cement+23.5%GGBS after 7 days of curing

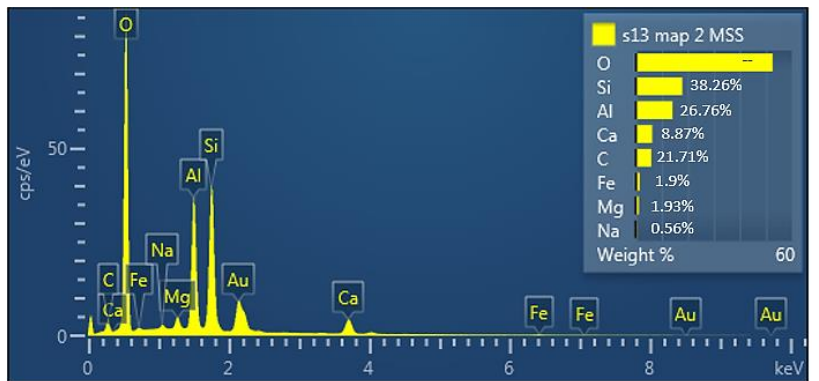
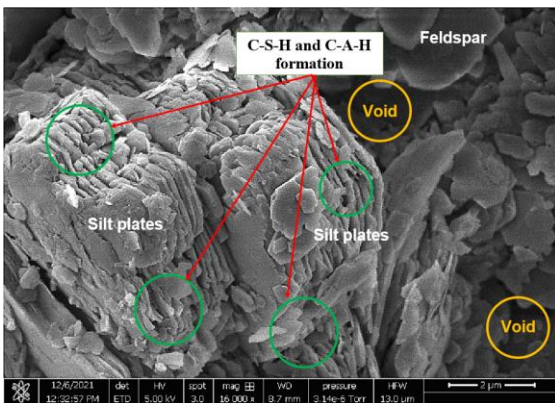
Appendixes



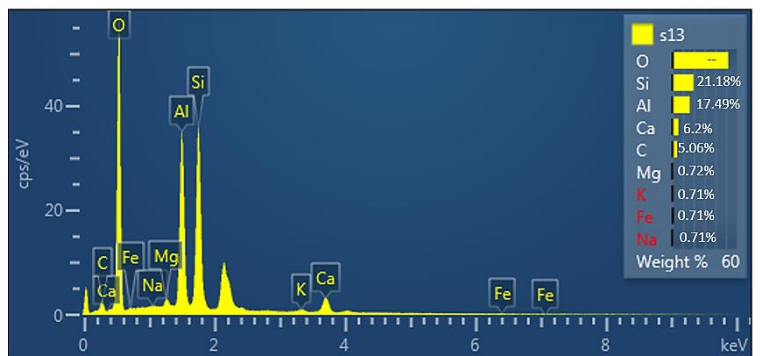
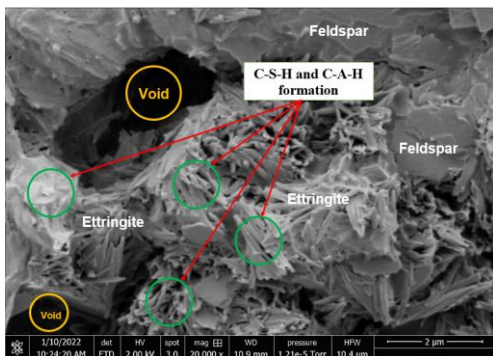
SEM image and EDX results for ASS2+2%Lime+2.5%Cement+23.5%GGBS after 28 days of curing



SEM image and EDX results for ASS1+2%Lime+2.5%Cement+23.5%Plastic after 7 days of curing

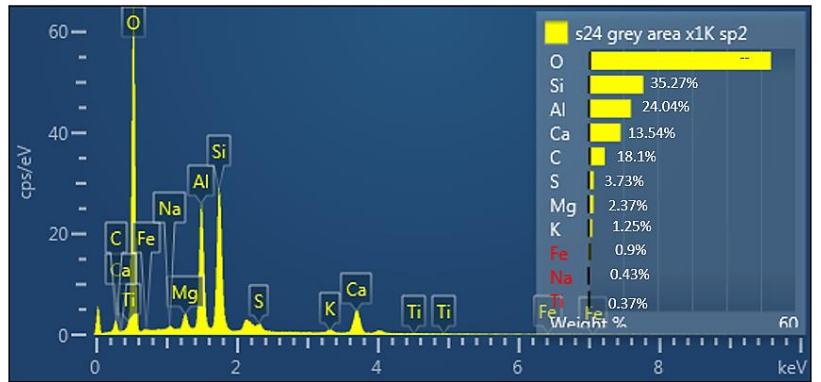
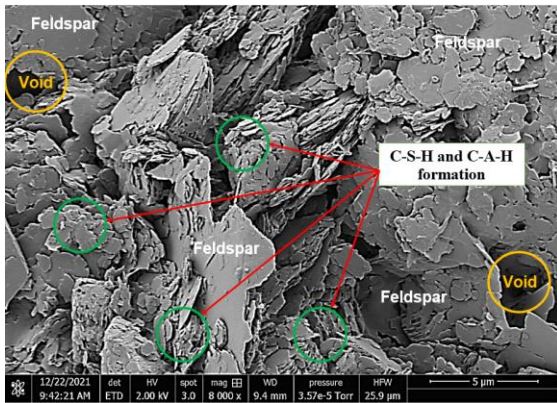


SEM image and EDX results for ASS1+2%Lime+2.5%Cement+23.5%Plastic after 28 days of curing

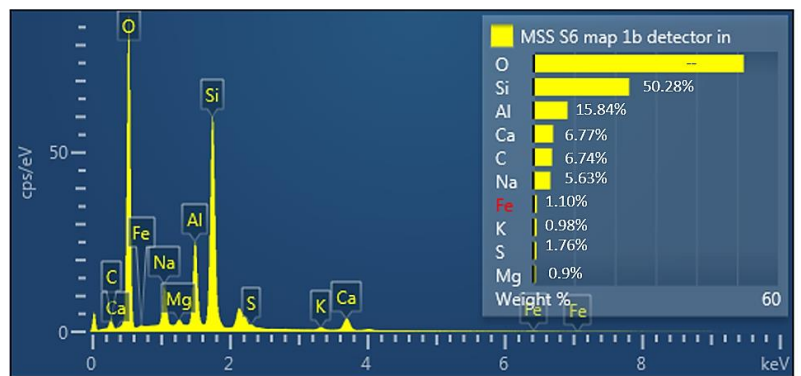
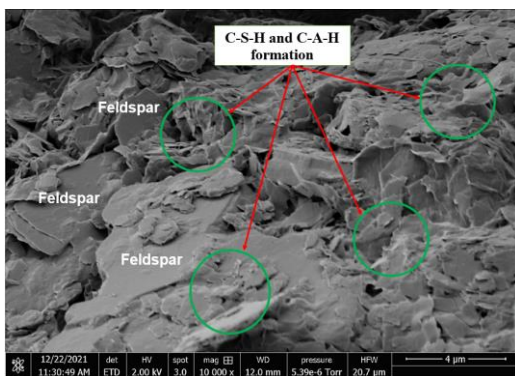


SEM image and EDX results for ASS2+2%Lime+2.5%Cement+23.5%Plastic after 7 days of curing

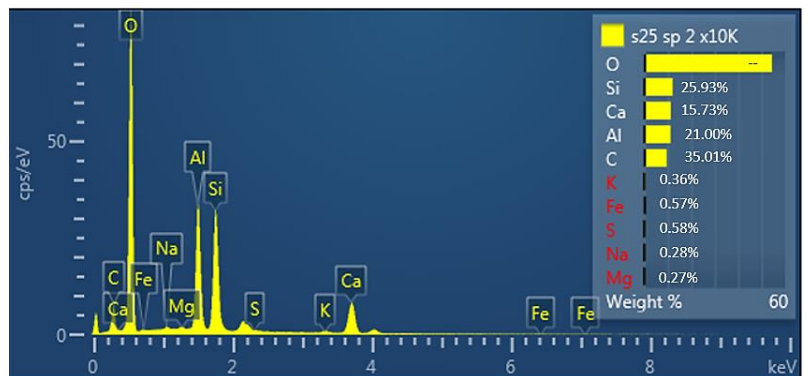
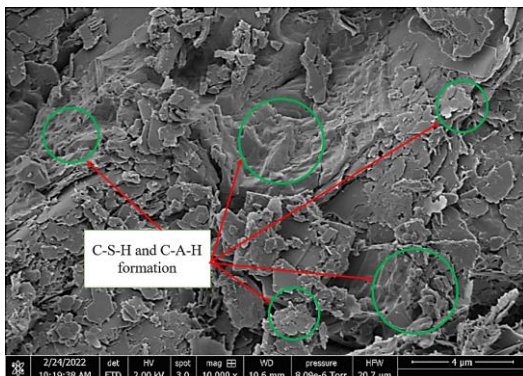
Appendix



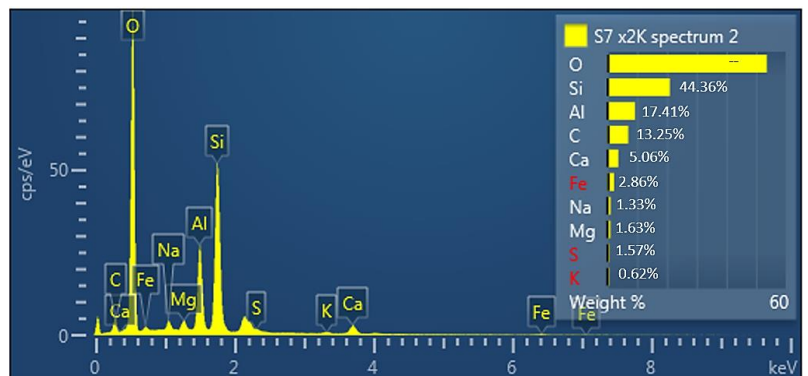
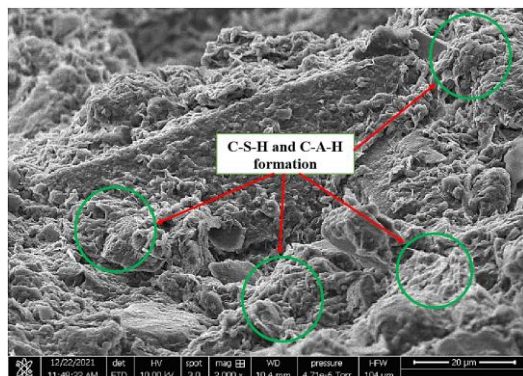
SEM image and EDX results for ASS2+2%Lime+2.5%Cement+23.5%Plastic after 28 days of curing



SEM image and EDX results for ASS1+2%Lime+2.5%Cement+23.5%Glass after 7 days of curing

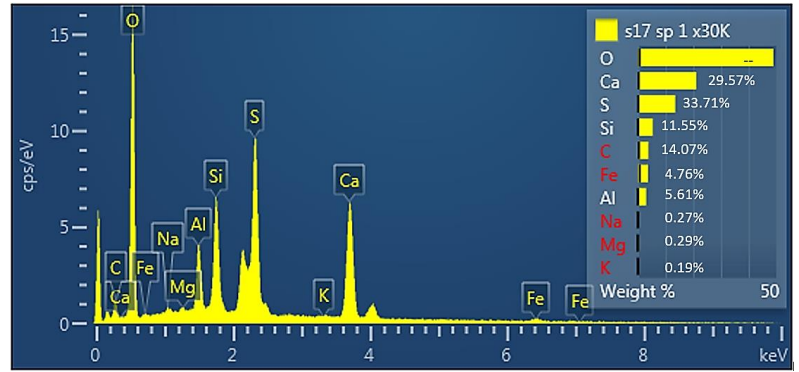
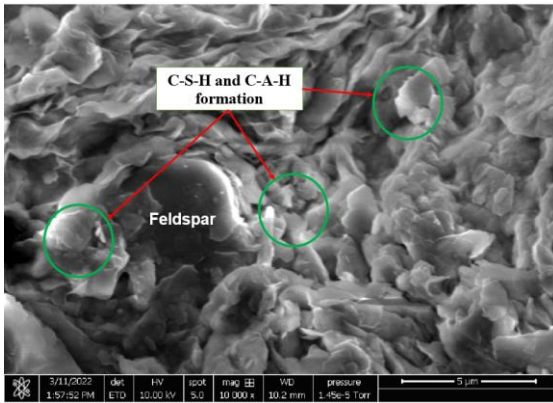


SEM image and EDX results for ASS1+2%Lime+2.5%Cement+23.5%Glass after 28 days of curing

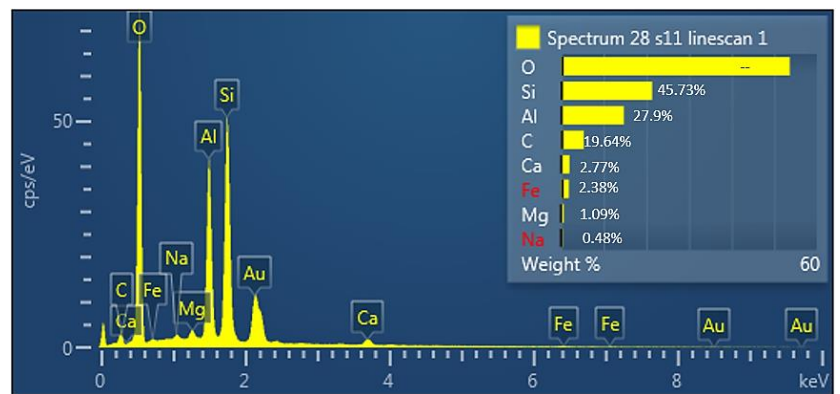
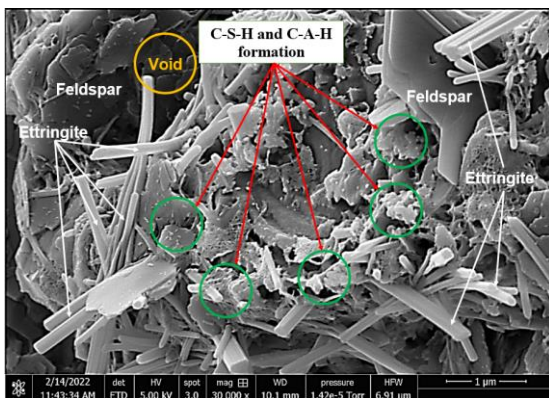


SEM image and EDX results for ASS2+2%Lime+2.5%Cement+23.5%Glass after 7 days of curing

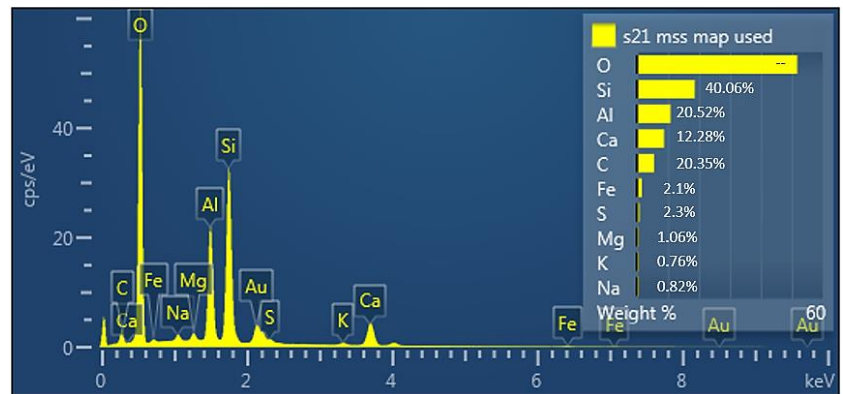
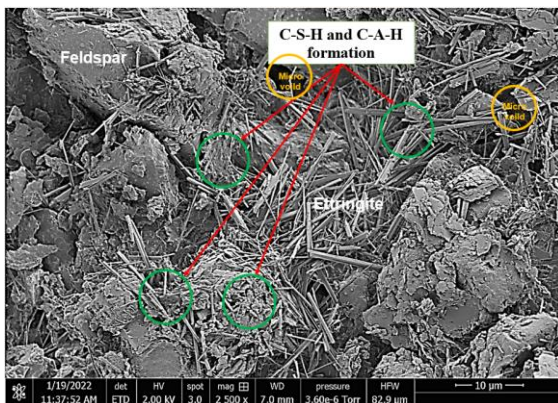
Appendix



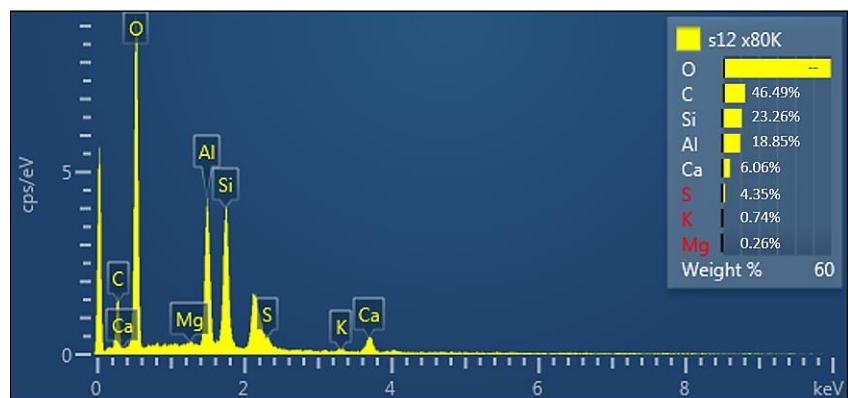
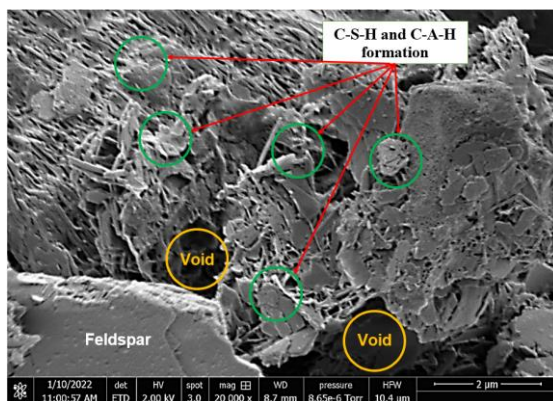
SEM image and EDX results for ASS2+2%Lime+2.5+Cement+23.5%Glass after 28 days of curing



SEM image and EDX results for ASS1+2%Lime+2.5%Cement+11.75%GGBS+11.75%Plastic after 7 days of curing

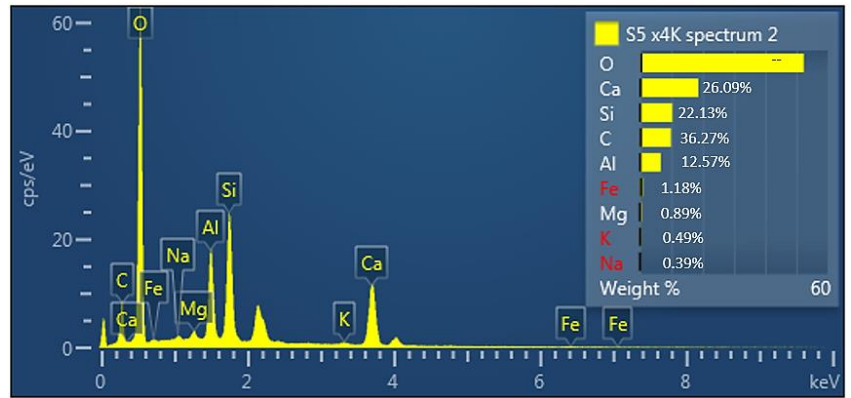
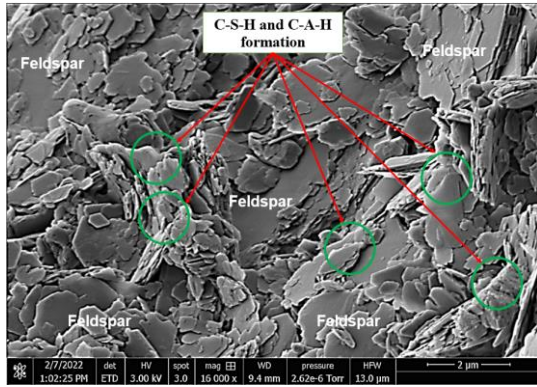


SEM image and EDX results for ASS1+2%Lime+2.5%Cement+11.75%GGBS+ 11.75%Plastic after 28 days of curing

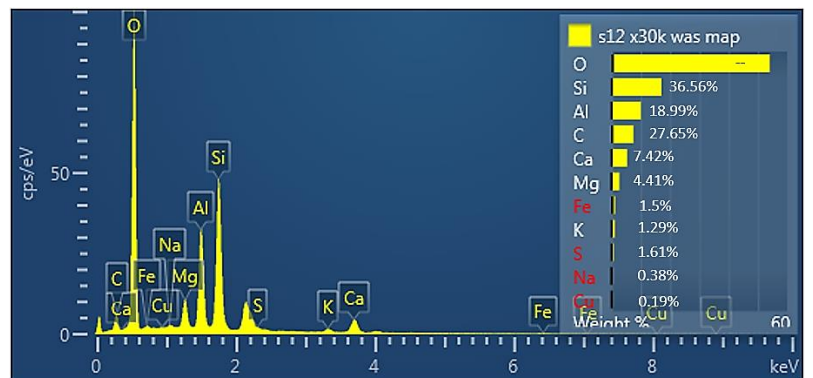
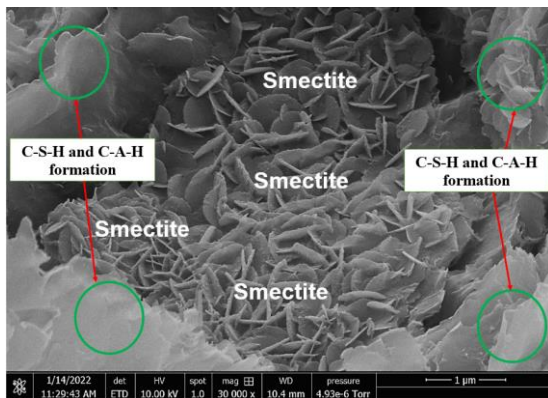


SEM image and EDX results for ASS2+2%Lime+2.5%Cement+11.75%GGBS+11.75%Plastic after 7 days of curing

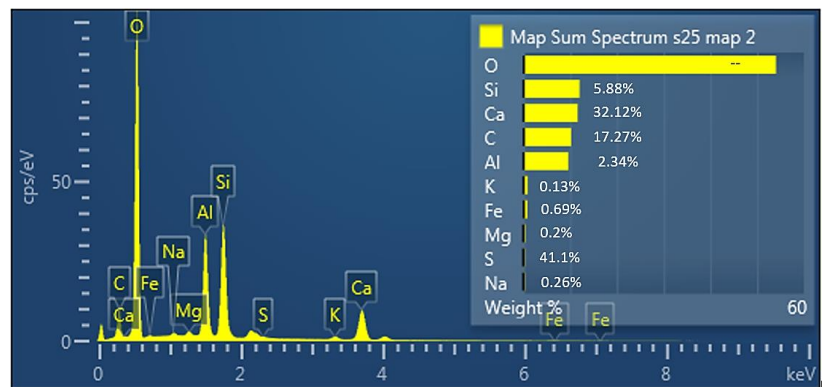
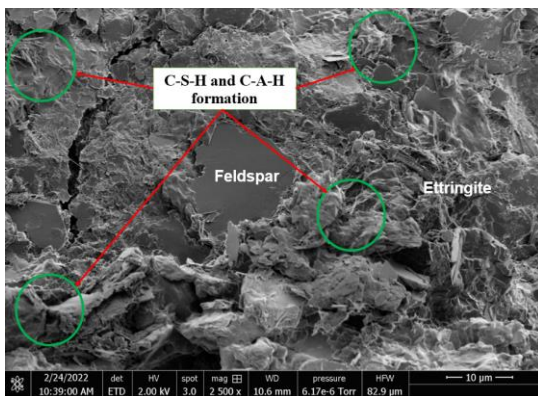
Appendix



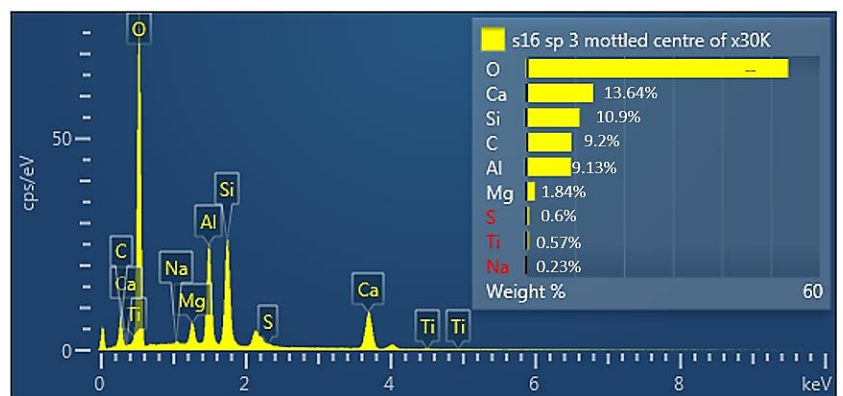
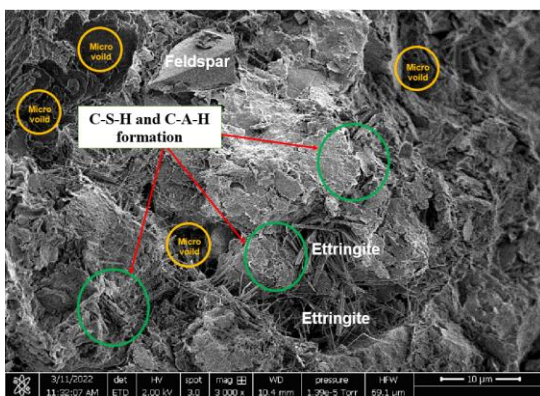
SEM image and EDX results for ASS2+2%Lime+2.5%Cement+11.75%GGBS+11.75%Plastic after 28 days of curing



SEM image and EDX results for ASS1+2%Lime+2.5%Cement+11.75%GGBS+11.75% Glass after 7 days of curing

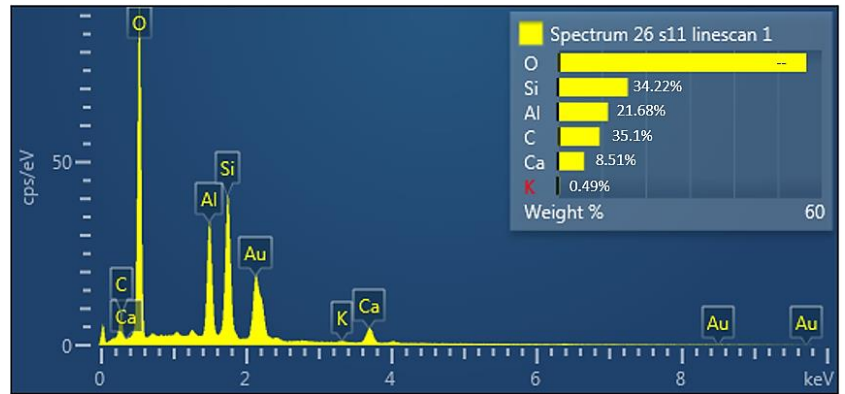
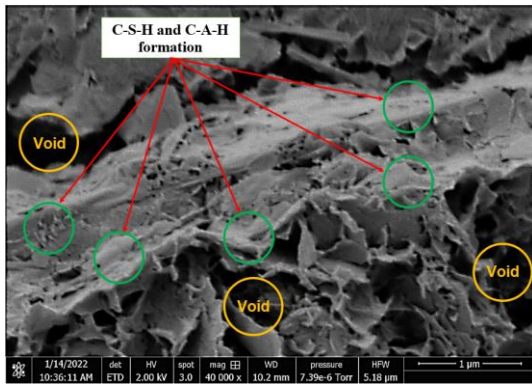


SEM image and EDX results for ASS1+2%Lime+2.5%cement+11.75%GGBS+11.75%Glass after 28 days curing

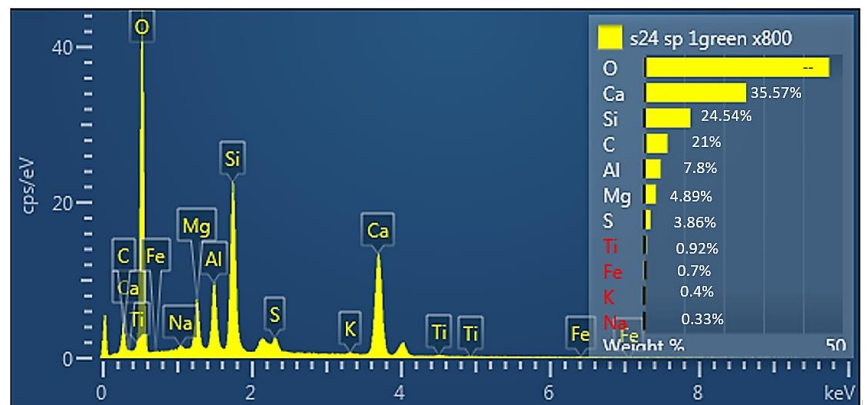
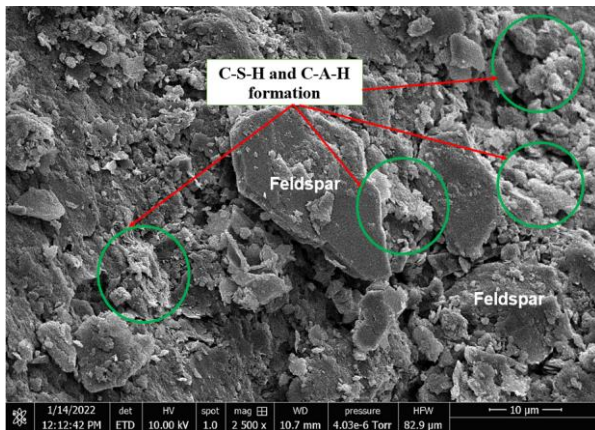


SEM image and EDX results for ASS2+2%Lime+2.5%Cement+11.75%GGBS+11.75%Glass after 7 days of curing

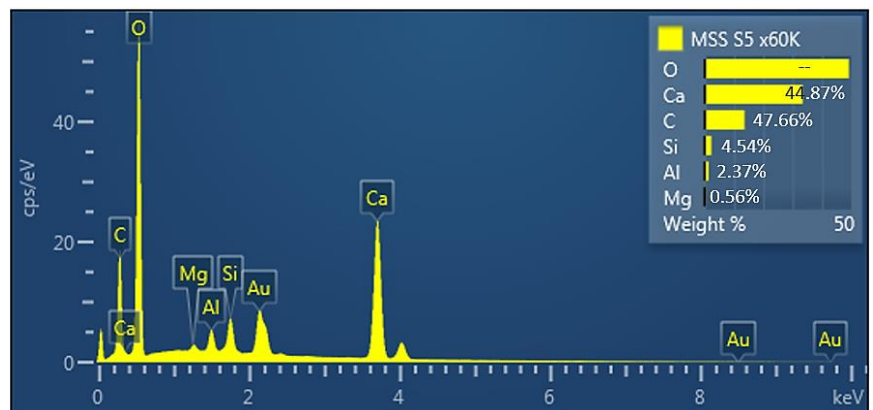
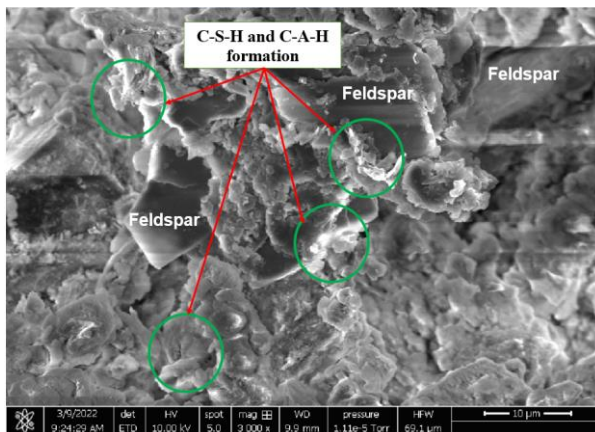
Appendixes



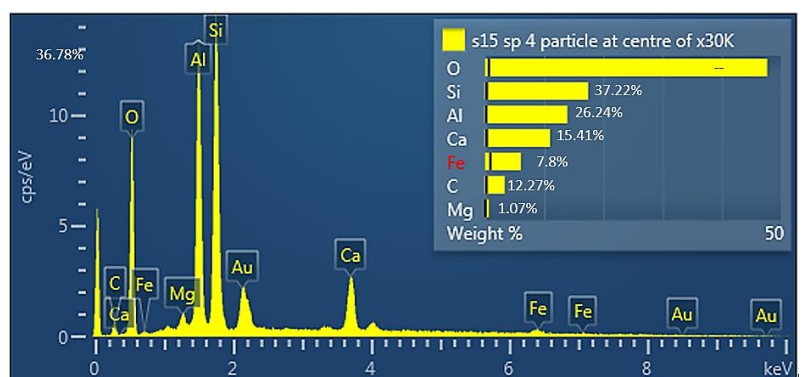
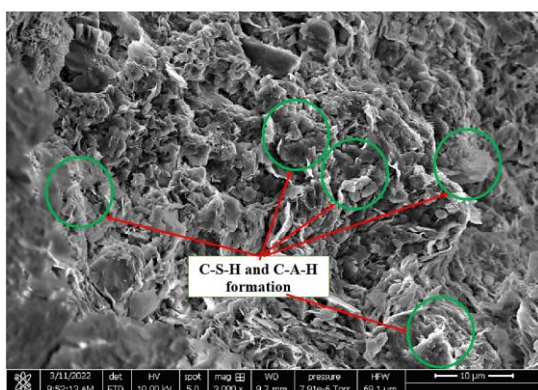
SEM image and EDX results for ASS2+2%Lime+2.5%Cement+11.75%GGBS+11.75%Glass after 28 days of curing



SEM image and EDX results for ASS1+2%Lime+2.5%Cement+11.75%GGBS+11.75%BDW after 7 days of curing

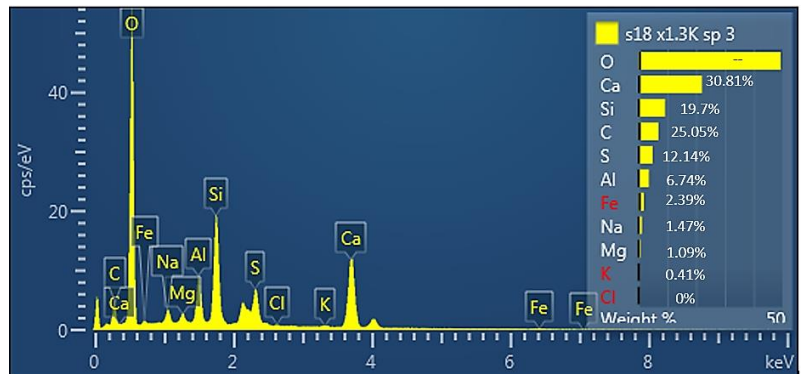
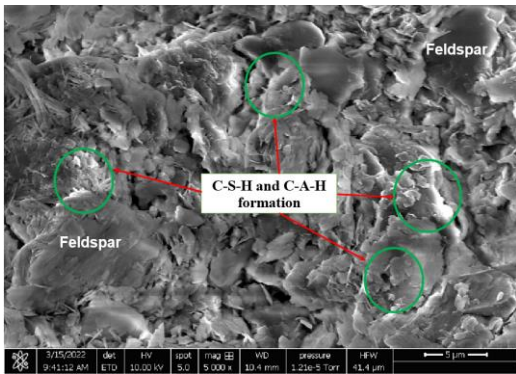


SEM image and EDX results for ASS1+2%Lime+2.5%cement+11.75%GGBS+11.75%BDW after 28 days of curing

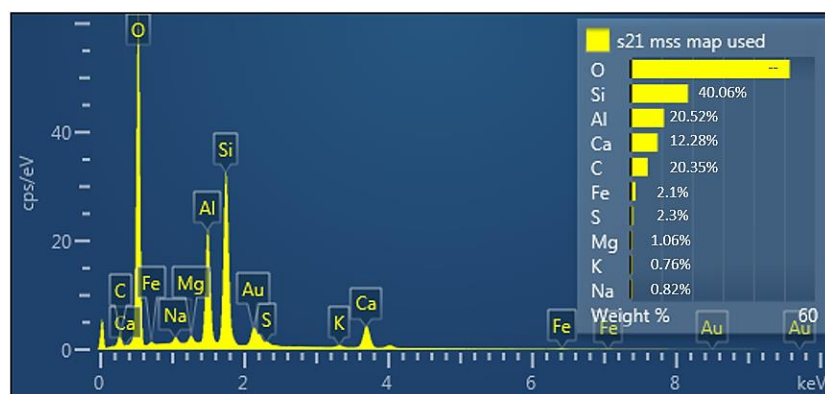
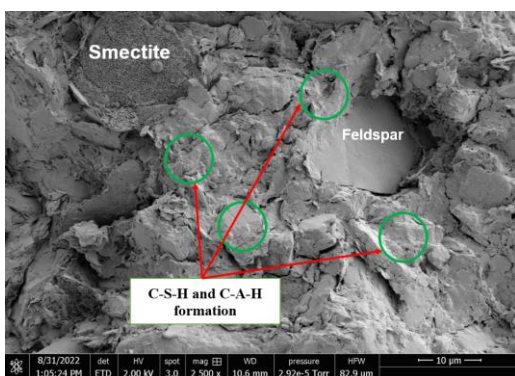


Appendixes

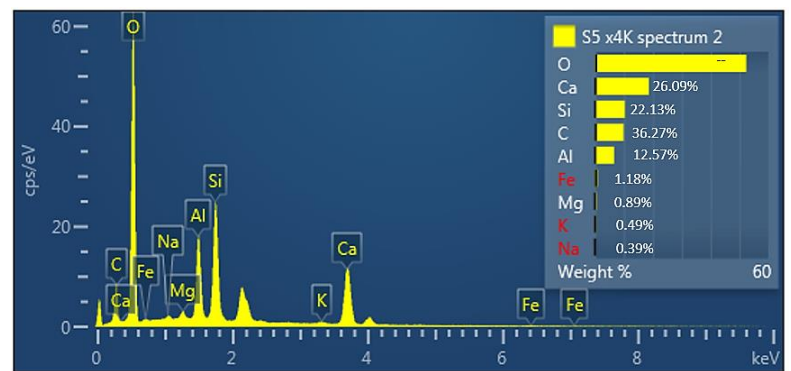
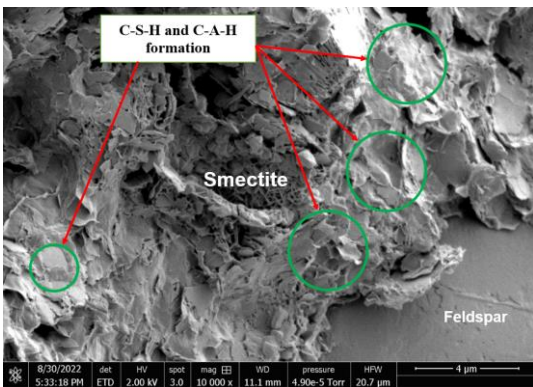
SEM image and EDX results for ASS2+2%Lime+2.5%Cement+11.75%GGBS+11.75%BDW after 7 days of curing



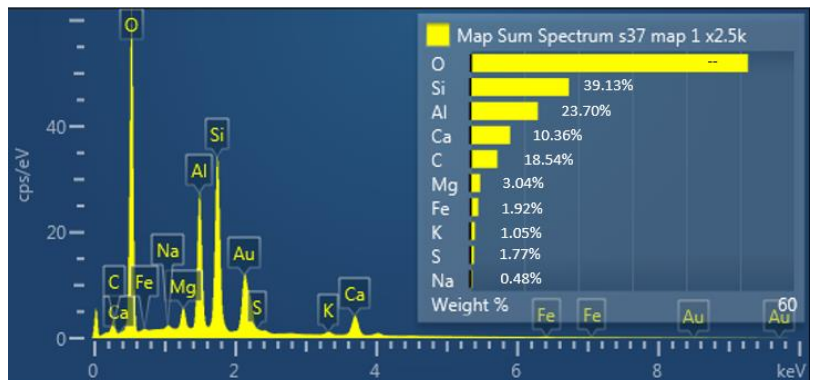
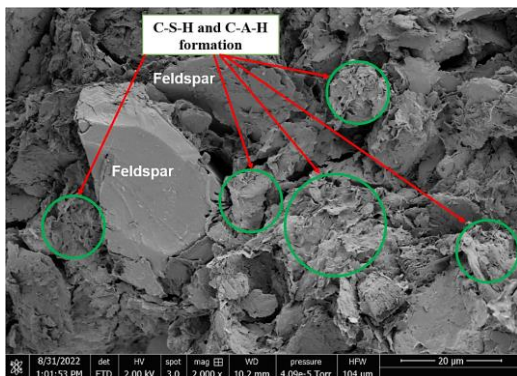
SEM image and EDX results for ASS2+2%Lime+2.5%Cement+11.75%GGBS+11.75%BDW after 28 days of curing



SEM image and EDX results for ASS1+2%Lime+2.5%Cement+11.75%GGBS+11.75%BDW after 90 days of curing

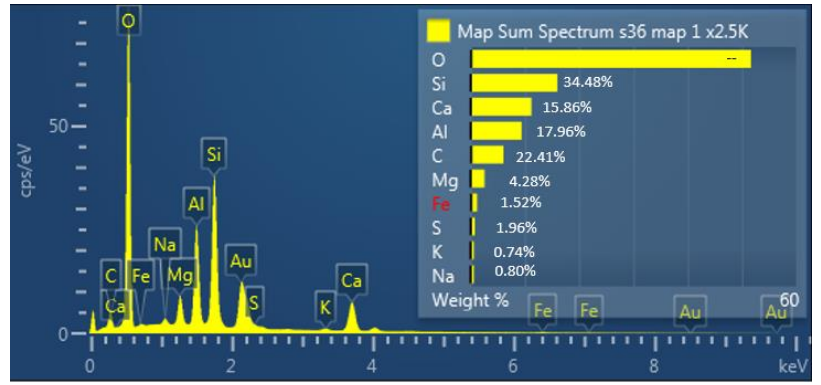
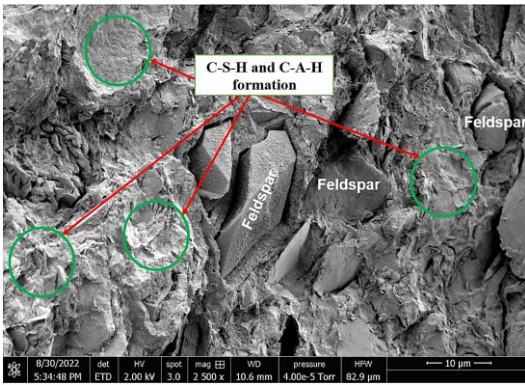


SEM image and EDX results for ASS2+2%Lime+2.5%cement+11.75%GGBS+11.75%BDW after 90 days of curing

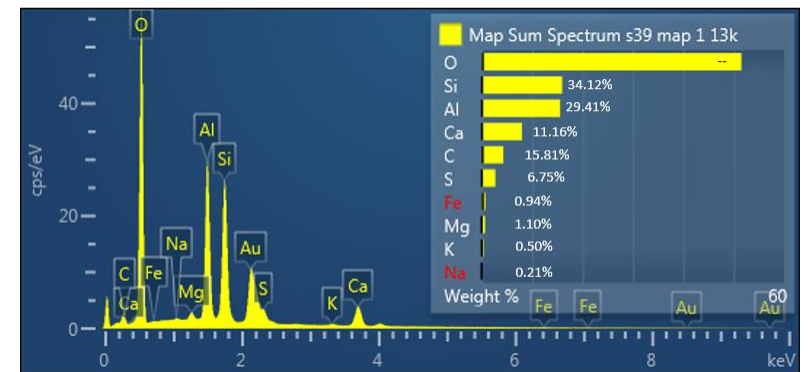
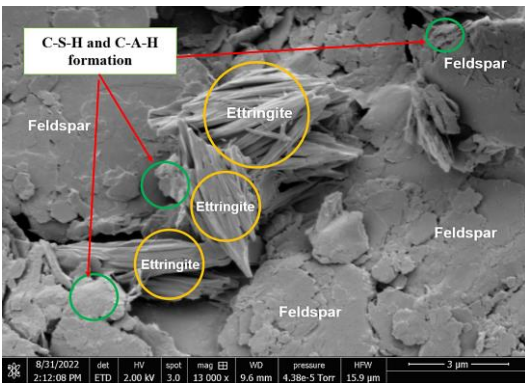


SEM image and EDX results for ASS1+2%Lime+2.5%Cement+23.5%GGBS after 90 days of curing

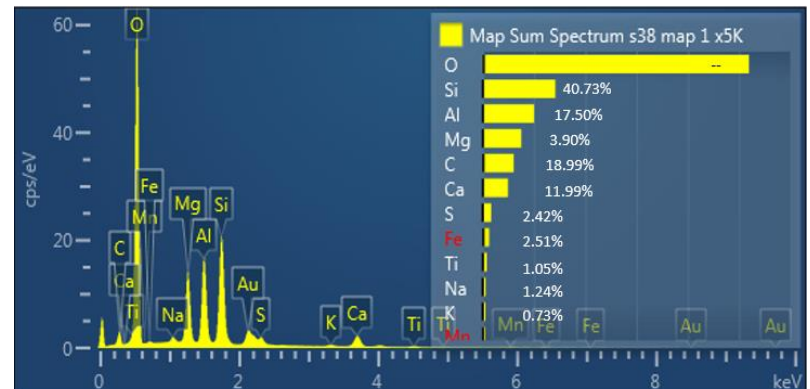
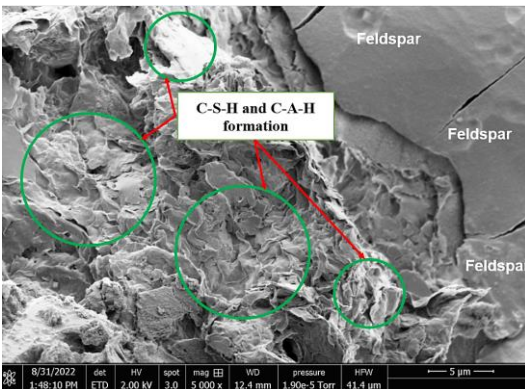
Appendixes



SEM image and EDX results for ASS2+2%Lime+2.5%Cement+23.5%GGBS after 90 days of curing



SEM image and EDX results for ASS1+2%Lime+26%GGBS after 90 days of curing



SEM image and EDX results for ASS2+2%Lime+26%GGBS after 90 days of curing

Appendix 8 Publications

Appendix 8.1 Publications (Journal)



Article

Performance of Sustainable Road Pavements Founded on Clay Subgrades Treated with Eco-Friendly Cementitious Materials

Samuel Y. O. Amakye ^{1,*}, Samuel J. Abbey ², Colin A. Booth ² and Jonathan Oti ³

¹ Department of Engineering, Design and Mathematics, Faculty of Environment and Technology, University of the West of England, Bristol BS16 1QY, UK

² Centre for Architecture and Built Environment Research (CABER), Faculty of Environment and Technology, University of the West of England, Bristol BS16 1QY, UK

³ School of Engineering, Faculty of Computing, Engineering and Science, University of South Wales, Pontypridd CF37 1DL, UK

* Correspondence: samuel.amakye@uwe.ac.uk



Citation: Amakye, S.Y.O.; Abbey, S.J.; Booth, C.A.; Oti, J. Performance of Sustainable Road Pavements Founded on Clay Subgrades Treated with Eco-Friendly Cementitious Materials. *Sustainability* **2022**, *14*, 12588. <https://doi.org/10.3390/su141912588>

Academic Editor: Edoardo Bocci

Received: 15 August 2022

Accepted: 30 September 2022

Published: 3 October 2022

Publisher's Note: MDPI stays neutral with regard to jurisdictional claims in published maps and institutional affiliations.



Copyright: © 2022 by the authors. Licensee MDPI, Basel, Switzerland. This article is an open access article distributed under the terms and conditions of the Creative Commons Attribution (CC BY) license (<https://creativecommons.org/licenses/by/4.0/>).

Abstract: Clays encountered during road construction are mostly weak and result in major pavement failures due to their low California bearing ratio (CBR) and high swelling potential. In this study, sustainable and eco-friendly waste materials including brick dust waste (BDW), ground granulated blastfurnace slag (GGBS), recycled plastic (RP) and recycled glass (RG) at varying proportions of 11.75% and 23.5% were used as partial replacement for cement and lime in clay treatment. After determining the water content by conducting Atterberg limit and compaction test, A CBR and swell characteristics of treated and untreated clay were also conducted. A road pavement design was conducted using the Design Manual for Road and Bridges (DMRB) as a guide to determine the performance of treated clay with varying CBR values. A road pavement failure analysis was also conducted to understand the defect formation within pavement structures supported by eco-friendly treated clay. The embodied carbon of treated clay was calculated and a life cycle cost analysis (LCCA) of flexible pavement with treated clay and road with imported materials was conducted. The results show a liquid limit of 131.26 and plastic limit of 28.74 for high plasticity index (clay 1) and liquid limit of 274.07 and a plastic limit of 45.38 for extremely high plasticity index (clay 2). An increase in CBR values from 8% and 9% to 57% and 97% with a reduction in swell values from 4.11% and 5.03% to 0.38% and 0.56% were recorded. This resulted in a reduction in pavement thickness and stresses within the road pavement leading to reduced susceptibility of the pavement to fatigue, rutting and permanent deformation. Very low embodied carbon was recorded for eco-friendly treated clay and a high life cycle cost (LCC) with clay removed and replaced with imported materials compared with clay treated using eco-friendly waste materials. The study concluded that carbon and overall construction costs can be reduced using waste materials in road construction. Owners and operators can save money when clay is treated and used in road construction instead of removing clay and replacing it with imported materials.

Keywords: brick dust waste; eco-friendly solutions; pavement; clay; economic appraisal; life cycle cost analysis; fatigue; rutting; deformation

1. Introduction

One of the vital components in the process of road projects is road pavement design. Road pavement design plays an important role in determining the layer composition, materials required and the cost of the projects based on the California bearing ratio (CBR) of clay (original ground). The California bearing ratio (CBR) is a penetration test to investigate the strength of subgrade and evaluate its bearing capacity to carry traffic load [1]. CBR plays an important role in determining the thickness and type of road pavement materials to select during the construction phase of a project [2]. In this study, the

Design Manual for Road and Bridges (DMRB) was used in the design of road pavement and road pavement failure investigation conducted using clay treated with waste and industrial by-products. Clay soils expand when wet and shrink when dry causing movement in the foundation due to the repeated expansion and shrinkage [3,4]. These movements within the road foundation cause defects in the road pavement structure leading to high cost of maintenance and sometimes a total reconstruction of the road [4]. This calls for modification and reengineering of the clay before construction. Traditional cement and lime are mostly used in clay treatment however, they are associated with high carbon dioxide (CO₂) emissions and are non-environmentally friendly [5]. This calls for the use of more sustainable and environmentally friendly binders in clay treatment.

In this study, waste materials including brick dust waste (BDW), ground granulated blastfurnance slag (GGBS), recycled plastic (RP) and recycled glass (RG) were used as binders to treat clay. Research has shown that waste materials can be used in clay treatment due to their ability to improve the engineering properties of clay through the production of calcium silicate hydrate (CSH) gel during the hydration process [6]. Materials including brick dust, synthetic fibre, thermal bituminous, rice husk, sugarcane bagasse, cow dung, geo-textiles, fabric and electrical waste have been used in soil treatment [6]. Waste materials including electric arc furnace (EAF) ladle furnace (LF) slags, coal fly (CF) ash, bottom ash, glass waste (GW) and reclaimed asphalt pavement (RAP) were used to improve the economic and environmental sustainability of road constructions [7]. Carbon reduction in pavement construction was observed when recycled plastic (RP) waste was used at varying proportions to enhance the engineering properties for eco-friendly pavement application [8]. Road pavements are superimposed layers of materials placed over the natural ground [9,10]. Development of stresses within road pavement caused by traffic load and geotechnical issues lead to damage to the road pavement [11]. According to [12], clay corrugates at the surface of the road and increases unevenness. The process of treating clay using cement and lime to improve its CBR to make them usable in road construction can lead to a high overall construction cost of road pavement [1,4]. Countries such as the United States and China have spent USD 30 billion on maintenance costs only due to road pavement defects caused by clay [2,4]. Road pavement defect that leads to permanent damage to the pavement was investigated in this study using a mixture of bentonite and kaolinite to form clay with varying plasticity index. Atterberg and compaction tests were conducted for untreated clay to determine its water content after which the clay was treated using waste materials. The CBR of treated clay was determined and the results were used in the pavement design and defect analysis conducted in this study. A life cycle cost analysis (LCCA) was conducted to determine the cost of treating clay compared with the cost of removing clay and replacing them with imported materials. LCCA serves as a tool to calculate the real cost of an asset over its useful design life [13,14]. In the 1930s the LCCA concept was introduced in highway projects and as part of federal legislation on flood control [13]. The nature and characteristics of clay (natural ground) can influence the LCC of road pavement [1].

2. Materials and Methods

Bentonite and kaolinite were mixed in varying proportions to form an Artificially Synthesised Clay (ASC): Clay 1 (25% bentonite + 75% kaolinite) of high plasticity index and Clay 2 (75% bentonite + 25% kaolinite) of extremely high plasticity index. Sustainable waste materials including brick dust waste (BDW), ground granulated blastfurnance slag (GGBS), recycled plastic (RP) and recycled glass (RG) at varying proportions of 11.75% and 23.5% were used in clay treatment. The process of water content determination (compaction and Atterberg limit tests), California bearing ratio (CBR) and swell tests, road pavement design, defect analysis and the design guidance used are as reported in the authors' previous study [3,15] using CBR values achieved in this study. Stresses within the various layers of the pavement were analysed using KENPAV software, and a detailed description of KENPAV software is as reported in the authors' previous study [3,15]. The suppliers'

information for the bentonite, kaolinite, cement and lime used in this study are as reported in the authors' previous study [2]. The brick dust waste (BDW) was supplied by Celtic Sustainable Ltd., Unit 9 Parc Teifi Business Park Cardigan, Wales, SA43 1EW UK and complies with BS EN 771-1:2011+A1:2015. Ground Granulated Blastfurnace Slag (GGBS) used was in compliance with BS EN 15167-1:2006 and supplied by Francis Flower, The White House, Gurney Slade, Radstock, Somerest, England, BA3 4UU. The plastic used was supplied by Poli Plastic Pellets Ltd., Monor farmhouse, Hawarden, Flintshire, Wales, CH5 3PL, UK. The recycled glass used was supplied by Centurywise Ltd., Unit 2 Bridge House, Stuart Road Bredbury, Stockport, Greater Manchester, England, SK6 2SR. The focused on conducting road pavement design using sustainably treated clay subgrade affects road pavement design. The study also carried out pavement defect analysis to investigate the effect of varying CBR values and traffic loads on sustainably treated clay subgrade in terms of failure. Further investigations of the life cycle cost (cost effects) of road pavement designed using sustainably treated clay subgrade materials were conducted and compared with the life cycle cost of road pavement designed using imported subgrade materials. Lastly, the study investigated the embodied carbon for each sustainable binder used in stabilising clay subgrade materials. The particle size distribution, oxide and chemical composition of all materials used in this study are shown in Figures 1 and 2 and Table 1.



Figure 1. Materials used in this study.

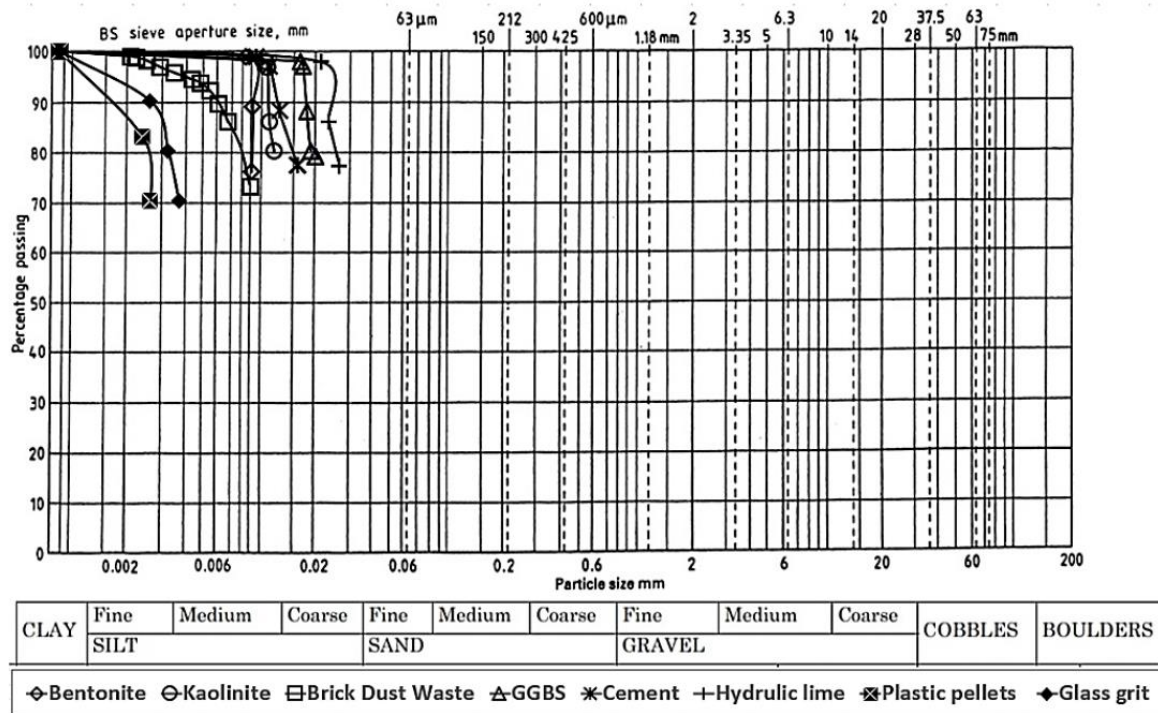


Figure 2. Particle size distribution of materials used in this study.

Table 1. Oxide and chemical composition of materials used.

Oxide	SiO ₂	Al ₂ O ₃	Fe ₂ O ₃	FeO	MgO	CaO	K ₂ O	SO ₃	TiO ₂	Na ₂ O	BaO	Cr ₂ O ₃	Trace	L.O.I
Bentonite Clay (%)	63.02	21.08	3.25	0.35	2.67	0.65	-	-	-	2.57	-	-	0.72	5.64
Kaolinite Clay (%)	48.5	36.0	1.00	-	0.30	0.05	2.15	-	0.06	0.15	-	-	-	11.7
Cement (%)	20	6.0	3.0	-	4.21	63	-	2.30	-	-	-	-	-	0.80
GGBS (%)	35.35	11.59	0.35	-	8.04	41.99	-	0.23	-	-	-	-	-	-
Lime (%)	3.25	0.19	0.16	-	0.45	89.2	0.01	2.05	-	-	-	-	-	-
BDW (%)	52	41	0.7	-	0.12	4.32	0.53	0.33	0.65	0.05	-	-	-	2.01
Plastic (%)	45.47	12.11	1.04	-	-	38.49	0.94	0.43	-	-	-	-	-	-
Glass (%)	72.20	1.50	0.07	-	1.30	10.90	0.45	0.16	0.06	13.30	0.04	0.02	-	-

3. California Bearing Ratio (CBR) and Swell

The sample preparation, testing procedure and standards used to determine the CBR and Swell for treated and untreated clay are as reported in the authors’ previous study [2]. A high-quality subgrade has a CBR value between 80% and 100% minimum [2,3]. A CBR value < 2% is unacceptable for use in road construction and would need modification or reengineering [2,3]. A subgrade swell > 2.5% is unacceptable for use in road construction and must be treated [2,3].

4. Life Cycle Cost Analysis (LCC)

Life cycle cost analysis (LCCA) was carried out in this study for the best performing mix design for a design period of 35 years in compliance with BS ISO 15686-5:2017 [16]. The LCC of clay treated using waste materials was compared with the LCC of clay removed and replaced with imported materials. The life cycle cost analysis performed in this study would help inform contractors on the choice of binders and binder proportions to adopt when they encounter clay with characteristics similar to what was used in this study. The cost of binders used was investigated using current market prices at the time of this study

to calculate the total cost of binders required to stabilize a square kilometre of clay based on the percentages of binders used in a mix-design. In establishing the real cost of treating a square kilometre of clay, plant cost was estimated using the Newmarket Plant Hire (NPH) [17] Group document and ecoinvent database [18] to get product and materials data for the analysis.

5. Results and Discussion

California Bearing Ratio (CBR) and Swell

After conducting California bearing ratio (CBR) and swell test for treated and untreated clay samples soaked and unsoaked, it was observed that CBR values increased for treated soaked and unsoaked clay samples compared with untreated soaked and unsoaked samples. The highest CBR value of 97% was recorded for Clay 1 treated with ground granulated blastfurnace slag (GGBS) and brick dust waste (BDW) after 28 days of curing. This confirms that waste materials can improve the engineering properties of clay. A CBR value > 250% was achieved in a study conducted by [19] using a minimum of 20% of high calcium waste dust from asphalt concrete manufacturing to stabilize low-quality soil used as subbase course material in road structures. The study concluded that, recycled waste dust from asphalt concrete in sustainable road construction. The lowest swell value of 0.38% was recorded for Clay 1 treated with GGBS and plastic. Table 2 shows CBR and swell values for treated and untreated clay samples.

Table 2. CBR and swell values for treated and untreated clay samples.

Clay Type	Mix Design	Treated	Soaked	Curing Days	CBR Values (%)	Swell Values (%)
1	25% B + 75% K	x	x	0	8	4.11
1	25% B + 75% K	x	√	0	0.6	
2	75% B + 25% K	x	x	0	9	5.03
2	75% B + 25% K	x	√	0	1.3	
1	2L% + 2.5% C + 23.5% GL	√	x	7	14	0.52
1	2L% + 2.5% C + 23.5% GL	√	√	7	17	
1	2L% + 2.5% C + 23.5% GL	√	x	28	16	0.46
1	2L% + 2.5% C + 23.5% GL	√	√	28	11	
2	2L% + 2.5% C + 23.5% GL	√	x	7	11	0.64
2	2L% + 2.5% C + 23.5% GL	√	√	7	3	
2	2L% + 2.5% C + 23.5% GL	√	x	28	8	0.57
2	2L% + 2.5% C + 23.5% GL	√	√	28	4	
1	2L% + 2.5% C + 23.5% PL	√	x	7	13	0.56
1	2L% + 2.5% C + 23.5% PL	√	√	7	12	
1	2L% + 2.5% C + 23.5% PL	√	x	28	13	0.51
1	2L% + 2.5% C + 23.5% PL	√	√	28	8	
2	2L% + 2.5% C + 23.5% PL	√	x	7	12	0.61
2	2L% + 2.5% C + 23.5% PL	√	√	7	6	
2	2L% + 2.5% C + 23.5% PL	√	x	28	8	0.59
2	2L% + 2.5% C + 23.5% PL	√	√	28	3	
1	2L% 2.5% C + 11.75% GGBS + 11.75% PL	√	x	7	44	0.38

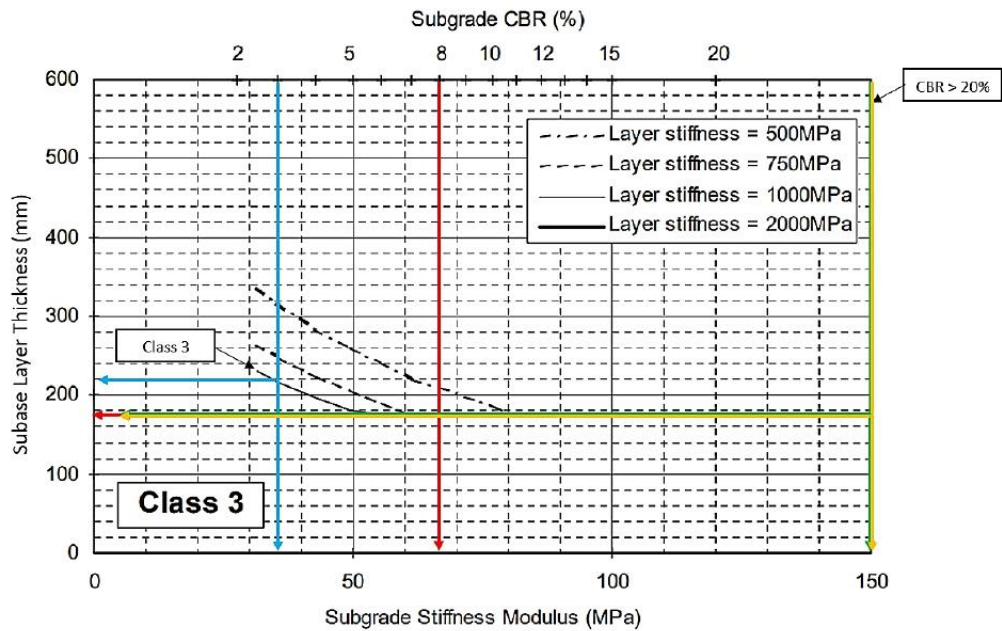
Table 2. Cont.

Clay Type	Mix Design	Treated	Soaked	Curing Days	CBR Values (%)	Swell Values (%)
2	2L% 2.5% C + 11.75% GGBS + 11.75% PL	✓	×	7	21	0.94
1	2L% 2.5% C + 11.75% GGBS + 11.75% GL	✓	✓	7	59	0.39
2	2L% 2.5% C + 11.75% GGBS + 11.75% GL	✓	✓	7	31	0.56
1	2L% + 2.5% C + 11.75% GGBS + 11.75% BDW	✓	✓	28	97	0.42
2	2L% + 2.5% C + 11.75% GGBS + 11.75% BDW	✓	×	7	27	0.54
2	2L% + 2.5% C + 11.75% GGBS + 11.75% BDW	✓	✓	7	16	0.49
2	2L% + 2.5% C + 11.75% GGBS + 11.75% BDW	✓	×	28	44	0.49
2	2L% + 2.5% C + 11.75% GGBS + 11.75% BDW	✓	✓	28	24	0.49

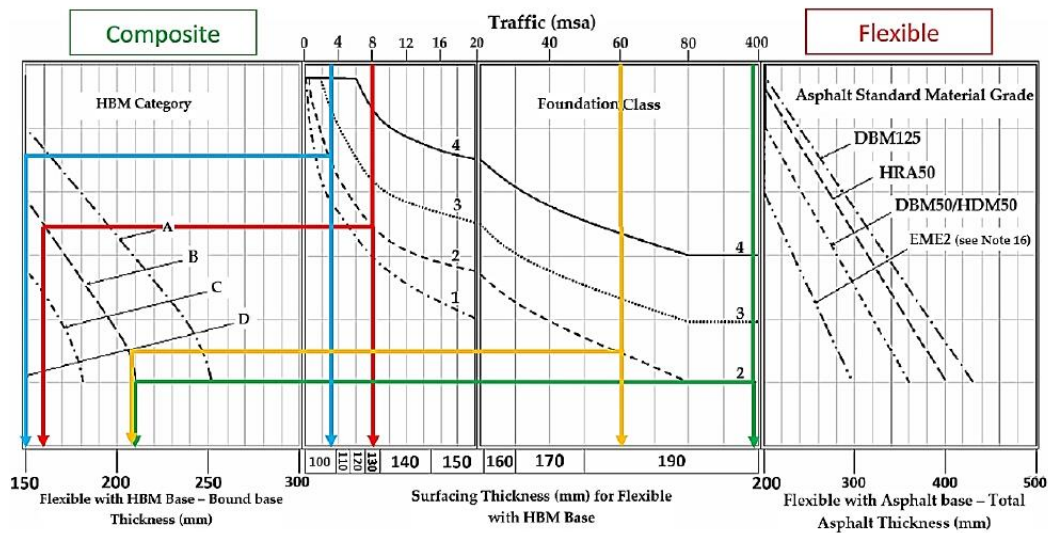
Where B = Bentonite, K= Kaolinite, L = Lime, C = Cement, GGBS = Ground Granulated Blastfurnace Slag, PL= Plastic, GL = Glass, BDW = Brick Dust waste.

6. DMRB Road Pavement Design Using Sustainable Treated Clay

Road pavement design was conducted in this study in accordance with DMRB CD 226 [20] using selected California bearing ratio (CBR) values achieved in this study. The procedure used and parameters adopted are as reported in the authors' previous study [13]. The design traffic load selected include 3 msa, 8 msa, 60 msa and 100 msa and the CBR values selected include 3% for Clay 2, 8% for Clay 1, 109% for Clay 1. A three-layer composite pavement was adopted for the design using class 3 design in accordance with DMRB CD 226 [20]. The results show a reduction in pavement thickness as CBR values increase for Clay 1 for all design traffic loads. A high CBR value resulted in reduced pavement thickness and the overall construction cost of a project [21]. A CBR value of 19% reflected in a reduction in the overall thickness and life cycle cost of road pavement in Uganda [4]. Ref. [22], stated in a study that pavement thickness is determined by the subgrade CBR. According to [23]. Pavements are built to a set thickness dependent on the clay quality, being dependent on anticipated traffic. After designing pavement using DMRB 226 [20], a slight change in pavement thickness was observed compared with using other standards. Changes in pavement thickness were significant for clay CBR values from 2–5% using DMRB [16]. This is so because the subbase layer forms a major part of pavement thickness and Class 3 subbase chart offers a thicker subbase layer only for CBR values between 2–10.5%, after which the sub-base thickness remains the same (180 mm). This means no significant pavement thickness was observed even with a CBR value of 100%. Using sustainable waste materials resulted in achieving very high CBR values and thinner pavement. The thickest pavement of 600 mm (100 msa) was recorded for clay with a CBR value of 3% and the thickest pavement of 418 mm (3 msa) was recorded for clay with a CBR value of 109%. Figure 3a,b shows Class 3 design–single foundation layer (IAN 73/06 [3,24]) (b) Nomograph for determining the design thickness for flexible pavement (DMRB CD 226 [3,20]). Figure 4a,b show the result of road pavement designed using DMRB for traffic 3 msa and 8 msa. (b) Result of road pavement designed using DMRB for traffic 60 msa and 100 msa.

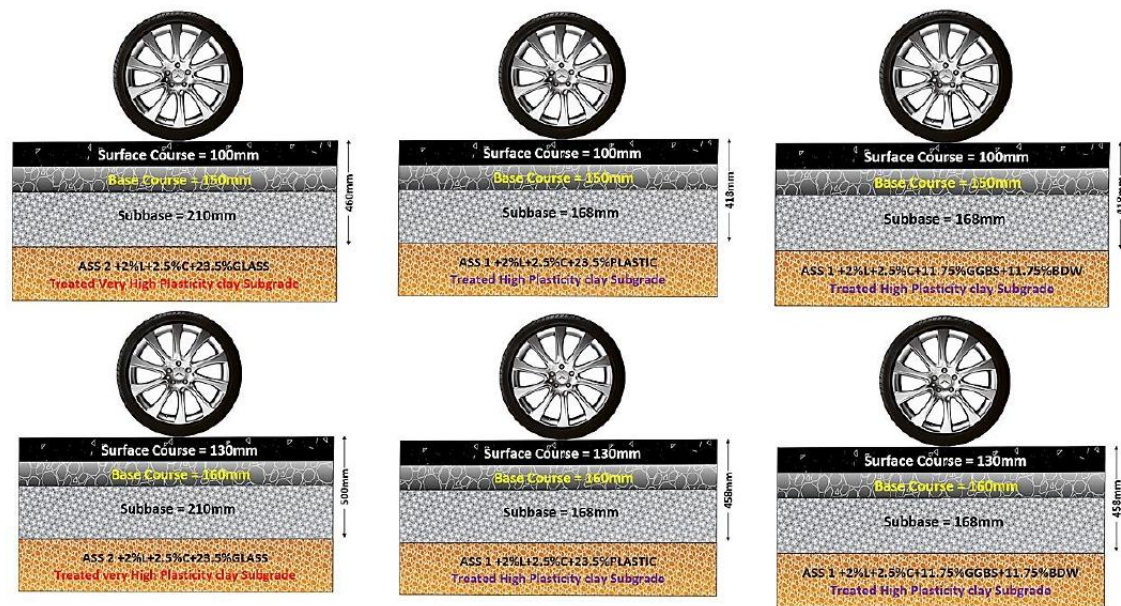
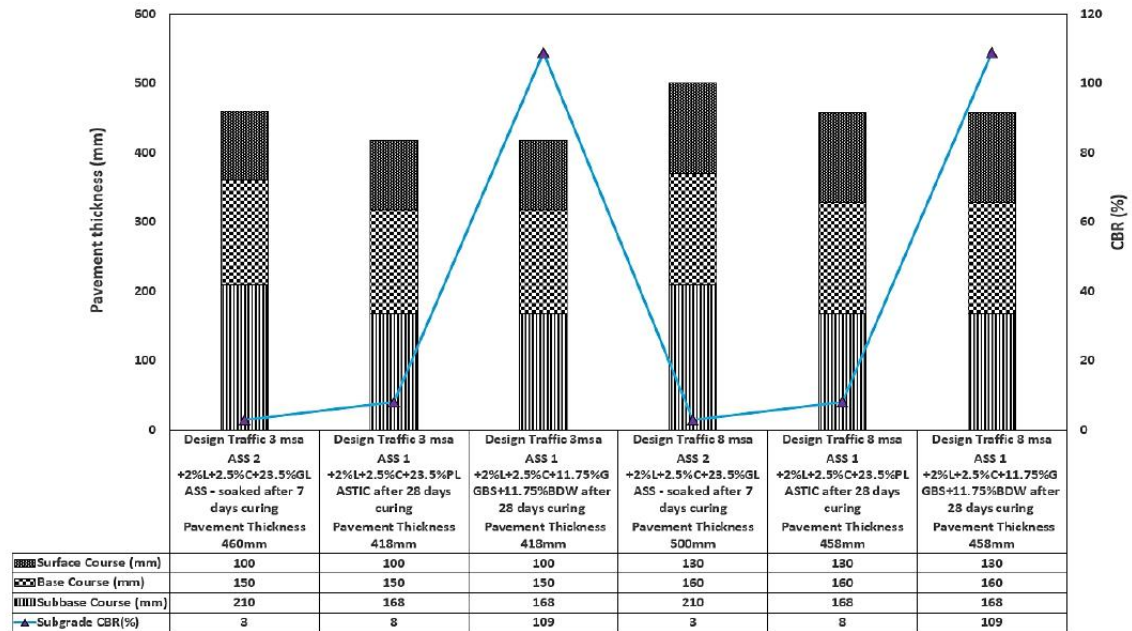


(a)



(b)

Figure 3. (a) Class 3 design—single foundation layer (IAN 73/06 [3,24]). (b) Nomograph for determining the design thickness for flexible pavement (DMRB CD 226 [3,20]).



(a)

Figure 4. Cont.

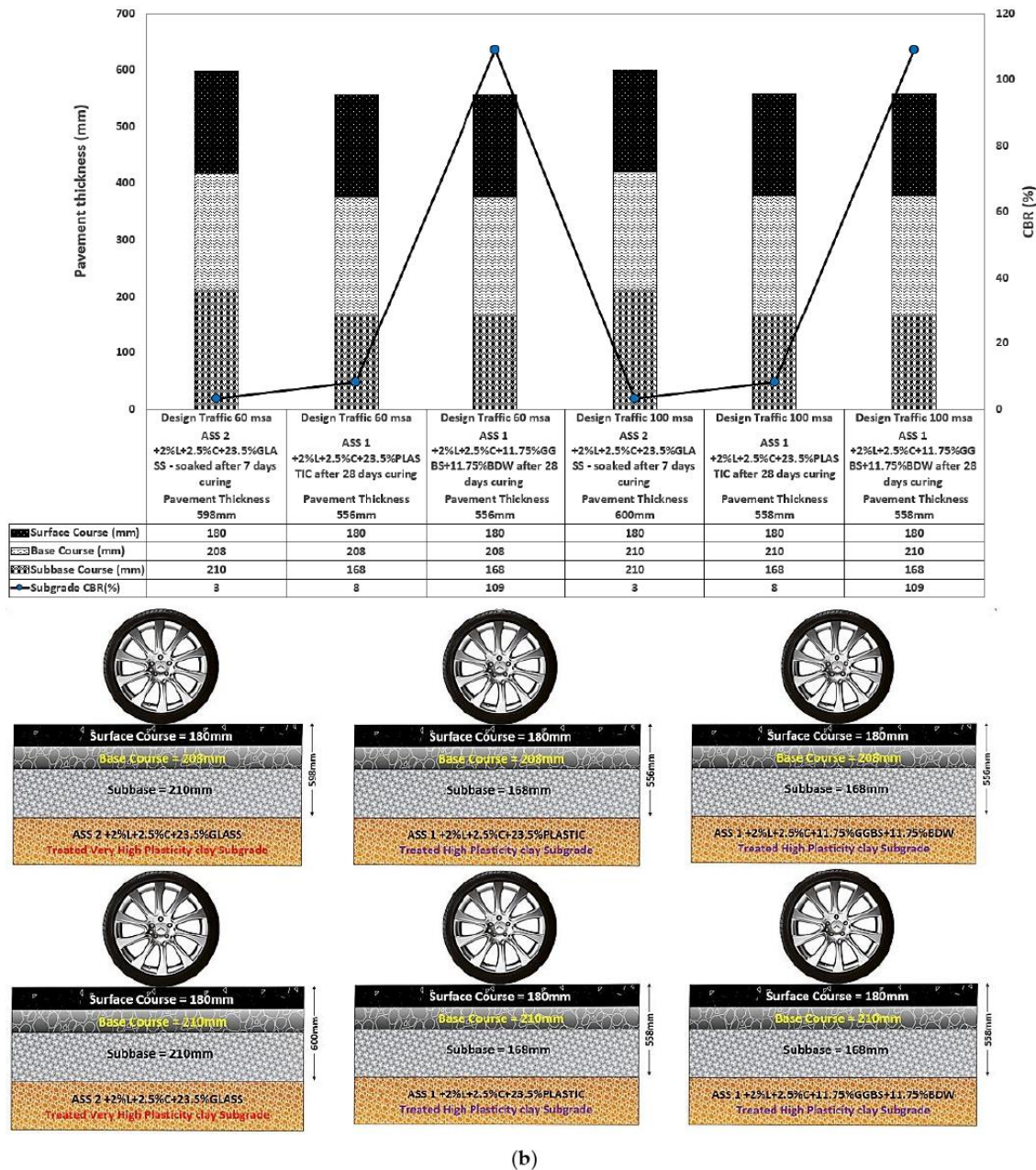


Figure 4. (a) Result of road pavement designed using DMRB for traffic 3 msa and 8 msa (b) Result of road pavement designed using DMRB for traffic 60 msa and 100 msa.

7. Road Pavement Failure Investigation

Road pavement defect investigations were conducted to determine the level of stresses within road pavement structures using selected CBR values achieved in this study for sustainably treated clay. The level of stress within road pavement structures is determined by the CBR values used in road construction [3,15]. For defects to occur in road pavement is dependent on the severity of the stresses within the road pavement [3]. The pavement defect

analysis conducted in this study includes fatigue, rutting and deformation. The stresses within the various layers of the road pavement were analysed using KENPAV software. The procedure used, selected pavement type, design traffic adopted and other parameters used in the defect analysis are as reported in the authors' previous study [3,15]. The equations used in calculating the allowable load repetition for fatigue, permanent deformation and rutting life of the road pavement are as reported in the authors' previous study [3]. After conducting defect analysis, it was observed that clay treated with sustainable waste with low CBR values recorded very high stresses compared with clay with high CBR values. According to [3,25,26], fatigue cracks are initiated in road pavement with high stresses within its clay. Hence, clay with low CBR values achieved in this study are susceptible to defects when used in road construction. However, clay with a high CBR value has less stress making them more durable for use in road construction. Asphalt layer thickness is required to limit stresses within the pavement and reduce the severity of reflective cracking. Due to the low CBR value of 5%, a thicker pavement was required to limit the rate of pavement deterioration due to stress from traffic load [27]. Thicker pavement was observed for clay with low CBR values. The results achieved shows that sustainable waste materials can be used in road clay treatment to reduce the occurrence of defect within a pavement structure. Plastics can be used in flexible pavement to improve its performance against rutting [3,28]. To compensate for clay with low CBR values, road pavements are made thicker to help reduce the stresses within the road structure to prevent defects from occurring. However, the thicker the road pavement the high the overall cost of construction. According to [3,29], road pavement with asphalt thickness below 180 mm deforms quicker but thicker pavement deforms at a lesser rate [3,29]. High elastic modulus was recorded for pavements with high clay CBR values resulting in reduced stresses hence less chances for deformation to occur. A reduction in allowable load repetition for fatigue, rutting and permanent deformation confirms that road pavement with clay treated with sustainable waste can withstand fatigue for a longer period before they occur. A reduction in CBR values reflected in a reduction in allowable repeated loads and an increase in CBR value resulted in an increase in allowable repeated loads for fatigue, rutting and permanent deformation. Failure occurs after a large number of cycles when load repetitions are high and applied stresses are low [3]. However, low load repetitions result in high stresses hence failure occurs after a few cycles due to high stresses above the materials' yield stress [3,25]. Stresses and KENPAVE results are shown in Figures 5–7 showing stresses and KENPAVE results for treated clay and Figure 8a,b shows results for permanent deformation and fatigue and rutting for sustainably treated clay using plastic, glass and brick dust waste.

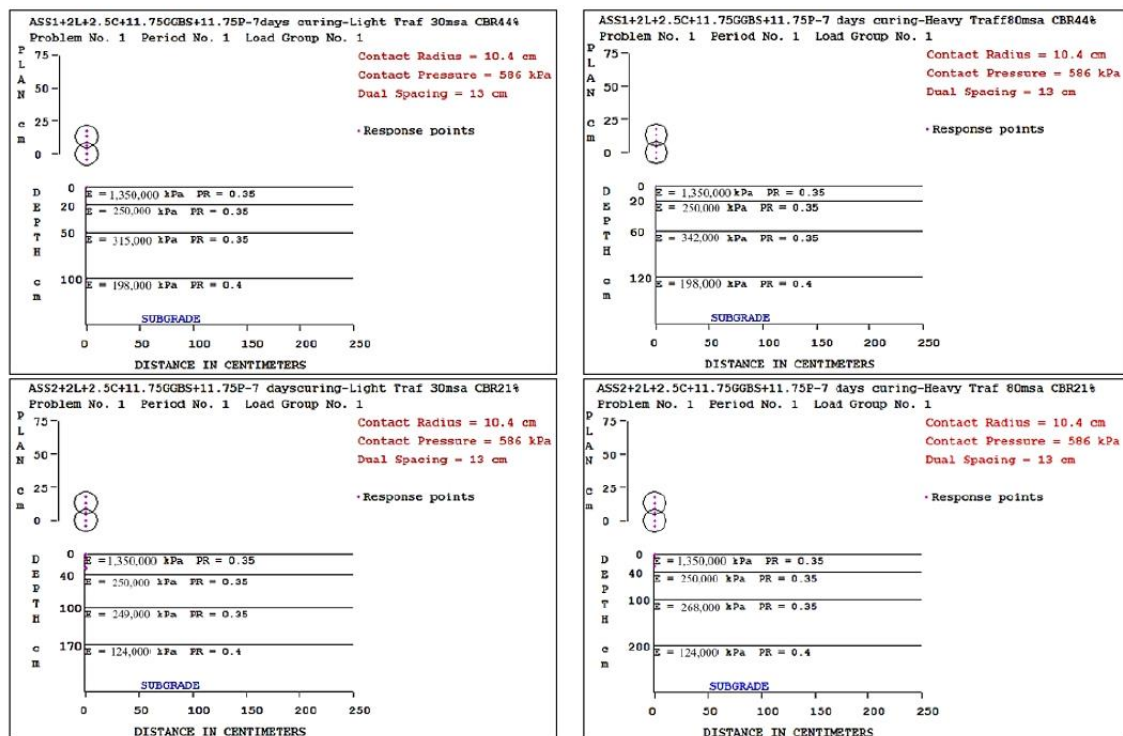
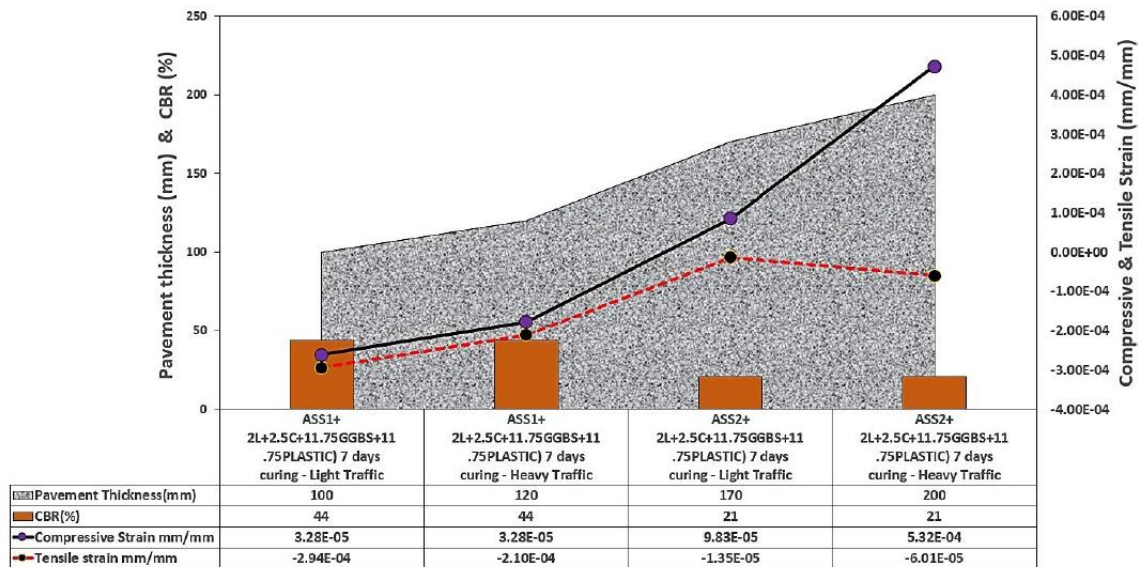


Figure 5. Stresses and KENPAVE results for clay treated using plastic waste.

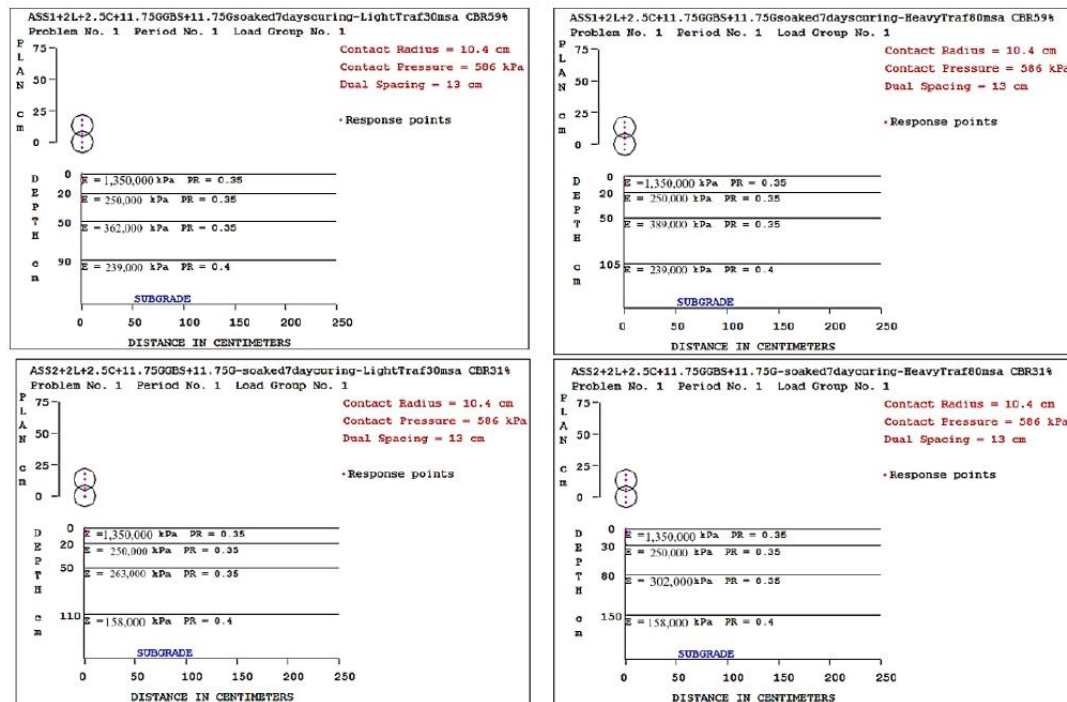
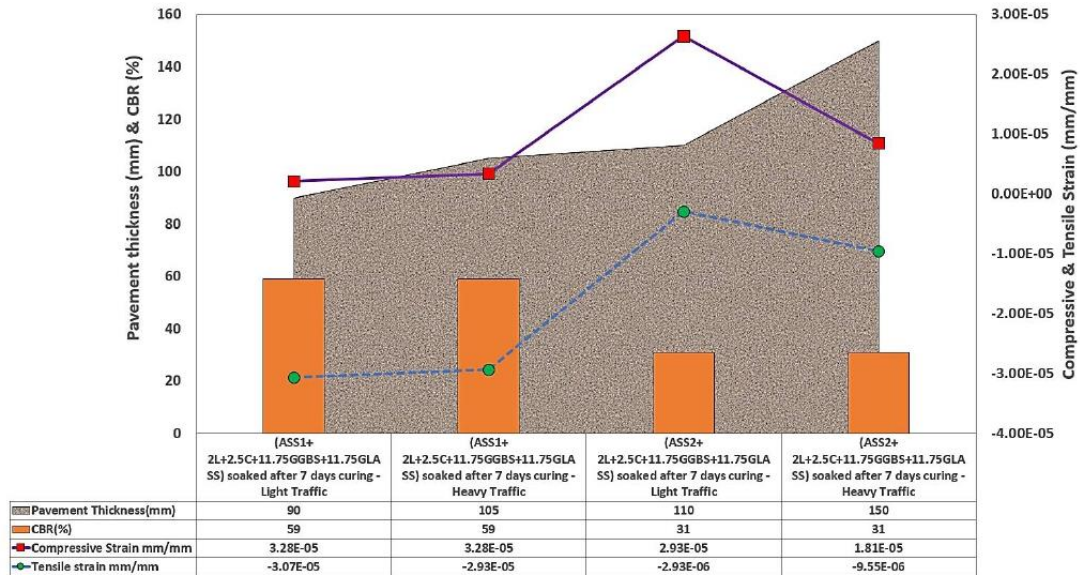


Figure 6. Stresses and KENPAVE results for clay treated using glass waste.

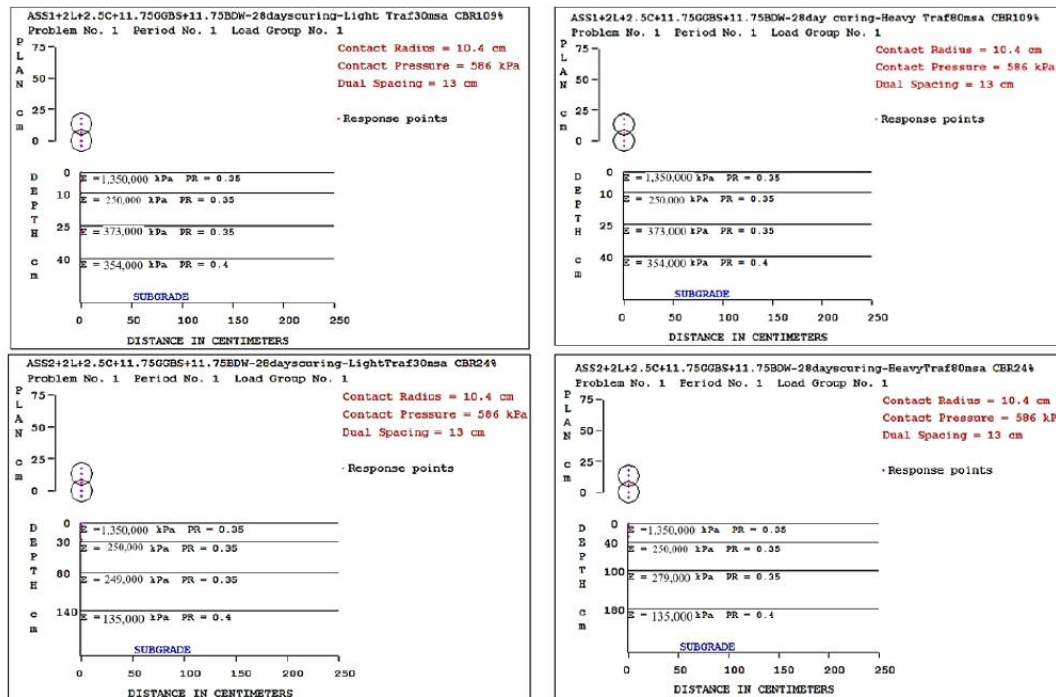
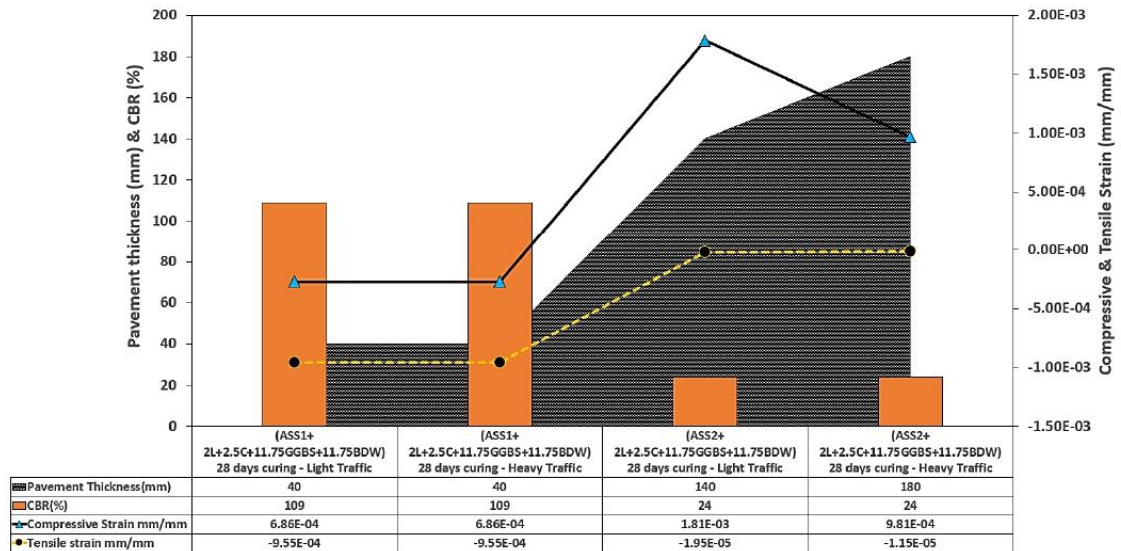
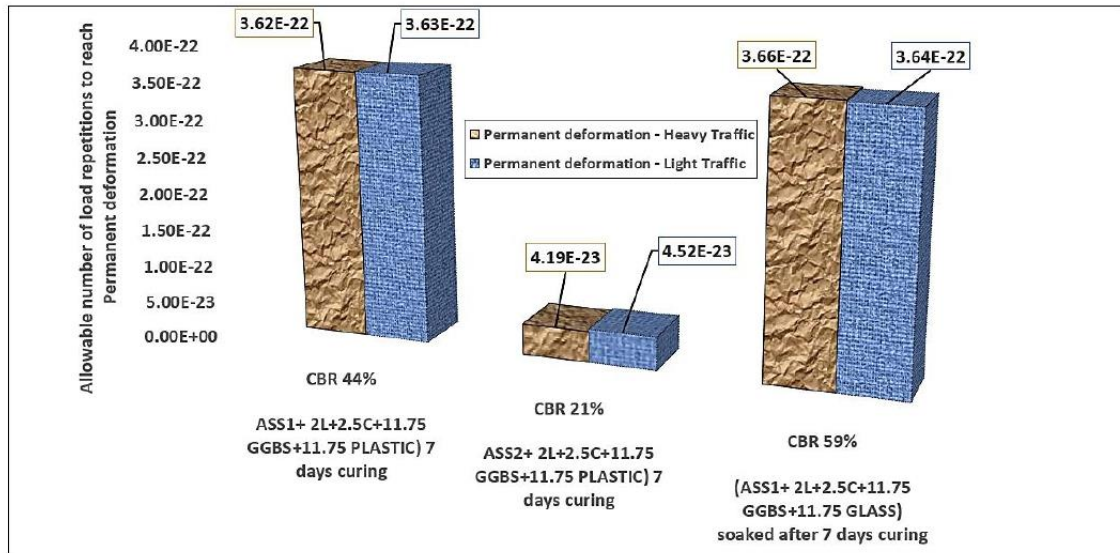
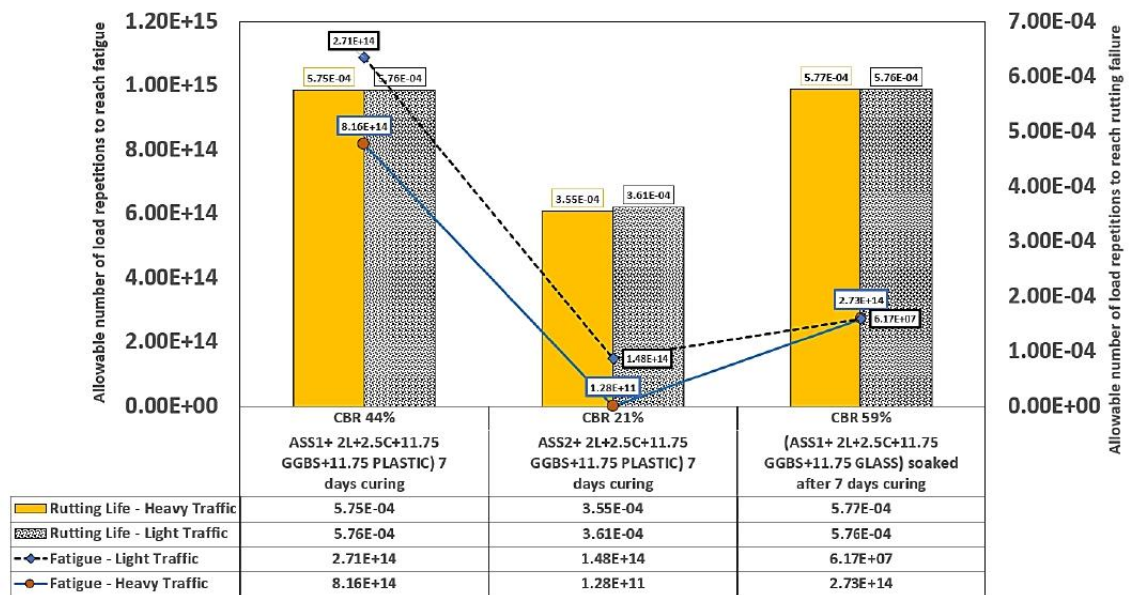


Figure 7. Stresses and KENPAVE results for clay treated using brick dust waste.



(a)



(b)

Figure 8. Cont.

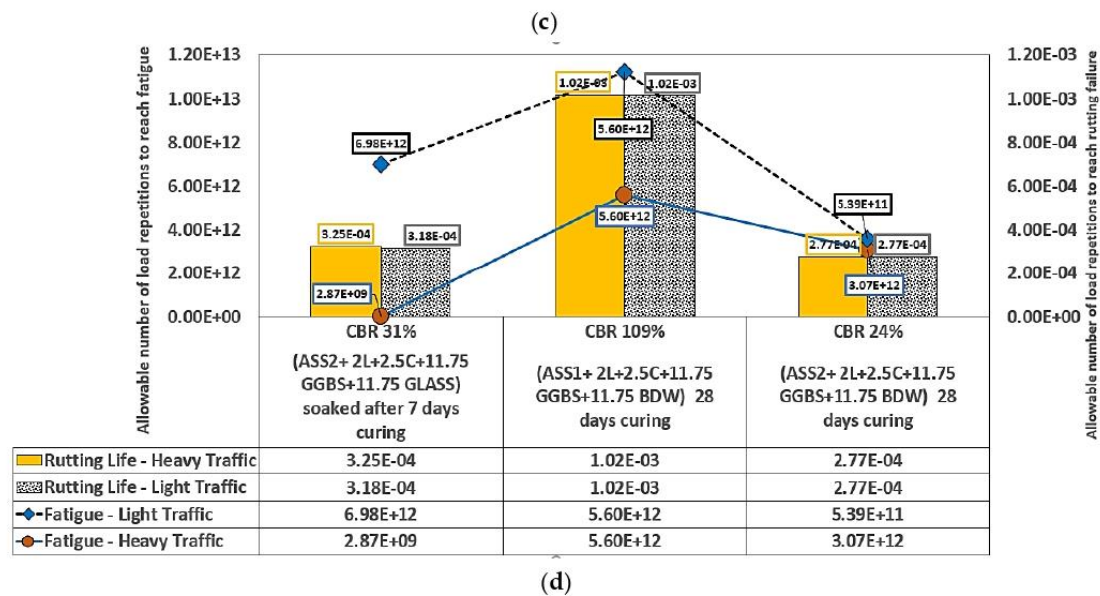
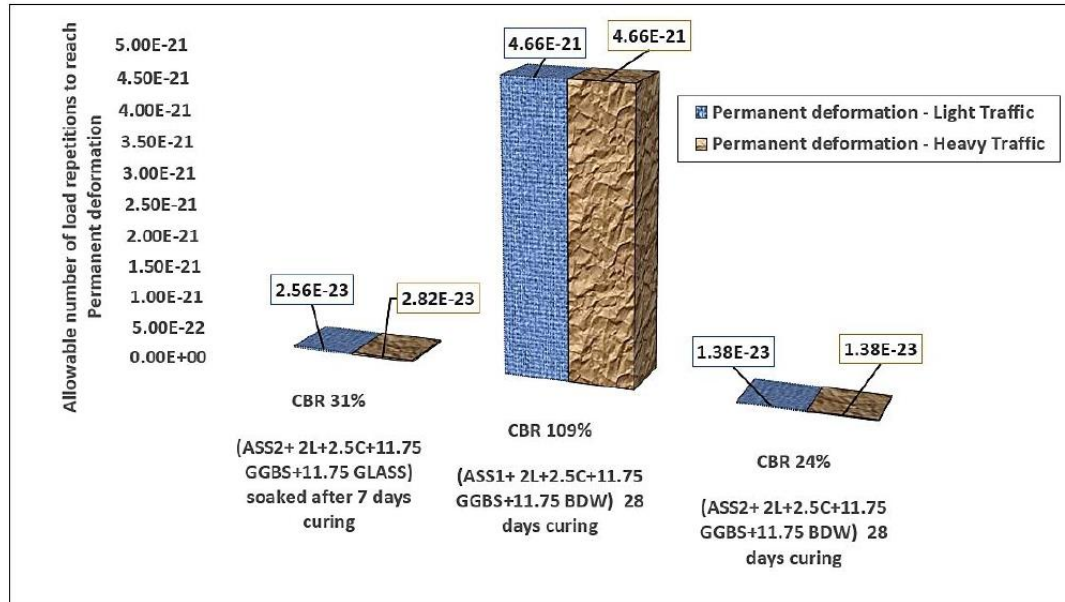


Figure 8. (a) results for permanent deformation for clay treated with plastic and glass waste (b) results for fatigue and rutting failure for clay treated with plastic and glass waste (c) results for permanent deformation for clay treated with glass and brick dust waste (d) results for fatigue and rutting clay treated with glass and brick dust waste.

8. Life Cycle Cost Analysis

Life Cycle Cost Analysis in this study was conducted using economic principles based on a range of design traffic to ascertain the long-term cost and economic effects of roads designed using CBR values achieved in this study. Due to the effectiveness of life cycle cost analysis in determining the cost-effectiveness of road pavement, The

United States has made efforts to record life cycle cost analysis state-of-practice for all highways construction [30]. A life cycle analysis (LCA) conducted for sustainable pavement demonstrated lower environmental impacts and is suitable for eco-design in the pavement sector [31]. According to [32], a key factor in multiyear prioritisation is emphasised the use of life cycle cost information in cost calculations. LCCA has gained recognition in the road construction sector as a practice in the sustainability of its infrastructural systems [33]. Life cycle cost analysis (LCCA) is an economic analysis process used to evaluate the cost-efficiency of alternatives based on the net present value (NPV) concept [34]. The LCCA approach was used to develop an inventory of quantitative asset-level models for predicting life cycle costs associated with the preservation and replacement of highway assets [35]. RealCost software was used as a tool to investigate the cost and economic effects, agency and user costs during the service life of the road. [36] used RealCost in life cycle cost analyses (LCCA) for infrastructure sustainability. RealCost software was proposed as the preferred software for use in life cycle cost analyses for road pavement [37]. The five sections of the RealCost Switchboard used for data input and results are shown in Figure 9. The initial costs, maintenance cost rehabilitation cost and salvage value of the road were projected using the net present value (NPV) indices in Equation (1). Using Equation (2), the present and future expenditure was converted into annual costs and used to calculate the equivalent uniform annual costs (EUAC) for future budget calculations while Equation (3) was used to calculate the discount rate. Table 3 shows the description of parameters used in LCCA.

$$NPV = \text{Initial Cons. Cost} + \sum_{k=1}^N \text{Future Cost}_k \left[\frac{1}{(1+i)^{n_k}} \right] - \text{Salvage Value} \left[\frac{1}{(1+i)^{n_c}} \right] \quad (1)$$

where:

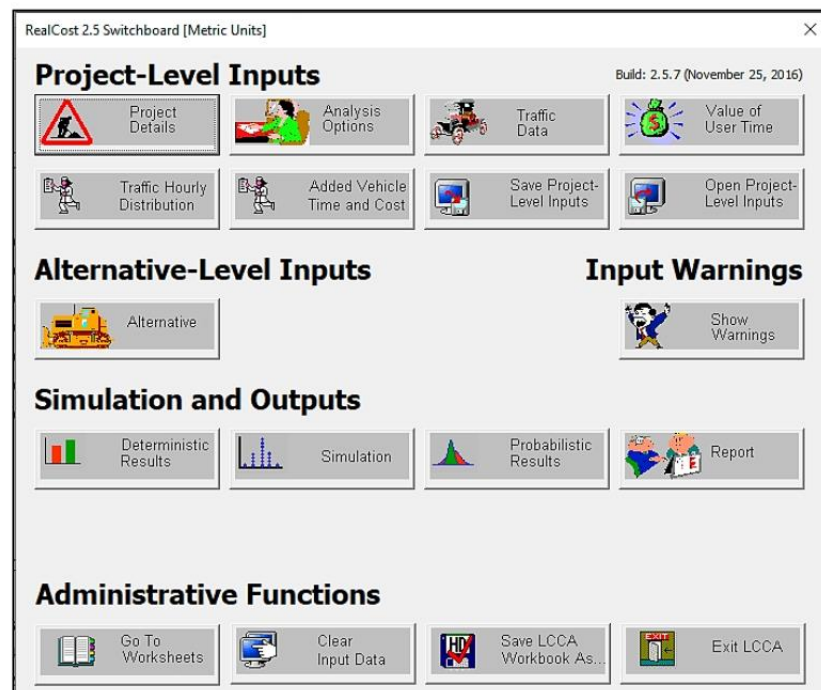


Figure 9. The five sections of the RealCost Switchboard used in this study.

Table 3. Description of parameters used in the LCCA.

Parameters	Description
Initial construction cost (ICC)	This is the cost presented in unit prices and derived from bid records of previous projects.
Maintenance and Rehabilitation cost (M&R)	This is the cost incurred to make sure the road is usable through its service life. This cost is normally M&R retrieved from previous projects.
Salvage value (SV)	Is the evaluation of the road beyond the period of analysis to ascertain the useful life of the road at the end of the analysis.
Discount rate (DR)	This is the rate used to estimate the real value of money based on the difference between inflation and interest rates.
Life Cycle Cost (LCC)	ICC + (M&R × DR)

N = number of future costs incurred over the analysis period

i = discount rate in the present

n_k = number of years from the initial construction to the K^{th} expenditure

n_e = analysis period in years.

$$EUAC = NPV \left[\frac{(1+i)^n}{(1+i)^n - 1} \right] \tag{2}$$

where:

i = discount rate

n = years of expenditure.

$$\text{Discount Rate} = \left[\frac{\text{interest} - \text{inflation}}{1 + \text{inflation}} \right] \tag{3}$$

where:

interest = Expected interest rate

inflation = Expected inflation rate.

A CBR value of 80% for clay 2 after 28 days achieved in this study was used to conduct the Life Cycle Analysis (LCCA). Two alternatives were considered during the analysis and the lowest NPV for user and agency costs derived from RealCost software was used to calculate the LCC for a period of 35 years. The initial construction cost composed of user and agency cost, cost of cement and lime treatment was calculated for a square kilometre of the road at year 0. Maintenance costs were calculated at years 6, 19 and 28 and rehabilitation costs were calculated at years 9, 21 and 30, respectively. The salvage cost of the road at year 35 in this study was based on a prorated cost of year 30 rehabilitation. The initial cost of construction was calculated based on a square kilometre of the road at year 0. Rehabilitation and maintenance costs including salvage value for clay removal and replacement were calculated for years 9, 21 and 30, respectively. This brought the Life Cycle Cost of a road with treated clay using cement and lime to GBP268,536,644.10 and Life Cycle Cost for a road with clay removed and replaced with imported materials to GBP488,754,774.64. A vast difference in life cycle cost (LCC) was observed between roads with clay treated using cement and lime and clay removed and replaced with imported materials. The LCC for the road with clay treated using cement and lime was less compared to the LCC for the road with clay removed and replaced with foreign materials. It was observed that the overall life cycle cost of the two types of roads was greatly influenced by the initial cost (user, agency cost and cost of clay treatment) at year 0. According to [38], land acquisition, renovation, modification, construction and equipment cost can increase the initial cost during Life cycle Cost Analysis (LCCA). The study proves that it is cheaper to construct roads using the existing clay compared to removing and replacing roads with clay during construction. It is more economical to design road pavement for the existing subgrade capacity than to import

or raise subgrade supports by using an extra-thicker subbase [39]. A gradual increase in maintenance and rehabilitation cost was seen for road pavement with treated clay after year 0. The high maintenance cost compared with rehabilitation cost translated into a drop in salvage value at year 35. Road pavement with clay removed and replaced recorded the highest initial cost at year 0 with a gradual increase in maintenance and rehabilitation cost and a later drop in salvage value. The total cost of treating a square kilometre of road clay using cement and lime against the total cost of removing and replacing a square kilometre of clay can be seen in Figure 10. The NPV derived from RealCost software for agency and user cost for alternatives 1 and 2 can be seen in Table 4. Estimated maintenance and rehabilitation cost and the discount rates used can be seen in Figures 11 and 12. Life Cycle Cost analysis for sustainability treated clay and Life Cycle Cost analysis for road clay removed and replaced with imported materials are shown in Figures 13 and 14.

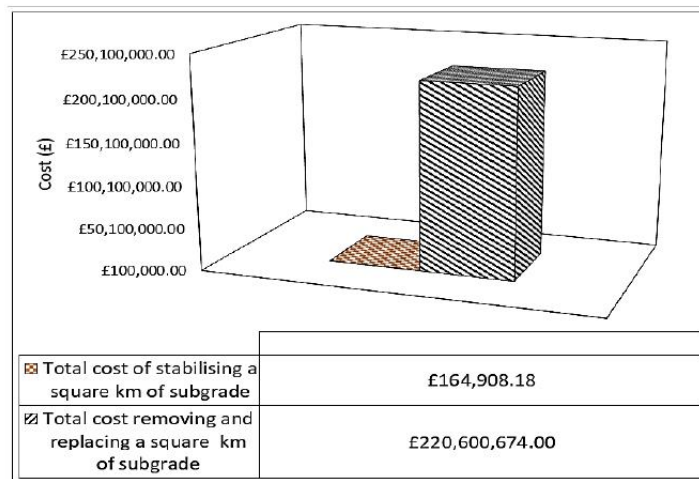


Figure 10. Cost of treating and removing clay.

Table 4. Agency and user cost for alternatives 1 and 1 derived from RealCost software.

Total Cost	Alternative 1		Alternative 2	
	Agency Cost	User Cost	Agency Cost	User Cost
Undiscounted Sum	GBP 6,000,000.00	GBP 80,000.06	GBP 7,200,000.00	GBP 133,000.43
Net Present Value	GBP 5,521,000.40	GBP 80,000.06	GBP 6,632,000.91	GBP 133,000.43
EUAC	GBP 295,000.82	GBP 4000.29	GBP 355,000.37	GBP 7000.15
Lowest Net Present Value Agency Cost	Alternative 1			
Lowest Net Present Value User Cost	Alternative 1			

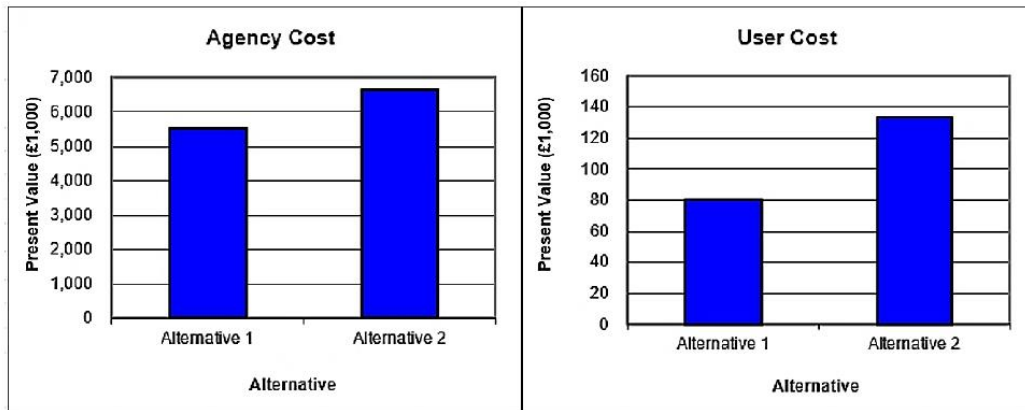


Figure 11. NPV results from RealCost software for agency and user cost for alternatives 1 and 2.

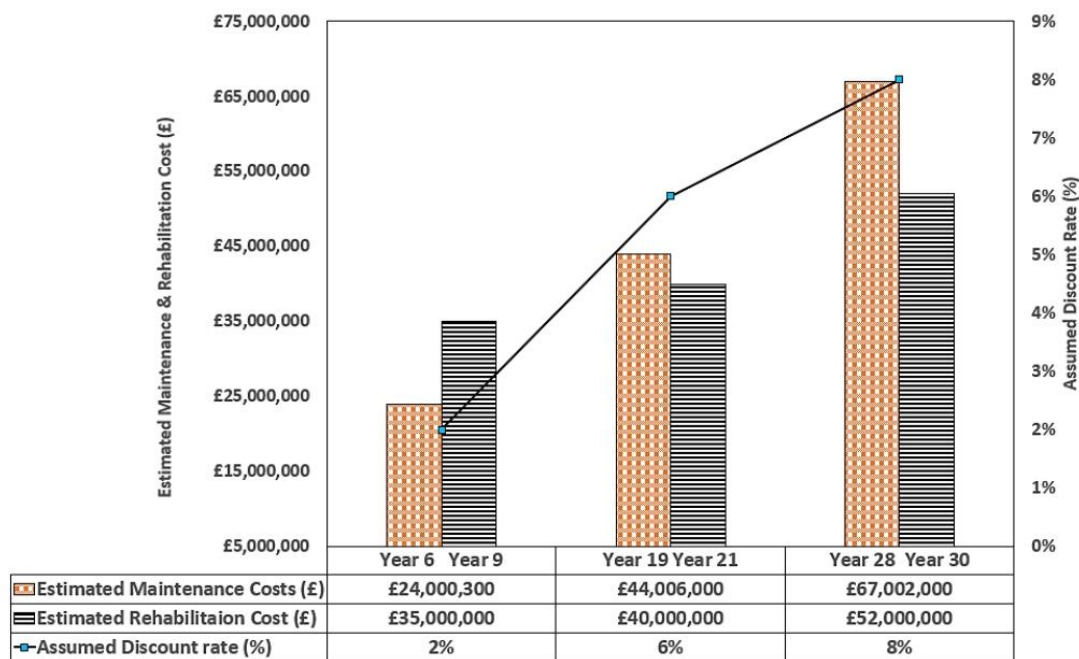


Figure 12. Discount rate, estimated maintenance and rehabilitation cost.

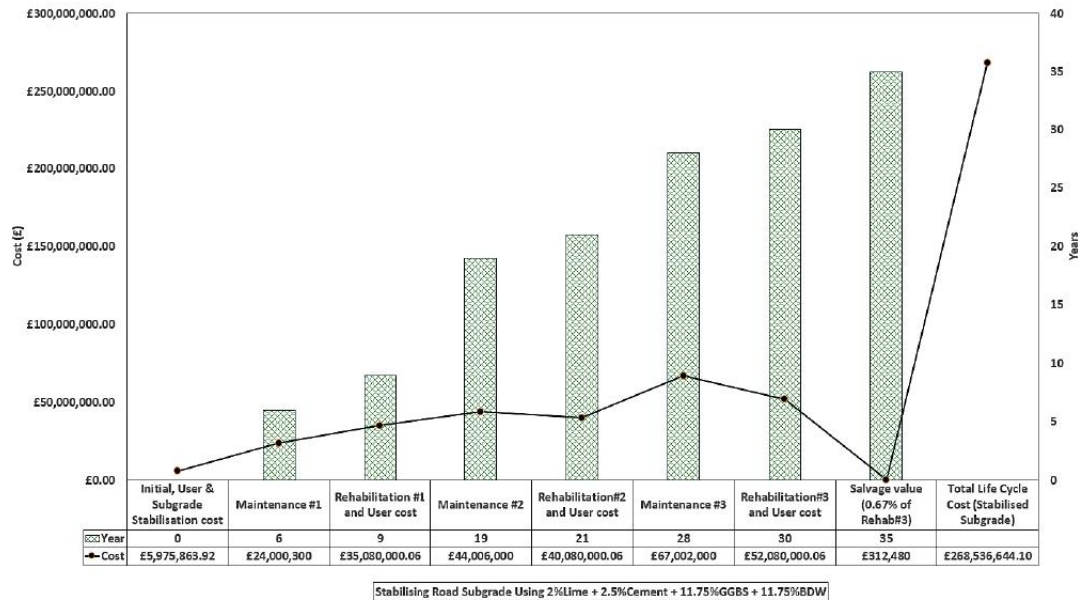


Figure 13. Life Cycle Cost analysis for sustainability treated clay.

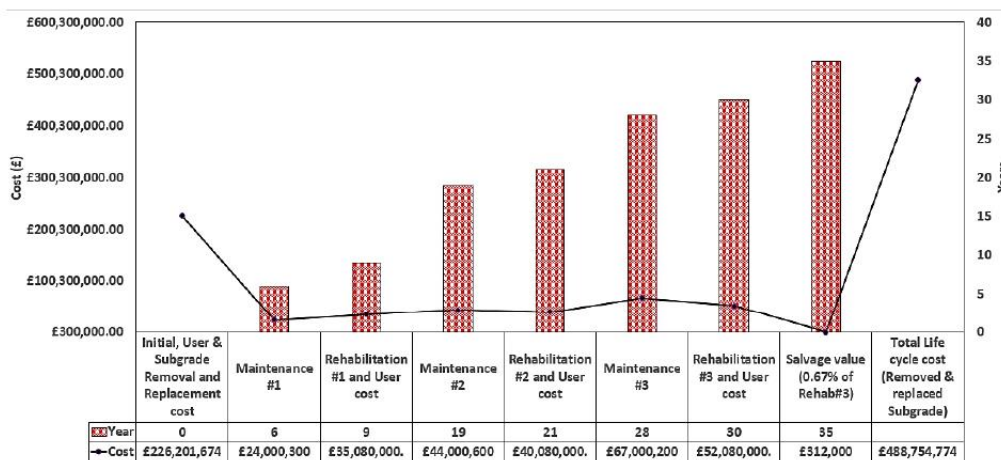


Figure 14. Life Cycle Cost analysis for road clay removed and replaced with imported materials.

9. Embodied Carbon Associated with Mix

The lowest embodied carbon was recorded for mix design 2% Lime + 2.5% Cement + 23.5% GGBS (0.0018 Co₂e/kg) compared with the control mix 8% Lime + 20% Cement of 0.0084 Co₂e/kg. However, sustainably treated mix recorded low embodied carbon except for mixed designs containing plastic. The highest embodied carbon of 0.0107 Co₂e/kg was recorded for 2% Lime +2.5% Cement +11.75% GGBS +11.75% Plastic as a result of the plastic because plastics have very high embodied carbon. [40] stated that plastics are carbon more specifically because almost all plastics are fossil carbon locked up in polymer form. Control mix 8% Lime + 20% Cement recorded the lowest Life Cycle Cost (£268,344,106.46) for treated clay followed by mix design 2% Lime + 2.5% Cement + 23.5% GGBS (£268,433,336.06). However, there was no significant difference in their LCC which makes using waste

materials in clay treatment the best option for achieving more sustainable construction. Even though traditional cement and lime are cheaper compared with sustainable waste-treated clay, they are none-environmentally friendly and unsustainable due to their high embodied carbon. Table 5 shows the classification of parameters and embodied Carbon.

Table 5. Classification of Parameters and Embodied Carbon.

S/N	Binder Composition	CBR Range (%)	Embodied Carbon for Binders (CO ₂ e/kg) (BSRIA Guide 2022 [41])	Life Cycle Cost (LCC) 35 Years	
				Treated Clay	Clay Removal and Replacement
1	8% L + 20% C (control)	38–96	0.0084	GBP268,344,106.46	GBP488,754,774.64
2	2% L + 2.5% C + 23.5% BDW	17–23	0.0036	GBP268,447,414.50	GBP488,754,774.64
3	2% L + 2.5% C + 23.5% GGBS	46–97	0.0018	GBP268,433,336.06	GBP488,754,774.64
4	2% L + 2.5% C + 23.5% PL	3–13	0.0195	GBP268,998,357.71	GBP488,754,774.64
5	2% L + 2.5% C + 23.5% GL	3–17	0.0069	GBP268,383,764.06	GBP488,754,774.64
6	2% L + 2.5% C + 11.75% GGBS + 11.75% BDW	16–109	0.0028	GBP268,536,644.10	GBP488,754,774.64
7	2% L + 2.5% C + 11.75% GGBS + 11.75% PL	44–93	0.0107	GBP269,087,587.31	GBP488,754,774.64
8	2% L + 2.5% C + 11.75% GGBS + 11.75% GLASS	21–80	0.0072	GBP268,472,993.66	GBP488,754,774.64

Where L = Lime, C = Cement, GGBS = Ground Granulated Blastfurnace Slag, PL= Plastic, GL = Glass, BDW = Brick Dust waste.

10. Conclusions

Conducting road pavement design, defect analysis and Life Cycle Cost Analysis (LCCA) using clay treated with eco-friendly waste materials achieved good results in this study therefore the study concludes on the following:

1. Road pavement thickness reduced with an increase in CBR value however, there was no significant difference between pavement thickness.
2. CBR values from 2–5% only recorded high pavement thickness as a result thicker subbase layer influences the overall thickness of the pavement.
3. Defects are less likely to occur due to high CBR values recorded resulting in low stresses within the pavement structure.
4. High allowable repeated loads were recorded for subgrade with high CBR value resulting in the ability of road pavement to withstand several cyclic loading before failure occurs.
5. The study reveals the possibility of treating clay using waste materials which would help reduce the problem of landfill and greenhouse gas emissions and the environmental effects associated with cement and lime production while reducing our overreliance on natural resources such as clinker used in cement production.
6. Road pavement constructed using clay removed and replaced with foreign materials recorded the highest Life Cycle Cost. Compared to the Life Cycle Cost of road pavement constructed using clay treated with waste. The study confirmed that road pavement constructed using clay treated with waste is cheaper and more economical compared with road pavement with clay removed and replaced with imported materials.
7. The Life Cycle Cost (LCC) of a road is greatly influenced by the initial cost such as agency, user cost and subgrade treatment cost. Year 0 to year 19 observed a gradual increase in maintenance and rehabilitation costs as road pavement age increased. Followed by a reduction in rehabilitation cost in year 21 with an increase in maintenance cost in year 28. Both road pavements recorded the same salvage value.
8. Decision-makers, road contractors and engineers can quickly refer to this study when deciding on the Life Cycle Cost (LCC) of road projects with subgrade characteristics and parameters similar to what was used in this study.

9. To save money in road construction, this study recommends that clay or weak subgrades should be treated for use in road construction instead of removing subgrades and replacing them with imported materials. The cost of road pavement can be reduced by achieving good CBR values and thinner pavement thickness through subgrade treatment using cement and lime as binders.
10. This study would encourage the use of waste materials dumped in landfills in ground improvement and road construction. This would promote greener, sustainable and eco-friendly ways of road construction to help battle the climate change problems faced today.

Author Contributions: S.J.A. and S.Y.O.A.; methodology, S.Y.O.A., J.O. and S.J.A.; validation, S.Y.O.A., J.O. and S.J.A.; formal analysis, S.Y.O.A.; investigation, S.Y.O.A.; re-sources, S.J.A. and C.A.B.; data curation, S.Y.O.A. and S.J.A.; writing—original draft preparation, S.Y.O.A.; writing—review and editing, S.Y.O.A., S.J.A. and C.A.B.; visualization, S.J.A., J.O. and C.A.B.; supervision, S.J.A., J.O. and C.A.B.; project administration, C.A.B. and S.J.A. All authors have read and agreed to the published version of the manuscript.

Funding: This research received no external funding.

Institutional Review Board Statement: Not applicable.

Informed Consent Statement: Not applicable.

Data Availability Statement: Data can be obtained from corresponding authors upon reasonable request.

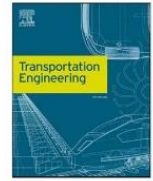
Acknowledgments: The authors acknowledge that the advice, comments and suggestions from anonymous reviewers significantly improved the quality of this paper.

Conflicts of Interest: The authors declare that they have no conflict of interest associated with this publication, and no financial support has been given to influence the outcome of this work.

References

1. Amakye, S.Y.; Abbey, S.J. Understanding the performance of Clay subgrade materials treated with non-traditional stabilisers: A Review. *Clean. Eng. Technol.* **2021**, *4*, 100159. [CrossRef]
2. Amakye, S.Y.O.; Abbey, S.J.; Booth, C.A.; Oti, J. Road Pavement Thickness and Construction Depth Optimization Using Treated and Untreated Artificially-Synthesized Clay Road Subgrade Materials with Varying Plasticity Index. *Materials* **2022**, *15*, 2773. [CrossRef]
3. Amakye, S.Y.; Abbey, S.J.; Booth, C.A. Booth. Road pavement defect investigation using treated and untreated Clay road subgrade materials with varying plasticity index. *Transp. Eng.* **2022**, *9*, 100123. [CrossRef]
4. Amakye, S.Y.; Abbey, S.J.; Booth, C.A.; Mahamadu, A.-M. Enhancing the engineering properties of subgrade materials using processed waste: A review. *Geotechnics* **2021**, *1*, 307–329. [CrossRef]
5. Abbey, S.J.; Eyo, E.U.; Ng’Ambi, S. Swell and microstructural characteristics of high-plasticity clay blended with cement. *Bull. Eng. Geol. Environ.* **2020**, *79*, 2119–2130. [CrossRef]
6. Abbey, S.J.; Ngambi, S.; Coakley, E. Effect of cement and by-product material inclusion on plasticity of deep mixing improved soils. *Int. J. Civ. Eng. Technol.* **2016**, *7*, 265–274.
7. Baldo, N.; Rondinella, F.; Daneluz, F.; Pasetto, M. Foamed Bitumen Mixtures for Road Construction Made with 100% Waste Materials: A Laboratory Study. *Sustainability* **2022**, *14*, 6056. [CrossRef]
8. Suksiripattanapong, C.; Phetprapai, T.; Singsang, W.; Phetchuay, C.; Thumrongvut, J.; Tabyang, W. Utilization of Recycled Plastic Waste in Fiber Reinforced Concrete for Eco-Friendly Footpath and Pavement Applications. *Sustainability* **2022**, *14*, 6839. [CrossRef]
9. Abbey, S.J.; Eyo, E.U.; Jeremiah, J.J. Experimental Study on Early Age Characteristics of Lime-GGBS-Treated Gypseous Clays under Wet–Dry Cycles. *Geotechnics* **2021**, *1*, 402–415. [CrossRef]
10. Rivera, J.F.; Orobio, A.; De Gutiérrez, R.M.; Cristelo, N. Clayey soil treatment using alkali-activated cementitious materials. *Mater. Construc.* **2020**, *70*, e211. [CrossRef]
11. Li, J.; Cameron, D.A.; Ren, G. Case study and back analysis of a residential building damaged by Clay soils. *Comput. Geotech.* **2014**, *56*, 89–99. [CrossRef]
12. The Constructor Building Ideas (TCBI). Available online: <https://theconstructor.org/transportation/flexible-pavement-design-cbr-method/11442/> (accessed on 14 November 2021).
13. Wild, W.J.; Waalkes, S.; Harrison, R. Life Cycle Analysis of Portland Cement Concrete Pavement. Research Report SWUTC/01/167205-1 Southwest Region University Transportation Center. University for Transport Research, The University of Texas at Austin. 2001. Available online: https://ctr.utexas.edu/wp-content/uploads/pubs/1739_1.pdf (accessed on 14 August 2022).

14. Life Cycle Cost Analysis. U.S. Department of Transportation, Federal Highway Administration. 2017. Available online: <https://www.fhwa.dot.gov/infrastructure/asstmgmt/lccasoft.cfm> (accessed on 14 August 2022).
15. Amakye, S.Y.O.; Amakye, S.J.; Booth, C.A. DMRB Flexible Road Pavement Design Using Re-Engineered Clay Road Subgrade Materials with Varying Plasticity Index. *Geotechnics* **2022**, *2*, 395–411. [CrossRef]
16. BS ISO 15686-5:2017; Building and Constructed Assets—Service Life Planning—Part 5: Life-Cycle Costing. ISO Standards. Available online: <https://www.iso.org/standard/61148.html> (accessed on 14 August 2022).
17. Newmarket Plant Hire (NPH) Group. Available online: <http://www.nphgroup.co.uk/wp-content/uploads/2016/07/Plant-Tools-Hire-Rates-Final-Copy.pdf> (accessed on 16 December 2021).
18. Ecoinvent. Available online: <https://ecoinvent.org/> (accessed on 27 February 2022).
19. Chaiyaput, S.; Sertsoongnern, P.; Ayawanna, J. Utilization of Waste Dust from Asphalt Concrete Manufacturing as a Sustainable Subbase Course Material in Pavement Structures. *Sustainability* **2022**, *14*, 9804. [CrossRef]
20. Design Manual for Roads and Bridges (DMRB) CD 226. Design for New Pavement Construction. Available online: <https://www.standardsforhighways.co.uk/ha/standards/> (accessed on 14 November 2021).
21. Otoko, G.R.; Pedro, P.P. Cement treatment of laterite and Chikoko soils using waste rubber fiber. *Int. J. Eng. Sci. Res. Technol.* **2014**, *3*, 1–7. Available online: https://www.researchgate.net/publication/267211553_Cement_Stabilization_of_Laterite_and_Chikoko_Soils_Using_Waste_Rubber_Fibre (accessed on 2 April 2022).
22. The Construction, Road Construction. 2022. Available online: https://www.designingbuildings.co.uk/wiki/Road_construction (accessed on 10 March 2022).
23. Dawson, A.; Kolisoja, P.; Vuorimies, N. Understanding Low-Volume Pavement Response to Heavy Traffic Loading. Institute of Earth & Foundation Structure. 2008. Tampere University of Technology. Available online: https://www.roadex.org/wp-content/uploads/2014/01/task-b2_designa_140408.pdf (accessed on 5 April 2022).
24. *Interim Advice Note (IAN) 73/06*; Design Guidance for Road Pavement Foundations. Available online: <https://www.standardsforhighways.co.uk/ha/standards/> (accessed on 14 November 2021).
25. Iowa State University. 2021. Available online: <https://www.nde-ed.org/Physics/Materials/Mechanical/FractureToughness.xhtml> (accessed on 14 February 2022).
26. Fleck, N.; Shin, C.; Smith, R. Fatigue crack growth under compressive loading. *Eng. Fract. Mech.* **1985**, *21*, 173–185. [CrossRef]
27. Parry, A.R.; Phillips, S.J.; Potter, J.F.; Nunn, M.E. Design and performance of flexible composite road pavements. *Proc. Inst. Civ. Eng. Transp.* **1999**, *135*, 9–16. [CrossRef]
28. Dhiman, A.; Arora, N. Improving rutting resistance of flexible pavement structure by using waste plastic. *IOP Conf. Ser. Earth Environ. Sci.* **2021**, *889*, 012030. [CrossRef]
29. Nunn, M.E.; Brown, A.; Weston, D.; Nicholls, J.C. Design of long-life flexible pavement for heavy traffic. *Br. Aggreg. Constr. Mat. Indust Refin. Bitum. Associ.* **1997**, *250*, 1–81.
30. Peterson, D.E. Life-Cycle Cost Analysis of Pavements. National Cooperative Highway Research Program Synthesis of Highway Practice. Transportation Research Board. 1985, Volume 122, pp. 1–145. Available online: http://onlinepubs.trb.org/Onlinepubs/nchrp/nchrp_syn_122.pdf (accessed on 14 November 2021).
31. Praticò, F.G.; Giunta, M.; Mistretta, M.; Gulotta, T.M. Energy and Environmental Life Cycle Assessment of Sustainable Pavement Materials and Technologies for Urban Roads. *Sustainability* **2020**, *12*, 704. [CrossRef]
32. Zimmerman, K.A.; Smith, K.D.; Grogg, M.G. Applying economic concepts from life-cycle cost analysis to pavement management analysis. *Transp. Res. Rec.* **2000**, *1699*, 58–65. [CrossRef]
33. Ozbay, K.; Jawad, D.; Parker, N.A.; Hussain, S. Life-cycle cost analysis: State of the practice versus state of the art. *Transp. Res. Rec.* **2004**, *1864*, 62–70. [CrossRef]
34. Babashamsi, P.; Yusoff, N.I.M.; Ceylan, H.; Nor, N.G.M.; Jenatabadi, H.S. Evaluation of pavement life cycle cost analysis: Review and analysis. *Int. J. Pavement Res. Technol.* **2016**, *9*, 241–254. [CrossRef]
35. Flannery, A.; Manns, J.; Venner, M. *NCHRP Synthesis of Highway Practice 494: Life-Cycle Cost Analysis for Management of Highway Assets*; Transportation Research Board of the National Academies: Washington, DC, USA, 2016.
36. Lee, E.-B.; Thomas, D.K.; Alleman, D. Incorporating Road User Costs into Integrated Life-Cycle Cost Analyses for Infrastructure Sustainability: A Case Study on Sr-91 Corridor Improvement Project (Ca). *Sustainability* **2018**, *10*, 179. [CrossRef]
37. Rangaraju, P.R.; Amirkhani, S.; Guven, S.Z. *Life Cycle Analysis for Pavement Type Section*; FHWA, South Carolina Department of Transportation: Clemson, SC, USA, 2008. Available online: <https://www.scdot.scltap.org/wp-content/uploads/2017/05/SPR656Final.pdf> (accessed on 14 November 2021).
38. Fuller, S. Life-Cycle Cost Analysis (LCCA). National Institute of Standard and Technology (NIST). 2006. Available online: <https://www.wbdg.org/resources/life-cycle-cost-analysis-lcca> (accessed on 8 March 2022).
39. Li, S. Heavy duty pavements. *S. D. Sch. Mines Technol.* **1964**, *25*, 1–4. Available online: https://www.concreteconstruction.net/_view-object?id=00000153-8b57-dbf3-a177-9f7feb540000 (accessed on 14 August 2022).
40. Zhu, X. The Plastic Cycle—An Unknown Branch of the Carbon Cycle. *Front. Mar. Sci.* **2021**, *7*, 1–4. Available online: <https://www.frontiersin.org/articles/10.3389/fmars.2020.609243/full> (accessed on 14 November 2021).
41. Carbon, E. The Inventory of Carbon and Energy (ICE) A BSRIA Guide. 2022. Available online: <https://greenbuildingencyclopaedia.uk/wp-content/uploads/2014/07/Full-BSRIA-ICE-guide.pdf> (accessed on 14 November 2021).



Road pavement defect investigation using treated and untreated expansive road subgrade materials with varying plasticity index

Samuel Y.O. Amakye^{*}, Samuel J. Abbey, Colin A. Booth

Civil Engineering Cluster, Department of Geography and Environmental Management, Faculty of Environment and Technology, University of the West of England, United Kingdom

ARTICLE INFO

Keywords:

Subgrade
Pavement
Defect
Swell
Compaction
California Bearing Ratio
Atterberg limit
Repeated load
Crack, Fatigue
Deformation
Rutting

ABSTRACT

Road pavement defect has been a major issue in the construction industry leading to a high cost of maintenance and sometimes a total reconstruction of the road. Expansive road subgrade materials are one of the major causes of these road defects. In this study subgrade materials with varying plasticity index were formulated at a ratio of 25% bentonite + 75% kaolinite, 35% bentonite + 65% kaolinite and 75% bentonite + 25% kaolinite respectively. Cement and lime were used as binders to improve the engineering properties of these expansive subgrade materials to make them usable in road construction. A road pavement defect analysis was conducted to investigate the effect of varying California Bearing Ratio (CBR) and traffic load on treated road subgrade in terms of failure. Atterberg limit, compaction, characteristics, mineral structure, California Bearing Ratio (CBR), Swell and microstructural properties (Scanning Electron Microscopy (SEM) and Energy Dispersive X-ray (EDX)) of the subgrade were also investigated in this study. The results show an increase in CBR value with a reduction in swell values translating to lesser stresses within the pavement structure which reduced rutting, fatigue and permanent deformation of the road. The study concluded that the service life of the pavement can be prolonged by reducing road pavement defects using cement and lime as binders in subgrade stabilisation.

1. Introduction

Layers of processed materials placed over the natural ground (subgrade) are referred to as road pavement. Road pavements distribute traffic load to the subgrade providing skid resistance, low noise and smooth riding. Most times, road pavement defects occur as a result of distress developed in the pavement under the combined effect of traffic loading, environmental conditions and geotechnical issues due to expansive subgrade [1]. The strength of road subgrade can be investigated by conducting California Bearing Ratio (CBR) test on the subgrade material. The California Bearing Ratio (CBR) of road subgrade can influence the overall thickness and depth of construction of the road pavement which greatly impacts the cost of construction [2] and [3]. According to Amakye et al., 2021 [4] road pavement defects are a result of expansive subgrade and the process of maintaining or repairing the pavement comes with a huge cost. The US and China incurred a cost of \$US30 billion as maintenance costs due to expansive subgrade [5]. The damage caused by expansive subgrade runs into millions of dollars and the UK spent more than £3 billion on infrastructural damages caused by expansive soils [6] and [7]. Other studies have used binders such as

Construction and Demolition Waste (CDW) [8,9,10,11] and [12] Crashed glass waste [13], waste ceramic tiles and zinc-coated steel milling waste [14] and [15], and recycled construction and demolition materials in road pavement subgrade [16].

However, in this study, Cement and lime were used as binders in subgrade stabilisation due to their ability to improve the engineering properties of subgrade materials. Portland cement and lime over the years have been used in subgrade stabilisation due to the ability to form Calcium Silicate Hydrate (C-S-H) gel responsible for strength gain [17]. Calcium Silicate Hydrate (C-S-H) gel act as a binding agent which binds subgrade particle together [3]. Cement and lime are suitable for subgrade stabilisation and a cement range of 4% and 15% was used to enhance the engineering properties of subgrade materials [18] and [19]. Using lime as a binder with the help of calcium releases a cementitious product called Calcium Silicate Hydrate (C-S-H) gel which can stabilise subgrade materials with plasticity index between 20% and 30% and a liquid limit from 25% to 50% [20] and [21]. Ingles et al., (1972) [22] achieved good California Bearing Ratio (CBR) and swell values using 80% lime in subgrade treatment and 3% – 8% lime to improve high plasticity index clays. 1%, 4% and 6% lime proportions were used in

^{*} Corresponding author.

E-mail address: Samuel.amakye@uwe.ac.uk (S.Y.O. Amakye).

<https://doi.org/10.1016/j.treng.2022.100123>

Received 22 March 2022; Received in revised form 24 June 2022; Accepted 28 June 2022

Available online 1 July 2022

2666-691X/© 2022 The Author(s). Published by Elsevier Ltd. This is an open access article under the CC BY-NC-ND license (<http://creativecommons.org/licenses/by-nc-nd/4.0/>).

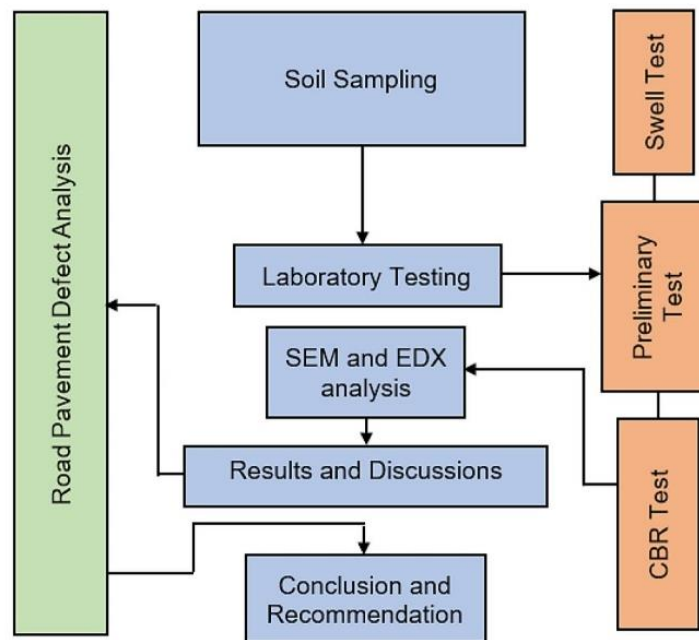


Fig. 1. Methodological process used in this study.



Fig. 2. SEM image, Map and EDX results for ASS1 after 7 days of curing.

various studies for subgrade treatment to achieve good performance [23,24] and [25]. The inclusion of cement increased the bearing capacity of subgrade materials during stabilisation at proportions of 10%, 15% and 20% by weight of soil. In this study road pavement defect analysis was conducted using varying design traffic load and California Bearing Ratio (CBR) values achieved in this study to determine their effect on the durability of the road pavement structure. The study seeks to explore the area of road pavement defects by investigating the causes of road pavement defects. The study investigated the factors responsible for these defects and attempt to eliminate or reduce these defects for road pavement with stabilised high plasticity index subgrade materials using chemical stabilisation techniques.

2. Materials and methods

Bentonite and kaolinite were used in this study to form subgrade materials with varying plasticity index. These Artificially Synthesised Subgrade (ASS) materials were referred to in this study as ASS 1 (25% bentonite + 75% kaolinite) high plasticity index subgrade, ASS 2 (35% bentonite + 65% kaolinite) very high plasticity index subgrade and ASS 3 (75% bentonite + 25% kaolinite) extremely high plasticity index subgrade respectively. These subgrade materials were treated using cement and lime to improve their engineering properties in accordance with relevant standards. The standards used in sample preparation, testing, details of suppliers, material oxide, mineralogical composition, chemical composition and particle size distribution of the materials used

are as reported in the authors' previous study [2]. Atterberg and compaction tests were conducted on untreated subgrade materials and California Bearing Ratio (CBR) and swell test was conducted on treated and untreated subgrade materials. The study also conducted micro-structural properties (Scanning Electron Microscopy (SEM) and Energy Dispersive X-ray (EDX)) for treated subgrade materials to determine the effect of the binder after treatment. The study analysed the occurrence of a potential defect within road pavement using California Bearing Ratio (CBR) values achieved in this study and adopted design traffic loads. KENPAVE software was used to analyse stresses at various response points within the road pavement layers. Fig. 1 show the methodology used in this study.

3. Results and discussion

3.1. California Bearing Ratio (CBR) and Microstructural Properties

Artificially Synthesised Subgrade (ASS 3) composed of high bentonite content achieved the highest CBR value for untreated subgrade materials soaked and unsoaked at 9% and 2% and Untreated ASS 1 and ASS 2 recorded CBR values of 0.9%, 5% and 0.8% for untreated soaked respectively. The CBR values achieved for untreated soaked subgrade materials are unacceptable for use in road construction. According to Amakye et al. [2,26], California Bearing Ratio (CBR) values <2% are unacceptable for use in road construction. California Bearing Ratio (CBR) values achieved for treated subgrade materials both soaked

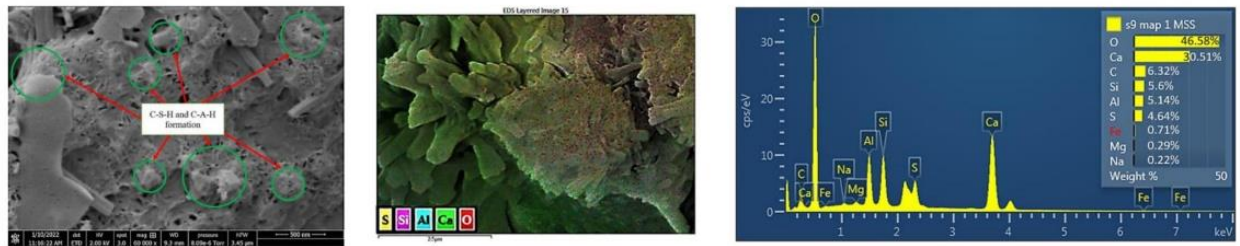


Fig. 3. SEM image, Map and EDX results for ASS2 after 7 days of curing.

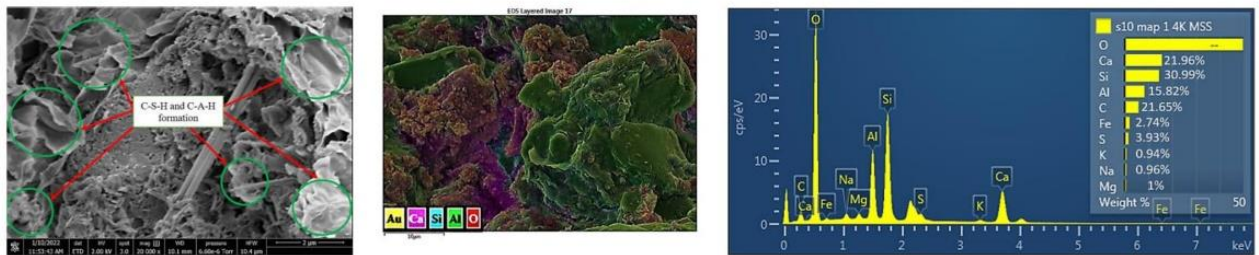


Fig. 4. SEM image, Map and EDX results for ASS3 after 7 days of curing.

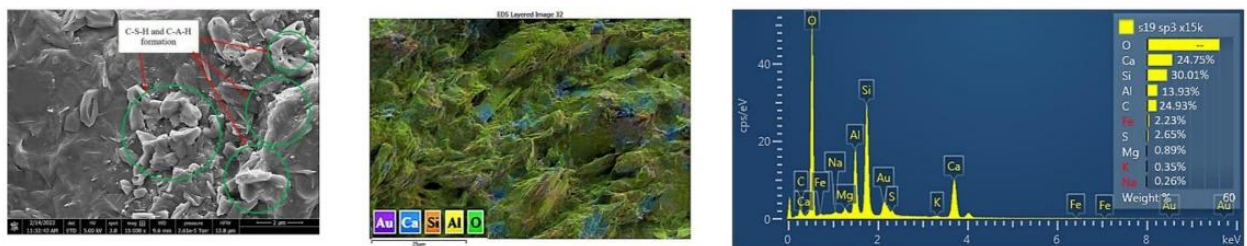


Fig. 5. SEM image, Map and EDX results for ASS1 after 28 days of curing.



Fig. 6. SEM image, Map and EDX results for ASS2 after 28 days of curing.

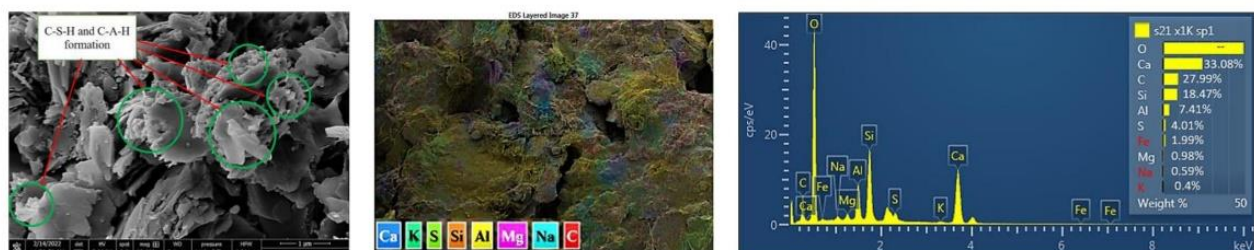


Fig. 7. SEM image, Map and EDX results for ASS3 after 28 days of curing.

Table 1
Selected CBR values used in defect analysis.

Subgrade Type	Mix Design	Treated	Soaked	Curing days	CBR (%)
ASS 1	(25%B + 75% K)	x	x	0	8
ASS 2	(35%B + 65% K)	x	x	0	5
ASS 3	(75%B + 25% K)	x	x	0	9
ASS 1	(8%L + 20% C)	✓	x	7	80
ASS 2	(8%L + 20% C)	✓	x	7	60
ASS 3	(8%L + 20% C)	✓	x	7	30
ASS 1	(8%L + 20% C)	✓	✓	7	50
ASS 2	(8%L + 20% C)	✓	✓	7	40
ASS 3	(8%L + 20% C)	✓	✓	7	30
ASS 1	(8%L + 20% C)	✓	x	28	90
ASS 2	(8%L + 20% C)	✓	x	28	100
ASS 3	(8%L + 20% C)	✓	x	28	80

Where B = Bentonite K = Kaolinite L = Lime and C = Cement

and unsoaked are greater than 2% and suitable for use in road construction. Further details on California Bearing Ratio (CBR) results are as reported in the authors' previous study [2]. The high CBR achieved for the treated subgrade in this study was a result of the formation of calcium silicate hydrate (C-S-H) gel during the hydration process of cement and lime. A gradual increase in CBR value and a reduction in swell was observed with an increase in curing age. Scanning microscopy (SEM) and Energy Dispersive X-ray (EDX) analysis conducted on treated subgrade samples showed an obvious formation of C-S-H gel in the mix. The EDX results show an increase in the formation of calcium (Ca) responsible for the formation of calcium silicate hydrate (C-S-H) gel for strength gain in the mix as curing age increases. At the end of curing day 7, EDX for ASS 1 reported a formation of 16.21% Calcium (Ca), 30.51% Calcium (Ca), for ASS 2 and 21.96% Calcium (Ca) for ASS 3. At the end of 28 days of curing, Calcium (Ca) formation increased drastically from 16.21% Calcium (Ca), for ASS1 to 24.75% Calcium (Ca), and 30.51% Calcium (Ca) to 32.56% Calcium (Ca) for ASS 2 and from 21.96% Calcium (Ca), to 33.08% for ASS 3 respectively. Fig. 2–7 show detailed results for SEM and EDX achieved in this study for selected subgrade

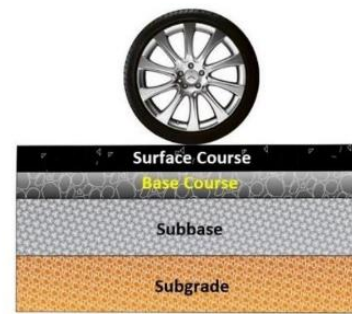


Fig. 9. Three-layer flexible composite pavement structure.

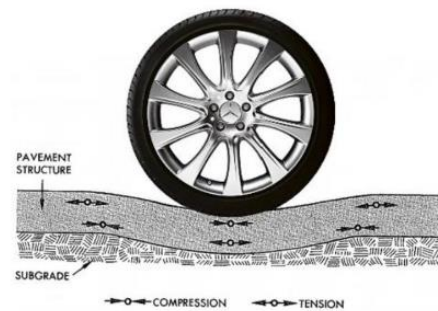


Fig. 10. Pavement deflection in tensile and compressive stress in a pavement structure [31].

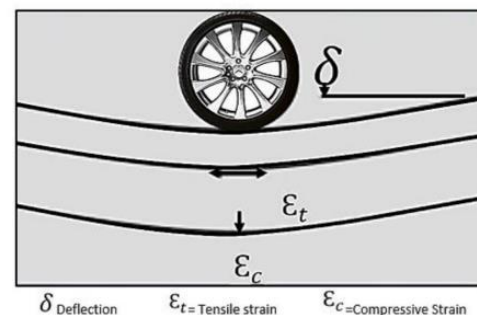


Fig. 11. Types of stress within a road pavement structure.

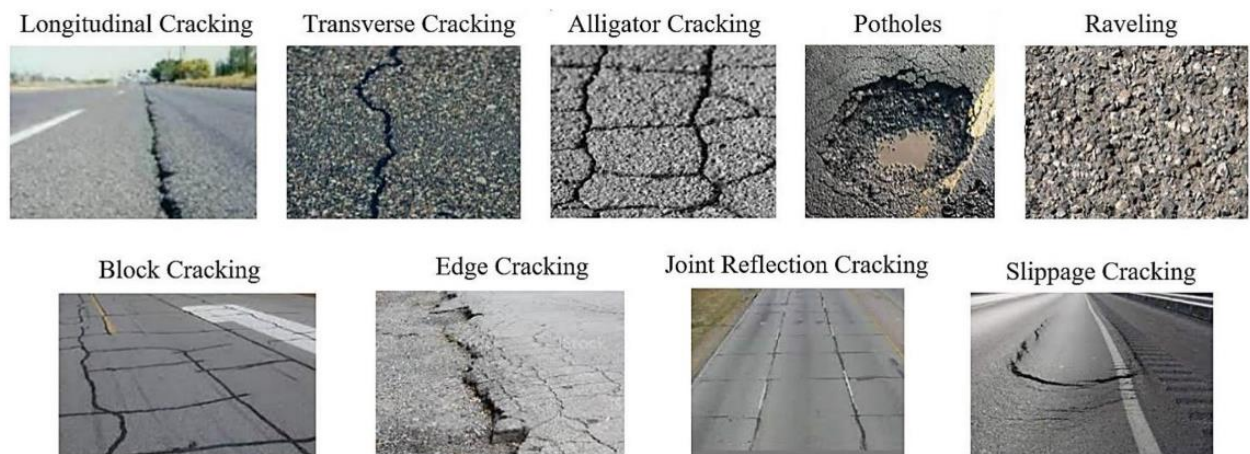


Fig 8. Types of road pavement failures [35–43].

ASS 1 Untreated -Unoaked -Light Traffic- Subgrade CBR 8% - Design Traffic 30msa				
Flexible Pavement Layers	Material	Thickness (mm)	Elastic Modulus MPa	Poisson's Ratio
Surface Course	TSCS	40	1350	0.35
Binder Course	DBM50	60	250	0.35
Subbase	DBM50	170	165	0.35
Subgrade CBR 8%	ASS	∞	67	0.4
Total pavement thickness		270		
NOTE: TSCS = Thin Surface Course System ASS = Artificially Synthesised Subgrade ASS				

Fig. 12. properties of flexible pavement layers used in this study.

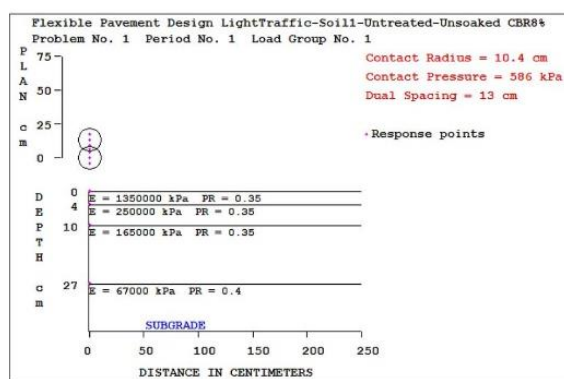


Fig. 13. KENPAVE analysis results.

materials used in defect analysis. Table 1 shows selected CBR values used in defect analysis in this study.

4. Road pavement defect analysis

Defect analysis in this study was conducted to establish the durability of road pavement structures using varying California Bearing Ratio (CBR) values achieved in this study. Subgrade California Bearing Ratio (CBR) values of a road pavement whether high or low would determine the stress and strain behaviours within the road pavement structure [27]. The intensity of these stress and strains can cause fatigue failure and would determine the type of road pavement defect that would occur in the pavement structure and how long it would take for these defects to occur. Some of these road pavement defects include the occurrence of fatigue, rutting and deformation in the pavement structure. Fatigue refers to the ability of an object or material to withstand concentrated stresses before it fails completely [27]. Rutting refers to the surface or longitudinal depression that occurs in the wheelpaths of flexible pavement and deformation is the change in a road surface from the originally intended profile. In this study, fatigue, rutting and permanent deformation analyses were conducted to determine the effect of varying CBR values and traffic loads and how they affect the pavement structure [27]. KENPAVE software was used to determine the stresses within the pavement structure based on the subgrade California Bearing Ratio (CBR) values achieved in this study [28]. KENPAVE provides a solution for elastic multilayer pavement systems under circular loaded areas [29]. The software is designed to analyse different wheel configurations under linear elastic, nonlinear elastic and visco-elastic layer behaviours. KENPAVE software was used to analyse a three-layer pavement system underneath the asphalt layer and the vertical compressive strain on the top of the subgrade. The loaded areas were determined using the same

radius and contact pressure (tyre inflation pressure). Materials adopted for the various layers include a bituminous surfacing material - Thin Surface Course System (TSCS), granular base and subbase material - Dense Macadam Binder and subbase Course (DBM50) respectively. The subgrade CBR values achieved for high plasticity subgrade stabilised using cement and lime were used in the analyses to see the effect of stabilised or treated high plasticity subgrade material on road pavement fatigue, rutting and permanent deformation.

A traffic design of 30msa (million standard axils) for light traffic and 80msa for Heavy traffic were adopted with a single axle dual wheel load configuration. A contact radius of 10.4cm and contact pressure of 586KPa on a circular loaded area was adopted. The pavement was assumed to behave as a linear elastic structure with Poisson's ratio of 0.35 for all layers and Poisson's ratio of 0.4 for the subgrade. The critical stress and strain are estimated in the pavement layers at radial distances of 13cm away from the centre of the wheel load. Vertical compression strain above the subgrade and tensile strain at the bottom of the bituminous layer were considered to be the critical conditions for the pavement system. Resilient modulus MR1, of the bituminous layer, was considered to be 1350MPa as used for a standard UK asphalt material at temperatures 20°C and 5Hz in accordance with DMRB CD 226 [30]. Resilient modulus of the subgrade, subbase and base were estimated using CBR values of Artificially Synthesised Subgrade (ASS) materials achieved in this study and were calculated using Eqs. (1), (2) and (3) (IRC, [31]). Resilient modulus refers to a measure of elastic behaviour of pavement under repeated loadings and helps in characterising different materials used in the construction of pavement under simulated field conditions. Values for long-term elastic stiffness modules 4700MPa of standard UK asphalt material Dense Macadam Binder (DBM50) used in the analytical design were adopted in accordance with DMRB [32]. Eqs. (4), (5) and (6) used by Asphalt Institute and IRC [31] were adopted to calculate the allowable load repetition for fatigue, permanent deformation and rutting life of the road pavement. Repeated loading refers to the number of loading required to initial fatigue crack. Before fatigue crack can be initiated, three basic factors are required (i) The loading pattern must contain minimum and maximum peak values with large enough variation or fluctuation [27]. The peak values may be in tension or compression which may change over time but the reverse loading cycle must be sufficient to initiate a crack [27]. (ii) peak stress must be very high, if peak stresses are low they may not initiate crack [27] (iii) the materials must experience a sufficiently large number of cycles of the applied stress [27]. So the higher the stress concentration the more likely a crack may initiate [12,27]. Fatigues are usually associated with tensile stresses but fatigue crakes have been reported due to compressive loads, hence the greater the applied stress range, the shorter the life [33]. Observations after carrying out pavement damage analysis on selected treated and untreated ASS materials from this study are as follows;

Appendixes

Table 2
Pavement details and response for actual tyre contact area for selected subgrade materials.

Subgrade Type	CBR (%)	Pavement Thickness (mm)	Design Traffic (msa)	Traffic Type	Tyre Inflation Pressure (kPa)	Radius of circular Contact Area (cm)	Tensile Strain (ϵ_t)	Compressive Strain (ϵ_c)	Allowable Load Repetition for Fatigue Prediction	Allowable Load Repetition for Permanent Deformation Prediction	Allowable Load Repetition for rutting Life Prediction
ASS 1-Untreated	8	270	30	Light	586	10.4	6.70E-04	9.74E-04	5.22E+06	2.34E+06	3.04E+06
ASS 1-Untreated	8	320	80	Heavy	586	10.4	6.32E-04	7.96E-04	5.70E+06	8.53E+05	8.62E+06
ASS 2-Untreated	5	350	30	Light	586	10.4	2.49E-04	2.02E-03	4.71E+06	4.15E+04	1.71E+06
ASS 2-Untreated	5	410	80	Heavy	586	10.4	5.28E-04	9.61E-04	4.99E+06	1.56E+05	2.30E+06
ASS 3-Untreated	9	220	30	Light	586	10.4	6.80E-04	9.74E-04	4.89E+06	7.28E+06	2.59E+06
ASS 3-Untreated	9	298	80	Heavy	586	10.4	6.58E-04	7.24E-04	5.82E+06	1.19E+06	1.09E+07
ASS 1-Treated-7 days curing	80	50	30	Light	586	10.4	5.58E-05	1.39E-03	1.07E+12	8.35E+03	3.70E+05
ASS 1-Treated-7 days curing	80	60	80	Heavy	586	10.4	4.46E-05	1.82E-03	1.38E+12	2.45E+04	1.10E+06
ASS 2-Treated-7 days curing	60	70	30	Light	586	10.4	1.66E-05	2.05E-03	2.06E+11	9.92E+02	4.28E+04
ASS 2-Treated-7 days curing	60	90	80	Heavy	586	10.4	2.27E-05	3.30E-03	9.79E+10	2.52E+03	1.10E+05
ASS 3-Treated-7 days curing	30	120	30	Light	586	10.4	2.60E-06	2.24E-03	6.76E+10	7.00E+01	1.07E+03
ASS 3-Treated-7 days curing	30	150	80	Heavy	586	10.4	1.21E-05	3.56E-03	4.71E+09	5.50E+02	7.92E+04
ASS 1-Treated-Soaked 7days curing	50	80	30	Light	586	10.4	5.61E-04	8.92E-04	1.00E+12	6.14E+04	2.79E+06
ASS 1-Treated-Soaked 7days curing	50	100	80	Heavy	586	10.4	2.25E-04	1.83E-03	2.33E+11	2.44E+03	1.43E+06
ASS 2-Treated-Soaked 7days curing	40	105	30	Light	586	10.4	3.04E-05	1.99E-03	1.24E+11	1.68E+03	7.29E+04
ASS 2-Treated-Soaked 7days curing	40	120	80	Heavy	586	10.4	3.21E-05	1.73E-03	1.18E+10	3.20E+03	1.40E+05
ASS 3-Treated-Soaked 7days curing	30	120	30	Light	586	10.4	1.66E-05	2.05E-03	3.05E+10	1.47E+03	6.38E+04
ASS 3-Treated-Soaked 7days curing	30	150	80	Heavy	586	10.4	1.21E-05	1.76E-03	2.17E+07	5.07E+03	7.92E+04
ASS 1-Treated-28 days curing	90	48	30	Light	586	10.4	6.47E-05	2.23E-03	1.03E+10	1.02E+03	4.41E+04
ASS 1-Treated-28 days curing	90	50	80	Heavy	586	10.4	6.01E-05	2.18E-03	1.31E+10	1.14E+03	4.91E+04
ASS 2-Treated-28 days curing	100	30	30	Light	586	10.4	4.10E-04	1.78E-03	2.25E+10	2.80E+03	1.22E+05
ASS 2-Treated-28 days curing	100	30	80	Heavy	586	10.4	4.10E-04	1.78E-03	2.25E+10	2.80E+03	1.22E+05
ASS 3-Treated-28 days curing	80	50	30	Light	586	10.4	5.58E-05	2.39E-03	2.62E+09	7.41E+02	3.18E+04
ASS 3-Treated-28 days curing	80	60	80	Heavy	586	10.4	4.46E-05	2.10E-03	1.04E+10	1.34E+03	5.82E+04

Where ASS = Artificially Synthesised Subgrade. msa = million standard axils

ASS 1= (25% Bentonite + 75% Kaolinite) High Plasticity, ASS 2= (35% Bentonite + 65% Kaolinite) Very High Plasticity, ASS 3= (75% Bentonite + 25% Kaolinite) Extremely High Plasticity

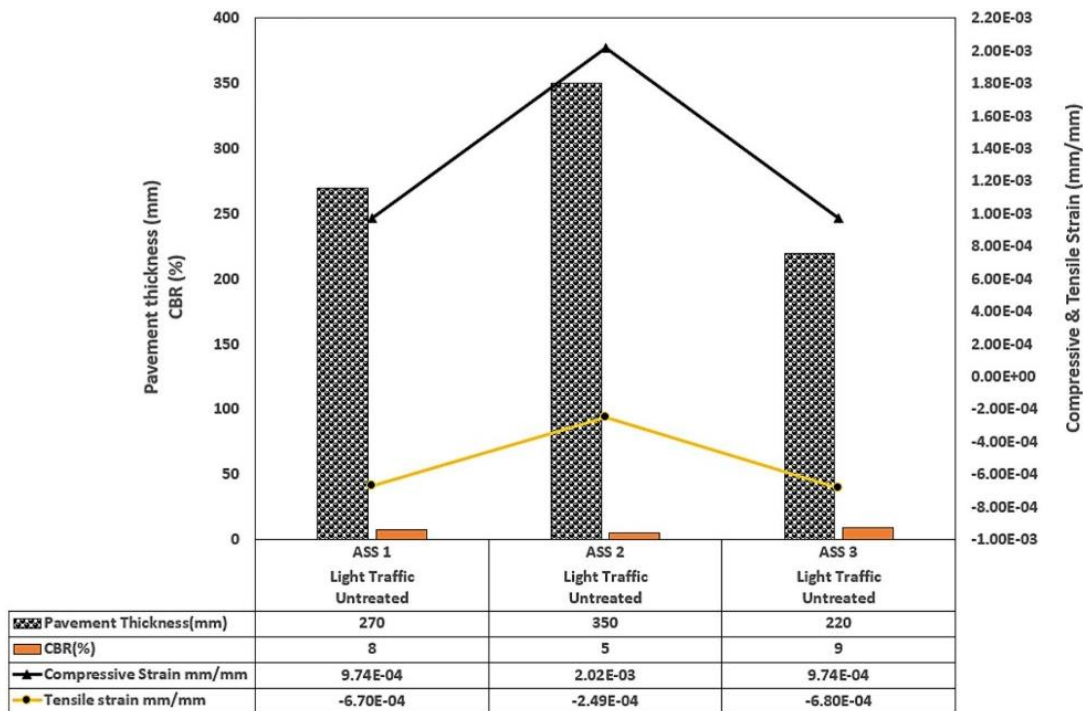


Fig. 14. Compressive and tensile strain results of light traffic for untreated ASS materials.

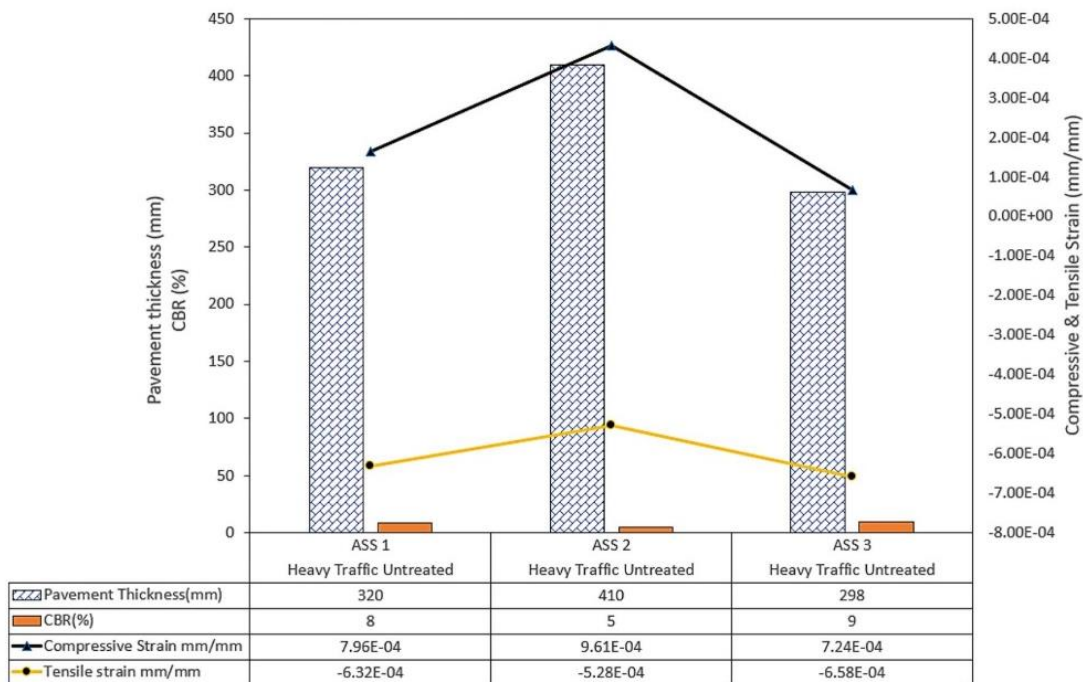


Fig. 15. Compressive and tensile strain results of heavy traffic for untreated ASS materials.

4.1. Effect of stresses on treated and untreated subgrade materials

A high potential for pavement defect was observed with an increase in compressive and tensile stresses for light traffic in untreated Artificially Synthesised Subgrade (ASS) material with California Bearing Ratio (CBR) values of 5% for ASS 2. These stresses began to decrease when California Bearing Ratio (CBR) values for ASS1 and 3 increased to

8% and 9% respectively. CBR values recorded for untreated ASS 1, 2 and 3 for heavy traffic exhibited high compressive and tensile strains responsible for pavement defects. However, these stresses reduced as CBR values increased. Overall, very high CBR values with low compressive and tensile strain responsible for pavement deformation were recorded for treated ASS materials for light and heavy traffic loads compared with that of untreated ASS materials. This means, treated ASS

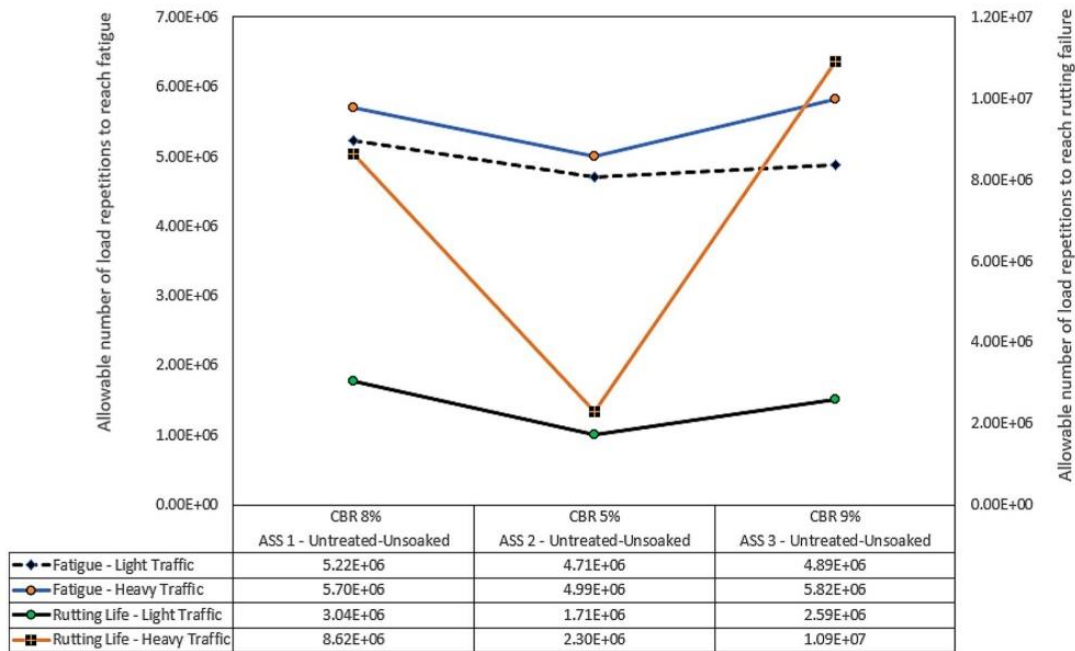


Fig. 16. Load repetition for fatigue and rutting of light and heavy traffic for untreated ASS materials.

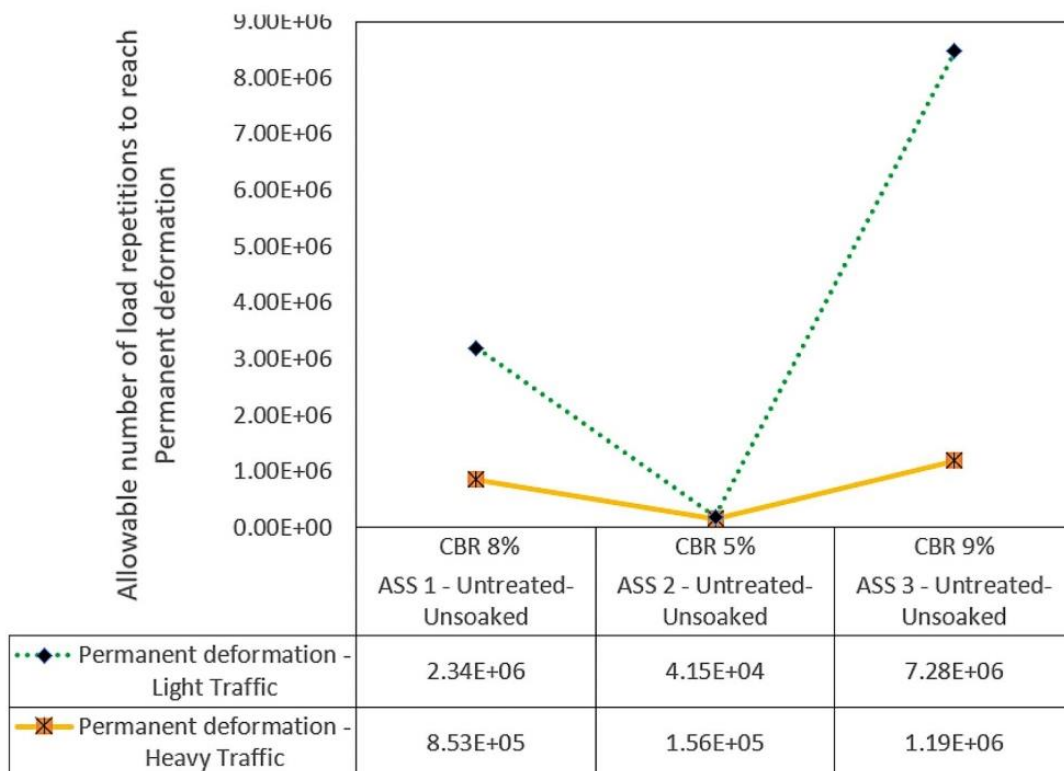


Fig. 17. Load repetition for permanent deformation of light and heavy traffic for untreated ASS materials.

materials with very high CBR values can withstand stresses in road pavement structure for a longer period before any defect occurs compared with untreated ASS with low CBR values. An increase in compressive and tensile stresses were observed with an increase in pavement thickness due to low California Bearing Ratio (CBR) values for light and heavy traffic load after 7 and 28 days of curing for treated ASS

materials. For fatigue crack to initiate in road pavement structure, peak stress (compressive and tensile) must be very high, if peak stresses are low they may not initiate a crack [27]. The higher the stress concentration the more likely a crack may initiate and the greater the applied stress range, the shorter the life of the pavement structure [27] and [33]. This means the higher the subgrade CBR value the least likely a defect

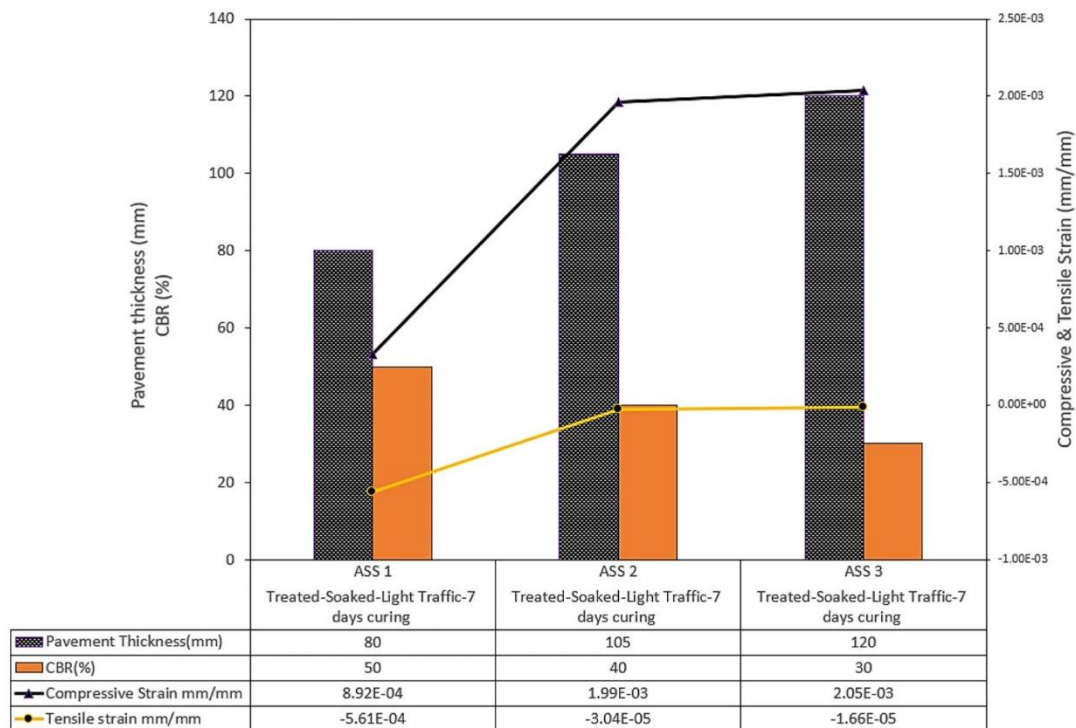


Fig. 18. Compressive and tensile strain results of light traffic for treated- soaked ASS materials 7 days curing.

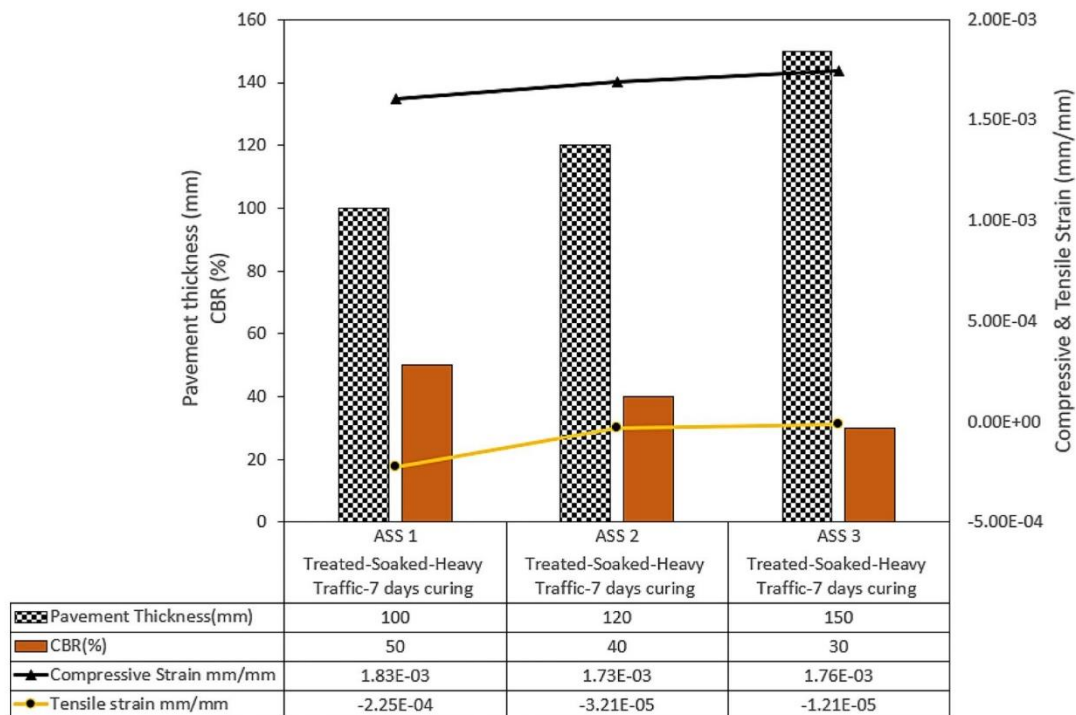


Fig. 19. compressive and tensile strain results of heavy traffic for treated-soaked ASS materials 7 days curing.

may occur in the road pavement structure. These are the reasons why pavement thickness increases with low subgrade CBR values to help cattail or reduced stresses in pavement structures to prolong the life of the road pavement. According to Nunn et al. [34], road pavement with thinner pavement thickness deforms at a higher rate compared with

pavement frith thicker asphalts.

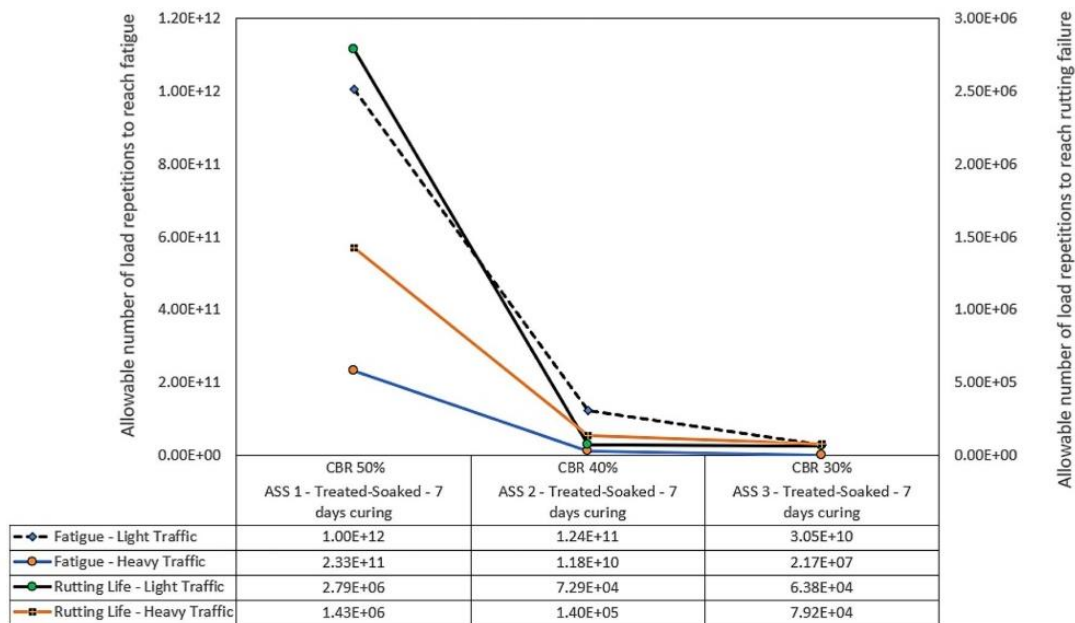


Fig. 20. Load repetition for fatigue and rutting of light and heavy traffic for treated-soaked ASS materials 7 days curing.

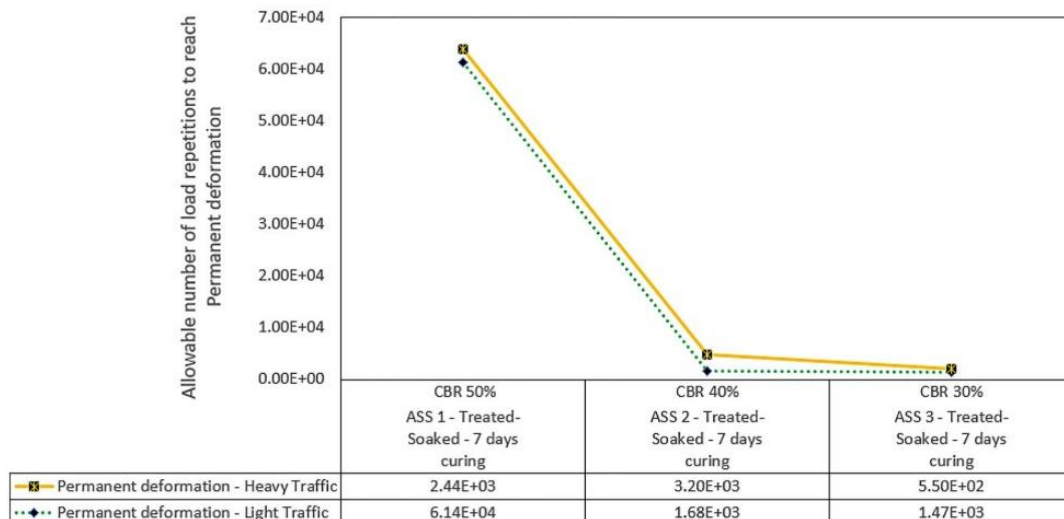


Fig. 21. Load repetition for permanent deformation of light and heavy traffic for treated-soaked ASS materials 7 days curing.

4.2. Effect of the application of repeated load on treated and untreated ASS materials

An allowable number of load repetitions to reach fatigue, rutting and permanent deformation for light and heavy traffic load were recorded for untreated Artificially Synthesised Subgrade (ASS 1) with CBR 8%. These repeated loads reduced when the California Bearing Ratio (CBR) value for untreated ASS 2 reduced to 5% and later increased when the CBR value for untreated ASS 3 increased to 9%. An allowable number of load repetitions to reach fatigue for light and heavy traffic load recorded for 7 days cured treated ASS 1 with CBR 80% and ASS 2 with CBR 60% decreased when CBR value decreased to 30% for 7 days cured treated ASS 3. An allowable number of load repetitions to reach rutting failure for light and heavy traffic load recorded for 7 days cured treated ASS 1 CBR 80% and ASS 2 60% also decreased when CBR value decreased to 30% for 7 days treated ASS 3. An allowable number of load repetitions to

reach permanent deformation for light and heavy traffic load recorded for 7 days treated ASS 1 CBR 80% and ASS 2 60% decreased with a decrease in CBR value to 30% for 7 days treated ASS 3. This was the case for treated 7 and 28 days CBR values, a reduction in the allowable number of load repetitions with a reduction in CBR value was observed with an increase in CBR value. This means subgrade materials with high California Bearing Ratio (CBR) could withstand fatigue, rutting and permanent deformation for a longer period of time before failure occurs compared with subgrade materials with low CBR values. High cyclic load repetition values mean the applied cyclical stresses are low and failure occurs after a very large number of cycles, typically more than 10,000 cycles [27]. Low cyclic load repetition involves higher applied cyclical stresses and failure may occur after fewer cycles because the stresses involved are above the materials yield stress both elastic and plastic deformation may occur [27]. Fig. 8 shows the types of road pavement failures. Figs. 9–11 shows the three-layer flexible composite

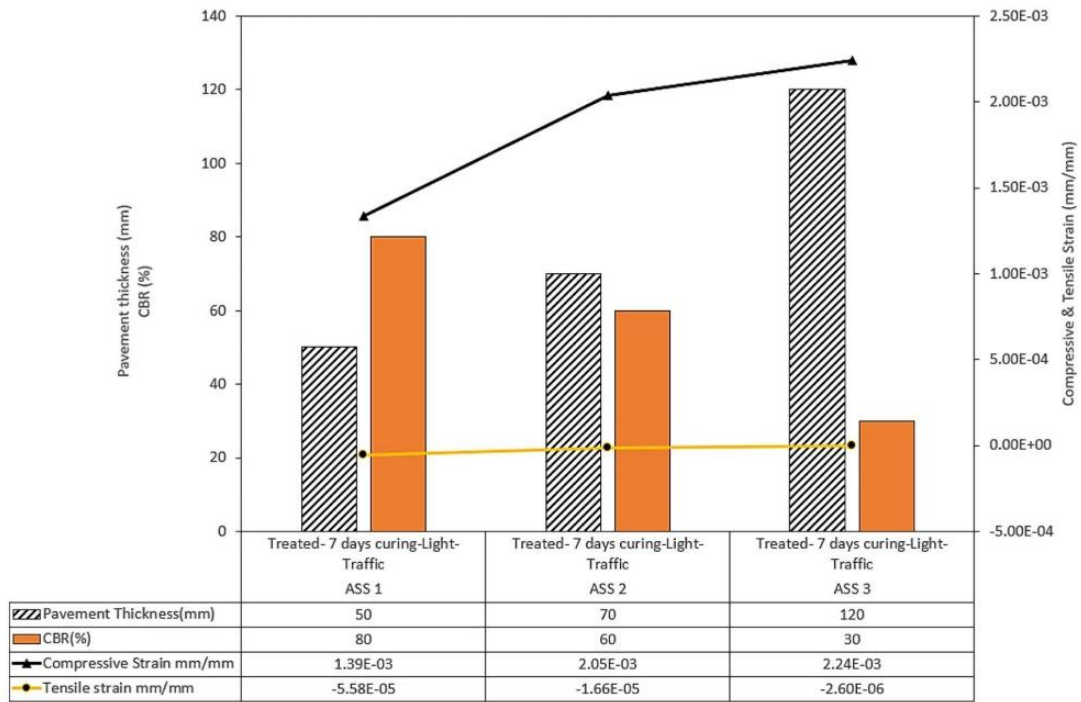


Fig. 22. Compressive and tensile strain results of light traffic for treated ASS materials 7 days curing.

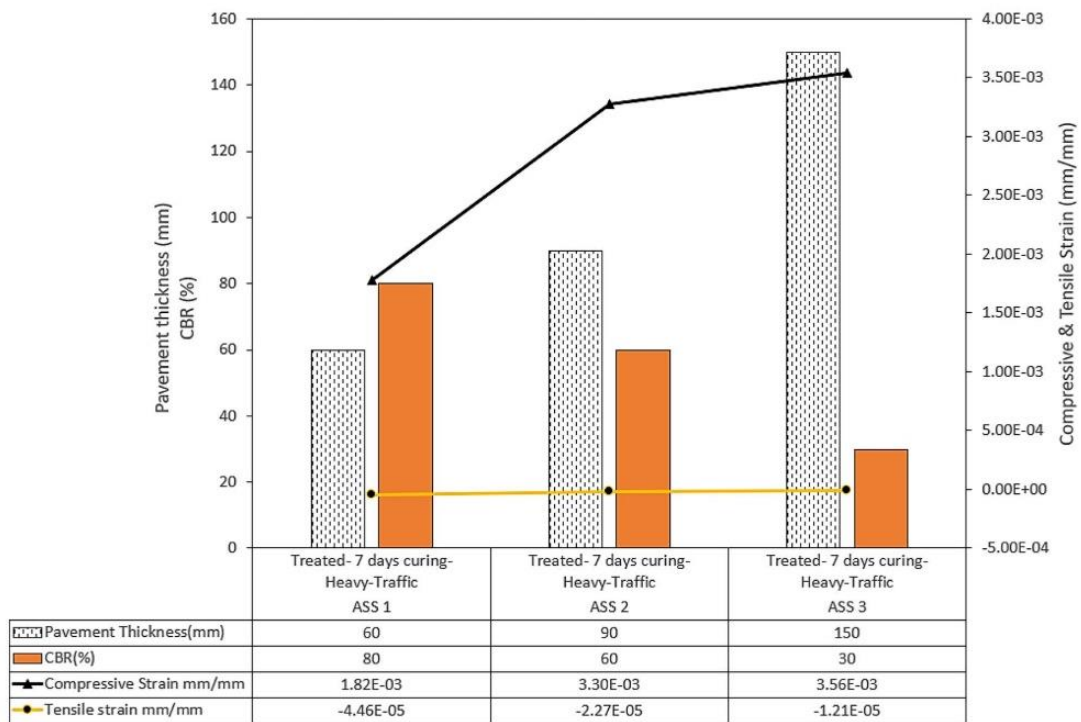


Fig. 23. compressive and tensile strain results of heavy traffic for treated ASS materials 7 days curing.

pavement structure adopted for and used in this study and the types of stress that could occur in a road pavement structure. Figs. 12 and 13 show the properties of flexible pavement layers used in this study and pavement analysis results from KENPAV for traffic load 8msa. Table 2 shows pavement details and responses for the actual tyre contact area for selected ASS materials. The results after defect analyses are shown in

Figs. 14–29.

$$MR1 = 17.6 \times CBR^{0.64} \tag{1}$$

$$MR2 = E3 \times 0.2 \times h^{0.45} \tag{2}$$

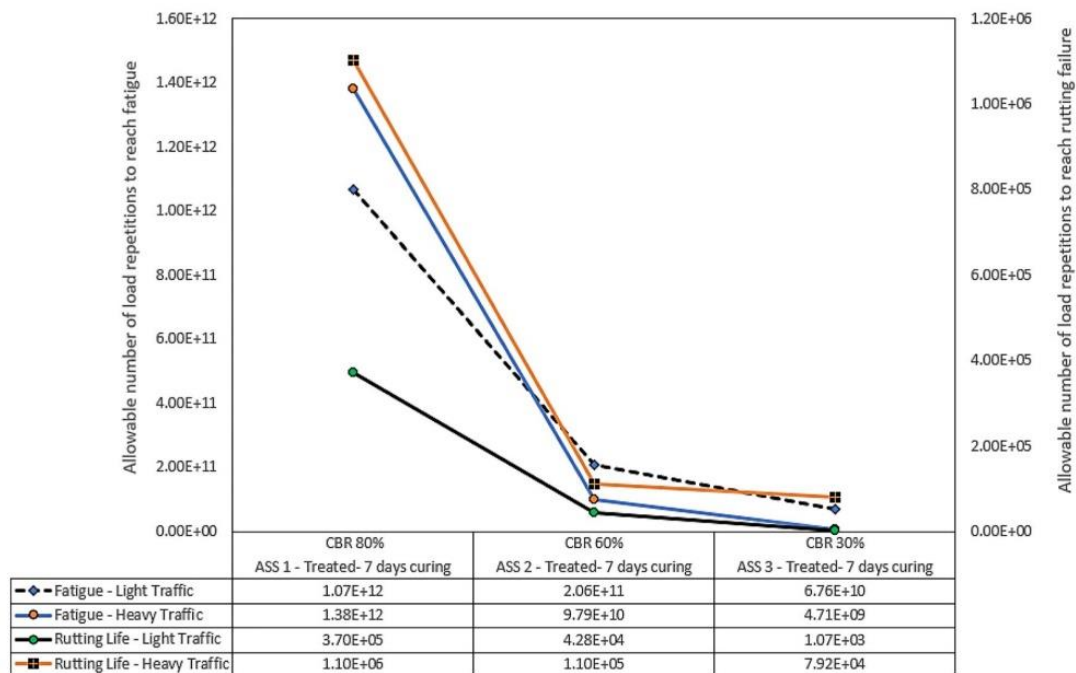


Fig. 24. Load repetition for fatigue and rutting of light and heavy traffic for treated ASS materials 7 days curing.

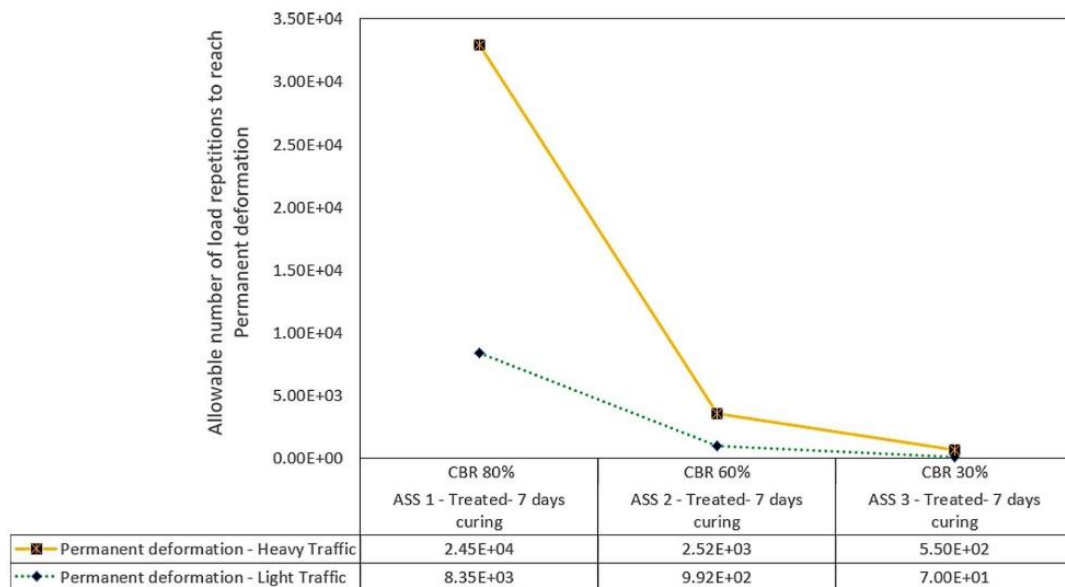


Fig. 25. Load repetition for permanent deformation of light and heavy traffic for treated ASS materials 7 days curing.

$$MR_3 = 17.6 \times CBR^{0.64} \tag{3}$$

Where M_R is resilient modulus of base course, M_{R2} resilient modulus of subbase course, M_{R3} resilient modulus of subgrade.

Damage Analysis

$$N_{fatigue} = f_1(\epsilon_t)^{-12}(E_1)^{-13} \tag{4}$$

$$N_{permanent\ deformation} = f_4 E^{-9}(\epsilon_c)^{-15} \tag{5}$$

Where ϵ_t is the tensile strain at the bottom of asphalt layer, and E_1 = the modulus of the asphalt layer, and ϵ_c = compressive strain at the top of the subgrade layer, and f_{1-5} are empirical values used by Asphalt

Institute for these calculations.

Rutting life Prediction

$$N = 4.1656 \times 10^{-08} \left[\frac{1}{\epsilon_c} \right]^{4.5337} \tag{6}$$

Where N = Number of cumulative standard axles
 ϵ_c = Compressive strain in the subgrade

5. Conclusion

Failures in road pavement structure were analysed in this study using treated and untreated subgrade CBR values achieved in this study and

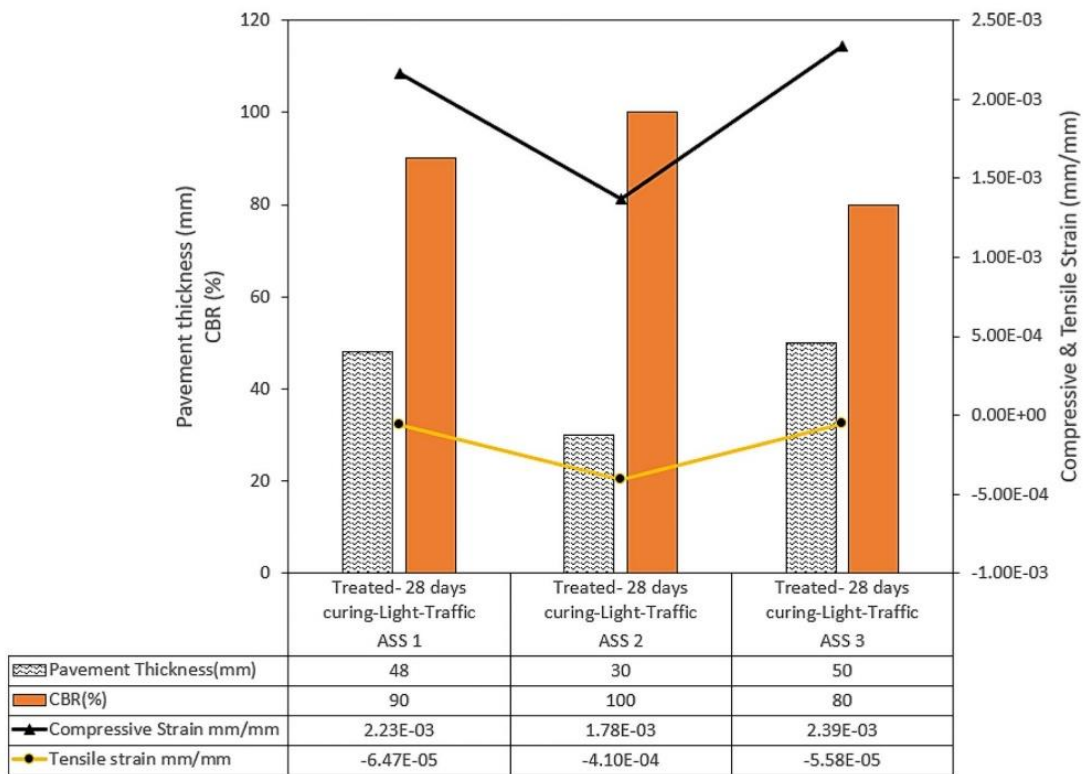


Fig. 26. Compressive and tensile strain results of light traffic for treated ASS materials 28 days curing.

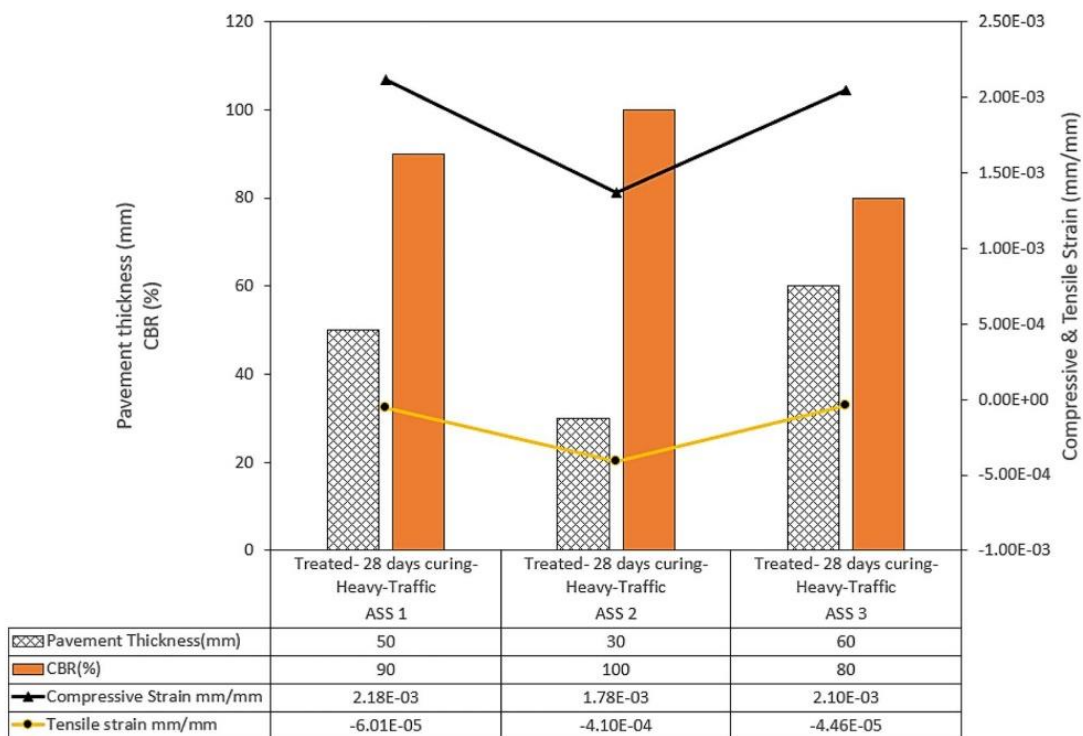


Fig. 27. Compressive and tensile strain results of heavy traffic for treated ASS materials 28 days curing.

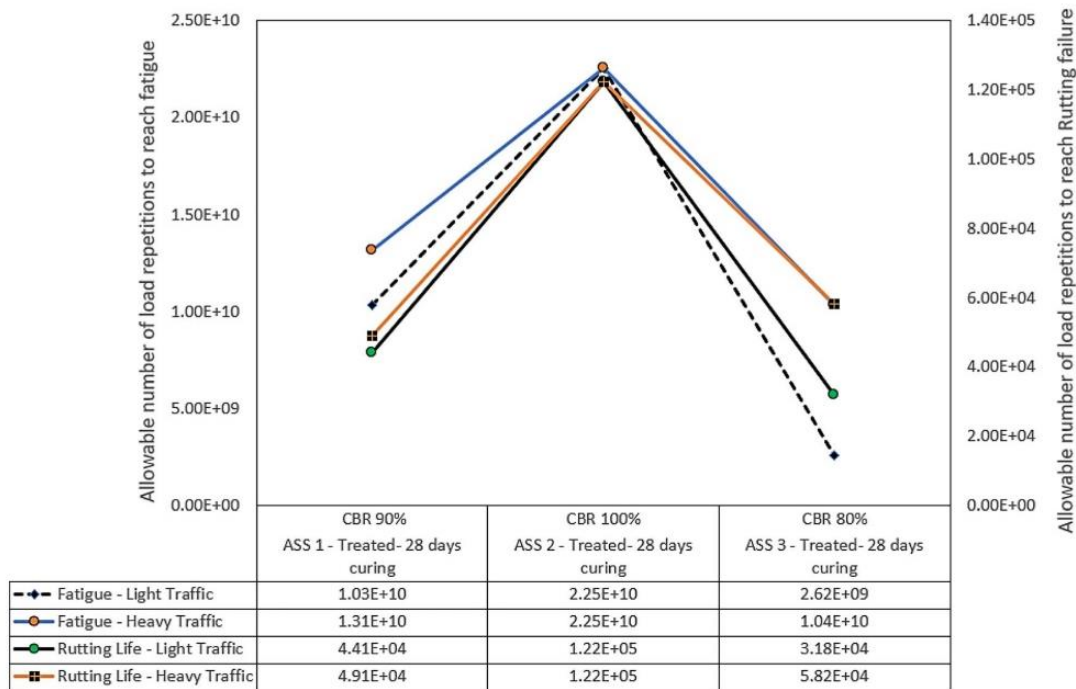


Fig. 28. Load repetition for fatigue and rutting of light and heavy traffic for treated ASS materials 28 days curing.

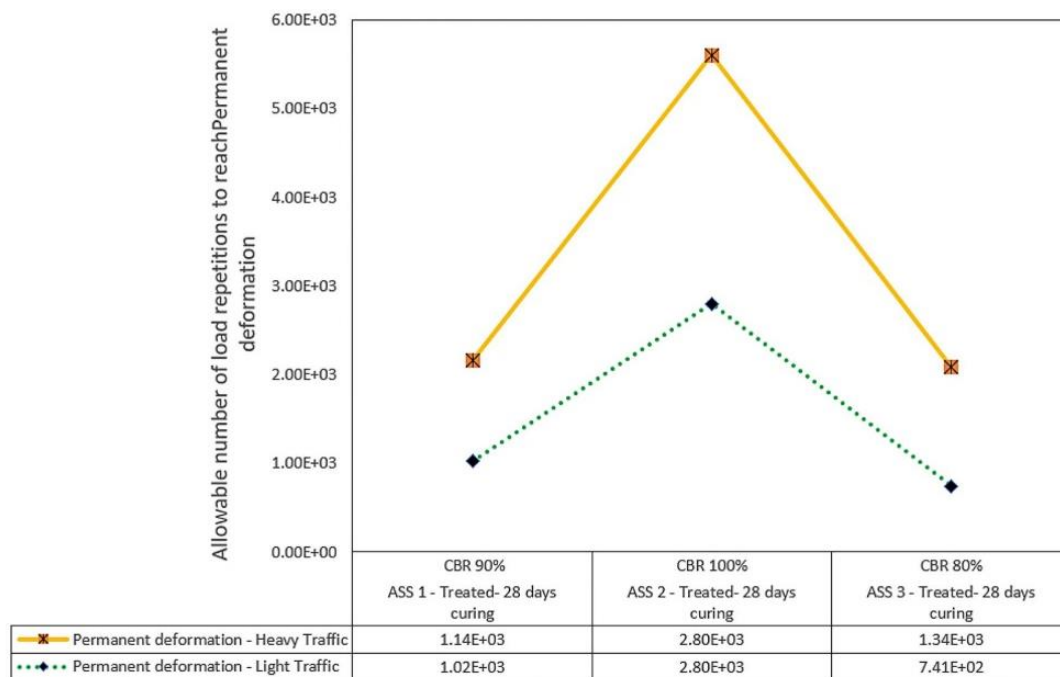


Fig. 29. Load repetition for permanent deformation of light and heavy traffic for treated ASS materials 28 days curing.

the findings are as follows;

1. A reduction in stresses responsible for failure within road pavement structure was observed. Low compressive and tensile stresses with an increasing CBR value were recorded this means it is unlikely defects may occur in the pavement with a high subgrade CBR value.
2. High allowable repeated loads were recorded for ASS materials with high CBR values and vice versa. This signifies the ability of road subgrade with high CBR values to withstand several cycles of loading (repeated traffic load) before failure occurs within the pavement.
3. A reduction or elimination of the tendency of defects to occur with road pavement structure was observed when CBR values increased after expansive subgrade was treated using cement and lime.
4. This study established the possibility of improving the engineering properties of expansive road subgrade using cement and lime.

5. The construction industry would benefit from this study as road contractors can refer to this study to predict the likelihood of defect occurrence within road pavement when they encounter subgrade materials with similar properties and characteristics as used in this study.
6. Overall construction costs can be reduced when weak or expansive subgrades are treated using cement and lime instead of removing and replacing subgrades with foreign materials.

Funding

This research did not receive any specific grant from funding agencies in the public, commercial, or not-for-profit sector.

Declaration of competing interest

The authors declare that they have no known competing financial interests or personal relationships that could have appeared to influence the work reported in this paper.

Acknowledgement

The authors acknowledge the advice, comments and suggestions from anonymous reviewers which significantly improved the quality of this paper.

References

- [1] Z.B Rashid, R. Gupta, Review paper on defects in flexible pavement and its maintenance, International Journal of Advanced Research in Education & Technology (IJARET) (2018). https://www.researchgate.net/publication/329642418_Review_Paper_On_Defects_in_Flexible_Pavement_and_its_Maintenance (Accessed 11 March 2022).
- [2] S.Y.O. Amakye, S.J. Abbey, C.A. Booth, J. Oti, Road Pavement Thickness and Construction Depth Optimization Using Treated and Untreated Artificially-Synthesized Expansive Road Subgrade Materials with Varying Plasticity Index, Materials 15 (2022) 2773, <https://doi.org/10.3390/ma15082773>.
- [3] SY Amakye, SJ. Abbey, Understanding the performance of expansive subgrade materials treated with non-traditional stabilisers: A, Review (2021) 100154–100159, <https://doi.org/10.1016/j.clet.2021.100159>.
- [4] Anakye SY, Abbey SJ, Booth CA, Mahamadu A. Enhancing the engineering properties of subgrade materials using processed waste: A review 2021;307-329-1 (2). <https://doi.org/10.3390/geotechnics1020015>.
- [5] Li J, Cameron DA, Ren G. Case study and back analysis of a residential building damaged by expansive soils 2014;89-99-56. <https://doi.org/10.1016/j.compgeo.2013.11.005>.
- [6] Jones LD, Jefferson I. Institution of Civil Engineers Manuals series 2019. http://nora.nerc.ac.uk/id/eprint/17002/1/C5_expansive_soils_Oct.pdf. (Accessed 29 November 2021).
- [7] T López-Lara, J Hernández-Zaragoza, J Horta-Rangel, E Rojas-González, S López-Ayala, V. Castaño, Expansion reduction of clayey soils through Surcharge application and Lime Treatment, Case Stud (2017) 102–109, <https://doi.org/10.1016/j.cscm.2017.06.003>.
- [8] A.F. Cabalar, M.D. Abdulnafaa, V. Isubga, Plate Loading Tests on Clay with Construction and Demolition Materials, Arab J Sci Eng 46 (2021) 4307–4317, <https://doi.org/10.1007/s13369-020-04916-6>.
- [9] A.F. Cabalar, M.D. Abdulnafaa, H. Isik, The role of construction and demolition materials in swelling of a clay, Arab J Geosci 12 (2019) 361, <https://doi.org/10.1007/s12517-019-4552-4>.
- [10] A.F. Cabalar, M.D. Abdulnafaa, Z. Karabash, Influences of various construction and demolition materials on the behavior of a clay, Environ Earth Sci 75 (2016) 841, <https://doi.org/10.1007/s12665-016-5631-4>.
- [11] Mohamadnia, A., Arul, A., Sanjayan, J., Disfani, M. m., Bo, M. W and Darmawan, S. (2015). Laboratory evaluation of the use of cement treated construction and demolition materials in pavement base and subgrade application. Vol 27, 6 [https://doi.org/10.1061/\(ASCE\)MT.1943-5533.0001148](https://doi.org/10.1061/(ASCE)MT.1943-5533.0001148).
- [12] A. Arulrajah, M.M. Disfani, S. Horpibulsuk, C. Suksiripattanonong, N Prongmanee, Physical properties and shear strength responses of recycled construction and demolition materials in unbound pavement base/subbase applications, Construction and Building Materials 58 (2014) 245–257, <https://doi.org/10.1016/j.conbuildmat.2014.02.025>. ISSN 0950-0618.
- [13] A. Mohajerani, J. Vajna, L.H.H. Cheung, H. Kurnus, A. Arulrajah, S. Horpibulsuk, Practical recycling applications of crushed waste glass in construction materials: A review, Construction and Building Materials 156 (2017) 443–467, <https://doi.org/10.1016/j.conbuildmat.2017.09.005>. ISSN 0950-0618.
- [14] Cabalar, A. F., Hassan, D. I., Abdulnafaa, M. D. (2016) Use of waste ceramic tiles for road pavement subgrade. Vol. 18 4. 882-896. doi: 10.1080/14680629.2016.1194884.
- [15] A.F. Cabalar, I.A. Ismael, A Yavuz, Use of zinc coated steel CNC milling waste for road pavement subgrade, Transportation Geotechnics (23) (2020), 100342, <https://doi.org/10.1016/j.trgeo.2020.100342>. ISSN 2214-3912.
- [16] Arulrajah, A., Piratheepan, J., Disfani, M.M., Bo, M. W. (2013) Geotechnical and geoenvironmental properties of recycled construction and demolition materials in pavement subbase applications. Vol. 25 8. [https://doi.org/10.1061/\(ASCE\)MT.1943-5533.0000652](https://doi.org/10.1061/(ASCE)MT.1943-5533.0000652).
- [17] AM. Neville, Properties of concrete, 5th edition, Harlow, England, New York, NY, 2011. <https://pdfcoffee.com/properties-of-concrete-fifth-edition-a-m-neville-pdf-pdf-free.html> (Accessed 02 October 2021).
- [18] P. Walker, Review and Experimental Comparison of erosion tests on Earth Blocks, in: Terra 2000 Postprints: 8th International Conference on the Study and Conservation of Earthen Architecture, Torquay, Devon, UK, James & James, London, UK, 2000.
- [19] Gooding DE, Thomas TH. The potential of cement stabilised or treated building blocks as an urban building material in developing countries. DTU working paper No.44. 2021. https://warwick.ac.uk/fac/sci/eng/research/group/structural/dtu/pubs/wp/wp44/wp44_.pdf (Accessed on 18 November 2021).
- [20] SJ Abbey, S Ngambi, AO Olubanwo, FK Tetteh, Strength and Hydraulic Conductivity of Cement and By-Product Cementitious Materials Improved Soil, International Journal of Applied Engineering Research ISSN 0973-4562 13 (10) (2018). Number.8684-8694-10.
- [21] DI Boardman, S Glendinning, C.D.F. Rogers, Development of stabilisation and solidification in lime-clay mixes, Geo-technique (2001).533-543-51.
- [22] OG Ingles, JB. Metcalf, Soil stabilisation, Butterworth Pty, Ltd Australia, 1972.
- [23] Ingles OH. Soil stabilisation. Chapter 38. In: Bell, F. G (Ed.), Ground Engineer's Reference Book. Butterworths, London 1987;38/1-38/26.
- [24] AK Jha, PV Sivapullajah, Lime stabilization of soil: a physico-chemical and micro-mechanistic perspective, Indian Geotech. J. (3) (2019) 339-347-50.
- [25] Y Wang, P Guo, X Li, H Lin, Y Liu, H Yuan, Behaviour of fibre reinforced and lime stabilised or treated clayey soil in triaxial test 2019, Appl. Sci 9 (5) (2019) 900.
- [26] S.Y.O. Amakye, S.J. Abbey, C.A. Booth, DMRB Flexible Road Pavement Design Using Re-Engineered Expansive Road Subgrade Materials with Varying Plasticity Index, Geotechnics 2 (2022) 395–411, <https://doi.org/10.3390/geotechnics2020018>.
- [27] Iowa State University. <https://www.nde-ed.org/Physics/Materials/Mechanics/1/FractureToughness.xhtml> (Accessed 14 February 2022).
- [28] S. Kiran, M. Kavitha, Rutting and Fatigue Analysis of Flexible Pavement using KENPAVE and IITPAVE: A Review, Journal of transportation Engineering and Traffic management, 39(1) (2022) 1–12, <https://doi.org/10.5281/zenodo.5830649>.
- [29] Pandey, S., Rawat, A., Sachan, A.K and Singh, S. (2021) Study of rigid pavement for varying conditions using KENPAVE. International Conference on Futuristic Technologies Paper No. FT-21047. https://www.researchgate.net/publication/350631768_STUDY_OF_RIGID_PAVEMENT_FOR_VARYING_CONDITIONS_USING_KENPAVE (accessed 23rd June 2022).
- [30] DMRB CD 226 – Design for new pavement construction. Design Manual for Roads and Bridges 2021.
- [31] IRC-37-2001, Guidelines for the design of flexible pavements, Indian Roads Congress, 2001.
- [32] DMRB CD 226 – Design for new pavement construction. Design Manual for Roads and Bridges 2021.
- [33] NA Fleck, SC Shin, RA. Smith, Fatigue crack growth under compressive loading, Engineering Fracture Mechanics (1) (1985) 173-185-21, [https://doi.org/10.1016/0013-7944\(85\)90063-3](https://doi.org/10.1016/0013-7944(85)90063-3).
- [34] Nunn, M.E, Brown, A, Weston, D, Nicholls, J.C. (1997). Design of long life flexible pavement for heavy traffic. British Aggregate Construction Mat. Indust, and the Refined Bitumen Associ. 1997.
- [35] T Ahmad, H Khawaja, Review of low temperature crack (LTC) Developments in Asphalt Pavements, The International Journal of Multiphysics 12 (2) (2018) 169–188, <https://doi.org/10.21152/1750-9548.12.2.169>.
- [36] Vale of Glamorgan Council Potholes. <https://www.valeofglamorgan.gov.uk/en/1iving/Roads/Potholes.aspx>. (accessed 23rd June 2022).
- [37] Alpha Paving Industries LLC: Alligator Cracking & Severity. <https://alphapavin.com/alligator-cracking-severity/> (accessed 23rd June 2022).
- [38] SURE-SEAL Pavement maintenance INC. Transverse/Thermal Cracking in Asphalt Pavement: Causes and Repair. <https://suresealpavement.com/transversethermal-cracking-asphalt-pavement-causes-repair/>. (accessed 23rd June 2022).
- [39] Pavement Preservation & Recycling Alliance (PPRA). Treatment Resource center: https://roadresource.org/treatment_resources/crack_seal?page=pre_site (accessed 23rd June 2022).
- [40] Indiana 2020 IDEA Block Cracking: <https://www.in.gov/indot/div/aviation/pavement-inspection/pci-review/distresses-ac/block-cracking.html> (accessed 23rd June 2022).

- [41] Infrastructure Management Services LLC. How to spot a failing asphalt street. <https://www.insanalysis.com/blog/how-to-spot-a-failing-asphalt-street>. (accessed 23rd June 2022).
- [42] Airfield Asphalt Pavement Technology program (AAPTP). 2009. Technical Guide AAPTP 05-04 techniques for Mitigation of Reflective Cracks. Auburn University. <https://eng.auburn.edu/research/centers/ncat/files/aaptp/Report.TechnicalGuide.05-04.pdf>. (accessed 23rd June 2022).
- [43] Coleri, E., HMAC layer adhesion through tack coat. Final Report. School of Civil and Construction Engineering. https://www.researchgate.net/publication/329105094_HMAC_Layer_Adhesion_Through_Tack_Coat. (accessed 23rd June 2022).



Article

DMRB Flexible Road Pavement Design Using Re-Engineered Expansive Road Subgrade Materials with Varying Plasticity Index

Samuel Y. O. Amakye ^{1,*}, Samuel J. Abbey ² and Colin A. Booth ²

- ¹ Civil Engineering Cluster, Department of Geography and Environmental Management, Faculty of Environment and Technology, University of the West of England, Bristol BS16 1QY, UK
- ² Faculty of Environment and Technology, University of the West of England, Bristol BS16 1QY, UK; samuel.abbey@uwe.ac.uk (S.J.A.); colin.booth@uwe.ac.uk (C.A.B.)
- * Correspondence: samuel.amakye@uwe.ac.uk



Citation: Amakye, S.Y.O.; Abbey, S.J.; Booth, C.A. DMRB Flexible Road Pavement Design Using Re-Engineered Expansive Road Subgrade Materials with Varying Plasticity Index. *Geotechnics* 2022, 2, 395–411. <https://doi.org/10.3390/geotechnics2020018>

Academic Editor: Raffaele Di Laora

Received: 23 April 2022

Accepted: 30 April 2022

Published: 12 May 2022

Publisher's Note: MDPI stays neutral with regard to jurisdictional claims in published maps and institutional affiliations.



Copyright: © 2022 by the authors. Licensee MDPI, Basel, Switzerland. This article is an open access article distributed under the terms and conditions of the Creative Commons Attribution (CC BY) license (<http://creativecommons.org/licenses/by/4.0/>).

Abstract: Pavement thickness is a very vital component during the design stage of a road construction project. Pavement design helps to determine the costs of the project over a certain period to ascertain how the cost of road pavement construction affect the life cycle cost of the road. Road pavements are designed based on the type of subgrade material and the expected traffic load to help clients and decision-makers make decisions on the project. In this study, expansive road subgrade materials were improved using lime and cement and their California Bearing Ratio (CBR) was used in road pavement design. The study used the Design and Manual for Roads and Bridges (DMRB) as a guide to investigating the effect of stabilised expansive road subgrade with varying CBR values on road pavement design. The mineral structure, characteristics, Atterberg limit, compaction CBR, swell and microstructural analysis (scanning electron microscopy (SEM) and Energy Dispersive X-ray (EDX)) of stabilised subgrade materials were investigated. The results show an increase in California Bearing Ratio (CBR) values and a reduction in swell values while curing age increased for stabilised subgrade materials. Treated samples show high Calcium Silicate Hydrate (C-S-H) gel formation after 7 and 28 days of curing. The thickness of road pavement was observed with an increase in CBR values. The study established that the thickness of road pavement and overall construction cost can be reduced using cement and lime as additives in subgrade stabilisation.

Keywords: Artificially Synthesised Subgrade; expansive subgrade; road pavement thickness; Atterberg limit; California Bearing Ratio

1. Introduction

In this study, flexible road pavement design was carried out for various traffic loads, and California Bearing Ratio CBR values were achieved in this study in accordance with the Design Manual for Road and Bridges (DMRB) for re-engineered Artificially Synthesised Subgrade (ASS). The impact of using treated and untreated expansive road subgrade with varying plasticity CBR values in flexible road pavement design used for light and heavy traffic were investigated. A mixture of untreated bentonite and kaolin at various percentages was used to form an Artificially Synthesised Subgrade (ASS) with properties similar to an already existing expansive subgrade. The study conducted Atterberg limits and compaction test for untreated ASS materials to determine their moisture content and characteristics. ASS materials were further stabilised using cement and lime to improve their engineering properties for use as subgrade materials in road construction. Road pavements are superimposed processed materials placed over natural subgrade to carry traffic load and provide adequate skid resistance. Pavements are designed based on various factors, such as traffic load, CBR and many more, which helps in decision-making by determining the cost of the road project based on the design [1,2]. Road pavement construction

takes more than 50% of the overall construction cost, especially where weak subgrade is involved, which can cause defects and failure, leading to a high cost of maintenance and sometimes a total reconstruction of the road [3,4]. China, the United States and the UK have spent up to \$US30 billion and £3 billion on maintenance costs due to infrastructure built on expansive soils [5,6]. Reference [7] stated that millions of dollars are spent on damage caused by expansive road subgrade. In this study, cement and lime were used as binders in subgrade stabilisation. Cement and lime have been used for decades in the improvement of subgrade materials due to their ability to form calcium silicate hydrate gel (C-S-H) gel during the hydration process responsible for strength gain [4,8]. C-S-H gel binds subgrade particles together, making cement suitable for subgrade stabilisation [3,9]. Reference [10] used cement in proportions of 4% and 15% in subgrade stabilisation. During lime hydration, C-S-H gel is produced on enhancing strength in a mix [11]. Lime stabilisation is recommended for subgrade with a liquid limit from 25% to 50% and plasticity between 20% and 30% [12]. Reference [13] achieved good CBR values after using 3–8% lime in subgrade stabilisation, while reference [14] used 1% of lime in expansive subgrade stabilisation. Figure 1a–d shows wet and dry expansive soil and road pavement defects caused by expansive subgrade. Figure 2 shows how the results achieved in this study can be applied in real-life road construction, and Table 1 shows the merits and demerits of treating road subgrade and subgrade removed and replaced with imported materials.

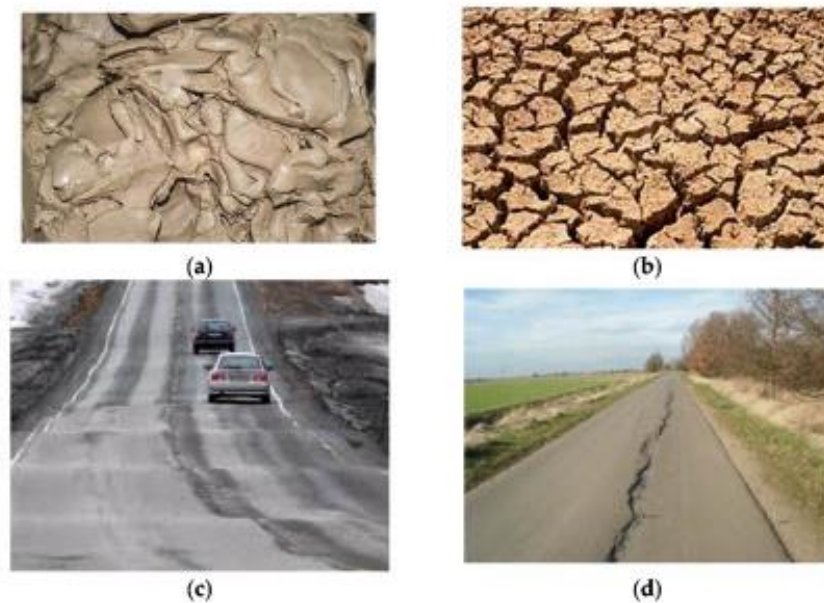


Figure 1. (a) Typical wet expansive soil [4]; (b) Typical dry expansive soil [4]; (c) Uplifting of flexible pavement [4]; (d) Typical longitudinal crack on road pavement due to expansive subgrade [4].

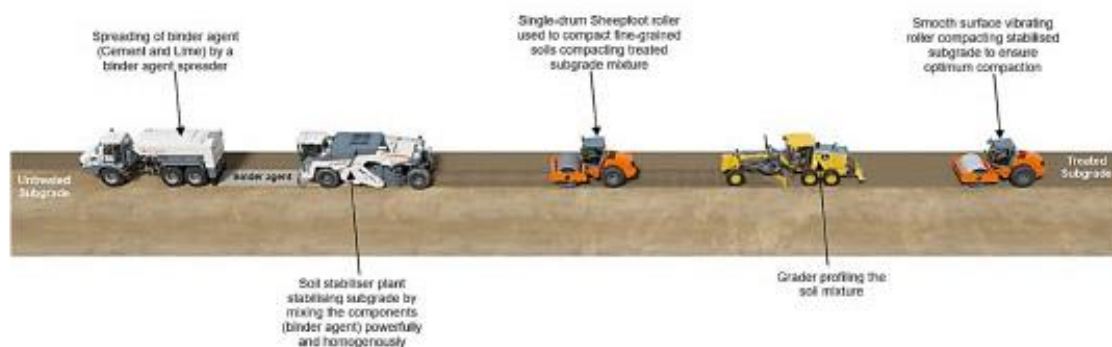





Figure 2. The application process of binder agent in real-life road construction.

Table 1. Merits of in situ stabilised subgrade and demerits of subgrade removal and replacement [15].

Cement/Lime Treated Subgrade	
<ul style="list-style-type: none"> • Less time, less cost and reduce environmental impact • Improves the workability of subgrade of soil • Reduces plasticity and shrink/swell potential • Reduce moisture susceptibility and migration • Increase speed of construction • Increase bearing capacity compared to untreated subgrade 	<ul style="list-style-type: none"> • Promotes soil drying • Provides significant improvement to the working platform • Uses onsite soil rather than removal and replacement • Provides permanent soil modification (no leaching) • Does not require mellowing period
	
<p>In situ soil stabilisation process (Wirtgen-group.com (accessed on 7 May 2022))</p>	<p>In situ soil treatment process in mixing chamber</p>
Removal and Replacement	
	<ul style="list-style-type: none"> • Time-consuming • Very costly • Greater environmental impact
<p>Removal and replace subgrade</p>	

2. Materials and Methods

In this study, bentonite and kaolinite were used to form ASS subgrade ASS 1 (25% bentonite + 75%kaolinite), ASS 2 (35% bentonite + 65% kaolinite) and ASS 3 (75% bentonite + 25% kaolinite). Details regarding the suppliers of the materials used, their oxide, chemical, mineralogy and particle size distribution can be found in reference [15]. Laboratory synthesised expansive road subgrade were formulated in accordance with BS 1924-1:2018 [16] and was used as the target material in this study. The Atterberg limits, compaction, swell and CBR tests were carried out on stabilised and unstabilised ASS materials to determine their bearing capacity and swell potentials for use in road construction. Microstructural properties were conducted for stabilised ASS to ascertain the effect of additives on strength development in subgrade materials. Further details including sample preparation and laboratory testing exercise are as reported in the authors’ previous study [15]. Flexible road pavement design was conducted using the CBR values achieved in this study in accordance with DMRB, CD 226 [17], DMRB HD 26/06 [18] and IAN 73/06 [19] using varying design traffic loads to determine the effect of varying traffic load and CBR on road pavement design. KENPAVE road pavement analysis software was used to analyse the stresses at various response points within the layers of the selected pavement structure. Compaction and Atterberg limits tests were conducted in accordance with BS EN 13286-2:2012 [20], BS EN ISO 17892-12:2021 [21], BS 1377-4:1990 [22], ASSHTO T265 [23], ASTM D2216-19 [24], ASTM D4318-17e1 [25], AASHTO T90 [26] and ASSHTO T89 [27] were used in their optimum moisture content (OMC) and maximum dry density (MDD)

determination. Figure 3 shows the methodological process used in this study to achieve the set aim of this study.

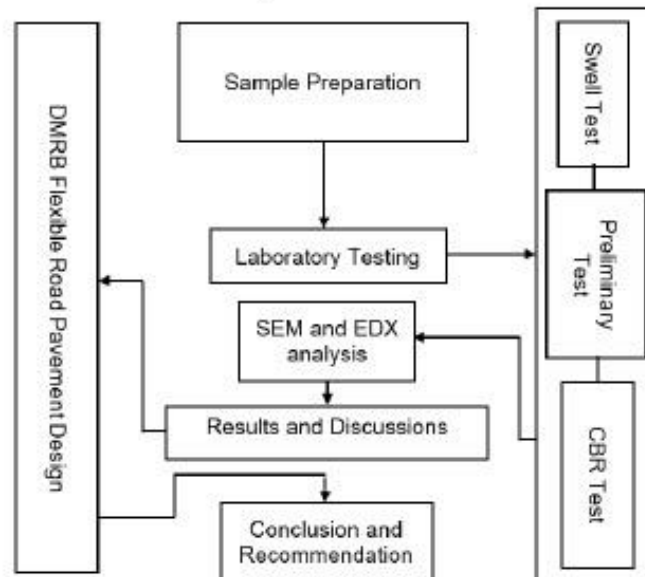


Figure 3. The methodological process used in this study.

3. Results and Discussion

California Bearing Ratio (CBR) and Microstructural Characteristics

Untreated ASS materials recorded the highest CBR values of 9% and 2% for unsoaked and soaked ASS 3 composed of high bentonite content, while ASS 1 recorded a CBR value of 8% for untreated and 0.9% for untreated soaked and ASS 2 observed 5% CBR for untreated and 0.8% for untreated soaked ASS samples. The CBR values achieved for soaked untreated ASS materials are unacceptable for use in road construction. Ref. [18] states that CBR values <2% are unacceptable for use in road construction. Treated ASS 2 recorded the highest CBR value of 100%, while ASS 1 and ASS 3 recorded CBR values of 90% and 80% after 28 days of curing. CBR value for treated ASS materials decreases with an increase in bentonite content. According to [15], high plasticity subgrade exhibits high bearing capacity. High plasticity soil has good CBR values [28]. After treating ASS samples using cement and lime, CBR values for ASS 1 (8%) increased to 80% and 90% after 7 and 28 days of curing; a CBR value of 5% was recorded for ASS 2, and increased to 60% and 100% after 7 and 28 days of curing; and a CBR value of 9% for ASS 3 increased to 30% and 80% after 7 and 28 days of curing. An overall decrease in CBR value was observed as bentonite content increased. The increase in CBR value observed after treating ASS materials using cement and lime was due to the formation of calcium silicate hydrate (C-S-H) gel in the mix, which is responsible for strength gain. C-S-H gel acts as a binder to hold soil particles together. Cement and lime produce C-S-H gel during the hydration process, which is responsible for strength gain [3,29]. The formation of C-S-H gel in treated samples increased with an increase in curing age. This accounts for the high increase in CBR values for treated ASS materials as curing age increases. The formation of C-S-H gel was observed after conducting Scanning Electron Microscopy (SEM) analysis on treated ASS materials. A clear formation of calcium silicate hydrate (C-S-H) gel and calcium aluminate hydrate (C-A-H) gel was observed in ASS samples, and the C-S-H formation in ASS samples increased as curing age increase. ASS 1 recorded calcium formation of 16.21%, ASS 2 at 30.51% and ASS 3 at 21.96% after 7 days of curing. After 28 days of curing, C-S-H gel formation increased with ASS 1 recording calcium formation of 24.75%, ASS 2 at 32.56% and ASS 3 at 33.08%, respectively [15]. This translated into an increase in CBR value with an increase in curing age. According to references [3] and [30], the continuous formation of C-S-H gel with an increase in curing age within a pore structure can contribute to strength development in a

mix. Further details including Energy Dispersive X-ray (EDX) results are reported in the authors' previous study [15]. Table 2 shows CBR results for treated and untreated ASS materials. Figure 4a–f shows SEM images of ASS sample after 7 and 28 days of curing.

Table 2. CBR results for treated and untreated ASS materials

Subgrade Type	Mix Design	Treated	Soaked	Curing Days	CBR Values (%)
ASS 1	(25%B + 75%K)	x	x	0	8
ASS 1	(25%B + 75%K)	x	✓	0	0.9
ASS 2	(35%B + 65%K)	x	x	0	5
ASS 2	(35%B + 65%K)	x	✓	0	0.8
ASS 3	(75%B + 25%K)	x	x	0	9
ASS 3	(75%B + 25%K)	x	✓	0	2
ASS 1	(8%L + 20%C)	✓	x	7	80
ASS 1	(8%L + 20%C)	✓	x	28	90
ASS 1	(8%L + 20%C)	✓	✓	0	50
ASS 2	(8%L + 20%C)	✓	x	7	60
ASS 2	(8%L + 20%C)	✓	x	28	100
ASS 2	(8%L + 20%C)	✓	✓	0	40
ASS 3	(8%L + 20%C)	✓	x	7	30
ASS 3	(8%L + 20%C)	✓	x	28	80
ASS 3	(8%L + 20%C)	✓	✓	0	30

Where B = Bentonite K = Kaolinite L = Lime and C = Cement.

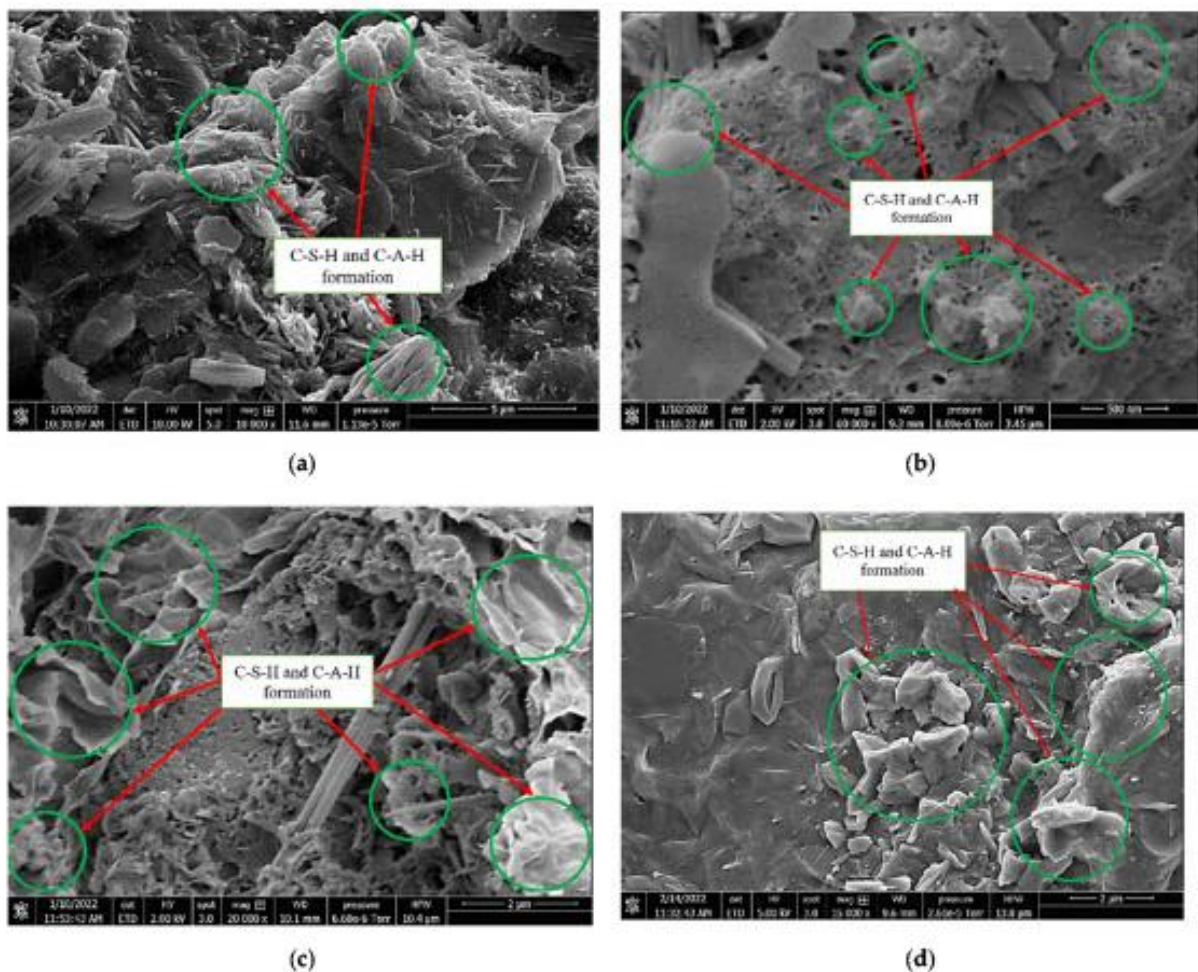


Figure 4. Cont.

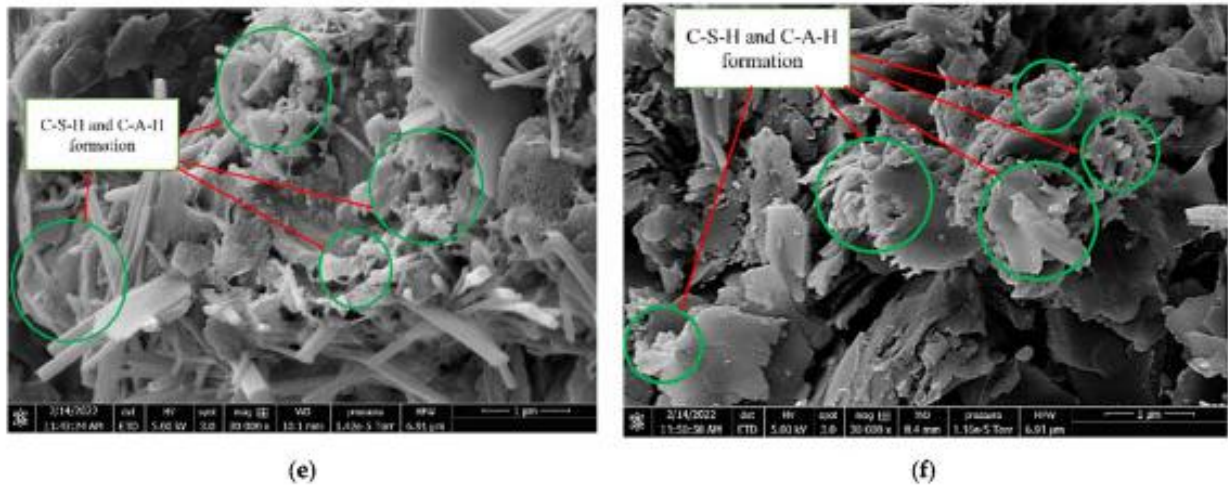


Figure 4. (a) Scanning Electron Microscopy (SEM) image results for ASS 1 after 7 days of curing; (b) SEM image results for ASS 2 after 7 days of curing; (c) SEM image results for ASS3 after 7 days of curing; (d) SEM image results for ASS 1 after 28 days of curing; (e) SEM image results for ASS 2 after 28 days of curing; (f) SEM image results for ASS 3 after 28 days of curing.

4. DMRB Road Pavement Design

Road pavement design is the process of determining the type and composition of road pavement structure based on various factors, such as type of traffic, the California Bearing Ratio (CBR) of subgrade and many more. Pavement design helps the client and decision-makers to determine the costs of the project over a certain period and investigate the effects of cost, service life and economic inputs on the life cycle cost of the road when making investment decisions [2]. Pavement designs are based on the principle that the flexural strength of the cement-bound roadbase should be greater than the combined traffic and thermal warping stresses experienced during service [31]. There are two major types of road pavement—these are flexible and rigid pavements. Flexible pavement is a pavement structure that includes a combination of aggregate and bitumen; it is heated and blended precisely and then placed and compacted on a bed of granular layer. Traffic load is transferred to the subgrade through the combination of layers. Flexible pavements require proper maintenance to avoid crumbling due to heavy traffic load because it is made up of asphalt, whose viscous nature permits plastic distortion. Although almost all asphalt pavements are constructed on a gravel base, some full-depth asphalt surfaces are constructed directly on the subgrade. There are three different classifications of asphalt depending on temperature: (i) hot mix asphalt (HMA), (ii) warm mix asphalt (WMA), and (iii) cold mix asphalt (CMA) [32]. Rigid pavement is a combination of aggregates and cement. It is blended precisely and then placed and compacted on a bed of granular layer. Rigid road pavement has no subbase and is non-flexible; they are constructed from reinforced concrete. Rigid road consists of three layers and is mostly used to build airport runways and highways and typically provide heavy-duty industrial floor slabs, ports and dock plant pavements and heavy, high traffic park or concluding pavements. Rigid pavements are designed to be long-lasting structures, with high-quality surfaces for the purpose of safe driving. The structural layers of rigid pavement transmit the traffic load to the subgrade. The differences between flexible and rigid pavement are shown in Figure 5.



Figure 5. Difference between flexible and rigid pavement [33].

In this study, flexible road pavement design was carried out based on the CBR values achieved for treated and untreated ASS materials in accordance with the Design Manual for Roads and Bridges (DMRB) CD 226 [17], DMRB HD 26/06 [18] and IAN 73/06 [19], respectively. In this study, a traffic design of 8 msa and 80 msa (million standard axles) were adopted for the pavement design to see the effect of heavy and light traffic design on pavement thickness using varying CBR values. Acceptable CBR values above 2% were achieved in this study, and a stiffness modulus above 30 MPa was adopted (Road Pavement Design Guide, 2000 [34] and IAN73/06 [20]).

A flexible composite pavement construction with performance design Class 3 was adopted due to its durability and cost-effectiveness, compared to a fully flexible pavement [31]. Heavy-duty road pavements are usually built using flexible composite pavement options because it is cheaper, can carry up to about 100 msa and provide the same quality as fully flexible pavement [31]. Composite pavement structures have a Cement Bound Granular Materials (CBGM) base with an asphalt overlay. In this study, a three-layer flexible composite pavement structure was adopted as shown in Figure 6.



Figure 6. Three-layer flexible composite pavement structure.

Surface Course: a carefully proportioned mixture of bitumen-bound minerals mixed to the required specification. It provides skid resistance, weather resistance and low traffic noise. It can withstand traffic load and transfer the load to lower layers [1].

Base Course: the area immediately under the wearing surface (surface course). The materials used in a base course are extremely high quality, as the base course lies close under the pavement surface and is subjected to severe loading [1].

Subbase Course: this is the lower layer of the road pavement and is made up of cement-bound granular materials containing crushed rock or gravel. It is the foundation of the road and it transfers the load from above to the lower layers [1].

Subgrade: the existing ground, whether improved by stabilisation or compacted to the appropriate level of strength required to carry traffic load. In situations where subgrade materials are not strong enough on their own, a capping course can be provided as a construction platform to work on [1]. Capping courses are generally a layer of granular product from crushed rock quarry and recycled materials. In some circumstances, depending on the particular need of the road being built, a pavement structure may require a binder course at the lower part of the surfacing. Binder course carries part of the load the surface course carries and helps to waterproof lower layers. Binder courses are made up of a type of asphalt concrete with different gradings of aggregate types and quantities [31]. Figure 7a,b were used to determine the thickness and stiffness modulus for the various pavement layers. Based on the design, a hydraulic-bound class (B) CBGM B-C8/10 (or T3) was adopted as subbase materials (See Table 3). A hydraulic bound mixture (HBM) category (B) was adopted as base material (Marked in Table 3) and a hot-rolled asphalt (HRA) was adopted as surface materials in accordance with DMRB CD 226 [17].

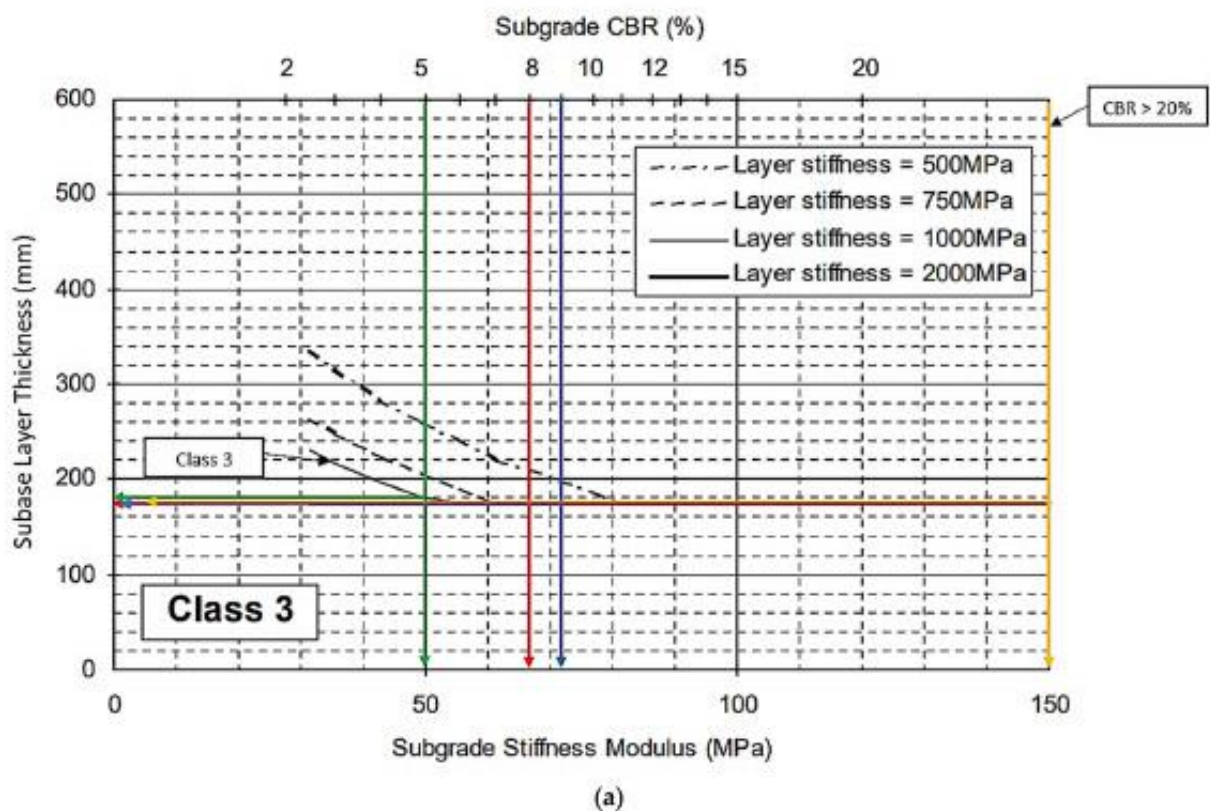


Figure 7. Cont.

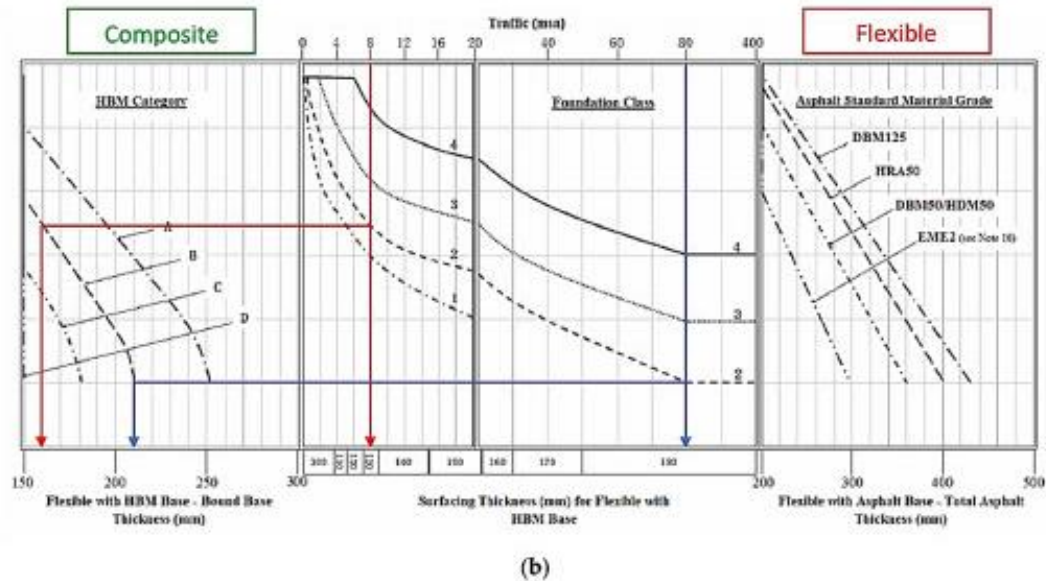


Figure 7. (a) Class 3 design—single foundation layer (Interim Advice Note (IAN) 73/06) [19]; (b) nomograph for determining the design thickness for flexible pavement (Design Manual for Roads and Bridges (DMRB) CD 226) [17].

Table 3. Examples of hydraulic bound base materials (HBM) (DMRB CD 226) [17].

HBM Category	A	B	C	D
Crushed rock coarse aggregate: (using aggregate with a coefficient of thermal expansion $< 10 \times 10^{-6}$ per $^{\circ}\text{C}$)	-	CBGM B-C8/10 (or T3) SBM B1-C9/12 (or T3) FABM1-C9/12 (or T3)	CBGM B-C12/15 (or T4) SBM B1-C12/16 (or T4) FABM1-C12/16 (or T4)	CBGM B-C16/20 (or T5) SBM B1-C15/20 (or T5) FABM1-C15/20 (or T5)
Gravel coarse aggregate: (using aggregate with a coefficient of thermal expansion $\geq 10 \times 10^{-6}$ per $^{\circ}\text{C}$)	CBGM B-C8/10 (or T3) SBM B1-C9/12 (or T3) FABM1-C9/12 (or T3)	CBGM B-C12/15 (or T4) SBM B1-C12/16 (or T4) FABM1-C12/16 (or T4)	CBGM B-C16/20 (or T5) SBM B1-C15/20 (or T5) FABM1-C15/120(or T5)	-
Pavement layers	Materials Description			
Surface course	Hot Rolled Asphalt (HRA)			
Base course	Hydraulic Bound Mixture (HBM)			
Subbase	Cement Bound Granular Mixture (CBGM)			

After carrying out road pavement design, the results obtained for traffic design 8 msa and 80 msa using subgrade CBR values 5, 8 and 9% obtained in this study are shown in Figure 8a–d. A pavement design software KENPAVE was used to analyse different wheel configurations under linear elastic layer behaviour to determine the behaviour of the layers at various response points in the pavement structure. The study has shown that a significant change in pavement thickness can only be observed for subgrade CBR values from 2–5% when using DMRB in road pavement design guidance. This is because the subbase layer forms a major of the road pavement structure, and class 3 subbase chart offers the thicker subbase layer only for subgrade CBR values between 2–10.5% after which the subbase thickness remains the same (180 mm). Hence, no significant change in pavement thickness was observed, even with a CBR value of 100% achieved for ASS 2 as shown in Table 4c,d. A reduction in road pavement thickness with a rise in subgrade CBR values was observed. Pavement design structure showing the thickness of various layers was carried out for untreated CBR values 5%, 8% and 9% as an example in this study. The results show

that a subgrade CBR value of 5% has a thicker pavement structure compared to that of subgrade CBR values of 8% and 9% for traffic design 8 msa and 80 msa, respectively. This shows a reduced pavement thickness with respect to high CBR values. Due to the low CBR values (5%), a thicker pavement is required to limit the rate of pavement deterioration due to stresses from traffic load. According to [31], the thickness of asphalt layers is required to limit stresses and reduce the severity of reflective cracking. Pavement design for the remaining CBR values for treated ASS samples achieved shows similar pavement thickness, with a small change in thickness achieved for the selected traffic design load and their corresponding layer thickness. A reduction in elastic modulus for various layers was observed with a reduction in the CBR value during analysis using KENPAVE, resulting in the determination of layer thickness. Layers with high elastic modulus require thinner layer thickness, and low elastic modulus require thicker layer thickness. Low elastic modulus in a pavement layer means stresses in that layer are high due to applied traffic load, and the thickness of that layer must be increased to reduce the stresses to avoid fatigue. The thickness of asphalt layers is required to limit stresses and reduce the severity of reflective cracking [31]. Pavement thickness for treated and soaked ASS samples are summarised in Table 4a–f of this study.

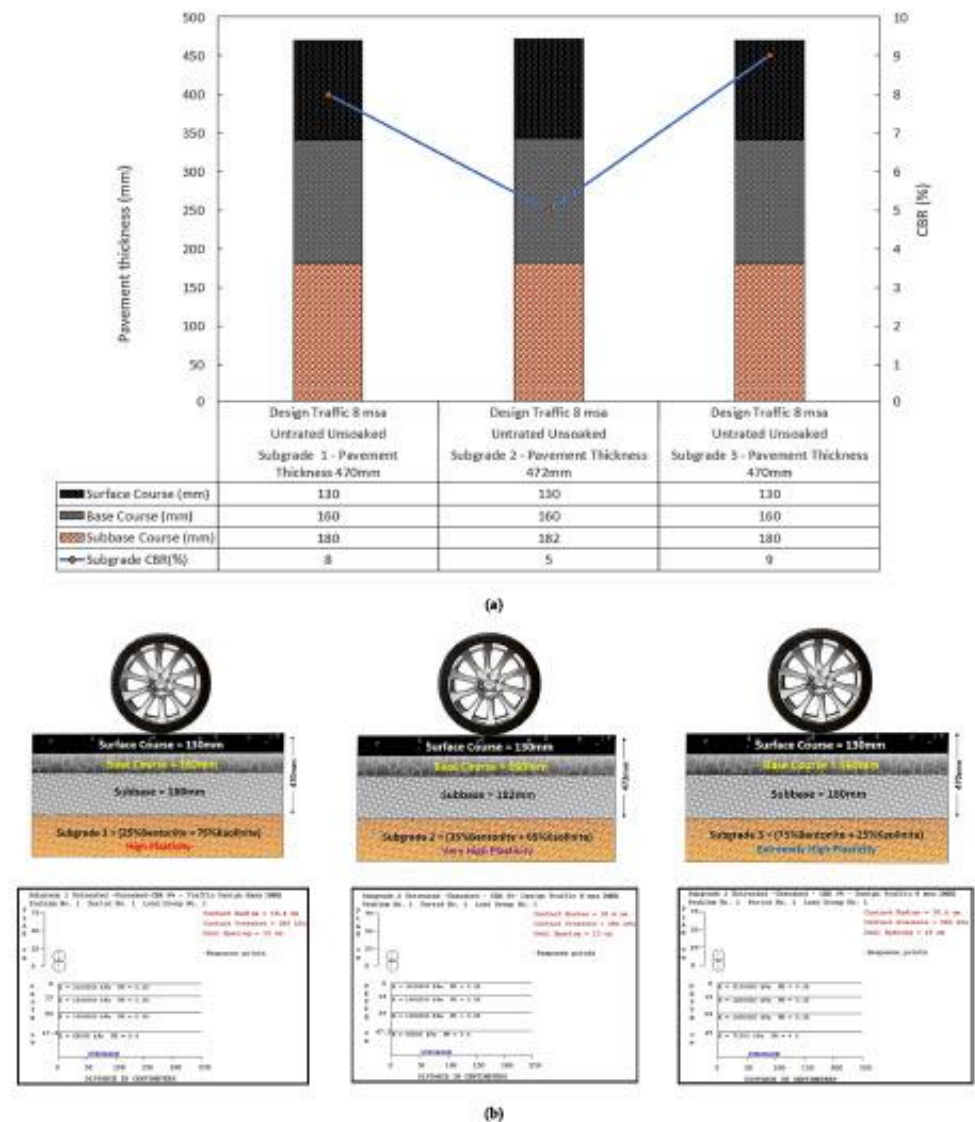


Figure 8. Cont.

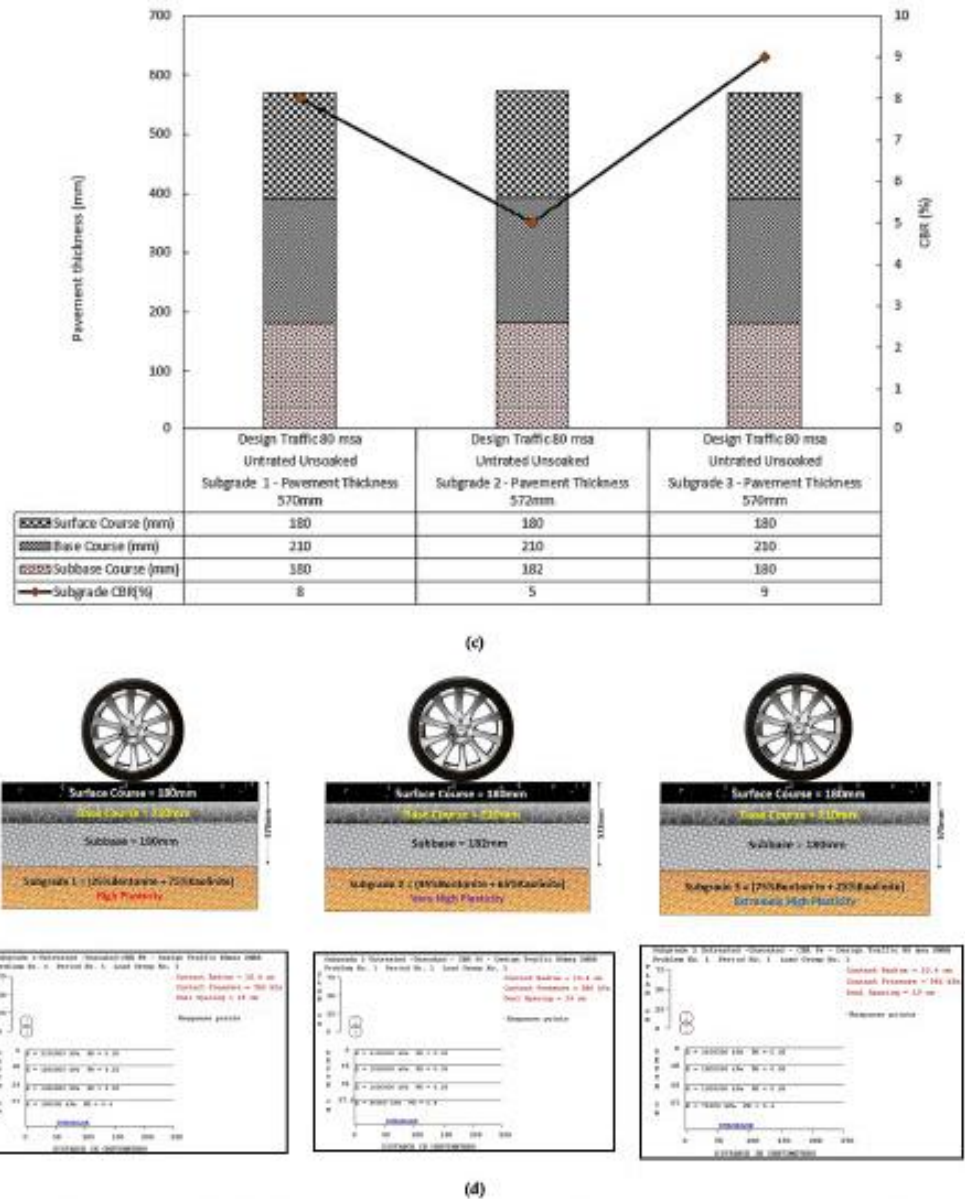


Figure 8. (a) Results for DMRB pavement design traffic 8 msa for untreated subgrade; (b) pavement thickness and three-layered flexible pavement system from KENPAVE for ASS 1, 2 and 3; (c) results for DMRB pavement design traffic 80 msa for untreated subgrade; (d) pavement thickness and three-layered flexible pavement system from KENPAVE for ASS 1, 2 and 3.

Table 4. (a) DMRB pavement design for traffic load 8 msa. (b) DMRB pavement design for traffic load 80 msa. (c) DMRB pavement design for traffic load 8 msa. (d) DMRB pavement design for traffic load 80 msa. (e) DMRB pavement design for traffic load 8 msa. (f) DMRB pavement design for traffic load 80 msa.

ASS 1 (25% Bentonite + 75% Kaolinite) High Plasticity						ASS 2 (35% Bentonite + 65% Kaolinite) Very High Plasticity						ASS 3 (75% Bentonite + 25% Kaolinite) Extremely High Plasticity													
Flexible Pavement Layers	Material	Thickness (mm)	Treated	Curing (Days)	Soaked	CBR (%)	Design Traffic (msa)	Flexible Pavement Layers	Material	Thickness (mm)	Treated	Curing (Days)	Soaked	CBR (%)	Design Traffic (msa)	Flexible Pavement Layers	Material	Thickness (mm)	Treated	Curing (Days)	Soaked	CBR (%)	Design Traffic (msa)		
Surface Course	HRA	130						Surface Course	HRA	130						Surface Course	HRA	130							
Base Course	HBM	160						Base Course	HBM	160						Base Course	HBM	160							
Subbase	CBGM	180						Subbase	CBGM	180						Subbase	CBGM	180							
Subgrade	ASS	∞	√	7	x	80	8	Subgrade	ASS	∞	√	7	x	60	8	Subgrade	ASS	∞	√	7	x	30	8		
Total pavement thickness		470						Total pavement thickness		470						Total pavement thickness		470							

ASS 1 (25% Bentonite + 75% Kaolinite) High Plasticity						ASS 2 (35% Bentonite + 65% Kaolinite) Very High Plasticity						ASS 3 (75% Bentonite + 25% Kaolinite) Extremely High Plasticity												
Flexible Pavement Layers	Material	Thickness (mm)	Treated	Curing (Days)	Soaked	CBR (%)	Design Traffic (msa)	Flexible Pavement Layers	Material	Thickness (mm)	Treated	Curing (Days)	Soaked	CBR (%)	Design Traffic (msa)	Flexible Pavement Layers	Material	Thickness (mm)	Treated	Curing (Days)	Soaked	CBR (%)	Design Traffic (msa)	
Surface Course	HRA	180						Surface Course	HRA	180						Surface Course	HRA	180						
Base Course	HBM	210						Base Course	HBM	210						Base Course	HBM	210						
Subbase	CBGM	180						Subbase	CBGM	180						Subbase	CBGM	180						
Subgrade	ASS	∞	√	7	x	80	80	Subgrade	ASS	∞	√	7	x	60	80	Subgrade	ASS	∞	√	7	x	30	80	
Total pavement thickness		570						Total pavement thickness		570						Total pavement thickness		570						

Table 4. Cont.

ASS 1 (25% Bentonite + 75% Kaolinite) High Plasticity						ASS 2 (35% Bentonite + 65% Kaolinite) Very High Plasticity						ASS 3 (75% Bentonite + 25% Kaolinite) Extremely High Plasticity												
Flexible Pavement Layers	Material	Thickness (mm)	Treated	Curing (Days)	Soaked	CBR (%)	Design Traffic (msa)	Flexible Pavement Layers	Material	Thickness (mm)	Treated	Curing (Days)	Soaked	CBR (%)	Design Traffic (msa)	Flexible Pavement Layers	Material	Thickness (mm)	Treated	Curing (Days)	Soaked	CBR (%)	Design Traffic (msa)	
Surface Course	HRA	130						Surface Course	HRA	130						Surface Course	HRA	130						
Base Course	HBM	160						Base Course	HBM	160						Base Course	HBM	160						
Subbase	CBGM	180						Subbase	CBGM	180						Subbase	CBGM	180						
Subgrade	ASS	∞	√	28	x	90	8	Subgrade	ASS	∞	√	28	x	100	8	Subgrade	ASS	∞	√	28	x	80	8	
Total pavement thickness		470						Total pavement thickness		470						Total pavement thickness		470						

ASS 1 (25% Bentonite + 75% Kaolinite) High Plasticity						ASS 2 (35% Bentonite + 65% Kaolinite) Very High Plasticity						ASS 3 (75% Bentonite + 25% Kaolinite) Extremely High Plasticity												
Flexible Pavement Layers	Material	Thickness (mm)	Treated	Curing (Days)	Soaked	CBR (%)	Design Traffic (msa)	Flexible Pavement Layers	Material	Thickness (mm)	Treated	Curing (Days)	Soaked	CBR (%)	Design Traffic (msa)	Flexible Pavement Layers	Material	Thickness (mm)	Treated	Curing (Days)	Soaked	CBR (%)	Design Traffic (msa)	
Surface Course	HRA	180						Surface Course	HRA	180						Surface Course	HRA	180						
Base Course	HBM	210						Base Course	HBM	210						Base Course	HBM	210						
Subbase	CBGM	180						Subbase	CBGM	180						Subbase	CBGM	180						
Subgrade	ASS	∞	√	28	x	90	80	Subgrade	ASS	∞	√	28	x	100	80	Subgrade	ASS	∞	√	28	x	80	80	
Total pavement thickness		570						Total pavement thickness		570						Total pavement thickness		570						

Table 4. Cont.

ASS 1 (25% Bentonite + 75% Kaolinite) High Plasticity							(e) ASS 2 (35% Bentonite + 65% Kaolinite) Very High Plasticity							ASS 3 (75% Bentonite + 25% Kaolinite) Extremely High Plasticity										
Flexible Pavement Layers	Material	Thickness (mm)	Treated	Curing (Day#)	Soaked	Design Traffic (msa)	Flexible Pavement Layers	Material	Thickness (mm)	Treated	Curing (Days)	Soaked	CBR (%)	Design Traffic (msa)	Flexible Pavement Layers	Material	Thickness (mm)	Treated	Curing (Day#)	Soaked	CBR (%)	Design Traffic (msa)		
Surface Course	HRA	130					Surface Course	HRA	130						Surface Course	HRA	130							
Base Course	HBM	160					Base Course	HBM	160						Base Course	HBM	160							
Subbase	CBGM	180					Subbase	CBGM	180						Subbase	CBGM	180							
Subgrade	ASS	∞	✓	3	✓	50 8	Subgrade	ASS	∞	✓	3	✓	40 8		Subgrade	ASS	∞	✓	3	✓	30 8			
Total pavement thickness		470					Total pavement thickness		470						Total pavement thickness		470							

ASS 1 (25% Bentonite + 75% Kaolinite) High Plasticity							(f) ASS 2 (35% Bentonite + 65% Kaolinite) Very High Plasticity							ASS 3 (75% Bentonite + 25% Kaolinite) Extremely High Plasticity										
Flexible Pavement Layers	Material	Thickness (mm)	Treated	Curing (Days)	Soaked	Design Traffic (msa)	Flexible Pavement Layers	Material	Thickness (mm)	Treated	Curing (Days)	Soaked	CBR (%)	Design Traffic (msa)	Flexible Pavement Layers	Material	Thickness (mm)	Treated	Curing (Days)	Soaked	CBR (%)	Design Traffic (msa)		
Surface Course	HRA	180					Surface Course	HRA	180						Surface Course	HRA	180							
Base Course	HBM	210					Base Course	HBM	210						Base Course	HBM	210							
Subbase	CBGM	180					Subbase	CBGM	180						Subbase	CBGM	180							
Subgrade	ASS	∞	✓	3	✓	50 80	Subgrade	ASS	∞	✓	3	✓	40 80		Subgrade	ASS	∞	✓	3	✓	30 80			
Total pavement thickness		570					Total pavement thickness		570						Total pavement thickness		570							

NOTE: HRA = Hot Rolled Asphalt, ASS = Artificially Synthesised Subgrade, HBM = Hydraulic Bound mixture, CBGM = Cement Bound Granular Mixture.

5. Conclusions

After conducting pavement design for re-engineered artificially synthesised expansive subgrade materials with varying plasticity index using DMRB design guidance, it was observed that pavement thickness increased or reduced in relation to CBR values and elastic modulus within the various layers of the pavement structure. The study also concluded with the following:

- There was no significant difference in pavement thickness for low and high CBR values when using DMRB in road pavement design. A significant change in pavement thickness can only be observed for subgrade CBR values from 2–5% when using DMRB in road pavement design. CBR values and elastic modulus influenced the overall thickness of road pavement.
- This study would benefit the industry in many ways, as road contractors can quickly refer to this study to determine road pavement layer thickness when they encounter subgrade materials with CBR characteristics similar to what was used in this study.
- ASS samples with high bentonite content recorded a high plasticity index with unacceptable swell values greater than 2.5% and acceptable CBR values below 2%.
- Lime and cement were able to improve the engineering properties of ASS materials and reduce swell to the lowest minimum of 0.04%.
- CBR value increased with an increase in bentonite content in treated and untreated ASS samples. This proves that bentonite has a high bearing capacity.
- Based on the finding in this study, it is recommended that subgrade materials are stabilised on-site to reduce the cost of construction instead of removing them and replacing them with imported materials.

Author Contributions: Conceptualisation, S.J.A. and S.Y.O.A.; methodology, S.Y.O.A. and S.J.A.; validation, S.Y.O.A. and S.J.A.; formal analysis, S.Y.O.A. and S.J.A.; investigation, S.Y.O.A. and S.J.A.; resources, S.J.A. and C.A.B.; data curation, S.Y.O.A. and S.J.A.; writing—original draft preparation, S.Y.O.A. and S.J.A.; writing—review and editing, S.Y.O.A., S.J.A. and C.A.B.; visualisation, S.J.A. and C.A.B.; supervision, S.J.A. and C.A.B.; project administration, C.A.B. and S.J.A. All authors have read and agreed to the published version of the manuscript.

Funding: This research did not receive any specific grant from funding agencies in the public, commercial or not-for-profit sector.

Institutional Review Board Statement: Not applicable.

Informed Consent Statement: Not applicable.

Data Availability Statement: The data presented in this study are openly available in *Materials* at <https://www.mdpi.com/1996-1944/15/8/2773>, accessed on 9 April 2022.

Acknowledgments: The authors acknowledge the advice, comments and suggestions from anonymous reviewers significantly improved the quality of this paper.

Conflicts of Interest: The authors declare that they have no conflict of interest associated with this publication, and no financial support has been given to influence the outcome of this work.

References

1. Paul, A. Pavement Design in Road Construction—Design Parameters. 2014. Available online: <https://civildigital.com/pavement-design-road-construction-design-parameters/> (accessed on 11 March 2022).
2. Wilson, S. *Whole Life Cycle Cost Analysis for various Pavement and Drainage Options*; Interpave—The Precast Concrete Paving and Kerb Association, a Product Association of BPCF Ltd.: Glenfield, UK, 2006.
3. Amakye, S.Y.; Abbey, S.J. Understanding the performance of expansive subgrade materials treated with non-traditional stabilisers: A Review. *Clean. Eng. Technol.* **2021**, *4*, 100159. [[CrossRef](#)]
4. Amakye, S.Y.; Abbey, S.J.; Booth, C.A.; Mahamadu, A. Enhancing the engineering properties of subgrade materials using processed waste: A review. *Geotechnics* **2021**, *1*, 0015. [[CrossRef](#)]
5. Li, J.; Cameron, D.A.; Ren, G. Case study and back analysis of a residential building damaged by expansive soils. *Comput. Geotech.* **2014**, *56*, 89–99. [[CrossRef](#)]

6. Jones, L.D.; Jefferson, I. Institution of Civil Engineers Manuals Series. 2019. Available online: http://nora.nerc.ac.uk/id/eprint/17002/1/C5_expansive_soils_Oct.pdf (accessed on 29 November 2021).
7. López-Lara, T.; Hernández-Zaragoza, J.; Horta-Rangel, J.; Rojas-González, E.; López-Ayala, S.; Castaño, V. Expansion reduction of clayey soils through Surcharge application and Lime Treatment. *Case Stud.* **2017**, *7*, 102–109. [CrossRef]
8. Neville, A.M. Properties of Concrete 5th Edition. New York, NY: Harlow, England. 2011. Available online: <https://pdfcoffee.com/properties-of-concrete-fifth-edition-a-m-neville-pdf-pdf-free.html> (accessed on 2 October 2021).
9. Walker, P. Review and Experimental Comparison of erosion tests on Earth Blocks. In Proceedings of the 8th International Conference on the Study and Conservation of Earthen Architecture, Torquay, UK, May 2000; James & James: London, UK, 2000.
10. Gooding, D.E.; Thomas, T.H. The Potential of Cement Stabilised or Treated Building Blocks as an Urban Building Material in Developing Countries. DTU Working Paper No.44. 1995. 2021. Available online: <https://warwick.ac.uk/fac/sci/eng/research/group/structural/dtu/pubs/wp/wp44/wp44.pdf> (accessed on 18 November 2021).
11. Abbey, S.J.; Ngambi, S.; Olubanwo, A.O.; Tetteh, F.K. Strength and Hydraulic Conductivity of Cement and By-Product Cementitious Materials Improved Soil. *Int. J. Appl. Eng. Res.* **2018**, *13*, 8684–8694.
12. Boardman, D.I.; Glendinning, S.; Rogers, C.D.F. Development of stabilisation and solidification in lime-clay mixes. *Geotechnique* **2001**, *51*, 533–543. [CrossRef]
13. Ingles, O.G.; Metcalf, J.B. *Soil Stabilisation*; Butterworth Pty, Ltd.: Sydney, Australia, 1972.
14. Ingles, O.H. Soil stabilisation. Chapter 38. In *Ground Engineer's Reference Book*; Bell, F.G., Ed.; Butterworths: London, UK, 1987; pp. 38/1–38/26.
15. Amakye, S.Y.O.; Abbey, S.J.; Booth, C.A.; Oti, J. Road Pavement Thickness and Construction Depth Optimization Using Treated and Untreated Artificially-Synthesized Expansive Road Subgrade Materials with Varying Plasticity Index. *Materials* **2022**, *15*, 2773. [CrossRef] [PubMed]
16. *British Standard, BS 1924-1:2018*; Stabilised or Treated Materials for Civil Engineering Purposes. Available online: <https://www.bsigroup.com/en-GB/> (accessed on 7 May 2022).
17. *Design Manual for Roads and Bridges (DMRB) CD 226*; Design for New Pavement Construction. Available online: <https://www.standardsforhighways.co.uk/ha/standards/> (accessed on 7 May 2022).
18. *Design Manual for Roads and Bridges DMRB HD 26/06*; Pavement Design. Available online: <https://pdf4pro.com/amp/view/hd-26-06-pavement-design-standards-for-highways-3ef7c2.html> (accessed on 7 May 2022).
19. *Interim Advice Note (IAN) 73/06*; Design Guidance for Road Pavement Foundations. Available online: <http://origin.standardsforhighways.co.uk/ha/standards/ians/pdfs/ian73.pdf> (accessed on 7 May 2022).
20. *British Standard, BS EN 13286-2-2012*; Unbound and Hydraulically Bound Mixtures—Test Methods for Laboratory Reference Density and Water Content. Proctor Compaction. Available online: <https://www.thenbs.com/PublicationIndex/Documents/Details?DocId=311925> (accessed on 7 May 2022).
21. *British Standard, BS EN ISO 17892-12-2021*; Geotechnical Investigation and Testing. Laboratory Testing of Soil—Determination of Water Content. Available online: <https://standardsdevelopment.bsigroup.com/projects/2020-00948#/section> (accessed on 7 May 2022).
22. *British Standard, BS 1377-4:1990*; Methods of Test for Soils for Civil Engineering Purposes—Compaction—Related Tests. Available online: <https://www.thenbs.com/PublicationIndex/documents/details?Pub=BSI&DocID=261911> (accessed on 7 May 2022).
23. AASHTO T 265; Standard Method of Test for Laboratory Determination of Moisture Content of Soils. 2015. Available online: <https://www.transportation.org/> (accessed on 7 May 2022).
24. ASTM D2216-19; 2019. Standard Test Methods for Laboratory Determination of Water (Moisture) Content of Soil and Rock by Mass. Available online: <https://www.astm.org/d2216-19.html> (accessed on 7 May 2022).
25. ASTM D4318-17e1; Standard Test Method for Liquid Limit, Plastic Limit, and Plasticity Index of Soils. 2017. Available online: <https://www.astm.org/> (accessed on 9 February 2022).
26. AASHTO T 90; Standard Method of Test for Determining the Plastic Limit, Liquid Limit and Plasticity Index. 2020. Available online: <https://standards.globalspec.com/std/14316709/aashto-t-90> (accessed on 7 May 2022).
27. AASHTO T 89; Standard Method of Test for Determining the Liquid Limit of Soils. 2013. Available online: https://global.ihc.com/doc_detail.cfm?document_name=AASHTO%20T%2089&item_s_key=00488948 (accessed on 7 May 2022).
28. Gratchev, I.; Pitawala, S.; Gurung, N.; Monteiro, E. A Chart to Estimate CBR of Plastic Soils. 2018. Available online: https://www.researchgate.net/publication/324557522_A_CHART_TO_ESTIMATE_CBR_OF_PLASTIC_SOILS (accessed on 9 February 2022).
29. Abbey, S.J.; Eyo, E.U.; Jeremiah, J.J. Experimental study on early age characteristics of lime-GGBS-Treated gypseous clays under wet-dry cycles. *Geotechnics* **2021**, *1*, 0019. [CrossRef]
30. Abbey, S.J.; Eyo, E.U.; Ng'ambi, S. Swell and microstructural characteristics of high-plasticity clay blended with cement. *Bull. Eng. Geol. Environ.* **2019**, *79*, 2119–2130. [CrossRef]
31. Parry, A.R.; Phillips, S.J.; Potter, J.F.; Nunn, M.E. Design and performance of flexible composite road pavements. *Proc. Inst. Civ. Eng.—Transp.* **1999**, *135*, 9–16. [CrossRef]
32. Oreto, C.; Veropalumbo, R.; Viscione, N.; Biacardo, A.; Russo, F. Investigating the environmental impacts and engineering performance of road asphalt pavement mixtures made up of jet grouting waste and reclaimed asphalt pavement. *Environ. Res.* **2021**, *198*, 111277. [CrossRef] [PubMed]

33. Allaboutengineering, 2022. Available online: <https://allabouteng.com/difference-between-flexible-pavement-and-rigid-pavement/> (accessed on 22 January 2022).
34. Road Pavement Design Guide. 2000. Available online: https://www.kent.gov.uk/__data/assets/pdf_file/0012/13035/Making-it-Happen-Road-pavement-design-guide-July-2000.pdf (accessed on 26 February 2022).

Article

Road Pavement Thickness and Construction Depth Optimization Using Treated and Untreated Artificially-Synthesized Expansive Road Subgrade Materials with Varying Plasticity Index

 Samuel Y. O. Amakye ^{1,*}, Samuel J. Abbey ¹, Colin A. Booth ¹ and Jonathan Oti ²
¹ Faculty of Environment and Technology, University of the West of England, Bristol BS16 1QY, UK; samuel.abbey@uwe.ac.uk (S.J.A.); colin.booth@uwe.ac.uk (C.A.B.)

² School of Engineering, Faculty of Computing, Engineering and Science, University of South Wales, Pontypridd CF37 1DL, UK; jonathan.oti@southwales.ac.uk

* Correspondence: samuel.amakye@uwe.ac.uk

Abstract: Road pavement thickness and their depth of construction take a chunk of the overall cost of road construction. This has called for a need for reduced road pavement thickness by improving the engineering properties of subgrade such as the California bearing ratio (CBR). The CBR of road subgrade has been a major determining factor for road pavement thickness, and expansive subgrades generally have a low CBR, resulting in major road defects. In this study, road pavement thickness and construction depth optimization were conducted using the CBR values achieved in this study. Additives proportions of 8% lime and 20% cement were used in expansive subgrade to improve their engineering properties, making them suitable for use in road construction. The study investigated the characteristics, mineral structure, Atterberg limit, compaction, CBR, swell and microstructural properties of expansive subgrade. The results show a reduction in road pavement thickness and a construction depth with an increase in CBR value. All CBR values for treated samples were above 2%, making them usable in road construction. A reduction in swell potential up to 0.04% was observed for treated expansive subgrade. The study concluded that pavement thickness and construction depth can be reduced by enhancing subgrade materials and using cement and lime as binders.

Keywords: expansive subgrade material; artificially-synthesized subgrade; California bearing ratio; road pavement thickness optimization; compaction test; swell test



Citation: Amakye, S.Y.O.; Abbey, S.J.; Booth, C.A.; Oti, J. Road Pavement Thickness and Construction Depth Optimization Using Treated and Untreated Artificially-Synthesized Expansive Road Subgrade Materials with Varying Plasticity Index. *Materials* **2022**, *15*, 2773. <https://doi.org/10.3390/ma15082773>

Academic Editor: F. Pacheco Torgal

Received: 16 March 2022

Accepted: 7 April 2022

Published: 9 April 2022

Publisher's Note: MDPI stays neutral with regard to jurisdictional claims in published maps and institutional affiliations.



Copyright: © 2022 by the authors. Licensee MDPI, Basel, Switzerland. This article is an open access article distributed under the terms and conditions of the Creative Commons Attribution (CC BY) license (<https://creativecommons.org/licenses/by/4.0/>).

1. Introduction

Road pavements are structures that consist of superimposed layers of processed materials placed over the natural subgrade. The primary function of road pavement is to distribute traffic load to the subgrade and provide a surface of acceptable riding quality, adequate skid resistance and low noise pollution [1]. During road construction, a huge sum of the total construction cost goes into road pavement construction, especially in situations where weak or expansive subgrade is involved. The California bearing ratio (CBR) value of road pavement subgrade can influence the overall thickness and depth of the construction of road pavement, which can greatly impact the overall construction cost [2]. Subgrade material is the natural soil underneath a road pavement structure [2]. California bearing ratio (CBR) is a penetration test to evaluate the strength of road subgrade materials to ascertain their bearing capacity for use as road subgrade materials during construction [2]. When soils exhibit evident volume changes with the potential to swell and shrink with changes in moisture content due to the presence of clay minerals, they are referred to as expansive subgrade [2]. Expansive subgrade materials do not have the capacity to support the weight of road pavement and traffic load and will normally require some form of modification or re-engineering to enhance their capacity to support the load [2]. Many

road pavement defects and failures are a result of expansive subgrade, and the process of repairing or maintaining these defects comes with a huge cost and sometimes requires a total reconstruction of the road [3]. Infrastructure built on expansive soils may experience structural failure or deformation, resulting in a combined annual repair and maintenance cost of 30 billion USD to the United States and China [4]. The UK economy, over the past ten years, has suffered a cost of over 3 billion GBP, making it the most damaging geohazard in Britain [5]. According to [6], the damage caused by expansive subgrade materials in road structures runs into millions of dollars compared to the damages caused by floods.

In this study, road pavement thickness and pavement depth optimization was carried out in accordance with the CBR, which is method recommended by the California state of highways to determine how varying CBR values affect road pavement thickness using laboratory artificially-synthesized subgrade (ASS) material. The aim of this study is to determine the effect of treated and untreated expansive road subgrade materials and how they affect their CBR values and pavement thickness using chemical stabilization techniques. Chemical subgrade stabilization is an effective technique to improve expansive subgrade, and it involves adding different types of admixtures such as lime and cement, among others, as binders to stabilize soil [7,8]. Chemical soil stabilization techniques have been reportedly used in addressing the problems associated with expansive subgrades [9,10]. The addition of these chemical binders changes the gradation and physico-synthetics within and around the soil particles, promoting cation exchange, which leads to the flocculation and agglomeration of the expansive soil particles [11]. In this study, the artificially-synthesized subgrade (ASS) materials used in this study are a mixture of untreated bentonite and kaolinite clays at various percentages to form subgrade materials with the properties of an expansive subgrade similar to that of a naturally existing expansive clay subgrade material. Atterberg limits, a compaction behavior test, was conducted on untreated bentonite and kaolinite clay soil before mixing them to determine their behavior, characteristics and strength at different moisture contents. The ASS was later treated using cement and lime to improve its strength for use as subgrade materials in road construction. The California bearing ratio (CBR) test was conducted for untreated and treated ASS to determine the strength and bearing capacity for use as road subgrade materials.

Cement is a finely ground powder that becomes solid when mixed with water through a process called hydration [2,12]. Over the years, Portland cement and lime have been used to improve the engineering properties of subgrade materials. Portland cement is a hydraulic binder derived through the crushing, milling and proportioning of raw material such as calcareous limestone/chalk rock and clay/shale after burning them in a large rotary kiln at a temperature of up to 1450 °C or 2600 °F. Cement solidifies when mixed with water through a process known as hydration [2]. Hydration is a chemical combination of Portland cement compounds and water to form sub-microscopic crystals. During the hydration process, a cement gel matrix is produced called calcium silicate hydrate (C-S-H), which binds subgrade particles together and is responsible for strength gain [2]. According to [13], cement is suitable for the stabilization of subgrade materials with low plasticity indexes. Cement is popularly used to improve the engineering properties of expansive subgrade materials [14]. A cement range of 4 to 15% was used to enhance the engineering properties of the subgrade materials [15]. The addition of 3% cement with 1% nano-silica and nano-alumina resulted in a 196% and 164% increase in the soaked CBR of the nontreated clay [16]. Cement, fly ash, bituminous, rice husk ash, lime, construction and demolition waste, electrical and thermal waste, geotextile fabrics and recycled waste can be used as admixtures in this process [8]. The addition of these materials as admixtures can alter the geotechnical properties of expansive soil such as the strength, bearing capacity, hydraulic conductivity, compressibility, workability, durability and swelling potentials [17]. Lime was mostly used in subgrade stabilization before the introduction of cement, and it has proven to be an effective modification agent for the stabilization of highway and airport pavement subgrade. A lime soil reaction takes place when soil mixed with lime changes the moisture and density relationship of the soil. This reaction triggers a lime hydration

process and, with the help of calcium, releases cementitious products (calcium-silicate-hydrate (C-S-H) and calcium-aluminate-hydrate (C-A-H)) responsible for the strength increase in the subgrade [2,14]. The use of limestone, which is a source of lime, as road fill is very important due to the ability of limestone to improve the bearing capacity of road subgrade during the formation of C-S-H gel in the lime hydration process [18,19]. An investigation into the application of the stabilization of wastewater sludge proves that cement, lime and bitumen can be used as subgrade materials [20]. During chemical road subgrade stabilization, the shear strength of the expansive subgrade improves when stabilizers react with water within the soil, leading to an increase in stiffness of the soil [7]. A further increase in strength and durability is observed depending on the curing time and temperature [2]. In civil engineering applications, subgrade materials with a plasticity between 20% and 30%, with a liquid limit from 25% to 50%, are recommended for lime stabilization [21]. Good CBR and swelling results were achieved when 80% lime was used in the expansive subgrade stabilization for flexible pavement, and 3–8% of lime was used to improve high plasticity clays [22]. Reference [23] used 1% of lime for every 10% of clay content in the soil. Reference [24] used 6% of lime to stabilize expansive subgrade. A lime proportion of 4–6% was adopted to achieve the best performance of expansive subgrade material [25]. The treatment of expansive subgrade using lime and other additives to improve its engineering properties has been effective for road pavement construction [26]. The addition of 8% lime to an expansive black clay mixture fell beyond the satisfactory range for use as sub-base materials for light-traffic roads [27]. Black cotton soil (BCS) stabilized with 3% lime + 15% volcanic ash (VA), which meets the performance requirements of roadbed materials [28]. The inclusion of cement increased the bearing capacity of subgrade material during subgrade stabilization at proportions of 10%, 15% and 20% [29]. Subgrade materials were improved by achieving a compressive strength from 564.78 kPa to 636.19 kPa [30]. Hydraulic lime is produced by burning a form of low-grade limestone containing silica and alumina, which are above certain temperatures, combined with calcium oxide. Lime is one of the most common binders used in road subgrade stabilization [2]. According to [31], an optimum lime dosage between 6–12% by dry weight is suitable to enhance the engineering properties of road subgrade materials. Figure 1a–d shows typical wet and dry expansive soil and road pavement defects caused by expansive subgrade. Table 1 shows the advantages of treating expansive subgrade and the disadvantages of the removal and replacement of weak subgrade.

Table 1. The advantages of in situ treated subgrade and the disadvantages of the removal and replacement of subgrade.

Cement/Lime Treated Subgrade	
<ul style="list-style-type: none"> • Less time, less cost and reduces environmental impact • Improves the workability of the subgrade of the soil • Reduces the plasticity and shrink/swell potential • Reduces moisture susceptibility and migration • Increases the speed of construction • Increases the bearing capacity compared to untreated subgrade 	<ul style="list-style-type: none"> • Promotes soil drying • Provides significant improvement to the working platform • Uses onsite soil rather than removal and replacement • Provides permanent soil modification (no leaching) • Does not require mellowing period
Subgrade Removal and Replacement	
Time-consuming, Very costly and Greater environmental impact	

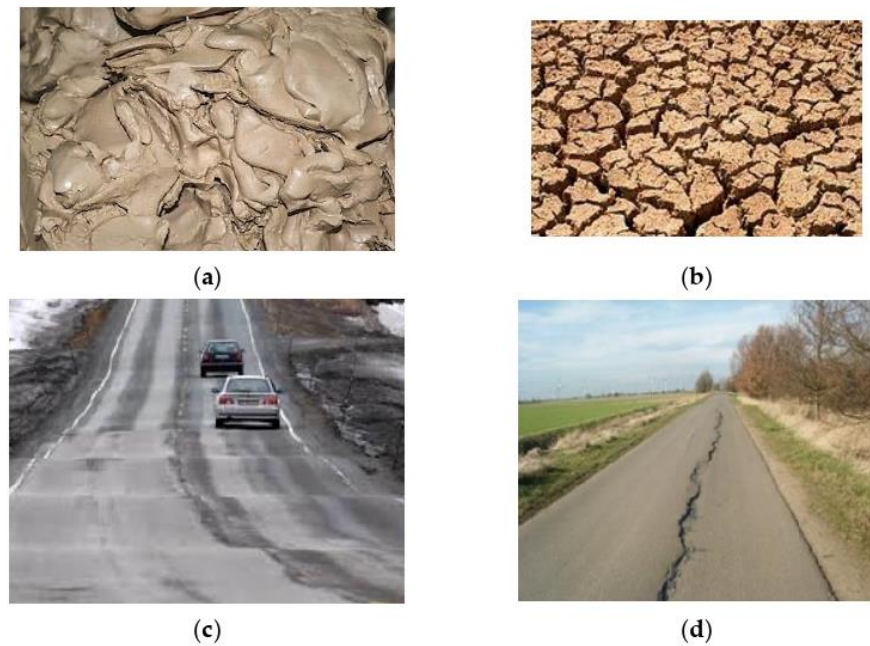


Figure 1. (a) Typical wet expansive soil [3]; (b) typical dry expansive soil [3]; (c) uplifting of flexible pavement [3]; (d) typical longitudinal crack on road pavement due to expansive subgrade [3].

2. Materials and Methods

Materials used in this study consist of bentonite clay and kaolinite clay to form subgrade 1 = ASS 1 (25% bentonite, 75% kaolinite), subgrade 2 = ASS 2 (35% bentonite, 65% kaolinite) and subgrade 3 = ASS 3 (75% bentonite, 25% kaolinite), respectively. The kaolinite used was supplied by Potclays Ltd. Brickkiln Lane, Etruria, Stoke-on-Trent, England, and the bentonite used was supplied by Potclays Ltd., Brickkiln Lane, Etruria, Stoke-on-Trent, England. The cement used (CEM I) complies with BS EN 197-1:2011 [32] and was supplied by CEMEX UK Operations Ltd., CEMEX House, Evreux Way, Rugby, Warwickshire, CV21 2DT, and the lime used was (quicklime), complies with BS EN 459-1-2015 [33] and was supplied by Singleton Birch Ltd., Melton Ross Quarries, Barnetby, North Lincolnshire. Tables 2 and 3 show the oxide and some of the chemical and mineralogical composition of bentonite and kaolinite. Table 4 shows consistency limits and physical properties of kaolinite and bentonite used in this study. Figure 2 shows the particle size distribution of bentonite, kaolinite, cement and lime used in this study.

Table 2. Oxide and some of the chemical composition of the bentonite and kaolinite clays.

Oxide	SiO ₂	Al ₂ O ₃	Fe ₂ O ₃	FeO	MgO	CaO	K ₂ O	SO ₃	TiO ₂	Na ₂ O	BaO	Cr ₂ O ₃	Trace	L.O.I
Bentonite clay	63.02	21.08	3.25	0.35	2.67	0.65	-	-	-	2.57	-	-	0.72	5.64
Kaolinite clay	48.5	36.0	1.00	-	0.30	0.2	2.15	-	0.06	0.15	-	-	-	11.7
Cement (%)	20	6.0	3.0	-	4.21	63	-	2.30	-	-	-	-	-	0.80
Lime (%)	3.25	0.19	0.16	-	0.45	89.2	0.04	2.05	-	-	-	-	-	-

Table 3. Mineralogical composition of bentonite and kaolinite.

Mineralogy	Kaolinite (%)	Quartz (%)	Na-Montmorillonite (%)	Feldspar (%)	Calcite (%)	Micaceous Materials (%)	Organic Material (%)
Chemical formula	Al ₂ Si ₂ O ₅ (OH) ₄	SiO ₂	Na ₃₃ Mg ₃₃ Al _{1.67} Si ₄ O ₁₀ (OH) ₂	CaAlSi ₃ O ₈	CaCO ₃	-	-
Bentonite clay	0	18		20	3	0	0
Kaolinite clay	84	48		0	0	13	2

Table 4. Consistency limits and physical properties of kaolinite and Bentonite.

Properties	Kaolinite Clay	Bentonite Clay
Consistency limits		
Liquid limit w_L (%)	59	310
Plastic limit w_P (%)	28	49
Plasticity index I_p (%)	31	261
Other physical properties		
Water absorption	-	16.0
Density $^\circ C$	2.4	2.5 at 20 $^\circ C$
Bulk density $glcc$	-	1.18
Maximum dry density (kN/m^3)	14.21	11.26
Relative density g/cm^3	1.8	2.7
Solubility in water (g/L)	Insoluble	Insoluble
Natural moisture content (%)	28	14

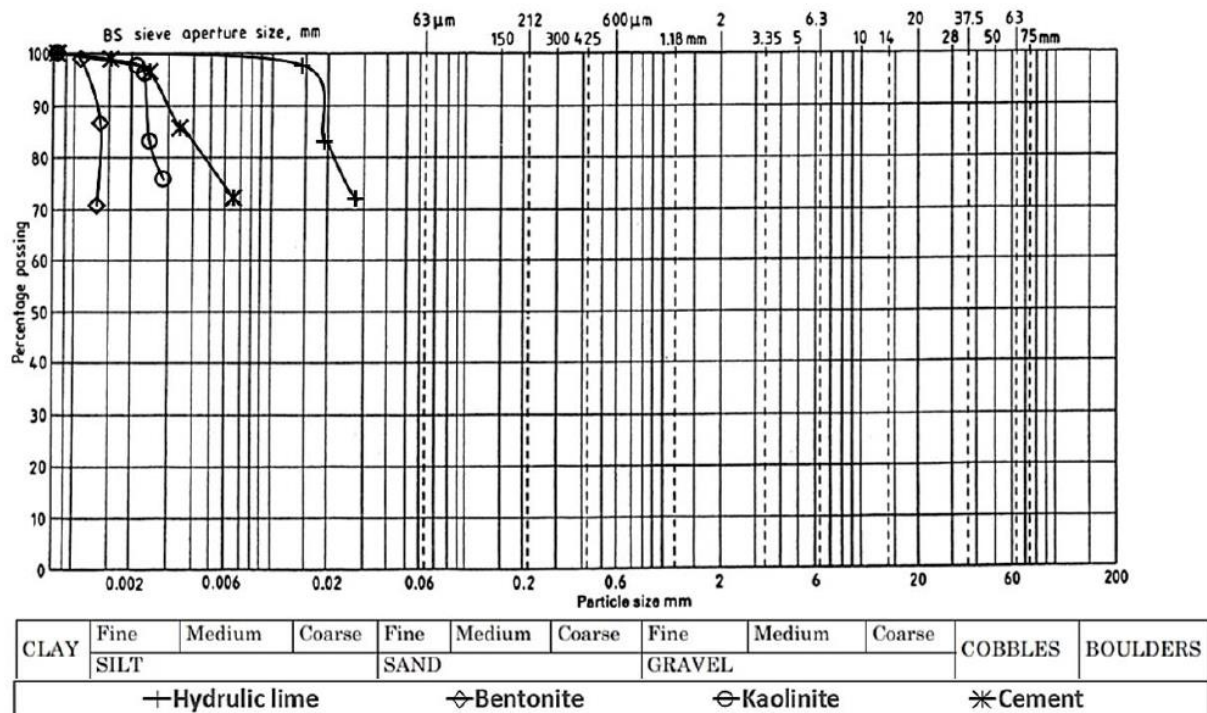


Figure 2. Particle size distribution of materials used in this study.

This study focused on road pavement thickness optimization using treated artificially-synthesized expansive subgrade composed of a mixture of bentonite and kaolinite at various percentages, in accordance with BS 1924-1:2018 [34]. The Atterberg limits and the compaction behavior of untreated bentonite and kaolinite clay were investigated. The California bearing ratio (CBR) for treated and untreated ASS was conducted to ascertain the strength and bearing capacity of treated expansive soil for use as road subgrade materials in road construction. SEM and EDX analyses were conducted for treated subgrade materials to see how the addition of binders affected the engineering properties of the subgrade materials. Based on the CBR values achieved in the laboratory test, pavement thickness and construction depth optimization were carried out in accordance with the CBR method recommended by the California state of highways to determine the effect of varying CBR values on pavement thickness and construction depth. The methodological process used to

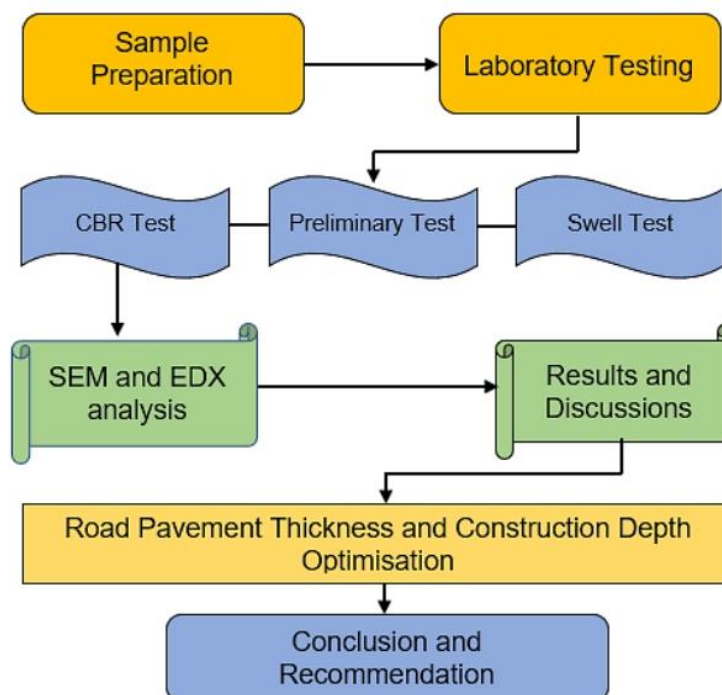


Figure 3. Methodological process.

Bentonite and kaolinite clays were mixed in various proportions by the weight of soil to form subgrade 1 = ASS 1 (25% bentonite, 75% kaolinite), subgrade 2 = ASS 2 (35% bentonite, 65% kaolinite) and subgrade 3 = ASS 3 (75% bentonite, 25% kaolinite). Compaction and Atterberg limit tests for the various proportions of the ASS were conducted in accordance with BS EN ISO 17892-1:2014 [35], BS EN ISO 17892-12:2018+A1:2021 [36], BS 1377-4:1990 [37], AASHTO T265 [38], ASTM D2216-19 [39], ASTM D4318-17e1 [40], AASHTO T90 [41] and AASHTO T89 [42] to determine their optimum moisture content (OMC) and maximum dry density (MDD).

2.1. California Bearing Ratio (CBR)

The California bearing ratio is a penetration test conducted to evaluate the strength and bearing capacity of road subgrade material. Knowing the CBR value of subgrade material prior to any road construction influences the design and construction of road pavement. According to BS EN 13286-47:2021 [43], the classification of a road in terms of pavement thickness and how much traffic a road can carry are dependent on the CBR value of the subgrade material. A typical CBR value of 2% equates to clay, while some sands may have a CBR value of 10%. A high-quality subgrade normally has a CBR value between 80–100% maximum [44]. Relevant road pavement design guidance documents such as the Design Manual for Roads and Bridges (DMRB) and the Indian Roads Congress—IRC-37-2001 [45] state that the higher the CBR value the thinner the road pavement, and the lower the CBR value the thicker the road pavement. During road pavement design, thicker pavements are recommended to compensate for the low CBR value of weak road subgrade material to enable it to carry a traffic load. According to [46], a document on flexible pavement design by the California bearing ratio method showed that a CBR value of 2% will require a road pavement thickness of 700 mm to carry heavy traffic (5443 kg), while a CBR value of 80% will require a pavement thickness of 70 mm to withstand a heavy traffic load (5443 kg). A subgrade with a CBR value < 2% is unacceptable for road construction and will require engineering or modification to make it suitable for use in road construction [46]. This means that CBR values affect the design, overall thickness and cost of road construction and has to be taken seriously during a road project.

CBR Sample Preparation and Testing

CBR test samples were prepared for all three ASS materials (treated and untreated). A total sample mass of 4 kg was required to achieve a fully compacted CBR mold. Based on total sample mass, bentonite and kaolinite at required proportions were weighed to form ASS 1 (25% bentonite, 75% kaolinite), ASS 2 (35% bentonite, 65% kaolinite) and ASS 3 (75% bentonite, 25% kaolinite). For treated ASS samples, various proportions of binders (8% lime and 20% cement) were selected based on a benchmark subgrade CBR value of 80%, capable of carrying a heavy traffic load of 5443 kg in accordance with the CBR method recommended by the California state of highways [46]. According to [44], a high-quality subgrade normally has a CBR value between 80–100% maximum. To achieve the target of 80% CBR, a range of cement and lime proportions were experimented with in subgrade mixtures using the intervals for cement and lime stabilization recommended by the Design Manual for Roads and Bridges (DMRB) HA 74/07 [47]. The cement and lime proportions were increased gradually (2%lime + 5%cement, 4%lime + 10%cement, 6%lime + 15%cement, etc.) until a CBR value of 80% was achieved for 8%lime 20%cement. The percentages of cement and lime were measured by weight of the total sample mass, and dry-mixed with the ASS materials until homogeneity was achieved. A measured amount of water was gradually added, based on the OMC for untreated ASS materials achieved during the proctor compaction test and mixed together to form a uniform mixture. Where the mixture looks and feels dry at OMC during the preparation of treated ASS materials due to the addition of binders (cement and lime), which imbibe water, a recommended amount of water within the range of 10–20% above the optimum moisture content (OMC) was added to the original moisture content (OMC) achieved during the proctor compaction test, in accordance with BS EN ISO 17892-1-2014 [35], BS EN 13286-47:2021 [43] and section 3/9 of the document [48]. A CBR mold (152 mm diameter × 178 mm high) was weighed on a scale without the collar, and the weight was recorded. The collar was later attached to the mold, and the uniformly mixed ASS material (4 kg) was divided into three equal parts and placed in layers in the mold during compaction. Each part was placed in the CBR mold and, with the help of a mechanical compactor, fitted with a 2.5 kg rammer; 62 blows were applied at different areas of the surface of each layer to ensure an even distribution of force. After the last layer was compacted, the mold containing the compacted sample was detached from the mechanical compactor. The collar was carefully removed, and the compacted ASS material was trimmed off using a pallet knife so that it was completely even with the top edge of the mold. The compacted ASS material with the mold and the base was weighed and the value recorded. At this stage, untreated ASS materials were tested for soaked and unsoaked CBR without curing. Treated (with binders) ASS samples and the mold were also wrapped in an airtight plastic bag, ready for curing at a room temperature of 20 ± 2 °C for 7 and 28 days, respectively. Figure 4a,b shows the mixing and testing process of the treated-unsoaked and treated-soaked CBR samples. Figure 5 shows the recommended OMC range recommended by [48].

CBR tests were carried out for all ASS material types (treated and untreated) to determine their bearing capacity in accordance with BS 13377-4:1990 [37] and BS EN 13286-47:2021 [43] using the Design Manual for Roads and Bridges (DMRB) CD 226 [49] and DMRB HA 74/07 [47] as a guide. The test was conducted to evaluate the subgrade strength of road and pavement by determining the ratio of force per unit area required to penetrate a soil mass with a standard circular plunger.

CBR test samples were prepared and tested for all three types of untreated ASS material in accordance with relevant standards. The aim of conducting a CBR test on untreated expansive artificially-synthesized (ASS) materials was to determine its bearing capacity for use as subgrade materials without any modification, re-engineering, or treatment. Untreated ASS samples prepared for all three types of ASS materials were tested for CBR immediately after compaction without soaking. The same samples were prepared and soaked for 96 h (4 days) immediately after compaction at a temperature of 20 ± 2 °C at a level that the sample was fully immersed in water in accordance with

BS EN 13286-47:2021 [43]. The idea of soaked CBR samples in this study was to investigate how the subgrade material would behave when the air voids in the sample are filled with water to simulate the effect and behavior of untreated expansive subgrade in the event of a flood. In this study, measured amounts of cement, lime and water were added to the ASS materials and mixed together until homogeneity. CBR test samples were prepared from the mix in accordance with the relevant standards. Samples were made for all three types of ASS material to be tested for unsoaked CBR after 7 and 28 days of curing at a room temperature of 20 ± 2 °C. Soaked CBR tests were conducted on samples soaked in water for 96 h (4 days) after 7 and 28 days curing at room temperature of 20 ± 2 °C in accordance with BS EN 13286-47:2021 [43]. The samples were fully immersed in water with a temperature of 20 ± 2 °C at a level that allows free access of the water to the top and bottom of the specimen. The idea of soaked CBR in this study was to investigate how treated subgrade material would behave when the air voids in the sample are filled with water to simulate the effect and behavior of stabilized or treated expansive road subgrade in the event of a flood.

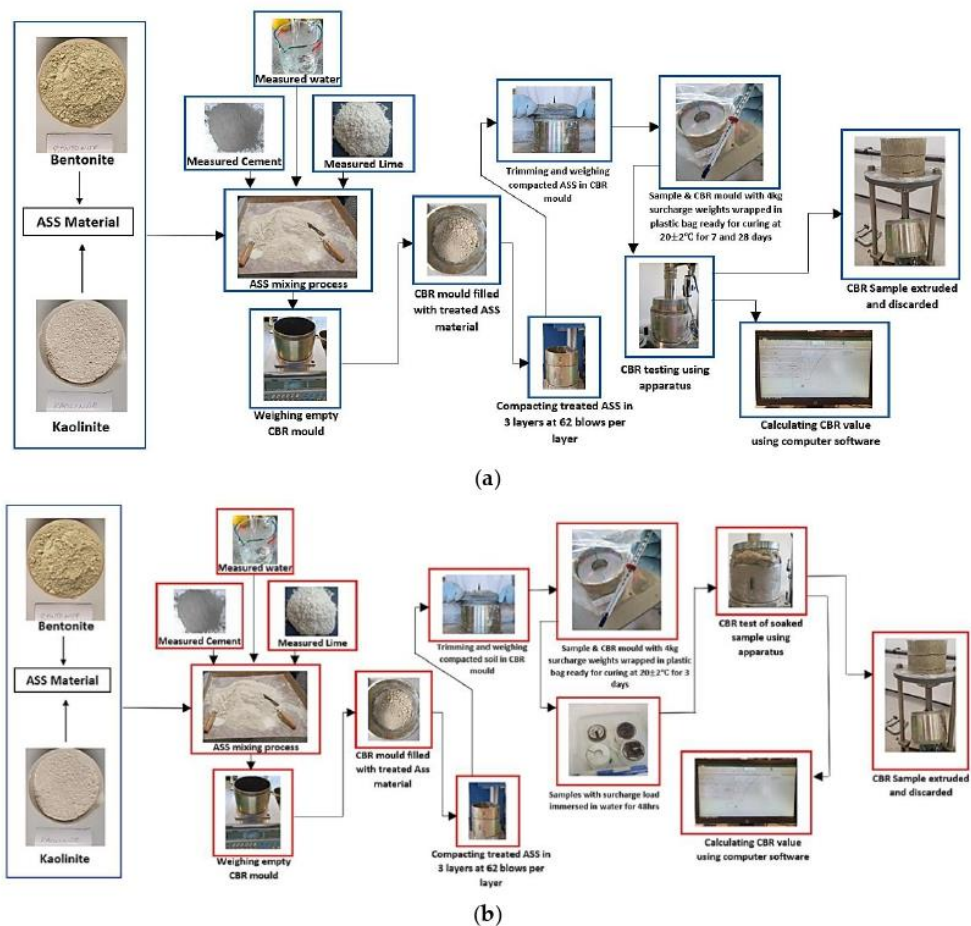
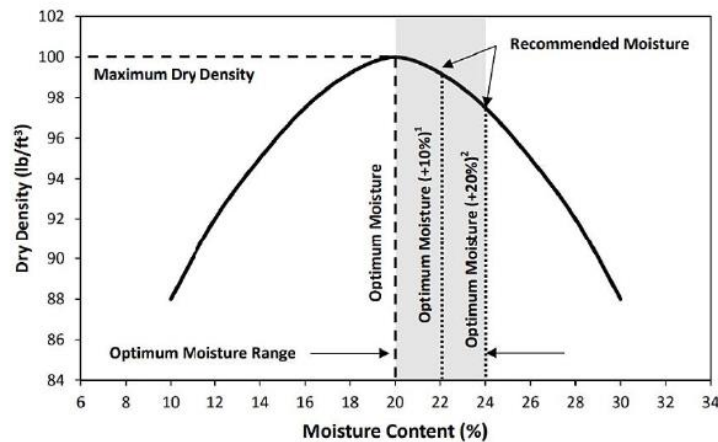


Figure 4. (a) The mixing and testing process of the treated-unsoaked CBR samples; (b) the mixing and testing process of the treated-soaked CBR samples.



¹Acceptable Range = Up to 20% above Optimum Moisture

²Recommended Range = 10% to 20% above Optimum Moisture

Figure 5. Moisture content control chart (Section 3/9 of [48]).

2.2. Swell Test of Treated and Untreated ASS Materials

Even though a significant and obvious amount of swell was observed after the soaking process of untreated ASS samples, a separate swell test was conducted on both untreated and treated ASS materials. The swell behavior for untreated and treated expansive ASS materials was tested using the linear expansion measurement method in accordance with BS EN 13286-49:2004 [50]. At this stage, the amount of swell or expansion observed in the various ASS materials was measured using a self-contained basic swell consolidometer (BSC) apparatus. The apparatus included a stainless-steel compaction ring with a diameter of 2.42, two porous stones (top porous stone with diameter 61.5 mm, 6.35 mm thick, and bottom porous stone diameter 84 mm, 6.35 mm thick), a loading weight of 2.87 kPa and a dial gauge. Treated and untreated ASS material with a total mass of 100 g with or without a binder inclusive was weighed. A measured amount of water was added at OMC, mixed uniformly and used to prepare samples for the swell test by compacting the ASS mixture into the stainless-steel compaction ring. The compacted samples were placed in the consolidometer between the two porous stones, which were already soaked in water to allow water to seep through them immediately at the start of the test. A loading weight to produce 2.87 kPa was placed on top of the porous stone on the sample, and a dial gauge indicator was set to the initial sample height with the tip of the plunger touching the top of the loading weight. The dial gauge reading was set to zero, and the consolidometer was filled with water to begin the test. Untreated ASS materials were tested for swell immediately after the compaction without curing. Treated ASS subgrade materials were wrapped in cling film and cured at a room temperature of $20 \pm 2^\circ\text{C}$ for 7 days before testing for swell. The aim of wrapping treated samples in cling film was to slow the rate of water evaporation and allow the binders (cement and lime) to chemically react in anticipation of reducing the swelling potential of the subgrade material. Dial gauge readings of the amount of swell were recorded daily for 28 days, and the data were analyzed to establish the swelling potentials of both treated and untreated ASS materials. Figure 6a–e shows the obvious swell after the soaked CBR test, including the consolidometer apparatus, compacted swell samples in the stainless-steel compaction ring and the swell set-up for treated and treated and untreated ASS samples after the swell test.



Figure 6. (a) Swell observed after soaking CBR untreated ASS samples; (b) consolidometer apparatus used in this study; (c) compacted swell samples in stainless-steel compaction ring; (d) swell set-up for treated and untreated ASS materials; (e) treated and untreated ASS samples after the swell test.

2.3. Microstructural Properties of Treated Subgrade Material

Microstructural properties are the properties that influence the physical properties of materials such as hardness, strength, high/low-temperature behavior, toughness, wear resistance and others [2]. Microstructural properties of materials can be determined in the laboratory by conducting a scanning electron microscopy (SEM) analysis, energy dispersive X-ray (EDX) analysis, radar detection, or a Mises strain test, among others [2]. A study conducted by [51] shows the SEM analysis results, which showed a high C-S-H gel development, resulting in high strength after adding 6% of limited leather waste ash (LLWA) in a mix. EDX patterns showed a high formation of calcium silicate hydrate (C-S-H) gel

after 28 days when the expansive soil was stabilized or treated with 20% GGBS [52]. A combination of SEM and EDX analysis provides a better understanding of the surface material and the elemental composition of a sample, allowing for a more quantitative result offering the chemical composition and elemental investigation to provide a comprehensive evaluation of the results. In this study, scanning electron microscopy (SEM) and energy dispersive X-ray (EDX) analysis were conducted to determine the elemental composition of the stabilized or treated ASS materials, providing high-resolution imaging for identifying and evaluating the material's surface structure, contaminants, flaws/corrosion and unknown particles and to determine the cause of failure and interaction between the materials. The SEM and EDX equipment used in this study include the FEI Quanta 650 field emission scanning electron microscope manufactured by Philips, supplied by Frost bank Tower, 401 Congress Avenue, Suite 1760, Austin, Texas USA and Oxford Instruments Aztec Energy EDX system using an X-Max 50 detector with a coverage area of 50 mm² and a sputter Coater Emscope SC500 gold sputter coating unit manufactured by Oxford Instruments Inc. and supplied by Science House, Church Farm Business Park, Corston, Bath, UK. Figure 7a–d describes how samples are mounted, shows the stub holder for the SEM chamber and the Gold Sputter Coating Unit and shows the treated ASS samples ready for the SEM and EDX test.

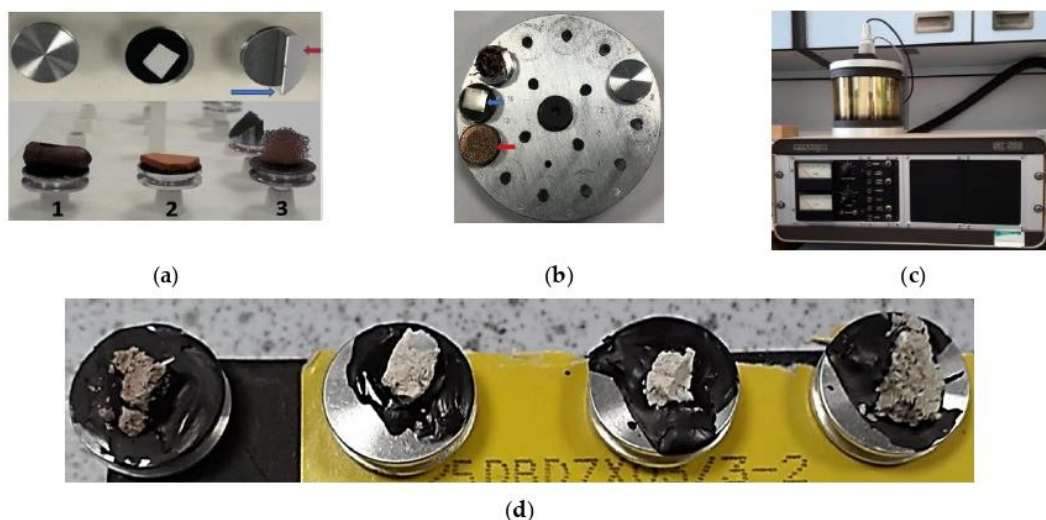


Figure 7. (a) (1) Samples are mounted on standard aluminum stubs 13 mm in diameter. The stub has a groove at the side to facilitate handling using forceps; (2) the aluminum stub with a double-sided adhesive black conductive carbon, tab. A piece of filter paper has been cut to size and pressed down at the corners using forceps onto the tab; (3) this stub allows one to see a transverse view. The sample is mounted against the vertical face (blue arrow). The red arrow indicates a 45° angle face. (b) The stub holder for the SEM chamber. The blue arrow indicates a piece of metal that requires no further preparation. The red arrow shows a non-conductive sample that has been sputter coated with gold to make it conductive; (c) gold sputter coating unit; (d) treated artificially-synthesized subgrade (ASS) samples mounted and ready for the SEM and EDX analysis.

3. Results and Discussion

3.1. Compaction and Atterberg Limits for Untreated ASS Materials

Results obtained after the proctor compaction and the Atterberg limit test show a high OMC, liquid limit (LL) and plastic limit (PL) recorded for ASS 3 (75% bentonite and 25% kaolinite), followed by ASS 2 (35% bentonite and 65% kaolinite) and ASS 1 (25% bentonite and 75% kaolinite). The increase and decrease in proctor compaction and Atterberg limit test results observed in the various ASS materials were a result of bentonite content in the mix. Bentonite clays are very expansive, with a high plasticity, and they imbibe a lot of water. After the preliminary test, the results showed a high plasticity for ASS 1

(25% bentonite and 75% kaolinite), a very high plasticity for ASS 2 (35% bentonite and 65% kaolinite) and an extremely high plasticity for ASS 3 (75% bentonite and 25% kaolinite), respectively. The gradual increase in plasticity as bentonite proportion increased is due to the high clay content in bentonite. According to [53], the gradual increase in the percentage of bentonite clay in a mix increases the plasticity index of the soil. Bentonite is highly water-absorbent and has high shrinkage and swell characteristics [54]. Figure 8 a–c shows the proctor compaction, Atterberg limit test results, Liquid and Plastic limit results against plasticity index and plasticity index chat for various ASS materials.

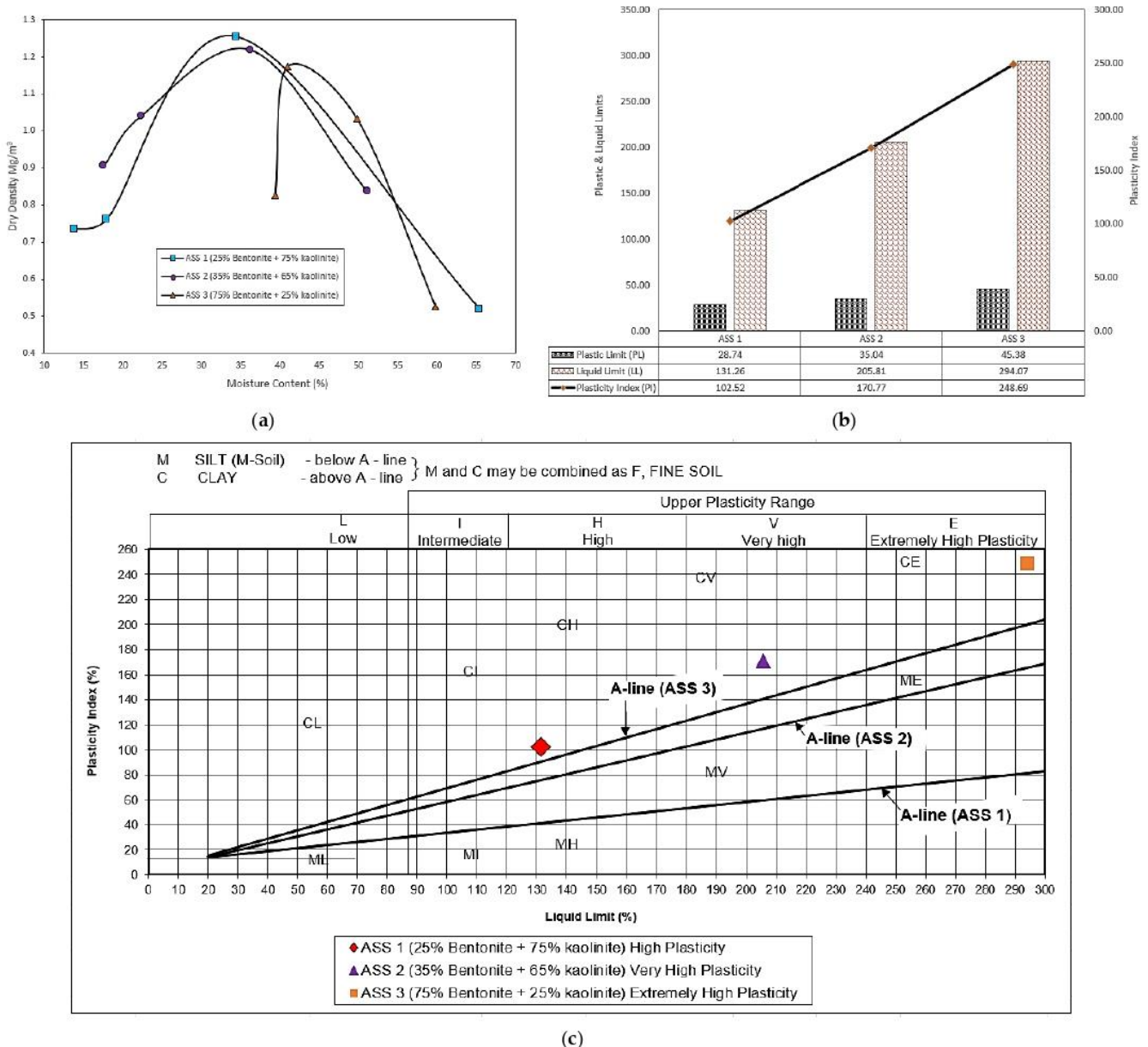


Figure 8. (a) Proctor compaction test results; (b) Atterberg limit test results against plasticity index; (c) plasticity index chat.

3.2. Moisture Content and Dry Density Test of CBR Sample

The moisture content and dry density test were conducted on untreated CBR samples after testing by taking samples from the top and bottom of the CBR sample. This test was to determine the variation in moisture content and dry density at the top and bottom of the ASS sample immediately after compaction. The results showed a higher moisture content at the bottom of the CBR sample compared to the top of the sample. This could be a result of the settlement of water to the base of the sample due to the influence of gravity and the vertical force applied by the rammer. This is called gravitational water drain, which acts as a relative amount of water (capillary water) that is held between the soil particles due to the force of cohesion (surface tension that attracts water molecules to each other) and adhesion (the attraction of water molecules to other surfaces) that are stronger than gravity [55]. The highest moisture content was recorded at the top and bottom for ASS 2 (35% bentonite and 65% kaolinite), and ASS 1 and 3 recorded similar moisture content values for both the top and bottom of the sample. The highest dry density was recorded at the top of ASS 3, followed by a drastic reduction in dry density at the bottom of ASS 3 (75% bentonite and 25% kaolinite). ASS 2 recorded similar dry densities for both the top and bottom of the sample. Figure 9a,b shows the results of the moisture content and dry density for the top and bottom of the CBR samples.

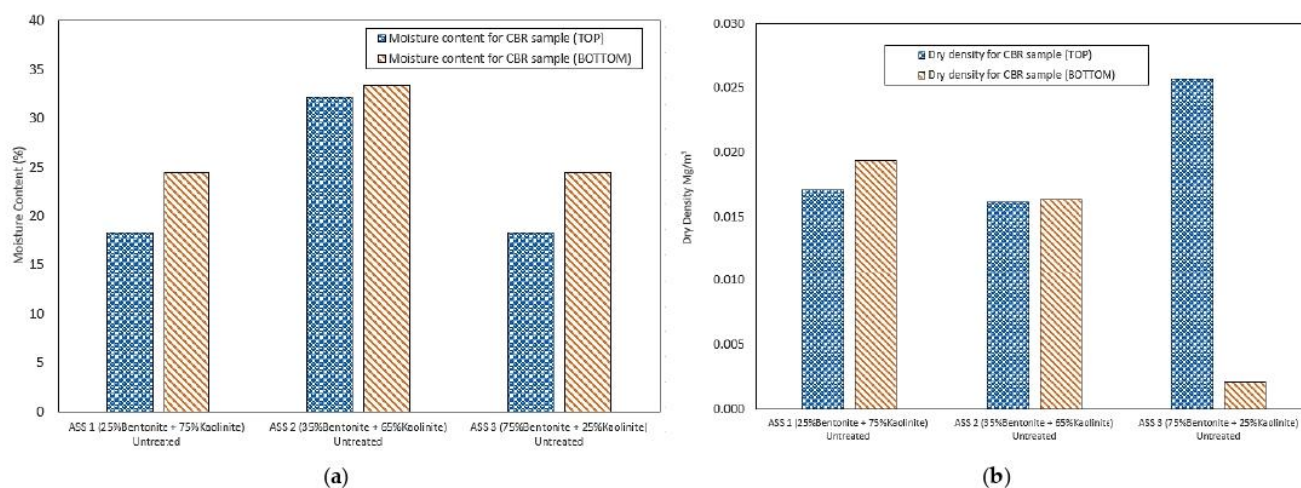


Figure 9. (a) Moisture content for the top and bottom of the CBR samples; (b) dry density for the top and bottom of the CBR samples.

3.3. California Bearing Ratio (CBR)

3.3.1. Untreated ASS Materials

A CBR of 9% and 2% was recorded for the untreated and untreated-soaked ASS 3 (75% bentonite and 25% kaolinite) samples, representing the highest CBR values for untreated and untreated-soaked ASS materials. The results showed that the high plasticity subgrade (high amount of bentonite present in ASS 3) naturally exhibited a reasonably high bearing capacity, even though it may have high shrink-swell potentials. However, this naturally-high bearing capacity of bentonite can be affected by the addition of cement and or lime as binders in the mixture. ASS 1 (25% bentonite and 75% kaolinite) also achieved a CBR value of 8% for untreated-unsoaked and 0.9% for untreated-soaked ASS materials, followed by ASS 2 (35% bentonite and 65% kaolinite) with an untreated-unsoaked value of 5% and an untreated-soaked of 0.8%, respectively. Very low CBR values were observed for all soaked ASS samples, and this indicated that high-plasticity subgrade materials have a low bearing capacity when wet. However, a gradual increase in CBR values was observed for soaked samples with an increase in bentonite content. A naturally high CBR value was observed for mixtures with high bentonite content without treatment. However, it was observed that the addition of lime and cement reduced the natural bearing capacity of

bentonite in the mixture. According to [56], pure bentonite has a high CBR value, which equates to 35.8%. This confirms the findings in this study that bentonite subgrade materials exhibit naturally high CBR values. Overall, the test results showed that the higher the presence of bentonite in ASS, the higher the CBR value and vice versa. Even though some value of CBR was recorded for ASS 1 soaked and ASS 2 soaked, these values were unacceptable for use in road construction, except for ASS 3 which hit the 2% mark. According to IAN73/06 [57], CBR values below 2% are not acceptable for use and will require some modification. Figure 9a shows the CBR results for the untreated ASS materials.

3.3.2. Treated ASS Materials

The highest CBR value of 100% was recorded for ASS 2 (35% bentonite and 65% kaolinite), followed by a CBR of 90% for ASS 1 (25% bentonite and 75% kaolinite) and then 80% for ASS 3 (75% bentonite and 25% kaolinite) all after 28 days of curing. CBR values took a nosedive from 80% for ASS 1, to 60% for ASS 2 and 30% for ASS 3 all after seven days of curing. This showed a decrease in CBR value as bentonite content increased. Reasonably high CBR values were observed with an increase in curing age for ASS 2 and ASS 3, which were of a very high and extremely high plasticity index. ASS 2 at 28 days recorded the highest CBR values due to the presence of bentonite in the mix. As mentioned earlier in Section 3.3.1, the naturally-high bearing capacity of bentonite can be affected by the addition of lime and cement during the stabilization process. Thus, the reduction in the CBR value for ASS 3 could be due to the high presence of bentonite content in the mixture, and the high CBR value for ASS 1 and ASS 2 could be a result of low bentonite content in the mix, as they both recorded very high CBR values of 90 and 100%. According to [58], the unconfined compressive strength of lime-treated soil increased considerably because of a low content of bentonite added in the mixture. Reference [59] also stated that limited percentages of bentonite in a mix using lime as a binder is enough to improve the soil strength. This shows that high-plasticity bentonite subgrade materials exhibit a high bearing capacity when they are dry after they come in contact with water, and they are very weak when wet. This attribute of high-plasticity subgrade materials was responsible for the high CBR values and high swell observed in this study. According to [60], soils with a high plasticity index exhibit reasonable CBR values. Even though soils with a high plasticity index exhibit high strength when dry after coming into contact with water, their strength potential can be affected by the binders used during the stabilization process. Unlike untreated ASS samples, CBR values for soaked-treated samples decreased with an increase in bentonite (highly plastic clay) content because clays are weak in compression when wet. However, the CBR values achieved for the soaked-treated samples were good enough for use in road construction. A study conducted by [61] showed a reduction in CBR values from 15.41% to 3.56% as the bentonite content in a mix increased from 5%, 10%, 15%, 20% and 25% respectively. CBR values (8%) for untreated ASS 1 increased to 80% and 90% after treatment with cement and lime and after they were cured for 7 and 28 days. CBR values (5%) for untreated ASS 2 increased to 60% and 100% after treatment with cement and lime and after they were cured for 7 and 28 days. CBR values (9%) for untreated ASS 3 increased to 30% and 80% after treatment with cement and lime and after they were cured for 7 and 28 days. CBR values (0.9%) for untreated-soaked ASS 1 increased to 50% when soaked for four days after treatment with cement and lime and they were cured for seven days. CBR values (0.8%) for untreated-soaked ASS 2 increased to 40% when soaked for four days after treatment with cement and lime and they were cured for seven days. CBR values (2%) for untreated-soaked ASS 3 increased to 30% when soaked for four days after treatment with cement and lime and they were cured for seven days. This trend indicates a significant increase in CBR values with an increase in curing age after the subgrade materials were treated with cement and lime. Although an increase in CBR values was observed for untreated-soaked ASS samples after they were treated with cement and lime and they were cured and soaked for four days, a gradual reduction in CBR values in treated-soaked samples was observed for all ASS materials. This shows that the CBR values for subgrade

materials with a high plasticity index can reduce when they are soaked in water for days. The CBR values achieved for treated-soaked and treated-uns soaked were above 2% and were suitable for use in road construction. This study has established that cement and lime have the ability to increase the bearing capacity of expansive road subgrade material. Overall, a decrease in CBR values was observed in treated ASS samples as bentonite content increased. Figure 10b shows the CBR results for the treated ASS materials.

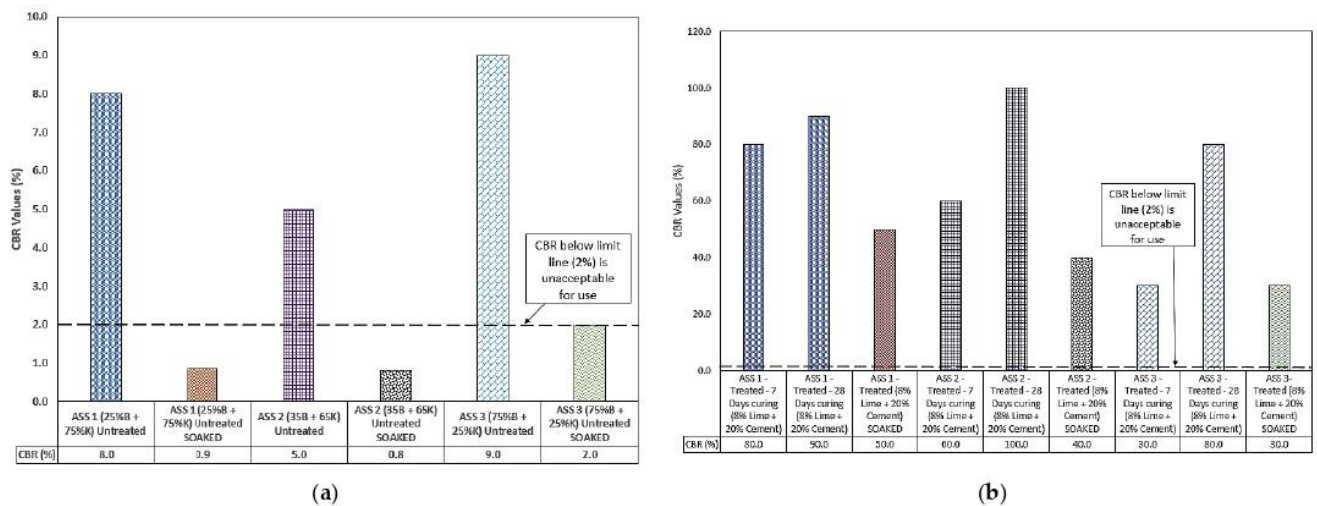


Figure 10. (a) Results for the untreated ASS materials, where B is bentonite and K is kaolinite; (b) treated artificially-synthesized subgrade.

3.4. Swell for ASS Materials

3.4.1. Untreated ASS Materials

ASS materials began to swell after day 1, and ASS 1 and ASS 2 continued to swell until day 14, when no further swell was observed. ASS 3 continued to swell until day 3, with a slight reduction in swell on day 4 and a rise in swell at day 5, until no further swell was recorded. The highest swell percentage of 56.76% was recorded for ASS 3 (75% bentonite and 25% kaolinite), and the lowest swell percentage was 35.92% for ASS 1 (25% bentonite and 75% kaolinite), while ASS 2 (35% bentonite and 65% kaolinite) recorded a swell percentage of 40.52% all after 28 days of curing. This shows a high swell with an increase in bentonite content. This proves that extremely high and high plasticity subgrade materials exhibit very high swell potentials. According to standard practice, a subgrade swell > 2.5% is unacceptable and would require treatment or removal and replacement [62]. Hence, untreated ASS materials in this study did not meet the standard for use as subgrade material. Figure 10a shows the swell results for untreated ASS materials. The maximum swell values obtained at day 4 compared with four days soaked untreated CBR values shows that ASS 3, composed of very high bentonite (extremely high plasticity index) content, recorded a swell percentage value of 55%, with the highest CBR value of 2% for untreated-soaked ASS materials, followed by ASS 2 and ASS 1 of 33% swell, 0.8% CBR and 29% swell, 0.9% CBR, respectively. This shows that the higher the swell the lower the CBR value, and it confirms the statement made in this study about bentonite exhibiting some reasonable amount of CBR, even though they have very high swelling potentials.

3.4.2. Treated ASS Materials

The swelling potential of ASS reduced drastically from 55% for untreated ASS 3 (75% bentonite and 25% kaolinite) to 0.2% after treating ASS materials using cement and lime. The lowest swell value of 0.04% was recorded for ASS 1 and ASS 2, with high kaolinite contents, compared to ASS 3 with a high bentonite content. However, a swell value of 0.2% (even though acceptable) recorded for ASS 3 was the highest recorded for treated ASS samples due to the high amount of bentonite (extremely high plasticity index) content. This

indicated very high swell potentials for subgrade materials with a high plasticity index. Swell values recorded for treated ASS materials in this study fell below the unacceptable 2.5% swell limit. Hence, all treated ASS materials in the study met the standard for use as subgrade materials in road construction. Figure 11b shows the results for treated ASS materials, and Figure 11c shows a combined swell result of both untreated and treated ASS materials for easy comparison. ASS 3, composed of a very high bentonite content, obtained the highest acceptable swell value of 0.2% against the lowest CBR value of 30% for treated-soaked ASS materials. This confirms the statement earlier made in this study, that binders (cement and lime) used during a road subgrade stabilization process can affect the bearing capacity of bentonite clay. After investigating the maximum swell values obtained after four days of soaking the treated CBR samples, a reduction in the CBR values with an increase in bentonite content, and an increase in swell values as bentonite content increased, was observed. Figure 11d and e shows the day 4 swell compared with the four-day soaked untreated CBR values and the day 4 swell compared with the four-day soaked treated CBR values.

3.5. Microstructural Properties of Treated Subgrade Material

In this study, the SEM image and EDX results for the treated ASS 1 (25% bentonite + 75% kaolinite + 8% lime + 20% cement), ASS 2 (35% bentonite + 65% kaolinite + 8% lime + 20% cement) and ASS 3 (75% bentonite + 25% kaolinite + 8% lime + 20% cement) show the formation of calcium silicate hydrate (C-S-H) gel and calcium aluminate hydrate (C-A-H) gel with an increase in curing age. A clear presence of high Ca-Si-Al elements responsible for the formation of tobermorite gel was observed from the SEM map for the various chemical compositions in different areas of the ASS materials. Tobermorite is a chemical composed of calcium silicate hydrate mineral, with the chemical formula $[Ca]_5 [Si]_6 O_{16} [(OH)]_2 \cdot 4H_2O$ or $[Ca]_5 [Si]_6 [(O,OH)]_{18} \cdot 5H_2O$, and it is responsible for the detoxification and strength gain in a mix. According to investigations conducted by [63], the relationship between the content of minerals formed in a mix and their detoxification efficiency shows that the formation of tobermorite helps to promote detoxification in a mix. This means the presence of toxic elements found in a mix due to the addition of binders (especially waste materials or industrial by-products, which can be very toxic due to leaching) can be detoxified due to the formation of a high amount of tobermorite (C-S-H and C-A-H gel) in the mix. During the hydration process in a cement/lime mix, cementitious products are released (C-S-H and C-A-H gel), which are responsible for the strength gain in the mixture [2,64]. The formation of C-S-H and C-A-H gel in this study acted as a binding agent responsible for the strength gain and the high CBR value of the subgrade materials. According to [2], Portland cement with lime in the presence of water forms hydraulic compounds: Portland cement + water \rightarrow calcium silicate hydrate = $Ca(OH)_2 + CO_2 \rightarrow CaCO_3 + H_2O$. Extra amounts of hydraulic cement are formed when the cement reacts with lime = Pozzolana + $Ca(OH)_2 + Water \rightarrow C-S-H$ gel. At the end of seven days of curing, a formation of 16.21% calcium (Ca) was found in ASS 1, 30.51% calcium (Ca) in ASS 2 and 21.96% calcium (Ca) in ASS 3, respectively. All ASS samples cured for 28 days and exhibited a very high presence of C-S-H and C-A-H gel. At the end of 28 days of curing, the formation of 16.21% calcium (Ca) found in the seven-day ASS 1 increased to 24.75%, the 30.51% calcium (Ca) in the seven-day ASS 2 increased to 32.56% and the 21.96% calcium (Ca) for ASS 3 increased to 33.08%, respectively. This shows that the formation of C-S-H gel increased with an increase in curing age. The continuous formation of C-S-H gel with an increase in curing age within a pore structure can contribute to strength development in a mix; the higher the C-S-H gel content, the higher the strength in the samples [2,53]. Figures 12a–f and 13a–f show the SEM image, mapping and EDX results for ASS 1, 2 and 3 at various points of the sample after 7 and 28 days of curing.

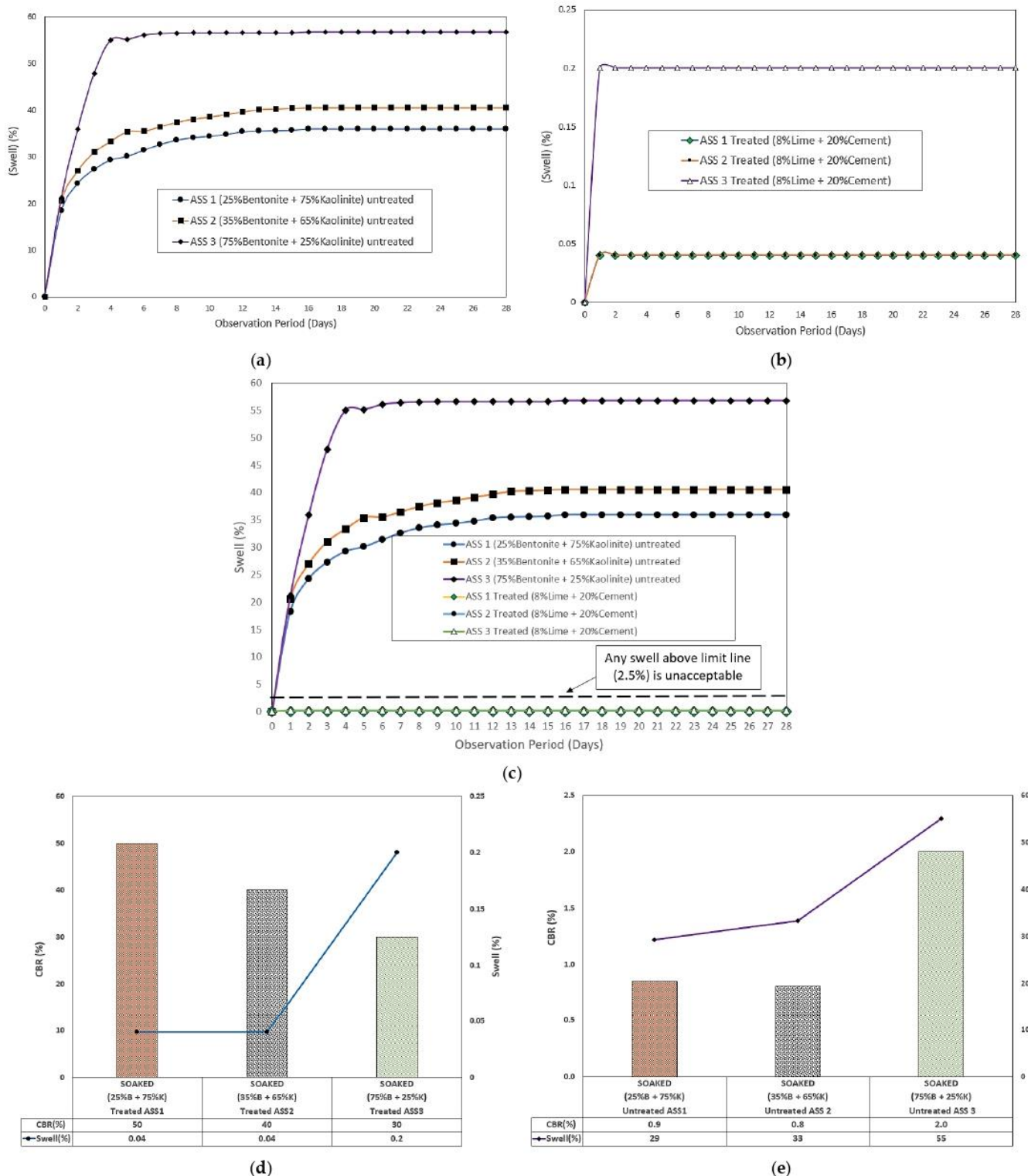


Figure 11. (a) Results for the untreated ASS materials; (b) results for the treated ASS; (c) combined swell result for untreated and treated ASS materials; (d) day 4 untreated-soaked CBR values against day 4 swell, where B = bentonite and K = kaolinite; (e) day 4 treated-soaked CBR values against day 4 swell, where B = bentonite and K = kaolinite.

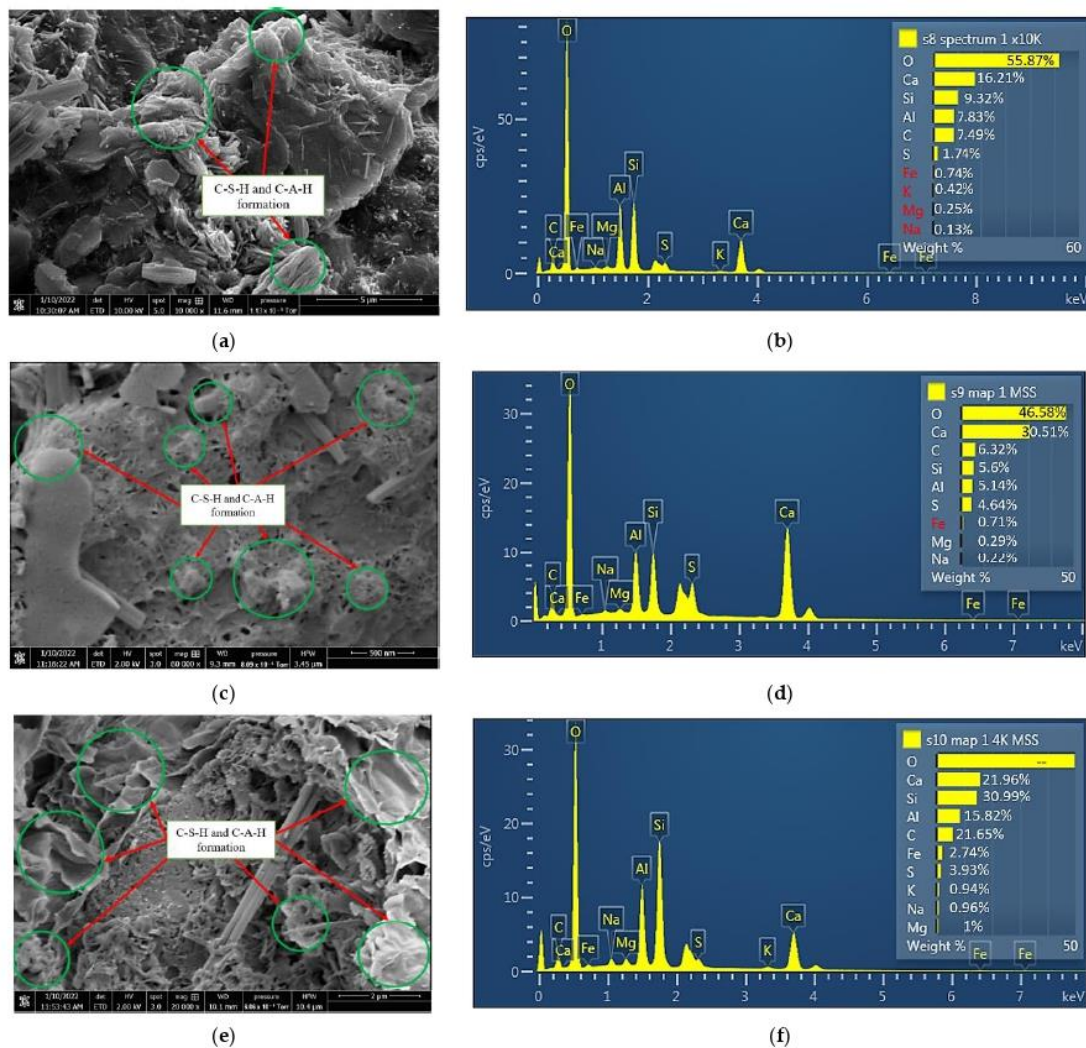


Figure 12. (a) SEM image results for ASS 1 after seven days of curing; (b) EDX results for ASS 1 after seven days of curing; (c) SEM image results for ASS 2 after seven days of curing; (d) EDX results for ASS 2 after seven days of curing; (e) SEM image results for ASS 3 after seven days of curing; (f) EDX results for ASS 3 after seven days of curing.

3.6. Road Pavement Thickness and Construction Depth Optimization

Road pavement thickness and construction depth optimization were conducted using the laboratory CBR values obtained for the various types of ASS materials in this study. The CBR values obtained in this study were analyzed with the aim of reducing the road pavement thickness and construction depth, while increasing the strength, durability and performance of the road pavement structure without compromising the relevant standards used in road design. According to [65], pavement thickness is determined by the subgrade strength, and it is good to make the subgrade as strong as possible. Road pavement thickness and construction depth optimization in this study was carried out in compliance with the CBR method recommended by the California state of highways for light traffic (3175 kg), medium traffic (4082 kg) and heavy traffic (5443 kg), respectively [46]. Relevant guidance, such as the Design Manual for Roads and Bridges (DMRB) CD 226 [49] and the Indian Roads Congress—IRC-37-2001 [45], used in flexible road pavement design, have shown that high CBR values are associated with a thinner road pavement thickness and a low CBR value results in a thicker pavement structure. The pavement thickness and construction depth determination chart recommended by the California state of highways

were used to determine the pavement thickness and associated construction depth for various CBR values.

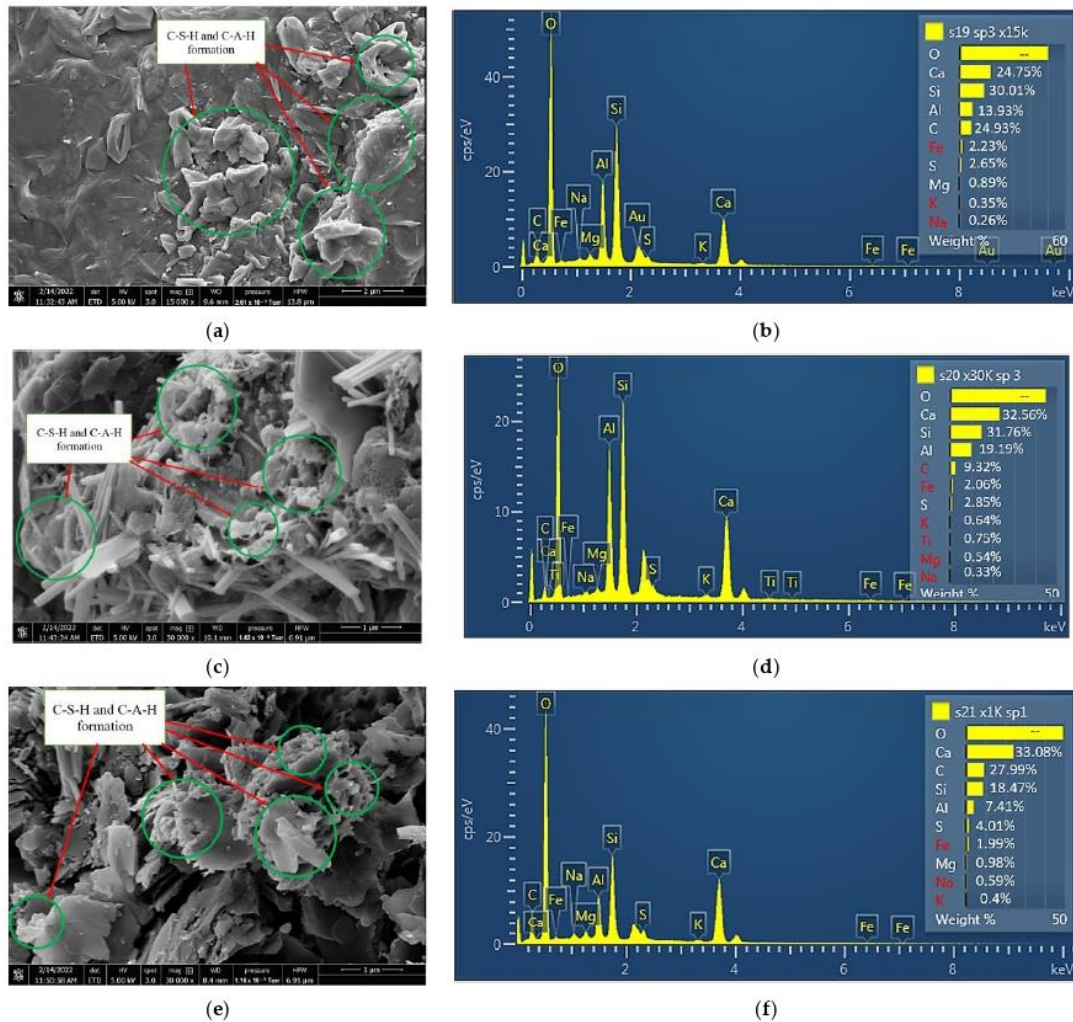


Figure 13. (a) SEM image results for ASS 1 after twenty-eight days of curing; (b) EDX results for ASS 1 after twenty-eight days of curing; (c) SEM image results for ASS 2 after twenty-eight days of curing; (d) EDX results for ASS 2 after twenty-eight days of curing; (e) SEM image results for ASS 3 after twenty-eight days of curing; (f) EDX results for ASS 3 after twenty-eight days of curing.

After pavement thickness optimization was conducted using the CBR values achieved in this study, it was observed that the pavement thickness reduced with an increase in CBR value. Hence, the higher the CBR value, the thinner the pavement thickness and vice versa. A significant difference in pavement thickness was observed between the lowest and the highest CBR value, and the pavement thickness for the CBR value deferred between the various traffic types. It was observed that a heavy traffic load required a thicker pavement, and a light traffic load required a thinner pavement, even though the same CBR value was used in their analysis. This is because heavy traffic requires thicker pavement to be able to carry a traffic load, reduce fatigue and control the deterioration of the road pavement. According to [66], road pavements are designed for predicted levels of traffic to control deterioration due to the accumulation of small amounts of damage caused by the passage of each vehicle. Pavement with less than about 180 mm of asphalt deforms at a high rate, but thicker pavement deforms at a lesser rate [66]. It is more economical to design road pavement for the existing subgrade capacity than to import or raise the subgrade support by using an extra-thick subbase [67]. The pavement thickness determination chart

recommended by the California state of highways was used as a guide to determine light, medium and heavy traffic classifications for the construction depth determination. It was observed that the pavement depth of construction reduced as the CBR value increased, and the pavement depth of construction increased with an increase in traffic load. The highest pavement depth of construction was recorded for the CBR value of 2% for a heavy traffic load above 4500 kN, and the least pavement depth of construction was recorded for the CBR value of 100% for a light traffic load between 15–45 kN. A huge difference between the pavement depth of heavy traffic compared to light and medium traffic was observed. This is because heavy traffic required a robust road pavement to transfer the traffic load into the ground and reduce the rate of pavement deterioration. Very low CBR values of 2% and 0.81% were recorded for untreated-soaked ASS samples, resulting in thicker pavements. According to relevant guidance such as the IAN73/06 [57], CBR values less than 2% are unacceptable for use in road construction and would require modification or treatment to improve their engineering properties. Figures 14 and 15 show the road pavement thickness and depths of construction optimization for CBR values achieved in this study. An increase in pavement thickness and construction depth was observed as the traffic load increased from light, medium to heavy traffic for both treated and untreated subgrade materials. It was also observed that ASS 3 (extremely high plasticity) recorded the thickest pavement with the lowest CBR value for treated and untreated ASS materials. An increase in swell and pavement thickness was observed as bentonite content increased in ASS materials, with ASS 3 (high bentonite content) recording the highest swell. Unacceptable CBR values for untreated ASS 1 and ASS 2 recorded a reasonably high swell; however, a high swell, pavement thickness and construction depth were recorded for the ASS 3 light, medium and heavy traffic loads. A gradual increase in pavement thickness and construction depth was observed with a rise in swell for ASS 1 to 3 light, medium and heavy traffic loads. Swell values increased drastically for treated-soaked ASS 3 for light, medium and heavy traffic loads (see Figures 14 and 15). Figure 16 shows the day 4 soaked pavement thickness and the depth of construction against day 4 swell values for the treated and untreated ASS samples.

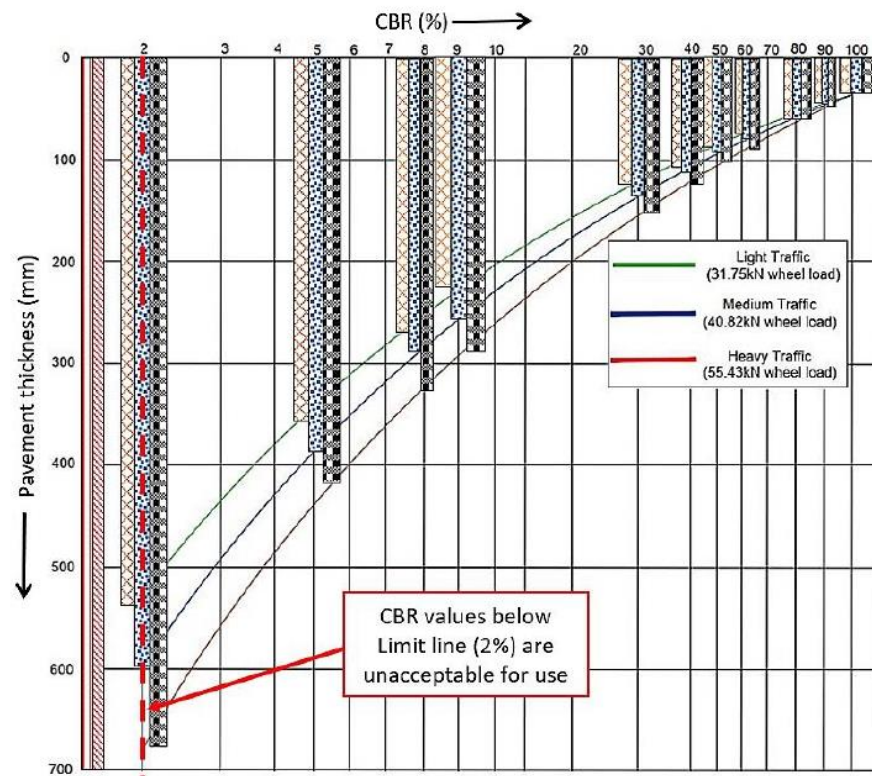


Figure 14. Cont.

<ul style="list-style-type: none"> ☐ ASS 1 CBR - 8% Untreated unsoaked - Light traffic - PAV Thickness 270mm ☒ ASS 1 CBR - 8% Untreated unsoaked - Medium traffic - PAV Thickness 290mm ☑ ASS 1 CBR - 8% Untreated unsoaked - Heavy traffic - PAV Thickness 320mm 	<ul style="list-style-type: none"> ☐ ASS 2 CBR - 60% Treated 7 days curing unsoaked - Light traffic - PAV Thickness 70mm ☒ ASS 2 CBR - 60% Treated 7 days curing unsoaked - Medium traffic - PAV Thickness 80mm ☑ ASS 2 CBR - 60% Treated 7 days curing unsoaked - Heavy traffic - PAV Thickness 90mm
<ul style="list-style-type: none"> ☐ ASS 1 CBR - 50% Treated soaked - Light traffic - PAV Thickness 80mm ☒ ASS 1 CBR - 50% Treated soaked - Medium traffic - PAV Thickness 90mm ☑ ASS 1 CBR - 50% Treated soaked - Heavy traffic - PAV Thickness 100mm 	<ul style="list-style-type: none"> ☐ ASS 2 CBR - 100% Treated 28 days curing unsoaked - Light traffic - PAV Thickness 30mm ☒ ASS 2 CBR - 100% Treated 28 days curing unsoaked - Medium traffic - PAV Thickness 30mm ☑ ASS 2 CBR - 100% Treated 28 days curing unsoaked - Heavy traffic - PAV Thickness 30mm
<ul style="list-style-type: none"> ☐ ASS 1 CBR - 80% Treated 7 days curing unsoaked - Light traffic - PAV Thickness 50mm ☒ ASS 1 CBR - 80% Treated 7 days curing unsoaked - Medium traffic - PAV Thickness 55mm ☑ ASS 1 CBR - 80% Treated 7 days curing unsoaked - Heavy traffic - PAV Thickness 60mm 	<ul style="list-style-type: none"> ☐ ASS 3 CBR - 9% Untreated unsoaked - Light traffic - PAV Thickness 220mm ☒ ASS 3 CBR - 9% Untreated unsoaked - Medium traffic - PAV Thickness 250mm ☑ ASS 3 CBR - 9% Untreated unsoaked - Heavy traffic - PAV Thickness 298mm
<ul style="list-style-type: none"> ☐ ASS 2 CBR - 5% Untreated unsoaked - Light traffic - PAV Thickness 350mm ☒ ASS 2 CBR - 5% Untreated unsoaked - Medium traffic - PAV Thickness 390mm ☑ ASS 2 CBR - 5% Untreated unsoaked - Heavy traffic - PAV Thickness 410mm 	<ul style="list-style-type: none"> ☐ ASS 3 CBR - 2% Untreated soaked - Light traffic - PAV Thickness 540mm ☒ ASS 3 CBR - 2% Untreated soaked - Medium traffic - PAV Thickness 600mm ☑ ASS 3 CBR - 2% Untreated soaked - Heavy traffic - PAV Thickness 680mm
<ul style="list-style-type: none"> ☐ ASS 2 CBR - 40% Treated soaked - Light traffic - PAV Thickness 105mm ☒ ASS 2 CBR - 40% Treated soaked - Medium traffic - PAV Thickness 110mm ☑ ASS 2 CBR - 40% Treated soaked - Heavy traffic - PAV Thickness 120mm 	<ul style="list-style-type: none"> ☐ ASS 3 CBR - 30% Treated 7 days curing unsoaked - Light traffic - PAV Thickness 120mm ☒ ASS 3 CBR - 30% Treated 7 days curing unsoaked - Medium traffic - PAV Thickness 130mm ☑ ASS 3 CBR - 30% Treated 7 days curing unsoaked - Heavy traffic - PAV Thickness 150mm
<ul style="list-style-type: none"> ☐ ASS 1 CBR - 90% Treated 28 days curing unsoaked - Light traffic - PAV Thickness 48mm ☒ ASS 1 CBR - 90% Treated 28 days curing unsoaked - Medium traffic - PAV Thickness 49mm ☑ ASS 1 CBR - 90% Treated 28 days curing unsoaked - Heavy traffic - PAV Thickness 50mm 	<ul style="list-style-type: none"> ☒ ASS 1 CBR - 0.85% Untreated soaked (unacceptable) ☒ ASS 2 CBR - 0.81% Untreated soaked (unacceptable)

Figure 14. Road pavement thickness optimization using the chart for pavement thickness determination.

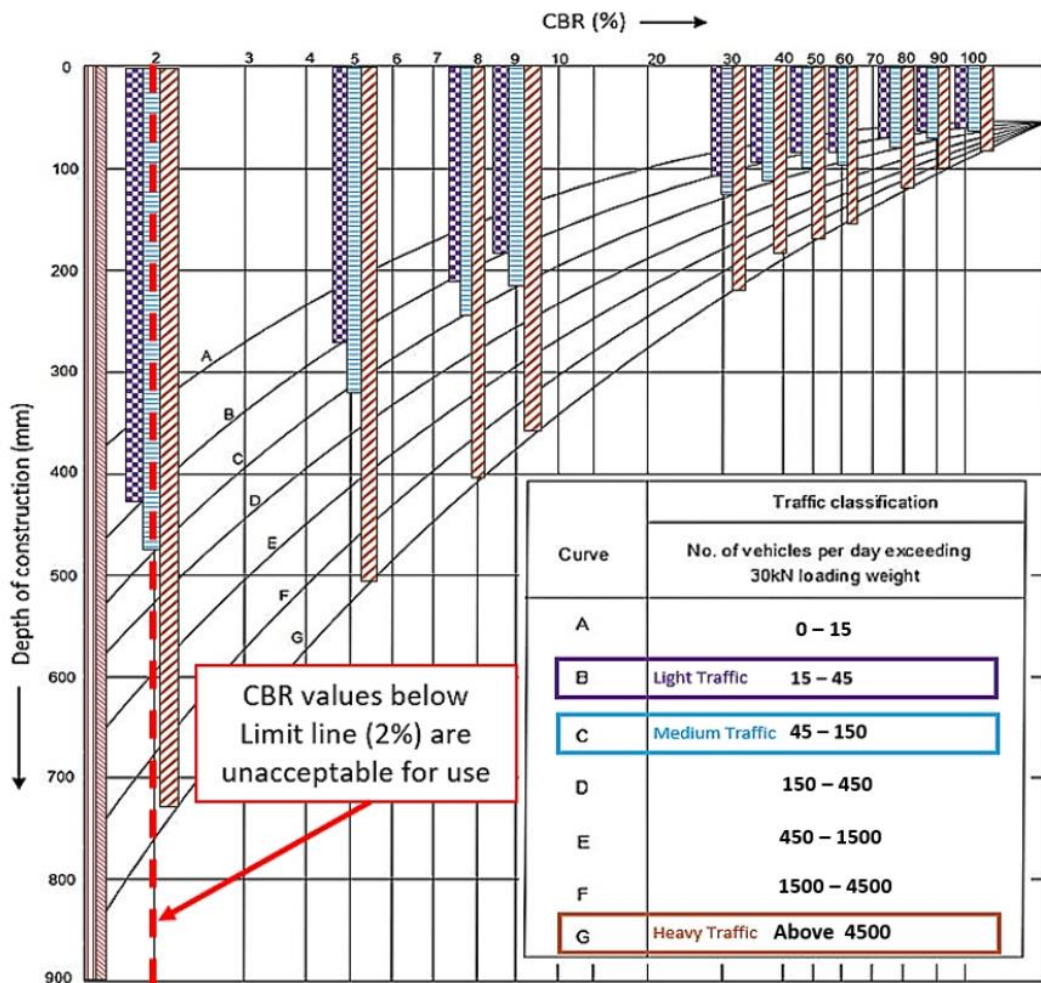


Figure 15. Cont.

<ul style="list-style-type: none"> ■ ASS 1 CBR - 8% Untreated unsoaked - Light traffic - Depth of Construction = 210mm □ ASS 1 CBR - 8% Untreated unsoaked - Medium traffic - Depth of Construction = 250mm ▨ ASS 1 CBR - 8% Untreated unsoaked - Heavy traffic - Depth of Construction = 405mm 	<ul style="list-style-type: none"> ■ ASS 3 CBR - 9% Untreated unsoaked - Light traffic - Depth of Construction = 190mm □ ASS 3 CBR - 9% Untreated unsoaked - Medium traffic - Depth of Construction = 220mm ▨ ASS 3 CBR - 9% Untreated unsoaked - Heavy traffic - Depth of Construction = 360mm
<ul style="list-style-type: none"> ■ ASS 1 CBR - 50% Treated soaked - Light traffic - Depth of Construction = 90mm □ ASS 1 CBR - 50% Treated soaked - Medium traffic - Depth of Construction = 100mm ▨ ASS 1 CBR - 50% Treated soaked - Heavy traffic - Depth of Construction = 170mm 	<ul style="list-style-type: none"> ■ ASS 2 CBR - 40% Treated soaked - Light traffic - Depth of Construction = 100mm □ ASS 2 CBR - 40% Treated soaked - Medium traffic - Depth of Construction = 120mm ▨ ASS 2 CBR - 40% Treated soaked - Heavy traffic - Depth of Construction = 190mm
<ul style="list-style-type: none"> ■ ASS 1 CBR - 80% Treated 7 days curing unsoaked - Light traffic - Depth of Construction = 60mm □ ASS 1 CBR - 80% Treated 7 days curing unsoaked - Medium traffic - Depth of Construction = 70mm ▨ ASS 1 CBR - 80% Treated 7 days curing unsoaked - Heavy traffic - Depth of Construction = 110mm 	<ul style="list-style-type: none"> ■ ASS 2 CBR - 60% Treated 7 days curing unsoaked - Light traffic - Depth of Construction = 80mm □ ASS 2 CBR - 60% Treated 7 days curing unsoaked - Medium traffic - Depth of Construction = 90mm ▨ ASS 2 CBR - 60% Treated 7 days curing unsoaked - Heavy traffic - Depth of Construction = 150mm
<ul style="list-style-type: none"> ■ ASS 1 CBR - 90% Treated 28 days curing unsoaked - Light traffic - Depth of Construction = 50mm □ ASS 1 CBR - 90% Treated 28 days curing unsoaked - Medium traffic - Depth of Construction = 70mm ▨ ASS 1 CBR - 90% Treated 28 days curing unsoaked - Heavy traffic - Depth of Construction = 100mm 	<ul style="list-style-type: none"> ■ ASS 3 CBR - 2% Untreated soaked - Light traffic - Depth of Construction = 430mm □ ASS 3 CBR - 2% Untreated soaked - Medium traffic - Depth of Construction = 480mm ▨ ASS 3 CBR - 2% Untreated soaked - Heavy traffic - Depth of Construction = 730mm
<ul style="list-style-type: none"> ■ ASS 2 CBR - 5% Untreated unsoaked - Light traffic - Depth of Construction = 270mm □ ASS 2 CBR - 5% Untreated unsoaked - Medium traffic - Depth of Construction = 310mm ▨ ASS 2 CBR - 5% Untreated unsoaked - Heavy traffic - Depth of Construction = 500mm 	<ul style="list-style-type: none"> ■ ASS 3 CBR - 30% Treated 7 days curing unsoaked - Light traffic - Depth of Construction = 110mm □ ASS 3 CBR - 30% Treated 7 days curing unsoaked - Medium traffic - Depth of Construction = 120mm ▨ ASS 3 CBR - 30% Treated 7 days curing unsoaked - Heavy traffic - Depth of Construction = 220mm
<ul style="list-style-type: none"> ■ ASS 2 CBR - 100% Treated 28 days curing unsoaked - Light traffic - Depth of Construction = 40mm □ ASS 2 CBR - 100% Treated 28 days curing unsoaked - Medium traffic - Depth of Construction = 50mm ▨ ASS 2 CBR - 100% Treated 28 days curing unsoaked - Heavy traffic - Depth of Construction = 80mm 	<ul style="list-style-type: none"> ■ ASS1 CBR - 0.85% Untreated soaked (unacceptable) □ ASS 2 CBR - 0.81% Untreated soaked (unacceptable)

Figure 15. Pavement depths determination using the chart for construction depth determination.

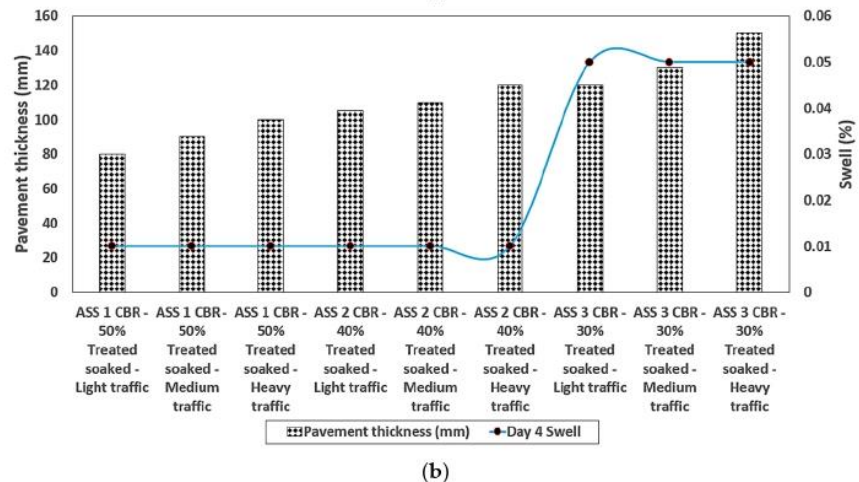
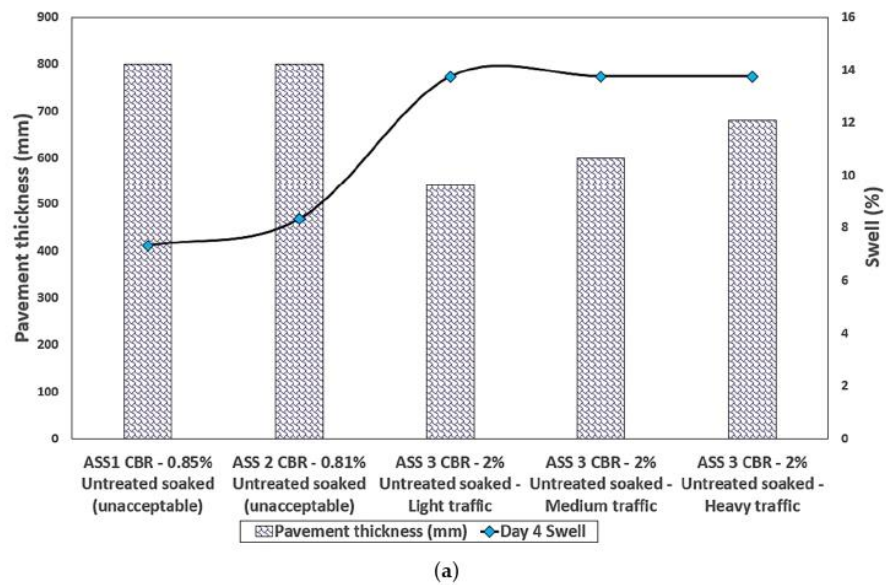


Figure 16. Cont.

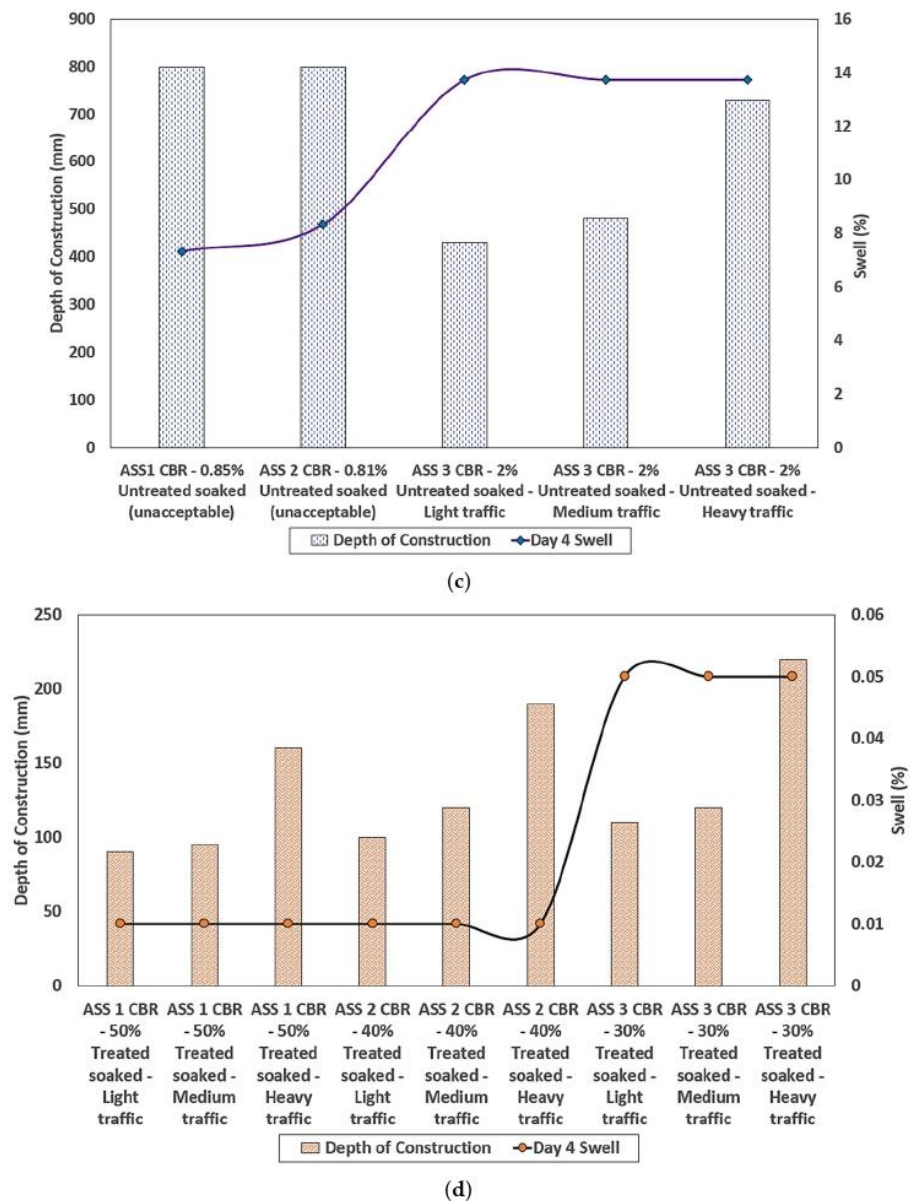


Figure 16. (a) Day 4 soaked pavement thickness against day 4 swell values for untreated ASS samples; (b) day 4 soaked pavement thickness against day 4 swell values for treated ASS samples; (c) day 4 soaked depth of construction against day 4 swell values for untreated ASS samples; (d) day 4 soaked depth of construction against day 4 swell values for treated ASS samples.

4. Conclusions

After conducting road pavement thickness and depth of construction optimization in this study, it was observed that the CBR values of the subgrade materials played a very vital role in determining the pavement thickness and construction depth of a road pavement structure. The conclusions arrived at after conducting the pavement thickness optimization for re-engineered artificially-synthesized expansive subgrade materials are as follows:

1. A reduction in pavement thickness with an increase in CBR value and a significant difference in pavement thickness between subgrade CBR values of 2% and 100% was observed. Pavement construction depth reduced as the CBR value increased, and pavement construction depth increased as traffic load increased. The deepest pavement depth value was recorded for the CBR value of 2% for heavy traffic, and

- the least pavement construction depth was recorded for the CBR value of 100% for the light traffic load.
2. Preliminary test results showed a high plasticity index, liquid limit and moisture content for the untreated subgrade materials with an increase in bentonite content in the mix. Swell values for all untreated CBR samples crossed the 2.5% unacceptable region, making them unsuitable for use as subgrade material, while all swell values for treated CBR samples fell below the 2.5% region, making them suitable for use in road construction. High swell values were recorded for samples with high bentonite content after 28 days of observation.
 3. The engineering properties of the expansive subgrade materials were improved after treatment using lime and cement as additives. High swell values were recorded for samples composed of high bentonite content compared with samples with high kaolinite content. Swell potentials of ASS materials were reduced drastically from 56.76% to 0.04%, below the unacceptable subgrade swell value of >2.5%, after treatment using lime and cement as binders.
 4. All untreated-soaked CBR samples fell below the 2% unacceptable region, making them unsuitable for use, while all treated-soaked and treated-unsoaked CBR samples crossed the acceptable 2% region, making them suitable for use in road construction. An increase in CBR values was observed as bentonite content increased for treated, untreated and soaked ASS samples. This shows that bentonite is strong in compression when it dries after coming in contact with water and is weak in compression when wet. It was established that the bearing capacity and strength of bentonite can be affected by binders (cement and lime) used during the stabilization process.
 5. The study recommends that expansive subgrade materials found on-site during road construction should be stabilized or treated to improve their engineering properties inserted by removing and replacing them with imported materials. Stabilizing weak subgrade materials can reduce the overall road construction costs compared to the cost of removal and replacement of weak subgrades. Road pavement construction costs can also be reduced by achieving high CBR values after stabilization, resulting in thinner road pavement thickness.

Author Contributions: Conceptualization, S.J.A. and S.Y.O.A.; methodology, S.Y.O.A. and S.J.A.; validation, S.Y.O.A. and S.J.A.; formal analysis, S.Y.O.A. and S.J.A.; investigation, S.Y.O.A. and S.J.A.; re-sources, S.J.A., C.A.B. and J.O.; data curation, S.Y.O.A. and S.J.A.; writing—original draft preparation, S.Y.O.A. and S.J.A.; writing—review and editing, S.Y.O.A., S.J.A. and C.A.B.; visualization, S.J.A., C.A.B. and J.O.; supervision, S.J.A., C.A.B. and J.O.; project administration, C.A.B., J.O. and S.J.A. All authors have read and agreed to the published version of the manuscript.

Funding: This research did not receive any specific grant from funding agencies in the public, commercial or not-for-profit sector.

Institutional Review Board Statement: Not applicable.

Informed Consent Statement: Not applicable.

Data Availability Statement: Data can be obtained from corresponding authors upon reasonable request.

Acknowledgments: The authors acknowledge that the advice, comments and suggestions from anonymous reviewers significantly improved the quality of this paper.

Conflicts of Interest: The authors declare that they have no conflict of interest associated with this publication, and no financial support has been given to influence the outcome of this work.

References


1. Dhir, R.K.; de Brito, J.; Silva, R.V.; Lye, C.Q. 12—Use of recycled aggregates in road pavement applications. In *Sustainable Construction Materials*; Elsevier: Amsterdam, The Netherlands, 2019; pp. 451–494. [CrossRef]
2. Amakye, S.Y.; Abbey, S.J. Understanding the performance of expansive subgrade materials treated with non-traditional stabilisers: A Review. *Clean. Eng. Technol.* **2021**, *4*, 100159. [CrossRef]
3. Amakye, S.Y.; Abbey, S.J.; Booth, C.A.; Mahamadu, A. Enhancing the engineering properties of subgrade materials using processed waste: A review. *Geotechnics* **2021**, *1*, 307–329. [CrossRef]
4. Li, J.; Cameron, D.A.; Ren, G. Case study and back analysis of a residential building damaged by expansive soils. *Comput. Geotech.* **2014**, *56*, 89–99. [CrossRef]
5. Jones, L.D.; Jefferson, I. Institution of Civil Engineers Manuals Series. 2019. Available online: http://nora.nerc.ac.uk/id/eprint/17002/1/C5_expansive_soils_Oct.pdf (accessed on 29 November 2021).
6. López-Lara, T.; Hernández-Zaragoza, J.; Horta-Rangel, J.; Rojas-González, E.; López-Ayala, S.; Castaño, V. Expansion reduction of clayey soils through Surcharge application and Lime Treatment. *Case Stud. Constr. Mater.* **2017**, *7*, 102–109. [CrossRef]
7. Phanikumar, B.R.; Raju, E.R. Compaction and strength characteristics of expansive clay stabilised with lime sludge and cement. *Soils Found.* **2020**, *60*, 129–138. [CrossRef]
8. Rivera, J.F.; Orobio, A.; Mejía de Gutiérrez, R.; Cristelo, N. Clayey soil stabilisation using alkali-activated cementitious materials. *Mater. Construcción* **2020**, *70*, e211. [CrossRef]
9. Jalal, F.E.; Xu, Y.; Jamhiri, B.; Memon, S.A. On the Recent Trends in Expansive Soil Stabilisation Using Calcium-Based Stabiliser Materials (CSMs): A Comprehensive Review. *Adv. Mater. Sci. Eng.* **2020**, *2020*, 1510969. [CrossRef]
10. Ikeagwuani, C.C.; Nwonu, D.C. Emerging trends in expansive soil stabilisation: A review. *J. Rock Mech. Geotech. Eng.* **2018**, *11*, 423–440. [CrossRef]
11. Jawad, I.T.; Taha, M.R.; Majeed, Z.H.; Khan, T.A. Soil Stabilisation Using Lime: Advantages, Disadvantages and Proposing a Potential Alternative Research. *J. Appl. Sci. Eng. Technol.* **2014**, *8*, 510–520. [CrossRef]
12. Neville, A.M. *Properties of Concrete*, 5th ed.; Pearson: Harlow, UK; New York, NY, USA; Available online: <https://pdfcoffee.com/properties-of-concrete-fifth-edition-a-m-neville-pdf-pdf-free.html> (accessed on 2 October 2021).
13. Walker, P. Review and Experimental Comparison of erosion tests on Earth Blocks. In *Terra 2000 Postprints: Proceedings of the 8th International Conference on the Study and Conservation of Earthen Architecture, Torquay, Devon, UK, May 2000*; James & James: London, UK, 2000.
14. Abbey, S.J.; Ngambi, S.; Olubanwo, A.O.; Tetteh, F.K. Strength and Hydraulic Conductivity of Cement and By-Product Cementitious Materials Improved Soil. *Int. J. Appl. Eng. Res.* **2018**, *13*, 8684–8694.
15. Gooding, D.E.; Thomas, T.H. The Potential of Cement Stabilised or Treated Building Blocks as an Urban Building Material in Developing Countries. DTU Working Paper No. 44. 1995. 2021. Available online: <https://warwick.ac.uk/fac/sci/eng/research/group/structural/dtu/pubs/wp/wp44/wp44.pdf> (accessed on 18 November 2021).
16. Karimiazar, J.; Teshnizi, E.S.; Mirzababaei, M.; Mahdad, M.; Arjmandzadeh, R. California bearing ratio of a reactive clay treated with nano-additives and cement. *J. Mater. Civ. Eng.* **2022**, *34*, 04021431. [CrossRef]
17. Cabezas, R.; Cataldo, C.; Choudhary, A.K. Influence of chemical stabilisation method and its effective additive concentration (EAC) in non-pavement roads. A study in andesite-based soils. *Cogent Eng.* **2019**, *6*, 1592658. [CrossRef]
18. Aliyazicioğlu, Ş.; Külekçi, G. Investigation of Usability of Limestone and Basalt Type Rocks as Road Infrastructure Filling, Trabzon Çatak Case. In Proceedings of the Internationally participated Cappadocia Geosciences Symposium, Niğde, Turkey, 24–26 October 2018; pp. 207–211.
19. Külekçi, G.; Yılmaz, A.O. The Investigation of Usage of Trabzon (Düzköy) Region Volcanites as Filling Material for Roads. In Proceedings of the 8th International Aggregates Symposium, Kutahya, Turkey, 13–14 October 2016; pp. 400–405.
20. Lucena, L.C.I.; Juca, J.F.T.; Soares, J.B.; Filho, P.G.T. Use of wastewater sludge for base and subbase of road pavements. *Trans. Res. Part D Trans. Env.* **2014**, *33*, 210–219. [CrossRef]
21. Boardman, D.I.; Glendinning, S.; Rogers, C.D.F. Development of stabilisation and solidification in lime-clay mixes. *Geotechnique* **2001**, *51*, 533–543. [CrossRef]
22. Ingles, O.G.; Metcalf, J.B. *Soil Stabilisation*; Butterworth Pty. Ltd.: Killara, Australia, 1972.
23. Ingles, O.H. Soil Stabilisation. Chapter 38. In *Ground Engineer's Reference Book*; Bell, F.G., Ed.; Butterworths: London, UK, 1987; pp. 38/1–38/26.
24. Jha, A.K.; Sivapullaiah, P.V. Lime stabilization of soil: A physico-chemical and micro-mechanistic perspective. *Indian Geotech. J.* **2019**, *50*, 339–347. [CrossRef]
25. Wang, Y.; Guo, P.; Li, X.; Lin, H.; Liu, Y.; Yuan, H. Behaviour of fibre-reinforced and lime-stabilised or treated clayey soil in triaxial test. *Appl. Sci.* **2019**, *9*, 900. [CrossRef]
26. Reddi, L.; Inyang, H.I. *Environmental Engineering: Principles and Applications*; CRC Press: Boca Raton, FL, USA, 2000; ISBN 9780824700454.
27. Etim, R.K.; Attah, I.C.; Ekpo, D.U.; Usanga, I.N. Evaluation on stabilisation role of lime and cement in expansive black clay-Oyster shell ash composite. *Transp. Infrastruct. Geotechnol.* **2021**, 1–35. [CrossRef]
28. Cheng, Y.; Huang, X. Effect of Mineral Additives on the Behavior of an Expansive Soil for Use in Highway Subgrade Soils. *Appl. Sci.* **2019**, *9*, 30. [CrossRef]

29. Liang, S.; Chen, J.; Guo, M.; Feng, D.; Liu, L.; Qi, T. Utilisation of pretreated municipal solid waste incineration fly ash for cement-stabilised or treated soil. *Waste Manag.* **2020**, *105*, 425–432. [CrossRef]
30. Nazari, Z.; Tabarsa, A.; Latifi, N. Effect of compaction delay on the strength and consolidation properties of cement-stabilised or treated subgrade soil. *Transp. Geotech.* **2021**, *27*, 100495. [CrossRef]
31. Lepore, B.J.; Thompson, A.M.; Petersen, A. Impact of polyacrylamide delivery method with lime or gypsum for oil and nutrient stabilisation. *J. Soil Water Conserv.* **2009**, *64*, 223–231. [CrossRef]
32. *BS EN 197-1*; Cement Composition, Specifications and Conformity Criteria for Common Cements. British Standards Institution: London, UK, 2011.
33. *BS EN 459-1*; Building Lime—Definitions, Specifications and Conformity Criteria. British Standards Institution: London, UK, 2015.
34. *BS 1924-1*; Stabilised or Treated Materials for Civil Engineering Purposes—General Requirements, Sampling, Sample Preparation and Test on Materials before Stabilization. British Standards Institution: London, UK, 2018.
35. *BS EN ISO 17892-1*; Geotechnical Investigation and Testing. Laboratory Testing of Soil—Determination of Water Content. British Standards Institution: London, UK, 2014.
36. *BS EN ISO 17892-12:2018+A1*; Geotechnical Investigation and Testing. Laboratory Testing of Soil Determination of Liquid and Plastic Limits. British Standards Institution: London, UK, 2021.
37. *BS 1377-4*; Methods of Test for Soils for Civil Engineering Purposes—Compaction—Related Tests. British Standards Institution: London, UK, 1990.
38. *AASHTO T265*; Standard Method of Test for Laboratory Determination of Moisture Content of Soil. AASHTO: Washington, DC, USA, 2015.
39. *ASTM D2216*; Standard Test Method for Laboratory Determination of Water (Moisture) Content of Soil and Rock by Mass. AASHTO: Washington, DC, USA, 2019. Available online: www.astm.org (accessed on 9 February 2022).
40. *ASTM D4318-17e1*; Standard Test Method for Liquid Limit, Plastic Limit, and Plasticity Index of Soils. AASHTO: Washington, DC, USA, 2017. Available online: www.astm.org (accessed on 9 February 2022).
41. *AASHTO T90*; Standard Method of Test for Determining the Plastic Limit and Plasticity Index of Soils. AASHTO: Washington, DC, USA, 2020.
42. *AASHTO T 89*; Standard Method of Test for Determining the Liquid Limit of Soils. AASHTO: Washington, DC, USA, 2013.
43. *BS EN 13286-47*; Unbound and Hydraulically Bound Mixtures—Test Methods for the Determination of California Bearing Ratio, Immediate Bearing Index and Linear Swelling. British Standards Institution: London, UK, 2021.
44. Southern Testing Environmental & Geotechnical. Available online: <https://www.southern-testing.co.uk/services/ground-site-investigation-consultants/cbr-test/> (accessed on 18 September 2021).
45. *IRC 37-2001*; Guidelines for the Design of Flexible Pavements. Indian Roads Congress: New Delhi, India, 2001.
46. The Constructor Building Ideas (TCBI). Available online: <https://theconstructor.org/transportation/flexible-pavement-design-cbr-method/11442/> (accessed on 14 November 2021).
47. *DMRB HA 74*; Treatment of Fill and Capping Materials using Either Lime or Cement or Both. Highways Agency: London, UK, 2007.
48. Virginia Department of Transport (VDOT). 2016. Available online: <https://pdf4pro.com/amp/view/construction-and-acceptance-testing-of-1fa6ed.html> (accessed on 14 November 2021).
49. *DMRB CD 226*; Design for New Pavement Construction. Highways Agency: London, UK, 2021.
50. *BS EN 13286-49*; Unbound and Hydraulically Bound Mixtures—Accelerated Swelling Test for Soil Treated by Lime and/or Hydraulic Binder. British Standards Institution: London, UK, 2004.
51. Parihar, N.S.; Gupta, A. *Strength and Microstructural Behaviour of Expansive Soil Treated with Limed Leather Waste Ash*; Blue Eyes Intelligence Engineering & Sciences Publication: Bhopal, India, 2020; Volume 9, ISSN 2278-3075. [CrossRef]
52. Sharma, A.K.; Sivapullaiah, P.V. Ground granulated blast furnace slag amended fly ash as an expansive soil stabiliser. *Soils Found.* **2015**, *56*, 205–212. [CrossRef]
53. Abbey, S.J.; Eyo, E.U.; Ng’ambi, S. Swell and microstructural characteristics of high-plasticity clay blended with cement. *Bull. Eng. Geol. Environ.* **2020**, *79*, 2119–2130. [CrossRef]
54. Asad, M.; Kar, S.; Ahmeduzzaman, M.; Hassan, M. Suitability of bentonite clay: An analytical approach. *Earth Sci.* **2013**, *2*, 88–95. [CrossRef]
55. O’Geen, A.T. Soil water dynamics. *Nat. Educ. Knowl.* **2013**, *4*, 9. Available online: <https://www.nature.com/scitable/knowledge/library/soil-water-dynamics-103089121/> (accessed on 30 November 2021).
56. Schanz, T.; Elsayy, M.B.D. Swelling characteristics and shear strength of highly expansive clay–lime mixtures: A comparative study. *Arab. J. Geosci.* **2015**, *8*, 7919–7927. [CrossRef]
57. *IAN 73*; Design Guidance for Road Pavement Foundations. Highways Agency: London, UK, 2006.
58. Hashemi, M.A.; Zine, N.; Massart, T.J. Lime-treatment of sand improved by bentonite addition. In Proceedings of the 2012 Conference: European Young Technical Engineers Conference (EYGE), Gothenburg, Sweden, 26–29 August 2012.
59. Parthiban, D.; Vijayan, D.S.; Hausik, J.; Rahman, A.A.; Veerachandru, K. Performance study on clayey soil stabilized by lime and geopolymer with partial replacement of sodium bentonite as an additive 2020. *AIP Conf. Proc.* **2020**, *2271*, 030003. [CrossRef]
60. Gratchev, I.; Pitawala, S.; Gurung, N.; Monteiro, E. A Chart to Estimate CBR of Plastic Soils. 2018. Available online: https://www.researchgate.net/publication/324557522_A_CHART_TO_ESTIMATE_CBR_OF_PLASTIC_SOILS (accessed on 9 February 2022).

61. Thakur, Y.; Yadav, R.K. Effect of bentonite clay on compaction, CBR and shear behaviour of Narmada sand. *Int. Res. J. Eng. Technol.* **2018**, *5*, 2087–2090.
62. Global Road Technology, Subgrade Reactivity Considerations in Pavement Design. 2021. Available online: <https://globalroadtechnology.com/subgrade-reactivity-considerations-pavement-design/> (accessed on 9 February 2022).
63. Shi, D.; Tong, H.; Lv, M.; Zhang, H.; Wang, H.; Luo, L.; Ma, J.; Ma, C.; Luo, D.; Zhao, X.; et al. Effect of Ca-Si-Al element proportion on the formation of Aluminosilicate minerals and detoxification of PAHs in fly ash from MSW incineration during the hydrothermal process. American Chemical Society. *Energy Fuels* **2021**, *35*, 9474–9488. [CrossRef]
64. Abbey, S.J.; Eyo, E.U.; Jeremiah, J.J. Experimental study on early age characteristics of lime-GGBS-Treated gypseous clays under wet-dry cycles. *Geotechnics* **2021**, *1*, 402–415. [CrossRef]
65. The Construction, Road Construction. 2022. Available online: https://www.designingbuildings.co.uk/wiki/Road_construction (accessed on 10 March 2022).
66. Nunn, M.E.; Brown, A.; Weston, D.; Nicholls, J.C. *Design of Long-Life Flexible Pavements for Heavy Traffic, Prepared for British Aggregate Construction Mat, Indust, and the Refined Bitumen Associ*; Transport Research Laboratory: Crowthorn, UK, 1997; Available online: <https://www.trl.co.uk/Uploads/TRL/Documents/TRL250---Design-of-long-life-flexible-pavements-for-heavy-traffic.pdf> (accessed on 10 March 2022).
67. Li, S. *Heavy Duty Pavements*; South Dakota School of Mines and Technology: Rapid City, SD, USA, 1964.

Review

Enhancing the Engineering Properties of Subgrade Materials Using Processed Waste: A Review

Samuel Y. Amakye ^{1,*}, Samuel J. Abbey ², Colin A. Booth ²  and Abdul-Majeed Mahamadu ²

¹ Department of Geography and Environmental Management, Faculty of Environment and Technology, University of the West of England, Bristol BS16 1QY, UK

² Faculty of Environment and Technology, University of the West of England, Bristol BS16 1QY, UK; samuel.abbey@uwe.ac.uk (S.J.A.); Colin.booth@uwe.ac.uk (C.A.B.); Abdul.Mahamadu@uwe.ac.uk (A.-M.M.)

* Correspondence: Samuel.amakye@uwe.ac.uk

Abstract: Subgrade materials refer to the original ground underneath a road pavement, when these materials are made up of expansive soil it is referred to as expansive subgrade. Sometimes, these materials do not have sufficient capacity to support the weight of the road pavement and traffic load, which means they require some form of modification and re-engineering to enhance their load capacity. Chemical modification techniques using traditional stabilisers (such as cement and lime) have proved to be an effective means of subgrade stabilisation. However, high costs and environmental concerns associated with the use and production of these additives have highlighted the need for more sustainable and environmentally friendly substitutes. This study reviews the use of industrial by-products and other waste materials used for subgrade stabilisation, focusing on the sustainability of using processed wastes and how they alter the engineering properties of weak subgrade, compared to the use of cement and also reviews the availability of processed waste materials in quantities sufficient to meet the current demand for subgrade stabilisation. The findings illustrate that, processed waste is less expensive and has better sustainability credentials compared to cement. Moreover, processed wastes are available in sufficient quantities to meet existing demands for subgrade stabilisation. Therefore, it is recommended that the use of processed wastes should be promoted and utilised to improve and enhance the geotechnical properties of weak subgrade materials where possible.

Keywords: expansive soil; subgrade stabilisation; engineering properties; California bearing ratio; unconfined compressive strength



Citation: Amakye, S.Y.; Abbey, S.J.; Booth, C.A.; Mahamadu, A.-M. Enhancing the Engineering Properties of Subgrade Materials Using Processed Waste: A Review. *Geotechnics* **2021**, *1*, 307–329. <https://doi.org/10.3390/geotechnics1020015>

Academic Editor: Daniel Dias

Received: 17 August 2021

Accepted: 8 October 2021

Published: 14 October 2021

Publisher's Note: MDPI stays neutral with regard to jurisdictional claims in published maps and institutional affiliations.



Copyright: © 2021 by the authors. Licensee MDPI, Basel, Switzerland. This article is an open access article distributed under the terms and conditions of the Creative Commons Attribution (CC BY) license (<https://creativecommons.org/licenses/by/4.0/>).

1. Introduction

Expansive subgrade materials in road pavement structures can cause defects and failure in road pavement structure leading to high cost of maintenance and sometimes total redesign and reconstruction of the road infrastructure. The damage caused by expansive subgrade in road structure runs into many billions of dollars, which is notably more than damages caused by flooding [1]. For instance, the UK economy alone over the past ten years has suffered costs in excess of GBP 3 billion, making it the most damaging geohazard [2,3]. Oftentimes, subgrade materials do not have sufficient capacity to support the weight of the road pavement and traffic load and will require some sort of modification and reengineering to enhance their load capacity. Chemical subgrade stabilisation techniques, using traditional binders (such as cement and lime) are regularly used to stabilise expansive subgrade materials and have proven to be an effective approach. However, using cement and lime in road subgrade stabilisation has proved very costly and also unsustainable due to environmental effects associated with the use of cement and its production [4,5]. Cement is the most widely used material on earth after water however, cement is considered the most destructive material on earth [2]. Cement production produces a large amount of (4–8%) the world's CO₂, destroying natural resources such as vegetation, with limestone

discharging wastewater and sludge from concrete batch plants having a harmful effect on the water ecosystem [6]. Processed wastes derived from industrial by-products that are often dumped in landfills can be used as additives in road subgrade stabilisation. The use of processed wastes to improve the engineering and geotechnical properties of expansive road subgrade is less costly than cement and lime and can reduce the amount of greenhouse gas emitted into the atmosphere. Processed waste (such as ground granulated blast furnace slag (GGBS), brick dust waste synthetic fibres, plastic waste and fly ash amongst other construction and demolition wastes) have been used in subgrade stabilisation to improve their engineering properties of road pavement and concomitantly reduce overall construction costs. Figure 1a,b shows areas in the UK and the US that are susceptible to swell–shrink effects, and Figure 1c,d shows a contours plot of swelling potential in Louisiana, while Figure 2a,b shows a typical wet and dry expansive soil with high potential to swelling and shrinkage. Figure 2c,d shows a road pavement defect caused by expansive subgrade. Tables 1 and 2 show the estimated cost of damage due to expansive soils in some countries and annual damage in the US from expansive soils.

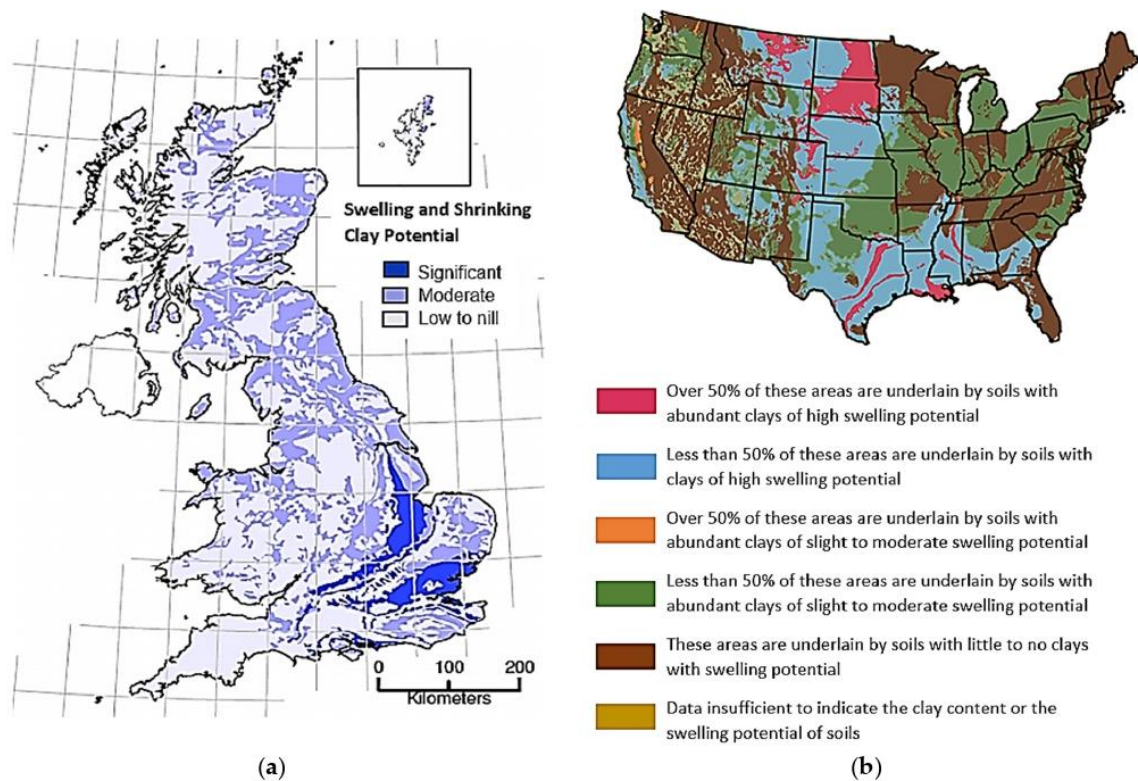


Figure 1. Cont.

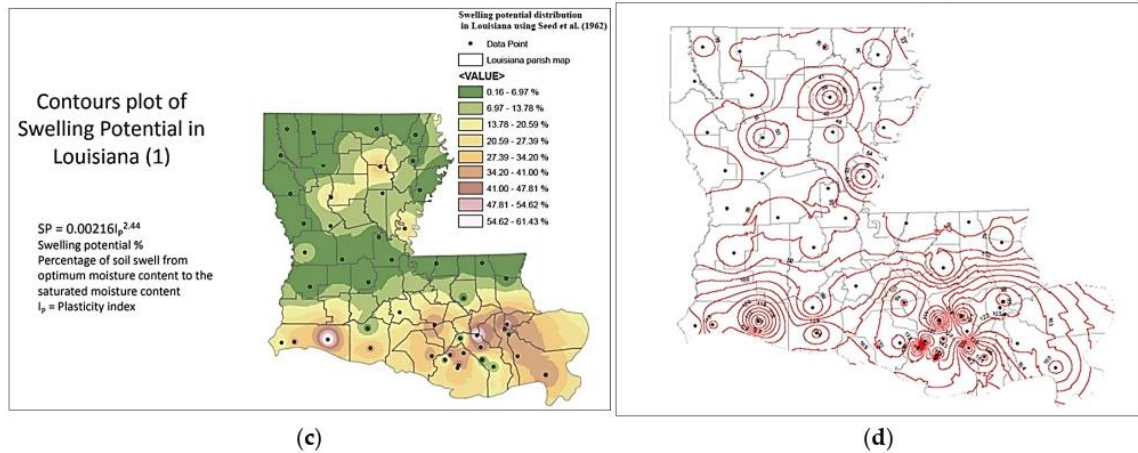


Figure 1. (a) Shrink–swell potential areas in the UK [3]; (b) Areas in the US where soils are susceptible to swelling [7]; (c) contours plot of swelling potential in Louisiana [7]; (d) contours plot of swelling potential in Louisiana [7].

Table 1. Estimated cost of damage due to expansive soils in some countries.

Country	Amount (USD)	Reference
UK	>3.7 billion	[8]
China	>1 billion	[9]
France	>2.71 billion	[10]
India	>73 million	[11]
Saudi Arabia	>300 million	[12]
Sudan	>6 million	[13]
USA	>9 billion annually	[9]

Table 2. Annual damage in the US from expansive soils [7].

Category	Annual Damage (US\$)
Highways and streets	4,550,000,000
Commercial buildings	1,440,000,000
Single family homes	1,200,000,000
Walks, drives and parking areas	440,000,000
Buried utilities and services	400,000,000
Multi-story buildings	320,000,000
Airport installations	160,000,000
Involved in urban landslides	100,000,000
Other	390,000,000
Total annual damage (1987)	9,000,000,000



Figure 2. Cont.



Figure 2. (a) Typical wet expansive soil [14]; (b) typical dry expansive soil [15]; (c) uplifting of flexible pavement due to expansive soil [16]; (d) typical longitudinal crack developed on pavements over expansive clays [17].

2. Scope of the Study

This study reviews the use of processed waste materials for road subgrade stabilisation, with a focus on their availability, the costs of processing the waste and revealing associated environmental effects compared to those of cement production. The study also reviews the effects of using processed waste materials on the engineering properties of road subgrade (such as unconfined compressive strength (USC), California bearing ration (CBR), tensile strength and shrink–swell of expansive subgrade materials stabilised using processed waste).

3. Characteristics and Minerals Structure of Clay Soil

The swelling ability of expansive subgrade materials depends on the total internal and external areas of its mineral particles, such as montmorillonite expandable illite and vermiculite or if the liquid limit of the soil exceeds 50% and the plasticity index exceeds 30% [2,11]. The types of expansive clay soils include smectite, bentonite, montmorillonite, beidellite, vermiculite, attapugite, nontronite and chlorite. The enlargement of the capillary films in clay minerals can cause swelling to occur when water is absorbed through their outer surface [18,19]. According to [20], expansive soils contain smectite clay materials which when view under a microscope looks like layered sheets due to their moisture-retaining abilities. When water is introduced to expansive soil, the water molecules are pulled into the gaps between the clay plates, which force the plates [21,22]. The hydraulic conductivity and other engineering properties of clayey soil are influenced by the diffused double layer. Clay minerals are major constituents of fine-grained sediments and rocks including mudrocks, shales, claystones, clayey siltstones, clayey oozes and argillites [2,23]. Clay minerals are defined by geologist as hydrous layer aluminosilicates with particle sizes $<2 \mu\text{m}$, whilst engineers defined clay as any mineral particle $<4 \mu\text{m}$ which are a diverse group of hydrous layer aluminosilicate that constitutes the greater part of the phyllosilicate family of minerals.

The physical structure of montmorillonite particles in clay is generally perceived in sheets and layers. Each layer is composed of two types of structural sheets namely octahedral and tetrahedral. The tetrahedral sheet is composed of silicon-oxygen tetrahedral linked to neighbouring tetrahedra by sharing three corners resulting in a hexagonal network. The remaining four corners of each tetrahedron form a part of the adjacent octahedral sheet which are normally composed of aluminium or magnesium in six-fold coordination with oxygen from the tetrahedral sheet and with hydroxyl [24,25]. Figure 3 shows the expansion of a single smectite grain after introducing water between clay layers, Table 3 shows swell potential of soil based on their liquid limit, Table 4 shows the classification of shrink potentials of expansive soil based on their plasticity index and Table 5 shows the relation of soil index properties and probable volume change for highly plastic soils, Table 6 shows typical values for cation exchange capacities. Figure 4a shows clay mineral structure, Figure 4b shows bentonite clay structure, Figure 4c shows kaolinite clay structure.

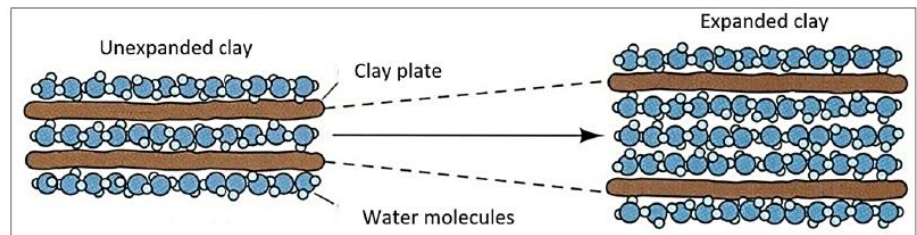


Figure 3. Expansion of a single smectite grain [20].

Table 3. Swelling potential of soils based on liquid limit [26].

Liquid Limit	Classification
0–20	Non-Swelling
20–35	Low-Swelling
35–50	Medium-Swelling
50–70	High-Swelling
70–90	Very High-Swelling
>90	Extra High-Swelling

Table 4. Classification of shrink potentials based on plasticity index [3].

PI (%)	Clay Fraction	Shrinkage Potential (<0.002 mm)
>35	>95	Very High
22–48	60–95	High
12–32	30–60	Medium
<18	<30	Low

PI = plasticity index.

Table 5. Relation of soil Index properties and probably volume change for highly plastic soils [27].

Data from Index Tests ¹			Estimation of Probable Expansion ² , Percent Total Volume Change (Dry to Saturated Condition)	Degree of Expansion
Colloid Content Percent Minus 0.00004 in. (0.001 mm) (ASTM D422)	Plasticity Index (ASTMD4318)	Shrinkage Limit Percent (ASTM D427)		
>28	>35	>11	>30	Very High
20–31	24–41	7–12	20–30	High
13–23	15–28	10–16	10–20	Medium
<15	<8	<15	<10	Low

¹ All three index tests should be considered in estimating expansive properties. ² Based on a vertical loading of 1.0 psi (0.007 MPa). For higher loadings the amount of expansion is reduced, depending on the load and on the clay characteristics.

Table 6. Typical values for cation exchange capacities [25].

Liquid Limit	meq/100 g
Kaolinite	3–18
Halloysite	5–40
Chlorite	10–40
Illite	10–40
Montmorillonite	60–150
Vermiculite	100–215

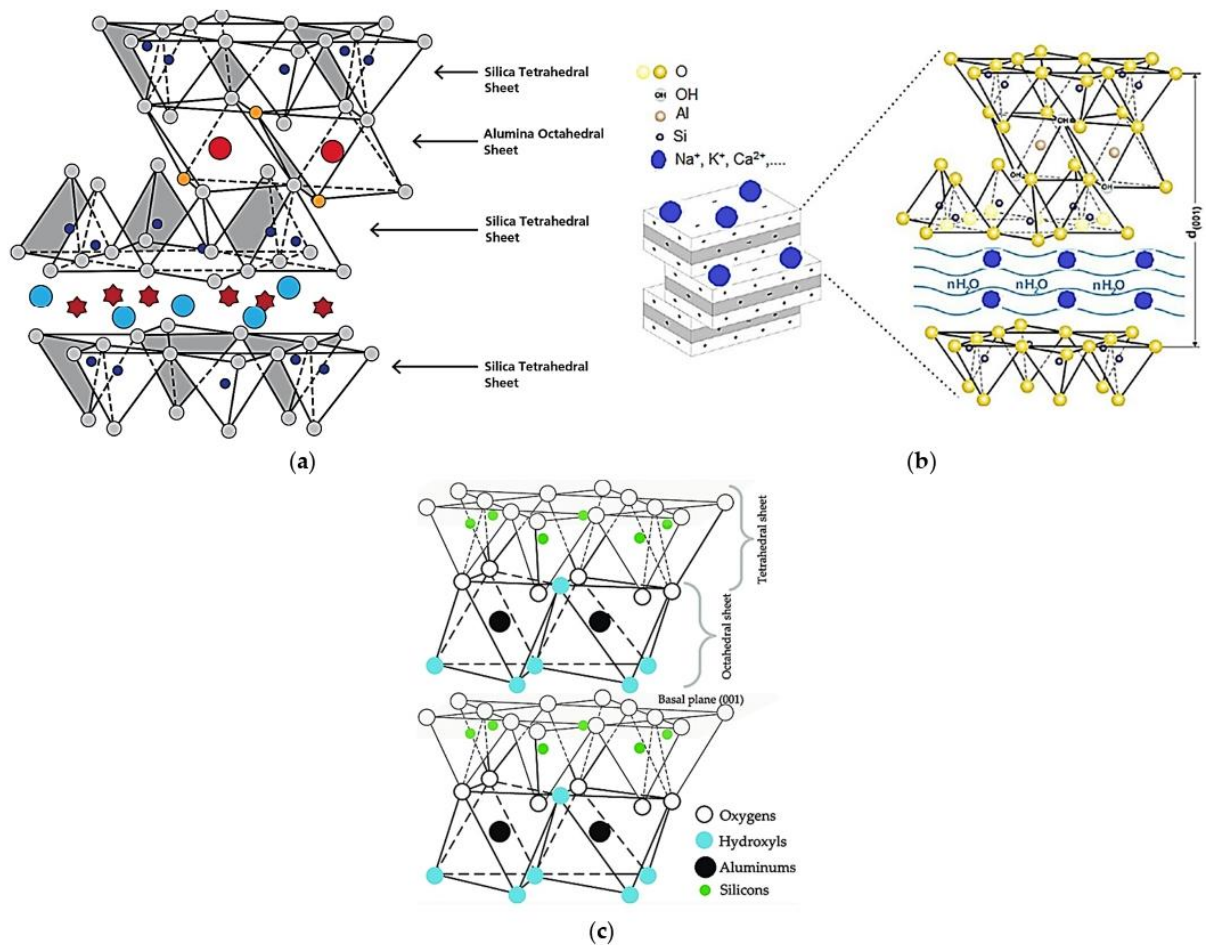


Figure 4. (a) Clay mineral structure [28]; (b) bentonite clay structure [29]; (c) kaolinite clay structure [30].

4. Characteristics and Manufacturing Process of Some Industrial Waste

Ground granulated blast furnace slag (GGBS) is an industrial by-product from the manufacturing of pig iron, during the production, the molten slag is cooled and solidified to a greasy state by rapid water quenching, where no air or little crystallisation occurs. This process results in the formation of sand size fragments with some flexible clinker-like materials known as GGBS. The chemical composition of the slag, its temperature at the time of water quenching and the method of production determines the physical structure and gradation of GGBS [31]. Silica fume is a by-product of silicon metal or ferrosilicon production in an electric furnace. The smoke generated from the furnace is collected and known as silica fume or micro silica. Silica fume is the most valuable by-product pozzolanic material due to its active and high pozzolanic properties [31]. Polypropylene fibre is produced by slurry solution or gas phase process where propylene monomers are subjected to heat and pressure in the presence of a catalyst system. Polypropylene is achieved at relatively low temperature and pressure yielding a translucent product known as polypropylene [32]. There are two varieties of glass fibre manufacturing: one involves the preparation of marble that is melted in the fibrilization stage and the other involves the direct melting route, where a furnace charges continuously with raw materials that are melted and refined as the glass reaches the forehearth above a set of platinum-rhodium brushing from which the fibres are drawn. Rice husk is a by-product of rice

milling commonly known as rice hull is the coating on the seed or grain of rice. It is formed from hard materials including silica and lignin to protect the seed during the growing season and can be used in soil stabilisation [33]. Metakaolin is one type of calcined clay, and it comes from the calcination of kaolin clay and has been explored as a partial substitute for cement [34]. Fly ash is a fine powder formed from the mineral matter in coal and consist of the non-combustible matter in coal and a small amount of carbon that remains from incomplete combustion. It is either cementitious or pozzolanic and can be used in soil stabilisation [35]. Particle size distribution of non-traditional stabiliser waste materials such as silica fume, metakaolin, rice husk ash and fly ash compared to traditional cement are shown in Figure 5. The manufacturing process and end product of GGBS, silica fume, polypropylene fibre and glass fibre are shown in Figure 6a–h. Some properties of waste materials used in soil stabilisation are shown in Table 7. Table 8 shows some mechanical properties of polypropylene fibre and Table 9 shows the main physical and chemical properties of plastic waste.

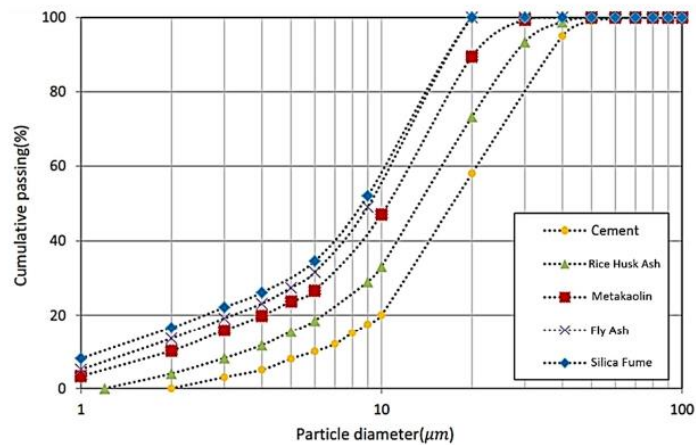


Figure 5. Particle size distribution curves of cement and pozzolanic materials [36].

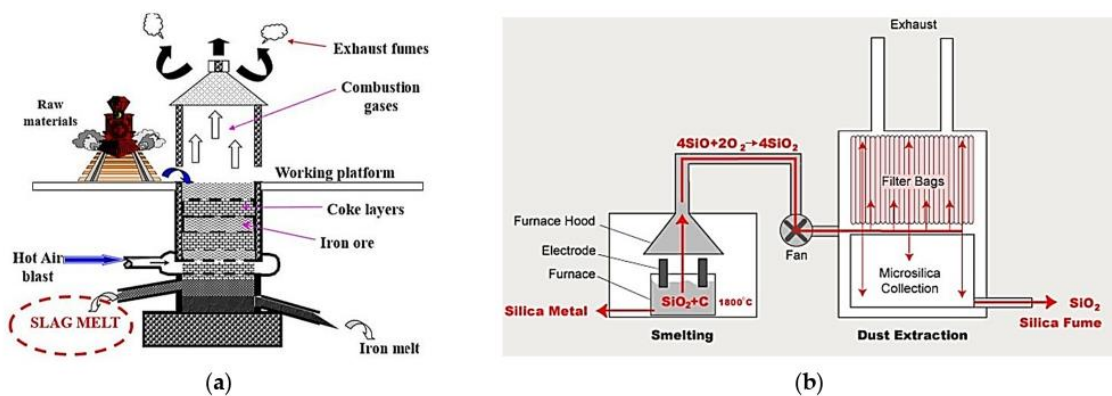


Figure 6. Cont.

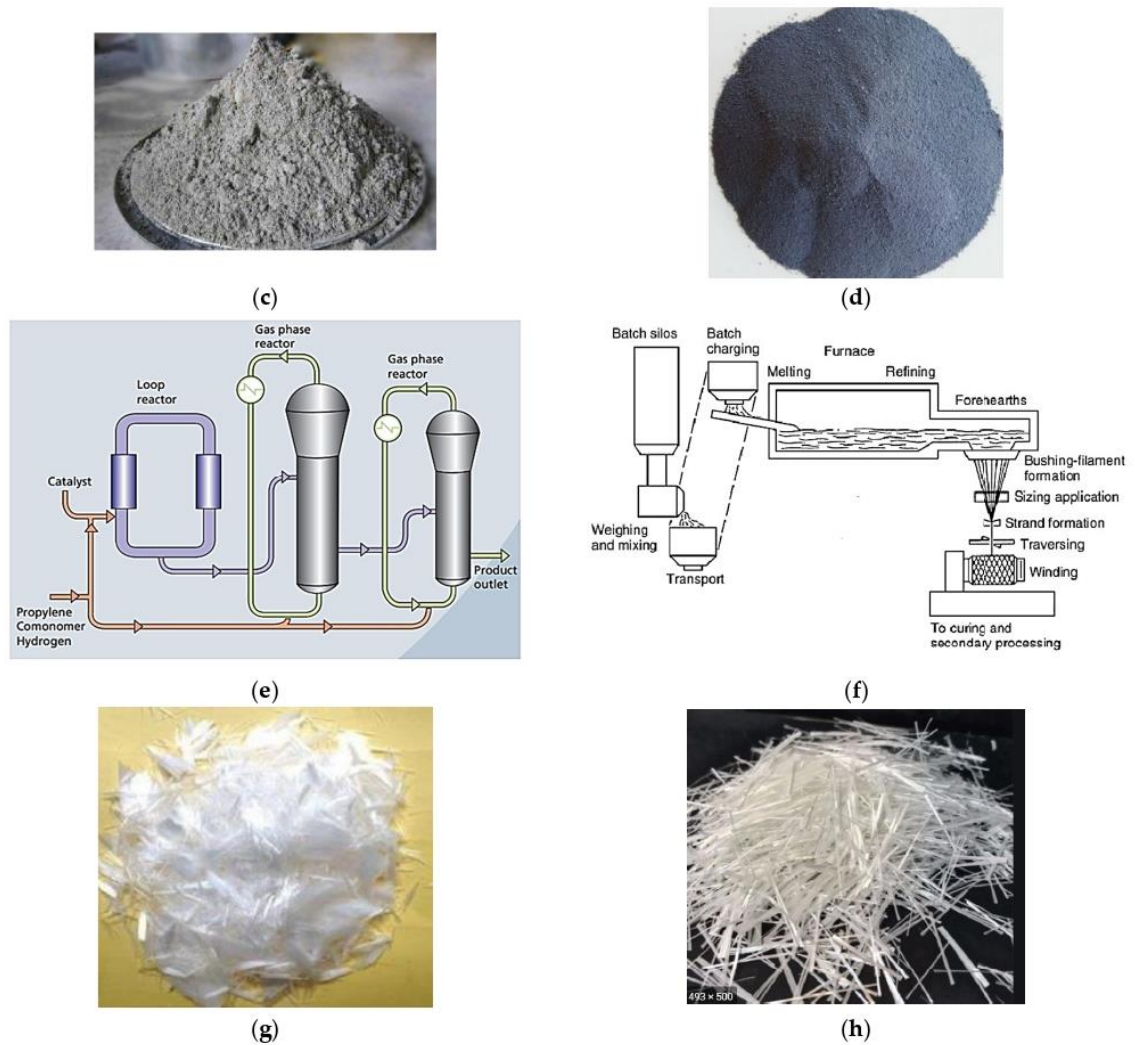


Figure 6. (a) Schematic diagram of the manufacturing process of GGBS [31]; (b) manufacturing process of silica fume [37]; (c) the end product of processed GGBS [38]; (d) the end product of processed silica fume [39]; (e) manufacturing process of polypropylene [40]; (f) schematics of marble melt process for glass fibre production [40]; (g) the end product of processed polypropylene fibre [41]; (h) the end product of processed glass fibre [42].

Table 7. Chemical composition mineralogy and physical properties of waste.

Oxide	SiO ₂	Al ₂ O ₃	Fe ₂ O ₃	MgO	CaO	K ₂ O	SO ₃	TiO ₂	Na ₂ O	Loss of Ignition	Source
BDW	52	41	0.7	0.12	4.32	0.53	0.33	0.65	0.05	2.01	[43]
GGBS	34.72	19.11	0.5	8.46	35.27	0.58	0.18	0.65	0.16	-	[44]
Silica fume	93.38	0.15	0.21	0.10	0.67	-	0.37	-	-	1.46	[45]
Glass fibre	45.47	12.11	1.04	-	38.49	0.94	0.43	-	-	-	[46]
RHA (Malaysia)	93.10	0.21	0.21	1.59	0.41	2.31	-	-	-	2.36	[47]
RHA (Brazil)	92.90	0.18	0.43	0.35	1.03	0.72	0.10	-	0.02	-	[47]
RHA (Netherlands)	86.90	0.84	0.73	0.57	1.40	2.46	-	-	0.11	5.14	[47]
RHA (India)	90.70	0.40	0.40	0.50	0.40	2.20	0.10	-	0.10	4.80	[47]

Table 7. Cont.

Oxide	SiO ₂	Al ₂ O ₃	Fe ₂ O ₃	MgO	CaO	K ₂ O	SO ₃	TiO ₂	Na ₂ O	Loss of Ignition	Source
RHA (Iraq)	86.80	0.40	0.19	0.37	1.40	3.84	1.54	-	1.15	3.30	[47]
RHA (USA)	94.50	Trace	Trace	0.23	0.25	1.10	1.13	-	0.78	-	[47]
RHA (Canada)	87.20	0.15	0.16	0.35	0.55	3.68	0.24	-	1.12	8.55	[47]
Paper Sludge Ash	60.57	2.06	0.92	3.59	14.94	0.16	1.07	-	0.22	-	[48]
Fly ash	48.28	27.72	7.19	2.51	10.51	-	3.16	1.28	-	-	[49]
Boron	21.64	0.75	0.19	9.40	-	-	-	16.77	7.88	35.38	[49]
Marble dust	0.2	0.07	0.11	0.3	54.5	-	0.08	-	0.01	44.52	[49]
Granite dust	89.30	0.19	0.23	0.46	0.58	-	0.06	-	0.37	8.26	[49]
Green Bayburt Stone	68.22	12.06	1.84	1.14	2.17	1.54	0.09	-	6.08	6.79	[50]

Table 8. Mechanical properties of polypropylene fibre [51].

Properties	Description
Tensile strength (gf/den)	3.5–5.5
Elongation (%)	40–100
Abrasion resistance	Good
Moisture absorption (%)	0–0.05
Softening point (°C)	140
Melting point (°C)	165
Chemical resistance	General excellent
Relative density	0.91
Thermal conductivity	6.0 (with air as 1.0)
Electric insulation	Excellent
Resistance to mildew and moth	Excellent

Table 9. Main physical and chemical properties of plastic waste [52].

Properties	Description
C (%)	85.0
H (%)	13.8
N (%)	0
S (%)	0
O (%)	0
Ashes (%)	1.0
Moisture (%)	0.2
Low heating value (kJ/kg)	45,500
Starting devolatilization temp (°C)	≈250
Devolatilization Temp (°C)	≈410
Diameter and thickness of fuel pellets (mm)	5.2
Particle density (kg/m ³)	940
Bulk density (kg/m ³)	570

5. Production of Processed Waste and Their Utilisation in Road Subgrade

Various kinds of waste materials are being generated worldwide as a result of human activities. Due to our inability to recycle all the waste society produces, a large section of these waste materials is dumped in landfills and others dumped in water bodies which have contributed to some of the environmental problems we face today. According to [53], the world generates 2.01 billion tonnes of municipal solid waste annually and it is expected to grow to 3.40 billion tonnes by 2050 Figure 7. In the approach to mitigate the problem, many strategies have been put in place including recycling incineration. However, these strategies are not enough to deal effectively with all the waste we produce. This has encouraged the use of processed waste in the engineering and construction sector for the construction of roads pavements and buildings. However, the availability of processed waste for use quantities and the environmental effect associated with waste processing

has been questioned. The [54] stated that, a huge amount of processed waste is produced around the world for use in various engineering activities. Before waste materials can be used in subgrade stabilisation, the waste must first of all be processed to remove toxic chemicals and contamination to make them suitable for use as an additive in road construction. The use of processed waste in subgrade stabilisation is arguably the new trend in chemical stabilisation of subgrade materials. This is aimed at reducing the amount of greenhouse gas emissions and the environmental effects associated with cement and lime production. A huge amount of processed waste is produced around the world for use in various engineering activities. However, many concerns have been raised with regard to the cost and environmental effects associated with the production process of these waste materials. These concerns include the amount of CO₂ emitted during waste processing and, are there enough processed waste available to meet the current demand for use in subgrade stabilisation?

Research has shown that there are enough processed industrial by-products and waste materials available to meet the current demands for soil stabilisation. The processing of these waste materials is cheaper and sustainable compared to the cost of cement and its production [55]. Over 20 million metric tonnes (22 million tonnes) of fly ash are used annually in a variety of engineering applications typically highway engineering [53]. Table 10 shows that 62 million metric tonnes (68 million tonnes) of fly ash was produced in 2001 and only 20 million metric tonnes (22 million tonnes) or 32% of the total production was used. The total production of hypo-sludge in Bangladesh which is capable of replacing cement is equivalent to $550,000 \times 6 = 3,300,000$ kg per year. A reduction in the amount of coal combustion products that must be disposed of in landfills has been observed due to their use in subgrade stabilisation [53]. The use of waste in soil stabilisation provides environmental and economic advantages [49]. Figure 7 shows projected waste generation, by region Mt per year. According to Figure 7, there has been a significant increase in the amount of waste generated by the various region since 2016 and it is projected to increase from 177 to 602 Mt by the year 2030 and from 255 to 714 Mt by the year 2050 respectively. Table 10 shows 61.84 million metric tonnes of fly ash was produced in 2001 and only 19.98 million metric tonnes were used (32.3%). Table 11 shows the annual production of major industrial solid wastes generated in India which are not fully utilised. Figure 8a,b shows the modes and utilisation of fly ash in various engineering sectors in India in the year 2014–2015, which includes the enhancement of the engineering properties of subgrade materials. Hence, there are no projections of waste shortage in the future by various statistics to hinder the reliance on the use of waste in subgrade stabilisation.

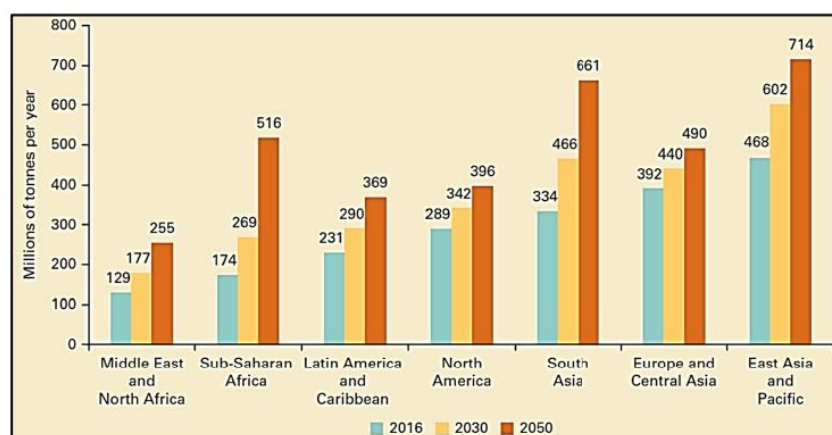


Figure 7. Projected waste generation, by region Mt per year [53].

Table 10. Fly ash production and use in the US in 2001 [53].

	Million Metric Tonnes	Million Short Tonnes	Percent
Produced	61.84	68.12	100
Used	19.98	22.00	32.3

Table 11. Major industrial solid wastes generated in India [56].

Solid Waste	Fly Ash	GGBS	Steel Slag	Red Mud	Lime Sludge	Lead-Zinc Slag	Phosphorus Furnace Slag	PG	Jarosite	Kimberlite	Mine Rejects
Annual production (million tonnes)	184.14	10	12	4.71	4.5	0.5	0.5	11	0.6	0.6	750

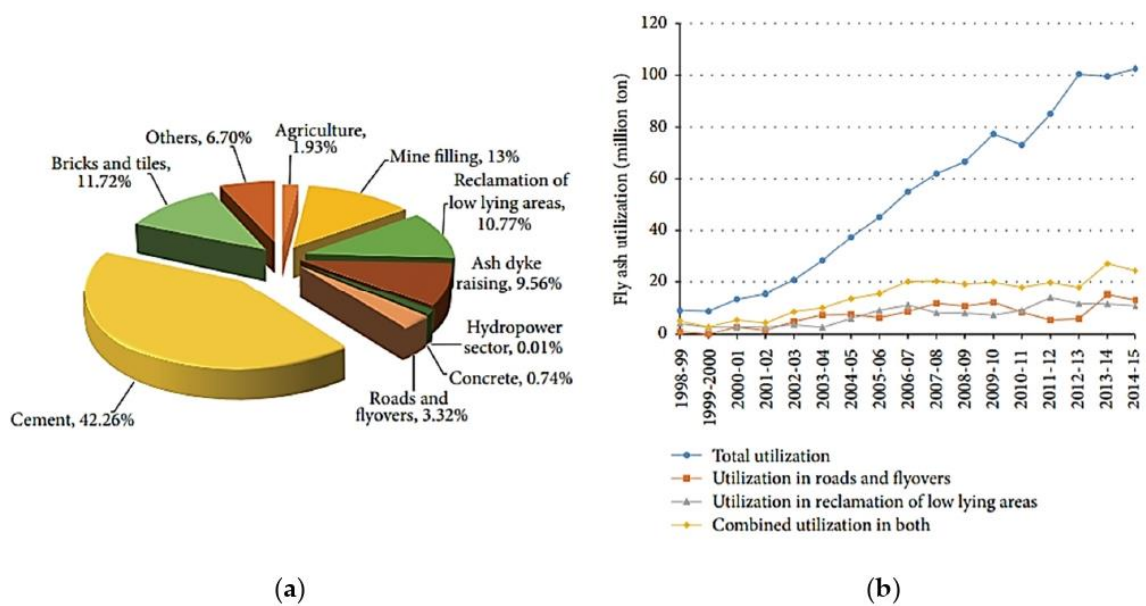


Figure 8. (a) Modes of the utilisation of fly ash in the years 2014–2015 [57]; (b) utilisation of Fly ash in areas of engineering [56].

According to the [57] report, about 1.3 billion tonnes of solid waste are generated by cities globally each year and the volume is expected to increase to about 2.2 billion tonnes by 2025 [58]. Statistics have shown that approximately 780 million tonnes of waste are generated worldwide. These wastes include coal combustion products (CCP) such as fly ash, bottom ash, cenospheres, conditioned ash and flue gas desulphurisation gypsum. Out of these, the largest CCP of 395 million tonnes were produced by China, 118 million tonnes by North America, 105 million tonnes by India, 52.6 million tonnes by Europe, 31.1 million tonnes by Africa and a minor contribution from the Middle East [59]. Table 12 shows CCP production around the world. According to [60], approximately 400 million tonnes of GGBS are produced annually worldwide while the production of steel slag is around 350 million tonnes. Studies have shown that an estimated amount of 70–120 million tonnes per year of red mud is produced worldwide [61], while an estimated 100–280 million tonnes of phosphogypsum is produced every year [62]. Cement kiln dust of approximately 510–680 million tonnes is produced yearly [63]. India had a fly ash production of about 163.56 million tonnes per year in 2014 which increased to 184.14 million tonnes in 2014 [57]. Meanwhile, the utilisation of fly ash in the year 2012–2013 in India was 100.37 million tonnes which are approximately 61.37% of the total waste produced that year [64]. About

41.18% of fly ash was utilised by cement the cement industry in India whiles 11.78% and 6% fly ash was utilised for reclamation of low-lying areas and as fill for road embankments. Table 13 shows some other industrial waste produces in India and Figure 9 shows modes of fly ash utilisation in India from 2012–2013.

Table 12. CCP production around the world [59].

Country/Region	CCP Production (Mt)	CCP Utilisation (Mt)	Utilisation Rate (%)	CCP Production/Person (Mt)	CCP Utilisation/Person (Mt)
Australia	13.1	6.0	45.8	0.60	0.27
Canada	6.8	2.3	33.8	0.20	0.07
China	395	265	67.1	0.20	0.20
Europe	52.6	47.8	90.9	0.11	0.10
India	105	14.5	13.8	0.09	0.01
Japan	11.1	10.7	96.4	0.09	0.08
Middle East and Africa	32.2	3.4	10.6	0.02	0.01
United States	118	49.7	42.1	0.37	0.16
Other Asia	16.7	11.1	66.5	0.05	0.03
Russian Federation	26.6	5.0	18.8	0.19	0.04

Table 13. Summary of findings of improved engineering properties of subgrade using waste.

Waste Type	Content (%) / Ratio	Information Source	Test	Results: UCS (kN/m ²), CBR (%), Swell (mm), Shrinkage (%)	Standards
Brick dust	30–50	[65]	CBR and UCS increased	CBR = 19 & UCS = 20	ASTM D1883-16
Brick dust	30–50	[66]	Shrinkage reduced	Shrinkage = 23.7 to 7.3	IS 2720
Brick dust	0–16	[67]	CBR increased	CBR = 7.9	ASTM D1883-16
Brick dust	10–30	[68]	CBR increased	CBR = 4.6	BS1377
Brick dust	5–25	[69]	UCS and CBR increased	UCS = 3544 & CBR = 21.90	IS:2720 part 16
Brick dust	0–30	[70]	UCS increased & swell decreased	UCS = 297.76 & Swell = 23.98	IS:2720 Part X1991
Brick dust	10–50	[71]	Swell reduced & CBR increased	Sewll = 0 & CBR = 12.54	IS 2720
Brick dust	10–30	[72]	CBR increased	CBR = 7.4	IS:2720 part 16
Brick dust	30–50	[73]	CBR improved from	CBR = 1.6 to 6.8	IS:2720 Part 16
Brick dust	10–40	[74]	UCS improved	UCS = 197	IS:2720 Part 16
Brick dust	10–20	[75]	UCS improved	UCS = 142.2	IS:2720 Part 16
Brick dust	10–20	[75]	CBR improved	CBR = 2.86	ASTM D1883-16
Brick dust	10–20	[75]	Swell decreased	Swell = 0.83	1977STM D1883-16
Brick dust	10–20	[75]	Shear strength improved	UCS = 67.15	BS 1377-1:2016
GGBS	5–10	[76]	UCS increased with	5% and 10% GGBS	IS:4332 Part 5 [1970]
GGBS	70 ratio	[77]	UCS increased	UCS = 450	IS:2720 Part 16
GGBS	0–30	[78]	CBR increased	CBR = 2.69	IS:2720 Part 10-1991
GGBS	0–30	[79]	UCS increased	UCS = 263.5	IS:2720 Part 16
GGBS	3–9	[80]	CBR increased	CBR = 2.05 to 8.29	IS:2720 Part 40-1977STM D1883-16
GGBS	3–12	[80]	Swell reduced	Swell = 67 and 21	IS:2720 Part 16
Plastic waste	0.0–1.0	[81]	CBR values increased	CBR = 1.967 to 2.479	IS-2720: Part 7
Plastic waste	0–1.5	[82]	UCS and CBR increased	UCS = 40 and CBR = 2.35	IS:2720 Part 16
Polypropylene	0.5–2	[78]	CBR increased	CBR = 8.51	IS 2720 part 10
Polypropylene	0.05–0.25	[83]	UCS increased	UCS = 1280	IS:2720 Part 40-1977
Polypropylene	0.2–0.5	[84]	Swell reduced considerably	Swell = 21.73	IS:2720 Part 40-1977
Polypropylene	0.5–2	[85]	Swell pressure reduced	Swell = 110 to 59	IS 2720 part 10
Polypropylene	0.1–1.3	[39]	UCS increased	UCS = 338.7	IS:4332 Part 5 [1970]
Polypropylene	0–1.4	[86]	UCS increased by	UCS = 29.87	IS:4332 Part 5 [1970]
Polypropylene	0.05–0.30	[87]	UCS decreased	UCS = 600 to 330	

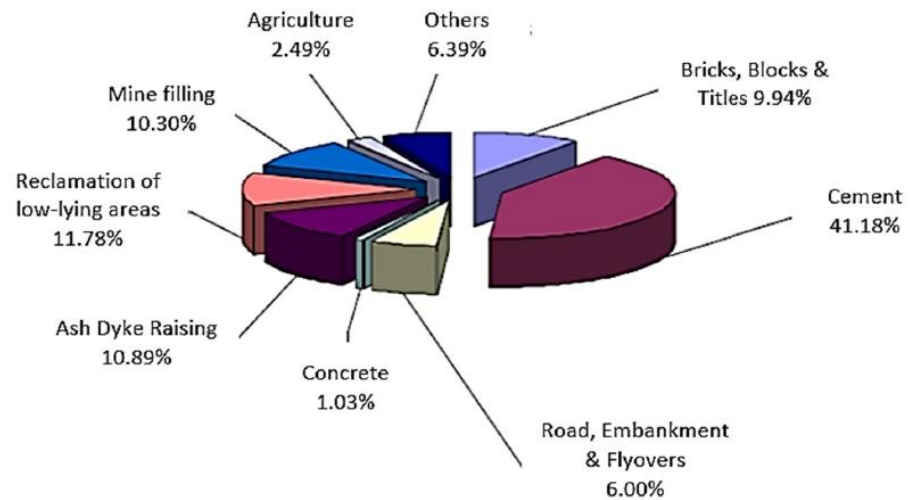


Figure 9. Modes of fly ash utilisation in 2012–2013 [64].

6. Sustainability of Using Processed Waste in Subgrade Stabilisation

Climate change has been a huge challenge to the world and many efforts have been made to remedy the situation by ensuring a more sustainable way of production especially in the construction sector to reduce greenhouse gas emissions [88]. Cement and lime are mostly used in subgrade stabilisation. However, there are many environmental effects associated with the production of cement and lime. The lime-drying process produces the biggest carbon emission (962.1 skg CO₂-eq/t sludge) accounting for 89.0% of the total emission [89]. According to [90], 7% of the world's CO₂ emission comes from cement production this is due to the high demand for cement. One tonne of CO₂ is emitted for every ton of cement produced. During cement production, 50% of the carbon emitted as a result of the calcination of the raw materials and 50% of the energy used [91]. Recent studies have shown the efforts made by many countries to mitigate carbon emissions in cement plants. However, the problem of greenhouse gas emission persists and the total replacement of cement with processed waste materials can help mitigate the problem and reduce the associated environmental problems.

Some concerns have been raised on the production of processed wastes including their associated environmental effects such as CO₂ emission and high energy consumption. However, the environmental impact associated with the production of processed waste is far less compared to the problems associated with the use of cement and its production. Using GGBS in high volumes as supplementary cementitious materials is good from the environmental point of view [92]. The higher the amount of GGBS used in replacing cement in soil stabilisation the lesser carbon footprint is expected due to the reduction in the use of cement [92]. The use of processed waste such as fly ash has significant environmental benefits including a net reduction in energy use and greenhouse gas emission. Figure 10 shows the contribution of the top ten countries in global CO₂ emission in 2008.

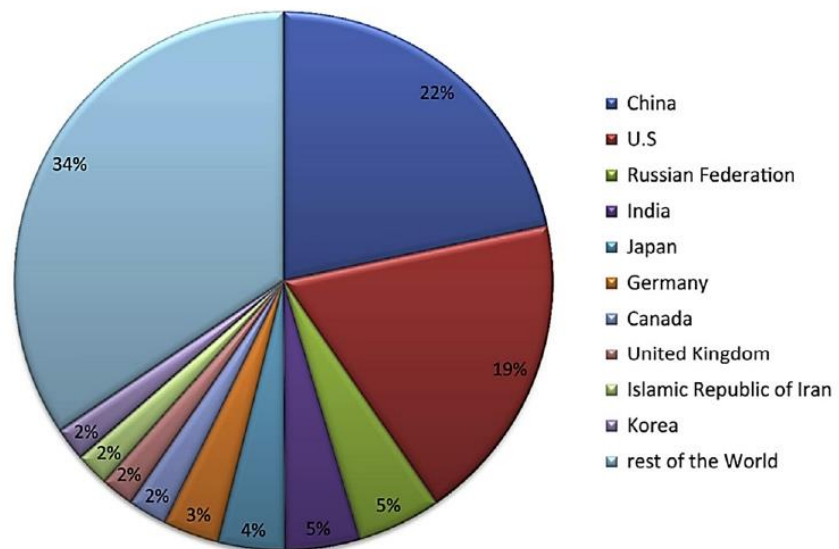


Figure 10. Contribution of the top 10 countries in global CO₂ emission in 2008 [93].

7. Effect of Process Waste on the Engineering Properties of Road Subgrade

Brick dust waste is mainly sourced from the cutting and demolition of brick and brick structures. Brick dust waste has been reportedly used in various studies to stabilise expansive road subgrade material. According to [94], the California bearing ratio (CBR) value increased to over 400% and a high unconfined compressive strength (UCS) was achieved when an optimum brick dust waste (BDW) content of 40% was used during expansive subgrade stabilisation. Compressive strength and CBR of soil reached their maximum values based on the standard compaction test when an optimum content of 40% BDW was used in subgrade stabilisation in accordance with ASTM D2166/D2166M-13 and ASTM D1883-14.

Other studies have shown an increase in CBR values at optimum BDW content from 5% to 20% [95]. The best stabilisation effects were obtained with brick dust waste at an optimum content of 50% [96]. A reduction in swell linear shrinkage and compaction water content was recorded when an optimum content of 50% brick dust waste was used in subgrade stabilisation [65]. Good CBR and swelling results were achieved when 20% of brick dust waste proportions were used in expansive subgrade stabilisation for flexible pavement [97]. Unconfined compressive strength increased with the addition of 30% brick dust waste and began to decrease at 40% brick waste in accordance with ASTM D2166/D2166M-13 [74]. Studies under the use of brick waste as a partial replacement for cement in expansive subgrade stabilisation have shown that the optimum or the highest proportion of brick waste used in subgrade stabilisation to achieve good engineering properties of soil is up to 50%. Brick dust waste proportion from 5%, 10%, 15%, 20% and 25% was used in subgrade stabilisation and the results obtained are as follows CBR 7.36, 8.54, 13.70, 19.13 and 7.36. UCS 0.60, 2.60, 4.31 and 2.84 kg/cm² respectively. Unconfined compressive strength increased with the addition of 30% brick dust waste and began to decrease at 40% brick waste [74].

GGBS is a by-product of the steel manufacturing process and has been successfully used in various studies as cement replacement to stabilise expansive road subgrade material. The first application of GGBS based stabiliser combination in road pavement construction in the UK was on the A421 Tingwick Bypass in Buckinghamshire, and on the A130 road near London [98]. The engineering properties of expansive soil was improved with the addition of up to 7.5% GGBS [99]. Subgrade materials were stabilised with 16% GGBS and the results obtained shows an increase in UCS value over time to 1500 kN/m² in

accordance with ASTM 1633 [100]. The addition of 6% GGBS to a lime treated soil reduced swell from 8% to 0% [101]. High compressive strength of 14.2, 89, 211.9 and 656 kPa was achieved when GGBS proportions of 6%, 12%, 18% and 24% were used in subgrade stabilisation after 28 days of curing [102]. Plastic waste has been successfully used in various studies as an additive to stabilise expansive road subgrade material. CBR value of 3.04 was achieved for soil stabilised with up to 2% plastic strip and UCS values of up to 316.4 kN were achieved [103]. Synthetic fibres such as polypropylene have been reportedly used in various studies as an additive to stabilise expansive road subgrade material. Plastic waste has been successfully used in various studies as an additive to stabilise expansive road subgrade material. CBR value of 3.04 was achieved for soil stabilised with up to 2% plastic strip and UCS values of up to 316.4 kN were achieved [103]. Synthetic fibres such as polypropylene have been reportedly used in various studies as an additive to stabilise expansive road subgrade material. Figure 11a shows the effect of polypropylene fibre on UCS; Figure 11b shows the UCS results of polypropylene fibre content, and Figure 11c shows the effect of brick dust waste on CBR. Table 13 shows a summary of findings of improved engineering properties of expansive subgrade stabilised using various types of processed waste.

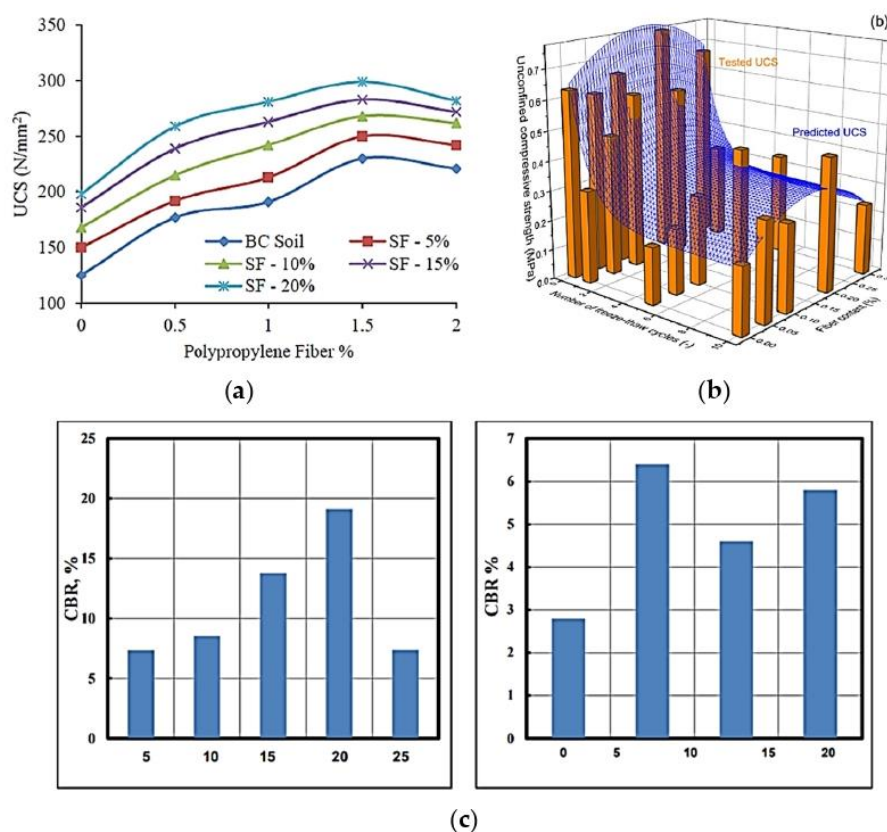


Figure 11. (a) Effect of polypropylene fibre on UCS [39]; (b) UCS results of poly-propylene fibre content [66] and (c) Effect of Brick dust waste on CBR [95].

8. Enhancement Mechanisms of Waste, Cement and Lime in Subgrade Stabilisation

8.1. Lime

Before cement, quick lime or hydraulic lime was the most common lime used in subgrade stabilisation. It has proven to be a good modification agent for the stabilisation of highway and airport pavement subgrade. When the soil is mixed with lime, a lime-soil

reaction takes place which may change the moisture and density relationship of the soil. The addition of lime as a binder to soil triggers a lime hydration process responsible for pH increase in soil. The lime hydration process with the aid of calcium, release cementitious products (calcium–silicate–hydrate (C–S–H) and calcium–aluminate–hydrate (C–A–H)) responsible for soil stabilisation. When lime is mixed with pozzolanic materials such as fly ash, a pozzolanic reaction takes place which releases cementitious products C–S–H and C–A–H gel. Pozzolanic materials are any material with the ability to react with calcium hydroxide to produce C–S–H and C–A–H gel. Pozzolanic reaction is the process where cement-like compounds are formed between lime and certain clay materials to bind soil particles together. This reaction further increases the strength and durability of stabilised subgrade depend on curing time and temperature [104]. Lime works well with clay minerals in soil with plasticity greater than 10% and a minimum clay content of 10%. A soil with a plasticity index between 20% and 30% with a liquid limit from 25% to 50% is recommended for lime stabilisation in most civil engineering applications [105]. Unlike cement, lime is slow in achieving its strength resulting in a long curing time. Long-term stabilisation effects are generated as a result of pozzolanic reactions which occur depending on the characteristics of the soil being treated.

8.2. Cement

Portland cement is a common subgrade stabilisation material used to improve the engineering properties of subgrade materials. It is a finely ground powder (hydraulic binder) that becomes solid when mixed with water through the process called hydration [106]. During the hydration process cement gel matrix is produced (C–S–H) which binds the soil particles together and is responsible for strength gain [107]. In subgrade stabilisation, the amount of cement used is in the range of 4% and 15% to increase the strength of subgrade materials [108]. According to [109], cement is suitable for the stabilisation of subgrade with a low plasticity index ranging between 2% and 30%. Additionally, a high pH can be recorded during cement hydration and C–S–H production as alkalis become solubilised due to pozzolanic reactions [110]. Figure 12a shows the pozzolanic reaction between clay particles and binder. Figure 12b shows cementitious hydration activity between clay particles and binder.

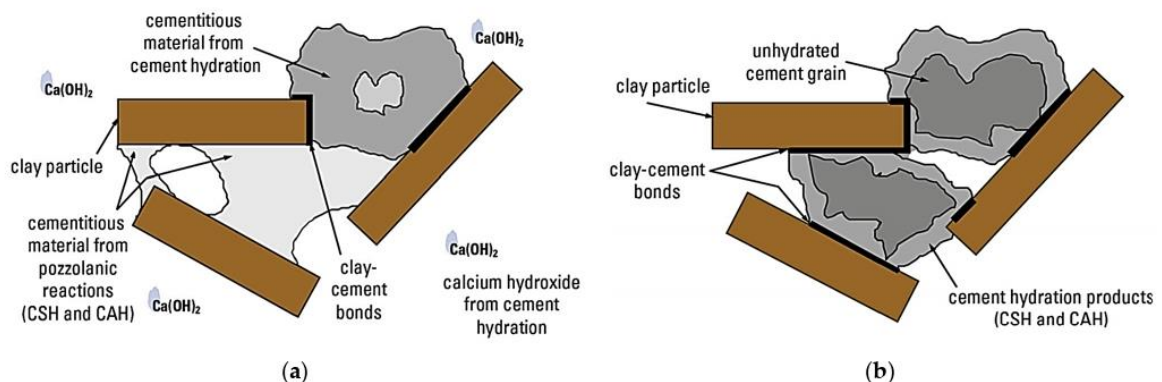


Figure 12. (a) Pozzolanic reaction between clay particles and binder [111]; (b) cementitious hydration activity between clay particles and binder [111].

8.3. Waste Materials

Any waste materials which possess pozzolanic properties has the ability to enhance the engineering properties of subgrade materials just like cement and lime. Waste materials are mostly used as a partial replacement for cement and lime for high strength gain and durability. The following pozzolanic waste materials reacts the same way as cement and

lime when used in subgrade stabilisation; fly ash, GGBS, silica fume, rice husk ash, phosphogypsum, ceramic wastes, and construction and demolition waste based on pozzolanic materials. GGBS is a latent hydraulic binder when rapidly quenched in water at the molten stage [112]. GGBS forms a supplementary binder in many cement applications to enhance durability. In subgrade stabilisation, the addition of GGBS introduces additional alumina, calcia, silica and magnesia to the system [113]. Construction and demolition waste such as brick dust are produced by the calcination of alumina-silicate clay which are ground into fines powder giving it pozzolanic properties and can be used as cement replacement in subgrade stabilisation [114]. Brick waste is pozzolanic, materials that contain alumina/silica which react to form new compounds (calcium silicate hydrate (C-S-H) and calcium aluminate hydrate (C-A-H). The addition of pozzolanic waste materials to a soil mix will enhance the engineering properties and speedup setting time with increased strength and durability. Rice husk ash and silica fume are rich in amorphous SiO_2 which have great pozzolanic properties [115]. Phosphogypsum has been used together with cement lime and fly ash to stabilise soil despite its high sulfate content [115]. Ceramic wastes possess pozzolanic properties because they are produced from clay and the thermal process leaves the Al and Si oxides in an amorphous state [115].

As much as partial replacement of cement and lime is important in the fight to reduce greenhouse gas emissions, the total replacement of cement and lime in subgrade stabilisation would speed up the global fight towards zero carbon. Recently, geopolymers have been used as cement replacement in subgrade stabilisation, providing an avenue for the total replacement of cement. The name “geopolymer” was coined by Davidovits, the inventor and developer of polymerisation to classify the newly discovered geosynthetic that produces inorganic polymeric materials now used in several industrial applications [116]. Geopolymers can be produced using waste materials such as fly ash, slag, silica fume, bentonite etc. amongst these waste materials, fly ash-based geopolymer cementitious binder has emerged as a promising new cement alternative in road subgrade stabilisation [117]. Fly ash-based geopolymers are produced by the chemical reaction of aluminosilicate oxides (Si_2O_5 , Al_2O_2) with alkali polysilicates yielding polymeric Si-O-Al bonds. Geopolymer can be produced with any waste materials containing silica, alumina and calcium content-rich composition. Preferably, low-calcium fly ash should be used than high calcium (ASTM class C) fly ash for the formation of geopolymers. This is because the presence of a high amount of calcium may affect the polymerisation process [118]. Fly ash with sodium hydroxide and sodium silicate as well as potassium hydroxide with potassium silicate combinations was used to produce geopolymer [119]. The presence of calcium content in fly ash significantly improved compressive strength development during subgrade stabilisation in a short curing time [120]. Using polymers in road subgrade stabilisation improves the density and load-bearing capacity of the pavement subgrade [2].

9. Limitations in the Use of Waste Compared to Cement and Lime in Subgrade Stabilisation

The use of waste as additives in subgrade stabilisation comes with some limitations that need to be addressed. Some of these limitations include contamination through the leaching of toxic substances into waste dumped in landfills. The engineering properties and performance of road subgrade can be affected due to these toxic materials found in the waste. Additionally, the cost-effectiveness of decontaminating these wastes can be a limitation to the use of waste materials in subgrade stabilisation. Many times, greenhouse gas emissions are associated with the production of cement and lime. However, there is a significant amount of carbon dioxide emission associated with the processing of waste materials for use as additives in subgrade stabilisation. Even though the processing of waste materials and cement and lime production produce some amount of carbon dioxide, the low cost of waste materials used in subgrade stabilisation holds promising keys to a sustainable future.

10. Summary of Findings and Future Focus

The effects of expansive subgrade materials in road pavement structure and the damage they cause to road pavement and other infrastructure has been reviewed. The study has shown that the problem of expansive subgrade is not limited to one geographical location, and the damage caused by expansive soils can run into billions of pounds as cost of maintenance or redesign of the road structure. The study has proven that cement and lime are mostly used in subgrade stabilisation. However, processed waste materials are effective for use as cement and lime replacement in road subgrade stabilisation using chemical stabilisation techniques. Waste materials and industrial by-products possess characteristics and engineering properties that can be found in cement and lime making these wastes materials a suitable substitute for cement and lime in road subgrade stabilisation.

It has been established in this study that the use of waste materials in subgrade stabilisation is cheaper compared to using cement and lime. Although the process of transforming waste materials used as additives in subgrade stabilisation is associated with some amount of greenhouse gas emission, this study has shown that the amount of greenhouse gas emitted during the processing of waste materials is far less compared to the carbon dioxide emitted during cement production. This makes the use of waste in subgrade stabilisation more sustainable, environmentally friendly and cost-effective. The availability of possessed waste materials to meet the current demand of subgrade stabilisation has been investigated and proven in this study, that there is enough processed waste available to meet the current demand. The future of sustainable engineering and achieving the United Nation Sustainable Development Goals (Goal 9: Industry, Innovation, and Infrastructure; Goal 12: Responsible Consumption and Production, and Goal 13: Climate Action) can be feasible when a conscious effort is made to use waste materials in road subgrade stabilisation [121].

11. Conclusion and Recommendations

Efforts have been made by many countries and organisations to tackle the challenges of climate change which is caused by human activities. Activities within the engineering and construction sector have contributed largely to the high amount of carbon dioxide in the atmosphere, which is the main cause of climate change. The use of traditional additives such as cement and lime in road subgrade stabilisation has contributed negatively to the environment due to the emission of greenhouse gas, pollution of water bodies, ecosystems and the destruction of natural resources during cement production. The greener ways of road subgrade stabilisation established in this study using non-traditional additives (such as waste materials and industrial by-products) in subgrade stabilisation have always been successful.

The study has proven that processed waste materials in subgrade stabilisation is sustainable, less costly, environmentally friendly and effective in enhancing the engineering properties of expansive subgrade materials. the availability of processed waste and industrial by-products to meet current demand has been established in this study. This study reveals the possibility of using waste materials like cement and lime replacement in road construction due to their cementitious properties, engineering properties and characteristics of these waste which as similar to cement and lime.

Based on the findings of this review, the following recommendations are proposed:

1. Research should be conducted to investigate new/novel and more sustainable waste materials that can be used in road subgrade stabilisation.
2. Companies and firms should encourage contractors by giving them some incentives for using sustainable waste materials in road construction. This will help achieve the global fight against climate change by 2050.
3. Strict rules or legislation should be put in place during the bidding process for contracts to ensure a certain amount of sustainable waste materials are used in construction.

4. Further investigation should be conducted into the whole life cycle cost of road stabilised with waste materials compared to cement and lime stabilised subgrade. This will provide a wider picture of the cost benefits of using waste materials in road construction
5. Further investigation can be carried out in the future to determine long-term durability and how elevated and freezing temperatures can affect subgrade materials stabilised using processed waste.

Author Contributions: Conceptualisation, S.J.A. and S.Y.A.; methodology, S.Y.A. and S.J.A.; validation, S.Y.A. and S.J.A.; formal analysis, S.Y.A. and S.J.A.; investigation, S.Y.A. and S.J.A.; resources, S.J.A., C.A.B. and A.-M.M.; data curation, S.Y.A. and S.J.A.; writing—original draft preparation, S.Y.A. and S.J.A.; writing—review and editing, S.Y.A., S.J.A. and C.A.B.; visualisation, S.J.A., C.A.B. and A.-M.M.; supervision, S.J.A., C.A.B. and A.-M.M.; project administration, C.A.B., A.-M.M. and S.J.A. All authors have read and agreed to the published version of the manuscript.

Funding: This research did not receive any specific grant from funding agencies in the public, commercial, or not-for-profit sector.

Institutional Review Board Statement: Not Applicable.

Informed Consent Statement: Not Applicable.

Acknowledgments: The authors acknowledge the advice, comments and suggestions from anonymous reviewers significantly improved the quality of this paper.

Conflicts of Interest: The authors declare that they have no conflict of interest associated with this publication and no financial support has been given to influence the outcome of this work.

References

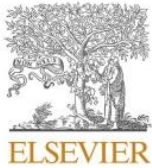
1. López-Lara, T.; Hernández-Zaragoza, J.; Horta-Rangel, J.; Rojas-González, E.; López-Ayala, S.; Castaño, V. Expansion reduction of clayey soils through Surcharge application and Lime Treatment. *Case Stud. Constr. Mater.* **2017**, *7*, 102–109. [CrossRef]
2. Amakye, S.Y.; Abbey, S.J. Understanding the performance of expansive subgrade materials treated with non-traditional stabilisers: A review. *Clean. Eng. Technol.* **2021**, *4*, 100159. [CrossRef]
3. Jones, L.D.; Jefferson, I. Institution of civil engineers manuals series. In *Expansive Soils*; ICE Publishing British Geological Survey: Nottingham, UK, 2012; pp. 413–441. [CrossRef]
4. Eyo, E.; Ng'Ambi, S.; Abbey, S.J. Incorporation of a nanotechnology-based additive in cementitious products for clay stabilisation. *J. Rock Mech. Geotech. Eng.* **2020**, *12*, 1056–1069. [CrossRef]
5. Abbey, S.J.; Ngambi, S.; Ganjian, E. Development of Strength Models for Prediction of Unconfined Compressive Strength of Cement/Byproduct Material Improved Soils. *Geotech. Test. J.* **2017**, *40*, 20160138. [CrossRef]
6. Federica, C.; Idiano, D.; Massimo, G. Sustainable management of waste-to-energy facilities. *Renew. Sustain. Energy Rev.* **2014**, *33*, 719–728.
7. Wang, J.X. Expansive Soil and Practice in Foundation Engineering. PhD. Thesis, P.E. Programs of Civil Engineering Programs Louisiana Tech University, Ruston, LA, USA, 2016. Available online: [https://www.ltrc.lsu.edu/ltrc_16/pdf/presentations/10-University%20Transportation%20Centers%20\[Part%201\]-Characterization%20of%20Expansive%20Soils%20in%20Northern%20Louisiana.pdf](https://www.ltrc.lsu.edu/ltrc_16/pdf/presentations/10-University%20Transportation%20Centers%20[Part%201]-Characterization%20of%20Expansive%20Soils%20in%20Northern%20Louisiana.pdf) (accessed on 7 March 2021).
8. Jones, L.D.; Jefferson, I. Institution of Civil Engineers Manuals Series 2019. Available online: http://nora.nerc.ac.uk/id/eprint/17002/1/C5_expansive_soils_Oct.pdf (accessed on 18 January 2021).
9. Jalal, F.E.; Xu, Y.; Jamhiri, B.; Memon, S.A. On the Recent Trends in Expansive Soil Stabilization Using Calcium-Based Stabilizer Materials (CSMs): A Comprehensive Review. *Adv. Mater. Sci. Eng.* **2020**, *2020*, 1–23. [CrossRef]
10. Sabat, A. A Study on Some Geotechnical Properties of Lime Stabilised Expansive Soil—Quarry Dust Mixes. *Int. J. Emerg. Trends Eng. Dev.* **2012**, *1*, 42–49.
11. Elarabi, H. Damage Mechanism of Expansive Soils Damage Mechanism of Expansive Soils 2010. Available online: [Gov.uk/pdf/GEHO1111BVDF-E-E.pdf](http://gov.uk/pdf/GEHO1111BVDF-E-E.pdf) (accessed on 13 April 2020).
12. Osinubi, K.; Ijimdiya, T.S.; Nmadu, I. Lime Stabilization of Black Cotton Soil Using Bagasse Ash as Admixture. *Adv. Mater. Res.* **2009**, *62–64*, 3–10. [CrossRef]
13. Nelson, J.D.; Miller, D.J. *Expansive Soils: Problems and Practice in Foundation and Pavement Engineering*, 1st ed.; Wiley: New York, NY, USA, 1992; ISBN 0471511862.
14. Hossain, A.S.M.F.; Sultana, N.; Bhowmic, S.; Hoque, M.S.; Shantana, F.A. Modification of expansive soil using recycled plastic bottle chips. *J. Geotech. Stud.* **2019**. [CrossRef]

15. British Geological Survey. Available online: <https://www.bgs.ac.uk/geology-projects/shallow-geohazards/clay-shrink-swell/> (accessed on 17 August 2021).
16. White, J.D.; Vennapusa, P. Low-cost rural surface alternatives: Literature review and recommendations 2013. InTrans Project Reports. 28. Available online: https://lib.dr.iastate.edu/intrans_reports/28 (accessed on 16 March 2021).
17. The geological society. 2012. Available online: <https://www.geolsoc.org.uk/Geoscientist/Archive/March-2014/Cracking-up-in-Lincolnshire> (accessed on 16 March 2021).
18. Eyo, E.U.; Ng'Ambi, S.; Abbey, S.J. Performance of clay stabilized by cementitious materials and inclusion of zeolite/alkaline metals-based additive. *Transp. Geotech.* **2020**, *23*, 100330. [CrossRef]
19. Al-Rawas, A.A.; Goosen, F.A. *Expansive Soils: Recent Advances in Characterization and Treatment*; Taylor & Francis: London, UK, 2006. [CrossRef]
20. Reda, A.; Ibrahim, E.; Houssami, L. A Cure for Swelling 2016. Available online: <https://dar.com/news/details/a-cure-for-swelling> (accessed on 21 February 2021).
21. Eyo, E.U.; Abbey, S.J.; Ngambi, S.; Ganjian, E.; Coakley, E. Incorporation of a nanotechnology-based product in cementitious binders for sustainable mitigation of sulphate-induced heaving of stabilised soils. *Eng. Sci. Technol. Int. J.* **2020**, *24*, 436–448. [CrossRef]
22. Zaid, A. Swelling Expansion and Dilation of Soil 2017. Available online: <https://www.slideshare.net/AhmedZaid11/swelling-expansion-and-dilation-of-soil> (accessed on 11 February 2021).
23. Huggett, J. *Clay Minerals*; Elsevier: Amsterdam, The Netherlands, 2015. [CrossRef]
24. Eyo, E.; Ng'Ambi, S.; Abbey, S. Investigative Study of Behaviour of Treated Expansive Soil Using Empirical Correlations. *IFCEE 2018* **2018**, 373–384. [CrossRef]
25. Uddin, F. *Montmorillonite: An Introduction to Properties and Utilization*; IntechOpen: London, UK, 2018. [CrossRef]
26. Dakshanamurthy, V.; Raman, V. A Simple Method of Identifying an Expansive Soil. *Soils Found.* **1973**, *13*, 97–104. [CrossRef]
27. ACPA Concrete Pavement Technology Series. Available online: <http://1204075.sites.myregisteredsite.com/downloads/TS/EB204P/TS204.2P.pdf> (accessed on 13 January 2021).
28. Murray, H.H. Chapter 2 structure and Composition of the Clay Minerals and their Physical and Chemical Properties. *Dev. Clay Sci.* **2006**, *2*, 7–31. [CrossRef]
29. Bananezhad, B.; Islami, M.R.; Ghonchepour, E.; Mostafavi, H.; Tikdari, A.M.; Rafiei, H.R. Bentonite clay as an efficient substrate for the synthesis of the super stable and recoverable magnetic nanocomposite of palladium (Fe₃O₄/Bentonite-Pd). *Polyhedron* **2019**, *162*, 192–200. [CrossRef]
30. Jaradat, K.A.; Darbari, Z.; Elbakhshwan, M.; Abdelaziz, S.L.; Gill, S.K.; Dooryhee, E.; Ecker, L.E. Heating-freezing effects on the orientation of kaolin clay particles. *Appl. Clay Sci.* **2017**, *150*, 163–174. [CrossRef]
31. Oti, J.E. The Development of Unfired Clay Building Materials for Sustainable Building Construction 2010. Available online: https://unilearn.southwales.ac.uk/webapps/blackboard/content/listContent.jsp?course_id=_141532_1&content_id=_2997727_1&mode=reset (accessed on 15 February 2021).
32. British Plastic Federation (2019). Polypropylene. Available online: <http://www.bpf.co.uk/plastipedia/polymers/pp.aspx> (accessed on 16 March 2021).
33. Behak, L. Soil Stabilization with Rice Husk Ash. *Rice Technol. Prod.* **2017**, *29*. [CrossRef]
34. Khatib, J.M.; Baalbaki, O.; ElKordi, A.A. Waste and supplementary cementitious materials in concrete. *Woodhead Publ. Ser. Civ. Struct. Eng.* **2018**, 493–511. [CrossRef]
35. Ghassemi, M.; Andersen, P.K.; Ghassemi, A.; Chianelli, R.R. Hazardous Waste from Fossil Fuels. *Encycl. Energy* **2004**, 119–131. [CrossRef]
36. Gholhaki, M.; Kheyroddin, A.; Hajforoush, M.; Kazemi, M. An investigation on the fresh and hardened properties of self-compacting concrete incorporating magnetic water with various pozzolanic materials. *Constr. Build. Mater.* **2018**, *158*, 173–180. [CrossRef]
37. Lafarge Cement UK. Manufacturing Process of Silica Fume 2012. Available online: <https://www.aggregate.com/> (accessed on 17 February 2021).
38. Miorslags. Available online: <http://miorslags.com/ggbs.html> (accessed on 14 February 2021).
39. Bianco Construction & Industrial Supplies. Available online: <https://www.bianco.com.au/product/view/7008> (accessed on 16 March 2021).
40. Guichon Valves. Manufacturing Process of Polypropylene 2019. Available online: <https://guichon-valves.com/pp-valves/> (accessed on 17 August 2021).
41. Tomar, A.; Sharma, T.; Singh, S. Strength properties and durability of clay soil treated with mixture of nano silica and Polypropylene fiber. *Mater. Today: Proc.* **2020**, *26*, 3449–3457. [CrossRef]
42. Mindiamart, 2021. Available online: <https://www.indiamart.com/proddetail/alkali-resistant-glass-fiber-21702650255.html> (accessed on 16 March 2021).
43. Amakye, S.Y.; Abbey, S.J.; Olubanwo, A.O. Consistency and mechanical properties of sustainable concrete blended with brick dust waste cementitious materials. *SN Appl. Sci.* **2021**, *3*, 1–12. [CrossRef]
44. Thakur, I.C.; Kisku, N.; Singh, J.P.; Kumar, S. Properties of concrete incorporated with GGBS. *Int. J. Res. Eng. Technol.* **2016**, *5*, 275–281. Available online: <https://ijret.org/volumes/2016v05/i08/IJRET20160508046.pdf> (accessed on 7 March 2021).

45. Kalantari, B.; Prasad, A.; Huat, B.B.K. Cement and Silica Fume Treated Columns to Improve Peat Ground. *Arab. J. Sci. Eng.* **2012**, *38*, 805–816. [CrossRef]
46. Khalil, A.A.; Siswomiharjo, W.; Sunarintyas, S. Effect of non dental glass fiber orientation on transverse strength of dental fiber reinforced composite. *J. Teknosains* **2017**, *5*, 104–110. [CrossRef]
47. Prasad, P.D.; Nagarnaik, P.B.; Gajbhiye, A.R. Utilization of solid waste for soil stabilization: A Review. *Electron. J. Geotech. Eng.* **2012**. Available online: https://www.researchgate.net/publication/267723862_Utilization_of_Solid_Waste_for_Soil_Stabilization_A_Review (accessed on 21 February 2021).
48. Ahmad, S. Study of Concrete Involving Use of Waste Paper Sludge Ash as Partial Replacement of Cement. *IOSR J. Eng.* **2013**, *3*, 6–15. [CrossRef]
49. Zorluer, L.; Afyon Kocatepe University; Gucek, S. The usability of industrial wastes on soil stabilization. *Rev. De La Construcción* **2020**, *19*, 80–89. [CrossRef]
50. Yilmaz, F.; Kamiloğlu, H.; Şadoğlu, E. Soil Stabilization with Using Waste Materials against Freezing Thawing Effect. *Acta Phys. Pol. A* **2015**, *128*, 80–89. [CrossRef]
51. RILON. Polypropylene Fibre: Main Characteristics, Application, products and Structure 2020. Available online: <https://rilonfibers.com/blog/polypropylene-fiber/> (accessed on 28 February 2021).
52. Arena, U.; Zaccariello, L.; Mastellone, M.L. Tar removal during the fluidized bed gasification of plastic waste. *Waste Manag.* **2009**, *29*, 783–791. [CrossRef] [PubMed]
53. US Department of Transportation. Available online: <https://www.fhwa.dot.gov/pavement/recycling/fach01.cfm> (accessed on 7 March 2021).
54. Chakraborty, S.; Mahmud, T.; Islam, M.M.; Islam, M.S. Use of paper industry waste in making low cost concrete 2014. 2nd International Conference on Advances in Civil Engineering. [ICACE-2014] CUET, Chittagong, Bangladesh. Available online: https://www.researchgate.net/publication/293810073_Use_of_Paper_Industry_Waste_in_Making_Low_Cost_Concrete (accessed on 19 March 2021).
55. James, J.; Pandian, P.K. Industrial Wastes as Auxiliary Additives to Cement/Lime Stabilization of Soils. *Adv. Civ. Eng.* **2016**, *2016*, 1–17. [CrossRef]
56. Central Electricity Authority. Report on fly ash generation at coal/lignite based thermal power station and its utilisation in the country for the year 2014-15, New Delhi, India. Available online: https://cea.nic.in/wp-content/uploads/2020/04/flyash_final_1415.pdf (accessed on 17 August 2021).
57. The World Bank. 2021. Available online: https://datatopics.worldbank.org/what-a-waste/trends_in_solid_waste_management.html (accessed on 16 March 2021).
58. Hoornweg, D.; Bhada-Tata, P. *What a Waste: A Global Review of Solid Waste Management*; World Bank: Washington, DC, USA, 2012.
59. Heidrich, C.; Feuerborn, H.; Weir, A. Coal combustion production: A Global Perspective. In Proceedings of the World of Coal Ash Conference, Lexington, KY, USA, 22–25 April 2013.
60. Motz, H.; Ehrenberg, A.; Mudersbach, D. Dry solidification with heat recovery of ferrous slag. In Proceedings of the Third International Slag Valorisation Symposium, Leuven, Belgium, 19–20 March 2013; pp. 37–55.
61. Mišík, M.; Burke, I.T.; Reismüller, M.; Pichler, C.; Rainer, B.; Mišíková, K.; Mayes, W.M.; Knasmueller, S. Red mud a byproduct of aluminum production contains soluble vanadium that causes genotoxic and cytotoxic effects in higher plants. *Sci. Total Environ.* **2014**, *493*, 883–890. [CrossRef]
62. Tayibi, H.; Choura, M.; López, F.A.; Alguacil, F.J.; López-Delgado, A. Environmental impact and management of phosphogypsum. *J. Environ. Manag.* **2009**, *90*, 2377–2386. [CrossRef]
63. Kumal, P.; Rajour, A.; Siddiqui, R. Biological remediation of alkaline cement kiln dust for sustainable development. In *Industrial, Medical and Environmental Application of Microorganisms*; Wageningen Academic Publishers: Madrid, Spain, 2014; pp. 52–58.
64. Central Electricity Authority. Report on fly ash generation at coal/lignite based thermal power station and its utilisation in the country for the year 2011-12 and 2012-14, New Delhi, India. Available online: https://cea.nic.in/wp-content/uploads/2020/04/fly_ash_final_111213.pdf (accessed on 17 August 2021).
65. Teja, S.L.; Kumar, S.S.; Needhidasan, S. Stabilisation of expansive soil using brick dust. *Int. J. Pure Appl. Math.* **2018**, *119*, 903–910. Available online: <https://acadpubl.eu/hub/2018-119-17/4/375.pdf> (accessed on 7 March 2021).
66. Bhavsar, S.; Patel, A. Analysis of Swellings and Shrinkage Properties of Expansive Soil Using Brick Dust as a Stabilizer. 2014. Available online: https://www.researchgate.net/publication/269762906_Analysis_of_Swelling_Shrinkage_Properties_of_Expansive_Soil_using_Brick_Dust_as_a_Stabilizer (accessed on 13 February 2021).
67. Kumar, J.K.; Kumar, V.P. *Experimental Analysis of Soil Stabilisation Using e-Waste*; Saveetha School of Engineering, SIMATS: Chennai, India, 2019; Volume 22, pp. 456–459.
68. Khan, T.A.; Taha, M.R.; Khan, M.M.; Shah, S.A.R.; Aslam, M.A.; Waqar, A.; Khan, A.R.; Waseem, M. Strength and Volume Change Characteristics of Clayey Soils: Performance Evaluation of Enzymes. *Minerals* **2020**, *10*, 52. [CrossRef]
69. Kumar, A.; Kumar, A.; Ved, P. Stabilization of Expansive Soil with Lime and Brick Dust. *Int. J. All Res. Educ. Sci. Methods* **2016**, *4*(9), 2455–6211. Available online: http://www.ijaresm.com/uploaded_files/document_file/Ajay_kumarNcca.pdf (accessed on 13 March 2021).
70. Pokale, K.R.; Borkar, Y.R.; Jichkar, R.R. Experimental Investigation for Stabilization of Black Cotton Soil By using waste material—Dust. *Int. Res. J. Eng. Technol.* **2015**, *2*, 726.

71. Neha, P.; Trivedi, M.K. Improvement of Pavement Soil Subgrade by Using Burnt Brick Dust. *Int. J. Res. Appl. Sci. Eng. Technol.* **2017**, *5*, 218–221.
72. Soil Stabilization using Brick Kiln Dust and waste Coir Fibre. *Int. J. Recent Technol. Eng.* **2019**, *8*, 2574–2578. [CrossRef]
73. Kinjal, C.C.; Padvi, H.S.; Patel, H.V.; Patel, J.A.; Tandel, J. Literature Review of Soil Stabilisation Using Different Materials. *Int. J. Tech. Innov. Mod. Eng. Sci.* **2018**. Available online: http://ijtimes.com/papers/finished_papers/IJTIMESV04I02150228175419.pdf (accessed on 21 February 2021).
74. Hairulla; Betaubun, P. The effect of using brick waste on the stabilisation of soft soil due to the unconfined compression. *J. Basic Appl. Sci. Res.* **2016**, *6*, 1–8. Available online: [https://www.textroad.com/pdf/JBASR/J.%20Basic.%20Appl.%20Sci.%20Res.,%206\[2\]1-8,%202016.pdf](https://www.textroad.com/pdf/JBASR/J.%20Basic.%20Appl.%20Sci.%20Res.,%206[2]1-8,%202016.pdf) (accessed on 12 February 2021).
75. Rank, K.; Bhandari, J.; Mehta, J.V. Using Brick Dust Manufacturing Waste and Cement Dust Manufacturing Waste as Stabilising Materials for Expansive Soil 2020. Available online: <http://www.jetir.org/papers/JETIR2002078.pdf> (accessed on 14 February 2021).
76. Estabragh, A.R.; Jahani, A.; Javadi, A.A.; Babalar, M. Assessment of different agents for stabilisation of a clay soil. *Int. J. Pavement Eng.* **2020**, 1–11. [CrossRef]
77. Sharma, A.K.; Sivapullaiah, P. Ground granulated blast furnace slag amended fly ash as an expansive soil stabilizer. *Soils Found.* **2016**, *56*, 205–212. [CrossRef]
78. Prasad, S.D.; Prasad, D.S.V.; Raju, G.V.R. Stabilisation of black cotton soil using ground granulated blast furnace slag and plastic fibres. *Int. J. Recent Technol. Eng.* **2019**. Available online: <https://www.ijrte.org/wp-content/uploads/papers/v7i6c2/F11150476C219.pdf> (accessed on 21 February 2021).
79. Duyu, H.; Tania, T.; Dhake, M. Study on the effect of ground granulated blast furnace slag on the properties of black cotton soil and red soil. *Int. J. Sci. Res.* **2015**. Available online: <https://www.ijsr.net/archive/v6i5/ART20173214.pdf> (accessed on 18 January 2021).
80. Yadu, L.; Tripathi, R.K. Effects of Granulated Blast Furnace Slag in the Engineering Behaviour of Stabilised Soft Soil 2013. Available online: <https://www.sciencedirect.com/science/article/pii/S1877705813000209> (accessed on 11 February 2021).
81. Ashraf, A.; Sunil, A.; Dhanya, J.; Joseph, M.; Varghese, M.; Veena, M. Soil stabilisation using plastic bottles. In Proceedings of the Indian Geotechnical Conference, Kochi, Kerala, India, 15–17 December 2011. Available online: https://www.researchgate.net/publication/279999540_SOIL_STABILISATION_USING_RAW_PLASTIC_BOTTLES (accessed on 12 February 2021).
82. Wani, I.A.; Sheikh, I.M.; Maqbool, T.; Kumar, V. Experimental investigation on using plastic wastes to enhance several engineering properties of soil through stabilization. *Mater. Today Proc.* **2021**, *45*, 4571–4574. [CrossRef]
83. Tang, C.-S.; Shi, B.; Gao, W.; Chen, F.; Cai, Y. Strength and mechanical behavior of short polypropylene fiber reinforced and cement stabilized clayey soil. *Geotext. Geomembranes* **2007**, *25*, 194–202. [CrossRef]
84. Ali, N.; Raj, V.S. Effect of polypropylene fibre on swelling behaviour of black cotton soil. *Mater. Today Proc.* **2020**. [CrossRef]
85. Murthi, P.; Saravanan, R.; Poongodi, K. Studies on the impact of polypropylene and silica fume blended combination on the material behaviour of black cotton soil. *Mater. Today Proc.* **2020**, *39*, 621–626. [CrossRef]
86. Vakili, A.H.; Ghasemi, J.; bin Selamat, M.R.; Salimi, M.; Farhadi, M.S. Internal erosional behaviour of dispersive clay stabilized with lignosulfonate and reinforced with polypropylene fiber. *Constr. Build. Mater.* **2018**, *193*, 405–415. [CrossRef]
87. Ding, M.; Zhang, F.; Ling, X.; Lin, B. Effects of freeze-thaw cycles on mechanical properties of polypropylene fibre and cement stabilised clay. *Cold Reg. Sci. Technol.* **2018**. [CrossRef]
88. Booth, C.A.; Hammond, F.N.; Lamond, J.E.; Proverbs, D.G. *Solutions to Climate Change Challenges in the Built Environment*; Wiley-Blackwells: Oxford, UK, 2012.
89. Ping, L.; Zhao, G.; Lin, X.; Gu, Y.; Liu, W.; Cao, H.; Huang, J.; Xu, J. Feasibility and Carbon Footprint Analysis of Lime-Dried Sludge for Cement Production. *Sustainability* **2020**, *12*, 2500. [CrossRef]
90. Benhelal, E.; Zahedi, G.; Shamsaei, E.; Bahadori, A. Global strategies and potentials to curb CO₂ emissions in cement industry. *J. Clean. Prod.* **2013**, *51*, 142–161. [CrossRef]
91. Geng, Y.; Wang, Z.; Shen, L.; Zhao, J. Calculating of CO₂ emission factors for Chinese cement production based on inorganic carbon and organic carbon. *J. Clean. Prod.* **2019**, *217*, 503–509. [CrossRef]
92. Onn, C.C.; Mo, K.H.; Radwan, M.K.H.; Liew, W.H.; Ng, C.G.; Yusoff, S. Strength, Carbon Footprint and Cost Considerations of Mortar Blends with High Volume Ground Granulated Blast Furnace Slag. *Sustainability* **2019**, *11*, 7194. [CrossRef]
93. International Energy Agency (IEA). CO₂ Emission for Combustion Highlights 2010. Available online: https://www.iea.org/co2_highlights (accessed on 24 March 2021).
94. Anand, K.B.G.; Agrawel, S.; Dobriyal, A. Stabilisation of Cohesive Soil Using Demolished Brick Waste 2014, Innovations and Advances in Civil Engineering towards Green and Sustainable Systems. Available online: https://www.researchgate.net/publication/326972521_Stabilization_of_Cohesive_Soil_using_Demolished_Brick_Waste (accessed on 12 February 2021).
95. Al-Baidhani, A.A.; Al-Taie, A. Review of brick waste in expansive soil stabilisation and other civil engineering applications. *J. Geotech. Stud.* **2019**, *4*, 14–23.
96. Sachin, N.B.; Hiral, B.J.; Priyanka, K.S.; Ankit, P. Effect of burnt brick dust on engineering properties on expansive soil. *Int. J. Res. Eng. Technol.* **2014**, *3*, 433–441.
97. Reddy, S.S.; Prasad, A.C.S.V.; Krishna, N.V. Lime-stabilised black cotton soil and brick powder mixture as subbase material. *Adv. Civ. Eng.* **2018**, *18*, 1–10.

98. Wild, S.; Kinuthia, J.M.; Jones, G.I.; Higgins, D.D. Effect of partial substitution of lime with ground granulated blast furnace slag (GGBS) on the strength properties of lime-stabilised sulphate-bearing clay soils. *Eng. Geol.* **1998**, *51*, 37–53. [[CrossRef](#)]
99. Corrêa-Silva, M.; Miranda, T.; Rouainia, M.; Araújo, N.; Glendinning, S.; Cristelo, N. Geomechanical behaviour of a soft soil stabilised with alkali-activated blast-furnace slags. *J. Clean. Prod.* **2020**, *267*, 122017. [[CrossRef](#)]
100. Obuzor, G.; Kinuthia, J.; Robinson, R. Soil stabilisation with lime-activated-GGBS—A mitigation to flooding effects on road structural layers/embankments constructed on floodplains. *Eng. Geol.* **2012**, *151*, 112–119. [[CrossRef](#)]
101. Celik, E.; Nalbantoglu, Z. Effects of ground granulated blastfurnace slag (GGBS) on the swelling properties of lime-stabilized sulfate-bearing soils. *Eng. Geol.* **2013**, *163*, 20–25. [[CrossRef](#)]
102. Gokul, V.; Steffi, D.A.; Kaviya, R.; Harni, C.; Dharani, S. Alkali activation of clayey soil using GGBS and NaOH. *Mater. Today: Proc.* **2020**, *43*, 1707–1713. [[CrossRef](#)]
103. Kassa, R.B.; Workie, T.; Abdela, A.; Fekade, M.; Saleh, M.; Dejene, Y. Soil Stabilization Using Waste Plastic Materials. *Open J. Civ. Eng.* **2020**, *10*, 55–68. [[CrossRef](#)]
104. Consoli, N.C.; Da Silva Lopes, L.; Foppa, D.; Heineck, K.S. Key parameters dictating strength of lime/cement-treated soils. *Proc. Inst. Civ. Eng. Geotech. Eng.* **2009**, *162*, 111–118. [[CrossRef](#)]
105. Boardman, D.I.; Glendinning, S.; Rogers, C.D.F. Development of stabilisation and solidification in lime-clay mixes. *Geotechnique* **2001**, *51*, 533–543. [[CrossRef](#)]
106. Neville, A.M. *Properties of Concrete*, 5th ed.; Wiley: New York, NY, USA; Harlow, England, 2011. Available online: <https://pdfcoffee.com/properties-of-concrete-fifth-edition-a-m-neville-pdf-pdf-free.html> (accessed on 13 September 2021).
107. Prusinski, J.R.; Bhattacharja, S. Effectiveness of Portland cement and lime in stabilising clay soils. *Transp. Res. Rec.* **1999**, *1652*, 215–227. [[CrossRef](#)]
108. Walker, P. Review and Experimental Comparison of erosion tests or Earth Blocks. In *Terra 2000 Postprints: 8th International Conference on the Study and Conservation of Earthen Architecture, Torquay, Devon, UK, May 2000*; James & James: London, UK, 2000.
109. Gooding, D.E.; Thomas, T.H. The potential of cement stabilised building blocks as an urban building material in developing countries. DTU working paper No.44. 1995. Available online: <https://warwick.ac.uk/fac/sci/eng/research/grouplist/structural/dtu/pubs/wp/wp44/wp44.pdf> (accessed on 17 August 2021).
110. Lea, F.M. *The Chemistry of Cement and Concrete*, 3rd ed.; Edward Arnold: London, UK, 1980.
111. Gross, J.; Adaska, W. Guide to Cement-Stabilised Subgrade Soils. 2020. Available online: https://intrans.iastate.edu/app/uploads/2020/05/guide_to_CSS.pdf (accessed on 23 September 2021).
112. Taylor, H.F.W. *Cement Chemistry*, 2nd ed.; Thomas Telford Publishing: London, UK, 1997; pp. 19–43.
113. Oner, A.; Akyuz, S. An experimental study on optimum usage of GGBS for the compressive strength of concrete. *Cem. Concr. Compos.* **2007**, *29*, 505–514. [[CrossRef](#)]
114. Kartini, K.; Rohaidah, M.N.; Zuraini, Z.A. Performance of ground clay bricks as partial cement replacement in grade 30 concrete. *Int. Sch. Sci. Res. Innov.* **2012**, *6*, 312–315.
115. Seco, A.; Ramirez, F.; Miqueleiz, L.; Urmeneta, P.; García, B.; Prieto, E.; Oroz, E.P.A.V. *Types of Waste for the Production of Pozzolanic Materials—A Review*; BoD – Books on Demand: Norderstedt, Germany, 2012. [[CrossRef](#)]
116. Davidovits, J. Geopolymers and gopolymeric materials. *J. Therm. Anal.* **1989**, *35*, 429–441. [[CrossRef](#)]
117. Srinivasan, K.; Sivakumar, A. Geopolymer Binders: A Need for Future Concrete Construction. *ISRN Polym. Sci.* **2013**, *2013*, 1–8. [[CrossRef](#)]
118. Gourley, J.T. Geopolymers, opportunities for environmentally friendly construction material. In *Proceedings of the International Conference and Exhibition on Adaptive materials for a Modern society (Materials '30)*, Sydney, Australia, 30–31 August 2003.
119. Palomo, A.; Grutzeck, M.W.; Blanco, M.T. Alkali-activated fly ashes: A cement for the future. *Cem. Concr. Res.* **1999**, *29*, 1323–1329. [[CrossRef](#)]
120. Van Jaarsveld, J.G.S.; Van Deventer, J.S.J.; Lukey, G.C. The characteristics of source materials in fly ash-based geopolymers. *Mater. Lett.* **2003**, *57*, 1272–1280. [[CrossRef](#)]
121. United Nation Sustainable Development Goals. Available online: <https://sdgs.un.org/goals/goal9> (accessed on 17 August 2021).



Contents lists available at ScienceDirect

Cleaner Engineering and Technology

journal homepage: www.sciencedirect.com/journal/cleaner-engineering-and-technology

Understanding the performance of expansive subgrade materials treated with non-traditional stabilisers: A review

Samuel Y. Amakye^{*}, Samuel J. Abbey

Department of Geography and Environmental Management, Faculty of Environment and Technology, University of the West of England, United Kingdom

ARTICLE INFO

Keywords:

Expansive soil
Subgrade stabilisation
Engineering properties
California bearing ratio
Unconfined compressive strength

ABSTRACT

Expansive soils are problematic soils which pose a risk to the safety of civil engineering structures. These soils can be treated by compaction or by adding additives to the soil. Where the strength and properties of expansive soil cannot be improved via mechanical stabilisation (Compaction), a desirable strength can be achieved through the use of chemical admixture techniques. The swelling and shrinkage of expansive soils cause movement in the soil mass resulting in a differential settlement in engineering structures such as roads and building leading to cracks and subsequent failure leading to high cost of maintenance. Calcium based additives such as cement and lime have been used in expansive subgrade stabilisation to enhance the strength, reduce swell and subsequent differential settlement. However, the growing concerns on carbon dioxide (CO₂) emission and climate change have reignited the need for a more sustainable soil stabilisation techniques using waste materials. In this study, non-traditional expansive subgrade treatment techniques using sustainable waste materials with respect to their efficiency in improving the geotechnical engineering properties of the subgrade materials have been investigated and reviewed. This study also discusses the engineering problems associated with expansive soils, proposing an effective, efficient, cheaper and sustainable application of non-traditional stabilisers in expansive soil stabilisation. The study concludes that, the addition of non-traditional stabilisers in expansive subgrade stabilisation using chemical stabilisation techniques can improve the engineering properties of expansive subgrade materials.

1. Introduction

An expansive soil is any soil that has the potential to swell when wet and shrink when dry. Clay mineral smectites found in expansive soils usually exhibits evident volume change with changes in moisture content, causing major structural and geotechnical challenges worldwide. Structures built on expansive soils develop defects due to swell and shrink activities causing fissures in the structure (Abbey et al., 2019). Each year the damage caused by expansive soil in buildings and infrastructural systems are more than the damage caused by floods, hurricanes, tornadoes and earthquakes combined (Wu et al., 2019). Over the past 10 years, effects from expansive soils have cost the UK economy an estimated amount of £3 billion making it the most damaging geohazard in Britain (Jones et al., 2019). Subgrade materials refer to the ground or soil underneath a road pavement. Oftentimes, these materials do not have sufficient capacity to support the weight of the road pavement and the traffic loads and will require some sort of modification and re-engineering to enhance its capacity to support the load. Expansive soils can lead to early distress causing the premature failure of the road

pavement structure. Chemical soil stabilisation techniques have been reportedly used in addressing the problems associated with expansive subgrades (Jalal et al., 2020). Chemical stabilisation involves adding different types of admixtures such as lime, cement lignin, lignosulfonate, xanthan gum among others as additives to improve the strength of expansive road subgrade (Rivera et al., 2020). Lignin, a by-product of paper and timber industry exhibited high mechanical performance when used as highway subgrade course material and road embankment in civil engineering infrastructure (Abbey et al., 2018). The mechanical responses, strength and durability of stabilised soil and natural silt were improved with the addition of Lignin (Zhang et al., 2020). Cement is popularly used to improve the engineering properties of expansive subgrade materials (Lucena et al., 2014). Stabilising road pavement subgrade has proved to be very costly and unsustainable due to the amount of carbon dioxide (CO₂) emitted during cement production (Abbey et al., 2017). However, the use of non-traditional stabilisers in road subgrade stabilisation will enhance the engineering properties of expansive subgrade materials while reducing environmental effects and overall construction cost (Kassa et al., 2020). Non-traditional stabilisers

^{*} Corresponding author.

E-mail addresses: samuel_amakye@outlook.com, Samuel.amakye@uwe.ac.uk (S.Y. Amakye), Samuel.abbey@uwe.ac.uk (S.J. Abbey).

<https://doi.org/10.1016/j.clet.2021.100159>

Received 20 August 2020; Received in revised form 15 May 2021; Accepted 4 June 2021

Available online 10 June 2021

2666-7908/© 2021 The Authors.

Published by Elsevier Ltd.

This is an open access article under the CC BY-NC-ND license

(<http://creativecommons.org/licenses/by-nc-nd/4.0/>).

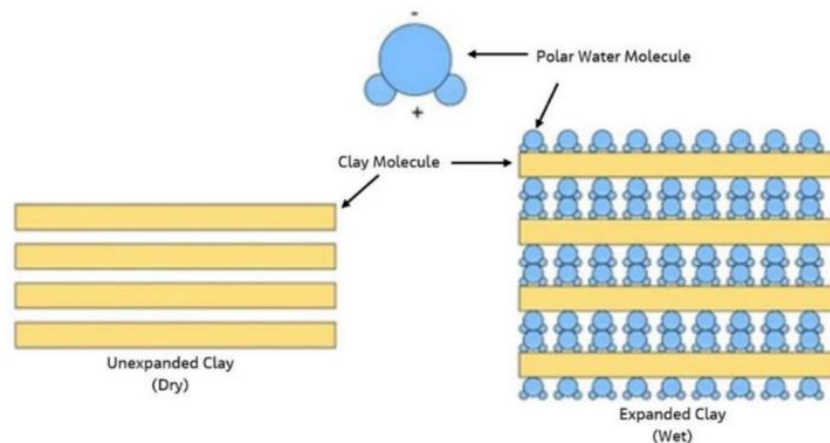


Fig. 1. Shrinking and Swelling of soils (Reda et al., 2016).

Table 1
Swelling potential of soils based on liquid limit (Dakshnamurthy et al., 1973).

Liquid limit	Classification
0–20	Non-Swelling
20–35	Low-Swelling
35–50	Medium-Swelling
50–70	High-Swelling
70–90	Very High-Swelling
>90 Extra	High-Swelling

Table 2
Classification of shrink potentials based on plasticity index (Jones and Jefferson, 2012).

I_p (%)	Clay Fraction(<0.002 mm)	Shrinkage potential
>35	>95	Very High
22–48	60–95	High
12–32	30–60	Medium
<18	<30	Low

Where I_p = Plasticity Index.

Table 3
Relation of Soil index Properties and Probably Volume Change for Highly Plastic Soils (ACPA Concrete Pavement Technology Series).

Data from Index Tests ¹			Estimation of probable expansion ² , percent total volume change (dry to saturated condition)	Degree of expansion
Colloid Content (percent minus 0.00004 in. (0.001 mm))	Plasticity Index	Shrinkage Limit Percent		
(ASTM D422)	(ASTM D4318)	(ASTM D427)		
>28	>35	>11	>30	Very High
20–31	24–41	7–12	20–30	High
13–23	15–28	10–16	10–20	Medium
<15	<8	<15	<10	Low

such as rice husk ash (RHA), ground granulated blast-furnace slag (GGBS), plastic waste, synthetic fibres, sugarcane bagasse ash (SCBA), cow dung ash (CDA), fly ash, bituminous, thermal, electrical, silica fume, geo-textile and fabrics, among others can be used in soil stabilisation (Rivera et al., 2020). The result obtained in subgrade stabilisation

using waste materials are suitable for application (Christopher et al., 2019). The current study presents a review on the use of non-traditional soil stabilisers and sustainable treatment of expansive subgrade materials.

2. Scope of the study

This current study presents an in-depth review into the characteristics and behaviour of expansive soils. The study focusses on expansive road pavement subgrade stabilisation providing information on geotechnical solutions based on current and non-traditional treatment of expansive subgrade stabilisation techniques. The main objective of this study was to review the engineering properties such as Unconfined Compressive Strength (UCS), California Bearing Ratio (CBR), Tensile Strength, Shrink-Swell and microstructural properties of expansive subgrade stabilised with non-traditional sustainable waste materials. This study will contribute to the existing knowledge on sustainable stabilisation of expansive subgrade using chemical stabilisation techniques.

3. Mechanisms of expansive soils

A soil is considered expansive when it has a high percentage of clay minerals such as montmorillonite expandable illite and vermiculite, or if the liquid limit of a soil exceeds 50% and the plasticity index exceeds 30% (Elarabi et al., 2010). The swelling ability of expansive soil is dependant on the total internal and external areas of its mineral particles. A small amount of swell can occur as a result of the enlargement of the capillary films in clay minerals when water is absorbed through their outer surface (Al-Rawas and Goosen, 2006). Water molecules in expansive soils are pulled into the gaps between the clay plates when the soil is introduced to water, causing the soil to absorb more water as the moisture content increase, forcing the plates further apart (Zaid, 2017). A study conducted by Reda, (2016) reveals that, expansive soils contain smectite clay materials which at the microscopic level looks like layered sheets due to their moisture-retaining abilities. The diffused double layer influences the engineering properties of clayey soil especially the hydraulic conductivity (Besq, 2003). Fig. 1 illustrates the mechanism of expansive soils. Table 1 shows swelling potential of soils based on liquid limit, classification of shrink potentials based on plasticity index are shown in Table 2, and relation of soil index properties and probably volume change for highly plastic soils are shown in Table 3.

Table 4
Estimated cost of damage due to expansive soils in some countries.

Country	Amount (US\$)	Reference
UK	>3.7 billion	Jones et al. (2019)
China	>1 billion	Jalal et al. (2020)
France	>3.3 billion	Toll et al. (2012)
India	Several millions	Gobena et al. (2019)
Saudi Arabia	>300 million	Adem et al. (2015)
Sudan	>6 million	Zumrawi et al. (2017)
USA	>15 billion annually	Jones et al. (2019)
Victoria, Australia	150 million	Adem et al. (2015)



Fig. 2. Road pavement defect (U.S. Department of Transport).



Fig. 3. Typical longitudinal crack developed on pavements over expansive clays (Zornberg and Gupta, 2015).

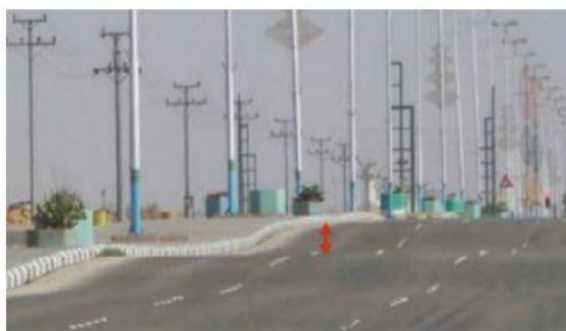


Fig. 4. Uplifting of flexible pavement due to expansive soil (Jalal et al., 2020).



Fig. 5. Slope failure of embankment caused by expansive soil (Jalal et al., 2020).

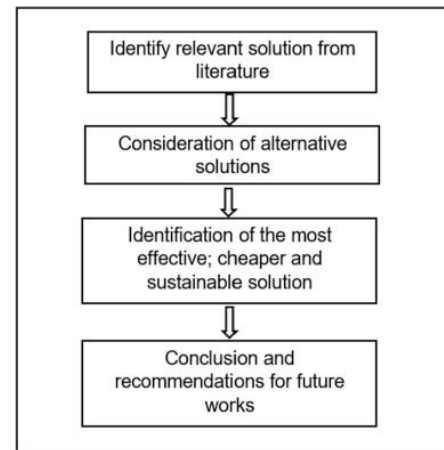


Fig. 6. Methodology for selecting literature.

4. Expansive pavement subgrade

Shrink swell behaviours of expansive subgrades are the major causes of pavement defects causing movement and differential settlement in pavement subgrade. The shrink-swell behaviour of weak subgrade materials when in contact with water can cause rutting, cracking, ravelling, formation of potholes and damage to pavements and light loaded civil engineering structures (Little et al., 2019). The economic effects caused by expansive subgrade in some countries are shown in Table 4, whiles Figs. 2–5 shows an overview of damage to road and embankments across different countries due to expansive subgrade (Mehmood et al., 2011).

5. Method for selecting literature

This section outlines how literature was selected for this current study and the method used to identify the most effective and sustainable solution for subgrade stabilisation using non-traditional stabilisers. Several works of literature on subgrade and soil stabilisation were investigated and alternative solutions considered to identify the cheaper and sustainable solution in expansive subgrade stabilisation. Fig. 6 visualises the methodology used.

6. Geotechnical solutions for expansive subgrade

Geotechnical solutions such as soil treatment and modification have been adopted to help overcome the problems of expansive subgrade

Table 5
Some methods and procedure of mechanical soil stabilisation (The Civil engineer, 2012).

Method	Procedure
Soil reinforcement	In this method, Geo-textiles and engineered plastic mechanical are used to help control soil moisture conditions and trap the soil. See Fig. 9.
Compaction	Pressure is exerted on soil material from above using heavyweight equipment to increase the density of the soil. See Fig. 10.
Mechanical remediation	In this method, expansive soil is removed and backfilled with more stable soil. See Fig. 11
Addition of graded aggregate materials	The engineering properties of expansive soil are improved by adding aggregates to the soil. See Fig. 12.

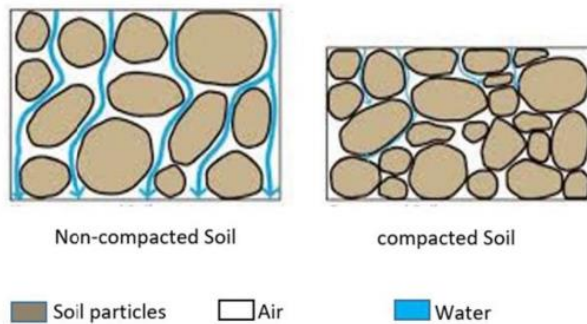


Fig. 7. Compacted and non-compacted soil(Tennessee stormwater Training).



Fig. 8. Different types of compactions (a) Pad-foot or tamping-foot roller (b) Smooth-drum vibratory roller (c) Walk-behind vibratory compactor and (d) Jumping-jack tamper (Meehan et al., 2009).

materials. Soil stabilisation techniques via mechanical, chemical and polymer techniques have been used in addressing the problems associated with expansive subgrade materials (Ikeagwuani et al., 2018).

6.1. Mechanical subgrade stabilisation

Subgrade compaction or densification using mechanical force is referred to as mechanical subgrade stabilisation (Afrin et al., 2017). Mechanical subgrade stabilisation involves the use of vibration, rammers, rollers and blasting to expulsion air voids within a soil mass and it is considered expansive compared to other forms of subgrade stabilisation (Nabil et al., 2020). Some methods and procedure of mechanical



Fig. 9. Soil reinforced with Geogrids(Kiganda, 2016).



Fig. 10. Compaction process(Compact Equipment).



Fig. 11. Soil removed and ready for backfill (Capital geotechnical services PLLC).



Fig. 12. Graded aggregate material (Longworth BRE Associate).



Fig. 15. Fly ash stabilisation process in road construction (Beeghly et al., 2003).



Fig. 13. Cement stabilisation process in road construction (Pleasants Construction, Inc).



Fig. 16. Construction and demolition waste, Geogrid and textile used in road construction (ABG Geosynthetics).



Fig. 14. Lime stabilisation process in road construction (Saranya et al., 2017).

subgrade stabilisation, before and after compaction and different types of compaction equipment are shown in Table 5, Figs. 7 and 8.

6.2. Chemical subgrade stabilisation

The process of adding chemicals to improve the engineering properties of expansive subgrade material is termed chemical subgrade stabilisation (Afrin et al., 2017) (see Fig. 15). The addition of these chemicals changes the gradation and physico-synthetics within and around the soil particles promoting cation exchange which leads to flocculation and agglomeration of the expansive soil particles (Jawad et al., 2014). Cement, fly ash, bituminous, rice husk ash, lime,

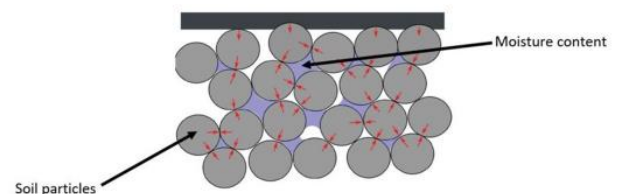


Fig. 17. Moisture content distribution inside an unpaved road (Cabezas et al., 2019).

construction and demolition waste, electrical and thermal waste, geotextile fabrics and recycled waste can be used as admixtures in this process as shown in Figs 13, 14, 15 and 16 (Rivera et al., 2020). The addition of this materials as admixtures can alter the geotechnical properties of expansive soil such as strength, bearing capacity, hydraulic conductivity, compressibility, workability, durability and swelling potentials (Cabezas et al., 2019). Chemical subgrade stabilisation is an effective technique to improve expansive subgrade (Phanikumar et al., 2020). An investigation into the application of stabilisation of wastewater sludge proves that cement, lime and bitumen can be used as subgrade materials (Lucena et al., 2014). During chemical road subgrade stabilisation, the shear strength of expansive subgrade is improved when stabilisers react with water within the soil leading to an increase in stiffness of the soil (Phanikumar et al., 2020) Fig. 17 shows moisture content distribution inside an unpaved road.



Fig. 18. Application of liquid polymer in road construction (Soil stabilisation Innovations).



Fig. 19. Soil stabilised with polymer for road construction (K31 Roads, 2018).

6.3. Polymer stabilisation

Polymers are large molecules composed of many repeated subunits. Polymer subgrade stabilisation involves the addition of polymer to expansive or unstable subgrade material to make it suitable for construction (AggreBind, 2020). Adding polymers as an admixture in subgrade stabilisation prevents the penetration of water that can cause failure in road pavement. The addition of polymer increases the density and load-bearing capacity of pavement subgrade after proper compaction (Midwest, 2020). Studies have shown that the application of polymer in subgrade stabilisation has favourable and improved engineering properties. Proportions of polymer (1%, 2%, 3% and 4%) and cement (10%, 20% 30% and 40%) were mixed with expansive soil to improve its engineering properties (Iyengar et al., 2012). The application of polymer in road construction and soil stabilised with polymer are shown in Figs. 18 and 19. A summary of some advantages and disadvantages of mechanical, chemical and polymer subgrade stabilisation techniques are shown in Table 6.

7. Sustainable stabilisation of expansive subgrades

Sustainable stabilisation of expansive subgrade in this study refers to the use of sustainable non-biodegradable waste materials as additives to stabilise expansive subgrade materials. This emerging trend in subgrade stabilisation focuses on the use of locally available industrial waste to improve the engineering properties of soil (Bhardwaj, 2020). Waste and secondary materials such as silica fume, volcanic ash, rice husk, bitumen, kiln dust, natural fibre, Ground Granulated Blast-furnace Slag (GGBS) among others can be used as a partial substitute in conventional subgrade stabilisation (Ijaz et al., 2020). These wastes can improve the

Table 6

Summary of advantages and disadvantages of mechanical, chemical and polymer subgrade stabilisation techniques(Christopher et al., 2019).

Technique	Advantages	Disadvantages
Mechanical	<ul style="list-style-type: none"> • Easy to apply and does not require skilled personnel. • No additives needed hence less time-consuming. • Environmentally friendly no potentially harmful materials involved. • It is an effective waste management alternative when waste materials are used. • Application is quicker when the engineering properties of soil are not critical. 	<ul style="list-style-type: none"> • It can be time-consuming when prolonged physical activities are involved. • Unexpected outcome can be achieved in cases of pre-wetting or drying cycles. • It is not efficient when soil condition is critical. • The method sometimes requires the support of chemical stabilisation.
Chemical	<ul style="list-style-type: none"> • Laboratory test process is involved to determine the results. • Quantity of binders required is usually small making it cost-effective. • It is less time consuming because chemical reaction occurs spontaneously. • The use of waste in the process promotes waste management. • It is effective in improving the engineering properties of soil. 	<ul style="list-style-type: none"> • In-situ application in this method may be inept if field conditions vary. • The process is mostly associated with the release of toxic components that can affect the environment. • Can be ineffective when the cost or amount of additives cannot be achieved. • Unfortunate conditions can lead to achieving adverse results.
Polymer	<ul style="list-style-type: none"> • Easy to apply and does not require highly skilled personnel. • They are environmentally friendly and energy-efficient to produce compared to traditional chemical additive. • It is effective irrespective of the engineering properties of the soil. • Gives maximum weather ability 	<ul style="list-style-type: none"> • They are not a permanent solution. • Ideal results are difficult to obtain in this process when the soil has a high percentage of clay. • In-situ application may be pragmatically inept in varying field condition. • Unsuitable when the cost or amount of additives needed cannot be achieved

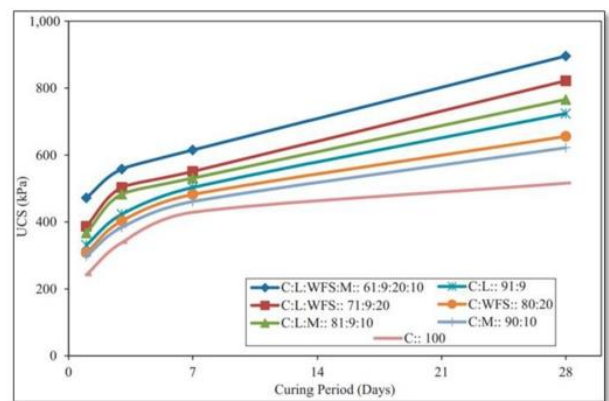


Fig. 20. UCS of clayey soil with different mixes (Bhardwaj et al., 2020).

workability and durability of expansive subgrade while getting economic benefits (Ijaz et al., 2020). Crushed waste and quarry dust was used in soil treatment in a study to improve the engineering properties of soil (Onyelowe et al., 2018). Other studies have shown an increase in the pH of sludge above 10 with the addition of 34% of cement kiln dust in expansive subgrade stabilisation (Singh et al., 2015). Bagasse ash, industrial waste sand and ground shell reinforced fibre has been successfully used to stabilise expansive subgrade material (Joe et al., 2015). Literature has shown that lime can be used in civil engineering to

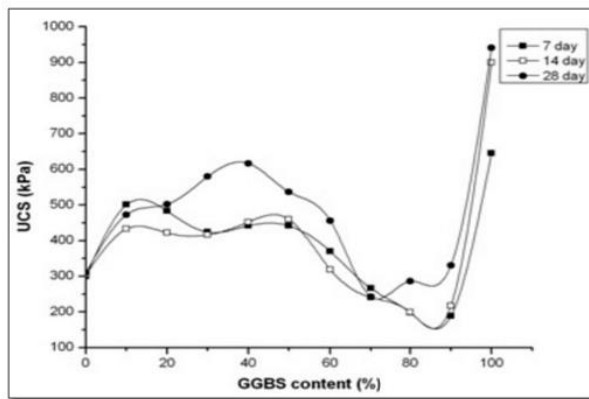


Fig. 21. Variation of UCS of black cotton soil with GGBS (Sharma et al., 2011).

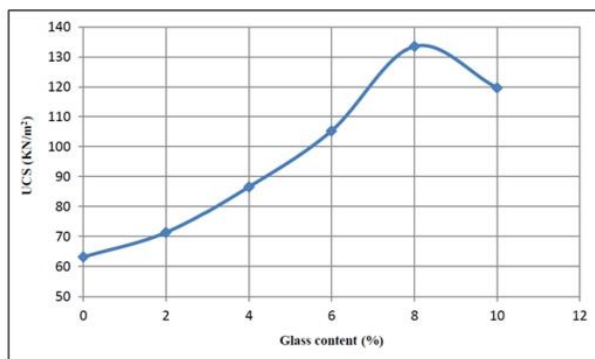


Fig. 22. Variation of UCS values for different glass powder content (Javed et al., 2020).

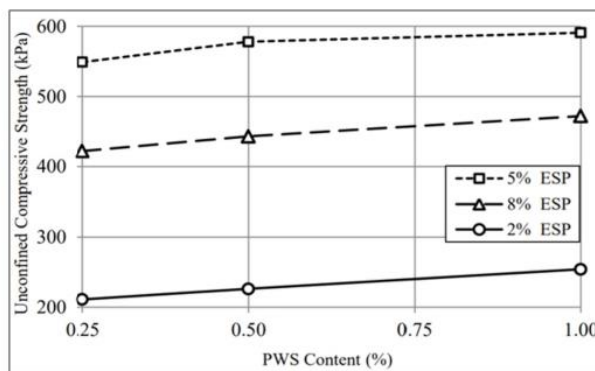


Fig. 23. UCS of ESP-PWS stabilised soil samples after 28 days of curing (Alzaidy et al., 2019).

stabilise subgrade, roadbeds, embankment, plies and foundations (Cai et al., 2006). In other studies, varying proportion of sawdust (4%, 8%, 12%, 16% and 20%) were added to black cotton soil to make it suitable for use as subgrade material (Ikeagwuani et al., 2018).

Peter et al. (2014) used palm oil fuel ash (POFA) to stabilise Sarawak peat composite for used as road subbase material and Foner et al. (1998) used fly ash in the construction of road embankment in Israel. Industrial waste such as copper slag was recommended for subgrade, subbase,

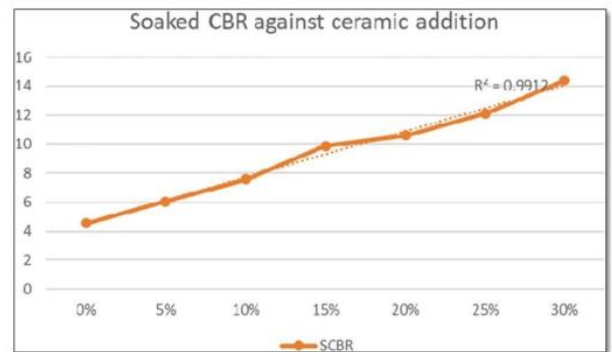


Fig. 24. Soaked CBR with ceramic dust addition (Onakunle et al., 2019).

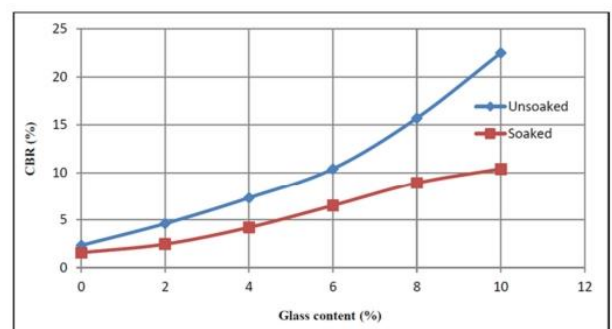


Fig. 25. Variation in CBR values for different glass powder content (Javed et al., 2020).

bitumen mixes (Chandrshekhar et al., 2015). Crushed glass, recycled concrete aggregate plus 0.5% fine rubber and 0.5% coarse rubber was used to stabilised road subgrade (Saberian et al., 2020). The mechanical characteristics and resistance factor of subbase and subgrade material in flexible pavement improved with the addition of steel slag, crushed limestone mixture and fly fiery debris (Andavan et al., 2019). Research conducted by Saltan et al. (2007) proves that pumice waste can be used as subbase material of highway and stabilisation material when building roads.

Construction and demolition waste (CDW) and various sizes of tyre derived aggregate (TDA) blended with crushed rocks (CR) at 1%, 2% and 3% by weight was used in pavement subbase application (Tavia et al., 2019). Crushed rubber and recycled concrete aggregate were used in pavement base/subbase application (Li et al., 2018). Reports have shown the use of by-product of acetylene gas and municipal incinerated bottom ash (MIBA) in highway subgrade and road pavement construction (Du et al., 2016). Recycling waste such as concrete aggregate was classified as excellent highway pavement and embankment material due to their gradation and Atterberg limits (Yap et al., 2019). Recycling screening waste mixed with recycled aggregate from construction and demolition waste were used in the construction of paved bike lanes (Yap et al., 2019). Using recycled waste as a substitute for expansive subgrade will improve the structural capacity and reduce rattle damage (Zhang et al., 2019). Studies have shown the use of coal wash (CW) and fly ash (FA) as base and subbase material in road construction (Wang et al., 2019). The engineering properties of subgrade material was improved when clay soil was mixed with oil palm shell at 10%, 20% and 30% after 7, 10 and 14 days of curing (Gungat et al., 2013).

Geotechnical properties of expansive subgrade with high plasticity was improved when quarry dust at proportions 5%, 10%, 15%, 20%, 25%, 30%, 35%, 40% and 50% was mixed with the soil (Duc et al.,

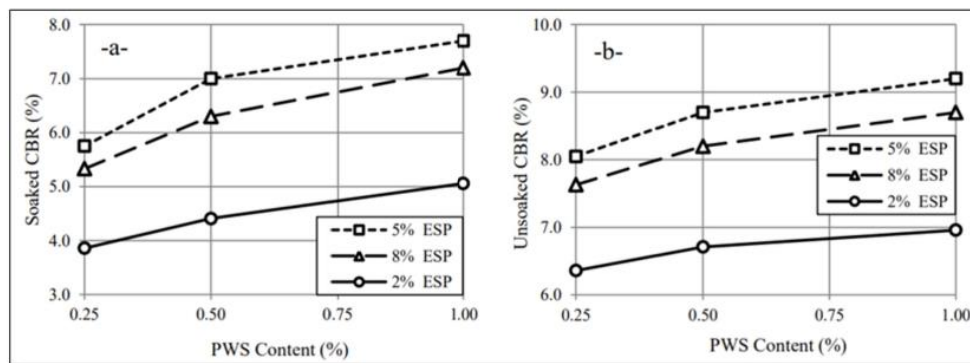


Fig. 26. CBR values for ESP-PWS stabilised soil samples, a -soaked, b- Unsoaked(Alzaidy et al., 2019).

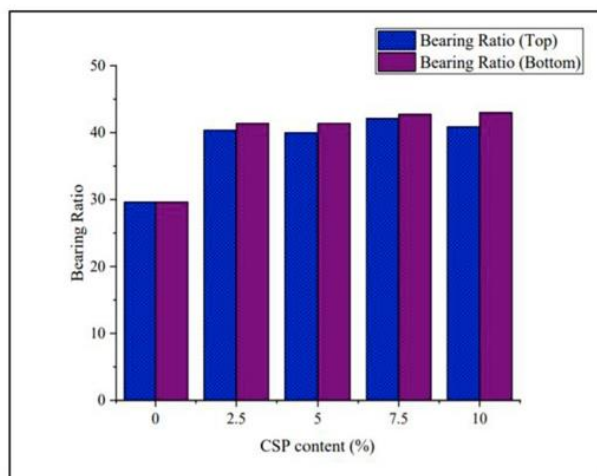


Fig. 27. CBR of stabilised marine clay with varying CSP content(Nujid et al., 2020).

2018). Better performance was observed in red mud soil used as subgrade material when dome fine, ground granulated blast furnace slag (GGBS), cement kiln dust, fly ash and recycled asphalt (RAP) was used as an additive (Mukiza et al., 2018). According toZhang et al. (2020), recycled aggregate from construction and demolition waste was used as alternative filling materials for highway subgrade. Reclaimed asphalt pavement (RAP) and crushed stone aggregate (CSA) were stabilised with varying percentages of cement (Saha et al., 2017). Waste fly ash, oil shale ash and a by-product of paper and timber industry (Lignin) were used to modify silty clay as a subgrade material (Wei et al., 2018). Improved strength was achieved when recycled PET fibre and fly ash wash mixed with expansive subgrade material at proportions 1.2% and 15% by weight of the soil (Mishra et al., 2018). Studies have shown satisfactory results in subgrade and embankment material when pond ash, rice husk ash and cement was used to stabilise expansive subgrade material at 30%–45% and 5%–20% proportion (Gupta et al., 2016). Industrial waste and lime sludge were used to stabilise expansive subgrade leading to a reduction in the lifecycle cost and overall road pavement thickness (Phanikumar et al., 2020). Although there are enough proof from the authors that waste materials can be used in subgrade stabilisation, concerns have been raised on the availability of these waste materials in large quantities to meet current demand. The manufacturing of processed waste however, has some environmental effects which need to be investigated.

8. Properties of waste materials stabilised expansive subgrade

8.1. Unconfined compressive strength (UCS)

Unconfined compressive strength (UCS) test are conducted to determine the stress-strain characteristics and strength of the subgrade material in accordance with relevant standards. Several studies have shown that the use of waste material dumped as landfill such as colliery spoil, waste steel slag among others used as additives yielded high UCS results in subgrade layer (Morales et al., 2019). It has been proven in a study that the addition of kiln dust is enough to achieve a significant increase in UCS values (Michael et al., 2016). The addition of rice husk ash, sugarcane bagasse ash and cow dung as an additive to stabilise subgrade material at 0%, 2.5%, 5%, 7.5%, 10% and 12.5% resulted in high UCS (Yadav et al., 2016). Weak soil was improved using deep mixing techniques by adding waste material such as pulverised fly ash (PFA) and GGBS at varying proportions of 5%, 10%, 15% and 20% (Abbey et al., 2017). An improvement in UCS and other mechanical properties of the subgrade material after 7, 14, 28 and 56 days of curing (Abbey et al., 2017). A study carried out by Bassani et al. (2019) shows an increase in UCS after 3, 7 and 28 days of curing. An investigation conducted on fine-grained by Abbey et al. (2018) shows improvement in UCS with the addition of pulverised fly ash (PFA) and GGBS.

Krishana et al., (2016) recorded an increase in UCS from 55 kN/m² to 98 kN/m² when ceramic dust content was increased from 3% to 30%. Zinc-coated steel milling waste significantly increases UCS vales to 298 kPa, 334 kPa and 390 kPa in road subgrade stabilisation (Cabalar et al., 2020). The Road and maritime Services Specification 3051 states that the unconfined compressive test of subgrade materials are required to be less than 1000 kPa to prevent highly brittle behaviour. The addition of plastic bottle strips at 0.5%, 1% and 2% in subgrade stabilisation recorded improved UCS values (Kassa et al., 2020). Unconfined compressive strength increases with the addition of 5% lime to fly ash stabilised expansive during subgrade whiles UCS increase up to 236 kN/m² in a similar study (Tan et al., 2020). An increase in UCS value in Fig. 20 was recorded after waste foundry sands (WFS) and Molasses along with Lime was added to improve the strength characteristics of clayey soil (Bhardwaj et al., 2020). Fig. 21 shown an increase in UCS values when 40% GGBS was used to stabilise black cotton soil after 7, 14 and 28 days (Sharma et al., 2011). Significant increase in UCS from 63.2 kN/m² to 133.5 kN/m² was recorded in Fig. 22 when glass powder content was increased to 8% (Javed et al., 2020). Results in Fig. 23 shows an increase in UCS when varying proportions of eggshell powder (2%, 5% and 8%) and plastic waste strips (0.25%, 0.5% and 1%) were used to stabilise expansive subgrade material (Alzaidy et al., 2019). A significant increase in UCS was achieved in most of the findings in this section, this shows the that waste materials can be used to improve the engineering properties of subgrade materials. Even though some UCS

Table 7
Summary of findings on UCS and CBR achieved in waste material used in expansive soil stabilisation.

Waste source	Waste Type	Curing Time (days)	Content (%/Ratio)	Information Source	Findings
Industrial	GGBS	7-28	5-15	Estabragh et al. (2020)	UCS strength increased with 5% and 10% GGBS content
	Silica fume	28	2.5-10	Saygili et al., (2019)	Increased UCS and promote the formation of CSH gel
	Rice husk ash	-	0-12.5	Yadav et al. (2017)	Maximum CBR value of 7.68% and UCS was 2.16 kg/cm ²
	Industrial waste sand	-	5-30	Joe et al. (2015)	Maximum UCS of 197 kN/m ² and CBR of 25% was achieved
	Copper slag	-	25-75	Mohanraj et al. (2017)	Maximum UCS achieved at 50% copper slag
	Cement kiln dust	7-28	7.5-15	Adeyanju et al. (2019)	CBR increased from 1.49% to 28.6%
	Brick dust	-	10-20	Rank et al. (2020)	UCS increased as Brick dust increase
	Polyvinyl waste	-	-	Michael et al. (2016)	UCS had 60% increment and CBR had about 50% increment
	Ceramic dust waste	-	-	Onakunle et al. (2019)	CBR increased from 6.82% to 21.97% with addition of 5% CDW
	Lignin	7-15	8-12	Zhang et al. (2016)	CBR values increased from 50.6% to 124% for 12% lignin
	Pumice waste	-	10-35	Saltan et al. (2007)	CBR increased by 93%, the best performing mixture is 30% pumice
	Plastic waste	-	0.5-2	Kassa et al. (2020)	UCS reduced at a high percentage of strip content
	Gypsum waste	-	0-15	Al-Adili et al. (2019)	UCS increased by adding up to 5% recycled gypsum
	Coal waste	14-60	0-20	Afrakoti et al. (2019)	UCS increased with the addition of CW at 28 and 60 days
	Sawdust	-	4-12	Ikeagwuani et al. (2018)	Optimum increase in CBR achieved at 16% sawdust content
	Milling waste spiral	-	5-25	Cabalar et al. (2020)	CBR of 11.22% and UCS of 390 kPa was achieved
	Fly ash	-	-	Andavan et al. (2019)	CBR and UCS values can be improved with RHA
	Construction	Limed leather waste	4-28	2-10	Parihar et al. (2020)
Recycled demolition waste		-	-	Zhang et al. (2020)	Gravel particles have sufficient CBR value
Crushed bricks		-	3-5	Perera et al. (2019)	CBR was higher than the minimum required doe subgrade
Unselected demolition waste		3-28	-	Bassani et al. (2019)	An increase in strength was achieved without thermal treatment
Electrical	E-waste	-	5-12	Kumar et al. (2019)	UCS increased by 56% and 60% in direct shear value
Others	Waste paper sludge ash	7-28	1:1	Mavroulidou et al. (2018)	High UCS was achieved with the addition of WPSA
	Calcium carbide residue	-	1-4	Varaprasad et al. (2020)	USC and CBR increased
	Burned sewage sludge	7-28	0-15	Amminudin et al. (2020)	UCS increased to 16.72N/mm ² , can be used in road construction
	Locust bean waste	-	0-12	Aliyu et al. (2019)	UCS increased up to 236 kN/m ² and CBR from 21% to 46%
	Bagasse ash	-	0-30	Maheshwar et al. (2020)	Compressive strength increases with increase in ash content
	Crumb rubber	-	5-15	Kumar et al. (2017)	UCS increased with the addition of crumb rubber
	Coir waste	-	0-3	Peter et al. (2014)	CBR values increased by 192% and 335%
	Bassanite	1-28	1:1	Ahmed et al. (2013)	Increase in CBR and UCS with increase in time was recorded
	Palm fuel ash	7-28	1-6	Abdeldjoud et al. (2019)	UCS strength increased largely after 28days curing
	Fuel ash desulphurisation	7-28	-	Salih et al. (2020)	UCS increased with increase in age with same red mud content
	Wood & sunflower waste	0-13	24hr	Wang et al. (2019)	UCS increased with the addition of 7% fly ash
	Waste glass powder	-	2-10	Javed et al. (2020)	CBR increased to 22.5% with increase in UCS of 133.5 kN/m ²

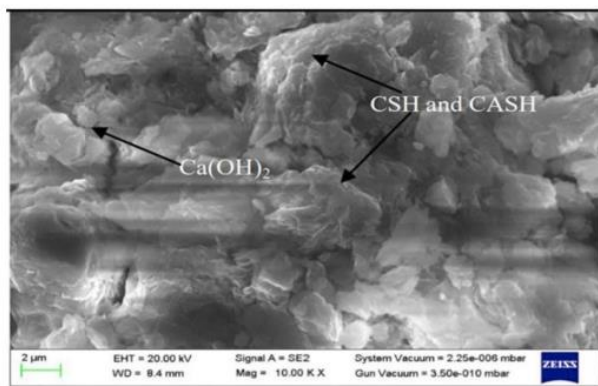


Fig. 28. SEM results of soil +6% LLWA cured(Parihar et al., 2020).

values were low, they are still useable in road construction.

8.2. California bearing ratio (CBR)

California bearing ratio is a penetration test to evaluate the strength of the stabilised subgrade materials to ascertain the bearing capacity of road subgrade in accordance with the relevant standards. Studies have

shown that CBR has been improved when waste materials were used to stabilise expansive subgrade. In recent study, CBR values were greater than 30% translating into an improved foundation during subgrade stabilisation using recycled concrete aggregate as an additive (Pooni et al., 2019). Amadi et al. (2014) in a study stated that CBR values increased to 13 when cement kiln dust content was increased to 4% and a significant increase in CBR of up to 48 was achieved at 16% cement kiln dust required for subgrade in a flexible pavement system. Its been proven in several studies that the addition of about 0%–25% cement kiln dust is enough to achieve a significant increase in CBR values (Michael et al., 2016). Results from a study show an increase in CBR value from 31 to 42 fold rated as good material for road subgrade construction (Mahmood et al., 2019). CBR values increased by 93% after the stabilisation process of subgrade material when pumice was added (Saltan et al., 2007). CBR value increased by 192% and 335% when 2% of coir pith, 0.6% of short coir fibre waste and adjusted and activated steel slag (ASS) was used as stabilising materials (Peter et al., 2014). High CBR was achieved when six polyethylene terephthalate (PET) plastic waste blend used as construction materials were higher than the minimum CBR required for use as subgrade material (Perera et al., 2019).

Using up to 40% reclaimed asphalt pavement (RAP) and basic oxygen furnace (BOF) aggregate in subgrade stabilisation satisfies the requirement for CBR and a maximum fly ash content of up to 13% can achieve high CBR in subgrade stabilisation (Chen et al., 2017). Mixing crushed stones aggregate and reclaimed asphalt pavement (RAP) from 20% to 100% is makes it suitable for subgrade in flexible pavement

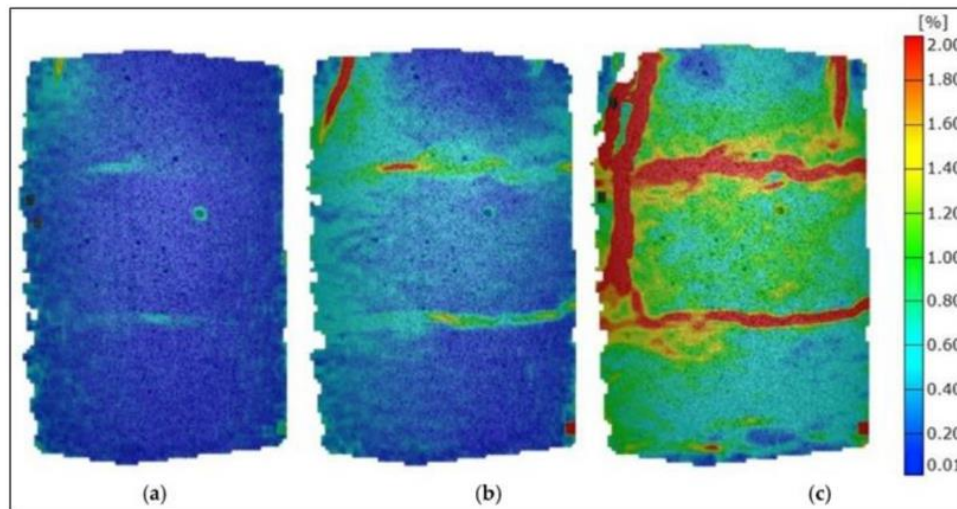


Fig. 29. Mises strain at various load stages with wheat fly ash. (a) 0.3 Fmax, (b) 0.6 Fmax, (C) 1.0 Fmax (Barisić et al., 2019).

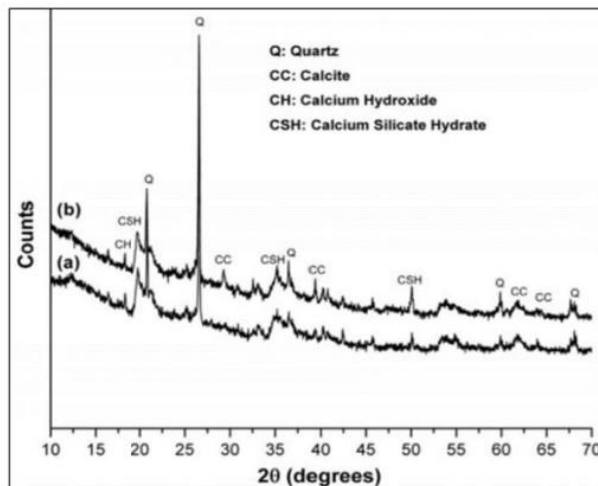


Fig. 30. X-ray diffraction patterns of the soil stabilised with 20% binder cured for 28 days (a) no lime (b) 1% lime(Sharma et al., 2015).

(Saha et al., 2017). According to Yap et al., (2019), CBR value of subgrade materials can be improved using recycled concrete aggregate (RCA). Crushed stone aggregate used as additives improved soaked CBR values substantially while municipal incinerated bottom ash (MIBA) achieved good CBR value of up to 90% in subgrade stabilisation (Saha et al., 2017). During expansive subgrade stabilisation, CBR values increased from both double and single layer of lime treated Cori geotextile by 399% and 435% respectively (Tiwari et al., 2019). CBR values of pavement subgrade increase with intensities of 1, 5, 10, 20 and 30 million standard axles leading to a reduction in pavement thickness above the subgrade material (Selvi et al., 2014). The addition of waste fly ash and oil shale ash at ratio 40:20:40 for oil shale ash (OSA), fly ash (FA and silty clay (SC) exhibited a higher CBR value and improved physical properties of silty clay (Wei et al., 2018). CBR value for treated and untreated soil increased from 3.4% to 48% when 20% cement kiln dust was added to poor subgrade material and cured for 14 days (Mosa et al., 2017).

A high CBR value and resilient modulus were recorded when calcium

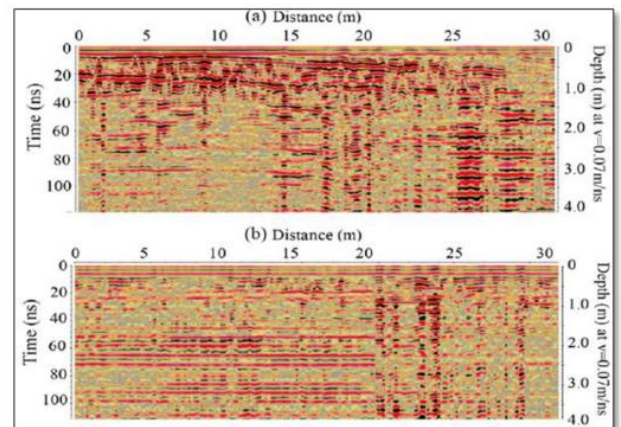


Fig. 31. Radar detection results of two subgrade section made of different materials: (a) CDW (b) Clay (Zhang et al., 2020).

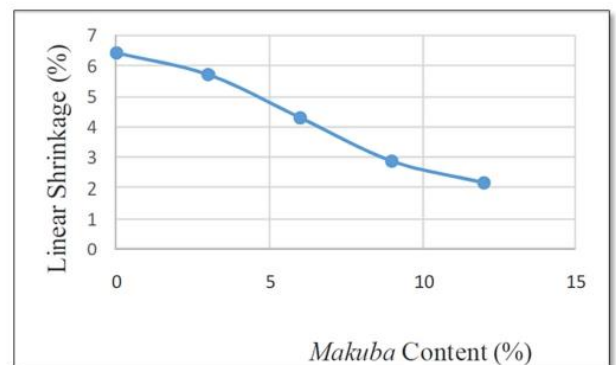


Fig. 32. Variation of linear shrinkage with Makuba content(Aliyu et al., 2019).

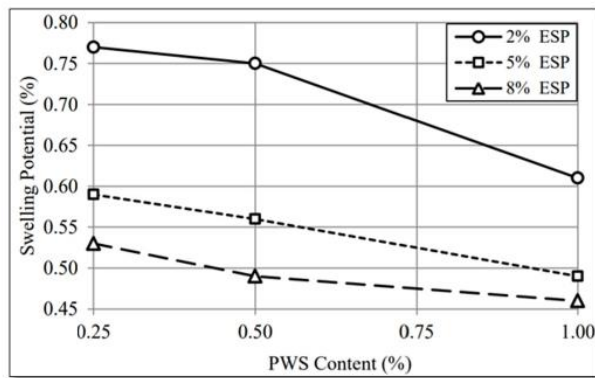


Fig. 33. Swell percent of ESP-PWS stabilised soil sample after 7 days (Alzaidy et al., 2019).

carbide residue was used to stabilise clayey soil concluded that, calcium carbide residue is a viable alternative binder for stabilising soft subgrade soil (Du et al., 2016). The highest CBR value was achieved in expansive subgrade material in pavement construction when 30% oil palm shell was used as an additive and cured for 20 days period (Gungat et al., 2013). The bottom zone layer of road pavement made up of 12% lignin stabilised silt exhibits high value of CBR when by-product of paper and timber industry (Lignin) was used an additive in a field trial (Zhang et al., 2016). Enhanced CBR values were achieved when recycled basanite produced from gypsum waste plasterboards was mixed with furnace slag cement at ratio 1:1 during weak road subgrade stabilisation (Ahmed et al., 2013). Polyethylene terephthalate (PET) and fly ash were mixed in proportions ranging from 0% to 20% by weight of the soil increased CBR value (Mishra et al., 2018). 19% increase in CBR reflected in a reduction in the overall thickness and life cycle cost of a road in Uganda were reduced in a study through the application of geogrids in pavement layers (Melling et al., 2017). Results from an investigation where pond ash (PA) and rice husk ash (RHA) was replaced at 30%–40% in expansive subgrade material shows high CBR values useable for road subgrade and embankment (Gupta et al., 2016). Other studies have shown increasing CBR values using waste plastic materials and industrial waste to stabilise expansive black cotton subgrade material with red mud used for subgrade pavement (Kassa et al., 2020). High CBR was achieved with the addition of sludge, a by-product of paper industry to stabilise and improve expansive soil characteristics (Phanikumar et al.,

2020). Lateritic soil mixed with ceramic dust with ratio from 0% to 30% achieved an increase in CBR from 6.82% to 21.97% and 4.55%–14.39% respectively as shown in Fig. 24 (Onakunle et al., 2019). CBR values increased at 2.32% and 1.56% when 10% glass powder was used as an additive to stabilise expansive subgrade at ratios 2%, 4%, 6%, 8% and 10% as shown in Fig. 25 (Javed et al., 2020). Results in Fig. 26 shows an increase in CBR value when eggshell powder (ESP) (2%, 5% and 8% and plastic waste strips (PWS) (0.25%, 0.5% and 1%) were used to stabilise expansive subgrade material (Alzaidy et al., 2019). CBR values increased with varying content of cockle shell powder (CSP) at 0%, 2%, 5.5%, 7.5% and 10% at 5.0 mm penetration as shown in Fig. 27 (Nujid et al., 2020). Table 7 shows a summary of findings on UCS and CBR achieved in waste material used in expansive subgrade stabilisation. CBR in road constructing is crucial, this is because, subbase thickness are selected based on the CBR values achieved after CBR test. CBR values achieved by the various findings when waste materials were used in this section are promising and can be used in road subgrade stabilisation.

8.3. Microstructural properties

Microstructural properties are the properties that influence the physical properties such as hardness, strength, high/low-temperature behaviour, toughness wear resistance etc. Microstructural properties of a material can be determined in the laboratory by conducting tests such as Scanning Electron Microscopy (SEM), X-ray, Radar detection, Mises strain test among others. A study conducted by Parihar et al. (2020) shows SEM analysis results after adding 6% of limited leather waste ash (LLWA) shows high CSH gel development resulting in high strength in Fig. 28. Wheat fly ash mixture from a 3D digital image correlation (DIC) measurement in Fig. 29 shows deformations transforming into a vertical and horizontal crack at maximum force (Fmax) (Barisic et al., 2019). The addition of 5% lime to fly ash in a study decreased the plasticity index of expansive soil by 64.9%, reducing the free-swelling ratio to about 10% while reducing the swell ratio to nearly 4% (Zhou et al., 2019). Fig. 30 shows XRY patterns of reaction products of soil stabilised with 20% binder after 28 day in a study where fly ash and GGBS was used to stabilise expansive soil (Sharma et al., 2015). The hydration products result in pozzolanic reaction primarily consist of C–S–H gel and calcium hydroxide (CH) as shown in Fig. 31 (Zhang et al., 2020).

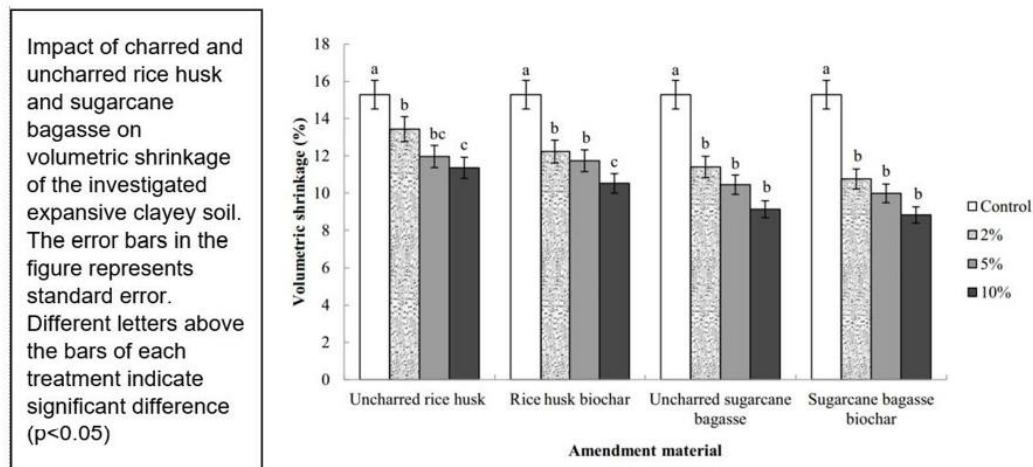


Fig. 34. Volumetric shrinkage against amendment material (Malongweni et al., 2019).

Table 8

Summary of findings on microstructural and tensile properties and shrink-swell of waste used in expansive subgrade stabilisation.

Waste source	Waste Type	Curing Time (days)	Content (%/Ratio)	Information Source	Findings
Industrial	GGBS	7–28	5–15	Estabragh et al. (2020)	Sem shows high strength between soil particles and stabilising agents.
	Silica fume	28	2.5–10	Saygilli et al., (2019)	SEM shows silica fume/lime addition promoted the creation of CSH gel.
	Cement kiln dust	7–28	7.5–15	Adeyanju et al. (2019)	Swell test shows a rise in geotechnical properties of stabilised soils
	Brick dust	–	10–20	Rank et al. (2020)	Swelling potential reduced with lower content
	Polyvinyl waste	–	–	Michael et al. (2016)	X-ray diffraction shows high montmorillonite content in the soil
	Ceramic dust waste	–	0–30	Onakunle et al. (2019)	Maximum dry density increased CWD
	Plastic waste	–	0.5–2	Kassa et al. (2020)	Swell behaviour of soil reduced
	Gypsum waste	–	0–15	Al-Adilli et al. (2019)	5% rise in swelling index decreased with increase in gypsum
	Coal waste	14–60	0–20	Afrakoti et al. (2019)	Tensile strength increased at short curing periods of 14 days
	Sawdust	–	4–12	Ikeagwuani et al. (2018)	X-ray diffraction test shows the occurrence of pozzolanic reactions
	Milling waste spiral	–	5–25	Cabalar et al. (2020)	Values decrease in swell index (Cs) and compression index (Cc)
Limed leather waste	4–28	2–10	Parihar et al. (2020)	SEM results confirm formation of CSH gel increases with curing time.	
Construction	Recycled demolition waste	–	–	Zhang et al. (2020)	Radar detection of subgrade section made of CDW and clay
	Unselected demolition waste	3–28	–	Bassani et al. (2019)	FESEM demonstrate the feasibility of using unselected CDW
Others	Waste paper sludge ash	7–28	1:1	Mavroulidou et al., (2018)	SEM shows developed reaction hydration coatings after 28days curing
	Burned sewage sludge	7–28	0–15	Amminudin et al. (2020)	XRF test shows DSS has good potential to replace cement in concrete.
	Bassanite	1–28	1:1	Abdeldjouad et al. (2019)	SEM-EDS shows strengthening in the mechanism of alkaline activation
	Palm fuel ash	7–28	1–6	Salih et al. (2020)	Highest tensile strength of 0.078 MPa was observed

8.4. Tensile and shrink-swell properties

Tensile strength in this study refers to the measure of the stress responses of stabilised subgrade material by applying a tensile or pulling force to the specimen and shrink-swell is the extent to which expansive subgrade will expand when wet and shrink when dry. Research has shown that indirect tensile strength values mixture satisfies the minimum requirements for granular mixture for subbase layer of road pavements when unselected construction and demolition waste (UCDW) was used as an additive (Bassani et al., 2019). Tensile strength and shrink-swell properties of expansive subgrade material can be improved using waste materials as additives. In a similar experiment, tensile strength values increased by adding 5% lime to fly ash was added to expansive subgrade material (Zhou et al., 2019). 52.19% cori geotextile mat in single layer and 81.89% in double-layer reduce road pavement thickness after expansive subgrade stabilisation (Zhou et al., 2019). Other studies have shown a reduction in shrink-swell potentials from 6.43% to 2.14% with an increase in powered locust bean pod in Fig. 32 (Aliyu et al., 2019). Swell potential was reduced when eggshell powder (ESP) 2%, 5% and 8% and Plastic waste strip PWS) was used to stabilise expansive subgrade material shown in Fig. 33 (Alzaidy et al., 2019). Tensile strength increased by 4.5 times when mud masonry blocks were stabilised using waste plastic fibres (Subramaniaprasad et al., 2014). High tensile strength was recorded in a study when waste fibres were used as an additive in clay soil stabilisation (Muntohar et al., 2012). Swell potentials of expansive subgrade were suppressed with an improvement in strength when waste steel slag was used to stabilise subgrade material for road construction (Wu et al., 2019). Other studies have also shown an improvement in the physico-mechanical properties related to swelling potentials of expansive subgrade when charred and uncharred rice husk and sugarcane bagasse were used as additives as shown in Fig. 34 (Malongweni et al., 2019). The application of lime has been reported to have strong bonds between soil particles resulting in reduced shrink-swell potentials (Kamaruddin et al., 2020). Swell ratio was increased from 3.4% for untreated soil to 48% for treated soil when 20% cement kiln dust was added to poor subgrade material after 14 days

of curing (Mosa et al., 2017). Recycled basanite produced from gypsum waste plasterboards was used to enhance tensile splitting strength of weak subgrade clay soil used in road construction (Ahmed et al., 2013). Summary of findings on micro and tensile properties and shrink-swell of waste used in expansive subgrade stabilisation are shown in Table 8. The results achieved in this section indicates that soils are weak in tension but strong in compression. On the other hand, shrink-swelling potentials of expansive subgrade materials were reduced with the addition of waste.

8.5. Limitations and future focus

There are limitations associated with the use of waste materials as additives in expansive subgrade stabilisation. Some of these limitations in waste materials dumped as landfill include contamination through leaching of toxic into the waste. Using contaminated waste in soil stabilisation can affect the performance and engineering properties of the soil. The cost effects of decontamination of these waste materials is a limitation to the use of waste materials in subgrade stabilisation. The application of additives to expansive soils insitu can be stabilised only to a shallow depth which is not suitable for deep soil stabilisation. However, the easy accessibility and the low cost of waste materials used in subgrade stabilisation hold promising keys to a sustainable future. Using waste in subgrade stabilisation focus on providing a better understanding of the use of new technology and materials in subgrade stabilisation to exploit any improvement in the future.

9. Conclusion

Current expansive subgrade stabilisation techniques is focused on using chemical agents such as cement and lime in subgrade stabilisation. However, these chemical agents have limitations and prove to be non-environmentally friendly and expensive. This has called for the use of non-traditional stabilisers as additive in subgrade stabilisation. The addition of non-traditional stabilisers in subgrade stabilisation using chemical stabilisation techniques has proven to be more

environmentally friendly, cheaper and effective in improving the engineering properties of expansive subgrade materials. Using non-traditional industrial waste materials in subgrade stabilisation will reduce overall project cost and greenhouse gas emission while saving landfill space. It is essential to carryout performance base testing to prove the effectiveness of non-traditional stabilising agents and focus on exploring other novel by-products that can be used in expansive subgrade stabilisation. It is crucial to carry out further research into the effects of climate change on stabilised expansive subgrade materials stabilised with non-traditional by-products and how they can improve.

Funding

This research did not receive any specific grant from funding agencies in the public, commercial, or not-for-profit sector.

Declaration of competing interest

The authors declare that they have no known competing financial interests or personal relationships that could have appeared to influence the work reported in this paper.

Acknowledgement

The authors acknowledge the advice, comments and suggestions from anonymous reviewers which significantly improved the quality of this paper.

References

- Abbey, S.J., Ngambi, S., Olubanwo, A.O., 2017. The effect of overlap distance and chord angle on performance of overlapping soil-cement columns. *Int. J. Civ. Eng. Technol.* 8 (5), 627–637.
- Abbey, S.J., Ngambi, S., Olubanwo, A.O., Tetteh, F.K., 2018. Strength and hydraulic conductivity of cement and by-product cementitious materials improved soil. *Int. J. Appl. Eng. Res.* ISSN: 0973-4562 13, 8684–8694. Number 10 (2018).
- Abbey, S., Ngambi, S., Ganjian, E., 2017. Development of strength models for prediction of unconfined compressive strength of cement/byproduct material improved soils. *Geotech. Test J.* 40 (6), 928–935, 2017. <https://doi.org/10.1520/GTJ20160138>. ISSN 0149-6115.
- Abbey, S.J., Eyo, E.U., Ng'ambi, S., 2019. Swell and microstructural characteristics of high-plasticity clay blended with cement. *Bull. Eng. Geol. Environ.* <https://doi.org/10.1007/s10064-019-01621-z>.
- Abdeljoud, L., Asadi, A., Ball, R., Nahazanan, H., Huat, B., 2019. Application of alkali-activated palm oil fuel ash reinforced with glass fibers in soil stabilisation. *Soils Found.* 59 (5), 1552–1561. <https://doi.org/10.1016/j.sandf.2019.07.008>.
- Abg Geosynthetics. Creative geosynthetic engineering. <http://www.abg-geosynthetics.com/products/abgrid.html>. (Accessed 15 June 2020).
- ACPA concrete pavement technology series. <http://1204075.sites.myregisteredsite.com/downloads/TS/EB204P/TS204.2P.pdf>. (Accessed 13 October 2020).
- Adem, H.H., 2015. Modulus of Elasticity Based Method for Estimating the Vertical Movement of Natural Unsaturated Expansive Soils. A Thesis Submitted to the Faculty of Graduate and Postdoctoral Studies in Partial Fulfillment of the Requirements for the Doctor in Philosophy Degree in Civil Engineering, pp. 1–267.
- Adeyanju, E.A., Okeke, C.A., 2019. Clay Soil Stabilisation Using Cement Kiln Dust. Department of Civil Engineering, Covenant University, Ogun State, Nigeria. <https://doi.org/10.1088/1757-899X/640/1/012080>, 2019 IOP Conf. Ser.: Mater. Sci. Eng. 640 012080.
- Afrakoti, Afrakoti, M.T., Choobasti, A.J., Ghadapour, M., 2019. Investigation of the effect of the coal waste on the mechanical properties of the cement-treated sandy soil. *Construct. Build. Mater.* <https://doi.org/10.1016/j.conbuildmat.2019.117848> (IF 4.046) Pub Date: 2019-12-26.
- Afrin, H., 2017. A review on different types soil stabilisation techniques. *International Journal of Transportation Engineering and Technology* 3 (2), 19–24. <https://doi.org/10.11648/jijet.20170302.12>, 2017.
- AggreBind, 2020. Online. <https://aggrebond.com/about/what-is-a-polymer-what-is-soil-stabilizing/>. (Accessed 29 May 2020).
- Ahmed, A., 2013. Recycled bassanite for enhancing the stability of poor subgrade clay soil in road construction project. *Construct. Build. Mater.* 48, 151–159. <https://doi.org/10.1016/j.conbuildmat.2013.05.089>.
- Al-Adili, A., Salim, N.M., Al-Soudany, Y., 2019. Response of soft soil mixing with recycled gypsum plasterboard as stabilised agent for soil underneath oil tank as a case study. In: IOP Conf. Ser.: Mater. Sci. Eng. <https://doi.org/10.1088/1757-899X/579/1/012048>, 579 012048.
- Aliyu, D.S., Ma'aruf, A., Farouq, M.M., Dawusu, S.U., 2019. Stabilisation of Lateritic Soil Using Powdered Locust Bean Pod 'Makuba'. *IJESR/ICRIT-IV/Special Issue/Article No-46/249-255* ISSN 2277-2685.
- Al-Rawas, A.A., Goosen, F.A., 2006. *Expansive Soils: Recent Advances in Characterization and Treatment*, ISBN 9780415396813. <https://doi.org/10.1201/9780203968079>, 544 Pages.
- Alzaidi, M.N., 2019. Experimental study for stabilising clayey soil with eggshell powder and plastic wastes. *Mater. Sci. Eng.* 518 (2019) <https://doi.org/10.1088/1757-899X/518/2/022008>, 022008.
- Amadi, A.A., 2014. Enhancing Durability of Quarry Fines Modified Black Cotton Soil Subgrade with Cement Kiln Dust Stabilisation. Department of Civil Engineering, Federal University of Technology, Minna, Nigeria, pp 3, 4 and 6.
- Amminudin, A.L., Ramadhansyah, P.J., Doh, S.I., Mangi, S.A., Mohd, W.I., 2020. Effect of dried sewage sludge on compressive strength of concrete. In: IOP Conf. Series: Materials Science and Engineering. <https://doi.org/10.1088/1757-899X/712/1/012042>, 712 (2020) 012042.
- Andavan, S., Pagadala, V., 2019. A study on soil stabilisation by addition of fly ash and lime. *Geotech. Geol. Eng.* <https://doi.org/10.1007/s10706-012-9532-3>, 10.1007/s10706-012-9532-3.
- Barisić, I., Grubeša, I., Dokšanović, T., Marković, B., 2019. Feasibility of agricultural biomass fly ash usage for soil stabilisation of road works, 12, p. 1375. <https://doi.org/10.3390/ma12091375>, 9.
- Bassani, M., Tefa, L., Coppola, B., Palmero, P., 2019. Alkali-activation of aggregate fines from construction and demolition waste: valorisation in view of road pavement subbase applications. <https://doi.org/10.1016/j.jclepro.2019.06.207>.
- Beeghly, J.H., 2003. Recent experiences with lime-fly ash stabilisation of pavement subgrade soils base, and recycled asphalt. In: *International Ash Utilisation Symposium*, p. 8.
- Besq, A., Malfoy, C., Pantet, A., Monnet, P., Righi, D., 2003. Physicochemical Characterisation and Flow Properties of Some Bentonite Muds, pp. 275–286. [https://doi.org/10.1016/S0169-1317\(03\)00127-3](https://doi.org/10.1016/S0169-1317(03)00127-3).
- Bhardwaj, A., Sharma, R., 2020. Effect of industrial wastes and lime on strength characteristics of clayey soil. *J. Eng. Des. Technol.* <https://doi.org/10.1108/JEDT-12-2019-0350>.
- Cabalar, A.F., Ismael, I.I., Yavuz, A., 2020. Use of zinc coated steel CNC milling waste for road pavement subgrade. *Transportation Geotechnics* 23. <https://doi.org/10.1016/j.trgeo.2020.100342>.
- Cabezas, R., Cataldo, C., Choudhary, A.K., 2019. Influence of chemical stabilisation method and its effective additive concentration (EAC) in non-pavement roads. A study in andesite-based soils. <https://doi.org/10.1080/23311916.2019.1592658>.
- Cai, Y., Shi, B., Ng, C., Tang, C., 2006. Effect of polypropylene fibre and lime admixture on engineering properties of clayey soil. *Eng. Geol.* 87 (3–4), 230–240. <https://doi.org/10.1016/j.enggeo.2006.07.007>.
- Capital geotechnical services Plc. <https://www.capitalgeotechnical.com/mitigating-clay.html>. (Accessed 15 June 2020).
- Chandrasekhar, J., Chokshi, T., Chauhan, D., 2015. A review on utilisation of waste material "copper slag" in geotechnical applications. *International Research Journal of Engineering and Technology (IRJET)*, ISSN: 2349-6010 249 (online).
- Chen, S., Lin, D., Luo, H., Lin, Z., 2017. Application of reclaimed basic oxygen furnace slag asphalt pavement in road base aggregate. <https://doi.org/10.1016/j.conbuildmat.2017.09.136>.
- Christopher, I.C., Chimboi, N.D., 2019. Emerging trends in expansive soil stabilisation: a review. *Journal of Rock Mechanics and Geotechnical Engineering* 11 (2). <https://doi.org/10.1016/j.jrmge.2018.08.013>.
- Compact equipment. <https://compactequip.com/hand-tools/best-compaction-equipment-utility-project/>. (Accessed 15 June 2020).
- Dakshanamurthy, V., Raman, V., 1973. A simple method of identifying an expansive soil. *Japanese Society of Soil Mechanics and Foundation Engineering* 13 (1), 97–104.
- Du, Y., Jiang, N., Liu, S., Horpibulsuk, S., Arulrajah, A., 2016. Field Evaluation of Soft Highway Subgrade Soil Stabilised with Calcium Carbide Residue. <https://doi.org/10.1016/j.sandf.2016.02.012>.
- Duc, B.V., Kennedy, O., 2018. Adsorbed complex and laboratory geotechnics of quarry dust stabilised lateritic soils. *Environmental Technology and Innovation*. DOI.org/10.1016/j.eti.2018.04.005.
- Elarabi, H., 2010. Damage Mechanism of Expansive Soils Damage Mechanism of Expansive soils.gov.uk/pdf/GEHO1111BVDf-E-E.Pdf. (Accessed 13 April 2020).
- Estabragh, A.R., Jahani, A., Javadi, A.A., Babalar, M., 2020. Assessment of different agent for soil stabilisation of clay soil. *Int. J. Pavement Eng.* <https://doi.org/10.1080/10298436.2020.1736293>.
- Foner, H.A., James, C., Graham, U.M., 1998. Characterization of fly ash from Israel with reference to its possible utilisation. <https://doi.org/10.1139/t93-024>.
- Gobena, J.A., Suppiah, S., 2019. Strength Characteristics of tropical expansive soil-A review. *International Journal of Science and Technology research*. ISSN: 2277-8616 8, 07.
- Gungat, L., Putri, E., Makinda, J., 2013. Effect of oil palm shell curing time to the load-bearing capacity of clay subgrade. *Procedia Engineering* 54, 690–697. <https://doi.org/10.1016/j.proeng.2013.03.063>.
- Gupta, D., Kumar, A., 2016. Performance evaluation of cement-stabilised pond ash-rice husk ash-clay mixture as a highway construction material. <https://doi.org/10.1016/j.jrmge.2016.05.010>.
- Ijaz, N., Dai, F., Rehman, Z., 2020. Paper and wood industry waste as a sustainable solution for environmental vulnerabilities of expansive soil: a novel approach. *J. Environ. Manag.* 262 <https://doi.org/10.1016/j.jenvman.2020.110285>.
- Ikegwuani, C.C., Nwonu, D.C., 2018. Emerging trends in expansive soil stabilisation: a review. *Journal of Rock Mechanics and Geotechnical Engineering* 11. <https://doi.org/10.1016/j.jrmge.2018.08.013>.
- Iyengar, S.R., Masad, E., Rodriguez, A.K., Bazzi, H.S., Little, D., Hanley, H.J.M., 2012. Pavement subgrade stabilisation using polymers: characterisation and performance.

- J. Mater. Civ. Eng. 25 (4), 472. [https://doi.org/10.1061/\(ASCE\)MT.1943-5533.0000612](https://doi.org/10.1061/(ASCE)MT.1943-5533.0000612).
- Jalal, F.E., Xu, Y., Jamhiri, B., Memon, S.A., 2020. On the recent trends in expansive soil stabilisation using calcium-based stabiliser materials (CSMs): a comprehensive review, 2020. <https://doi.org/10.1155/2020/1510969>. |Article ID 1510969 | 23 pages |
- Javed, S.A., Chakraborty, S., 2020. Effects of waste glass powder on subgrade soil improvement. World Scientific News. An international scientific journal. WSN 144, 30–42, 2020, 2392-2192.
- Jawad, I.T., Taha, M.R., Majeed, Z.H., Khan, T.A., 2014. Soil stabilisation using lime: advantages, disadvantages and proposing a potential alternative. Res. J. Appl. Sci. Eng. Technol. 8 (4), 510–520, 2014 ISSN: 2040-7459; e-ISSN: 2040-7467.
- Joe, M., Rajesh, A.M., 2015. Soil stabilisation using industrial waste and lime. International Journal of scientific research Engineering & Technology (IRJET). ISSN: 2278-0882 1–6.
- Jones, L.D., Jefferson, I., 2012. Institution of civil engineers' manuals series. In: Expansive Soils. ICE Publishing, pp. 413–441. <https://www.icevirtuallibrary.com/doi/abs/10.1680/moge.57074.0413>. (Accessed 14 April 2020).
- Jones, L.D., Jefferson, I., 2019. Institution of Civil Engineers Manuals Series. http://nora.nerc.ac.uk/id/eprint/17002/1/C5_expansive_soils_Oct.pdf. (Accessed 30 March 2020).
- K31 roads. <https://www.youtube.com/watch?v=SO3u5uf8Xsc>. (Accessed 15 June 2020).
- Kamaruddin, F.A., Nahazanan, H., Huat, B.K., Anggraini, V., 2020. Improvement of marine clay soil using lime and alkaline activation stabilised with inclusion of treated coir fibre. Appl. Sci. <https://doi.org/10.3390/app10062129>.
- Kassa, R.B., Workie, T., Abdela, A., Fekade, M., Saleh, M., Dejene, Y., 2020. Soil stabilisation using waste plastic Materials. Open J. Civ. Eng. 10, 55–68. https://doi.org/10.4236/ojce.2020.101006_01.
- Kiganda, A., 2016. Soil reinforcement with geogrids. Construction Review online. <https://constructionreviewonline.com/2016/05/soil-reinforcement-with-geogrids/>. (Accessed 15 June 2020).
- Kumar, J.K., Kumar, V.P., 2019. In: Experimental Analysis of Soil Stabilisation Using E-Waste. Saveetha School of Engineering, SIMATS, Chennai, India. Proceedings 22 (2020), pp. 456–459.
- Kumar, P., Goel, R., Yadav, V., 2017. Stabilisation of soil using crumb rubber. http://www.ijarse.com/images/fullpdf/1503486120_IJTEBangalore810.pdf. (Accessed 15 June 2020).
- Li, J., Saberian, M., Nguyen, B.T., 2018. Effect of crumb rubber on the mechanical properties of crushed recycled pavement material. J. Environ. Manag. 218, 291–299. <https://doi.org/10.1016/j.jenvman.2018.04.062>.
- Longworth, I., Hardcore for Supporting Ground Floors of Buildings. BRE association. <http://www.nhbc.co.uk/zmedia/filedownload.58508.en.pdf>. (Accessed 14 May 2020).
- Lucena, L.C.I., Juca, J.F.T., Soares, J.B., Filho, P.G.T., 2014. Use of wastewater sludge for base and subbase of road pavements. Transport. Res. Transport Environ. 33, 210–219. <https://doi.org/10.1016/j.trd.2014.06.007>.
- Maheshwar, R., Sivarakash, A., Prasanth, A., Sivaboopath, S., 2020. Strength and durability study on agro waste based on mud block. International Research Journal of Engineering and Technology (IRJET) 7 (1) e-ISSN: 2395-0056, Jan 2020. www.irjet.net. p-ISSN: 2395-0072.
- Mahmood, A.A., Hussain, M.K., Mohamed, S.N.A., 2019. Use of palm oil fuel ash (POFA)-stabilised Sarawak peat composite for road subbase. Materials today proceedings 20 (Part 4, 2020), 505–511. <https://doi.org/10.1016/j.matpr.2019.09.178>.
- Malongweni, S.O., Kihara, Y., Sato, K., 2019. Impact of agricultural waste on the shrink-swell behaviour and cracking dynamics of expansive soils. Int. J. Recycl. Org. Waste Agric. 8, 339–349. <https://doi.org/10.1007/s40093-019-0265-7>.
- Mavroulidou, M., 2018. Use of Waste Paper Sludge Ash as a Calcium-Based Stabiliser for Clay Soils, vol. 36. London South Bank University, 103 Borough Road, London SE1 0AA, UK, pp. 1066–1072. <https://doi.org/10.1177/0734242X18804043>, 11.
- Meehan, C., Tehrani, F.S., 2009. An Investigation of Continuous Compaction Control Systems. Delaware Center for Transportation, pp. 831–1446. University of Delaware 355 DuPont Hall Newark, Delaware 19716 (302).
- Mehmood, E., Ilyas, M., Farooq, K., 2011. Effect of initial placement conditions on swelling characteristics of expansive soils. In: Proceedings of the Geo-Frontiers 2011: Advances in Geotechnical Engineering, pp. 2397–2403.
- Melling, H., Tusabe, K., Jjuuko, S., Kalumba, D., 2017. Designing a paved road using geogrids to reduce the thickness of the pavement layers. <https://www.researchgate.net/publication/320774837>. (Accessed 19 May 2020).
- Michael, T., Singh, S., Kumar, A., 2016. Expansive Soil Stabilisation Using Industrial Solid Waste A Review. International Conference on Recent Trends in Engineering & Science. Shree Ramchandra College of Engineering, Pune (India), pp. 508–516. Midwest. <https://midwestind.com/soil-sement-engineered-formula/>. (Accessed 30 May 2020).
- Mishra, B., Gupta, M., 2018. Use of randomly oriented polyethylene terephthalate (PET) fiber in combination with fly ash in subgrade of flexible pavement. Construct. Build. Mater. 190, 95–107.
- Mohanraj, P., Muthupandi, G., Kumar, K.N., 2017. Experimental study on stabilisation of soil using copper slag and lime waste. South Asian Journal of Engineering and Technology 3 (7), 134–141, 2017.
- Morales, D., Romero-Esquinas, A., Fernández-Ledesma, E., Fernández, J., Jiménez, J., 2019. Feasible use of colliery spoil as subbase layer for low-traffic roads. Construct. Build. Mater. <https://doi.org/10.1016/j.conbuildmat.2019.116910>.
- Mosa, A.M., Taher, A.H., Al-Jaberi, L.A., 2017. Improvement of poor subgrade soil using cement kiln dust. Case Studies in Construction Materials 7 (C). <https://doi.org/10.1016/j.cscm.2017.06.005>.
- Mukiza, E., Zhang, L., Liu, X., Zhang, N., 2019. Utilization of red mud in road base and subgrade materials: a review. Resour. Conserv. Recycl. 141, 187–199. Pp 1 and 11.
- Muntohar, A.S., 2012. Influence of plastic waste fibres on the strength of lime-fly ash stabilised clay. Civil Engineering Dimension 11 (1), 32–40.
- Nabil, M., Mustapha, A., Rios, S., 2020. Impact of wetting–drying cycles on the mechanical properties of lime-stabilised soils. Int. J. Pavement Res. Technol. 13, 83–92. <https://doi.org/10.1007/s42947-019-0088-y>, 2020.
- Nujid, M.M., Idrus, J., Tholibon, D.A., Bapwadi, N.F., Firoozi, A.A., 2020. Bearing capacity of soft marine soil stabilisation with cockle shell powder (CSP). Int. J. Eng. Adv. Technol. ISSN: 2249-8958 9 (3).
- Onakunle, O., Omole, D.O., Ogiye, A.S., Choudhary, A.K., 2019. Stabilisation of lateritic soil from Agbara Nigeria with ceramic waste dust. Cogent Engineering 6, 1. <https://doi.org/10.1080/23311916.2019.1710087>.
- Onyelowe, K., Van, D.B., 2018. Structural analysis of consolidation settlement behaviour of soil treated with alternative cementing materials for foundation purposes. Environmental Technology and Innovation. DOI.org/10.1016/j.eti.2018.05.005.
- Parihar, N.S., Gupta, A.K., 2020. Strength and microstructural behaviour of expansive soil stabilised with limed leather waste ash. Int. J. Innovative Technol. Explor. Eng. ISSN: 2278-3075 9 (4).
- Perera, S., Arulrajah, A., Wong, Y., Horpibulsuk, S., Maghoo, I.F., 2019. Utilizing recycled PET blends with demolition waste as construction materials. Construct. Build. Mater. 221, 200–209. <https://doi.org/10.1016/j.conbuildmat.2019.06.047>, 2019.
- Peter, L., Jayasree, P., Balan, K., Raj, S., 2016. Laboratory investigation in the improvement of subgrade characteristics of expansive soil stabilised with coir waste. Transportation Research Procedia 17, 1–8. <https://doi.org/10.1016/j.trpro.2016.11.110>.
- Phanikumar, B.R., Raju, E.R., 2020. Compaction and strength characteristics of expansive clay stabilised with lime sludge and cement. Soils Found. <https://doi.org/10.1016/j.sandf.2020.01.007>.
- Pleasant Construction, Inc. Soil stabilisation and soil modification. <https://pleasantconstruction.com/services/soil-cement-soil-stabilization/>. (Accessed 15 June 2020).
- Pooni, J., Giustozzi, F., Robert, D., Setunge, S., O'Donnell, B., 2019. Durability of enzyme stabilised expansive soil in road pavements subjected to moisture degradation. Transportation Geotechnics 5.
- Rank, K., Bhandari, J., Mehta, J.V., 2020. Using brick dust manufacturing waste and cement dust manufacturing waste as stabilising material for expansive soil. <http://www.jetir.org/papers/JETIR2002078.pdf>. (Accessed 15 June 2020).
- Reda, A., Ibrahim, E., Houssami, L., 2016. A cure for swelling. <https://dar.com/news/d-etails/a-cure-for-swelling>. (Accessed 30 March 2020).
- Rivera, J.F., Orobio, A., Mejía de Gutiérrez, R., Cristelo, N., 2020. Clayey soil stabilisation using alkali-activated cementitious materials. Mater. Construcción 70, e211. <https://doi.org/10.3989/mc.2020.07519>, 337.
- Road and Maritime Services, Specification 3051, 2014. Granular base and subbase materials for surface road pavement. <https://www.rms.nsw.gov.au/business-industry/partners-suppliers/documents/specifications/3051.pdf>. (Accessed 8 February 2020).
- Saberian, M., Li, J., Boroujeni, M., Law, D., Li, C., 2020. Application of demolition waste mixed with crushed glass and crumb rubber in pavement base/subbase. Resour. Conserv. Recycl. 156 (2020) <https://doi.org/10.1016/j.resconrec.2020.104722>, 104722.
- Saha, D., Mandal, J., 2017. Laboratory investigations on Recycled Asphalt Pavement (RAP) for using it as base course of flexible pavement. Process Eng. 189 (2017), 434–439. <https://doi.org/10.1016/j.proeng.2017.05.069>.
- Salih, W.T., Yu, W., Dong, X., Hao, W., 2020. Study on stress-strain-resistivity and microscopic mechanism of red mud waste modified by desulphurization gypsum-fly ash under drying-wetting cycles. <https://doi.org/10.1016/j.conbuildmat.2020.118772>.
- Saltan, M., Findik, F., 2007. Stabilisation of subbase layer materials with waste pumice in flexible pavement. Build. Environ. 43 (2008), 415–421. <https://doi.org/10.1016/j.buildenv.2007.01.007>. Pp 1 and 7.
- Saranya, K., Jeevitha, J., Varshini, T., 2017. A review on application of chemical additives in soil stabilisation. International Research Journal of Engineering and Technology (IRJET) 4 (3) e-ISSN: 2395-0056, Mar -2017. p-ISSN: 2395-0072.
- Selvi, P., 2014. Fatigue and rutting strain analysis on lime stabilised subgrades to develop a pavement design chart. Transp Geotech 2 (2015), 86–98.
- Sharma, A.K., Sivapullaiah, P.V., 2015. Ground granulated blast furnace slag amended fly ash as an expansive soil stabiliser. Article in Soils and Foundations -Tokyo. <https://doi.org/10.1016/j.sandf.2016.02.004>. March 2016.
- Sharma, A., Puvvadi, S., 2011. Soil stabilisation with waste materials based binder. In: Proceedings of Indian Geotechnical Conference. December 15-17, 2011, Kochi (Paper No. H-119).
- Singh, V., Jain, R., 2015. Effect of cement kiln dust (CKD) on engineering properties of black cotton soil. International Journal for Innovative Research in Science & Technology 1 (12), 86–90.
- Soil stabilisation innovations- the industry leaders in the soil erosion control and dust control solutions. <https://dustcontrolsolutions.wordpress.com/2019/01/05/how-ss-i-polymers-are-better-than-the-others-polymers-used-in-the-soil-stabilization-industry/>. (Accessed 15 June 2020).
- Subramaniaprasad, C.K., Abraham, B.M., Kunhanandan Nambiar, E.K., 2014. Influence of embedded waste-plastic fibres on the improvement of the tensile strength of stabilised mud masonry blocks. J. Mater. Civ. Eng. 27 (7), 04014203.
- Tan, J.F., Adajar, M.A.Q., 2020. Recycled gypsum and rice husk ash as additives in the stabilisation of expansive soil. International Journal of GEOMATE 18 (70), 197–202.

- <https://doi.org/10.21660/2020.70.9201>. ISSN: 2186-2982 (P), 2186-2990 (O), Japan.
- Tennessee permanent stormwater management and design guidance manual. Chapter 5, 5.3.2 soil restoration. <https://tpermanentstormwater.org/manual/07%20Chapter%205%20Permanent%20Stormwater%20Management%20Measures%20-%20Sections%205.0-5.3.pdf>. (Accessed 13 April 2020).
- The Civil Engineer, 2012. Mechanical and cement stabilisation of soil (DAMS). <https://constructionduniya.blogspot.com/2012/02/mechanical-and-cement-stabilization-of.html>. (Accessed 27 April 2020).
- Tiwari, N., Satyam, N., 2020. An experimental study on the behaviour of lime and silica fume treated coir geotextile reinforced expansive soil subgrade. <https://doi.org/10.1016/j.jestch.2019.12.006>. (Accessed 20 April 2020).
- Toll, D.G., Abedin, Z., Buma, J., Cui, Y., Osman, A.S., Phoon, K.K., 2012. The Impact of Changes in Water Table and Soil Moisture on Structural Stability of Buildings and Foundation Systems: Systematic Review CEE10-005 (SR90). Technical report. Collaboration for Environmental Evidence.
- U.S. Department of Transport. Federal Highway administration: chapter 3.0 Geotechnical aspects of pavements reference manual [online]. Available at: <http://www.fhwa.dot.gov/engineering/geotech/pubs/05037/03a.cfm>. (Accessed 13 April 2020).
- Varaprasady, B.J., Reddy, J.J., Reddy, S.J., 2020. Remediation of expansive soils using mango kernel ash and calcium carbide residue. *Int. J. Environ. Waste Manag.* <https://doi.org/10.1504/IJEW.2020.105351>.
- Wang, D., Tawk, M., Indraratna, B., Heitor, A., Rujikiatkamjorn, C., 2019. A mixture of coal wash and fly ash as a pavement substructure material. *Transportation Geotechnics*. <https://doi.org/10.1016/j.trgeo.2019.100265>, 21 100265-1-100265-10, Pp 1 and 4.
- Wei, H., Zhang, Y., Cui, J., Han, L., Li, Z., 2018. Engineering and environmental evaluation of silty clay modified by waste fly ash and oil shale ash as road subgrade material. *Construct. Build. Mater.* 196, 204–213, 2019.
- Wu, J., Liu, Q., Deng, Y., Yu, X., Feng, Q., Yan, C., 2019. Expansive Soil Modification by Waste Steel Slag and its Application in Subbase Layer of Highways Soil. <https://doi.org/10.1016/j.sandf.2019.03.009>. (Accessed 12 June 2020).
- Yadav, A., Gauravx, K., Kishor, R., Suman, S., 2017. Stabilisation of alluvial soil for subgrade using rice husk ash, sugarcane bagasse ash and cow dung ash for rural roads. *International Journal of Pavement Research and Technology* 10, 254–261, 2017.
- Zaid, A., 2017. Swelling expansion and dilation of soil. *Linkedin*. <https://www.slideshare.net/AhmedZaid11/swelling-expansion-and-dilation-of-soil>. (Accessed 30 March 2020).
- Zhang, J., Ding, L., Li, F., Peng, J., 2020. Recycled aggregate from construction and demolition waste as alternative filling materials for highways subgrade in China. *J. Clean. Prod.* 255, 120223. <https://doi.org/10.1016/j.jclepro.2020.120223>. (Accessed 10 May 2020).
- Zhang, J., Gu, F., Zhang, Y., 2019a. Use of building-related construction and demolition wastes in highway embankment: laboratory and field evaluations. *laboratory and field evaluations*. *J. Clean. Prod.* <https://doi.org/10.1016/j.jclepro.2019.05.182>.
- Zhang, L., Little, D.N., Hariharan, N., Kim, Y., 2019. Prediction of climate specific vertical movement of pavements with expansive soil based on long-term 2D numerical simulation of rainwater infiltration. *Comput. Geotech.* <https://doi.org/10.1016/j.compgeo.2019.103172>.
- Zhang, T., Cai, G., Liu, S., 2016. Application of lignin-based by-product stabilised silty soil in highway subgrade: a field investigation. *J. Clean. Prod.* 142, 4243–4257. <https://doi.org/10.1016/j.jclepro.2016.12.002>, 2017.
- Zhou, S., Zhou, D., Zhang, Y., Wang, W., 2019. Study on physical-mechanical properties and microstructure of expansive soil stabilised with fly ash and lime. *Adv. Civ. Eng.* 2019 <https://doi.org/10.1155/2019/4693757>. Article ID 4693757.
- Zornberg, J.G., Gupta, R., 2015. Reinforcement of pavements over expansive clay subgrades. <https://www.researchgate.net/publication/242465167>. (Accessed 15 April 2020).
- Zumrawi, M., Abdelmarouf, A.O., Abubakr, E., Gameil, A., 2017. Damage of buildings on expansive soils: diagnosis and avoidance. *Int. J. Multidisciplinary and Scientific Emerging Research, IJMSER*. ISSN: 2349-6037 6 (2), 108–116.
- Zhang, T., Yang, Y., Liu, S., 2020. Application of Biomass By-Product Lignin Stabilised Soils as Sustainable Geomaterials: A Review. *Science of the Total Environment*. <https://doi.org/10.1016/j.scitotenv.2020.138830>.
- Zhang, T., Liu, S., Zhan, H., Ma, C., Cai, G., 2019. Durability of silty soil stabilised with recycled lignin for sustainable engineering materials. *J. Clean. Prod.* <https://doi.org/10.1016/j.jclepro.2019.119293>.



Short Communication

Consistency and mechanical properties of sustainable concrete blended with brick dust waste cementitious materials

S. Y. Amakye¹ · S. J. Abbey¹ · A. O. Olubanwo²Received: 3 August 2020 / Accepted: 24 February 2021 / Published online: 4 March 2021
© The Author(s) 2021 **OPEN**

Abstract

The reuse of waste materials in civil engineering projects has become the topic for many researchers due to their economic and environmental benefits. In this study, brick dust waste (BDW) derived from cutting of masonry bricks and demolition waste which are normally dumped as land fill is used as partial replacement of cement in a concrete mix at 10%, 20% and 30% respectively, with the aim of achieving high strength in concrete using less cement due to the environmental problems associated with the cement production. To ascertain the effects of BDW on the consistency and mechanical performance of concrete mix, laboratory investigations on the workability of fresh concrete and the strength of hardened concrete were carried out. Slump and compaction index test were carried out on fresh concrete mix and unconfined compressive strength (UCS) test and tensile strength test were conducted on hardened concrete specimen after 7, 14 and 28 days of curing. The results showed high UCS and tensile strength with the addition of 10% BDW to the concrete mix, hence achieving the set target in accordance with the relevant British standards. A gradual reduction in strength was observed as BDW content increases, however, recording good workability as slump and compaction index results fell within the set target range in accordance with relevant British standards. Findings from this study concluded that BDW can partially replace cement in a concrete mix to up to 30% igniting the path to a cleaner production of novel concrete using BDW in construction work.

Keywords Brick dust waste · Partial cement replacement · Construction demolition waste · Unconfined compressive strength · Tensile splitting strength · Workability · Green concrete

1 Introduction

Recent growth in the world's population has triggered an increase in the demand for concrete products for the construction of more building for use as homes and other infrastructure. This has led to the consumption of billions of tons of our natural resources such as clinker, water and aggregates by construction industries to produce cement; therefore, increasing the problems associated with cement production such as high greenhouse gas (GHG) emission and environmental pollution [1].

Cement consumption in 2014 in developed economies increased by about 9.2 million metric tons followed by 9 million metric tons in 2015 and is expected to grow from 2.3% in 2019 and 1.7% in 2020 [2]. The world cement vision predicted a rise in GHG emission in 2020 due to a rise in demand for cement worldwide [3]. According to [4] approximately one ton of CO₂ is produced in preparation of one ton of cement. The negative impact of cement production has raised concerns to push towards a more sustainable practice of using recycled waste materials. By-products pozzolanic materials such

✉ S. Y. Amakye, Samuel.amakye@uwe.ac.uk; S. J. Abbey, Samuel.abbey@uwe.ac.uk; A. O. Olubanwo, aa7878@coventry.ac.uk | ¹Civil Engineering Cluster, Department of Geography and Environmental Management, Faculty of Environment and Technology, University of the West of England, Bristol, UK. ²School of Energy, Construction and Environment, Faculty of Engineering, Environment and Computing, Coventry University, Coventry, UK.



as marble dust has been used in concrete production [5]. Quarry dust, fly ash and billet scale are successfully used in a study as cement replacement in a concrete mix [6]. Cementitious materials such as fly ash, rice hush ground granulated blast furnace slag, and bagasse ash can be used in concrete mix due to their pozzolanic properties [7]. Clay bricks ground to cement fineness was partially replaced with cement at 0% 10%, 20% and 30% in standard mortar [8].

About 14% of construction and demolition waste is made up of bricks and reasonable results have been achieved when Brick dust waste (BDW) was used as a substitute for cement at 5%, 10% and 15% [9].

Brick dust waste is a pozzolanic material when mixed with cement produces calcium silicate hydrate gel (C–S–H) which determines the strength of concrete. Any materials with a siliceous and aluminous content that reacts with calcium hydroxide when in contact with water to form cementitious hydration product are referred to as Pozzolans [10]. Ancient structures in Rome and Egypt used pozzolans as part of the cement used in their construction [11]. Excessive dumping of construction and demolition waste as landfill has influenced current research to consider the use of construction and demolition waste as partial replacement for cement due to the negative environmental impact associated with landfill. Using waste materials in the construction sector will reduce the overall cost of construction and the negative environmental effects associated with cement production leading to a more sustainable construction industry. Bricks are manufactured by the calcination of alumina-silicate clay and ground to suitable fineness to possess pozzolanic properties and made brittle by subjecting it to a high temperature of about 1000 to 1100 °C and the creation of a liquid glassy phase when cooling indicate high pozzolanic properties [8]. Although kaolinite loses its structural water around 600 °C to form metakaolin, this new material is used as pozzolan in finely divided form in cement-based system [12]. In this study, detailed investigation into the consistency and mechanical properties of concrete made from partially replaced cement with brick dust waste at varying proportions is presented, and it highlights the tests conducted along with the appropriate standards adopted. The study will outline the experimental methods used, describing the samples preparation, design mix and various tests conducted on fresh and hardened concrete. Results and discussion section will focus on presenting and discussing the results obtained from the various tests conducted, which subsequently provides the key findings given in the conclusions and recommendations for future work.

2 Scope of the study

This study will contribute to the understanding of partially replacing cement with BDW focusing on the workability of fresh concrete and the strength of hardened concrete. Slump and compaction index test were carried out on wet concrete and unconfined compressive test and tensile splitting test were conducted on hardened concrete. The study focuses on the replacement of cement with brick dust waste and its effect on strength and workability. CEM II cement was used and a strength class of RC 35/45 was adopted. A target Class S3 was set for the slump test as recommended by BS EN 206:2013 + A1:2016(E) which suggest a slump range of 100 to 150 mm. A target Class C3 was set for compaction index test as recommended by BS EN 206:2013 + A1:2016(E) which suggest a degree of compatibility range of 1.10 to 1.04 in accordance with BS 8500-2-2015 + A1:2016. Unconfined compressive strength test was conducted in line with BS EN 12390-3:2019 and ASTM C109/C109M-20b after the samples were cured in water for 7, 14 and 28 days. A tensile splitting test was conducted after 28 days of curing the samples in water in accordance with BS EN 12390-6-2009 and ASTM C496/C496M-17. The results from the tests will be compared with the target values provided by British Standards (BS) and the American Society for Testing and Materials (ASTM).

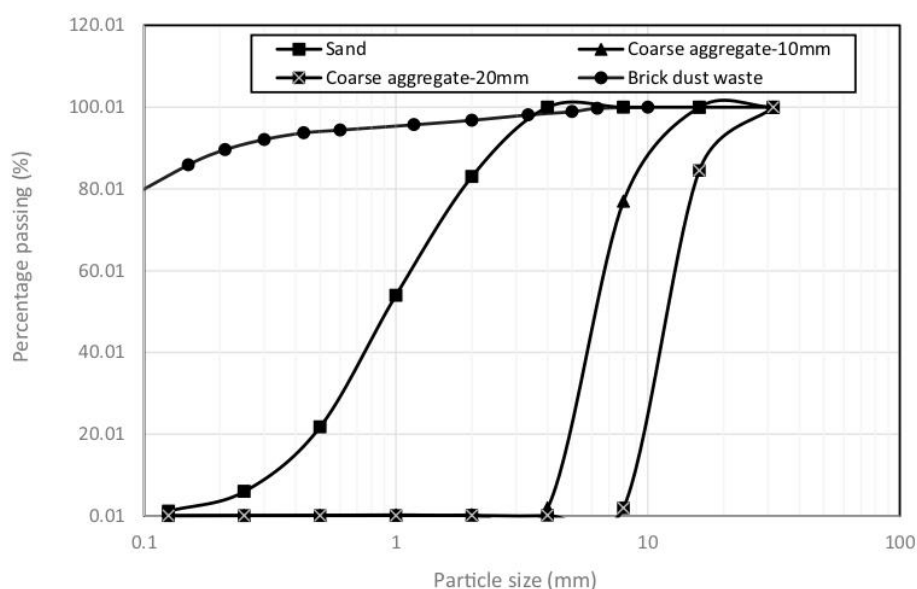
3 Materials and method

The materials used in this study include brick dust waste, Portland cement, limestone aggregate (coarse) 10 mm (10/4) and 20 mm (20/10) grade, natural sea-dredged sand (fine aggregate). Brick dust used in the study is a waste from cutting of fired bricks supplied by Brick Fabrication Ltd, Gemini works, Pontypool, South Wales, UK. Portland cement type BS EN 197-1 CEM II/B-V 32.5R with a minimum compressive strength of 32.5 N/mm² was used in accordance with BS EN 197-1:2011a and supplied by Lafarge Cement UK through a local contractor. Fine and coarse aggregate used in the study was supplied by a local contractor in line with PD 6682-1-:2009. Sieve analysis was conducted by the local supplier in accordance with BS EN 12620:2002+A1:2008 and BS EN 933-1:2012. Consistency limit and particle size distribution of brick dust waste (BDW) are shown in Table 1 and Fig. 1, Chemical composition mineralogy and physical properties of BDW and PC are shown in Table 2 and Particle size distribution (Figs. 2, 3, 4), chemical composition and other properties of sand and stone are shown in Table 3.

Table 1 Consistency limit and particle size distribution of BDW

Consistency limits BDW	Description
Liquid limit w_L (%)	–
Plastic limit w_p (%)	–
Plasticity index I_p (%)	Non-plastic
Others	Value
Specific gravity	2.5
Bulk density (kg/m^3)	1837
Maximum dry density (MDD) Mg/ m^3	1.5
Optimum moisture content (OMC) (%)	17
Blaine fineness (m^2/kg)	369
Colour	Brick red

Fig. 1 Particle size distribution of aggregates and brick dust waste used



3.1 Experimental Method

3.1.1 Mix design and sample preparation

Based on BS 8500-2:2015+A1-2016, concrete type RC35/45 was adopted and four batches of concrete mix were prepared with ratio 1:2:3 and water-cement ratio (w/c) 0.5, cement was partially replaced with BDW based in the control mix. Nine (9) cubes (100 mm × 100 mm × 100 mm) and two (2) cylindrical specimens (100 mm diameter and 200 mm height) were made per mix. Based on the design criteria for control mix in Table 4, Mix composition (MC)1–3 were designed by replacing cement with BDW at 10%, 20% and 30% by weight of various materials.

Based on the mix design, dry materials were mixed using a concrete mixer and a measured amount of water

added. An oiled steel cube and cylindrical moulds filled with fresh concrete and vibrated for up to 40 Hz for 5 s using a vibrating table until no further settlement was observed, and a compact and air free concrete achieved. The surface was levelled and store without any seal in a room for 24 h with a temperature of about 20 ± 5 °C. With the help of a powered tool, the dry concrete samples were de-moulded and cured in water to be tested after 7, 14 and 28 days.

3.1.2 Fresh concrete testing

3.1.2.1 Slump test Slump test was carried out for all mix compositions in line with BS EN 12,350-2:2009. During the test, a metal cone mould with height 300 mm, base diameter 200 mm and top diameter 100 mm with two handles

Table 2 Chemical composition mineralogy and physical properties of BDW and PC

Chemical composition										
Oxide	SiO ₂	Al ₂ O ₃	Fe ₂ O ₃	MgO	CaO	K ₂ O	SO ₃	TiO ₂	Na ₂ O	Loss of ignition
% BDW	52	41	0.7	0.12	4.32	0.53	0.33	0.65	0.05	2.01
% PC	20.00	6.00	3.00	4.21	63.00	-	2.30	-	-	0.80
Mineralogy of brick dust waste										
Com- pound	Kaolinite	Aunite	Quartz	Illite						
Percent- age	54	5	41	-						
Physical Properties of PC										
Properties	Insoluble residue	Bulk density (m ³ /kg)	Relative density	Blaine fineness (m ³ /kg)	Colour					
Description	0.5	1400	3.1	365	Grey					

and two fool rest were used. The cone was placed on a non-absorbent surface with the top diameter 100 mm facing up. With a firm grip of the handle and footrest, the mould was filled with fresh concrete in three layers. Each layer of concrete was tapped 25 times with a standard steel rod (16 mm diameter and 600 mm length). The rod was rolled horizontally over the top of the mould to level the concrete. The mould was lifted slowly using the handle leaving unsupported concrete to slump. The metal cone is placed next to the slumped concrete and the 600 mm long rod was placed on top of the empty cone mould to set as a target. The distance between the set target and the slumped concrete was measured using a measuring ruler. The value of the measurement is the slump value of fresh concrete. Figs. 5 and 6 show the slump test and the types of slump.

3.1.2.2 Compaction index (CI) test Compaction index was carried out to determine the degree of compaction of fresh concrete. This test was carried out for all mix compositions in accordance with BS 12350-4:2009. A measuring ruler, hand trowel, vibrating table, 600 mm long steel rod and a rectangular metal container with internal dimensions 400 mm height and 200 mm base were used in this test. With the help of a hand trowel, the rectangular container was filled with fresh concrete to the top and levelled by rolling a 600 mm steel rod over the top of the mould. The mould with concrete was then vibrated for up to 40 Hz using a vibrating table until no further settlement was observed. The distance (S) from the surface of the compacted fresh concrete to the top edge of the metal mould was measured with a measuring ruler and the values recorded. Compaction index was determined using Eq. 1. Compaction index test process is shown in Figs. 7, 8 and 9.

$$CI = \frac{H}{H - S} \tag{1}$$

where, H= Internal height of the container and S= Mean value of 'S'.

3.1.3 Hardened concrete testing

3.1.3.1 Unconfined compressive strength (UCS) Hardened concrete cube was tested for compressive strength after 7, 14 and 28 days of curing in line with BS EN 12,390-3:2019 and ASTM C109/C109M-20b. Using compressive test equipment, a vertical force was applied to cube specimen at a rate of 6kN/sec until failure and the failure load was recorded. Base on recorded failure loads for various mix composition, unconfined compressive strength was determined using Eq. 2.

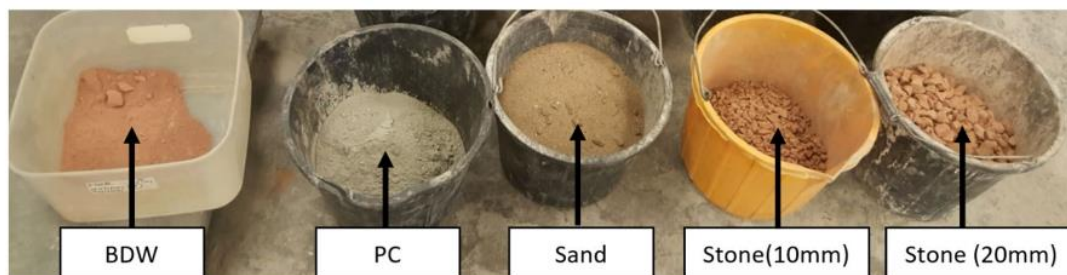


Fig. 2 Materials used in the study



Fig. 3 Fresh concrete in a steel mould



Fig. 4 Concrete cubes and cylinder specimen in a curing tank

$$UCS (N/mm^2) = \frac{F}{A_c} \quad (2)$$

where, F=Maximum failure load (N) and A_c = Cross-sectional area of specimen (mm^2).

3.1.3.2 Tensile splitting strength (TSS) Tensile splitting test was conducted on the cylindrical test specimen after 28 days of curing. The splitting tensile method was used in line with BS EN 12,390-6-2009 and ASTM C496/

C496M-17. The cylinder specimen was put into a steel frame and places horizontally between the platens of a compressive test machine. A constant vertical force was applied along the length of the specimen at a stress rate of 1.57kN/sec until failure and the failure load was recorded as shown in Figs. 10, 11 and 12. Tensile splitting strength was determined using Eq. 3.

$$TSS(N/mm) = \frac{2F}{\pi Ld} \quad (3)$$

where, F= Maximum load at failure (N), L= length of specimen (mm), d= diameter of specimen (mm).

4 Results and discussion

The results obtained from the laboratory test conducted on the consistency and mechanical properties of concrete composed of varying brick dust waste proportions show good consistency and workability for fresh concrete and improved strength for hardened concrete. A true slump and good compaction index values were achieved. However, low slump was recorded for mix composition MC2 composed of 20%BDW and MC3 composed of 30% BDW and low compaction index value recorded for MC 3 composed of 30% BDW. A gradual reduction in slump and compaction index was observed with an increase in brick duct waste content. High compressive and tensile strengths were achieved for all mix compositions which signify strength improvement with the addition of brick dust waste as partial replacement for cement. Compared to the control mix, no significant difference in splitting tensile strength was achieved indicating good performance. The overall results obtained from this experiment prove that brick dust waste has the ability to improve the strength and consistency of concrete.

Table 3 Chemical composition and other properties of sand and stone

Chemical composition of sand		Chemical composition of stone	
Elements	(%) weight of sand		(%) weight of stone
O	56.37		60.04
Mg	0.46		10.82
Al	1.20		1.10
Si	35.04		2.33
S	-		0.10
K	0.64		0.44
Ca	3.1		23.49
Fe	3.19		1.68
Total	100		100

Some geometrical, mechanical and physical properties of limestone				
Property	Sand		Stone (20/10)	
	Sand	Stone (10/4)	Stone (10/4)	Stone (20/10)
Water absorption (%)	0.85	1.5	1.5	1.1
Saturated density (Mg/m ³)	2.82	2.68	2.68	2.65
Dry density (Mg/m ³)	2.71	2.57	2.57	2.54
Shape index (%)	-	12	12	7
Impact value (%)	-	23	23	15
Flakiness index (%)	-	-	-	-

Table 4 Mix proportions and material

Mix Composition	Replacement (%)	PC (kg)	BDW (kg)	Sand (kg)	Limestone		
					10 mm (kg)	20 mm (kg)	water (litres)
Control Mix	0	5	0	10	6	9	3
MC 1	10	4.4	0.5	10	6	9	3
MC 2	20	3.9	1	10	6	9	3
MC 3	30	3.5	1.5	10	6	9	3

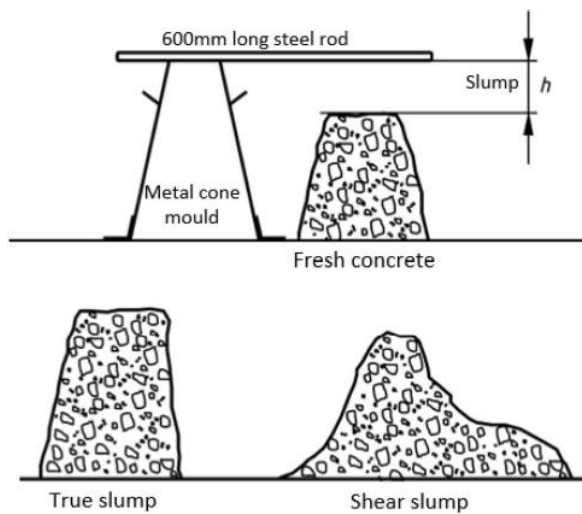


Fig. 5 Slump test and types of slumps (British Standard)



Fig. 7 Filling mould with fresh concrete



Fig. 6 Laboratory slump test



Fig. 8 Levelling the top of the mould

4.1 Fresh concrete

4.1.1 Slump and Compaction Index

A variation in slump was observed for each mix composition and a drastic reduction in slump of 110 mm (MC 1) to 40 mm (MC 2) was observed. However, a true slump was



Fig. 9 Measuring distance (s)



Fig. 12 Cylindrical specimen locked in steel frame



Fig. 10 Applying vertical force to cube specimen



Fig. 13 Applying vertical force on the cylindrical test specimen



Fig. 11 Failed cube specimen with cracks

achieved with MC 1 comprising of 10% BDW as shown in Fig. 13 in accordance with BS EN 12350-2:2009. The results show that MC 2 and MC 3 did not achieved the set target range, however, they can still be used in construction work. All mix compositions fell within the set target range for compaction index in line with BS 12350-4:2009. However, a gradual reduction in compaction index was observed as BDW content increases. Variations in slump value of the concrete mix are as a result of the physical properties of BDW influencing the consistency of fresh concrete with varying brick dust content [13]. In a similar study where BDW was added to a concrete mix at 10%, 20% and 30%, similar trend of results were observed by [9]. The study indicates that every percentage increase in ground clay bricks results in a gradual reduction in slump value [12]. However, the reduction in slump cannot be attributed to the increase in BDW content alone, changes in water-cement ratio (w/c) and rate of water absorption by BDW in different mix compositions also play a major role. A study conducted by [8] revealed that 25% of PC replacement by

ground brick in the concrete mix had no significant effect on water demand. An increase in absorption properties of concrete increased with an increased coconut shell content. In [14], it's observed that water absorption in concrete mix increased when brick dust waste was used as a partial substitute for cement from between 5 and 30%. Fluidity in the mix composition generally reduced under the same w/c for varying mix compositions of brick dust waste, leading to higher stiffness and subsequent reduction in slump. In [15] it's shown that BDW has 25% more fineness compared to cement, and therefore requires a high amount of water during hydration when ground waste clay is used as a partial replacement. The gradual increase in percentages of BDW between 10% and 30% in fresh concrete influenced the 'S' value in their study. 'S' value is the mean value of the four sides distance from the edge top of the steel container to the surface of the compacted concrete. It thus follows that the lower the slump the higher the 'S' value and vice versa. Clear factors

affecting compaction index include w/c, cement content, mix proportions, aggregate shape and size. All compaction index values achieved in the current study are within the target range as shown in Fig. 14 with the highest compaction index of 1.18 mm recorded for MC 1.

4.2 Hardened concrete

4.2.1 Unconfined compressive strength (UCS)

A high compressive strength was achieved at later stages for all mix compositions in the current study. It's observed that at the early age of curing, a low compressive strength was generally observed but was followed by a predominate increase in compressive strength for all mix composition after curing age 7, 14 and 28 days as shown in Fig. 15. But in a similar study conducted by [4] at different replacement of 5%, 10% and 15%, a higher compressive strength was obtained with 15% brick dust waste. Another study by [16] revealed that a high compressive strength could be achieved when sand is replaced with up to 15% of BDW. Hardened concrete with BDW generally shows lower compressive strength at early ages, but a comparable strength with cement only concrete at later ages [12]. In the current study, MC 1 achieved the set target with a compressive strength of 36 N/mm², while desirable strength values of about 75% and 65% of the control strength were achieved with MC 2, MC 3 composed of 30% less cement did not achieve the desired compressive strength at even at 28 days. The results showed an increase in strength as curing age increases as the formation of calcium silicate hydrate gel (C-S-H) developed during the hydration process shown in Fig. 16. The presence of pozzolans reacts with the calcium hydroxide during hydration and forms calcium silicate hydrate gel (C-S-H) [17]. The pozzolanic characteristics are responsible for high



Fig. 14 Failed cylindrical specimen

Fig. 15 Slump values of concrete mix with BDW

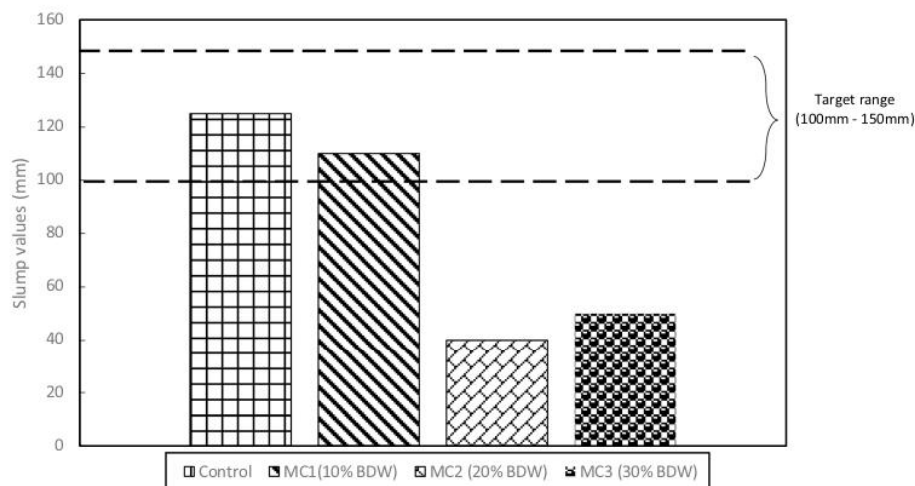
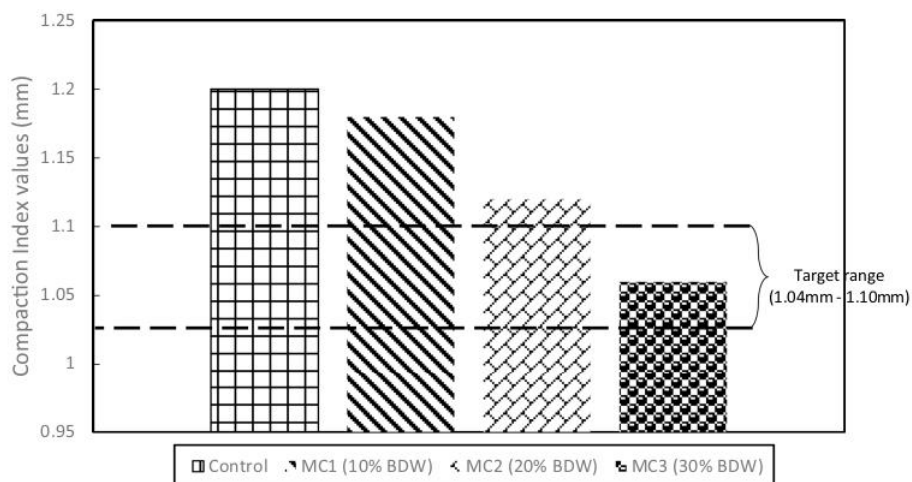


Fig. 16 Compaction index of concrete mix with BDW



compressive strength at 50% brick waste replacement ratio [5]. The chemical reaction of brick dust in concrete shows a reaction of pozzolana with lime in the presence of water to form hydraulic compounds. The pozzolanic behaviour of ground clay brick (GCB) is similar to conventional materials such as fly ash and calcined clay at later age of 28 days [17]. The continuous of C–S–H gel within a pore structure contribute to strength development in concrete [14]. Results achieved in recent study show an increase in compressive strength as curing age increased due to the formation of C–S–H gel [18]. In line with this current study; development of additional C–S–H gel was observed when clay brick waste was used in mortar and concrete in an experimental study [19]. The high strength recorded for MC 1 can be attributed to the presence of pozzolanic material (brick waste) which contribute to high strength at a later age due to the rapid increase in silicon dioxide (SiO₂) leading to dicalcium silicate (2S) which is responsible for high strength at later age. This is because

MC 1 has a lower cement replacement level which has resulted in high strength. Cement is responsible for the early strength of concrete and pozzolana from brick dust waste is responsible for strength at later ages by providing an extra amount of C–S–H gel [4]. Figure 17 shows the compressive test result. 3

4.2.2 Tensile splitting strength (TSS) test

MC 1 which is composed of 10% BDW achieved the highest TSS of 3.6 N/mm² in Fig. 18 compared to MC 2 and MC 3. The results show no significant difference in tensile strength for all mix compositions. However, a gradual reduction in strength as BDW percentage increase was observed for MC 2 and MC 3. High tensile strength was recorded when cement was replaced with 15% brick dust [4]. The close interval in tensile strength between mix compositions indicates a significant contribution to the increase in strength with the addition of BDW as a

Fig. 17 Compressive strength of concrete mix with BDW

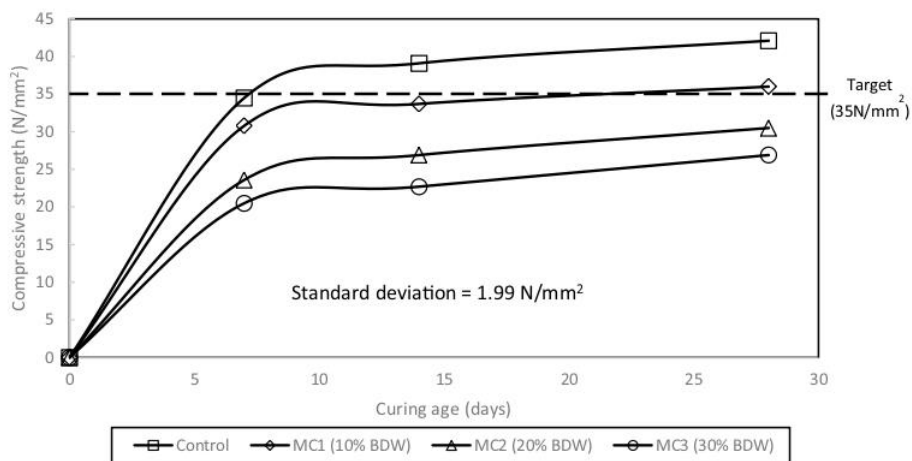
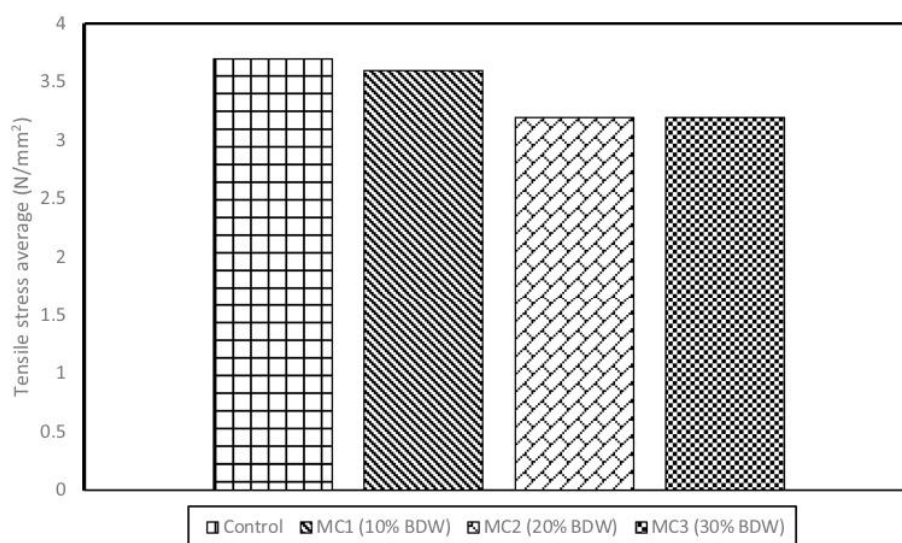


Fig. 18 Tensile strength of concrete mix with BDW

partial replacement for cement. The high tensile strength observed could be attributed to the angular shape of the aggregate coupled with the presents of pozzolans from BDW responsible for the production of high C–S–H gel during hydration [19]. Properties like tensile strength were significantly enhanced when waste materials were used to replace cement [4]. According to [17] tensile strength increased when brick waste was added to a concrete mix. The slow early strength observed in TSS is due to the presents of brick dust, however, the strength gain is higher compared to traditional concrete mix [17].

5 Conclusion and recommendation

The consistency and mechanical behaviour of concrete with varying proportions of brick dust waste content was investigated, discussed and the results showed high strength and good workability for all mix composition. MC 1 composed of 10% BDW achieved the highest UCS and TSS after 28 days of curing. MC 1 achieved all targets set in accordance with the relevant standard. A reduction in strength was observed with an increase in BDW percentage, However, the strengths achieved in this study are usable in construction. The strength pattern of concrete with BDW is similar to conventional concrete with cement only. A drastic reduction in slump was observed in MC 2. However, the concrete is still usable for construction. Results showed that brick dust waste has high water absorption abilities which can lead to variation in slump compared to traditional concrete. An increase in strength with increase in curing age was observed for all mix compositions. Some limitations associated with using brick dust waste in concrete mix is the process of harvesting. Brick dust waste

are mostly contaminated with various construction and demolition materials such as concrete, steel and wood, this makes it difficult to and time-consuming during separation. Grinding bricks into powder using heavy crushing machine generate lots of noise, dust, heat and carbon dioxide (CO₂) which affects the environment. However, this is low compared to the problems associated with cement production. After careful consideration on the results, it's recommended that at least 10% of cement can be replaced with BDW in concrete mix in real-life construction, in order to reduce overall construction cost. Future investigation into the effect of BDW on the durability and rheological properties of fresh concrete and steel reinforcement in concrete can be carried out.

Declaration

Conflict of interest The authors declare that they have no conflict of interest associated with this publication and no financial support has been given to influence the outcome of this work.

Open Access This article is licensed under a Creative Commons Attribution 4.0 International License, which permits use, sharing, adaptation, distribution and reproduction in any medium or format, as long as you give appropriate credit to the original author(s) and the source, provide a link to the Creative Commons licence, and indicate if changes were made. The images or other third party material in this article are included in the article's Creative Commons licence, unless indicated otherwise in a credit line to the material. If material is not included in the article's Creative Commons licence and your intended use is not permitted by statutory regulation or exceeds the permitted use, you will need to obtain permission directly from the copyright holder. To view a copy of this licence, visit <http://creativecommons.org/licenses/by/4.0/>.

References

1. European Environmental state and outlook, 2020. [online]. <https://www.eea.europa.eu/publications/soer-2020>. Accessed: 21 Jul 2020
2. Portland Cement Association, 2020. [online]. <https://www.cement.org/economics/forecasts>. Accessed: 21 Jul 2020
3. World cement. [online]. <https://www.worldcement.com/special-reports/15012020/2020-vision/>. Accessed: 21 Jul 2020
4. Muhammed NA, Nabeel L, Ibrar A, Abdul B, Muhammad U, Muhammad AK (2018) Effect of brick dust on strength and workability of concrete. *IOP Conf Ser Mater Sci Eng* 414:012005. <https://doi.org/10.1088/1757-899X/414/1/012005>
5. Ali AA, Abde. M, Esraa MA. (2014) Re-use of waste marble dust in the production of cement and concrete. *constr. Build Mater.* <https://doi.org/10.1016/j.conbuildmat.2013.09.005>
6. Alaa S, Sivakumar N, Kamal NM (2013) Properties of bricks made using fly ash, quarry dust and billet scale. *Constr Build Mater.* <https://doi.org/10.1016/j.conbuildmat.2012.11.077>
7. Praveenkumar S, Sankarasubramanian G (2019) Mechanical and durability properties of bagasse ash-blended high-performance concrete. *Sci, SN Appl.* <https://doi.org/10.1007/s42452-019-1711-x>
8. O'Farrell M, Wild S, Sabir B (2001) Cement composites-pore size distribution and compressive strength of waste clay brick mortar 23(1):82. [https://doi.org/10.1016/S0958-9465\(00\)00070-6](https://doi.org/10.1016/S0958-9465(00)00070-6)
9. Muhammad BS, Abdullah A, Muhammad AT, Muhammad Y (2013) Performance of pozzolanic concrete using different mineral admixtures. *Pak J Eng Appl Sci* 12:73–81
10. Walker R and Pavia S: (2011) Physical properties of pozzolans and their influence on the properties of lime-pozzolan paste, materials and structural, [online]. <http://hdl.handle.net/2262/58454>. Accessed: 16 Jul 2020
11. Spence RJS, Cook DJ (1983) *Building materials in developing countries*. Wiley, London
12. Viviana FR, Mónica AT, Alejandra T, Claudia CC, Milena P, Jaroslav P, Edgardo FI, Ondřej J, Zbyšek P (2019) Complex characterisation and behaviour of waste fired brick powder-Portland cement system. *Materials.* <https://doi.org/10.3390/ma12101650>
13. Golaszewski J (1999) The influence of ground brick on the physical properties of mortar and concrete. In: *Proceedings, Modern Concrete Materials: Binders, Additions and admixtures*, Dundee, Thomas Telford, London, pp 119–130.
14. Sharda S, Ritesh M, Khalid R (2014) Effect of waste brick kiln dust with partial replacement of cement with adding superplasticizer in construction of paver blocks. *Int J Sci Eng Technol Res* 3(9):2261–2266
15. Kartini K, Rohaidah M, N, and Zuraini Z. A. (2012) Performance of ground clay bricks as partial cement replacement in grade 30 concrete. *Int Scholarly Sci Res Innov* 6(8):312–315
16. Rajesh KB, Patel RD (2014) A study on low performance concrete using mineral admixtures (brick kiln dust and silica fume). *Int J Sci Res Dev* 2(10):217–221
17. Faith (2007): Use of ground clay brick as a supplementary cementitious material in concrete hydration characteristics, mechanical properties, and ASR durability. PhD thesis. Iowa state University. [online]. <https://lib.dr.iastate.edu/cgi/viewcontent.cgi?referer=&httpsredir=1&article=1091&context=rt-d>. Accessed: 20 Jul 2020.
18. Yassin NIM, Adnan SH, Shahidan S, Ayop SS, Kamarulzaman NA, Osman MH, Jamelloddin Z, Majid M, Salleh N, Alisibramulisi A, Wehee AMNA (2020) Effects of curing conditions on properties of lightweight concrete brick containing expanded polystyrene and palm oil fuel ash. *IOP Conf Ser: Mater Sci Eng* 713:012006
19. Lihua Z, Zengmie Z (2020) Reuse of clay brick waste in mortar and concrete. *Hindawi. Adv Mater Sci Eng.* 2020, Article ID 6326178, pp 7, 5. <https://doi.org/https://doi.org/10.1155/2020/6326178>.

Publisher's Note Springer Nature remains neutral with regard to jurisdictional claims in published maps and institutional affiliations.

Article

Mechanical Properties and Microstructure of Fibre-Reinforced Clay Blended with By-Product Cementitious Materials

Samuel J. Abbey ^{1,*} , Eyo U. Eyo ² , Jonathan Oti ³ , Samuel Y. Amakye ⁴ and Samson Ngambi ²

¹ Civil Engineering Cluster, Department of Geography and Environmental Management, Faculty of Environment and Technology, University of the West of England, Bristol BS16 1QY, UK

² School of Energy, Construction and Environment, Faculty of Engineering, Environment and Computing, Coventry University, Coventry CV1 5FB, UK; eyoe@uni.coventry.ac.uk (E.U.E.); apx290@coventry.ac.uk (S.N.)

³ School of Engineering, Faculty of Computing, Engineering and Science, University of South Wales, Trefforest, Pontypridd CF37 1DL, South Wales, UK; jonathan.oti@southwales.ac.uk

⁴ Ph.D. Candidate Civil Engineering Cluster, Department of Geography and Environmental Management, Faculty of Environment and Technology, University of the West of England, Bristol BS16 1QY, UK; Samuel.Amakye@uwe.ac.uk

* Correspondence: samuel.abbey@uwe.ac.uk

Received: 6 May 2020; Accepted: 19 June 2020; Published: 21 June 2020



Abstract: Clayey soils endure adverse changes in strength and volume due to seasonal changes in moisture content and temperature. It has been well recognised that high cement content has been successfully employed in improving the mechanical properties of clayey soils for geotechnical infrastructural purposes. However, the environmental setbacks regarding the use of high cement content in soil reinforcement have necessitated the need for a greener soil reinforcement technique by incorporating industrial by-product materials and synthetic fibres with a reduced amount of cement content in soil-cement mixtures. Therefore, this study presents an experimental study to investigate the mechanical performance of polypropylene and glass fibre-reinforced cement-clay mixtures blended with ground granulated blast slag (GGBS), lime and micro silica for different mix compositions and curing conditions. The unconfined compressive strength, linear expansion and microstructural analysis of the reinforced soils have been studied. The results show that an increase in polypropylene and glass fibre contents caused an increase in unconfined compressive strength but brought on the reduction of linear expansion of the investigated clay from 7.92% to 0.2% at fibre content up to 0.8% for cement-clay mixture reinforced with 5% Portland cement (PC). The use of 0.4–0.8% polypropylene and glass fibre contents in reinforcing cement-clay mixture at 5% cement content causes an increase in unconfined compressive strength (UCS) values above the minimum UCS target value according to American Society for Testing and Materials (ASTM) 4609 after 7 and 14 days curing at 20 °C to 50 °C temperature. Therefore, this new clean production of fibre-reinforced cement-clay mixture blended with industrial by-product materials has great potential for a wide range of applications in subgrade reinforcement.

Keywords: cement-clay mixture; ground granulated blast slag; micro silica; polypropylene fibre; glass fibre; elevated temperature

1. Introduction

Soil stabilization has been proven to be a technically effective and economically viable means of achieving a safe and stable ground for crucial development activities [1–4]. It is essentially a

method of ground improvement that involves the chemical alteration of weak soil properties in order to meet some specific mechanical or engineering requirements such as strength, swelling and durability [5]. The chemicals or binders often used traditionally for the stabilization of problematic soils are lime and cement and it is pertinent to state that the usage of these traditional binders has raised key environmental issues as a result of their high energy consumption and outputs, carbon dioxide emission and the depletion of resources [6]. In recent decades, potential substitutes (industrial wastes, by-products materials, polymers, organics products) to the traditional binders (lime and cement) have been considered by researchers and industries for the stabilization of soft expansive soils [2,7–11]. These materials have now become very competitive economically and technically, and their usage does ensure environmental sustainability. Even though some of these materials are pozzolanic as far as soil stabilization is concerned, others may still require activators to enable them to be more effective in their functions. Ground granulated blast furnace slag (GGBS) for instance is a common by-product generated in the steel production process and has been used as an agent either solely or in combination with lime, cement, etc. for the stabilization of weak expansive soils [5,12–14]. Attention has also shifted to the consideration of polymers for use in stabilization in geotechnical engineering in recent years and their applications in soil improvement spans various areas including in expansive soils, tunneling, landfill lining, geological barriers etc. [15–18]. The utilization of geosynthetic or polypropylene for instance as reinforcement in compacted expansive soils has led to the reduction in tension cracking and controlled volume changes as a result of swelling and shrinkage [19–30]. In these studies, fibre length was suggested as one of the main factors that can bear a significant influence on the properties of the stabilized soil. but it has been proven that relatively long fibres could weaken the soil and encourage swelling of the soil [31]. Glass fibre is another material with excellent properties including strong heat resistance, good corrosion resistance, high tensile strength [32]. It is commonly used as a reinforcement material in a composite material [32]. The use of glass fibre as an agent in the improvement of weak soils are found in literature [33,34]. Another potentially desirable soil binder is micro silica which is a by-product material resulting basically from the reduction of high-purity quartz with coal in an electric arc furnace during the manufacture of silicon or ferro-silicon alloy can be used as a pozzolana. This product is processed and sold in powdered form even though it is more commonly available in liquid. Few research works have investigated the effect of using micro silica on the geotechnical properties of expansive soils [35–40]. Al-zazzawi et al. [36] investigated the effect of micro-silica on the soil subgrades of inadequate natural stability. The clay-micro-silica mixtures were compacted at their various optimal conditions and then subjected to engineering tests. Micro-silica led to an increase in improvement of the consistency limit properties and a decrease in the specific gravity for all the clay samples tested and with 4% of the additive. A significant improvement in swell performance and compressive strength of composite samples were also noted by using micro-silica. The swell pressure reduced by 87% when micro-silica was increased from 5% to 15% by weight of the samples. Undoubtedly, cement in the range of 8–20% [41] has been widely used in enhancing the mechanical behaviour of weak and expansive soils but despite being a fantastic building material, there have been some sustainability concerns with Portland cement (PC), especially in relation to the growth in greenhouse gas (GHG) emissions. Which can be attributed to the intensive energy requirement for its production with an approximate of 1 tonne of carbon dioxide (CO₂) released into the environment for each tonne of cement produced. In 2018, there was an increase in global GHG emissions of about 2% mainly due to a 2% increase in global fossil CO₂ emissions from the combustion of fossil-fuel and those from industrial non-combustion processes including cement production. Therefore, motivated by the environmental setbacks regarding the use of high cement content in soil stabilization and the limited research in the use of a combination of green industrial by-products (GGBS and micro silica) and synthetic fibres, in the soil stabilization process, this study has set out to study the performance of polypropylene and glass fibre reinforced cement-clay mixtures blended with GGBS, lime and micro silica for different mix compositions and curing conditions.

2. Scope of Study

This study is intended to contribute to the understanding of unconfined compressive strength (UCS) and linear expansion of polypropylene and glass fibre reinforced clay blended with GGBS, micro silica and lime. The clay was stabilised with a low binder content and reinforced with polypropylene and glass fibres. To this end, three types of test were carried out: unconfined compressive strength (UCS) tests, linear expansion test, and scanning electron-microscope test (SEM). The study focuses on the analysis of the effect of accelerated curing temperature, binder quantity, both with and without fibres and the effect of the fibre quantity on the compressive and swelling behaviour of the reinforced clay. At reduced cement content and inclusion complimentary cementitious binders and fibres, the UCS values of the reinforced clay were compared with the minimum target of UCS for stabilised soils as recommended by the American Society for Testing and Materials (ASTM) 4609. The ASTM D 4609 (Standard Guide for Evaluating Effectiveness of Admixtures for Soil Stabilization) suggests that if an increase in UCS of 345 kPa or more due to treatment occurs, or if no significant strength is lost due to soaking, then the treatment may be considered effective. Therefore, the UCS values of the fibre treated soil in the present study will be compared to the value provided by the ASTM D 4609 to ascertain the level of improvement.

3. Materials and Method

The materials used in this study were kaolin clay, Portland cement (PC), lime, supplementary cementing materials (SCM) (GGBS and micro silica (MS)), and polypropylene (PPF) and glass fibre (GF). In terms of their main constituents, the PC and lime used comply with BS EN 197-1:2011 (BSI, 2011a) and BS EN 459-1:2015, and the chemical properties of the materials are as provided by the manufacturers respectively. Two by-product supplementary cementitious materials (GGBS and micro silica) were used for this study to contribute to the properties of the treated soil through hydraulic or pozzolanic activity. Preliminary classification test such as Atterberg limit and compaction test conducted on the clay soil is presented in Table 1. Figure 1 shows result of the particle size distribution test conducted on the materials using the laser particle size analysis method. The chemical compositions of the materials are presented in Table 2. The polypropylene used is a synthetic material with resistance to alkalis, chloride and chemical and are non-corrosive and hydrophobic, and was supplied by Helios drive, Baglan Energy, Port Talbot, UK. The glass fibre used is also an alkali-resistant glass fibre and was supplied by Fibre Technologies International Avonmouth, Bristol. Glass fibre is a material with excellent properties, it has random network structure composed of SiO_4 tetrahedra. It has a perfect insulating behaviour, excellent corrosion resistance, strong heat resistance and high tensile strength (1950–2050 MPa). A 12 mm length and 12–13 μm diameter polypropylene fibres and 10 mm length and 14 μm diameter glass fibres were used.

Table 1. Consistency limits and other properties of kaolin clay.

Soil Property	Value
Consistency Limits	
Liquid limit w_L (%)	56
Plastic limit w_P (%)	26
Plasticity index I_p (%)	30ZZ
Others	
Specific gravity	2.6
Expansion index, EI	58.4
Potential expansion	Medium
Maximum dry Density (kg/m^3)	1430
timum moisture content (%)	27

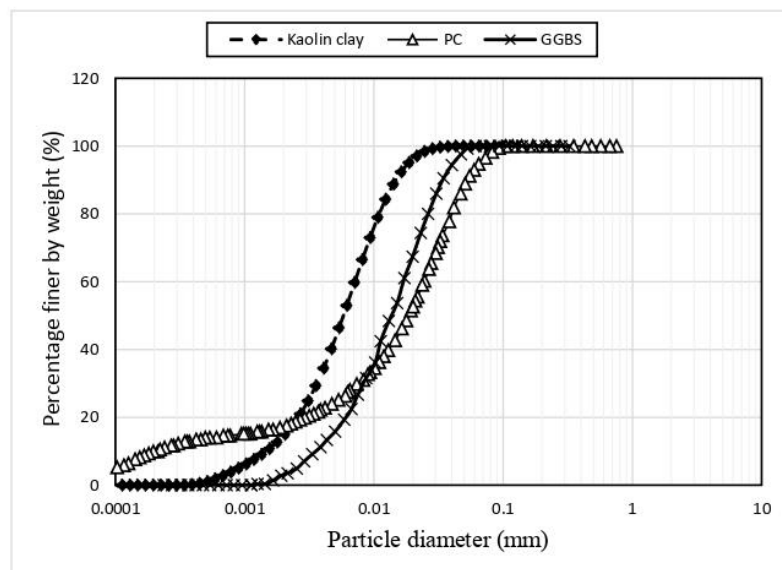


Figure 1. Distribution of particle size.

Table 2. Chemical composition of materials.

Materials Used	Oxides (%)											
	SiO ₂	TiO ₂	Al ₂ O ₃	Fe ₂ O ₃	MnO	MgO	CaO	Na ₂ O	K ₂ O	P ₂ O ₅	SO ₃	LOI
Clay	48.00	0.02	37.00	0.65	-	0.300	0.07	-	1.60	-	-	12.5
Portland cement	20.00	-	6.00	3.0	0.09	4.21	63.0	-	-	0.20	2.30	0.80
GGBS	33.28	0.57	13.12	0.32	0.316	7.74	37.16	0.33	0.474	0.009	2.21	4.42
Micro silica	90.6	<0.1	1.47	1.93	-	0.42	1.52	0.63	1.31	0.28	0.41	1.33

4. Experimental Program

4.1. Mix Compositions and Sample Preparation

The mix compositions were developed to improve the strength and linear expansion of the investigated clay with further consideration of possible reduction in cement and the inclusion of SCM and fibres. In the first stage of mixing, the clay was mixed with 5% of PC by dry weight of soil. In the other stages of mixing, several mix compositions were considered with their corresponding average optimal moisture content (OMC) as shown in Table 3. The aim was to reduce cement content and replace with GGBS, lime, micro silica and synthetic fibres to develop an economic and environmentally friendly binder combination for soil treatment. Dry materials were mixed thoroughly at optimal moisture content in a variable speed Kenwood Chef Excel mixer for 2 min to enhance homogeneity before slowly adding the calculated amount of water. After proper mixing, wet mixed materials were placed into a cylindrical steel mould (50 mm in diameter and 100 mm in length) fitted with a collar to help accommodate all the material required for one sample. Samples placed in the cylindrical steel mould were equally compacted to maximum dry density (MDD) at optimal moisture (ASTM D698, 2012), using a hydraulic jack. The prefabricated mould ensured that the material was not over compacted. The cylinders were extruded using a steel plunger, wrapped in several runs of cling film, labelled and placed in polythene bags before being placed on a platform in sealed plastic containers. Water was always maintained below the platform to ensure that there was no evaporation from the samples. The plastic containers were then placed in an environmental chamber capable of maintaining temperatures to 20 °C until they are ready for testing after 7- and 14-days moist curing period. Additional curing was carried out after 14 days, this time samples were cured under elevated temperatures (ET) of 30°, 40° and 50 °C for 48 h.

Table 3. Mix proportion and materials.

Mix Composition	Materials							Average OMC
	Clay	Portland cement	Glass fibre	Polyprop-ylene fibre	Lime	GGBS	Micro silica	
Untreated soil	√	-	-	-	-	-	-	28.2
5%PC + 0%F	√	√	-	-	-	-	-	24.6
5%PC + 0.4%GF	√	√	√	-	-	-	-	24.4
5%PC + 0.4%PPF	√	√	-	√	-	-	-	
5%PC + 0.6%GF	√	√	√	-	-	-	-	
5%PC + 0.6%PPF	√	√	-	√	-	-	-	
5%PC + 0.8%GF	√	√	√	-	-	-	-	
5%PC + 0.8%PPF	√	√	-	√	-	-	-	
2%PC + 3%SCM + 2%Lime + 0%F	√	√	-	-	√	√	-	
2%PC + 3%SCM + 2%Lime + 0.4%GF	√	√	√	-	√	√	-	23.2
2%PC + 3%SCM + 2%Lime + 0.4%PPF	√	√	-	√	√	√	-	
2%PC + 3%SCM + 2%Lime + 0.6%GF	√	√	√	-	√	√	-	
2%PC + 3%SCM + 2%Lime + 0.6%PPF	√	√	-	√	√	√	-	
2%PC + 3%SCM + 2%Lime + 0.8%GF	√	√	√	-	√	√	-	
2%PC + 3%SCM + 2%Lime + 0.8%PPF	√	√	-	√	√	√	-	
2%PC + 3%SCM + 0%F	√	√	-	-	-	-	√	
2%PC + 3%SCM + 0.4%GF	√	√	√	-	-	-	√	23.5
2%PC + 3%SCM + 0.4%PPF	√	√	-	√	-	-	√	
2%PC + 3%SCM + 0.6%GF	√	√	√	-	-	-	√	
2%PC + 3%SCM + 0.6%PPF	√	√	-	√	-	-	√	
2%PC + 3%SCM + 0.8%GF	√	√	√	-	-	-	√	
2%PC + 3%SCM + 0.8%PPF	√	√	-	√	-	-	√	

4.2. Laboratory Testing

4.2.1. Unconfined Compression Test

At the end of each of the moist curing periods, the treated samples were subjected to UCS tests. The UCS test was conducted in two stages after each curing periods. Firstly, the UCS test was conducted on samples cured under 20 °C after 7 and 14 days respectively. The second phase of UCS test was conducted on 14 days cured samples subjected to elevated curing temperatures of 30°, 40° and 50 °C for 48 h, and tested before cooling and after 24 h cooling period, to investigate the effect of a sudden rise and fall in curing temperature on UCS of the treated soils. Samples were placed on the platens of the HounMSiled compression test machine and loaded until failure at a strain rate of 1 mm/min in accordance with BS EN 12390-4:2000 and ASTM D2166/D2166M (2013).

4.2.2. Swell Test

The samples tested for swelling were placed on a platform in a glass tank and covered with a lid fitted with dial gauges. The cylindrical samples were partially immersed in water to a depth of 10 mm above the sample base and swell was monitored for 7 days after 7- and 14-days moist curing periods. The tank was placed in the environmental chamber where conditions were maintained at 20 °C and 100% relative humidity. Values of linear axial swelling were recorded daily until no further expansion occurred, (BS EN 13286-49:2004). Both the moist curing environment and the soaking environment were closed sealed systems to reduce the availability of carbon dioxide and prevent carbonation of the lime, and clearly, excessive carbonation of the lime would reduce the amount of lime available for pozzolanic reaction and is, therefore, undesirable [12].

4.3. Scanning Electron Microscope (SEM)

Microscopic examination and measurement of soil pores have gained so much interest in recent years, partly because the analysis of images of soil fabric provides a straightforward investigation and analysis of soil void and porosity including clay particle degree of arrangement [42,43]. In this study, the micro-structural characteristics of the investigated soils were studied using scanning electron microscopy (SEM) to allow for microscopic examination and measurement of soil pores and orientation. Observations were made on dried and highly vacuumed samples using an acceleration voltage of up to 5 kV. In order to examine the micro-structural characteristics of the samples, scanning electron micrograph (SEM) was conducted on samples mixed with 5%PC, 2%PC + 3%GGBS and 2%PC + 3%MS to understand the effect of cementation effect on soil pores and orientation.

5. Results and Discussion

5.1. Unconfined Compressive Strength (UCS) of Samples Cured under Normal Temperature

The effectiveness of the investigated mix compositions has been evaluated and presented in terms of UCS as an index in defining the extent of improvement of soils due to chemical treatment. According to the (ASTM D 4609), an effective soil stabilisation process using binders, should give a minimum target value of UCS equals 345 kPa. The UCS of the fibre reinforced clay blended with cement, lime, GGBS and micro silica, cured under 20 °C is presented in Figures 2–4. The results plotted in Figure 2 shows that after 14days curing period, the UCS of samples mixed with 5% cement increases from 707 kPa at 0% fibre content to 957 kPa) and 964kPa at 0.4% polypropylene and 0.8% glass fibre contents respectively. The increase in UCS with increasing cement and fibre contents agrees with the results of Chore and Vaidya, and Cheng et al. [44,45]. Over time, the high strength observed in the samples containing 5%PC and 0 to 0.8% fibre is due to the formation of calcium silicate hydrate gel (C-S-H gel) as expected. This result also shows that the presence of fibre does not interfere with the strength development and hence increased UCS. The reduction in cement content to 2%PC and inclusion of 3% GGBS and 2% lime at 14days, show the UCS increased above the minimum target of UCS for a stabilised soil as recommended by the ASTM 4609, as shown in Figure 3, which again explains the effectiveness of the mix composition with reference to ASTM 4609. The observed increase in UCS is due to the cementation effect and the inclusion of lime to the pozzolanic supplementary cementitious material. However, from Figure 4, it is evident that the UCS of the mixture containing 2%PC and 3% micro silica falls below the minimum target irrespective of the fibre type and content due to reduced cement paste and bonding effect of soil-cement particles in the presence of a siliceous material with lower cementitious value, [46] after 7 and 14 days, respectively.

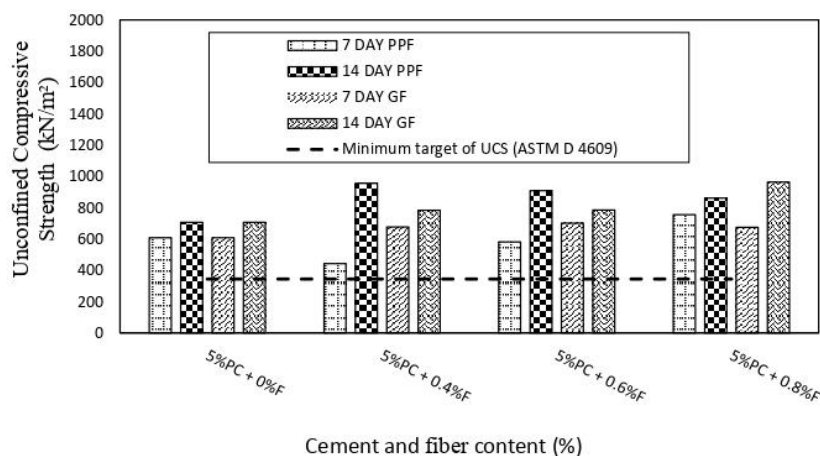


Figure 2. Unconfined compressive strength (UCS) test results for 5%PC and fibre for 7 and 14 days of curing.

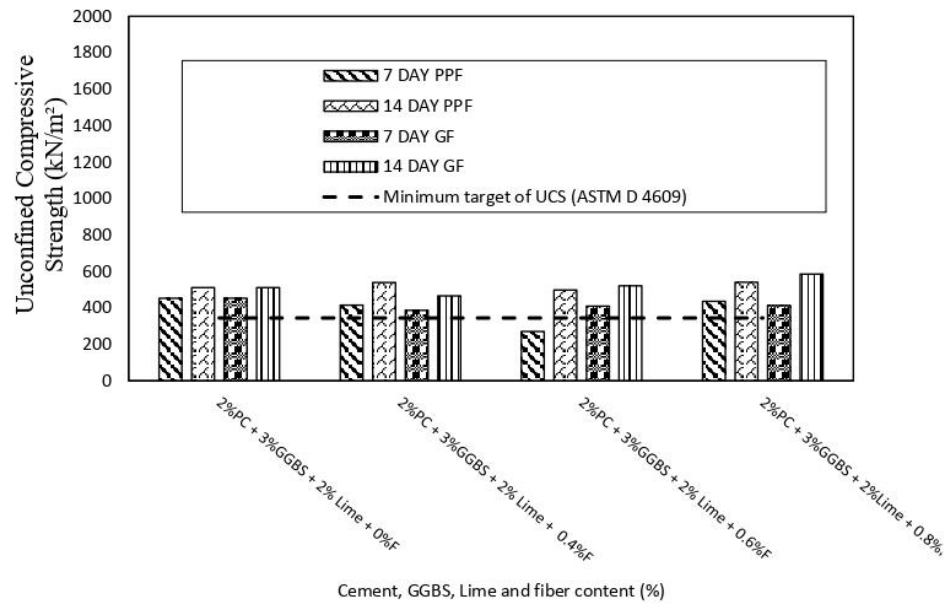


Figure 3. UCS results for 2%PC, 3%GGBS, 2%Lime and Fibre content after 7 and 14 days of curing.

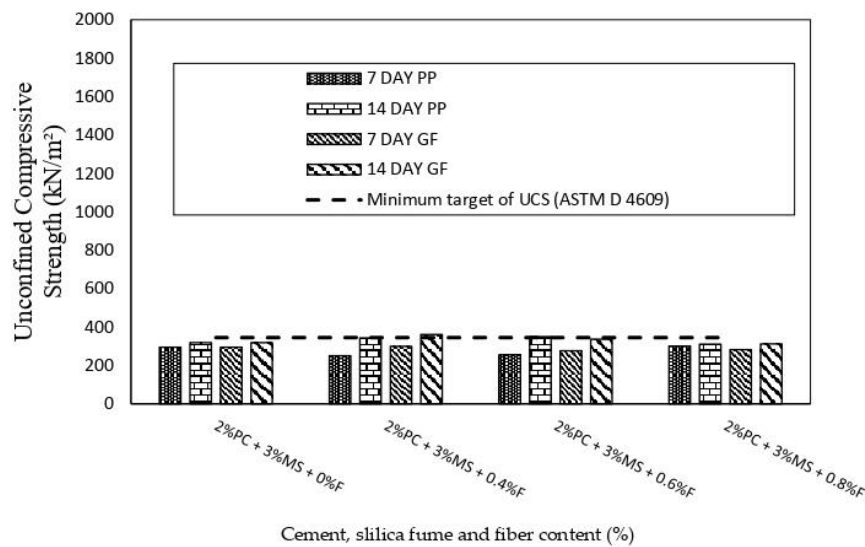


Figure 4. UCS results for 2%PC, 3%MS and fibre content after 7 and 14 days of curing.

Effect of Elevated Temperature on UCS

The UCS of samples cured for an additional 48 h under elevated curing temperatures of 30°, 40° and 50 °C after 14 days of curing under 20 °C, were tested in two stages. Firstly, the effect of elevated curing temperature on UCS was investigated for samples tested immediately after the 48 h of ET curing and secondly, for samples tested after 24 h cooling period, respectively. The results of the effectiveness of the investigated clay-binder mixtures in terms of UCS are presented in Figures 5–8. The results presented in Figures 5–8 show that at a higher curing temperature between 30 and 50 °C, and binder-fibre contents, the UCS of the reinforced clay increases in most cases under both testing conditions. Figures 5 and 6 show that in most cases, as temperature increases, the UCS of polypropylene fibre reinforced clay increases with an increase in cement and fibre contents respectively. However, the increase in UCS of the fibre-reinforced cemented clay can be attributed more to the bonding effect of the cement and other used cementitious materials (Lime, GGBS and MS) than the contribution of the polypropylene and glass fibres respectively. The UCS increases from 900 kPa to 1200 kPa and

from 1200 kPa to 1300 kPa at 5% cement and 0.8% polypropylene fibre contents for samples tested immediately after ET curing and samples tested after 24 h cooling period. This is due to an increase in the rate of hydration reaction at 30, 40 and 50 °C and the bonding effect of the clay-binder-fibre system. According to Clare et al. [47] curing temperature up to 45 °C is enough to result in an accelerated increase in strength of stabilised clay, and “the nature of the strength/age relationships obtained with the cohesive soils means that at temperatures up to 45 °C one mechanism of hardening is involved; and that this is accelerated by increased temperature”.

The UCS of the glass fibre-reinforced clay-binder mixtures reaches a maximum value of 1300 kPa and 1400 kPa at 5% cement and 0.8% glass fibre for samples tested immediately after ET curing and samples tested after 24 h cooling period respectively. The inclusion of fibres along with the cement only enhances the UCS as the curing time increases [27]. This statement is in line with the observations made in the present studies however, the present study has also considered an increase in temperature during the time the treated soils were cured, and it was found that the combination of the temperature effect and curing time, closely bonded and parked the particles together. Under the ET curing and cooling periods, the UCS of the investigated fibre-reinforced clay-binder samples increases more than that of the samples cured for 14 days under 20 °C. It was observed that the dimensions of the samples (50 mm diameter and 100 mm length) remained unchanged after curing under the investigated elevated temperatures due to the ability of polypropylene and glass fibres to control both volume change and any associated increase in porosity. The increase in UCS of the clay-binder-fibre system after cooling as shown in Figures 6 and 8 is an indication of the absence of both dehydration of the C-S-H gel and breakdown of the structure of the cement paste after curing under elevated temperatures up to 50 °C. This means that the presence of polypropylene and glass fibres in a clay-binder-fibre system does not interfere with the tricalcium silicate (C_3S) responsible for early strength development and the bulk of C-S-H gel and calcium hydroxide ($Ca(OH)_2$) produced during the hydration process but rather reinforces and increases resistance to deformation. The reduction in cement content and inclusion of lime, GGBS and micro silica resulted in UCS values greater than the minimum target of UCS for evaluation of the effectiveness of any soil treatment activity as stated by the ASTM D 4609. The interaction between cement, GGBS, and lime with polypropylene and glass fibres under elevated curing temperatures, and the pozzolanic property and extreme fineness of micro silica all contributed to the enhanced performance of the fibre-reinforced clay-binder mixtures in terms of UCS. The increase in UCS above the minimum target of UCS can also be attributed to the ability of micro silica to bind and coat all clay particles which possess very little cementitious value [48].

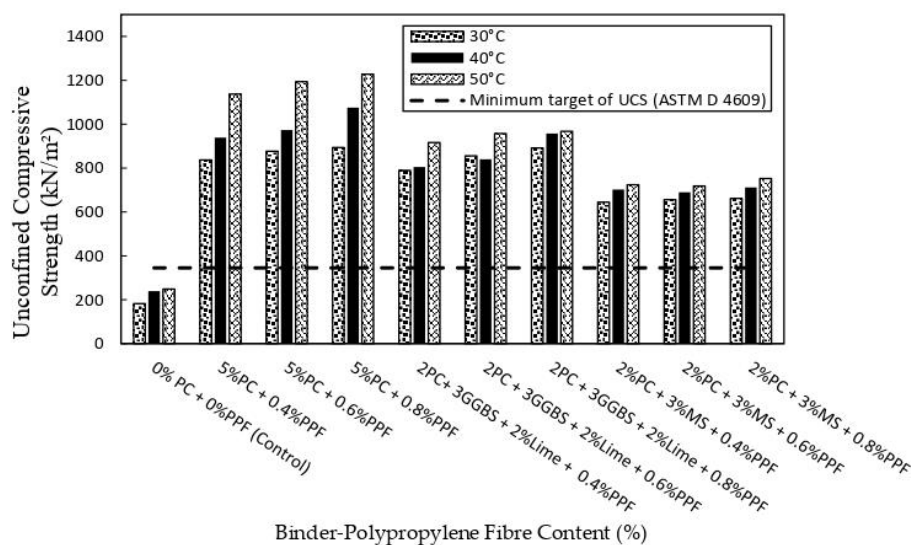


Figure 5. UCS of polypropylene and clay-binder mixtures tested immediately after 48 h elevated temperatures (ET) curing.

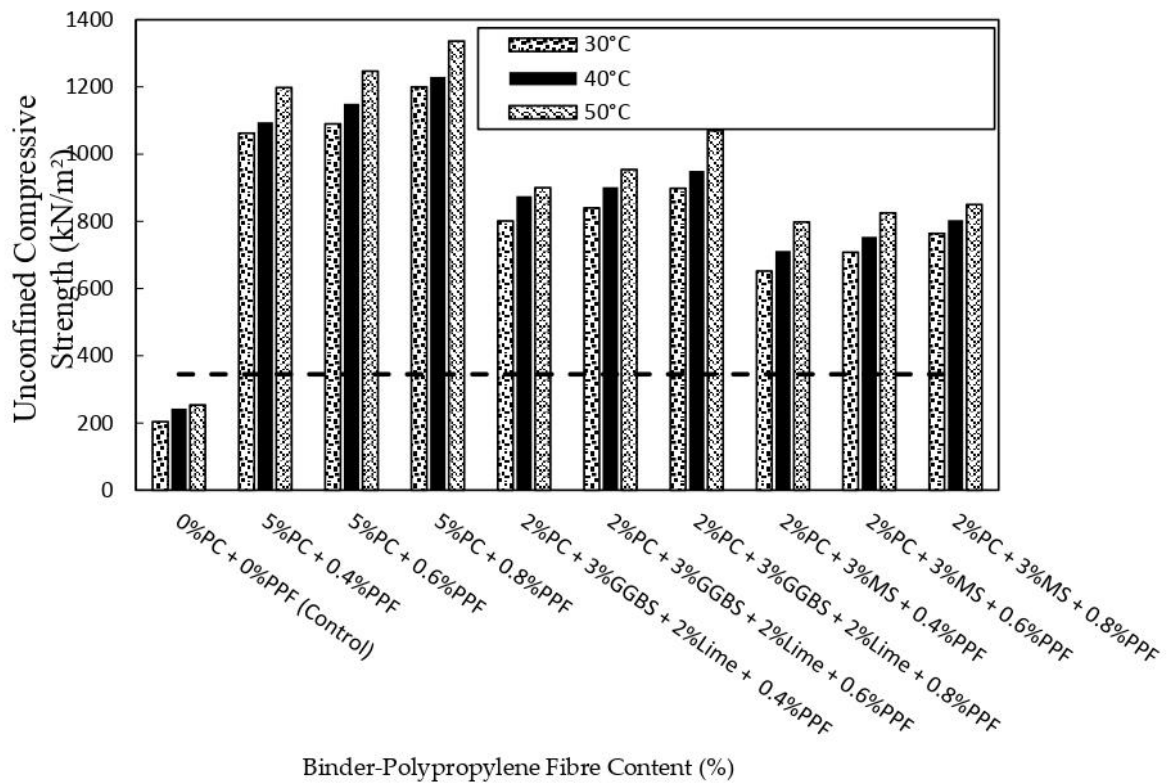


Figure 6. UCS of polypropylene-reinforced clay-binder mixtures tested after 24 h cooling period.

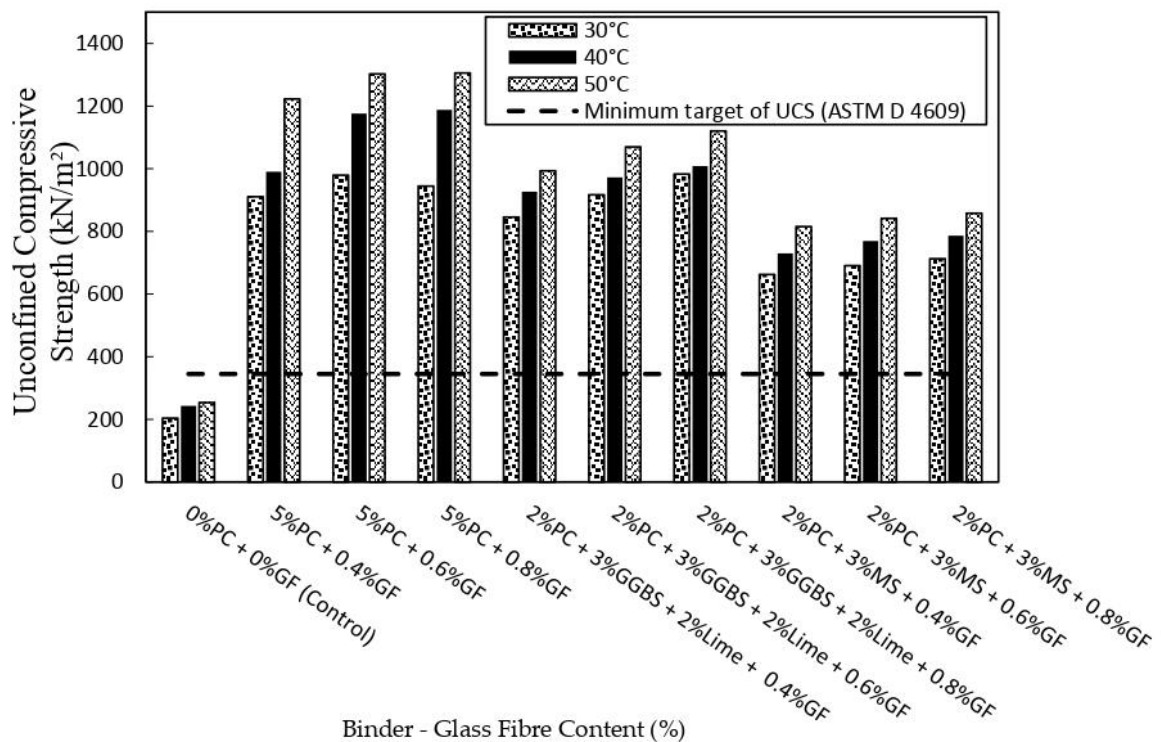


Figure 7. UCS of glass fibre-reinforced clay-binder mixtures tested immediately after ET curing.

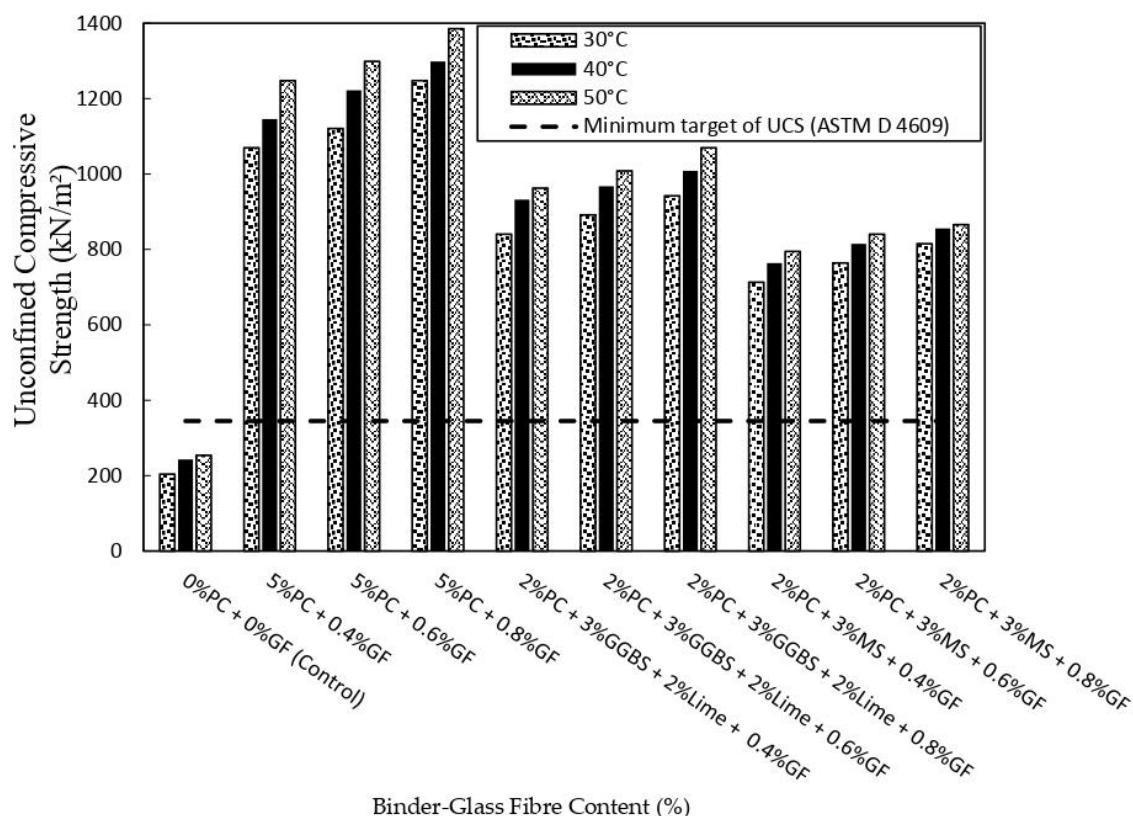


Figure 8. UCS of glass fibre-reinforced clay-binder mixtures tested after 24 h cooling period.

5.2. Linear Expansion

The Control mix with 0%PC and 0%F achieved the highest linear expansion value of 7.92% after 7 days soaking period as shown in Figure 9a due to intercrystalline swelling of kaolinite clay in the presence of water. This clay seems to absorb much water within the first 2 days after which the expansion plateaus, indicating an equilibrium condition. However, the addition of 5%PC and 0% fibre resulted to a drastic decrease in expansion from 7.92% to 0.2% as shown in Figure 9a,b. Similarly, the inclusion of polypropylene and glass fibres show the linear expansion reduces from 7.92% to 0.48% and 0.32% at 0.8% polypropylene and 0.6% glass fibre contents, respectively. The results presented in Figure 9c to f show that a reduction in cement content to 2%PC and the inclusion of 3% micro silica and 3% GGBS and 2% lime, also reduces the linear expansion of the fibre reinforced clay compared to the linear expansion of the unreinforced control sample. At reduced cement content, the inclusion of 3% GGBS and 2% lime, reduce the linear expansion of the unreinforced kaolin clay from 7.92% to 0.87% at 0% fibre content. However, the inclusion of polypropylene and glass fibre reinforcements reduces the linear expansion of the unreinforced clay from 7.92% to 1.21% and 0.92% at 0.4% polypropylene and glass fibre content respectively. The reduction in expansion in the presence of cement, lime and GGBS can be attributed to the hydration process in PC when soaked in water and the formation of more calcium silicate hydrate gel (C-S-H gel) due to the presence of high amount of tricalcium silicate (C_3S) in Portland cement leading to early strength gain and particle bonding, [49]. Also, the addition of fibres in the soil means that when swelling occurs the fibres are stretched creating tension in the fibres which causes it to resist swelling. According to Soltani et al. [30], the greater the contact between the fibres and soil particles, the greater the resistance to swelling. However, it was observed that the application of polypropylene and glass fibres reduces linear expansion of the unreinforced clay but, the mix compositions with 0% fibre content achieved fairly lower expansion than other mixtures except for mix composition containing (2%PC + 3%MS + 0%GF) due to low silic fume content as seen in

Figure 9e,f. However, Al-Soudany [50] reported that free swell and swell pressure can decrease by increasing the percentage of micro silica between 3% and 7%. In the present study, the inclusion of polypropylene and glass fibres resulted to a reduction in swell at higher fibre contents compared to the swell potential of the original soil. Therefore, polypropylene and glass fibres have the potential of reducing swelling in clay when mixed with GGBS, micro silica, 2% lime and 2% cement.

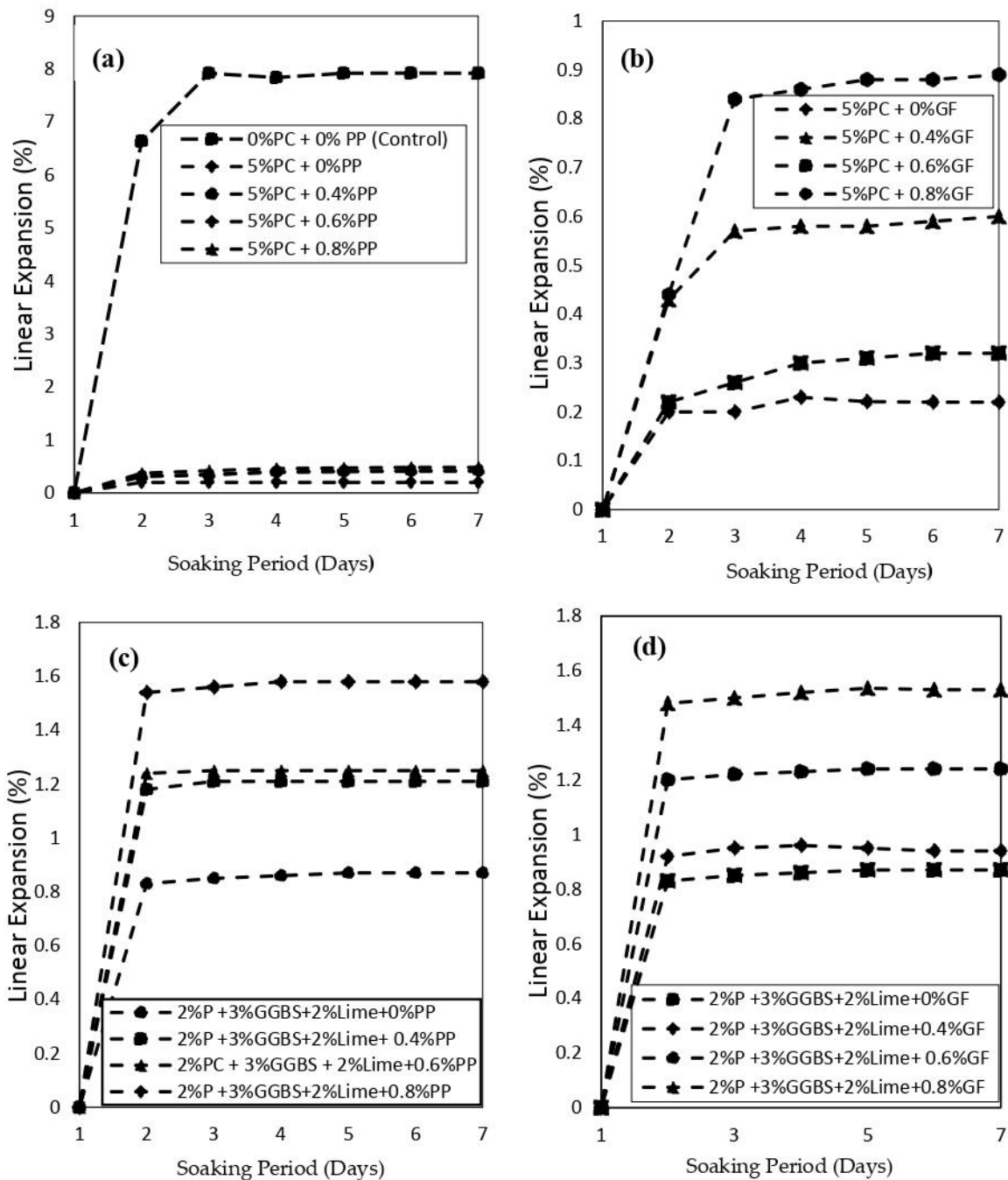


Figure 9. Cont.

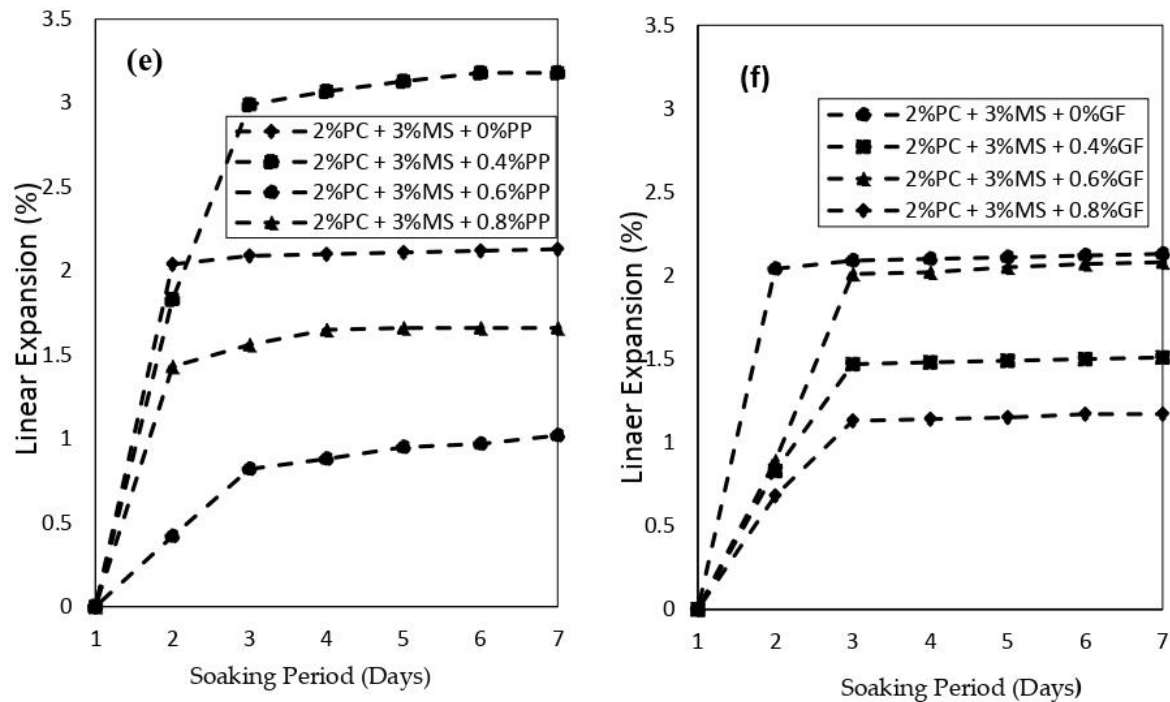


Figure 9. (a–f) Linear expansion of the clay-binder mixtures versus soaking time.

5.3. Scanning Electron Microscopy (SEM) of Treated Soils

The SEM images presented in Figure 10a–d, show the micro-structural orientation of the unreinforced and reinforced clay blended with PC and supplementary cementitious materials such as GGBS and micro silica. Figure 10a shows the presence of pore and hollow cavities, for the unreinforced kaolin clay while several aggregated soil particles of varying shape and size, gel formation are observed with the addition of 5%PC as shown in Figure 10b. Information on particle size distribution of the investigated clay is as previously presented in Figure 1. The formation of the cementitious hydrated compound can be attributed to the development of a cementitious compound called calcium silicate hydrate (CSH gel) during the hydration of cement. This increases the bonding between particles, closing up and filling pores and leading to the formation of a more closely packed soils with higher strength and lower expansion. According to Jha and Sivapullaiah, [42], the binding and coating of aggregated soil particles leads to the formation of densely packed and compacted structure, whereas relatively lesser white patches are observed, reflecting the consumption of cementitious gel in filling and binding of particles. The hydration products of cement hydration surround and connect clay particles together to form a denser structure and reduced voids. Figure 10c shows the SEM image of the reinforced clay with 2%PC + 3%GGBS + 2%lime + 0%F, with a dense matrix which in turn resulted to a reduction in expansion. At reduced cement content of 2%PC and inclusion of 3% micro silica, the microstructure of the reinforced clay shows more of a conglomerated attributes living some pore and hollow cavity at 0% fibre content as shown in Figure 10d.

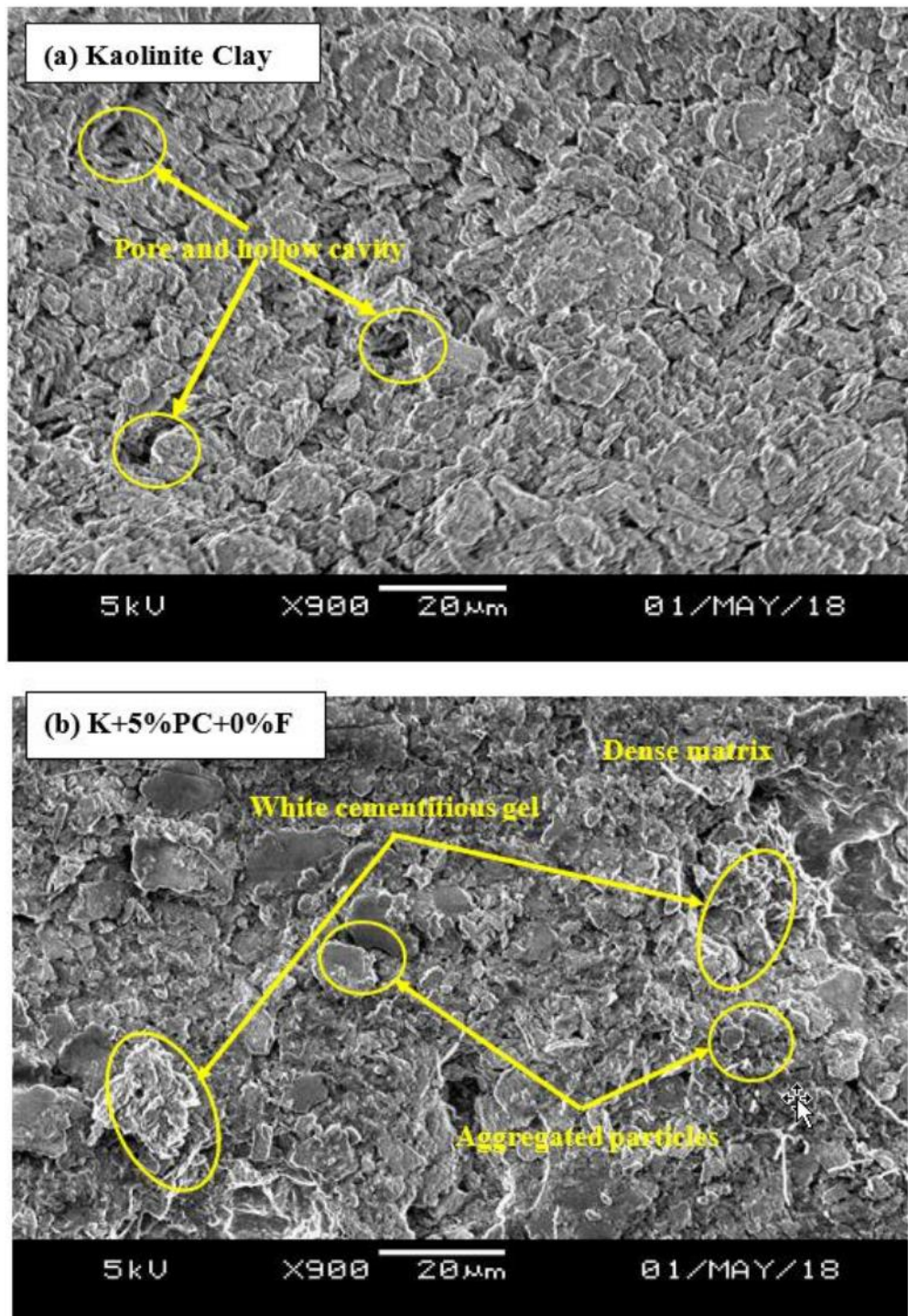


Figure 10. Cont.

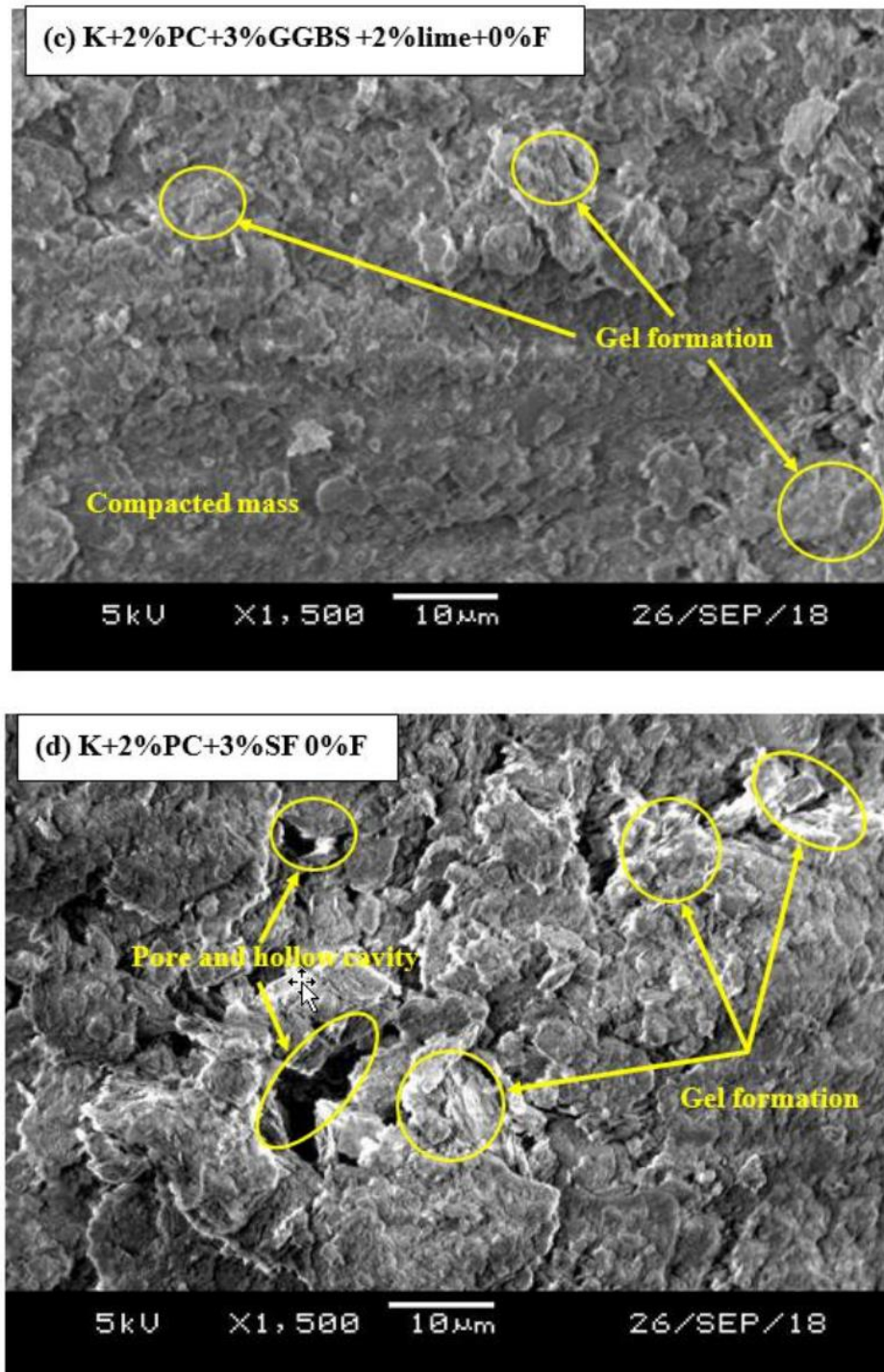


Figure 10. (a–d) SEM images of fibre-reinforced clay blended with PC and SCM.

5.4. Geological Engineering Significance

Clay soils often present difficulties in construction operations such as sliding and swelling during or after construction and can lead to significant geological disasters and geological environmental damages. However, the susceptibility of clayey soils to sliding and swelling can be controlled by enhancing the engineering properties of the clay by the addition of small percentages, by weight,

of cement to produce an improved clay-cement material that can be used for construction purposes. The experimental results obtained from the present study indicate that the susceptibility of swelling clays to landsliding during construction activities can be reduced drastically by stabilisation with synthetic fibres blended with GGBS and micro silica based on the level of improvement achieved. Compared to that of the untreated clay which will exhibit significant swelling and shrinkage behaviour in the presence of water due to the amounts of swelling clay minerals. The unconfined compressive strengths and shear strengths of untreated clay soils will decrease dramatically upon saturation which may lead to landsliding, for example, during construction of high-speed railways. However, the present study has shown that the use of synthetic fibre and by-product cementitious materials have the ability to increase the strength of clay soils when mixed together at optimal moisture content due to the binding and cementation of clay particles by the cementitious by-products in the presence of reduced amount of cement. This implies that synthetic fibres blended with by-product cementitious materials can find application in stabilisation and improvement of the engineering properties of clayey soil slopes to eliminate possible geological disasters and geological environmental damages that may occur during or after construction. Nonetheless, it is important also to state that the properties of clay in a clay-cement mixture can be affected by the type of minerals present in the clay. Therefore, the clay type used in this study (kaolin clay) may appear to have little effect on the hydration and hardening process and hence, the significant increase in strength and reduction in swelling potential. It is recommended that the application of these synthetic fibres blended with GGBS and micro silica mixed with a small amount of cement be extended to the stabilisation of clay of dominantly montmorillonite due to higher expansive lattice and possibly more significant influence on the hardening process.

6. Conclusions

In the present study, a series of tests has been performed on clayey soil mixed with different percentages of stabilisers; cement, lime and micro silica and synthetic fibres; polypropylene and glass fibres to investigate the characteristics of the stabilized soils. The mechanical properties and microstructure of the fibre-reinforced clay blended with cement, lime, GGBS and micro silica were studied. The following conclusions may be drawn:

1. An increase in polypropylene and glass fibre contents caused an increase in UCS but brought on the reduction of linear expansion at fibre content up to 0.8% for cement-clay mixture reinforced with 5%PC. The use of 0.4–0.8% polypropylene and glass fibre contents in reinforcing cement-clay mixture at 5% cement content caused an increase in UCS values above minimum UCS target value according to ASTM 4609 after 7 and 14 days curing at 20 to 50 °C temperature.
2. At reduced cement content of 2%, cement-clay mixtures blended with lime and GGBS required 14 days curing period under 20 °C to achieve UCS value greater than minimum UCS target value according to ASTM 4609; however, at elevated curing temperature of 30 to 50 °C, higher UCS values were obtained after 7 days' curing period. For the samples cured under elevated curing temperature, the observed increase in unconfined compressive strength upon reduction in cement content implies that less PC should be needed to stabilise clay soils under tropical than under temperate conditions.
3. At reduced cement content of 2%PC and inclusion of 3% micro silica, the microstructure of the fibre-reinforced clay showed a denser matrix with closely parked particles at 0.8% fibre content compared to a microstructure with pore and hollow cavity at 0% fibre content for 2%PC + 3%MS mixture.
4. At elevated curing temperature up to 50 °C, the addition of polypropylene and glass fibres in cement-clay mixtures blended with GGBS and micro silica caused an increase in UCS even at reduced cement content of 2%.
5. The increase in UCS is due to the development of a cementitious compound called the calcium silicate hydrate (CSH gel) during the hydration of cement and subsequent increases in the bonding

between particles, filling of pores and formation of a more closely packed soils. Therefore, this new clean production of fibre-reinforced cement-clay mixture blended with industrial by-product materials can be applied in a wide range of soil reinforcements.

Compliance with Ethical Standards

Author Contributions: Conceptualization, S.J.A., J.O., S.Y.A. and S.N.; Data curation, S.J.A. and S.Y.A.; Formal analysis, S.J.A., E.U.E., J.O. and S.Y.A.; Investigation, S.J.A., E.U.E., S.Y.A. and S.N.; Methodology, S.J.A., J.O. and E.U.E.; Project administration, S.J.A., E.U.E., J.O. and S.N.; Resources, S.J.A., E.U.E., J.O., S.Y.A. and S.N.; Supervision, J.O. and S.N.; Validation, S.N.; Writing—original draft, S.J.A.; Writing—review & editing, S.J.A., E.U.E., J.O., S.Y.A. and S.N. All authors have read and agreed to the published version of the manuscript.

Funding: The authors have not received any external funding for this work.

Conflicts of Interest: The authors declare that they have no conflict of interest.

References

1. Modarres, A.; Nosoudy, Y.M. Clay Stabilization Using Coal Waste and Lime—Technical and Environmental Impacts. *Appl. Clay Sci.* **2015**, *116–117*, 281–288. [[CrossRef](#)]
2. Abbey, S.J.; Ngambi, S.; Coakley, E. Effect of Cement and By-Product Material Inclusion on Plasticity of Deep Mixing Improved Soils. *Int. J. Civ. Eng. Technol.* **2016**, *7*, 265–274.
3. Farouk, A.; Shahien, M.M. Ground Improvement Using Soil-Cement Columns: Experimental Investigation. *Alexandria Eng. J.* **2013**, *52*, 733–740. [[CrossRef](#)]
4. Abbey, S.J.; Eyo, E.U.; Ng'ambi, S. Swell and Microstructural Characteristics of High-Plasticity Clay Blended with Cement. *Bull. Eng. Geol. Environ.* **2019**. [[CrossRef](#)]
5. Nidzam, R.M.; Kinuthia, J.M. Sustainable Soil Stabilisation with Blastfurnace Slag—A Review. *Proc. Inst. Civ. Eng.-Constr. Mater.* **2010**, *163*, 157–165. [[CrossRef](#)]
6. Higgins, D. *Soil Stabilisation with Ground Granulated Blastfurnace Slag*; UK Cementitious Slag Makers Association (CSMA): London, UK, 2005.
7. Eyo, E.U.; Ngambi, S.; Abbey, S.J. Investigative Study of Behaviour of Treated Expansive Soil Using Empirical Correlations. In *International Foundation Congress and Equipment Expo 5–10 March*; American Society of Civil Engineers (ASCE): Orlando, FL, USA, 2018; pp. 373–384.
8. Abbey, S.J.; Ng'ambi, S.; Ganjian, E. Development of Strength Models for Prediction of Unconfined Compressive Strength of Cement/by-Product Material Improved Soils. *Geotech. Test. J.* **2017**, *40*, 928–935. [[CrossRef](#)]
9. Eyo, E.U.; Ngambi, S.; Abbey, S.J. Investigative Modelling of Behaviour of Expansive Soils Improved Using Soil Mixing Technique. *Int. J. Appl. Eng. Res.* **2017**, *12*, 3828–3836.
10. Eyo, E.U.; Ngambi, S.; Abbey, S.J. Performance of Clay Stabilized by Cementitious Materials and Inclusion of Zeolite / Alkaline Metals-Based Additive. *Transp. Geotech.* **2020**, *23*. [[CrossRef](#)]
11. Abbey, S.J.; Ngambi, S.; Olubanwo, A.O. Effect of Overlap Distance and Chord Angle on Performance of Overlapping Soil-Cement Columns. *Int. J. Civ. Eng. Technol.* **2017**, *8*, 627–637.
12. Wild, S. Effects of Ground Granulated Blast Furnace Slag (GGBS) on the Strength and Swelling Properties of Lime-Stabilized Kaolinite in the Presence of Sulphates. *Clay Miner.* **1996**, *31*, 423–433. [[CrossRef](#)]
13. Cokca, E.; Yazici, V.; Ozaydin, V. Stabilization of Expansive Clays Using Granulated Blast Furnace Slag (GBFS) and GBFS-Cement. *Geotech. Geol. Eng.* **2009**, *27*, 489–499. [[CrossRef](#)]
14. James, R.; Kamruzzaman, A.H.M.; Haque, A.; Wilkinson, A. Behaviour of Lime-Slag-Treated Clay. *Proc. Inst. Civ. Eng.-Gr. Improv.* **2008**, *161*, 207–216. [[CrossRef](#)]
15. Azzam, W.R. Utilization of Polymer Stabilization for Improvement of Clay Microstructures. *Appl. Clay Sci.* **2014**, *93–94*, 94–101. [[CrossRef](#)]
16. Soltani, A.; Taheri, A.; Khatibi, M.; Estabragh, A.R. Swelling Potential of a Stabilized Expansive Soil: A Comparative Experimental Study. *Geotech. Geol. Eng.* **2017**, *35*, 1717–1744. [[CrossRef](#)]
17. Haase, H.; Schanz, T. Compressibility and Saturated Hydraulic Permeability of Clay-Polymer Composites—Experimental and Theoretical Analysis. *Appl. Clay Sci.* **2016**, *130*, 62–75. [[CrossRef](#)]

18. Correia, A.A.S.; Venda Oliveira, P.J.; Custódio, D.G. Effect of Polypropylene Fibres on the Compressive and Tensile Strength of a Soft Soil, Artificially Stabilised with Binders. *Geotext. Geomembr.* **2015**, *43*, 97–106. [[CrossRef](#)]
19. Olgun, M. Effects of Polypropylene Fiber Inclusion on the Strength and Volume Change Characteristics of Cement-Fly Ash Stabilized Clay Soil. *Geosynth. Int.* **2013**, *20*, 263–275. [[CrossRef](#)]
20. Tang, C.-S.; Shi, B.; Cui, Y.-J.; Liu, C.; Gu, K. Desiccation Cracking Behavior of Polypropylene Fiber-Reinforced Clayey Soil. *Can. Geotech. J.* **2012**, *49*, 1088–1101. [[CrossRef](#)]
21. Puppala, A.J.; Musenda, C. Effects of Fiber Reinforcement on Strength and Volume Change in Expansive Soils. *Transp. Res. Rec. J. Transp. Res. Board* **2007**, *1736*, 134–140. [[CrossRef](#)]
22. Abdi, M.R.; Parsapajouh, A.; Arjomand, M.A. Effects of Random Fiber Inclusion on Consolidation, Hydraulic Conductivity, Swelling, Shrinkage Limit and Desiccation Cracking of Clays. *Int. J. Civ. Eng.* **2008**, *6*, 284–292.
23. Ikizler, S.B.; Aytekin, M.; Nas, E. Laboratory Study of Expanded Polystyrene (EPS) Geofabric Used with Expansive Soils. *Geotext. Geomembr.* **2008**, *26*, 189–195. [[CrossRef](#)]
24. Al-Akhras, N.M.; Attom, M.F.; Al-Akhras, K.M.; Malkawi, A.I.H. Influence of Fibers on Swelling Properties of Clayey Soil. *Geosynth. Int.* **2008**, *15*, 304–309. [[CrossRef](#)]
25. Punthutaecha, K.; Puppala, A.J.; Vanapalli, S.K.; Inyang, H. Volume Change Behaviors of Expansive Soils Stabilized with Recycled Ashes and Fibers. *J. Mater. Civ. Eng.* **2006**, *18*, 616–617. [[CrossRef](#)]
26. Wang, Y.; Cui, Y.J.; Tang, A.M.; Tang, C.S.; Benahmed, N. Effects of Aggregate Size on Water Retention Capacity and Microstructure of Lime-Treated Silty Soil. *Geotechnique Lett.* **2015**, *5*, 269–274. [[CrossRef](#)]
27. Tang, C.; Shi, B.; Gao, W.; Chen, F.; Cai, Y. Strength and Mechanical Behavior of Short Polypropylene Fiber Reinforced and Cement Stabilized Clayey Soil. *Geotext. Geomembr.* **2007**, *25*, 194–202. [[CrossRef](#)]
28. Zaimoglu, A.S.; Yetimoglu, T. Strength Behavior of Fine Grained Soil Reinforced with Randomly Distributed Polypropylene Fibers. *Geotech. Geol. Eng.* **2012**, *30*, 197–203. [[CrossRef](#)]
29. Consoli, N.C.; Arcari Bassani, M.A.; Festugato, L. Effect of Fiber-Reinforcement on the Strength of Cemented Soils. *Geotext. Geomembr.* **2010**, *28*, 344–351. [[CrossRef](#)]
30. Soltani, A.; Deng, A.; Taheri, A. Swell-Compression Characteristics of a Fiber-Reinforced Expansive Soil. *Geotext. Geomembr.* **2018**, *46*, 183–189. [[CrossRef](#)]
31. Viswanadham, B.V.S.; Phanikumar, B.R.; Mukherjee, R.V. Swelling Behaviour of a Geofiber-Reinforced Expansive Soil. *Geotext. Geomembr.* **2009**, *27*, 73–76. [[CrossRef](#)]
32. Syed, M.; Guharay, A. Stabilization of Expansive Soil Reinforced with Polypropylene and Glass Fiber in Cement and Alkali Activated Binder. In *Advancements in Unsaturated Soil Mechanics*; Hoyos, L., Shehata, H., Eds.; Springer International Publishing: Cham, Switzerland, 2020; pp. 41–55.
33. Ateş, A. Mechanical Properties of Sandy Soils Reinforced with Cement and Randomly Distributed Glass Fibers (GRC). *Compos. Part B Eng.* **2016**, *96*, 295–304. [[CrossRef](#)]
34. Ahmad, F.; Mujah, D.; Hazarika, H.; Safari, A. Assessing the Potential Reuse of Recycled Glass Fibre in Problematic Soil Applications. *J. Clean. Prod.* **2012**, *35*, 102–107. [[CrossRef](#)]
35. Ali, G.; Saeed, K.; Parham, R. Stabilization of Silty Sand Soils with Lime and Micro silica Admixture in Presence of Sulfates. In Proceedings of the 14th Pan-American Conference on Soil Mechanics and Geotechnical Engineering, Toronto, ON, Canada, 2–6 October 2011.
36. Al-azzawi, A.A.; Daud, K.A.; Abdul Sattar, M.A. Effect of Micro silica Addition on the Behavior of Silty-Clayey Soils. *J. Eng. Dev.* **2012**, *16*, 92–105.
37. Long, G.; Li, L.; Li, W.; Ma, K.; Dong, W.; Bai, C.; Zhou, J.L. Enhanced Mechanical Properties and Durability of Coal Gangue Reinforced Cement-Soil Mixture for Foundation Treatments. *J. Clean. Prod.* **2019**, *231*, 468–482. [[CrossRef](#)]
38. Kalkan, E. Influence of Micro silica on the Desiccation Cracks of Compacted Clayey Soils. *Appl. Clay Sci.* **2009**, *43*, 296–302. [[CrossRef](#)]
39. Goodarzi, A.R.; Akbari, H.R.; Salimi, M. Enhanced Stabilization of Highly Expansive Clays by Mixing Cement and Micro silica. *Appl. Clay Sci.* **2016**, *132–133*, 675–684. [[CrossRef](#)]
40. Alrubaye, A.J.; Hasan, M.; Fattah, M.Y. Stabilization of Soft Kaolin Clay with Micro silica and Lime. *Int. J. Geotech. Eng.* **2017**, *11*, 90–96. [[CrossRef](#)]
41. ACI, C. 230. State-of-the-Art Report on Soil-Cement. *Mater. J.* **1990**, *87*, 395–417.
42. Jha, A.K.; Sivapullaiah, P.V. Mechanism of Improvement in the Strength and Volume Change Behavior of Lime Stabilized Soil. *Eng. Geol.* **2015**, *198*, 53–64. [[CrossRef](#)]

43. Jamshowang, P.; Nuansrithong, N.; Voottipruex, P.; Songpiriyakij, S. Laboratory Investigations on the Swelling Behavior of Composite Expansive Clays Stabilized with Shallow and Deep Clay-Cement Mixing Methods. *Appl. Clay Sci.* **2017**, *148*, 83–94. [[CrossRef](#)]
44. Chore, H.S.; Vaidya, M.K. Strength Characterization of Fiber Reinforced Cement–Fly Ash Mixes. *Int. J. Geosynth. Gr. Eng.* **2015**, *1*, 1–8. [[CrossRef](#)]
45. Cheng, Q.; Zhang, J.; Zhou, N.; Guo, Y.; Pan, S. Experimental Study on Unconfined Compression Strength of Polypropylene Fiber Reinforced Composite Cemented Clay. *Crystals* **2020**, *10*, 247. [[CrossRef](#)]
46. Mohammed, Y.F.; Aamal, A.A.; Mather, M.J. Characteristics of Clays Stabilized with Lime-Silica Fume Mix. *Ital. J. Geosci.* **2015**, *134*, 104–113. [[CrossRef](#)]
47. Clare, K.E.; Pollard, A.E. The Effect of Curing Temperature on the Compressive Strength Of Soil-Cement Mixtures. *Géotechnique* **1954**, *4*, 97–106. [[CrossRef](#)]
48. Abd El-Aziz, M.; Abo-Hashema, M.; El-Shourbagy, M. “The effect of Lime Silica Fume Stabilizer on Engineering Properties of Clay Subgrade”. In Proceedings of the Fourth Mansoura International Engineering Conference (4th IEC), Faculty of Engineering, Mansoura, Egypt, 1–4 April 2004.
49. Saghiri, M.A.; Orangi, J.; Asaturian, A.; Gutmann, J.L.; Garcia-Godoy, F.; Lotfi, M.; Sheibani, N. Calcium silicate-based cements and functional impacts of various constituents. *Dent. Mater. J.* **2017**, *36*, 8–18. [[CrossRef](#)] [[PubMed](#)]
50. Al-Soudany, K. Remediation of Clayey Soil Using Silica Fume. In Proceedings of the 3rd International Conference on Buildings, Construction and Environmental Engineering, BCEE3-2017, Sharm el-Sheikh, Egypt, 23–25 October 2017. [[CrossRef](#)]



© 2020 by the authors. Licensee MDPI, Basel, Switzerland. This article is an open access article distributed under the terms and conditions of the Creative Commons Attribution (CC BY) license (<http://creativecommons.org/licenses/by/4.0/>).